FOUNDATION ANALYSIS AND DESIGN

Fifth Edition

Joseph E. Bowles, P.E., S.E.
Consulting Engineer/Software Consultant
Engineering Computer Software
Peoria, Illinois

The McGraw-Hill Companies, Inc.

New York St. Louis San Francisco Auckland Bogotá Caracas
Lisbon London Madrid Mexico City Milan Montreal New Delhi
San Juan Singapore Sydney Tokyo Toronto

McGraw-Hill

A Division of The McGraw-Hill Companies

FOUNDATION ANALYSIS AND DESIGN
International Edition 1997

10 09 08 07
20 09 08 07 06
BJE

Library of Congress Cataloging-in-Publication Data
Bowles, Joseph E.
Foundation analysis and design / Joseph E. Bowles. –5th ed.
p. cm.
Includes index.
ISBN 0-07-912247-7 (set)
1. Foundations. 2. Soil mechanics. I. Title.
TA775.B63 1996
624.'5—dc20 95-37880

When ordering this title, use ISBN 0-07-118844-4

Printed in Singapore

PREFACE

This fifth edition continues the format of the previous four editions for providing current state-of-art (SOA) and state-of-practice (SOP) methods in Foundation Engineering. From author-user interaction I have concluded that SOP tends to lag SOA on the average of about 10 years. There is a range, however, where a few larger organizations are at the cutting edge of technology and many—particularly the smaller firms—are at varying intermediate stages.

This textbook, which is also widely used as a practitioner's reference, includes SOP material but with major emphasis on SOA. The latter is accomplished by including a mix of practice, "how to," and latest suggested design/analysis methodology. This produces a text compatible with the general goals of the American Society of Civil Engineers (ASCE) and other professional organizations, which have determined that technical graduates have a postgraduate period of only 5 to 7 years before obsolescence becomes a factor in their practice.

Design methods tend to vary between geographic regions, partly from instructors' influences and partly because there are few "design absolutes." As a consequence it is necessary to include the generally accepted alternative methods but to temper these with recommendations and suggestions on their use. This allows the user access to regional differences and provides "averaged" design results or the option to select the most appropriate alternative on a site-specific basis. Although these comments may appear overly practice-oriented, the fact is that the student must be aware of these real-world conflicts, geographical differences, and alternatives so as to be productive upon graduation.

This book emphasizes computer methods and the Finite-Element Method (FEM), involving matrix methods given in the previous editions, to reflect the widespread use of the personal computer and of the FEM in practice. Be aware, however, that the finite-element method does not have a unique definition. To some practitioners it is any mathematical representation of the continua (beams, plates, or solids) using discrete (or finite) elements. To other practitioners the FEM definition is reserved only for modeling the soil mass and the interfacing structural elements—sometimes this is called "soil-structure interaction" modeling.

In this textbook the former definition is used, for it is the one that is most widely practiced and given in most textbooks devoted solely to the FEM.

This textbook gives sufficient background theory for a FEM model so that the average user should have little difficulty using this method for design/analysis of those types of soil-structure interfacings used herein. It does make the modest assumption that most students at the level of this textbook have been exposed to some FEM and matrix methodology in statics; elementary structures; and the required university-level math courses. As a further aid there are computer programs (already compiled on an accompanying diskette) so the user does not have to become involved in FEM programming to use the methodology given.

WHAT'S NEW

This book has been substantially revised to include appropriate new material and expanded discussion of previous material. A large number of figures have been modified and several new ones added. I was able to do this with only a small increase in the total page count since providing the computer programs on diskette freed for text pages that had been used for program listings. Specifically these changes include but are not limited to the following:

a. Revision of text examples and problems so they are *all* in SI. Only two or three exceptions occur in examples that were originally published in Fps and for which a user would have to put forth too much effort to reconvert the material for verification.

b. I added five additional computer programs to the basic package so there are now 16 on the diskette. Nearly all of the data sets for the examples used in the textbook that can be used with the included programs are also on the program diskette. These will be extremely valuable for users to obtain computer output quickly in a more readable size. A number of problems at the ends of chapters are based on the user making a copy of the included data file for editing and execution.

c. I have revised the problems so that if an applicable computer program is on the diskette it will have to be used.

d. I have corrected several equations and figures from the previous edition.

e. I have revised the method for footings with overturning (in Chapter 8) to use the methodology first proposed by Meyerhof in 1953 for both bearing capacity and for the actual base design.

f. I have enlarged the discussion on lateral pressures in Chapter 11.

g. I have generally improved on the example format so that the computations are easier to follow.

The book is not a literature survey, but an extensive reference list is required to supplement and lend authority to the material presented as well as to give professional credit to those contributing to the advance in knowledge and practice. Because of text space I have had to limit use of references to seldom more than one or two for any topic covered. However, I tried to cite references that contained the most recent and most extensive reference lists so that the interested reader can easily make any follow-up verification or background fill-in with only a minimal literature search effort. If limiting the reference list has omitted any important contribution, I am sincerely regretful. Also I hope that junior authors are not offended by the practice of using "et al." where there are more than two coauthors.

A broad range of subject matter is necessary if one is to achieve reasonabe coverage of the subject of Foundation Engineering as defined by the text scope given in Chapter 1. The subject matter ranges in computational difficulty from requiring use of advanced programmable calculators through digital computers. This range of material allows the book to be used in Civil, Structural, Architectural, and Construction Engineering curricula through a judicious selection of topics and for a minimum of two courses.

This edition—although almost completely rewritten—retains most of the organization of the fourth edition since that edition was also substantially rewritten. This edition has focused more on cleaning up and clarifying those topics requested by users or deemed necessary by the author.

A principal difference between this and the fourth edition is to provide the computer programs from that edition on a diskette in compiled format. All of the programs were edited to allow the user to input data from screen requests. Where the data file is extensive, the user has the option of creating the data file and saving it to disk for later revision using a screen editor so that parametric studies can be easily made. Other than adding the screen routines, the programs are essentially those of the fourth edition. The reason for this is a number of instructors obtained copies of those programs in source code from the author (others had their students type in the programs) so it would be counterproductive to revise the programs substantially so that program users do not get quite the same output order using fifth edition programs compared with those from the fourth edition. Also, when those users obtained the programs in source code, a user's manual was provided giving the input variable names, order of input, and units.

As in previous editions a very substantial number of examples are included. The examples carried over have been extensively reworked and/or new ones added with a reasonably detailed explanation of steps in arriving at the solution. As in previous editions I have attempted to include examples that are realistic—at least within limits of available text space. Often they have been cited from published works so the instructor can require the student to do some background research to gain an appreciation of the difficulty associated with trying to use the published work of others from professional journals. Where the example is hand-worked, comments and discussion of the results and what the next step in the design process might be are usually given. Where computer output is used, some comments are always given on how to make output checks to see if a correct solution has been obtained for that model. This practice supplements the prior text discussion about the computer program.

I wish to express appreciation to the many users of this text, both in the United States and abroad, who have written or called with comments or constructive criticism or simply to make inquiry about a procedure. I should also like to thank those who took part in the McGraw-Hill user survey to provide input for this revision including Y. S. Chae, Rutgers University—Busch Campus; K. L. Bergesen, Iowa State University; M. Gunaratne, University of Southern Florida; C. W. Lovell, Purdue University; Mete Oner, Oklahoma State University; and Stein Sture, University of Colorado.

Finally I have to acknowledge the very considerable contribution of my wife, Faye, who helped with figure and reference checking and the myriad other busy work details necessary to produce the manuscript.

Joseph E. Bowles

ABOUT THE COMPUTER PROGRAMS

Software to accompany this text is available separately.
To obtain, please contact McGraw-Hill office nearest you or your local bookstore.

When ordering the diskette, please quote PART NO. 0-07-114811-D.

The 16 computer programs on the diskette in *fname*.**EXE** format *will execute either with or without a math coprocessor on your system.* These programs will execute on any IBM or compatible system that uses PC-DOS or MS-DOS for the operating system. They will operate in Windows™ environment but as "DOS" programs. A computer system with a hard disk is recommended but not required. There is an installation program on the diskette to assist you in putting the programs onto your system.

The 16 programs are in Subdirectory EXE as follows:

BEARING	Program to compute bearing capacity factors for Hansen, Meyerhof, and Vesić methods (new)
FAD3DPG	3-dimensional pile group analysis using a "rigid" pile cap (**B-10**)
FADBEMLP	Beam on elastic foundation and lateral pile analysis (**B-5**)
FADDYNF1	Dynamic base analysis with uncoupled modes (**B-11**)
FADMAT	Mat/plate analysis using the FGM (**B-6**)
FADSPABW	Sheet-pile/braced excavation wall analysis (**B-9**)
FFACTOR	To compute a number of factors (K_a, K_p, I_s, I_f, earthquake, etc.) used in Foundation Design (new)
LAYERSOL	for bearing capacity on a layered soil (**B-1**)
SMBLP1	Boussinesq lateral pressure for a number of surcharge load cases (**B-8**)
SMBRGNP	Bearing capacity factors for base on a slope (**B-2**)
SMBWVP	Vertical pressure using either Boussinesq or Westergaard method (**B-4**, but Westergaard option is new)
SMNMWEST	Vertical pressure beneath corner of a rectangle using either the Newmark or Westergaard method (**B-3**)

SMTWEDGE	Trial-wedge method for lateral wall force (**B-7**)
UFACTOR	Obtain Terzaghi consolidation percent U versus time factor T (new)
WEDGE	Obtain passive earth force for horizontal and sloping dredge lines for adjusting modulus of subgrade reaction k_s (new)
WORK	Work method (see in Chap. 2) for estimating preconsolidation pressure for a curved e versus log p plot (new)

There are 50 data sets included with the programs in subdirectory DATA. The data sets are keyed to the program output in the text. Note that if these programs accept a disk file as input, they output the file name with the output for a project record.

There is additional user's information about some of the above programs and a summary of other programs noted in the text (programs B-12 through B-31 and several others that are available from the author) in the disk file README.DOC, which you should read and print out. Note that "new" indicates new programs—others with B-numbers are essentially the same as listed in the fourth edition of this textbook.

There is some information on input data organization, parameter identifications, and limitations in the disk file USERMANL.DOC, which you should also print. Consider putting these two printouts in a file folder for rapid reference.

SPECIAL USER NOTE

For more rapid turn-around of inquiries, downloading of program lists/costs, errata, possible formation of a users group, and similar purposes, use the following Web page address (it has e-mail capabilities):

http://www.bcscom.com/fad5e/

If you are on the Internet, you should use this contact method instead of the regular mail address and telephone number in the README.DOC file on the diskette.

LIST OF PRIMARY SYMBOLS USED IN TEXT

The following is a list of symbols used throughout the text. Additionally, most symbols are identified where they are used, or first used if use is different than given below. Not all symbols or subscripts are shown.

A = area, or used as a coefficient; may be subscripted
ADM = ACI 318-: *A*lternate *D*esign *M*ethod (uses actual unfactored design loads)
a = area or is used as a coefficient
B = least lateral base dimensions (sometimes is $2B$); pile group width
B_p = pedestal diameter
B' = $B/2$ when base dimension = B
B_q = cone pore pressure increase ratio
C_C = compression index (Chaps. 2 and 5)
C'_C = compression ratio (Chap. 2)
C_r = recompression index (Chaps. 2 and 5)
C_p = percent clay (material finer than 0.002 mm)
C_α = secondary compression index
CD = consolidated drained
CU = consolidated undrained
CPT = cone penetration test
CIUC = consolidated isotropically undrained compression test
CK_oUC = consolidated in K_o-conditions, undrained compression test
CK_oUE = consolidated in K_o-conditions, undrained extension test
CK_oDSS = consolidated in K_o-conditions, direct simple shear test

c = cohesion of soil
c.g. = center of gravity (or mass)
c_i = damping constants used in Chap. 20 ($i = x, y, z,$ and θ_i)
c_v = coefficient of consolidation (Chap. 2)
D = depth of footing or pile base; pile diameter or width
D_b = diameter of anchor bolt circle for industrial bases
D_c = total thickness of a concrete base slab
D_r = relative density
DMT = flat *d*ilato*m*eter *t*est
d = effective depth of a concrete base slab (to c.g.'s of rebars)
E_c = modulus of elasticity of concrete
E_p = modulus of elasticity of pile material (Chap. 20)
E_s = stress-strain modulus or modulus of deformation (also modulus of elasticity) of soil; may include additional subscripts to indicate method of determination
E_i = energy coefficient symbols used in Chap. 3 to identify SPT values
e = void ratio
e_o = in situ void ratio
F_o, F = dynamic forces as used in Chap. 20; F_o = basic value; F = value at ωt
$f'c$ = 28-day compressive strength of concrete
f_y = yield strength of steel rebars, piles and other steel members
f_a = allowable steel stress
FVST = field vane shear test (*also* VST *or* FVT)
FEM = finite element method; *also* fixed-end-moment, *see context of usage*
G' = shear stress-strain modulus of soil or other material computed using Eq. (*b*) of Sec. 2-14 or by dynamic methods given in Chap. 20
G = specific gravity, for any material other than soil
G_s = specific gravity of soil grains making up a given soil mass
GWT = groundwater table
H = influence depth of footing (Chap. 5); stratum thickness; also used for wall height in Chaps. 11–15, and for hydraulic head in Chap. 2
I = moment of inertia of cross-section
ID = inside diamter of a round section
I_i = settlement influence coefficients used in Chap. 5
I_P = plasticity index = $w_L - w_P$
$I_{\theta i}$ = mass inertia for rotation modes in Chap. 20
J_a = coefficient defined in Chap. 20
J = torsion moment of inertia
J = Joules (an energy term), N · m, but not a bending moment, which is also N · m
K = ratio of lateral to vertical stress
K_o = in situ (or at rest) lateral/vertical stress ratio

K_a = active earth pressure coefficient = $\tan^2(45 - \phi/2)$
K_p = passive earth pressure coefficient = $\tan^2(45 + \phi/2)$
K_z = vertical soil spring for beam-on-elastic foundations, mats and vibrating bases
K_i = horizontal dynamic soil springs; $i = x, y$ as used in Chap. 20
$K_{\theta i}$ = rotational dynamic springs; $i = x, y$, and z used in Chap. 20
k = coefficient of permeability; k_x, k_y = horizontal and vertical values
k_s = modulus of subgrade reaction either vertical or horizontal
k'_s = $k_s B$ used as a beam loading in Chap. 9
L = base or footing length; also pile length; may be subscripted with p = pile, etc.
LF = load factor
M = computed moment from loads
M_u = ultimate (factored) moment as used for ACI Strength Design
m = exponent; also used for mass = W/g in Chap. 20
N = SPT blow count
N_b = number of anchor bolts in a circle of diameter D_b
N_i = SPT blow count at i = efficiency of 55, 60, 70, etc., percent; also used as stability number
N'_i = corrected SPT blow count at i = efficiency
N_k = cone bearing factor
N_{kt} = adjusted cone bearing factor
n = porosity; also used as an exponent; number of piles in a group
OD = outside diamter of a circular section
OCR = overconsolidation ratio
OMC = optimum moisture content—usually in percent
P_a = wall force due to active earth pressure
P_p = wall force due to passive earth pressure
p_o = in situ vertical pressure at some depth z
p'_o = effective vertical pressure at some depth z
p'_c = effective preconsolidation pressure at some depth z
Q = vertical force (also V and sometimes P)
q = overburden pressure = γz used interchangeably with p_o
$\bar{q}$ = effective overburden pressure (same as p'_o) but symbol usually used when computing bearing capacity
q_c = cone bearing pressure
q_T = cone bearing pressure corrected for any pore pressure effects
q_o = footing (or base) contact pressure
q_{ult} = ultimate computed bearing pressure
q_a = allowable bearing pressure
q_u = unconfined compression strength (**always**)
R = resultant force—usually against a wall, as in Chap. 11

RQD = rock quality designation (a ratio)
S = degree of saturation (defined in Chap. 2)—**always**
S = section modulus
S_t = sensitivity of clay (Chap. 2)
SCP = soil-cement-pile (usually produced in-place)
SF = safety factor (also called a stability number)
s = shear strength; pile spacing
s_u = undrained shear strength (often $s_u = q_u/2$)
SPT = standard penetration test
T = time factor for consolidation analyses; Torque measured in a field vane shear test (FVST)
t_f = flange thickness of a rolled section
t_w = web thickness of a rolled section
U = undrained soil state
U = percent consolidation
USD = ultimate strength design (ACI 318-) and uses ϕ-factors
u = pore water (or neutral) pressure
u_c = measured pore pressure at the tip of a piezocone
V_b' = bearing capacity factor used on Fig. 3-22
w = water content; w_N = natural (in situ); w_L = liquid limit; w_P = plastic limit
$\bar{x}$ = horizontal location of load resultant R in x–y plane
$\bar{y}$ = vertical location of load resultant R in x–y plane; eccentricity of a rotating mass in Chap. 20 as $F = m_e\bar{y}\omega^2$
Z_i = Hetenyi plate bending factors
z = depth of interest from ground surface
α = angle used in Chap. 4; cohesion reduction factor in Chap. 16
β = slope angle of ground or backfill; skin resistance factor in Chap. 16
β_d = part of solution of differential equation or internal damping coefficient used in Chap. 20
γ = unit weight of material; subscript is used with γ to identify type or state, as c = concrete, dry, wet, sat, etc.
γ' = effective unit weight computed, as $\gamma' = \gamma - \gamma_W$.
δ = angle of friction between materials, as pile-to-soil, etc.
ΔH = settlement of foundation as used in Chap. 5 and Chap. 18
ΔH_g = pile group settlement (Chap. 18)
ΔH_p = single-pile settlement (Chap. 18)
Δq = stress increase in stratum from footing or pile load
Δu = excess pore water pressure
ϵ = strain = $\Delta q/E_s$ (or q/E_s) or $\Delta L/L_o$
η = base tilt angle in Chap. 4; factor in Chap. 18
κ_i = multipliers for dynamic springs K_i in Chap. 20

λ = multiplier for Chap. 16; with subscripts is dynamic damping multiplier of Chap. 20; also used in Chap. 18

μ = Poisson's ratio (used throughout—defined in Chap. 2)

ρ = mass density of soil or other material; also used as rupture angle of soil wedge retained by a wall; also factor used in Chap. 18 for pile settlement computations

σ_i = pressure or stress; i = direction as x, y, or z

σ_o = effective *mean* normal pressure computed as $(\sigma_1 + \sigma_2 + \sigma_3)/3$

ϕ = angle of internal friction

ϕ' = effective angle of internal friction

ω = frequency as used in Chap. 20

τ = sometimes used instead of s to indicate shear strength

Contents

CHAPTER 1

INTRODUCTION

1-1 FOUNDATIONS: THEIR IMPORTANCE AND PURPOSE

All engineered construction resting on the earth must be carried by some kind of interfacing element called a *foundation.*[1] The foundation is the part of an engineered system that transmits to, and into, the underlying soil or rock the loads supported by the foundation and its self-weight. The resulting soil stresses—except at the ground surface—are in addition to those presently existing in the earth mass from its self-weight and geological history.

The term *superstructure* is commonly used to describe the engineered part of the system bringing load to the foundation, or substructure. The term *superstructure* has particular significance for buildings and bridges; however, foundations also may carry only machinery, support industrial equipment (pipes, towers, tanks), act as sign bases, and the like. For these reasons it is better to describe a foundation as that part of the engineered system that interfaces the load-carrying components to the ground.

It is evident on the basis of this definition that a foundation is the most important part of the engineering system.

1-2 FOUNDATION ENGINEERING

The title *foundation engineer* is given to that person who by reason of training and experience is sufficiently versed in scientific principles and engineering judgment (often termed "art") to design a foundation. We might say engineering judgment is the creative part of this design process.

The necessary scientific principles are acquired through formal educational courses in geotechnical (soil mechanics, geology, foundation engineering) and structural (analysis, de-

[1]This is also sometimes called the *substructure.*

sign in reinforced concrete and steel, etc.) engineering and *continued self-study* via short courses, professional conferences, journal reading, and the like.

Because of the heterogeneous nature of soil and rock masses, two foundations—even on adjacent construction sites—will seldom be the same except by coincidence. Since every foundation represents at least partly a venture into the unknown, it is of great value to have access to others' solutions obtained from conference presentations, journal papers, and textbook condensations of appropriate literature. The amalgamation of experience, study of what others have done in somewhat similar situations, and the site-specific geotechnical information to produce an economical, practical, and safe substructure design is application of engineering judgment.

The following steps are the minimum required for designing a foundation:

1. Locate the site and the position of load. A rough estimate of the foundation load(s) is usually provided by the client or made in-house. Depending on the site or load system complexity, a literature survey may be started to see how others have approached similar problems.
2. Physically inspect the site for any geological or other evidence that may indicate a potential design problem that will have to be taken into account when making the design or giving a design recommendation. Supplement this inspection with any previously obtained soil data.
3. Establish the field exploration program and, on the basis of discovery (or what is found in the initial phase), set up the necessary supplemental field testing and any laboratory test program.
4. Determine the necessary soil design parameters based on integration of test data, scientific principles, and engineering judgment. Simple or complex computer analyses may be involved. For complex problems, compare the recommended data with published literature or engage another geotechnical consultant to give an outside perspective to the results.
5. Design the foundation using the soil parameters from step 4. The foundation should be economical and be able to be built by the available construction personnel. Take into account practical construction tolerances and local construction practices. Interact closely with all concerned (client, engineers, architect, contractor) so that the substructure system is not excessively overdesigned and risk is kept within acceptable levels. A computer may be used extensively (or not at all) in this step.

The foundation engineer should be experienced in and have participation in all five of the preceding steps. In practice this often is not the case. An independent geotechnical firm specializing in soil exploration, soil testing, design of landfills, embankments, water pollution control, etc. often assigns one of its geotechnical engineers to do steps 1 through 4. The output of step 4 is given to the client—often a foundation engineer who specializes in the design of the structural elements making up the substructure system. The principal deficiency in this approach is the tendency to treat the design soil parameters—obtained from soil tests of variable quality, heavily supplemented with engineering judgment—as precise numbers whose magnitude is totally inviolable. Thus, the foundation engineer and geotechnical consultant must work closely together, or at least have frequent conferences as the design progresses. It should be evident that both parties need to appreciate the problems of each other and, particularly, that the foundation design engineer must be aware of the approximate methods used

to obtain the soil parameters being used. This understanding can be obtained by each having training in the other's specialty.

To this end, the primary focus of this text will be on analysis and design of the interfacing elements for buildings, machines, and retaining structures and on those soil mechanics principles used to obtain the necessary soil parameters required to accomplish the design. Specific foundation elements to be considered include shallow elements such as footings and mats and deep elements such as piles and drilled piers. Retaining structures will also be considered in later chapters.

Geotechnical considerations will primarily be on strength and deformation and those soil-water phenomena that affect strength and deformation. With the current trend to using sites with marginal soil parameters for major projects, methods to improve the strength and deformation characteristics through soil improvement methods will be briefly considered in Chap. 6.

1-3 FOUNDATIONS: CLASSIFICATIONS AND SELECT DEFINITIONS

Foundations may be classified based on where the load is carried by the ground, producing:

Shallow foundations—termed bases, footings, spread footings, or mats. The depth is generally $D/B \leq 1$ but may be somewhat more. Refer to Fig. 1-1*a*.

Deep foundations—piles, drilled piers, or drilled caissons. $L_p/B \geq 4+$ with a pile illustrated in Fig. 1-1*b*.

Figure 1-1 illustrates general cases of the three basic foundation types considered in this text and provides some definitions commonly used in this type of work. Because all the definitions and symbols shown will be used throughout the text, the reader should give this figure careful study.

The superstructure brings loads to the soil interface using column-type members. The load-carrying columns are usually of steel or concrete with allowable design compressive stresses on the order of 140^+ MPa (steel) to 10^+ MPa (concrete) and therefore are of relatively small cross-sectional area. The supporting capacity of the soil, from either strength or deformation considerations, is seldom over 1000 kPa but more often on the order of 200 to 250 kPa. This means the foundation is interfacing two materials with a strength ratio on the order of several hundred. As a consequence the loads must be "spread" to the soil in a manner such that its limiting strength is not exceeded and resulting deformations are tolerable. Shallow foundations accomplish this by spreading the loads laterally, hence the term *spread footing*. Where a spread footing (or simply *footing*) supports a single column, a *mat* is a special footing used to support several randomly spaced columns or to support several rows of parallel columns and may underlie a portion of or the entire building. The mat may also be supported, in turn, by piles or drilled piers. Foundations supporting machinery and such are sometimes termed *bases*. Machinery and the like can produce a substantial load intensity over a small area, so the base is used as a load-spreading device similar to the footing.

Deep foundations are analogous to spread footings but distribute the load vertically rather than horizontally. A qualitative load distribution over depth for a *pile* is shown in Fig. 1-1*b*. The terms *drilled pier* and *drilled caisson* are for the pile type member that is constructed by drilling a 0.76^+-m diameter hole in the soil, adding reinforcing as necessary, and backfilling

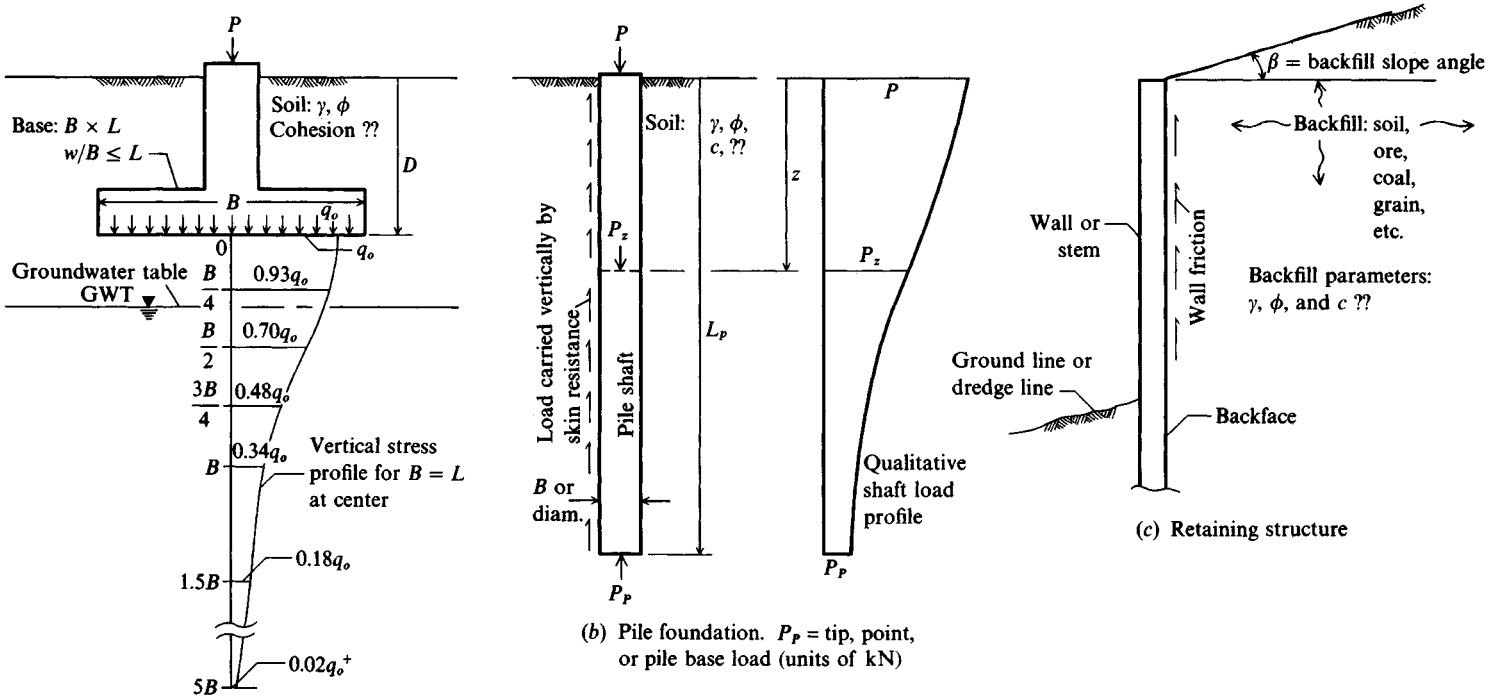

(*a*) Spread foundation. Base contact pressure

$$q_o = \frac{P}{BL} \text{ (units of kPa, usually)}$$

(*b*) Pile foundation. P_P = tip, point, or pile base load (units of kN)

(*c*) Retaining structure

Figure 1-1 Definition of select terms used in foundation engineering. Refer to "tabulated" list of primary symbols after preface for unrecognized terms.

the cavity with concrete. Design and construction of piles and caissons will be considered in more detail in Chaps. 16–19.

A major consideration for both spread footings (and mats) and piles is the distribution of stresses in the stress influence zone beneath the foundation [footing or pile tip (or point)]. The theoretical distribution of vertical stress beneath a square footing on the ground surface is shown in Fig. 1-1*a*. It is evident that below a critical depth of about *5B* the soil has a negligible increase in stress (about $0.02q_o$) from the footing load. This influence depth depends on B, however. For example, if $B = 0.3$ m, the critical stress zone is $5 \times 0.3 = 1.5$ m, and if $B = 3$ m, the zone is 15 m for a zonal influence depth ratio of 1 : 10. Because these B values are in a possible range beneath a large building, any poor soils below a depth of 2 m would have a considerable influence on the design of the wider footings.

Any structure used to retain soil or other material (see Fig. 1-1*c*) in a geometric shape other than that naturally occurring under the influence of gravity is a retaining structure. Retaining structures may be constructed of a large number of materials including geotextiles, wood and metal sheeting, plain or reinforced concrete, reinforced earth, precast concrete elements, closely spaced pilings, interlocking wood or metal elements (crib walls), and so on. Sometimes the retaining structure is permanent and in other cases it is removed when it is no longer needed.

The foundations selected for study in this text are so numerous that their specialized study is appropriate. Every building in existence rests on a foundation whether formally designed or not. Every basement wall in any building is a retaining structure, whether formally designed or not. Major buildings in areas underlain with thick cohesive soil deposits nearly always use piles or drilled caissons to carry the loads vertically to more competent strata, primarily to control settlement. Note that nearly every major city is underlain by clay or has zones where clay is present and requires piles or caissons. Numerous bridges have retaining structures at the abutments and spread foundations carrying the intermediate spans. Usually the abutment end reactions are carried into the ground by piles. Harbor and offshore structures (used primarily for oil production) use piles extensively and for both vertical and lateral loads.

1-3.1 Other Foundations

Many other types of "foundations" that the geotechnical/foundation engineer may encounter are not readily classified. These may include reinforcing the foundation of an existing building if it has undergone excessive settlement or so it can carry additional load if additional height is added. They may involve removing an existing foundation (whole or in part) and replacing it with a basement or other structure, i.e., putting the new foundation at a lower depth. They may involve routing a tunnel (subway or utility) beneath an existing structure or for some type of vibration control. In some of these cases no new foundation is designed. Rather, the engineer must determine the magnitude of any potential adverse effect on the existing structure. If the adverse effect is intolerable, the engineer may need to devise a remedial design.

These several types of "foundations" are so diverse—and are so often one of a kind—that their study is not suitable for a general foundation engineering textbook. These types of design require a geotechnical engineer with a solid base in geotechnical fundamentals (generally with an advanced degree), some experience, a willingness to venture into the unknown, and a willingness to draw on the experience of others through membership in the appropriate technical societies.

1-4 FOUNDATIONS: GENERAL REQUIREMENTS

Foundation elements must be proportioned both to interface with the soil at a safe stress level and to limit settlements to an acceptable amount. In the past 50^+ years few buildings (but numerous embankment types) have failed as a result of overstressing the underlying soil. However, excessive settlement problems are fairly common and somewhat concealed since only the most spectacular ones get published.

Few modern buildings collapse from excessive settlements; however, it is not uncommon for a partial collapse or a localized failure in a structural member to occur. More common occurrences are unsightly wall and floor cracks, uneven floors (sags and slopes), sticking doors and windows, and the like.

The variability of soil in combination with unanticipated loads or subsequent soil movements (e.g., earthquakes) can result in settlement problems over which the designer may have little control. In other words, current state-of-the-art design methods may greatly reduce the likelihood (risk factor) of settlement problems but do not generally provide a risk-free project. In fairness, though, some problems are the direct result of poor design—either simple carelessness or lack of engineering ability. Yes, just as there are both competent and incompetent doctors, lawyers, and other professionals, so there are competent and incompetent engineers!

A major factor that greatly complicates foundation design is that the soil parameters used for the design are obtained before the project is started. Later when the foundation is in place, it is on (or in) soil with properties that may be considerably modified from the original, either from the construction process or from installing the foundation. That is, the soil may be excavated and/or replaced and compacted; excavations tend to remove load and allow the underlying soil to expand; driving piles usually makes soil more dense, etc. Any of these events either directly alters the soil (replacement) or modifies the initially estimated soil strength parameters.

As a result of the uncertainties in loads, in soil properties, and in attempts to account for variability and any other factors, it is common practice to be conservative in designing this part of the system. We may quickly note, however, that this being the most important part but the most difficult to access if problems later develop, a conservative design or even an overdesign has a better return on investment here than in other parts of the project.

Another factor that encourages conservative design is the fact that many geotechnical engineers tend to imply that their talents (and design recommendations) are better than those of the competition. This generates a false sense on the part of the client that using that geotechnical engineer will produce a minimum cost foundation. When this happens and problems later occur (unanticipated soil strata, water, excessive settlements, or whatever), the client is very likely to litigate (i.e., sue). This possibility means that geotechnical engineers should be candid about the status of the state of the art in this specialty and make the client fully aware that precise soil parameters are difficult if not impossible to quantify *and* that at least some design conservatism is prudent.

Design conservatism means that any two design firms are unlikely to come up with exactly the same soil parameters and final foundation design. It would not be unusual for one firm to recommend the base contact pressure q_o of Fig. 1-1*a* to be, say, 200 kPa whereas another might recommend 225 or even 250 kPa—both with the use of spread footings. There might be a problem in ethics, however, if one firm recommended 200 kPa and the other recommended only 100 kPa, which would require a mat foundation or the use of piles. One of the recommendations is either overly optimistic (the 200 kPa) or realistic; the other is either realistic or

overly conservative. Being excessively conservative is an ethics problem, unless the client is made aware of the several alternatives and accepts the more conservative recommendation as being in his or her best interests.

In summary, a proper design requires the following:

1. Determining the building purpose, probable service-life loading, type of framing, soil profile, construction methods, and construction costs
2. Determining the client/owner's needs
3. Making the design, but ensuring that it does not excessively degrade the environment, and provides a margin of safety that produces a tolerable risk level to all parties: the public, the owner, and the engineer

1-5 FOUNDATIONS: ADDITIONAL CONSIDERATIONS

The previous section outlined in general terms requirements to be met in designing a foundation in terms of settlement and soil strength. We will now outline a number of additional considerations that may have to be taken into account at specific sites.

1. Depth must be adequate to avoid lateral squeezing of material from beneath the foundation for footings and mats. Similarly, excavation for the foundation must take into account that this can happen to existing building footings on adjacent sites and requires that suitable precautions be taken. The number of settlement cracks that are found by owners of existing buildings when excavations for adjacent structures begin is truly amazing.
2. Depth of foundation must be below the zone of seasonal volume changes caused by freezing, thawing, and plant growth. Most local building codes will contain minimum depth requirements.
3. The foundation scheme may have to consider expansive soil conditions. Here the building tends to capture upward-migrating soil water vapor, which condenses and saturates the soil in the interior zone, even as normal perimeter evaporation takes place. The soil in a distressingly large number of geographic areas tends to swell in the presence of substantial moisture and carry the foundation up with it.
4. In addition to compressive strength considerations, the foundation system must be safe against overturning, sliding, and any uplift (flotation).
5. System must be protected against corrosion or deterioration due to harmful materials present in the soil. Safety is a particular concern in reclaiming sanitary landfills but has application for marine and other situations where chemical agents that are present can corrode metal pilings, destroy wood sheeting/piling, cause adverse reactions with Portland cement in concrete footings or piles, and so forth.
6. Foundation system should be adequate to sustain some later changes in site or construction geometry and be easily modified should changes in the superstructure and loading become necessary.
7. The foundation should be buildable with available construction personnel. For one-of-a-kind projects there may be no previous experience. In this case, it is necessary that all concerned parties carefully work together to achieve the desired result.

TABLE 1-1
Foundation types and typical usage

Foundation type	Use	Applicable soil conditions
	Shallow foundations (generally $D/B \leq 1$)	
Spread footings, wall footings	Individual columns, walls	Any conditions where bearing capacity is adequate for applied load. May use on a single stratum; firm layer over soft layer or soft layer over firm layer. Check settlements from any source.
Combined footings	Two to four columns on footing and/or space is limited	Same as for spread footings above.
Mat foundations	Several rows of parallel columns; heavy column loads; use to reduce differential settlements	Soil bearing capacity is generally less than for spread footings, and over half the plan area would be covered by spread footings. Check settlements from any source.
	Deep foundations (generally $L_p/B \geq 4^+$)	
Floating pile	In groups of 2^+ supporting a cap that interfaces with column(s)	Surface and near-surface soils have low bearing capacity and competent soil is at great depth. Sufficient skin resistance can be developed by soil-to-pile perimeter to carry anticipated loads.
Bearing pile	Same as for floating pile	Surface and near-surface soils not relied on for skin resistance; competent soil for point load is at a practical depth (8–20 m).
Drilled piers or caissons	Same as for piles; use fewer; For large column loads	Same as for piles. May be floating or point-bearing (or combination). Depends on depth to competent bearing stratum.
	Retaining structures	
Retaining walls, bridge abutments	Permanent material retention	Any type of soil but a specified zone (Chaps. 11, 12) in backfill is usually of controlled fill.
Sheeting structures (sheet pile, wood sheeting, etc.)	Temporary or permanent for excavations, marine cofferdams for river work	Retain any soil or water. Backfill for waterfront and cofferdam systems is usually granular for greater drainage.

8. The foundation and site development must meet local environmental standards, including determining if the building is or has the potential for being contaminated with hazardous materials from ground contact (for example, radon or methane gas). Adequate air circulation and ventilation within the building are the responsibility of the mechanical engineering group of the design team.

Although not all of the preceding are applicable to a given project, it is readily apparent that those that are tend to introduce much additional uncertainty into the system. This makes the application of engineering judgment an even more important ingredient in the design process.

1-6 FOUNDATIONS: SELECTION OF TYPE

Table 1-1 tabulates the use and application of the several general foundation types shown in Fig. 1-1. Design of these several types will be taken up in detail in later chapters, but it is useful at this point to obtain a general overview of when and where a particular type of foundation is used.

Where the groundwater table (GWT) is present (see Fig. 1-1*a*), it is common to lower it below the construction zone either permanently or for the duration of the construction work. The GWT shown on Fig. 1-1*a* is below the footing and would probably be below the construction zone. If the GWT later rises above the footing level, the footing will be subject to uplift or flotation, which would have to be taken into account.

If the groundwater table must be lowered either temporarily or permanently, it is usually necessary to get approval from environmental protection agencies. Also there is a potential problem of causing ground subsidence in the area surrounding the construction site if there is significant lowering of the GWT. For this reason it is a common practice to construct water barriers around the site perimeter and only pump out the interior.

1-7 THE INTERNATIONAL SYSTEM OF UNITS (SI) AND THE FOOT-POUND-SECOND (Fps) SYSTEM[2]

We may define a system of units for computational purposes in terms of the fundamental quantities of length, mass, and time as follows:

a. Meter, kilogram, second = mks; SI

b. Foot, pound, second = Fps; widely used in the United States through 1993–1995 but almost nowhere else since about 1975.

Table 1-2 lists computational units (*see also table inside back cover*) and the abbreviations that will be consistently used throughout the text. Refer to this table if you are not already familiar with the abbreviation when later used. Units in this table generally follow those used

[2] This section has been retained for "historical" purposes and for those few users who may need some aid in making units conversions.

by the American Society for Testing and Materials (ASTM) Committee D-18 (soils and soil testing), of which the author is a member.

The value of the gravitational constant g shown in the table is at approximately 45° latitude and sea level. It varies about 0.5 percent based on latitude and elevation, but its use as a constant will produce a negligible error for foundation work in most geographic locations on the Earth.

In the general case the force is computed as

$$F = \frac{\text{Mass} \times \text{acceleration}}{\text{Constant of proportionality } \eta} = \frac{m \cdot a}{\eta}$$

TABLE 1-2
Units* and abbreviations used in this text

Unit	Abbreviations used	Comments
Length		
foot	ft	
inch	in.	
meter	m	May use cm = centimeter = m/100 or millimeter = m/1000
Force		
gram force	g_f	May prefix with k for kilo = 1000 g = kg = preferred SI unit, Mg = 10^6 g, etc.
pound force	lb_f	May use kilopound = kip = 1000 pounds
Mass—symbol = m		
gram	g	May prefix a kg, Mg, etc.
pound	lb	
pound force/g	slug	g = gravitational constant of 32.2 ft/s^2 or 9.807 m/s^2
Weight/volume—symbol = γ		May have subscript as w = water, etc.
pound/ft^3	pcf	Or kips/ft^3 = kcf
Newton/m^3	N/m^3	May use kN/m^3, MN/m^3, etc.; for soil use kN/m^3 as preferred unit
Pressure		
Newton/m^2	Pa	Pa = Pascal = N/m^2; may use kPa, Mpa; kPa for soil pressure
pound/in^2	psi	May use kip/in.^{2} = ksi
pound/ft^2	psf	May use kip/ft^2 = ksf preferred for soil pressure
Density—symbol = ρ		
mass/volume	kg/m^3 slug/ft^3	May use g/cm^3 = gram/cu cm

*Fps units primarily for historical purposes.

For the system units of primary interest, a number of sources (including most college physics textbooks) give the following:

System	Mass	Length	Time	Force F	η
SI (mks)	kg	m	s	N	$1\ \text{kg}\cdot\text{m/N}\cdot\text{s}^2$
US (Fps)	slug	ft	s	lb_f	$1\ \text{slug}\cdot\text{ft/lb}\cdot\text{s}^2$
US (Fps)	lb_m	ft	s	$1\ \text{lb}_\text{f}$	$32.2\ \text{lb}_\text{m}\cdot\text{ft/lb}\cdot\text{s}^2$
Metric	kg	m	s	kg_f	$9.807\ \text{kg}\cdot\text{m/kg}_\text{f}\cdot\text{s}^2$

With this table, let us look at a $1\ \text{ft}^3$ volume of sand that weighs and has a mass of 100 pounds (lb_f *and* lb_m obtained from $F = m\cdot a/\eta = 100\times 32.2/32.2$) as determined by placing it on a set of laboratory scales. Using this 100 lb_m, we have (using table in book cover) the following:

$$\text{Mass in kilograms} = 100\ \text{lb}_\text{m}\times 0.4536\ \text{kg/lb}_\text{m} = \mathbf{45.36}\ \text{kg}$$

$$\text{Volume in cubic meters} = 1\ \text{ft}^3\times(0.3048\ \text{m/ft})^3 = \mathbf{0.02832}\ \text{m}^3$$

If this sand is placed in a weightless bag and suspended by a spring in the laboratory, what is the spring force? The vertical acceleration is, of course, g, and

$$\text{SI:}\quad F = m(g)/\eta = 45.36\ \text{kg}(9.807\ \text{m/s}^2)/1\ \text{kg}\cdot\ \text{m/N}\cdot\text{s}^2 = \mathbf{444.8}\ \text{N}$$

$$\text{Fps:}\quad F = 100(32.2)/32.2 = \mathbf{100}\ \text{lb}_\text{f}\ \text{(usually written as 100 lb)}$$

It is this latter computation that causes confusion—obtaining 100 lb of force from a 100 lb mass. Closer inspection, however, shows this conclusion is valid only because $g = \eta$. In those cases where this equality does not exist, we have $\text{lb}_\text{m} \neq \text{lb}_\text{f}$. Let us also look at the weight/volume and density relationships for this case:

Unit weight γ = $\text{weight}_\text{force}$/volume

$$\text{SI:}\quad \gamma = 444.8\ \text{N}/0.028\ 32\ \text{m}^3 = 15\ 706.2\ \text{N/m}^3 = \mathbf{15.71}\ \text{kN/m}^3$$

$$\text{Fps:}\quad \gamma = 100\ \text{lb}_\text{f}/1\ \text{ft}^3 = 100\ \text{lb}_\text{f}/\text{ft}^3\ \text{(or pcf)} = 0.100\ \text{kcf}$$

Density ρ = mass/volume

$$\text{SI}\quad \rho = 45.36\ \text{kg}/0.028\ 32\ \text{m}^3 = 1601.7\ \text{kg/m}^3 = 1.602\ \text{tonnes/m}^3$$
$$= 1.602\ \text{Mg/m}^3 = \mathbf{1.602}\ \text{g/cm}^3$$

An alternative computation in SI with application in soil dynamics computations is to define density as

$$\text{SI:}\quad \rho = \frac{\text{kN/m}^3}{g} = \frac{1.602\times 9.807}{9.807} = \mathbf{1.602\ kN\cdot s^2/m^4}$$

$$\text{Fps:}\quad \rho = 100/1\ \text{ft}^3 = 100\ \text{pcf} = 0.100\ \text{kcf}$$

Also since the unit weight of water $\gamma_w = 62.4\ \text{pcf} = 9.807\ \text{kN/m}^3$, we can compute the unit weights between systems as

$$\text{SI:}\quad \gamma = \frac{\gamma_\text{Fps}}{\gamma_w}\times 9.807 = \frac{100}{62.4}\times 9.807 = \mathbf{15.71\ kN/m^3}$$

$$\text{Fps:}\quad \gamma = \frac{15.71}{9.807} \times 62.4 = \mathbf{100\ pcf}$$

These unit weight relationships are particularly useful in converting between SI and Fps. Also note the connection between the unit weight of soil/unit weight of water, giving directly the soil density ρ as

$$\rho = \frac{\gamma}{\gamma_w} = \frac{15.71}{9.807} = \frac{100}{62.4} = 1.602\ \text{g/cm}^2$$
$$= 1601.7\ \text{kg/m}^3$$
$$= \mathbf{1.602\ kN \cdot s^2/m^4}$$

The first two forms for mass density just given are not dimensionally correct and require conversion factors, which are not shown since they cancel. The last form, in units of $\text{kN}\cdot\text{s}^2/\text{m}^4$, is dimensionally correct as given.

Some commonly used approximations are obtained from the table on the inside back cover as follows:

Base Value	Suggest using
1 ksf = 47.88 kPa	50 kPa
2 ksf = 1 ton/ft^2 = 95.76 kPa	100 kPa
1 kg/cm^2 = 0.976 ton/ft^2	1 ton/ft^2 or 1 tsf

The last value of 1 kg/cm^2 $\simeq$ 1 tsf is the origin of the one-time common use of tons and tsf by many engineers for pile loads and soil pressure. With SI being used, the ton[3] and tsf units are obsolete.

1-8 COMPUTATIONAL ACCURACY VERSUS DESIGN PRECISION

Pocket or desktop calculators and digital computers compute with 7 to 14 digits of accuracy. This gives a fictitiously high precision to computed quantities whose input values may have a design precision only within 10 to 30 percent of the numerical value used. The reader should be aware of this actual versus computed precision when checking the example data and output. The author has attempted to maintain a checkable precision by writing the intermediate value (when a pocket calculator was used) to the precision the user should input to check the succeeding steps. If this intermediate value is not used, the computed answer can easily differ in the 1.0 to 0.1 position. The reader should also be aware that typesetting, transcribing, and typing errors inevitably occur, particularly in misplaced parentheses and misreading 3 for 8, etc.

[3]This is the 2000 lb ton. The "metric" ton of 1000 kg is still used to some extent but is usually identified as "tonne."

The text user should be able to reproduce most of the digits in the example problems to 0.1 or less unless a typesetting (or other) error has inadvertently occurred. There may be larger discrepancies if the reader uses interpolated data and the author used "exact" data from a computer printout without interpolating. Generally this situation will be noted so that the reader is alerted to potential computational discrepancies. The example problems have been included primarily for procedure rather than numerical accuracy, and the user should be aware of this underlying philosophy when studying them.

1-9 COMPUTER PROGRAMS IN FOUNDATION ANALYSIS AND DESIGN

A large number of foundation engineering problems can be efficiently analyzed and/or designed using a digital computer. Particular advantages of using a computer accrue from these features:

1. One is able to try a range of problem variables to obtain a feel for the effect of specifying, or using, a particular set of soil parameters.
2. One can avoid having to use tabulated data or plotted curves, which usually require interpolation and excessive simplification of the foundation model.
3. One can minimize computational errors from these sources:
   a. Erroneous key entry when using a calculator. The bad entry is (or should be) output to paper using a computer so the input can be checked.
   b. Omission of computational steps. A working computer program usually includes all the design steps. A set of hand computations may not include every step for any number of reasons (forget, not be aware of, carelessness, etc.).
   c. Calculator chip malfunction not readily detected except by using two calculators. Computer chips are often internally checked on power-up, or output is so bad that chip errors are visually detected.
4. With output to a printer one has a paper record of the problem for office files without the necessity of transcribing data from intermediate steps. This avoids copy errors such as 83 for 38 and the like.

The major disadvantage of using a computer program is that it is difficult to write a first generation, error-free program of real use in a design office. Program usability tends to increase with each revision (or history) level.

With the current wide availability of computer programs—many, such as those on the included diskette, having a "history"—the advantages gained from program use far exceed any perceived disadvantages. The author suggests that both geotechnical and foundation engineers should use computer programs whenever possible—and certainly be aware of what computer program(s) each is likely to use for the given project.

This statement is made with full awareness of the possibility of program errors (or "bugs"). Fortunately, most geotechnical software is task-specific so that the possibility of program errors or their not being detected is not so likely as for some of the large finite-element or structural analysis programs that purport to solve a wide range of tasks. In any case, the

author cannot recall a single reported foundation design failure that can be attributed to a bad[4] computer program.

It should be evident that computer programs vary widely in *perceived quality,* perceived quality being defined here as problem limitations and "ease of use." Both users and programmers should be aware that it is difficult to predefine the full range of problem parameters likely to be encountered in practice, so nearly any geotechnical program of significant value is likely to have some built-in limitations. Ease of use is highly subjective and depends more on user familiarity with a program than how easy it really is to use—many users like pull-down menus and graphics whereas others are quite content without these features. As a final comment on computer programs, be aware that although business applications and games usually have a market in the hundreds of thousands, geotechnical programs have a potential market of only a few thousand. This small market means geotechnical software is likely to be more expensive than other software and, to minimize development costs, it is not likely to have many so-called user-friendly features.

One should routinely check the output from any computer program used for design or analysis. The user is responsible for his or her design since it is impossible to write a computer program with any usefulness that cannot be misused in some manner. Primarily for this reason most computer programs are sold or licensed with a disclaimer making the user responsible.

Fortunately, most computer programs can be written to be somewhat self-checking, either by writing back the input data or by providing output that can be readily identified as correct (or incorrect) *if the user understands or knows how to use the program.* It should go without saying that, if you do not know much about the specific problem being designed or analyzed, you should first do some preliminary study before using a computer program on it.

This textbook encourages computer use in foundation engineering. Select programs are furnished on the enclosed computer diskette in compiled format to save time for the text user. All of the programs used or suggested for use are identified from the author's program library and are available in source code with user's manuals individually or in a package on IBM PC/AT type diskettes ($5\frac{1}{4}$-in. or 3.5-in.) at a reasonable[5] cost from the author.

---

[4]Generally if the program is "bad," the user finds this out by performing some kind of independent check and does not use that program further in the design.

[5]Please note that "reasonable" does not mean "free." There is a substantial cost just in reproducing a diskette, providing a user's manual, and shipping.

CHAPTER 2

GEOTECHNICAL AND INDEX PROPERTIES: LABORATORY TESTING; SETTLEMENT AND STRENGTH CORRELATIONS

2-1 INTRODUCTION

This chapter reviews those physical and engineering properties of soils of principal interest for the analysis and design of foundation elements considered in this text. These primarily include the following:

1. Strength parameters[1]
   Stress-strain modulus (or modulus of elasticity), E_s; shear modulus, G', and Poisson's ratio, μ; angle of internal friction, ϕ; soil cohesion, c
2. Compressibility indexes for amount and rate of settlement
   Compression: index, C_c, and ratio, C'_c; recompression: index, C_r, and ratio, C'_r; coefficient of consolidation, c_v; coefficient of secondary compression, C_α
3. Gravimetric-volumetric data
   Unit weight, γ; specific gravity, G_s; void ratio, e, or porosity, n; water content, w_i (where $i = N$ for natural, L for liquid limit, or P for plastic limit; e.g., w_P = plastic limit)

[1]Symbols and definitions generally follow those of ASTM D 653 except E_s, G', and μ (refer also to "List of primary symbols" following the Preface). It is common to subscript E for soil as E_s, for concrete E_c, etc. G' will be used for shear modulus, as G_s is generally used for specific gravity. The symbol μ is commonly used for Poisson's ratio; however, ASTM D 653 suggests ν, which is difficult to write by hand.

4. Permeability, also called *hydraulic conductivity* (sometimes required)
   k = coefficient of permeability (or hydraulic conductivity)

The symbols shown here will be consistently used throughout the text and will not be subsequently identified/defined.

The more common laboratory tests also will be briefly commented on. For all laboratory tests we can immediately identify several problems:

1. Recovery of good quality samples. It is not possible to recover samples with zero disturbance, but if the disturbance is a minimum—a relative term—the sample quality may be adequate for the project.
2. Necessity of extrapolating the results from the laboratory tests on a few small samples, which may involve a volume of ± 0.03 m^3, to the site, which involves several thousands of cubic meters.
3. Laboratory equipment limitations. The triaxial compression text is considered one of the better test procedures available. It is easy to obtain a sample, put it into the cell, apply some cell pressure, and load the sample to failure in compression. The problem is that the cell pressure, as usually used, applies an even, all around (isotropic) compression. In situ the confining pressure prior to the foundation load application is usually anisotropic (vertical pressure is different from the lateral value). It is not very easy to apply anisotropic confining pressure to soil samples in a triaxial cell—even if we know what to use for vertical and lateral values.
4. Ability and motivation of the laboratory personnel.

The effect of these several items is to produce test results that may not be much refined over values estimated from experience. Items 1 through 3 make field testing a particularly attractive alternative. Field tests will be considered in the next chapter since they tend to be closely associated with the site exploration program.

Index settlement and strength correlations are alternatives that have value in preliminary design studies on project feasibility. Because of both test limitations and costs, it is useful to have relationships between easily determined index properties such as the liquid limit and plasticity index and the design parameters. Several of the more common correlations are presented later in this chapter. Correlations are usually based on a collection of data from an extensive literature survey and used to plot a best-fit curve or to perform a numerical regression analysis.

2-2 FOUNDATION SUBSOILS

We are concerned with placing the foundation on either *soil* or *rock*. This material may be under water as for certain bridge and marine structures, but more commonly we will place the foundation on soil or rock near the ground surface.

Soil is an aggregation of particles that may range very widely in size. It is the by-product of mechanical and chemical weathering of rock. Some of these particles are given specific names according to their sizes, such as gravel, sand, silt, clay, etc., and are more completely described in Sec. 2-7.

Soil, being a mass of irregular-shaped particles of varying sizes, will consist of the particles (or solids), voids (pores or spaces) between particles, water in some of the voids, and air taking up the remaining void space. At temperatures below freezing the pore water may freeze, with resulting particle separation (volume increase). When the ice melts particles close up (volume decrease). If the ice is permanent, the ice-soil mixture is termed *permafrost.* It is evident that the pore water is a variable state quantity that may be in the form of water vapor, water, or ice; the amount depends on climatic conditions, recency of rainfall, or soil location with respect to the GWT of Fig. 1-1.

Soil may be described as *residual* or *transported.* Residual soil is formed from weathering of parent rock at the present location. It usually contains angular rock fragments of varying sizes in the soil-rock interface zone. Transported soils are those formed from rock weathered at one location and transported by wind, water, ice, or gravity to the present site. The terms *residual* and *transported* must be taken in the proper context, for many current residual soils are formed (or are being formed) from transported soil deposits of earlier geological periods, which indurated into rocks. Later uplifts have exposed these rocks to a new onset of weathering. Exposed limestone, sandstone, and shale are typical of indurated transported soil deposits of earlier geological eras that have been uplifted to undergo current weathering and decomposition back to soil to repeat the geological cycle.

Residual soils are usually preferred to support foundations as they tend to have better engineering properties. Soils that have been transported—particularly by wind or water—are often of poor quality. These are typified by small grain size, large amounts of pore space, potential for the presence of large amounts of pore water, and they often are highly compressible. Note, however, exceptions that produce poor-quality residual soils and good-quality transported soil deposits commonly exist. In general, each site must be examined on its own merits.

2-3 SOIL VOLUME AND DENSITY RELATIONSHIPS

The more common soil definitions and gravimetric-volumetric relationships are presented in this section. Figure 2-1 illustrates and defines a number of terms used in these relationships.

Void ratio e. The ratio of the volume of voids V_v to the volume of soils V_s in a given volume of material, usually expressed as a decimal.

$$e = \frac{V_v}{V_s} \qquad 0 < e \ll \infty \tag{2-1}$$

For soils, e ranges from about 0.35 in the most dense state to seldom over 2 in the loosest state.

Porosity n. The ratio of the volume of voids to the total volume V_t, expressed as either a decimal or a percentage.

$$n = \frac{V_v}{V_t} \tag{2-2}$$

Water content w. The ratio of the weight of water W_w to the weight of soil solids W_s, expressed as a percentage but usually used in decimal form.

$$w = \frac{W_w}{W_s} \times 100 \qquad (\%) \tag{2-3}$$

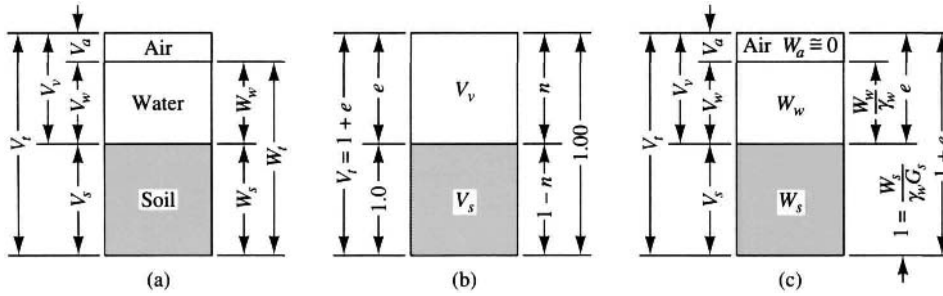

Figure 2-1 Block diagrams showing: (*a*) Weight/volume relationships for a soil mass; (*b*) volume/void relationships; (*c*) volumes expressed in terms of weights and specific gravity.

Unit density (or **mass***)* ρ. The ratio of mass per unit of volume. In the Fps system the values are the same as unit weight following. The SI system gives units of kg/m^3 but a preferred usage unit is g/cm^3. Note that 1 g/cm^3 = 1 Mg/m^3 = 1 tonne/m^3. Often unit density is called "density."

Unit weight γ. The weight of a unit volume of soil (or other material) in force units. The general expression is

$$\gamma = \frac{W_t}{V_t} \tag{2-4}$$

Commonly used units are kN/m^3 or pcf, kcf. The symbol may be subscripted to identify particular state values as $\gamma_{dry} = W_s/V_t$, etc. The unit weight can vary from a minimum at the dry state to a maximum at the saturated (voids full of water) state for a given particle arrangement.

Degree of saturation S. The ratio of the volume of water to the total volume of soil voids, expressed as a percentage but used as a decimal.

$$S = \frac{V_w}{V_v} \times 100 \qquad (\%) \tag{2-5}$$

A "saturated" soil as obtained from beneath the groundwater table may have a computed S of between 95 and 100 percent.

Specific gravity G. The usual definition for soil is the same as found in most elementary physics textbooks. The unit weight of distilled water is standard at 4°C, but the usual laboratory temperatures in the range of 15 to 25°C do not introduce serious errors. G is usually subscripted to identify the quantity; for soil grains, obtain G_s as

$$G_s = \frac{W_s/V_s}{\gamma_w} = \frac{\gamma_s}{\gamma_w} \tag{2-6}$$

The unit weight of water may be taken as 9.807 kN/m^3, 62.4 pcf, or more commonly as 1 g/cm^3 so that the factor γ_w drops out of the calculations—as long as γ_s is also in units of g/cm^3.

These six basic definitions in equation form are sufficient to develop any needed relationships for geotechnical engineering problems. For example, a useful relationship between void ratio e and porosity n can be obtained from the block diagram of Fig. 2-1*b* as follows:

Let the volume of solids $V_s = 1.00$ (since values are symbolic anyway). This relation gives directly that $e = V_v$ from Eq. (2-1). Placing these values on the left side of the block diagram (as shown) gives the total volume directly as $V_t = 1 + e$. Now using Eq. (2-2), we have

$$n = \frac{V_v}{V_t} = \frac{e}{1+e} \tag{2-7}$$

and, solving Eq. (2-7) for e, we obtain

$$e = \frac{n}{1-n} \tag{2-8}$$

A useful expression for dry unit weight can be obtained similarly by making reference to the block diagram of Fig. 2-1*a* (right side). By inspection we have $W_t = W_s + W_w$ (the air has negligible weight). From Eq. (2-3) we have $W_w = wW_s$ (where w is in decimal form). Also, dividing W_s and W_t by V_t gives the dry and wet unit weights so

$$\gamma_{\text{dry}} + w\gamma_{\text{dry}} = \gamma_{\text{wet}}$$

which gives

$$\gamma_{\text{dry}} = \frac{\gamma_{\text{wet}}}{1+w} \tag{2-9}$$

A useful relation for the void ratio in terms of S, w, and G_s is obtained by using $\gamma_w = 1$ g/cm^3 as follows:

1. From Eq. (2-6) and referring to the block diagram of Fig. 2-1*c*, obtain

$$G_w = \frac{W_w}{V_w \gamma_w}$$

   and because $G_w = \gamma_w = 1$, the weight of water W_w (in grams) $= V_w \gamma_w G_w = V_w$ (in cubic centimeters, cm^3).
2. Let $V_s = 1.0$ cm^3, and from Eq. (2-1) obtain $V_v = eV_s = e$.
3. From Eq. (2-5) and using S as a decimal, obtain directly

$$V_w = SV_v$$

   Substitution of W_w for V_w from step 1 and V_v from step 2 gives

$$W_w = Se$$

4. From Eq. (2-6) obtain the weight of soil solids as

$$W_s = V_s \gamma_w G_s.$$

   which for $V_s = 1$ cm^3 gives $W_s = G_s$.
5. From Eq. (2-3) for water content and using above step 3 for W_w and step 4 for W_s, obtain

$$w = \frac{W_w}{W_s} = \frac{Se}{G_s}$$

6. Solving step 5 for the void ratio e, we obtain

$$e = \frac{w}{S}G_s \tag{2-10}$$

and when $S = 1$ (a saturated soil), we have $e = wG_s$.

The dry unit is often of particular interest. Let us obtain a relationship for it in terms of water content and specific gravity of the soil solids G_s. From Fig. 2-1*c* the volume of a given mass $V_t = 1 + e$, and with e obtained from Eq. (2-10) we have

$$V_t = 1 + \frac{w}{S}G_s$$

Also, in any system of units the weight of the soil solids is

$$W_s = V_s\gamma_w G_s = \gamma_w G_s \quad \text{when } V_s = 1 \quad \text{as used here}$$

The dry unit weight is

$$\gamma_{\text{dry}} = \frac{W_s}{V_t} = \frac{\gamma_w G_s}{1 + (w/S)G_s} \tag{2-11}$$

and for $S = 100$ percent,

$$\gamma_{\text{dry}} = \frac{\gamma_w G_s}{1 + wG_s} \tag{2-11a}$$

From Eq. (2-9) the wet unit weight is

$$\gamma_{\text{wet}} = \gamma_{\text{dry}}(1 + w)$$

$$\gamma_{\text{wet}} = \frac{\gamma_w G_s(1 + w)}{1 + (w/S)G_s} \tag{2-12}$$

These derivations have been presented to illustrate the use of the basic definitions, together with a basic block diagram on which is placed known (or assumed) values. It is recommended that a derivation of the needed relationship is preferable to making a literature search to find an equation that can be used.

Example 2-1. A cohesive soil specimen (from a split spoon; see Chap. 3 for method) was subjected to laboratory tests to obtain the following data: The moisture content $w = 22.5$ percent; $G_s = 2.60$. To determine the approximate unit weight, a sample weighing 224.0 g was placed in a 500-cm^3 container with 382 cm^3 of water required to fill the container. The reader should note the use of standard laboratory units.

Required.

1. The wet unit weight, γ_{wet}
2. The dry unit weight, γ_{dry}
3. Void ratio e and porosity n

4. Degree of saturation S
5. Dry bulk specific gravity

Solution.

Step 1. The wet unit weight is obtained from total sample weight as

$$\rho_{\text{wet}} = \frac{W_t}{V_t} = \frac{224.0 \text{ g}}{(500 - 382) \text{ cm}^3} = \mathbf{1.898} \text{ g/cm}^3 \qquad \text{(wet density)}$$

and from Sec. 1-7 we have

$$\gamma_{\text{wet}} = 1.898 \times 9.807 = \mathbf{18.61} \text{ kN/m}^3$$

Step 2. The dry unit weight is obtained using Eq. (2-9):

$$\gamma_{\text{dry}} = \frac{18.61}{1.225} = \mathbf{15.19} \text{ kN/m}^3$$

Step 3. The void ratio e and porosity n require some volume computations as follows:

$$V_s = \frac{W_s}{G_s \gamma_w} = \frac{1.898/1.225}{2.60(1.0)} = 0.596 \text{ cm}^3 \text{ (or m}^3\text{)}$$

$$V_v = V_t - V_s = 1.000 - 0.596 = 0.404 \text{ cm}^3 \text{ (using cm)}$$

$$e = \frac{V_v}{V_s} = \frac{0.404}{0.596} = \mathbf{0.678}$$

$$n = \frac{V_v}{V_t} = \frac{0.404}{1.00} = \mathbf{0.404} \text{ (or 40.4\%)}$$

Step 4. To find the degree of saturation S it will be necessary to find the volume of water in the voids. The weight of water W_w is the difference between the dry and wet weights; therefore,

$$W_w = 1.898 - \frac{1.898}{1.225} = 0.349 \text{ g (in 1 cm}^3 \text{ of soil)}$$

From Eq. (2-6) for G_w obtain $V_w = W_w$ when using g and cm^3; therefore,

$$S = \frac{V_w}{V_v} \times 100 = \frac{0.349}{0.404} \times 100 = \mathbf{86.4\%}$$

Step 5. The dry bulk specific gravity is obtained as (dimensionless)

$$G_b = \frac{\gamma_{\text{dry}}}{\gamma_w} = \frac{15.19}{9.807} = \mathbf{1.549}$$

////

2-4 MAJOR FACTORS THAT AFFECT THE ENGINEERING PROPERTIES OF SOILS

Most factors that affect the engineering properties of soils involve geological processes acting over long time periods. Among the most important are the following.

Natural Cementation and Aging

All soils undergo a natural cementation at the particle contact points. The process of aging seems to increase the cementing effect by a variable amount. This effect was recognized very early in cohesive soils but is now deemed of considerable importance in cohesionless deposits as well. The effect of cementation and aging in sand is not nearly so pronounced as for clay but still the effect as a statistical accumulation from a very large number of grain contacts can be of significance for designing a foundation. Care must be taken to ascertain the quantitative effects properly since sample disturbance and the small relative quantity of grains in a laboratory sample versus site amounts may provide difficulties in making a value measurement that is more than just an estimate. Field observations have well validated the concept of the cementation and aging process. Loess deposits, in particular, illustrate the beneficial effects of the cementation process where vertical banks are readily excavated.

Overconsolidation

A soil is said to be *normally consolidated* (nc) if the current overburden pressure (column of soil overlying the plane of consideration) is the largest to which the mass has ever been subjected. It has been found by experience that prior stresses on a soil element produce an imprint or stress history that is retained by the soil structure until a new stress state exceeds the maximum previous one. The soil is said to be *overconsolidated* (or *preconsolidated*) if the stress history involves a stress state larger than the present overburden pressure.

Overconsolidated cohesive soils have received considerable attention. Only more recently has it been recognized that overconsolidation may be of some importance in cohesionless soils. A part of the problem, of course, is that it is relatively easy to ascertain overconsolidation in cohesive soils but very difficult in cohesionless deposits. The behavior of overconsolidated soils under new loads is different from that of normally consolidated soils, so it is important—particularly for cohesive soils—to be able to recognize the occurrence.

The *overconsolidation ratio* (OCR) is defined as the ratio of the past effective pressure p'_c to the present overburden pressure p'_o:

$$\text{OCR} = \frac{p'_c}{p'_o} \tag{2-13}$$

A **normally consolidated** soil has OCR = 1 and an **overconsolidated** soil has OCR > 1. OCR values of 1–3 are obtained for lightly overconsolidated soils. Heavily overconsolidated soils might have OCRs > 6 to 8.

An **underconsolidated** soil will have OCR < 1. In this case the soil is still consolidating. Over- or preconsolidation may be caused by a geologically deposited depth of overburden that has since partially eroded away. Of at least equally common occurrence are preconsolidation effects that result from shrinkage stresses produced by alternating wet and dry cycles. These readily occur in arid and semiarid regions but can occur in more moderate climates as well. Chemical actions from naturally occurring compounds may aid in producing an overconsolidated soil deposit. Where overconsolidation occurs from shrinkage, it is common for only the top 1 to 3 meters to be overconsolidated and the underlying material to be normally consolidated. The OCR grades from a high value at or near the ground surface to 1 at the normally consolidated interface.

Mode of Deposit Formation

Soil deposits that have been transported, particularly via water, tend to be made up of small grain sizes and initially to be somewhat loose with large void ratios. They tend to be fairly uniform in composition but may be stratified with alternating very fine material and thin sand seams, the sand being transported and deposited during high-water periods when stream velocity can support larger grain sizes. These deposits tend to stabilize and may become very compact (dense) over geological periods from subsequent overburden pressure as well as cementing and aging processes.

Soil deposits developed where the transporting agent is a glacier tend to be more varied in composition. These deposits may contain large sand or clay lenses. It is not unusual for glacial deposits to contain considerable amounts of gravel and even suspended boulders. Glacial deposits may have specific names as found in geology textbooks such as moraines, eskers, etc.; however, for foundation work our principal interest is in the uniformity and quality of the deposit. Dense, uniform deposits are usually not troublesome. Deposits with an erratic composition may be satisfactory for use, but soil properties may be very difficult to obtain. Boulders and lenses of widely varying characteristics may cause construction difficulties.

The principal consideration for residual soil deposits is the amount of rainfall that has occurred. Large amounts of surface water tend to leach materials from the upper zones to greater depths. A resulting stratum of fine particles at some depth can affect the strength and settlement characteristics of the site.

Quality of the Clay

The term *clay* is commonly used to describe any cohesive soil deposit with sufficient clay minerals present that drying produces shrinkage with the formation of cracks or fissures such that block slippage can occur. Where drying has produced shrinkage cracks in the deposit we have a *fissured clay.* This material can be troublesome for field sampling because the material may be very hard, and fissures make sample recovery difficult. In laboratory strength tests the fissures can define failure planes and produce fictitiously low strength predictions (alternatively, testing intact pieces produces too high a prediction) compared to in situ tests where size effects may either bridge or confine the discontinuity. A great potential for strength reduction exists during construction where opening an excavation reduces the overburden pressure so that expansion takes place along any fissures. Subsequent rainwater or even local humidity can enter the fissure so that interior as well as surface softening occurs.

A clay without fissures is an *intact clay* and is usually normally consolidated or at least has not been overconsolidated from shrinkage stresses. Although these clays may expand from excavation of overburden, the subsequent access to free water is not so potentially disastrous as for fissured clay because the water effect is more nearly confined to the surface.

Soil Water

Soil water may be a geological phenomenon; however, it can also be as recent as the latest rainfall or broken water pipe. An increase in water content tends to decrease the shear strength of cohesive soils. An increase in the pore pressure in any soil will reduce the shear strength. A sufficient increase can reduce the shear strength to zero—for cohesionless soils the end result

is a viscous fluid. A saturated sand in a loose state can, from a sudden shock, also become a viscous fluid. This phenomenon is termed *liquefaction* and is of considerable importance when considering major structures (such as power plants) in earthquake-prone areas.

When soil water just dampens sand, the surface tension produced will allow shallow excavations with vertical sides. If the water evaporates, the sides will collapse; however, construction vibrations can initiate a cave-in prior to complete drying. The sides of a vertical excavation in a cohesive soil may collapse from a combination of rainfall softening the clay together with excess water entering surface tension cracks to create hydrostatic water pressure.

In any case, the shear strength of a cohesive soil can be markedly influenced by water. Even without laboratory equipment, one has probably seen how cohesive soil strength can range from a fluid to a brick-like material as a mudhole alongside a road fills during a rain and subsequently dries. Ground cracks in the hole bottom after drying are shrinkage (or tension) cracks.

Changes in the groundwater table (GWT) may produce undesirable effects—particularly from its lowering. Since water has a buoyant effect on soil as for other materials, lowering the GWT removes this effect and effectively increases the soil weight by that amount. This can produce settlements, for all the underlying soil "sees" is a stress increase from this weight increase. Very large settlements can be produced if the underlying soil has a large void ratio. Pumping water from wells in Mexico City has produced areal settlements of several meters. Pumping water (and oil) in the vicinity of Houston, Texas, has produced areal settlements of more than 2 meters in places. Pumping to dewater a construction site can produce settlements of 30 to 50 mm within short periods of time. If adjacent buildings cannot tolerate this additional settlement, legal problems are certain to follow.

2-5 ROUTINE LABORATORY INDEX SOIL TESTS

Some or all of the following laboratory tests are routinely performed as part of the foundation design process. They are listed in the descending order of likelihood of being performed for a given project.

Water Content w

Water content determinations are made on the recovered soil samples to obtain the natural water content w_N. Liquid (w_L) and plastic (w_P) tests are commonly made on cohesive soils both for classification and for correlation studies. Water content determinations are also commonly made in soil improvement studies (compaction, using admixtures, etc.).

Atterberg Limits

The *liquid* and *plastic limits* are routinely determined for cohesive soils. From these two limits the *plasticity index* is computed as shown on Fig. 2-2*a*. The significance of these three terms is indicated in Fig. 2-2*a* along with the qualitative effect on certain cohesive soil properties of increasing either I_P or w_L. The plasticity index is commonly used in strength correlations; the liquid limit is also used, primarily for consolidation estimates.

The liquid and plastic limit values, together with w_N, are useful in predicting whether a cohesive soil mass is preconsolidated. Since an overconsolidated soil is more dense, the void

ratio is smaller than in the soil remolded for the Atterberg limit tests. If the soil is located below the groundwater table (GWT) where it is saturated, one would therefore expect that smaller void ratios would have less water space and the w_N value would be smaller. From this we might deduce the following:

If w_N is close to w_L,	soil is normally consolidated.
If w_N is close to w_P,	soil is some- to heavily overconsolidated.
If w_N is intermediate,	soil is somewhat overconsolidated.
If w_N is greater than w_L,	soil is on verge of being a viscous liquid.

Although the foregoing gives a qualitative indication of overconsolidation, other methods must be used if a quantitative value of OCR is required.

We note that w_N can be larger than w_L, which simply indicates the in situ water content is above the liquid limit. Since the soil is existing in this state, it would seem that overburden pressure and interparticle cementation are providing stability (unless visual inspection indicates a liquid mass). It should be evident, however, that the slightest remolding disturbance has the potential to convert this type of deposit into a viscous fluid. Conversion may be localized, as for pile driving, or involve a large area. The larger w_N is with respect to w_L, the greater the potential for problems. The *liquidity index* has been proposed as a means of quantifying this problem and is defined as

$$I_L = \frac{w_N - w_P}{w_L - w_P} = \frac{w_N - w_P}{I_P} \tag{2-14}$$

where, by inspection, values of $I_L \geq 1$ are indicative of a liquefaction or "quick" potential. Another computed index that is sometimes used is the *relative consistency,*[2] defined as

$$I_C = \frac{w_L - w_N}{I_P} \tag{2-14a}$$

Here it is evident that if the natural water content $w_N \leq w_L$, the relative consistency is $I_C \geq 0$; and if $w_N > w_L$, the relative consistency or consistency index $I_C < 0$.

Where site evidence indicates that the soil may be stable even where $w_N \geq w_L$, other testing may be necessary. For example (and typical of highly conflicting site results reported in geotechnical literature) Ladd and Foott (1974) and Koutsoftas (1980) both noted near-surface marine deposits underlying marsh areas that exhibited large OCRs in the upper zones with w_N near or even exceeding w_L. This is, of course, contradictory to the previously given general statements that if w_N is close to w_L the soil is "normally consolidated" or is about to become a "viscous liquid."

Grain Size

The grain size distribution test is used for soil classification and has value in designing soil filters. A soil filter is used to allow drainage of pore water under a hydraulic gradient with

[2]This is the definition given by ASTM D 653, but it is more commonly termed the *consistency index,* particularly outside the United States.

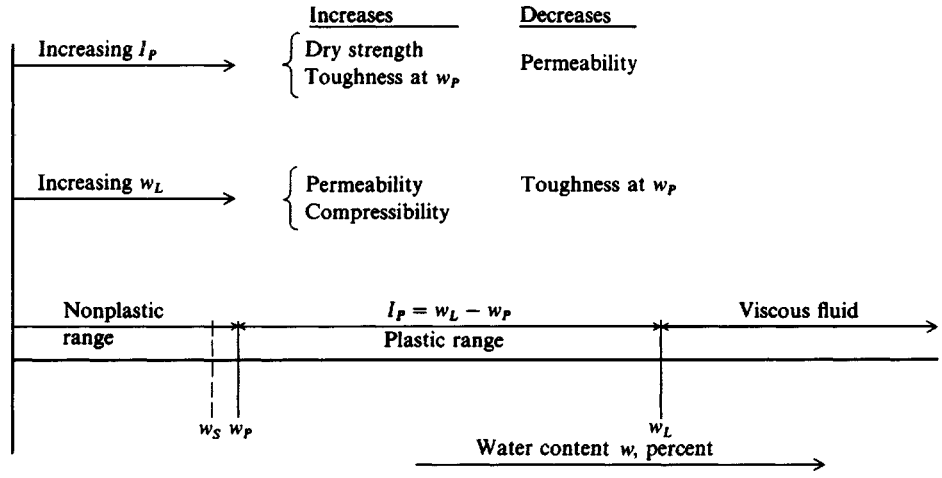

(*a*) Relative location of Atterberg limits on a water content scale. Note that w_S may be to the right of w_P for some soils.

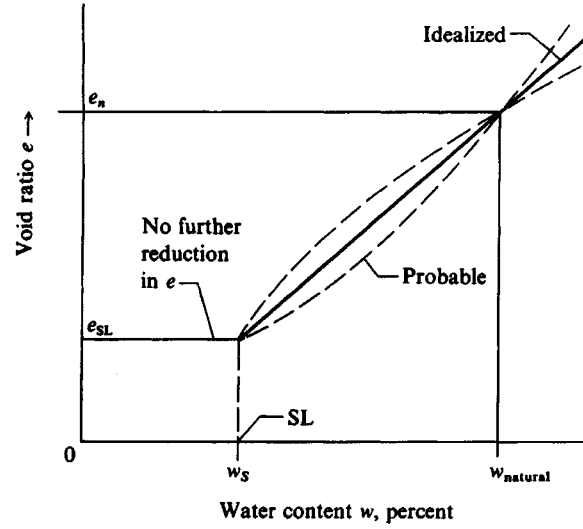

(*b*) Qualitative definition of the shrinkage limit.

Figure 2-2 The Atterberg limits and some relationships to soil mass properties.

erosion of soil fines minimized. Frequently, the grain size test is used to determine the D_{85}, D_{60}, D_{10} fractions (or percents). For example, on Fig. 2-3*a*, *b* the D_{85} (size for which 85 percent of sample is smaller) is about 1.1 mm for the "well-graded" soil. The D_{10} size is about 0.032 mm and was determined from the hydrometer test branch of the curve. The percent clay (particles smaller than 0.002 mm) can be determined from a grain size curve

U.S. as of 1994		British (B.S.)		German DIN		French	
Sieve no.	mm	Sieve no.	mm	Sieve no.	mm	Sieve no.	mm
4	4.76	—		—		—	
10*	2.00	8*	2.057	—		34*	2.000
20	0.841	16	1.003	—		31	1.000
30	0.595	30	0.500	500	0.500	28	0.500
		36†	0.422	400†	0.400	27†	0.400
40†	0.420	—		—		—	
50	0.297	52	0.295	—		—	
60	0.250	60	0.251	250	0.250	25	0.250
80	0.177	85	0.178	160	0.160	23	0.160
100	0.149	100	0.152	125	0.125	22	0.125
200	0.074	200	0.076	80	0.080	20	0.080
270	0.053	300	0.053	50	0.050	18	0.050

* Breakpoint between sand and gravel.
† Use for Atterberg limits.

(*a*)

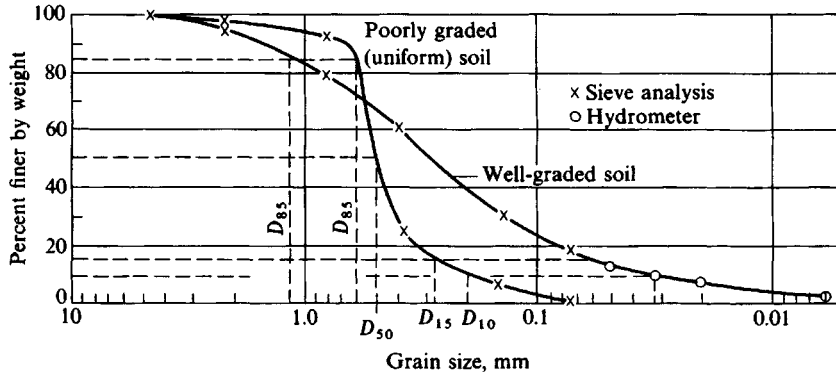

(*b*)

Figure 2-3 (*a*) Various standard sieve numbers and screen openings; (*b*) grain size distribution curves.

such as this, which uses a combination of sieves and a hydrometer test. Typical sieve sizes as used for sands and silts are shown in Fig. 2-3*a*.

Unit Weight γ

Unit weight γ is fairly easy to estimate for a cohesive soil by trimming a block (or length of a recovered tube sample) to convenient size, weighing it, and then placing it in a volumetric jar and measuring the quantity of water required to fill the container. The unit weight is simply

$$\gamma_{\text{wet}} = \frac{\text{Weight of sample}}{\text{Volume of jar} - \text{volume of water to fill jar}}$$

If the work is done rapidly so that the sample does not have time to absorb any of the added water a very reliable value can be obtained. The average of several trials should be used if possible.

The unit weight of cohesionless samples is very difficult (and costly) to determine. Estimated values as outlined in Chap. 3 are often used. Where more accurate values are necessary, freezing and injection methods are sometimes used; that is, a zone is frozen or injected with a hardening agent so that a somewhat undisturbed block can be removed to be treated similarly as for the cohesive sample above. Where only the unit weight is required, good results can be obtained by recovering a sample with a piston sampler (described in Chap. 3). With a known volume initially recovered, later disturbance is of no consequence, and we have

$$\gamma_{\text{wet}} = \frac{\text{Weight of sample recovered}}{\text{Initial volume of piston sample}}$$

The unit weight is necessary to compute the in situ overburden pressure p_o used to estimate OCR and is necessary in the computation of consolidation settlements of Chap. 5. It is also used to compute lateral pressures against soil-retaining structures and to estimate skin resistance for pile foundations. In cohesionless materials the angle of internal friction ϕ depends on the unit weight and a variation of only 1 or 2 kN/m^3 may have a substantial influence on this parameter.

Relative Density D_r

Relative density is sometimes used to describe the state condition in cohesionless soils. Relative density is defined in terms of natural, maximum, and minimum void ratios e as

$$D_r = \frac{e_{\max} - e_n}{e_{\max} - e_{\min}} \tag{2-15}$$

It can also be defined in terms of natural (in situ), maximum, and minimum unit weight γ as

$$D_r = \left(\frac{\gamma_n - \gamma_{\min}}{\gamma_{\max} - \gamma_{\min}}\right)\left(\frac{\gamma_{\max}}{\gamma_n}\right) \tag{2-16}$$

The relative density test can be made on gravelly soils if the (−) No. 200 sieve (0.074 mm) material is less than 8 percent and for sandy soils if the fines are not more than about 12 percent according to Holtz (1973).

The relative density D_r is commonly used to identify potential liquefaction under earthquake or other shock-type loadings [Seed and Idriss (1971)]; however, at present a somewhat more direct procedure is used [Seed et al. (1985)]. It may also be used to estimate strength (Fig. 2-30).

It is the author's opinion that the D_r test is not of much value since it is difficult to obtain maximum and minimum unit weight values within a range of about ±0.5 kN/m^3. The average maximum value is about this amount under (say 20.0 kN/m^3 − 0.5) and the minimum about this over (say, 15.0 kN/m^3 + 0.5). The definition is for the maximum and minimum values, but average values are usually used. This value range together with the uncertainty in obtaining the in situ value can give a potential range in computed D_r of up to 30 to 40 percent (0.3 to 0.4). Chapter 3 gives the common methods of estimating the in situ value of D_r. A simple

laboratory procedure is given in Bowles (1992) (experiment 18) either to compute D_r or to obtain a unit weight for quality control.

Specific Gravity G_s

The specific gravity of the soil grains is of some value in computing the void ratio when the unit weight and water content are known. The test is of moderate difficulty with the major source of error deriving from the presence of entrapped air in the soil sample. Since G_s does not vary widely for most soils, the values indicated here are commonly estimated without performing a test.

Soil	G_s
Gravel	2.65–2.68
Sand	2.65–2.68
Silt, inorganic	2.62–2.68
Clay, organic	2.58–2.65
Clay, inorganic	2.68–2.75

A value of $G_s = 2.67$ is commonly used for cohesionless soils and a value of 2.70 for inorganic clay. Where any uncertainty exists of a reliable value of G_s, one should perform a test on a minimum of three small representative samples and average the results. Values of G_s as high as 3.0 and as low as 2.3 to 2.4 are not uncommon.

Shrinkage Limit w_S

This is one of the Atterberg limit tests that is sometimes done. The shrinkage limit is qualitatively illustrated in Fig. 2-2*b*. It has some value in estimating the probability of expansive soil problems. Whereas a low value of w_S indicates that only a little increase in water content can start a volume change, the test does not quantify the amount of ΔV. The problem of making some kind of estimate of the amount of soil expansion is considered in Sec. 7-9.4.

2-6 SOIL CLASSIFICATION METHODS IN FOUNDATION DESIGN

It is necessary for the foundation engineer to classify the site soils for use as a foundation for several reasons:

1. To be able to use the database of others in predicting foundation performance.
2. To build one's own local database of successes (or any failures).
3. To maintain a permanent record that can be understood by others should problems later develop and outside parties be required to investigate the original design.
4. To be able to contribute to the general body of knowledge in common terminology via journal papers or conference presentations. After all, if one is to partake in the contributions of others, one should be making contributions to the general knowledge base and not be just a "taker."

The Unified Soil Classification System (USCS) of Table 2-1 is much used in foundation work. A version of this system has been standardized by ASTM as D 2487 (in Volume 04.08: *Soil and Rock; Dimension Stone; Geosynthetics*). The standardized version is similar to the original USCS as given by Casagrande (1948) but with specified percentages of sand or gravel passing specific sieves being used to give the "visual description" of the soil. The original Casagrande USCS only classified the soil using the symbols shown in Table 2-1 (GP, GW, SM, SP, CL, CH, etc.), based on the indicated percentages passing the No. 4 and No. 200 sieves and the plasticity data. The author has always suggested a visual description supplement such as the following:

Soil data available	Soil description (using Table 2-1)
Sand, $C_u = 7$; $C_c = 1.3$, 95% passing No. 4 sieve, brown color	Well-graded, brown sand with a trace of gravel, SW
Gravel, 45% passes No. 4, 25% passes No. 200; $w_L = 42$, $w_P = 22$, tan color	Tan clayey gravel with sand, GC
70% passes No. 4 and 18% passes No. 200 sieve; $w_L = 56$; $w_P = 24$. Sample is firm and dark in color with a distinct odor	Organic gravelly, clayey sand, SC

It is evident in this table that terms "trace" and "with" are somewhat subjective. The soil color, such as "blue clay," "gray clay," etc., is particularly useful in soil classification. In many areas the color—particularly of cohesive soils—is an indication of the presence of the

Figure 2-4 Typical soil profiles at locations indicated. Values for soil properties indicate order of magnitude; they should not be used for design. Depths shown are in meters.

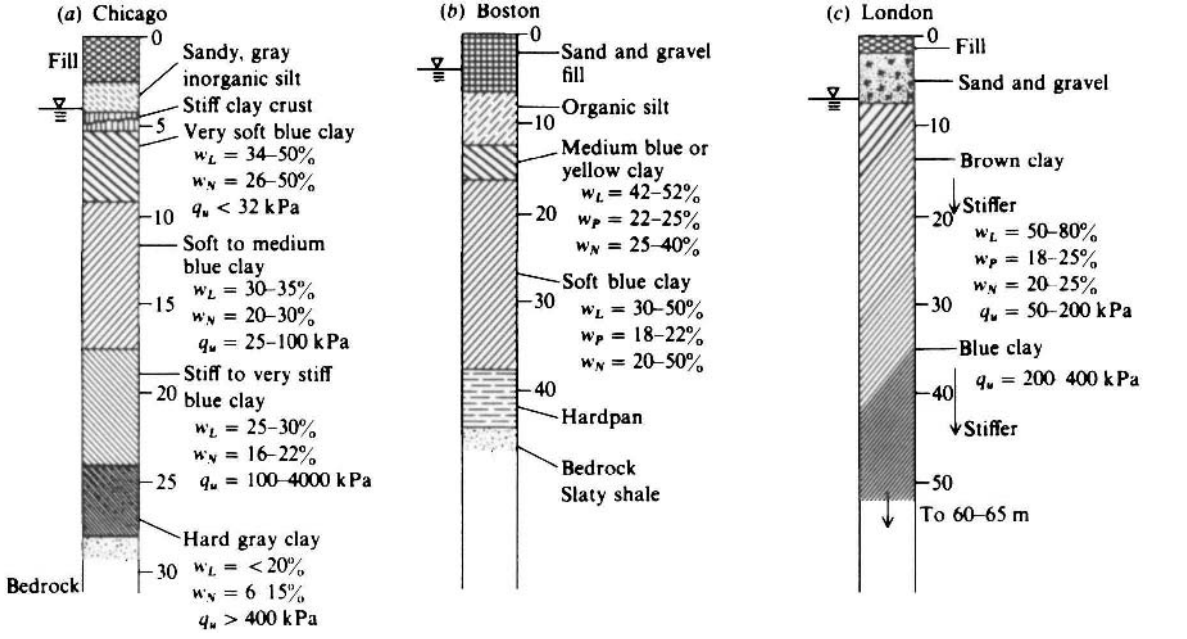

same soil stratum as found elsewhere. For example the "soft blue clay" on the soil profile of Fig. 2-4 for Chicago has about the same properties at any site in the Chicago area.

In foundation work the terms *loose, medium,* and *dense,* as shown in Table 3-4, and consistency descriptions such as *soft, stiff, very stiff,* etc., as shown in Table 3-5, are also commonly used in foundation soil classification. Clearly, all of these descriptive terms are of great use to the local geotechnical engineer but are somewhat subjective. That is, there could easily be some debate over what is a "medium" versus a "dense" sand, for example.

The D 2487 standard removed some of the subjectiveness of the classification and requires the following terminology:

$< 15\%$ is sand or gravel	use name (organic clay, silt, etc.)
$15\% < x < 30\%$ is sand or gravel	describe as clay or silt with sand, or clay or silt with gravel
$> 30\%$ is sand or gravel	describe as sandy clay, silty clay, or gravelly clay, gravelly silt

The gravel or sand classification is based on the percentage retained on the No. 4 (gravel) sieve or passing the No. 4 and retained on the No. 200 (sand) sieves. This explanation is only partial, as the new standard is too lengthy for the purpose of this textbook to be presented in detail.

Although not stated in D 2487, the standard is devised for using a computer program[3] to classify the soil. Further, not all geotechnical engineers directly use the ASTM standard, particularly if their practice has a history of success using the original USC system.

General Comments on Using Table 2-1

1. When the w_L-I_P intersection is very close to the "A" or $w_L = 50\%$ line, use dual symbols such as SC-SM, CL-ML, organic OL-OH, etc. to indicate the soil is borderline.
2. If the w_L-I_P intersection is above the "U" line one should carefully check that the tests and data reduction are correctly done. It may require redoing the limits tests as a check. The reason for this caution is that this line represents the upper limit of real soils so far analyzed.

Peat and Organic Soils

Strictly, *peat* is not a soil but rather an organic deposit of rotting wood from trees, plants, and mosses. If the deposit is primarily composed of moss, it may be termed a sphagnum peat. If the deposit has been somewhat contaminated with soil particles (silt, clay, sand) it may be named for the soil particles present as peaty silt, peaty sand, peaty clay, and so on. If the soil contamination is substantial (in a relative sense) the soil is more likely to be termed an

[3] A compiled computer program for use with D 2487 (along with several others) is available with the laboratory text *Engineering Properties of Soils and Their Measurement,* 4th ed., (1992), McGraw-Hill Book Company, New York, NY 10020; Tel.: (212) 512-2012.

TABLE 2-1
Unified soil classification [Casagrande (1948)]

Major divisions			Group symbols		Typical names	Laboratory classification criteria		
Coarse-grained soils (More than half of material is larger than No. 200 sieve size)	Gravels (More than half of coarse fraction is larger than No. 4 sieve size)	Clean gravels (Little or no fines)	GW		Well-graded gravels, gravel-sand mixtures, little or no fines	Determine percentages of sand and gravel from grain-size curve. Depending on percentages of fines (fraction smaller than No. 200 sieve size), coarse-grained soils are classified as follows: Less than 5% GW, GP, SW, SP; More than 12% GM, GC, SM, SC; 5 to 12 % *Borderline* cases requiring dual symbols†	$C_u = \frac{D_{60}}{D_{10}}$ greater than 4; $C_c = \frac{(D_{30})^2}{D_{10} \times D_{10}}$ between 1 and 3	
			GP		Poorly graded gravels, gravel-sand mixtures, little or no fines		Not meeting C_u or C_c requirements for GW	
		Gravels with fines (Appreciable amount of fines)	GM*	*d*	Silty gravels, gravel-sand-silt mixtures		Atterberg limits below "A" line or I_P less than 4	Limits plotting in hatched zone with I_P between 4 and 7 are *borderline* cases requiring use of dual symbols.
				u			Atterberg limits above "A" line with I_P greater than 7	
			GC		Clayey gravels, gravel-sand-clay mixtures			
	Sands (More than half of coarse fraction is smaller than No. 4 sieve size)	Clean sands (Little or no fines)	SW		Well-graded sands, gravelly sands, little or no fines		$C_u = \frac{D_{60}}{D_{10}}$ greater than 6; $C_c = \frac{(D_{30})^2}{D_{10} \times D_{60}}$ between 1 and 3	
			SP		Poorly graded sands, gravelly sands, little or no fines		Not meeting C_u or C_c requirements for SW	
		Sands with fines (Appreciable amount of fines)	SM*	*d*	Silty sands, sand-silt mixtures		Atterberg limits below "A" line or I_P less than 4	Limits plotting in hatched zone with I_P between 4 and 7 are *borderline* cases requiring use of dual symbols.
				u			Atterberg limits above "A" line with I_P greater than 7	
			SC		Clayey sands, sand-clay mixtures			

Fine-grained soils (More than half of material is smaller than No. 200 sieve)	Silts and clays (Liquid limit less than 50%)	ML	Inorganic silts and very fine sands, rock flour, silty or clayey fine sands, or clayey silts with slight plasticity
		CL	Inorganic clays of low to medium plasticity, gravelly clays, sandy clays, silty clays, lean clays
		OL	Organic silts and organic silty clays of low plasticity
	Silts and clays (Liquid limit greater than 50%)	MH	Inorganic silts, micaceous or diatomaceous fine sandy or silty soils, elastic silts
		CH	Inorganic clays of high plasticity, fat clays
		OH	Organic clays of medium to high plasticity, organic silts
	Highly organic soils	Pt	Peat and other highly organic soils

For all soils plotting nearly on "A" line use dual symbols, i.e., $I_P = 29.5$, $w_L = 60$ gives CH-OH or CH-MH. When w_L is near 50 use CL/CH, ML/MH. Take "nearly on" as ±2 percent.

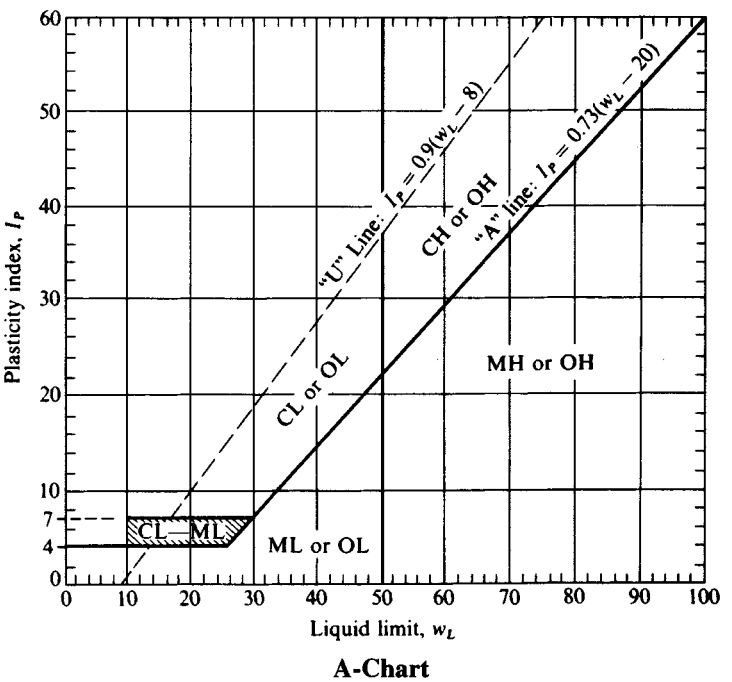

A-Chart

*Division of GM and SM groups into subdivisions of *d* and *u* are for roads and airfields only. Subdivision is based on Atterberg limits; suffix *d* used when w_L is 28 or less and the I_P is 6 or less; suffix *u* used when w_L is greater than 28.

†Borderline classifications, used for soils possessing characteristics of two groups, are designated by combinations of group symbols. For example: GW-GC, well-graded gravel-sand mixture with clay binder.

organic soil. Generally a "peat" deposit is classified as such from visual inspection of the recovered samples.

There have been a number of attempts to quantify various engineering properties of peat (or peaty) deposits; however, it is usually necessary to consider the properties of each site. Several engineering properties such as unit weight, compressibility, and permeability will be heavily dependent on the type, relative quantity, and degree of decomposition (state) of the organic material present. Several recent references have attempted to address some of these problems:

Landva and Pheeney (1980)
Berry and Vickers (1975)
Edil and Dhowian (1981)
Lo et al. (1990)
Fox et al. (1992)
Stinnette (1992)

Organic soils are defined as soil deposits that contain a mixture of soil particles and organic (peat) matter. They may be identified by observation of peat-type materials, a dark color, and/or a woody odor. ASTM (D 2487 Section 11.3.2) currently suggests that the organic classification (OL, OH shown on the "A" chart of Table 2-1) be obtained by performing the liquid limit on the natural soil, then oven-drying the sample overnight and performing a second liquid limit test on the oven-dry material. If the liquid limit test after oven drying is less than 75 percent of that obtained from the undried soil, the soil is "organic." Oven drying of organic soils requires special procedures as given in ASTM D 2974.

After performing the liquid and plastic limits, one classifies an organic soil using the "A" chart of Table 2-1. The soil may be either an organic silt OL, OH, or an organic clay OL, OH depending on the liquid limit w_P and plasticity index I_P and where these values plot on the "A" chart. It is necessary to use both the qualifier "organic silt" or "organic clay" **and** the symbol OL or OH.

Approximate Field Procedures for Soil Identification

It is sometimes useful to be able to make a rapid field identification of the site soil for some purpose. This can be done approximately as follows:

1. Differentiate gravel and sand by visual inspection.
2. Differentiate fine sand and silt by placing a spoonful of the soil in a deep jar (or test tube) and shaking it to make a suspension. Sand settles out in $1\frac{1}{2}$ minutes or less whereas silt may take 5 or more minutes. This test may also be used for clay, which takes usually more than 10 minutes. The relative quantities of materials can be obtained by observing the depths of the several materials in the bottom sediment.
3. Differentiate between silt and clay as follows:
   a. Clay lumps are more difficult to crush using the fingers than silt.
   b. Moisten a spot on the soil lump and rub your finger across it. If it is smooth it is clay; if marginally streaked it is clay with silt; if rough it is silt.

c. Form a plastic ball of the soil material and shake it horizontally by jarring your hand. If the material becomes shiny from water coming to the surface it is silt.

4. Differentiate between organic and inorganic soils by visual inspection for organic material or a smell test for wood or plant decay odor.

2-7 SOIL MATERIAL CLASSIFICATION TERMS

The soil classification terms shown in Table 2-1 are widely used in classification. A number of other terms are used both by engineers and construction personnel, or tend to be localized. A few of these terms will be defined here as a reader convenience.

Bedrock

This is a common name for the parent rock, but generally implies a rock formation at a depth in the ground on which a structure may be founded. All other rocks and soils are derived from the original bedrock formed from cooling of molten magma and subsequent weathering. Bedrock extends substantially downward to molten magma and laterally in substantial dimensions. The lowermost part is igneous rock formed by cooling of the molten magma. This may, or may not, be overlain by one or more layers of more recently formed sedimentary rocks such as sandstone, limestone, shale, etc. formed from indurated soil deposits. The interface layers between igneous and sedimentary rocks may be metamorphic rocks formed from intense heat and pressure acting on the sedimentary rocks. In some cases a bedding rock layer—usually sedimentary in origin—may overlie a soil deposit. In earthquake areas the parent rock may be much fractured. Past areal uplifts may have produced zones of highly fragmented parent rock at the bedrock level.

Considering these factors, one might say that generally, bedrock makes a satisfactory foundation, but good engineering practice requires that one check the geological history of the site. In this context it is fairly common to refer to the bedrock with respect to the geological age of estimated formation as Cambrian, pre-Cambrian, etc.

Boulders

Boulders are large pieces of rock fractured from the parent material or blown out of volcanos (called bombs in this case). They may have volumes ranging from about $\frac{1}{2}$ to 8 or 10 m^3 and weigh from about one-half to several hundred tonnes. They may create disposal or excavation problems on or near the ground surface and problems in soil exploration or pile driving at greater depths when suspended in the soil matrix, as in glacial till. Large ones may be suitable to found pile or caissons on; however, size determination may be difficult, and placing a large load on a small suspended boulder may be disastrous.

Gravels and Smaller

Rock fragments smaller than boulders grade into cobbles, pebbles, gravel, sand, silt, and colloids in order of size as shown on Table 2-2. *Crushed stone* is gravel manufactured by crushing rock fragments from boulders or obtained from suitable rock formations by mining. *Bank-run gravel* is a common term for naturally occurring gravel lenses deposited along

TABLE 2-2
Usual size range for general soil classification terminology

Material	Upper, mm	Lower, mm	Comments
Boulders, cobbles	1000 +	75 -	
Gravel, pebbles	75	2 – 5	No. 4 or larger sieve
Sand	2 – 5	0.074	No. 4 to No. 200 sieve
Silt	0.074 – 0.05	0.006	Inert
Rock flour	0.006	?	Inert
Clay	0.002	0.001	Particle attraction, water absorption
Colloids	0.001	?	

rivers or from glaciers. *Pea gravel* is gravel screened to contain only sizes in a certain range (usually about 6 down to 3 mm) and is poorly graded because the > 6 mm and < 3 mm sizes are missing.

Gravels, sands, and silts are cohesionless materials that exist in deposits ranging from a state of loose to dense and coarse to fine. Most deposits, however, are in a medium to fairly dense state. These materials can have cohesion from clay minerals in the fine sand and silt filler that may be present.

Silt

Silts and clays are of particular interest in foundation engineering because they tend to be most troublesome in terms of strength and settlements. Silts and rock flour in the particle range of 0.074 mm down to about 0.001 mm are inert by-products of rock weathering. They may be *organic silts* (OL, OH) if contaminated with organic materials or inorganic (ML, MH) otherwise. Damp silt has an apparent cohesion from the cumulative effect of surface tension on the many small particles, but on drying minimal shrinkage (unless organic) takes place and the resulting dry lumps are easily broken by finger pressure.

Most silt deposits, however, are contaminated with clay minerals so that they have cohesion (dry lumps are not so easily broken). As little as 5 to 8 percent clay can give a silt deposit considerable cohesion, depending on the silt grain sizes and the type of clay mineral. At higher percentages of clay, or depending on its visual effects, a silt deposit may be loosely termed "clay," particularly by construction personnel. From an engineering viewpoint, however, we can see from the "A" chart of Table 2-1 that it is quite possible for a "clay" to have lower plasticity characteristics than a silt, i.e., a CL of say $w_L = 35$ and $I_P = 15$ versus a MH of $w_L = 60$ and $I_P = 25$.

Clay

The clay size (particles 0.002 mm and smaller) overlaps the silt sizes somewhat. The essential difference between the two, however, is that a clay mineral is not inert. It is a complex hydroaluminum silicate,

$$Al_2O_3 \cdot nSiO_2 \cdot kH_2O$$

where n and k are numerical values of attached molecules and vary for the same mass. The clay mineral has a high affinity for water, and individual particles may absorb 100^+ times the particle volume. The presence or absence (during drying) of water can produce very large volume and strength changes. Clay particles also have very strong interparticle attractive forces, which account in part for the very high strength of a dry lump (or a clay brick). Water absorption and interparticle attraction collectively give the *activity* and cohesion to clay (and to soils containing clay minerals).

The three principal identified clay minerals can be characterized in terms of activity and plasticity:

Montmorillonite (or *smectite*)—Most active of the identified minerals. The activity, in terms of affinity for water and swell, makes this material ideal for use as a drilling mud in soil exploration and in drilling oil wells. It is also commonly injected into the ground around basement walls as a water barrier (swells to close off water flow paths) to stop basement leaks. It is also blended with local site material to produce water barriers to protect the GWT from sanitary landfill drainage. The I_P of an uncontaminated montmorillonite is 150^+.

Illite—A clay mineral that is intermediate in terms of activity. The I_P of a pure illite ranges from about 30 to 50.

Kaolinite—The clay mineral with the least activity. This material is commonly used in the ceramic industry and for brick manufacture. It is sometimes used as an absorbent for stomach medicine. The I_P of a pure kaolinite ranges from about 15 to 20.

Montmorillonite deposits are found mostly in arid and semiarid regions. All clay minerals weather into less active materials, e.g., to illite and then to kaolinite. As a consequence most "clay" deposits contain several different clay minerals. Only deposits of relatively pure clay have commercial value. Most of the remainder represent engineering problems. For example, in temperate regions it is not unusual for deposits to contain substantial amounts of montmorillonite or even lenses of nearly pure material.

Clay deposits with certain characteristics are common to certain areas and have been named for the location. For example the "Chicago blue clay," "Boston blue clay," "London clay" shown in Fig. 2-4 are common for those areas. Leda clay is found in large areas of Ottawa Province in Canada and has been extensively studied and reported in the *Canadian Geotechnical Journal.*

Local Terminology

The following are terms describing soil deposits that the geotechnical engineer may encounter. Familiarity with their meaning is useful.

a. *Adobe.* A clayey material found notably in the Southwest.
b. *Caliche.* A conglomeration of sand, gravel, silt, and clay bonded by carbonates and usually found in arid areas.
c. *Glacial till* or *glacial drift.* A mixture of material that may include sand, gravel, silt, and clay deposited by glacial action. Large areas of central North America, much of Canada, northern Europe, the Scandinavian countries, and the British Isles are overlain with glacial

till or drift. The term *drift* is usually used to describe any materials laid down by the glacier. The term *till* is usually used to describe materials precipitated out of the ice, but the user must check the context of usage, as the terms are used interchangeably. Moraines are glacial deposits scraped or pushed ahead (terminal), or alongside the glacier (lateral). These deposits may also be called ground moraines if formed by seasonal advances and retreats of a glacier. The Chicago, Illinois, area, for example, is underlain by three identifiable ground moraines.

d. Gumbo. A clayey or loamy material that is very sticky when wet.

e. Hardpan. This term may be used to describe caliche or any other dense, firm deposits that are excavated with difficulty.

f. Loam. A mixture of sand, clay, silt; an organic material; also called *topsoil.*

g. Loess. A uniform deposit of silt-sized material formed by wind action. Often found along the Mississippi River, where rising damp air affects the density of the air transporting the material, causing it to deposit out. Such deposits are not, however, confined to the Mississippi Valley. Large areas of Nebraska, Iowa, Illinois, and Indiana are covered by loess. Large areas of China, Siberia, and southeastern Europe (southern Russia and Ukraine) and some areas of western Europe are covered with loess. Loess is considered to be a *transported* soil.

h. Muck. A thin watery mixture of soil and organic material.

i. Alluvial deposits. Soil deposits formed by sedimentation of soil particles from flowing water; may be lake deposits if found in lake beds; deltas at the mouths of rivers; marine deposits if deposited through saltwater along and on the continental shelf. Alluvial deposits are found worldwide. For example, New Orleans, Louisiana, is located on a delta deposit. The low countries of The Netherlands and Belgium are founded on alluvial deposits from the Rhine River exiting into the North Sea. Lake deposits are found around and beneath the Great Lakes area of the United States and Canada. Large areas of the Atlantic coastal plain, including the eastern parts of Maryland, Virginia, the Carolinas, the eastern part and most of south Georgia, Florida, south Alabama, Mississippi, Louisiana, and Texas consist of alluvial deposits. These deposits formed when much of this land was covered with the seas. Later upheavals such as that forming the Appalachian mountains have exposed this material. Alluvial deposits are fine-grained materials, generally silt-clay mixtures, silts, or clays and fine to medium sands. If the sand and clay layers alternate, the deposit is a *varved* clay. Alluvial deposits are usually soft and highly compressible.

j. Black cotton soils. Semitropical soils found in areas where the annual rainfall is 500 to 750 mm. They range from black to dark gray. They tend to become hard with very large cracks (large-volume-change soils) when dry and very soft and spongy when wet. These soils are found in large areas of Australia, India, and southeast Asia.

k. Laterites. Another name for residual soils found in tropical areas with heavy rainfalls. These soils are typically bright red to reddish brown in color. They are formed initially by weathering of igneous rocks, with the subsequent leaching and chemical erosion due to the high temperature and rainfall. Collodial silica is leached downward, leaving behind aluminum and iron. The latter becomes highly oxidized, and both are relatively insoluble in the high-pH environment (greater than 7). Well-developed laterite soils are generally porous and relatively incompressible. Lateritic soils are found in Alabama, Georgia, South

Carolina, many of the Caribbean islands, large areas of Central and South America, and parts of India, southeast Asia, and Africa.

l. Saprolite. Still another name for residual soils formed from weathered rock. These deposits are often characterized by a particle range from dust to large angular stones. Check the context of use to see if the term is being used to describe laterite soils or residual soils.

m. Shale. A fine-grained, sedimentary rock composed essentially of compressed and/or cemented clay particles. It is usually laminated, owing to the general parallel orientation of the clay particles, as distinct from claystone or siltstone, which are indurated deposits of random particle orientation. According to Underwood (1967), shale is the predominant sedimentary rock in the Earth's crust. It is often misclassified; layered sedimentary rocks of quartz or argillaceous materials such as argillite are not shale. Shale may be grouped as (1) compaction shale and (2) cemented (rock) shale. The compaction shale is a transition material from soil to rock and can be excavated with modern earth excavation equipment. Cemented shale can sometimes be excavated with excavation equipment but more generally requires blasting. Compaction shales have been formed by consolidation pressure and very little cementing action. Cemented shales are formed by a combination of cementing and consolidation pressure. They tend to ring when struck by a hammer, do not slake in water, and have the general characteristics of good rock. Compaction shales, being of an intermediate quality, will generally soften and expand upon exposure to weathering when excavations are opened. Shales may be clayey, silty, or sandy if the composition is predominantly clay, silt, or sand, respectively. Dry unit weight of shale may range from about 12.5 kN/m^3 for poor-quality compaction shale to 25.1 kN/m^3 for high-quality cemented shale.

2-8 IN SITU STRESSES AND K_o CONDITIONS

Any new foundation load—either an increase (+) from a foundation or a decrease (−) from an excavation—imposes new stresses on the existing state of "locked in" stresses in the foundation soil mass. The mass response is heavily dependent on the previous stress history, so one of the most important considerations in foundation engineering is to ascertain this stress imprint. The term *imprint* is used since any previously applied stresses that are larger than those currently existing have been locked into the soil structure and will affect subsequent stress-response behavior until a new set of larger stresses are applied to produce a new imprint. Of course, the stress history is lost in varying degrees (or completely) when the soil is excavated/remolded or otherwise disturbed as in sample recovery. Factors contributing to loss of stress history during sampling are outlined in Sec. 3-5.

In situ, the vertical stresses act on a horizontal plane at some depth z. These can be computed in any general case as the sum of contributions from n strata of unit weight γ_i and thickness z_i as

$$p_o = \sum_{i=1}^{n} \gamma_i z_i \qquad (a)$$

The unit weight for a homogeneous stratum is of the general form

$$\gamma = A_1 + A_2 z^m \qquad (b)$$

with the constants A_1, A_2, and m determined by obtaining weight values at several depths z and plotting a best-fit curve. In practice, at least for reasonable depths on the order of 5 to 10 meters, a constant value is often (incorrectly) used. An alternative is to divide the deposit into several "layers" and use a constant unit weight γ_i for each as in Eq. (*a*).

In most cases involving geotechnical work, the *effective stress* p'_o is required so that below the GWT one uses the effective soil unit weight computed as

$$\gamma' = \gamma_{\text{sat}} - \gamma_w \tag{c}$$

For any soil deposit formation the plan area is usually rather large and the depth continually increases until either deposition or interior weathering stops. This change produces a gradual vertical compression of the soil at any given depth; similarly, γ increases under compression so that in nearly all cases unit weight $\gamma = f$ (depth). Since the lateral dimension is large there is little reason for significant lateral compression to occur. For this reason it is logical to expect that vertical locked-in *effective stresses* p'_o would be larger than the effective lateral stresses σ'_h at the same point. We may define the ratio of the horizontal to vertical stresses as

$$K = \frac{\sigma_h}{p_o} \tag{d}$$

which is valid for any depth z at any time.

Over geological time the stresses in a soil mass at a particular level stabilize into a steady state and strains become zero. When this occurs the vertical and lateral stresses become principal stresses acting on principal planes.[4] This effective stress state is termed the *at-rest* or K_o condition with K_o defined as

$$K_o = \frac{\sigma'_h}{p'_o} \tag{2-17}$$

Figure 2-5 qualitatively illustrates the range of K_o and the relationship of p_o and σ_h in any homogeneous soil. Note the qualitative curves for preconsolidation in the upper zone of some soil from shrinkage/chemical effects. This figure (see also Fig. 2-45) clearly illustrates the anisotropic ($\sigma_v \neq \sigma_h$) stress state in a soil mass.

Because of the sampling limitations given in Sec. 3-5 it is an extremely difficult task to measure K_o either in the laboratory or in situ. A number of laboratory and field methods are cited by Abdelhamid and Krizek (1976); however, from practical limitations the direct simple shear device (Fig. 2-26*b*) is the simplest for direct laboratory measurements. Field methods will be considered in the next chapter, but note that they are very costly for the slight improvement—in most cases—over using one of the simple estimates following. In these equations use the effective angle of internal friction ϕ' and not the total stress value.

Jaky (1948) presented a derived equation for K_o that is applicable to both soil and agricultural grains (such as corn, wheat, oats, etc.) as

$$K_o = \frac{1 - \sin\phi'}{1 + \sin\phi'}\left(1 + \frac{2}{3}\sin\phi'\right) \tag{2-18}$$

[4]Stresses acting on planes on which no strains or shearing stresses exist are defined as principal stresses, and the planes are principal planes.

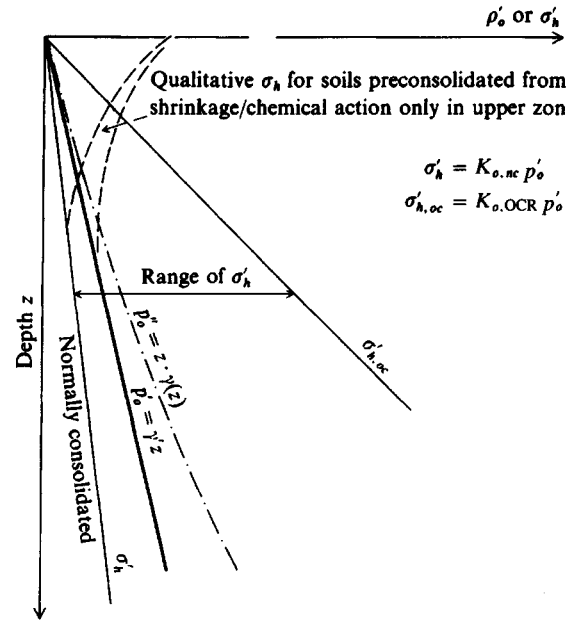

Figure 2-5 Qualitative vertical and lateral pressures in a soil. Although the linear vertical (also called geostatic) pressure profile is commonly used, the p''_o effective pressure profile is more realistic of real soils since γ usually increases with depth. The lateral pressure profile range is for the geostatic pressure profile and would be curved similarly to the p''_o curve for real soils.

which has been simplified—and erroneously called "Jaky's equation"—to the following:

$$K_o = 1 - \sin\phi' \tag{2-18a}$$

This equation is very widely used and has proved reasonably reliable [see extensive regression analysis by Mayne and Kulhawy (1982)] in comparing initial to back-computed K_o values in a number of cases and for normally consolidated materials. Kezdi (1972) suggests that for sloping ground Jaky's equation can be used as follows:

$$K_o = \frac{1 - \sin\phi'}{1 + \sin\beta} \tag{2-19}$$

where β is the angle with the horizontal with sign so that K_o is either increased or reduced as site conditions dictate. This reference also gives a partial derivation of the Jaky equation for any interested user.

Brooker and Ireland (1965) (for normally consolidated clay) suggest

$$K_o = 0.95 - \sin\phi' \tag{2-20}$$

Alpan (1967) (for normally consolidated clay) suggests

$$K_o = 0.19 + 0.233 \log_{10} I_P \tag{2-21}$$

An equation similar to Eq. (2-21) is given by Holtz and Kovacs (1981, on Fig. 11.69) as

$$K_o = 0.44 + 0.0042 I_P \tag{2-21a}$$

where I_P is in percent for both Eqs. (2-21).

We can readily derive a value for K_o in terms of Poisson's ratio based on the definition of K_o being an effective stress state at zero strain. From Hooke's law [Eq. (2-64)] the lateral

strain in terms of the effective horizontal (x, z) and vertical (y) stresses is

$$\epsilon_x = 0 = \frac{1}{E_s}(\sigma_x - \mu\sigma_y - \mu\sigma_z) = \epsilon_z$$

With $\sigma_x = \sigma_z = K_o\sigma_y$ we obtain, on substitution into the preceding and canceling,

$$K_o = \frac{\mu}{1 - \mu} \tag{2-22}$$

For a cohesionless soil μ is often assumed as 0.3 to 0.4, which gives $K_o = 0.43$ to 0.67, with a value of 0.5 often used.

It is extremely difficult to obtain a reliable estimate of K_o in a normally consolidated soil, and even more so in overconsolidated soils (OCR > 1). A number of empirical equations based on various correlations have been given in the literature [see the large number with cited references given by Mesri and Hayat (1993)]. Several of the more promising ones are:

Alpan (1967) and others have suggested that the overconsolidated consolidation ratio $K_{o,\text{OCR}}$ is related to the normally consolidated value $K_{o,\text{nc}}$ in the following form

$$K_{o,\text{OCR}} = K_{o,\text{nc}} \times \text{OCR}^n \tag{2-23}$$

where $n = f(\text{test, soil, locale})$ with a value range from about 0.25 to 1.25. For *overconsolidated sand, n* can be estimated from Fig. 2-6. For *cohesive* soil, Wroth and Houlsby (1985, p. 12) suggest n as follows:

$$n = 0.42 \text{ (low plasticity—}I_P < 40\%\text{)}$$
$$n = 0.32 \text{ (high plasticity—}I_P > 40\%\text{)}$$

However, $n \approx 0.95$ to 0.98 was obtained from in situ tests on several clays in eastern Canada [Hamouche et al. (1995)].

Mayne and Kulhawy (1982) suggest that a *mean* value of $n = 0.5$ is applicable for both sands and clays and that $n = \sin\phi'$ is also a good representation for sand. Their sugges-

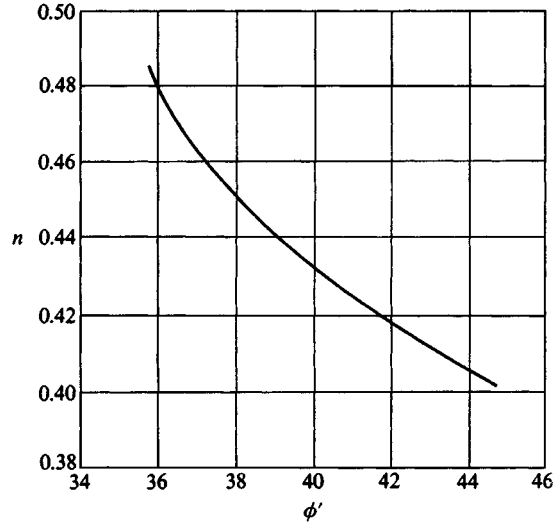

Figure 2-6 Exponent n for sands. [*After Alpan (1967).*]

tions are based on a semi-statistical analysis of a very large number of soils reported in the literature.

The exponent n for *clays* was also given by Alpan (1967) in graph format and uses the plasticity index I_P (in percent). The author modified the equation shown on that graph to obtain

$$n = 0.54 \times 10^{-I_P/281} \tag{2-24}$$

And, as previously suggested (for sands), we can use

$$n = \sin\phi' \tag{2-24a}$$

The n-values previously given by Wroth and Houlsby (1985) can be obtained from Eq. (2-24) using an average "low plasticity" I_P of about 30 ($n = 0.42$) and a "high plasticity" I_P of about 65 percent ($n = 0.32$).

Mayne (1984) suggests that the range of valid values for the overconsolidated $K_{o,\text{OCR}}$ using Eq. (2-23) for cohesive soils depends on the normalized strength ratio s_u/p'_c being less than 4—at least for noncemented and intact clays. Therefore, this ratio is indirectly used for Eq. (2-23), but it will be directly used in the following section.

2-8.1 Overconsolidated K_o Conditions

The equation for the overconsolidation ratio (OCR) was given in Sec. 2-4, and it is repeated here for convenience:

$$\text{OCR} = \frac{p'_c}{p_o} \tag{2-13}$$

In this equation the current overburden pressure p'_o can be computed reasonably well, but the value of the preconsolidation pressure p'_c is at best an estimate, making a reliable computation for OCR difficult. The only method at present that is reasonably reliable is to use the consolidation test described in Sec. 2-10 to obtain p'_c. The alternative, which is likely to be less precise, is to use some kind of in situ testing to obtain the s_u/p'_i ratio (where $i = o$ or c) and use a chart such as Fig. 2-36 given later in Sec. 2-11.9.

There are a number of empirical correlations for OCR based on the s_u/p'_o ratio (the undrained shear strength, s_u, divided by the current in situ effective overburden pressure p'_o) and on in situ tests that are defined later in Chap. 3. The following were taken from Chang (1991):

For the field vane test:

$$\text{OCR} = 22(s_u/p'_o)_{\text{fv}}(I_P)^{-0.48}$$

$$\text{OCR} = \frac{(s_u/p'_o)_{\text{fv}}}{0.08 + 0.55I_P}$$

For the cone penetrometer test:

$$S = \frac{s_u}{p'_o} = \frac{(q_c - p_o)}{p'_o} \cdot \frac{1}{N_k}$$

$$S_1 = 0.11 + 0.0037I_P \quad \text{[see Eq. (2-60)]}$$

These two S-values are then used to compute the OCR as

$$\text{OCR} = (S/S_1)^{1.13+0.04(S/S_1)}$$

Section 3-11.1 gives an alternative method to compute the OCR from a cone penetration test using Eqs. (3-17).

For the flat dilatometer test:

$$\text{OCR} = 0.24K_D^{1.32}$$

In these equations I_P = plasticity index in percentage; q_c = cone resistance; p_o = total (not effective) overburden pressure; N_k = cone factor that is nearly constant at $N_k = 12$ for OCR ≤ 8; K_D = horizontal stress index for the dilatometer. All of these terms (see Symbol list) are either used later in this chapter or in Chap. 3. There are a number of other equations given by Chang but these tend to summarize his discussion best.

With the value of OCR and the current in situ effective pressure p'_o one can use Eq. (2-13) to back-compute the preconsolidation pressure p'_c.

An estimate for $K_{o,\text{OCR}}$ is given by Mayne (1984) based on the analysis of a number of clay soils reported in the literature. The equation is as follows:

$$K_{o,\text{OCR}} = K_{o,\text{nc}}(A + s_u/p'_o) \tag{2-25}$$

In this equation note that the ratio s_u/p'_o uses the effective current overburden pressure p'_o. The variable A depends on the type of laboratory test used to obtain the s_u/p'_c ratio as follows:

Test	A	Comments
CK_oUC	0.7	K_o-consolidated—undrained compression
CIUC	0.8	Isotropically consolidated
CK_oDSS	1.0	Direct simple shear test

The upper limit of $K_{o,\text{OCR}}$ appears to be the passive earth pressure coefficient K_p (defined in Chap. 11), and a number of values reported in the literature range from 1.5 to 1.7. It would appear that the upper limit of any normally consolidated soil would be $K_{o,\text{nc}} \leq 1.0$ since a fluid such as water has $K_o = 1.0$ and no normally consolidated soil would have a value this large.

Example 2-2. Compare K_o by the several approximate methods given in this section for both a normally consolidated (nc) clay and for a clay with a known value of OCR = 5.0.

Other data: $\phi' = 20°$ $I_P = 35\%$ (nc)
$\phi' = 25°$ $I_P = 32\%$ (OCR = 5)

Solution. For the normally consolidated case, we may write the following:

1. Use Brooker and Ireland's Eq. (2-20):

$$K_{o,\text{nc}} = 0.95 - \sin\phi' = 0.95 - \sin 20 = 0.61$$

2. Use Eqs. (2-21):

$$\text{(2-21)}: \quad K_{o,\text{nc}} = 0.19 + 0.233 \log I_P$$
$$= 0.19 + 0.233 \log 35 = 0.55$$
$$\text{(2-21a)}: \quad K_{o,\text{nc}} = 0.44 + 0.0042 I_P = 0.59$$

In the absence of better data, use the average of these as

$$K_{o,\text{nc}} = \frac{0.61 + 0.55 + 0.59}{3} = \mathbf{0.58}$$

For the overconsolidated case, we calculate as follows:

1. Use Eq. (2-23), but first use Eq. (2-24) to find exponent n:

$$n = 0.54 \times 10^{-I_P/281} \rightarrow n = 0.42 \quad \text{for } I_P = 32\%$$

Now, $K_{o,\text{OCR}} = K_{o,\text{nc}} \times \text{OCR}^n \rightarrow$ use $K_{o,\text{nc}} = 0.58$ just found

$$K_{o,\text{OCR}} = 0.58 \times \text{OCR}^{0.42} = 0.58 \times 5^{0.42} = 1.14$$

2. Use Eq. (2-24*a*) for an alternative n:

$$n = \sin\phi' = \sin 25 = 0.423$$

$$K_{o,\text{OCR}} = 0.58 \times 5^{0.423} = 1.15 \text{ (vs. 1.14 just computed)}$$

3. Use Eq. (2-25) and assume CIUC testing so $A = 0.8$. Also estimate a value for s_u/p'_c. For this use Eq. (2-59) following:

$$\frac{s_u}{p'_o} = 0.45\sqrt{I_P} \quad \text{[Eq. (2-59)]}$$

$$= 0.45(0.35)^{0.5} = 0.27 \quad \text{(using nc value for } I_P\text{)}$$

Substitution into Eq. (2-25) gives

$$K_{o,\text{OCR}} = 0.58(0.8 + 0.27) = 0.62$$

We can obtain a best estimate using all three values to obtain

$$K_{o,\text{OCR}} = \frac{1.14 + 1.15 + 0.62}{3} = \mathbf{0.97}$$

or, since 0.62 is little different from the average nc value of 0.58, we might only use the two values of 1.14 and 1.15 to obtain

$$K_{o,\text{OCR}} = \frac{1.14 + 1.15}{2} = \mathbf{1.14}$$

One should use a value of about **1.1**, as 1.14 implies more precision than is justified by these procedures.

Conventional usage is to call all values K_o. For computations such as in this example it is necessary to distinguish between the normally consolidated value $K_{o,\text{nc}}$ and the overconsolidated value $K_{o,\text{OCR}}$ as a compact means of identification in equations such as Eqs. (2-23) and (2-25).

////

Previous Page

2-9 SOIL WATER; SOIL HYDRAULICS

The presence or absence of soil water can have a considerable effect on soil strength and the duration of settlements. In estimating the time for foundation settlements to take place, or for water flow studies, permeability (or *hydraulic conductivity*) is the property of interest. We may define permeability as the facility for water flow through a soil mass. It is quantified as a coefficient k in units of flow (ft/s, m/s, etc.).

All natural soil deposits contain free water in their voids. After prolonged dry periods the amount of water may be quite small in the soil near the ground surface, but immediately after a rain the voids may be nearly filled. There is a transition zone of variable water content down to the groundwater table (GWT); however, at and near the water table, the soil remains very nearly saturated. Soil below the GWT is saturated; however, recovered samples may compute saturation values somewhat less than 100 percent as a result of drainage or loss of hydrostatic pressure during recovery, which allows dissolved air to come out of solution and occupy some of the sample void space.

Water below the GWT surface is usually flowing under a hydraulic gradient, defined as the slope of the free water surface in the direction of flow. This slope could be defined by installing a series of vertical tubes (called piezometers) in the soil along the flow direction. In some cases depressions in impervious soils will capture the groundwater to form essentially underground lakes called *perched water tables.* These may be lost by well pumping or by making drill holes through their impervious bottoms that allow the water to drain down—inadvertently or otherwise.

As previously stated the soil zone above the GWT is transient in terms of pore water; however, a zone of some depth immediately adjacent to the GWT may be nearly saturated by capillary water. Capillary water is not free to move, as it is held in place by surface tension, and its presence produces an increase in the unit weight. The height of capillary rise can be estimated from computations as shown in Fig. 2-7. Theoretically this rise can be substantial, but few laboratory measurements have found values much over 1 to 2 m. Below the GWT the free water exerts a buoyant or flotation effect on the soil.

If one places a small tube to some depth into the soil below the GWT, free water will rise in the tube to the GWT level at that point. If we apply a load to the soil such that the void ratio in the vicinity of this piezometer tube decreases, there will be a rise in the elevation of the tube water. This rise is the increase in pore pressure caused by the void reduction and produces

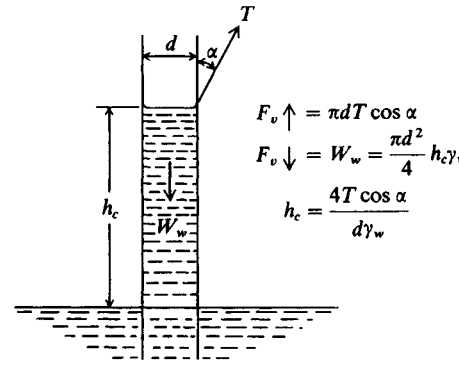

Figure 2-7 Computation of height of capillary rise in a capillary tube of diameter d and surface tension T for water.

excess free water, which will eventually drain away at a rate depending on the permeability of the soil. As this excess pore water drains, the water level in the piezometer tube will fall and when all of the excess has drained, the tube level is back to that of the outside GWT. If the tube is inserted into the capillary zone or above, no water level shows in the piezometer tube. This state may change, however, if some loading produces sufficient void ratio reduction that an excess of pore water develops. From this discussion it is evident that we have some chance of measuring a pore pressure when the soil starts from a saturated condition. When the soil is not saturated, the change in voids may produce excess pore pressures in some voids while adjacent voids are still not filled with water; thus, any pore pressure measurement would depend on the chance location of the piezometer. In other words, if the soil is partially saturated, pore pressure measurements are difficult-to-impossible to make. In passing, note that if the voids increase under load, the water level in the piezometer tube may drop, and we say the soil develops *suction,* which is another term used for a negative pore pressure.

This discussion enables us to define the *pore pressure* as "the hydrostatic pressure from the column of water in a piezometer tube above the tube tip." If the water level is different from the static water level outside the tube we have an *excess pore pressure* Δu. The excess pressure is from the elevation difference and may be (+) if the water level in the tube is above or (−) if the tube level is below the outside static level.

Effective Pressure

The effective pressure on a plane is developed from grain-to-grain contacts (but computed as a nominal area contact of *P/A*). The effective pressure produces friction resistance between soil particles, a component of soil strength, and produces the stresses necessary to cause particle rolling and sliding into a more dense structure called settlement. When the soil mass is below the free water surface (the GWT), it is buoyed according to Archimedes' principle. This buoyant effect is readily computed since it is the same for any submerged body. The upward buoyant force is computed as

$$P_{\text{up}} = \gamma_w z_w A$$

When the body is under the water a depth z'_w there is likewise a downward water force acting on top, computed just as above. Since a unit area ($A = 1$) is commonly used, we tend to use pressures rather than forces. So we have

$$\sigma_{\text{up}} = \gamma_w z'_w + \gamma_w z_n = \gamma_w (z'_w + z_n) = \gamma_w z_w$$

since $z'_w + z_n = z_w$ = depth to bottom of soil of thickness z_n.

The concept of effective pressure will be illustrated from the conditions shown in Fig. 2-8. This figure should be carefully studied, as it illustrates several features common to analyzing for effective pressure. As a preliminary discussion, note that we know the average natural water content w_N in the top 2 m of the sand stratum. We would probably estimate $G_s = 2.65$ as shown, and it is common to assume a constant unit weight value rather than make allowance for any probable increase—even small—with depth. The unit weight of the sand soil below the water table might be obtained from a tube (or more likely a piston) sample or estimated using procedures from Chap. 3. From these data we can estimate the wet unit weight of the soil above the water table using computations similar to those shown in the figure. Note the use of the block diagram, which displays known relationships and known quantities (total

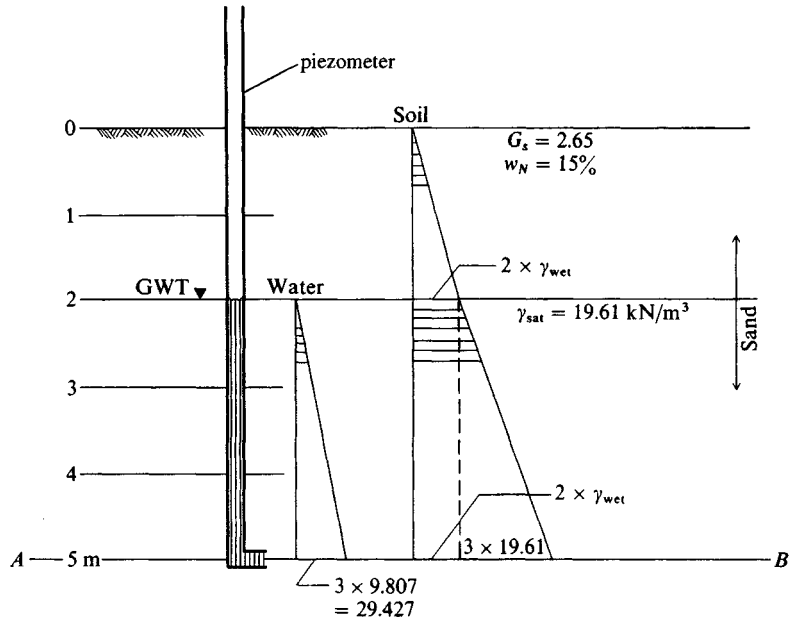

It is necessary to find γ_{wet} of the top 2m.
Refer to block diagram for same soil
below GWT.

$W_s = \gamma_w G_s V_s = 9.807 \times 2.65 V_s = 25.989 V_s$

$W_w = \gamma_w G_w V_w = 9.807 \times 1 \times V_w = 9.807 V_w$

By inspection: $V_s + V_w = 1 \rightarrow V_w = 1 - V_s$

$W_s + W_w = 19.61$

and substituting for W_s and W_w

$25.989\, V_s + 9.807(1 - V_s) = 19.61$

$$V_s = \frac{9.803}{16.182} = \mathbf{0.6058\ m^3}$$

$$\gamma_{dry} = \frac{\gamma_w G_s V_s}{V_t} = \frac{9.807 \text{ x } 2.65 \text{ x } 0.6058}{1} = 15.74 \text{ kN/m}^3$$

From Eq. (2-9) $\gamma_{wet} = 15.74(1 + 0.15) = \mathbf{18.10\ kN/m^3}$

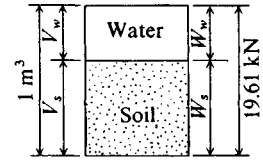

We can derive an equation for γ_{dry} in terms of G_s, γ_{sat}, γ_w once for all as $\gamma_{dry} = \dfrac{G_s(\gamma_{sat} - \gamma_w)}{G_s - 1}$

Figure 2-8 Soil and soil-water geometry to illustrate effective pressure concepts. Computations shown are typical to obtain the unit weight when the saturated unit weight is known, and either a measured or estimated value for specific gravity G_s is available.

volume and unit weight of soil below the water table), to obtain the dry unit weight of the sand from saturated conditions in order to be able to compute the wet unit weight of the sand above the GWT. From these computations we obtain the wet unit weight (shown on the figure) as

$$\gamma_{wet} = 18.10 \text{ kN/m}^3 \qquad \gamma_{sat} = 19.61 \text{ kN/m}^3 \quad \text{(given in Fig. 2-8)}$$

The sand above the GWT being pervious (has large k), the water table will seek a minimum energy profile, and the GWT represents this water level. In general, the GWT slopes, but over relatively short distances it is nearly horizontal and is generally shown that way (as here).

Our question, however, is, what is the effective pressure on plane AB? It is customary to use in the computations a column of soil that is square with $A = 1$ unit. We have placed a

piezometer tube in the soil with the tip at plane AB to measure the water pressure at this point, which in this case is obviously the static head of 3 meters. The piezometer is to illustrate site conditions and would not be likely to be installed in a real case.

The *total* pressure on plane AB can be readily computed using Eq. (a) but is intuitively obtained from stacking the several soil cubes overlying the point of interest (here plane AB) of unit area and unit height to obtain

$$\sigma_{\text{down}} = 2 \text{ cubes} \times \gamma_{\text{wet}} + 3 \text{ cubes} \times \gamma_{\text{sat}}$$

The use of fractional cube heights (as 1.2, 2.3, 2.7, etc.) is permissible, but here all cube heights are integers. Since we have used a unit area, we see that the product of γ, kN/m^3 $\times$ h, m gives kN/m^2 = kPa, which is pressure. Inserting numbers in the foregoing equation we have the total pressure on plane AB as

$$\sigma_{\text{down}} = 2(18.10) + 3(19.61) = \mathbf{95.03} \text{ kPa}$$

The water (or pore) pressure at the piezometer tip acts in all directions so that the upward component "floats" or reduces the total downward pressure, with the net difference being the effective pressure p'_o or, in equation form,

$$p'_o = p_o - \text{pore pressure} \qquad (\geq 0)$$

A negative effective pressure would indicate tension stresses, in which the soil particles are separated or on the verge of separation, and is meaningless. The pore pressure is usually designated as u (or when it is in excess of the GWT as Δu) so that the "effective" pressure on plane AB is

$$p'_o = 95.03 - 3(9.807) = \mathbf{65.61} \text{ kPa}$$

Excess Pore Pressure Δu

What height of water h (above the GWT) in the piezometer tube would reduce the effective pressure on plane AB to zero? Since the water height in the piezometer is above the GWT, this is a (+) *excess pore pressure,* and from the method of computing effective pressures just used we can write

$$p'_o = 0 = p_o - u - \Delta u$$

and, inserting values,

$$0 = 95.03 - 3(9.807) - \Delta h(9.807)$$

$$\Delta h = \frac{65.61}{9.807} = 6.69 \text{ m (above the GWT)}$$

In other words, if we quickly poured water into the tube to a height of $6.69 - 2 = 4.69$ m above the existing ground surface, the effective pressure on plane AB would be zero. With no grain-to-grain contact pressure the sand is in a state of liquefaction, similar to a liquid (here a viscous fluid). In this state sand is most dangerous, either to simply walk on or to use construction equipment on it or in the immediate vicinity.

Also observe we stated that we would "quickly pour" the water into the tube. This qualifier is made because sand has a relatively large coefficient of permeability and water would drain

out the tip. If it drained as fast as we poured it in, we could not develop the excess pore pressure.

The water table tends to flow laterally under its hydraulic gradient. When water is poured into the piezometer tube, we create a vertical hydraulic gradient, for the tube represents the minimum flow distance to reduce the excess pressure. The length of time for the water in the tube to return to the GWT level outside the tube would depend on the permeability of the soil. For sands and gravels this time would be relatively short. For cohesive soils and sands and gravels with appreciable fines this time could be considerable.

There is a real-life analog to pouring water into the piezometer tube. That is where we have a saturated soil mass that is loaded by a building, fill, or other engineered works. Under load the soil compresses and voids reduce with the squeezed-out water producing the excess pore pressure until it gradually drains away—taking the shortest possible flow path. This excess pore pressure would show a rise of water level in a piezometer tube just as if we had poured water into it in the case just analyzed.

Hydraulic Gradient

When a piezometer tube is inserted into the soil and the water level rises to the GWT outside the tube we have a static case, and any flow is in the direction of the hydraulic grade line of the GWT. When we pour water into the tube, we produce an excess pore pressure with a higher energy level inside than outside the tube and, according to the Bernoulli principle, flow will start from the high to the lower energy level (the GWT). This creates a vertical hydraulic grade line that has a varying energy level until the excess pore pressure is dissipated. It is customary to assume this line has a linear variation over the flow path, although in a real soil only the condition of the endpoints is known. With a linear variation the hydraulic gradient is simply

$$i = \frac{\Delta h}{L}$$

The *critical hydraulic gradient* i_c is defined as that which reduces the effective pressure p'_o to zero and can be derived as shown on Fig. 2-9. From the equation shown it follows that, if the saturated unit weight $\gamma_{sat} = 19.61$ kN/m^3, the critical hydraulic gradient across a 1-m depth L is

$$i_c = \frac{19.61 - 9.807}{9.807} = \frac{9.803}{9.807} \cong 1$$

That is, if the column of water above the top of the soil $\Delta h = 1$ m, we have

$$i_c = \frac{\Delta h}{L} = \frac{1}{1} = \mathbf{1}$$

It is evident that if $L = 2$ m then $\Delta h = 2$ m, etc. In real soils the alternative form for i_c using G_s and void ratio e in Fig. 2-9 gives a range of about 0.8 to 1.25, so for most practical cases it is satisfactory to use $i_c = 1$ for the critical hydraulic gradient.

Hydrostatic Uplift

When the GWT is confined beneath an impermeable stratum, for example, a gravelly sand (the aquifer) containing water that cannot rise to the free groundwater level because of

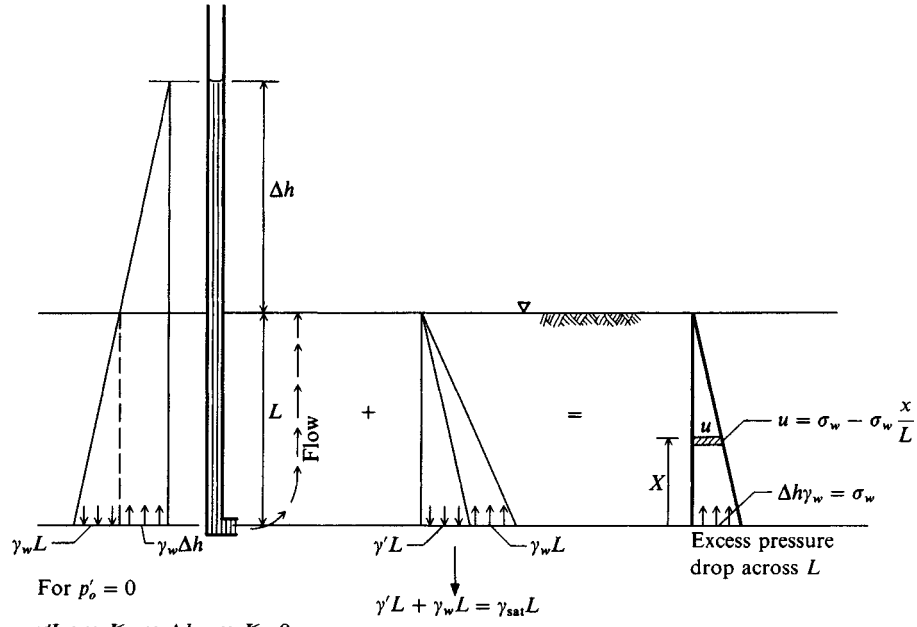

For $p'_o = 0$

$$\gamma' L + \gamma_w L - \gamma_w \Delta h - \gamma_w L = 0$$

after cancelling as shown we obtain

$$\gamma_w \Delta h = \gamma' L \quad (1) \qquad \text{Also: } \gamma' = \gamma_w \frac{(G_s - 1)}{1 + e} \quad (2)$$

Define critical hydraulic gradient as pressure slope producing $p'_o = 0$ at depth L:

From (1): $i_c = \dfrac{\Delta h}{L} = \dfrac{\gamma'}{\gamma}$ (3)

From (1) and (2): $i_c = \dfrac{G_s - 1}{1 + e}$ (4)

Figure 2-9 Development of critical hydraulic gradient. By inspection of usual range of G_s(2.6 to 2.8) and by using void ratios of 0.35 to 0.8, the critical hydraulic gradient is found to be around 1.0.

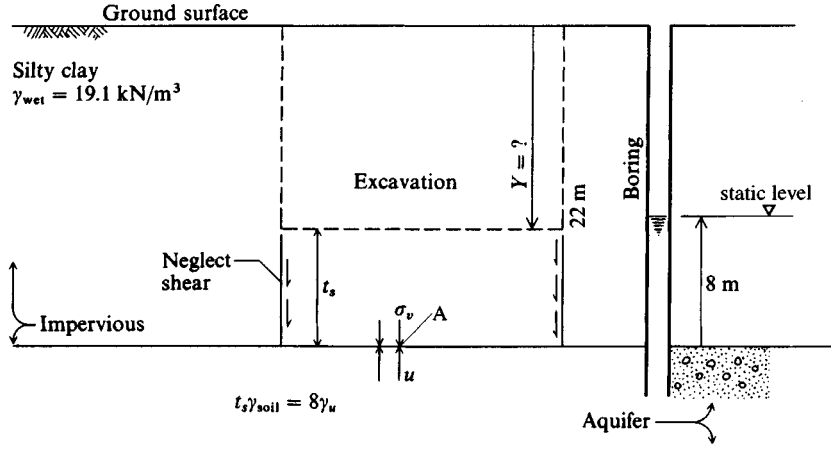

Figure 2-10 Groundwater conditions producing hydrostatic uplift.

confinement, the Δh between the bottom of the impermeable layer and the free water surface represents uplift pressure on the confining stratum. The following case will be used to illustrate this concept:

A silty clay layer extends from the ground surface to a depth of 22 m and has an average unit weight of 19.1 kN/m^3. The confining pressure in the sandy soil containing the water table is such that water would rise 8 m in a borehole extending into the aquifer. How deep could an excavation proceed before there is a danger that the hydrostatic uplift pressure would lift the remaining soil? Referring to Fig. 2-10 and neglecting any side shear, we can compute the thickness of soil t_s from a freebody analysis equating upward and downward pressures at point A as

$$\sigma_{\text{down}} = \sigma_v = t_s(19.1) \qquad \sigma_{\text{up}} = u = 8(9.807)$$

Equating and solving for t_s, we have

$$t_s = \frac{8(9.807)}{19.1} = 4.1 \text{ m}$$

$$Y = 22 - t_s = \mathbf{17.9} \text{ m}$$

At this depth there is incipient uplift (termed a *blow in*) and site safety is in jeopardy. A safe thickness would be more on the order of 7–8 m to allow for measurement uncertainties and worm holes, etc., which produce weakened points where water could more readily enter the excavation.

It is evident that very costly remedial measures might be necessary if the site exploration program had not discovered this confined aquifer.

Permeability

Flow of soil water for nonturbulent conditions has been expressed by Darcy as

$$v = ki \tag{2-26}$$

where i = hydraulic gradient h/L, as previously defined
k = coefficient of permeability (or hydraulic conductivity) as proposed by Darcy, length/time

Table 2-3 lists typical order-of-magnitude (exponent of 10) values for various soils. The quantity of flow q through a cross section of area A is

$$q = kiA \qquad \text{volume/time}$$

TABLE 2-3
Order-of-magnitude values for permeability k, based on description of soil and by the Unified Soil Classification System, m/s

10^0	10^{-2}	10^{-5}	10^{-9}	10^{-11}
Clean gravel GW, GP	Clean gravel and sand mixtures GW, GP SW, SP GM	Sand-silt mixtures SM, SL, SC	Clays	

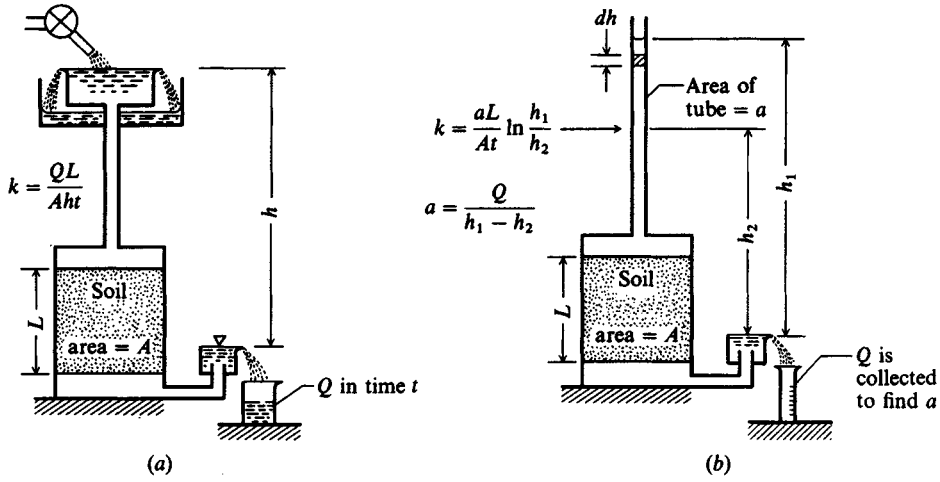

Figure 2-11 Schematic for permeability determination. (*a*) Constant-head permeameter; (*b*) falling-head permeameter; t = time for head to change from h_1 to h_2.

Two tests commonly used in the laboratory to determine k are the *constant-head* and *falling-head* methods.[5] Figure 2-11 gives the schematic diagrams and the equations used for computing k. The falling-head test is usually used for $k < 10^{-5}$ m/s (cohesive soils), and the constant-head test is usually used for cohesionless soils.

It is often necessary to determine the field value of k since it is usually larger than the laboratory-determined value, often by a factor of 2. An accurate[6] determination of the field k is beyond the scope of this textbook but some procedures and equipment are described by Leroueil et al. (1988).

Flow Nets

The flow of water through soil under an energy potential can be mathematically expressed by a Laplace equation as

$$k_x \frac{\partial^2 h}{\partial x^2} + k_y \frac{\partial^2 h}{\partial y^2} = 0$$

where k_x, k_y = coefficients of permeability parallel to the x, y axes, respectively
h = energy potential

The preceding equation is for two-dimensional flow, which with appropriate axis rotation will apply to most seepage problems. A graphical solution of this equation results in families

[5]The general method is given in Bowles: (1992) *Engineering Properties of Soils and Their Measurement,* 4th ed., McGraw-Hill Book Co., New York, NY, 10020.

[6]Actually only true if the field soil is fully saturated.

of intersecting orthogonal curves that are called a flow net. One set of the curves represents equipotential lines (lines of constant piezometric head) and the other set, intersecting at right angles, represents flow paths. The flow net consists of squares of varying dimension if $k_x = k_y$ and rectangles otherwise. In general, for reasonably homogeneous soil a graphical solution of the Laplace equation provides seepage quantities that are at least as correct as one is likely to measure the coefficients of permeability k_i.

Seepage quantities are often required for foundation engineering work. They are needed to determine the pumping requirements to dewater excavation sites and cofferdams. They can be estimated from a flow net as

$$Q = k'H\frac{n_f}{n_d}Wt \qquad (\text{m}^3 \text{ in time } t) \tag{2-27}$$

where k' = transformed coefficient of permeability when $k_x \neq k_y$ and so the resulting flow net consists of squares, $k' = \sqrt{k_x k_y}$ in units of H and t
H = differential head of fluid across system, m
n_f, n_d = numbers of flow paths and equipotential drops, respectively, in system
W = width of seepage flow, m
t = time base (1 hour, 1 day, 1 week, etc.)

Although for academic purposes considerable effort is often expended to produce neat flow nets consisting of well-formed squares, in practice flow quantities to a precision far in excess of the accuracy of k' can be obtained with rather crude approximations (see Fig. 2-12) as long as the problem geometry is to scale. Great effort to refine the ratio of n_f/n_d above to, say, 4.3/7.5 versus a rough value of 4/7 is simply a waste of time.

It is evident that using squares of side dimensions $s \times s$ produces a flow path of dimension $n_f s$ and length $n_d s$. The ratio $H/n_d s$ is the hydraulic gradient used earlier. Of course, we simply cancel s since it is with both n_d and n_f. As a result, we must use the hydraulic gradient defined by a constant loss of ΔH across each length $n_d s$. For $n_d = 4$, each n_d value represents a 25 percent loss of the total pressure head H across the length $n_d s = L$.

Figure 2-12*a* illustrates a flow net for one side of a cofferdam-type structure, which will be of most interest in this text. We may use the flow net to estimate how much drawdown may be allowed on the construction side of the wall or how much excavation can be performed before the construction side becomes "quick."

For other seepage problems the user is referred to any text on soil mechanics [e.g., Bowles (1984)].

Example 2-3. From Fig. 2-12*a* assume the following data:

$$H = 6.0 \text{ m} \qquad k_x = k_y = 4 \times 10^{-5} \text{ m/s} \qquad \gamma_{sat} = 19.80 \text{ kN/m}^3 \text{ (sand)}$$

Distances: $AB = 2$ m, $BC = 2$ m, $CD = 1.5$ m, $DE = 1$ m

Required. *a.* Flow quantity/day per meter of wall (1 day = 86 400 s)
b. Effective pressure at point C

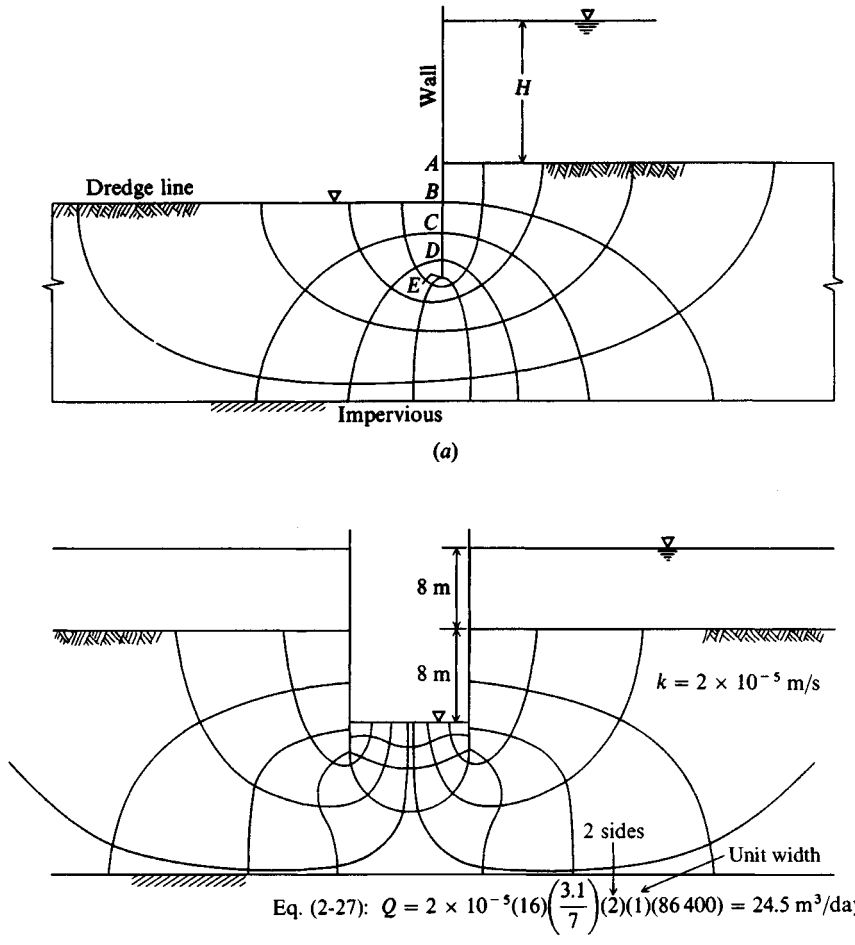

Figure 2-12 Typical flow nets as used for sheet pile or cofferdam structures. (*a*) Single sheet pile wall or other wall is too far away to influence net. (*b*) Double-wall cofferdam as used for bridge piers, etc.

Solution. *a.* Flow quantity (estimate $n_f = 4.1$). Also with tailwater at the dredge line $H_t = 6+2 = 8$ m; $W = 1$ m

$$Q = kH_t\frac{n_f}{n_d}Wt = 4 \times 10^{-5}(8)\left(\frac{4.1}{8}\right)\overset{W}{\overset{\swarrow}{(1)}}(86\,400) = \mathbf{14.2}\ \text{m}^3/\text{day}$$

b. Effective pressure at C with one ΔH remaining (of 8 total).

Total pressure at C: $p_o = 2(19.8) = 39.6$ kPa

Static pore pressure at C: $u_s = 2(9.807) = 19.61$ kPa

Excess pore pressure at C: $\Delta u = \frac{1}{8}(8)(9.807) = 9.81$ kPa

$u = 29.4$

$$p_o' = p_o - (u_s + \Delta u) = 39.6 - 29.4 = \mathbf{10.2}\ \text{kPa}$$

Since $p_o' > 0$, the soil is not "quick."

Previous Page

2-10 CONSOLIDATION PRINCIPLES

When a soil is loaded by any new load condition (a foundation, fill, embankment, etc.), settlements always occur. They may be insignificant or large enough to require special construction procedures. These settlements are not elastic, as one would have by compressing a column of steel or concrete, but rather are the vertical statistical accumulation of particle rolling, sliding, and slipping into the void spaces together with some particle crushing (or fracturing) at the contact points. This portion of the settlement is a state change and is largely nonrecoverable upon any removal of load. Any elastic compression of the soil particles is a settlement component that is recoverable upon removal of load. Because this component is usually very small, the so-called elastic settlement[7] recovery upon removal of the load is small.

As noted in the preceding section, particle displacement and void reduction can produce a temporary excess pore pressure depending on the amount and distribution of pore water present—very large values of Δu if the soil is saturated ($S \rightarrow$ 100 percent) and negligible for $S \rightarrow 0$ percent.

If we have a relationship between stresses and strains for the soil we can compute a stress-strain modulus E_s, also called *modulus of deformation* or, more commonly (but incorrectly), the *modulus of elasticity.* With this modulus we can use an integration over the influence depth L_o to compute the deformation or settlement ΔH as

$$\Delta H = \int_0^{L_o} \frac{\Delta q}{E_s}\, dz = \int_0^{L_o} \epsilon\, dz \tag{2-28}$$

For the usual integration over a sufficiently small length L_o that the compressive stress Δq and the stress-strain modulus E_s can be taken as a constant, the preceding integration becomes

$$\Delta H = \epsilon L_o \tag{2-28a}$$

The stress-strain modulus E_s used here is not a simple parameter to obtain for any soil, for it varies with soil type, state, *confinement,* and depth. The stress increment Δq may be known reasonably well at the foundation interface, but it decreases within the stress influence zone in such a manner that it is difficult-to-impossible to obtain accurately. Approximations are commonly used for both E_s and Δq because of these difficulties.

When the soil contains water, a further complication arises because settlement is not complete until the excess pore pressure Δu dissipates (and often for some additional time beyond). Because this involves the hydraulic conductivity k of the stratum (or strata), time may be a significant factor.

Thus, for most soil foundations we have two problems:

1. How much settlement will occur? (The answer usually depends on whether the soil is normally consolidated or overconsolidated.)
2. How long will it take for most of the settlement to occur?

---

[7]Elastic settlement recovery is the preferred description here since substantial base expansion often occurs in excavations made in cohesive soil deposits. This expansion, however, is not an "elastic" phenomenon but results primarily from water absorption around the clay particles. This type of expansion is usually called *heave* and is most difficult to predict or quantify.

For example, the settlement computed from Eq. (2-28) for ΔH may take three or four years to occur. As a rather extreme example, the Leaning Tower of Pisa (in Italy) is, and has been, settling (but not uniformly, so it leans) for over 700 years. Most time-dependent settlements occur in the range of 3 to 10 years but engineering projects usually require that the time-of-settlement estimate be more narrowly bracketed.

In saturated coarse-grained or nonsaturated fine-grained soils, pore drainage is nearly instantaneous,[8] so we can use a form of Eq. (2-28) without time being of concern. In fine-grained *saturated* soils time is a concern, so we need to obtain both an estimate for ΔH and a time parameter.

The settlements for waste disposal ponds and dredged fills are usually very large (sometimes 50^+ percent of original thickness). These are usually called "consolidation" settlements, and both the amount and time duration are of considerable importance. That type of consolidation is considered briefly in Sec. 2-10.5.

The consolidation theory presented in the rest of this section applies reasonably well to fully saturated soils and to those cases where the settlement ΔH is not large relative to the mass thickness.

2-10.1 Elements of Consolidation Theory

It is assumed that the reader has been exposed to some of the basic elements of consolidation theory; however, as a convenience, select elements are included here. The following assumptions are essential for the general development of the consolidation theory as first given by Terzaghi ca. the mid-1920s.

1. Soil in the consolidating layer is homogenous.
2. Soil is completely saturated ($S = 100\%$).
3. Compressibility of either water or soil grains is negligible.
4. Strains are infinitesimal. An element of dimensions dx, dy, and dz has the same response as one with dimensions x, y, and z.
5. Flow is one-dimensional.
6. Compression is one-dimensional.
7. Darcy's law is valid ($v = ki$).
8. Soil properties are constants.
9. The void ratio e vs. pressure p response is linear.

Of these, assumptions 8 and 9 are the most serious; however, number 4 can be of consequence. The total laboratory strain using a 20-mm thick test sample may approach $\epsilon = \Delta H/H = 0.5$, whereas the field strain may be nearly infinitesimal for a 2- to 3-m thick consolidating layer.

[8]Drainage may not be nearly instantaneous for fine-grained nonsaturated soils, depending on the degree of saturation. However, if S is not known there is no theory that can do more than estimate pore-pressure dissipation.

The basic expression for three-dimensional (3-D) flow volume V in a saturated earth mass is

$$\left(k_x\frac{\partial^2 h}{\partial x^2} + k_y\frac{\partial^2 h}{\partial y^2} + k_z\frac{\partial^2 h}{\partial z^2}\right) dx\, dy\, dz = \frac{dV}{dt}$$

This expression depends on assumptions 1–4 and 7. For 1-D flow (in the z or vertical direction) the first two terms drop out. If for convenience we use $k = k_z$, we have the volumetric flow defined as

$$k\frac{\partial^2 h}{\partial z^2}\, dx\, dy\, dz = \frac{dV}{dt} \tag{2-29}$$

The element volume is $dx\, dy\, dz$ and the pore volume is $(dx\, dy\, dz)[e/(1 + e)]$. All volume changes V are pore volume changes from assumption 3, so we can write the time rate of volume change as

$$\frac{\partial}{\partial t}\left(dx\, dy\, dz\frac{e}{1+e}\right) = \frac{dV}{dt} \tag{2-29a}$$

Since $(dx\, dy\, dz)/(1 + e)$ is the constant volume of solids, we can rewrite Eq. (2-29a) as $[(dx\, dy\, dz)/(1+e)](\partial e/\partial t)$. Equating this to Eq. (2-29) and canceling dx, dy, and dz, we obtain

$$k\frac{\partial^2 h}{\partial z^2} = \frac{1}{1+e}\frac{\partial e}{\partial t} \tag{2-29b}$$

Only a pressure head u in excess of the hydrostatic head will cause flow (and volume change); and since $h = \Delta u/\gamma_w$ we can rewrite Eq. (2-29b) as

$$\frac{k}{\gamma_w}\frac{\partial^2 u}{\partial z^2} = \frac{1}{1+e}\frac{\partial e}{\partial t} \tag{2-30}$$

Now let us define, from the slope of the linear part of an arithmetic plot of void ratio e or strain ϵ versus pressure p, the *coefficient of compressibility* a_v and the *compressibility ratio* a_v' as

$$\begin{aligned} a_v &= \frac{\Delta e}{\Delta p} = \frac{de}{dp} \\ a_v' &= \frac{\Delta \epsilon}{\Delta p} = \frac{d\epsilon}{dp} \end{aligned} \tag{2-31}$$

with negative signs ignored. Before any pore pressure dissipates we have $dp = du$, so we can write $de = a_v\, du$, which can then be substituted into Eq. (2-30) to give

$$\left[\frac{k(1+e)}{a_v\gamma_w}\right]\frac{\partial^2 u}{\partial z^2} = \frac{\partial u}{\partial t} \tag{2-32}$$

We may define the bracketed terms as the *coefficient of consolidation* c_v or

$$c_v = \frac{k(1+e)}{a_v\gamma_w} \tag{2-33}$$

Let us also define the *coefficient of volume compressibility* m_v (and introducing the initial in situ void ratio e_o for e) as

$$m_v = \frac{a_v}{1 + e_o} = a'_v \tag{2-34}$$

The reciprocal of m_v has the units of stress-strain modulus (kPa or MPa). It is often referred to as the *constrained modulus* and is the E_s of Eq. (2-28). We can rewrite c_v in a form suitable for finite element analysis as

$$c_v = \frac{k(1 + e_o)}{a_v \gamma_w} = \frac{k}{m_v \gamma_w} \tag{2-35}$$

We can also write Eq. (2-32) as

$$c_v \frac{\partial^2 u}{\partial z^2} = \frac{\partial u}{\partial t} \tag{2-36}$$

The solution of Eq. (2-36) is not trivial and uses a Taylor series expansion. Without going into the several details that can be found in Taylor (1948) and Holtz and Kovacs (1981, Appendix B2) it is as follows:

$$u = \sum_{n=1}^{n=\infty} \left(\frac{1}{H} \int_0^{2H} u_i \sin \frac{n\pi z}{2H} \, dz \right) \left(\sin \frac{n\pi z}{2H} \right) \exp \left(\frac{n^2 \pi^2 c_v t}{4H^2} \right) \tag{2-37}$$

This equation is general and applies for any case of initial hydrostatic pressure u_i in a stratum of depth or thickness $z = 2H$ and with z measured from the upper surface of the stratum downward↓ . The notation $\exp x = e^x$ where $e = 2.71828\ldots$. Since the coefficient of consolidation c_v is constant and time t is a multiple of $c_v H$, we can introduce a dimensionless time factor T defined as

$$T_i = \frac{c_v t_i}{H^2} \tag{2-38}$$

It is convenient to let $n = (2m + 1)$, where m = integer 0, 1, 2, 3, . . . , and to define

$$M = \frac{\pi}{2}(2m + 1)$$

With these parameters one can rewrite Eq. (2-37) to read

$$u = \sum_{m=0}^{m=\infty} \frac{2u_i}{M} \left(\sin \frac{Mz}{H} \right) \exp(-M^2 T) \tag{2-39}$$

Although Eq. (2-39) gives the pore pressure at various depth ratios z/H, it is preferable in most cases to estimate the average amount of consolidation that has taken place after some elapsed time. Finite-element programs usually obtain the average amount of consolidation U_i after some elapsed time, as in the following equation:

$$U_i = 1.0 - \frac{\text{Area of current excess pore-pressure profile}}{\text{Area of initial excess pore-pressure profile}}$$

Table 2-4 Time factors for indicated pressure distribution

	U,%	Case I	Case II
$U=\sqrt{\frac{4T}{\pi}}$	0	0.000	0.000
	10	0.008	0.048
	20	0.031	0.090
	30	0.071	0.115
	40	0.126	0.207
	50	0.197	0.281
$U=1-\frac{8}{\pi^2}e^{\frac{-\pi^2 T}{4}}$	60	0.287	0.371
	70	0.403	0.488
	80	0.567	0.652
	90	0.848	0.933
	100	∞	∞

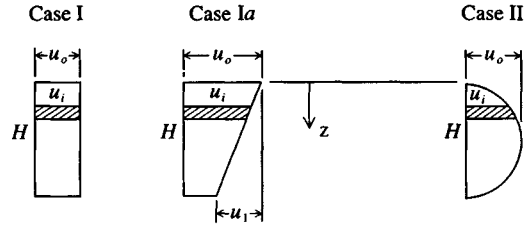

Pore-pressure distribution for case I usually assumed for case I*a* [Taylor (1948)]

Pore-pressure distribution for case II

The initial and current pore-pressure profiles are obtained using numerical integration (such as average end area, trapezoidal rule, Simpson's $\frac{1}{3}$ rule, etc.). Equation (2-39) can be integrated for select cases to obtain $U_i = 1 - u_i/u_o$ where i = some elapsed time after the initial application of pressure that produces the initial pore-pressure profile u_o. For the special case of u_o being constant or linearly decreasing with depth (Case I or I*a* of Table 2-4),

$$U_i = 1 - \sum_{m=0}^{m=\infty} \frac{2}{M^2} \exp(-M^2 T) \tag{2-40}$$

A number of approximations for Eq. (2-40) were made to simplify computations prior to wide availability of personal computers. Equation (2-40) seldom requires over three values of m (0, 1, and 2 except for very small values of U). The approximations are useful in order to obtain specific values of either T or U. Among the most widely used are those given by Fox (1948*a*) as follows:

$$U_i = \sqrt{\frac{4T_i}{\pi}} \qquad 0 \le T \le 0.197$$

$$U_i = 1 - \frac{8}{\pi^2} e^{-\pi^2 T/4} \qquad T > 0.197$$

These equations are useful alternatives to programming Eq. (2-40). They can be used to extend the range of Table 2-4 for certain operations.

2-10.2 The One-Dimensional Consolidation Test

A one-dimensional (1-D) consolidation test[9] is widely used to obtain the settlement and time parameters. A 1-D test confines the soil laterally in a metal ring so that settlement and drainage can occur only in the vertical direction. These conditions are reasonably close to what occurs in situ for most loading cases. Actually some radial displacement and lateral drainage probably occur but, based on experience, these appear to be small enough that a 1-D analysis gives adequate accuracy in most cases.

There is some opinion that field consolidation is sufficiently three-dimensional that a 1-D analysis is inadequate, prompting some researchers to propose theories (or computational models) to attempt to solve this case. The three-dimensional finite-element model (FEM) is sometimes used. The 3-D FEM method, however, has several disadvantages: First, it requires substantial computer resources; it requires estimating the stress-strain modulus E_s and Poisson's ratio μ and, when time is involved, the coefficient of permeability k_i for the three directions (k_x, k_y, k_z). Second, interpretation of the output is difficult, as is assessing the accuracy. There are, of course, occasions where a client may be willing to pay the extra expense of a 3-D analysis, or it may be required for the uniqueness of the project. A 3-D consolidation may occur where a series of spread footings (or a mat) overlies a very thick consolidating layer with lateral dimensions much larger than the loaded area(s).

Terzaghi's general consolidation theory is based heavily on the premise that the soil is saturated. A number of persons have attempted to develop a suitable theory both for 3-dimensional consolidation and for the general case, in which the soil may be either saturated or only partially saturated. The most recent attempt known to the author is that of Tekinsoy and Haktanir (1990), who give a differential equation. Their solution, however, requires estimation of several critical parameters, so there is little to recommend it.

In most cases, the 1-D consolidation test is suitable and is certainly the most economical and, compared to 3-D FEM models, it is better understood. This test is reasonably simple and has a large experience base, having been widely used since it was first developed by Terzaghi in the mid-1920s [see state-of-art report by Olson (1986)].

The 1-D test is used to obtain a compression parameter for the amount of settlement and the consolidation parameter c_v for the settlement rate estimate. The preconsolidation pressure p'_c and thus the OCR can also be determined from this test.

The test is performed on an "undisturbed" soil sample[10] that is placed in a consolidation ring available in diameters ranging from 45 to 115 mm. The sample height is between 20 and 30 mm; 20 mm is the most commonly used thickness to reduce test time. The larger-diameter samples give better parameters, since the amount of disturbance (recovery, trimming, insertion into the test ring, etc.) is about the same for any size of sample, with the

[9]This test is described in most laboratory test manuals and in specific detail in ASTM as test D 2435 or in Bowles (1992). It is also sometimes called an *oedeometer* test.

[10]There is no such thing as an "undisturbed" soil sample. In geotechnical work "undisturbed" means a sample where care has been taken to minimize sample damage.

relative effects less for the larger samples. The most common test ring diameter is 64 mm, since this best balances the costs of sample recovery and disturbance effects. Tube diameters larger than 76 mm may result in a premium charge for the sample, particularly if a larger borehole must be made.

The consolidation test proceeds by applying a series of load increments (usually in the ratio of $\Delta p/p = 1$ in a pressure range from about 25 to either 1600 or 3200 kPa) to the sample and recording sample deformation by using either an electronic displacement device or a dial gauge at selected time intervals.

Sometimes the $\Delta p/p$ ratio is reduced to 0.5 or less in the region of the current overburden pressure p_o to attempt to better define the transition zone between preyield and postyield stresses in the test sample.

Controlled rate of strain (CRS) consolidation test. The standard consolidation test is a controlled stress test (CST), since a constant load increment is used for each stage of the test. A modified version of the test that applies the load through a controlled rate of strain (CRS) has been standardized as ASTM D 4186. Silvestri et al. (1985) give a comparison of the CRS and the CST on a sensitive Canadian clay and claim that the CRS may have some advantage over the CST for certain clays. In this test, special equipment is used that can apply a very slow strain rate to develop the consolidation load. The consolidation ring has porous stones on both sample faces so that pore pressure at the sample base can be measured if required. The load is applied as a constant strain [on the order of about 20 percent total and a rate $d\epsilon/dt = 1 \times 10^{-7}(s^{-1})$] but at a rate such that the excess pore pressure (measured at the sample base) is kept in a range of from 3 to 30 percent of the loading pressure developed by that strain rate. The results are plotted as strain ϵ vs. $\log p$ (i.e., take displacement strain accumulations ϵ and pressure readings—with monitoring of the base pore pressure so that strain rate can be adjusted—at select time intervals similar to the CST). Proponents of this test claim that, for sensitive soils or where the soil would produce an ϵ vs. $\log p$ curve similar to Fig. 2-17*b*, the CRS provides a better estimate of the preconsolidation pressure p_c' and a somewhat higher compression index. Inspection of Fig. 2-17*b* indicates that test results will be subject to considerable personal interpretation, since a plot of ϵ vs. $\log p$ is very nearly identical to a plot of e vs. $\log p$. Because of the special equipment required and the problem of interpretation of the data plot, the CRS is not as widely used (as of 1995) as its proponents would like and will not be considered further in this text.

Sufficient laboratory data should be obtained to allow computation of the natural (or in situ) water content w_N and the specific gravity G_s so that the initial void ratio e_o and the void ratio e_i at the end of any load increment can be computed.

With these data there are several ways one can obtain t_i values that are used to compute the coefficient of consolidation c_v given by Eq. (2-38), which can be rearranged to $c_v = T_i H^2/t_i$. This textbook will describe five of them.

The Original Casagrande Method (Method 1)

This method was developed by Casagrande [see Taylor (1948), p. 241] in the early 1930s and utilizes a semilog plot of sample compression δ vs. time.[11] In using the Casagrande Method,

[11] The method is sometimes called the *Logarithm of Time Fitting Method.*

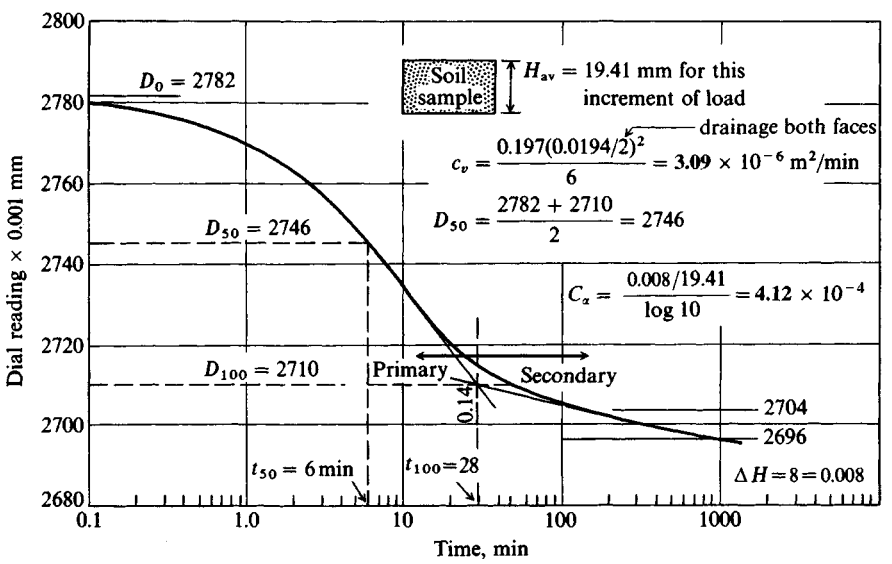

(a) Casagrande's semi log method of presenting time–settlement data. Method is required if it is necessary to obtain a secondary compression coefficient C_α as shown.

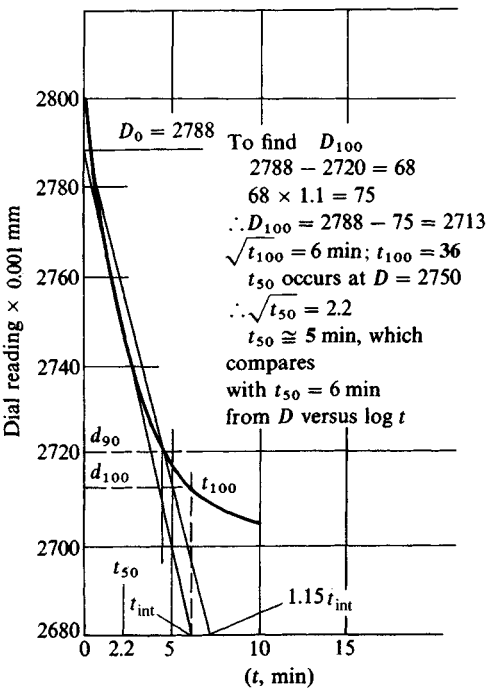

(b) Taylor's $\sqrt{\text{time}}$ method to directly obtain d_{90}

Figure 2-13 Two common methods of presenting time-settlement data from a consolidation (or oedometer) test. Note the use of dial readings instead of ΔH since the difference between any two dial readings × dial sensitivity (here 0.001 mm/div) is ΔH. If you directly read ΔH, plot that instead of dial readings.

time-deformation data are plotted on a semilogarithmic plot as illustrated in Fig. 2-13*a*. This type of plot is based on the similarity between a semilog plot of *displacement* versus $\log t$ and a semilog plot of U versus $\log T$ values shown in Table 2-4 (Case I or I*a*). This semilog plot gives an identifiable 3-branch curve: (1) an initial parabolic curved part [see equation in Table 2-4 ($T \approx \pi U^2/4$ for $U < 0.60$)]; (2) a midpart that is relatively straight, and (3) a curved part for the end[12] portion. If tangents are drawn on the mid and end two branches (or parts), their intersection is at approximately $\log T = 1$, which represents a state of 100 percent consolidation.

It has been found that at least some consolidation tests plot a δ versus $\log t$ curve with a shape very similar to the U versus T plot. When this is the case[13] one should be able to plot the laboratory δ versus $\log t$ curve and obtain the δ displacement at 100 percent consolidation (i.e., $U = 100$ or 1.0). We obtain this displacement by projecting from the intersection to the displacement axis (see Fig. 2-13*a*). We will call this displacement D_{100}. The D_{100} theoretically occurs when excess pore pressure Δu developed under that load increment becomes 0. Practically, Δu may only $\rightarrow 0$ as a result of time limitations for the test and the procedure used to obtain D_{100} graphically. A poor D_{100} value can also be obtained if the δ versus $\log p$ plot does not have a readily identifiable three-branch or S shape.

The next needed data item is the apparent initial displacement[14] of the sample, which we will call D_0. With these two values it is a trivial task to compute the displacement at any time of interest.

Since one cannot plot $\log t = 0$ ($\log 0 = -\infty$), it is necessary to resort to the characteristics of the semilog plot of a parabola. If the initial shape is not approximately parabolic on the semilog plot, you should either use a different method (of the five given here) or simply take D_0 as the initial displacement reading at the start of the load increment at $t = 0$. If the initial shape is parabolic, use the following sequence to obtain the D_0 estimate:

1. Select a time t_1 in the parabolic portion of the plot.
2. Select a second time $t_2 = 4t_1$, also in the parabolic part.
3. Obtain the vertical distance (or reading) between t_1 and t_2.
4. Plot this vertical distance above t_1 to obtain D_0. If possible one should repeat these steps for other t_1 values and put an "average" horizontal line through the points for a "best" D_0.

The time t_i at some deformation D_i is obtained from the D_0 and D_{100} deformation values. That D_i value is projected to the settlement curve to obtain t_i from the time axis. The t_{50} value occurs at the $D_{50} = (D_{100} + D_{50})/2$ point projected to the time versus settlement curve.

This value is the one most commonly used but others such as D_{60}, D_{30}, ... can be used. Whatever value is used, it should be one for which there is a T value in Table 2-4 (unless you

[12]Table 2-4 shows T only up to 0.848. Thus, it is necessary to use the equation shown in the table and compute additional points between $U = .90$ and $U = 1.00$ (or 100 percent—table uses percentages). Alternatively, use the computer program UFACTOR on your diskette for sufficient data to plot a reasonably accurate curve.

[13]If the δ versus $\log p$ is not S-shaped, you can enlarge the vertical δ scale and do the best you can. Preferably you should use one of the alternative procedures and possibly average the two time values for your "best estimate."

[14]It is usual to plot dial gauge readings versus log time; however, the actual displacements are plotted if electronic displacement equipment (usually a Linear Voltage Displacement Transducer, or LVDT) is used.

increase the table range). In considering the precision of this method, the value range given in Table 2-4 is probably adequate.

Taylor's $\sqrt{Time}$ Method (Method 2)

An alternative method to obtain t_i is to plot deformation versus $\sqrt{t}$ with time on the abscissa [see Taylor (1948)] as in Fig. 2-13*b*. This method uses the fact that if one plots the Table 2-4 values (again, Case I) using U on the ordinate versus $\sqrt{T}$ on the abscissa, the resulting curve has a straight initial portion and a curved end portion. Locate the 90 percent value of Table 2-4 on this curve at the $\sqrt{0.848} = 0.921$ plotted point. Now draw a straight line from $U = 0$ through the linear part of the plot and continue to the $\sqrt{T}$ axis (abscissa). Now draw a second straight line from $U = 0$ through the 90 percent point previously located on the U versus $\sqrt{T}$ plot and continue it to the abscissa. It is found that the latter line will have an intercept on the abscissa that is approximately 15 percent larger than the initial line.

Based on this observation, Taylor (1948) suggested that since many of the actual laboratory δ versus $\log t$ curves resembled Case I of Table 2-4, a similar analogy should exist between a plot of U versus $\sqrt{T}$ and the actual δ versus $\sqrt{t}$. The steps in the Taylor method are these:

1. Take deformation and time readings as with the Casagrande Method. As these are taken, begin a plot of δ (or dial reading) versus $\sqrt{t}$; i.e., if elapsed time = 16 min, you would plot $\sqrt{16} = 4.0$ versus whatever the displacement is at time = 16 min (see Fig. 2-13*b*).
2. Continue this plot until enough data are obtained to estimate the straight line reasonably (probably four to six points). Now draw the straight line through the best average of the points and project to both axes. Again, if this part of the curve does not exhibit any linearity, do the best you can or else use one of the other methods given.
3. Obtain D_0 as the intersection of the straight line and the δ axis. Also obtain the intersection on the abscissa and multiply the abscissa reading by 1.15 (i.e., if the intercept is 2.5, calculate $2.5 \times 1.15 = 2.875$). Locate the point (here it would be at 2.875 on the abscissa). Now from the D_0 point draw a second straight line to intercept this point.
4. Continue taking deformation time readings and plotting the results. When the actual curve of δ versus $\sqrt{t}$ intersects the 1.15 line, that point projected horizontally to the δ axis is the D_{90} reading.
5. With the D_0 and D_{90} values you can now obtain any t_i value of interest such as t_{50}, t_{90}, etc. Remember the time values from this plot are $\sqrt{t}$ values and must be squared (i.e., if you find $\sqrt{t_{50}} = 5.0$, the actual $t_{50} = 5^2 = 25$ min).
6. It is usual to stop taking δ versus t data once the laboratory curve is beyond the t_{90} location, add the next pressure increment, and continue the test. These steps are repeated as necessary until all of the pressure increments have been applied.

It has been found that, although theoretically any t_i value (say, t_{50}) should be the same using the Casagrande semilog fitting and Taylor $\sqrt{t}$ methods, in practice the $\sqrt{t}$ method usually gives *smaller* values, often less than one-half the t_{50} obtained from a semilog plot. As a result, smaller c_v values are computed using the $\sqrt{t}$ value of t_{50}. A possible explanation is that the semilog plot includes some secondary compression time whereas the t_{90} obtained from the $\sqrt{t}$ plot may be more realistic.

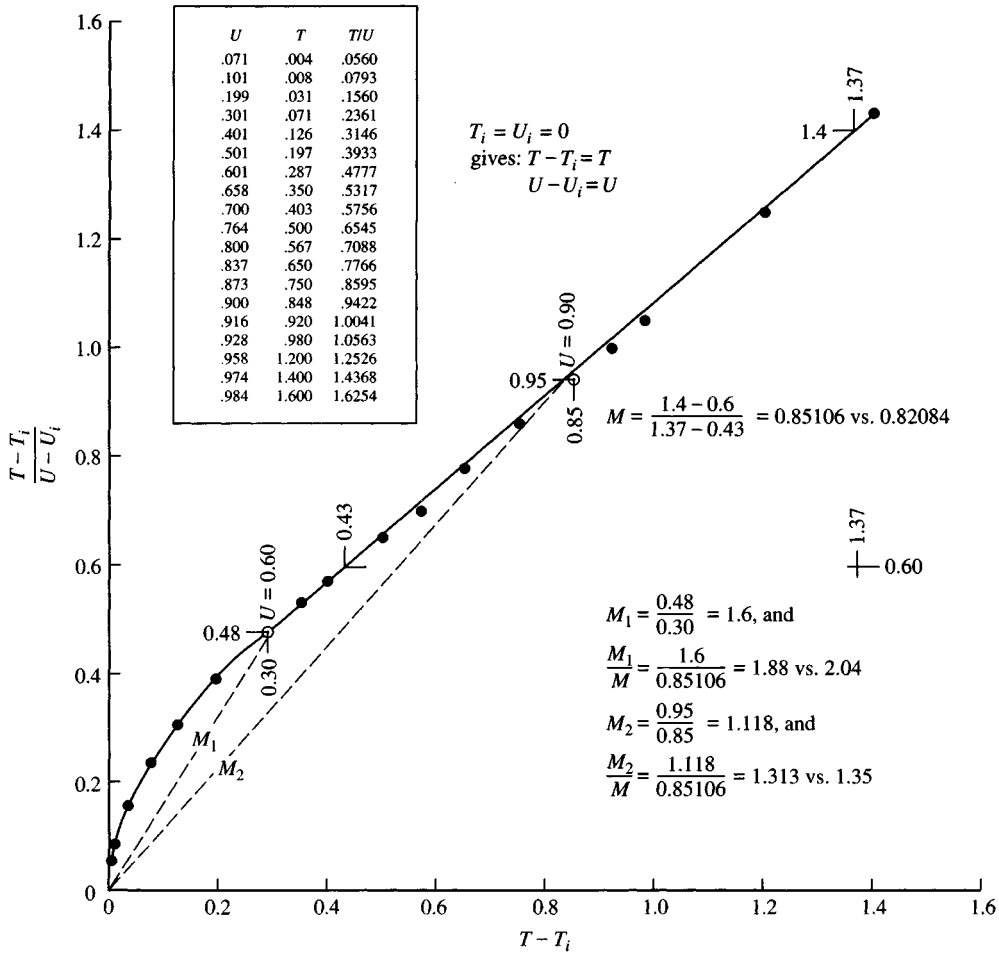

Figure 2-14*a* The rectangular hyperbola method for estimating the coefficient of consolidation c_v. [*After Sridharan and Prakash (1985).*] Theoretical plot of T vs. T/U. Note the slight differences between values given in reference and those computed here. You can make your own plot using the table of values shown.

The Rectangular Hyperbola Method (Method 3)

This method has been suggested by Sridharan and Rao (1981) and Sridharan and Prakash (1985). The method involves (see also Sec. 2-10.4) the following:

1. From a *normalized* plot of T/U versus T (both arithmetic scales) obtain the slope of a curve through the origin and to selected points on the *linear* part of the normalized plot (see Fig. 2-14*a*). The linear part of the plot lies in the region of $60 \leq U \leq 90^+$ percent. You should make a plot and check the values given on Fig. 2-14*a*, which was plotted by the author.

   Also measure the slope of the straight line between $U = 60$ and 90 percent. The references coauthored by Sridharan give this slope in an equation (from using U in percent,

t, days	δ, mm	t/δ, day/mm	t, days	δ, mm	t/δ, day/mm	t, days	δ, mm	Select Computations	$t-t_i$ days	$\delta-\delta_i$ mm	$\frac{t-t_i}{\delta-\delta_i}$
1	7.5	0.13	12	55.0	0.22	60	148.0	70 − 60 = 10	0	0	0.0
2	15.0	0.13	14	60.0	0.23	70	160.0	177 − 148 = 29	10	12.0	0.83
3	19.0	0.16	16	69.0	0.23	90	177.0	120 − 60 = 60	30	29.0	1.03
4	22.0	0.18	22	85.0	0.25	120	191.0	200 − 148 = 52	60	43.0	1.39
7	35.0	0.20	31	107.0	0.29	150	200.0	90/52 = 1.73	90	52.0	1.73
8	40.0	0.20	45	130.0	0.35	300	230.0		240	82.0	2.90
9	42.0	0.21	55	145.0	0.38						
10	46.0	0.22	60	148.0	0.40						
11	52.0	0.21									

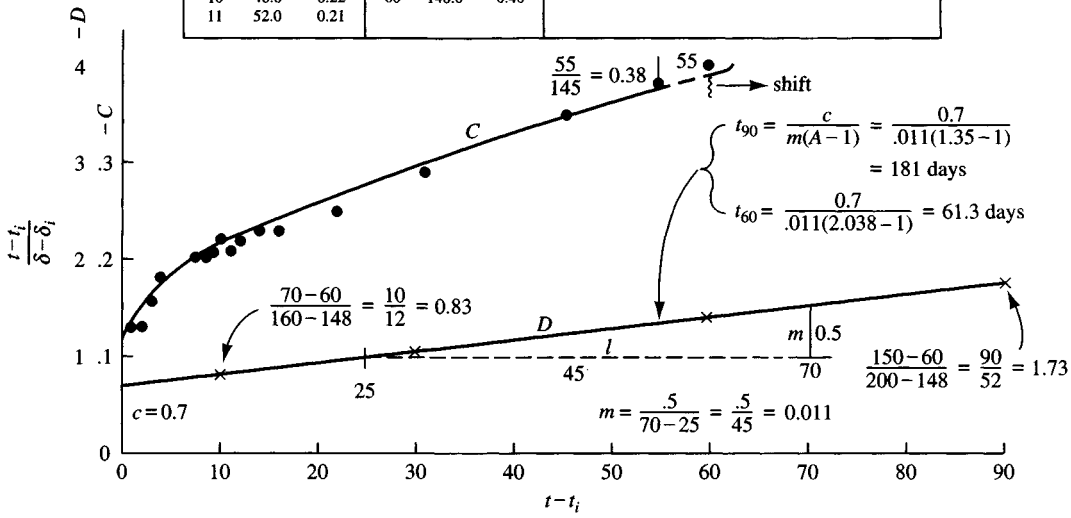

Figure 2-14*b* The rectangular hyperbola method for estimating the coefficient of consolidation c_v. [*After Sridharan and Prakash (1985).*] Plot of actual data from a consolidation test using data in above table to estimate the time for 60 and 90 percent consolidation. Refer to part (*a*) and see if you need to adjust A in the above equation for plotting differences.

where the author used U as a decimal) as

$$T/U = M + C = 0.008208T + 0.00244$$

From this we have $M = 0.008208T$ and $C = 0.00244$. The constant C is the intercept of the straight line part of the plot extended back to intercept the ordinate.

If you do not obtain equivalent values from your plot, you may need to adjust the A and B values given in the text and taken from the reference cited.

2. On the plot from step 1, draw a line from the origin to the point on Fig. 2-14*a* represented by $U = 60$ percent, computed as follows: $U = 60$ percent; $T = 0.287$; $T/U = 0.287/0.60 = 0.48$. Plot 0.48 on the ordinate versus 0.287 on the abscissa and label the point as $U = 60$ percent. Measure the slope of M_1; then, from the origin to $U = 90$ percent obtain a slope M_2. Compare these values to those of the author, 1.88 versus 2.038 and 1.31 versus 1.35. If your values are intermediate, use an average of the three values. If they are close to the reference, use the reference values; and if close to the author's, use an average of your values and the author's.
3. Now plot your normalized δ versus *time* data in the form of t/δ versus t (equal time intervals are suggested—perhaps every 5 or 10^+ minutes). As soon as the plot displays a linear part, measure the slope as m and the intercept on the ordinate as c. Refer to Fig. 2-14*b* and note on that plot with furnished data how the plot is "folded."

4. By analogy we have

$$\frac{T/U}{t/\delta} \approx \frac{MT + C}{mt + c}$$

From this consideration and the previous observation that a straight line from the origin to $U = 60$ percent had a slope $M_1 = 2.038M$ (or your value) and to $U = 90$ percent had a slope of $M_2 = 1.35M$, it follows that the slopes from the origin of the laboratory t/δ versus t curve should have those slopes as well. Using this concept with the origin as the starting point, one can say

$$t/\delta = Amt$$

Here A is a function of the degree of consolidation U, which can be readily computed. Several are listed here:

U, %	A	B
60	2.038*	0.2972
70	1.873	0.2972
80	1.524	0.2972
90	1.350*	0.2972

*used for t_{60}, t_{90} on Fig. 2-14*b*

For intermediate values in this table either compute or make a plot. From $t/\delta = mt + c$ and $t/\delta = Amt$, one can obtain

$$t = \frac{c}{m(A - 1)}$$

In this equation, $t = t_{60}, t_{70}, \ldots$, etc., depending on the value of A used. For example, from a t/δ versus t plot obtain $m = 0.0015$ and $c = 0.030$ (t/δ in min/mm). Then obtain for t_{60}

$$t_{60} = \frac{c}{m(A - 1)} = \frac{0.03}{0.0015(2.038 - 1)} = 19.3 \text{ min}$$

For t_{70} you would use $A = 1.873$, and so on.

Special note: If the t/δ versus t curve exhibits more than one straight line part, use the first linear part for these computations.

5. You can also compute the coefficient of consolidation, previously defined as $c_v = TH^2/t_i$, by substitution for t_i from the previous step to obtain $c_v = TH^2(A - 1)m/c$. Let $B = T(A - 1)$ and obtain B from the previous table. For a sample height of 18 mm and two-way drainage (and using m and c from Step 4) obtain

$$c_v = \frac{BmH^2}{c}$$

$$= \frac{0.2972(0.0015)0.009^2}{0.03} = 1.204^{-6} \text{ m}^2/\text{min} \rightarrow 1.73^{-3} \text{ m}^2/\text{day}$$

Since c_v = constant, any t_i can be used. Note from the table that B = constant.

6. You can do an axis shift as described in Sec. 2-10.5.

The Velocity Method (Method 4)

This method [Parkin (1978); Lun and Parkin (1985)] consists basically of the following steps:

1. Plot a curve of consolidation rate $\log \dot{U}$ versus log time factor T with $\dot{U}$ on the ordinate (see Fig. 2-15) on a sheet of 216 × 280 mm tracing paper laid over a similar size sheet of 3 × 3 cycle log-log paper. The consolidation rate $\dot{U}$ is the derivative of U, but one can approximate it by two branches as

$$\dot{U} = \frac{1}{\sqrt{\pi T}} \qquad T \approx 0.197 \ (U \leq 50\%; \text{ see equations on Table 2-4})$$

$$\dot{U} = 2e^{-(\pi^2 T/4)} \qquad T > 0.197 \ (U > 50\%)$$

   This plot has an initial slope of approximately 1:2 up to about $U = 50$ percent (slope defined by two log cycles horizontal and one log cycle vertical), and then the slope increases continuously toward ∞. Make a heavy vertical line on the plot at the point $T = 1$ (corresponding to $U = 100$ percent). Parkin scaled this plot by dividing the $\dot{U}$ values by 10 so that the resulting ordinate values are closer to the δ/t values of the following step, but this is not necessary.

2. From your δ versus t data compute δ/t and make a similar plot using $\log \delta/t$ on the ordinate versus $\log t$ and three-cycle log-log paper. There should be an initial straight line part in this plot that is also 1:2. If the plot is not overly distorted, you should arbitrarily make this slope 1:2 after plotting enough points to verify that it will be reasonably close. Now superimpose the tracing (step 1) onto this plot (use a light table, a lighted window, or darker lines if you have difficulty seeing the lower plot).

   You may have to do some curve fitting here. First, align the 1:2 slopes, compare the theoretical and laboratory curves, and try to obtain a best fit. In doing this step you may shift the tracing horizontally (but be careful not to rotate the axes) to obtain a best fit over as much of the two curves as possible. When your best fit is obtained, read through the tracing at $T = 1$ to the time scale on the abscissa of the lower (δ/t) plot to obtain t_{100}.

3. Use this t_{100} and, directly substituting into the coefficient of consolidation equation [Eq. (2-38)], rearrange to obtain

$$c_v = \frac{TH^2}{t_{100}} = \frac{1H^2}{t_{100}}$$

   If $H = 18$ mm (two-way drainage) and $t_{100} = 15$ min (obtained from Fig. 2-15*a*,*b*), the coefficient of consolidation is obtained as follows: Compute $H = 18/2 = 9$ mm = 0.009 m; $T = 1$. Use the preceding equation to solve for c_v:

$$c_v = [1(0.009^2)/15] \times 1440 = \mathbf{0.0078\ m^2/day}$$

   The 1440 is used to convert m^2/min to m^2/day.

The Finite-Element Method (Method 5)

The finite-element method (FEM) requires a computer program. The general methodology for 1-D consolidation is given in Desai (1979). The author's program FEMCONSL utilizes

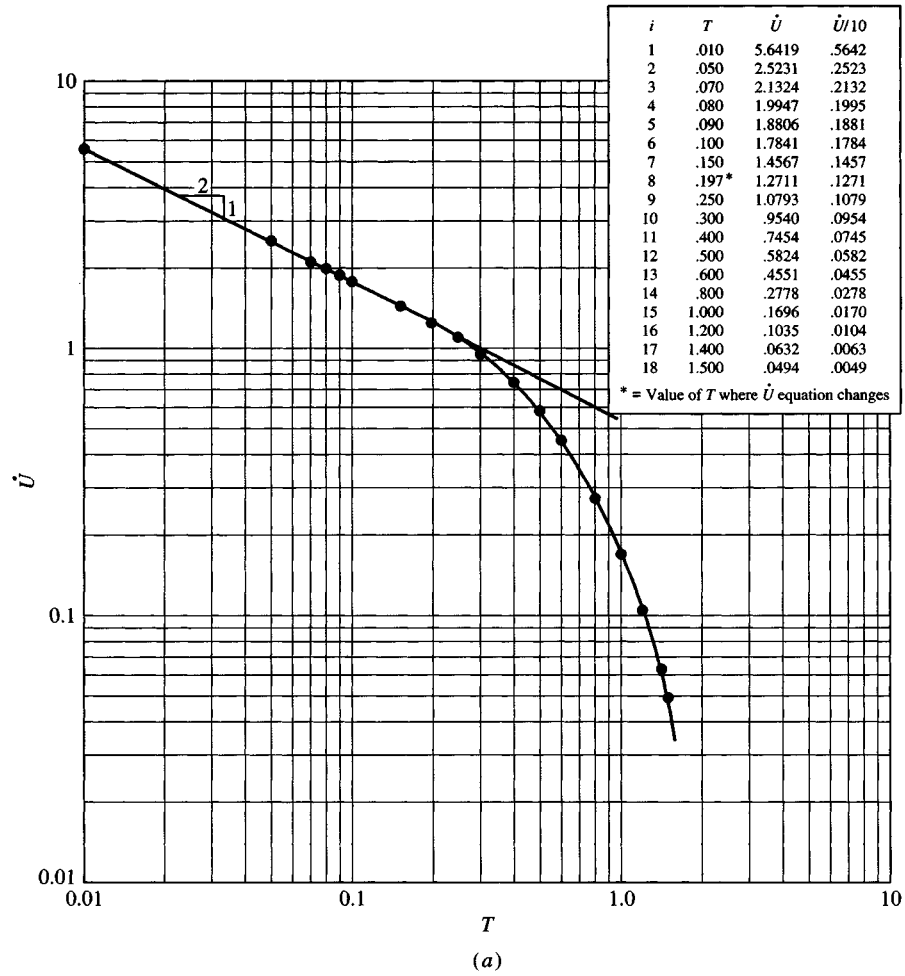

i	T	$\dot{U}$	$\dot{U}/10$
1	.010	5.6419	.5642
2	.050	2.5231	.2523
3	.070	2.1324	.2132
4	.080	1.9947	.1995
5	.090	1.8806	.1881
6	.100	1.7841	.1784
7	.150	1.4567	.1457
8	.197*	1.2711	.1271
9	.250	1.0793	.1079
10	.300	.9540	.0954
11	.400	.7454	.0745
12	.500	.5824	.0582
13	.600	.4551	.0455
14	.800	.2778	.0278
15	1.000	.1696	.0170
16	1.200	.1035	.0104
17	1.400	.0632	.0063
18	1.500	.0494	.0049

* = Value of T where $\dot{U}$ equation changes

Figure 2-15*a* The velocity method to estimate a time value for computing the coefficient of consolidation c_v. [*After Lun and Parkin (1985).*] Theoretical log-log plot of $\dot{U}$ versus T. This should be put on a sheet of tracing paper to use as an overlay to plots such as (*b*).

this method, which is integrated into program SMSETTLE (see the README.DOC file on your diskette).

Basically the FEM requires that the user subdivide the stratum or strata (including intermediate sand layers) where consolidation settlements will occur into at least two elements. This step yields at least a top, a midheight, and a bottom node point so that one can plot the layer pore-pressure distribution profile if desired.

For each stratum (including sandwiched sand layers) the coefficient of permeability (or hydraulic conductivity) k_v in the vertical direction must be input along with the coefficient of volume compressibility m_v (given in the previous section). Since hydraulic conductivity is a time-dependent parameter, the user must select some time intervals, usually starting with 1 day, then perhaps 7, 10, 100, . . . , n days as input data.

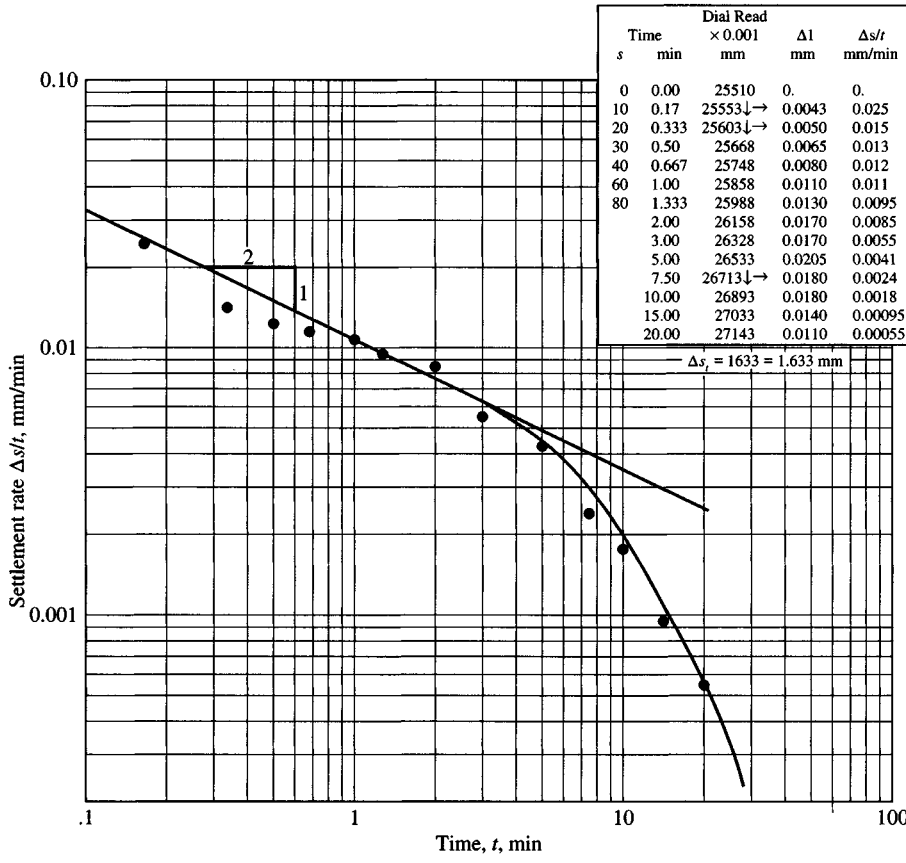

(*b*)

Figure 2-15*b* A log-log plot of settlement rate $\Delta s/t$ versus t. Use a tracing of (*a*) as an overlay and shift it laterally until a best fit is obtained over as much of the curve as possible, and then read t_{100} where the $T = 1$ ordinate intersects the abscissa on the test curve.

One must also estimate an initial pore-pressure distribution in the consolidating strata. One might use a method given in Chap. 5 to obtain the stress at each vertical node caused by the foundation loading. Another option is to use the pressure produced by the vertical load on the uppermost node as a constant pressure for the consolidation depth. Other similar options are available.

On the basis of the pressure profile used and the time increments, together with the input k_v and m_v, the program computes for each time value a pressure profile, the percent consolidation U (using the numerical integration method), and a time factor T. Several trial sets of time values may be required before a suitable data set is obtained. The output for each trial is the percent consolidation U and a pressure profile and time factor T_i for each of the input times. The last output values should represent the time for, say, $U = 90$ to 95 percent consolidation to have taken place. If the largest U value for the trial is only 70 or 80 percent, you would certainly want to make another trial with some of the later times increased.

Which of These Several Methods Should One Use?

If secondary compression is to be estimated, the semilog plot method must be used with sufficient δ versus time data recorded so that the end branch of the one or more curves from pressure increments closest to the design value can be plotted with an identifiable slope. This will enable you to compute a secondary compression index even though there might not be a well-identified t_{100} value for when it begins.

For the usual computation of c_v and with these five methods available, which one should be used?

a. Methods 1 and 2 are most widely used.
b. Some users prefer Method 2 (the $\sqrt{t}$ method) since it is often somewhat faster (i.e., change pressure increments as soon as the plot has passed the D_{90} point).
c. Method 3 will be almost as fast as Method 2 since you can stop data collection for that pressure increment as soon as a linear plot region is obtained.
d. All but the FEM depend upon the assumption that the measured δ versus time curve is similar to the U versus T curve.
e. Method 5 is suggested when several strata contribute to the total consolidation, since this method tends to *couple* stratum effects somewhat, where Eq. (2-38) considers each stratum separately. Coupling is also necessary if there are sand layers interspersed between clay layers.
f. You might also consider using Methods 3 and 4 where Methods 1 and/or 2 do not seem to provide readily identifiable t_i values and if an enlarged vertical scale using Method 1 does not give any apparent improvement in results.
g. Use the method that has the greatest local acceptance.

2-10.3 The Compression Index and Ratio

The amount of primary consolidation settlement is computed using either the compression index C_c obtained from a plot of void ratio e versus log pressure (Fig. 2-16*a*) or from a compression ratio C_c' obtained from a plot of strain ϵ versus log pressure as on Fig. 2-16*b*. The void ratio or strain is computed based on initial sample conditions and the compression ΔH under the current load increment to D_{100}.

Some persons have used the total compression under the load increment to compute the current void ratio or strain, but current practice favors using only the sample ΔH from D_0 to D_{100}. This latter value computes a slightly larger (and more conservative) value for the compression index C_c or ratio C_c'.

The plot of ϵ versus log p is more rapid than using e versus log p. Because the strain ϵ is based on the *initial sample height* H_i and the accumulated compression $\sum \Delta H$ to the D_{100} value of the current load increment, the plot can proceed with the test ($\epsilon = \sum \Delta H/H_i$). The e versus log p plot requires considerably more computations, some of which can only be done at the completion of the test, but (until recently) it has been more used.

The initial branch of the e or ϵ versus log p plot represents recompression of the sample back to the in situ state from the expansion that occurred during recovery (refer also to Figs. 2-16 and 2-17). This is also called the *preyield* stress range. The approximately linear curve portion beyond the in situ state is called the *postyield* stress range.

The discontinuity between the pre- and postyield curve branches represents the previously consolidated stress state (or previous stress history imprint). The discontinuity is seldom abrupt but usually transitions along a curve that is a characteristic of that particular soil under the test procedure(s) being used. Experience on both "undisturbed" and remolded samples of the same soil, and using loading and unloading curve parts, gives the following:

1. If the discontinuity occurs at approximately the current in situ overburden pressure p'_o, the soil is *normally consolidated.*
2. If the discontinuity occurs at a pressure p'_c greater than the existing overburden pressure, the soil is *overconsolidated* and the OCR $= p'_c/p'_o > 1$.
3. If the discontinuity occurs at a pressure p'_c less than p'_o, the soil is probably recently (on a geologic scale) deposited and may still be undergoing consolidation.
4. When preconsolidation and existing overburden pressures are within about ± 10 percent of each other you will have to make a subjective determination of the preconsolidation state (*under-, normally,* or *overconsolidated*). Base the determination on experience, sample quality, test procedure, and any other helpful information that might apply.
5. The remolded soil consolidation curve is always below the "undisturbed" soil curve, as shown by the labeled, dashed line on Fig. 2-17*a*. This observation, together with the transition back to the "virgin" curve at the point where an unload curve branch is done, is the basis for defining C_r and locating the preconsolidation pressure p'_c.

If the soil is preconsolidated, that slope between current p'_o and p'_c, drawn by eye as a best fit since it is usually curved, is designated the recompression index C_r or recompression ratio C'_r. You may get some guidance for this slope if you do a rebound and reload curve branch as in Fig. 2-17*a*. For computing C_r with rebound data sometimes the average of the initial recompression branch and the reload branch is used.

At the end of primary consolidation for the current load increment—usually taken as 24 hr—the dial gauge (or displacement device) reading for settlement measurement should have not changed appreciably for a considerable (range of 2 to 6 hr) period of time. We say this state represents the end of primary consolidation when the excess pore pressure Δu in the sample is zero, or very nearly so, and we are somewhat into secondary compression (to be considered later). The value of D_{100} described in the previous section is arbitrarily taken as the primary settlement and the corresponding time when it occurs is t_{100}.

It should be evident that all stresses involved here are effective stresses. In situ we have K_o conditions, and in the laboratory by definition the excess pore pressure Δu is zero when we complete the data for any given load increment on the sample. At this pore-pressure state the soil grain contact points carry the applied stress, and by definition this is the *effective pressure* state.

The transition point between pre- and postyield may be a gradual curve, a well-defined one, or a sharp break. There are several methods available to obtain this transition as a "point" so that the preconsolidation pressure p'_c defined by this point can be compared with the current in situ overburden pressure p'_o to ascertain whether the soil is preconsolidated (OCR $= p'_c/p'_o > 1$).

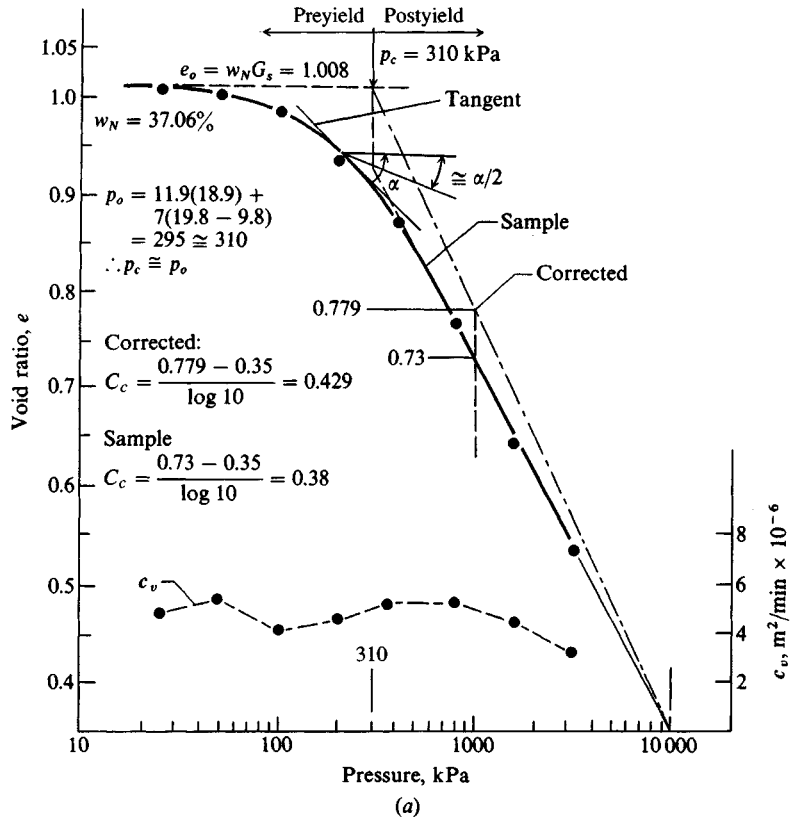

Figure 2-16*a* Two common methods of presenting pressure-settlement data using semilog plots. Plot of e versus log p using data shown on (*b*). Note pre- and postyield regions. The Casagrande method is used to estimate preconsolidation pressure p'_c. The compression index C_C is computed as shown. A correction for C_C using the method of Schmertmann (1955) is also shown. Note c_v is plotted using the average pressure increment and the average sample H_i in the pressure increment.

Method 1: By Eye

We may identify the transition as a most probable value by eye, which is a rather common practice, particularly with some experience (see Fig. 2-16*b* and Example 5-12). The shape of the discontinuous (curved region) portion of the curve is used as a guide.

Method 2: Using Casagrande's Method

Casagrande[15] (1936) proposed a procedure as shown on Fig. 2-16*a* to determine p'_c. Steps in the "Casagrande Method" are as follows:

[15]At the Settlement Conference at Northwestern University in 1964, Casagrande (during his oral presentation) stated he had never used this method himself.

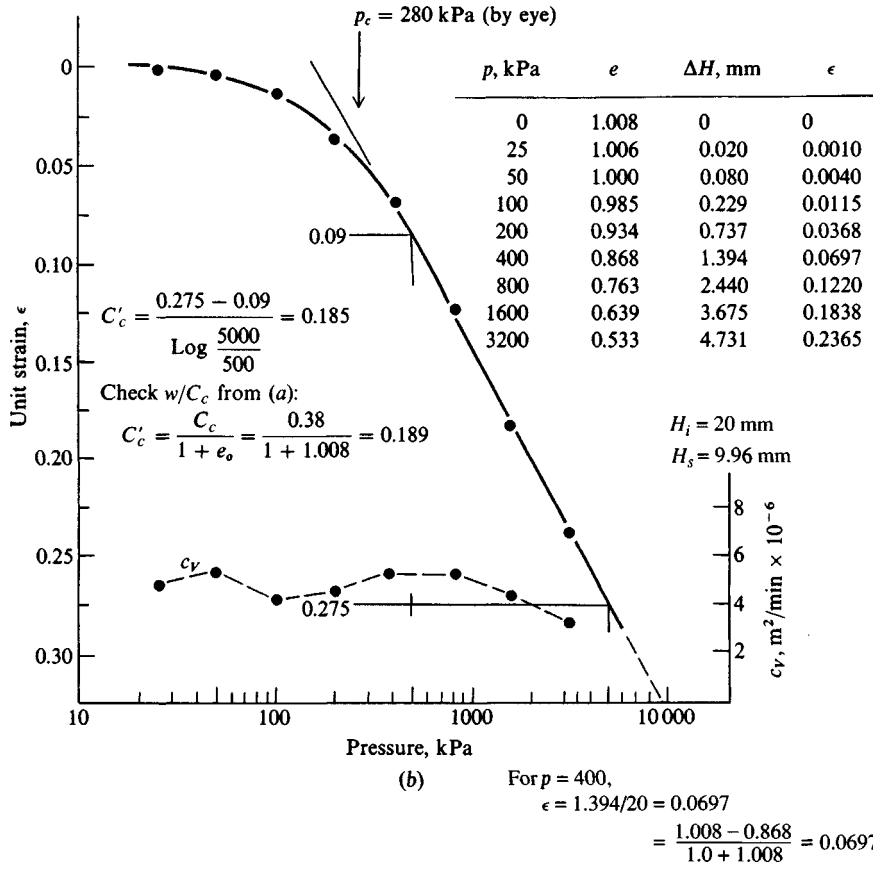

Figure 2-16*b* Plot of ϵ versus log p. Note the substantial similarity with the plot of e versus log p. You should verify that $\epsilon = \sum(\Delta H_i)/H_i = \sum(H_i)/20 = \sum(\Delta e)/(1 + e_o) = \sum(\Delta e)/(1 + 1.008)$.

1. Determine by eye the sharpest curvature in the transition zone and draw a tangent.
2. Draw a horizontal line through this tangent point and bisect the angle α thus produced.
3. Extend the "straight line" or virgin slope of the e or ϵ versus log p curve to intersect the bisector of step 2.
4. Take the intersection of step 3 as the preconsolidation pressure p'_c. Remember the e or ϵ versus log p is an "effective" stress plot since the load at D_{100} is fully carried by the grain-to-grain contact pressure.

The value of p'_c (see Fig. 2-16) from the curve is then compared to the existing overburden effective pressure p'_o to see if OCR > 1.

Method 3: The Method of Work

There are cases where the e versus log p plot has a large, gently curved region as illustrated in Fig. 2-18 so that the "Casagrande Method" for finding the preconsolidation pressure cannot be

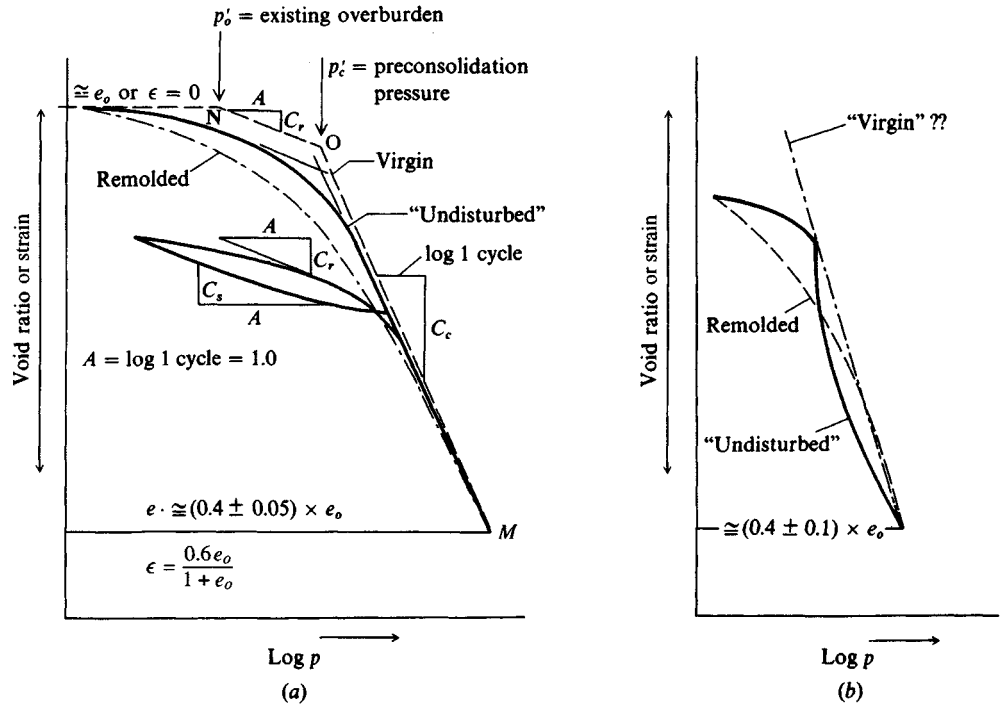

Figure 2-17 Two curves of e versus log p. Both curves have a reasonably well-identified break between pre- and postyield regions. (*a*) General plot for a preconsolidated soil with the Schmertmann (1955) method for correction for sample disturbance. Note use of an unload cycle to compute C_r, which is transferred (parallel) to produce slope NO. Note also the suggested use of log p using 1 log cycle so $\log p_2/p_1 = 1$. (*b*) A test where the sample "collapses" in the postyield region. There will be some difficulty in estimating the preconsolidation pressure p_c' and in computing the compression index C_C (or C_c'). Refer also to Fig. 2-18.

applied with much confidence. The curved plot of Fig. 2-18 can also occur when consolidation tests are done using a load ratio $\Delta p/p < 1$. When this occurs you should first estimate the in situ effective pressure p_o' and note where it falls on the plot.

If this point does not appear reasonable you might use a method of work given by Becker et al. (1987) based on the work input in the test.[16] The basic methodology is as follows:

1. The work input is $W = \int (\sigma_1\, d\epsilon_1 + \sigma_2\, d\epsilon_2 + \sigma_3\, d\epsilon_3)$ where ϵ and σ are the strain and stress in the direction subscripted. We will take the subscript 1 as the vertical direction.
2. In a consolidation test we have the following:
   a. There are no ϵ_2 or ϵ_3 strains because of the ring confinement, and,
   b. Since the vertical strain ϵ_1 is nonlinear, one cannot easily integrate $\int \sigma_1\, d\epsilon_1$, but instead one can use finite increments (that is, replace $d\epsilon_1$ with Δ increments and replace the integral $\int$ with a $\sum$.

[16]This method was criticized by Morin (1988) as being incorrect; however, his "correct" method gives differences so small that they are well within method accuracy. The method was also criticized by Li (1989) as being influenced by the scale of the plot.

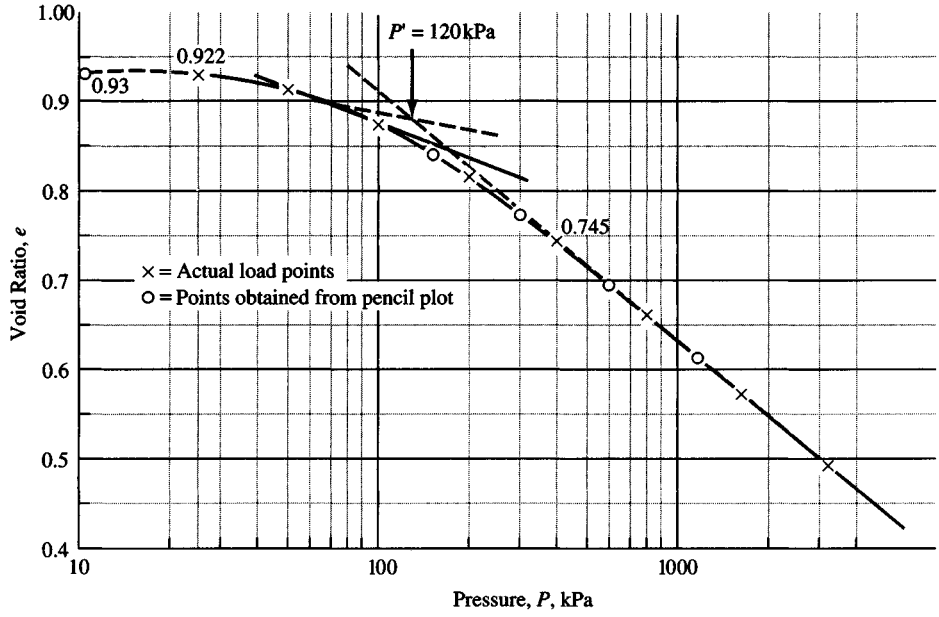

Figure 2-18 A consolidation test where the full e versus log p plot is curved so that the Casagrande method to obtain p'_c is not very reliable. Note some additional points were inserted after the initial plot and curve were drawn. These points are useful in the methods of work (Fig. 2-19) and the log-log plot of Fig. 2-20. The e and p data for the above are given on Fig. 2-19.

These conditions yield the following equation:

$$\Delta W_i = \left[\frac{\sigma'_i + \sigma_{i+1}}{2}\right](\epsilon_{i+1} - \epsilon_i) \tag{2-41}$$

We can interpret the [ ] term as the average stress on the sample for any two loads. The ( ) term is the difference in strain between the same two loads used for the [ ]. The work ΔW_i is the product of $\sigma \times \epsilon$, and the cumulative work is computed as $\sum(\Delta W_i)$. This is plotted on the ordinate of an arithmetic plot of $\sum W$ versus $\sigma = p$. The vertical stress p is the value *at the end of the relevant load increment* (the σ_{i+1} stress). The plot is done using arithmetic scales. Because of the limitations of the standard (216 × 280 mm) graph sheet, do the following:

i. Make a plot that uses most of the page with minimal points plotted for small values of work. From the end region where the work values are larger, make your best estimate of the straight line end portion (see Fig. 2-19*a*). Select about three points arbitrarily (as points 1, 2, and 3 on Fig. 2-19*a*) along this straight line and record their values.

ii. Make a smaller insert (see Fig. 2-19*b*) where you can expand the vertical scale somewhat (but not excessively). Plot the two or three points from step 1 and draw a straight line through them. Call this line *BC*. Next plot the several accumulated work values in the low region and draw a best-fit straight line (*OA*) through them as well, and intersecting with line *BC*. Take the intersection as the preconsolidation pressure p'_c and compare the value at the intersection to p'_o and compute the OCR.

iii. Note that if you use a very large vertical scale the line *OA* may appear curved.

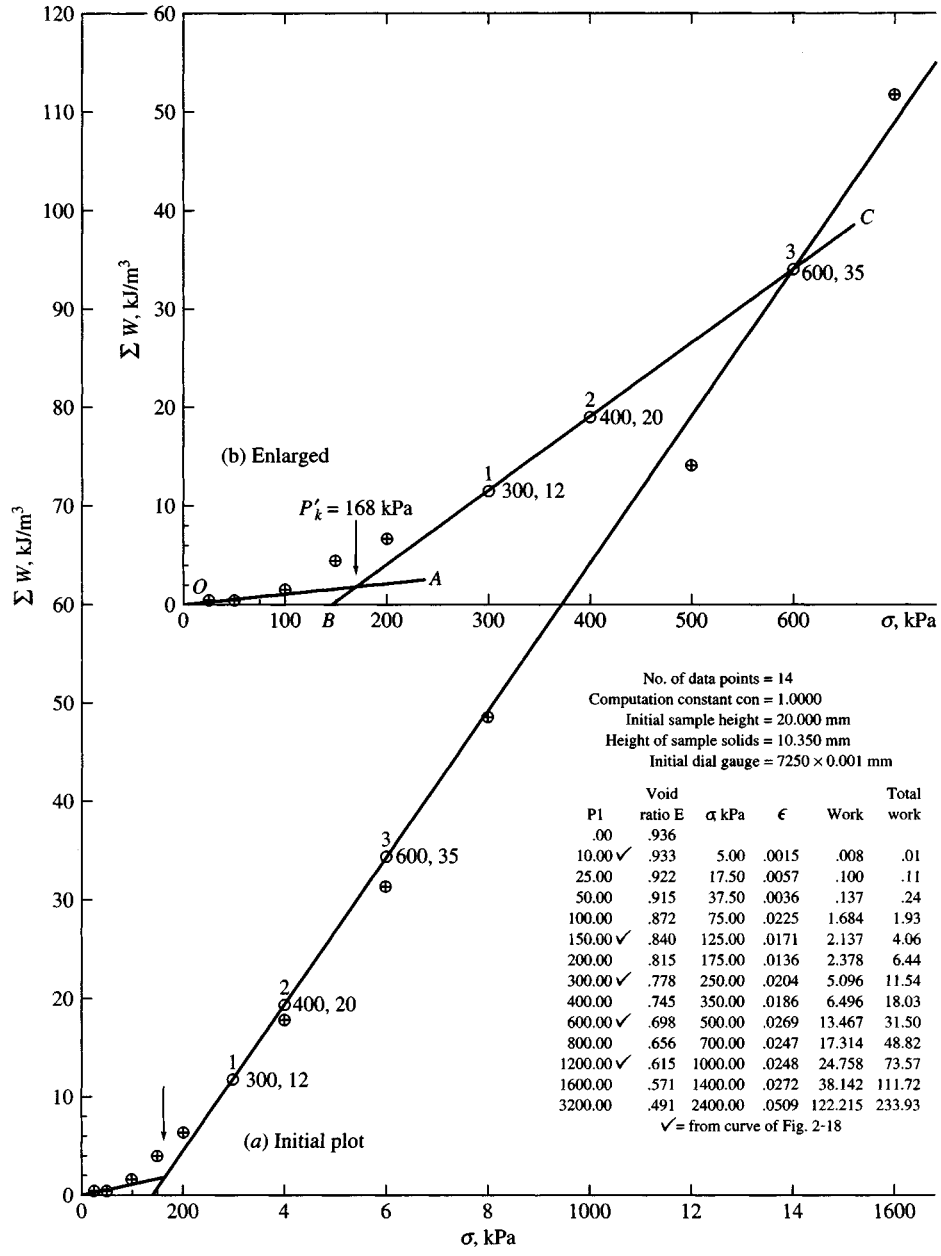

P1	Void ratio E	σ kPa	ϵ	Work	Total work
.00	.936				
10.00✓	.933	5.00	.0015	.008	.01
25.00	.922	17.50	.0057	.100	.11
50.00	.915	37.50	.0036	.137	.24
100.00	.872	75.00	.0225	1.684	1.93
150.00✓	.840	125.00	.0171	2.137	4.06
200.00	.815	175.00	.0136	2.378	6.44
300.00✓	.778	250.00	.0204	5.096	11.54
400.00	.745	350.00	.0186	6.496	18.03
600.00✓	.698	500.00	.0269	13.467	31.50
800.00	.656	700.00	.0247	17.314	48.82
1200.00✓	.615	1000.00	.0248	24.758	73.57
1600.00	.571	1400.00	.0272	38.142	111.72
3200.00	.491	2400.00	.0509	122.215	233.93

✓= from curve of Fig. 2-18

Figure 2-19 The method of work used to verify the preconsolidation pressure obtained from Fig. 2-18. The e and p data used to plot this curve are presented on the graph. The curve is plotted using a short computer program and the extra points collected from Fig. 2-18 [*After Becker et al. (1987).*]

This procedure has been used [see, for example, Crawford and Campanella (1991)] with reasonable results. Note, however, that this method implies that the e or ϵ versus log p curve can be plotted using two straight lines—one from the start of the test to the yield point defined by the location of the p'_c point and the other the postyield line from this point to the end of the test. As a final cautionary note, do not use too large a scale enlargement in the preyield region. Because the initial part of the curve is usually curved, trying to obtain the preconsolidation pressure p'_c will not be very accurate. When using this procedure, be sure to refer to an e versus log p plot so that you do not produce an intersection that is well into the postyield region. Rarely can the pre- and postyield lines be drawn through the exact points, so some judgment must be used to obtain these two straight lines and their intersection. Typical work computations using the data on Fig. 2-19 follow:

From 0 to 10 kPa:

$$e_o = 0.936 \qquad e_i = 0.933$$
$$\Delta e = 0.936 - 0.933 = 0.003$$
$$\epsilon = \frac{\Delta e}{1 + e_o} = \frac{0.003}{1 + 0.936} = 0.0015$$
$$W = \Delta\sigma \times \epsilon = \left(\frac{10 + 0}{2}\right)(0.0015) = 0.008$$
$$\sum W = 0 + 0.008 = 0.008 \rightarrow \mathbf{0.01}$$

From 10 to 25 kPa:

$$e_o = 0.933 \qquad e_i = 0.922$$
$$\Delta e = 0.933 - 0.922 = 0.011$$
$$\epsilon = \frac{0.011}{1 + 0.933} = 0.0057$$
$$W = \left(\frac{25 + 10}{2}\right)(0.0057) = 0.998 \approx 0.1$$
$$\sum W = 0.01 + 0.10 = \mathbf{0.11} \qquad \text{and so on}$$

These computations can be done using the program WORK on your diskette.

Method 4: The Log-Log Method

This alternative method might also be used when the e or ϵ versus log p curve does not have a clearly defined transition point. The method was proposed by Jose et al. (1989) and Sridharan et al. (1991) and is essentially as follows:

a. Collect the 1-D consolidation test data and compute for each load increment the void ratio e.

b. Use a computer plotting program and construct a four-cycle log plot along the abscissa of a sheet of paper.

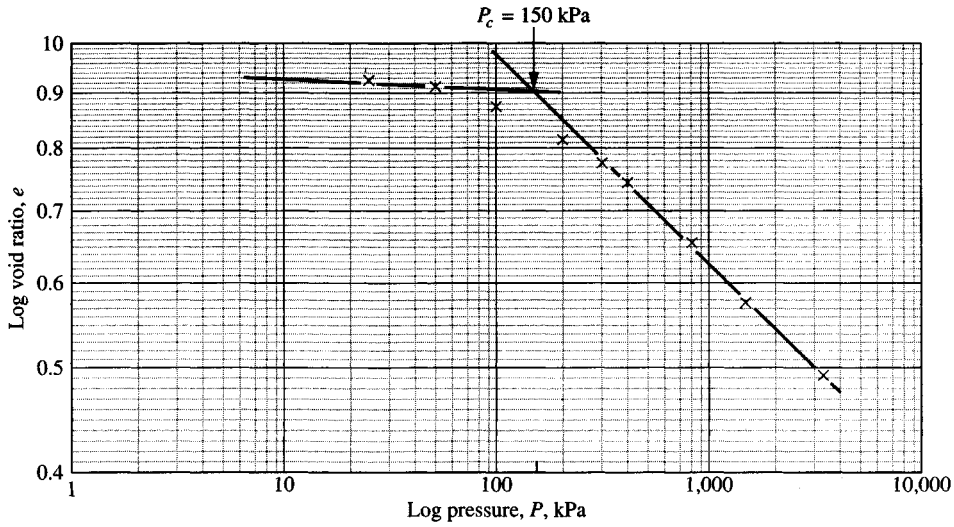

Figure 2-20 The log-log method to estimate the preconsolidation pressure p'_c. The e and p data to generate this plot are in the table on Fig. 2-19. A computer program was used to generate the log-log scales, but minor subdivisions on the log e axis were completed by hand. [*After Sridharan et al. (1991).*]

c. If the plotting program has the facility to plot an enlarged log scale on the ordinate of this graph sheet similar to that in Fig. 2-20, do so. If the plotting program cannot produce such an enlarged scale you may use a sheet of one-cycle log-log paper to transfer a suitable log scale to the ordinate of the graph paper.[17] Make several copies for future use.

d. Now plot log e versus log p and draw straight lines as a best fit in both the pre- and postyield regions as illustrated in Fig. 2-20 (using the data on Fig. 2-19). Their intersection is the preconsolidation pressure p'_c. Using remolded laboratory samples, both aged and young, that had been *preconsolidated to known values,* the authors of this procedure claim that it gave the most nearly correct p'_c of any of the four methods given here.

What Is the Correct Value of p'_c for General Design Use?

The text has presented a set of consolidation test data and used four methods to obtain p'_c as follows:

By eye	—
Casagrande (Fig. 2-18)	120 kPa
Method of work (Fig. 2-19)	168 kPa
Log-log method (Fig. 2-20)	150 kPa

[17]The transfer procedure is found in most elementary engineering drawing/drafting textbooks. Tape one corner of the scale to the control point on your graph and fix the other end at an angle to the ordinate. Use a pair of triangles and align a point on the scale to your ordinate and proceed to place control marks on the ordinate. Use a straight edge to complete the ordinate grid.

The author would probably use 150 kPa. Interestingly, the average of the three methods is 146 (which was used as a guide in "recommending" the use of $p'_c = 150$ kPa). The Casagrande Method commonly gives somewhat low values. You should routinely verify the Casagrande Method by use of at least one of the other methods. The log-log method is trivial if you have suitable log-log paper, and the work method is trivial if you have a short computer program.

2-10.4 Computation of the Settlement Indexes and Settlements

The settlement indexes are computed from the slope of the void ratio or strain versus log p curve along the virgin (or postyield) branch (see Fig. 2-16*a* or *b*) as

$$C_c = \frac{\Delta e}{\log p_2/p_1} \qquad C'_c = \frac{\Delta \epsilon}{\log p_2/p_1} \tag{2-42}$$

The *recompression indexes* C_r, C'_r are computed similarly but for the branch between p'_o and p'_c. It is common, where possible, to extend the virgin slope to intercept one log cycle so that $\log p_2/p_1 = \log 10 = 1$ to simplify computations.

During the initial development and verification of the consolidation theory, it was found that a completely remolded sample produced a curve that always falls beneath an "undisturbed" sample, as qualitatively shown on Fig. 2-17*a*. It was also noted that soils with an unstable structure (often with $w_N > w_L$) may exhibit behavior as in Fig. 2-17*b* where, beyond the current in situ load, the soil structure collapses. This latter soil requires considerable engineering judgment in making any settlement estimate. It is possible, however, to make an improvement in the compression index C_c or ratio C'_c for the soils shown in Figs. 2-16*a* and 2-17*a* using a method proposed by Schmertmann (1955), who analyzed a large number of consolidation tests to develop the following procedure:

1. Extend the straight line portion of the end branch until it intersects the void ratio abscissa at about 0.4 (this is about the minimum void ratio for most real soils—see point M of Fig. 2-17*a*). Use the equivalent strain location with an ϵ versus log p plot.
2. In some manner obtain the initial void ratio e_o of the in situ soil. The rebound (or swell) value is too high, but you can probably get a fair estimate using G_s and w_N (compute $e_o = w_N G_s$). This estimate assumes the in situ soil is saturated.
3. In some manner determine the in situ effective overburden pressure p'_o. Refer to Section 2-9 and Fig. 2-8 for typical computations. You may have to estimate some or all of the soil unit weights.
4. At the intersection of p'_o and e_o (Fig. 2-16*a*) extend a straight line to intersect the point M located in step 1.
5. The slope of the line drawn in step 4 is the corrected value of C_c for a normally consolidated clay.

For a preconsolidated soil one may estimate a corrected C_c as follows:

1–3. These are the same as for a normally consolidated clay.

4. At the intersection of p'_o and e_o draw a line NO with a slope C_r (see Fig. 2-17*a*) that is parallel to the actual e versus log p curve as a best fit by eye. Use an average of the recompression and the reload slope for computing C_r for slope of NO if an unload-reload test branch has been produced.

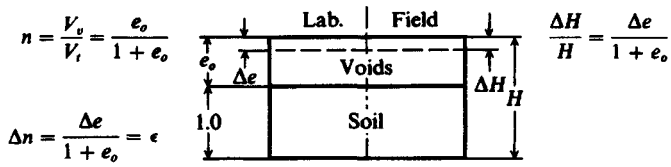

Figure 2-21 Soil relationships for settlement equations. The left side is laboratory; the right side is field relationships.

5. At the intersection of step 4 and p'_c (point O) draw a line OM to the point M established in step 1.
6. The slope of the line from step 5 is the approximate corrected value of C_c for the curve branch beyond p'_c.

Sample disturbance always reduces the field value of C_c to a lesser value, with a completely remolded sample representing the minimum. As a consequence even corrected values tend to be somewhat lower than the true values. Holtz et al. (1986) reported results from block samples carved by hand versus high-quality piston samples. Although there was not a great difference between these two recovery procedures, it appeared that any disturbance reduced C_c. In passing, note that if we take a hand-carved block and obtain two consolidation test samples, one with a horizontal H orientation and one with a vertical V orientation, we can compute K_o as

$$K_o = \frac{p'_{c,H}}{p'_{c,V}}$$

From the settlement ratio shown on Fig. 2-21 one can compute the settlement (either lab or field) with the aid of Eqs. (2-31) and (2-34) as

$$\Delta H = \frac{\Delta e}{1 + e_o} H = m_v(\Delta p)H \tag{2-43}$$

If we substitute Eq. (2-31) into Eq. (2-43); use $\Delta e = de$, $\Delta p = dp$; and observe that $m_v = 1/E_s$, we obtain

$$\Delta H = \frac{\Delta p}{E_s} H = \epsilon H$$

From this expression and inspection of Eq. (2-43) it is evident that the strain is $\epsilon = \Delta e/(1 + e_o)$.[18] This relationship is most useful, since it depends only on the change in void ratio Δe and the initial void ratio e_o. Now we can write Eq. (2-43) as

$$\Delta H = \epsilon H \tag{2-43a}$$

[18]This ϵ is referenced to the initial height. Note that the incremental ϵ computed in the table shown on Fig. 2-19 uses $\Delta e = e_{i-1} - e_i$ and $1 + e_{i-1}$, that is, the void ratio at the beginning of the load increment so that $1 + e_{i-1}$ is H_i.

More commonly we use C_c in computing ΔH in an equation obtained by substitution for Δe from Eq. (2-42) into Eq. (2-43) to give

$$\Delta H = \frac{C_c H}{1 + e_o} \log \frac{p'_o + \Delta p}{p_o} \tag{2-44}$$

This is simply another form of Eq. (2-43*a*) with the terms identified as follows:

C_c = compression index from the e versus log p plot (corrected as necessary)

e_o = in situ void ratio in the stratum where C_c was obtained

H = stratum thickness. If the stratum is very thick (say 6^+ m) it should be subdivided into several sublayers of $H_i = 2$ to 3 m, with each having its own e_o and C_c. Compute the several values of ΔH_i and then sum them to obtain the total consolidation settlement ΔH.

p'_o = effective overburden pressure at midheight of H

Δp = average increase in pressure from the foundation loads in layer H and in the same units as for p'_o

The computed settlement from Eq. (2-44) will be in the units of H.

From the definition of the compression ratio C'_c previously given and using $\Delta H = \epsilon H$ we can obtain the settlement as

$$\Delta H = C'_c H \log \frac{p'_o + \Delta p}{p'_o} \tag{2-45}$$

By equating Eqs. (2-44) and (2-45) a very useful relationship between C_c and C'_c is obtained as

$$C'_c = \frac{C_c}{1 + e_o} \tag{2-46}$$

These equations are directly applicable for normally consolidated soils. When the soil is preconsolidated they should be adjusted as follows (and with reference to Fig. 2-22). Taking the stress increase as

$$\Delta p = \Delta p_1 + \Delta p_2$$

where Δp_2 is any part of Δp that is along the C_c zone to the right of p'_c, we have the total settlement consisting of two parts—that from p_o to p'_c and that (if any) from p'^+_c. These are computed from Eq. (2-44) as follows:

$$\text{Part 1:} \quad \Delta H_i = \frac{C_r H}{1 + e_o} \log \frac{p'_o + \Delta p}{p'_o} \qquad (p'_o + \Delta p_1 \leq p'_c)$$

$$\text{Part 2: (if any)} \quad \Delta H_2 = \frac{C_c H}{1 + e_o} \log \frac{p'_c + \Delta p_2}{p'_c} \qquad (\Delta p_2 = \Delta p - p'_c > 0) \tag{2-44a}$$

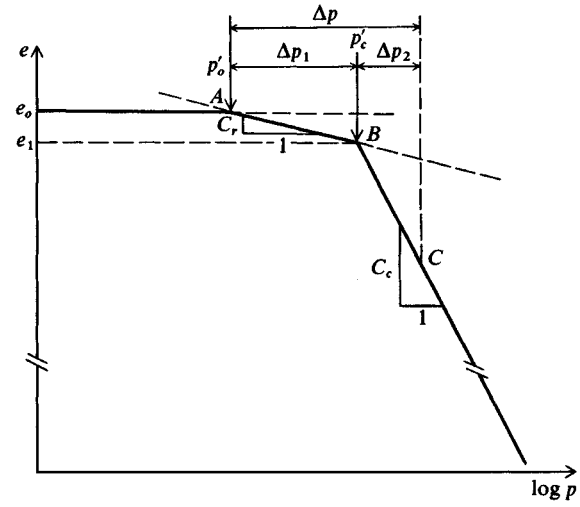

Figure 2-22 Enlargement of upper part of Fig 2-17*a* to compute the settlement from a stress increase Δp along path *ABC*.

The total *primary consolidation* settlement is

$$\Delta H_p = \Delta H_1 + \Delta H_2$$

You may substitute the equivalent forms of Eq. (2-45) when you use a plot of ϵ versus $\log p$ to obtain the total settlement ΔH. Carefully note that primary consolidation is defined as that state when the excess pore pressure $\Delta u \rightarrow 0$. Settlement usually continues beyond this point for some time.

2-10.5 Large Strain Consolidation

Recall that the Terzaghi consolidation theory is applicable only for small strains (or settlement). When the consolidating material is in a sludge pond or dredged hydraulic fills, and a settlement estimate (which may be over half of the fill depth) is wanted—together with a time estimate—some alternative means of estimating the total consolidation settlement is required.

Quantifying the settlement of sludge ponds and hydraulic fills is particularly difficult because initially one has a sedimentation problem. The elapsed time for much of this depends on Stokes' law (as used in hydrometer tests) and may be speeded somewhat if some kind of flocculating agent can be used so that the small particles form larger clumps that can settle faster.

After sedimentation there is some thickness of solids with a very high natural water content and large void ratio e (which can be 20 or more). The consolidation of this material is from the self-weight computed as $\gamma_s - \gamma_f$ (difference between the solids and fluid unit weights). Since γ_s can and usually does vary considerably over both depth and time, it is clearly evident this is a most formidable problem, which can be solved analytically only by making a number of assumptions. For this reason it is most useful to assemble a database on the settlement response of different types of sludges and hydraulic fills. Databases such as these, which would be based on field verification using settlement-measuring devices, enable one to make better estimates of time and consolidation than with no database.

Townsend and McVay (1990, see also the discussion in January 1992) focused on using some type of computer program for the estimates of time and ΔH, and they cite a total of 10. This rather large number of computer programs results from the great difficulty in defining the problem in a form suitable for a computer model. As a consequence the greatest confidence likely to be had in any of these programs is by its author.

Tan et al. (1991) suggest using a hyperbolic method. The general form of the hyperbolic method (which is almost identical to that presented earlier in Sec. 2-10.2, where $\alpha = C$ and $\beta = M$) is

$$s = \frac{t}{\alpha + \beta t} \tag{2-47}$$

If time $t \to \infty$ the settlement limit $s\ (= \Delta H) = 1/\beta$. It is useful to rearrange Eq. (2-47) and obtain

$$\frac{t}{s} = \alpha + \beta t \tag{2-47a}$$

which is a straight line plot of t/s versus t (see Fig. 2-23). It is more useful, however, to rearrange again to obtain

$$\begin{aligned} \frac{t - t_i}{s - s_i} &= \alpha + \beta(t - t_i) \\ \frac{\Delta t}{\Delta s} &= \alpha + \beta(\Delta t) \end{aligned} \tag{2-47b}$$

or in $U - T$ space

$$\frac{T - T_i}{U - U_i} = \alpha + \beta(T - T_i) \tag{2-47c}$$

where t = some time after initial time t_i
s = settlement (usually symbolized as ΔH but it is convenient here to use the symbol s) at some time t with s_i = settlement at time t_i
α = constant determined from the linear plot at $t = \Delta t = 0$
β = slope of the straight line part of the plot of $\Delta t/\Delta s$ curve
U, T = as previously defined in Sec. 2-10.1

The hyperbolic method is used as follows:

1. Take elapsed time (usually days) and settlement (usually millimeters or centimeters) data for the consolidating location and start a plot of t/s versus t. When the plotted points produce a reasonably straight line (termed the *hyperbolic line*) you can obtain α by projecting to the ordinate and simply measuring the slope to obtain β. Note that if you start $t = s = 0$, the plot values are directly measured.
2. It is necessary to take t and s data for a sufficiently long time that the curve does not deviate from the straight line [see Carrier (1993)]. After what you deem a suitable time lapse, use the plot to obtain the data to substitute into Eq. (2-47) to compute the settlement $s\ (= \Delta H)$ for the consolidating mass at some arbitrary time based on data taken to this point.

t, day	s, cm	t, day	s, cm	t, day	s, cm	$t - t_0$	$s - s_0$	$\Delta t/\Delta s$
1	0.9	10	4.8					
2	1.5	11	5.3	43	13.5	13	2.5	5.2
3	1.9	12	5.6	56	15.0	26	4.0	6.5
4	2.5	14	6.4	70	16.1	40	5.1	7.8
7	3.7	16	7.0	90	17.0	60	6.0	10.0
8	4.1	22	8.7					
9	4.4	30	11.0					

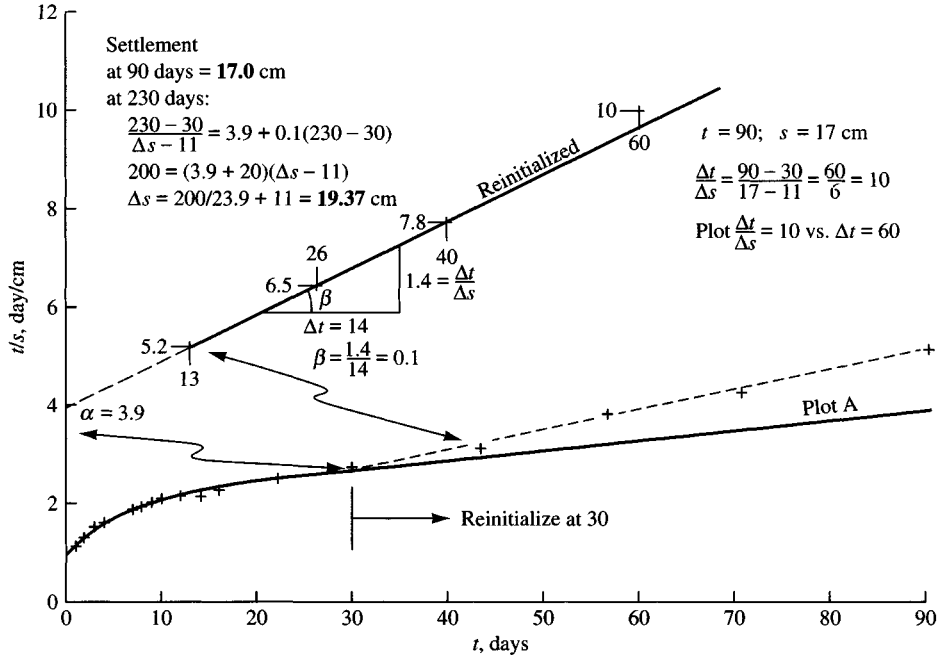

Figure 2-23 Hyperbolic plot of time versus settlement. The "hyperbolic" line deviates in full plot *A* but is reasonably linear when reinitialized using $t_o = 30$ days and $s_o = 11$ cm so that the slope of the reinitialized line gives $\alpha \approx 3.9$ and slope $\beta = 0.1$. From computations on the figure at 230 days the settlement is 19.37 cm (you should verify at 1,030 days that the settlement $\approx$ 20.6 cm). Clearly, most of the settlement has occurred in the 90-day time increment.

3. If a new "straight" section deviates from the initial straight line after some elapsed time t, there is usually a cause such as adding or removing surcharge (or fill), water table lowering, or the like. When this deviation occurs, *reinitialize* the previous curve. Reinitialization consists in using the time and settlement values at some time in the vicinity of the deviation of the points from the straight line and recomputing the plot points. For example, Fig. 2-23 shows linear deviation at $t = 43$ days, $s = 13.5$ cm. We will arbitrarily reinitialize the curve at

$$t = 30 \text{ days} \qquad s = 11 \text{ cm}$$

as shown in typical computations on the figure. These become t_i and s_i, so the new plot continues on Fig. 2-23 in the form of

$$\frac{t-30}{s-11} \text{ versus } (t-30)$$

For measured data of $t = 56$ days, $s = 15.0$ cm, obtain plot points of

$$\frac{56-30}{15-11} = \frac{26}{4} = 6.5$$

Plot $t/s = 6.5$ versus $t = 26$ days as shown on Fig. 2-23.

To make a final settlement estimate, obtain α and β from the linear hyperbolic curve and compute a table of settlement values s using several arbitrarily selected time values t in Eq. (2-47*b*) until time increases result in almost no increase in settlement s. Plot these values on a graph of time t versus settlement s. The approximate asymptote represents the maximum estimated settlement. With care and enough t and s field data you may be able to estimate the final total settlement within 10 to 20 percent.

2-10.6 Secondary Consolidation

After primary consolidation the soil structure continues to adjust to the load for some additional time. This settlement is termed *secondary consolidation* or *secondary compression* and may continue for many years, but at an approximately logarithmic rate. At the end of secondary consolidation the soil has reached a new K_o state. The total settlement when accounting for both primary ΔH_p and secondary ΔH_s compression is

$$\Delta H_{\text{total}} = \Delta H_p + \Delta H_s$$

The slope of a plot of *deformation* versus log *time* beyond the D_{100} location is used (see Fig. 2-13*a*) to obtain the secondary compression index C_α, computed as

$$C_\alpha = \frac{\Delta H_{ls}/H_{li}}{\log t_2/t_1} = \frac{\Delta \epsilon}{\log t_2/t_1} \tag{2-48}$$

Now using this C_α index, the field secondary compression (or settlement) ΔH_s after some time $t_2 = t_1 + \Delta t$ is computed as

$$\Delta H_s = H_f C_\alpha \log \frac{t_2}{t_1} \tag{2-49}$$

where for the preceding two equations

H_{li} = thickness of laboratory sample at time t_i

ΔH_{ls} = change in sample thickness at some time t_2 taken from the *deformation* versus log *time* curve; try to use one log cycle

t_2 = time at end of primary consolidation $t_1 + \Delta t$ as just defined and consistent with c_v. Find the initial field time t_1 using Eq. (2-38), then rearrange to find t_{90} (use $T = 0.848$ from Table 2-4) and $t_{100} \approx t_{90}/0.9$; for Δt choose some convenient time lapse.

H_f = thickness of field-consolidating stratum at the end of primary consolidation. Commonly one uses initial thickness unless the primary consolidation is very large, say, more than 10 percent of the initial thickness.

The slope of the secondary branch of the deformation versus log time curve is very nearly a constant for a remolded soil but varies with the load for "undisturbed" soil samples. For "undisturbed" field samples you should obtain C_α as the slope of that curve from that laboratory pressure closest to the estimated field loading.

Secondary consolidation (or settlement) is only a small component of the total settlement for most inorganic soils. For highly organic soils (for example, very peaty) the secondary settlement component may be larger than the primary consolidation value.

2-10.7 Compression Index Correlations

A laboratory consolidation test takes a considerable amount of time and is both labor- and computation-intensive (unless the test has been automated[19]). In any case it is rather expensive, and in most cases at least two—and preferably three—tests should be performed in each critical stratum. Because of these factors a substantial effort has been undertaken to attempt to correlate the compression indexes to some other more easily determined soil index properties. Also, if the first laboratory consolidation test correlates reasonably well with one or more of the following expressions, additional verification tests may not be required.

Correlations have particular value in preliminary site studies before extensive soil exploration and testing is undertaken for a final design

Table 2-5 lists several equations, along with their sources, that might be used to make compression index estimates. If the compression ratio C_c' or other ratios are used, they can be obtained from expressions such as Eq. (2-46); but you must somehow estimate the in situ void ratio e_o (usually from an estimated G_s in the range of 2.68 to 2.72).

It appears that better values are obtained when more than one index property is used (remember that I_P uses *both* the liquid and plastic limits).

Because the compression settlement also depends on the initial in situ void ratio e_o, it is probably better to use those equations that include e_o either directly or indirectly (γ or w_N).

Here are suggestions for using Table 2-5:

1. It might be more useful if you have done at least one consolidation test and then use a correlation to verify it (say within ± 10 percent).
2. If you have not done any consolidation tests, you should use at least two table equations and average the results.
3. You should start compiling a local database so that you can identify one of the equations, with minor adjustments to the numerical constants, as defining the local soil.

[19] A computer program such as that in Bowles (1992) is helpful in consolidation test data reduction.

TABLE 2-5
Correlation equations for soil compressibility/consolidation

Compression index, C_c	Comments	Source/Reference
$C_c = 0.009(w_L - 10)$ (±30% error)	Clays of moderate S_t	Terzaghi and Peck (1967)
$C_c = 0.37(e_o + 0.003w_L + 0.0004w_N - 0.34)$	678 data points	Azzouz et al. (1976)
$C_c = 0.141G_s\left(\frac{\gamma_{sat}}{\gamma_{dry}}\right)^{2.4}$	All clays	Rendon-Herrero (1983)
$C_c = 0.0093w_N$	109 data points	Koppula (1981)
$C_c = -0.0997 + 0.009w_L + 0.0014I_P + 0.0036w_N + 0.1165e_o + 0.0025C_P$	109 data points	Koppula (1981)
$C_c = 0.329[w_N G_s - 0.027w_P + 0.0133I_P(1.192 + C_P/I_P)$	All inorganic clays	Carrier (1985)
$C_c = 0.046 + 0.0104I_P$	Best for $I_P < 50\%$	Nakase et al. (1988)
$C_c = 0.00234w_L G_s$	All inorganic clays	Nagaraj and Srinivasa Murthy (1985, 1986)
$C_c = 1.15(e_o - 0.35)$	All clays	Nishida (1956)
$C_c = 0.009w_N + 0.005w_L$	All clays	Koppula (1986)
$C_c = -0.156 + 0.411e_o + 0.00058w_L$	72 data points	Al-Khafaji and Andersland (1992)
Recompression index, C_r		
$C_r = 0.000463w_L G_s$		Nagaraj and Srinivasa Murthy (1985)
$C_r = 0.00194(I_P - 4.6)$	Best for $I_P < 50\%$	Nakase et al. (1988)
$= 0.05$ to $0.1C_c$	In desperation	
Secondary compression index, C_α		
$C_\alpha = 0.00168 + 0.00033I_P$		Nakase et al. (1988)
$= 0.0001w_N$		NAFAC DM7.1 p. 7.1–237
$C_\alpha = 0.032C_c$	$0.025 < C_\alpha < 0.1$	Mesri and Godlewski (1977)
$= 0.06$ to $0.07C_c$	Peats and organic soil	Mesri (1986)
$= 0.015$ to $0.03C_c$	Sandy clays	Mesri et al. (1990)

Notes: 1. Use w_L, w_P, w_N, I_P as percent, not decimal.
2. One may compute the in situ void ratio as $e_o = w_N G_s$ if $S \rightarrow 100$ percent.
3. C_P = percent clay (usually material finer than 0.002 mm).
4. Equations that use e_o, w_N, and w_L are for both normally and overconsolidated soils.

2-10.8 Compression Index Correlations and Preconsolidation

A reliable estimate of the *effective preconsolidation pressure* p'_c is difficult without performing a consolidation test. There have been a few correlations given for p'_c of which one was given by Nagaraj and Srinivasa Murthy (1985, 1986) for saturated soils preconsolidated by overburden pressure (as opposed to shrinkage or chemical factors):

$$\log_{10} p'_c = 5.97 - 5.32(w_N/w_L) - 0.25 \log_{10} p'_o \tag{2-50}$$

As an example, for

$$w_N = 25\%; \quad w_L = 50\% \text{ (liquid limit)};$$
$$p'_o = \gamma'_s z = 16 \times 3 \text{ m} = 48 \text{ kPa}$$

we have

$$\log_{10} p_c' = 5.97 - 5.32(0.25/0.50) - 0.25 \log_{10} 48$$
$$= 2.89 \rightarrow p_c' = 10^{2.89} = \mathbf{776}\ \text{kPa}$$

The OCR = 776/48 = **16**. While this is a very large OCR, we could have predicted that there would be some overconsolidation, with $w_N = w_L/2$—certainly a case where w_N is closer to w_P than to w_L.

For soils preconsolidated by cementation and shrinkage Nagaraj and Srinivasa Murthy (1985, 1986) suggest

$$p_c' = 3.78 s_u - 2.9 \text{ (units of kPa)} \tag{2-51}$$

where s_u = in situ undrained shear strength as defined in Sec. 2-11.4 and determined by the field vane shear test described in Sec. 3-12.

As previously noted, it is possible to estimate whether a soil is preconsolidated from overburden pressure by noting the position of the natural water content w_N with respect to the Atterberg limits of w_P and w_L on Fig. 2-2*a*:

1. If w_N is closer to the liquid limit w_L than to w_P the soil is likely to be *normally consolidated.*
2. If w_N is closer to the plastic limit w_P than to w_L the soil is likely to be *preconsolidated.*

Unfortunately this information cannot be used in a quantitative manner or for over- or preconsolidation caused by shrinkage or chemical action. All that can be said with any certainty is that if the soil is preconsolidated it is not likely to settle as much under a foundation load as a similar soil in a normally consolidated state.

2-11 SHEAR STRENGTH

Soil strength is the resistance to mass deformation developed from a combination of particle rolling, sliding, and crushing and is reduced by any pore pressure that exists or develops during particle movement. This resistance to deformation is the shear strength of the soil as opposed to the compressive or tensile strength of other engineering materials. The shear strength is measured in terms of two soil parameters: interparticle attraction or *cohesion* c, and resistance to interparticle slip called the *angle of internal friction* ϕ. Grain crushing, resistance to rolling, and other factors are implicitly included in these two parameters. In equation form the shear strength in terms of *total* stresses is

$$s = c + \sigma \tan \phi \tag{2-52}$$

and, using *effective* strength parameters,

$$s = c' + \sigma' \tan \phi' \tag{2-52a}$$

where terms not identified earlier are

s = shear strength (sometimes called τ), kPa, ksf, etc.
σ = normal stress on shear plane (either total σ or effective σ'), kPa, ksf, etc.
$\sigma' = \sigma - u$ = effective normal stress (defined in Sec. 2-9)

we have

$$\log_{10} p'_c = 5.97 - 5.32(0.25/0.50) - 0.25 \log_{10} 48$$
$$= 2.89 \rightarrow p'_c = 10^{2.89} = \mathbf{776}\ \text{kPa}$$

The OCR = 776/48 = **16**. While this is a very large OCR, we could have predicted that there would be some overconsolidation, with $w_N = w_L/2$—certainly a case where w_N is closer to w_P than to w_L.

For soils preconsolidated by cementation and shrinkage Nagaraj and Srinivasa Murthy (1985, 1986) suggest

$$p'_c = 3.78 s_u - 2.9 \text{ (units of kPa)} \tag{2-51}$$

where s_u = in situ undrained shear strength as defined in Sec. 2-11.4 and determined by the field vane shear test described in Sec. 3-12.

As previously noted, it is possible to estimate whether a soil is preconsolidated from overburden pressure by noting the position of the natural water content w_N with respect to the Atterberg limits of w_P and w_L on Fig. 2-2*a*:

1. If w_N is closer to the liquid limit w_L than to w_P the soil is likely to be *normally consolidated.*
2. If w_N is closer to the plastic limit w_P than to w_L the soil is likely to be *preconsolidated.*

Unfortunately this information cannot be used in a quantitative manner or for over- or preconsolidation caused by shrinkage or chemical action. All that can be said with any certainty is that if the soil is preconsolidated it is not likely to settle as much under a foundation load as a similar soil in a normally consolidated state.

2-11 SHEAR STRENGTH

Soil strength is the resistance to mass deformation developed from a combination of particle rolling, sliding, and crushing and is reduced by any pore pressure that exists or develops during particle movement. This resistance to deformation is the shear strength of the soil as opposed to the compressive or tensile strength of other engineering materials. The shear strength is measured in terms of two soil parameters: interparticle attraction or *cohesion* c, and resistance to interparticle slip called the *angle of internal friction* ϕ. Grain crushing, resistance to rolling, and other factors are implicitly included in these two parameters. In equation form the shear strength in terms of *total* stresses is

$$s = c + \sigma \tan \phi \tag{2-52}$$

and, using *effective* strength parameters,

$$s = c' + \sigma' \tan \phi' \tag{2-52a}$$

where terms not identified earlier are

s = shear strength (sometimes called τ), kPa, ksf, etc.
σ = normal stress on shear plane (either total σ or effective σ'), kPa, ksf, etc.
$\sigma' = \sigma - u$ = effective normal stress (defined in Sec. 2-9)

The strength parameters are often used as constants, but they are quite dependent on the type of laboratory test, previous stress history, and current state (particle packing, grain shape, and water content). As a consequence, obtaining accurate values is not a trivial task, and the values obtained actually apply only to the current soil state. Also whereas Eq. (2-52) has a linear form, in real soils for the reasons just cited this equation is often a curve.

The shear envelope defined by Eq. (2-52), obtained from the locus of tangent points to a series of Mohr's circles (see Fig. 2-24), constitutes the limiting states of soil stresses. Since there are two parameters in these equations (c, ϕ), at least two soil tests must be performed to obtain their values using either simultaneous equations or, most commonly, a graphical solution. From the Mohr's circle[20] of Fig. 2-24, the normal stress on the shear plane in terms of principal stresses σ_1 and σ_3 is

$$\sigma_n = \frac{\sigma_1 + \sigma_3}{2} + \frac{\sigma_1 - \sigma_3}{2} \cos 2\theta \tag{2-53}$$

The principal stress difference $\sigma_1 - \sigma_3$ (also called the *deviator stress* $\Delta\sigma_1$) used above and as shown on Fig. 2-24 at failure is the instant increase in compression stress starting from σ_3. The vertical stress increase Δp from foundation loads in situ from p'_o is also the *deviator stress.*

Figure 2-24 Mohr's failure stress circle for a triaxial compression test series with only a single test shown for clarity and to include shear strength terminology. Also shown is orientation of the shear plane in sample and shear and normal stresses on plane. Note conventional use of first quadrant for stress plot even though stresses are all compressive. In-depth theory of Mohr's circle construction is available in introductory geotechnical, mechanics of materials, and statics textbooks.

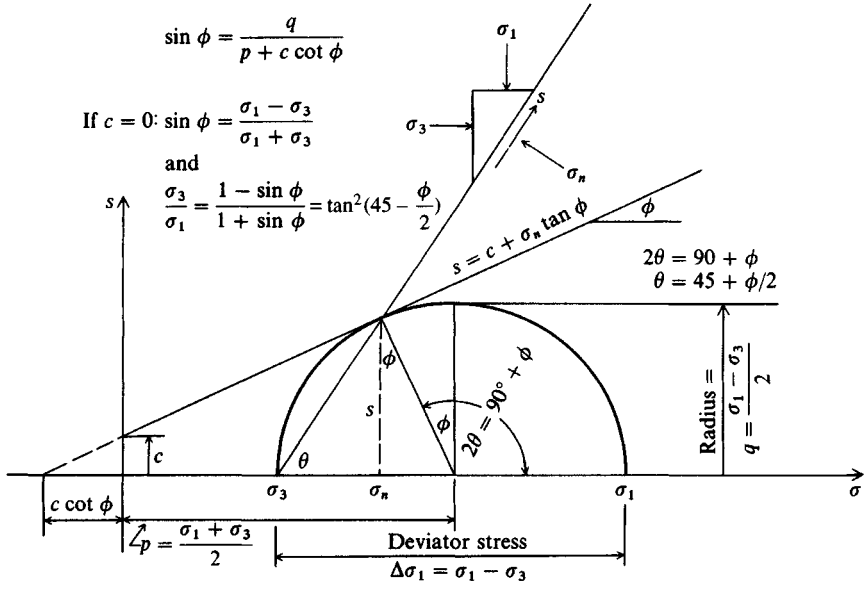

[20]It is usual in geotechnical practice to plot Mohr's circles in the first quadrant since both principal stresses are compressive but consistently used as (+) values.

Solving Eq. (2-53) for the principal stresses and using Eq. (2-52) and the trigonometric relationship that

$$\frac{1 - \sin\phi}{1 + \sin\phi} = \tan^2\left(45° - \frac{\phi}{2}\right)$$

we obtain the following two equations to which reference is made a number of times in this textbook:

$$\sigma_1 = \sigma_3 \tan^2\left(45° + \frac{\phi}{2}\right) + 2c \tan\left(45° + \frac{\phi}{2}\right) \tag{2-54}$$

$$\sigma_3 = \sigma_1 \tan^2\left(45° - \frac{\phi}{2}\right) - 2c \tan\left(45° - \frac{\phi}{2}\right) \tag{2-55}$$

The shear strength of a soil is heavily dependent on the type of test and on pore water conditions, which may be generalized as follows:

1. *Unconsolidated-undrained (UU or U) tests.* The sample is placed in a compression testing machine and immediately loaded to failure. The failure stress is the unconfined compression strength q_u for clay soils. This test can also be performed in a shear box, where the shearing stress is begun as soon as the vertical load is applied. In this latter case the shear stress is plotted versus the normal stress to obtain the undrained shear strength s_u (see Fig. 2-27*b*). The sample is free to drain, but with a low coefficient of permeability k not enough occurs to say the sample has drained.

   For cohesionless soils this test must be performed in a triaxial cell or shear box. For these soils the drained shear strength parameter ϕ' is obtained, even if the soil is saturated, unless the test is performed at an unrealistic rate of speed with a sample so fine-grained it has a very low coefficient of permeability k.

   Sometimes clay samples are put in a triaxial cell, a cell pressure is applied, and the compression is done immediately. This procedure is not recommended because of the time involved and additional sample disturbance produced.

2. *Consolidated-undrained (CU) tests.* The sample is consolidated with drain lines open until no further drainage occurs (it has consolidated). The drain lines are then closed, and the sample is tested to failure (undrained). In cohesive soils this test generally produces both a cohesion intercept c and a ϕ angle that is intermediate between 0 and ϕ' depending on the degree of saturation S.

   The test may be given a designation based on the type of cell consolidation pressure used:

   I = isotropic (constant all around, as usually obtained in the triaxial cell)

   K_o = consolidated with some vertical pressure and with lateral pressure set to an estimate of the field value of $K_o\sigma_v$. This test requires special equipment and is seldom done.

   A = anisotropically consolidated (vertical not same as lateral but lateral is not $K_o\sigma_v$)

   These types of consolidation give a test designation as CIUC (consolidated isotropically and undrained compression) or CK_oUE (consolidated to K_o and tested in undrained extension). There are others, but this explanation should give you a general idea when you see these test designations in the literature.

3. *Consolidated-drained (CD) tests.* In these tests (seldom done) the sample is consolidated by one of the methods for the consolidated-undrained test, and when drainage is com-

plete the test is commenced—but at such a slow rate that the excess pore pressure can be neglected. There is always some excess pore pressure above the static level, as it is impossible for there to be any strain or particle movement without this pressure taking place.

This brings us to the crux of the problem. When a site soil is loaded by some new load and consolidates under water to a "consolidated" state, the pore pressure is not zero. Rather, the pore pressure is the static head ($\gamma_w h_w$), which can be—depending on h_w—significant. This is not a consolidated-drained state but rather one of a number of consolidated-undrained states that can develop in this mass. It just happens that at this instant the pore pressure is the static head.

This current state is based on some pressure that caused a particle rearrangement from the previous (also consolidated-undrained) state. The pressure that caused this current state is now a new historical imprint.

The common laboratory procedure to obtain CU-parameters is to consolidate about three or four samples isotropically in a triaxial cell using a different cell pressure for each sample and, from the several *deviator* stresses and cell pressures, plot data to draw a best-fit Mohr's stress envelope so that an "undrained" value of c and ϕ are obtained. If the total pore pressure is measured, one can obtain both "undrained" CU and "drained" CD parameters $c \approx 0$; $\phi \rightarrow \phi'$ (see Fig. 2-32*b*).

Actual field conditions usually involve increasing the stress from some initial value to some new value. After some time elapses the pore pressure returns to the static level and strain stops, with some increase in soil density. A new stress increase results in this process repeating, . . . , etc. The soil is certainly not going from one consolidated-drained state to another one. There is only one set of strength parameters for the consolidated-drained state, but here we have values depending on the current stress level versus the previous one, . . . , etc.

Laboratory tests tend to be categorized as *compression* if the sample is compressed or *shear* if the sample is sheared to obtain the desired strength information.

Shear strength tends to be anisotropic (horizontal strength not the same as vertical) as a result of the way a soil mass develops from sedimentation (or even in residual soils from weathering and leaching). In view of this observation, current practice suggests that one look at the location of the likely failure mode (shear, compression) and perform a laboratory test consistent with the general orientation of the failure zone as illustrated in Fig. 2-25.

2-11.1 Shear Tests

These tests are made using either direct shear (Fig. 2-26*a*), which is most common, or direct simple shear (Fig. 2-26*b*) equipment. For controlled pore water conditions and for stress reversal studies, the direct simple shear device is used. There are several configurations of the direct simple shear test, but the most common uses a round sample 2.0 cm in height with an area of 50 cm^2. The wire-reinforced rubber membrane (see Fig. 2-26*b*) prevents lateral deformation during consolidation from vertical load P_v. Moving the top cap laterally produces shear stresses, and by monitoring the deformations and adjusting the vertical load the sample can be sheared at a constant volume and water content. Attaching the cap to a load-cycling machine to produce shear stress reversals allows the device to be used in dynamic and liquefaction studies. Using the direct simple shear device produces DSS tests (see Fig. 2-25 for typical use).

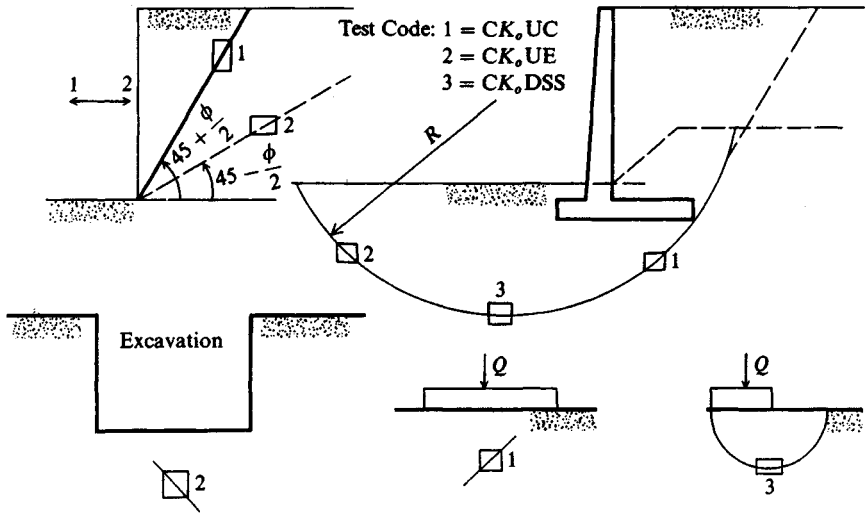

Figure 2-25 Strength tests corresponding to field shear. [*After Ladd et al. (1977) and Johnson (1975).*] The unconfined compression test is commonly used for all cases.

Both test devices shown on Fig. 2-26 allow one to consolidate a sample to K_o conditions. A compression load on the laterally confined sample produces a state of zero lateral strain with consolidation complete when vertical strain → zero for a reasonable time period. This is by definition a K_o state with principal stresses on the vertical and horizontal planes. Whether this is the same K_o as in situ is speculative, but if an in situ vertical consolidation stress is used it is about the best that can be done. "Undisturbed" samples can be obtained for cohesive soils; however, cohesionless samples are usually completely remolded between recovery and insertion into the shear box so that any geological history (aging, cementation, structure, etc.) is lost. A replication of void ratio does not necessarily reproduce the in situ soil structure.

The stress state in direct shear type tests is somewhat indeterminate (there is wide disagreement [see Saada and Townsend (1981)] among engineers about the value of these tests), but those who use the test assume that applying the lateral shearing load to the sample produces a plane strain condition with a shear stress s of known magnitude on the horizontal plane and an effective normal stress σ_n computed from the sample load P_v and original cross-sectional area. This is somewhat in error, however, from the required rotation of principal planes during shear as shown on Fig. 2-26*a*.

We may perform several tests (always more than two) at several values of σ_n or vertical loads and make plots as in Fig. 2-27 to obtain graphically the P_h maximum and the soil parameters ϕ and c—which may be total or effective—depending on whether excess pore pressure existed on the shear plane at the failure load or if Δu was measured.

2-11.2 Compression Tests

Although we often perform compression tests on soil samples, the data are always presented in terms of shear strength or used to obtain a stress-strain relationship as the stress-strain modulus or modulus of deformation E_s.

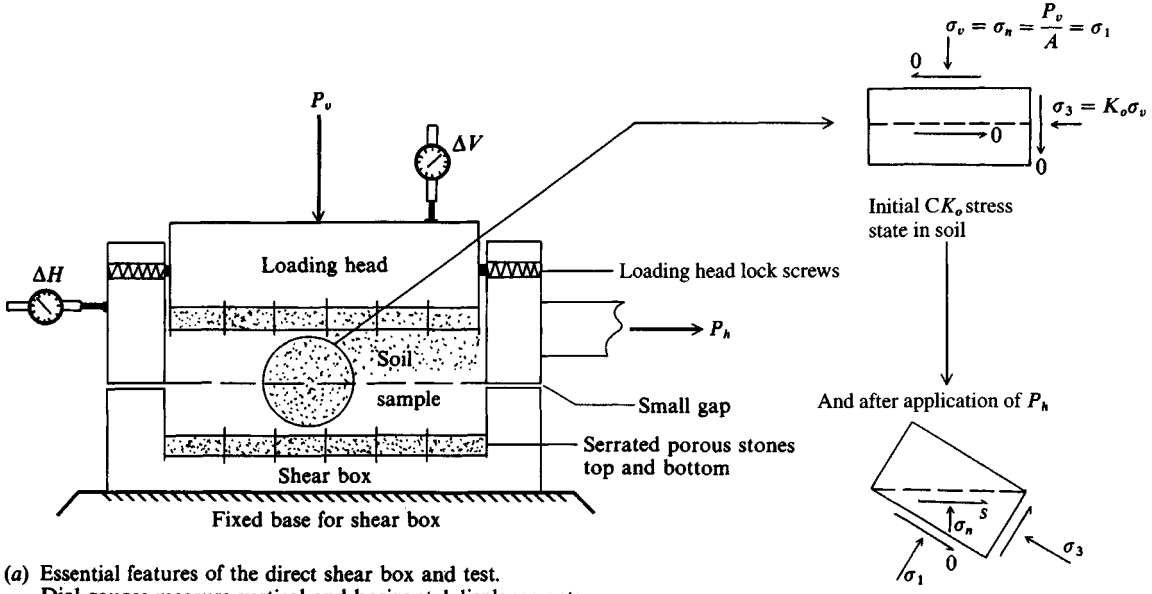

(*a*) Essential features of the direct shear box and test. Dial gauges measure vertical and horizontal displacements. Thin sample (about 20 mm), porous stones, and box gap produces CU data in nearly all cases unless P_h is applied at a very high rate.

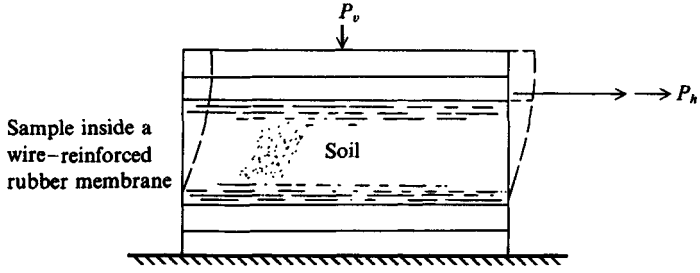

(*b*) Direct simple shear DSS device. Note pore water state can be controlled. Application of P_v produces a CK_o state.

Figure 2-26 The two most common direct shear type devices for laboratory testing.

Unconfined compression tests to obtain a compressive strength, *always termed* q_u, can be performed using almost any type of compression-loading device on cohesive samples. The compression device must have a reasonable load accuracy at the low loads at which soil samples usually fail. In the test a length of sample (usually length/diameter > 2) is placed in the device and compressed to failure. Load and deformation data are taken periodically to plot a stress-strain curve (as on Fig. 2-28) if desired. From the average of several peak (or residual) strength values a Mohr's circle may be drawn to obtain the undrained shear strength $s_u = q_u/2$ = cohesion. If the Mohr's circle uses the residual strength (see Fig. 2-27*a*), the "residual" strength parameters are obtained.

Confined compression tests are similar to unconfined tests except for the sample confinement during testing. These tests are usually considered to be of better quality but at higher

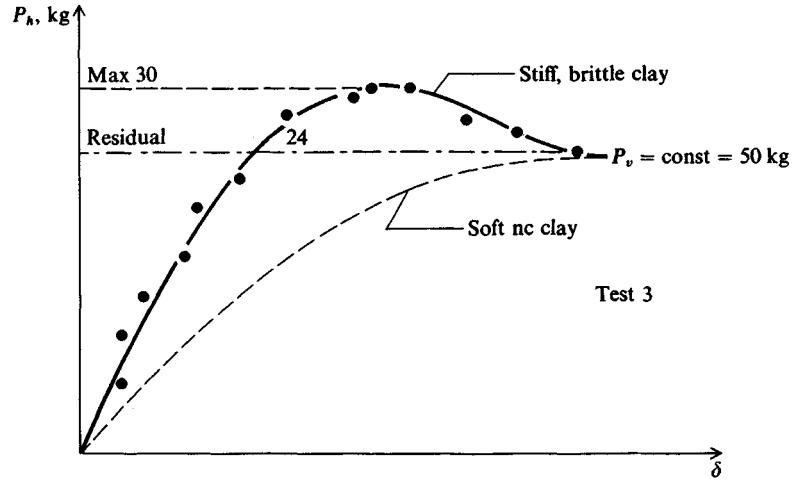

(*a*) Typical shear force P_h versus horizontal displacement δ for one of a series of direct shear tests. Note peak and residual values and use of kilograms.

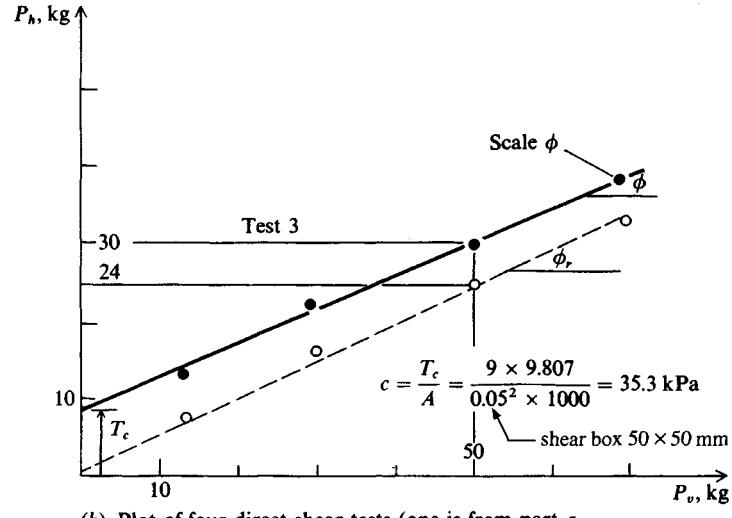

(*b*) Plot of four direct shear tests (one is from part *a* above) so ϕ and c can be directly scaled. Both peak and residual values are shown. Note plot of force with c converted to stress for design as last step.

Figure 2-27 Typical direct shear tests and data reduction for shear strength parameters ϕ and cohesion c.

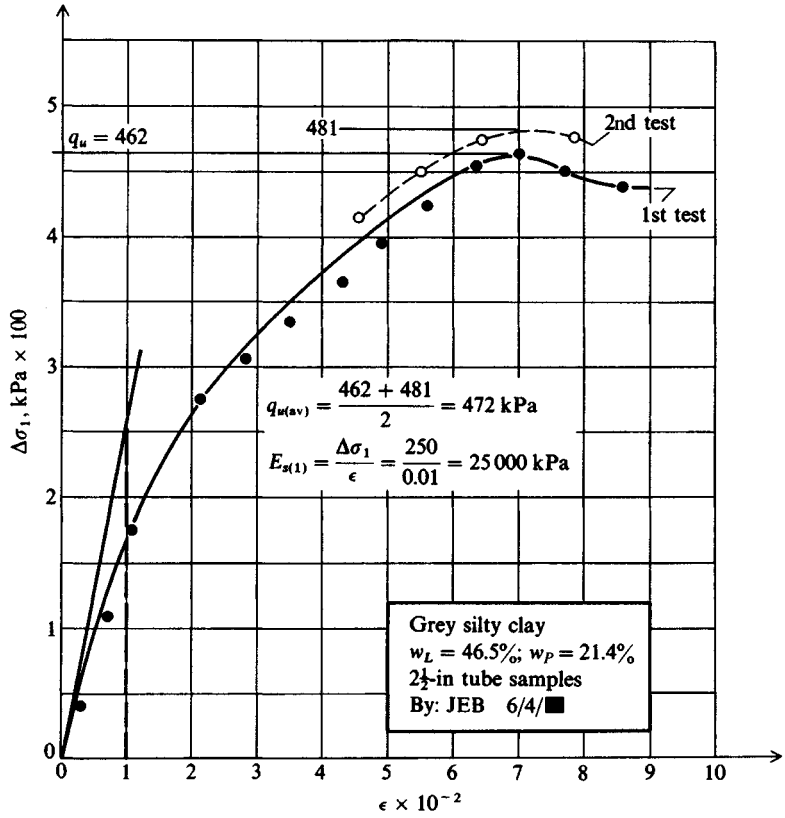

(*a*) Stress-strain plot to obtain q_u. Stress $\Delta\sigma_1$ is computed using equation shown on Fig. 2-23.

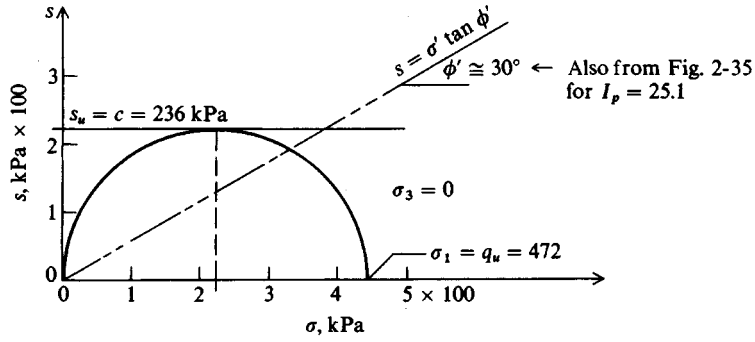

(*b*) Plot of Mohr's circle using **average** q_u from (*a*) above.

Figure 2-28 Unconfined compression test using compression machine.

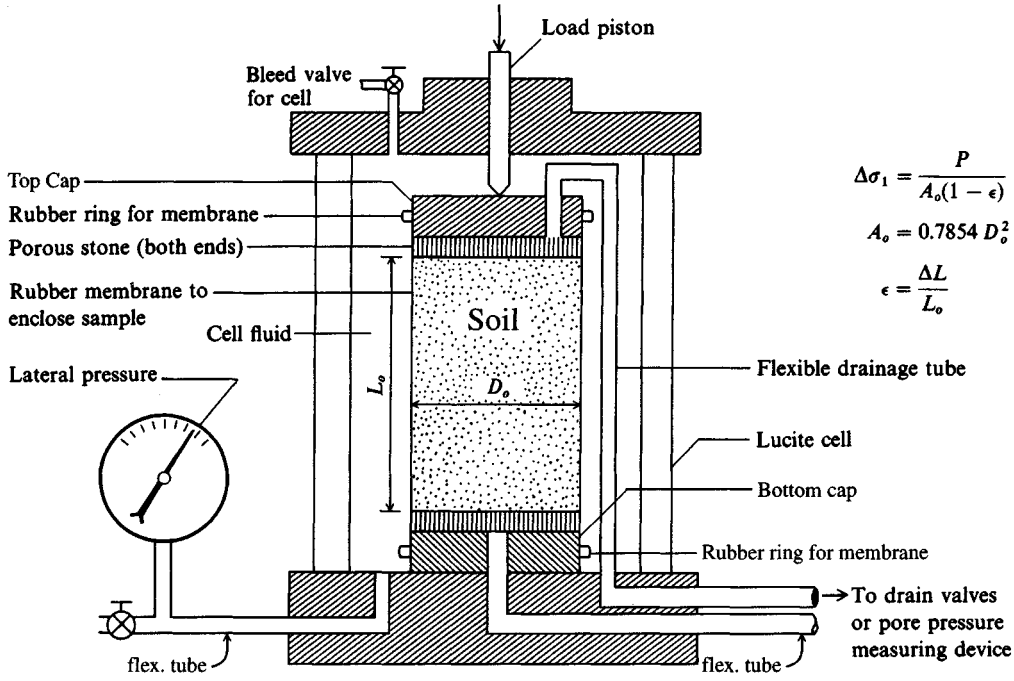

Figure 2-29 Principal line details of triaxial cell. Currently, ASTM D 4767 requires that a membrane strength correction be used with commercial rubber membranes. See Bowles (1992) for methodology and computer program which includes this adjustment.

costs in terms of sample recovery and the extra time for sample preparation, testing, and data reduction. A confining (triaxial) cell (see Fig. 2-29) is required with the compression machine. The triaxial cell should have the facility to do the following:

1. Apply a confining pressure to the sample, which is usually encased in a rubber membrane. This pressure may be from air or from using a liquid such as water (with rust inhibitor) or a mixture of water and glycerine where greater viscosity is needed to control seepage at higher pressures and where volume displacements are measured or controlled. This facility allows one to test either cohesionless or cohesive soil samples.
2. Be able to seal the sample so that interior pore water conditions can be somewhat controlled. That is, one must have the facility to drain or saturate the sample. Sample saturation is a time-consuming process for cohesive samples, so it is necessary to be able to pressurize the pore fluid (termed "back pressure") so that saturation occurs at a faster rate. The use of back pressure also allows one to perform the test at the in situ pore pressure. The pore-pressure lines require facility for drainage control so that volume changes during sample consolidation can be measured. Also by opening the sample drain lines one may perform a "drained" test. Alternatively, by saturating the sample and lines and then closing the top one of Fig. 2-29 and attaching a pore-pressure (pressure transducer) measuring device, we can measure the excess pore pressure (at that end of the sample) developed during a CU test so that we can correct the total stress parameters to obtain the effective stress parameters ϕ' and c'.

Reasonably "undisturbed" cohesive samples can be tested if we accept "undisturbance" as including sample recovery + transporting to the laboratory + sample preparation and insertion into the rubber membrane. It is evident that an undisturbed cohesionless sample is not possible—it is difficult even to reproduce the in situ density.

Worst-case conditions (or soil parameters) are usually obtained from testing saturated soils; however, $S = 100$ percent is not a necessary test condition. One should try to test the soil in the worst water content case likely to occur at the site during the life of the engineered works.

Triaxial extension tests can also be performed and for certain situations (see Fig. 2-25, code 2) will provide better strength parameters. These usually require stress-controlled equipment whereas the common triaxial equipment from most laboratory supply organizations provides strain-controlled devices. In strain control an electric motor advances the loading head at a constant strain rate (mm/min). To perform an extension test we should be able to hold the vertical stress and either increase or decrease the cell pressure. Normally, of course, we hold the cell pressure and increase the vertical load (or pressure σ_1).

The cell pressure $\sigma_3 = \sigma_c$ in a triaxial test may be one of the following:

$$\sigma_c = mp'_o$$

$$\sigma_c = mp'_o \frac{1 + 2K_o}{3} \qquad \text{(termed the } \textit{mean normal stress}\text{)}$$

The multiplier m may range from $\frac{1}{2} \leq m < 2$ to $3 \times \text{OCR}$.

2-11.3 Cohesionless Soils

Cohesionless soils are always tested in a consolidated-drained condition so that effective stress ϕ' values are obtained. They are consolidated either from the normal pressure in direct shear tests or from the cell pressure in a triaxial test. As they have a high permeability, it takes very little time for consolidation pore pressures to dissipate. It is only necessary, then, to perform the test at a strain rate low enough that the remaining water does not produce excess pore pressure of consequence. Testing a saturated cohesionless sample in U or CU conditions is meaningless.

In addition to other factors previously discussed, the angle of internal friction of cohesionless soils depends on the density or relative density (see Fig. 2-30) and the confining pressure (Fig. 2-31). This latter is of some importance for pile points founded at great depths in the sand with high confining pressures from overburden.

It has been found that the angle of internal friction from a triaxial test (ϕ_{tr}) is from 1 to 5 degrees smaller than that from a plane strain test (ϕ_{ps}). Plane strain is, of course, what a direct shear test purports to produce. In the field when a long wall leans forward under lateral soil pressure, plane strain conditions develop along the length except at the ends. Similarly, a long footing for a wall is a plane strain case versus a triaxial case for a square footing. Several adjustments have been proposed to obtain the plane strain ϕ from triaxial values. An early proposal was

$$\phi_{\text{ps}} = 1.1\phi_{\text{tr}} \qquad (\phi_{\text{tr}} \geq 30^\circ) \tag{2-56}$$

This was also suggested by Lee (1970). Meyerhof modified this equation slightly to transition from a full triaxial to a full plane strain case for footings using $1.1 - 0.1B/L$. Later Lade and

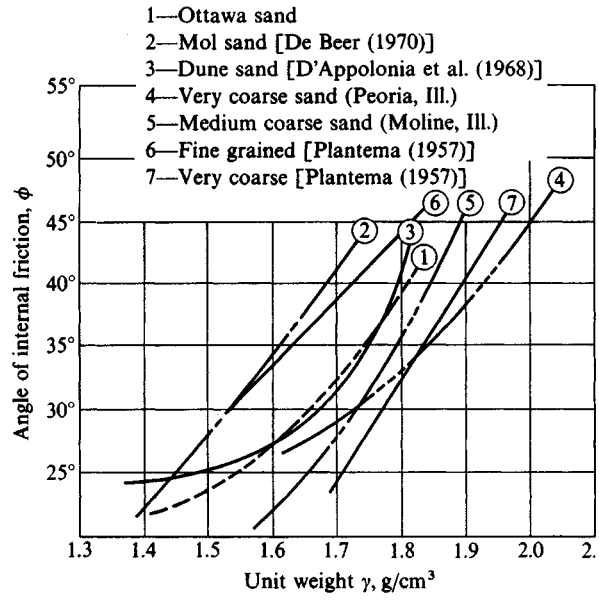

(*a*) ϕ vs. γ for several soils. [*From Bowles (1974a).*]

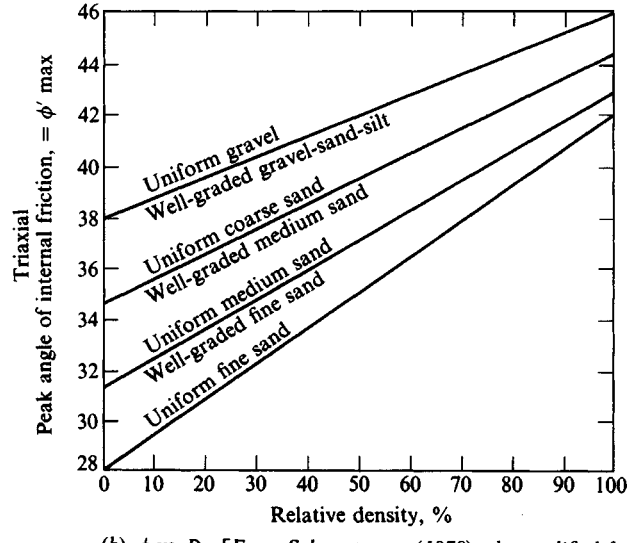

(*b*) ϕ vs. D_r. [*From Schmertmann (1978) who modified from D. M. Burmister (1948), "The Importance and Practical Use of Relative Density in Soil Mechanics", ASTM Proceedings, vol. 48.*]

Figure 2-30 Relationships between angle of internal friction ϕ and unit weight γ or relative density D_r.

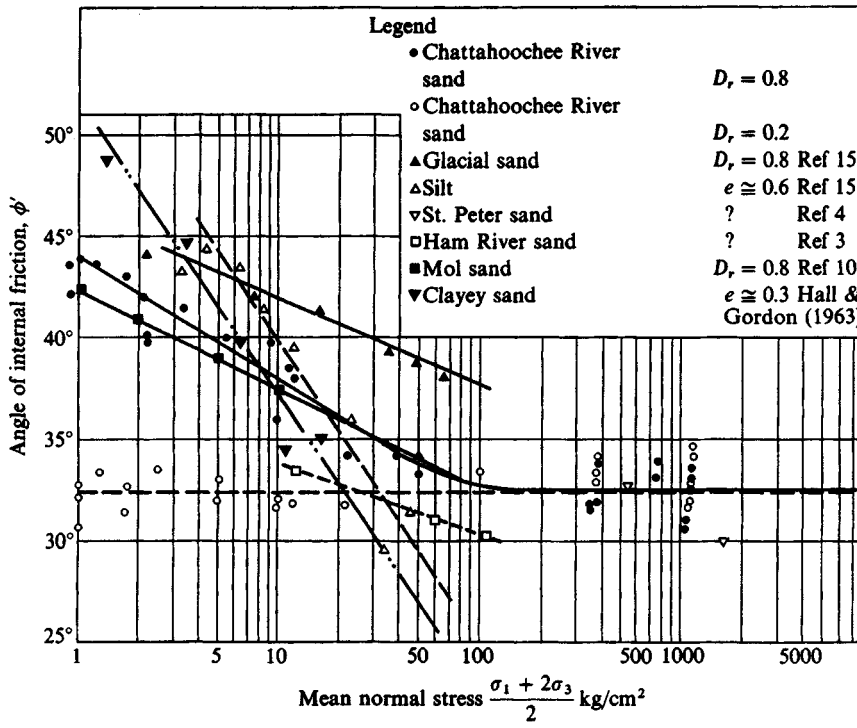

Figure 2-31 Reduction in angle of internal friction with increase in mean normal confining stress. Modified from Vesić and Clough (1968) and using reference numbers from that cited list.

Lee (1976) revised Eq. (2-56) to

$$\phi_{ps} = 1.5\phi_{tr} - 17° \qquad (\phi_{tr} > 34°) \tag{2-57}$$

In general, it is not recommended to adjust ϕ_{tr} unless it is larger than 32–35°, and the adjustment should be limited to not more than 5°. If values are larger, give consideration to performing plane strain tests.

The angle of internal friction, as previously noted, implicitly includes factors in addition to interparticle friction. If ϕ only measured interparticle friction the angle would probably range from about 26 to 30 degrees. Also, contrary to some early opinion, water does not provide a measurable lubrication effect—its primary effects are surface tension and excess pore pressures.

2-11.4 Normally Consolidated Clay ($S \rightarrow$ 100 percent)

The unconfined compression test gives the compressive strength q_u. The test can be made on any cohesive sample (regardless of water content) and is routinely made on recovered cohesive samples during field boring operations. It is estimated that recovery of thin-walled tube samples (the better-quality samples) produces disturbance that reduces the strength 20 to 60 percent with much of the reduction from loss of overburden pressure. However, when this loss occurs the sample tends to expand and negative pore pressures are developed, which tend to confine the sample and produce some strength increase. From this combination, some

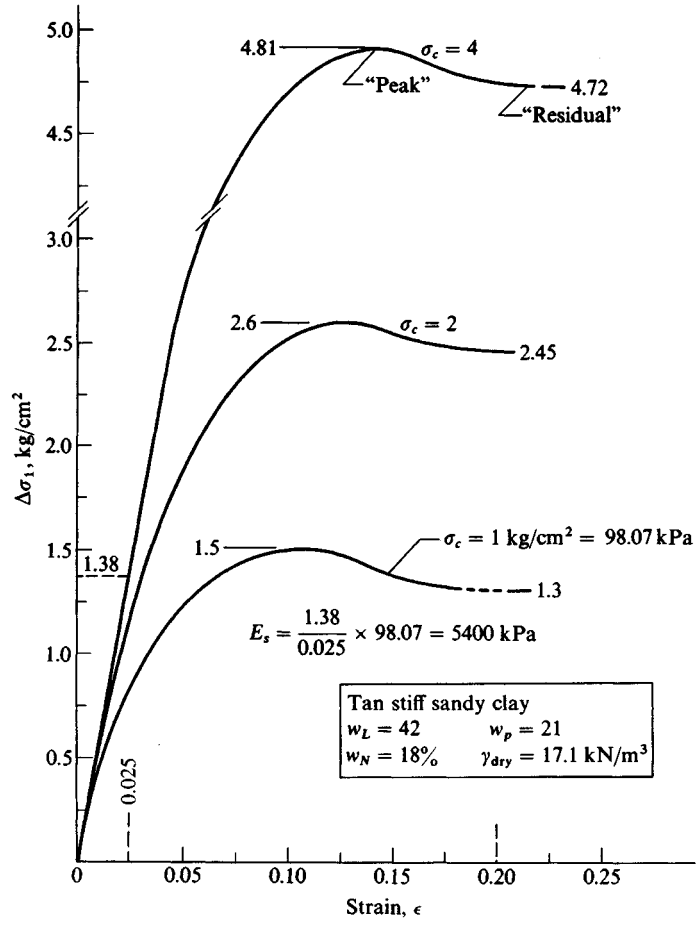

(*a*) Stress-strain data with an initial tangent stress-strain modulus E_s computed.

Figure 2-32*a* CU triaxial test with pore pressure measured for a normally consolidated cohesive soil.

authorities claim the unconfined compression strength is near the true value. Others estimate that at best q_u is not more than about 80 percent of the "true" strength. In usual design, several values of q_u from the same stratum are averaged as the design value. For bearing capacity a factor of safety (or uncertainty) of 3 is commonly applied to q_u.

One could test a sample in the triaxial cell as a U test using a cell pressure of $\sigma_c = 0$; however, since the result is q_u there is no point in the extra effort. We do, however, commonly perform a CK_oU or CIU test series (three or more tests) using increasing values of cell pressure σ_c. With consolidation at different stress levels, even for undrained testing, there is often a measurable set of total stress parameters ϕ and c as on Fig. 2-32. If the excess pore pressure at failure (Δu_f) is measured, we may adjust the total stress Mohr's circles as shown on Fig. 2-32*b* to obtain the effective stress envelope with a cohesion intercept of approximately zero and the effective angle of internal friction ϕ' (here of 33°). The slope of the

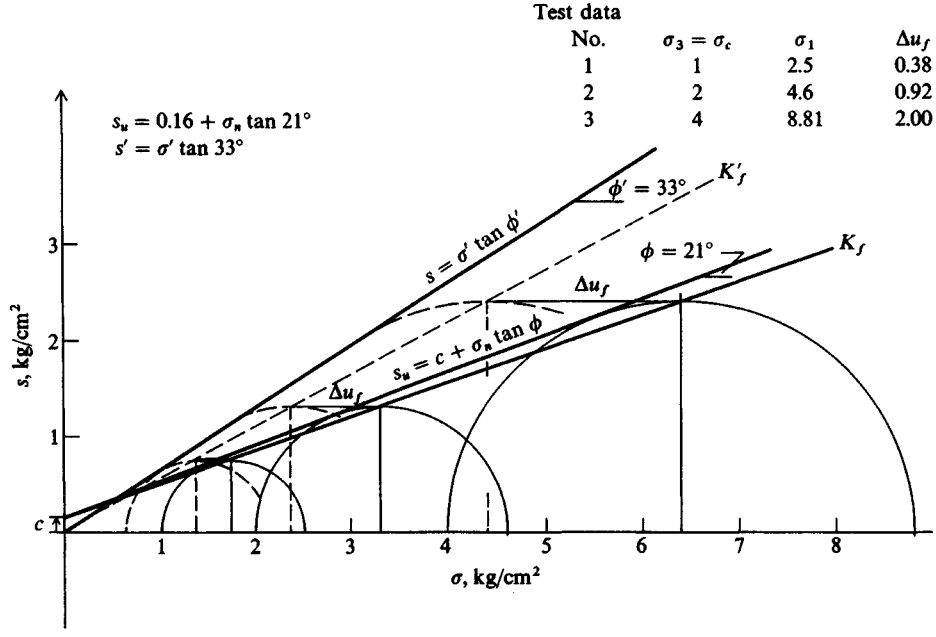

Figure 2-32*b* Mohr's circle plotted for both total (solid) and effective (dashed) stresses from data shown on part (*a*). Shown are both the K_f-line from a *p-q* plot and the Mohr's circle envelope. ASTM D 4767 currently requires a *p-q* plot as part of the data presentation.

stress-strain curves is used to obtain E_s (as shown earlier on Fig. 2-28*a*). Usually the initial tangent value is used, but a secant modulus may be more appropriate in the general range of field loading.

In general, the shear strength for normally consolidated clays is as follows:

Unconfined compression: $s_u = c = q_u/2$ (a $\phi = 0$ state or case)
Consolidated-undrained: $s_u = c + \sigma \tan \phi$
Consolidated-drained (or CU adjusted for Δu_f): $s_d = \sigma' \tan \phi'$

Carefully note that there is no measurable cohesion in the drained strength s_d case for a normally consolidated clay. Referring to the Mohr's circle of Fig. 2-28*b* for q_u, we see that the drained strength goes from a case of $c = q_u/2$ to a case of $c = 0$ and $\phi' > 0$. In some region along the abscissa it is evident that the drained strength is less than the undrained strength. Some embankment failures have been attributed to this phenomenon. From this, one may conclude that the undrained shear strength is a behavior and not a unique soil property and depends on the test method as well as sample state (*e*, *w*, etc.).

2-11.5 Overconsolidated Intact Clay ($S \rightarrow$ 100 percent)

The undrained or CU test tends to give a higher strength s_u for overconsolidated clays than for normally consolidated clays, e.g., the Mohr's circles of Figs. 2-28 and 2-32 have a larger

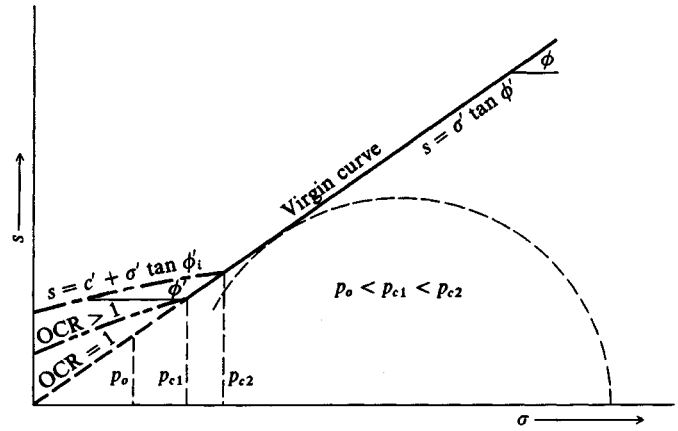

Figure 2-33 Qualitative rupture envelopes for three OCR ratios. Not all Mohr's circles to produce rupture line are shown. The initial branch of rupture line is usually curved for OCR > 1 and is discontinuous at intersection with virgin curves.

diameter. The increase in stress is attributed to a combination of increased density from the consolidating pressure and negative pore pressures developed when the sample tends to expand from loss of overburden pressure during recovery. Any negative (suction) pressure tends to hold grains in closer contact, so the friction and particle displacement resistances are larger.

The CU test will give higher values also if the cell pressure $\sigma_3 < p_c'$ and if the OCR is larger than about 4. This phenomenon is attributed to negative pore pressures from sample recovery and to the negative pressures that develop during shear on the shearing plane as the sample expands (or dilates). Any strength increases produced by negative pore pressures are unsafe for field use. This is because negative pressures are destroyed when environmental free water is absorbed. Experimental evidence indicates that if $\sigma_3 < p_c'$ and the OCR is less than about 4, then negative pore pressures do not develop during the CU test.

When the cell pressure σ_3 is greater than the preconsolidation pressure p_c' the sample responds as if the clay is normally consolidated. This fact is illustrated in Fig. 2-33. Note again that for normally consolidated clays there is a negligible cohesion intercept under drained conditions. For overconsolidated clays at initial stress conditions (σ_3 of cell) less than the preconsolidation pressure there is a measurable cohesion intercept for both drained and undrained conditions. It should also be noted that for overconsolidated clays, the initial branch of the shear stress envelope is seldom a straight line, so that one must make a best estimate of the value of ϕ or ϕ'.

2-11.6 Fissured Clays

Fissures or cracks form in surficial clays during alternate cycles of wetting and drying. Over geological periods a deposit may contain an aggregation of clay blocks in loose to close attachment and much crack contamination from windblown silt, sand, organic materials, or a combination. One may readily observe shrinkage cracks in the soil at the bottoms of dry water holes, in yards, and other ground surfaces after prolonged (or intense) dry periods. Sometimes these visible fissures may be several meters in length, one or more meters in depth, and from

5 to 30^+ mm in width. These clays are usually found above the water table, but regional geological changes may relocate deposits of fissured clays at some depth or below existing lakes or oceans.

In any case, both sample recovery and strength testing are very difficult on fissured clays. Sampling is difficult because the apparent preconsolidation may be 8 or more, and the soil—especially above the GWT—may be very hard and brittle. Driving pressures in sample recovery can collapse thin-walled tubes, and the use of thick-walled tubes tends to produce excessive sample disturbance. Where the sampler cuts fissures, the recovery may be a tube of bits and pieces of soil. If an "intact" sample is recovered, the strength may be affected by any fissures in the sample (sometimes covered by smearing of adjacent soil). Depending on fissuring, any foundation bridging, and moisture control, testing an intact sample may give an unrealistically high strength, and a fissured sample an unrealistically low strength.

For these several reasons, considerable engineering judgment is required to interpret the design parameters for a fissured clay. A principal consideration is control of environmental water after the foundation is installed since the fissures allow ready access to the interior of the soil mass for a general, rather than surface, softening and/or swell.

Fissured clays are found over wide regions worldwide, and in the United States over large areas of the Southwest. Some of the problems in the Southwest are considered by McManis and Arman (1986) and Mahar and O'Neill (1983).

2-11.7 Residual Strength and Critical Void Ratio

Soil failures in situ result in volume changes along the shear plane and a considerable remolding of the soil so that a significant strength reduction takes place. Since soil in any remolded state has some strength that we may term the *residual* strength, its value may be of interest in select foundation problems. A case of considerable interest is the strength of a mass of soil (or other particulate material) that must be held in place by a retaining wall.

Since all failures are from loads that exceed the shear strength of the soil, particle displacements during shear result in one of the following:

1. Increase in volume (or void ratio e) for dense soils. Thus, if pore water is present there is an increase in water content on the failure plane. In a laboratory compression test the failure plane is clearly identified on dense or brittle soil samples.
2. Decrease in volume (or e) for loose soils and a reduction in water content along the failure plane. An identifiable failure plane is seldom observed in a compression test for these samples—they shorten and thicken.
3. No change in volume if the present void ratio is at a value termed the *critical void ratio.* This void ratio seldom exists in situ, but dense and loose samples converge to this value of e at some strain level. The strength value where the several curves of different initial soil states converge (as Fig. 2-34 or Fig. 2.27*a*) for the dense and loose soil samples is termed the *residual strength.*

In the laboratory tests the soil may fail suddenly or gradually. Sudden failures occur at some relatively low strain when the soil is dense and/or the particles are well-bonded. This brittle effect may be from natural aging and cementation, from being at a somewhat dry state,

from being well-compacted (for remolded samples), or from a combination of factors. Gradual failures at large strains occur when the soil is loose or wet and/or when one is using wet remolded samples. Normally consolidated saturated, uncemented, clays tend to have gradual failures; overconsolidated or cemented (aged) clays tend to brittle failures.

These failures are typified by the stress-strain curves of Fig. 2-34*a* and of Figs. 2-27*a* and 2-32*a*. Brittle or sudden failures produce stress-strain curves with a definable peak. Gradual failures produce stress-strain curves with no definable peak (such as curve *b* of Fig. 2-34*a*). With no definable peak the maximum deviator stress is often defined at some percent strain. A value of 15 percent ($\epsilon = 0.15$) is commonly used.

At the residual strength the soil is sufficiently remolded that there is negligible cohesion [but there may be excess (+) or (−) pore-pressure contributions to the stress reduction], and the principal resistance is from friction produced by interparticle friction and rolling resistance. We may term this parameter the residual angle of internal friction ϕ_r and define the residual shear strength in general terms as

$$s_r = c_r + \sigma \tan \phi_r \tag{2-58}$$

The residual strength parameters c_r and ϕ_r can be obtained by plotting residual P_h versus P_v of the direct shear test (Fig. 2-27*b*) or from the residual deviator stresses $\Delta\sigma_r$ from a triaxial test as on Fig. 2-34*b*. Equation (2-58) represents the lower bound strength of any soil. Some are of the opinion that ϕ_r is the true angle of internal friction of the soil.

2-11.8 Design Shear Strength Values

From the preceding discussion the question of what to use for the design strength parameters ($s_{u,d}$ or ϕ and c values) naturally arises. The answers are various.

1. The expression $s_{u,d} = c = q_u/2$ is very widely used and generally provides a conservative value where field loading conditions and water content are duplicated by the rapid test loading. The worst-case strength is when the test sample is saturated. Rapid loading occurs when an embankment is constructed within about 2 weeks or when the foundation loading from the superstructure occurs in about 2–3 weeks. Figure 2-28*b* illustrates that if it is possible for "drained" conditions to exist, the drained strength can be substantially less than s_u—depending on the current normal pressure σ_n.
2. Parameters from CIUC tests are probably the next most widely used. The test is easier but gives s_u/p'_o ratios somewhat higher than CK_oUC tests. Instead of triaxial tests, direct shear or direct simple shear (CK_o-type) tests may be made. CIU and shear tests are of about equal difficulty and cost.
3. Use drained strength (CIUC with pore-pressure measurements) when drained field loading occurs or to check long-term stability under the load.
4. Use $s_{u,d} = \frac{1}{3}(s_{u,C} + s_{u,E} + s_{u,D})$ where $s_{u,C}$ is from CK_oUC, $s_{u,E}$ is from CK_oUE triaxial tests, and $s_{u,D}$ is from the direct simple shear test. According to Aas et al. (1986) (who also cite others) this may be the best value and is applicable for embankments, excavations, and shallow foundations. This strength parameter is also the most costly to obtain.

Although the foregoing comments may be used as a guide, each project must be evaluated separately for the strength recommendation. There are simply too many project-dependent

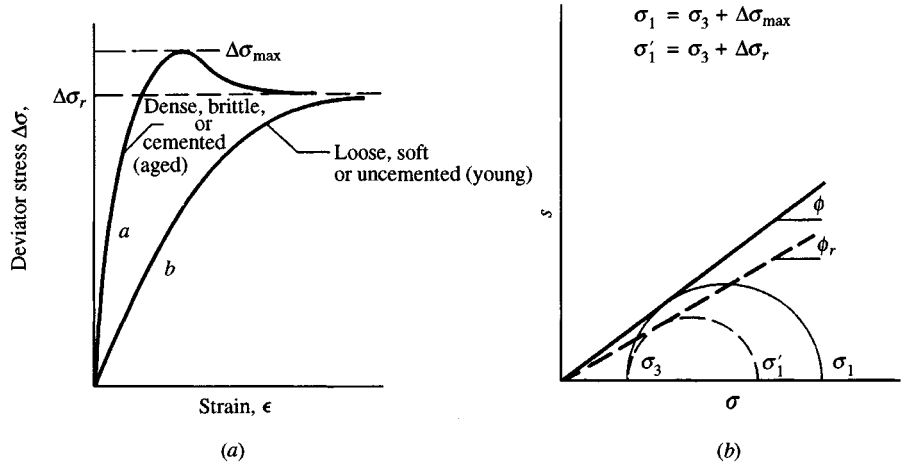

Figure 2-34 Residual soil strength. (*a*) Stress-strain plot applicable for any soil. (*b*) Mohr's circle qualitatively shown for a dense sand. For "loose" or "soft" soils σ_{max} may be defined at a specified strain (for example, 20 percent).

considerations to make a blanket recommendation to use either this or that particular strength value in any general-use publication such as this.

2-11.9 Shear Strength Correlations and the s_u/p_o' Ratio

Shear strength correlations or parameters are widely used for both preliminary and final design studies. For example, shear tests on cohesionless soils are seldom made to obtain ϕ. Instead, tabulated values as in Table 2-6 or values from in situ testing as in Table 3-4 are commonly used.

The drained angle of internal friction of cohesive soils can be estimated from correlations such as those in Fig. 2-35. This figure represents a best-fit set of curves from plotting a very large number of tests. The scatter is substantial, and some of the more extreme values have been plotted to alert the user. Note that, whereas some of the scatter is inevitable as a result of the heterogeneity of soils, some is due to the difficulty in reproducing w_L and w_P values between different laboratory technicians and laboratories. This difficulty is due both to technician skill and poorly adjusted liquid limit test equipment.

Normalized material behavior is obtained when a parameter of significance divided by another parameter gives a unique relationship. Generally normalization is discovered by simple trial, with the objective of reducing the property of interest to some quantity that displays a definite trend (a plot without substantial scatter of data points). The modulus of elasticity is a normalized parameter that is common for all elastic materials. The s_u/p_o' ratio is one that has been in use since the late 1940s, when many clay soils were found (by trial) to exhibit normalized behavior between the ratio of the undrained shear strength s_u, the in situ overburden pressure p_o', and some index property I_i in a generalized form as

$$s_u/p_o' = A_o + f(I_i)^k$$

TABLE 2-6
Representative values for angle of internal friction ϕ

Soil	Type of test*		
	Unconsolidated-undrained, U	Consolidated-undrained, CU	Consolidated-drained, CD
Gravel			
Medium size	40–55°		40–55°
Sandy	35–50°		35–50°
Sand			
Loose dry	28–34°		
Loose saturated	28–34°		
Dense dry	35–46°		43–50°
Dense saturated	1–2° less than dense dry		43–50°
Silt or silty sand			
Loose	20–22°		27–30°
Dense	25–30°		30–35°
Clay	0° if saturated	3–20°	20–42°

*See a laboratory manual on soil testing for a complete description of these tests, e.g., Bowles (1992).

Notes:

1. Use larger values as γ increases.
2. Use larger values for more angular particles.
3. Use larger values for well-graded sand and gravel mixtures (GW, SW).
4. Average values for gravels, 35–38°; sands, 32–34°.

Figure 2-35 Correlation between ϕ' and plasticity index I_p for normally consolidated (including marine) clays. Approximately 80 percent of data falls within one standard deviation. Only a few extreme scatter values are shown [*Data from several sources: Ladd et al. (1977), Bjerrum and Simons (1960), Kanja and Wolie (1977), Olsen et al. (1986).*]

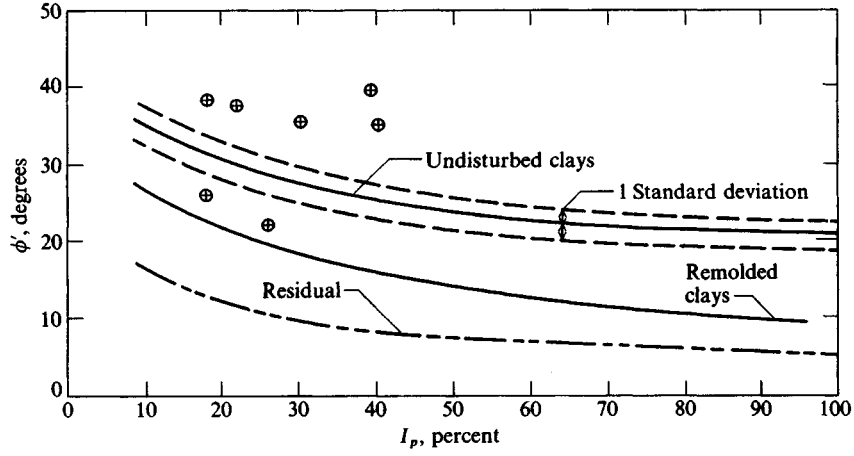

Following are several correlations of this general form for *normally consolidated* clays:

1. Bjerrum and Simons (1960) provided Eq. (2-59) as a best fit to curves given in Figs. 7 and 8 of their work:

$$s_u/p'_o = 0.45(I_P)^{1/2} \qquad I_P > 0.5 \tag{2-59}$$

This equation has a scatter in the range of ±25 percent. Using the liquidity index [see Eq. (2-14)] they derived an approximation of

$$s_u/p'_o = 0.18(I_L)^{1/2} \qquad I_L > 0.5 \tag{2-59a}$$

In both of these equations, use the plasticity index and liquidity index as *decimal entries.* Equation (2-59*a*) has an estimated scatter of ±30 percent.

2. A linear equation[21] for the s_u/p'_o ratio for nc clays was presented earlier in curve form by Skempton and Henkel (1953, Figs. 8 and 9) which can be approximated from the plots as

$$s_u/p'_o = 0.11 + 0.0037I_P \tag{2-60}$$

In this equation use I_P in *percent* and *not decimal.*

3. Karlsson and Viberg (1967) suggest

$$s_u/p'_o = 0.5w_L \qquad w_L > 0.20 \tag{2-61}$$

where the liquid limit w_L is a *decimal value.* This equation has a scatter of about ±30 percent.

All of the preceding equations are for a *normally consolidated* soil. For design purposes use as many of these equations as possible and average the several values (unless there is a large scatter) for a best design value. If there is a substantial scatter in the computed values give strong consideration to doing some laboratory testing.

A specific methodology termed SHANSEP[22] that is based on normalization of select soil properties has been proposed and used since the mid-1970s at the Massachusetts Institute of Technology (MIT). Ladd et al. (1977) give an extensive discussion on normalizing soil parameters for use in the SHANSEP method.

ESTIMATING THE s_u/p'_o RATIO FOR PRECONSOLIDATED SOILS. The Ladd et al. (1977) reference also gave a means of estimating the OCR strength, as illustrated in Fig. 2-36, based on direct simple shear (DSS) tests. The original plot used five soils: three from the northeastern United States, one from Louisiana, and one from Bangkok, Thailand. The liquid limits (for all but the varved clay) ranged from 41 to 95 percent, and I_L ranged from 0.8 to 1.0. These clays were tested in CK_oUDSS at OCR from 1 to large values with the undrained shear strength s_u results normalized using the laboratory (or existing) **effective** overburden pressure p'_o as follows:

Compute $A = s_{u,nc}/p'_o$ and $B = s_{u,OCR}/p'_o$.
Compute B/A and plot this versus OCR.

[21]This equation has been attributed to a later Skempton reference by Anderson (1982) and others. It is rounded somewhat and given by Peck et al. (1974) but attributed to a different source.

[22]An acronym for Stress History And Normalized Soil Engineering Properties (or Parameters)

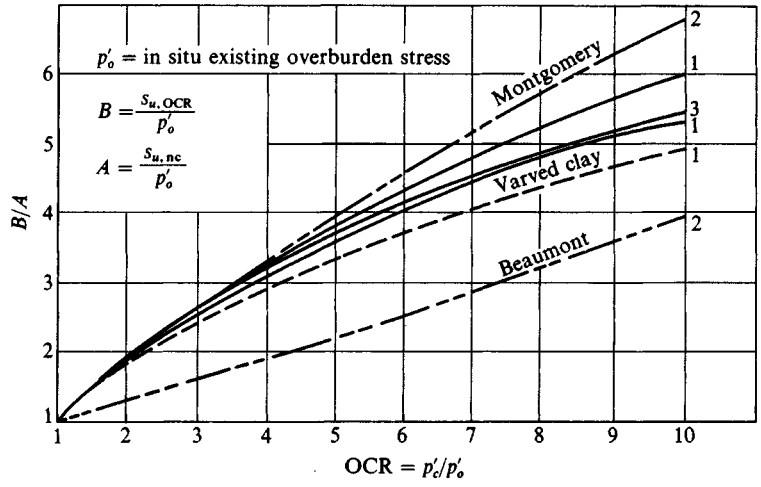

Code	Source
1	CK_o UDSS [Ladd et al. (1977) and Koutsoftas and Fischer (1976)]
2	CIUC [Mahar and O'Neill (1983)]
3	CIUC [Simons, 1960]

Figure 2-36 Ratio (B/A) of overconsolidated to normally consolidated clays. Clays range from inorganic to organic and highly dessicated (code 2). Code 1 covers five clays, code 2 is same locale but two separate strata, code 3 is from Oslo, Norway.

It is evident that at OCR = 1 we would obtain $B/A = 1$ (at least within test limitations). Also with the overburden pressure p'_o the same for both OCR = 1 and OCR > 1, we have the relationship

$$B/A = s_{u,\text{OCR}}/s_{u,\text{nc}}$$

The more general form of B/A allows one to use a laboratory value of p'_o that may be different from the field value. The initial curve has only a modest scatter and would appear useful for almost any clay. Other test data from Mahar and O'Neill (1983) and Simons (1960) have been plotted by the author onto this curve (codes 2 and 3), and it is evident that both test procedure[23] and type of soil may be significant. The general curve trends are still present and these curves may be useful for similar soils and the same local test method. This set of curves will become more valuable as users contribute to the data base so that additional soils with OCR > 1 can be plotted on it.

This type of curve has two uses, as illustrated by the following examples, which implicitly assume the solid curves (test code 1 of Fig. (2-25), are representative.

For both normally and overconsolidated soils, Mayne (1982) gives an equation for correlation with CIUC, CK_oUC, and (anisotropically consolidated) CAUC triaxial compression

[23]The s_u/p'_o ratio for normally consolidated clays is on the order of 5 to 12 percent larger in CIU tests than in CK_oU tests [see Mitachi and Kitago (1976), who also cite other sources].

and extension tests as

$$\frac{s_u}{p'_o} = \frac{M}{2}\left(\frac{\text{OCR}}{2.71828}\right)^{(1-C_s/C_c)} \tag{2-62}$$

The M term is the slope of the critical state line and is defined by the following equations:

$$M_{\text{comp}} = \frac{6\sin\phi'}{3-\sin\phi'} \qquad M_{\text{exten}} = \frac{6\sin\phi'}{3+\sin\phi'}$$

The terms C_s (swell or rebound) and C_c (compression index) are conventional consolidation test parameters that have been previously defined [see Fig. 2-17*a* and Mayne (1980)].

Example 2-4.

Given. From a consolidation test one obtained $p'_c = 250$ kPa. From field exploration at the depth of interest p'_o was 50 kPa. From the depth of interest $s_{u,\text{nc}}$ of a *remolded* K_o consolidated sample is 60 kPa (consolidation pressure used $= p'_o = 60$).

Required. Estimate the field value of $s_{u,\text{OCR}}$. (One might question why we did not obtain a sample and measure s_u directly, but assume for the example we did not.)

Solution. For the normally consolidated case $s_{u,\text{nc}} = 60$ kPa. Also, OCR $= p'_c/p'_o = 250/50 = 5$.

From Fig. 2-36 obtain $B/A = 3.7$ (visual interpolation between solid curve lines at OCR $= 5$). Thus,

$$s_{u,\text{OCR}} = 3.7(s_{u,\text{nc}}) = 3.7(60) = \mathbf{220\ kPa}\ \text{(rounded)}$$

////

Example 2-5.

Given. Same data as in Example 2-4 except we did not do a consolidation test and we did obtain an average value of $s_{u,\text{OCR}} = 220$ kPa.

Required. Estimate the in situ OCR.

Solution. Compute $A = s_{u,\text{nc}}/p'_o = 60/50 = 1.2$. Compute $B = s_{u,\text{OCR}}/p'_o = 220/50 = 4.4$. Compute $B/A = 4.4/1.2 = 3.7$ and enter abscissa of Fig. 2-36 and project to the average of the two curves and down to obtain OCR $\cong$ **5**.

It is evident that if this latter value of OCR is approximately the in situ value, then Fig. 2-36 has much value, for this determination of OCR is much less expensive than performing a consolidation test—unless the consolidation data are needed for settlement studies.

////

Example 2-6. Redo the OCR part of Example 2-2 and see if Eq. (2-25) has more merit than indicated in that example.

Given.

OCR $= 1$	$\phi' = 20°$	$I_P = 35$ percent
OCR $= 5$	$\phi' = 25°$	$I_P = 32$ percent

Previously found in Example 2-2.

$$K_{o,\text{nc}} = 0.58 \qquad K_{o,\text{OCR}} = 1.14 \text{ and } 1.15$$

and $K_{o,\text{OCR}} = 0.62$ from Eq. (2-25) using $0.58(0.8 + 0.27) = 0.62$.

Solution. Here, use Fig. 2-36 with Eq. (2-59) to find $s_{u,\text{nc}}/p'_o$:

$$s_{u,\text{nc}}/p'_o = 0.45(I_P)^{1/2} = 0.45(0.35)^{1/2} = 0.267$$

This is also the A in the B/A ratio used in Fig. 2-36.

From Fig. 2-36, using OCR = 5 and the average of the upper four curves, obtain

$$B/A \cong 3.5 \rightarrow B/0.267 = 3.5$$
$$B = 3.5(.267) = \mathbf{0.93}$$

Substituting into Eq. (2-25), we have

$$K_{o,\text{OCR}} = 0.58(0.8 + 0.93) = \mathbf{1.00} \text{ (and does not appear unreasonable)}$$

Now the "best" estimate is

$$K_{o,\text{OCR}} = \frac{1.00 + 1.15 + 1.14}{3} = \mathbf{1.10}$$

One would probably use some value between 1.00 and 1.12 since Eq. (2-25) is based on regression on a large base of reported data and similarly for Fig. 2-36 so that 1.00 may be more nearly correct than either 1.15 or 1.14. In other words, give this value more "weight" for design.

////

2-12 SENSITIVITY AND THIXOTROPY

The ratio of the undisturbed shear strength of a cohesive soil to the remolded strength at the same water content is defined as the *sensitivity* S_t:

$$S_t = \frac{\text{Undisturbed strength}}{\text{Remolded strength}} \tag{2-63}$$

For the unconfined compression test this is

$$S_t = \frac{q_{u,\text{undisturbed}}}{q_{u,\text{remolded}}} \tag{2-63a}$$

Clays may be classified as follows:

	S_t	Comments
Insensitive	≤ 4	Majority of clays
Sensitive	$4 < S_t \leq 8$	
Extrasensitive	> 8	Use with caution

Marine and lake clays and organic silts with high water content may have no measurable remolded strength. In any case, if disturbance causes a significant strength reduction, great

care is required in using the site, since an unanticipated disturbance (perhaps as little as driving a heavy tractor over it) has the potential of converting the deposit into a viscous fluid.

Thixotropy is the regain of strength from the remolded state with time. All clays and other soils containing cementing agents exhibit thixotropic properties. When the strength gain is from pore-pressure dissipation, this is not thixotropy. Piles driven into a soft clay deposit often have very little load-carrying capacity until a combination of aging/cementation (thixotropy) and dissipation of excess pore pressure (consolidation) occurs. Remolded quick clays ($S_t >$ 16) have been found to recover very little of the original strength in reasonable time lapses (on the order of under four months [Skempton and Northey (1952)].)

2-13 STRESS PATHS

A stress path is a locus of stress points developed by stress changes in the soil and can be either obtained from, say, points obtained from Mohr's stress circle or directly computed. Stress paths can be used to plot stress changes both in laboratory soil samples and in situ. They have value in giving insight into probable soil response—particularly if a part of the previous history stress path can be either reproduced or estimated. A careful study of the stress path concept may lead to a better organized laboratory test program. A particular advantage of a stress path is that it provides greater clarity than what one obtains from a series of Mohr's circles, which often overlap.

Stress paths can be plotted in a number of ways; however, the method now most widely used [apparently first used by Simons (1960)] and later called a stress path by Lambe (1964, 1967) uses p-q coordinates defined on Fig. 2-37. Stress path coordinates may be in terms of total (TSP) or effective (ESP) values. Since the effective stresses are

$$\sigma_1' = \sigma_1 - u \qquad \text{and} \qquad \sigma_3' = \sigma_3 - u$$

on adding and subtracting, respectively, and dividing by 2 we find

$$p' = p - u \qquad \text{and} \qquad q' = q$$

Thus, the effective stress path is shifted along the p axis by the pore pressure, which may be (+) or (−). The pore pressure used above should include the static value u_s as well as any excess developed during shear, usually designated Δu.

As shown on Fig. 2-37 for test 3(p_3', q_3'), the p-q values locate the origin (p) and the diameter (q) of a Mohr's circle. It is evident that $2q$ = deviator stress at some value of cell pressure and axial stress in a triaxial test. The q parameter is also the current maximum shear stress.

Stress path concepts will be illustrated in Figs. 2-37 through 2-41. Figure 2-37 is the stress path (here the K_o line) as developed in situ for a normally consolidated sedimented deposit. It must start from $q = p = 0$ because the first deposition has no overburden pressure and thus $\sigma_v = \sigma_h = 0$. Mohr's circles can be plotted as the deposit depth z increases (as partially shown for clarity) and the locus of p-q points thus traced representing the K_o stress path. Note that this is an effective stress path from the definition of K_o previously given.

Figure 2-38 is a triaxial CK_oUC test of a normally consolidated clay. The K_o consolidation uses σ_3 = in situ value (obviously somewhat estimated) and increasing σ_1 to the present effective overburden value p_o'. By definition of K_o consolidation, the excess pore pressure Δu is zero at this point. For the plot we will have adjusted total stresses by the static pore

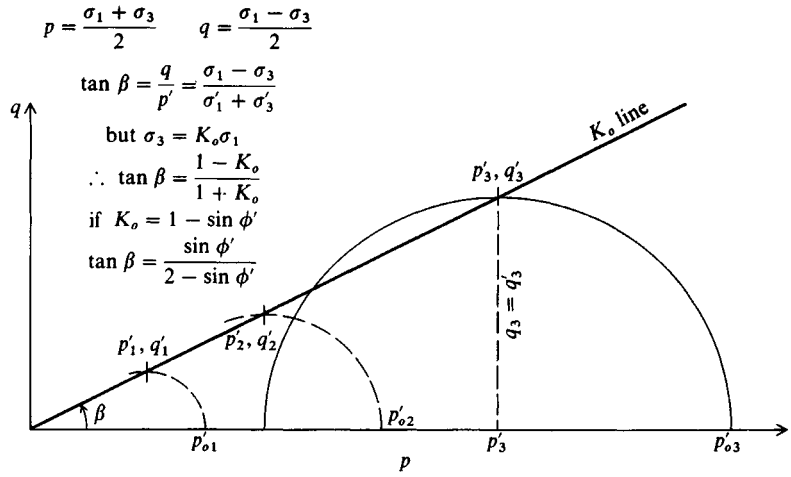

(*a*) Mohr's circles and resulting ESP (K_o line).

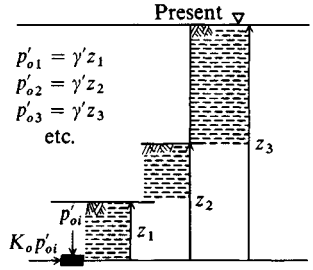

(*b*) Deposit formation.

Figure 2-37 Stress path (with Mohr's circles partially shown) for several stages of deposition in a normally consolidated soil deposit.

pressure u_s, so what is shown are effective stresses. Now as we start the test from the K_o point we increase the axial stress $\Delta\sigma_1$, which, in undrained compression, produces excess pore pressures Δu. If these Δu values are plotted they produce a TSP[24] as shown. By measuring Δu we can plot ESP (or approximate it) with a straight line if we only measure the pore pressure at peak (failure) stress Δu_f. The TSP from several tests allows one to draw a best-fit K_f line and from ESP points a best-fit K'_f line. These lines represent the ratio of q/p at failure and for either total or effective stresses and corresponding principal stress values. Observe the difficulty with data plotting and interpretation for a single test at several load stages in Fig. 2-38*a* compared to the relatively clean stress path plots of Fig. 2-38*b*. From this stress path plot note these features:

1. The path AB' is of little interest here as it merely reproduces the in situ stresses. Its slope along with the rest of the TSP is 45°. From the graphics shown, it should be evident that the TSP always has this slope.

[24]Actually a (total $- u_s$) stress path symbolically given as ($T - u_s$) SP.

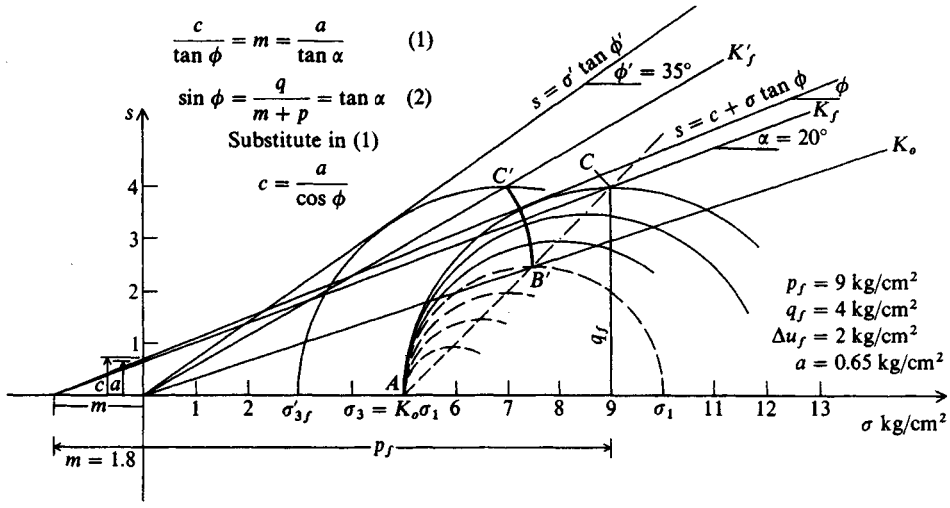

(*a*) Mohr's circles for test 2 of a CK_oUC series on a normally consolidated clay. It should be evident why additional tests are not shown on plot for general reader interest.

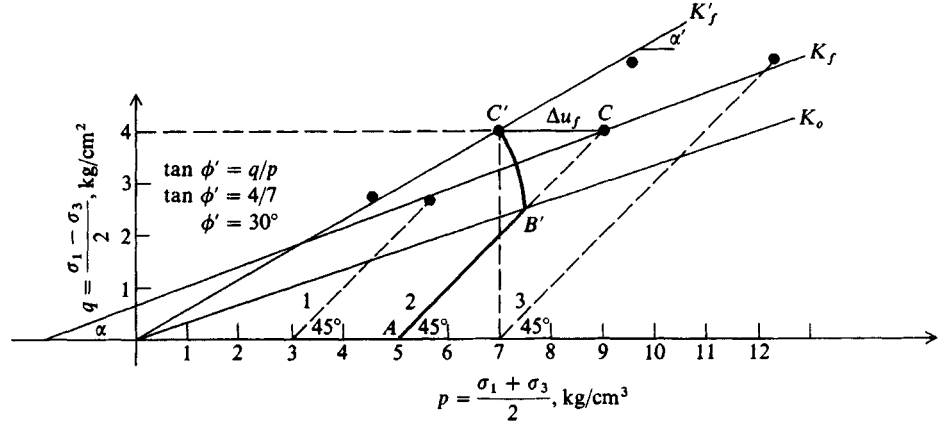

(*b*) Stress path plot or $p = q$ of part *a* plus two additional tests not shown on part *a*.

Figure 2-38 Triaxial tests (CK_oUC) for normally consolidated clay displayed using Mohr's circles and as a stress path plot.

2. The ESP is $B'C'$ and the TSP is $B'C$. These two stress paths are of interest. $B'C$ is usually curved if intermediate values of Δu are obtained. Otherwise there are only the two endpoints (starting and ending) if only Δu_f is measured.
3. There is usually an intercept a from the K_f line for cohesive soils but a is very nearly zero for the K'_f line for normally consolidated soils and all cohesionless soils. From a and slope angle α we can compute total shear stress parameters c and ϕ as shown on Fig. 2-38*a*. We can also compute effective stress parameters in a similar manner. The distance m is common to both the s line and the K_f line as shown here.

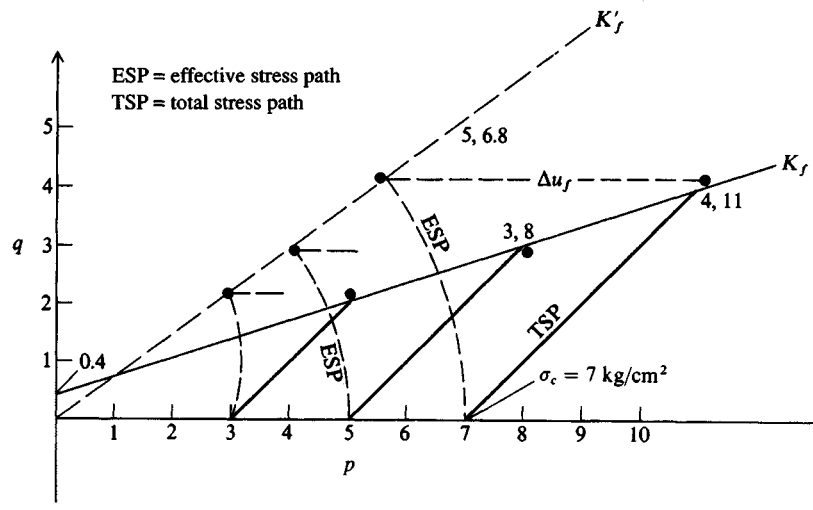

Figure 2-39 A series of CIU triaxial tests on a cohesive soil. This is the usual method of making triaxial tests; however, pore-pressure measurements are less common.

Figure 2-39 is the more usual case of a consolidated undrained triaxial test that uses isotropic consolidation (CIU test). Inspection of this and Fig. 2-38 indicates that the principal difference between an isotropic and an anisotropic consolidation (aside from the great difficulty of carrying out the consolidation) is that the CK_oU test starts at $q > 0$ whereas the CIU test always starts at $q = 0$ and p = cell pressure σ_c. In both cases $\Delta u = 0$ at the end of consolidation and the start of applying a stress change. Again the starting point is (or should be) adjusted for static pore pressure $u_s = \gamma_w h_w$.

Figure 2-40 illustrates the four possibilities for stress changes in a triaxial test and the corresponding field applications. Observe that point A may be at the end of either isotropic (shown) or anisotropic consolidation (as point B' of Fig. 2-38). Note that cases 2 and 4 are not easy since changing σ_h (if it is a cell pressure) requires simultaneous adjustment of the axial stress σ_v so that it is kept constant.

These four cases will be quantitatively illustrated in Fig. 2-41 using the numerical data for the tests as indicated, together with the following comments:

Test 1. Initial cell pressure $\sigma_1 = \sigma_3 = 470$ kPa. Decrease lateral pressure and maintain constant vertical pressure = 470 kPa (compression test with decreasing lateral pressure). Sample "fails" at $\sigma_3 = 118$ kPa.

Test 2. Initial cell pressure = 470 kPa. Increase vertical pressure with lateral pressure = 470 kPa (standard compression test). Sample "fails" at $\sigma_1 = 1176$ kPa.

Test 3. Initial cell pressure = 470 kPa. Decrease vertical pressure and hold lateral pressure constant (extension test—decreasing vertical pressure).

Test 4. Initial cell pressure = 470 kPa. Increase horizontal pressure to 1176 kPa and hold vertical pressure constant (extension test with constant vertical pressure).

From these several plots, it should be evident that the K_f line of slope q/p always intersects the p axis, but may be at a $(-)p$ value (m distance). It should also be evident that this

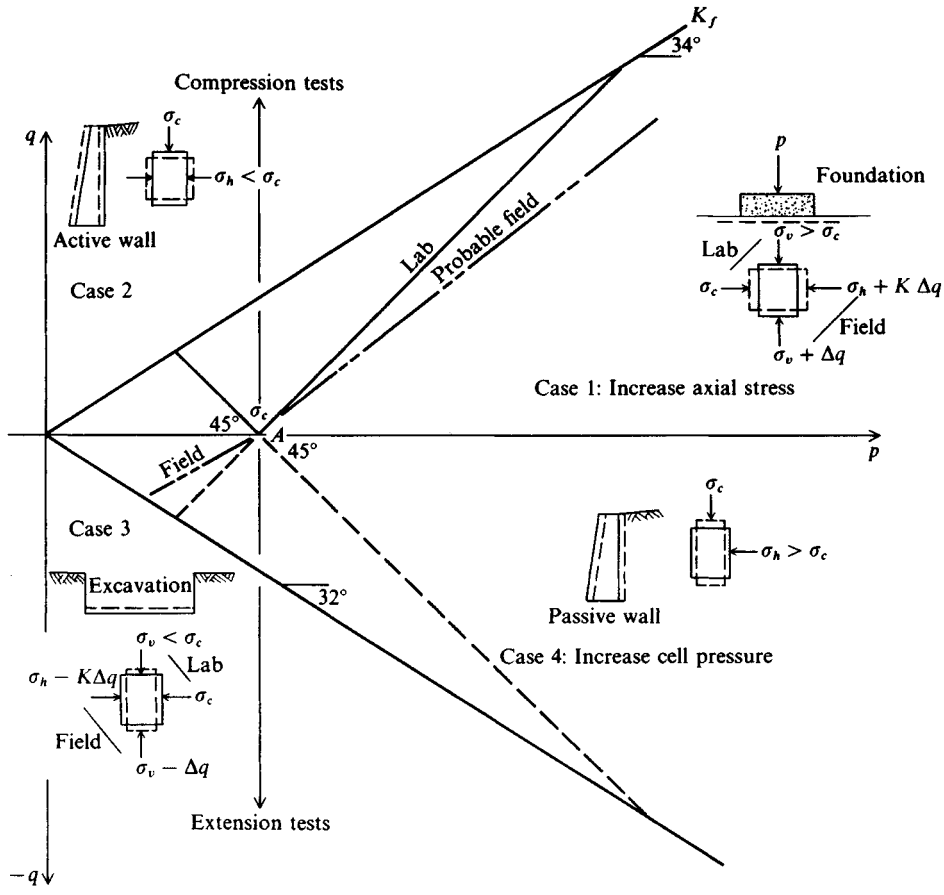

Figure 2-40 Four possible stress paths from either compression or extension triaxial tests and the corresponding field cases. Note that case 1 and case 3 can be duplicated by laboratory tests only with great difficulty as the vertical stress field changes result in lateral stress changes of some amount K (not K_o or K_f) as shown so that the resulting stress path is not 45° from horizontal as are cases 2 and 4.

intersection point is also common to the shear stress envelope s because of the Mohr's circle relationship.

Figure 2-42 illustrates the stress path to produce an overconsolidated cohesive soil using a consolidation (or oedometer) test as an illustration. This is similar to field overconsolidation from sedimentation. Steps are as follows:

1. Sample is K_o consolidated at point A under a vertical stress of 50 kPa, which produces a lateral stress σ_h against the confining ring of $K_o\sigma_v = 28$ kPa. It is computed or directly scaled form Mohr's circle as σ_3 if the slope of the K_o line is known so that it can be drawn prior to any Mohr's circles since a 45° slope from $\sigma_1 (= 50$ kPa) intersects K_o at A.
2. Now we add the next load increment of 50 kPa (doubling the stress) so that $\sigma_v = \sigma_1 = 100$ kPa. This moves the stress circle at constant diameter laterally along the p axis 50 kPa, because without immediate pore drainage the $\Delta\sigma_1$ is carried by the pore water as excess pore pressure $\Delta u = 50$ kPa. As drainage occurs, Mohr's circles form with a

Test	σ_1	σ_3, kPa	p	q
1	470	118	294	176
2	1176	470	823	353
3	118	470	294	−176
4	470	1176	823	−353

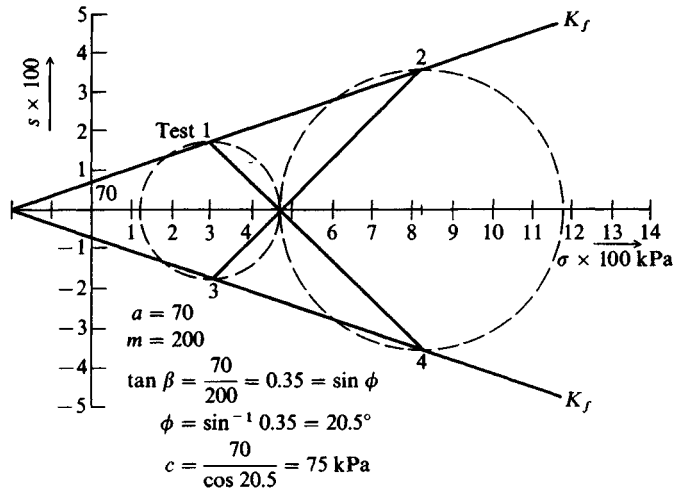

Figure 2-41 Stress paths for the four basic triaxial tests.

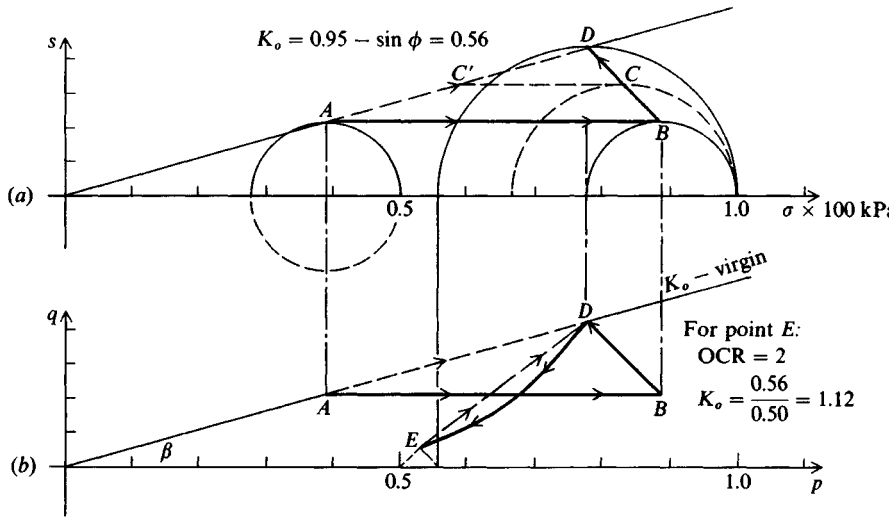

Figure 2-42 Stress paths for a consolidation test.

locus of TSP points along path *BD*. The ESP is, of course, along the K_o line from to *A* to *D* (definition of K_o). After some time elapses, the *p-q* coordinates of point *D* are developed and consolidation is complete with

$$\sigma_v = 100 \text{ kPa}$$
$$\sigma_h = K_o\sigma_v = 56 \text{ kPa (scaled or computed)}$$

3. We will now remove 50 kPa (leaving a total vertical stress of $\sigma_v = 50$ kPa). At this point we have known effective stresses of $\sigma_v = 50$ kPa and a "locked in" lateral stress of 56 kPa represented by point *E*. The stress path from *D* to *E* is uncertain because of sample swell and some slight reduction in lateral stress from ring tension previously developed, but we can approximate it as shown (or by a straight line). Point *E* is located using 45° slopes from $\sigma_v = 50$ and $\sigma_h = 56$ kPa as shown.

If we then reapplied the 50 kPa stress increment we would traverse the dashed line from *E* back to approximately the point *D* previously located. We say approximately for two reasons:

a. In a consolidation test the ring will expand and contract under lateral stresses from hoop tension.

b. There are secondary compression (or creep) effects.

In any case, remolded laboratory samples tested in this manner never exactly reproduce the "preconsolidation" point *D*. Usually the recovered point is to the right of the original (or below it on an *e* versus log *p* plot).

This unload-reload cycle is similar to recovery of an in situ sample, except sample recovery reduces σ_v to zero and the subsequent application of load increments extends beyond the original preconsolidation load. In Fig. 2-42 we know the OCR at stage 3 (point *E*) and can compute it and the current $K_{o,E}$, which is not the same as $K_{o,D}$. Note that from the figure $K_{o,\text{nc}} = 0.56$ and for OCR = 2 the overconsolidated value is $K_{o,\text{OCR}} = 1.12$. The test procedure here produced the same change in K_o as the OCR. In field soils, secondary compression and other factors do not maintain this ratio (as previously observed in Sec. 2-8). Another essential consideration is that the static pore pressure u_s in the lab on a 20–25 mm thick sample is negligible, where in the field it probably is not.

The use of stress paths will be illustrated in the following example.

Example 2-7.

Given. A square footing 4 m × 4 m overlies a dense sand of $\gamma = 20$ kN/m^3. The footing contact pressure is $q_o = 250$ kPa. Taking $K_o = 0.4$ [from Eq. (2-18*a*)] estimate the stress path at 2-m depth for a similar triaxial test to obtain strain data for this load ϵ_2 so that a settlement increment from 1 to 3 m can be computed as $\Delta H_2 = \epsilon_2$ (2 m).

Solution. Refer to Fig. E2-7.

1. Plot K_o.
2. Compute $\Delta q_{v,2}$ from the vertical stress profile of Fig. 1-1*a* at $D/B = 2/4 = 0.5$ ($D = 0.5B$),

$$\Delta q_{v,2} = \text{factor} \times q_o = 0.7(250) = 175 \text{ kPa}$$

3. Compute $\Delta q_{h,2} = K_o\Delta q_{v,2} = 0.4(175) = 70$ kPa.

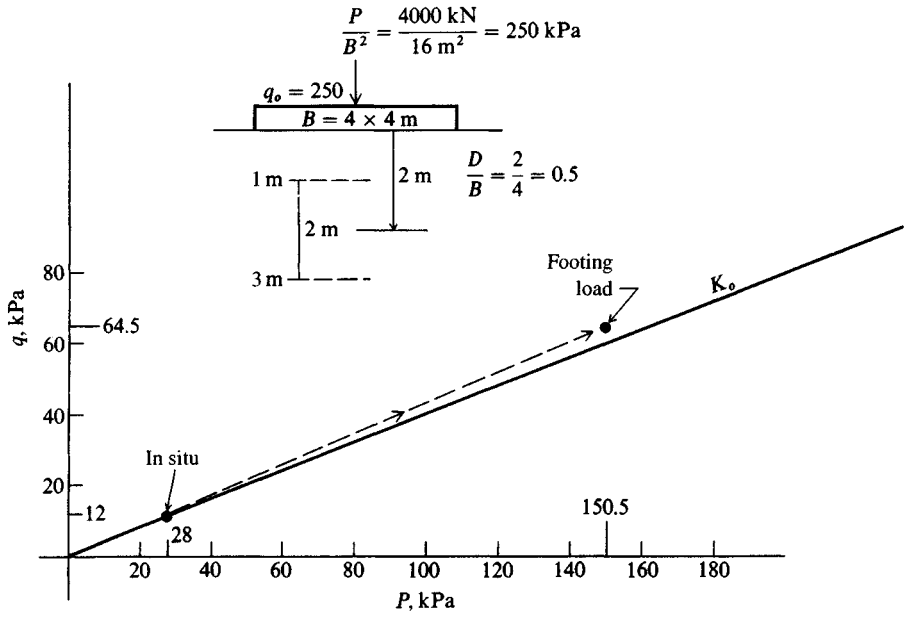

Figure E2-7

4. Compute initial in situ p_o and σ_h:

$$p_o = \gamma z = 20(2) = 40 \text{ kPa}$$
$$\sigma_h = K_o p_o = 0.4(40) = 16 \text{ kPa}$$

5. Initial conditions p and q (using equations on Fig. 2-37) are

$$p = \frac{p_o + \sigma_h}{2} = \frac{40 + 16}{2} = \mathbf{28}$$
$$q = \frac{p_o - \sigma_h}{2} = \frac{40 - 16}{2} = \mathbf{12}$$

6. The footing stress q_o increases both the vertical and lateral stresses at this point by the amounts computed in step 2 above, so the endpoints of the stress path are computed as

$$p_e = \frac{(p_o + \Delta q_{v,2}) + (\sigma_h + \Delta q_{h,2})}{2} = \frac{(40 + 175) + (16 + 70)}{2} = \mathbf{150.5}$$
$$q_e = \frac{(40 + 175) - (16 + 70)}{2} = \mathbf{64.5}$$

7. The process of plotting $p = 28$, $q = 12$ (is on K_o line) and endpoints $p = 150.5$ and $q = 64.5$ and connecting with a straight line gives the dashed stress path as shown on Fig. E2-7.
8. Perform a triaxial test to duplicate this stress path as nearly as possible for data to make a stress-strain plot to obtain ϵ_2.

////

2-14 ELASTIC PROPERTIES OF SOIL

Hooke's generalized stress-strain law is commonly used in solving geotechnical problems of stress and settlement. In equation form Hooke's stress-strain law for any homogeneous, isotropic, elastic material is

$$\epsilon_x = \frac{1}{E_s}(\sigma_x - \mu\sigma_y - \mu\sigma_z)$$
$$\epsilon_y = \frac{1}{E_s}(\sigma_y - \mu\sigma_x - \mu\sigma_z) \tag{2-64}$$
$$\epsilon_z = \frac{1}{E_s}(\sigma_z - \mu\sigma_x - \mu\sigma_y)$$

The signs here are based on using (+) μ of Eq. (*b*) following.

In matrix notation Eq. (2-64) can be written as

$$\boldsymbol{\epsilon} = \mathbf{D}\boldsymbol{\sigma} \tag{2-64a}$$

where the matrix **D** is the following

$$\mathbf{D} =$$

ϵ \ σ	1	2	3
1	1	$-\mu$	$-\mu$
2	$-\mu$	1	$-\mu$
3	$-\mu$	$-\mu$	1

The *shear modulus* G' (which may be subscripted) is defined as the ratio of shear stress s_s to shear strain ϵ_s.[25] It is related to E_s and μ as

$$G'_s = \frac{s_s}{\epsilon_s} = \frac{E_s}{2(1+\mu)} \tag{a}$$

Poisson's ratio μ is used in both pressure and settlement studies and is defined as the ratio of axial compression ϵ_v to lateral expansion ϵ_L strains, or

$$\mu = \frac{\epsilon_L}{\epsilon_v} \tag{b}$$

The μ ratio has a (+) sign in this equation if ϵ_v is compressive strain and the lateral strain ϵ_L causes the lateral dimension to increase. In a tension test the sign is (+) if the sample ϵ_v produces elongation while the lateral dimension(s) decrease. The shearing strain ϵ_s is defined as the change in right angle of any corner of an element in compression as illustrated in

[25]The shear modulus in structural mechanics literature often uses the symbol G_i, where i may be s = steel; c = concrete; etc. Since G_s is used in geotechnical work for the specific gravity of the soil solids, the closest symbol to the "literature" is G'.

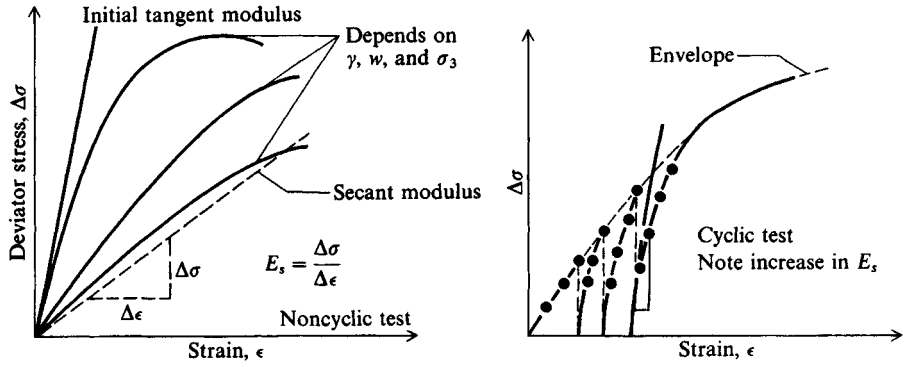

(*a*) Stress-strain modulus.

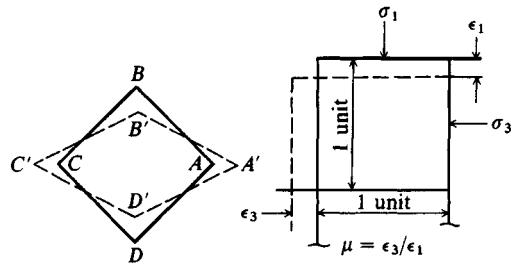

(*b*) Poisson's ratio, μ [(+) as shown].

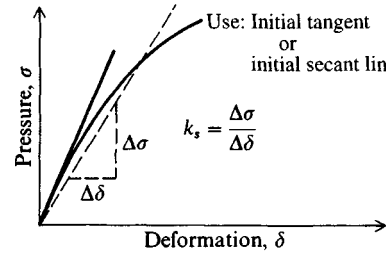

(*c*) Modulus of subgrade reaction.

Figure 2-43 Elastic properties of soil.

Fig. 2-43*b* such that

$$\epsilon_s = \text{angle } BCD - \text{angle } B'C'D' \tag{c}$$

Another concept occasionally used is the volumetric strain, ϵ_v defined using initial mass volume V and volumetric change ΔV as

$$\epsilon_v = \frac{\Delta V}{V} = \epsilon_1 + \epsilon_2 + \epsilon_3 \tag{d}$$

The subscripts x, y, and z may be substituted for 1, 2, and 3 in this equation.

In confined compression tests (such as the consolidation test described in Sec. 2-10 or for the compression beneath the tip of a pile in situ) the lateral strain (ϵ_2, ϵ_3) is taken as 0.0. Making these substitutions in Eqs. (2-64) and solving for $\epsilon_1 = \epsilon_v$, one can obtain the following:

$$\epsilon_v = \frac{(1+\mu)(1-2\mu)\sigma_1}{E_s(1-\mu)} = \frac{1-2\mu}{2(1-\mu)}\frac{\sigma_1}{G'} \tag{e}$$

Since this textbook uses the z axis as the vertical axis, you may use σ_z for σ_1 in this equation. Of interest is that for $\mu = 0.5$, this equation gives the volumetric strain $\epsilon_v = 0.0$; i.e., there is no volume change in the soil. Also, for $\mu = 0$ the volumetric strain is $\epsilon_v = \sigma_z/E_s = \epsilon_z$. The volumetric strain was used to plot ϵ versus log p of Fig. 2-16*b*.

TABLE 2-7
Values or value ranges for Poisson's ratio μ

Type of soil	μ
Clay, saturated	0.4–0.5
Clay, unsaturated	0.1–0.3
Sandy clay	0.2–0.3
Silt	0.3–0.35
Sand, gravelly sand	−0.1–1.00
commonly used	0.3–0.4
Rock	0.1–0.4 (depends somewhat on type of rock)
Loess	0.1–0.3
Ice	0.36
Concrete	0.15
Steel	0.33

Another material property concept is the *bulk modulus* E_b, which is defined as the ratio of hydrostatic stress to the volumetric strain ϵ_v and is given as

$$E_b = \frac{2}{3}G' \frac{1+\mu}{1-2\mu} = \frac{E_s}{3(1-2\mu)} \qquad (f)$$

For an *elastic* material the shear modulus G' cannot be $(-)$, so Eq. (a) sets the lower limit of $\mu > -1$. Equation (f) sets the upper limit at $\mu < 0.5$. It appears that the range of μ for soils (that are not "elastic") is from about -0.1 to 1.00. Table 2-7 gives a range of values for select materials. It is very common to use the following values for soils:

μ	Soil type
0.4–0.5	Most clay soils
0.45–0.50	Saturated clay soils
0.3–0.4	Cohesionless—medium and dense
0.2–0.35	Cohesionless—loose to medium

Although it is common to use $\mu = 0.5$ for saturated clay soils, the reader should be aware that this represents a condition of no volume change under the applied stress σ_z. Over time, however, volume change does occur as the pore fluid drains. Equation (e) defines the Poisson's ratio that develops initially ($\epsilon_v = 0$) and also later when $\epsilon_v > 0$. Since the strain is produced from stress and Fig. 1-1 indicates a vertical variation, it necessarily follows that μ is stress-dependent from Eq. (e).

A special case in geotechnical work is that of *plane strain.* This arises where strains occur parallel to two of the coordinate axes (say the x and z) but the strain is zero perpendicular to the x-z plane (along the y axis). If we set $\epsilon_y = 0$ in the set of equations for Hooke's law [(Eqs. (2-64)] and solve for the resulting values of E_s and μ, we obtain the following:

$$E_s' = \frac{E_s}{1-\mu^2} \qquad \mu' = \frac{\mu}{1-\mu} \qquad (2\text{-}65)$$

If we take $\mu = 0.5$ and solve for the plane strain value μ', we have

$$\mu' = \frac{\mu}{1 - \mu} = \frac{0.5}{(1 - 0.5)} = 1.0$$

which is greater than the "elastic" value of 0.5. The plane strain μ' should be used in plane strain problems—and with E_s' if applicable.

The *modulus of subgrade reaction* (also *subgrade modulus* or *subgrade reaction*) is defined as (see Fig. 2-43*c*)

$$k_s = \frac{\Delta\sigma}{\Delta\delta} \tag{2-66}$$

where $\Delta\sigma$ is the increment of contact pressure and $\Delta\delta$ is the corresponding change in settlement or deformation. These data can be obtained from a plate (or footing) load test and a plot drawn as Fig. 2-43*c*. The δ versus σ plot is generally not linear, and one must obtain k_s as the slope of either a tangent or secant line. Either a tangent (solid line) or secant (dashed) line slope of Fig. 2-43*c* can be used for k_s. Usually, initial values (through the origin) are used; however, one can choose any tangent point or an averaged value using the two points cut by a secant line along the curve. The secant slope defined by the origin ($\delta = 0$) and at $\delta = 0.0254$ m (25 mm or 1 in.) giving $\Delta\delta = 0.0254$ m is recommended as an initial selection for Eq. (2-66).

The stress-strain modulus E_s, Poisson's ratio μ, and the modulus of subgrade reaction k_s are the elastic properties of most interest. These values are commonly used in computing estimates of foundation settlements. The shear modulus G' is commonly used in vibration problems of Chap. 20 to estimate foundation frequency and displacement amplitudes.

The stress-strain modulus can be obtained from the slope (tangent or secant) of stress-strain curves from triaxial tests (see Figs. 2-43*a* and 2-32). It is often estimated from field tests that are described in Chap. 3 (see also Table 5-6). Typical value ranges for several soils are given in Table 2-8. It can be seen that E_s for soils is only $\frac{1}{10}$ to $\frac{1}{100}$ that of steel and concrete.

For the CD or CU triaxial test with a cell pressure of σ_3 and a deviator stress $\Delta\sigma_1 = \sigma_1 - \sigma_3$ (the pressure applied at various load stages during the test) we may rewrite one of Eq. (2-64), say $\epsilon_z = \epsilon_1$, as

$$\epsilon_1 = \frac{1}{E_s}(\Delta\sigma_1 - 2\mu\sigma_3) \tag{g}$$

It is usual to plot ϵ_1 (computed directly as $\Delta\sigma_1/L$) versus $\Delta\sigma_1$ as shown in Fig. 2-43*a*. From this plot we should be able to solve Eq. (*g*) above for both E_s and μ by taking several pairs of points along the curve such that the curve slope is approximately constant in the interval between point pairs. If we do this, we find that $\mu > 0.5$ at very small strains and that both E_s and μ are stress-dependent. Of course, we could directly inspect Fig. 2-43*a* and readily observe that if the curve is not linear, then the stress-strain modulus E_s is not linear. This result again gives reason to term the curve "slope" the stress-strain modulus, and not the *modulus of elasticity.*

Equation (*g*) also gives clear reason why unconfined compression tests with $\sigma_3 = 0$ give larger strains (and smaller E_s) than confined compression tests. Since the soil is "confined"

TABLE 2-8
Value range* for the static stress-strain modulus E_s for selected soils (see also Table 5-6)

Field values depend on stress history, water content, density, and age of deposit

Soil	E_s, MPa
Clay	
Very soft	2–15
Soft	5–25
Medium	15–50
Hard	50–100
Sandy	25–250
Glacial till	
Loose	10–150
Dense	150–720
Very dense	500–1440
Loess	15–60
Sand	
Silty	5–20
Loose	10–25
Dense	50–81
Sand and gravel	
Loose	50–150
Dense	100–200
Shale	150–5000
Silt	2–20

*Value range is too large to use an "average" value for design.

in situ, it is reasonable for confined compression tests to produce better "elastic" parameters. Although it is difficult to compare laboratory and field E_s values, there is some evidence that field values are often four to five times larger than laboratory values from the unconfined compression test. For this reason, current practice tends to try to obtain "field" values from in situ testing whenever possible. This topic will be taken up in more detail in the next chapter.

Table 2-8 gives a range of E_s values that might be obtained. Note that the range is very large, owing to the foregoing factors as well as those factors given on the table. With this wide range of values the reader should not try to use "averaged" values from this table for design.

If laboratory test plots similar to Fig. 2-43*a* are used, it is most common to use the initial tangent modulus to compute the stress-strain modulus E_s for the following reasons:

1. Soil is elastic only near the origin.
2. There is less divergence between all plots in this region.
3. The largest values are obtained—often three to five times larger than a tangent or secant modulus from another point along the curve.

In spite of these several shortcomings for E_s the value along the curve is commonly used in finite-element analyses based on the computed stress level. This computation may require that the problem be iterated several times until the computed stress level matches the stress level that was used on the previous cycle to obtain E_s.

A number of investigators [Leonards (1968), Soderman et al. (1968), Makhlouf and Stewart (1965), Larew and Leonards (1962)] have suggested that a better initial tangent modulus for settlement analyses might be obtained by cycling the deviator stress $\Delta\sigma_1$ to about half the estimated failure stress several times [Leonards (1968) suggests at least five cycles] and then compressing the sample to failure in the CU triaxial test. The initial tangent modulus (may be called E_r) by this method may be three to five times larger than E_s obtained on the first cycle (see Fig. 2-43*a*). The increase in stiffness depends on the initial soil state and on sample disturbance. This stress-strain modulus is a static value.

Cyclic tests using low-amplitude strains and frequencies (or stress reversals) in the range of $\frac{1}{6}$ to 10 Hz are used to obtain dynamic values of E_s and G'. The dynamic values (considered in more detail in Chap. 20) may be from two to ten times the static value.

Both E_s and Poisson's ratio μ are heavily dependent on the following:

1. Method of laboratory test (confined, unconfined, undrained, drained).
2. Degree of confinement. E_s increases from a minimum value in the unconfined compression test to very large values depending on cell pressure σ_c.
3. Overconsolidation ratio OCR—usually increases with OCR.
4. Soil density—E_s usually increases with depth in situ because the density usually increases (in the same stratum).
5. Water content—lower water contents tend to higher E_s. Brittle fractures at low strains occur at low water contents.
6. Strain rate (ϵ/time)—E_s is lower by a factor of 2 or more compared with values obtained at high strain rates [see Richardson and Whitman (1963)]. Field strain rates are usually, but not always, lower than in the laboratory.
7. Sample disturbance—usually reduces E_s from in situ value.

These several factors mean that considerable judgment is required to obtain a reasonably reliable value for design use.

The stress-strain curve for all soils is nonlinear except in a very narrow region near the origin. Kondner (1963) proposed that the stress-strain curve (Fig. 2-44*a*) could be represented by a hyperbolic equation of the form

$$\sigma_1 - \sigma_3 = \frac{\epsilon}{a + b\epsilon}$$

which could be rewritten with $\Delta\sigma_1 = \sigma_1 - \sigma_3$ in linear form as

$$\frac{\epsilon}{\Delta\sigma_1} = a + b\epsilon \tag{2-67}$$

Note the similarity of Eq. (2-67) to Eq. (2-47). The left side of Eq. (2-67) can be computed for various values of deviator stress and the corresponding strain to make a linear plot as shown in Fig. 2-44*b*. Extension of the plot across the discontinuity at $\epsilon \rightarrow 0$ gives the coefficient

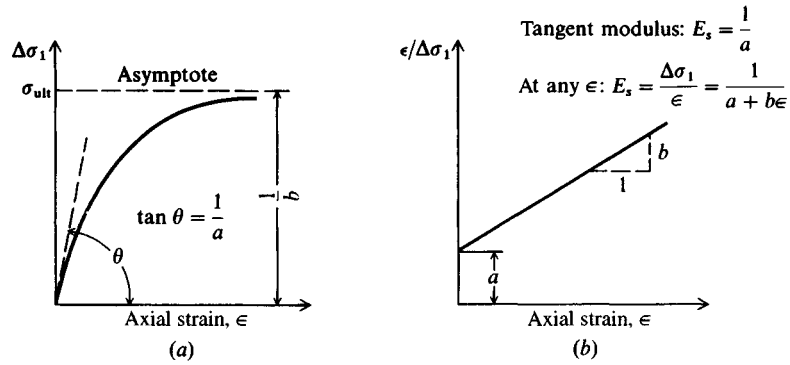

Figure 2-44 (*a*) Usual stress-strain plot—hyperbolic-curve approximation; (*b*) transformed representation of stress-strain—gives approximate linear curve as shown. [*After Kondner (1963).*].

a, and the slope is b. Although Kondner proposed this procedure for clay soils, it should be applicable for all soils with similar stress-strain curves [see Duncan and Chang (1970)]. The form of Eq. (2-67) rearranged and shown on Fig. 2-44*b* has particular value in finite-element method (FEM) analyses since it is much easier to program an equation to compute E_s based on current output ϵ than to make a search along a stress-strain curve (using a number of values of ϵ versus $\Delta\sigma_1$ input as an array). Computation time is greatly reduced when a large number of elements are in the FEM model.

The following empirical correlations may be used to estimate E_s for cohesive soils:

Normally consolidated sensitive clay:

$$E_s = (200 \text{ to } 500) \times s_u \tag{2-68}$$

Normally consolidated insensitive and lightly overconsolidated clay:

$$E_s = (750 \text{ to } 1200) \times s_u \tag{2-69}$$

Heavily overconsolidated clay

$$E_s = (1500 \text{ to } 2000) \times s_u \tag{2-70}$$

Several equations will be presented in the next chapter, based on in situ testing, that may also be used for both cohesive and cohesionless soils to compute E_s.

2-15 ISOTROPIC AND ANISOTROPIC SOIL MASSES

An *isotropic* material is one in which the elastic properties (E_s and μ) are the same in all directions. The elastic properties for *anisotropic* materials are different in the different directions. A material is homogeneous when the physical and compositional properties such as γ, void ratio, and silt or clay content are the same throughout the volume of interest.

Almost all naturally occurring soil deposits are anisotropic and nonhomogeneous. The anisotropy is produced from a combination of particle placement during deposition/formation (also called geometrical or inherent anisotropy) and from overburden pressures. In natural soils this commonly results in horizontal bedding planes that have both strength and elastic

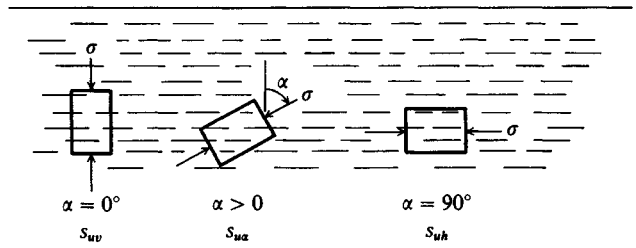

Anisotropy ratio $R = s_{uv}/s_{uh}$

$s_{u\alpha} = s_{uh}[1 + (R - 1)\cos^2 \alpha]$

s_u = undrained shear strength (see above for orientation)

Figure 2-45 Undrained shear strength for anisotropic soils.

properties different for samples stressed perpendicular and parallel to the bedding planes. This property of anisotropy has been known for some time [Casagrande and Carrillo (1944)], but only more recently have attempts been made to quantify the effects [see Yong and Silvestri (1979), Law and Lo (1976), Arthur and Menzies (1972), and Yamada and Ishihara (1979)]. Figure 2-45 illustrates anisotropy and the possible range in strength that occurs when the stress orientation is at some angle with respect to the bedding plane. This figure should also be compared with Fig. 2-25 to see how anisotropy can qualitatively affect in situ shear resistance depending on the intersection angle between the bedding plane and the potential shear plane.

Nonhomogeneous deposits are produced from particle packing versus depth, mass contamination during deposition, and lenses or strata of different materials in the depth of interest. The increase in particle packing and confining pressure with depth nearly always produces a stress-strain modulus increase in depth, which is usually nonlinear. It has been common, however, to assume a soil mass is semi-infinite, homogeneous, and isotropic, even in layered deposits, as a computational convenience. The current state-of-art is such that a soil mass can be somewhat more realistically modeled than this, albeit at some additional time and expense.

Anisotropy is an important consideration in finite-element analyses of soils, since elastic properties are input parameters. Where two elastic constants define the stress-strain relationship [Eq. (2-64)] of an isotropic material, five constants are required when a homogeneous soil is deposited in layers so that one can assume symmetry about a vertical axis. A soil deposit that meets this criterion is termed *cross-anisotropic.* Strictly, a soil is not cross-anisotropic because of depth variations, but this simplification, which may not introduce serious computational errors, has the effect of reducing 21 elastic constants of the general case to seven.

The seven elastic constants for a cross-anisotropic material (actually only five are independent) are defined as follows (*the x-z plane of isotropy is horizontal and the y axis is vertical*):

E_V = stress-strain modulus in the vertical direction

E_H = stress-strain modulus in the horizontal plane, i.e., in the plane of isotropy

$\mu_1 = \epsilon_z/\epsilon_x$ when the applied stress is σ_x

$\mu_2 = \epsilon_x/\epsilon_y$ when the applied stress is σ_y

$\mu_3 = \epsilon_y/\epsilon_x$ when the applied stress is σ_x

G'_H = shear modulus in the horizontal plane

G'_V = shear modulus in the vertical plane
τ_i = shear stress on i-plane

But

$$G'_H = \frac{E_H}{2(1 + \mu_1)}$$

and

$$\frac{\mu_2}{E_V} = \frac{\mu_3}{E_H} \tag{a}$$

So the five elastic constants for a cross-anisotropic material are G'_V, E_V, E_H, μ_1, and μ_2. A more detailed discussion on cross-anisotropic behavior of soil deposits can be found in Bhatacharya (1968).

The generalized Hooke's law for cross-anisotropic material takes the following form:

$$\left.\begin{aligned} \epsilon_x &= \frac{\sigma_x}{E_H} - \mu_2\frac{\sigma_y}{E_V} - \mu_1\frac{\sigma_z}{E_H} \\ \epsilon_y &= \frac{\sigma_y}{E_V} - \mu_3\frac{\sigma_x}{E_H} - \mu_3\frac{\sigma_z}{E_H} \\ \epsilon_z &= \frac{\sigma_z}{E_H} - \mu_1\frac{\sigma_x}{E_H} - \mu_2\frac{\sigma_y}{E_V} \\ \gamma_{xy} &= \frac{\tau_{xy}}{G'_V} \qquad \gamma_{xz} = \frac{\tau_{xz}}{G'_H} \quad \gamma_{yz} = \frac{\tau_{yz}}{G'_V} \end{aligned}\right\} \tag{b}$$

For problems of plane strain (when $\epsilon_z = \gamma_{xz} = \gamma_{yz} = 0$),

$$\sigma_z = \mu_1\sigma_x + \mu_2\frac{E_H}{E_V}\sigma_y \tag{c}$$

By substituting Eq. (*c*) in Eqs. (*b*), using Eq. (*a*) to obtain μ_3, and noting that $\gamma_{xz} = \gamma_{yz} = 0$, the following form of the generalized Hooke's law for cross-anisotropic material in plane strain is obtained:

$$\begin{aligned} \epsilon_x &= A\sigma_x + B\sigma_y \\ \epsilon_y &= B\sigma_x + C\sigma_y \\ \gamma_{xy} &= \frac{\tau_{xy}}{G'_V} \end{aligned}$$

where

$$\left.\begin{aligned} A &= \frac{1 - \mu_1^2}{E_H} \qquad B = \frac{-\mu_2 - \mu_1\mu_2}{E_V} \\ C &= \frac{1 - n\mu_2^2}{E_V} \qquad n = \frac{E_H}{E_V} \end{aligned}\right\} \tag{d}$$

Hence, the **D** matrix for plane-strain problems of cross-anisotropic materials is

$$\mathbf{D} = \begin{array}{|c|c|c|c|} \hline \epsilon \backslash \sigma & 1 & 2 & 3 \\ \hline 1 & A & B & 0 \\ \hline 2 & B & C & 0 \\ \hline 3 & 0 & 0 & \dfrac{1}{G'_V} \\ \hline \end{array} \qquad (e)$$

Thus, for plane-strain problems of cross-anisotropic materials it is only necessary to know the four parameters A, B, C, and G'_V, which can be determined [Chowdhury (1972)] as follows:

1. Perform a set of plane-strain triaxial tests with a constant cell pressure on a sample with the plane of isotropy horizontal.
2. Plot the deviator stress versus axial strain.
3. Plot the deviator stress versus lateral strain. The lateral strain can be computed from the axial strain and volume-change measurements.
4. Compute $1/B$ = slope of curve of step 3.
   $1/C$ = slope of curve of step 2.
5. Perform a plane-strain triaxial test with a constant cell pressure on a sample with the plane of isotropy vertical such that the direction of plane strain is parallel to the plane of isotropy.
6. Plot steps 2 and 3 above to obtain a second set of curves.
7. Compute $1/B$ = slope of curve of step 3 (should check reasonably with step 4).
   $1/A$ = slope of curve of step 2.
8. Test a sample with the plane of isotropy inclined at 45° to the horizontal (samples may be difficult to obtain except from a test pit).
9. Plot the deviator stress versus axial strain. The slope $d\sigma/d\epsilon$ of this curve is related to G'_V by the following equation:

$$G'_V = \frac{1}{4/\text{slope} - (A - 2B + C)} \qquad (f)$$

Thus, the four constants required to solve the plane-strain problems of cross-anisotropic soil can be obtained from three sets of plane-strain triaxial tests; one set of tests is on soil samples with the plane of isotropy horizontal; the second set is on samples with the plane of isotropy vertical; and the third set is on samples with the plane of isotropy 45° inclined to the horizontal. Effective or total stresses may be used as appropriate, but all values should be consistent. Since the value of G'_V is particularly critical [Raymond (1970)], all four constants A, B, C, and G'_V must be correctly determined if one wants to consider the cross anisotropy of the soil. If the correct evaluation of each of the four constants is not possible, the soil should be treated as an isotropic material.

PROBLEMS

Problems are presented in order of topic coverage; select partial answers are purposely not identified.

General Soil Mechanics

2-1. A soil has a unit weight of 19.12 kN/m^3. For $G_s = 2.67$ and $w = 12.1$ percent, find γ_{dry}, void ratio e, porosity n, and degree of saturation S.
Partial answer: 0.349, 60.5

2-2. A soil has $\gamma = 19.57$ kN/m^3. If $G_s = 2.70$ and the soil is *saturated,* find γ_{dry}, void ratio e, porosity n, and water content w.
Partial answer: 98.6, 0.709

2-3. A soil has an in situ void ratio $e_o = 1.80$ and $w_N = 60.0$ percent; from laboratory tests and estimation we have $G_s = 2.68$, $w_L = 55$ percent, and $I_P = 30$. What are the wet unit weight γ_{wet}, the liquidity index I_L, I_C, and S?
Partial answer: 15.02, 89.4, −0.17

2-4. A sample of saturated clay has a mass of 1,853.5 g, and 1,267.4 g after drying. The dry unit weight is 14.71 kN/m^3. What are (*a*) γ_{wet}; (*b*) e; (*c*) G_s; and (*d*) γ_{wet} for $S = 50$ percent?

2-5. Classification tests were performed on the following two soils:

	Soil 1	Soil 2
Percent passing sieve		
No. 4	84	
No. 40	36.5	
No. 200	18.8	≅ 100
w_L	41.2	72.2 (after oven drying is 49.2)
w_P	23.6	34.1
Color	Light brown	Dark gray with very slight odor

Classify these two soils.

2-6. Data were obtained from a relative density test using information from six separate laboratory tests:

	Limiting γ	Average for tests, kN/m^3
γ_{max}	18.07	17.52
γ_{min}	14.77	15.56
	$\gamma_{field} = 16.5$ (average of 2 tests)	

Compute the range of D_r.
Hint: Use data sheet from Bowles (1992, see p. 215).
Answer: About 40 to 70 percent.

K_o and Soil Hydraulics

2-7. For soil No. 1 of Prob. 2-5, estimate K_o for the normally consolidated case and for a known OCR $= p'_c/p'_o = 4$.

2-8. Recompute $K_{o,nc}$ for Example 2-2 if $\phi' = 30°$ and $I_P = 25$.

2-9. For Fig. P2-9, (*a*) estimate h' at which the sand would be expected to become "quick"; (*b*) if $h' = 0.25$ m, what is the effective pressure p'_o at point A?

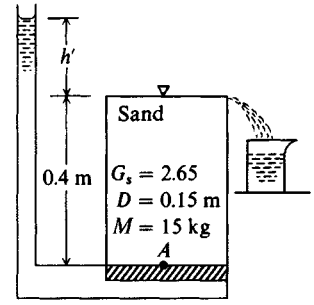

Figure P2-9

2-10. What H in Example 2-3 (as shown on Fig. 2-12*a*) will produce a "quick" condition at a point halfway between C and B?

Answer: $H = 14.3$ m

2-11. What depth of excavation Y will provide a safety factor of 1.25 for the condition of Fig. 2-10?

Answer: $Y = 16.9$ m

Consolidation

2-12. A consolidation test was performed on a sample with initial dimensions of $H = 20.00$ mm and ring diameter $= 63.00$ mm. At the end of the test the sample height was 13.3 mm and the oven-dry weight of the soil cake was 78.3 g. Assuming $G_s = 2.66$, find the initial and final void ratios e_o, e_f, and total sample strain ϵ_f.

Partial answer: 1.12, 0.335

Dial readings (× 0.0025)

Time, min	25 kPa	50 kPa	100 kPa
0	2240	2188	2127
0.25	2234	2180	2119
0.50	2230	2172	2113
1.0	2227	2162	2105
2.0	2222	2153	2094
4.0	2218	2144	2083
8.0	2213	2139	2073
16.0	2208	2135	2062
30.0	2204	2132	2055
60.0	2200	2131	2050
120.0	2197	2130	2047
240.0	2193	2129	2046
480.0	2190	2128	2045
1440.0	2188	2127	2044

2-13. The accompanying data are given from a consolidation test. For the assigned load increment,

(*a*) Plot dial reading versus log time and find t_{50}.

(*b*) Plot dial reading versus $\sqrt{t}$, find t_{50}, and compare to step (*a*).

(*c*) Assuming two-way drainage and the initial sample height $H = 20.00$ mm, compute c_v.

(*d*) Compute the secondary compression index C_α.

Note: On your plot clearly show where values are obtained and/or any slopes. Show steps *c* and *d* directly on the dial reading versus log time plot.

2-14. The accompanying consolidation data were obtained from tests on samples from locations shown on Fig. P2-14. The samples were consolidated from $H_i = 20.00$ mm and ring diameter = 63.00 mm.

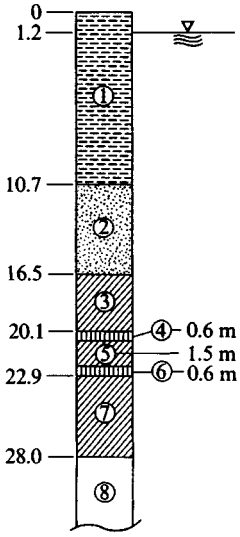

Figure P2-14

	Void ratio, *e*		
Test load, kPa	**Soil No. 3**	**Soil No. 5**	**Soil No. 7**
0	1.405	1.195	1.151
8	1.395	1.190	1.140
16	1.393	1.187	1.135
32	1.390	1.180	1.130
64	1.385	1.175	1.105
140	1.380	1.125	1.080
280	1.360	1.050	1.060
560	1.180	0.925	0.965
680	1.110		
1020	0.925	0.760	0.805
2040	0.725	0.625	0.680
w_L	77.0%	53.0%	69.0%
w_P	24.0	26.0	24.0
G_s	2.74	2.70	2.66
e_o	1.38	1.18	1.12 (as $w_N G_S$)
ΔH_1	0.0832 mm	0.0456	0.1023 (0–8 kPa)
ΔH_f	5.6550 mm	5.1936	4.3794 (0–2040 kPa)

Soil†	1	2	3	4	5	6	7
γ_{sat}, kN/m^3	15.72	18.31	*	18.62	*	18.73	*

*Compute from e_o and G_s given above.

†Soil description: Soil No. 1, organic silt and clay; soil No. 2, medium dense sand; soils No. 3, 5, and 7, clay; soils No. 4 and 6, thin silt seams.

(*a*) Plot *e* versus log *p* curves as assigned, compute C_c and p'_o, and estimate p'_c.

(*b*) Using the strain data given, together with data on *e* from this table, plot ϵ versus log *p*. Compare C'_c with the computed value from (*a*).

Partial answer:

Soil 3: $C_c \cong 0.76$ $\quad p'_o = 137.3$ $\quad C'_c \cong 0.32$

Soil 5: $C_c \cong 0.44$ $\quad p'_o = 161.2$

Soil 7: $C_c \cong 0.43$ $\quad p'_o = 191.9$ $\quad p'_c = 250$

2-15. Make a plot of U versus $\sqrt{T}$ and see if Taylor's 15 percent offset for 90 percent consolidation is about correct. If you get 13 percent, that is "about" correct.

Shear Strength and Stress Paths

2-16. An unconfined compression test was performed with the following data: $L = 110.00$ mm; diameter = 50.00 mm; $\Delta L = 8.00$ mm at failure; $P_{\text{failure}} = 0.140$ kN. Compute the undrained shear strength s_u. *Hint:* Refer to stress computations on Fig. 2-29.

Answer: $s_u = c = 38.5$ kPa.

2-17. A CIU triaxial test gave the following data:

Test no.	σ_c	$\Delta\sigma_1$	Δu, kPa
1	100	238	36
2	200	307	108
3	300	389	197

Compute total and effective stress parameters.

Partial answer: $\phi = 15°$; $\phi' = 41°$.

2-18. Plot the following CK_oU direct shear test data (50-mm square sample) and find the undrained shear strength parameters ϕ and c.

Test no.	P_v, kN	P_h, kN
1	0.05	0.047
2	0.20	0.114
3	0.30	0.136

Partial answer: $\phi \cong 22°$ (best fit by eye).

2-19. Plot the total stress data of Fig. 2-32*a* on a *p-q* diagram and obtain the undrained strength parameters.

2-20. Plot the residual soil strength data of Fig. 2-32*a* on either a *p-q* diagram or using Mohr's circles and obtain the residual strength parameters.

Partial answer: $c \cong 10$ kPa.

2-21. Plot the data of Prob. 2-17 using a *p-q* diagram for the total and effective strength parameters.

2-22. Replot Fig. 2-42 and verify that reloading to 100 kPa recovers point D (theoretically) and then add another 100 kPa (total load = 200) and locate resulting point F (it should fall on the K_o line).

2-23. Explain how you would set up a laboratory triaxial test for the stress path of Example 2-6.

2-24. Estimate the s_u/p'_o ratio for the soil of Prob. 2-3. If $p'_o = 50$ kPa, what is the estimated in situ undrained shear strength s_u?

2-25. Estimate the in situ s_u for the soil of Prob. 2-3 if $p'_o = 50$ kPa and $p'_c = 150$.

2-26. Estimate Poisson's ratio for a dense, saturated sand; a saturated clay; and a loose, dry sand.

2-27. Plot the assigned triaxial test data of Prob. 5-16. Make a smooth curve through the points and, starting with a strain = 0.005, compute E_s and μ using Eq. (*g*) of Section 2-14. Stop the computations when $\mu < -0.1$ or $\mu > 1.0$. Can you make any comments on strain level and values?

CHAPTER 3

EXPLORATION, SAMPLING, AND IN SITU SOIL MEASUREMENTS

3-1 DATA REQUIRED

Investigation of the underground conditions at a site is prerequisite to the economical design of the substructure elements. It is also necessary to obtain sufficient information for feasibility and economic studies for a proposed project. Public building officials may require soil data together with the recommendations of the geotechnical consultant prior to issuing a building permit, particularly if there is a chance that the project will endanger the public health or safety or degrade the environment.

To eliminate the site exploration, which usually ranges from about 0.5 to 1.0 percent of total construction costs, only to find after construction has started that the foundation must be redesigned, is certainly false economy. This fact is generally recognized, and it is doubtful that any major structures are currently designed without site exploration being undertaken. Small structures are sometimes designed without site exploration; however, the practice is not recommended. The condition of the adjacent structures is an indication, but certainly no guarantee, that a site is satisfactory.

Suitable building sites in urban areas are becoming difficult to find, and often sites targeted for urban renewal are used. These sites can be quite hazardous from demolition of previously existing structures and backfilling of former basements during landscaping. Often this type of backfill is done with little supervision or quality control, so there can be significant soil variation at these sites within a few meters in any direction.

The elements of a site investigation depend heavily on the project but generally should provide the following:

1. Information to determine the type of foundation required (shallow or deep).
2. Information to allow the geotechnical consultant to make a recommendation on the allowable load capacity of the foundation.

3. Sufficient data/laboratory tests to make settlement predictions.
4. Location of the groundwater table (or determination of whether it is in the construction zone). For certain projects, groundwater table fluctuations may be required. These can require installation of piezometers and monitoring of the water level in them over a period of time.
5. Information so that the identification and solution of construction problems (sheeting and dewatering or rock excavation) can be made.
6. Identification of potential problems (settlements, existing damage, etc.) concerning adjacent property.
7. Identification of environmental problems and their solution.

An exploration program may be initiated on an existing structure where additions are contemplated. The current safety of an existing structure may require investigation if excessive settlements or cracks have occurred. The required remedial measures may be undertaken based on new-found information or on the damage evidence and a reinterpretation of the original data.

Part of the geotechnical program may include on-site monitoring, both during and after construction, to make certain that recommendations are being followed. Where excavation reveals conditions requiring design changes, monitoring of progress will ensure that change orders are initiated early enough to keep costs to a minimum. Postconstruction monitoring of building performance is particularly desirable from the geotechnical consultant's view, since this allows for a review of the design procedures and builds a database for future work. Unfortunately, few owners are willing to make this investment or even allow property entry should the foundation consultant be willing to underwrite the cost.

Although the primary focus of this chapter is on site exploration for buildings and other structures where the cost per unit area is high (compact site), many of the methods are applicable to roads; airfields; water, sewer, pipe, and power lines; and other extended sites. Extended site exploration is useful to establish line and grade, locate groundwater level and rock line, delineate zones of poor-quality soil, and establish borrow pits.

3-2 METHODS OF EXPLORATION

The most widely used method of subsurface investigation for compact sites as well as for most extended sites is boring holes into the ground, from which samples may be collected for either visual inspection or laboratory testing. Several procedures are commonly used to drill the holes and to obtain the soil samples. These will be taken up in more detail later.

Generally we may categorize the site exploration as in Table 3-1, where disturbed or undisturbed samples are collected. On the basis of preliminary borings (or prior site knowledge) a decision is made whether to base additional site design information on in situ tests or to recover "undisturbed" samples for laboratory tests or, in the usual case, to use a combination.

Table 3-2 lists the wide variety of in situ tests currently available. Prior to 1960 this list would have included only the standard penetration test (SPT), the mechanical cone test (CPT), vane shear test, and plate load test. Many of the devices listed here have been developed since the early 1970s. Some are new and others, such as several of the "cones," are claimed improvements on the original mechanical cone. Many of the test methods and equip-

TABLE 3-1
The several exploration methods for sample recovery*

Method	Depths	Applicability
Disturbed samples taken		
Auger boring†	Depends on equipment and time available, practical depths being up to about 35 m	All soils. Some difficulty may be encountered in gravelly soils. Rock requires special bits, and wash boring is not applicable. *Penetration testing* is used in conjunction with these methods, and disturbed samples are recovered in the split spoon. Penetration counts are usually taken at 1- to 1.5 m increments of depth
Rotary drilling Wash boring Percussion drilling	Depends on equipment, most equipment can drill to depths of 70 m or more	
Test pits and open cuts	As required, usually less than 6 m; use power equipment	All soils
Undisturbed samples taken		
Auger drilling, rotary drilling, percussion drilling, wash boring	Depends on equipment, as for disturbed sample recovery	Thin-walled tube samplers and various piston samplers are used to recover samples from holes advanced by these methods. Commonly, samples of 50- to 100-mm diameter can be recovered
Test pits	Same as for disturbed samples	Hand-trimmed samples. Careful trimming of sample should yield the least sample disturbance of any method

* Marine sampling methods not shown.
† Most common method currently used.

ment have only a very limited number of users, and some are little beyond the development stage.

A summary such as this is useful, however, since needs are often sudden and require an almost instant solution. From this list one has several choices in making an in situ determination of any of the desired engineering design parameter(s).

The more widely used in situ test methods given in Table 3-2 will be described in some detail. For information on those less widely used or still somewhat in development, the reader is referred to the cited reference (which usually contains a large reference list that will be useful for a starting point). Also of interest would be the ASCE Geotechnical Special Publication No. 6: *Use of In Situ Tests in Geotechnical Engineering* (1986), footnoted in Table 3-2.

3-3 PLANNING THE EXPLORATION PROGRAM

The purpose of the exploration program is to determine the stratification and engineering properties of the soils underlying the site. The principal properties of interest will be the strength, deformation, and hydraulic characteristics. The program should be planned so that the maximum amount of information can be obtained at minimum cost.

It may be more economical to provide a conservative foundation design than to expend large sums on an elaborate exploration and testing program. On the other hand, sufficient

TABLE 3-2
In situ test methods and general application*

	Soil Identification	Establish vertical profile	Relative density D_r	Angle of friction ϕ	Undrained shear strength S_u	Pore pressure u	Stress history OCR and K_o	Modulus: E_s, G'	Compressibility m_v and C_c	Consolidation§ c_h and c_v	Permeability k	Stress-strain curve	Liquefaction resistance	Reference (in chapter if not given)
Acoustic probe	C	B	B	C	C	—	C	C	—	—	—	—	C	Koerner and Lord (1986)†
Borehole permeability	C	—	—	—	—	A	—	—	—	B	A	—	—	ASTM STP No. 322, ASTM STP 417
Cone														
Dynamic	C	A	B	C	C	—	C	—	—	—	—	—	C	
Electrical friction	B	A	B	C	B	—	C	B	C	—	—	—	B	
Electrical piezo	A	A	B	B	B	A	A	B	B	A	B	B	A	
Electrical piezo/ friction	A	A	A	B	B	A	A	B	B	A	B	B	A	
Impact	C	B	C	C	C	—	C	C	C	—	—	—	C	Dayal and Allen (1973)
Mechanical	B	A	B	C	B	—	C	B	C	—	—	—	B	
Seismic CPT down-hole	C	C	C	—	—	—	—	A	—	—	—	B	B	
Dilatometer (DMT)	B	A	B	C	B	—	B	B	C	—	—	C	B	
Hydraulic Fracture	—	—	—	—	—	B	B	—	—	C	C	—	—	
K_o stepped blade	—	—	—	—	—	—	B	—	—	—	—	—	—	
Nuclear tests	—	—	A	B	—	—	—	C	—	—	—	—	C	ASTM STP 412
Plate load tests	C	C	B	B	C	—	B	A	B	C	C	B	B	ASTM D 1194
Pressure meter														
Ménard	B	B	C	B	B	—	C	B	B	—	—	C	C	
Self-boring	B	B	A	A	A	A	A	A	A	A	B	A	A	
Screw plate	C	C	B	C	B	—	B	A	B	C	C	B	B	Patrick et al. (1980), Dahlberg (1974, 1974*a*)
Seismic														
Cross-hole	C	C	B	—	—	—	—	A	—	—	—	B	B	Woods (1986)†
Down-hole	C	C	C	—	—	—	—	A	—	—	—	B	B	Woods (1986)†
Surface refraction	C	C	—	—	—	—	—	B	—	—	—	—	B	Leet (1950)
Shear														
Borehole	C	C	—	B	B	—	C	C	—	—	—	C	—	
Vane	B	C	—	—	A	—	B	—	—	—	—	—	—	
Standard penetration test (SPT)	B	B	B	C	C	—	—	—	C	—	—	—	A	

* After Wroth (1984).

† In ASCE Conference: Use of In Situ Tests in Geotechnical Engineering, GT SP No. 6 (1986).

§ c_h = vertical consolidation w/horizontal drainage; c_v = vertical consolidation w/vertical drainage.

Code: A = most applicable; B = may be used; C = least applicable.

exploration should be undertaken so that the geotechnical consultant is not in the position of making an expensive recommendation to protect against uncertainties that could have been detected by a reasonable program. It should be understood that an overly conservative recommendation made by the consultant for the sole purpose of self-protection after an adequate exploration has been undertaken is not ethical.

If the soil is highly erratic, there should only be sufficient borings to establish a general picture of the underground conditions. An extensive boring (and laboratory testing) program is not justified in erratic soils, and the final design should be conservatively based on the properties of the poorer soils. Again, a question of ethics is involved if an excessive number of borings are taken under these circumstances, unless specifically requested by the client.

In planning the program the foundation consultant must have a good knowledge of current and accepted methods of both field exploration and laboratory testing and their limitations. A competent consultant will also have sufficient understanding of equipment function and soil behavior to make adjustments so that nonstandard equipment or test methods can be used (if necessary) to obtain the desired information.

In planning the program full advantage should be taken of any existing information, including the geotechnical engineer's own database for the area. It is obviously most helpful to have done site exploration on adjacent sites, or at least in the general area. It will also be most advantageous to have made the initial borings if this is a part of a detailed site exploration follow-up from an earlier feasibility study. Even if the consultant does not have a database from which to work, considerable information on underground conditions may exist—particularly in urban areas—in various government and utility offices, the owner's files, or the files of the engineer/architect who has retained the geotechnical consultant. In any case the borings should be used for a correlation and extension of the existing database if at all possible. In an undeveloped area where no database currently exists the program is in fact *exploratory.*

The actual planning of a subsurface exploration program includes some or all of the following steps:

1. *Assembly of all available information* on dimensions, column spacing, type and use of the structure, basement requirements, any special architectural considerations of the proposed building, and tentative location on the proposed site. Foundation regulations in the local building code should be consulted for any special requirements.

   For bridges the soil engineer should have access to type and span lengths as well as pier loadings and their tentative location. This information will indicate any settlement limitations and can be used to estimate foundation loads.

2. *Reconnaissance of the area.* This may be in the form of a field trip to the site, which can reveal information on the type and behavior of adjacent structures such as cracks, noticeable sags, and possibly sticking doors and windows. The type of local existing structures may influence to a considerable extent the exploration program and the best type of foundation for the proposed adjacent structure. Since nearby existing structures must be maintained in their "as is" condition, excavations or construction vibrations will have to be carefully controlled, and this can have considerable influence on the "type" of foundation that can be used.

   Erosion in existing cuts (or ditches) may also be observed, but this information may be of limited use in the foundation analysis of buildings. For highways, however, runoff patterns, as well as soil stratification to the depth of the erosion or cut, may be observed. Rock outcrops may give an indication of the presence or the depth of bedrock.

   The reconnaissance may also be in the form of a study of the various sources of information available, some of which include the following:

Geological maps. Either U.S. government or state geological survey maps.

Agronomy maps. Published by the Department of Agriculture (U.S., state, or other governmental agency).

Aerial photographs. Investigator may require special training to interpret soil data, but the nonspecialist can easily recognize terrain features.

Water and/or oil well logs.

Hydrological data. Data collected by the U.S. Corps of Engineers on streamflow data, tide elevations, and flood levels.

Soil manuals by state departments of transportation.

State (or local) university publications. These are usually engineering experiment station publications. Information can be obtained from the state university if it is not known whether a state study has been undertaken and published.

3. *A preliminary site investigation.* In this phase a few borings (one to about four) are made or a test pit is opened to establish in a general manner the stratification, types of soil to be expected, and possibly the location of the groundwater table. If the initial borings indicate that the upper soil is loose or highly compressible, one or more borings should be taken to rock or competent strata. This amount of exploration is usually the extent of the site investigation for small structures.

   A feasibility exploration program should include enough site data and sample recovery to establish an approximate foundation design and identify the construction procedures. Certain construction procedures (sheeting, bracing, tiebacks, slurry walls, rock excavation, dewatering, etc.) can represent a very significant part of the foundation cost and should be identified as early as practical.

   It is common at this stage to limit the recovery of good-quality samples to only three or four for laboratory testing. These tests, together with strength and settlement correlations using index properties such as liquid limit, plasticity index, and penetration test data as well as unconfined compression tests on disturbed samples recovered during penetration testing, are usually adequate for determining if the site is suitable.

4. *A detailed site investigation.* Where the preliminary site investigation has established the feasibility and overall project economics, a more detailed exploration program is undertaken. The preliminary borings and data are used as a basis for locating additional borings, which should be confirmatory in nature, and determining the additional samples required.

   Note that if the soil is relatively uniformly stratified, a rather orderly spacing of borings at locations close to critical superstructure elements should be made (requires client furnish the necessary location data). On occasion additional borings will be required to delineate zones of poor soil, rock outcrops, fills, and other areas that can influence the design and construction of the foundation.

   Sufficient additional soil samples should be recovered to refine the design and for any unusual construction procedure required by the contractor to install the foundation. These samples allow the foundation engineer and contractor to avoid an excessive (uncertainty factor) bid for the foundation work, cost overruns, and/or damage to adjacent property owners from unanticipated soil conditions discovered when the excavation is opened.

   In the detailed program phase it is generally considered good practice to extend at least one boring to competent rock if the overlying soil is soft to medium stiff. This is particularly true if the structure is multiple-storied or requires settlement control.

3-4 SOIL BORING

Exploratory holes into the soil may be made by hand tools, but more commonly truck- or trailer-mounted power tools are used.

Hand Tools

The earliest method of obtaining a test hole was to excavate a test pit using a pick and shovel. Because of economics, the current procedure is to use power excavation equipment such as a backhoe to excavate the pit and then to use hand tools to remove a block sample or shape the site for in situ testing. This is the best method at present for obtaining quality *undisturbed* samples or samples for testing at other than vertical orientation (see Fig. 2-45). For small jobs, where the sample disturbance is not critical, hand or powered augers (Fig. 3-1) held by one or two persons can be used. Hand-augered holes can be drilled to depths of about 35 m, although depths greater than about 8 to 10 m are usually not practical. Commonly, depths are on the order of 2 to 5 m, as on roadways or airport runways, or investigations for small buildings.

Mounted Power Drills

For numerous borings to greater depths and to collect samples that are *undisturbed,* the only practical method is to use power-driven equipment. *Wash boring* is a term used to describe one of the more common methods of advancing a hole into the ground. A hole is started by driving casing (Fig. 3-2) to a depth of 2 to 3.5 m. Casing is simply a pipe that supports the hole, preventing the walls from sloughing off or caving in. The casing is cleaned out by means of a chopping bit fastened to the lower end of the drill rod. Water is pumped through the drill rod and exits at high velocity through holes in the bit. The water rises between the casing and drill rod, carrying suspended soil particles, and overflows at the top of the casing through a **T** connection into a container, from which the effluent is recirculated back through the drill rod. The hole is advanced by raising, rotating, and dropping the bit into the soil at the bottom of the hole. Drill rods, and if necessary casing, are added as the depth of the boring increases. Usually 6 m or less of casing is required at a hole site. This method is quite rapid for advancing holes in all but very hard soil strata. Wash boring is more widely used in South America, Africa, and Asia than in Europe, Australia, or North America.

Rotary drilling is another method of advancing test holes. This method uses rotation of the drill bit, with the simultaneous application of pressure to advance the hole. Rotary drilling is the most rapid method of advancing holes in rock unless it is badly fissured; however, it can also be used for any type of soil. Drilling mud may be used in soils where the sides of the hole tend to cave in. Drilling mud is usually a water solution of a thixotropic clay (such as bentonite[1]), with or without other admixtures, that is forced into the sides of the hole by the rotating drill. The mud cake thus formed provides sufficient strength in conjunction with the hydrostatic pressure of the mud suspension ($\rho \approx 1.1$ to 1.2 g/cm^3) against the wall and soil "arching" so that the cavity is maintained. The mud pressure also tends to seal off the water

[1] A trade name for clay containing large amounts of montmorillonite clay minerals.

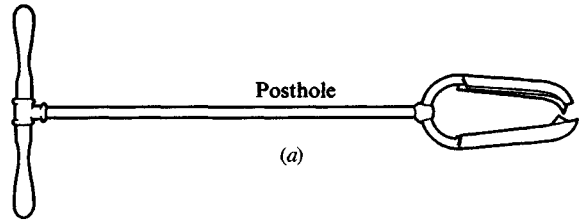

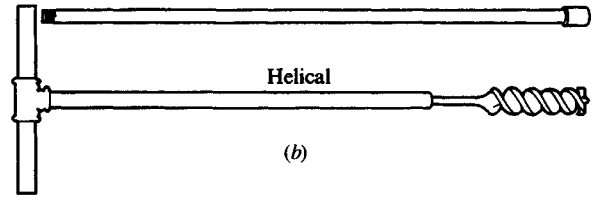

Figure 3-1 Hand tools for soil exploration. (*a*), (*b*) Hand augers; (*c*) gasoline-engine-powered hand auger with additional auger flights in the foreground together with hand-driven sample tube.

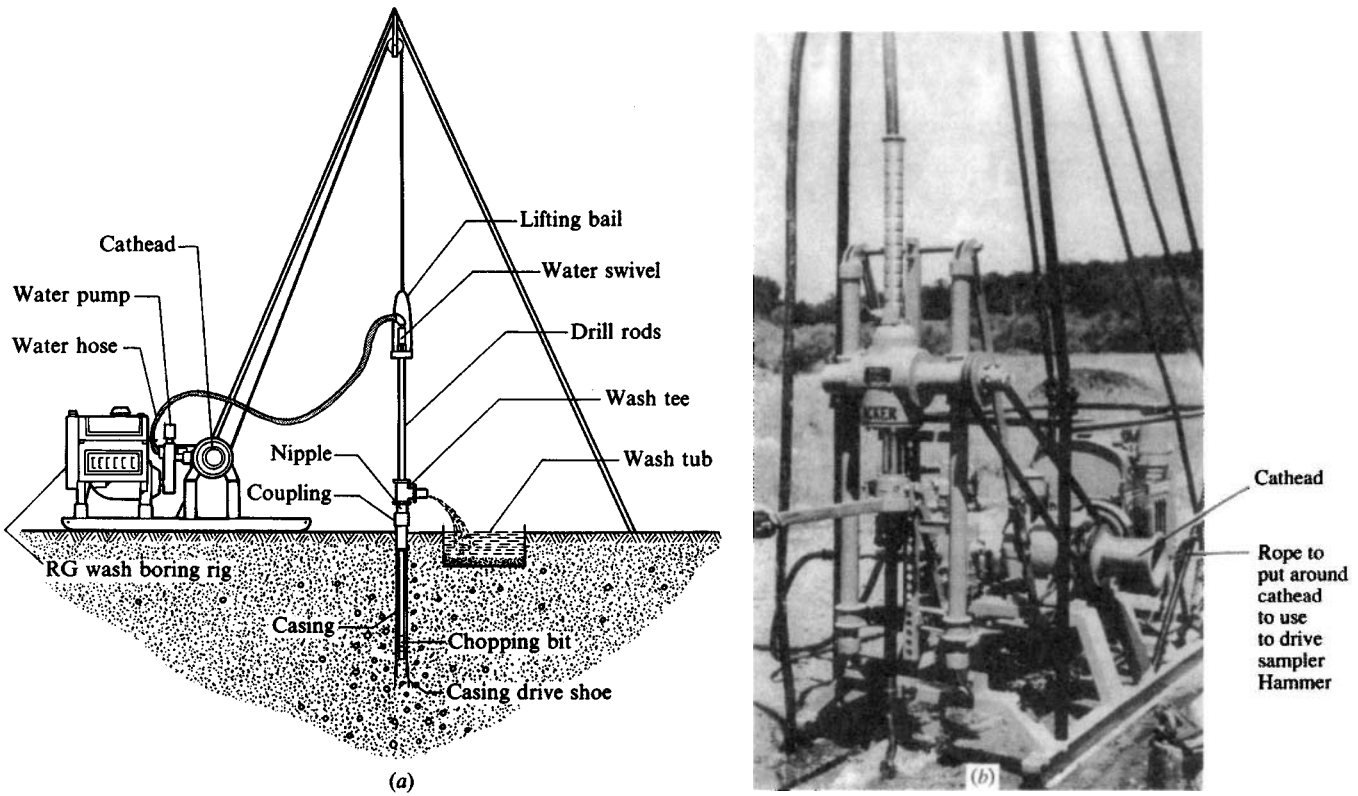

Figure 3-2 (*a*) Schematic of wash-boring operations; (*b*) photograph of wash-boring operation. Note weight in lower right foreground to advance the casing and to take penetration numbers when the chopping bit is replaced with the split spoon. (*The Acker Drill Company.*)

Figure 3-3 Soil drilling using a continuous-flight auger.

flow into the hole from any permeable water-bearing strata. Various drill heads are available, such as auger heads for shallow highway and borrow pit exploration, grinding heads for soil and rock, and coring bits for taking cores from rock as well as from concrete and asphalt pavements.

Continuous-flight augers with a rotary drill[2] are probably the most popular method of soil exploration at present (Fig. 3-3) in North America, Europe, and Australia. The flights act

[2]This drill assemblage can also be used as a rotary drill to obtain rock cores. The auger head is replaced with a rock core drill.

as a screw conveyor to bring the soil to the surface. The method is applicable in all soils, although in saturated sand under several feet of hydrostatic pressure the sand tends to flow into the lead sections of the auger, requiring a washdown prior to sampling. Borings up to nearly 100 m can be made with these devices, depending on the driving equipment, soil, and auger diameter.

The augers may be *hollow-stem* or *solid* with the hollow-stem type generally preferred, as penetration testing or tube sampling may be done through the stem. For obvious reasons, borings do not have to be cased using continuous-flight augers, and this feature is a decided economic advantage over other boring methods.

Continuous-flight augers are available in nominal 1- to 1.5-m section lengths (with rapid attachment devices to produce the required boring depth) and in several diameters including the following:

Solid stem							
OD, mm	67	83	102	115	140	152	180
Hollow stem							
ID/OD, mm	64/160	70/180	75/205	90/230	100/250	127/250	152/305

Inspection of this list of auger diameters indicates that a wide range of tube sample diameters may be used in sample recovery. Tube samples are generally limited to about 100-mm diameter, however, to obtain the best balance between sample quality and cost of drilling the hole.

The actual hole diameter will be on the order of 12 mm larger than the auger size. In practice a cutting head is attached to an auger flight, with or without a head plug depending on the soil; and the hole is advanced with top sections added as required. At the desired depth the plug is removed (if used), a penetration test is performed, and/or a tube sample recovered. If a plug is not used, soil cuttings that have accumulated at the bottom have to be removed so that the test can be made or a sample recovered. Caution should be exercised in removing the plug below the water table, since a difference in water level inside and outside the auger stem may create a temporary quick condition in the base soil until the water level stabilizes inside the auger stem.

Percussion drilling is still another method of forming a hole. In this method the drill is lifted, rotated slightly, and dropped onto the bottom of the hole. Water is circulated to bring the soil cuttings to the ground surface; casing is required as well as a pump to circulate the water.

3-5 SOIL SAMPLING

The most important engineering properties for foundation design are strength, compressibility, and permeability. Reasonably good estimates of these properties for cohesive soils can be made by laboratory tests on *undisturbed* samples, which can be obtained with moderate difficulty. It is nearly impossible to obtain a truly undisturbed sample of soil, so in general usage the term *undisturbed* means a sample where some precautions have been taken to minimize disturbance of the existing soil skeleton. In this context, the quality of an "undisturbed" sample varies widely between soil laboratories. The following represent some of the factors

that make an undisturbed sample hard to obtain:

1. *The sample is always unloaded from the in situ confining pressures,* with some unknown resulting expansion. Lateral expansion occurs into the sides of the borehole, so in situ tests using the hole diameter as a reference are "disturbed" an unknown amount. This is the reason K_o field tests are so difficult.
2. Samples collected from other than test pits are disturbed by volume displacement of the tube or other collection device. The presence of gravel greatly aggravates sample disturbance.
3. Sample friction on the sides of the collection device tends to compress the sample during recovery. Most sample tubes are (or should be) swaged so that the cutting edge is slightly smaller than the inside tube diameter to reduce the side friction.
4. There are unknown changes in water content depending on recovery method and the presence or absence of water in the ground or borehole.
5. Loss of hydrostatic pressure may cause gas bubble voids to form in the sample.
6. Handling and transporting a sample from the site to the laboratory and transferring the sample from sampler to testing machine disturb the sample more or less by definition.
7. The quality or attitude of drilling crew, laboratory technicians, and the supervising engineer may be poor.
8. On very hot or cold days, samples may dehydrate or freeze if not protected on-site. Furthermore, worker attitudes may deteriorate in temperature extremes.

Cohesionless Soil Sampling

It is nearly impossible to obtain undisturbed samples of cohesionless material for strength testing. Sometimes samples of reasonable quality can be obtained using thin-walled piston samplers in medium- to fine-grained sands. In gravelly materials, and in all dense materials, samples with minimal disturbance are obtained only with extreme difficulty. Dilation occurs in dense sands as a combination of volume displacement of the sampler and any pieces of gravel that catch on its cutting edge to give a larger apparent volume. Some attempts have been made to recover cohesionless materials by freezing the soil, freezing a zone around the sample (but not the sample), or injecting asphalt that is later dissolved from the sample; but most commonly thin-walled piston samplers are used to obtain "undisturbed" samples. A survey of freezing methods and an analysis of an attempt at frozen-sample recovery is given by Singh et al. (1982).

A test pit may be used to recover a quality sample, but the large amount of hand work will make it difficult to justify the expense. The devices shown in Fig. 3-4 can be used to recover disturbed samples from a boring for visual classification, sieve analyses, and chemical tests.

The primary use of "undisturbed" cohesionless samples is to obtain the unit weight γ or relative density D_r. The weight of soil in the known volume of the sampler allows a reasonable determination of unit weight, even if the sample has been later disturbed by transporting it from the site to the laboratory. An attempt to transfer a cohesionless sample from a tube to a testing machine for strength determination is not likely to meet with much success. A sample rebuilt in the laboratory to the in situ weight is lacking in both natural cementation

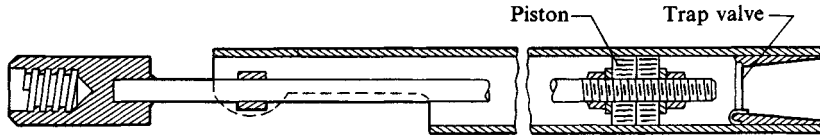

(*a*) Sand-pump sampler which utilized pumping action to recover a sample;

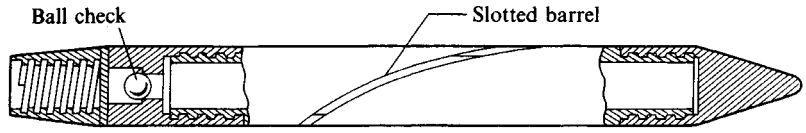

(*b*) spiral-slot sampler;

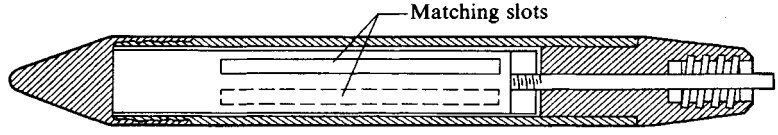

(*c*) parallel slot sampler.

Figure 3-4 Special sampling tools.

and anisotropy, which are significant factors in both strength and permeability estimates for most soil deposits.

Some geotechnical laboratories are of the opinion that anisotropic samples can be built to duplicate the in situ state and that the samples can be "aged" to recover some natural cementation. Even assuming this can be done, few projects could justify the expense for the small increase obtained in confidence level.

Since it is nearly impossible to recover undisturbed samples from cohesionless deposits, density, strength, and compressibility estimates are usually obtained from penetration tests or other in situ methods. Permeability may be estimated from well pumping tests or, approximately, by bailing the boring and observing the time for the water level to rise some amount.

Disturbed Sampling of All Soils

Disturbed samples are adequate to locate suitable borrow, where compaction characteristics and index tests for classification are usually sufficient. In this case a larger-diameter auger (usually only shallow depths) may be used so that bags of representative soil may be obtained for laboratory compaction tests, sieve analyses, and Atterberg limits.

In recognizing the difficulty and resulting expense of obtaining undisturbed samples, it is common practice on most foundation projects to rely on penetration tests and, depending on the method, recovery of disturbed samples for obtaining an estimate of the soil conditions. The standard penetration test (SPT) of Sec. 3-7 is nearly universally used,

even though highly disturbed samples are recovered. Other types of tests, particularly cones, are also widely used, although these latter devices do not recover a soil sample. For very complex projects, more than one type of test equipment may be used (such as the standard penetration test together with a cone penetration test).

Figure 3-5 illustrates the *sampling device* (also called a *split spoon*) most commonly used with the SPT. It is made up of a driving shoe, to ensure a reasonable service life from driving into the soil, and a barrel. The barrel consists of a piece of tube split lengthwise (split spoon) with a coupling on the upper end to connect the drill rod to the surface. Inserts (see Fig. 3-5*c*) are used when samples of thin mud and sand are to be recovered.

Some split spoons of the type shown in Fig. 3-5 have provision for a liner that contains the soil sample from a test. At present this method of obtaining a soil sample for laboratory testing is little used, primarily because the recovered sample is excessively disturbed.

In a test the sampler is driven into the soil a measured distance, using some kind of falling weight producing some number of blows (or drops). The number of blows N to drive the specified distance is recorded as an indication of soil strength.

The sampler is then slightly twisted to shear the soil at the base of the tube and withdrawn. The shoe and coupling are unscrewed and the two halves of the barrel are opened to expose the sample (unless a liner is used). If a liner is used, both ends are sealed—usually with melted wax—for later laboratory testing. If a liner is not used, on-site unconfined compression q_u tests are routinely made on cohesive samples. The wall thickness of the driving shoe (Fig. 3-5a) indicates that any samples recovered by this device are likely to be highly disturbed.

Representative samples from the soil in the sampler barrel are stored in sample jars and returned to the laboratory for inspection and classification. The field technician marks the jar with the job and boring number, sample depth, and penetration blow count; the test details are given in Sec. 3-7.

These jar samples are usually large enough to provide sufficient material for the Atterberg limits and natural water content. In routine work these index properties, used with correlation tables and charts and with q_u, are sufficient to select the foundation type, estimate the allowable bearing capacity, and make some kind of estimates of probable settlement.

This is particularly true if the soil is stiff, is above the water table, or is overconsolidated and fissured where it is difficult to push a thin-walled sample tube and/or obtain an intact sample for a compression test. The penetration number N (a measure of resistance) is usually sufficient for making estimates of both strength and settlement in cohesionless soils. Where the geotechnical consultant has obtained sufficient experience to build a reasonable database, strength/settlement predictions made in this manner are quite adequate for about 85 to 90 percent of foundation work.

It is the other 10 to 15 percent of the work that taxes the ingenuity of the geotechnical engineer. In recognizing the difficulty both of obtaining a quality sample and of trying to return it to the K_o condition for a laboratory test, in situ tests described in later sections may be used. This is particularly true for important structures founded on fine to medium sands and where strata of very soft cohesive and/or organic soils are present. Even thin seams (or layers) of these latter soils may be sufficient to cause great problems, even where the primary deposit is sand or other better-quality material. In any case, unless competent lower strata are close enough to decide a viable foundation alternative immediately, some testing of (or in) these poor soils will be required.

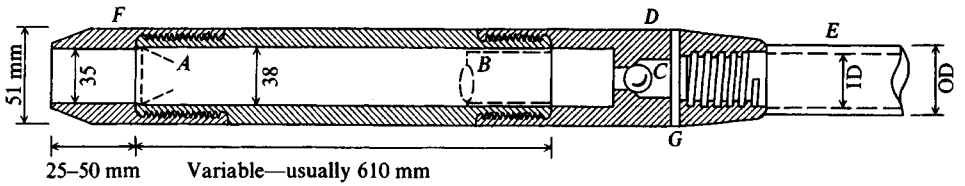

A—insert if used *B*—liner if used
C—ball check valve (provide suction on sample)
D—sampler-to-drill rod coupling
E—drill rod (A or AW)
F—drive shoe *G*—vent holes (used with *C*)

Drill rod sizes:

A: 41 OD × 29 ID mm	5.51 kg/m
AW: 44 OD × 32 ID mm	6.25 kg/m

(a) Standard split barrel sampler (also called a split spoon). Specific sampler dimensions may vary by ± 0.1 to 1.0 mm.

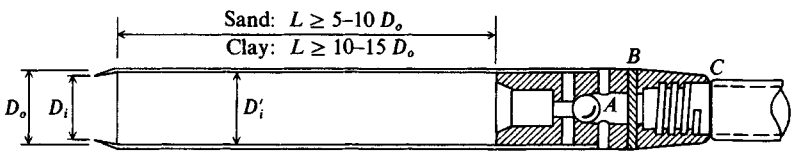

A—ball check valve to hold sample in tube on withdrawal
B—tube-to-drill rod coupling
C—drill rod

$$\text{Inside clearance ratio} = \frac{D_i' - D_i}{D_i}$$

Common D_o: 51, 64, 76, and 89 mm

(*b*) Thin wall tube sampler.

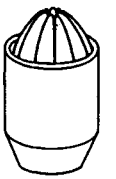

Basket shoe; the flexible fingers open to admit the sand then close when the tube is withdrawn

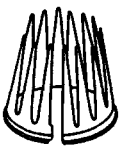

Spring sample retainer

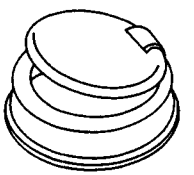

Trap valve sample retainer used to recover muds and watery samples

(*c*) Split barrel sampler inserts.

Figure 3-5 Commonly used in situ testing and sample recovery equipment. For both split barrel and thin wall tube details see ASTM D 1586 and D 1587.

Undisturbed Sampling in Cohesive Soils

As the field boring progresses and soft layers are encountered that may influence the foundation selection/design, undisturbed samples are usually taken so that consolidation and more refined laboratory strength tests can be made.

Recovery of "undisturbed" samples in cohesive soils is accomplished by replacing the split spoon on the drill rod with specially constructed thin-walled (1.63 to 3.25 mm) seamless steel tubing (610 mm in length × 51 to 89 mm in diameter), which should be pushed, but is sometimes driven, the tube length into the soil. The tube is slightly rotated (or a previously attached special cutting device is used) to cut the sample off. Friction holds the sample in the tube as the sample is withdrawn; however, there are also special valve or piston (Fig. 3-6) arrangements that use a pressure differential (suction) to retain the sample in the tube.

A special sampler termed a *foil sampler* (Fig. 3-6*b*) was developed in Sweden [see Hvorslev (1949, p. 269), Kjellman (1948)] to overcome two principal deficiencies of the usual sampling tubes and piston samplers. These deficiencies are short sample length and side friction between the inside tube wall and soil as soil is forced into the sampler. Reducing side friction requires using short sample tubes. If one is in a soil suspected of being particularly troublesome, it may be necessary to take continuous samples. These are not practical with samplers of, say, 1 m maximum length because of continually having to pull the drill rods to attach a new tube. The foil sampler is a means of recovering samples 10 to 20 m in length with a minimal friction effect. The interested reader should consult the cited references for exact details, but essentially the sampler operates by first being placed on the bottom of the borehole. Next it is pushed into the soil; as the sample enters the tube, it is surrounded by 16 foil strips (thin metal strips about 13-mm wide by 0.5- to 1.0-mm thick), which carry it up the tube. Friction between soil and foils results in reducing the compressive stress in the sample as the length of recovered sample increases in the tube.

If the soil is extremely soft, or experience indicates that in situ tests should be made (and the necessary equipment is available), only a few "undisturbed" tube samples for consolidation tests should be taken. As a general rule, tube samples for consolidation tests should be at least 12 mm larger than the consolidation ring (to allow trimming the disturbed perimeter); in practice, a 76-mm tube sample is often collected for use in the 64-mm diameter consolidometer. Sometimes a 51-mm tube sample is used with a 48-mm diameter consolidometer, but this size test diameter is so small that it is not recommended. Tube samples larger than 76 mm can be obtained, but if they are much larger than 100 mm a premium may be charged for the extra drilling effort and tube cost—particularly if stainless steel tubes are used for rust control.[3]

Although sample disturbance depends on factors such as rate of penetration, whether the cutting force is obtained by pushing or driving, and presence of gravel, it also depends on the ratio of the volume of soil displaced to the volume of collected sample, expressed as an *area ratio* A_r:

$$A_r = \frac{D_o^2 - D_i^2}{D_i^2} \times 100 \tag{3-1}$$

[3]Ordinary steel tubes rust rapidly, with resulting great difficulty in sample extrusion. ASTM D 1587 requires an inside protective coating if a sample is to be contained in the tube more than 72 hr.

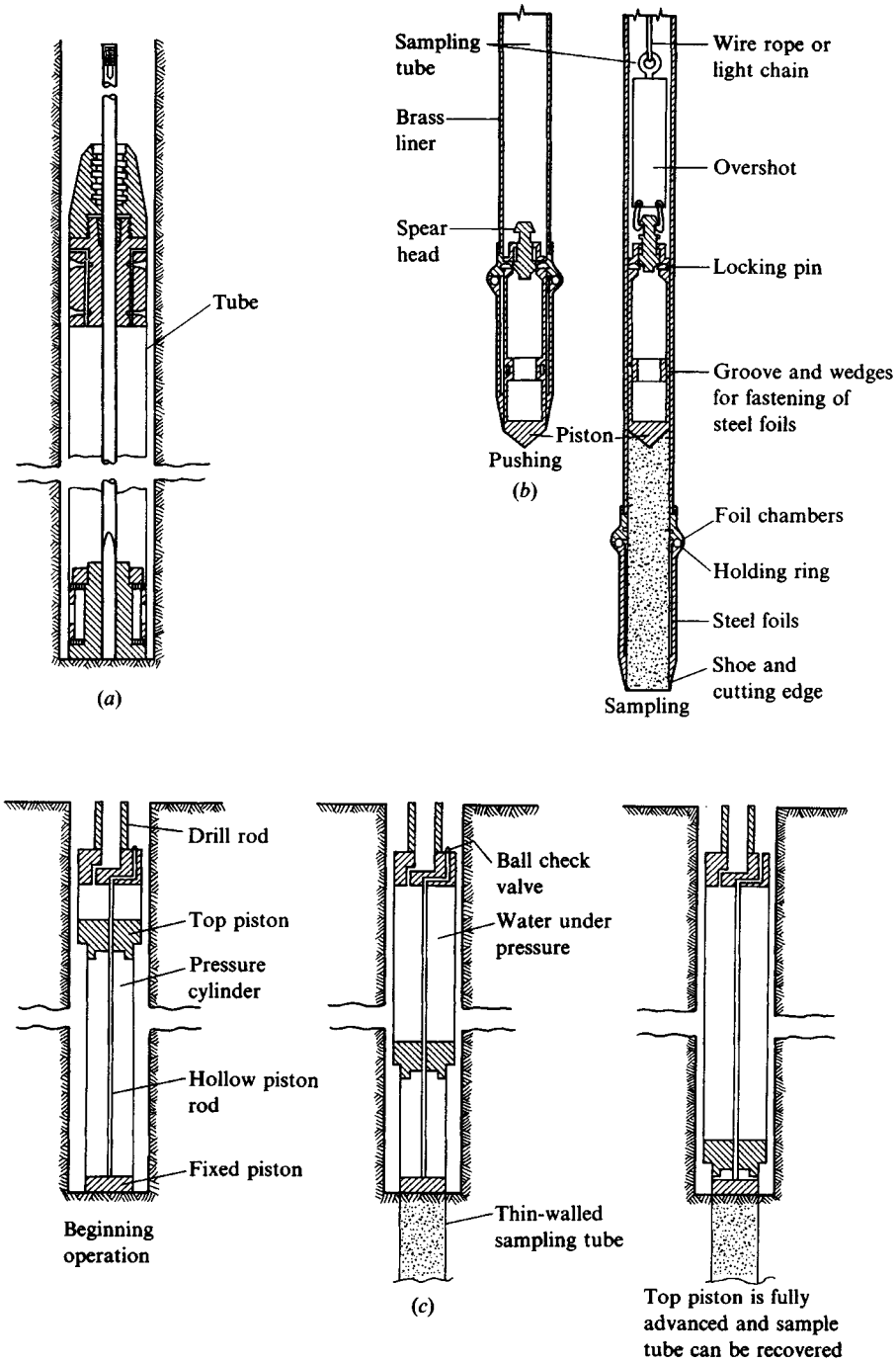

Figure 3-6 Typical piston samplers. (*a*) Stationary piston sampler for recovery of "undisturbed" samples of cohesive soils. Piston remains stationary on soil and tube is pushed into the soil; piston is then clamped and sample is recovered; (*b*) Swedish foil sampler; (*c*) Osterberg piston sampler. [*Hvorslev (1949)*].

where D_o = outside diameter of tube
D_i = inside diameter of cutting edge of tube

Well-designed sample tubes should have an area ratio of less than about 10 percent. The widely used 51-mm thin walled tube has an A_r of about 13 percent as computed in Example 3-1.

Another term used in estimating the degree of disturbance of a cohesive or rock core sample is the recovery ratio L_r:

$$L_r = \frac{\text{Actual length of recovered sample}}{\text{Theoretical length of recovered sample}} \tag{3-2}$$

A recovery ratio of 1 (recovered length of the sample = the length sampler was forced into the stratum) indicates that, theoretically, the sample did not become compressed from friction on the tube. A recovery ratio greater than 1.0 would indicate a loosening of the sample from rearrangement of stones, roots, removal of preload, or other factors.

In the final analysis, however, engineering judgment must be relied upon to extrapolate the results of tests on "undisturbed" samples to the prediction of field behavior.

Example 3-1. What is the area ratio of the 51-mm diam. thin walled sample tube?

Solution. Using dimensions from a supplier's catalog, obtain OD = 50.8 mm and ID = 47.7 mm. (The actual ID of the tube is slightly larger than the ID of the cutting edge to reduce side friction on the sample as the tube is pushed into the soil.) Direct substitution into Eq. (3-1) gives

$$A_r = \frac{D_o^2 - D_i^2}{D_i^2} \times 100 = \frac{50.8^2 - 47.7^2}{47.7^2} \times 100 = 13.4\%$$

////

3-6 UNDERWATER SAMPLING

Common constructions that require some kind of underwater exploration program include bridge piers, port structures, pipelines, oil well platforms, land recovery (fills to extend the shore line or for an island), and the like.

It is usually necessary to collect enough data to make a strength estimate. Soil shear strength determines how much pile embedment is required or whether a fill will require special construction procedures. Estimates of settlement are also often required—both how much and how long it will take. This is very critical for land recovery operations, since the client will want to know when enough settlement has occurred so that construction of surface facilities can begin.

The in situ testing and recovery procedures for underwater samples, either in a freshwater or a saltwater environment, are not much different from those for dry land for water depths up to about 45 m. The principal differences are that the testing or drilling equipment is mounted on a barge that is towed to the test location and securely anchored and that casing is used, at least to the water bed and possibly 1 or 2 meters into the bed. The casing strength is the principal cause for limiting the depth to about 45 m. For this situation the barge is securely anchored using four to six anchors so it does not shift or twist. Sometimes divers are used to observe visually if any construction difficulty will be encountered or if there are any existing underwater obstructions.

A barge-mounted drilling rig (drilling over the side) is a common method for drilling in rivers, in lake beds, and in the shallower water along the continental shelf for bridges, port structures, or land recovery. Penetration, vane, and pressuremeter tests described in the following sections can be made in the borings.

In deeper water (up to 1,000+ m) wave action requires alternative exploration equipment, such as a small ship converted to a drilling platform by installing a center well of 460 to 610 mm diameter from the deck through the hull and adding a drill rig. This configuration is sometimes called a *drill ship.* Submarine-type vessels (sometimes called *submersibles*) are also used. In very deep water a platform might be constructed, off of which the exploration crew might work. Any of these equipment options will allow recovery of samples of reasonable quality.

Where wave action occurs, it is necessary to use casing with flexible joints, and a casing diameter large enough to allow passage of the sampling (or test device) tube. In deeper water the drill pipe may act as the casing (again using flexible joints). In this case the lower end of the pipe holds the auger bit, which produces an over-sized hole. At the desired level a sampler is lowered through the drill pipe to the base of the hole and either driven or pushed into the soil below the bit.

There are also projectile-type devices that are lowered to the ocean floor from the drill ship to recover soil samples. Servomechanisms commanded from the surface may be used to force a sample tube into the soil using the weight of either the surface vessel or some kind of reaction device placed on the seafloor. A projectile device may contain a gas or explosive charge to propel a sample tube into the soil, again using the weight of the total device as a reaction. Most of these types of devices are patented and/or proprietary. Deepwater divers are sometimes used to recover samples or to inspect the reaction device.

In situ tests are currently considered preferable to sample recovery, particularly for strength testing. It is difficult to recover good-quality samples from underwater because of the change in pore pressure when the sample is brought above water. As a minimum, air bubbles tend to come out of the pore water and occupy a greater volume, causing the sample to expand or even explode. If the sample is still in the sample tube, the expansion may cause the sample to extend out of the tube end(s).

Depending on the equipment, the sample recovery tube (about 50- to 75-mm ID and 610 to 1000^+ mm in length) may be pushed or driven. A pushed sample is generally of better quality than one obtained by driving the tube into the soil. Shorter tube lengths generally produce better-quality samples, since side friction is significant with all tube samples; if the sample is too long, it may become compressed from side friction between the sample and the inside walls of the sampler.

At a given site a few samples should be recovered for visual inspection and possibly some index tests (w_N, w_L, I_P).

A driven-tube recovered sample will often have excessive disturbance for strength testing, but the blow count to drive the tube gives some indication of soil strength, somewhat like the SPT test described in the next section.

A number of underwater exploration methods are described in ASTM (1971) and appear among the references cited by Focht and Kraft (1977), which the interested reader may wish to consult. Using the in situ vane test (of Sec. 3-12) for underwater exploration is described in ASTM (1988). Olsen et al. (1986) described an elaborate marine sampling and testing program undertaken in 1979–1980.

3-7 THE STANDARD PENETRATION TEST (SPT)

The standard penetration test, developed around 1927, is currently the most popular and economical means to obtain subsurface information (both on land and offshore). It is estimated that 85 to 90 percent of conventional foundation design in North and South America is made using the SPT. This test is also widely used in other geographic regions. The method has been standardized as ASTM D 1586 since 1958 with periodic revisions to date. The test consists of the following:

1. Driving the standard split-barrel sampler of dimensions shown in Fig. 3-5*a* a distance of 460 mm into the soil at the bottom of the boring.
2. Counting the number of blows to drive the sampler the last two 150 mm distances (total = 300 mm) to obtain the N number.[4]
3. Using a 63.5-kg driving mass (or hammer) falling "free" from a height of 760 mm. Several hammer configurations are shown in Fig. 3-7.

The exposed drill rod is referenced with three chalk marks 150 mm apart, and the guide rod (see Fig. 3-7) is marked at 760 mm (for manual hammers). The assemblage is then seated on the soil in the borehole (after cleaning it of loose cuttings). Next the sampler is driven a distance of 150 mm to seat it on undisturbed soil, with this blow count being recorded (unless the system mass sinks the sampler so no N can be counted). The sum of the blow counts for the next two 150-mm increments is used as the penetration count N unless the last increment cannot be completed. In this case the sum of the first two 150-mm penetrations is recorded as N.

The boring log shows *refusal* and the test is halted if

1. 50 blows are required for any 150-mm increment.
2. 100 blows are obtained (to drive the required 300 mm).
3. 10 successive blows produce no advance.

When the full test depth cannot be obtained, the boring log will show a ratio as

$$70/100 \quad \text{or} \quad 50/100$$

indicating that 70 (or 50) blows resulted in a penetration of 100 mm. Excessive equipment wear, as well as greatly reduced daily drilling meterage, results when blow counts are high. Standardization of refusal at 100 blows allows all drilling organizations to standardize costs so that higher blow counts result in a negotiation for a higher cost/length of boring or a requirement for some type of coring operation.

SPT testing prior to about 1967 (according to ASTM) only required the sampler to be seated and then driven 300 mm. This stipulation could reduce the N count nearly 50 percent

[4]Strictly, the driving distance should be 305 mm since the original test was based on a driving distance of 12 inches. Owing to the approximate nature of the test it will be adequate to use a distance of 300 mm and divide it into two 150-mm increments. The rationale is that the driving depth is never exact, since one cannot drive using a fractional hammer drop. If the last hammer drop produces more than 300 mm of penetration, it is still considered 300 mm.

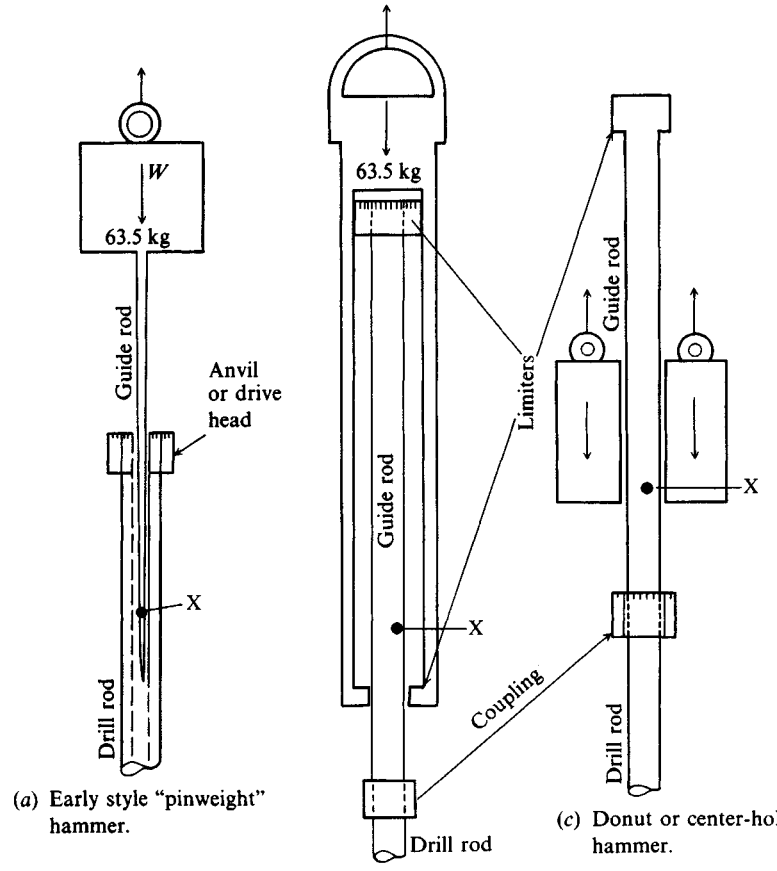

Figure 3-7 Schematic diagrams of the three commonly used hammers. Hammer (*b*) is used about 60 percent; (*a*) and (*c*) about 20 percent each in the United States. Hammer (*c*) is commonly used outside the United States. Note that the user must be careful with (*b*) and (*c*) not to contact the limiter and "pull" the sampler out of the soil. Guide rod *X* is marked with paint or chalk for visible height control when the hammer is lifted by rope off the cathead (power takeoff).

since the first 150 mm of required seating produces substantial friction resistance on the sampler for the next 300 mm. It is unfortunate that many current SPT correlations are based on *N* values from this earlier procedure.

Both before and after ASTM standardization it was regularly observed that *N* values from adjacent boreholes or from using different equipment in adjacent holes were not reproducible. Because of wide SPT use, this problem received much attention—first by Gibbs and Holtz (1957), who considered that overburden pressure and length of drill rod were the principal causes of nonreproducibility. Beyond this, not much was done until de Mello (1971) presented a comprehensive literature survey that started a focus on the driving energy [Schmertmann (1975)].

Discrepancies can arise from factors such as using a warped or worn driving shoe, pushing a rock (usually detected by an experienced driller), and allowing a quick condition in the hole bottom resulting from too rapid withdrawal of auger or bit plug or from a differential in water

level between GWT and in hole (or stem of hollow auger). A quick condition is avoided by attention to the ASTM 1586 standard. The status of the drive shoe can be ensured by regular inspection, especially after hard driving.

Proper attention to these causes of discrepancies leaves the input driving energy and its dissipation around the sampler into the surrounding soil as the principal factors for the wide range in N values. It should be evident that the blow count would be directly related to the driving energy, which is theoretically computed as follows:

$$E_{\text{in}} = \frac{1}{2}mv^2 = \frac{1}{2}\frac{W}{g}v^2 \qquad (a)$$

$$v = (2gh)^{1/2} \qquad (b)$$

and substituting Eq. (b) into Eq. (a), we obtain

$$E_{\text{in}} = \frac{1}{2}\frac{W}{g}(2gh) = Wh \qquad (c)$$

where W = weight or mass of hammer and h = height of fall. This gives, for the standard 63.5 kg hammer and h = 762 mm (30 in.), the *theoretical* input driving energy of

$$E_{\text{in}} = 63.5 \times 9.807 \times 0.762 = 474.5 \text{ (say, 475 J)}$$

Kovacs and Salomone (1982) found that the actual input driving energy E_a to the sampler to produce penetration ranged from about 30 to 80 percent; Riggs et al. (1983) obtained energy inputs ranging from about 70 to 100 percent. These discrepancies appear to arise from factors such as the following:

1. Equipment from different manufacturers. A large variety of drilling rigs are in current use; however, the rotary auger of Fig. 3-3*a* with the safety hammer of Fig. 3-7*b* is the most common in North American practice.
2. Drive hammer configurations of Fig. 3-7. The anvil also seems to have some influence on the amount of energy input to the sampler.
3. Whether
   a. the hammer uses an automatic trip with the drop height h controlled to within ±25 mm, or
   b. the system used is a rope-cathead (low-speed power takeoff pulley) (see Fig. 3-8) with E_a dependent on
      (*i*) diameter and condition of rope
      (*ii*) diameter and condition of cathead (rusty, clean, etc., and whether using 125- or 200-mm diameter—200-mm is common in North America)
      (*iii*) number of turns of rope around cathead, as $1\frac{1}{2}$, 2, 3, etc. It appears that a nominal 2 turns is optimum and in wide use. There may be some influence on whether the rope is pulled from the top ($1\frac{3}{4}$ turns) or from the bottom ($2\frac{1}{2}$ turns) of the cathead.
      (*iv*) the actual drop height at which the operator releases the rope to allow the hammer to "free" fall. Riggs (1986) suggests the operator commonly overlifts an average of 50 mm (actual drop height = 810 mm). This results from the operator pulling the rope into the spinning cathead (Fig. 3-8), visually observing the lift to a mark

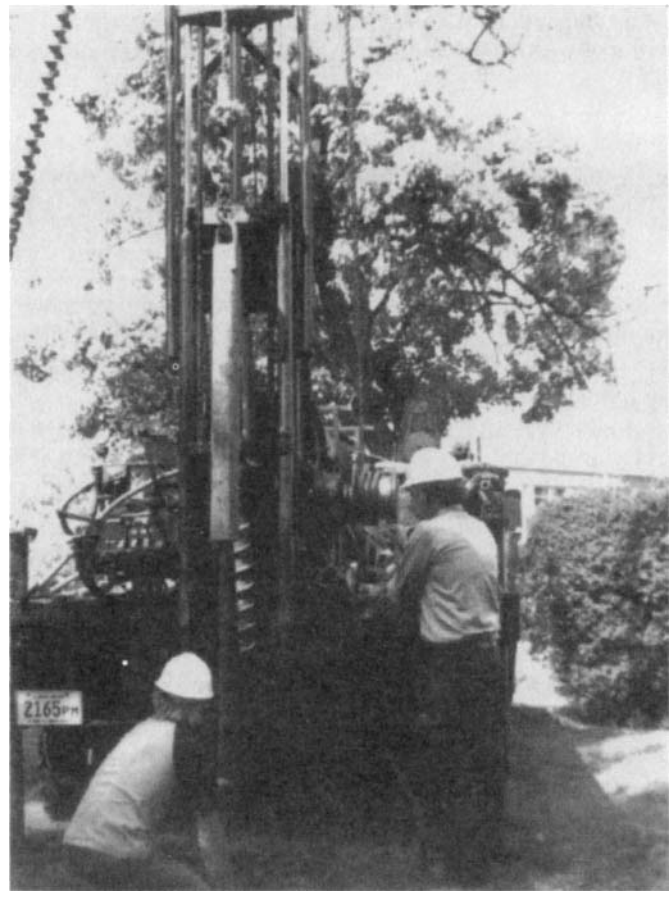

Figure 3-8 Drilling operator performing the SPT test using a safety hammer with rope-cathead lift. Rope is coming off the bottom of cathead and operator is observing for height mark on hammer guide rod. Helper in foreground is taking count and observing penetration.

(see Fig. 3-7) on the guide rod, and then releasing the rope back toward the cathead so it loosens and allows the hammer to fall. Reaction time and mark visibility result in this overlift. The operator commonly obtains 40 to 50 blows/minute.

4. Whether a liner is used inside the split barrel sampler. Side friction increases the driving resistance (and N) and is less without the liner (shown in Fig. 3-5*a*). It is common practice not to use a liner. Also it would appear that N values should be larger for soils with OCR > 1 (and larger relative density D_r) than for normally consolidated soils.
5. Overburden pressure. Soils of the same density will give smaller N values if p'_o is smaller (as near the ground surface). Oversize boreholes on the order of 150 to 200 mm will also reduce N unless a rotary hollow-stem auger is used with the auger left in close contact with the soil in the hole bottom. Degree of cementation may also be significant in giving higher N counts in cemented zones that may have little overburden pressure.
6. Length of drill rod. Above about 10 m the rod length does not seem critical; however, for shorter lengths and $N < 30$ it is. This effect was first examined by Gibbs and Holtz

(1957) and later by McLean et al. (1975) and others [see Schmertmann (1979)], who used a computer model to analyze the influence of rod length as well as other factors such as sampler resistance.

From the several recent studies cited (and their reference lists) it has been suggested that the SPT be standardized to some energy ratio E_r which should be computed as

$$E_r = \frac{\text{Actual hammer energy to sampler, } E_a}{\text{Input energy, } E_{\text{in}}} \times 100 \qquad (d)$$

There are proposals to compute E_{in} based on the measured hammer velocity at impact with the anvil or as the measured energy in the drill rod just below the anvil. It would appear, however, that using the theoretical value given by Eq. (*c*) for E_{in} would be preferable as it is not equipment-dependent.

Since there is a wide scatter in E_r and the resulting blow count N when it is reasonable to expect there should be a unique N for the soil at some depth, it is suggested the drill system-dependent E_r of Eq. (*d*) be referenced to a standard energy ratio value E_{rb}. In this way a drill rig with, say, $E_r = 45$ would, on adjustment to the standard E_{rb}, compute approximately the same N count as from a drill rig with $E_r = 70$. There are several current suggestions for the value of the standard energy ratio E_{rb} as follows:

E_{rb}	Reference
50 to 55 (use 55)	Schmertmann [in Robertson et al. (1983)]
60	Seed et al. (1985); Skempton (1986)
70 to 80 (use 70)	Riggs (1986)

The author will use 70 since the more recent data using current drilling equipment with a safety or an automatic hammer and with driller attention to ASTM D 1586 details indicate this is close to the actual energy ratio E_r obtained in North American practice. If a different standard energy ratio E_{rb} is specified, however, it is a trivial exercise to convert to the different base, as will be shown next.

The standard blow count N'_{70} can be computed from the measured N as follows:

$$N'_{70} = C_N \times N \times \eta_1 \times \eta_2 \times \eta_3 \times \eta_4 \qquad (3\text{-}3)$$

where η_i = adjustment factors from (and computed as shown) Table 3-3

N'_{70} = adjusted N using the subscript for the E_{rb} and the $'$ to indicate it has been adjusted

C_N = adjustment for effective overburden pressure p'_o (kPa) computed [see Liao and Whitman (1986)][5] as

$$C_N = \left(\frac{95.76}{p'_o}\right)^{1/2}$$

[5]There are a number of overburden corrections for N (this reference lists six); however, this equation plots at very nearly the average of all those proposed and is the simplest to use.

TABLE 3-3
Factors η_i For Eq. (3-3)*

Hammer for η_1					Remarks
	Average energy ratio E_r				
	Donut		Safety		
Country	R-P	Trip	R-P	Trip/Auto	R-P = Rope-pulley or cathead $\eta_1 = \mathbf{E}_r/\mathbf{E}_{rb} = E_r/70$ For U.S. trip/auto $w/\mathbf{E}_r = 80$ $\eta_1 = 80/70 = 1.14$
United States/ North America	45	—	70–80	80–100	
Japan	67	78	—	—	
United Kingdom	—	—	50	60	
China	50	60	—	—	

Rod length correction η_2			
Length	> 10 m	$\eta_2 = 1.00$	N is too high for $L < 10$ m
	6–10	= 0.95	
	4–6	= 0.85	
	0–4	= 0.75	

Sampler correction η_3			
	Without liner	$\eta_3 = 1.00$	Base value
With liner:	Dense sand, clay	= 0.80	N is too high with liner
	Loose sand	= 0.90	

Borehole diameter correction η_4			
Hole diameter:†	60–120 mm	$\eta_4 = 1.00$	Base value; N is too small when there is an oversize hole
	150 mm	= 1.05	
	200 mm	= 1.15	

* Data synthesized from Riggs (1986), Skempton (1986), Schmertmann (1978*a*) and Seed et al. (1985).
† $\eta_4 = 1.00$ for all diameter hollow-stem augers where SPT is taken through the stem.

Note that larger values of $\boldsymbol{E}_r$ *decrease* the blow count N nearly linearly, that is, $\boldsymbol{E}_{r45}$ gives $N = 20$ and $\boldsymbol{E}_{r90}$ gives $N = 10$; however, using the "standard" value of $\boldsymbol{E}_{r70}$ gives an N value for use in Eq. (3-3) of $N = 13$ for either drilling rig. We obtain this by noting that the energy ratio × blow count should be a constant for any soil, so

$$\boldsymbol{E}_{r1} \times N_1 = \boldsymbol{E}_{r2} \times N_2 \tag{e}$$

or

$$N_2 = \frac{\boldsymbol{E}_{r1}}{\boldsymbol{E}_{r2}} \times N_1 \tag{3-4}$$

For the arbitrarily chosen $\boldsymbol{E}_{r1} = 70$, this gives, in general,

$$N_2 = \frac{70}{\boldsymbol{E}_{r2}} \times N_1$$

For the previous example of N_2 for $\boldsymbol{E}_{r45} = 20 = \boldsymbol{E}_{r2}$ we obtain

$$20 = \frac{70}{45} \times N_1 \qquad \text{giving} \qquad N_1 = \frac{45}{70}(20) = 13 \quad \text{(use integers)}$$

If we convert N_{70} to N_{60} we have

$$N_2 = N_{60} = \frac{70}{60}(13) = 15 \quad \text{[which is larger as predicted by Eq. } (e)\text{]}$$

Using the relationship given by Eq. (e) we can readily convert any energy ratio to any other base, but we do have to know the energy ratio at which the blow count was initially obtained.

It is evident from Table 3-3 that all $\eta_i = 1$ in Eq. (3-3) for the case of a small bore hole, no sampler liner, length of drill rod over 10 m (30 ft) and the given drill rig has $\boldsymbol{E}_r = 70$. In this case the only adjustment N'_{70} is for overburden pressure using C_N. This observation is made since there are several opinions on N corrections:

1. Do nothing, which, with current equipment and conditions, may be nearly correct. This may have an advantage of detecting increases of soil stiffness (E_s) with depth, and upper variations may indicate cementation or OCR > 1.
2. Adjust *only* for overburden pressure (all $\eta_i = 1$ and C_N = some value).
3. Use Eq. (3-3). This is probably the best method but requires equipment calibration for $\boldsymbol{E}_r$—both equipment and operator. It will also require regular recalibration of the individual drilling rigs to account for wear and general equipment changes with use. This procedure will probably become mandatory to extrapolate N data across geographic regions where different equipment (and $\boldsymbol{E}_r$) is used.

Conventional practice is to do an SPT every 1 or 2 m after penetrating the topsoil or starting the first test at about 1- to $1\frac{1}{2}$-m depth. For each test there is a sample recovery of about 460 mm including the seating depth to provide a visual profile of around 50 percent of the boring depth.

Cohesionless samples are visually inspected and a portion is saved in a glass jar on which is marked job, boring number, depth, and field N. Cohesive samples are treated similarly, except q_u tests are routinely made—most often taking several values using a pocket penetrometer (see Fig. 3-9) with the average recorded. A small compression machine can be taken to the field for q_u tests; however, because of the area adjustment for strain (shown on Fig. 2-29) this is not commonly done. As a supplement in cohesive soils it is usual practice to take several thin-walled tube samples for laboratory testing as necessary (and to verify the field q_u).

The original SPT was developed for sand; however, at present it is commonly done at the given depth for all soils.

Several examples will illustrate the use of Eq. (3-3).

Example 3-2.

Given. $N = 20$; rod length = 12 m; hole diam. = 150 mm; $p'_o = 205$ kPa; use safety hammer with $\boldsymbol{E}_r = 80$; dense sand; no liner

Required. What are the "standard" N'_i and N'_{60} based on the following?

$$\boldsymbol{E}_{rb} = 70 \quad \text{and} \quad \boldsymbol{E}_{rb} = 60 \quad C_N = \left(\frac{95.76}{205}\right)^{1/2} = 0.68$$

$$\eta_i = 1.14 \quad \text{See sample computation shown in Table 3-3}$$

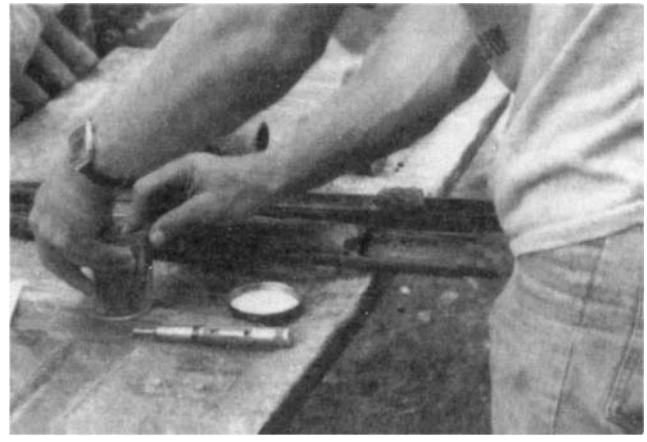

Figure 3-9 Field SPT sampling sequence. (*a*) Split tube opened to display sample and for taking a pocket penetrometer test for q_u. (*b*) Placing representative sample into jar for laboratory use. (*c*) Sample in jar with identification label. Pocket penetrometer in foreground. Dark band is marker for q_u on calibrated stem.

$$\eta_2 = 1.00 \quad L > 10 \text{ m}$$
$$\eta_3 = 1.00 \quad \text{usual United States practice of no liner}$$
$$\eta_4 = 1.05 \quad \text{slight oversize hole}$$

Use Eq. (3-3) and direct substitution in order:

$$N'_{70} = 0.68 \times 20 \times 1.14 \times 1 \times 1 \times 1.05$$
$$= \mathbf{16} \text{ (only use integers)}$$

for $\boldsymbol{E}_{rb} = \boldsymbol{E}_{r2}$ use Eq. (3-4), giving

$$N_2 = N'_{60} = \frac{70}{60} \times 16 = \mathbf{19}$$

////

Example 3-3. Same as Example 3-2 but with sample liner and $\boldsymbol{E}_r = 60$.

$$C_N = 0.68 \text{ as before}$$

$$\eta_1 = \frac{60}{70} = 0.86 \qquad \eta_2 = 1$$

$$\eta_3 = 0.80 \quad \text{(dense sand given with liner)} \qquad \eta_4 = 1.05$$
$$N'_{60} = 0.68 \times 20 \times 0.86 \times 0.80 \times 1.05 = \mathbf{10}$$

$$N_2 = N'_{70} = \frac{60}{70} \times 10 = \mathbf{9} \text{ using [Eq. (3-4)]}$$

////

Example 3-4. Same as Example 3-2 but $\boldsymbol{E}_r = 55$; $p'_c = 100$ kPa; 205 mm hollow stem auger, hole depth = 6 m.

$$C_N = \left(\frac{95.76}{100}\right)^{1/2} = 0.98 \quad (\text{using } p'_o = p'_c)$$

$$\eta_1 = 55/70 = 0.79 \qquad \eta_2 = 0.95 \quad (\text{since } 6 < 10 \text{ m})$$
$$\eta_3 = 1.0 \quad (\text{no liner}) \qquad \eta_4 = 1.0 \quad (\text{using hollow-stem auger})$$
$$N'_{70} = 0.98 \times 20 \times 0.79 \times 0.95 \times 1.0 \times 1.0 = \mathbf{15}$$
$$N_2 = N'_{60} = \frac{70}{60} \times 15 = \mathbf{17}$$

////

3-8 SPT CORRELATIONS

The SPT has been used in correlations for unit weight γ, relative density D_r, angle of internal friction ϕ, and undrained compressive strength q_u. It has also been used to estimate the bearing capacity of foundations (see Chap. 4, Sec. 4-10) and for estimating the stress-strain modulus E_s (see Chap. 5, Table 5-6).

For reasons given in the preceding sections many of these correlations are questionable. Some are based on a small database or on specific soils. Where a large database was used, there is the question of what $\boldsymbol{E}_r$ was used, this being very critical since many databases were obtained from published literature that might range from the early 1940s to the present for a corresponding range of $\boldsymbol{E}_r$ on the order of 35 to 80 percent.

TABLE 3-4
Empirical values for ϕ, D_r, and unit weight of granular soils based on the SPT at about 6 m depth and normally consolidated [approximately, $\phi = 28° + 15°D_r$ ($\pm 2°$)]

Description	Very loose	Loose	Medium	Dense	Very dense
Relative density D_r	0	0.15	0.35	0.65	0.85
SPT N'_{70}: fine	1–2	3–6	7–15	16–30	?
medium	2–3	4–7	8–20	21–40	> 40
coarse	3–6	5–9	10–25	26–45	> 45
ϕ: fine	26–28	28–30	30–34	33–38	
medium	27–28	30–32	32–36	36–42	< 50
coarse	28–30	30–34	33–40	40–50	
γ_{wet}, kN/m^3	11–16*	14–18	17–20	17–22	20–23

* Excavated soil or material dumped from a truck has a unit weight of 11 to 14 kN/m^3 and must be quite dense to weigh much over 21 kN/m^3. No existing soil has a $D_r = 0.00$ nor a value of 1.00. Common ranges are from 0.3 to 0.7.

The following are several SPT N-value correlations for angle of friction ϕ. The top two of Eq. (3-5) are from Shioi and Fukui (1982), who obtained them from the Japanese Railway Standards:

$$\begin{aligned} \phi &= \sqrt{18N'_{70}} + 15 \\ \phi &= 0.36N_{70} + 27 \\ \phi &= 4.5N_{70} + 20 \text{ (in general)} \end{aligned} \tag{3-5}$$

The top equation of this set is for roads and bridges, and the second is for buildings (refer also to Table 3-4).

A relationship for N and D_r was proposed indirectly by Meyerhof (1957) as

$$\frac{N}{D_r^2} = A + Bp_o \tag{3-5a}$$

For this equation Skempton (1986), using a database of five different soils, found that A and B are site-dependent with a range in A of 15 to about 54 and in B from 0.306 to 0.204 (using the N'_{70} base). This spread is such that using average values for A and B is somewhat risky; however, using averages we obtain

$$\frac{N'_{70}}{D_r^2} = 32 + 0.288p'_o \tag{3-5b}$$

with p'_o in kPa. For an average unit weight γ of 16 to 17 kN/m^3 and a depth of about 6 m one obtains $N'_{70}/D_r^2 \approx 60$, which was also used as a guide in designating the N values for normally consolidated sands of Table 3-4. For overconsolidated sands (OCR > 1), Skempton (1986) suggested the following adjustment:

$$\frac{N'_{70}}{D_r^2} = A + BC_{\text{OCR}}p'_o \tag{3-5c}$$

In this equation we define the new symbol C_{OCR} as follows:

1. Let the mean effective normal stress (as used in Sec. 2-11.2) be defined as

$$\overline{\sigma}_z = \frac{\sigma_x + \sigma_y + \sigma_z}{3} \qquad \sigma_x = \sigma_y = K_o\sigma_z$$

2. Now on substitution into the above and using p'_o for σ_z obtain the mean effective normal stress in situ (for a normally consolidated soil) as

$$C_{OCR}p'_o = \overline{p}'_{o,nc} = \frac{1 + 2K_{o,nc}}{3}p'_o$$

3. By usage definition the factor

$$C_{OCR} = \frac{\overline{p}'_{o,nc}}{\overline{p}'_{o,OCR}}$$

and we can, by using the appropriately subscripted $K_{o,i}$ and canceling p'_o from both the numerator and denominator because this is the existing effective overburden pressure, obtain

$$C_{OCR} = \frac{1 + 2K_{o,nc}}{1 + 2K_{o,OCR}} \tag{3-6}$$

This value of C_{OCR} is used in Eq. (3-5*c*). Note that this equation gives $C_{OCR} = 1$ for a *normally consolidated sand.* Use any of Eqs. (2-18) through (2-25) to obtain the lateral pressure coefficient $K_{o,i}$.

By using D_r from Eq. (3-5*c*) we can estimate ϕ (Meyerhof, 1959) as

$$\phi = 28 + 0.15D_r \qquad (D_r = \%) \tag{3-7}$$

or use the following equation, suggested by Yoshida et al. (1988), to compute D_r and then back-compute ϕ:

$$D_r = C_0 \cdot p'^{\,-C_1}_o \cdot N_{60}^{C_2} \tag{3-8}$$

In this equation D_r is in percent, and effective overburden pressure p_o is in kPa. The SPT N_{60} value is suggested by the author because little guidance is given in the cited reference. Yoshida et al. (1988) give a range of C_0 of 18 to 25 for soils with a best fit for all the soils of 25; a range for exponent C_2 from 0.44 to 0.57 with a best fit of 0.46; and a range for C_1 from 0.12 to 0.14 with a best fit of 0.12. These give

$$D_r = 25 \cdot p'^{\,-0.12}_o \cdot N_{60}^{0.46} \tag{3-8a}$$

and for a soil of $\gamma = 20$ kN/m^3 at a depth of 5 m with $N_{60} = 16$, obtain $p'_o = \gamma z = 20$ kN/m^3 $\times$ 5 m $= 100$ kPa and compute $D_r = 51.5 \rightarrow 52$ percent, and using Eq. (3-7), obtain $\phi \simeq 36°$.

The data shown in Table 3-4 for D_r and ϕ relate approximately to N'_{70} for borehole depths on the order of 4 to 6 m, as these might be the depth zone for spread footings. Additionally, one can use the preceding equations for guidance.

TABLE 3-5
Consistency of saturated cohesive soils*

Consistency			N'_{70}	q_u, kPa	Remarks
Very soft	NC	Young clay	0–2	<25	Squishes between fingers when squeezed
Soft			3–5	25–50	Very easily deformed by squeezing
Medium			6–9	50–100	? ?
Stiff	Increasing OCR	Aged/ cemented	10–16	100–200	Hard to deform by hand squeezing
Very stiff			17–30	200–400	Very hard to deform by hand squeezing
Hard			>30	>400	Nearly impossible to deform by hand

* Blow counts and OCR division are for a guide—in clay "exceptions to the rule" are very common.

Before using this table for design you should see a sample of the soil and have determined an average blow count N_i. With these data, use values from the table cautiously, because of the variables such as aging, natural cementation, water table location, and angularity of the soil grains. Additionally, terms such as *fine, medium,* and *coarse* are somewhat subjective, so any table value will be difficult to defend. With this precautionary note, we use the table but include any additional site information that is available.

A correlation for N versus q_u is in the general form of

$$q_u = kN \tag{3-9}$$

where the value of k tends to be site-dependent; however, a value of $k = 12$ has been used (i.e., for $N'_{70} = 10$, $q_u = 120$ kPa). Correlations for N'_{70} and consistency of cohesive soil deposits (soft, stiff, hard, etc.) are given in Table 3-5.

With the current practice of recovering samples and routinely inspecting them, performing on-site q_u tests with a pocket penetrometer, or using an unconfined compression test device, it is not necessary to use strength or consistency correlations. This is particularly true because of variations in OCR, aging, sample water content (or GWT location), presence or absence of drilling fluid, and site variations in terms of history, method of deposit formation and presence of gravel, and so on.

Most SPT correlations are based on modifying the coefficients of Eq. (3-5*a*) or using a different k in Eq. (3-9).

3-9 DESIGN N VALUES

Early recommendations were to use the smallest N value in the boring or an average of all of the values for the particular stratum. Current practice is to use an average N but in the zone of major stressing. For example, for a spread footing the zone of interest is from about one-half the footing width B above the estimated base location to a depth of about $2B$ below. Weighted averaging using depth increment × N may be preferable to an ordinary arithmetic average; that is, $N_{av} = \sum N \cdot z_i / \sum z_i$ and not $\sum N_i/i$.

For pile foundations there may be merit in the simple averaging of blow count N for any stratum unless it is very thick—thick being a relative term. Here it may be better to subdivide the thick stratum into several "strata" and average the N count for each subdivision.

The average corrected N'_{70} (or other base value) can then be computed from the average field-measured N and stratum data, or individual corrected N'_{70} values can be computed and then averaged.

Before the mid-1960s N values were adjusted[6] when they were taken from below the GWT. Current practice is not to adjust N values, because they are already reduced from being taken below the GWT (i.e., the blow count N is reduced from excess pore pressure as the sampler is driven). Work by Drozd (1974) indicates a reduced blow count is possible below the GWT but depends on the relative density. For example, reading approximately from one of his graphs (note: one cannot use a fraction of a blow), the following values were obtained:

D_r,%	N_{dry}	N_{sat}
40	4	1
50	5	2
60	8	4
70	9	6
80^+	Same values for either soil state	

For a sand state intermediate between "dry" and "saturated," the blow counts were sometimes larger than "dry" values of N. Although Drozd used a model split spoon (one-third the size of standard), he used seven different sands. The particle sizes ranged from 0.05 to 5 mm. The trend is evident that wet and saturated sands do not give values that are obtainable in "dry" sands.

If one is to use N values to obtain the stress-strain modulus E_s, which generally increases with depth (at least in any individual stratum), great care is required in how one adjusts N.

Using the factor C_N in Eq. (3-3) would modify any N to a value corresponding to a depth producing $\sigma_v = 95.76$ kPA and eliminate much of the depth effect. On the other hand, if we want a value of N for a zone of, say, $2B$ beneath a spread footing, we should use C_N after the averaged N_{av} is computed.

3-10 OTHER PENETRATION TEST METHODS

A number of other penetration methods are in use. The cone penetration test (CPT) of the next section appears to be one of the most popular. In a particular locale, though, one of the other tests may be preferable.

Figure 3-10 represents a Swedish weight sounding method used in most of Scandinavia, some countries in eastern Europe, and Japan and China. The test seems suited only for very soft silt or soft clay deposits. Basically, the test consists in pushing the device to some depth and then adding sufficient mass until the screw tip begins to self-turn and move downward. The mass and number of half-turns to advance some specified distance (usually 1 m or the tip length) are recorded. If the maximum mass of 100 kg does not start the penetrometer turning, it is turned by hand (or a driving motor), and the number of half-turns to advance the specified distance is recorded. The soil type is related to the plot of weight versus turn number as for example, a soft, medium, or stiff clay, or other. Usually the test is supplemented by some method that allows sample recovery for a visual comparison of the sounding test data to the soil type. This test is not standardized, so correlations would only apply to the area—and for that tip configuration.

[6]Usually as $N' = N + \frac{1}{2}(N - 15)$ for $N > 15$; $N' = N$ for $N \leq 15$.

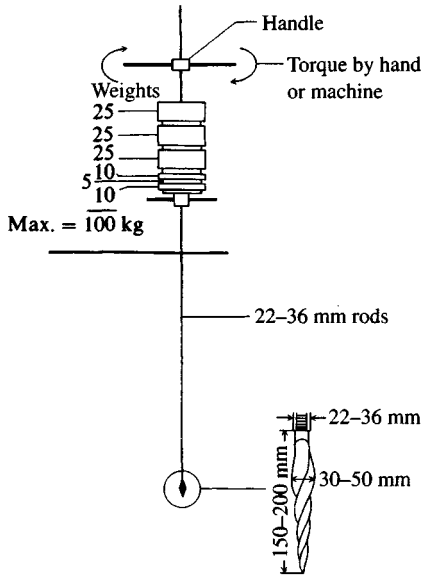

Figure 3-10 A type of Swedish weight sounding equipment.

Tombi-type trip release as used in Japan for the SPT as well as for dynamic cone

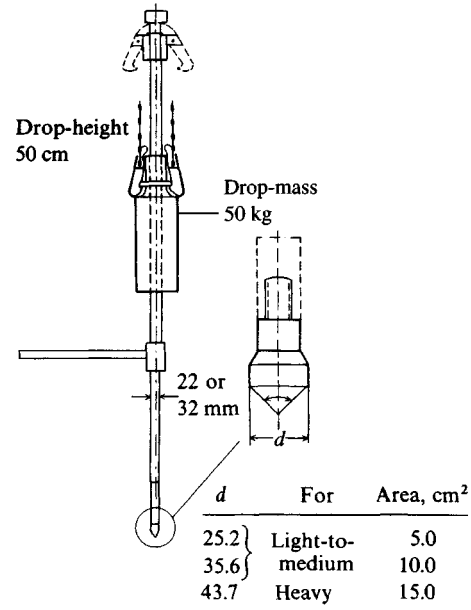

Figure 3-11 One type of dynamic cone penetration test.

Figures 3-11 and 3-12 are dynamic cone penetrometers that are used for *dynamic penetration testing*. This type test has some use in Europe and Asia but not much in North and South America. This test consists in driving the tip to some depth and recording the number of blows (somewhat similar to the SPT). Correlations exist but are usually specific to a locale because neither the conical-shaped tip nor the driving mass is standardized. Dynamic penetration testing is most suited to gravelly soil deposits.

Figure 3-13 is an illustration of a hand-held penetrometer developed by the U.S. Waterways Experiment Station (it can be purchased from most soil laboratory equipment suppliers). The device has most application at shallow depths where the user can push the cone tip into the ground and simultaneously read the resistance from deformation of the load ring. Typical applications include soil where a spread footing is to be placed and soil being monitored for quality control of compacted fills.

3-11 CONE PENETRATION TEST[7] (CPT)

The CPT is a simple test that is now widely used in lieu of the SPT—particularly for soft clays, soft silts, and in fine to medium sand deposits. The test is not well adapted to gravel deposits or to stiff/hard cohesive deposits. This test has been standardized by ASTM as D 3441. In outline, the test consists in pushing the standard cone (see Figs. 3-14 and 3-15) into

[7]Several thousand pages of literature on this test have been published since 1980.

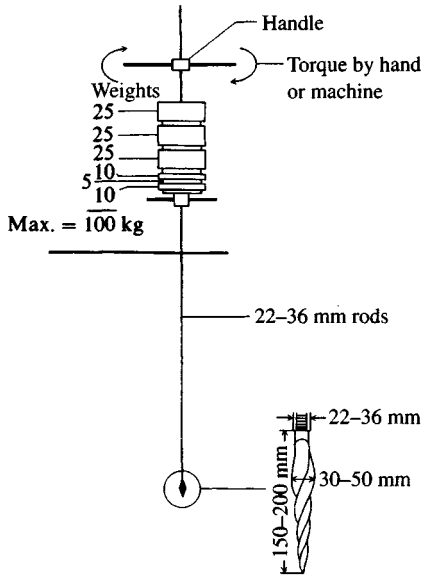

Figure 3-10 A type of Swedish weight sounding equipment.

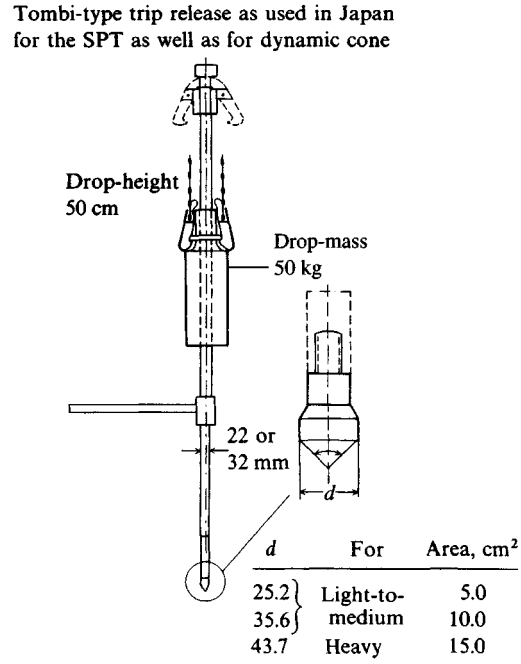

Figure 3-11 One type of dynamic cone penetration test.

Figures 3-11 and 3-12 are dynamic cone penetrometers that are used for *dynamic penetration testing*. This type test has some use in Europe and Asia but not much in North and South America. This test consists in driving the tip to some depth and recording the number of blows (somewhat similar to the SPT). Correlations exist but are usually specific to a locale because neither the conical-shaped tip nor the driving mass is standardized. Dynamic penetration testing is most suited to gravelly soil deposits.

Figure 3-13 is an illustration of a hand-held penetrometer developed by the U.S. Waterways Experiment Station (it can be purchased from most soil laboratory equipment suppliers). The device has most application at shallow depths where the user can push the cone tip into the ground and simultaneously read the resistance from deformation of the load ring. Typical applications include soil where a spread footing is to be placed and soil being monitored for quality control of compacted fills.

3-11 CONE PENETRATION TEST[7] (CPT)

The CPT is a simple test that is now widely used in lieu of the SPT—particularly for soft clays, soft silts, and in fine to medium sand deposits. The test is not well adapted to gravel deposits or to stiff/hard cohesive deposits. This test has been standardized by ASTM as D 3441. In outline, the test consists in pushing the standard cone (see Figs. 3-14 and 3-15) into

[7]Several thousand pages of literature on this test have been published since 1980.

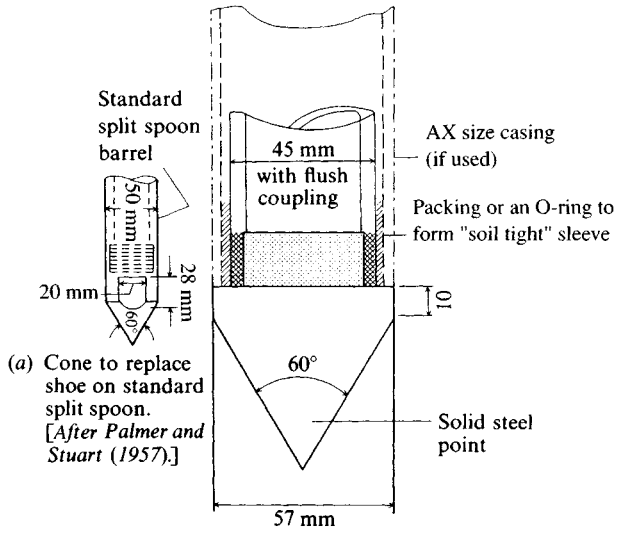

Figure 3-12 Two dynamic-type cones driven using the SPT or larger drive weights.

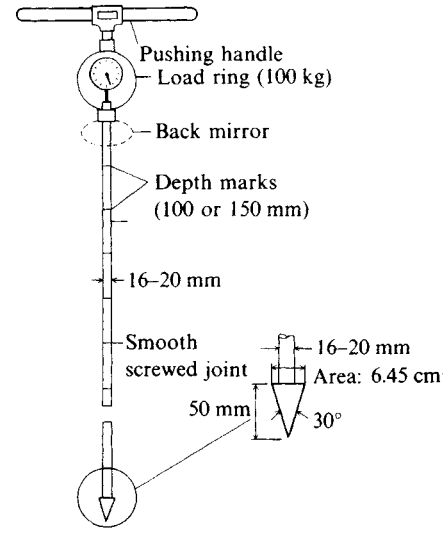

Figure 3-13 Hand-held penetrometer for shallow depths. The resistance necessary to push the cone 50 mm into soil is read in mirror from load ring gauge.

the ground at a rate of 10 to 20 mm/s and recording the resistance. The total cone resistance is made up of side friction on the cone shaft perimeter and tip pressure. Data usually recorded are the cone side resistance q_s, point resistance q_c, and depth. Pore pressures, vertical alignment, and temperature may also be taken if allowed by the equipment configuration (see Fig. 3-15).

The tip (or cone) usually has a projected cross-sectional area of 10 cm^2, but larger tips are also used and may provide more reliable pore pressure readings. The cone diameter does not seem to be a significant factor for tip areas between 5 and 15 cm^2.

A CPT allows nearly continuous testing at many sites, which is often valuable. If the soil is stratified, the test may be performed in parallel with a drilling machine. In this case the hole is drilled to soft material, a CPT is done, boring recommences, and so on. This test is rather popular for sites where there are deep deposits of transported soil such as in flood plains, river deltas, and along coastlines.

There are at least five cone types in use, although the ASTM D 3441 standard lists only three.

1. Mechanical—the earliest type, often called the *Dutch cone* since it was first developed and used in The Netherlands. A typical later configuration with a friction sleeve is shown in Fig. 3-14.
2. Electric friction—first modification using strain gauges to measure q_c (point resistance) and q_s (side friction) (see Fig. 3-15*a*).
3. Electric piezo—a modification of the electric friction cone to allow measuring the pore water pressure during the test at the cone tip (see Fig. 3-15*b*).
4. Electric piezo/friction—a further modification to measure point resistance, sleeve friction, and pore pressure.

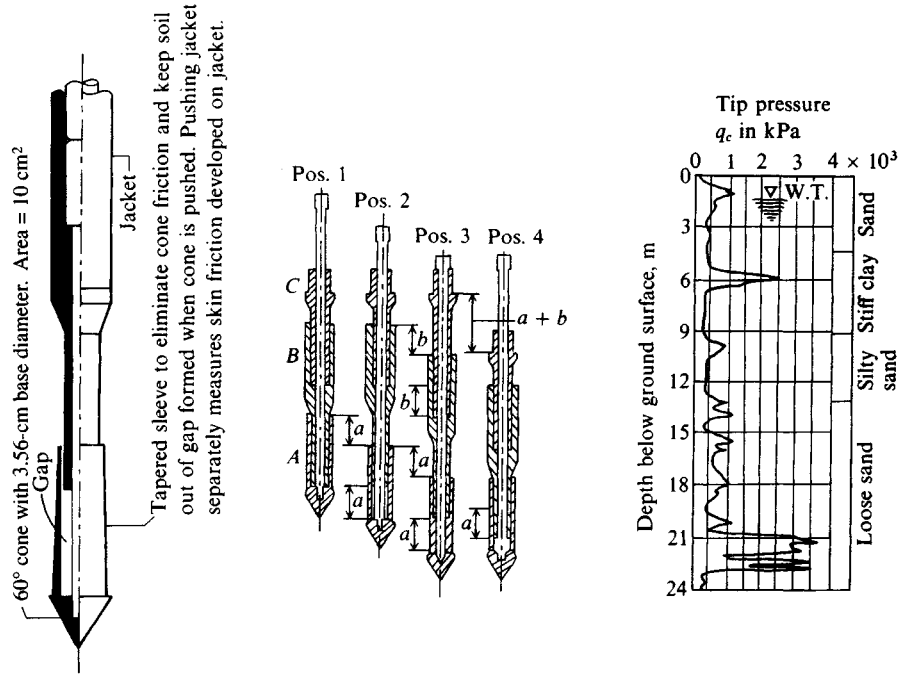

(*a*) Dutch cone modified to measure both point resistance q_c and skin friction q_f.

(*b*) Positions of the Dutch cone during a pressure record.

(*c*) Typical output (usually electronically made).

Figure 3-14 Mechanical (or Dutch) cone, operations sequence, and tip resistance data.

5. Seismic cone—a further modification to include a vibration sensor to obtain data to compute the shear wave velocity from a surface hammer impact so that the dynamic shear modulus can be computed [Campanella et al. (1986)].

There are several configurations of the *piezocone* of Fig. 3-15*a*, and it is critical that the friction sleeve diameter tolerance be 0 to not more than 0.25 mm larger than the cone tip diameter—if smaller, the side friction is too low. The piezometer (pore pressure sensor) element may be made from sintered metal, ceramics, or stone. It may be located at the "tip," somewhere along the cone face, or at the cone base—and sometimes both in the tip and at the cone base. Both the location of the tip and the type of material to be used in it are important, as any roughness will reflect into the tip resistance. Cone usage in sandy materials quickly roughens the tip. A serious concern using pore pressure sensors is that they be kept saturated, for any air that is present will substantially reduce the pressure that is recorded. The base location generally produces a lower measured pore pressure than for the tip (or cone face) location.

Some of the electrical cones may also be provided with inclinometer electronics to measure deviation from the vertical alignment, usually caused from encountering a hard stratum or large stones. Data deteriorate as the cone slope increases from the vertical. When this occurs, the test is usually halted, the equipment moved a few meters away, and a new test begun.

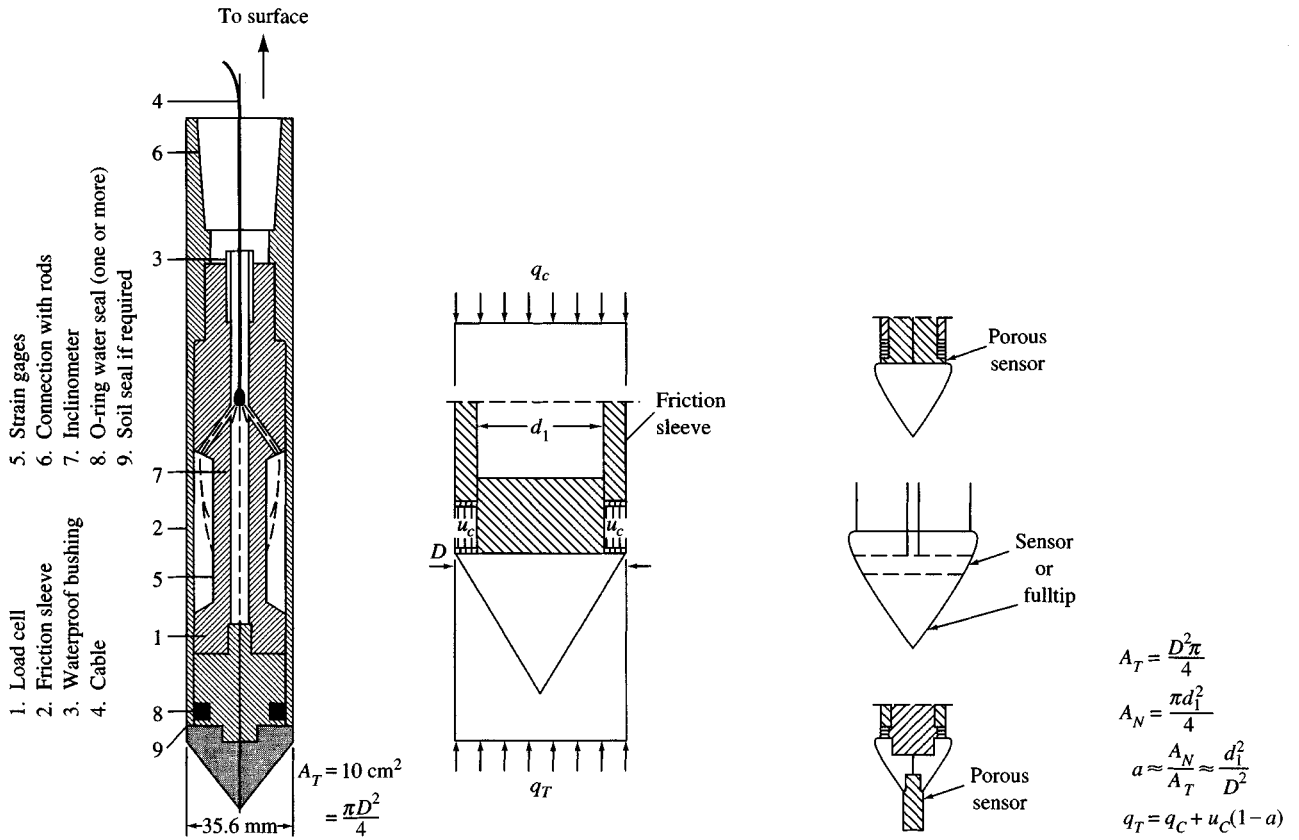

(*a*) Typical electric cone. (*b*) Pore-pressure definitions for cones. (*c*) Cone pore pressure sensor locations.

Figure 3-15 Electric cone and CPT data. There is some controversy involving both the piezometer material and tip configuration.

A temperature sensor may be located near the tip so that a calibration based on the in situ (usually cooler than laboratory) value can be made. If the cone electronics are calibrated in the laboratory at a temperature different from the soil, the output will be in error some amount.

The original mechanical cone test is illustrated in Fig. 3-14*b* with the step sequence as follows:

1. The cone system is stationary at position 1.
2. The cone is advanced by pushing an inner rod to extrude the cone tip and a short length of cone shaft. This action measures the tip resistance q_c.
3. The outer shaft is now advanced to the cone base, and skin resistance is measured as the force necessary to advance the shaft q_s.
4. Now the cone and sleeve are advanced in combination to obtain position 4 and to obtain a q_{total}, which should be approximately the sum of the $q_c + q_s$ just measured. The cone is now positioned for a new position 1.

By using an electrical cone configuration, a start-stop operation of the mechanical cone is not required (except to add push rod extensions). The test consists in making a continuous push with the output recorded electronically.

The test (on land) is usually done from a truck-mounted cone with an opening in the truck bed (or from the end gate) and the pushing equipment located so that the cone with suitable drill rods attached can be pushed into the soil. The system may also be mounted on all-terrain vehicles so that remote areas can be accessed. The mass of the vehicle and pushing equipment provides the reaction, but this mass may on occasion require additional anchorage—usually soil screw anchors.

When the pushing is continuous, it is advantageous to connect the cone output directly to a dedicated computer. Doing so makes it much easier both to compute necessary output and to plot results.

A test over water is similar to a land test. The vehicle or equipment is placed on a barge (or drill ship) that is moved to the site and securely anchored, both to resist wave action and to allow for any additional reaction.

Piezocone output is generalized in Fig. 3-16, where pore pressure is measured along with cone pressure q_c. Figure 3-17 illustrates two cone test records in soil as indicated.

The CPT test data are used to classify a soil, to establish the allowable bearing capacity of shallow foundation elements, or to design piles. They have been extensively used in the design of piles for offshore oil-drilling platforms. The data generally require some supplemental information derived from other exploration methods (i.e., SPT usually) unless the geotechnical consultant has done previous work in nearby areas. The supplemental data are required because CPT data can be quite erratic. Inspection of Fig. 3-17 reveals a number of "peaks," so that for the data to be useful some kind of resistance averaging must be done. The averaging is usually based on the user's judgement and inspection of the several plots. If the data are stored in a computer, an installed program might be used to obtain averages in the several strata.

The measured point resistance q_c and sleeve friction (or side friction) are used to compute the friction ratio f_r as

$$f_r = \frac{q_s}{q_c} \times 100 \qquad (\%) \tag{3-10}$$

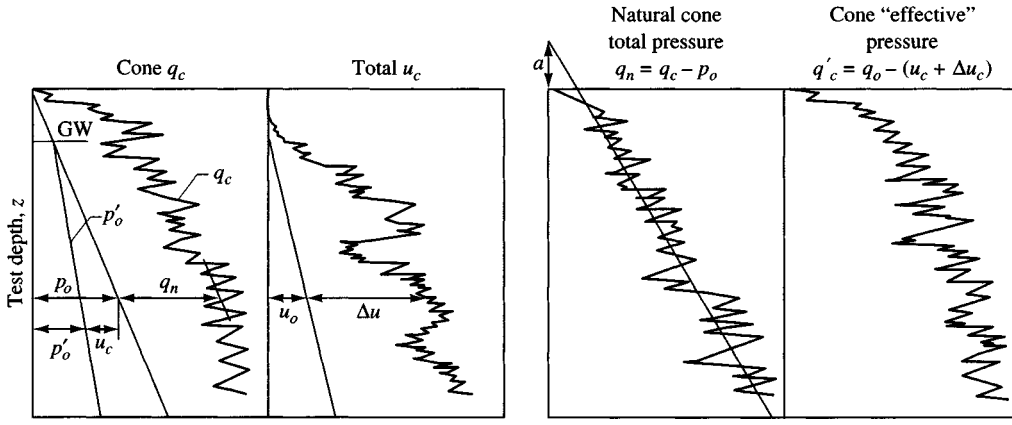

(*a*) Measured data and pore-pressure components. (*b*) Computed data using values from (*a*).

Figure 3-16 Qualitative items recorded or needed to interpret a CPT. *[After Senneset et al. (1982).]*

The friction ratio is primarily used for soil classification, as illustrated in Figs. 3-18*a* and *b*. It may also be used to give an estimate of the soil sensitivity, S_t [see Eq. (2-63)] with the correlation being approximately [see Robertson and Campanella (1983*a*)]

$$S_t \approx \frac{10}{f_r}$$

In this equation use f_r in percent. The constant 10 (a value of 15 was formerly used) is an approximation that may be improved with data from specific areas.

3-11.1 CPT Correlations for Cohesive Soil

Cone resistance may be directly used in design, but usually it is incorporated as some multiple of q_c. Instead of directly using q_c, one may obtain the required design parameter from one of the many correlations that use a relationship between q_c and the quantity of interest. Those correlations that seem to have most acceptance are given here; however, since they are generalized, a user should use them cautiously, because they may not be applicable locally. What a practitioner should do is plot local correlations onto these charts as practical, and as a trend develops, revise the equations.

One correlation between the cone bearing resistance q_c and undrained shear strength s_u is based on the bearing capacity equation (of Chap. 4) and is as follows:

$$q_c = N_k s_u + p_o$$

Solving for the undrained shear strength s_u, one obtains

$$s_u = \frac{q_c - p_o}{N_k} \tag{3-11}$$

where $p_o = \gamma z$ = overburden pressure point where q_c is measured as previously defined and used. This parameter is in the units of q_c and same type of pressure (i.e., if q_c is an effective pressure, use p'_o).

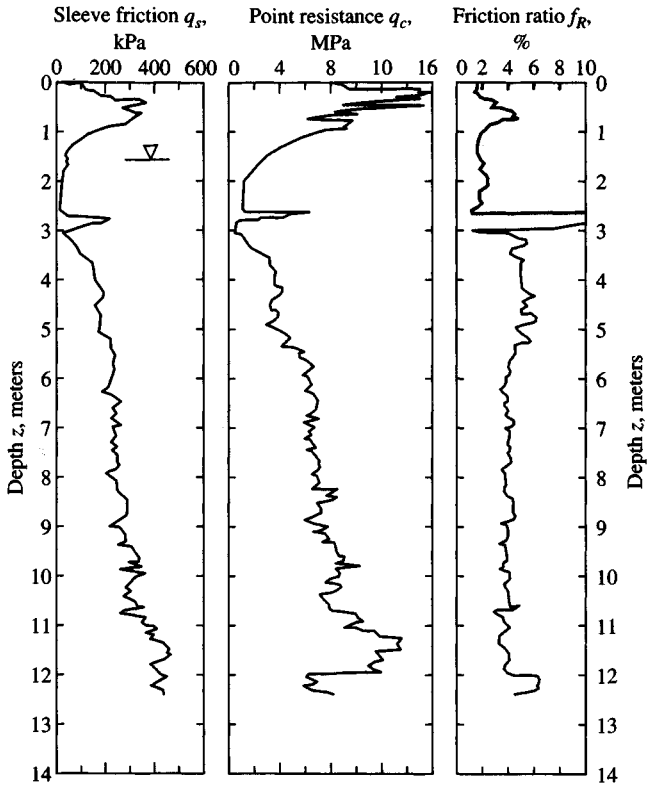

(*a*) Cone penetration record for a "clay" soil without pore pressure.

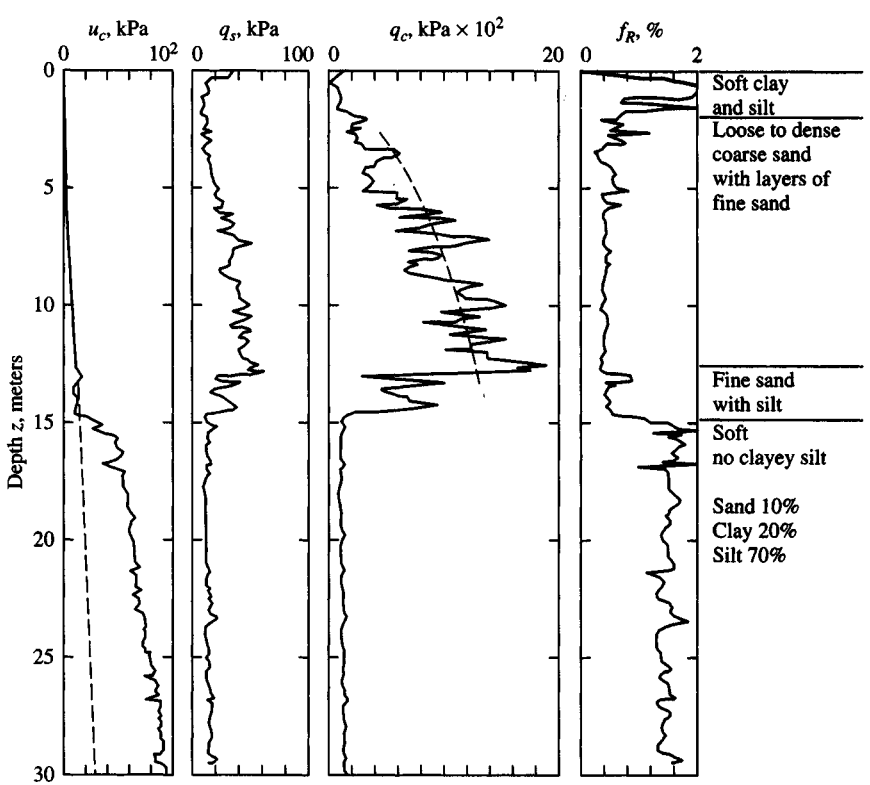

(*b*) CPT with pore pressure recorded.

Figure 3-17 Two CPT logs.

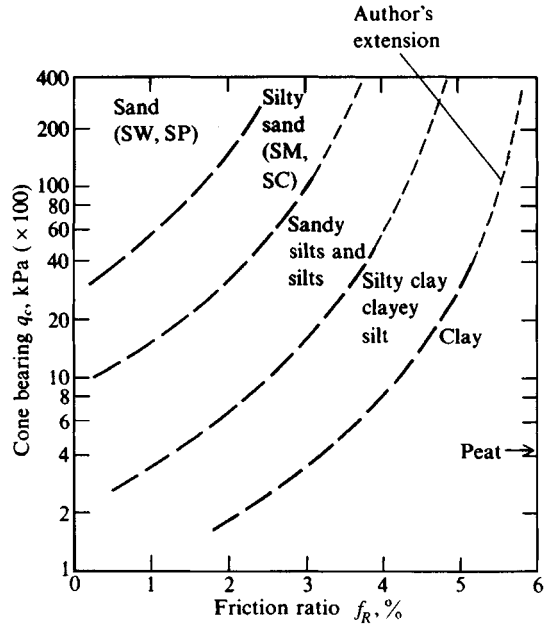

Figure 3-18*a* Soil classification charts. Use with caution and/or together with recovered tube samples.

(*a*) Using a standard electric or mechanical cone. [*After Robertson and Campanella (1983).*]

N_k = cone factor (a constant for that soil). N_k has been found to range from 5 to 75; however, most values are in the 10 to 30 range and, further, most values are in the 15 to 20 range. Figure 3-19 is a correlation based on the plasticity index I_P which might be used.

Because of the wide scatter in N_k, a number of persons have suggested correcting the piezocone resistance q_c with the measured pore pressure u_c to reduce the scatter [see Aas et al. (1986), but it was suggested earlier by Robertson and Campanella (1983*a*)]. The adjustment of q_c to a corrected total tip resistance q_T is

$$q_T = q_c + u_c(1 - a) \tag{3-12}$$

where a = an area ratio that depends on the cone type. It can be computed (see Fig. 3-15*b* or inset of Fig. 3-18*b*) as

$$\frac{\pi D^2/4 - k\pi d_1^2/4}{\pi D^2/4} \rightarrow 1 - \frac{kd_1^2}{D^2} \rightarrow 1 - a$$

If calibration is not used, it is common to assume $k = 1$ above, giving $a = (d_1/D)^2$; from calibration, a has been found to range from about 0.4 to 0.9, but for the "standard cone," with a 10 cm^2 area, the range is from about 0.6 to 0.9. A given cone can be calibrated[8] by inserting the system in a container of water

[8]Schaap and Zuidberg (1982) describes calibration procedures for the interested reader.

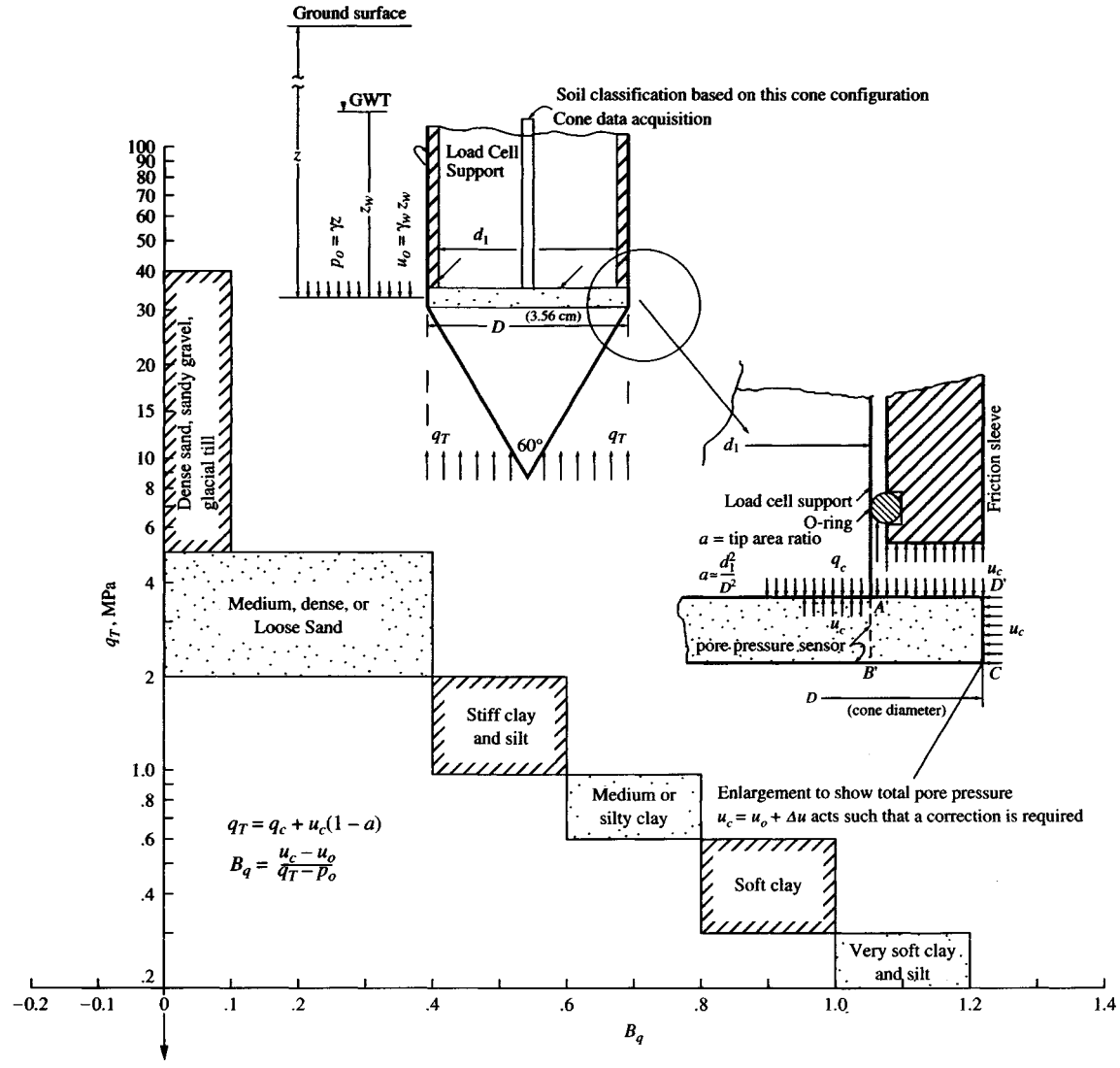

Figure 3-18*b* Using the CPT with a piezocone as shown above (note use of q_T). *[After Campanella and Robertson (1988).].*

with a wood block under the tip for protection and apply some known load q_T while recording both the pore pressure $u_c = u_o$ and the net cone pressure q_c and computing a as

$$a = [q_T - (q_c + u_o)]/u_o$$

u_c = measured pore pressure from the pressure sensor and in same units as q_c.

With this adjustment the undrained shear strength s_u is

$$s_u = \frac{q_T - p_o}{N_{kT}} \tag{3-13}$$

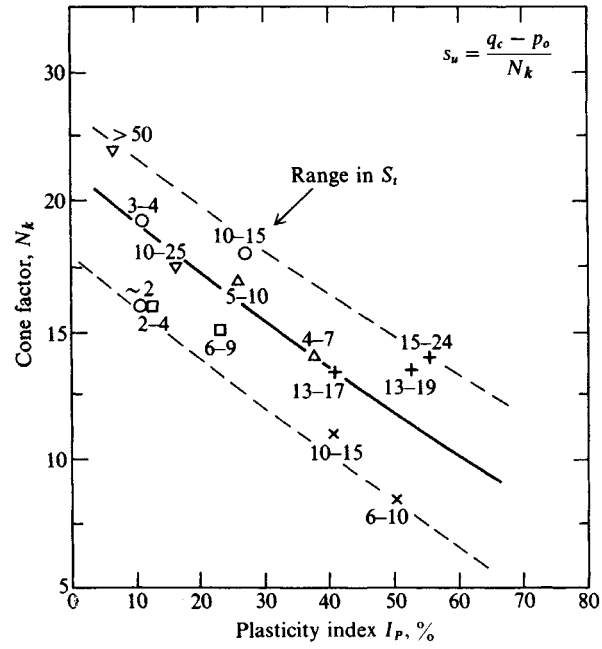

Figure 3-19 Cone factor N_k versus I_P plotted for several soils with range in sensitivity noted. [*After Lunne and Eide (1976).*]

The N_{kT} value is introduced here to identify that the adjusted cone bearing pressure q_T is being used. This seems to reduce the scatter to a range of about 10 to 20, which is a narrow enough range that the following equation (author's interpretation) can be used:

$$N_{kT} = 13 + \frac{5.5}{50} I_P \qquad (\pm 2) \tag{3-14}$$

Thus, for clay with a plasticity index $I_P = 20$, we compute $N_{kT} = 15.2 \pm 2$, or N_{kT} is between 13.2 and 17.2.

It is also possible to estimate the soil type as clay or cohesionless by inspection of the ratio of pore-pressure change Δu (see Fig. 3-16) and the measured cone resistance as

$$\Delta u / q_c$$

Very small values of this ratio represent cohesionless materials, for which the coefficient of permeability will be large enough that the excess pressure Δu generated by the probe displacement quickly dissipates. In cohesive deposits pore pressure does not dissipate very rapidly so the $\Delta u/q_c$ ratio is usually larger. The $\Delta u/q_c$ ratio is generally lower for overconsolidated cohesive soils (OCR > 1) than for normally consolidated deposits.

In general one should obtain several undisturbed tube samples and obtain s_u values to establish the likely value(s) of N_k or N_{kT}, since factors such as OCR, grain size, unit weight, cementing, aging, etc., are significant variables. For normally consolidated clays of low sensitivity (say $S_t < 4$) and $I_P < 30$ a value of N_k of about 18 and N_{kT} of 14 may be satisfactory to use in Eq. (3-11) or Eq. (3-13).

Correlations based on a relationship between q_c and either I_P or the consistency index I_c [as given in Eq. (2-14*a*)] have been attempted without much success. Also some attempts at a correlation between q_u and q_c have been proposed. Two of these correlations are obtained

from Sarac and Popović (1982) as follows:

$$\begin{aligned} q_c &= a + bI_c \\ q_c &= 612.6 + 587.5I_c \text{ kPa} \\ q_c &= a + bq_u \\ q_c &= 525.1 + 1.076q_u \text{ kPa} \end{aligned} \tag{3-15}$$

In these equations I_c is a decimal quantity, and both q_u and q_c are in kPa. These two correlations can be as much as ±30 percent in error—for example, if the computed value is 1000 kPa, the field value can be anywhere in a range of 700 to 1300 kPa.

Sully et al. (1988) give a correlation for the OCR using a piezocone as shown in Fig. 3-15*a* with pore pressure sensors installed at the cone base and either on the tip or in the lower half of the cone face. During a test the tip sensor should read a higher pore pressure than the sensor at the cone base. Defining this pore pressure difference as PPD gives us

$$\text{PPD} = \left(\frac{u_c}{u_o}\right)_{\text{tip}} - \left(\frac{u_c}{u_o}\right)_{\text{base}} \tag{3-16}$$

where u_o = in situ static pore pressure $\gamma_w z$ in the same units as the pore pressures u_c measured at the cone tip and base. A least squares analysis using a number of soils gives

$$\text{OCR} = 0.66 + 1.43\,\text{PPD} \tag{3-17}$$

with a correlation coefficient of $r = 0.98$ (1.0 would be exact). Sully (1988*a*) revised Eq. (3-17) to

$$\text{OCR} = 0.49 + 1.50\,\text{PPD} \qquad (r = 0.96) \tag{3-17a}$$

Again, on a much larger database, Sully (1990) revised Eq. (3-17) to

$$\text{OCR} = 0.50 + 1.50\,\text{PPD} \tag{3-17b}$$

The best range of this equation is for OCR < 10. Equations (3-17) were developed using pore-pressure data in clays, so they probably should not be used for sands. See Eq. (3-19*a*) for another equation for OCR applicable for both clay and sand.

3-11.2 CPT Correlations for Cohesionless Soils

Figure 3-20 is a plot of the correlation between cone pressure q_c and relative density D_r. This figure represents the author's composite from references given. The curves are for normally consolidated cohesionless material. If the soil is overconsolidated, D_r requires correction according to Schmertmann (and others). The correction uses the following equations:

$$\frac{q_{c,\text{OCR}}}{q_{c,\text{nc}}} = 1 + k\left(\frac{K_{o,\text{OCR}}}{K_{o,\text{nc}}} - 1\right) \tag{3-18}$$

Schmertmann (1978) suggested that the k term in this equation be 0.75, however, in other locales a different value may produce a better correlation.

In Eq. (3-18) the K_o ratio might be obtained from Eq. (2-23) rearranged and given here as a reader convenience:

$$\frac{K_{o,\text{OCR}}}{K_{o,\text{nc}}} = \text{OCR}^n \tag{2-23}$$

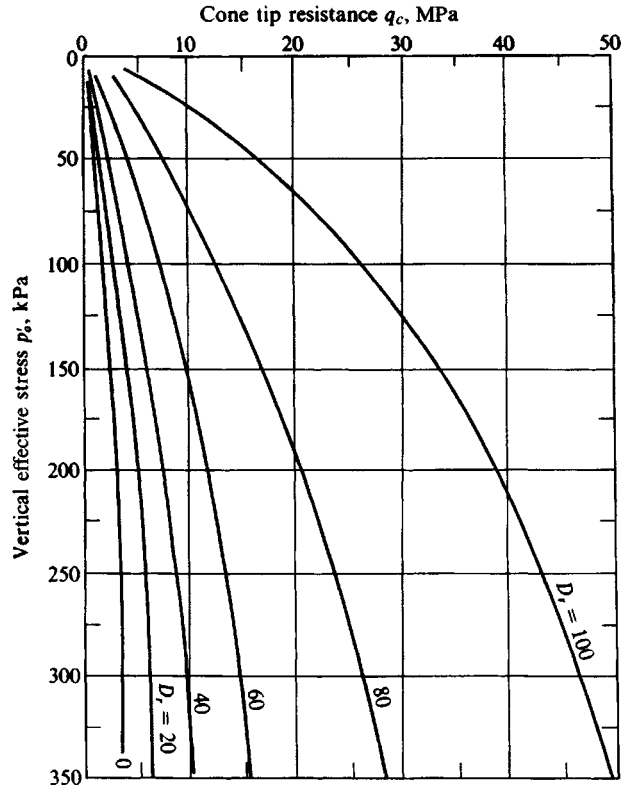

Figure 3-20 Approximate relationship between cone q_c and relative density D_r, as a composite from Schmertmann (1978) and Villet and Mitchell (1981) for normally consolidated saturated recent (noncemented) deposits.

Schmertmann suggested using $n = 0.42$, but later data suggest that n is site-dependent and may be from 0.32 to 0.52+, perhaps 0.4 for medium dense, 0.48 for dense, and 0.52 for very dense sands.

If the soil is normally consolidated, Fig. 3-20 can be used directly. For example: at $z = 10$ m, $\gamma' = 10$ kN/m^3 measure $q_c = 10$ MPa; now compute effective stress $p'_o = \gamma' z = 10$ kN/m$^3 \times 10$ m $= 100$ kPa; and using Fig. 3-20 at the intersection of $q_c = 10$ and $p'_o = 100$ interpolate and obtain $D_r \approx 70\%$).

When the cohesionless deposit is overconsolidated (OCR > 1) the CPT gives $q_{c,\text{OCR}}$ which must be converted using Eq. (3-18) to an equivalent $q_{c,\text{nc}}$ in order to use Fig. 3-20. Do this as follows:

1. First plot Eq. (3-18) using several values of the K_o ratio such as 0.5, 1, 1.5, 2, 2.5, 3,... about 5 to 6.
2. Find the K_o ratio for the site using one of the procedures given.
3. Enter the chart and project from the plot to the q_c-ratio axis and obtain the ratio $q_{c,\text{OCR}}/q_{c,\text{nc}}$ as Val.

4. Now solve

$$\frac{q_{c,\text{OCR}}}{q_{c,\text{nc}}} = \text{Val}$$

$$q_{c,\text{nc}} = \frac{q_{c,\text{OCR}}}{\text{Val}}$$

Use this value of $q_{c,\text{nc}}$ as the *cone tip resistance* term q_c and using the computed value of in-situ p'_o enter Fig. 3-20 and obtain the overconsolidated value of D_r.

5. Save the plot so that you can plot local data on it to see whether a better correlation can be obtained.

When the relative density D_r is estimated, use Table 3-4 or Eq. (3-7) to estimate the angle of internal friction ϕ.

Figure 3-21 may be used to estimate the OCR for both sands and clays. A pressure ratio B_q is computed using the measured cone pore pressure and *total* overburden pressure $p_o = \gamma z$ as

$$B_q = \frac{u_c - u_o}{q_T - p_o} = \frac{\Delta u}{q_T - p_o} \tag{3-19}$$

where terms are identified either on Fig. 3-15*b* or Fig. 3-18*b*. Use this equation to compute B_q, enter Fig. 3-21 for OCR, and then back-compute Eq. (2-23) for the K_o ratio if a suitable exponent n can be estimated. An equation for the relationship between OCR and B_q for clays

Figure 3-21 A relationship between B_q and OCR. Relationship may be site-specific but it is based on soils from a number of geographic locations. [*After Keaveny and Mitchell (1986).*]

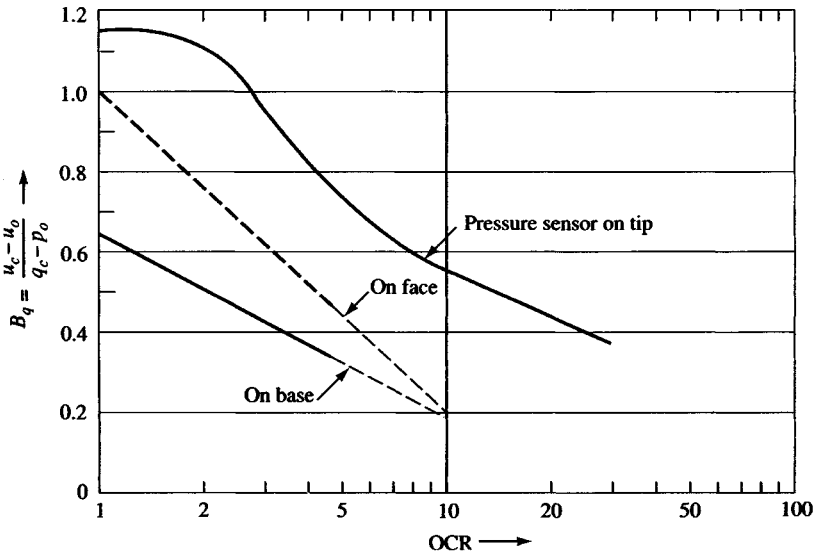

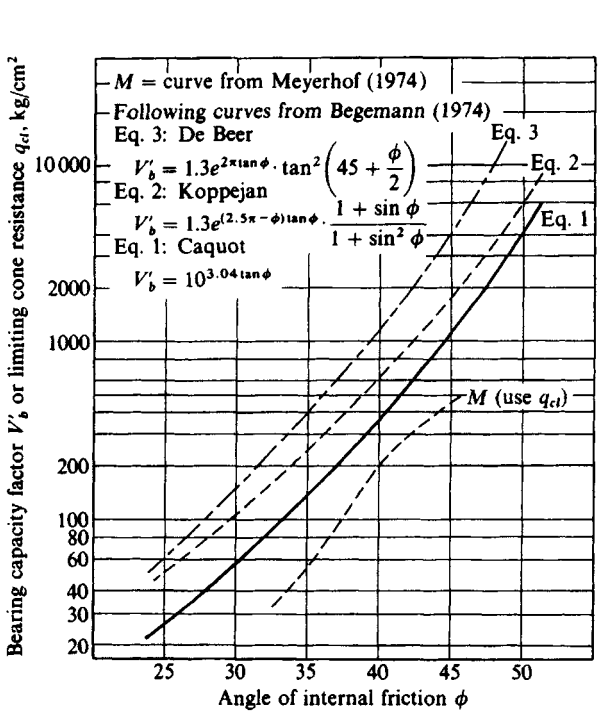

(*a*) Cone-bearing versus ϕ relationship.

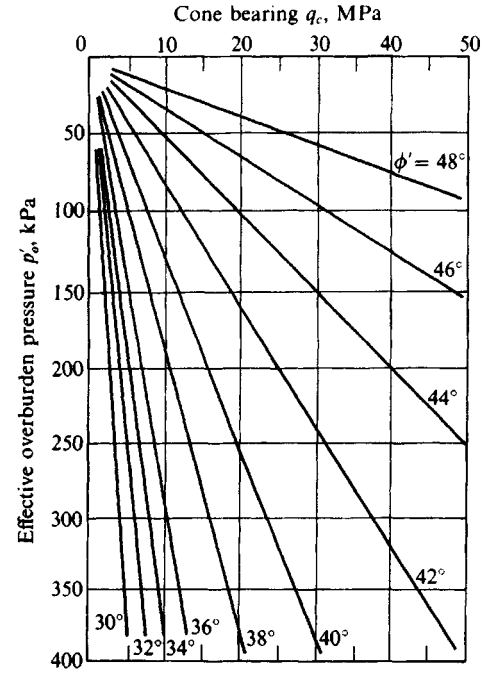

(*b*) Correlation between peak friction angle ϕ' and q_c for uncemented quartz sands. *Data from Robertson and Campanella (1983) and others.*

Figure 3-22 Correlations between cone data and angle of internal friction ϕ. The Meyerhof plot in (*a*) is a replot from five sources but valid only in the range of $30 \leq \phi \leq 45°$.

of sensitivity $S_t < 8$ is given by Chang (1991) as

$$\text{OCR} = \frac{2.3B_q}{3.7B_q - 1} \tag{3-19a}$$

Figure 3-22 is an alternative means to estimate the friction angle ϕ using the bearing capacity factor V'_b shown on the figure that is defined as

$$V'_b = \frac{q'_c}{p'_o}$$

where $p'_o = \gamma' z$ and q'_c are both "effective" stresses. The Meyerhof M curve is similar to those labeled "Eq. 1, 2, and 3" (on Fig. 3-22*a*), except that the limiting *total* cone pressure q_{cl} is used instead of V'_b for the ordinate axis. In most cases—particularly if the CPT is a continuous push—q_{cl} is the "limiting" total cone bearing pressure q_{cl}.

In the range shown the Meyerhof M curve tends to give larger ϕ-angles for the same pressure ratio. In practice one should probably use both figures (*a*) and (*b*) and average the values to obtain a design angle of internal friction ϕ. An approximate equation for ϕ using the total cone bearing pressure q_c (in MPa) is the following (with corrections shown):

$$\phi = 29° + \sqrt{q_c} \qquad + 5° \text{ for gravel;} \qquad - 5° \text{ for silty sand}$$

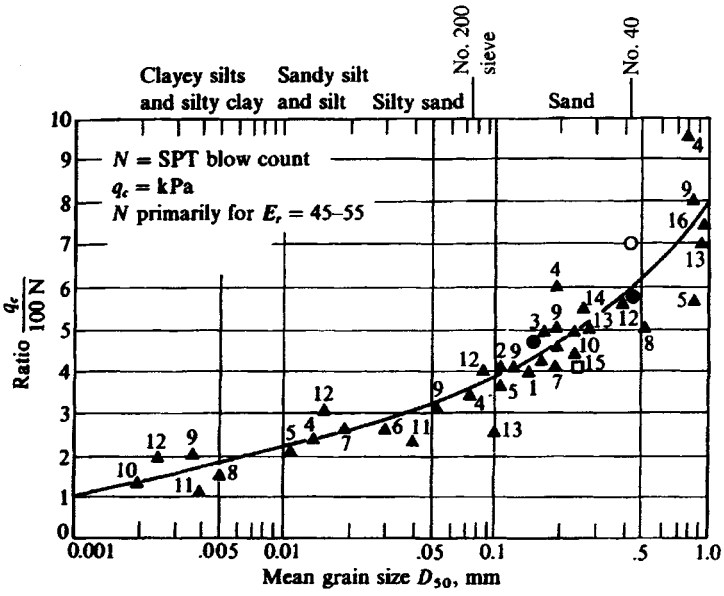

Example From sieve analysis $D_{50} = 0.5$ mm
From in situ CPT $q_{c,av} = 60$ kg/cm^2 (6000 kpa)

Required Estimate N_{55}

Solution Enter chart at $D_{50} = 0.5$ project vertically to curve then horizontally to read

$$\frac{q_c}{100N_{55}} \approx 6.2$$

$$N_{55} = \frac{6000}{100 \times 6.2} = 9.6 \rightarrow \mathbf{10} \text{ blows/0.3m}$$

Check using Eq. (4 – 20):

$$N_{55} \approx \frac{q_c}{4} = \frac{60}{4} = \mathbf{15}$$

Figure 3-23 Relationship between mean grain size (D_{50}) and q_c/N ratio. Note the energy ratio E_r on which the relationship is based. *[After Robertson et al. (1983) and Ismael and Jeragh (1986); reference numbers correspond to references in original sources.]*

A number of correlations have been proposed for making an SPT N-blow count estimate using CPT resistance in both clay and cohesionless materials. The reasons for this are that there is a larger database of N numbers than q_c pressures *and* that the SPT produces recovered (but disturbed) soil samples for visual inspection.

All of these correlations used various bridging parameters [desired quantity $= A + BN$; $r = f(N)$], but it was (and still is) difficult to produce anything that one can use with much confidence. The widespread use of the CPT makes it less important to put much additional development effort into this type of correlations—rather, plot local data on existing curves to improve their correlation reliability as much as possible.

Figure 3-23 is the most reliable of the q_c-N correlations presently in use. It uses the D_{50} grain size (the grain size where 50 percent is finer—see Fig. 2-3) as the bridging parameter. It appears that grain size gives better correlation than any other parameter in coarse-grained soils.

Some correlations for both clay and cohesionless soils use a generic form of

$$q_c = kN \tag{3-20}$$

where q_c is in units of MPa and coefficient k tends to range from 0.1 to about 1.0 as in the following table [from Ramaswamy et al. (1982) with some author revisions] which uses N'_{60}:

Soil type	q_c/N_{60}
Silts, sandy silts, and slightly cohesive silt-sand mixtures	0.1–0.2
Clean fine to medium sands and slightly silty sands	0.3–0.4
Coarse sands and sands with little gravel	0.5–0.7
Sandy gravels and gravel	0.8–1.0

To illustrate the scatter in q_c versus N'_{70}, one study found that a best fit for a fine silty sand was $k = 0.77$ [see Denver (1982)]. Comparing this value to the foregoing table, where one might obtain something between 0.1 and 0.4 (since $q_c/N'_{70} > q_c/N'_{60}$), we can see that there could be a substantial difference in what the soil is typed as.

Example 3-5.

Given. $q_c = 300$ kg/cm^2 at depth $z = 8$ m in sand, $\gamma' = 11.15$ kN/m^3.

Required. Estimate angle of internal friction ϕ.

Solution.

$$p'_o = 8 \times 11.15 = 89.2 \text{ kPa} \qquad \text{(effective pressure)}$$

$$q_c = V'_b p'_o \qquad \text{(from Fig. 3-22}a\text{)}$$

$$V'_b = \frac{q_c}{p'_o} = 300 \times \frac{98.07}{89.2} = 330 \qquad \text{(98.07 converts kg/cm}^2 \text{ to kPa)}$$

From Fig. 3-22a at $V'_b = 330$, we project to curves and down and obtain $\phi = 34.5$ to 39.5°, say, $\phi = 37°$. According to Fig. 3-20, q_c versus p'_o plots into the upper right corner above $D_r = 100$ and since the maximum $D_r = 100$ we can with $D_r = 100$ use Fig. 2-24b to obtain $\phi = 42$ to 46°, say, $\phi = 44°$. From Fig. 3-22b and $q_c = 300 \times 98.07/1000 = 29.4$ MPa, we obtain $\phi \approx 46°$.

We could use $\phi = 44°$ (which is high; also, it is somewhat doubtful whether the soil really has $D_r = 100$). A better estimate might be

$$\phi = \frac{(37 + 44 + 46)}{3} = \mathbf{42°}$$

The author would probably not use over 40°. Question: Could this soil have OCR > 1?

////

Example 3-6. Classify the soil on Fig. 3-17a at the 10- to 12-m depth. Also estimate the undrained shear strength s_u if the average $\gamma = 19.65$ kN/m^3 for the entire depth of the CPT. It is known that the profile is entirely in cohesive soil.

Solution. Enlarge the figure on a copy machine and estimate $q_c = 11$ MPa at the depth of interest by eye (with this data digitized into a microcomputer we could readily compute the average q_c as the depth increments $\times$ q_c summed and divided by the depth interval of 2 m).

From $q_c = 11$ MPa $= 11\,000$ kPa and $f_R = 4$ percent (from adjacent plot), use Fig. 3-18a and note the plot into the "silty sand" zone. This zone is evidently stiff from the large q_c, so classify as

Soil: stiff, sandy silt (actual soil is a gray, stiff clay, CH)

For s_u,

$$\text{Compute } p_o = \gamma \times \text{average depth} = 19.65 \times 11 = 216 \text{ kPa}$$

From Fig. 3-19 estimate $N_k = 18$ (using our just-made classification for a stiff sandy silt, we would expect an I_P on the order of 10 or less). With this estimate we can use Eq. (3-11) directly to obtain

$$s_u = \frac{11\,000 - 216}{18} = \mathbf{600} \text{ kPa}$$

(From laboratory tests s_u was approximately 725 kPa.)

////

3-12 FIELD VANE SHEAR TESTING (FVST)

The vane shear test VST is a substantially used method to estimate the in situ undrained shear strength of very soft, sensitive, fine-grained soil deposits. It also has considerable application in offshore soil exploration, particularly when used with sample recovery equipment. Offshore equipment configurations are similar to those for the SPT and CPT methods.

The FVST is closely related to the laboratory consolidated-undrained shear strength test; to identify this test the vane shear strength is usually given the symbol $s_{u,v}$. The *undrained strength* basis is justified from the observation that the vane test starts from the current consolidated state (unless, of course, the site has been recently filled and is still consolidating).

The test is performed by inserting the vane into the soil and applying a torque after a short time lapse, on the order of 5 to 10 minutes. If the time lapse is less than this, the insertion effects reduce the measured $s_{u,v}$, and if much over this time the soil tends to *set up* or consolidate, with an increase in $s_{u,v}$.

The vane may be inserted into the stratum being tested from the bottom of a borehole or pushed without a hole by using a vane sheath similar to a cone penetration test, with the vane then extended below (and out of) the sheath for the actual test. The vane test is done at a depth of at least five sheath diameters below the sheath or at least five diameters below the bottom of a drill hole. Equipment details vary somewhat; however, the vane device shown in Fig. 3-24*a* is fairly typical.

Vane blades are on the order of 1.5 to 2.5 mm thick, the shaft body is from about 12.7 to 22 mm in diameter, and the tip is sharpened using a 45° cut (90° vee). The dimensions are selected to minimize soil disturbance from its insertion—but there is always a small amount (on the order of 15 to 25 percent) of strength loss. The torque is usually applied through a suitable gearing device so that a rate of about 6° of rotation per minute can be achieved. The test is sometimes done using an ordinary torque wrench to apply (and measure) the torque. Commercial suppliers can provide the torque equipment, extension rods, and bearings as well as the vane in a package. The angle of rotation θ and the shear stress τ in the shaft from torque can be quite large if the vane depth is on the order of 6 meters or more. The following equations for θ and τ are given in most mechanics of materials textbooks as

$$\theta = \frac{TL}{GJ} \qquad \tau = \frac{Tr_r}{J}$$

where θ = the angle measured at the surface (in radians if computed from the equation)
τ = shear stress in shaft extension rods; should not exceed the elastic limit of the rod material
T = measured torque
L = extension rod lengths from surface to vane
G = shear modulus of elasticity of rods
r_r = minimum radius of vane rod
J = torsional moment of inertia of the rods

Use consistent units for all of T, L, G, r_r, and J.

Other test details consist in calibrating the torque to account for friction between the extension rods and support bearings and for soil contamination of the system. The torque to

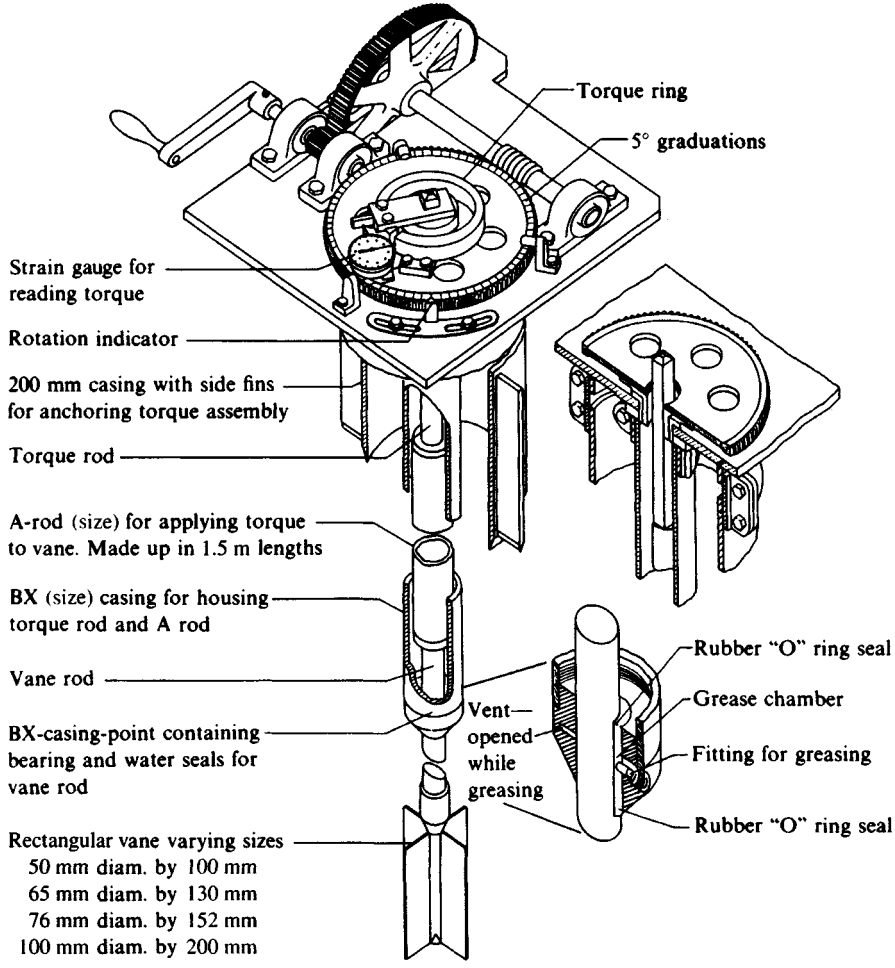

(*a*) The Bureau of Reclamation vane shear test apparatus. *Gibbs et al. (1960), courtesy of Gibbs and Holtz of the USBR.*]

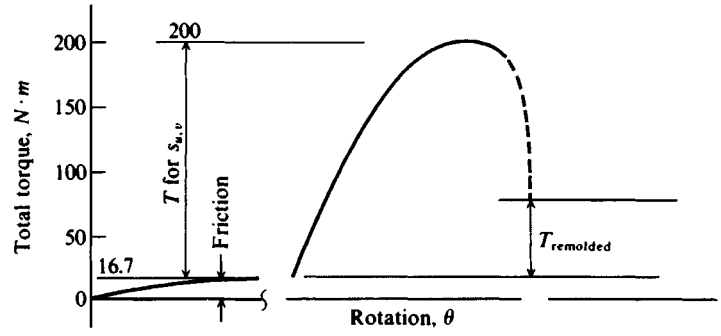

(*b*) Typical vane shear data.

Figure 3-24 Vane shear testing.

shear the soil around the perimeter is corrected by calibration, as illustrated in Fig. 3-24*b*. It is common to continue the vane rotation for 10 to 12 complete revolutions after the peak value (which occurs at soil rupture) so that the soil in the shear zone is substantially remolded. A rest period of 1 to 2 min is taken, then a second torque reading is made to obtain the residual (or remolded) strength. The ratio of these two strengths should be approximately the soil sensitivity S_t.

This test has been standardized by ASTM as D 2573, which allows either a rectangular or a tapered vane and specifies the ratio of $h/d = 2$.

The generalized test torque (after calibration corrections) for a *rectangular*-shaped vane can be written as

$$T = \pi\left(\frac{s_{u,vv}d^2h}{2} + \frac{s_{u,vh}ad^3}{4}\right) \tag{3-21}$$

where d, h = diameter and height of vane blades and in the ratio $h/d = 2$

a = constant for type of cylinder end shear assumed by user (see Fig. 3-25*b*)

= $\frac{2}{3}$ for uniform end shear

= $\frac{3}{5}$ for parabolic end shear

= $\frac{1}{2}$ for triangular end shear

$s_{u,vv}$ = shear in vertical plane from the perimeter of the vertical vane edges (earlier in text called $s_{u,v}$)

$s_{u,vh}$ = shear in horizontal plane from the horizontal (or tapered) vane edges. For a tapered vane this is a combination of the vertical and horizontal shear strengths

There is some opinion that the shear stress distribution on the vane perimeter parts is as shown in Fig. 3-25, with stress concentrations at the corners. It is usual to use a constant shear stress for the cylindrical part (since it would be extremely difficult to ascertain the stress concentrations). For the ends the stress is commonly described as

$$\tau' = \tau_m\left(\frac{2r}{d}\right)^n \tag{a}$$

where for easier writing τ' = shear stress at some distance r from the center of rotation and τ_m is the maximum shear on the end at $d/2$. Values to use for τ_m and n are shown in table form on Fig. 3-25.

For the rectangular vane and *uniform end shear* τ'' ($= s_{u,vh}$ in Fig. 3-25) a general equation is derived as follows.

The cylinder part (for either a rectangular or tapered vane) is always $\tau_1 = s_{u,vv}$, computed as

$$T_1 = \tau_1 \times \pi d \times d/2 \times h \tag{b}$$

The top and base resistances for a rectangular vane using a constant shear strength [$n = 0$ in Eq. (*a*)] and ignoring the rod diameter, is

$$T_e = 2\tau'' \int_0^{d/2} 2\pi r^2\, dr$$

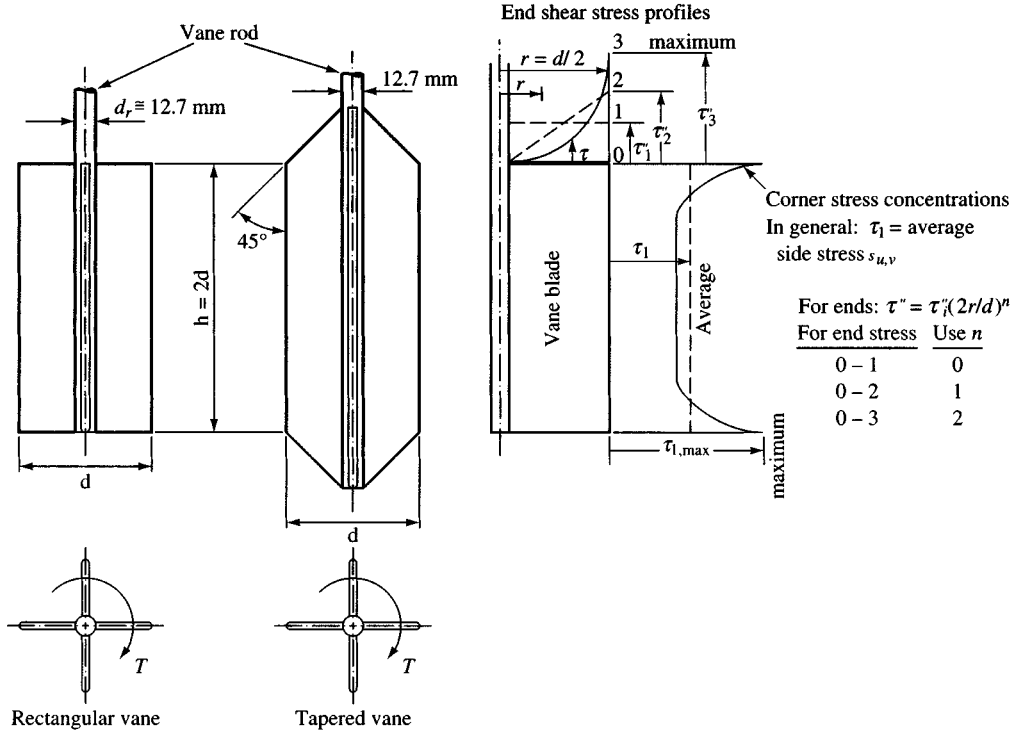

Figure 3-25 Vane shapes (ASTM D 2573) and approximations for the shear stress distribution on the vane ends and sides. *[After Chandler (1988).]*

$$T_e = 4\pi\tau'' \frac{r^3}{3}\Big|_0^{d/2}$$

$$= 4\pi\tau'' \frac{d^3}{(3)(8)} = \frac{2}{3}\pi\tau'' \frac{d^3}{4} \qquad (c)$$

$$= a\pi\tau'' \frac{d^3}{4} \qquad \left(a = \frac{2}{3}\right)$$

The total torque is the sum of the cylindrical [Eq. (*b*)] and the two end torques [Eq. (*c*)], giving

$$\frac{T}{\pi} = \frac{\tau_1 h d^2}{2} + \frac{a\tau'' d^3}{4} \qquad (3\text{-}22)$$

If we assume that $\tau_1 = \tau''$ (let $s_{u,vv} = s_{u,vh}$) and solve Eq. (3-22) for the shear strength, we obtain

$$s_{u,vv} = 0.2728 \frac{T}{d^3} \qquad (3\text{-}22a)$$

If $s_{u,vh} = 0.6s_{u,vv}$, one obtains

$$s_{u,vv} = 0.2894\frac{T}{d^3} \tag{3-22b}$$

Wroth (1984) and later Chandler (1988) suggest that Eq. (3-22*b*) defines the vane shear strength better than does Eq. (3-22*a*). On the other hand, Silvestri and Aubertin (1988) used different-sized vanes and found that, on average,

$$s_{u,vh}/s_{u,vv} \approx 1.14 \text{ to } 1.40$$

meaning the horizontal shear stress is about 15 to 40 percent larger than the vertical. This result would mean that anisotropy is significant, at least in some soft soil deposits.

In these equations use T and d in consistent units. For example in Eq. (3-22*a*), if T = 300 N·m and d = 65 mm (0.065 m) we have the shear stress $s_{u,vv} = (0.2728)(0.30)/0.065^3 =$ 298 kN/m^2 (kPa). Here, by use of Eq. (3-22*a*) it is explicitly assumed the soil is "isotropic" with $s_{u,vv} = s_{u,vh}$.

For the *tapered* vane, Eq. (*b*) is still valid; however, the end slopes (always 45° as in Fig. 3-25) produce two truncated cones. The shear stress equation is developed as follows.

The average radius r_{av} and moment arm of any truncated cone is

$$r_{av} = \frac{d + d_1}{2}$$

The lengths of the 45° conical slope are

$$s = \frac{d - d_1}{2}\sqrt{2}$$

The bottom cone base (small-diameter circular area) moment is

$$bc_m = \pi\frac{d_1^3}{12}$$

The torque (assuming $s_{u,vv}$ = average shear stress on all the parts) is

$$\begin{aligned} T &= \text{cylinder} + 2 \text{ ends} + \text{cone base} \\ &= \frac{s_{u,vv}\pi h d^2}{2} + 2(\pi r_{av}s)r_{av}s_{u,vv} + \frac{s_{u,vv}\pi d_1^3}{12} \end{aligned}$$

and substituting for r_{av} and s, we obtain

$$\frac{T}{\pi} = s_{u,vv}\left[\frac{hd^2}{2} + \frac{\sqrt{2}}{4}(d^3 - dd_1^2 + d_1d^2 - d_1^3) + \frac{d_1^3}{12}\right] \tag{3-23}$$

Rearranging, combining terms where possible, and solving for the undrained vane shear strength $s_{u,v}$, and with $h = 2d$; $1/\pi = 0.3183$; $\sqrt{2}/4 = 0.354$; and $1/12 = 0.0833$, we obtain

$$s_{u,v} = s_{u,vv} = \frac{0.3183T}{1.354d^3 + 0.354(d_1d^2 - dd_1^2) + 0.2707d_1^3} \tag{3-24}$$

where in all these equations d = vane diameter
d_1 = shaft diameter at vane, usually about 12 to 22 mm. Equation (3-24) is greatly simplified if the dd_1 terms are neglected.
T = measured torque

Use consistent units of T in N·m with d in m, or T in N·mm with d in mm. Use kN instead of N if numbers become very large.

Somewhat similar to the SPT, the vane test is usually performed every 0.5 to 1 m of depth in soft clays and fine silty sands. The test is not well suited for dense, hard, or gravelly deposits.

The generic forms of Eq. (3-24) allow the user to perform two tests in the stratum using different vane dimensions to obtain estimates of both $s_{u,vv}$ and $s_{u,vh}$. This is seldom done, however, and either the soil is assumed isotropic or the horizontal shear strength $s_{u,vh}$ is some fraction (say, 0.5, 0.6, etc.) of the vertical strength $s_{u,vv}$.

It appears that the FVST does not identify the OCR very well. This fact was ascertained from plotting the vane strength ratio $V_r = s_{u,vv}/CK_oUC$ triaxial test versus I_P to obtain

$$V_r = 0.55 + 0.008I_P \tag{3-25}$$

which is only marginally dependent on the OCR ratio. The normalized field vane strength may be approximated [see Chandler (1988)] as

$$\frac{s_{u,vv}}{p_o} = S_1(\text{OCR})^m \tag{3-26}$$

For normally consolidated clays $m \approx 0.95$ (with a range of 0.8 to 1.35) and $S_1 \approx 0.25$ (with a range of 0.16 to 0.33), which for the database used gives values within ±25 percent.

The FVST seems to give a value of $s_{u,v}$ that is too large for design. Bjerrum (1972) back-computed a number of embankment failures on soft clay and suggested using

$$s_{u,\text{design}} = \lambda s_{u,v} \tag{3-27}$$

where the reduction factor λ is given on Fig. 3-26 and $s_{u,v}$ is the $s_{u,vv}$ used to this point. Ladd et al. (1977) added additional data to support Fig. 3-26 but observed that there was substantial scatter in the points. Aas et al. (1986) restudied the Bjerrum chart, to include OCR and aging, and produced the revised chart of Fig. 3-26*b*. Both charts are included, since Bjerrum's chart has been widely used; however, the revised Aas chart appears more rational. Lefebvre et al. (1988) studied two soft, sensitive clays with a low I_P and found that for cases where $I_P < 20$ the Bjerrum λ-factor of Eq. (3-27) might be larger than 1. This study also found that the original Bjerrum curve (Fig. 3-26*a*) might be more nearly correct than the Aas revision (Fig. 3-26*b*). Evidently correlations between $s_{u,v}$ from the vane test and from the laboratory (or other field methods) are very dependent on test methodology (type of test, soil strain rate from the test method, soil type, history, etc.) as well as other factors. For example, others [see Arman et al. (1975) and Foott et al. (1980)] have found the measured vane strength $s_{u,v}$ to be too large—on the order of $2q_u$. Walker (1986), however, found a reasonable correlation between $s_{u,v}$ and laboratory triaxial tests (with the caveat that the vane test is difficult to perform at depths much over 10 m).

Some professionals in this field believe that anisotropy is a significant factor in the measured versus design values of $s_{u,v}$. Thus, generic forms of the equations are provided should

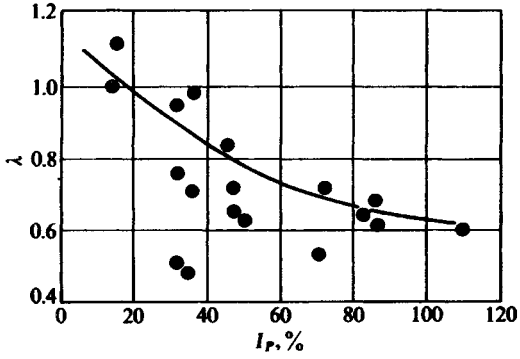

(*a*) Bjerrum's correction factor for vane shear test. [*After Bjerrum (1972) and Ladd et al. (1977).*]

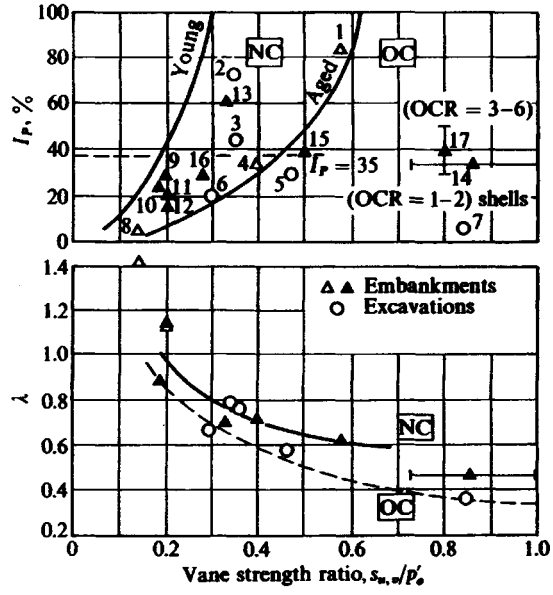

(*b*) Reinterpretation of the Bjerrum chart of part *a* by Aas et al. (1986) to include effects of aging and OCR. For interpretation of numbers and symbols on data points see cited reference.

Example: $p'_o = 150$; $s_{u,v} = 75$ kPa; $I_P = 35$; and need λ.
By Bjerrum's chart (*a*) obtain $\lambda = 0.85$ at $I_P = 35$.
$s_{u,\text{design}} = \lambda s_{u,v} = 0.85 \times 75 = 65$ kPa
By Aas et al. charts (*b*), enter top chart at $I_P = 35$ and project horizontally to $s_{u,v}/p'_o = 75/150 = 0.5$ (appears in overconsolidated zone) and vertically to the OC curve to obtain $\lambda = 0.5$
$s_{u,\text{design}} = 0.5 \times 75 = 37$ kPa
In this case, probably use $s_{u,\text{design}} = 40$ to 50 kPa.

Figure 3-26 Vane shear correction factor λ.

there be a need to attempt to obtain separate values for the vertical and horizontal shear strengths, somewhat similar to that attempted by Garga and Khan (1992).

Since the FVST, like the CPT, does not recover samples for visual classification or for confirmation tests, it is usually necessary to obtain samples by some alternative test method. This step might be omitted if the geotechnical engineer has done other work in the vicinity of the current exploration.

3-13 THE BOREHOLE SHEAR TEST (BST)

This test consists in carefully drilling a 76-mm diameter hole (usually vertical but may be inclined or horizontal) to a depth somewhat greater than the location of interest. Next the shear head is carefully inserted into the hole to the point where the shear strength is to be measured.

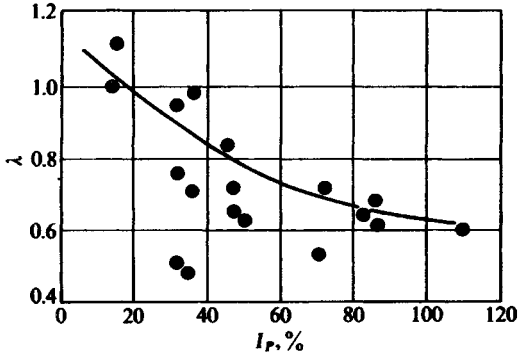

(*a*) Bjerrum's correction factor for vane shear test. [*After Bjerrum (1972) and Ladd et al. (1977).*]

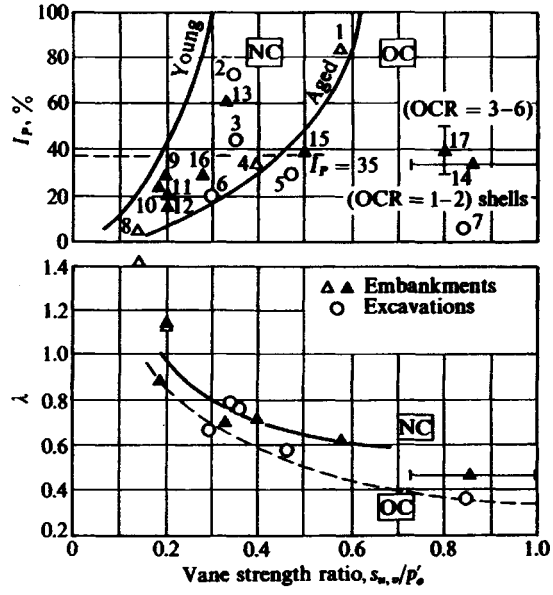

(*b*) Reinterpretation of the Bjerrum chart of part *a* by Aas et al. (1986) to include effects of aging and OCR. For interpretation of numbers and symbols on data points see cited reference.

Example: $p'_o = 150$; $s_{u,v} = 75$ kPa; $I_P = 35$; and need λ.
By Bjerrum's chart (*a*) obtain $\lambda = 0.85$ at $I_P = 35$.
$s_{u,\text{design}} = \lambda s_{u,v} = 0.85 \times 75 = 65$ kPa
By Aas et al. charts (*b*), enter top chart at $I_P = 35$ and project horizontally to $s_{u,v}/p'_o = 75/150 = 0.5$ (appears in overconsolidated zone) and vertically to the OC curve to obtain $\lambda = 0.5$
$s_{u,\text{design}} = 0.5 \times 75 = 37$ kPa
In this case, probably use $s_{u,\text{design}} = 40$ to 50 kPa.

Figure 3-26 Vane shear correction factor λ.

there be a need to attempt to obtain separate values for the vertical and horizontal shear strengths, somewhat similar to that attempted by Garga and Khan (1992).

Since the FVST, like the CPT, does not recover samples for visual classification or for confirmation tests, it is usually necessary to obtain samples by some alternative test method. This step might be omitted if the geotechnical engineer has done other work in the vicinity of the current exploration.

3-13 THE BOREHOLE SHEAR TEST (BST)

This test consists in carefully drilling a 76-mm diameter hole (usually vertical but may be inclined or horizontal) to a depth somewhat greater than the location of interest. Next the shear head is carefully inserted into the hole to the point where the shear strength is to be measured.

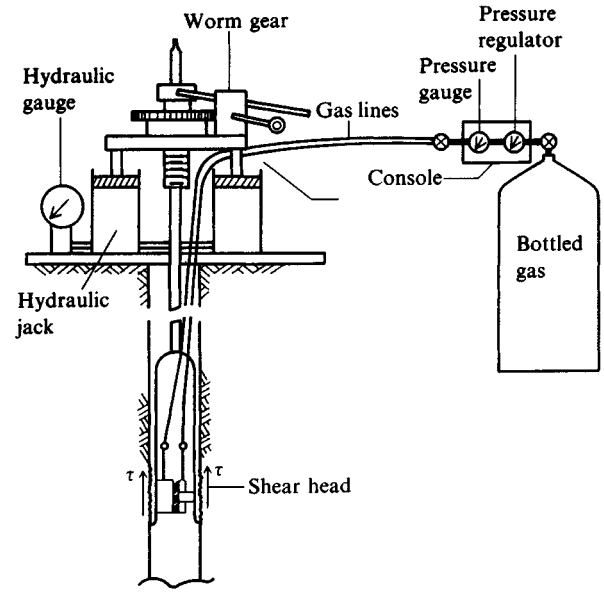

Figure 3-27 Borehole shear device. *[After Wineland (1975).]*

The test proceeds by expanding the serrated cylinder halves into the soil by applying pressure from the surface through a piping system. Next the cylinder is pulled with the pulling load and displacements recorded. The expansion pressure is σ_n and the pulling load can be converted to the shear strength s to make a plot as in Fig. 2-27*b* to obtain the in situ strength parameters ϕ and c.

Figure 3-27 illustrates the essential details of the test, which was developed by Dr. R. Handy at Iowa State University around 1967 and is sometimes called the *Iowa Borehole Shear Test.* The test undoubtedly is a drained shear test where the soil is relatively free-draining, since the drainage path from the shear head serrations is short *and* if the test is performed in the displacement range of about 0.5 mm/min or less. This rate might be too fast, however, for saturated clays, and Demartinecourt and Bauer (1983) have proposed adding a pore-pressure transducer to the shear heads and motorizing the pull (which was initially done by hand cranking with reduction gearing). With pore pressure measurements it is possible to obtain both total and effective stress parameters from any borehole shear test. Handy (1986) describes the BST in some detail, including its usefulness in collecting data for slope stability analyses.

The BST is applicable for all fine-grained soils and may be done even where a trace of gravel is present. It has particular appeal if a good-quality borehole can be produced and for modest depths in lieu of "undisturbed" sample recovery and laboratory testing.

3-14 THE FLAT DILATOMETER TEST (DMT)

This test consists of inserting the dilatometer probe of Fig. 3-28 to the depth of interest z by pushing or driving. The CPT pushing equipment can be used for insertion of the device, and in soils where the SPT N is greater than 35 to 40 the device can be driven or pushed from the bottom of a predrilled borehole using SPT drilling and testing equipment.

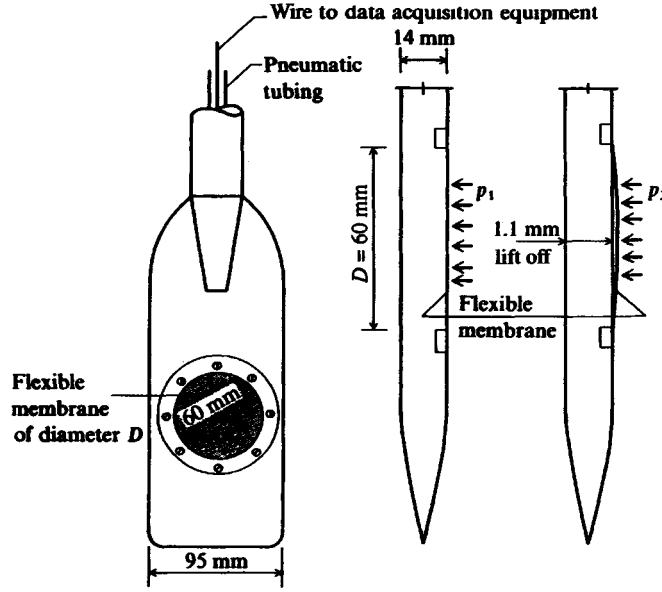

(*a*) Marchetti dilatometer [*After Marchetti (1980)*].

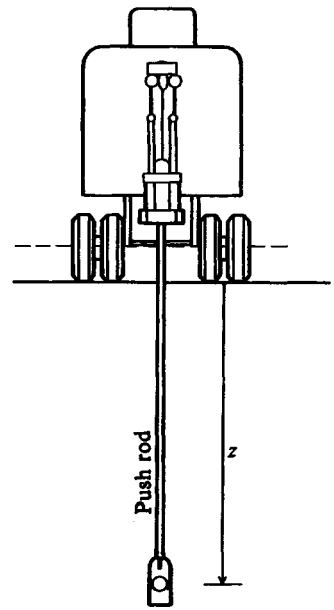

(*b*) The dilatometer pushed to depth z for test.

Figure 3-28 The flat dilatometer test (DMT).

Making a DMT after insertion to the depth of interest uses the following steps:

1. Take a pressure reading at the membrane in the dilatometer just flush with the plate (termed at *liftoff*), make appropriate zero corrections, and call this pressure p_1. The operator gets a signal at liftoff.
2. Increase the probe pressure until the membrane expands $\Delta d = 1.1$ mm into the adjacent soil and correct this pressure as p_2. Again the operator receives a signal so the pressure reading can be taken.
3. Decrease the pressure and take a reading when the membrane has returned to the liftoff position and correct for p_3. According to Schmertmann (1986) this latter reading can be related to excess pore pressure.

The probe is then pushed to the next depth position, which is from 150 to 200 mm (or more) further down, and another set of readings taken. A cycle takes about 2 minutes, so a 10-m depth can be probed in about 30 minutes including setup time.

Data are reduced to obtain the following:

1. Dilatometer modulus E_D. According to Marchetti (1980) we have

$$\Delta d = \frac{2D(p_2 - p_1)}{\pi}\left(\frac{1 - \mu^2}{E_s}\right)$$

and for $\Delta d = 1.1$ mm, $D = 60$ mm (see Fig. 3-28) we have on rearranging

$$E_D = \frac{E_s}{1 - \mu^2} = 34.7(p_2 - p_1) \tag{3-28}$$

2. The lateral stress index K_D is defined as

$$K_D = \frac{p_1 - u}{p_o'} = \frac{p_1}{p_o} \tag{3-29}$$

3. The material or deposit index I_D is defined as

$$I_D = \frac{p_2 - p_1}{p_2 - u} \tag{3-30}$$

The effective overburden pressure $p_o' = \gamma' z$ must be computed in some manner by estimating the unit weight of the soil or taking tube samples for a more direct determination. The pore pressure u may be computed as the static pressure from the GWT, which must also be known or estimated.

The DMT modulus E_D is related to E_s as shown in Eq. (3-28) and includes the effect of Poisson's ratio μ, which must be estimated if E_s is computed. The E_D modulus is also related to m_v of Eq. (2-34) from a consolidation test and thus has some value in making an estimate of consolidation settlements in lieu of performing a laboratory consolidation test.

The lateral stress index K_D is related to K_o and therefore indirectly to the OCR. Determination of K_o is approximate since the probe blade of finite thickness has been inserted into the soil. Figure 3-29 may be used to estimate K_o from K_D. Baldi et al. (1986) give some equations that they claim offer some improvement over those shown in Fig. 3-29; however,

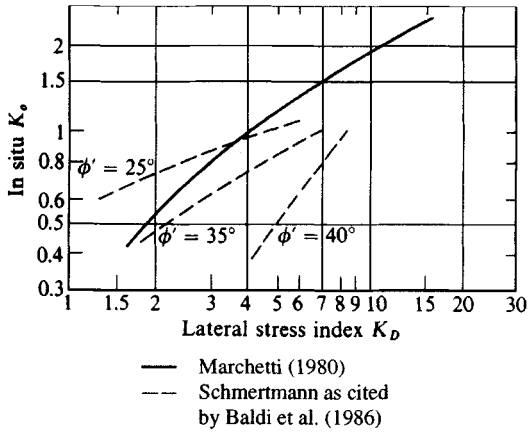

The Marchetti (1980) equation:

General Equation format: $K_o = \left(\frac{K_D}{\beta_D}\right)^{\alpha} - C_D$

where	β_D	α	C_D	
Marchetti	1.5	0.47	0.6	($K_D < 8$)
Others	1.25–??	0.44–0.64	0–0.6	
---	7.4	0.54	0	
Sensitive clay	2.0	0.47	0.6	

General Equation format: $OCR = (nK_D)^m$

where	n	m	
Marchetti	0.5	1.56	($K_D < 8$; $I_D < 1.2$)
Others	0.225–??	1.30–1.75	
I_D	0.225	1.67	(also $I_D < 1.2$)

Figure 3-29 Correlation between K_D and K_o. Note for the Schmertmann curves one must have some estimate of ϕ. *[After Baldi et al. (1986).]*

they are based heavily on laboratory tests that include D_r. In the field D_r might be somewhat difficult to determine at any reasonable test depth.

The material or deposit index I_D is related (with E_D) as illustrated in Fig. 3-30 to the soil type and state or consistency.

Proper interpretation of the DMT requires that the user have some field experience in the area being tested or that the DMT data be supplemented with information obtained from

Figure 3-30 Correlation between soil type and I_D and E_D. *[After Lacasse and Lunne (1986).]*

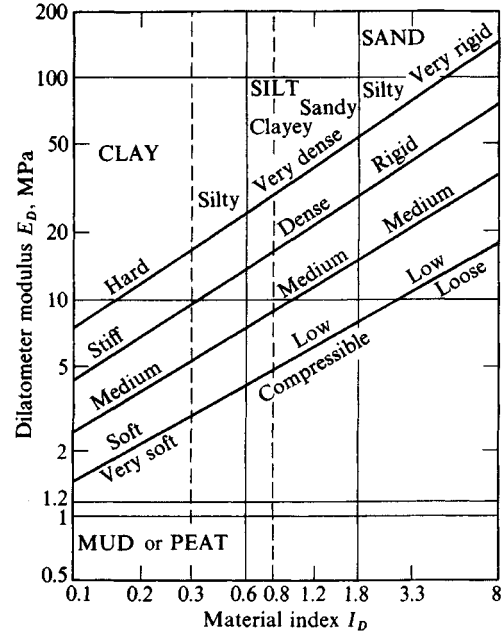

borings and sample recovery for visual verification of soil classification and from laboratory (or other) tests to corroborate the findings.

A typical data set might be as follows:

z, m (depth)	T, kg (rod push)	p_1, bar	p_2, bar	u, bar
2.10	1,400	2.97	14.53	0.21
2.40	1,250	1.69	8.75	0.24
2.70	980	1.25	7.65	0.26

1 bar ≈ 100 kPa

Here the depths shown are from 2.1 to 2.7 m. The probe push ranged from 1,400 kg to 980 kg (the soil became softer) and, as should be obvious, values of p_2 are greater than p_1. With the GWT at the ground surface the static pore pressure u is directly computed as $9.807z/100$ to obtain u in bars.

According to both Marchetti (1980) and Schmertmann (1986) the DMT can be used to obtain the full range of soil parameters (E_D, K_o, OCR, s_u, ϕ, and m_v) for both strength and compressibility analyses.

3-15 THE PRESSUREMETER TEST (PMT)

The borehole pressuremeter test is an in situ test developed ca. 1956 [Ménard (1956)] where a carefully prepared borehole that is sufficiently—but not over about 10 percent—oversized is used. The pressuremeter probe consisting of three parts (top, cell, and bottom) as shown in Fig. 3-31*a* is then inserted and expanded to and then into the soil. The top and bottom guard cells are expanded to reduce end-condition effects on the middle (the cell) part, which is used to obtain the volume versus cell pressure relationship used in data reduction.

A pressuremeter test is not a trivial task, as fairly high pressures are involved and calibrations for pressure and volume losses must be made giving data to plot curves as in Fig. 3-32*a*. These data are used to correct the pressure-volume data taken during a test so that a curve such as Fig. 3-32*b* can be made. It is evident that a microcomputer can be used to considerable advantage here by installing the calibration data in memory. With the probe data directly input, the data can be automatically reduced and, with a plot routine, the curve can be developed as the test proceeds.

The interested reader should refer to Winter (1982) for test and calibration details and to Briaud and Gambin (1984) for borehole preparation (which is extremely critical). It should be evident that the PMT can only be performed in soils where the borehole can be shaped and will stand open until the probe is inserted. Although the use of drilling mud/fluid is possible, hole quality cannot be inspected and there is the possibility of a mud layer being trapped between the cell membrane and the soil. Another factor of some to considerable concern is that the soil tends to expand into the cavity when the hole is opened so that the test often has considerable disturbance effects included.

To overcome the problems of hole preparation and soil expansion, self-boring pressuremeters were almost simultaneously developed in France [Baguelin et al. (1974)] and England [Wroth (1975)]. The self-boring pressuremeter test (SBPMT) is qualitatively illustrated in Fig. 3-31*b* and *c*.

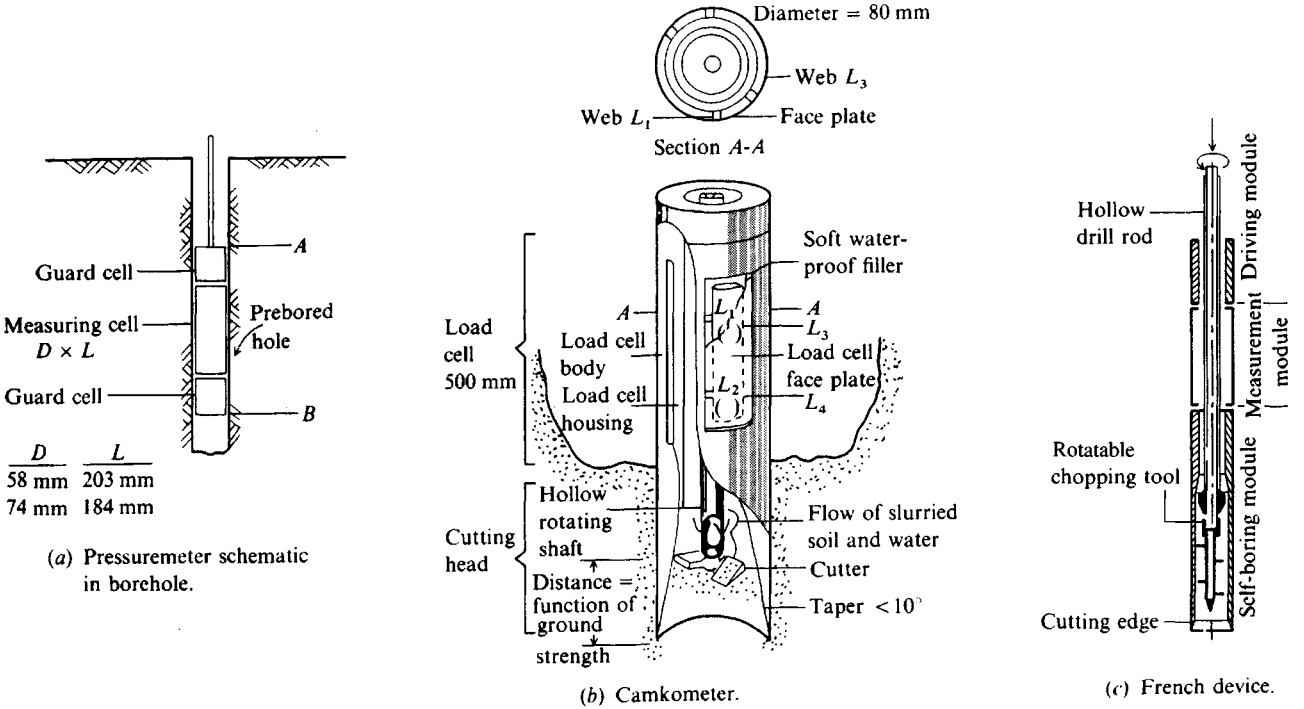

(*a*) Pressuremeter schematic in borehole.

(*b*) Camkometer.

(*c*) French device.

Figure 3-31 Pressuremeter testing; (*b*) and (*c*) above are *self-boring*, or capable of advancing the distance *AB* of (*a*) so that in situ lateral stress is not lost.

The pressuremeter operates on the principle of expanding a rigid cylinder into the soil and being resisted by an infinitely thick cylinder (the soil). The basic equation in terms of volumetric strain ϵ_v is

$$\epsilon_v = \frac{\Delta r}{r_1} = p\left(\frac{1-\mu}{E_s}\right) \tag{3-31}$$

where terms not previously defined are

$r_1, \Delta r$ = initial radius at contact with hole and change in hole radius, respectively
p = cell expansion pressure in units of E_s

In practice we obtain the slope $(\Delta V/\Delta p)$ from the linear part of the cell pressure versus volume plot and rearrange Eq. (3-31) to obtain the lateral static shear modulus as

$$G' = \frac{E_{sp}}{2(1+\mu)} = V_o' \frac{\Delta p}{\Delta V} \tag{3-32}$$

where V_o' = volume of the measuring cell at average pressure $\Delta p = V_o + V_c$
$\Delta p, \Delta V$ = as defined on Fig. 3-32*b* along with a sample computation for G'

The pressuremeter modulus E_{sp} is then computed using an estimated value of μ as $E_{sp} = E_s = G'[2(1+\mu)]$. Unless the soil is isotropic this lateral E_s is different from the vertical value usually needed for settlement analyses. For this reason the pressuremeter modulus E_{sp} usually has more application for laterally loaded piles and drilled caissons.

The value p_h shown on Fig. 3-32*b* is usually taken as the expansion pressure of the cell membrane in solid contact with the soil and is approximately the in situ lateral pressure (depending on procedure and insertion disturbance). If we take this as the in situ lateral pressure, then it is a fairly simple computation to obtain K_o as

$$K_o = \frac{p_h}{p_o} \tag{3-33}$$

which would be valid using either total or effective stresses (total is shown in the equation). It is necessary to estimate or somehow determine the unit weight of the several strata overlying the test point so that p_o can be computed.

With suitable interpretation of data as shown on Fig. 3-32*b* and replotting, one can estimate the undrained shear strength $s_{u,p}$ for clay [see Ladanyi (1972) for theory, example data, and computations] and the angle of internal friction ϕ [Ladanyi (1963), Winter and Rodriguez (1975)] for cohesionless soils.

It appears that the pressuremeter gives $s_{u,p}$ which are consistently higher than determined by other methods. They may be on the order of 1.5 to $1.7s_{u,v}$ (and we already reduce the vane shear strength by $\lambda s_{u,v}$). The PMT also appears to give values on the order of 1.3 to $1.5s_{u,\text{triaxial}}$.

The pressuremeter seems to have best applications in the same soils that are suitable for the CPT and DMT, that is, relatively fine-grained sedimentary deposits. In spite of the apparently considerable potential of this device, inconsistencies in results are common. Clough [see Benoit and Clough (1986) with references] has made an extensive study of some of the variables, of which both equipment configuration and user technique seem to be critical parameters.

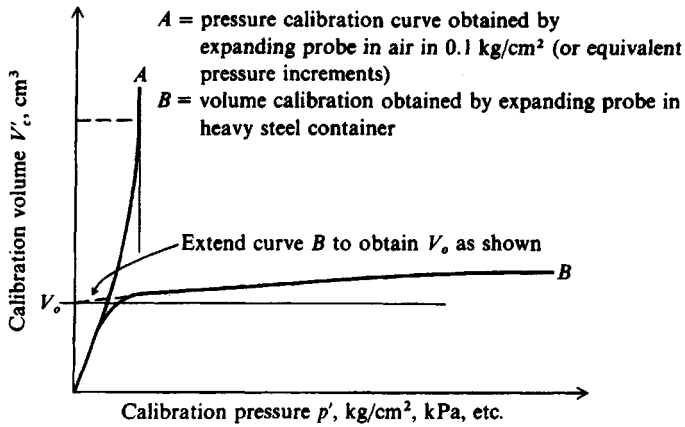

(*a*) Calibration curves for pressuremeter. This data may be put in a microcomputer so (*b*) can be quickly obtained.

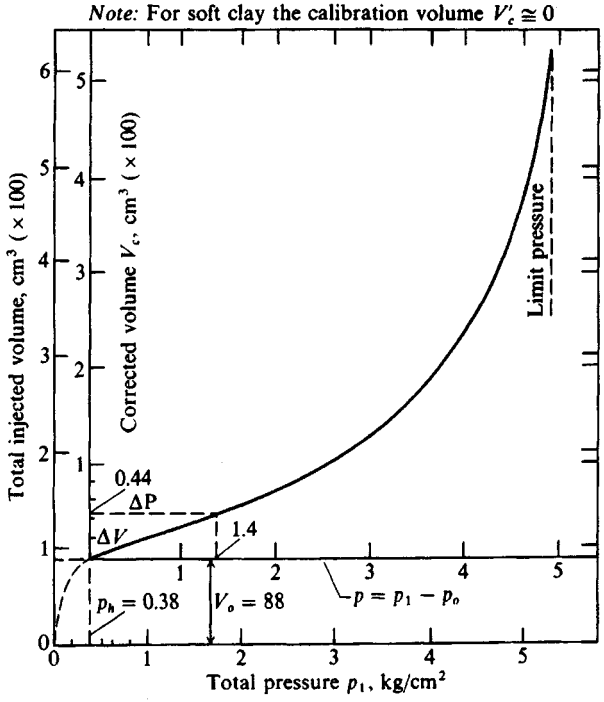

(*b*) Data from a pressuremeter test in soft clay.

Figure 3-32 Pressuremeter calibration and data.

Example:

$p_o = 4 \times 19.81 = 79.24$ kPa (in situ)

$$K_o = \frac{p_h}{p_o} = \frac{0.38 \times 98.07}{79.24} = \mathbf{0.47}$$

average over Δp

$$V_o' = \frac{0.44}{2} \times 100 + 88 = 110\,\text{cm}^3$$

For $S = 100\%$ take $\mu = 0.5$

$$E_{sp} = 2(1+\mu)V_o'\frac{\Delta p}{\Delta V} \quad \text{(Eq. (3-32))}$$

$$= 2(1.5)(110)\left(\frac{1.4}{44}\right)98.07 = \mathbf{1030\ kPa}$$

$$G' = \frac{E_{sp}}{2(1+\mu)} = \frac{1030}{3} = 343.3 \rightarrow \mathbf{345\ kPa}$$

3-16 OTHER METHODS FOR IN SITU K_o

The *Glötzl cell* of Fig. 3-33 is a device to measure K_o in soft clays. It is pushed to about 300 mm above the test depth in the protective metal sheath, then the blade is extended to the test depth. The device is 100 × 200 mm long × 4 mm thick [Massarsch (1975)]. The cell contains oil, which is pressurized from the surface to obtain the expansion pressure = lateral pressure. According to Massarsch (1975) and Massarsch et al. (1975), one should wait about a week for the excess pore pressure from the volume displacement to dissipate. It may be noted that the DMT, which has a displacement volume of about four times this device, uses no time delay for pore-pressure dissipation.

The *Iowa stepped blade* [Handy et al. (1982)] of Fig. 3-34 can be used to estimate K_o somewhat indirectly. In use the first step (3-mm part) is inserted at the depth of interest and a pressure reading taken. The blade is then pushed so the next step is at the point of interest and a reading taken, etc., for the four steps. Data of pressure versus blade thickness t can be plotted using a semilog scale as in Fig. 3-34. The best-fit curve can be extended to $t = 0$ to obtain the in situ lateral pressure p_h so that K_o can be computed using Eq. (3-33).

Lutenegger and Timian (1986) found that for some soils the thicker steps gave smaller pressure readings than for the previous step (with thinner blade). This result was attributed to the soil reaching its "limiting pressure" and resulted in increasing the original three-step blade to one now using four steps. This limit pressure is illustrated on the pressuremeter curve of Fig. 3-32*b*. Noting the stepped blade goes from 3 to 7.5 mm and the flat dilatometer

Figure 3-33 Glötzl earth-pressure cell with protection frame to measure lateral earth pressure after the protection frame is withdrawn.

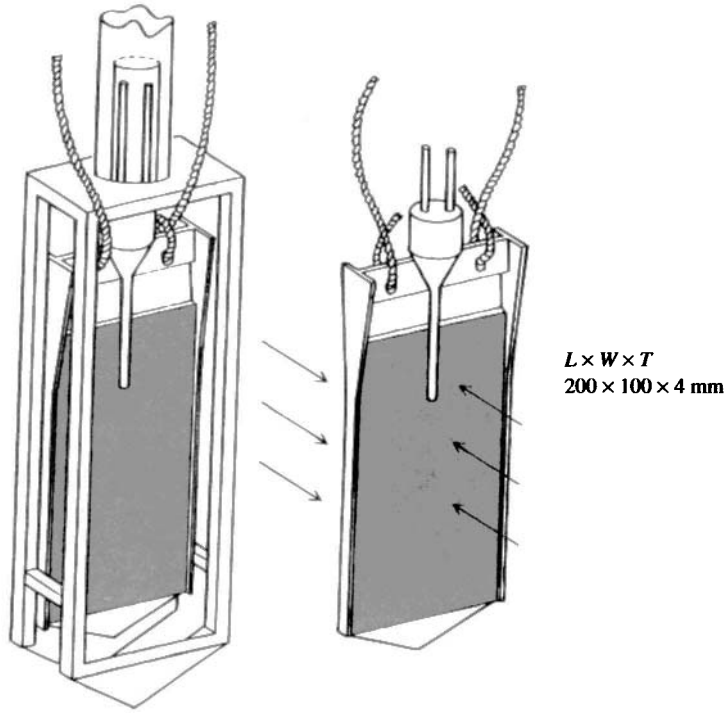

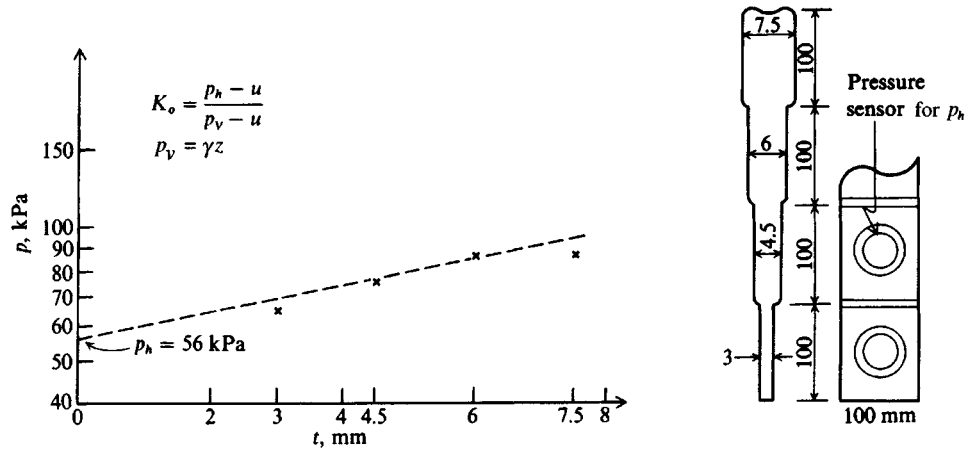

(*a*) Typical log - log data plot. (*b*) Dimensions, mm.

Figure 3-34 Iowa stepped blade for K_o estimation.

has a thickness of 14 mm we can well ask why this apparent limit pressure does not develop with the thicker—but tapered—dilatometer blade. It may be that the blade steps produce a different stress pattern in the ground than the tapered DMT blade.

Hydraulic fracture is a method that may be used in both rock and clay soils. It cannot be used in cohesionless soils with large coefficients of permeability. Water under pressure is pumped through a piezometer that has been carefully installed in a borehole to sustain considerable hydraulic pressure before a breakout occurs in the soil around the piezometer point. At a sufficiently high hydraulic pressure a crack will develop in the soil at the level of water injection. At this time the water pressure will rapidly drop and level off at an approximate constant pressure and flow rate. Closing the system will cause a rapid drop in pressure as the water flows out through the crack in the wall of the boring. The crack will then close as the pressure drops to some value with a resulting decrease in flow from the piezometer system. By close monitoring of the system and making a plot as in Fig. 3-35*b*, one can approximate the pressure at which the crack opens.

Steps in performing a fracture test are as follows (refer to Fig. 3-35*a*):

1. Prepare a saturated piezometer with a 6-mm standpipe tube filled with deaerated water with the top plugged and pushed to the desired depth L using a series of drill rods. The plug will keep water from flowing into the system under excess pore pressure developed by pushing the piezometer into the ground.
2. Measure L_w and L_f, and compute depth of embedment of piezometer and transducer voltage V.
3. After about $\frac{1}{2}$ hr unplug the 6-mm standpipe tube and connect the fracture apparatus to the standpipe using an appropriate tube connector at G.
4. Fill the fracture system with deaerated water from the 1- or 2-liter reservoir bottle by opening and closing the appropriate valves. Use the hand-operated pump/metering device to accomplish this.
5. Take a zero reading on the pressure transducer—usually in millivolts, mV.

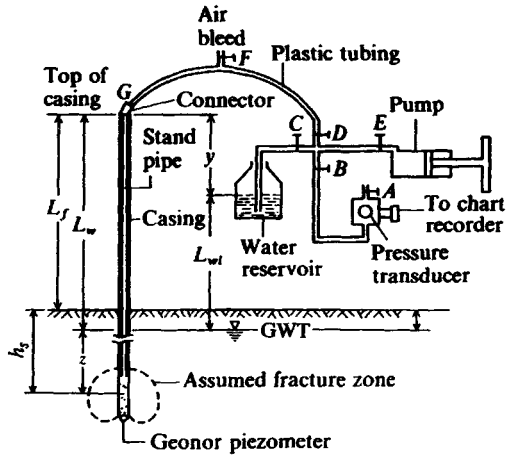

(*a*) Schematic of hydraulic fracture test setup

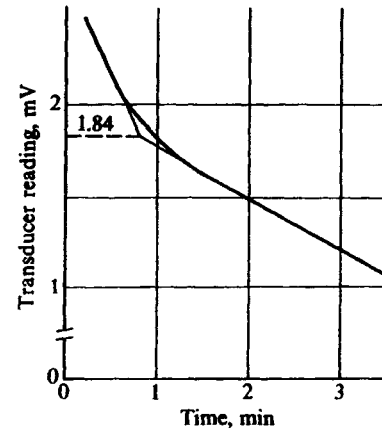

(*b*) Qualitative data plot from fracture test. Value of 1.84 is used in Example 3-7. [After Bozozuk (1974).]

Figure 3-35

6. Apply system pressure at a slow rate using the hand pump until fracture occurs as observed by a sudden drop-off in pressure.
7. Quickly close valve *E*.
8. From the plot of pressure transducer readings versus time, the break in the curve is interpreted as relating to σ_3.

Lefebvre et al. (1991) used a series of field tests in soils with apparently known OCRs in the range of 1.6 to 4.8 to see the effect of piezometer tip size and what range of K_o might be obtained. The tests appear to establish that $K_o \rightarrow 1.0$ when the OCR is on the order of 2.1. The K_o values ranged from about 0.59 to 3.70 and were generally higher as OCR increased, but not always for the smaller OCR. In the low-OCR region a $K_o = 0.59$ was found for OCR = 1.7, whereas a value of 0.88 was found for OCR = 1.6. These variations were likely due to soil anomalies or correctness of the "known" OCR.

This test may also be performed in rock, but for procedures the reader should consult Jaworski et al. (1981).

The following example is edited from Bozozuk (1974) to illustrate the method of obtaining K_o from a fracture test in soil.

Example 3-7. Data from a hydraulic fracture test are as follows (refer to Fig. 3-35):

Length of casing used = $L_w + z = \mathbf{6.25}$ m
Distance from top of casing to ground $L_f = 1.55$ m
Distance L_w measured inside drill rods (or standpipe) with a probe = 2.02 m
Saturated unit weight of soil, assuming groundwater nearly to surface and
$S = 100$ percent for full depth, $\gamma_{sat} = 17.12$ kN/m^3

y measured when fracture apparatus connected = 0.265 m

The pressure transducer output is calibrated to **12.162** kPa/mV.

Required. Find the at-rest earth-pressure coefficient K_o.

Solution.

$z = 6.25 - 2.02 = \mathbf{4.23}$ m (see Fig. 3-35*a*)

$L_{wi} = L_w - y = 2.02 - 0.265 = \mathbf{1.755}$ m

Total soil depth to piezometer tip, $h_s = L_w + z - L_f$

$= 6.25 - 1.55 = 4.70$ m

Total overburden pressure, $p_o = \gamma_{sat} h_s$

$= 17.12(4.70) = 80.46$ kPa

This p_o assumes soil is saturated from the ground surface. Now we compute the static pore pressure u_o before test starts:

$$u_o = z\gamma_w = 4.23(9.807) = \mathbf{41.98} \text{ kPa}$$

The effective pressure is expressed as

$$p'_o = p_o - u_o$$
$$= 80.46 - 41.48 = \mathbf{38.98} \text{ kPa}$$

Since $h_s = 4.70$ and $z = 4.23$ m, the GWT is 0.47 m below ground surface. With some capillary rise, the use of $\gamma_{sat} = 17.12$ kN/m^3 for full depth of h_s produces negligible error.
The fracture pressure is a constant $\times$ the reading (of 1.84), giving

$$\text{FP} = (12.162 \text{ kPa/mV})(1.84 \text{ mV}) = 22.38 \text{ kPa}$$

The additional pore pressure from water in the piezometer above the existing GWT is

$$u_{wi} = L_{wi}\gamma_w = 1.755(9.807) = 17.21 \text{ kPa}$$

Total pore pressure u_t is the sum of the measured value FP and the static value of u_{wi} just computed, giving

$$u_t = \text{FP} + u_{wi} = 22.38 + 17.21 = \mathbf{39.59} \text{ kPa}$$
$$K_o = q_h/q_v$$

And using $u_t = q_h$ and $q_v = p'_o$, we can compute K_o as

$$K_o = \text{total pore pressure}/p'_o = u_t/p'_o$$
$$= 39.59/38.98 = \mathbf{1.03}$$

This value of K_o is larger than 1.00, so this example may not be valid. To verify these computations, use a copy machine to enlarge Fig. 3-35*a*, then put the known and computed values on it.

////

Considerable research has been done on hydraulic fracture theory to produce a method that can be used to predict hydraulic fracture in soil more reliably. In addition to estimating the OCR and k_o there is particular application in offshore oil production, where a large head of drilling fluid may produce hydraulic fracture (and loss of fluid) into the soil being drilled. A recent summary of this work is given by Anderson et al. (1994).

3-17 ROCK SAMPLING

In rock, except for very soft or partially decomposed sandstone or limestone, blow counts are at the refusal level ($N > 100$). If samples for rock quality or for strength testing are required it will be necessary to replace the soil drill with rock drilling equipment. Of course, if the rock is close to the ground surface, it will be necessary to ascertain whether it represents a competent rock stratum or is only a suspended boulder(s). Where rock is involved, it is useful to have some background in geology. A knowledge of the area geology will be useful to detect rock strata versus suspended boulders, whose size can be approximately determined by probing (or drilling) for the outline. A knowledge of area geology is also useful to delineate both the type of rock and probable quality (as sound, substantially fractured from earth movements, etc.). This may save considerable expense in taking core samples, since their quantity and depth are dependent on both anticipated type and quality of the rock.

Rock cores are necessary if the soundness of the rock is to be established; however, cores smaller than those from the AWT core bit (Table 3-6) tend to break up inside the drill barrel. Larger cores also have a tendency to break up (rotate inside the barrel and degrade), especially if the rock is soft or fissured. Drilling small holes and injecting colored grout (a water-cement mixture) into the seams can sometimes be used to recover relatively intact samples. Colored grout outlines the fissure, and with some care the corings from several adjacent corings can be used to orient the fissure(s).

Unconfined and high-pressure triaxial tests can be performed on recovered cores to determine the elastic properties of the rock. These tests are performed on pieces of sound rock from the core sample and may give much higher compressive strengths in laboratory testing than the "effective" strength available from the rock mass, similar to results in fissured clay.

Figure 3-36 illustrates several commonly used drill bits, which are attached to a piece of hardened steel tube (casing) 0.6 to 3 m long. In the drilling operation the bit and casing rotate while pressure is applied, thus grinding a groove around the core. Water under pressure is forced down the barrel and into the bit to carry the rock dust out of the hole as the water is circulated.

The recovery ratio term used earlier also has significance for core samples. A recovery ratio near 1.0 usually indicates good-quality rock. In badly fissured or soft rocks the recovery ratio may be 0.5 or less.

TABLE 3-6
Typical standard designation and sizes for rock drill casing (barrel) and bits*

Casing OD, mm	Core bit OD, mm	Bit ID, mm
RW 29	EWT 37	23
EW 46	AWT 48	32
AW 57	BWT 60	44
BW 73	NWT 75	59
NW 89	HWT 100	81
PW 140	194	152

* See ASTM D 2113 for the complete range in core bit, casing, and drill rod sizes in current use. Sizes are nominal—use actual diameter of recovered core.

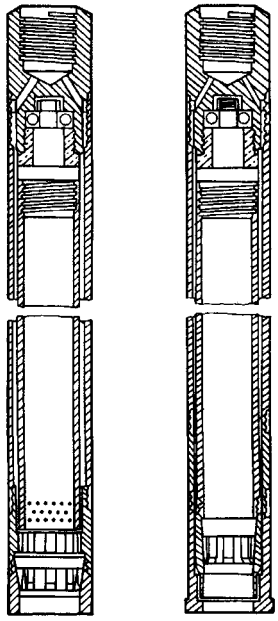

(*a*) Core barrels to collect rock cores

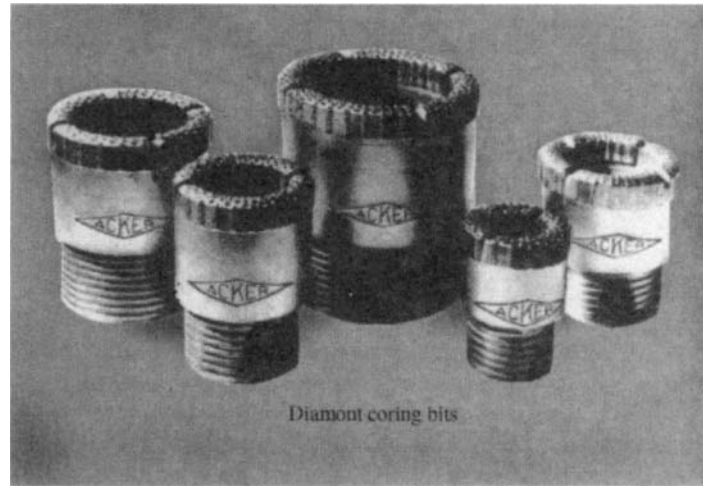

(*b*) Coring bits to attach to core barrel. (The Acker Drill Company)

Figure 3-36 Rock coring equipment. See such sources as DCDMA (1991) for standard dimensions, details, and a more complete list of available equipment for both rock and soil exploration.

Rock quality designation (RQD) is an index or measure of the quality of a rock mass [Stagg and Zienkiewicz (1968)] used by many engineers. RQD is computed from recovered core samples as

$$\text{RQD} = \frac{\sum \text{Lengths of intact pieces of core} > 100 \text{ mm}}{\text{Length of core advance}} \tag{3-34}$$

For example, a core advance of 1500 mm produced a sample length of 1310 mm consisting of dust, gravel, and intact pieces of rock. The sum of lengths of pieces 100 mm or larger[9] (pieces vary from gravel to 280 mm) in length is 890 mm. The recovery ratio $L_r = 1310/1500 = 0.87$ and RQD = 890/1500 = **0.59**.

The rating of rock quality may be used to approximately establish the field reduction of modulus of elasticity and/or compressive strength and the following may be used as a guide:

[9]Some persons use a modified RQD in which the pieces 100 mm and longer are sufficiently intact if they cannot be broken into shorter fragments by hand.

RQD	Rock description	E_f/E_{lab}*
<0.25	Very poor	0.15
0.25–0.50	Poor	0.20
0.50–0.75	Fair	0.25
0.75–0.90	Good	0.3–0.7
>0.90	Excellent	0.7–1.0

* Approximately for field/laboratory compression strengths also.

Depth of Rock Cores

There are no fast rules for rock core depths. Generally one should core approximately as follows:

1. A depth sufficient to locate sound rock or to ascertain that it is fractured and jointed to a very great depth.
2. For heavily loaded members such as piles or drilled piers, a depth of approximately 3 to 4 m below the location of the base. The purpose is to check that the "sound" rock does not have discontinuities at a lower depth in the stress influence zone and is not a large suspended boulder.

Local building codes may give requirements for coring; however, more often they give allowable bearing pressures that can be used if one can somehow ascertain the rock quality without coring.

Adjacent core holes can be used to obtain relative rock quality by comparing cross-hole seismic wave velocities in situ to laboratory values on intact samples. If the field value is less, it indicates fractures and jointing in the rock mass between holes. Down-hole and surface methods are of little value in this procedure, since a part of the wave travel is in the overlaying soil and separating the two with any confidence is nearly impossible.

3-18 GROUNDWATER TABLE (GWT) LOCATION

Groundwater affects many elements of foundation design and construction, so the GWT should be established as accurately as possible if it is within the probable construction zone; otherwise, it is only necessary to determine where it is not. For the latter case the location within ±0.3 to 0.5 m is usually adequate.

Soil strength (or bearing pressure) is usually reduced for foundations located below the water table. Foundations below the water table will be uplifted by the water pressure, and of course some kind of dewatering scheme must be employed if the foundations are to be constructed "in the dry."

The GWT is generally determined by directly measuring to the stabilized water level in the borehole after a suitable time lapse, often 24 to 48 hr later. This measurement is done by lowering a weighted tape down the hole until water contact is made. In soils with a high permeability, such as sands and gravels, 24 hr is usually a sufficient time for the water level to stabilize unless the hole wall has been somewhat sealed with drilling mud.

In soils with low permeability such as silts, fine silty sands, and clays, it may take several days to several weeks (or longer) for the GWT to stabilize. In this case an alternative is to

install a *piezometer* (small vertical pipe) with a porous base and a removable top cap in the borehole. Backfill is then carefully placed around the piezometer so that surface water cannot enter the boring. This procedure allows periodic checking until the water level stabilizes, that is, the depth to the water has not changed since the previous water level measurement was taken. Clearly this method will be expensive because of the additional labor involved in the installation and subsequent depth checks.

In theory we might do the following:

1. Plot the degree of saturation S with depth if it is possible to compute it reliably. A direct plot of the in situ water content may be useful, but for $S = 100$ percent w_N can decrease as the void ratio decreases from overburden pressure.
2. Fill the hole and bail it out. After bailing a quantity, observe whether the water level in the hole is rising or falling. The true level is between the bailed depth where the water was falling and the bailed depth where it is rising. This method implies a large permeability, so it would be more practical simply to bail the hole, then move to the next boring location while the GWT stabilizes.

One may apply a computational method; however, this requires capping the hole and taking periodic depth measurements to the water table (as done for direct measurements), and since no one (to the author's knowledge) computes the depth, the computational method is no longer given. This method was given in the first through third editions of this book.

3-19 NUMBER AND DEPTH OF BORINGS

There are no clear-cut criteria for determining directly the number and depth of borings (or probings) required on a project in advance of some subsurface exploration. For buildings a minimum of three borings, where the surface is level and the first two borings indicate regular stratification, may be adequate. Five borings are generally preferable (at building corners and center), especially if the site is not level. On the other hand, a single boring may be sufficient for an antenna or industrial process tower base in a fixed location with the hole made at the point.

Four or five borings are sufficient if the site soil is nonuniform (both to determine this and for the exploration program). This number will usually be enough to delineate a layer of soft clay (or a silt or peat seam) and to determine the properties of the poorest material so that a design can be made that adequately limits settlements for most other situations.

Additional borings may be required in very uneven sites or where fill areas have been made and the soil varies horizontally rather than vertically. Even though the geotechnical engineer may be furnished with a tentative site plan locating the building(s), often these are still in the stage where horizontal relocations can occur, so the borings should be sufficiently spread to allow this without having to make any (or at least no more than a few) additional borings.

In practice, the exploration contract is somewhat open as to the number of borings. The drilling operation starts. Based on discovery from the first holes (or CPT, DMT, etc.) the drilling program advances so that sufficient exploration is made for the geotechnical engineer to make a design recommendation that has an adequate margin of safety *and* is economically feasible for the client. Sometimes the exploration, particularly if preliminary, discloses that the site is totally unsuitable for the intended construction.

Borings should extend below the depth where the stress increase from the foundation load is significant. This value is often taken as 10 percent (or less) of the contact stress q_o. For the square footing of Fig. 1-1*a* the vertical pressure profile shows this depth to be about $2B$. Since footing sizes are seldom known in advance of the borings, a general rule of thumb is $2 \times$ the least lateral plan dimensions of the building or 10 m below the lowest building elevation.

Where the $2 \times$ width is not practical as, say, for a one-story warehouse or department store, boring depths of 6 to 15 m may be adequate. On the other hand, for important (or high-rise) structures that have small plan dimensions, it is common to extend one or more of the borings to bedrock or to competent (hard) soil regardless of depth. It is axiomatic that at least one of the borings for an important structure terminate into bedrock if there are intermediate strata of soft or compressible materials.

Summarizing, there are no binding rules on either the number or the depth of exploratory soil borings. Each site must be carefully considered with engineering judgment in combination with site discovery to finalize the program and to provide an adequate margin of safety.

3-20 DRILLING AND/OR EXPLORATION OF CLOSED LANDFILLS OR HAZARDOUS WASTE SITES

Seldom is a soil exploration done to place a structure over a closed landfill or hazardous waste site. Where exploration is necessary, extreme caution is required so that the drilling crew is not exposed to hazardous materials brought to the surface by the drill. Various gases that may be dangerous if inhaled or subject to explosion from a chance spark may also exit the drill hole. In addition to providing the drilling crew with protective clothing it may be necessary also to provide gas masks.

When drilling these sites, it is necessary to attempt to ascertain what types of materials might be buried in the fill. It is also of extreme importance that the drilling procedure not penetrate any protective lining, which would allow leachate contained in the fill to escape into the underlying soil or groundwater. If the boring is to penetrate the protective liner, it is absolutely essential to obtain approval from the appropriate governmental agencies of the procedure to use to avoid escape of the fill leachate. This approval is also necessary to give some protection against any litigation (which is very likely to occur). At the current (1995) level of drilling technology there is no known drilling procedure that will give an absolute guarantee that leachate will not escape if a drill hole is advanced through a protective liner, even if casing is used.

3-21 THE SOIL REPORT

When the borings or other field work has been done and any laboratory testing completed, the geotechnical engineer then assembles the data for a recommendation to the client. Computer analyses may be made where a parametric study of the engineering properties of the soil is necessary to make a "best" value(s) recommendation of the following:

1. Soil strength parameters of angle of internal friction ϕ and cohesion c
2. Allowable bearing capacity (considering both strength and probable or tolerable settlements)
3. Engineering parameters such as E_s, μ, G', or k_s.

A plan and profile of the borings may be made as on Fig. 3-37, or the boring information may be compiled from the field and laboratory data sheets as shown on Fig. 3-38. Field and data summary sheets are far from standardized between different organizations [see Bowles (1984), Fig. 6-6 for similar presentation], and further, the ASTM D 653 (Standard Terms and Symbols Relating to Soil and Rock) is seldom well followed.

In Fig. 3-38 the units are shown in Fps because the United States has not converted as of this date (1995) to SI. On the left is the visual soil description as given by the drilling supervisor. The depth scale is shown to identify stratum thickness; the glacial silty clay till is found from 6 in. to nearly 12 ft (about 11 ft thick). The SS indicates that split spoon samples were recovered. The N column shows for each location the blows to seat the sampler 6 in. (150 mm) and to drive it for the next two 6-in. (150-mm) increments. At the 3-ft depth it took five blows to drive the split spoon 6 in., then 10 and 15 each for the next two 6-in. increments—the total N count $= 10 + 15 = 25$ as shown. A pocket penetrometer was used to obtain the unconfined compression strength of samples from the split spoon (usually 2^+ tests) with the average shown as Q_p. At the 3-ft depth $Q_p = q_u = 4.5^+$ ton/ft^2 (430^+ kPa). The pocket penetrometers currently in use read directly in both ton/ft^2 and kg/cm^2, the slight difference between the two units being negligible (i.e., 1 ton/ft^2 $\approx$ 1 kg/cm^2) and ignored. The next column is the laboratory-determined $Q_u = q_u$ values, and for the 3-ft depth $q_u = 7.0$ tsf (670 kPa). Based on the natural water content $M_c = w_N = 15$ percent, the dry unit weight $D_d = \gamma_d = 121$ lb/ft^3 (or 19.02 kN/m^3). The GWT appears to be at about elevation 793.6 ft. Note that a hollow-stem continuous-flight auger was used, so that the SPT was done without using casing.

The client report is usually bound with a durable cover. The means of presentation can range from simple stapling to binding using plastic rings. At a minimum the report generally contains the following:

1. Letter of transmittal.
2. Title.
3. Table of contents.
4. Narrative of work done and recommendations. This may include a foldout such as Fig. 3-37. The narrative points out possible problems and is usually written in fairly general terms because of possible legal liabilities. The quality varies widely. The author used one in which the four-page narrative consisted of three pages of "hard sell" to use the firm for some follow-up work.
5. Summary of findings (and recommendations). This is usually necessary so that after the generalities of the narrative the client can quickly find values to use. Some clients may not read the narrative very carefully.
6. Appendices that contain log sheets of each boring, such as Fig. 3-35; laboratory data sheets as appropriate (as for consolidation, but not usually stress-strain curves from triaxial tests—unless specifically requested); and any other substantiating material.

The sample jars may be given to the client or retained by the geotechnical firm for a reasonable period of time, after which the soil is discarded. How the soil samples are disposed of may be stated in the contract between client and consultant.

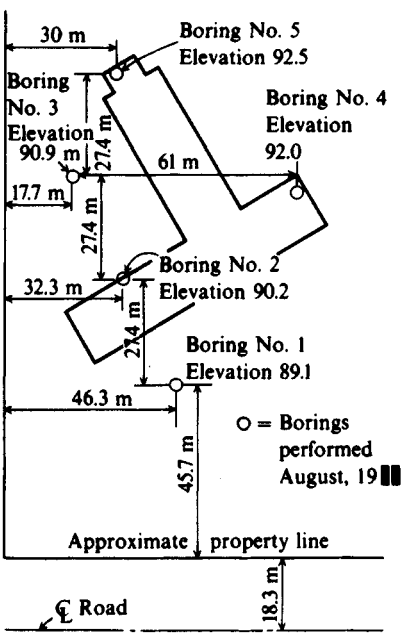

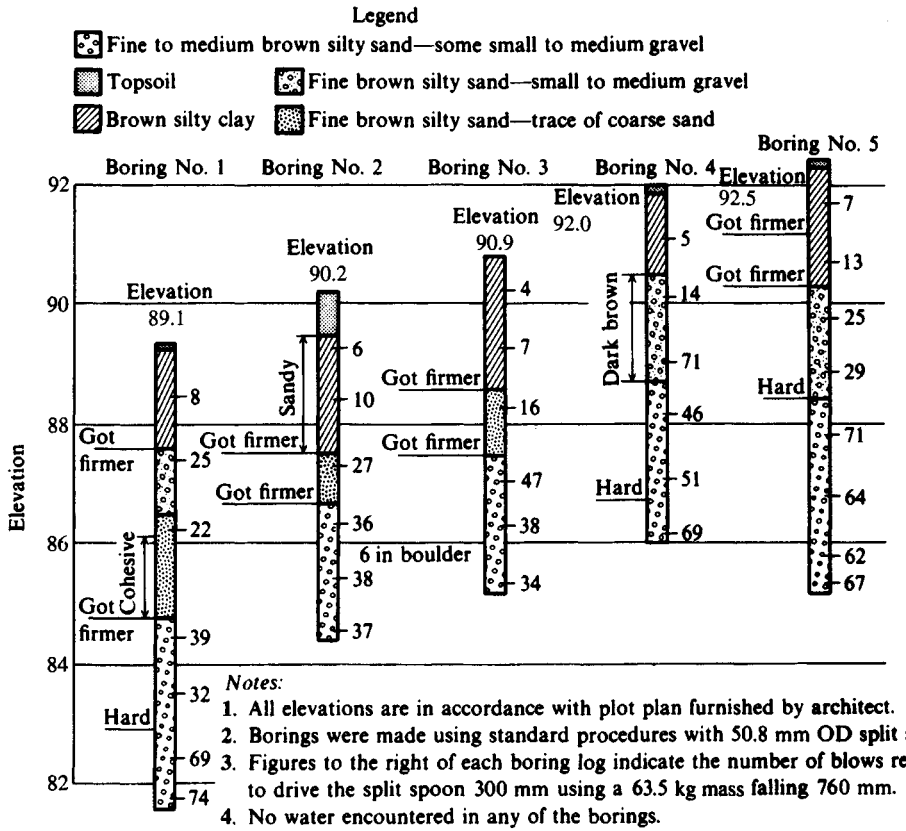

Notes:

1. All elevations are in accordance with plot plan furnished by architect.
2. Borings were made using standard procedures with 50.8 mm OD split spoon.
3. Figures to the right of each boring log indicate the number of blows required to drive the split spoon 300 mm using a 63.5 kg mass falling 760 mm.
4. No water encountered in any of the borings.

Figure 3-37 A method of presenting the boring information on a project. All dimensions are in meters unless shown otherwise.

WHITNEY & ASSOCIATES
INCORPORATED
2406 West Nebraska Avenue
PEORIA, ILLINOIS 61604

BORING LOG

BORING NO. B-04
DATE 12-03-92
W. & A. FILE NO. 55
SHEET 4 OF 7

PROJECT OHIO-AMERICAN ELEVATED WATER STORAGE TANK
LOCATION Ohio
BORING LOCATION See Plot Plan Sheet
DRILLED BY Winslow
BORING TYPE Hollow-Stem Auger
WEATHER CONDITIONS Partly Cloudy & Cool
SOIL CLASSIFICATION SYSTEM U.S.B.S.C.
SEEPAGE WATER ENCOUNTERED AT ELEVATION None
GROUND SURFACE ELEVATION 804.2
GROUND WATER ELEVATION AT 24+ HRS. 793.6
BORING DISCONTINUED AT ELEVATION 787.2
GROUND WATER ELEVATION AT COMPLETION 793.4

DESCRIPTION	DEPTH IN FEET	SAMPLE TYPE	N	Qp	Qu	Dd	Mc
Brown SILTY CLAY LOAM Organic Topsoil	6"						
Hard, Brown, Weathered GLACIAL SILTY CLAY TILL	03	SS	5 10 15(25)	4.5+	7.0	121	15
	06	SS	8 12 18(30)	4.5+	6.0	118	14
	09	SS	9 14 19(33)	4.5+	5.1	119	15
		SS	8 13 18(31)	4.5+	6.2	124	13
Hard, Gray, Unweathered GLACIAL SILTY CLAY TILL	12	SS	5 7 11(18)	4.5+	5.1	113	18
Very Stiff, Gray, Unweathered GLACIAL SILTY CLAY TILL	15	SS	5 5 8(13)	2.3	2.2	109	20
Hard, Gray LIMESTONE EXPLORATORY BORING DISCONTINUED	18						

N - BLOWS DELIVERED PER FOOT BY A 140 LB. HAMMER FALLING 30 INCHES
SS - SPLIT SPOON SAMPLE
ST - SHELBY TUBE SAMPLE

Qp - CALIBRATED PENETROMETER READING - T.S.F.
Qu - UNCONFINED COMPRESSIVE STRENGTH - T.S.F.
Dd - NATURAL DRY DENSITY - P.C.F.
Mc - NATURAL MOISTURE CONTENT - %

WHITNEY & ASSOCIATES
PEORIA, ILLINOIS

Figure 3-38 Boring log as furnished to client. N = SPT value; Q_p = pocket penetrometer; Q_u = unconfined compression test; D_d = estimated unit weight γ_s; M_c = natural water content w_N in percent.

PROBLEMS

Problems are in order of text coverage.

3-1. Sound cohesive samples from the SPT (returned to the laboratory in glass jars) were obtained for a γ determination using a 500 mL (mL = cm^3) volume jar as follows:

Boring	Depth, m	Trimmed weight, g	Water added, cm^3
B-1	6.00	142.3	426
B-3	8.00	145.2	427

i.e., weighed samples put in volume jar and water shown added. Volume of first sample = 500 − 426 = 74 cm^3

Required: Estimate the average unit weight of the clay stratum from depth = 5 to 9 m. If the GWT is at 2 m depth, what is γ_{dry}? *Hint:* Assume G_s.

Answer: $\gamma_{sat} \approx 19.18$ kN/m^3; $\gamma_{dry} = 14.99$ kN/m^3.

3-2. What are p_o and p'_o at the 9-m depth of Prob. 3-1 if $\gamma = 17.7$ kN/m^3 for the first 2 m of depth above the GWT?

Answer: $p'_o = 101.0$ kPa.

3-3. Compute the area ratio of the standard split spoon dimensions shown on Fig. 3-5*a*. What ID would be required to give $A_r = 10$ percent?

3-4. The dimensions of two thin-walled sample tubes (from supplier's catalog) are as follows:

OD, mm	ID, mm	Length, mm
76.2	73	610
89	86	610

Required: What is the area ratio of each of these two sample tubes? What kind of sample disturbance might you expect using either tube size?

Answer: $A_r = 8.96, 7.1$ percent

3-5. A thin-walled tube sampler was pushed into a soft clay at the bottom of a borehole a distance of 600 mm. When the tube was recovered, a measurement down inside the tube indicated a recovered sample length of 585 mm. What is the recovery ratio, and what (if anything) happened to the sample? If the 76.2 mm OD tube of Prob. 3-4 was used, what is the probable sample quality?

3-6. Make a plot of C_N (of Sec. 3-7) for p'_o from 50 to 1000 kPa.

3-7. From a copy of Table 3-4 remove the N'_{70} values and replace them with N'_{60} values. Comment on whether this improves or degrades the value of the table.

3-8. Discuss why Table 3-5 shows that the clays from consistency "medium" to "hard" show probable OCR > 1 where the soft clays are labeled "young."

3-9. If $N'_{70} = 25$ and $p'_o = 100$ kPa, for Eq. (3-5*a*), what is D_r? What is your best estimate for D_r if the OCR = 3? Estimate ϕ from Table 3-4 for a medium (coarse) sand.

3-10. Referring to Fig. P3-10 and Table 3-4, make reasonable estimates of the relative density D_r and ϕ for the sand both above (separately) and below the GWT shown. Assume $E_r = 60$ for the N values shown. Assume the unit weight of the sand increases linearly from 15 to 18.1 kN/m^3 from

near surface to the water table and $\gamma_{sat} = 19.75$ kN/m^3 below the GWT. Estimate the N value you would use for a footing that is 2×2 m located at the -2 m depth.

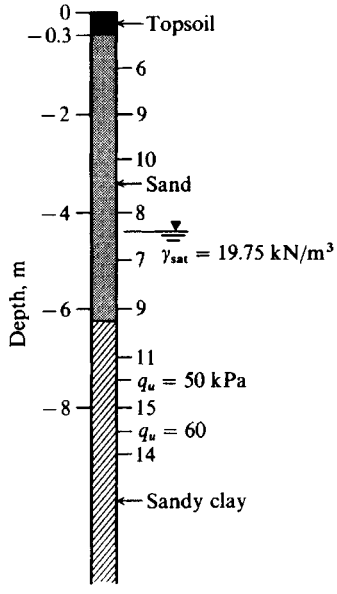

Figure P3-10

TABLE P3-11

Depth, m	q_c, MPa	q_s, kPa	Soil classification
0.51	1.86	22.02	Sandy silt
1.52	1.83	27.77	Silt and clayey silt
1.64	1.16	28.72	Very silty clay
2.04	1.15	32.55	Very silty clay
2.56	2.28	24.89	Silty sand
3.04	0.71	22.02	Silty clay
3.56	0.29	12.44	Clay
4.08	0.38	15.32	Clay
4.57	1.09	21.06	Very silty clay
5.09	1.22	31.60	Very silty clay
5.60	1.57	28.72	Silt and clayey silt
6.09	1.01	30.64	Very silty clay
6.61	6.90	28.72	Sand
7.13	5.41	39.26	Sand
7.62	10.50	26.81	Sand
8.13	4.16	27.77	Sand
8.65	2.45	43.09	Silt and clayey silt
9.14	8.54	26.11	Sand
9.66	24.19	76.60	Sand
10.18	32.10	110.12	Sand
10.66	23.34	71.82	Sand
11.18	5.86	62.24	Silty sand
11.70	4.17	57.45	Sandy silt
12.19	17.93	86.18	Sand
12.71	24.71	73.73	Sand
13.22	25.79	76.60	Sand
13.71	13.27	85.22	Sand
14.23	1.41	43.09	Very silty clay
14.75	2.73	196.30	Clay
15.24	1.75	108.20	Clay
15.75	1.02	78.52	Clay
16.27	0.82	36.38	Clay
16.76	1.88	72.77	Very silty clay
17.28	1.46	106.29	Clay
17.80	1.15	51.71	Clay

3-11. Plot the CPT data including f_R of Table P3-11 and estimate s_u at depth = 5.6 m if $I_P = 30$; also estimate ϕ at depth 7.62 m. Assume an average $\gamma = 16.5$ kN/m^3 to GWT at depth = 3 m and $\gamma = 19.81$ kN/m^3 for soil below the GWT.

3-12. Enlarge Fig. 3-15*b*. If $w_L = 45$, $w_P = 25$, estimate s_u at the depth of 7–8 m.

3-13. For the vane shear data on Fig. 3-21 estimate $s_{u,v}$ and $s_{u,\text{remolded}}$ if a 100-mm diameter vane is used with $h/d = 2$ (rectangular). Also estimate λ if $I_P = 35$ and $p'_o = 125$ kPa.

3-14. Assuming the dilatometer data in Sec. 3-14 for the depths 2.10 to 2.70 m are already "corrected," estimate E_D, K_D, and I_D, tentatively classify the soil, and estimate K_o for the individually assigned depth value.

3-15. Plot the following corrected pressuremeter data and estimate p_h, E_{sp}, and K_o. For E_{sp} take μ = 0.2 and 0.4. Also assume average γ = 17.65 kN/m^3 and test depth = 2.60 m. What is the "limiting pressure"?

V, cm^3	55	88	110	130	175	195	230	300	400	500
p, kPa	10	30	110	192	290	325	390	430	460	475

Answer: Based on V_o' = 123, μ = 0.2, obtain E_s = 860 kPa, K_o = 1.09.

3-16. What would the hydraulic fracture K_o have been if the transducer reading was ±5 percent of the 1.84 value shown on Fig. 3-35?

3-17. Referring to the boring log of Fig. 3-38, state what value you would use for q_u at the 6-ft depth.

3-18. Research the in situ test procedure you have been assigned from Table 3-2. You should find at least five references—preferably in addition to any cited/used by the author. Write a short summary of this literature survey, and if your conclusions (or later data) conflict with that in this text, include this in your discussion. If you find additional data that have not been used in any correlations presented, you should plot these data over an enlargement of the correlation chart for your own later use.

CHAPTER 4

BEARING CAPACITY OF FOUNDATIONS

4-1 INTRODUCTION

The soil must be capable of carrying the loads from any engineered structure placed upon it without a shear failure and with the resulting settlements being tolerable for that structure. This chapter will be concerned with evaluation of the limiting shear resistance, or ultimate bearing capacity q_{ult}, of the soil under a foundation load. Chapter 5 will be concerned with estimation of settlements. A soil shear failure can result in excessive building distortion and even collapse. Excessive settlements can result in structural damage to a building frame, nuisances such as sticking doors and windows, cracks in tile and plaster, and excessive wear or equipment failure from misalignment resulting from foundation settlements.

Seldom has a structure collapsed or tilted over from a base shear failure in recent times. Most reported base failures have occurred under embankments or similar structures where a low factor of safety was deemed acceptable. Most structural distress attributed to poor foundation design is from excessive settlements. Even here, however, structural collapse seldom occurs. This may in part be due to settlements being time-dependent, so that when cracks or other evidence first appears, there is sufficient time to take remedial measures.

It is necessary to investigate both base shear resistance and settlements for any structure. In many cases settlement criteria will control the allowable bearing capacity; however, there are also a number of cases where *base shear* (in which a base punches into the ground—usually with a simultaneous rotation) dictates the recommended bearing capacity. Structures such as liquid storage tanks and mats are often founded on soft soils, which are usually more susceptible to base shear failure than to settlement. Base shear control, to avoid a combination base punching with rotation into the soil, is often of more concern than settlement for these foundation types. These base types are often uniformly loaded so that nearly uniform settlements are produced across the base. Uniform settlements—even if relatively large—can usually be tolerated for either rigid mats (beneath buildings) or flexible mats beneath liquid storage tanks.

We should note that although our primary focus here is on estimating the ultimate bearing capacity for framed structures and equipment foundations, the same principles apply to obtaining the bearing capacity for other structures such as tower bases, dams, and fills. It will be shown that the ultimate bearing capacity is more difficult to estimate for layered soils, foundations located on or near slopes, and foundations subjected to tension loads.

The recommendation for the allowable bearing capacity q_a to be used for design is based on the *minimum* of either

1. Limiting the settlement to a tolerable amount (see Chap. 5)
2. The ultimate bearing capacity, which considers soil strength, as computed in the following sections

The allowable bearing capacity based on shear control q_a is obtained by reducing (or dividing) the ultimate bearing capacity q_{ult} (based on soil strength) by a safety factor SF that is deemed adequate to avoid a base shear failure to obtain

$$q_a = \frac{q_{ult}}{SF} \tag{4-1}$$

The safety factor is based on the type of soil (cohesive or cohesionless), reliability of the soil parameters, structural information (importance, use, etc.), and consultant caution. Possible safety factors are outlined in Sec. 4-15.

4-2 BEARING CAPACITY

From Fig. 4-1*a* and Fig. 4-2 it is evident we have two potential failure modes, where the footing, when loaded to produce the maximum bearing pressure q_{ult}, will do one or both of the following:

a. Rotate as in Fig. 4-1*a* about some center of rotation (probably along the vertical line *Oa*) with shear resistance developed along the perimeter of the slip zone shown as a circle
b. Punch into the ground as the wedge *agb* of Fig. 4-2 or the approximate wedge *ObO'* of Fig. 4-1*a*

It should be apparent that both modes of potential failure develop the limiting soil shear strength along the slip path according to the shear strength equation given as

$$s = c + \sigma_n \tan \phi \tag{2-52}$$

Although this is the equation of the Mohr's circle rupture envelope, its physical meaning is illustrated in Fig. 4-1*b* as it applies along the slip lines. It is common to use *total* stress parameters in this equation; however, for certain loading cases the *effective* stress parameters may be more appropriate, i.e., long-term slowly applied loadings.

The problem of how to obtain a reliable value of q_{ult} to develop the limiting shear resistance has been extensively covered in the literature, and several approximate methods have some following. We will examine briefly some approximations for q_{ult} to illustrate the complexity

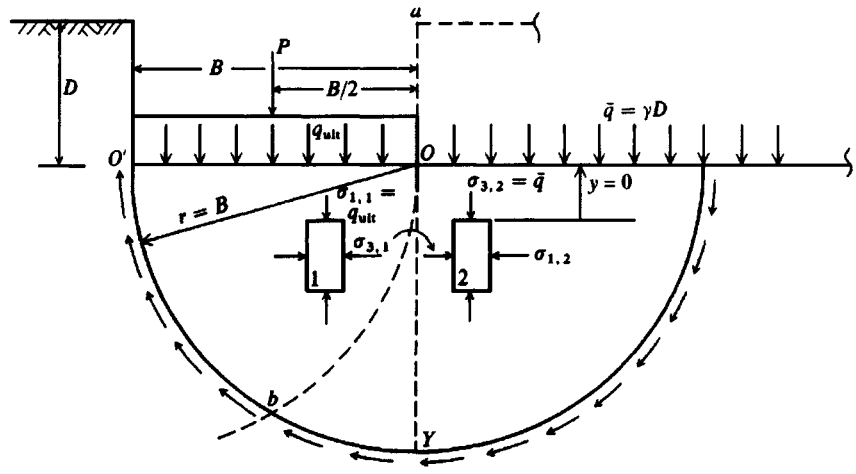

(*a*) Footing on $\phi = 0°$ soil.

Note: $\bar{q} = p'_o = \gamma' D$, but use $\bar{q}$, since this is the accepted symbol for bearing capacity computations.

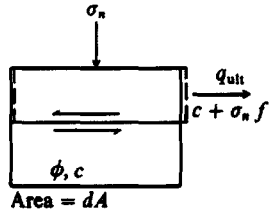

Area = dA

Friction = $\sigma_n \tan \phi = \sigma_n f$

Cohesion = $\dfrac{c\,dA}{dA}$

(*b*) **Physical meaning of Eq. (2-52) for shear strength.**

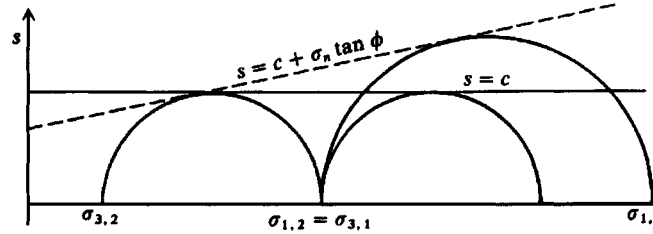

(*c*) **Mohr's circle for (*a*) and for a ϕ–c soil.**

Figure 4-1 Bearing capacity approximation on a $\phi = 0$ soil.

of the problem, and then in the next section look at several of the more popular bearing-capacity methods.

For Fig. 4-1*a* and a $\phi = 0$ soil we may obtain an approximate lower-bound solution for a unit width strip of a footing $B \times L(\rightarrow \infty)$ as in the following.

When the foundation pushes into the ground, stress block 1 to the left of vertical line OY has principal stresses as shown. The push into the ground, however, displaces the soil on the right side of the line OY laterally, resulting in the major principal stress on block 2 being horizontal as shown. These block stresses can be shown on the Mohr's circles of Fig. 4-1*c*. When the two blocks are adjacent to each other at the vertical line OY, it is evident that $\sigma_{3,1} = \sigma_{1,2}$ but with a principal stress rotation of 90° between blocks. From Chap. 2

$$\sigma_1 = \sigma_3 \tan^2\left(45 + \frac{\phi}{2}\right) + 2c \tan\left(45 + \frac{\phi}{2}\right) \qquad (2\text{-}54)$$

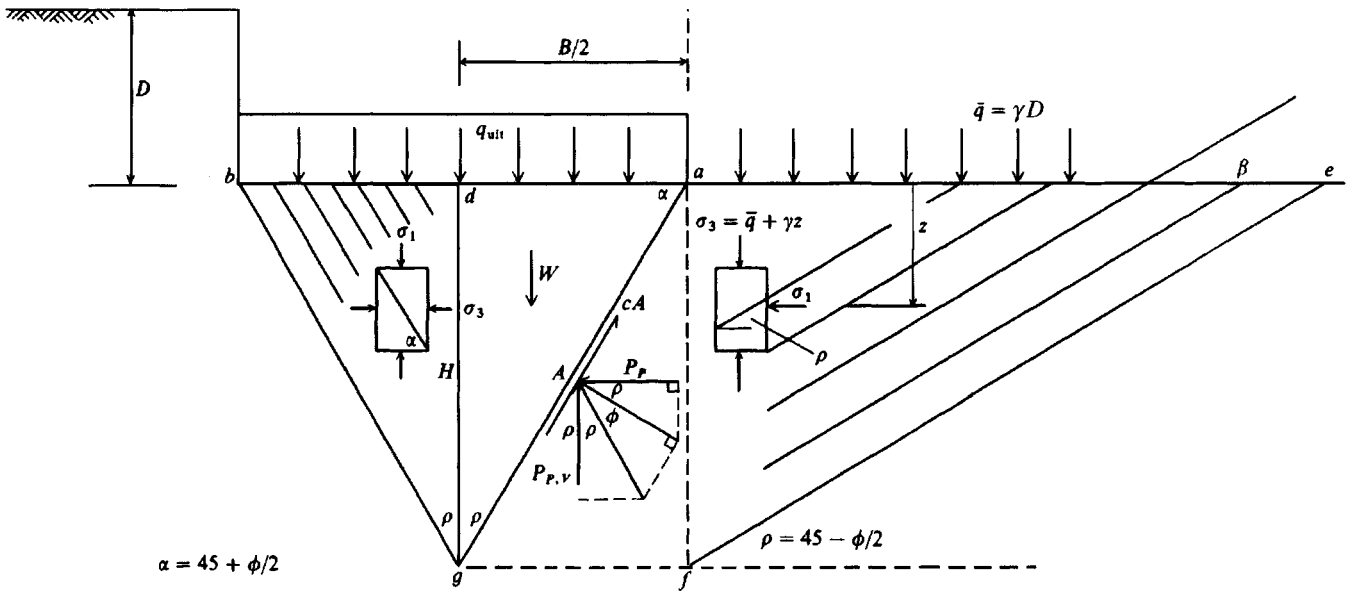

$$\alpha = 45 + \phi/2$$

$$H = \frac{B}{2}\tan\alpha$$

$$A = \frac{B}{2\cos\alpha}$$

$$P_{p,v} = \frac{P_p}{\cos\phi}$$

$$W = \frac{1}{2}\cdot\gamma\frac{B}{2}\cdot\frac{B}{2}\tan\alpha$$

$$K_p = \tan^2\left(45 + \frac{\phi}{2}\right)$$

$$K_a = \tan^2\left(45 - \frac{\phi}{2}\right)$$

Figure 4-2 Simplified bearing capacity for a ϕ–c soil.

We have for $\phi = 0$, $\tan(45 + \phi/2) = \tan^2(45 + \phi/2) = 1$, and for block 2 at point O (corner of footing) $\sigma_{3,2} = \bar{q} = \gamma D$.[1] Using these values in Eq. (2-54), we get the major principal stress as

$$\sigma_{1,2} = \sigma_{3,1} = \bar{q}(1) + 2c(1) \tag{a}$$

For block 1 just under the footing and again using Eq. (2-54), we have the major principal stress $\sigma_{1,1}$ as

$$\sigma_{1,1} = q_{\text{ult}} = \sigma_{3,1}(1) + 2c(1) \tag{b}$$

Substituting $\sigma_{3,1}$ from Eq. (*a*) into Eq. (*b*), we obtain

$$q_{\text{ult}} = \bar{q} + 2c + 2c = 4c + \bar{q} \tag{c}$$

This equation has two possibilities:

1. Use for bearing capacity
2. Use for critical excavation depth in clay (see Y distance of Fig. 2-10)

For bearing capacity and with the footing located on the ground surface so that $aO = 0 \rightarrow \bar{q} = 0$ of Fig. 4-1*a*, we obtain the ultimate bearing pressure q_{ult} as

$$q_{\text{ult}} = 4c \tag{d}$$

For a critical excavation depth, where a wall is used to support the soil along line aO and it is necessary to estimate the depth of excavation D so that the overburden pressure does not squeeze the soil from the toe of the wall into the excavation, we set $q_{\text{ult}} = 0$ and solve Eq. (*c*) to obtain

$$q_{\text{ult}} = 0 = 4c + \bar{q} = 4c + \gamma D$$

The critical depth of excavation D_c (Safety Factor = 1) is then

$$D_c = \frac{4c}{\gamma}$$

This equation will be used later in Chap. 11.

For a possible upper-bound solution we will take a footing rotation about point O. We observe that the rotation could be about O' as well, and for some case where the soils in the two rotation zones were exactly equal in strength the wedge ObO' would punch into the ground. It is statistically highly improbable, owing to worm holes, roots, or other inclusions, that rotation will not develop first (which is substantiated by observed field failures). Summing moments about point O, we have the peripheral shear resistance + overburden pressure $\bar{q}$ resisting the footing pressure q_{ult}; thus,

$$q_{\text{ult}} \frac{B \times B}{2} = c\pi B \times B - \frac{\bar{q} B \times B}{2} = 0 \tag{e}$$

[1] The $\bar{q}$ term may be either an *effective* or a *total* stress value. The reader must look at the context of usage. If there is any doubt, use $\bar{q}$ = effective overburden pressure.

Solving for q_{ult}, we obtain

$$q_{ult} = 2\pi c + \bar{q} \tag{f}$$

Equation (f) gives $q_{ult} = 6.28c$ when $\bar{q} = 0$. The average from Eqs. (d) and (f) is $(4c + 6.28c)/2 = 5.14c$, which is, coincidentally, $\pi + 2 = 5.14$, given by theory of plasticity. Actually, if one makes a search along and to the right of line Oa for a minimum q_{ult}, a value of about $5.5c < 2\pi c$ can be found.

Footing on a ϕ–c Soil

Figure 4-2 is a possible case for the footing on a soil with both cohesion c and angle of internal friction ϕ. Here a wedge failure is shown based on both theoretical considerations and observations of model footings [see Jumikis (1962), Ko and Davidson (1973)]. When the wedge displaces into the ground, lateral pressures are developed along line ag, which tends to translate block agf horizontally against wedge afe. The pressures along vertical line af are shown by the stress block on the right side of that line. It can be shown using Mohr's circles that the wedge agb develops stress slip lines, as shown on the small inset stress block, at $\alpha = 45 + \phi/2$ with the horizontal and for a footing with a smooth base so that ab is a principal plane. Similarly, wedge afe has slip line angles of $\beta = 45 - \phi/2$ that exit at line ae (also taken as a principal plane) at an angle of β.

From the stress block on the right of vertical line af (of length H) we can compute the total resisting earth pressure as force P_p by integrating Eq. (2-54),

$$P_p = \int_0^H \sigma_1(dz) = \int_0^H \left\{ (\gamma z + \bar{q}) \tan^2\left(45 + \frac{\phi}{2}\right) + 2c \tan\left(45 + \frac{\phi}{2}\right) \right\} dz \tag{g}$$

Using the definition given in Fig. 4-2 for K_p and integrating (necessary since σ_1 varies from a to f based on depth z), we obtain

$$P_p = \frac{\gamma H^2}{2} \cdot K_p + \bar{q} H \cdot K_p + 2cH \cdot \sqrt{K_p} \tag{h}$$

To find q_{ult} one must sum forces in the vertical direction for the half-wedge adg of unit width using the forces shown on the figure to obtain

$$\underbrace{q_{ult} \times \frac{B}{2}}_{\text{Footing pressure}} + \underbrace{\gamma \frac{B}{2} \cdot \frac{H}{2}}_{\text{Wedge weight}} - \underbrace{cA \cos \rho}_{\text{Cohesion}} - \underbrace{\frac{P_p}{\sin \rho \cos \phi}}_{\text{Lateral pressure}} = 0 \tag{i}$$

On substitution of values for H and A as shown on Fig. 4-2, we obtain

$$q_{ult} = c\left[\frac{2K_p}{\cos \phi} + \sqrt{K_p}\right] + \bar{q}\frac{\sqrt{K_p} K_p}{\cos \phi} + \frac{\gamma B}{4}\left[\frac{K_p^2}{\cos \phi} - \sqrt{K_p}\right] \tag{j}$$

Replacing the c, $\bar{q}$, and γB multipliers with N factors, we can write Eq. (j) in the commonly used format as

$$q_{ult} = cN_c + \bar{q}N_q + \gamma B N_\gamma \tag{k}$$

As we shall see in the next section, Eq. (*j*) underestimates q_{ult} substantially for several reasons:

1. Zone *afg* is neglected.
2. The footing interface is usually rough and contributes a roughness effect.
3. The shape of block *agfe* poorly defines the zone resisting the wedge movement into the soil. A logarithmic spiral better defines the slip surface from *g* to *f* and partly along *f* to *e*.
4. Solution is for a unit width strip across a very long footing, so it has to be adjusted for round, square, or finite-length footings (i.e., it needs a shape factor).
5. The shear resistance from plane *ae* to the ground surface has been neglected, thus requiring some kind of adjustment (i.e., a depth factor).
6. Other factors will be needed if q_{ult} is inclined from the vertical (i.e., inclination factors).

These derivations are only to illustrate the problems in defining the ultimate bearing capacity of a soil and are not intended for design use. Equations given in the following section should be used for any design. For a historical perspective on bearing-capacity efforts see Jumikis (1962), who presents a survey of a number of early proposals, which were primarily in German.

4-3 BEARING-CAPACITY EQUATIONS

There is currently no method of obtaining the ultimate bearing capacity of a foundation other than as an estimate. Vesić (1973) tabulated 15 theoretical solutions since 1940—and omitted at least one of the more popular methods in current use. There have been several additional proposals since that time.

There has been little experimental verification of any of the methods except by using model footings. Using models of $B = 25$ to 75 mm $\times$ $L = 25$ to 200 mm is popular because the "ultimate" load can be developed on a small prepared box of soil in the laboratory using commonly available compression machines on the order of 400 kN capacity. Full-size footings as small as 1 m $\times$ 1 m can develop ultimate loads of 3000 to 4000 kN so that very expensive site preparation and equipment availability are necessary to develop and measure loads of this magnitude.

Models—particularly on sand—do not produce reliable test results compared to full-scale prototypes because of scale effects. That is, the model reaction involves only a statistically small quantity of soil grains compared with that involved with the full-scale element. For example, sand requires confinement to develop resistance. The confined zone beneath a 25 $\times$ 50 mm model is almost nil compared with the confined zone beneath a small, say 1 m $\times$ 2 m, footing. It is also evident from both Fig. 1-1 and Fig. 4-2 that the depth of influence is considerably different in the two cases. In spite of this major defect in testing, the use of models is widespread and the literature regularly reports on the results of a new test program.

Centrifuge testing is used by some laboratories that can afford the expensive equipment. In this type of test the model footing is placed on a simulation of the foundation soil and spun in a centrifuge. Almost any practical multiple (or fraction) of the gravitational force can be modeled by adjusting the spin rate of the centrifuge. For a number of practical reasons—primarily soil simulation—this test has not received a wide following.

The Terzaghi Bearing-Capacity Equation

One of the early sets of bearing-capacity equations was proposed by Terzaghi (1943) as shown in Table 4-1. These equations are similar to Eq. (*k*) derived in the previous section, but Terzaghi used shape factors noted when the limitations of the equation were discussed. Terzaghi's equations were produced from a slightly modified bearing-capacity theory devel-

TABLE 4-1
Bearing-capacity equations by the several authors indicated

Terzaghi (1943). See Table 4-2 for typical values and for $K_{p\gamma}$ values.

$$q_{ult} = cN_c s_c + \bar{q}N_q + 0.5\gamma B N_\gamma s_\gamma$$

$$N_q = \frac{a^2}{a\cos^2(45 + \phi/2)}$$

$$a = e^{(0.75\pi - \phi/2)\tan\phi}$$

$$N_c = (N_q - 1)\cot\phi$$

$$N_\gamma = \frac{\tan\phi}{2}\left(\frac{K_{p\gamma}}{\cos^2\phi} - 1\right)$$

For:	strip	round	square
s_c =	1.0	1.3	1.3
s_γ =	1.0	0.6	0.8

Meyerhof (1963).* See Table 4-3 for shape, depth, and inclination factors.

Vertical load: $q_{ult} = cN_c s_c d_c + \bar{q}N_q s_q d_q + 0.5\gamma B' N_\gamma s_\gamma d_\gamma$

Inclined load: $q_{ult} = cN_c d_c i_c + \bar{q}N_q d_q i_q + 0.5\gamma B' N_\gamma d_\gamma i_\gamma$

$$N_q = e^{\pi\tan\phi}\tan^2\left(45 + \frac{\phi}{2}\right)$$

$$N_c = (N_q - 1)\cot\phi$$

$$N_\gamma = (N_q - 1)\tan(1.4\phi)$$

Hansen (1970).* See Table 4-5 for shape, depth, and other factors.

General:† $q_{ult} = cN_c s_c d_c i_c g_c b_c + \bar{q}N_q s_q d_q i_q g_q b_q + 0.5\gamma B' N_\gamma s_\gamma d_\gamma i_\gamma g_\gamma b_\gamma$

when $\phi = 0$

use $q_{ult} = 5.14 s_u(1 + s'_c + d'_c - i'_c - b'_c - g'_c) + \bar{q}$

N_q = same as Meyerhof above

N_c = same as Meyerhof above

$N_\gamma = 1.5(N_q - 1)\tan\phi$

Vesić (1973, 1975).* See Table 4-5 for shape, depth, and other factors. Use Hansen's equations above.

N_q = same as Meyerhof above

N_c = same as Meyerhof above

$N_\gamma = 2(N_q + 1)\tan\phi$

*These methods require a trial process to obtain design base dimensions since width B and length L are needed to compute shape, depth, and influence factors.

†See Sec. 4-6 when $i_i < 1$.

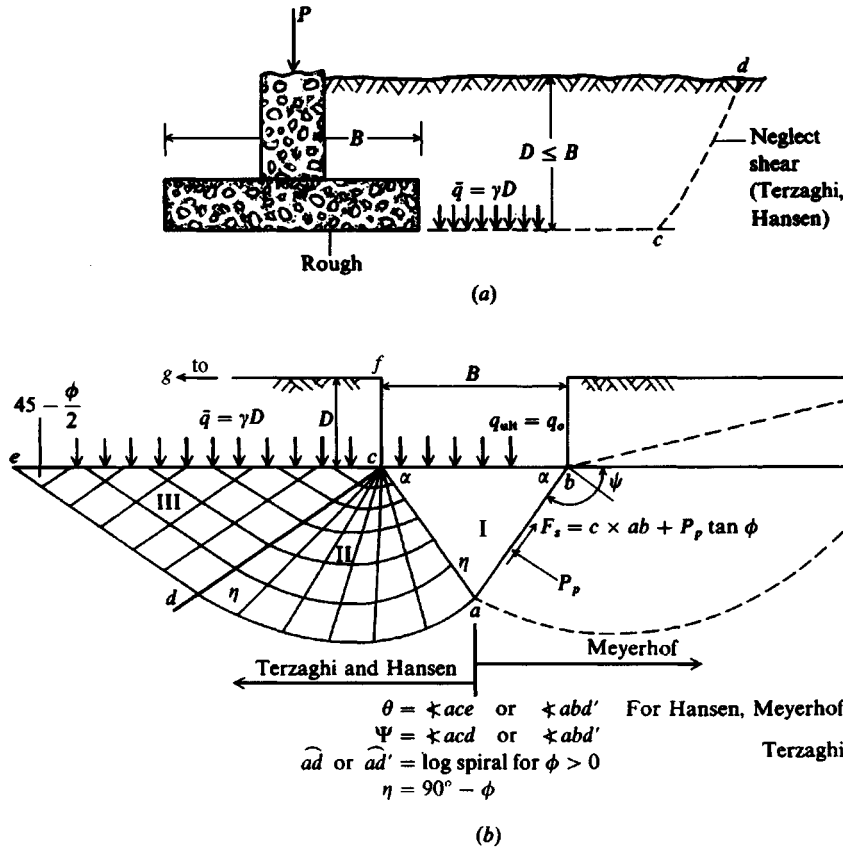

Figure 4-3 (*a*) Shallow foundation with rough base defined. Terzaghi and Hansen equations of Table 4-1 neglect shear along *cd*; (*b*) general footing-soil interaction for bearing-capacity equations for strip footing—left side for Terzaghi (1943), Hansen (1970), and right side Meyerhof (1951).

oped by Prandtl (ca. 1920) from using the theory of plasticity to analyze the punching of a rigid base into a softer (soil) material. Similar to Eq. (*k*), the basic equation was for the case in which a unit width from a long strip produced a plane strain case, all shape factors $s_i = 1.00$, but the N_i factors were computed differently. Terzaghi used $\alpha = \phi$ in Figs. 4-2 and 4-3 whereas most other theories use the $\alpha = 45 + \phi/2$ shown. We see in Table 4-1 that Terzaghi only used shape factors with the cohesion (s_c) and base (s_γ) terms. The Terzaghi bearing-capacity equation is developed, as was Eq. (*k*), by summing vertical forces on the wedge *bac* of Fig. 4-3. The difference in N factors results from the assumption of the log spiral arc *ad* and exit wedge *cde* of Fig 4-3. This makes a very substantial difference in how P_p is computed, which in turn gives the different N_i values. The shear slip lines shown on Fig. 4-3 qualitatively illustrate stress trajectories in the plastic zone beneath the footing as the ultimate bearing pressure is developed.

Terzaghi's bearing-capacity equations were intended for "shallow" foundations where

$$D \leq B$$

TABLE 4-2
Bearing-capacity factors for the Terzaghi equations

Values of N_γ for ϕ of 0, 34, and **48°** are original Terzaghi values and used to back-compute $K_{p\gamma}$

ϕ, deg	N_c	N_q	N_γ	$K_{p\gamma}$
0	5.7*	1.0	0.0	10.8
5	7.3	1.6	0.5	12.2
10	9.6	2.7	1.2	14.7
15	12.9	4.4	2.5	18.6
20	17.7	7.4	5.0	25.0
25	25.1	12.7	9.7	35.0
30	37.2	22.5	19.7	52.0
34	52.6	36.5	36.0	
35	57.8	41.4	42.4	82.0
40	95.7	81.3	100.4	141.0
45	172.3	173.3	297.5	298.0
48	258.3	287.9	780.1	
50	347.5	415.1	1153.2	800.0

*$N_c = 1.5\pi + 1$. [See Terzaghi (1943), p. 127.]

TABLE 4-3
Shape, depth, and inclination factors for the Meyerhof bearing-capacity equations of Table 4-1

Factors	Value	For
Shape:	$s_c = 1 + 0.2K_p\frac{B}{L}$	Any ϕ
	$s_q = s_\gamma = 1 + 0.1K_p\frac{B}{L}$	$\phi > 10°$
	$s_q = s_\gamma = 1$	$\phi = 0$
Depth:	$d_c = 1 + 0.2\sqrt{K_p}\frac{D}{B}$	Any ϕ
	$d_q = d_\gamma = 1 + 0.1\sqrt{K_p}\frac{D}{B}$	$\phi > 10$
	$d_q = d_\gamma = 1$	$\phi = 0$
Inclination:	$i_c = i_q = \left(1 - \frac{\theta°}{90°}\right)^2$	Any ϕ
R V $\theta < \phi$ H	$i_\gamma = \left(1 - \frac{\theta°}{\phi°}\right)^2$	$\phi > 0$
	$i_\gamma = 0$ for $\theta > 0$	$\phi = 0$

Where $K_p = \tan^2(45 + \phi/2)$ as in Fig. 4-2
θ = angle of resultant R measured from vertical without a sign; if $\theta = 0$ all $i_i = 1.0$.
B, L, D = previously defined

so that the shear resistance along cd of Fig. 4-3a could be neglected. Table 4-1 lists the Terzaghi equation and the method for computing the several N_i factors and the two shape factors s_i. Table 4-2 is a short table of N factors produced from a computer program and edited for illustration and for rapid use by the reader. Terzaghi never explained very well how he obtained the $K_{p\gamma}$ used to compute the bearing-capacity factor N_γ. He did, however, give a small-scale curve of ϕ versus N_γ and three specific values of N_γ at $\phi = 0$, 34, and 48° as shown on Table 4-2. The author took additional points from this curve and used a computer to back-compute $K_{p\gamma}$ to obtain a table of best-fit values from which the tabulated values of N_γ shown in Table 4-2 could be computed from the equation for N_γ shown in Table 4-1. Inspection of Table 4-4 indicates that the Meyerhof $N_{\gamma(M)}$ values are fairly close except for angles of $\phi > 40°$. Other approximations for N_γ include the following:

$$N_\gamma = 2(N_q + 1)\tan\phi \qquad \text{Vesić (1973)}$$

$$N_\gamma = 1.1(N_q - 1)\tan 1.3\phi \qquad \text{Spangler and Handy (1982)}$$

The N_γ value has the widest suggested range of values of any of the bearing-capacity N factors. A literature search reveals

$$38 \le N_\gamma \le 192 \qquad \text{for } \phi = 40°$$

In this textbook values from Tables 4-2 and 4-4 give a range from about 79 to 109.

Recently Kumbhojkar (1993) presented a series of values of N_γ with the claim they are better representations of the Terzaghi values than those of Table 4-2. An inspection of these

N_γ values shows the following:

ϕ	Terzaghi* (1943)	Bolton and Lau (1993)	Kumbhojkar (1993)	Table 4-2 (this text)
34°	36	43.5	32	36
48	780	638	650.7	780.1

*See Terzaghi (1943), Fig. 38 and page 128.

Fortunately the N_γ term does not make a significant contribution to the computed bearing capacity, so any of the values from Tables 4-2 or 4-4 can be used (or perhaps an average).

Bolton and Lau (1993) produced new N_q and N_γ values for strip and circular footings for both smooth and rough ground interfacings. Their N_q values for either smooth or rough strips are little different from the Hansen values for rough strips. The N_q values for circular footings range to more than two times the strip values. The N_γ values for rough footings compare well with the Vesić values in Table 4-4. Since the Table 4-4 values have shape s_i and depth d_i factors to be applied, it appears that these "new" values offer little advantage and are certainly more difficult to compute (see comparison with Terzaghi values in preceding table).

Meyerhof's Bearing-Capacity Equation

Meyerhof (1951, 1963) proposed a bearing-capacity equation similar to that of Terzaghi but included a shape factor s_q with the depth term N_q. He also included depth factors d_i and

TABLE 4-4
Bearing-capacity factors for the Meyerhof, Hansen, and Vesić bearing-capacity equations

Note that N_c and N_q are the same for all three methods; subscripts identify author for N_γ

ϕ	N_c	N_q	$N_{\gamma(H)}$	$N_{\gamma(M)}$	$N_{\gamma(V)}$	N_q/N_c	$2\tan\phi(1-\sin\phi)^2$
0	5.14*	1.0	0.0	0.0	0.0	0.195	0.000
5	6.49	1.6	0.1	0.1	0.4	0.242	0.146
10	8.34	2.5	0.4	0.4	1.2	0.296	0.241
15	10.97	3.9	1.2	1.1	2.6	0.359	0.294
20	14.83	6.4	2.9	2.9	5.4	0.431	0.315
25	20.71	10.7	6.8	6.8	10.9	0.514	0.311
26	22.25	11.8	7.9	8.0	12.5	0.533	0.308
28	25.79	14.7	10.9	11.2	16.7	0.570	0.299
30	30.13	18.4	15.1	15.7	22.4	0.610	0.289
32	35.47	23.2	20.8	22.0	30.2	0.653	0.276
34	42.14	29.4	28.7	31.1	41.0	0.698	0.262
36	50.55	37.7	40.0	44.4	56.2	0.746	0.247
38	61.31	48.9	56.1	64.0	77.9	0.797	0.231
40	75.25	64.1	79.4	93.6	109.3	0.852	0.214
45	133.73	134.7	200.5	262.3	271.3	1.007	0.172
50	266.50	318.5	567.4	871.7	761.3	1.195	0.131

* $= \pi + 2$ as limit when $\phi \to 0°$.

Slight differences in above table can be obtained using program BEARING.EXE on diskette depending on computer used and whether or not it has floating point.

inclination factors i_i [both noted in discussion of Eq. (*j*)] for cases where the footing load is inclined from the vertical. These additions produce equations of the general form shown in Table 4-1, with select N factors computed in Table 4-4. Program BEARING is provided on disk for other N_i values.

Meyerhof obtained his N factors by making trials of the zone abd' with arc ad' of Fig. 4-3*b*, which include an approximation for shear along line cd of Fig. 4-3*a*. The shape, depth, and inclination factors in Table 4-3 are from Meyerhof (1963) and are somewhat different from his 1951 values. The shape factors do not greatly differ from those given by Terzaghi except for the addition of s_q. Observing that the shear effect along line cd of Fig. 4-3*a* was still being somewhat ignored, Meyerhof proposed depth factors d_i.

He also proposed using the inclination factors of Table 4-3 to reduce the bearing capacity when the load resultant was inclined from the vertical by the angle θ. When the i_γ factor is used, it should be self-evident that it does not apply when $\phi = 0°$, since a base slip would occur with this term—even if there is base cohesion for the i_c term. Also, the i_i factors all = 1.0 if the angle $\theta = 0$.

Up to a depth of $D \approx B$ in Fig. 4-3*a*, the Meyerhof q_{ult} is not greatly different from the Terzaghi value. The difference becomes more pronounced at larger D/B ratios.

Hansen's Bearing-Capacity Method

Hansen (1970) proposed the general bearing-capacity case and N factor equations shown in Table 4-1. This equation is readily seen to be a further extension of the earlier Meyerhof (1951) work. Hansen's shape, depth, and other factors making up the general bearing-capacity equation are given in Table 4-5. These represent revisions and extensions from earlier proposals in 1957 and 1961. The extensions include base factors for situations in which the footing is tilted from the horizontal b_i and for the possibility of a slope β of the ground supporting the footing to give ground factors g_i. Table 4-4 gives selected N values for the Hansen equations together with computation aids for the more difficult shape and depth factor terms. Use program BEARING for intermediate N_i factors, because interpolation is not recommended, especially for $\phi \gtrsim 35°$.

Any of the equations given in Table 4-5 not subscripted with a V may be used as appropriate (limitations and restrictions are noted in the table). The equations shown in this table for inclination factors i_i will be considered in additional detail in Sec. 4-6.

Note that when the base is tilted, V and H are perpendicular and parallel, respectively, to the base, compared with when it is horizontal as shown in the sketch with Table 4-5.

For a footing on a slope both the Hansen and Vesić g_i factors can be used to reduce (or increase, depending on the direction of H_i) the bearing capacity using N factors as given in Table 4-4. Section 4-9 considers an alternative method for obtaining the bearing capacity of footings on a slope.

The Hansen equation implicitly allows any D/B and thus can be used for both shallow (footings) and deep (piles, drilled caissons) bases. Inspection of the $\bar{q}N_q$ term suggests a great increase in q_{ult} with great depth. To place modest limits on this, Hansen used

$$\left.\begin{aligned} d_c &= 1 + 0.4\frac{D}{B} \\ d_q &= 1 + 2\tan\phi(1 - \sin\phi)^2\frac{D}{B} \end{aligned}\right\} \frac{D}{B} \leq 1$$

$$\left.\begin{aligned} d_c &= 1 + 0.4 \tan^{-1} \frac{D}{B} \\ d_q &= 1 + 2 \tan \phi (1 - \sin \phi)^2 \tan^{-1} \frac{D}{B} \end{aligned}\right\} \frac{D}{B} > 1$$

These expressions give a discontinuity at $D/B = 1$; however, note the use of $\leq$ and $>$. For $\phi = 0$ (giving d_c') we have

$D/B =$	0	1	1.5*	2	5	10	20	100
$d_c' =$	0	0.40	0.42	0.44	0.55	0.59	0.61	0.62

*Actually computes 0.39

We can see that use of $\tan^{-1} D/B$ for $D/B > 1$ controls the increase in d_c and d_q that are in line with observations that q_{ult} appears to approach a limiting value at some depth ratio D/B, where this value of D is often termed the critical depth. This limitation on q_{ult} will be further considered in Chap. 16 on piles.

Vesić's Bearing-Capacity Equations

The Vesić (1973, 1975*b*) procedure is essentially the same as the method of Hansen (1961) with select changes. The N_c and N_q terms are those of Hansen but N_γ is slightly different (see Table 4-4). There are also differences in the i_i, b_i, and g_i terms as in Table 4-5*c*. The Vesić equation is somewhat easier to use than Hansen's because Hansen uses the i terms in computing shape factors s_i whereas Vesić does not (refer to Examples 4-6 and 4-7 following).

Which Equations to Use

There are few full-scale footing tests reported in the literature (where one usually goes to find substantiating data). The reason is that, as previously noted, they are very expensive to do and the cost is difficult to justify except as pure research (using a government grant) or for a precise determination for an important project—usually on the basis of settlement control. Few clients are willing to underwrite the costs of a full-scale footing load test when the bearing capacity can be obtained—often using empirical SPT or CPT data directly—to a sufficient precision for most projects.

Table 4-6 is a summary of eight load tests where the footings are somewhat larger than models and the soil data are determined as accurately as possible. The soil parameters and q_{ult} (in kg/cm^2) are from Milović (1965). The several methods used in this text [and the Balla (1961) method used in the first edition, which is a subroutine in supplemental computer program B-31 noted on your diskette] have been recomputed using plane strain adjustments where $L/B > 1$. Comparing the computed q_{ult} to the measured values indicates none of the several theories/methods has a significant advantage over any other in terms of a best prediction. The use of ϕ_{ps} instead of ϕ_{tr} when $L/B > 1$ did improve the computed q_{ult} for all except the Balla method.

Since the soil wedge beneath round and square bases is much closer to a triaxial than plane strain state, the adjustment of ϕ_{tr} to ϕ_{ps} is recommended only when $L/B > 2$.

TABLE 4-5*a*

Shape and depth factors for use in either the Hansen (1970) or Vesić (1973, 1975*b*) bearing-capacity equations of Table 4-1. Use s'_c, d'_c when $\phi = 0$ only for Hansen equations. Subscripts H, V for Hansen, Vesić, respectively.

Shape factors	Depth factors
$s'_{c(H)} = 0.2\dfrac{B'}{L'}$ $(\phi = 0°)$ $s_{c(H)} = 1.0 + \dfrac{N_q}{N_c} \cdot \dfrac{B'}{L'}$ $s_{c(V)} = 1.0 + \dfrac{N_q}{N_c} \cdot \dfrac{B}{L}$ $s_c = 1.0$ for strip	$d'_c = 0.4k$ $(\phi = 0°)$ $d_c = 1.0 + 0.4k$ $k = D/B$ for $D/B \le 1$ $k = \tan^{-1}(D/B)$ for $D/B > 1$ k in radians
$s_{q(H)} = 1.0 + \dfrac{B'}{L'}\sin\phi$ $s_{q(V)} = 1.0 + \dfrac{B}{L}\tan\phi$ for all ϕ	$d_q = 1 + 2\tan\phi(1 - \sin\phi)^2 k$ k defined above
$s_{\gamma(H)} = 1.0 - 0.4\dfrac{B'}{L'} \ge 0.6$ $s_{\gamma(V)} = 1.0 - 0.4\dfrac{B}{L} \ge 0.6$	$d_\gamma = 1.00$ for all ϕ

Notes:

1. Note use of "effective" base dimensions B', L' by Hansen but not by Vesić.
2. The values above are consistent with either a vertical load or a vertical load accompanied by a horizontal load H_B.
3. With a vertical load and a load H_L (and either $H_B = 0$ or $H_B > 0$) you may have to compute two sets of shape s_i and d_i as $s_{i,B}$, $s_{i,L}$ and $d_{i,B}$, $d_{i,L}$. For i, L subscripts of Eq. (4-2), presented in Sec. 4-6, use ratio L'/B' or D/L'.

TABLE 4-5*b*

Table of inclination, ground, and base factors for the Hansen (1970) equations. See Table 4-5*c* for equivalent Vesić equations.

Inclination factors	Ground factors (base on slope)
$i'_c = 0.5 - \sqrt{1 - \dfrac{H_i}{A_f C_a}}$	$g'_c = \dfrac{\beta°}{147°}$
$i_c = i_q - \dfrac{1 - i_q}{N_q - 1}$	$g_c = 1.0 - \dfrac{\beta°}{147°}$
$i_q = \left[1 - \dfrac{0.5H_i}{V + A_f c_a \cot\phi}\right]^{\alpha_1}$ $2 \le \alpha_1 \le 5$	$g_q = g_\gamma = (1 - 0.5\tan\beta)^5$
	Base factors (tilted base)
$i_\gamma = \left[1 - \dfrac{0.7H_i}{V + A_f c_a \cot\phi}\right]^{\alpha_2}$	$b'_c = \dfrac{\eta°}{147°}$ $(\phi = 0)$
$i_\gamma = \left[1 - \dfrac{(0.7 - \eta°/450°)H_i}{V + A_f c_a \cot\phi}\right]^{\alpha_2}$ $2 \le \alpha_2 \le 5$	$b_c = 1 - \dfrac{\eta°}{147°}$ $(\phi > 0)$ $b_q = \exp(-2\eta\tan\phi)$ $b_\gamma = \exp(-2.7\eta\tan\phi)$ η in radians

Notes:

1. Use H_i as either H_B or H_L, or both if $H_L > 0$.
2. Hansen (1970) did not give an i_c for $\phi > 0$. The value above is from Hansen (1961) and also used by Vesić.
3. Variable c_a = base adhesion, on the order of 0.6 to 1.0 × base cohesion.
4. Refer to sketch for identification of angles η and β, footing depth D, location of H_i (parallel and at top of base slab; usually also produces eccentricity). Especially note V = force *normal* to base and is not the resultant R from combining V and H_i.

Notes: $\beta + \eta$ 90° (Both β and η have signs (+) shown.)

β ϕ

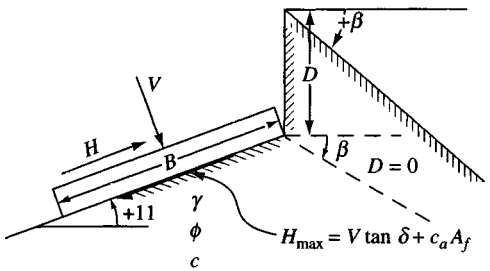

For: $L/B \le 2$ use ϕ_{tr}

$L/B > 2$ use $\phi_{ps} = 1.5\,\phi_{tr} - 17°$

$\phi_{tr} \le 34°$ use $\phi_{tr} = \phi_{ps}$

δ = friction angle between base and soil ($.5\phi \le \delta \le \phi$)

$A_f = B'L'$ (effective area)

c_a = base adhesion (0.6 to 1.0c)

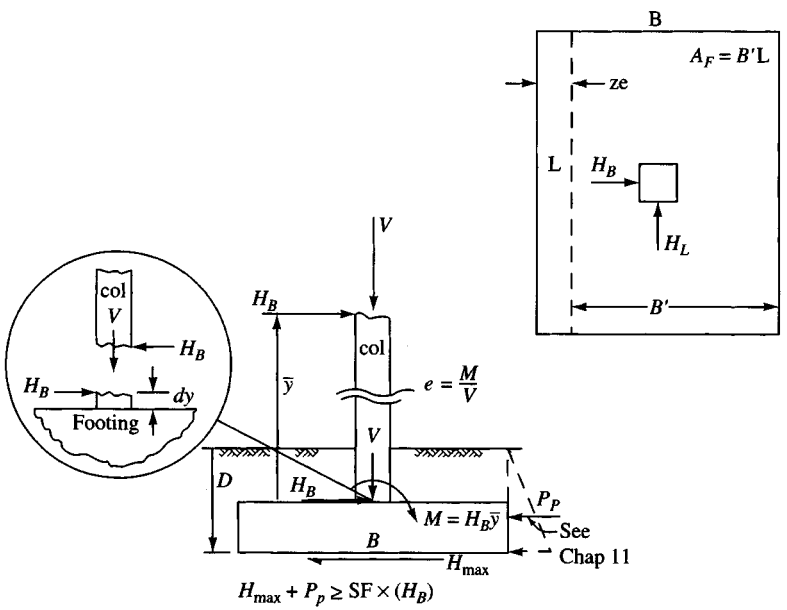

TABLE 4-5*c*

Table of inclination, ground, and base factors for the Vesić (1973, 1975*b*) bearing-capacity equations. See notes below and refer to sketch for identification of terms.

Inclination factors	Ground factors (base on slope)
$i'_c = 1 - \dfrac{mH_i}{A_f c_a N_c}$ $(\phi = 0)$	$g'_c = \dfrac{\beta}{5.14}$ β in radians
$i_c = i_q - \dfrac{1 - i_q}{N_q - 1}$ $(\phi > 0)$	$g_c = i_q - \dfrac{1 - i_q}{5.14 \tan \phi}$ $\phi > 0$
i_q, and m defined below	i_q defined with i_c
$i_q = \left[1.0 - \dfrac{H_i}{V + A_f c_a \cot \phi}\right]^m$	$g_q = g_\gamma = (1.0 - \tan \beta)^2$
	Base factors (tilted base)
$i_\gamma = \left[1.0 - \dfrac{H_i}{V + A_f c_a \cot \phi}\right]^{m+1}$	$b'_c = g'_c$ $(\phi = 0)$
$m = m_B = \dfrac{2 + B/L}{1 + B/L}$	$b_c = 1 - \dfrac{2\beta}{5.14 \tan \phi}$
$m = m_L = \dfrac{2 + L/B}{1 + L/B}$	$b_q = b_\gamma = (1.0 - \eta \tan \phi)^2$

Notes:

1. When $\phi = 0$ (and $\beta \neq 0$) use $N_\gamma = -2 \sin(\pm\beta)$ in N_γ term.
2. Compute $m = m_B$ when $H_i = H_B$ (H parallel to B) and $m = m_L$ when $H_i = H_L$ (H parallel to L). If you have both H_B and H_L use $m = \sqrt{m_B^2 + m_L^2}$. Note use of B and L, not B', L'.
3. Refer to Table sketch and Tables 4-5*a*,*b* for term identification.
4. Terms N_c, N_q, and N_γ are identified in Table 4-1.
5. Vesić always uses the bearing-capacity equation given in Table 4-1 (uses B' in the N_γ term even when $H_i = H_L$).
6. H_i term ≤ 1.0 for computing i_q, i_γ (always).

The Terzaghi equations, being the first proposed, have been very widely used. Because of their greater ease of use (one does not need to compute all the extra shape, depth, and other factors) they are still used—probably more than they should be. They are only suitable for a concentrically loaded footing on horizontal ground. They are not applicable for footings carrying a horizontal shear and/or a moment or for tilted bases (see Example 4-7 following).

Both the *Meyerhof* and *Hansen* methods are widely used. The *Vesić* method has not been much used [but is the suggested procedure in the API RP2A (1984) manual]. As previously noted there is very little difference between the Hansen and Vesić methods, as illustrated by the computed q_{ult} values shown in Table 4-6 (see also Example 4-7).

From these observations one may suggest the following equation use:

Use	Best for
Terzaghi	Very cohesive soils where $D/B \leq 1$ or for a quick estimate of q_{ult} to compare with other methods. *Do not use* for footings with moments and/or horizontal forces or for tilted bases and/or sloping ground.
Hansen, Meyerhof, Vesić	Any situation that applies, depending on user preference or familiarity with a particular method.
Hansen, Vesić	When base is tilted; when footing is on a slope or when $D/B > 1$.

It is good practice to use at least two methods and compare the computed values of q_{ult}. If the two values do not compare well, use a third method, a trivial exercise where the equations have been programmed for computer use. Use either an arithmetic or weighted average[2] value for the q_a provided for design (unless settlement is controlling).

4-4 ADDITIONAL CONSIDERATIONS WHEN USING THE BEARING-CAPACITY EQUATIONS

One should avoid using tables of N factors that require interpolation over about 2°. It is a trivial exercise to program the equations (or use program BEARING) to obtain N values for any angle. For angles larger than 35° the factors change rapidly and by large amounts. Interpolation can have a sizable error (or difference), so someone checking the work may not be able to verify q_{ult}.

The methods used to develop the bearing-capacity equations do not satisfy moment equilibrium but do satisfy $\sum F_H = \sum F_V = 0$. This error is not serious since statics is obviously

[2]Weighting is as follows: If you have values of 2 and 4 but believe 2 is 1.5 times as good as the 4, a weighted average gives

$$\text{Val} = \frac{2(1.5) + 4}{1 + 1.5} = \frac{7}{2.5} = 2.8$$

An arithmetic average is simply $(2 + 4)/2 = 3$.

TABLE 4-6

Comparison of computed theoretical bearing capacities and Milović's and Muh's experimental values*

Bearing-capacity method	Test 1	2	3	4	5	6	7	8
	D = 0.0 m	0.5	0.5	0.5	0.4	0.5	0.0	0.3
	B = 0.5 m	0.5	0.5	1.0	0.71	0.71	0.71	0.71
	L = 2.0 m	2.0	2.0	1.0	0.71	0.71	0.71	0.71
	γ = 15.69 kN/m^3	16.38	17.06	17.06	17.65	17.65	17.06	17.06
	ϕ = 37°(38.5°)	35.5(36.25)	38.5(40.75)	38.5	22	25	20	20
	c = 6.37 kPa	3.92	7.8	7.8	12.75	14.7	9.8	9.8
Milović (tests)				q_{ult}, kg/cm^2 = 4.1		5.5	2.2	2.6
Muhs (tests)	q_{ult} = 10.8 kg/cm^2	12.2	24.2	33.0				
Terzaghi	q_{ult} = 9.4*	9.2	22.9	19.7	4.3*	6.5*	2.5	2.9*
Meyerhof	8.2*	10.3	26.4	28.4	4.8	7.6	2.3	3.0
Hansen	7.2	9.8	23.7*	23.4	5.0	8.0	2.2*	3.1
Vesić	8.1	10.4*	25.1	24.7	5.1	8.2	2.3	3.2
Balla	14.0	15.3	35.8	33.0*	6.0	9.2	2.6	3.8

*After Milovic (1965) but all methods recomputed by author and Vesić added.

Notes:

1. ϕ = triaxial value ( ) = value adjusted as $\phi_{ps} = 1.5\phi_{tr} - 17$ (Eq. 2-57).
2. Values to nearest 0.1.
3. γ, c converted from given units to above values.
4. All values computed using computer program B-31 with subroutines for each method. Values all use ϕ_{ps} for $L/B > 1$.
5. * = best → Terzaghi = 4; Hansen = 2; Vesić and Balla = 1 each.

satisfied at ultimate loading but, of course, the interaction model may not be the same. The soil stress state is indeterminate at the design stress level q_a, similar to the stress state in a triaxial (or other) shear test. It is only at failure (q_{ult}) that the stress state is determined.

The bearing-capacity equations tend to be conservative most of the time, because the common practice is to use conservative estimates for the soil parameters. Additionally, after obtaining a conservative q_{ult} this is further reduced to the allowable soil pressure q_a using a safety factor. This means the probability is very high that q_a is "safe."

When Terzaghi (1943) developed his bearing-capacity equations, he considered a general shear failure in a dense soil and a local shear failure for a loose soil. For the local shear failure he proposed reducing the cohesion and ϕ as

$$c'' = 0.67c$$
$$\phi'' = \tan^{-1}(0.67 \tan \phi)$$

Terzaghi (and others) consider both smooth and rough base contact with the soil. It is doubtful that one would place a footing on a loose soil, and concrete footings poured directly on the soil will always be rough. Even metal storage tanks are not smooth, since the base is always treated with paint or an asphalt seal to resist corrosion.

There is some evidence, from using small footings up to about 1 m for B, that the BN_γ term does not increase the bearing capacity without bound, and for very large values of B both Vesić (1969) and De Beer (1965) suggest that the limiting value of q_{ult} approaches that of a deep foundation. The author suggests the following reduction factor:

$$r_\gamma = 1 - 0.25 \log\left(\frac{B}{\kappa}\right) \qquad B \geq 2 \text{ m (6 ft)}$$

where $\kappa = 2.0$ for SI and 6.0 for fps. This equation gives the following results:

B =	2	2.5	3	3.5	4	5	10	20	100 m
r_γ =	1.0	0.97	0.95	0.93	0.92	0.90	0.82	0.75	0.57

One can use this reduction factor with any of the bearing-capacity methods to give

$$0.5\gamma B N_\gamma s_\gamma d_\gamma r_\gamma$$

This equation is particularly applicable for large bases at small D/B ratios where the BN_γ term is predominating.

General observations about the bearing-capacity equations may be made as follows:

1. The cohesion term predominates in cohesive soil.
2. The depth term ($\bar{q}N_q$) predominates in cohesionless soils. Only a small D increases q_{ult} substantially.
3. The base width term $0.5\gamma BN_\gamma$ provides some increase in bearing capacity for both cohesive and cohesionless soils. In cases where $B < 3$ to 4 m this term could be neglected with little error.
4. No one would place a footing on the surface of a cohesionless soil mass.

5. It is highly unlikely that one would place a footing on a cohesionless soil with a D_r (Table 3-4) less than 0.5. If the soil is loose, it would be compacted in some manner to a higher density prior to placing footings in it.
6. Where the soil beneath the footing is not homogeneous or is stratified, some judgment must be applied to determine the bearing capacity. In the case of stratification, later sections will consider several cases.
7. When a base must be designed for a particular load, except for the Terzaghi method, one must use an iterative procedure since the shape, depth, and inclination factors depend on B. A computer program such as B-31 is most useful for this type problem. It should be set to increment the base by 0.010-m or 0.25-ft (3-in.) steps as this is a common multiple of base dimensions.
8. Inspection of Table 4-1 indicates that the Terzaghi equation is much easier to use than the other methods (see also Example 4-1) so that it has great appeal for many practitioners, particularly for bases with only vertical loads and $D/B \leq 1$. Its form is also widely used for deep foundations but with adjusted N factors.
9. Vesić (1973) recommends that depth factors d_i not be used for shallow foundations ($D/B \leq 1$) because of uncertainties in quality of the overburden. However, he did give the values shown in Table 4-5 despite this recommendation.

4-5 BEARING-CAPACITY EXAMPLES

The following examples illustrate the application of the bearing-capacity equations to some typical problems.

Example 4-1. Compute the allowable bearing pressure using the Terzaghi equation for the footing and soil parameters shown in Fig. E4-1. Use a safety factor of 3 to obtain q_a. Compare this with the value obtained from using Eq. (*j*). The soil data are obtained from a series of undrained U triaxial tests. Is the soil saturated?

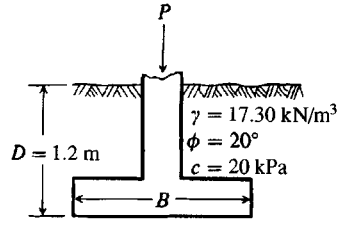

Figure E4-1

Solution.

1. The soil is not saturated, since a U test gives a ϕ angle. A CU test might give similar data for a saturated soil.
2. Find the bearing capacity. Note that this value is usually what a geotechnical consultant would have to recommend (B not known but D is). From Table 4-2 obtain

$$N_c = 17.7 \qquad N_q = 7.4 \qquad N_\gamma = 5.0$$
$$s_c = 1.3 \qquad s_\gamma = 0.8 \qquad \text{(from Table 4-1, square footing)}$$
$$q_{ult} = cN_c s_c + \bar{q}N_q + 0.5\gamma B N_\gamma s_\gamma$$

$$= 20(17.7)(1.3) + 1.2(17.3)(7.4) + 0.5(17.3)(B)(5)(0.8)$$
$$= (613.8 + 34.6B) \text{ kPa}$$

The allowable pressure (a SF = 3 is commonly used when $c > 0$) is

$$q_a = \frac{q_{ult}}{SF}$$
$$= \frac{613.8 + 34.6B}{3} = (205 + 11.5B) \text{ kPa}$$

Since B is likely to range from 1.5 to 3 m and at 3 m $r_\gamma = 0.95$,

$$q_a = 205 + 11.5(1.5) \quad = 220 \text{ kPa} \quad \text{(rounding)}$$
$$q_a = 205 + 11.5(3)(0.95) = 240 \text{ kPa}$$
$$\text{Recommend } q_a \cong \mathbf{200–220} \text{ kPa}$$

3. Using Eq. (*j*), we have

$$q_{ult} = c\left(\frac{2\sqrt{K_p}}{\cos\phi} + \sqrt{K_p}\right) + \bar{q}\frac{\sqrt{K_p}K_p}{\cos\phi} + \frac{\gamma B}{4}\left(\frac{K_p^2}{\cos\phi} - \sqrt{K_p}\right)$$

$$\cos\phi = \cos 20° = 0.940$$
$$\tan(45° + \phi/2) = \sqrt{K_p} = \tan 55° = 1.428$$
$$\tan^2(45° + \phi/2) = K_p = \tan^2 55° = 2.04$$
$$N_c = \left(\frac{2K_p}{\cos\phi} + \sqrt{K_p}\right) = \frac{2(2.04)}{0.940} + 1.428 = 5.8$$
$$N_q = \frac{1.428(2.04)}{0.940} = 3.1$$
$$N_\gamma = 0.25\left(\frac{2.04^2}{0.940} - 1.428\right) = 0.75$$
$$q_{ult} = 20(5.8) + 1.2(17.3)(3.1) + 17.3B(0.75)$$
$$= 180 + 13.0B$$
$$q_a = 60 + 4.3B \qquad (SF = 3)$$

For a reasonable size footing Eq.(*j*) gives $q_a \cong 60$ kPa. For this soil with $\phi = 30°$, $B = 1.5$ m, and SF = 3.0, we get

$$\text{Terzaghi: } q_{ult} = 967.2 + 467.1 + 204.5 = 1638.8$$
$$q_a = 1638.8/3 \approx \mathbf{550} \text{ kPa}$$
$$\text{Eq. } (j)\text{: } q_{ult} = 20(8.7) + 1.2(17.3)(6.0) + 17.3B(2.2)$$
$$\cong 174 + 125 + 38B = 299 + 38B$$
$$q_a = 100 + 13B \cong \mathbf{110} \text{ kPa}$$

We can see Eq. (*j*) is so conservative as to be nearly useless.

////

Example 4-2. A footing load test made by H. Muhs in Berlin [reported by Hansen (1970)] produced the following data:

$$D = 0.5\text{ m} \qquad B = 0.5\text{ m} \qquad L = 2.0\text{ m}$$

$$\gamma' = 9.31\text{ kN/m}^3 \qquad \phi_{\text{triaxial}} = 42.7^\circ \qquad \text{Cohesion } c = 0$$

$$P_{\text{ult}} = 1863\text{ kN (measured)} \qquad q_{\text{ult}} = \frac{P_{\text{ult}}}{BL} = \frac{1863}{0.5 \times 2} = 1863\text{ kPa (computed)}$$

Required. Compute the ultimate bearing capacity by both Hansen and Meyerhof equations and compare these values with the measured value.

Solution.

a. Since $c = 0$, any factors with subscript c do not need computing. All g_i and b_i factors are 1.00; with these factors identified, the Hansen equation simplifies to

$$q_{\text{ult}} = \gamma' D N_q s_q d_q + 0.5\gamma' B N_\gamma s_\gamma d_\gamma$$

$$L/B = \frac{2}{0.5} = 4 \rightarrow \phi_{\text{ps}} = 1.5(42.5) - 17 = 46.75^\circ$$

$$\text{Use } \phi = 47^\circ$$

From a table of ϕ in 1° increments (table not shown) obtain

$$N_q = 187 \qquad N_\gamma = 299$$

Using linear interpolation of Table 4-4 gives 208.2 and 347.2. Using Table 4-5*a* one obtains [get the $2\tan\phi(1 - \sin\phi)^2$ part of d_q term from Table 4-4] the following:

$$s_{q(H)} = 1 + \frac{B'}{L'}\sin\phi = 1.18 \qquad s_{\gamma(H)} = 1 - 0.4\frac{B'}{L'} = 0.9$$

$$d_q = 1 + 2\tan\phi(1 - \sin\phi)^2\frac{D}{B'} = 1 + 0.155\frac{D}{B'}$$

$$= 1 + 0.155\left(\frac{0.5}{0.5}\right) = 1.155 \qquad d_\gamma = 1.0$$

With these values we obtain

$$q_{\text{ult}} = 9.31(0.5)(187)(1.18)(1.155) + 0.5(9.31)(0.5)(299)(0.9)(1)$$

$$= \mathbf{1812}\text{ kPa vs. 1863 kPa measured}$$

b. By the Meyerhof equations of Table 4-1 and 4-3, and $\phi_{\text{ps}} = 47^\circ$, we can proceed as follows:

Step 1. Obtain $N_q = 187$

$$N_\gamma = (N_q - 1)\tan(1.4\phi) = 413.6 \rightarrow 414$$

$$K_p = \tan^2\left(45 + \frac{\phi}{2}\right) = 6.44 \rightarrow \sqrt{K_p} = 2.54$$

$$s_q = s_\gamma = 1 + 0.1K_p\frac{B}{L} = 1 + 0.1(6.44)\frac{0.5}{2.0} = 1.16$$

$$d_q = d_\gamma = 1 + 0.1\sqrt{K_p}\frac{D}{B} = 1 + 0.1(2.54)\frac{0.5}{0.5} = 1.25$$

Step 2. Substitute into the Meyerhof equation (ignoring any c subscripts):

$$\begin{aligned} q_{\text{ult}} &= \gamma' D N_q s_q d_q + 0.5\gamma B N_\gamma s_\gamma d_\gamma \\ &= 9.31(0.5)(187)(1.16)(1.25) + 0.5(9.31)(0.5)(414)(1.16)(1.25) \\ &= 1262 + 1397 = \mathbf{2659}\ \text{kPa} \end{aligned}$$

////

Example 4-3. A series of large-scale footing bearing-capacity tests were performed on soft Bangkok clay [Brand et al. (1972)]. One of the tests consisted of a 1.05-m-square footing at a depth $D = 1.5$ m. At a 1-in. settlement the load was approximately 14.1 tons from interpretation of the given load-settlement curve. Unconfined compression and vane shear tests gave U strength values as follows:

$$q_u = 3.0\ \text{ton/m}^2 \qquad s_u = 3.0\ \text{ton/m}^2 \qquad s_u, \text{vane} = 2.4\ \text{ton/m}^2$$

These data were obtained by the author's interpretation of data presented in several plots and in the zone from 1 to 2 m below footing. Plasticity data were $w_L = 80$ and $w_p = 35$ percent. The units of this problem are those of the test as reported in the cited source. These and other load-settlement data are in Prob. 4-17.

Required. Compute the ultimate bearing capacity by the Hansen equations and compare with the load-test value of 14.1 tons.

Solution. Obtain N, s_i', and d_i' factors. Since $\phi = 0°$ for a U test, we have $N_c = 5.14$ and $N_q = 1.0$. From Fig. 3-26*a* and $I_p = 45$, obtain a reduction factor of 0.8 (there are not enough data to use Fig. 3-26*b*).

$$\begin{aligned} s_{u,\text{des}} &= \lambda s_{u,\text{vane}} = 0.8(2.4) = 1.92\ \text{ton/m}^2 \\ s_c' &= 0.2\frac{B}{L} = 0.2\frac{1}{1} = 0.2 \\ d_c' &= 0.4\tan^{-1}\frac{D}{B} = 0.4\tan^{-1}\frac{1.5}{1.05} = 0.38 \qquad (D > B) \end{aligned}$$

Neglect $\bar{q}N_q$, since there was probably operating space in the footing excavation. Thus,

$$\begin{aligned} q_{\text{ult}} &= 5.14 s_u(1 + s_c' + d_c') \qquad \text{Table 4-1 for } \phi = 0 \text{ case} \\ q_{\text{ult}} &= 5.14(1.92)(1 + 0.2 + 0.38) = \mathbf{15.6}\ \text{ton/m}^2 \\ \text{From load test, } q_{\text{actual}} &= \frac{14.1}{1.05^2} = 12.8\ \text{ton/m}^2 \end{aligned}$$

If we use the unconfined compression tests and take $s_u = q_u/2$, we obtain

$$q_{\text{ult}} = \frac{1.5}{1.92}(15.6) = \mathbf{12.2}\ \text{ton/m}^2$$

////

Example 4-4.

Given. A series of unconfined compression tests in the zone of interest (from SPT samples) from a boring-log give an average $q_u = 200$ kPa.

Required. Estimate the allowable bearing capacity for square footings located at somewhat uncertain depths and B dimensions unknown using both the Meyerhof and Terzaghi bearing-capacity equations. Use safety factor SF = 3.0.

Solution. (The reader should note this is the most common procedure for obtaining the allowable bearing capacity for cohesive soils with limited data.)

a. By Meyerhof equations,

$$c = \frac{q_u}{2} \text{ (for both equations)} \qquad s_c = 1.2$$

$$q_{\text{ult}} = 1.2cN_c + \bar{q}N_q$$

$$q_a = \frac{q_{\text{ult}}}{3} = 1.2\frac{q_u}{2}(5.14)\frac{1}{3} + \frac{\bar{q}}{3} = 1.03q_u + 0.3\bar{q}$$

b. By Terzaghi equations, we can take $s_c = 1.3$ for $\phi = 0$.

$$q_a = \frac{q_{\text{ult}}}{3} = \frac{q_u}{2}(5.7)(1.3)\frac{1}{3} + \frac{\bar{q}}{3} = 1.24q_u + 0.3\bar{q}$$

It is common to neglect $0.3\bar{q}$ and note that either 1.03 or 1.24 is sufficiently close to 1.0 (and is conservative) to take the allowable bearing pressure as

$$q_a = q_u = \mathbf{200} \text{ kPa}$$

The use of $q_a = q_u$ for the allowable bearing capacity is *nearly universal* when SPT samples are used for q_u. Since these samples are in a very disturbed state, the true SF may well be on the order of 4 or 5 instead of close to 3.0 as used above. This method of obtaining q_a is not recommended when q_u is less than about 75 kPa or 1.5 ksf. In these cases s_u should be determined on samples of better quality than those from an SPT.

////

DISCUSSION OF EXAMPLES. Examples 4-1 and 4-4 illustrate the simplicity of the Terzaghi bearing-capacity method. They also illustrate that the approximate Eq. (*j*) is much too conservative for use in design.

Examples 4-2 and 4-3 illustrate how to use the equations and how to check load test values.

Example 4-4 also illustrates the common practice of using the simple version of

$$q_{\text{ult}} = cN_c \cong 3q_u; \qquad q_a = q_u$$

Note that for a "deep" foundation (say $D/B = 15$) in a cohesive soil $s_u = c$ for either a round or square base, and using the Hansen or Vesić equations, we have

$$d_c' = 0.4 \tan^{-1}\frac{D}{B} = 0.4(1.47) = 0.59$$

$$s_c' = 0.2\left(\frac{B}{L}\right) = 0.2$$

and for the equation in Table 4-1 for $\phi = 0$ we have

$$q_{\text{ult}} = 5.14c(1 + 0.59 + 0.2) = \mathbf{9.2}c$$

The value of $q_{ult} = 9c$ is used worldwide with local values (from load tests) ranging from about 7.5 to 11. The Terzaghi equation gives $7.41c$ but Meyerhof's method is not valid since it gives a value of $25c$.

4-6 FOOTINGS WITH ECCENTRIC OR INCLINED LOADINGS

A footing may be eccentrically loaded from a concentric column with an axial load and moments about one or both axes as in Fig. 4-4. The eccentricity may result also from a column that is initially not centrally located or becomes off-center when a part of the footing is cut away during remodeling and/or installing new equipment. Obviously the footing cannot be cut if an analysis indicates the recomputed soil pressure might result in a bearing failure.

Footings with Eccentricity

Research and observation [Meyerhof (1953, 1963) and Hansen (1970)] indicate that *effective* footing dimensions obtained (refer to Fig. 4-4) as

$$L' = L - 2e_x \qquad B' = B - 2e_y$$

should be used in bearing-capacity analyses to obtain an effective footing area defined as

$$A_f = B'L'$$

and the center of pressure when using a rectangular pressure distribution of q' is the center of area BL' at point A'; i.e., from Fig 4-4*a*:

$$2e_x + L' = L$$
$$e_x + c = L/2$$

Substitute for L and obtain $c = L'/2$. If there is no eccentricity about either axis, use the actual footing dimension for that B' or L'.

The effective area of a round base can be computed by locating the eccentricity e_x on any axis by swinging arcs with centers shown to produce an area *abcd*, which is then reduced to an equivalent rectangular base of dimensions $B' \times L'$ as shown on Fig. 4-4*b*. You should locate the dimension B' so that the left edge (line $c'd'$) is at least at the left face of the column located at point O.

For design (considered in Chap. 8) the minimum dimensions (to satisfy ACI 318-) of a rectangular footing with a central column of dimensions $w_x \times w_y$ are required to be

$$B_{min} = 4e_y + w_y \qquad B' = 2e_y + w_y$$
$$L_{min} = 4e_x + w_x \qquad L' = 2e_x + w_x$$

Final dimensions may be larger than B_{min} or L_{min} based on obtaining the required allowable bearing capacity.

The ultimate bearing capacity for footings with eccentricity, using either the Meyerhof or Hansen/Vesić equations, is found in *either* of two ways:

Method 1. Use either the Hansen or Vesić bearing-capacity equation given in Table 4-1 with the following adjustments:

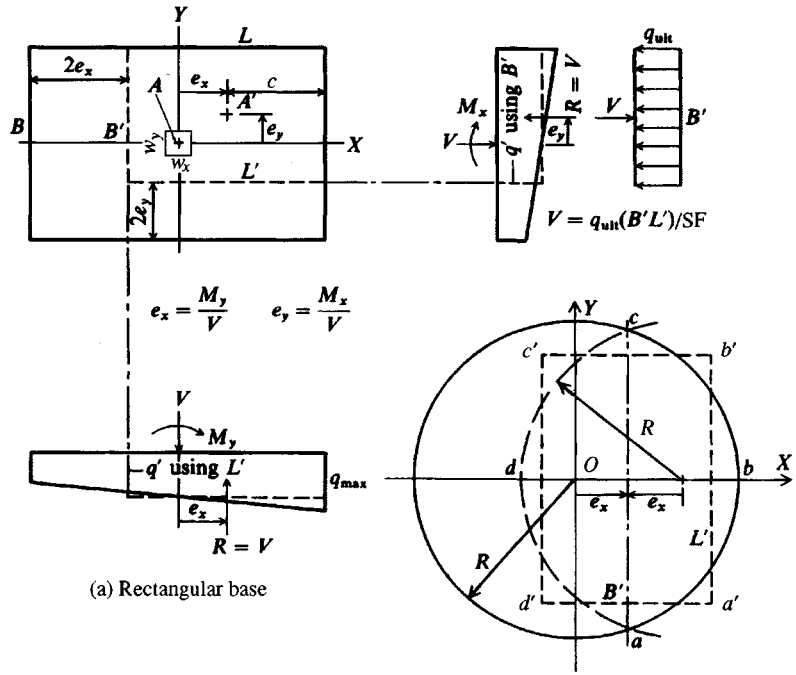

Figure 4-4 Method of computing effective footing dimensions when footing is eccentrically loaded for both rectangular and round bases.

a. Use B' in the γBN_γ term.

b. Use B' and L' in computing the shape factors.

c. Use actual B and L for all depth factors.

The computed ultimate bearing capacity q_{ult} is then reduced to an allowable value q_a with an appropriate safety factor SF as

$$q_a = q_{ult}/\text{SF} \qquad (\text{and } P_a = q_a B'L')$$

Method 2. Use the Meyerhof general bearing-capacity equation given in Table 4-1 and a reduction factor R_e used as

$$q_{ult,des} = q_{ult,comp} \times R_e$$

Since Meyerhof (1953) suggested this method, it should be used only with the Meyerhof equation to compute the bearing capacity. The original Meyerhof method gave reduction curves; however, the following equations are suitable for obtaining the reduction factor:

$$R_e = 1 - 2e/B \qquad \text{(cohesive soil)}$$

$$R_e = 1 - \sqrt{e/B} \qquad \text{(cohesionless soil and for } 0 < e/B < 0.3)$$

It should be evident from Fig. 4-4 that if $e/B = 0.5$, the point A' falls at the edge of the base and an unstable foundation results. In practice the e/B ratio is seldom greater than 0.2 and is

usually limited to $e \leq B/6$. In these reduction factor equations the dimensions B and L are referenced to the axis about which the base moment occurs. Normally, greatest base efficiency is obtained by using the larger or length dimension L to resist overturning. For *round bases* use B as the diameter, and for *octagonal* shapes use B as the effective base diameter.

Alternatively, one may directly use the Meyerhof equation with B' and L' used to compute the shape and depth factors and B' used in the $0.5\gamma B'N_\gamma$ term. This method is preferred by the author.

Example 4-5. A square footing is 1.8×1.8 m with a 0.4×0.4 m square column. It is loaded with an axial load of 1800 kN and $M_x = 450$ kN · m; $M_y = 360$ kN · m. Undrained triaxial tests (soil not saturated) give $\phi = 36°$ and $c = 20$ kPa. The footing depth $D = 1.8$ m; the soil unit weight $\gamma = 18.00$ kN/m^3; the water table is at a depth of 6.1 m from the ground surface.

Required. What is the allowable soil pressure, if SF = 3.0, using the Hansen bearing-capacity equation with B', L'; Meyerhof's equation; and the reduction factor R_e?

Solution. See Fig. E4-5.

$$e_y = 450/1800 = 0.25 \text{ m} \qquad e_x = 360/1800 = 0.20 \text{ m}$$

Both values of e are $< B/6 = 1.8/6 = 0.30$ m. Also

$$B_{\min} = 4(0.25) + 0.4 = 1.4 < 1.8 \text{ m given}$$
$$L_{\min} = 4(0.20) + 0.4 = 1.2 < 1.8 \text{ m given}$$

Now find

$$B' = B - 2e_y = 1.8 - 2(0.25) = 1.3 \text{ m} \qquad (B' < L')$$
$$L' = L - 2e_x = 1.8 - 2(0.20) = 1.4 \text{ m} \qquad (L' > B')$$

By Hansen's equation. From Table 4-4 at $\phi = 36°$ and rounding to integers, we obtain

$$N_c = 51 \qquad N_q = 38 \qquad N_\gamma = 40$$
$$N_q/N_c = 0.746 \qquad 2\tan\phi(1 - \sin\phi)^2 = 0.247$$
$$\text{Compute } D/B = 1.8/1.8 = 1.0$$

Now compute

$$s_c = 1 + (N_q/N_c)(B'/L') = 1 + 0.746(1.3/1.4) = 1.69$$
$$d_c = 1 + 0.4D/B = 1 + 0.4(1.8/1.8) = 1.40$$
$$s_q = 1 + (B'/L')\sin\phi = 1 + (1.3/1.4)\sin 36° = 1.55$$
$$d_q = 1 + 2\tan\phi(1 - \sin\phi)^2 D/B = 1 + 0.247(1.0) = 1.25$$
$$s_\gamma = 1 - 0.4\frac{B'}{L'} = 1 - 0.4\frac{1.3}{1.4} = 0.62 > 0.60 \quad \text{(O.K.)}$$
$$d_\gamma = 1.0$$
$$\text{All } i_i = g_i = b_i = 1.0 \text{ (not 0.0)}$$

The Hansen equation is given in Table 4-1 as

$$q_{\text{ult}} = cN_c s_c d_c + \bar{q}N_q s_q d_q + 0.5\gamma B'N_\gamma s_\gamma d_\gamma$$

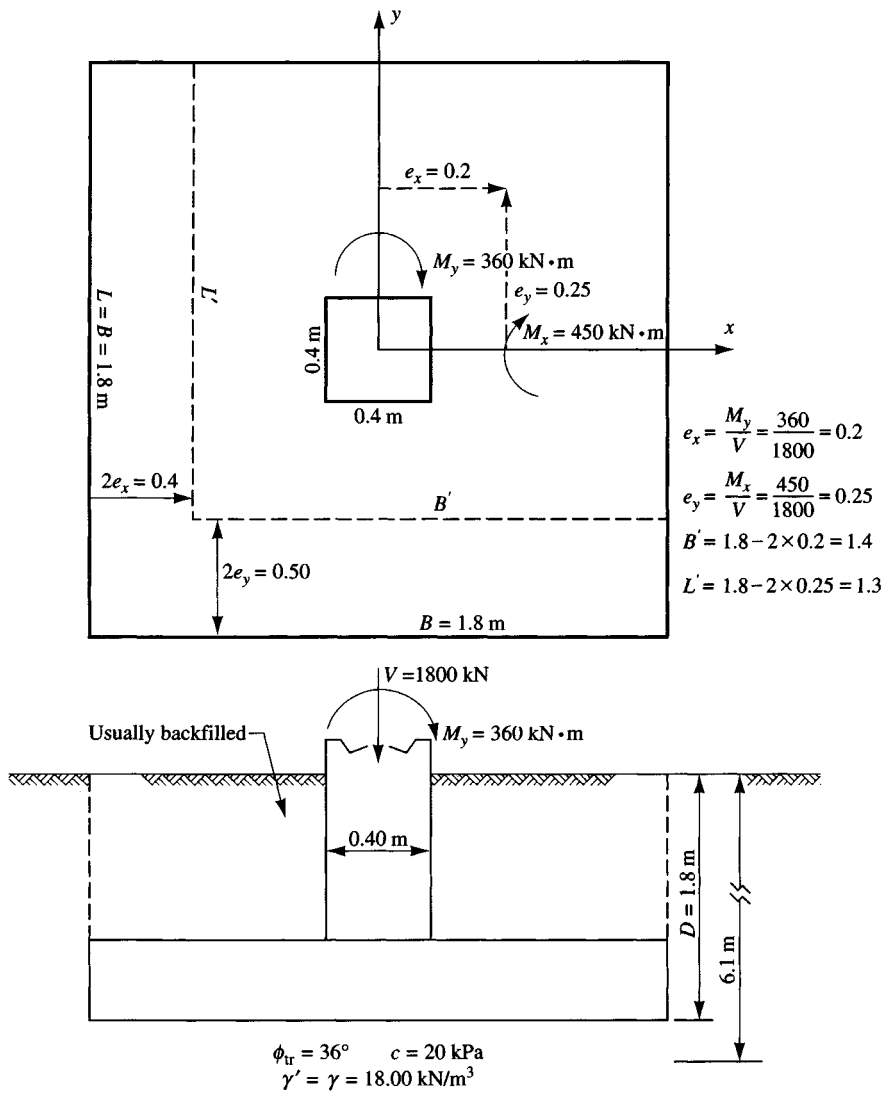

Figure E4-5

Inserting values computed above with terms of value 1.0 not shown (except d_γ) and using $B' = 1.3$, we obtain

$$q_{ult} = 20(51)(1.69)(1.4) + 1.8(18.0)(38)(1.55)(1.25) + 0.5(18.0)(1.3)(40)(0.62)(1.0)$$
$$= 2413 + 2385 + 290 = 5088 \text{ kPa}$$

For SF = 3.0 the allowable soil pressure q_a is

$$q_a = 5088/3 = 1696 \rightarrow \mathbf{1700} \text{ kPa}$$

The actual soil pressure is

$$q_{act} = \frac{1800}{B'L'} = \frac{1800}{1.3 \times 1.4} = \mathbf{989}\ \text{kPa}$$

Note that the allowable pressure q_a is very large, and the actual soil pressure q_{act} is also large. With this large actual soil pressure, settlement may be the limiting factor. Some geotechnical consultants routinely limit the maximum allowable soil pressure to around 500 kPa in recommendations to clients for design whether settlement is a factor or not. Small footings with large column loads are visually not very confidence-inspiring during construction, and with such a large load involved this is certainly not the location to be excessively conservative.

By Meyerhof's method and R_e. This method uses actual base dimensions $B \times L$:

$$K_p = \tan^2(45 + \phi/2) = \tan^2(45 + 36/2) = 3.85$$
$$\sqrt{K_p} = 1.96$$

From Table 4-3,

$$N_c = 51 \qquad N_q = 38 \text{ (same as Hansen values)} \qquad N_\gamma = 44.4 \rightarrow 44$$

Also

$$s_c = 1 + 0.2K_p\frac{B}{L} = 1 + 0.2(3.85)\frac{1.8}{1.8} = 1.77$$
$$s_q = s_\gamma = 1 + 0.1K_p\frac{B}{L} = 1.39$$
$$d_c = 1 + 0.2\sqrt{K_p}\frac{D}{B} = 1 + 0.2(1.96)\frac{1.8}{1.8} = 1.39$$
$$d_q = d_\gamma = 1 + 0.1(1.96)(1.0) = 1.20$$

Now direct substitution into the Meyerhof equation of Table 4-1 for the vertical load case gives

$$q_{ult} = 20(51)(1.77)(1.39) + 1.8(18.0)(38)(1.39)(1.20) + 0.5(18.0)(1.8)(44)(1.39)(1.20)$$
$$= 2510 + 2054 + 1189 = 5752\ \text{kPa}$$

There will be two reduction factors since there is two-way eccentricity. Use the equation for cohesionless soils since the cohesion is small (only 20 kPa):

$$R_{eB} = 1 - \left(\frac{e_y}{B}\right)^{0.5} = 1 - \sqrt{0.25/1.8} = 1 - 0.37 = 0.63$$
$$R_{eL} = 1 - \left(\frac{e_x}{L}\right)^{0.5} = 1 - \sqrt{0.2/1.8} = 0.67$$

The reduced $q_{ult} = 5752(R_{eB}R_{eL}) = 5752(0.63 \times 0.67) = 2428$ kPa. The allowable (SF = 3) soil pressure = $2428/3 = 809 \rightarrow$ **810** kPa. The actual soil pressure = $1800/(BL) = 1800/(1.8 \times 1.8) = 555$ kPa.

Meyerhof's reduction factors were based on using small model footings (B on the order of 50 mm), but a series of tests using a 0.5×2 m concrete base, reported by Muhs and Weiss (1969), indicated that the Meyerhof reduction method is not unreasonable.

Comments. The Hansen method gives high soil pressures but indicates the base is satisfactory. The Meyerhof method also indicates the base is satisfactory but with a very different q_a. Now the

question is, what does one do? The author would most probably limit the soil pressure to $q_a = 500$ kPa (which is less than either Meyerhof or Hansen) and back-compute a base as follows:

$$\text{New } B'L' = 1800/500 = 3.6 \text{ m}^2$$
$$\text{Original ratio of } B'/L' = 1.3/1.4 = 0.929$$
$$0.929L'^2 = 3.6 \rightarrow L' = 1.97 \text{ m} \quad \text{then} \quad B' = 1.83 \text{ m}$$

From these find

$$B = 1.83 + 2(0.25) = 2.33 \quad \text{and} \quad L = 1.97 + 2(0.2) = 2.37$$

Thus, make the base square with dimensions **2.40** × **2.40** m. ////

Footings with Inclined Loads

Inclined loads are produced when the footing is loaded with both a vertical V and a horizontal component(s) H_i of loading (refer to Table 4-5 and its figure). This loading is common for many industrial process footings where horizontal wind loads are in combination with the gravity loads. The retaining wall base design of Chap. 12 is a classic case of a foundation with both a horizontal (the lateral earth pressure) and vertical loading. Eccentricity results from the vertical load not being initially located at $B/2$ and from the lateral earth pressure effects.

Rolling equipment (as in steel mills) and a number of other types of industrial foundations are subjected to horizontal loads from material going through the equipment mounted on the foundation or from pulls or pushes applied to the foundation from servicing, repair/replacement, or normal operations. In any case the load inclination results in a bearing-capacity reduction over that of a foundation subjected to a vertical load only.

The inclination factors of Tables 4-3 and 4-5 can be used with the Meyerhof, Hansen, or Vesić bearing-capacity equations. The Terzaghi equations have no direct provision for a reduction in cases where the load is inclined.

The Meyerhof inclination factors $i_{i,M}$ are reasonably self-explanatory. The Hansen values are shown with the exponent of α_1 for i_q and α_2 for i_γ. The α_1 terms are used because Hansen (1970) gives $\alpha_1 = 5$, however. In the late 1950s Hansen had suggested using the exponent of 2 for i_q and $i_\gamma = (i_q)^2$. In the interim Vesić had concluded that the exponent should depend somewhat on the L/B (or B/L) ratio, giving the m exponents in Table 4-5*c*, with a lower limiting value of $m = 2$ and an upper limit not much larger than 2. The Vesić values were based in part on published exponents ranging from $2 \leq i_c \leq 5$ to $3 \leq i_q = i_\gamma \leq 5$.

The author suggests that the Hansen (1970) exponents of 5 are too large (using as a guide both the Vesić and the earlier Hansen values). Instead, the following less conservative exponents should be used in the Hansen equations:

$$\text{For } i_q \text{ use exponent} = 2 \text{ to } 3$$
$$\text{For } i_\gamma \text{ use exponent} = 3 \text{ to } 4$$

Using the Inclination Factors

In the general case of inclined loading there is a horizontal component parallel to each base dimension defined as

$$H = H_B \text{ parallel to the } B \text{ dimension}$$

$$\text{For } H_B = 0.0;\ i_{c,B}, i_{q,B}, i_{\gamma,B} \text{ are all } 1.0$$
$$H = H_L \text{ parallel to the } L \text{ dimension}$$
$$\text{For } H_L = 0.0;\ i_{c,L}, i_{q,L}, i_{\gamma,L} \text{ are all } 1.0$$

These H_i values are used to compute inclination factors for the Hansen equation as follows.

1. Compute the inclination factors using the equations given in Table 4-5 and using either the exponent given in that table or the one suggested in the previous paragraph.
2. Use the inclination factors just computed to compute Hansen shape factors as

$$s'_{c,B} = 0.2Bi_{c,B}/L \qquad s'_{c,L} = 0.2Li_{c,L}/B \qquad (\phi = 0 \text{ case})$$
$$s_{c,B} = 1.0 + \frac{N_q}{N_c} \cdot \frac{B'i_{c,B}}{L'} \qquad s_{c,L} = 1.0 + \frac{N_q}{N_c} \cdot \frac{L'i_{c,L}}{B'}$$
$$s_{q,B} = 1 + \sin\phi \cdot B'i_{q,B}/L' \qquad s_{q,L} = 1 + \sin\phi \cdot L'i_{q,L}/B'$$
$$s_{\gamma,L} = 1 - 0.4B'i_{\gamma,B}/L'i_{\gamma,L} \qquad s_{\gamma,L} = 1 - 0.4L'i_{\gamma,L}/B'i_{\gamma,B}$$
$$\text{Limitation: } s_{\gamma,i} \geq 0.6 \text{ (if less than 0.6 use 0.60)}$$

These are used in the following modifications of the "edited" Hansen bearing capacity equation:[3]

$$\left.\begin{aligned} q_{\text{ult}} &= cN_cs_{c,B}d_ci_{c,B} + \bar{q}N_qs_{q,B}d_qi_{q,B} + 0.5\gamma B'N_\gamma s_{\gamma,B}i_{\gamma,B} \\ &\text{or} \\ q_{\text{ult}} &= cN_cs_{c,L}d_ci_{c,L} + \bar{q}N_qs_{q,L}d_qi_{q,L} + 0.5\gamma L'N_\gamma s_{\gamma,L}i_{\gamma,L} \end{aligned}\right\} \qquad (4\text{-}2)$$

Use the smaller value of q_{ult} computed by either of Eqs. (4-2).

The Vesić equation for bearing capacity with inclined loads takes into account the load direction (H_B, H_L) in computing the m exponents for the inclination factors i_i of Table 4-5. The i factors are *not* used in computing the s factors, and Vesić always used the least "actual" lateral dimension as B' in the N_γ term of the general bearing-capacity equation.

Passive Earth Pressure and Bearing Capacity

With a horizontal load component a base must be stable against both sliding and bearing capacity. For sliding, the general equation can be written using partial safety factors SF_i (usually $\text{SF}_i = \text{SF}$) as

$$H_{B \text{ or } L} = \frac{V \tan\delta + c_aB'L'}{\text{SF}_1} + \frac{P_p}{\text{SF}_2} \qquad (4\text{-}3)$$

where all terms except P_p are defined in Table 4-5 or on its figure. The *passive pressure* P_p is defined in Chap. 11. If the passive pressure term is included, the user must decide whether

[3]Include the base b_i and ground g_i factors if applicable. They are not given in the equation for purposes of clarity. Remember that all $d_\gamma = 1.0$.

the full depth from ground surface to base of footing D_f can be relied upon or if only the base depth (footing thickness) D_c should be used to resist sliding. If you elect to use the passive pressure as a component of sliding resistance, the base must be in intimate contact with the soil around the base perimeter. Also, if you use the passive pressure in this manner, you should compute the bearing capacity based on all $d_i = 1.0$ (all depth factors = 1.0).

Example 4-6. You are given the data shown on the sketch of a load test (see Fig. E4-6):

$$H_{L,\text{ult}} = 382 \text{ kN}$$
$$V_{\text{ult}} = 1060 \text{ kN}$$

Required.

a. Find the ultimate bearing capacity by the Hansen method.

b. Find the ultimate bearing capacity by the Vesić method.

Solution. Since we are given $\phi_{\text{tr}} = 43$ and $L'/B' = L/B = 2/0.5 = 4$, use ϕ_{ps}, that is,

$$\phi_{\text{ps}} = 1.1\phi_{\text{tr}} = 1.1(43) = 47.3° \quad \text{[Eq. (2-56)]}$$
$$\phi_{\text{ps}} = 1.5\phi_{\text{tr}} - 17° = 1.5(43) - 17 = 47.5° \quad \text{[Eq. (2-57)]}$$

Use $\phi_{\text{ps}} = 47°$.

(*a*) Hansen's method. Compute the following:

$$N_q = 187 \qquad N_\gamma = 300 \quad \text{(rounding to integers)}$$
$$\text{Also } 2\tan\phi(1 - \sin\phi)^2 = 0.155 \qquad N_q/N_c = 1.078$$

All $b_i = g_i = 1.0$ (not 0.0), since both the base and ground are horizontal. Because $H_B = 0$, we have

$$d_{q,B} = 1 + 2\tan\phi(1 - \sin\phi)^2 D/B = 1 + 0.155(0.5/0.5) = 1.155 \rightarrow \mathbf{1.16}$$
$$d_{q,L} = 1 + 2\tan\phi(1 - \sin\phi)^2 D/L = 1 + 0.155(0.5/2.0) = \mathbf{1.04}$$
$$d_{\gamma,B} = d_{\gamma,L} = 1.00$$

Figure E4-6

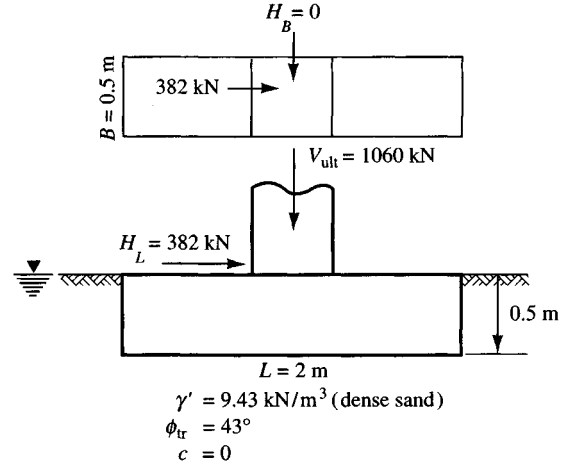

$$i_{q,B} = \left[1 - \frac{0.5H_B}{V + A_f c_a \cot\phi}\right]^{2.5} = \mathbf{1.0} \qquad (H_B = 0 \text{ and using } \alpha_1 = 2.5)$$

$$i_{\gamma,B} = \left[1 - \frac{0.7H_B}{V + A_f c_a \cot\phi}\right]^{3.5} = \mathbf{1.0} \qquad (\beta = \eta = 0 \text{ and using } \alpha_2 = 3.5)$$

$$i_{q,L} = [1 - 0.5H_L/(V + 0)]^{2.5} = [1 - 0.5(382)/1060]^{2.5}$$
$$= \mathbf{0.608} \qquad (\textit{Note}\text{: the } A_f c_a \cot\phi \text{ term} = 0 \text{ since cohesion} = 0.)$$

$$i_{\gamma,L} = \left[1 - \frac{0.7H_L}{V + 0}\right]^{3.5} = [1 - (0.7(382)/1060]^{3.5}$$
$$= 0.7477^{3.5} = \mathbf{0.361}$$

$$s_{q,B} = 1 + \sin\phi(Bi_{q,B}/L) = 1 + \sin 47[0.5(1)/2] = \mathbf{1.18}$$
$$s_{q,L} = 1 + \sin\phi(Li_{q,L}/B) = 1 + \sin 47[2(0.608)/0.5] = \mathbf{2.78}$$

$$s_{\gamma,B} = 1 - 0.4(Bi_{\gamma,B}/Li_{\gamma,L})$$
$$= 1 - 0.4[(0.5 \times 1)/(2 \times 0.361)] = \mathbf{0.723} > 0.6 \qquad \text{(O.K. to use)}$$
$$s_{\gamma,L} = 1 - 0.4(Li_{\gamma,L}/Bi_{\gamma,B})$$
$$= 1 - 0.4[(2 \times 0.361)/(0.5 \times 1)] = 0.422 < 0.6 \quad (\text{use } \mathbf{0.60})$$

Now substitute values into the two equations of Eq. (4-2) (cohesion term not shown to save space and is **0.0** anyway since cohesion $c = 0.0$ kPa):

First Eq. (4-2):

$$q_{ult} = \cancel{cN_c s_{c,B} d_{c,B} i_{c,B}}^{0.0} + \bar{q}N_q s_{q,B} d_{q,B} i_{q,B} + \tfrac{1}{2}\gamma' B N_\gamma s_{\gamma,B} d_{\gamma,B} i_{\gamma,B}$$
$$= 0.5(9.43)(187)(1.18)(1.16)(1)$$
$$+ 0.5(9.43)(0.5)(300)(0.732)(1)(1)$$
$$= 1206.9 + 511.3 = 1718.2 \rightarrow \mathbf{1700} \text{ kPa}$$

Second Eq. (4-2):

$$q_{ult} = \bar{q}N_q s_{q,L} d_{q,L} i_{q,L} + \tfrac{1}{2}\gamma' B' N_\gamma s_{\gamma,L} d_{\gamma,L} i_{\gamma,L} \qquad \text{(again, cohesion term} = 0)$$
$$= 0.5(9.43)(187)(2.78)(1.04)(0.608)$$
$$+ 0.5(9.43)(2.0)(300)(0.60)(1.0)(0.361)$$
$$= 1549.9 + 612.76 = 2162.7 \rightarrow \mathbf{2150} \text{ kPa}$$

Using the smaller computed value, we find the Hansen method seems to give $q_{ult} = 1700$ kPa $\gg$ 1060 kPa of load test.

(*b*) Vesić's method.

$$N_q = 187 \qquad N_\gamma = 404 \qquad \text{all } b_i = g_i = 1.0 \text{ (not 0)}$$
$$B/L = B'/L' = 0.5/2 = 0.25 \qquad D/B' = D/B = 0.5/0.5 = 1.0$$
$$s_q = 1 + \frac{B'}{L'}\tan\phi = 1 + \frac{0.5}{2.0}\tan 47^\circ = \mathbf{1.268} \rightarrow 1.27$$
$$s_\gamma = 1 - 0.4B'/L' = 1 - 0.4(0.25) = \mathbf{0.90} > 0.6 \qquad \text{(O.K.)}$$
$$k = D/B' = 1.0 \qquad L'/B' = 2/0.5 = \mathbf{4.0}$$
$$d_q = 1 + 2\tan\phi(1 - \sin\phi)^2 k = 1 + 0.155(1) = 1.155 \rightarrow \mathbf{1.16}$$

$$d_\gamma = 1.0 \qquad m = \frac{2 + L'/B'}{1 + L'/B'} = \frac{2+4}{1+4} = \frac{6}{5} = \mathbf{1.2}$$

$$i_q = \left[1 - \frac{H_i}{V + A_f c_a \cot\phi}\right]^m = [1 - 382/(1060 + 0)]^{1.2} = \mathbf{0.585}$$

$$i_\gamma = \left[1 - \frac{H_i}{V + A_f c_a \cot\phi}\right]^{m+1} = [1 - 382/(1060 + 0)]^{1.2+1} = \mathbf{0.374}$$

Substitute into the following equation (cohesion term = 0.0 and is not shown):

$$\begin{aligned} q_{\text{ult}} &= \bar{q} N_q s_q d_q i_q + \tfrac{1}{2}\gamma' B' N_\gamma s_\gamma d_\gamma i_\gamma \\ &= 0.5(9.43)(187)(1.27)(1.16)(0.585) + 0.5(9.43)(0.5)(404)(0.9)(1)(0.374) \\ &= 759.9 + 320.6 = 1080.5 \rightarrow \mathbf{1080}\ \text{kPa} \end{aligned}$$

This result compares with the load test pressure $q_{\text{ult}} = 1060\ (= V)$ kPa. Refer also to Probs. 4-6 and 4-7.

You should not conclude from this example that either the Hansen or Vesić equation is better to use. For one thing, a 1° change in ϕ_{tr} will change both results significantly. For important projects one should compute the bearing capacity by at least two methods to verify your result and to make a design recommendation for the allowable soil pressure $q_a = q_{\text{ult}}/\text{SF}$. In many cases the allowable soil pressure is based on settlement considerations rather than on q_{ult}/SF.

////

Example 4-7.

Given. A 2 × 2 m square footing has the ground slope of $\beta = 0$ for the given direction of H_B, but we would use $\beta \approx -80°$ (could use $-90°$) if H_B were reversed along with passive pressure P_P to resist sliding and base geometry shown in Fig. E4-7.

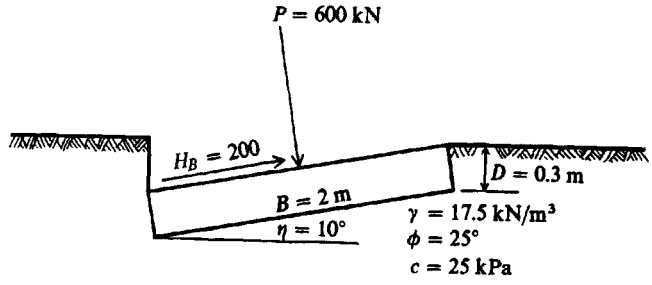

Figure E4-7

Required. Are the footing dimensions adequate for the given loads if we use a safety (or stability) factor SF = 3?

Solution. We may use any of Hansen's, Meyerhof's, or Vesić's equations.

Hansen's method. Initially let us use Hansen's equations (to illustrate further the interrelationship between the i_i and s_i factors).

Assumptions: $\delta = \phi \qquad c_a = c \qquad D = 0.3$ m (smallest value)

$$A_f = B \times L = 2 \times 2 = \mathbf{4}\ \text{m}^2$$

First check sliding safety (and neglect the passive pressure P_P for $D = 0.3$ m on right side)

$$F_{max} = A_f c_a + V \tan\phi = (4)(25) + 600\tan 25 = 379.8 \text{ kN}$$

Sliding stability (or SF) $= F_{max}/H = 379.8/200 = \mathbf{1.90}$ (probably O.K.)

From Table 4-4 (or computer program) obtain the *Hansen* bearing capacity and other factors (for $\phi = 25°$) as

$$N_c = 20.7 \quad N_q = 10.7 \quad N_\gamma = 6.8 \quad N_q/N_c = 0.514$$
$$2\tan\phi(1 - \sin\phi)^2 = 0.311$$

Compute $D/B = D/B' = D/L' = 0.3/2 = \mathbf{0.15}$.

Next compute depth factors d_i:

$$d_\gamma = \mathbf{1.00}$$
$$d_c = 1 + 0.4D/B = 1 + 0.4(0.3/2) = \mathbf{1.06}$$
$$d_q = 1 + 2\tan\phi(1 - \sin\phi)^2(D/B) = 1 + 0.311(0.15) = 1.046 \rightarrow \mathbf{1.05}$$

Compute the inclination factors i_i so we can compute the shape factors:

$$V + A_f c_a \cot\phi = 600 + (2 \times 2)(25)\tan 25 = 600 + 214.4 = 814.4$$

We will use exponents $\alpha_1 = 3$ and $\alpha_2 = 4$ (instead of 5 for both—see text):

$$i_{q,B} = \left[1 - \frac{0.5H_B}{V + A_f c_a \cot\phi}\right]^3 = [1 - 0.5(200)/814.4]^3 = \mathbf{0.675}$$

$$i_{\gamma,B} = \left[1 - \frac{(0.7 - \eta/450°)H_B}{V + A_f c_a \cot\phi}\right]^4 = [1 - (0.7 - 10/450)(200)/814.4]^4$$
$$= [1 - 0.68(200)/814.4]^4 = \mathbf{0.481}$$
$$i_{\gamma,L} = 1.00 \text{ (since } H_L = 0.0)$$

We can now compute $i_{c,B}$ as

$$i_{c,B} = i_q - \frac{1 - i_q}{N_q - 1} = 0.675 - (1 - 0.675)/(10.7 - 1) = \mathbf{0.641}$$

Using the just-computed i factors, we can compute shape factors $s_{i,B}$ as follows. With $H_L = 0.0$ and a square base it is really not necessary to use double subscripts for the several shape and inclination factors, but we will do it here to improve clarity:

$$s_{c,B} = 1 + \frac{N_q}{N_c} \cdot \frac{B' i_{c,B}}{L} = 1 + 0.514[2(0.641)]/2 = \mathbf{1.329}$$

$$s_{q,B} = 1 + \sin\phi\left(\frac{B' i_{q,B}}{L}\right) = 1 + \sin 25°[2(0.675)/2.0] = \mathbf{1.285}$$

$$s_{\gamma,B} = 1 - 0.4\left(\frac{B' i_{\gamma,B}}{L i_{\gamma,L}}\right) = 1 - 0.4[(2 \times 0.481)/(2 \times 1)] = \mathbf{0.808} > 0.60$$

Next we will compute the b_i factors:

$$\eta° = 10° = 0.175 \text{ radians}$$
$$b_{c,B} = 1 - \eta°/147° = 1 - 10/147 = \mathbf{0.93}$$
$$b_{q,B} = \exp(-2\eta\tan\phi) = \exp[-2(.175)(\tan 25)] = \mathbf{0.849}$$
$$b_{\gamma,B} = \exp(-2.7\eta\tan\phi) = e^{-2.7 \times 0.175 \times 0.466} = \mathbf{0.802}$$

We can now substitute into the Hansen equation, noting that with a horizontal ground surface all $g_i = 1$ (not 0):

$$q_{ult} = cN_c s_{c,B} d_{c,B} i_{c,B} b_{c,B} + \bar{q} N_q s_{q,B} d_{q,B} i_{q,B} b_{q,B} + \tfrac{1}{2}\gamma B' N_\gamma s_{\gamma,B} d_{\gamma,B} i_{\gamma,B} b_{\gamma,B}$$

Directly substituting, we have

$$\begin{aligned} q_{ult} &= 25(20.7)(1.329)(1.06)(0.641)(0.93) + \\ &\quad 0.3(17.5)(10.7)(1.285)(1.05)(0.675)(0.849) + \\ &\quad \tfrac{1}{2}(17.5)(2.0)(6.8)(0.808)(1.0)(0.481)(0.802) \\ &= 434.6 + 43.4 + 37.1 = 515.1 \text{ kPa} \end{aligned}$$

For a stability number, or SF, of 3.0,

$$q_a = q_{ult}/3 = 515.1/3 = 171.7 \rightarrow \mathbf{170} \text{ kPa} \qquad \text{(rounding)}$$

$$P_{allow} = A_f \times q_a = (B \times L) q_a = (2 \times 2 \times 170) = 680 \text{ kPa} > 600 \qquad \text{(O.K.)}$$

Vesić method. In using this method note that, with $H_L = 0.0$ and a square footing, it is only necessary to investigate the B direction without double subscripts for the shape, depth, and inclination terms. We may write

$$N_c = 20.7; \qquad N_q = 10.7 \text{ as before but } N_\gamma = 10.9$$

$$N_q/N_c = 0.514 \qquad 2\tan\phi(1 - \sin\phi)^2 = 0.311$$

The Vesić shape factors are

$$s_c = 1 + \frac{N_q}{N_c} \cdot \frac{B'}{L'} = 1 + 0.514(2/2) = \mathbf{1.514}$$

$$s_q = 1 + \frac{B'}{L'} \tan\phi = 1 + (2/2)\tan 25^\circ = \mathbf{1.466}$$

$$s_\gamma = 1 - 0.4\frac{B'}{L'} = 1 - 0.4(1.0) = \mathbf{0.60}$$

All d_i factors are the same as Hansen's, or

$$d_c = \mathbf{1.06} \qquad d_q = \mathbf{1.05} \qquad d_\gamma = \mathbf{1.00}$$

For the Vesić i_i factors, we compute m as

$$m = \frac{2 + B'/L'}{1 + B'/L'}$$

$$= \frac{2 + 2/2}{1 + 2/2} = \frac{3}{2} = \mathbf{1.5}$$

$$V + A_f c_a \cot\phi = 814.4 \text{ kN}; \; H = 200 \text{ kN}$$

$$i_q = \left[1 - \frac{H}{V + A_f c_a \cot\phi}\right]^m = (1 - 200/814.4)^{1.5} = \mathbf{0.655}$$

$$i_\gamma = \left[1 - \frac{H}{V + A_f c_a \cot\phi}\right]^{m+1} = (1 - 200/814.4)^{1.5+1} = \mathbf{0.494}$$

$$i_c = i_q - \frac{1 - i_q}{N_q - 1} = 0.655 - \frac{1 - 0.655}{10.7 - 1} = \mathbf{0.619}$$

The b_i factors are

$$b_c = 1 - \frac{2\beta}{5.14\tan\phi} = \mathbf{1.0} \qquad \text{(since ground slope } \beta = 0\text{)}$$

$$b_q = b_\gamma = (1 - \eta\tan\phi)^2 = (1 - 0.175\tan 25)^2 = \mathbf{0.843}$$

The Vesić equation is

$$q_{ult} = cN_c s_c d_c i_c b_c + \bar{q}N_q s_q d_q i_q b_q + \tfrac{1}{2}\gamma B N_\gamma s_\gamma d_\gamma i_\gamma b_\gamma$$

Directly substituting ($B = 2.0$ m, $\gamma = 17.5$ kN/m^3, and $D = 0.3$ m), we have

$$\begin{aligned} q_{ult} &= 25(20.7)(1.514)(1.06)(0.619)(1.0) + \\ &\quad 0.3(17.5)(10.7)(1.466)(1.05)(0.655)(0.843) + \\ &\quad \tfrac{1}{2}(17.5)(2.0)(10.9)(0.60)(1.0)(0.494)(0.843) \\ &= 514.1 + 47.7 + 47.7 = 609.5 \text{ kPa} \\ q_a &= q_{ult}/3 = 609.5/3 = 203.2 \rightarrow \mathbf{200} \text{ kPa} \end{aligned}$$

There is little difference between the Hansen (170 kPa) and the Vesić (200 kPa) equations. Nevertheless, let us do a confidence check using the Meyerhof equation/method.

Meyerhof method. Note Meyerhof does not have ground g_i or tilted base factors b_i.

$$\phi = 25° > 10° \text{ O.K.} \qquad D/B' = 0.3/2.0 = \mathbf{0.15}$$

$$\sqrt{K_p} = \tan(45° + \phi/2) = \tan 57.5° = \mathbf{1.57}; K_p = \mathbf{2.464}$$

See Meyerhof's equation in Table 4-1 and factors in Table 4-3:

$$s_c = 1.0, s_q = s_\gamma = 1 + 0.1K_p\frac{B}{L} = 1 + 0.1(2.464)(2/2) = \mathbf{1.25}$$

$$d_c = 1 + 0.2\sqrt{K_p}\cdot\frac{D}{B'} = 1 + 0.2(1.57)(0.15) = \mathbf{1.05}$$

$$d_q = d_\gamma = 1 + 0.1\sqrt{K_p}\cdot\frac{D}{B'} = 1 + 0.1(1.57)(0.15) = \mathbf{1.02}$$

Let us define the angle of resultant θ as

$$\theta = \tan^{-1}(H/V) = \tan^{-1}(200/600) = \mathbf{18.4°}$$

Use θ to compute Meyerhof's inclination factors:

$$\begin{aligned} i_c = i_q &= (1 - \theta°/90°)^2 = (1 - 18.4/90)^2 = \mathbf{0.633} \\ i_\gamma &= (1 - \theta/\phi)^2 = (1 - 18.4/25)^2 = 0.0696 \rightarrow \mathbf{0.07} \end{aligned}$$

Using Meyerhof's equation for an inclined load from Table 4-1, we have

$$q_{ult} = cN_c s_c d_c i_c s + \bar{q}N_q s_q d_q i_q + \tfrac{1}{2}\gamma N_\gamma s_\gamma d_\gamma i_\gamma$$

Making a direct substitution (Meyerhof's N_i factors are the same as Hansen's), we write

$$\begin{aligned} q_{ult} &= 25(20.7)(1)(1.05)(0.633) + 0.3(17.5)(10.7)(1.25)(1.02)(0.633) + \\ &\quad \tfrac{1}{2}(17.5)(2.0)(6.8)(1.25)(1.02)(0.07) \\ &= 344.0 + 45.3 + 10.6 = 399.9 \text{ kPa} \end{aligned}$$

The allowable $q_a = q_{ult}/3 = 399.9/3 = 133.3 \rightarrow \mathbf{130}$ kPa.

Terzaghi equation. As an exercise let us also use the Terzaghi equation:

$$N_c = 25.1 \qquad N_q = 12.7 \qquad N_\gamma = 9.7 \qquad \text{(from Table 4-2 at } \phi = 25°\text{)}$$

Also, $s_c = 1.3$ $\quad s_\gamma = 0.8$ $\quad$ (square base).

$$\begin{aligned} q_{\text{ult}} &= cN_c s_c + \overline{q}N_q + \tfrac{1}{2}\gamma B N_\gamma s_\gamma \\ &= (25)(25.1)(1.3) + 0.3(17.5)(12.7) + \tfrac{1}{2}(17.5)(2.0)(9.7)(0.8) \\ &= 815.8 + 66.7 + 135.8 = 1018.3 \rightarrow \mathbf{1018}\ \text{kPa} \\ q_a &= q_{\text{ult}}/3 = 1018/3 = 339 \rightarrow \mathbf{340}\ \text{kPa} \end{aligned}$$

Summary. We can summarize the results of the various methods as follows:

Hansen	170 kPa
Vesić	225
Meyerhof	130
Terzaghi	340

The question is, what to use for q_a? The Hansen-Vesić-Meyerhof average seems most promising and is $q_{a,\text{av}} = (170 + 225 + 130)/3 = \mathbf{175}$ kPa. The author would probably recommend using $q_a = \mathbf{175}$ kPa. This is between the Hansen and Vesić values; Meyerhof's equations tend to be conservative and in many cases may be overly so. Here the Terzaghi and Meyerhof equations are not appropriate, because they were developed for horizontal bases vertically loaded. It is useful to make the Terzaghi computation so that a comparison can be made, particularly since the computations are not difficult.[4]

////

4-7 EFFECT OF WATER TABLE ON BEARING CAPACITY

The *effective* unit weight of the soil is used in the bearing-capacity equations for computing the ultimate capacity. This has already been defined for $\overline{q}$ in the $\overline{q}N_q$ term. A careful inspection of Fig. 4-3 indicates that the wedge term $0.5\gamma BN_\gamma$ also uses the effective unit weight for the soil.

The water table is seldom above the base of the footing, as this would, at the very least, cause construction problems. If it is, however, the $\overline{q}$ term requires adjusting so that the surcharge pressure is an effective value. This computation is a simple one involving computing the pressure at the GWT using that depth and the wet unit weight + pressure from the GWT to the footing base using that depth × effective unit weight γ'. If the water table is at the ground surface, the effective pressure is approximately one-half that with the water table at or below the footing level, since the effective unit weight γ' is approximately one-half the saturated unit weight.

When the water table is below the wedge zone [depth approximately $0.5B\tan(45 + \phi/2)$], the water table effects can be ignored for computing the bearing capacity. When the water table lies within the wedge zone, some small difficulty may be obtained in computing the

[4] A major reason the Terzaghi equation is widely used (and often misused) is that it is much easier to calculate than the other equations.

Terzaghi equation. As an exercise let us also use the Terzaghi equation:

$$N_c = 25.1 \qquad N_q = 12.7 \qquad N_\gamma = 9.7 \qquad \text{(from Table 4-2 at } \phi = 25°\text{)}$$

Also, $s_c = 1.3$ $\quad s_\gamma = 0.8$ $\quad$ (square base).

$$\begin{aligned} q_{ult} &= cN_c s_c + \bar{q}N_q + \tfrac{1}{2}\gamma B N_\gamma s_\gamma \\ &= (25)(25.1)(1.3) + 0.3(17.5)(12.7) + \tfrac{1}{2}(17.5)(2.0)(9.7)(0.8) \\ &= 815.8 + 66.7 + 135.8 = 1018.3 \rightarrow \mathbf{1018}\ \text{kPa} \\ q_a &= q_{ult}/3 = 1018/3 = 339 \rightarrow \mathbf{340}\ \text{kPa} \end{aligned}$$

Summary. We can summarize the results of the various methods as follows:

Hansen	170 kPa
Vesić	225
Meyerhof	130
Terzaghi	340

The question is, what to use for q_a? The Hansen-Vesić-Meyerhof average seems most promising and is $q_{a,av} = (170 + 225 + 130)/3 = \mathbf{175}$ kPa. The author would probably recommend using $q_a = \mathbf{175}$ kPa. This is between the Hansen and Vesić values; Meyerhof's equations tend to be conservative and in many cases may be overly so. Here the Terzaghi and Meyerhof equations are not appropriate, because they were developed for horizontal bases vertically loaded. It is useful to make the Terzaghi computation so that a comparison can be made, particularly since the computations are not difficult.[4]

////

4-7 EFFECT OF WATER TABLE ON BEARING CAPACITY

The *effective* unit weight of the soil is used in the bearing-capacity equations for computing the ultimate capacity. This has already been defined for $\bar{q}$ in the $\bar{q}N_q$ term. A careful inspection of Fig. 4-3 indicates that the wedge term $0.5\gamma B N_\gamma$ also uses the effective unit weight for the soil.

The water table is seldom above the base of the footing, as this would, at the very least, cause construction problems. If it is, however, the $\bar{q}$ term requires adjusting so that the surcharge pressure is an effective value. This computation is a simple one involving computing the pressure at the GWT using that depth and the wet unit weight + pressure from the GWT to the footing base using that depth × effective unit weight γ'. If the water table is at the ground surface, the effective pressure is approximately one-half that with the water table at or below the footing level, since the effective unit weight γ' is approximately one-half the saturated unit weight.

When the water table is below the wedge zone [depth approximately $0.5B\tan(45 + \phi/2)$], the water table effects can be ignored for computing the bearing capacity. When the water table lies within the wedge zone, some small difficulty may be obtained in computing the

[4] A major reason the Terzaghi equation is widely used (and often misused) is that it is much easier to calculate than the other equations.

effective unit weight to use in the $0.5\gamma BN_\gamma$ term. In many cases this term can be ignored for a conservative solution since we saw in Example 4-1 that its contribution is not substantial (see also following Example). In any case, if B is known, one can compute the average effective weight γ_e of the soil in the wedge zone as

$$\gamma_e = (2H - d_w)\frac{d_w}{H^2}\gamma_{\text{wet}} + \frac{\gamma'}{H^2}(H - d_w)^2 \tag{4-4}$$

where $H = 0.5B\tan(45° + \phi/2)$
d_w = depth to water table below base of footing
γ_{wet} = wet unit weight of soil in depth d_w
γ' = submerged unit weight below water table = $\gamma_{\text{sat}} - \gamma_w$

Example 4-8. A square footing that is vertically and concentrically loaded is to be placed on a cohesionless soil as shown in Fig. E4-8. The soil and other data are as shown.

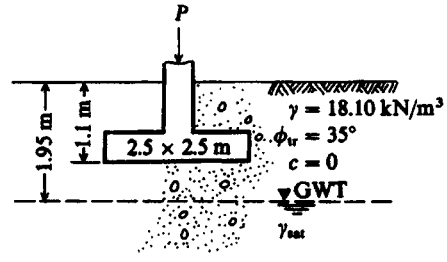

Figure E4-8

Required. What is the allowable bearing capacity using the Hansen equation of Table 4-1 and a SF = 2.0?

Solution. We should note that B would, in general, not be known but would depend on the column load and the allowable soil pressure. We could, however, compute several values of q_a and make a plot of q_a versus B. Here we will compute a single value of q_a.

Step 1. Since the effective soil unit weight is required, let us find these values. Estimate that the "wet" soil has w_N = 10 percent and G_s = 2.68.

$$\gamma_{\text{dry}} = \frac{\gamma_{\text{wet}}}{1 + w} = \frac{18.10}{1 + 0.10} = 16.45 \text{ kN/m}^3$$

$$V_s = \frac{\gamma_{\text{dry}}}{G_s(9.807)} = \frac{16.45}{2.68(9.807)} = 0.626 \text{ m}^3$$

$$V_v = 1.0 - V_s = 1.0 - 0.626 = 0.374 \text{ m}^3$$

The saturated unit weight is the dry weight + weight of water in voids, or

$$\gamma_{\text{sat}} = 16.45 + 0.374(9.807) = 20.12 \text{ kN/m}^3$$

From Fig. E4-8 we obtain d_w = 0.85 m and $H = 0.5B\tan(45° + \phi/2)$ = 2.40 m. Substituting into Eq. (4-4), we have

$$\gamma_e = (2 \times 2.4 - 0.85)\frac{0.85 \times 18.10}{2.4^2} + \frac{20.12 - 9.807}{2.4^2}(2.40 - 0.85)^2$$
$$= 14.85 \text{ kN/m}^3$$

Step 2. Obtain bearing-capacity factors for the Hansen equation using Tables 4-1 and 4-4. Do not compute ϕ_{ps}, since footing is square. For $\phi = 35°$ use program BEARING on your diskette and obtain

$$N_q = 33 \qquad N_\gamma = 34 \qquad 2\tan\phi\cdots = 0.255 \qquad \text{(also in Table 4-4)}$$

$$s_q = 1 + \frac{B'}{L'}\sin\phi = 1.57 \qquad s_\gamma = 1 - 0.4\frac{B'}{L'} = 0.6$$

$$d_q = 1 + 2\tan\cdots\frac{D}{B}$$

$$d_q = 1 + 0.255\frac{1.1}{2.5} = 1.11 \qquad d_\gamma = 1.10$$

From Table 4-1 and dropping any terms that are not used or are 1.0, we have

$$q_{ult} = \gamma D N_q s_q d_q + 0.5\gamma_e B' N_\gamma s_\gamma d_\gamma$$

Substituting values (note γ = soil above base), we see

$$q_{ult} = 1.1(18.10)(33)(1.57)(1.11) + 0.5(14.86)(2.5)(34)(0.6)(1.0)$$
$$= 1145 + 379 = 1524 \text{ kPa}$$

$$q_a = \frac{1524}{2} = \mathbf{762} \text{ kPa (a very large bearing pressure)}$$

It is unlikely that this large a bearing pressure would be allowed—a possible maximum is 500 kPa (about 10 ksf). We might simply neglect the $\gamma_e B N_\gamma$ term to obtain $q_a = 570$ kPa (still large). If the latter term is neglected, the computations are considerably simplified; and doing so has little effect on what would normally be recommended as q_a (around 500 kPa in most cases).

////

4-8 BEARING CAPACITY FOR FOOTINGS ON LAYERED SOILS

It may be necessary to place footings on stratified deposits where the thickness of the top stratum from the base of the footing d_1 is less than the H distance computed as in Fig. 4-2. In this case the rupture zone will extend into the lower layer(s) depending on their thickness and require some modification of q_{ult}. There are three general cases of the footing on a layered soil as follows:

Case 1. Footing on layered clays (all $\phi = 0$) as in Fig. 4-5*a*.
- *a.* Top layer weaker than lower layer ($c_1 < c_2$)
- *b.* Top layer stronger than lower layer ($c_1 > c_2$)

Case 2. Footing on layered ϕ–c soils with *a, b* same as case 1.

Case 3. Footing on layered sand and clay soils as in Fig. 4-5*b*.
- *a.* Sand overlying clay
- *b.* Clay overlying sand

Experimental work to establish methods to obtain q_{ult} for these three cases seems to be based mostly on models—often with $B < 75$ mm. Several analytical methods exist as well, and apparently the first was that of Button (1953), who used a circular arc to search for an approximate minimum, which was found (for the trial circles all in the top layer) to give $N_c = 5.5 < 2\pi$ as was noted in Sec. 4-2.

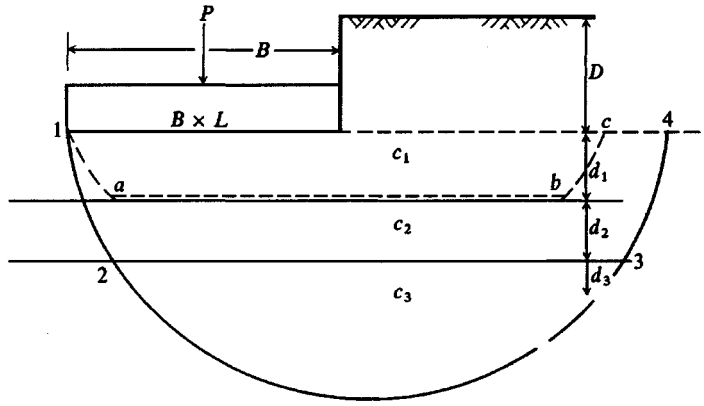

(*a*) Footing on layered clay soil. For very soft c_1 failure may occur along sliding block 1*abc* and not a circular arc and reduce N_c to a value less than 5.14.

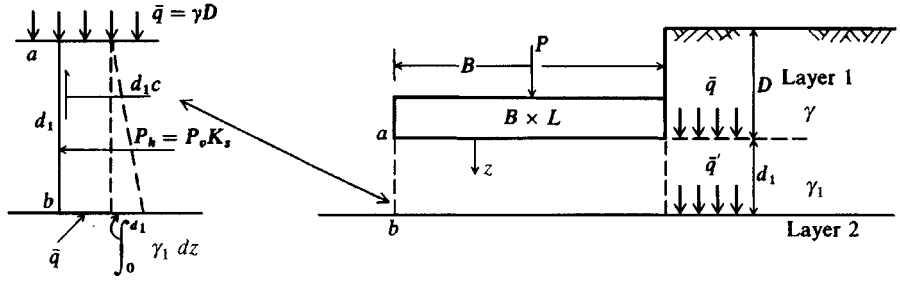

$\bar{q}' = \bar{q} + \gamma_1 d_1$

Figure 4-5 Footings on layered soil.

The use of trial circular arcs can be readily programmed for a computer (see program B-1 on diskette) for two or three layers using s_u for the layers. Note that in most cases the layer s_u will be determined form q_u tests, so the circle method will give reasonably reliable results. It is suggested that circular arcs be limited to cases where the strength ratio $C_R = c_2/c_1$ of the top two layers is on the order of

$$0.6 < C_R \leq 1.3$$

Where C_R is much out of this range there is a large difference in the shear strengths of the two layers, and one might obtain N_c using a method given by Brown and Meyerhof (1969) based on model tests as follows:

For $C_R \leq 1$

$$N_{c,s} = \frac{1.5d_1}{B} + 5.14C_R \qquad \leq 5.14 \qquad \text{(for strip footing)} \tag{4-5}$$

For a circular base with B = diameter

$$N_{c,r} = \frac{3.0d_1}{B} + 6.05C_R \qquad \leq 6.05 \qquad \text{(for round base)} \tag{4-6}$$

When $C_R > 0.7$ reduce the foregoing $N_{c,i}$ by 10 percent.

For $C_R > 1$ compute:

$$N_{1,s} = 4.14 + \frac{0.5B}{d_1} \quad \text{(strip)} \tag{4-7}$$

$$N_{2,s} = 4.14 + \frac{1.1B}{d_1} \tag{4-7a}$$

$$N_{1,r} = 5.05 + \frac{0.33B}{d_1} \quad \text{(round base)} \tag{4-8}$$

$$N_{2,r} = 5.05 + \frac{0.66B}{d_1} \tag{4-8a}$$

In the case of $C_R > 1$ we compute both $N_{1,i}$ and $N_{2,i}$ depending on whether the base is rectangular or round and then compute an averaged value of $N_{c,i}$ as

$$N_{c,i} = \frac{N_{1,i} \cdot N'_{2,i}}{N_{1,i} + N_{2,i}} \cdot 2 \tag{4-9}$$

The preceding equations give the following typical values of $N_{c,i}$, which are used in the bearing-capacity equations of Table 4-1 for N_c.

	C_R = 0.4		2.0		
d_1/B	Strip	Round	$N_{1,s}$	$N_{2,s}$	$N_{c,s}$
0.3	2.50	3.32	5.81	7.81	6.66
0.7	3.10	4.52	4.85	5.71	5.13
1.0	3.55	5.42	4.64	5.24	4.92

When the top layer is very soft with a small d_1/B ratio, one should give consideration either to placing the footing deeper onto the stiff clay or to using some kind of soil improvement method. Model tests indicate that when the top layer is very soft it tends to squeeze out from beneath the base and when it is stiff it tends to "punch" into the lower softer layer [Meyerhof and Brown (1967)]. This result suggests that one should check this case using the procedure of Sec. 4-2 that gave the "lower-bound" solution—that is, if $q_{ult} > 4c_1 + \bar{q}$ of Eq. (*c*) the soil may squeeze from beneath the footing.

Purushothamaraj et al. (1974) claim a solution for a two-layer system with ϕ–c soils and give a number of charts for N_c factors; however, their values do not differ significantly from N_c in Table 4-4. From this observation it is suggested for ϕ–c soils to obtain modified ϕ and c values as follows:

1. Compute the depth $H = 0.5B \tan(45 + \phi/2)$ using ϕ for the top layer.
2. If $H > d_1$ compute the modified value of ϕ for use as[5]

$$\phi' = \frac{d_1\phi_1 + (H - d_1)\phi_2}{H}$$

[5]This procedure can be extended to any number of layers as necessary, and "weighting" may be used.

3. Make a similar computation to obtain c'.
4. Use the bearing-capacity equation (your choice) from Table 4-1 for q_{ult} with ϕ' and c'.

If the top layer is soft (low c and small ϕ) you should check for any squeezing using Eq. (*c*) of Sec. 4-2.

For bases on sand overlying clay or clay overlying sand, first check if the distance H will penetrate into the lower stratum. If $H > d_1$ (refer to Fig. 4-5) you might estimate q_{ult} as follows:

1. Find q_{ult} based on top-stratum soil parameters using an equation from Table 4-1.
2. Assume a punching failure bounded by the base perimeter of dimensions $B \times L$. Here include the $\bar{q}$ contribution from d_1, and compute q'_{ult} of the lower stratum using the base dimension B. You may increase q'_{ult} by a fraction k of the shear resistance on the punch perimeter $(2B + 2L) \times ks_u$ if desired.
3. Compare q_{ult} to q'_{ult} and use the smaller value.

In equation form the preceding steps give the controlling q'_{ult} as

$$q'_{ult} = q''_{ult} + \frac{pP_vK_s \tan\phi}{A_f} + \frac{pd_1c}{A_f} \qquad \leq q_{ult} \tag{4-10}$$

where q_{ult} = bearing capacity of top layer from equations in Table 4-1

q''_{ult} = bearing capacity of lower layer computed as for q_{ult} but also using B = footing dimension, $\bar{q} = \gamma d_1$; c, ϕ of lower layer

p = total perimeter for punching [may use $2(B + L)$ or $\pi \times$ diameter]

P_v = total vertical pressure from footing base to lower soil computed as $\int_0^{d_1} \gamma h\, dh + \bar{q}d_1$

K_s = lateral earth pressure coefficient, which may range from $\tan^2(45 \pm \phi/2)$ or use K_o from Eq. (2-18*a*)

$\tan\phi$ = coefficient of friction between P_vK_s and perimeter shear zone wall

pd_1c = cohesion on perimeter as a force

A_f = area of footing (converts perimeter shear forces to a stress)

This equation is similar to that of Valsangkar and Meyerhof (1979) and applies to all soils.

Note that there will not be many cases of a two- (or three-) layer cohesive soil with clearly delineated strata. Usually the clay gradually transitions from a hard, overconsolidated surface layer to a softer one; however, exceptions may be found, primarily in glacial deposits. In these cases it is a common practice to treat the situation as a single layer with a worst-case s_u value. A layer of sand overlying clay or a layer of clay overlying sand is somewhat more common, and the stratification is usually better defined than for the two-layer clay.

A possible alternative for ϕ–c soils with a number of thin layers is to use average values of c and ϕ in the bearing-capacity equations of Table 4-1 obtained as

$$c_{av} = \frac{c_1H_1 + c_2H_2 + c_3H_3 + \cdots + c_nH_n}{\sum H_i} \tag{a}$$

$$\phi_{av} = \tan^{-1} \frac{H_1 \tan \phi_1 + H_2 \tan \phi_2 + \cdots + H_n \tan \phi_n}{\sum H_i} \qquad (b)$$

where c_i = cohesion in stratum of thickness H_i; c may be 0
ϕ_i = angle of internal friction in stratum of thickness H_i; ϕ may be zero

Any H_i may be multiplied by a weighting factor (1.0 is used in these equations) if desired. The effective shear depth of interest is limited to approximately $0.5B \tan(45° + \phi/2)$. One or two iterations may be required to obtain the best average ϕ–c values, since B is not usually fixed until the bearing capacity is established.

One can use a slope-stability program such as that written by Bowles (1974*a*) to obtain the bearing capacity for layered soils. The program given in that reference has been modified to allow the footing pressure as a surcharge (program B-22). An increase in shear strength with depth could be approximated by addition of "soils" with the same ϕ and γ properties but increased cohesion strength. The ultimate bearing capacity is that value of q_o producing $F = 1$.

Example 4-9. A footing of $B = 3 \times L = 6$ m is to be placed on a two-layer clay deposit as in Fig. E4-9.

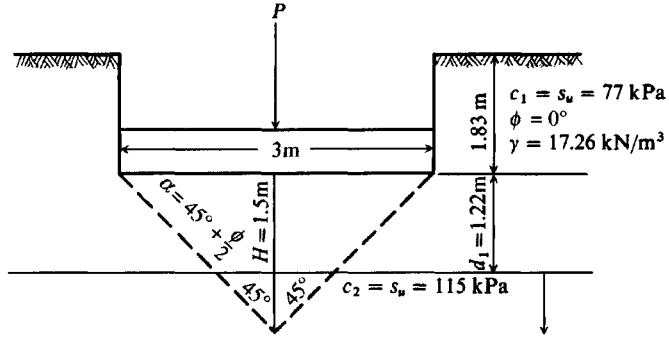

Figure E4-9

Required. Estimate the ultimate bearing capacity.

Solution.

$$H = 0.5B \tan\left(45° + \frac{\phi}{2}\right)$$
$$= 0.5(3) \tan 45 = 1.5 \text{ m}$$
$$C_R = \frac{c_2}{c_1} = \frac{115}{77} = 1.5 > 1.0$$
$$\frac{d_1}{B} = \frac{1.22}{3} = 0.4$$

Using Eqs. (4-7), (4-6*a*), and (4-8), we obtain (similar to table)

$N_{1,s} = 5.39 \qquad N_{2,s} = 6.89$
$N_c = 6.05$ (some larger than 5.14 that would be used for a one-layer soil)

Also

$$s'_c = \frac{0.2B}{L} = 0.2\left(\frac{3}{6}\right) = 0.1$$

$$d'_c = \frac{0.4D}{B} = 0.4\left(\frac{1.83}{3}\right) = 0.24$$

$$s_q = d_q = 1$$

Substituting values into Hansen's equation, we obtain

$$\begin{aligned} q_{ult} &= cN_c(1 + s'_c + d'_c) + \bar{q}N_q s_q d_q \\ &= 77(6.05)(1 + 0.1 + 0.24) + 1.83(17.26)(1)(1) \\ &= 624.2 + 31.5 = 655.7 \text{ kPa} \end{aligned}$$

Squeezing is not likely as d_1 is fairly large compared to H and we are not using an N_c value much larger than that for a one-layer soil.

////

Example 4-10. You are given the soil footing geometry shown in Fig. E4-10. Note that, with the GWT on clay, it would be preferable to keep the footing in sand if possible.

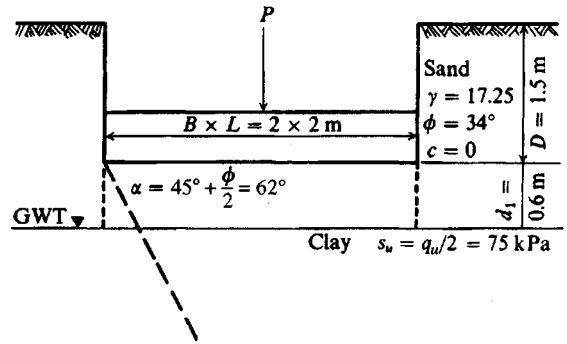

Figure E4-10

Required. What is ultimate bearing capacity and q_a if SF = 2 for sand and 3 for clay?

Solution. We will use Hansen's method. For the sand layer, we have

$$N_q = 29.4 \qquad N_\gamma = 28.7 \qquad \text{(using Table 4-4)}$$

$$s_q = 1 + \tan 34° = 1.67 \qquad s_\gamma = 0.6$$

$$d_q = 1 + 0.262\left(\frac{1.5}{2}\right) = 1.2 \qquad d_\gamma = 1$$

Substituting into Hansen's equation and rounding the N factors (and using $s_u = c = q_u/2 = 75$ kPa), we may write

$$\begin{aligned} q_{ult} &= 1.5(17.25)(29)(1.67)(1.2) + 0.5(17.25)(2)(29)(0.6)(1) \\ &= 1804 \rightarrow \mathbf{1800} \text{ kPa} \end{aligned}$$

For clay, we have

$$N_c = 5.14 \qquad \text{(using Table 4-4)}$$

$$s'_c = 0.2\left(\frac{B}{L}\right) = 0.2\left(\frac{2}{2}\right) = 0.2 \qquad s_q = d_q = 1$$

$$d'_c = 0.4\tan^{-1}\frac{D}{B} = 0.4\tan^{-1}\left(\frac{2.1}{2}\right) = 0.32 \qquad \left(\frac{D}{B} > 1\right)$$

$$q''_{ult} = 5.14(75)(1 + 0.2 + 0.32) + 2.1(17.25)(1)(1)$$
$$= \mathbf{622}\ \text{kPa}$$

Note: This s_u is common for the strength parameter for clay.

Now obtain the punching contribution. For the perimeter shear force on a strip 1 m wide, we write

$$P_v = \bar{q}d_1 + \int_0^{d_1} \gamma h\, dh \qquad \text{(kN/m)}$$

$$P_v = 1.5(17.25)(0.6) + 17.25\frac{h^2}{2}\Big|_0^{0.6}$$
$$= 15.5 + 3.1 = 18.6\ \text{kN/m}$$

Estimate $K_s = K_o = 1 - \sin\phi$ [from Eq. (2-18*a*)] $= 1 - \sin 34° = 0.44$. By inserting values into Eq. (4-10), the revised maximum footing pressure based on the clay soil and including punching is

$$q'_{ult} = q''_{ult} + \frac{pP_vK_s\tan 34°}{A_f} + \frac{pd_1c}{A_f}$$

But cohesion is zero in sand and the perimeter is $2(2 + 2) = 8$ m, so

$$q'_{ult} = 622 + \frac{8(18.6)(0.44)\tan 34°}{2 \times 2} = \mathbf{633}\ \text{kPa} < q_{ult}\ \text{of}\ 1800$$

The maximum footing pressure is controlled by the clay layer, giving $q_{ult} = 634$ kPa. The allowable footing contact soil pressure is

$$q = \frac{633}{3} = \mathbf{211} \qquad \text{(say, 200 kPa)}$$

////

FOOTINGS ON ANISOTROPIC SOIL. This situation primarily occurs in *cohesive* soils where the undrained vertical shear strength $s_{u,v}$ is different (usually larger) from the horizontal shear strength $s_{u,h}$. This is a frequent occurrence in cohesive field deposits but also is found in cohesionless deposits. To account for this situation ($\phi = 0$), Davis and Christian (1971) suggest the following:

When you measure both vertical and horizontal shear strength ($c = s_u$), compute the bearing capacity as

$$q_{ult} = 0.9N_c \cdot \frac{s_{u,v} + s_{u,h}}{2} + \bar{q}'$$

When you only have $s_{u,v}$, compute the bearing capacity as

$$q_{\text{ult}} = 0.85 s_{u,v} N_c + \overline{q'}$$

In these two equations take $N_c = 5.14$ (Hansen's value). You may include Hansen's s_i, d_i, and other factors at your own discretion, *but they were not included* by Davis and Christian (1971).

4-9 BEARING CAPACITY OF FOOTINGS ON SLOPES

A special problem that may be encountered occasionally is that of a footing located on or adjacent to a slope (Fig. 4-6). From the figures it can be seen that the lack of soil on the slope side of the footing will tend to reduce the stability of the footing.

The author developed Table 4-7 using program B-2 on your diskette to solve the footing on or adjacent to a slope as follows:

1. Develop the exit point E for a footing as shown in Fig. 4-6. The angle of the exit is taken as $45° - \phi/2$ since the slope line is a principal plane.
2. Compute a reduced N_c based on the failure surface $ade = L_0$ of Fig. 4-3 and the failure surface $adE = L_1$ of Fig. 4-6*a* to obtain

$$N_c' = N_c \frac{L_1}{L_0}$$

3. Compute a reduced N_q based on the ratio of area *ecfg* (call it A_o) of Fig. 4-3 to the equivalent area $Efg = A_\phi$ of Fig. 4-6*a*, or the alternative $Efgh = A_\phi$ of Fig. 4-6*b*, to obtain the following:

$$N_q' = N_q \frac{A_1}{A_0}$$

Figure 4-6 Footings on or adjacent to a slope.

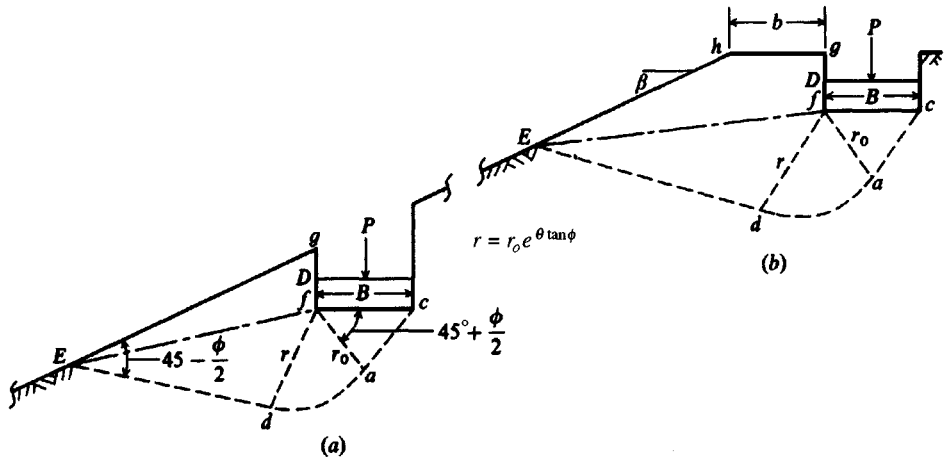

Note that when the distance b of Fig. 4-6*b* is such that $A_1 \geq A_0$ we have $N'_q = N_q$. This distance appears to be about $b/B > 1.5$ (or possibly 2).

4. The overall slope stability should be checked for the effect of the footing load using your favorite slope-stability program or program B-22. At least a few trial circles should touch point c of Fig. 4-6*a,b* as well as other trial entrance points on top of and on the slope.

The ultimate bearing capacity may be computed by any of the equations of Table 4-1; however, the author suggests using the Hansen equation modified to read as follows:

$$q_{ult} = cN'_c s_c i_c + \bar{q}N'_q s_q i_q + \tfrac{1}{2}\gamma B N'_\gamma s_\gamma i_\gamma$$

Obtain the N'_c and N'_q factors from Table 4-7 [or use the included computer program B-2 if interpolation is not desired]. The d_i factors are not included in the foregoing equation since the depth effect is included in the computations of ratios of areas. It will be conservative to use shape factors $s_c = s_q = 1$ (but compute s_γ).

The N_γ factor probably should be adjusted to N'_γ to account for the reduction in passive pressure on the slope side of the wedge *caf* of Fig. 4-6 when the base is either within the $b/B < 2$ zone on top of the slope or when $b/B = 0$. Saran et al. (1989) proposed an analytical solution to account for this reduction; however, the results do not seem adequately conservative and additionally there are too many algebraic manipulations for there to be great confidence in the end result. A simpler solution that compares reasonably well with test results (on models) is as follows:

1. Assume no reduction of N_γ for $b/B \geq 2$ of Fig. 4-6*b*. Use computer program B-2 for D/B and $b/B < 2$, for interpolation is not very accurate, especially for larger ϕ angles.
2. Use the Hansen N_γ factor and adjust as follows:
   a. Compute the Coulomb passive pressure coefficients for the slope angle β using $\beta = (-)$ for one computation and $(+)$ for the other. See Chap. 11 (and use program FFACTOR on furnished diskette). Use the friction angle $\delta = \phi$ for both computations. When you use $\beta = (+ \text{ or } 0)$ you are computing the passive pressure coefficient $K_p = K_{max}$ on the base side away from the slope and when $\beta = (-)$ you are computing $K_p = K_{min}$.
   b. Now using K_{max} and K_{min} compute an R ratio as

$$R = K_{min}/K_{max}$$

   c. Obtain the Hansen value of N_γ from Table 4-4 (or compute it). Now divide by 2 (allow for a contribution of $\frac{1}{2}$ from either side of the wedge *caf* of Fig. 4-6*a* or *b*). The side away from the wedge will contribute the full $\frac{1}{2}$ of N_γ, but the contribution from the slope side will be a fraction depending on the foregoing R ratio and the distance b/B.
   d. Now set up the following:

$$N'_\gamma = \frac{N_\gamma}{2} + \frac{N_\gamma}{2}\left[R + \frac{b}{2B}(1 - R)\right]$$

This equation is easily checked:

$$\text{At } b/2B = 0\text{: } N'_\gamma = N_\gamma/2 + N_\gamma R/2 \quad \text{(on slope)}$$

$$\text{At } b/2B = 2\text{: } N'_\gamma = 2N_\gamma/2 = N_\gamma \quad \text{(top of slope and out of slope influence)}$$

TABLE 4-7

Bearing capacity N'_c, N'_q for footings on or adjacent to a slope

Refer to Fig. 4-4 for variable identification. Base values ($\beta = 0$) may be used when length or area ratios > 1 or when $b/B > 1.5$ to 2.0 (approximate). Values given should cover usual range of footing locations and depths of embedment.

	$D/B = 0$ $b/B = 0$					$D/B = 0.75$ $b/B = 0$					$D/B = 1.50$ $b/B = 0$				
$\beta\downarrow$	$\phi = 0$	10	20	30	40	0	10	20	30	40	0	10	20	30	40
0° $N'_c =$	5.14	8.35	14.83	30.14	75.31	5.14	8.35	14.83	30.14	75.31	5.14	8.25	14.83	30.14	75.31
$N'_q =$	1.03	2.47	6.40	18.40	64.20	1.03	2.47	6.40	18.40	64.20	1.03	2.47	6.40	18.40	64.20
10°	4.89	7.80	13.37	26.80	64.42	5.14	8.35	14.83	30.14	75.31	5.14	8.35	14.83	30.14	75.31
	1.03	2.47	6.40	18.40	64.20	0.92	1.95	4.43	11.16	33.94	1.03	2.47	5.85	14.13	40.81
20°	4.63	7.28	12.39	23.78	55.01	5.14	8.35	14.83	30.14	66.81	5.14	8.35	14.83	30.14	75.31
	1.03	2.47	6.40	18.40	64.20	0.94	1.90	4.11	9.84	28.21	1.03	2.47	5.65	12.93	35.14
25°	4.51	7.02	11.82	22.38	50.80	5.14	8.35	14.83	28.76	62.18	5.14	8.35	14.83	30.14	73.57
	1.03	2.47	6.40	18.40	64.20	0.92	1.82	3.85	9.00	25.09	1.03	2.47	5.39	12.04	31.80
30°	4.38	6.77	11.28	21.05	46.88	5.14	8.35	14.83	27.14	57.76	5.14	8.35	14.83	30.14	68.64
	1.03	2.47	6.40	18.40	64.20	0.88	1.71	3.54	8.08	21.91	1.03	2.47	5.04	10.99	28.33
60°	3.62	5.33	8.33	14.34	28.56	4.70	6.83	10.55	17.85	34.84	5.14	8.34	12.76	21.37	41.12
	1.03	2.47	6.40	18.40	64.20	0.37	0.63	1.17	2.36	5.52	0.62	1.04	1.83	3.52	7.80

	$D/B = 0$			$b/B = 0.75$		$D/B = 0.75$			$b/B = 0.75$		$D/B = 1.50$			$b/B = 0.75$	
$\beta\downarrow$	0	10	20	30	40	0	10	20	30	40	0	10	20	30	40
10°	5.14	8.33	14.34	28.02	66.60	5.14	8.35	14.83	30.14	75.31	5.14	8.35	14.83	30.14	75.31
	1.03	2.47	6.40	18.40	64.20	1.03	2.34	5.34	13.47	40.83	1.03	2.47	6.40	15.79	45.45
20°	5.14	8.31	13.90	26.19	59.31	5.14	8.35	14.83	30.14	71.11	5.14	8.35	14.83	30.14	75.31
	1.03	2.47	6.40	18.40	64.20	1.03	2.47	6.04	14.39	40.88	1.03	2.47	6.40	16.31	43.96
25°	5.14	8.29	13.69	25.36	56.11	5.14	8.35	14.83	30.14	67.49	5.14	8.35	14.83	30.14	75.31
	1.03	2.47	6.40	18.40	64.20	1.03	2.47	6.27	14.56	40.06	1.03	2.47	6.40	16.20	42.35
30°	5.14	8.27	13.49	24.57	53.16	5.14	8.35	14.83	30.14	64.04	5.14	8.35	14.83	30.14	74.92
	1.03	2.47	6.40	18.40	64.20	1.03	2.47	6.40	14.52	38.72	1.03	2.47	6.40	15.85	40.23
60°	5.14	7.94	12.17	20.43	39.44	5.14	8.35	14.38	23.94	45.72	5.14	8.35	14.83	27.46	52.00
	1.03	2.47	6.40	18.40	64.20	1.03	2.47	5.14	10.05	22.56	1.03	2.47	4.97	9.41	20.33
	$D/B = 0$			$b/B = 1.50$		$D/B = 0.75$			$b/B = 1.50$		$D/B = 1.50$			$b/B = 1.50$	
10°	5.14	8.35	14.83	29.24	68.78	5.14	8.35	14.83	30.14	75.31	5.14	8.35	14.83	30.14	75.31
	1.03	2.47	6.40	18.40	64.20	1.03	2.47	6.01	15.39	47.09	1.03	2.47	6.40	17.26	49.77
20°	5.14	8.35	14.83	28.59	63.60	5.14	8.35	14.83	30.14	75.31	5.14	8.35	14.83	30.14	75.31
	1.03	2.47	6.40	18.40	64.20	1.03	2.47	6.40	18.40	53.21	1.03	2.47	6.40	18.40	52.58
25°	5.14	8.35	14.83	28.33	61.41	5.14	8.35	14.83	30.14	72.80	5.14	8.35	14.83	30.14	75.31
	1.03	2.47	6.40	18.40	64.20	1.03	2.47	6.40	18.40	55.20	1.03	2.47	6.40	18.40	52.97
30°	5.14	8.35	14.83	28.09	59.44	5.14	8.35	14.83	30.14	70.32	5.14	8.35	14.83	30.14	75.31
	1.03	2.47	6.40	18.40	64.20	1.03	2.47	6.40	18.40	56.41	1.03	2.47	6.40	18.40	52.63
60°	5.14	8.35	14.83	26.52	50.32	5.14	8.35	14.83	30.03	56.60	5.14	8.35	14.83	30.14	62.88
	1.03	2.47	6.40	18.40	64.20	1.03	2.47	6.40	18.40	46.18	1.03	2.47	6.40	16.72	36.17

One should not adjust ϕ_{tr} to ϕ_{ps}, as there are considerable uncertainties in the stress state when there is loss of soil support on one side of the base, even for strip (or long) bases.

The use of these factors and method will be illustrated in Example 4-11, which is based on (and compared with) load tests from the cited source.

Example 4-11.

Given. Data from a strip footing load test for a base located on the top of a slope [from Shields et al. (1977)]. Other data are as follows:

Slope β = 26.5° (1 on 2) and "compact" sand
ϕ_{tr} = 36° (estimated from the author's interpretation of the reference figure of ϕ vs. σ_3 (the confining pressure)
c = 0 (no cohesion)
γ = 14.85 kN/m^3 (effective value and not very dense)

Consider two test cases:

Case I: $b/B = 0.75$ $D/B = 1.50$
Case II: $b/B = 1.50$ $D/B = 0.0$

Required. Compare the author's suggested method with Shield's test curves. Also for Case II compare the author's method with Hansen's method using the ground factor g_i.

Solution.

Case I:

(*a*) *By Shields' method.*

$$q_{ult} = cN_c + \tfrac{1}{2}\gamma B N_{\gamma q} \qquad \text{(but } c = 0\text{)}$$

From curves, obtain

$$N_{\gamma q} \approx 120 \qquad \text{[Fig. 11 of Shields et al. (1977)]}$$

and

$$q_{ult} = \tfrac{1}{2}(14.85)B(120) = \mathbf{891}B$$

(*b*) *By Table 4-7 and using Hansen's N'_γ.* We will not adjust ϕ_{tr} to ϕ_{ps} for reasons stated earlier in this section. For a strip base all $s_i = 1.0$. Also here, since $H_i = 0$, all $i_i = 1.0$; because the base is horizontal, $b_i = 1$; and we take $g_i = 1$ since this method already accounts for the slope angle β.

From side computations of Chap. 11 (using program FFACTOR) obtain the Coulomb earth pressure coefficients (using $\phi = 36°$, $\delta = 36°$, vertical wall, $\alpha = 90°$) as

$$K_{max} = 128.2 \quad (\beta = 26.5°) \qquad K_{min} = 2.8 \quad (\beta = -26.5°)$$

$$R = K_{min}/K_{max} = 2.8/128.2 = 0.022 \qquad 1.000 - R = 0.978$$

N_γ = 40.0 and (refer to step *d* given just before this Example)

$$N'_\gamma = \frac{40}{2} + \frac{40}{2}\left[0.022 + \frac{b}{2B}(0.978)\right]$$

$$= 20 + 20\left[0.022 + \frac{0.75}{2}(0.978)\right] = 20 + 20(0.388)$$

$$= 27.8 \rightarrow \mathbf{28} \text{ (and is less than 40 as expected)}$$

At $b/B = 1.5$ (which we will use for Case II), we compute

$$N'_\gamma = 20 + 20(0.756) = \mathbf{35} \qquad \text{(rounded)}$$

For Case I Bowles' method gives

$$q_{ult} = \bar{q}N'_q + \tfrac{1}{2}\gamma BN'_\gamma \qquad (D/B = 1.5, \text{ so } D = 1.5B)$$

$$\text{Also } N'_q = \mathbf{27} \qquad \text{[rounded and using program B-2 (or Table 4-7)]}$$

$$q_{ult} = 14.85(1.5B)(27) + \tfrac{1}{2}(14.85)(B)(28)$$

$$= 601B + 207B = \mathbf{808}B < 891B \text{ kPa}$$

This result compares reasonably well to (within 10 percent) the $891B$ actually measured.

Case II Let $D/B = 0.0$ (base on surface; $\bar{q} = 0$) and $b/B = 1.5$ from edge of slope. From Shields et al. (1977) we obtain approximately

$$q_{ult} = \tfrac{1}{2}(14.85)B(35) = \mathbf{260}B \text{ kPa}$$

By Bowles' method and noting $N'_q = 27$ as before and $N'_\gamma = 35$, we obtain

$$q_{ult} = \cancel{14.85(0B)}(27) + \tfrac{1}{2}(14.85)(B)(35) = 259.9B \rightarrow \mathbf{260}B \text{ kPa}$$

By Hansen's method only the $\frac{1}{2}\gamma BN_\gamma g_\gamma$ term applies (since $c = \bar{q} = 0$), so

$$g_\gamma = (1 - 0.5\tan\beta)^5 = (1 - 0.5\tan 26.5°)^5 = 0.238$$

Directly substituting, we find

$$q_{ult} = 0 + 0 + \tfrac{1}{2}(14.85)B(35)(1)(1)(0.238) = \mathbf{61.8} \text{ kPa}$$

Inspection of the Vesić computation for g_γ gives $g_\gamma = 0.251 > 0.238$.

These computations indicate that Bowles' method appears to give the best solution based on the limited load-test data available. Both the Hansen and Vesić methods appear too conservative but were all that was available at the time they were proposed. Keep in mind that most real slopes exist in soils with both c and ϕ and not just sand, as in the model test used here for confirmation of methodology. In any case the use of a sand model has severely tested the several methods.

////

4-10 BEARING CAPACITY FROM SPT

The SPT is widely used to obtain the bearing capacity of soils directly. One of the earliest published relationships was that of Terzaghi and Peck (1967). This has been widely used, but an accumulation of field observations has shown these curves to be overly conservative. Meyerhof (1956, 1974) published equations for computing the allowable bearing capacity for a 25-mm settlement. These could be used to produce curves similar to those of Terzaghi and Peck and thus were also very conservative. Considering the accumulation of field observations and the stated opinions of the authors and others, this author adjusted the Meyerhof equations for an approximate 50 percent increase in allowable bearing capacity to obtain the following:

$$q_a = \frac{N}{F_1}K_d \qquad B \le F_4 \tag{4-11}$$

$$q_a = \frac{N}{F_2}\left(\frac{B + F_3}{B}\right)^2 K_d \qquad B > F_4 \tag{4-12}$$

where q_a = allowable bearing pressure for ΔH_o = 25-mm or 1-in. settlement, kPa or ksf
$K_d = 1 + 0.33\frac{D}{B} \leq 1.33$ [as suggested by Meyerhof (1965)]

F factors as follows:

	N_{55}		N'_{70}	
	SI	**Fps**	**SI**	**Fps**
F_1	0.05	2.5	0.04	2.0
F_2	0.08	4	0.06	3.2
F_3	0.3	1	Same	Same
F_4	1.2	4		

These equations have been in existence for quite some time and are based primarily on N values from the early 1960s back and, thus, $\mathbf{E}_r$ is likely on the order of 50 to 55 and not 70^+ as suggested in Sec. 3-7. Since lower $\mathbf{E}_r$ produces higher blow counts N if the preceding equations are standardized to N'_{70}, we must use revised values for factors F_1 and F_2 as shown in the table of F factors. Summarizing, use the left values under N_{55} and the given F factors, or standardize N to N'_{70} and use the right columns of F factors in Eqs. (4-11), (4-12), and (4-13). Figure 4-7 is a plot of Eqs. (4-11) and (4-12) based on $\cong N_{55}$.

In these equations N is the statistical average value for the footing influence zone of about $0.5B$ above footing base to at least $2B$ below. If there are consistently low values of N below this zone, settlements may be troublesome if N is not reduced somewhat to reflect this event. Figure E4-12 is a method of presenting q_a versus N for design office use.

We note in these equations that footing width is a significant parameter. Obviously if the depth of influence is on the order of $2B$ a larger footing width will affect the soil to a greater depth and strains integrated over a greater depth will produce a larger settlement. This is taken into account somewhat for mats, which were considered also by Meyerhof (and adjusted by the author for a 50 percent increase) to obtain

$$q_a = \frac{N}{F_2} K_d \tag{4-13}$$

In these equations the allowable soil pressure is for an assumed 25-mm settlement. In general the allowable pressure for any settlement ΔH_j is

$$q'_a = \frac{\Delta H_j}{\Delta H_o} q_a \tag{4-14}$$

where ΔH_o = 25 mm for SI and 1 in. for Fps. ΔH_j is the actual settlement that can be tolerated, in millimeters or inches. On a large series of spread footings on sand D'Appolonia et al. (1968) found that use of the Meyerhof equations (4-11) and (4-12) when N_{55} was corrected using C_N of Eq. (3-3) predicted settlements very well. The sand involved, however, was either overconsolidated or compacted to a very dense state. This soil state should have produced somewhat higher blow counts (or N-values) than for a less dense state.

Parry (1977) proposed computing the allowable bearing capacity of *cohesionless* soils as

$$q_a = 30N_{55} \quad \text{(kPa)} \qquad (D \leq B) \tag{4-15}$$

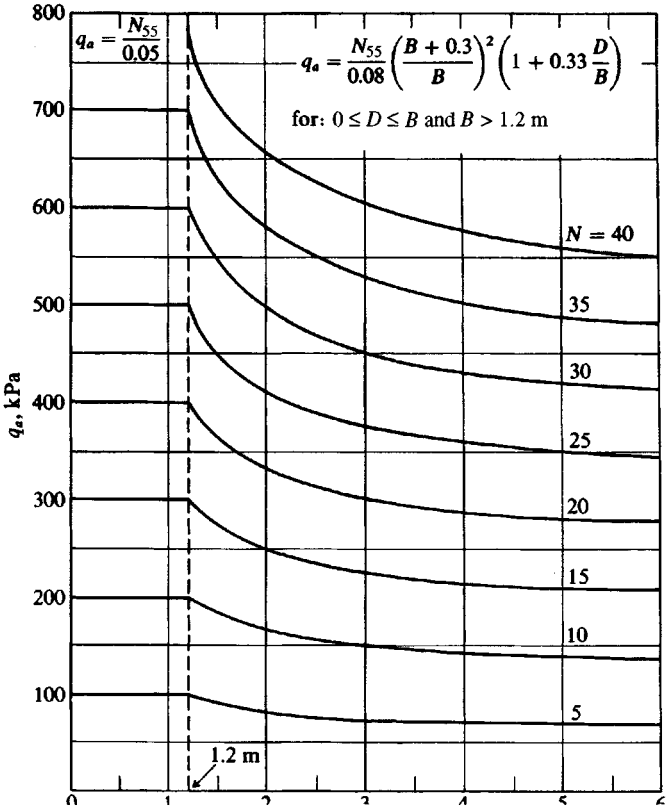

Figure 4-7 Allowable bearing capacity for **surface-loaded** footings with settlement limited to approximately 25 mm. Equation used is shown on figure.

Example.
Use chart to find q_a

$$N_{70} = 24$$

Footing depth $D = 1$ m
Footing width $B = 3$ m

Solution. $F_3 = 0.3$

$F_2 = 0.08$

$N_{55} = 24 \times 70/55 \sim \mathbf{30} > 24$

At ground surface:
(refer to chart)

$$q_a = \frac{30}{0.08}\left(\frac{3+0.3}{3}\right)^2 \sim \mathbf{450}\ \text{kPa}$$

At $D = 1$ m :
$K_d = 1 + 0.33(1/3) = 1.11$
$q_a = 450 \times K_d = 450 \times 1.11 \sim \mathbf{500}$ kPa

where N_{55} is the average SPT value at a depth about $0.75B$ below the proposed base of the footing. The allowable bearing pressure q_a is computed for settlement checking as

$$q_a = \frac{N_{55}}{15B} \quad \text{(kPa)} \qquad \text{(for a } \Delta H_o = 20 \text{ mm)} \tag{4-15a}$$

Use a linear ratio ($\Delta H/20$) to obtain q_a for settlements $\Delta H \neq 20$ mm (B is in meters, q_a in kPa). Use the smaller of the computed values from Eqs. (4-15) and (4-15*a*) for design.

Equation (4.15) was based on back-computing N_q and N_γ using an angle of internal friction ϕ based on N_{55} as

$$\phi = 25 + 28\left(\frac{N_{55}}{\bar{q}}\right)^{1/2} \tag{4-16}$$

Here $\bar{q}$ is the effective overburden pressure at the location of the average N_{55} count. The footing depth D must be such that there is an overburden ($\bar{q}N_q$) term.

Example 4-12

Given. The average N'_{70} blow count = 6 in the effective zone for a footing located at D = 1.6 m (blow count average in range from 1- to 4-m depth).

Required. What is the allowable bearing capacity for a 40-mm settlement? Present data as a curve of q_a versus B.

Solution. From Table 3-4 we can see D_r is small, soil is "loose," and settlement may be a problem. Should one put a footing on loose sand or should it be densified first?

Program Eqs. (4-12)–(4-14) with $F_2 = 0.06$ and $F_3 = 0.30$ (including K_d) on a programmable calculator or personal computer and obtain the following table, which is plotted as Fig. E4-12. Note $q'_a = q_a(40/25)$.

ΔH = 25		40 mm
B, m	q_a, kPa	q_a, kPa
1.5 > 1.2	192	310
2	167	267
3	142	228
4	131	209
5	124	199
6	120	192
10	112	179

For final design round q_a to multiples of 25 kPa.

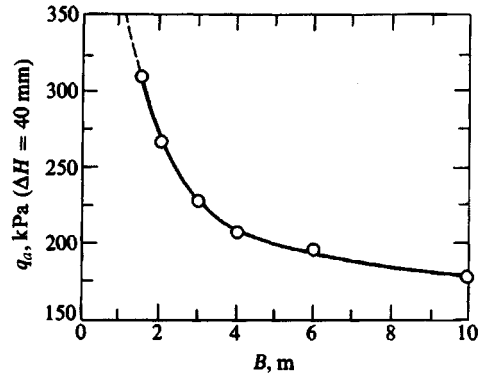

Figure E4-12

////

4-11 BEARING CAPACITY USING THE CONE PENETRATION TEST (CPT)

The bearing capacity factors for use in the Terzaghi bearing-capacity equation of Table 4-1 can be estimated [see Schmertmann (1978)] as

$$0.8N_q \cong 0.8N_\gamma \cong q_c \tag{4-17}$$

where q_c is averaged over the depth interval from about $B/2$ above to $1.1B$ below the footing base. This approximation should be applicable for $D/B \leq 1.5$. For cohesionless soils one may use

$$\text{Strip} \quad q_{ult} = 28 - 0.0052(300 - q_c)^{1.5} \quad (\text{kg/cm}^2) \tag{4-18}$$

$$\text{Square} \quad q_{ult} = 48 - 0.009(300 - q_c)^{1.5} \quad (\text{kg/cm}^2) \tag{4-18a}$$

For clay one may use

$$\text{Strip} \quad q_{ult} = 2 + 0.28q_c \quad (\text{kg/cm}^2) \tag{4-19}$$

$$\text{Square} \quad q_{ult} = 5 + 0.34q_c \quad (\text{kg/cm}^2) \tag{4-19a}$$

Equations (4-18) through (4-19*a*) are based on charts given by Schmertmann (1978) credited to an unpublished reference by Awakti.

According to Meyerhof (1956) the allowable bearing capacity of sand can be computed using Eqs. (4-11) and (4-12), making a substitution for q_c as

$$N_{55} \cong \frac{q_c}{4} \tag{4-20}$$

and with q_c in units of kg/cm^2. If q_c is in units other than kg/cm^2($\cong$ tsf) you must convert to these units prior to using Eq. (4-20). Note also that making the foregoing conversion of q_c to N_{55} to use Eqs. (4-11) and (4-12) adjusts the original Meyerhof recommendations to a 50 percent increase of the allowable bearing capacity as similarly done for directly obtained SPT N values.

It is evident that one can use the CPT correlations of Sec. 3-11 to obtain ϕ or s_u so that the bearing capacity equations of Table 4-1 can be used more directly.

4-12 BEARING CAPACITY FROM FIELD LOAD TESTS

Obviously the most reliable method of obtaining the ultimate bearing capacity at a site is to perform a load test. This would directly give the bearing capacity if the load test is on a full-size footing; however, this is not usually done since an enormous load would have to be applied. Such a load could be developed from two piles driven into the ground with a very large girder spanning between them so a hydraulic jack could be placed on the footing to jack against the girder for the footing load. This is very costly as one consideration; another factor is that the bearing capacity obtained is for that size only and if there is more than one size then additional tests would be required. For the test just described the cost could be very high.

4-12.1 Standard Method

The usual practice is to load-test small steel plates (although one could also pour small concrete footings, which would be troublesome to remove if that location were needed for other purposes) of diameters from 0.3 to 0.75 m or squares of side 0.3 × 0.3 and perhaps 0.6 × 0.6 m. These sizes are usually too small to extrapolate to full-size footings, which may be 1.5 to 4 or 5 m^2. Several factors cause the extrapolation to be questionable:

1. The significant influence depth of approximately $4B$ is substantially different for the model-versus-prototype footing. Any stratification below the H depth of Fig. 4-2 or Fig. 4-3*b* has minimal effect on the model but may be a major influence on the full-size footing.
2. The soil at greater depths has more overburden pressure acting to confine the soil so it is effectively "stiffer" than the near-surface soils. This markedly affects the load-settlement response used to define q_{ult}.
3. Previous discussion has noted that as B increases there is a tendency to a nonlinear increase in q_{ult}. It develops that for small models of say, 0.3, 0.45, and 0.6 m, the plot of B versus q_{ult} is nearly linear (as it is for using two sizes of, say, 2 m and 2.5 m). It takes a larger range of sizes to develop the nonlinear curve for that soil deposit.

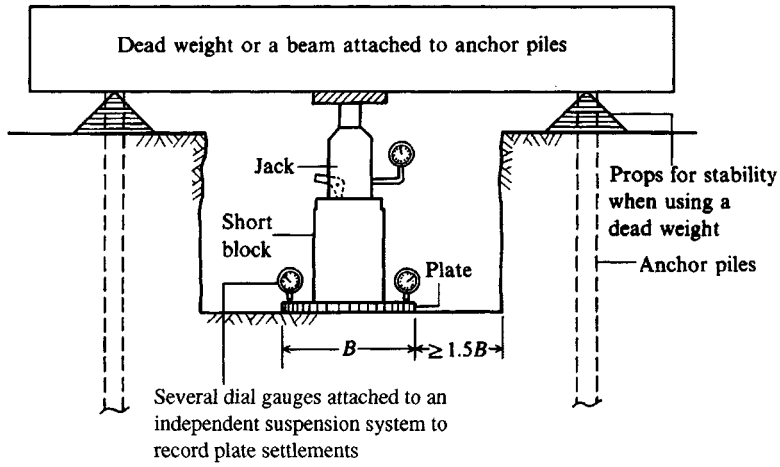

Figure 4-8 Plate-load testing. The method of performing this test is outlined in some detail in ASTM D 1194.

In spite of these major shortcomings, load tests are occasionally used. The procedure has been standardized as ASTM D 1194, which is essentially as follows:

1. Decide on the type of load application. If it is to be a reaction against piles, they should be driven or installed first to avoid excessive vibration and loosening of the soil in the excavation where the load test will be performed.
2. Excavate a pit to the depth the test is to be performed. The test pit should be at least four times as wide as the plate and to the depth the foundation is to be placed. If it is specified that three sizes of plates are to be used for the test, the pit should be large enough so that there is an available spacing between tests of $3D$ of the largest plate.
3. A load is placed on the plate, and settlements are recorded from a dial gauge accurate to 0.25 mm. Observations on a load increment should be taken until the rate of settlement is beyond the capacity of the dial gauge. Load increments should be approximately one-fifth of the estimated bearing capacity of the soil. Time intervals of loading should not be less than 1 h and should be approximately of the same duration for all the load increments.
4. The test should continue until a total settlement of 25 mm is obtained, or until the capacity of the testing apparatus is reached. After the load is released, the elastic rebound of the soil should be recorded for a period of time at least equal to the time duration of a load increment.

Figure 4-8 presents the essential features of the load test. Figure 4-9*a* is a typical semilog plot of time versus settlement (as for the consolidation test) so that when the slope is approximately horizontal the maximum settlement for that load can be obtained as a point on the load-versus-settlement curve of Fig. 4-9*b*. Where the load-versus-settlement approaches the vertical, one interpolates q_{ult}. Sometimes, however, q_{ult} is obtained as that value corresponding to a specified displacement (as, say, 25 mm).

Extrapolating load-test results to full-size footings is not standard. For clay soils it is common to note that the BN_γ term is zero, so that one *might* say that q_{ult} is independent of footing

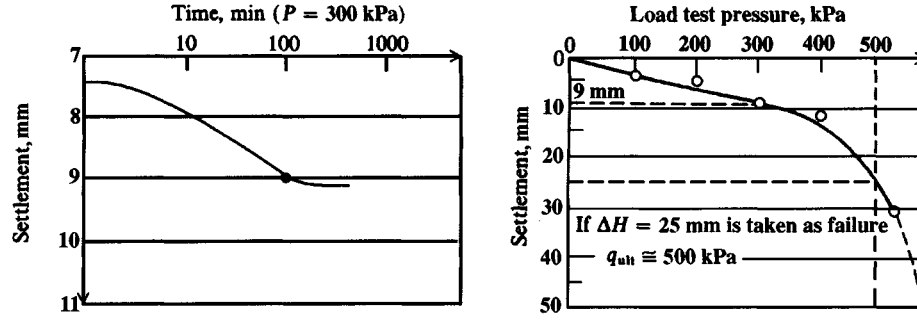

a) Plot of settlement vs. log time to determine the maximum settlement for a load increment (300 kPa in this case)

b) Load vs. settlement plot to establish the maximum design pressure.

Figure 4-9 Plate load test data.

size, giving

$$q_{\text{ult,foundation}} = q_{\text{ult,load test}}$$

In cohesionless (and ϕ–c) soils all three terms of the bearing-capacity equation apply and, noting that the N_γ term includes the footing width, one *might* say

$$q_{\text{ult,foundation}} = M + N\frac{B_{\text{foundation}}}{B_{\text{load test}}}$$

where M includes the N_c and N_q terms and N is the N_γ term. By using several sizes of plates this equation can be solved graphically for q_{ult}. Practically, for extrapolating plate-load tests for sands (which are often in a configuration so that the N_q term is negligible), use the following

$$q_{\text{ult}} = q_{\text{plate}}\left(\frac{B_{\text{foundation}}}{B_{\text{plate}}}\right) \tag{4-21}$$

The use of this equation is not recommended unless the $B_{\text{foundation}}/B_{\text{plate}}$ is not much more than about 3. When the ratio is 6 to 15 or more the extrapolation from a plate-load test is little more than a guess that could be obtained at least as reliably using an SPT or CPT correlation.

4-12.2 Housel's Method for Bearing Capacity from Plate-Load Tests

Housel (1929) and Williams (1929) both[6] gave an equation for using at least two plate-load tests to obtain an allowable load P_s for some settlement as

$$P_s = Aq_1 + pq_2 \qquad \text{(kPa or ksf)} \tag{4-22}$$

[6]Housel is generally given credit for this equation; however, when Williams presented it no credit was given, so the equation may have been proposed simultaneously by both persons.

where A = area of plate used for the load test, m^2 or ft^2
p = perimeter of load-test plate, m or ft
q_1 = bearing pressure of interior zone of plate, kPa or ksf
q_2 = edge shear of plate, kN/m or k/ft

Equation (4-22) is used as follows:

1. Perform two or more load tests using plates with different A and p. Plot curves of either load P or bearing pressure q versus settlement ΔH.
2. At the desired settlement obtain from these plots the load P_s ($= q \cdot A$ if the plot is pressure q versus settlement ΔH). One possible set of values is at $\frac{1}{2}P_{ult}$; however, values at plate settlements of 6, 10, or 15 mm might also be used.
3. Using P_s, plate area, and perimeter solve Eq. (4-22) for q_1, q_2. For more than two tests make as many solutions as possible and average the results for q_1, q_2.

For example, consider these data:

Test #	B, m	A, m^2	p, m	P_s, kN
1	0.45	$0.45^2 = 0.2025$	$4 \times .45 = 1.8$	30.4
2	0.60	$0.60^2 = 0.3600$	$4 \times .60 = 2.4$	45.1

which give

$$0.2025q_1 + 1.8q_2 = 30.4$$
$$0.3600q_1 + 2.4q_2 = 45.1$$

On solving, we obtain $q_1 = 50.83$ kPa and $q_2 = 11.17$ kN/m.

It is now necessary to solve by trial to find footing dimensions for a given design load. The following illustrates the approach.

The allowable P_a for a base that is 3×3 m is

$$P_a = (3\times3)50.83 + (4\times3)11.17 = \mathbf{591.5}\text{ kN}$$

If the design load $P_d \approx 591.5$ kN, use this trial B. If the design load is less, use a smaller B and make another trial computation, etc., until the computed footing load has converged within reasonable limits. Remember that your selection of the P_s values has approximately set the settlement for that base of dimension B.

This method is generally called *Housel's method.* It was widely used until the early 1950s even though Terzaghi (1929) did not approve of it and did not even mention it in Terzaghi (1943), where the *Terzaghi bearing-capacity method* was first introduced.

4-13 BEARING CAPACITY OF FOUNDATIONS WITH UPLIFT OR TENSION FORCES

Footings in industrial applications—such as for the legs of elevated water tanks, anchorages for the anchor cables of transmission towers, and bases for legs of power transmission

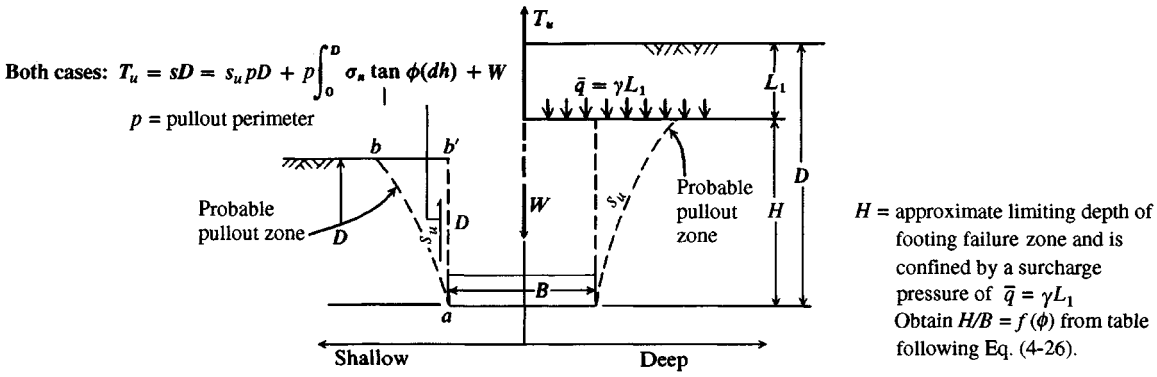

Figure 4-10 Footings for tension loads.

towers—and in a number of industrial equipment installations are subjected to uplift or tension forces. Uplift may be the principal mode of resistance or may be among several possible load combinations. Drilled shafts, with or without enlarged bases, are most commonly used to resist uplift because they are more economical to install. The analysis of these members will be considered in Sec. 16-14.

Footings to develop tension resistance are idealized in Fig. 4-10. Balla (1961) considered this problem. He assumed a failure surface (the dashed line *ab* in Fig. 4-10) as circular and developed some highly complicated mathematical expressions that were verified on model tests in a small glass jar and by some larger tests of others. The only footings he considered were circular. Meyerhof and Adams (1968) also considered the problem and proposed the conditions of Fig. 4-10, namely, that footings should be considered as either shallow or deep since deep footings could develop only to some limiting pull-out force. Circular and rectangular footings were considered and in both cohesive and cohesionless soils. They compared the theory (following equations) with models as well as full-scale tests on circular footings and found considerable scatter; however, with a factor of safety of 2 to 2.5 these equations should be satisfactory.

The following equations are developed by neglecting the larger pull-out zone observed in the tests (as *ab* of Fig. 4-10) and using an approximation of shear resistance along line *ab'*. Shape factors are used together with a limiting depth ratio *D/B* or *H/B* to make the simplified equations adequate for design use. In the general case we have for the ultimate tension

$$T_u = \text{Perimeter resistance, } s_u pD + \text{Base weight } W$$

with adjustments for depth and shape (whether perimeter is round or rectangular). This equation gives (***only for footings in sands***) the following:

For shallow footings

Round:
$$T_u = \pi B s_u D + s_f \pi B \gamma \left(\frac{D^2}{2}\right) K_u \tan\phi + W \tag{4-23}$$

Rectangular:
$$T_u = 2s_u D(B + L) + \gamma D^2(2s_f B + L - B)K_u \tan\phi + W \tag{4-24}$$

where the side friction adjustment factor $s_f = 1 + mD/B$.

For deep footings (base depth $D > H$)

Round: $$T_u = \pi s_u BH + s_f \pi B\gamma(2D - H)\left(\frac{H}{2}\right)K_u \tan\phi + W \tag{4-25}$$

Rectangular: $$T_u = 2s_u H(B + L) + \gamma(2D - H)(2s_f B + L - B)HK_u \tan\phi + W \tag{4-26}$$

where $s_f = 1 + mH/B$.

For footing shape

Round: B = diameter

Square: $L = B$

Rectangular: use B and L

Obtain shape factor s_f, ratios m and H/B [all $f(\phi)$] from the following table—interpolate as necessary:

		ϕ						
ϕ =		20°	25°	30°	35°	40°	45°	48°
Limiting	H/B	2.5	3	4	5	7	9	11
	m	0.05	0.10	0.15	0.25	0.35	0.50	0.60
Maximum	s_f	1.12	1.30	1.60	2.25	4.45	5.50	7.60

For example: $\phi = 20°$ so obtain $s_f = 1.12$, $m = 0.05$, and $H/B = 2.5$. Therefore, $H = 2.5B$, and total footing depth to be a "deep" footing $D > 2.5B$. If $B = 1$ m, D of Fig. 4-10 must be greater than 2.5 m, or else use "shallow footing" equations [Eqs. (4-23) or (4-24)].

The lateral earth pressure coefficient K_u can be taken as one of the following:

$$K_u = \tan^2\left(45° + \frac{\phi}{2}\right) = K_p \qquad K_u = \tan\left(45° + \frac{\phi}{2}\right) = \sqrt{K_p}$$

$$K_u = \tan^2\left(45° - \frac{\phi}{2}\right) = K_a \qquad K_u = 0.65 + 0.5\phi \quad (\phi \text{ in radians})$$

$$K_u = K_o = 1 - \sin\phi$$

With these several choices the user must make a judgment analysis for K_u. Using K_o or an average of K_p, K_o, and K_a may be reasonable.

The equations for a rectangular footing in tension are based on an assumption made by Meyerhof that the shape factor is acting on the end parts in a zone of $B/2$ along L and the interior part of $(L - B)$ is similar to a long strip footing with $s_f = 1$. Most tension footings, however, are round (common) or square.

For footings founded in very poor soils, Robinson and Taylor (1969) found that a satisfactory design resistance for transmission tower anchorages could be obtained by using only the weight term W in Eqs. (4-23) through (4-26) and with a safety factor slightly greater than one. Compute the footing weight W based on the volume of the footing concrete plus the weight of any soil that will be uplifted when the base is pulled up. If the footing is a poured concrete shaft (with or without an enlarged base) in clay, use about 80 percent of the shaft length to

compute a perimeter area. The perimeter is based on $\pi B'$, where B' is either the diameter of the shaft or that of the base if it is larger or belled. This perimeter area is used with adhesion defined as $k \cdot s_u$ between shaft perimeter zone and foundation soil. The use of $0.8D$ allows for soil damage or tension cracks in the upper zone of the embedment depth. The tension force is now computed as

$$T_u = W + \pi B'(0.8D)k \cdot s_u$$

In general, one reduces the ultimate tension resistance to the design value T_a as

$$T_a = \frac{T_u}{\text{SF}}$$

where the safety factor may range from, say, 1.2 to 4 or 5 depending on the importance of the footing, reliability of the soil parameters, and the likelihood that quality backfill over the footing will produce a reliable W term and a reasonably adequate shear zone along line ab'.

Example 4-13. A footing $1.2 \times 1.2 \times 0.6$ m is placed at a depth of 1.80 m in a soil of $\gamma = 17.29$ kN/m^3; $\phi = 20°$; $s_u = 20$ kPa.

Required. Estimate the allowable uplift force for a SF = 2.5.

Solution. $D/B = 1.8/1.2 = 1.5 < H/B = 2.5$ for $\phi = 20°$; therefore, the footing is classed as shallow and we will use Eq. (4-24) to calculate T_u.

$$T_u = 2s_u D(B + L) + \gamma D^2(2s_f B + L - B)K_u \tan\phi + W$$

$$s_f = 1 + \frac{mD}{B} = 1 + 0.05(1.5) = 1.075 < 1.12 \text{ in table preceding this example}$$

Several values of K_u are as follows:

$$K_u = \tan^2\left(45° + \frac{20°}{2}\right) = 2.04 = K_p$$

$$K_u = \sqrt{K_p} = 1.43$$

$$K_u = 0.65 + 0.5\phi = 0.82$$

$$K_u = K_o = 1 - \sin 20° = 0.658$$

$$\text{Average } K_u = (2.04 + 1.43 + 0.82 + 0.66)/4 = \mathbf{1.24}$$

$$W = \text{Weight of concrete} + \text{Weight of soil uplifted}$$

$$W = 1.2(1.2)(0.6)(23.6) + 1.2(1.2)(1.8 - 0.6)(17.29) = \mathbf{50.3} \text{ kN}$$

Substituting values into Eq. (4-23), we find

$$T_u = 2(20)(1.8)(1.2 + 1.2) + 17.29(1.8)^2[2(1.075)(1.2) + 1.2 - 1.2](1.24)\tan 20° + 50.3$$

$$= 172.8 + 65.2 + 50.3 = 288.3 \text{ kN}$$

$$T_a = \frac{288.3}{2.5} = \mathbf{115} \text{ kN}$$

The structural design of this anchor footing would be on the basis of $T_a \times$ some SF (or load factor).

////

4-14 BEARING CAPACITY BASED ON BUILDING CODES (PRESUMPTIVE PRESSURE)

In many cities the local building code stipulates values of allowable soil pressure to use when designing foundations. These values are usually based on years of experience, although in some cases they are simply used from the building code of another city. Values such as these are also found in engineering and building-construction handbooks. These arbitrary values of soil pressure are often termed *presumptive* pressures. Most building codes now stipulate that other soil pressures may be acceptable if laboratory testing and engineering considerations can justify the use of alternative values. Presumptive pressures are based on a visual soil classification.

Table 4-8 indicates representative values of building code pressures. These values are primarily for illustrative purposes, since it is generally conceded that in all but minor construction projects some soil exploration should be undertaken. Major drawbacks to the use of presumptive soil pressures are that they do not reflect the depth of footing, size of footing, location of water table, or potential settlements.

TABLE 4-8
Presumptive bearing capacities from indicated building codes, kPa
Soil descriptions vary widely between codes. The following represents author's interpretations.

Soil description	Chicago, 1995	Natl. Board of Fire Underwriters, 1976	BOCA,* 1993	Uniform Bldg. Code, 1991†
Clay, very soft	25			
Clay, soft	75	100	100	100
Clay, ordinary	125			
Clay, medium stiff	175	100		100
Clay, stiff	210		140	
Clay, hard	300			
Sand, compact and clean	240		140	200
Sand, compact and silty	100			
Inorganic silt, compact	125			
Sand, loose and fine			140	210
Sand, loose and coarse, or sand-gravel mixture, or compact and fine		140 to 400	240	300
Gravel, loose and compact coarse sand	300		240	300
Sand-gravel, compact			240	300
Hardpan, cemented sand, cemented gravel	600	950	340	
Soft rock				
Sedimentary layered rock (hard shale, sandstone, siltstone)			6000	1400
Bedrock	9600	9600	6000	9600

Note: Values converted from psf to kPa and rounded.

*Building Officials and Code Administrators International, Inc.

†Author interpretation.

4-15 SAFETY FACTORS IN FOUNDATION DESIGN

Buildings are designed on the basis of determining the service loads and obtaining a suitable ratio of material strength to these loads, termed either a safety or a load factor. None of the quantities in this factor is precisely known, so that codes or experience are relied upon to develop the ratio as, one hopes, a lower-bound value—the real value is this or something larger. Engineering materials such as steel and concrete are manufactured with strict quality control; nevertheless, in strength design for concrete the effective ultimate strength is taken as 85 percent of the unconfined compressive strength. The yield stress for steel and other metals is a lower-bound value—in the case of steel on the order of 10 to 20 percent less than the general range of measured yield strengths. Thus, a "safety factor" of sorts is already applied.

Code values used to develop live and other loads are a compromise between upper and near-upper bound. Building self-weight, or dead load, is reasonably identified (at least after the structure is designed). Either the service loads are multiplied by a suitable set of load factors and compared with the "ultimate strength," or the structural material or the yield strength is divided by a suitable safety or load factor[7] and compared with the loads. We note in passing that in concrete strength design the load factors for dead and live loads represent in a limited way the different degrees of uncertainty associated with each type of loading.

There are more uncertainties in determining the allowable strength of the soil than in the superstructure elements. A number of these uncertainties can be deduced from discussions in Chaps. 2 and 3. These may be summarized as follows:

Complexity of soil behavior
Lack of control over environmental changes after construction
Incomplete knowledge of subsurface conditions
Inability to develop a good mathematical model for the foundation
Inability to determine the soil parameters accurately

These uncertainties and resulting approximations have to be evaluated for each site and a suitable safety factor directly (or indirectly) assigned that is not overly conservative but that takes into account at least the following:

1. Magnitude of damages (loss of life, property damage, and lawsuits) if a failure results
2. Relative cost of increasing or decreasing SF
3. Relative change in probability of failure by changing SF
4. Reliability of soil data
5. Changes in soil properties from construction operations, and later from any other causes
6. Accuracy of currently used design/analysis methods

It is customary to use overall safety factors on the order of those shown in Table 4-9. Shear should be interpreted as bearing capacity for footings. Although the SF values in Table 4-9

[7] At this writing (1995), the terms usually used are *load factor* for designing the superstructure elements and *safety factor* for estimating the allowable soil pressure.

TABLE 4-9
Values of stability numbers (or safety factors) usually used

Failure mode	Foundation type	SF
Shear	Earthworks	
	Dams, fills, etc.	1.2–1.6
Shear	Retaining structure	
	Walls	1.5–2.0
Shear	Sheetpiling cofferdams	1.2–1.6
	Temporary braced excavations	1.2–1.5
Shear	Footings	
	Spread	2–3
	Mat	1.7–2.5
	Uplift	1.7–2.5
Seepage	Uplift, heaving	1.5–2.5
	Piping	3–5

do not appear larger than for, say, steel design, the uncertainties in developing the allowable shear stress (in most cases) produce larger real safety factors than shown. For example, as shown in Example 4-4 using $q_a = q_u$, the apparent SF $\cong 3^+$. But q_u is obtained from very disturbed samples, so that the value may only be 50 to 60 percent of the in situ value resulting in the true SF being much larger. Further, where settlement controls, the allowable bearing capacity will be further reduced—which in turn further increases the real safety factor.

Some persons [Hansen (1967), Meyerhof (1970)] advocate consideration of partial safety factors for the soil parameters, e.g., using a value of, say, 1.2 to 1.3 on ϕ and 1.5 to 2.5 on cohesion. The latter are larger, since cohesion is somewhat more state-dependent.

The design load is obtained from the most critical of several possible cases. Using the load-term abbreviations of Table 4-10 and code-load factors R_i, the following might be investigated:

$$\text{Design load} = R_D\text{DL} + R_L\text{LL} + R_S S + \text{HS} \qquad (\text{SF} = 3.0)$$

TABLE 4-10
Foundation loads

Load	Includes
Dead load (DL)	Weight of structure and all permanently attached material
Live load (LL)	Any load not permanently attached to the structure, but to which the structure may be subjected
Snow load (S)	Acts on roofs; value to be used generally stipulated by codes
Wind load (W)	Acts on exposed parts of structure
Earthquake (E)	A lateral force (usually) that acts on the structure
Hydrostatic (HS)	Any loads due to water pressure; may be either (+) or (−)
Earth pressure (EP)	Any loads due to earth pressures—commonly lateral but may be in other directions

$$\text{Design load} = R_D\text{DL} + R_L\text{LL} + R_W W + \text{HS} \qquad (\text{SF} = 2.0)$$
$$\text{Design load} = R_D\text{DL} + R_L\text{LL} + R_E E + R_S S \qquad (\text{SF} = 2.0)$$

A number of other possible load combinations, including 0.5LL and DL, E and HS, etc. are commonly investigated. It is usual to use smaller safety factors for transitory loads such as wind and earthquake but this requirement is not absolute.

We should especially note that the geotechnical consultant will make a recommendation for an allowable strength (bearing capacity, etc.) that has the safety factor already included. The structural designer then factors this value or factors the loads to produce the design. In general the structural designer should not arbitrarily assume the geotechnical consultant used a specific value of SF as in Table 4-9. Rather the recommendation is what should be used. If the designer has a high load intensity from some transitory load combination the recommended bearing pressure should not be arbitrarily increased one-third, or whatever, without first discussing this with the geotechnical consultant.

4-16 BEARING CAPACITY OF ROCK

With the exception of a few porous limestone and volcanic rocks and some shales, the strength of bedrock in situ will be greater than the compressive strength of the foundation concrete. This statement may not be true if the rock is in a badly fractured, loose state where considerable relative slip between rock fragments can occur. The major problem is to identify the rock soundness and on occasion take cores for unconfined compression testing of the intact fragments. On very important projects and where it is economically feasible, one may make in situ strength tests.

Settlement is more often of concern than is the bearing capacity, and most test effort is undertaken to determine the in situ deformation modulus E and Poisson's ratio so that some type of settlement analysis can be made. This comment is made since most rock loads are from piles or drilled piers with the points embedded to some depth into the rock mass. Thus, one must make an analysis based on a load on the interior of a semi-infinite elastic body. The finite-element method FEM is sometimes used, but if the rock is fractured results are speculative unless one has measured data that can be used to revise the model. Even if the rock is not fractured the FEM seldom provides good results because uncertain elastic parameters are used.

It is common to use building code values for the allowable bearing capacity of rock; however, geology, rock type, and quality (as RQD) are significant parameters, which should be used together with the recommended code value. It is common to use large safety factors in rock capacity. The SF should be somewhat dependent on RQD defined in Sec. 3-17; i.e., an RQD of 0.80 would not require as high an SF as for RQD = 0.40. It is common to use SF from 6 to 10 with the higher values for RQD less than about 0.75 unless RQD is used to reduce the ultimate bearing capacity (as shown following). Table 4-11 may be used as a guide to estimate bearing capacity from code values or to obtain trial elastic parameters for preliminary FEM analyses.

One may use bearing-capacity equations of the form given by Terzaghi in Table 4-1 to obtain the bearing capacity of rocks using the angle of internal friction and cohesion of the rock from high-pressure triaxial tests. According to Stagg and Zienkiewicz (1968, p. 151)

TABLE 4-11
Range of properties for selected rock groups; data from several sources

Type of rock	Typical unit wt., kN/m³	Modulus of elasticity E, MPa × 10^3	Poisson's ratio, μ	Compressive strength, MPa
Basalt	28	17–103	0.27–0.32	170–415
Granite	26.4	14–83	0.26–0.30	70–276
Schist	26	7–83	0.18–0.22	35–105
Limestone	26	21–103	0.24–0.45	35–170
Porous limestone		3–83	0.35–0.45	7–35
Sandstone	22.8–23.6	3–42	0.20–0.45	28–138
Shale	15.7–22	3–21	0.25–0.45	7–40
Concrete	15.7–23.6	Variable	0.15	15–40

*Depends heavily on confining pressure and how determined; E = tangent modulus at approximately 50 percent of ultimate compression strength.

the bearing-capacity factors for sound rock are approximately

$$N_q = \tan^6\left(45° + \frac{\phi}{2}\right) \qquad N_c = 5\tan^4\left(45° + \frac{\phi}{2}\right) \qquad N_\gamma = N_q + 1 \tag{4-27}$$

Use the Terzaghi shape factors of Table 4-1 with these bearing-capacity factors. The rock angle of internal friction is seldom less than 40° (often 45° to 55°) and rock cohesion ranges from about 3.5 to 17.5 MPa (500 to 2500 psi). It is evident from Eq. (4-27) that very high values of ultimate bearing capacity can be computed. The upper limit on allowable bearing capacity is, as previously stated, taken as f'_c of the base concrete or not more than the allowable bearing pressure of metal piles.

The angle of internal friction of rock is pressure-dependent, similar to soil. Also, inspection of rock parameters from a number of sources indicates that, similar to sand, we could estimate $\phi = 45°$ for most rock except limestone or shale where values between 38° and 45° should be used. Similarly we could in most cases estimate $s_u = 5$ MPa as a conservative value. Finally we may reduce the ultimate bearing capacity based on RQD as

$$q'_{\text{ult}} = q_{\text{ult}}(\text{RQD})^2$$

In many cases the allowable rock-bearing pressure is taken in the range of one-third to one-tenth the unconfined compression strength obtained from intact rock samples and using RQD as a guide, for example, as one-tenth for a small RQD. Others simply use an allowable bearing pressure from the local building code (as in Table 4-8) based on rock type from a visual inspection of the rock cores.

Few building foundations such as mats or spread bases are placed directly on rock. Most situations involving rock-bearing capacity require large-diameter drilled shafts (termed drilled piers as in Chap. 19), which are socketed 2 to 3 shaft diameters into the rock. Recent load tests on this type of foundation [see Rowe and Armitage (1987)] indicate the allowable bearing pressure is on the order of

$$q_a = q_u \text{ to } 2.5q_u$$

where q_u = unconfined compression strength of intact rock core samples. This value is substantially larger than the values of one-third and one-tenth previously cited. The large increase

in allowable pressure can be at least partially attributed to the triaxial confining effect developing at the pier base from the embedment depth. The lower values previously suggested are applicable for foundations located at the rock surface.

When rock coring produces no intact pieces of consequence (RQD $\rightarrow$ 0) one should treat as a soil mass and obtain the bearing capacity using equations from Table 4-1 and best estimates of the soil parameters ϕ and c.

Example 4-14. We have a drilled pier with a diam. = 1 m to be founded at a depth of 3.5 m into a rock mass to get through the surface irregularities and the weathered rock zone as determined by coring to a depth of 6.5 m into the rock. From the cores the average RQD = 0.50 (or 50 percent) below the pier point.

Required. Estimate the allowable bearing capacity for the pier base. For the pier concrete we will use f'_c = 28 MPa (allowable f_c is, of course, somewhat less).

Solution. Assume from inspection of the rock cores that $\phi = 45°$ and take c = 3.5 MPa (both reasonably conservative—cohesion may be overly so).

The Terzaghi shape factors are s_c = 1.3 and s_γ = 0.6. Assume the unit weight of the dense rock γ_{rock} = 25.15 kN/m^3. Compute the following:

$$N_c = 5\tan^4\left(45° + \frac{45°}{2}\right) = 170$$

$$N_q = \tan^6\left(45° + \frac{45°}{2}\right) = 198$$

$$N_\gamma = N_q + 1 = 199$$

We will omit the soil overburden pressure to the soil-rock interface. Substituting in, and dividing by 1000 where necessary to convert to MPa, we have

$$\begin{aligned} q_{ult} &= cN_c s_c + \bar{q}N_q + 0.5\gamma B N_\gamma s_\gamma \\ &= (3.5)(170)1.3 + \frac{3.5(25.15)(198)}{1000} + \frac{0.5(25.15)(1)(199)(0.6)}{1000} \\ &= 773.5 + 17.4 + 1.5 = \mathbf{792.4}\ \text{MPa} \end{aligned}$$

Use a SF = 3 and RQD = 0.5 to obtain the reduced allowable bearing pressure as

$$q_a = \frac{q_{ult}(0.5)^2}{3} = \frac{792.4(0.25)}{3} = \mathbf{66}\ \text{MPa}$$

This appears O.K., because 66 $\cong$ 2.4 $\times$ f'_c

Recommend $q_a \cong$ 30 MPa as this is approximately f'_c.

Comments. Since f'_c is seldom over 40 MPa for drilled piers we see bearing capacity of rock is seldom a controlling factor. It may be more critical for steel **HP** piles, however—depending on whether one uses the actual or projected area for bearing.

////

We might question in the previous example why unconfined or triaxial compression tests were not performed to obtain the strength parameters. These could have been done since the cores are available; however, the following are major considerations:

1. For either type of test, several rock samples with an $L/d > 2$ would have to be cut with the ends accurately flat and perpendicular to the longitudinal axis. This is costly.
2. Tests on intact rock samples where the RQD = 0.5 can give an incorrect strength for the mass.
3. Testing an intact sample for q_u would give $c = q_u/2$ but no ϕ angle, so the N_c term of Eq. (4-27) could not be obtained ($\tan^6 45° = 1$ is not a good estimate). A q_u strength is too low for intact rock.
4. Testing a triaxial sample requires access to high-pressure cell capabilities or else the results are little better than q_u values. This still requires making an estimate of lateral cell pressure to duplicate in situ confinement. Using an estimate for cell pressure makes it difficult to justify the test expense.

As a final note, what can one do if the bearing pressure is inadequate? In this case we have options. We can go deeper into the rock or we can utilize skin resistance of the shaft-to-rock interface (considered in more detail in Chap. 19). We can abandon the site, or we can treat the rock. Rock treatment usually involves drilling a number of small holes and pressure-injecting cement grout to fill the cracks to provide mass continuity after the grout hardens. The latter requires further coring to see if the joints have been adequately grouted.

PROBLEMS

4-1. What is the allowable bearing capacity using the Hansen, Vesić, Meyerhof, and Terzaghi methods for the assigned problem in the following data set?
Other data: Use $B = 1.83$ m or 6.0 ft and $D = 0.75B$. The average unit weight in the zone of interest is 17.3 kN/m^3 or 110 pcf and the water table is not a problem.

				Partial answers*			
ϕ_{tr}		Cohesion c		H	V	M	T
(*a*)	20	15 kPa	(0.30 ksf)	232/5	—	—	—
(*b*)	25	10	(0.20)	—	323	—	250
(*c*)	30	5	(5.0)	9	—	436	341
(*d*)	34	0	—	—	—	919/19	667
(*e*)	38	0	—	1366	1582	1781	1194

**Note:* Answer rounded to nearest integer.

4-2. Redo the assigned problem from the data of Prob. 4-1 if $L/B = 2.5$. Note that answers are from computer output and rounded only sightly for checking.

	Partial answers			
Problem	H	V	M	T
(*a*)	4/198	—	—	—
(*b*)	—	280	—	250
(*c*)	7.5	—	367	341
(*d*)	—	—	775/16	667
(*e*)	1221	1411	1464	1194/25

4-3. Find the required size of *square* footing using the soil data of Prob. 4-1 if $D = 1.3$ m and the footing load is as given below. Use SF = 3 for soil with cohesion and 2 for cohesionless soil.

Problem	Load, kN	Partial answers			
		H	*V*	*M*	*T*
(*a*)	1200	2.40	—	—	—
(*b*)	1200	—	1.6	—	—
(*c*)	1200	—	—	1.4	—
(*d*)	2500	—	—	—	1.95
(*e*)	4000	—	1.45	—	—

4-4. Referring to Fig. P4-4, find the size of square footing to carry the inclined load (with V and H components shown). Use Meyerhof's, Vesić's, or Hansen's method as assigned and a SF = 5.0 on q_{ult}. Column is square of size shown. Use $\alpha_1 = 2.5$ and $\alpha_2 = 3.5$ in Hansen's method.

Partial answer: $H = 2.95$ m; $V = 2.95$ m; $M = 3.05$ m.

4-5. Redo Prob. 4-4 if there is also a moment of 600 kN · m. Use SF = 5.0 as previously. Use the Meyerhof, Hansen, or Vesić equation as assigned.

Answer (all 3 methods):

$$H = 2.20 \times 3.00 \text{ m} \qquad V = 2.80 \times 3.65 \text{ m} \qquad M = 3.00 \times 3.80 \text{ m}$$

4-6. Redo Example 4-6 using $\phi_{ps} = 44°$ and 46°. Comment on the effect of small changes in ϕ on the computed bearing capacity.

Answer: $\phi = 46 \rightarrow 1442$ kPa; $\phi = 44 \rightarrow 1035$ kPa

4-7. Redo Example 4-6 using $\phi_{ps} = 47°$ but vary $\alpha_1 > 2.5$ and vary $\alpha_2 > 3.5$ (values of 2.5 and 3.5 used in example). Comment on the effect of these two parameters on allowable bearing pressure q_a.

Answer: Using $\alpha_1 = 4$ and $\alpha_2 = 5 \rightarrow q_{ult} = 807$ kPa

4-8. Redo Example 4-7 if the force H is reversed (acts from right to left). Estimate ground slope $\beta = -80°$. Also use the Vesić method if it is assigned by your instructor for a comparison of methods.

4-9. A footing is located in the slope shown in Fig. P4-9. What is the allowable bearing capacity using Table 4-7 and the Hansen or Vesić bearing-capacity equations? What value of q_a do you recommend? Why?

4-10. Redo Example 4-7. Let the depth to the water table be 1.4 m instead of the 1.95 m shown in the example. Can you draw any conclusions about the effect of the water table location on the basis of this q_a and that from Example 4-7?

Figure P4-4

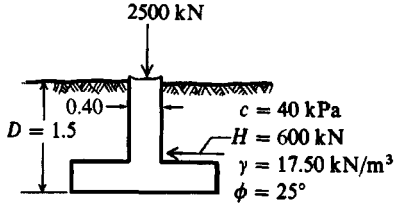

Figure P4-9

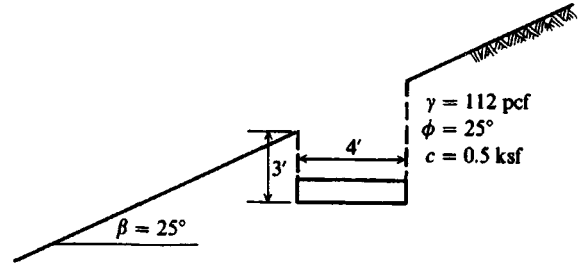

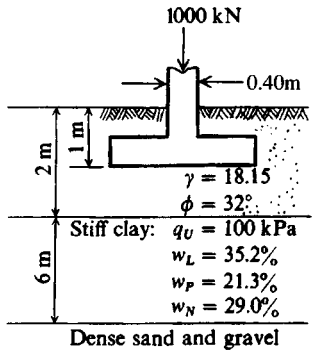

Figure P4-11

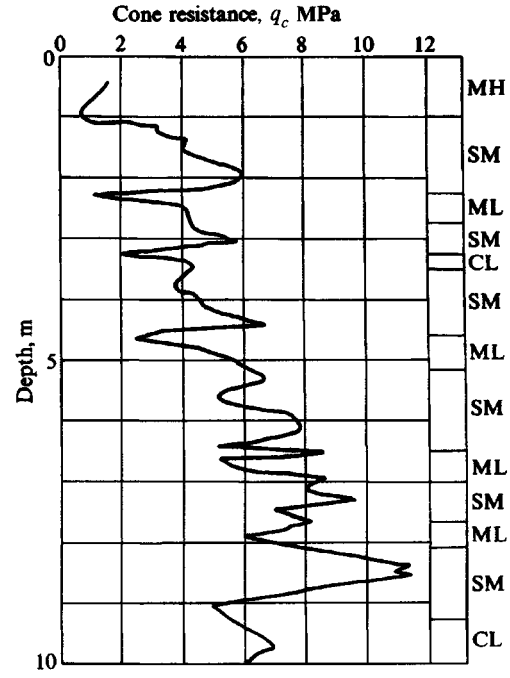

Figure P4-17

4-11. For the square footing on the layered soil of Fig. P4-11 find B to carry the 1000 kN load using a SF = 3.

4-12. Redo Prob. 4-11 if the layers are reversed, i.e., the upper layer is the "stiff" clay with a 2 m thickness and the footing is at D = 1 m.

4-13. Prepare a set of design charts of q_a/N_{70} versus B for the maximum range of D/B using Eqs. (4-11) and (4-12). Should you use an arithmetic or semilog plot?

4-14. Prepare a set of design charts of q_a/q_c versus B for the maximum range of D/B using appropriate equations. *Hint:* Take $q_c = 4N$.

4-15. For the SPT data shown in Fig. 3-34, estimate the allowable bearing pressure at −6.0 ft. Will the GWT be a problem?

4-16. For the boring log shown in Fig. P3-10 what do you recommend as q_a for footings located in the vicinity of the 2-meter depth? What does Table 4-8 suggest for q_a using the BOCA code?

4-17. A portion of a cone-penetration test is in Fig. P4-17. Estimate the allowable bearing pressure at the 2- and 5-m depths.

Answer: About 425 kPa at the 5-m depth using SF = 6.

4-18. For the portion of the CPT test shown in Fig. 3-14*c*, estimate the allowable bearing pressure at the 2-m depth. Will water be a problem?

4-19. Using the CPT data of Table P3-11, estimate the allowable bearing pressure at the 2-m and 15-m depths.

4-20. The following load-test data are obtained from Brand et al. (1972). The footings are all square with the given dimensions and located approximately 1.5 m below the ground surface. Plot the assigned load test and estimate the failure or "ultimate" load. Compare this estimated load with q_{ult} computed using the Meyerhof equations. Comment on your assumptions and results. See Example 4-3 for a computation of q_{ult} for the 1.05-m footing and additional comments. The

TABLE P4-20
Displacements, inches

Load, tons	Square plate size, m			
	1.05	0.9	0.75	0.60
0	0.000	0.000	0.000	0.000
2	0.030	0.043	0.062	0.112
3				0.212
4	0.075	0.112	0.175	0.406
5			0.243	0.631
6	0.134	0.187	0.325	0.912
7			0.450	1.456
8	0.212	0.306	0.606	
9		0.394	0.862	
10	0.331	0.500	1.293	
11		0.625		
12	0.537	0.838		
13		1.112		
14	0.706	1.500		
15	1.143			
16	1.425			

displacements in Table P4-20 are in inch units (for example, 0.030 inches, 0.043 inches, etc.). Use $s_u = 1.5$ tsf.

4-21. What is the required footing dimension of the Housel method of Sec. 4-12.1 if the design load $P_d = 500$ kN?

Answer: 2.75×2.75 m

4-22. What would you use for q_a in Example 4-14 if $c = 0.8$ ksi? What does your local building code suggest?

4-23. What is the fraction of q_u used in Example 4-14 to obtain q_a, assuming the cohesion parameter was obtained from an unconfined compression test?

CHAPTER 5

FOUNDATION SETTLEMENTS

5-1 THE SETTLEMENT PROBLEM

Foundation settlements must be estimated with great care for buildings, bridges, towers, power plants, and similar high-cost structures. For structures such as fills, earth dams, levees, braced sheeting, and retaining walls a greater margin of error in the settlements can usually be tolerated.

Except for occasional happy coincidences, soil settlement computations are only best estimates of the deformation to expect when a load is applied. During settlement the soil transitions from the current body (or self-weight) stress state to a new one under the additional applied load. The stress change Δq from this added load produces a time-dependent accumulation of particle rolling, sliding, crushing, and elastic distortions in a limited influence zone beneath the loaded area. *The statistical accumulation of movements in the direction of interest is the settlement.* In the vertical direction the settlement will be defined as ΔH.

The principal components of ΔH are particle rolling and sliding, which produce a change in the void ratio, and grain crushing, which alters the material slightly. Only a very small fraction of ΔH is due to elastic deformation of the soil grains. As a consequence, if the applied stress is removed, very little of the settlement ΔH is recovered. Even though ΔH has only a very small elastic component, it is convenient to treat the soil as a pseudo-elastic material with "elastic" parameters E_s, G', μ, and k_s to estimate settlements. This would appear reasonable because a stress change causes the settlement, and larger stress changes produce larger settlements. Also experience indicates that this methodology provides satisfactory solutions.

There are two major problems with soil settlement analyses:

1. *Obtaining reliable values of the "elastic" parameters.* Problems of recovering "undisturbed" soil samples mean that laboratory values are often in error by 50 percent or more. There is now a greater tendency to use in situ tests, but a major drawback is they tend to obtain horizontal values. *Anisotropy* is a common occurrence, making vertical elastic

values (usually needed) different from horizontal ones. Often the difference is substantial. Because of these problems, correlations are commonly used, particularly for preliminary design studies. More than one set of elastic parameters must be obtained (or estimated) if there is *stratification* in the zone of influence H.

2. *Obtaining a reliable stress profile from the applied load.* We have the problem of computing both the correct numerical values and the effective depth H of the influence zone. Theory of Elasticity equations are usually used for the stress computations, with the influence depth H below the loaded area taken from $H = 0$ to $H \rightarrow \infty$ (but more correctly from 0 to about $4B$ or $5B$). Since the Theory of Elasticity usually assumes an isotropic, homogeneous soil, agreement between computations and reality is often a happy coincidence.

The values from these two problem areas are then used in an equation of the general form

$$\Delta H = \int_0^H \epsilon \, dH$$

where ϵ = strain = $\Delta q/E_s$; but $\Delta q = f(H, \text{load})$, $E_s = f(H, \text{soil variation})$, and H (as previously noted) is the *estimated* depth of stress change caused by the foundation load. The principal focus in this chapter will be on obtaining Δq, E_s and H.

It is not uncommon for the ratio of measured to computed ΔH to range as $0.5 \leftarrow \frac{\Delta H_{\text{meas}}}{\Delta H_{\text{comp}}} \rightarrow 2$. Current methodology tends to minimize "estimation" somewhat so that most ratios are in the 0.8 to 1.2 range. Note too that a small computed ΔH of, say, 10 mm, where the measured value is 5 or 20 mm, has a large "error," but most practical structures can tolerate either the predicted or measured value. What we do not want is an estimate of 25 mm and a subsequent settlement of 100 mm. If we err in settlement computations it is preferable to have computed values larger than the actual (or measured) ones—but we must be careful that the "large" value is not so conservative that expensive (but unneeded) remedial action is required.

Settlements are usually classified as follows:

1. *Immediate,* or those that take place as the load is applied or within a time period of about 7 days.
2. *Consolidation,* or those that are time-dependent and take months to years to develop. The Leaning Tower of Pisa in Italy has been undergoing consolidation settlement for over 700 years. The lean is caused by the consolidation settlement being greater on one side. This, however, is an extreme case with the principal settlements for most projects occurring in 3 to 10 years.

Immediate settlement analyses are used for all fine-grained soils including silts and clays with a degree of saturation $S \lessapprox 90$ percent and for all coarse-grained soils with a large coefficient of permeability [say, above 10^{-3} m/s (see Table 2-3)].

Consolidation settlement analyses are used for all saturated, or nearly saturated, fine-grained soils where the consolidation theory of Sec. 2-10 applies. For these soils we want estimates of both settlement ΔH and how long a time it will take for most of the settlement to occur.

Both types of settlement analyses are in the form of

$$\Delta H = \epsilon H = \sum_{H_i}^{H_{i+1}} \frac{\Delta q_i}{E_{si}} \qquad (i = 1 \text{ to } n) \tag{5-1}$$

where the reader may note that the left part of this equation is also Eq. (2-43*a*). In practice the summation form shown on the right may be used where the soil is subdivided into layers of thickness H_i and stresses and properties of that layer used. The total settlement is the sum obtained from all n layers. The reader should also note that E_S used in this equation is the constrained modulus defined from a consolidation test as $1/m_v$ or from a triaxial test using Eq. (*e*) of Sec. 2-14, written as

$$E_s = \frac{1}{m_v} = \frac{(1-\mu)E_{s,\text{tr}}}{(1+\mu)(1-2\mu)} \tag{5-1a}$$

where $E_{s,\text{tr}}$ = triaxial value [also used in Eq. (5-16)]. Note, however, that if the triaxial cell confining pressure σ_3 approximates that developed in situ when the load is applied, the triaxial E_s will approximate $1/m_v$. In most cases the actual settlements will be somewhere between settlements computed using the equivalent of $1/m_v$ as from a consolidation test [see Eq. (5-1*a*)] and E_s from a triaxial test. Unfortunately the use of Eq. (5-1*a*) also requires estimating a value of Poisson's ratio μ.

5-2 STRESSES IN SOIL MASS DUE TO FOOTING PRESSURE

As we see from Eq. (5-1), we need an estimate of the pressure increase Δq from the applied load. Several methods can be used to estimate the increased pressure at some depth in the strata below the loaded area. An early method (not much used at present) is to use a 2 : 1 slope as shown in Fig. 5-1. This had a great advantage of simplicity. Others have proposed the slope angle be anywhere from 30° to 45°. If the stress zone is defined by a 2 : 1 slope, the

Figure 5-1 Approximate methods of obtaining the stress increase q_v in the soil at a depth z beneath the footing.

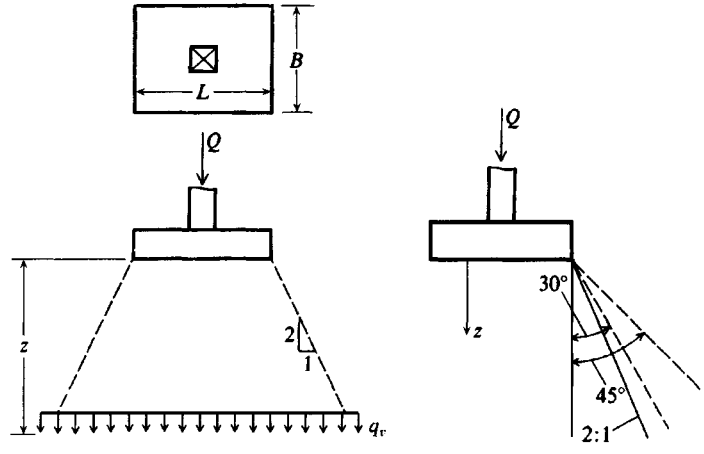

pressure increase $q_v = \Delta q$ at a depth z beneath the loaded area due to base load[1] Q is

$$\Delta q = q_v = \frac{Q}{(B + z)(L + z)} \tag{5-2}$$

which simplifies for a square base ($B \times B$) to

$$q_v = \frac{Q}{(B + z)^2} \tag{5-2a}$$

where terms are identified on Fig. 5-1. This 2 : 1 method compares reasonably well with more theoretical methods [see Eq. (5-4)] from $z_1 = B$ to about $z_2 = 4B$ but should not be used in the depth zone from $z = 0$ to B. The *average* stress increase in a stratum ($H = z_2 - z_1$) is

$$\Delta q_v H = \int_{z_1}^{z_2} \frac{Q}{(B + z)^2}\, dz \rightarrow q_v = \frac{1}{H}\left| -\frac{Q}{B + z} \right|_{z_1}^{z_2} \tag{5-2b}$$

5-3 THE BOUSSINESQ METHOD FOR q_v

One of the most common methods for obtaining q_v is the Boussinesq (ca. 1885) equation based on the Theory of Elasticity. Boussinesq's equation considers a point load on the surface of a semi-infinite, homogeneous, isotropic, weightless, elastic half-space to obtain

$$q_v = \frac{3Q}{2\pi z^2} \cos^5 \theta \tag{5-3}$$

where symbols are identified on Fig. 5-2*a*. From this figure we can also write $\tan\theta = r/z$, define a new term $R^2 = r^2 + z^2$, and take $\cos^5 \theta = (z/R)^5$. With these terms inserted in Eq.

Figure 5-2 (*a*) Intensity of pressure q based on Boussinesq approach; (*b*) pressure at point of depth z below the center of the circular area acted on by intensity of pressure q_o.

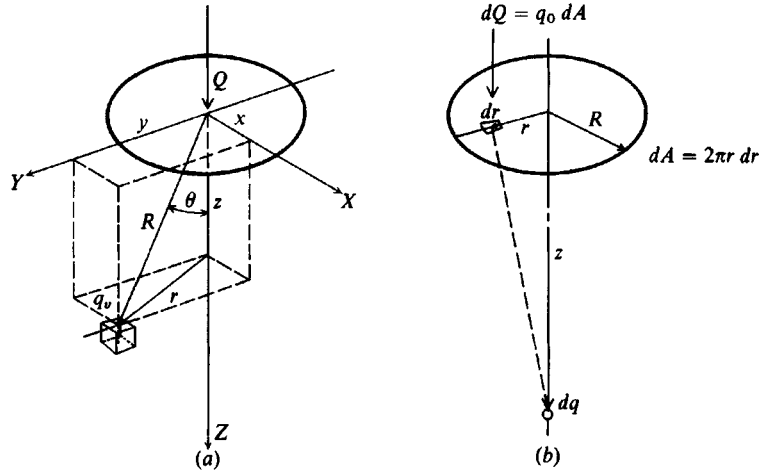

[1]The vertical base load uses P, V, and Q in this textbook and in the published literature; similarly, stress increases from the base load are q_v, Δq_v, p, and Δp.

(5-3) we obtain

$$q_v = \frac{3Qz^3}{2\pi R^5} \tag{5-4}$$

which is commonly written as

$$q_v = \frac{3Q}{2\pi z^2} 1/[1 + (r/z)^2]^{5/2} = \frac{Q}{z^2} A_b \tag{5-5}$$

Since the A_b term is a function only of the r/z ratio we may tabulate several values as follows:

$\pm r/z$	0.000	0.100	0.200	0.300	0.400	0.500	0.750	1.000	1.500	2.000
A_b	0.477	0.466	0.433	0.385	0.329	0.273	0.156	0.084	0.025	0.008

////

These values may be used to compute the vertical stress in the stratum as in the following two examples.

Example 5-1. What is the vertical stress beneath a point load $Q = 225$ kN at depths of $z = 0$ m, 0.6 m, 1.2 m, and 3.0 m?

Solution. We may write $q_v = (Q/z^2)A_b = 0.477Q/z^2$ (directly beneath Q we have $r/z = 0$). Substituting z-values, we obtain the following:

z, m	$q_v = 0.477(225)/z^2$, in kPa
0	∞
0.6	298 kPa
1.2	74.5
3.0	11.9

Example 5-2. What is the vertical stress q_v at point A of Fig. E5-2 for the two surface loads Q_1 and Q_2?

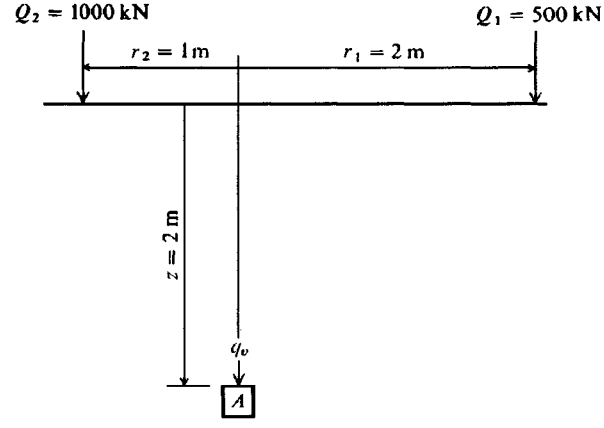

Figure E5-2

Solution.

$$q_v = \text{sum of stresses from the two loads}$$

$$Q_1: \frac{r}{z} = \frac{2}{2} = 1 \qquad A_b = 0.084$$

$$Q_2: \frac{r}{z} = -\frac{1}{2} = -0.5 \qquad A_b = 0.273$$

$$q_v = \frac{Q_1}{z^2}A_{b1} + \frac{Q_2}{z^2}A_{b2} = \frac{500(0.084)}{2 \times 2} + \frac{1000(0.273)}{2 \times 2} = \mathbf{78.8}\ \text{kPa}$$

////

Chart Methods

The purpose of foundations is to spread loads so that "point" loads with the accompanying very high stresses at the contact point ($z = 0$ of Example 5-1) are avoided. Thus, direct use of the Boussinesq equation is somewhat impractical until z is at a greater depth where computations indicate the point and spread load stress effects converge. We can avoid this by considering the contact pressure q_o to be applied to a circular area as shown in Fig. 5-2*b* so the load Q can be written as

$$Q = \int_0^A q_o \, dA$$

The stress on the soil element from the contact pressure q_o on the surface area dA of Fig. 5-2*b* is

$$dq = \frac{3q_o}{2\pi z^2} \frac{1}{[1 + (r/z)^2]^{5/2}} dA \qquad (a)$$

but $dA = 2\pi r \, dr$, and Eq. (*a*) becomes

$$q_v = \int_0^r \frac{3q_o}{2\pi z^2} \frac{1}{[1 + (r/z)^2]^{5/2}} 2\pi r \, dr \qquad (b)$$

Performing the integration and inserting limits, we have

$$q_v = q_o \left\{ 1.0 - \frac{1}{[1 + (r/z)^2]^{3/2}} \right\} \qquad (5\text{-}6)$$

This equation can be used to obtain the stress q_v directly at depth z for a round footing of radius r (now r/z is a depth ratio measured along the base center). If we rearrange this equation, solve for r/z, and take the positive root,

$$\frac{r}{z} = \sqrt{\left(1 - \frac{q_v}{q_o}\right)^{-2/3} - 1} \qquad (c)$$

The interpretation of Eq. (*c*) is that the r/z ratio is also the relative size of a circular bearing area such that, when loaded, it gives a unique pressure ratio q_v/q_o on the soil element at a depth z in the stratum. If values of the q_v/q_o ratio are put into the equation, corresponding

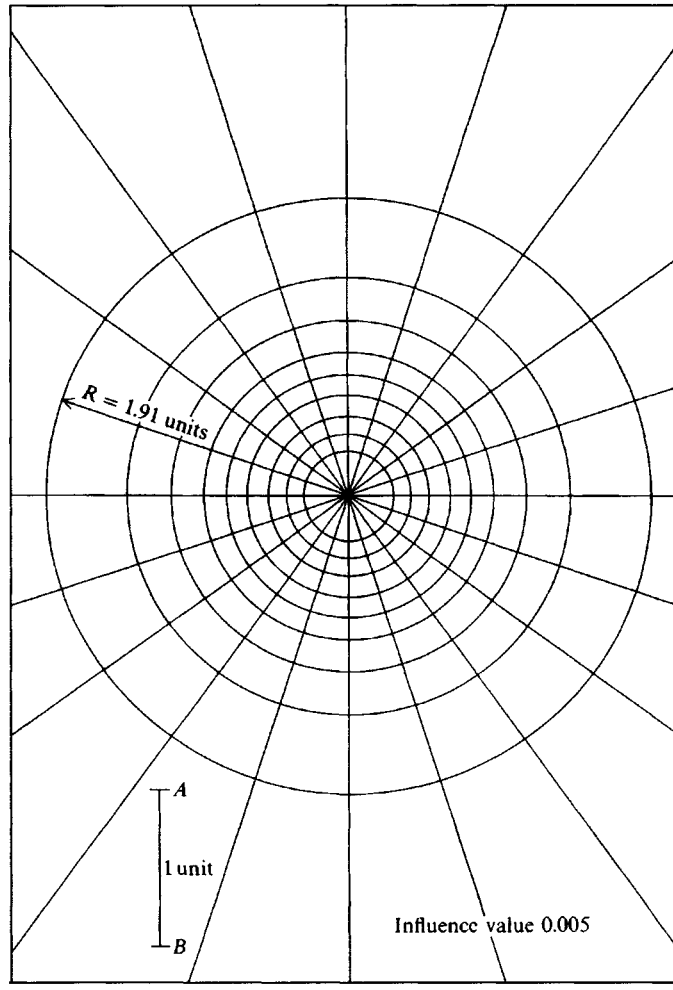

Figure 5-3 Influence chart for vertical pressure. *[After Newmark (1942).]*

values of r/z may be obtained as follows:

q_v/q_o =	0.0	0.100	0.200	0.300	0.400	0.500	0.600	0.700	0.800	0.900	1.00
$\pm r/z$ =	0.0	0.270	0.400	0.518	0.637	0.766	0.918	1.110	1.387	1.908	∞

These values may be used to draw the Newmark (1942) chart in Fig. 5-3. The use of the chart is based on a factor termed the *influence value*, determined from the number of units into which the chart is subdivided. For example, if the series of rings is subdivided so that there are 400 units, often made approximate squares, the influence value is 1/400 = 0.0025. In making a chart it is necessary that the sum of the units between two concentric circles multiplied by the influence value be equal to the change in the q_v/q_o of the two rings (i.e., if the change in two rings is 0.1 q_v/q_o, then the influence value I multiplied by the number of units M should equal 0.1). This concept enables one to construct a chart of any influence value. Figure 5-3 is

subdivided into 200 units; therefore, the influence value is 1/200 = 0.005. Smaller influence values increase the number of squares and the amount of work involved, since the sum of the squares used in a problem is merely a mechanical integration of Eq. (*a*). It is doubtful if much accuracy is gained using very small influence values, although the amount of work is increased considerably.

The influence chart may be used to compute the pressure on an element of soil beneath a footing, or from pattern of footings, and for any depth z below the footing. It is only necessary to draw the footing pattern to a scale of z = length AB of the chart. Thus, if z = 5 m, the length AB becomes 5 m; if z = 6 m, the length AB becomes 6 m; etc. Now if AB is 20 mm, scales of 1 : 250 and 1 : 300, respectively, will be used to draw the footing plans. These footing plans will be placed on the influence chart with the point for which the stress $\Delta q (< q_v)$ is desired at the center of the circles. The units (segments or partial segments) enclosed by the footing or footings are counted, and the increase in stress at the depth z is computed as

$$\Delta q = q_o M I \tag{5-7}$$

where Δq = increased intensity of soil pressure due to foundation loading at depth z in units of q_o
q_o = foundation contact pressure
M = number of units counted (partial units are estimated)
I = influence factor of the particular chart used

The influence chart is difficult to use, primarily because the depth z results in using an odd scale factor based on line AB in the figure. It has some value, however, in cases where access to a computer is not practical and there are several footings with different contact pressures or where the footing is irregular-shaped and Δq (or q_v) is desired for some point.

For single circular footings, a vertical center pressure profile can be efficiently obtained by using Eq. (5-6) on a personal computer. For square or rectangular footings the concept of the pressure bulb as shown in Fig. 5-4 is useful. The pressure bulbs are isobars (lines of constant pressure) obtained by constructing vertical pressure profiles (using similar to that of Fig. 1-1*a*) at selected points across the footing width B and interpolating points of equal pressure intensity (0.9, 0.8, 0.7q_o, etc.).

Numerical Methods for Solving the Boussinesq Equation

There are two readily available methods to obtain a vertical pressure profile using the Boussinesq equation and a computer. The first method is that used in program SMBWVP on your diskette (also applicable to the Westergaard equation of Sec. 5-5) as follows:

a. The square or rectangular base (for a round base convert to an equivalent square as $B = \sqrt{\pi r^2}$) with a contact pressure of q_o is divided into small square (or unit) areas of side dimension a so a series of "point" loads of $Q = q_o a^2$ can be used. Use side dimensions a on the order of 0.3 × 0.3 m (1 × 1 ft). Using very small a dimensions does not improve the result. The vertical pressure contributions from several bases can be obtained. The pressure at a point beneath a base such as the center, mid-side, or corner can be obtained from that footing as well as contributions from adjacent footings.

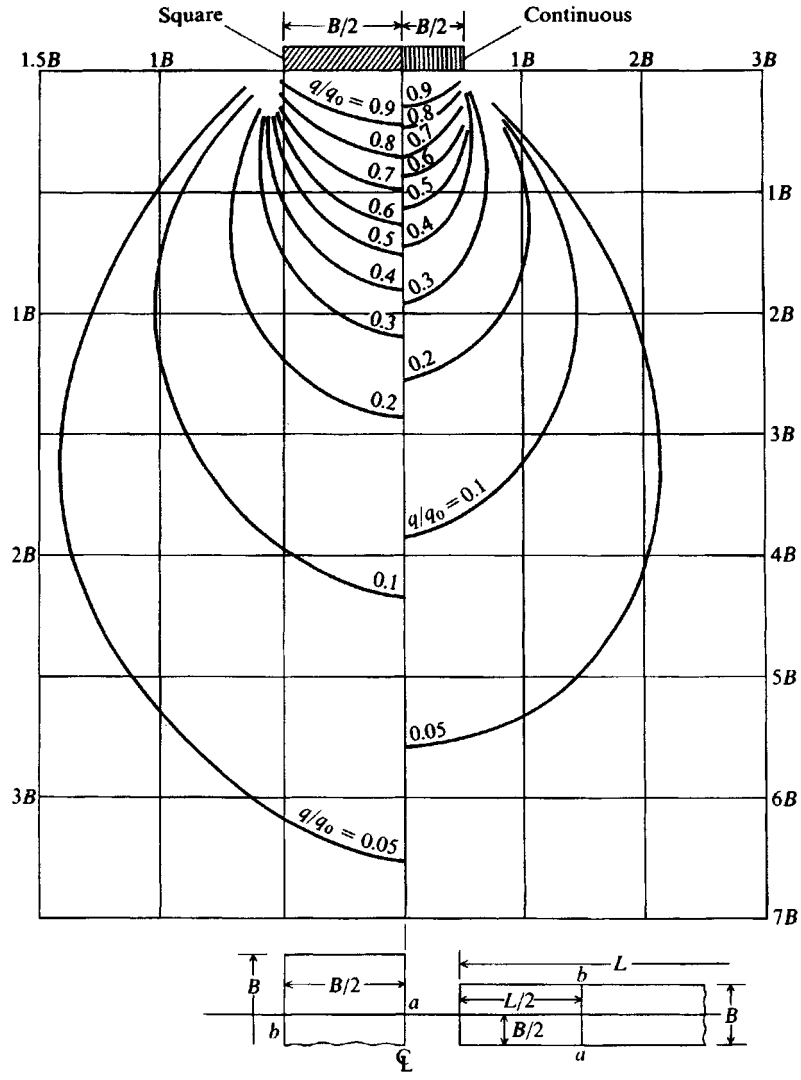

Figure 5-4 Pressure isobars (also called pressure bulbs) based on the Boussinesq equation for square and long footings. Applicable only along line *ab* from center to edge of base.

b. Input the location where the vertical pressure is wanted. Usually the x, z coordinates of this point are taken as the origin. Other bases (and this one if the point is under it) are referenced to the point where the vertical pressure is to be computed by distance DIST (see DTWAL of Fig. 11-19*a*) to the *far* side of the base and a perpendicular distance DOP [(+) to right side of DIST] to the base edge. Other bases that may contribute pressure are similarly referenced but in most cases bases not directly over the point can be treated as *point loads*. The pressures may be computed at any starting input depth Y_o; this may be at the ground surface or some point below. You can obtain a pressure profile using equally spaced depth increments DY or the vertical pressure at a single depth ($DY = 0$). For five

depth increments input number of vertical points NVERT = 6; for 10 input NVERT = 11, etc.

c. The program computes the center x, y coordinates of each unit area making up a base. The program recognizes the base dimensions in terms of the number of unit squares in each direction NSQL, NSQW that is input for that base. In normal operation you would input both DIST and DOP as (+) values along with the side dimensions of the square SIZE and contact pressure q_o (QO). The program then locates the x, z coordinates of the center of the first square (farthest from point and to right) and so on. These would be used with a point load of $Q = q_o a^2$ in Eq. (5-4) to obtain one pressure contribution. There would be NSQW × NSQL total contributions for this footing.

A point load would use a single unit (NSQW = 1; NSQL = 1) area of $a = 0.3$ m. For example, if we have a point load at a distance of $z = 1.1$ m from the pressure point, we would input NSQW = 1, NSQL = 1, DIST = 1.1 + 0.3/2 = 1.25, and DOP = 0 + 0.3/2 = 0.15 m. The program would locate the point load correctly on the DIST line at $z = 1.1$ m and $x = 0.15 - 0.3/2 = 0$ using a single unit area (0.3 × 0.3 m). These values of 1.1, 0.0, YO and pressure $q_o = QO = Q_{act}/a^2$ would give the vertical pressure at the point of interest; i.e.,if $Q = 90$ kN, input $QO = 90/(0.3 \times 0.3) = 1000$ kPa.

For several contributing footings this process would be repeated as necessary to get the total increase in vertical pressure Δq at this depth YO.

d. The depth is incremented if more vertical points are required to a new $YO = YO + DY$, the process repeated, and so on.

The program has an option to output the pressure (and some checking data) for each depth increment and to output the pressure profile in compact form. It also gives the average pressure increase in the stratum (sum of pressures divided by number of points) for direct use in settlement computations.

Another method that is applicable to square or rectangular bases (and round ones converted to equivalent squares) is to use the Boussinesq equation integrated over a rectangle of dimensions $B \times L$. This is not a simple integration, but it was done by a number of investigators in Europe in the 1920s, although the most readily available version is in Newmark (1935) and commonly seen as in the charts by Fadum (1948). The equation given by Newmark—*applicable beneath the corner of an area* $B \times L$—is

$$q_v = q_o \frac{1}{4\pi}\left[\frac{2MN\sqrt{V}}{V+V_1}\frac{V+1}{V} + \tan^{-1}\left(\frac{2MN\sqrt{V}}{V-V_1}\right)\right] \tag{5-8}$$

where $M = \dfrac{B}{z}$ $\quad N = \dfrac{L}{z}$ $\quad (q_v = q_o \text{ for } z = 0)$

$$V = M^2 + N^2 + 1$$

$$V_1 = (MN)^2$$

When $V_1 > V$ the $\tan^{-1}$ term is (−) and it is necessary to add π. In passing, note that $\sin^{-1}$ is an alternate form of Eq. (5-8) (with changes in V) that is sometimes seen. This equation is in program B-3 (SMNMWEST) on your diskette and is generally more convenient to use than Fadum's charts or Table 5-1, which usually requires interpolation for influence factors. The vertical stress at any depth z can be obtained for any reasonable proximity to or beneath the base as illustrated in Fig. 5-5 and the following examples.

TABLE 5-1

Stress influence values I_σ from Eq. (5-8) to use in Eq. (5-8*a*) to compute stresses at depth ratios $M = B/z$; $N = L/z$ beneath the *corner* of a base $B \times L$.

M and *N* are interchangeable.

N \ M	.100	.200	.300	.400	.500	.600	.700	.800	.900	1.000
.1	.005	.009	.013	.017	.020	.022	.024	.026	.027	.028
.2	.009	.018	.026	.033	.039	.043	.047	.050	.053	.055
.3	.013	.026	.037	.047	.056	.063	.069	.073	.077	.079
.4	.017	.033	.047	.060	.071	.080	.087	.093	.098	.101
.5	.020	.039	.056	.071	.084	.095	.103	.110	.116	.120
.6	.022	.043	.063	.080	.095	.107	.117	.125	.131	.136
.7	.024	.047	.069	.087	.103	.117	.128	.137	.144	.149
.8	.026	.050	.073	.093	.110	.125	.137	.146	.154	.160
.9	.027	.053	.077	.098	.116	.131	.144	.154	.162	.168
1.0	.028	.055	.079	.101	.120	.136	.149	.160	.168	.175
1.1	.029	.056	.082	.104	.124	.140	.154	.165	.174	.181
1.2	.029	.057	.083	.106	.126	.143	.157	.168	.178	.185
1.3	.030	.058	.085	.108	.128	.146	.160	.171	.181	.189
1.4	.030	.059	.086	.109	.130	.147	.162	.174	.184	.191
1.5	.030	.059	.086	.110	.131	.149	.164	.176	.186	.194
2.0	.031	.061	.089	.113	.135	.153	.169	.181	.192	.200
2.5	.031	.062	.089	.114	.136	.155	.170	.183	.194	.202
3.0	.031	.062	.090	.115	.137	.155	.171	.184	.195	.203
5.0	.032	.062	.090	.115	.137	.156	.172	.185	.196	.204
10.0	.032	.062	.090	.115	.137	.156	.172	.185	.196	.205

N \ M	1.100	1.200	1.300	1.400	1.500	2.000	2.500	3.000	5.000	10.000
.1	.029	.029	.030	.030	.030	.031	.031	.031	.032	.032
.2	.056	.057	.058	.059	.059	.061	.062	.062	.062	.062
.3	.082	.083	.085	.086	.086	.089	.089	.090	.090	.090
.4	.104	.106	.108	.109	.110	.113	.114	.115	.115	.115
.5	.124	.126	.128	.130	.131	.135	.136	.137	.137	.137
.6	.140	.143	.146	.147	.149	.153	.155	.155	.156	.156
.7	.154	.157	.160	.162	.164	.169	.170	.171	.172	.172
.8	.165	.168	.171	.174	.176	.181	.183	.184	.185	.185
.9	.174	.178	.181	.184	.186	.192	.194	.195	.196	.196
1.0	.181	.185	.189	.191	.194	.200	.202	.203	.204	.205
1.1	.186	.191	.195	.198	.200	.207	.209	.211	.212	.212
1.2	.191	.196	.200	.203	.205	.212	.215	.216	.217	.218
1.3	.195	.200	.204	.207	.209	.217	.220	.221	.222	.223
1.4	.198	.203	.207	.210	.213	.221	.224	.225	.226	.227
1.5	.200	.205	.209	.213	.216	.224	.227	.228	.230	.230
2.0	.207	.212	.217	.221	.224	.232	.236	.238	.240	.240
2.5	.209	.215	.220	.224	.227	.236	.240	.242	.244	.244
3.0	.211	.216	.221	.225	.228	.238	.242	.244	.246	.247
5.0	.212	.217	.222	.226	.230	.240	.244	.246	.249	.249
10.0	.212	.218	.223	.227	.230	.240	.244	.247	.249	.250

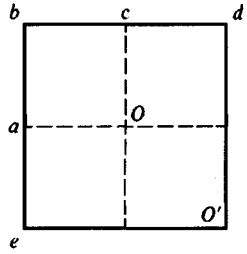

(*a*) Square loaded area = *O'ebd.*
For point *O*: use 4 × *Oabc.*
For point *O'*: use *O'ebd.*

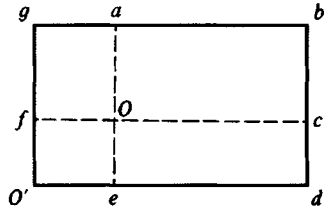

(*b*) Rectangle with loaded area = *O'gbd.*
For point *O*: use *Oabc* + *Ocde* + *OeO'f* + *Ofga.*
For point *O'*: use *O'gbd.*

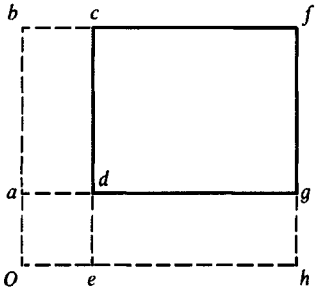

(*c*) Point outside loaded area = *dcfg.*
For point *O*: use *Obfh* − *Obce* − *Oagh* + *Oade.*

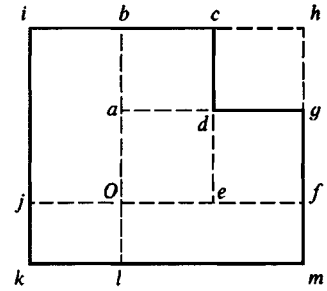

(*d*) For loaded area: *kicdgm.*
For point *O*: *Obce* + *Oagf* + *Ofml* + *Olkj* + *Ojib* − *Oade.*

Figure 5-5 Method of using Eq. (5-8) to obtain vertical stress at point indicated.

In general use, and as in the following examples, it is convenient to rewrite Eq. (5-8) as

$$\Delta q = q_o m I_\sigma \tag{5-8a}$$

where I_σ is all terms to the right of q_o in Eq. (5-8) as tabulated for selected values of M and N in Table 5-1.

The Boussinesq method for obtaining the stress increase for foundation loads is very widely used for all types of soil masses (layered, etc.) despite it being specifically developed for a semi-infinite, isotropic, homogeneous half-space. Computed stresses have been found to be in reasonable agreement with those few measured values that have been obtained to date.

Example 5-3. Find the stress beneath the center (point *O*) and corner of Fig. 5-5*a* for the following data:

$B \times B = 2\text{ m} \times 2\text{ m}$ $\quad Q = 800\text{ kN}$
At corner $z = 2\text{ m}$
At center for $z = 0, 1, 2, 3,$ and 4 m

Solution. It is possible to use Table 5-1; however, program SMNMWEST (B-3) on your diskette is used here for convenience (Table 5-1 is used to check the programming).

1. For the corner at $z = 2$ m

$$M = 2/2 = N = 1 \qquad \text{giving the table factor } 0.175 = I_\sigma$$

$$\Delta q = q_o m(0.175) = \frac{800}{2 \times 2} \times 1 \times 0.175 = \mathbf{35}\ \text{kPa}$$

2. For the center $B' = 2/2 = 1$; $L' = 2/2 = 1$ and with $m = 4$ contributions; for $M = N = \infty$ use 10.

z	M	N	Δq, kPa
0	∞	∞	$200 \times 0.250 \times 4 =$ **200** kPa*
1	1	1	$200 \times 0.175 \times 4 =$ **140**
2	0.5	0.5	$200 \times 0.084 \times 4 =$ **67**
3	0.333	0.333	$200 \times 0.045 \times 4 =$ **36**
4	0.25	0.25	$200 \times 0.027 \times 4 =$ **22**

*at $z = 0$, $\Delta q = 800/(2 \times 2) = 200$ kPa

////

Example 5-4. Find the stress at point O of Fig. 5-5*c* if the loaded area is square, with $dg = dc = 4$ m, $ad = 1$ m, and $ed = 3$ m for $q_o = 400$ kPa and depth $z = 2$ m.

Solution. From the figure the stress I_σ is the sum of $Obfh - Obce - Oagh + Oade$, and $m = 1$.

For	M	N	I_σ
Obfh	5/2	7/2	+0.243
Obce	1/2	7/2	−0.137
Oagh	3/2	5/2	−0.227
Oade	1/2	3/2	+0.131
			$I_\sigma =$ **+0.010**

$q_v = 400(1)(0.010) = \mathbf{4}$ kPa

////

5-4 SPECIAL LOADING CASES FOR BOUSSINESQ SOLUTIONS

On occasion the base may be loaded with a triangular or other type of load intensity. A number of solutions exist in the literature for these cases but should generally be used with caution if the integration is complicated. The integration to obtain Eq. (5-8) is substantial; however, that equation has been adequately checked (and with numerical integration using program SMBWVP on your program diskette) so it can be taken as correct. Pressure equations for triangular loadings (both vertical and lateral) are commonly in error so that using numerical procedures and superposition effects is generally recommended where possible. Equations for the cases of Fig. 5-6 have been presented by Vitone and Valsangkar (1986) seem to be correct since they give the same results as from numerical methods. For Fig. 5-6*a* we have

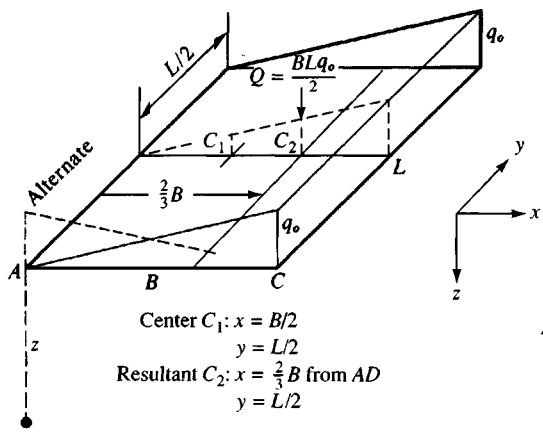

(*a*) One-way linear load variation. intensity = q_o

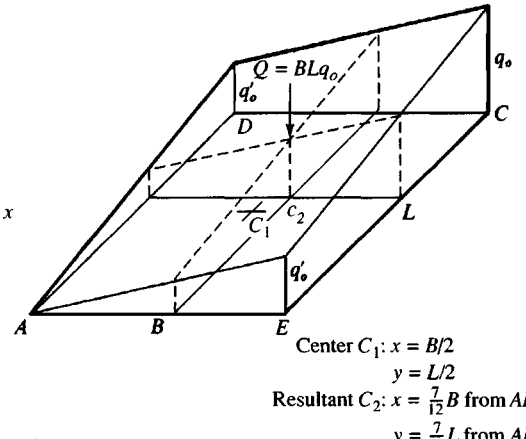

(*b*) Two-way linear load variation. intensity = q_o; $q'_o = q_o/2$

Figure 5-6 Special Boussinesq loading cases. Always orient footing for B and L as shown (B may be $>$ or $<$ L).

At point A,

$$\Delta q = \frac{q_o L}{2\pi B}\left(\frac{z}{R_L} - \frac{z^3}{R_B^2 R_D}\right) \tag{5-9}$$

At point C,

$$\Delta q = \frac{q_o L}{2\pi B}\left\{\frac{zR_D}{R_L^2} - \frac{z}{R_L} + \frac{B}{L}\sin^{-1}\left(\frac{BL}{(B^2L^2 + R_D^2 z^2)^{1/2}}\right)\right\} \tag{5-10}$$

For Fig. 5-6*b* (there is a limitation on the intermediate corners that $q'_o = q_o/2$), we have

At point A,

$$\Delta q = \frac{q_o}{4\pi}\left\{\frac{L}{B}\left(\frac{z}{R_L} - \frac{z^3}{R_D R_B^2}\right) + \frac{B}{L}\left(\frac{z}{R_B} - \frac{z^3}{R_D R_L^2}\right)\right\} \tag{5-11}$$

At point C,

$$q = \frac{q_o}{4\pi}\left\{\frac{L}{B}\left(\frac{zR_D}{R_L^2} - \frac{z}{R_L}\right) + \frac{B}{L}\left(\frac{zR_D}{R_B^2} - \frac{z}{R_B}\right) + 2\sin^{-1}\left(\frac{BL}{(B^2L^2 + R_D^2 z^2)^{1/2}}\right)\right\} \tag{5-12}$$

where $R_B^2 = B^2 + z^2$

$R_L^2 = L^2 + z^2$

$R_D^2 = B^2 + L^2 + z^2$

These equations can be checked by computing the stresses at A and C and summing. The sum should equal that at any depth z for a rectangular uniformly loaded base. This check is illustrated in Example 5-5.

Example 5-5. Given the footing example in the ASCE Journal of Geotechnical Engineering Division, vol. 110, No. 1, January 1984, p. 75 (which has an error), find the vertical pressure beneath the corners A and C at $z = 10$ ft. This footing is $L = 8$ ft $\times$ $B = 6$ ft with a linearly varying load from 0 at A to 1 ksf at C across the 6-ft width.

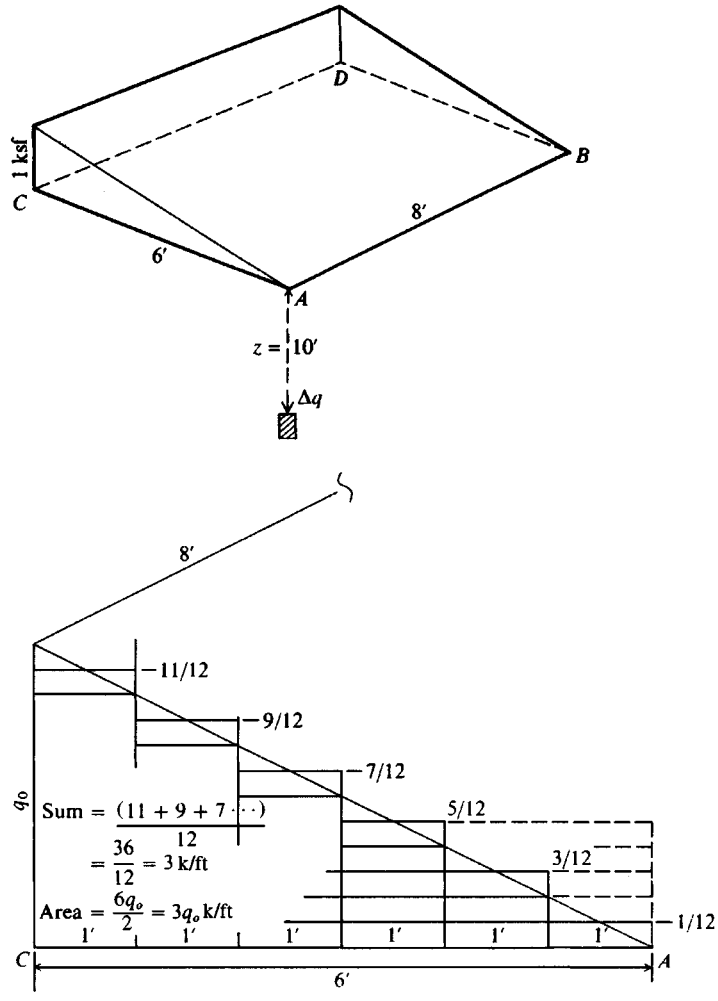

Figure E5-5

Solution. We will use the Newmark Eq. (5-8) and check it using Eqs. (5-9) and (5-10). For the Newmark method, draw the side view of the footing as shown in Fig. E5-5 and step the load intensity, so we have a series of strips loaded uniformly with the intensity fraction shown. The first strip is 1 ft $\times$ 8 ft, the second 2 ft $\times$ 8 ft, etc., so that we will have to subtract from strips after the first a fraction of the previous strip load to obtain the net strip contribution to the point at depth $z = 10$ ft. We will find the stresses at both A and C and use the sum as a check since it can be readily seen that

the sum is exactly equivalent to a uniform load of 1 ksf on the footing. Note that I_σ = constant but load intensity varies going from A to C and from C to A. A table will be convenient (again refer to Fig. E5-5):

			For point A (A to C)		For point C (C to A)	
Strip No.	$M = B/z$	$N = L/z$	I_σ	$\Delta q = q_o I_o$		$\Delta q = q_o I_o$
1	1/10	8/10	0.0257 × 1/12 − 0.000	= 0.002 14	×11/12−0	= 0.023 6
			+3/12		0.0257 × 9/12	
2	2/10	8/10	0.0504 × 3/12 − 0.006 425	= 0.006 18	× 9/12−0.019 28	= 0.018 5
			+5/12		0.0504 × 7/12	
3	3/10	8/10	0.0730 × 5/12 − 0.021 0	= 0.009 42	× 7/12−0.029 40	= 0.013 18
			+7/12		0.0730 × 5/12	
4	4/10	8/10	0.0931 × 7/12 − 0.042 58	= 0.011 73	× 5/12−0.030 42	= 0.008 37
			+9/12		0.0931 × 3/12	
5	5/10	8/10	0.1103 × 9/12 − 0.069 83	= 0.012 90	× 3/12−0.023 28	= 0.004 30
			+11/12		0.1103 × 1/12	
6	6.10	8/10	0.1245 × 11/12 − 0.101 11	= 0.013 20	× 1/12−0.009 19	= 0.001 20
				Total Δq = 0.055 56 ksf		Total Δq = 0.069 13 ksf

Summing, we have at A and C = 0.055 56 + 0.069 13 = 0.124 69 ksf. A uniform load of 1 ksf gives $\Delta q_a = \Delta q_c$ = 0.124 7 ksf based on Table 5-1 at M = 0.6, N = 0.8. Using Eq. (5-9), we have R_D = 14.14; R_B^2 = 136; R_L^2 = 164 and by substitution of values we obtain Δq = 0.055 36 ksf for point A and 0.069 33 ksf for point C.

////

Example 5-6. Let us assume that we are to redo Example 5-5. We do not have access to the Newmark methodology or Eq. (5-9) but do have access to Eq. (5-4). From the data given in Example 5-5 we have B = 6 ft; L = 8 ft; and depth z = 10 ft. We are to use Fps units consistent with both the reference and Example 5-5.

Solution. Referring to Fig. 5-6*a*, we see the *center of the resultant* is at

$$x = \frac{2}{3}B = \frac{2}{3}\cdot 6 = 4.0 \text{ ft} \qquad y = \frac{L}{2} = \frac{8}{2} = 4.0 \text{ ft} \qquad z = 10 \text{ ft}$$

$$R_A = \sqrt{x^2 + y^2 + z^2} = \sqrt{4^2 + 4^2 + 10^2} = 11.489 \text{ ft (to corner } A)$$

$$R_C = \sqrt{2^2 + 4^2 + 10^2} = 10.954 \text{ ft (to corner } C)$$

$$Q = BLq_o/2 = (6)(8)(1)/2 = \mathbf{24} \text{ kips}$$

From Eq. (5-4) we have

$$q_v = \frac{3Qz^3}{2\pi R^5}$$

Separating terms and computing $3Qz^3/2\pi$, we find

$$\frac{3 \cdot 24 \cdot 10^3}{2\pi} = 11\,459.129$$

$$q_{vA} = 11\,459.129/11.489^5 = 0.0572 \text{ ksf}$$

$$q_{vC} = 11\,459.129/10.954^5 = 0.0727 \text{ ksi}$$

The results from Example 5-5 and this example are next compared:

	Point *A*	**Point *B***
Boussinesq [Eq. (5-4)]	0.0572	0.0727 ksf
Example 5-5	0.0566	0.0691
Difference	0.0016	0.0035

Refer to Table E5-6 for a complete comparison of pressure profiles. For the computational purist some of the differences shown in Table E5-6 are substantial, but may be adequate—even conservative—for design purposes in an engineering office—and certainly the point load equation [Eq. (5-4)] is the easiest of all methods to use.

TABLE E5-6

Comparison of stress values from the Boussinesq point load equation (Eq. 5-4) and Eq. (5-4) converted to a numerical format using program SMBWVP

Refer to example Fig. E5-5 for location of points *A* and *C*.

	Points for Boussinesq equation		**Points for numerical method**	
***z*, ft**	***A***	***C***	***A***	***C***
0.0	0.0000	1.0000*	0.0000	1.0000*
2.0	0.0118	0.0325	0.0479	0.1972
4.0	0.0459	0.0943	0.0710	0.1527
6.0	0.0649	0.1055	0.0730	0.1168
8.0	0.0650	0.0907	0.0654	0.0895
10.0†	0.0572	0.0727	0.0555	0.0691
12.0	0.0482	0.0575	0.0463	0.0546
14.0	0.0401	0.0459	0.0384	0.0437
16.0	0.0333	0.0371	0.0321	0.0355
18.0	0.0279	0.0304	0.0270	0.0293

*Not from computations but known value.

†Depth used in Examples 5-5 and 5-6.

////

A SIMPLE METHOD FOR ALL SPECIAL LOADING CASES. Example 5-6 illustrates that when the load pattern is difficult (for example, a base covered with an uneven pile of material

producing a nonuniform load), the following procedure is adequate for design:

1. Locate the load resultant as best you can so critical footing locations such as corners, the center, and so forth can be located using x, y coordinates with respect to the load resultant.
2. For the case of depth $z = 0$, use the computed contact pressure as your best estimate. You must do this since $z = 0$ computes a value of $q_v = 0$ or undefined (∞) in Eq. (5-4).
3. For depth $z > 0$ compute the value R and use Eq. (5-4). For cases where $R < z$, Eq. (5-4) will not give very good values but may be about the best you can do. In Example 5-6 note that R is not much greater than z, but the answers compare quite well with the known values.
4. Consider using Table E5-6 as a guide to increase proportionately your Boussinesq pressures, as computed by Eq. (5-4), to approximate more closely the "exact" pressure values obtained by the numerical method. For example you actually have an $R = 2.11$ m (which corresponds exactly to the 4.0 ft depth on Table E5-6, so no interpolation is required), and you have a computed $q_{v,\text{comp}} = 9.13$ kPa at point A. The "corrected" (or at least more nearly correct) q_v can be computed as follows:

$$q_v = \frac{q_{v,\text{nm}}}{q_{v,b}} \times q_{v,\text{comp}}$$

where $q_{v,\text{nm}}$ = vertical pressure from numerical method (most correct)

$q_{v,b}$ = vertical pressure from Boussinesq Eq. (5-4)

so in our case above, we have

$$q_v = \frac{0.0710}{0.0459} \times 9.13 = 1.54 \times 9.13 = \mathbf{14.13}\ \text{kPa}$$

Pressures at other depth points would be similarly scaled. You might note that at the depth of 3.05 m (10 ft) the ratio is 0.0555/0.0572 = **0.970** at point A.

5-5 WESTERGAARD'S METHOD FOR COMPUTING SOIL PRESSURES

When the soil mass consists of layered strata of fine and coarse materials, as beneath a road pavement, or alternating layers of clay and sand, some authorities are of the opinion the Westergaard (1938) equations give a better estimate of the stress q_v.

The Westergaard equations, unlike those of Boussinesq, include Poisson's ratio μ, and the following is one of several forms given for a point load Q:

$$q_v = \frac{Q}{2\pi z^2} \frac{\sqrt{a}}{[a + (r/z)^2]^{3/2}} \tag{5-13}$$

where $a = (1 - 2\mu)/(2 - 2\mu)$ and other terms are the same as in the Boussinesq equation. We can rewrite this equation as

$$q_v = \frac{Q}{z^2} A_w \tag{5-13a}$$

as done for the Boussinesq equation. For $\mu = 0.30$ we obtain the following values:

r/z	0.000	0.100	0.200	0.300	0.400	0.500	0.750	1.000	1.500	2.000
A_w	0.557	0.529	0.458	0.369	0.286	0.217	0.109	0.058	0.021	0.010

Comparing the Boussinesq values A_b from Eq. (5-5), we see that generally the Westergaard stresses will be larger. This result depends somewhat on Poisson's ratio, however, since $\mu = 0$ and $r/z = 0.0$ gives $A_w = \mathbf{0.318}$ (versus $A_b = 0.477$); for $\mu = 0.25$ and $r/z = 0.0$ obtain $A_w = \mathbf{0.477}$.

Similarly as for the Boussinesq equation [Eq. (*a*) and using Fig. 5-2*b*] we can write

$$q = \frac{q_o\sqrt{a}}{2z^2}\int_0^A \left[a + \left(\frac{r}{z}\right)^2\right]^{-3/2} (2r)\,dr$$

After integration we have the direct solution for round footings analogous to Eq. (5-6):

$$q = q_o\left(1 - \sqrt{\frac{a}{(r/z)^2 + a}}\right) \tag{5-14}$$

From some rearranging and using the (+) root,

$$\frac{r}{z} = +\sqrt{\frac{a}{(1 - q/q_o)^2} - a}$$

If this equation is solved for selected values of Poisson's ratio and incremental quantities of q/q_0, as was done with the Boussinesq equation, values to plot a Westergaard influence chart may be computed. Since the Westergaard equation is not much used, construction of an influence chart (done exactly as for the Boussinesq method but for a given value of μ) is left as an exercise for the reader.

If use of the Westergaard equations is deemed preferable, this is an option programmed into SMBWVP on your diskette. For programming, the integration of stresses for a rectangle of $B \times L$ gives the following equation [used by Fadum (1948) for his stress charts] for the corner of a rectangular area (and programmed in SMNMWEST) as

$$q_v = \frac{q_o}{2\pi}\tan^{-1}\left(\frac{MN}{\sqrt{a}(M^2 + N^2 + a)^{1/2}}\right) \tag{5-15}$$

where M, N are previously defined with Eq. (5-8) and a has been defined with Eq. (5-13). The $\tan^{-1}$ term is in radians. This equation can be readily used to obtain a vertical stress profile as for the Boussinesq equation of Eq. (5-8) for rectangular and round (converted to equivalent square) footings. To check programming, use the following table of values:

μ	M	N	I_σ
0.45	1.0	1.0	0.1845
0.45	1.0	0.5	0.1529

At $z = 0$ we have a discontinuity where we arbitrarily set $\Delta q = q_o$ for any base-on-ground location.

5-6 IMMEDIATE SETTLEMENT COMPUTATIONS

The settlement of the corner of a rectangular base of dimensions $B' \times L'$ on the surface of an elastic half-space can be computed from an equation from the Theory of Elasticity [e.g., Timoshenko and Goodier (1951)] as follows:

$$\Delta H = q_o B' \frac{1-\mu^2}{E_s}\left(I_1 + \frac{1-2\mu}{1-\mu} I_2\right) I_F \tag{5-16}$$

where q_o = intensity of contact pressure in units of E_s

B' = least lateral dimension of contributing base area in units of ΔH

I_i = influence factors, which depend on L'/B', thickness of stratum H, Poisson's ratio μ, and base embedment depth D

E_s, μ = elastic soil parameters—see Tables 2-7, 2-8, and 5-6

The influence factors (see Fig. 5-7 for identification of terms) I_1 and I_2 can be computed using equations given by Steinbrenner (1934) as follows:

$$I_1 = \frac{1}{\pi}\left[M \ln \frac{(1+\sqrt{M^2+1})\sqrt{M^2+N^2}}{M(1+\sqrt{M^2+N^2+1})} + \ln \frac{(M+\sqrt{M^2+1})\sqrt{1+N^2}}{M+\sqrt{M^2+N^2+1}}\right] \tag{a}$$

$$I_2 = \frac{N}{2\pi} \tan^{-1}\left(\frac{M}{N\sqrt{M^2+N^2+1}}\right) \quad (\tan^{-1} \text{ in radians}) \tag{b}$$

where $M = \dfrac{L'}{B'}$

Figure 5-7 Influence factor I_F for footing at a depth D. Use actual footing width and depth dimension for this D/B ratio. Use program FFACTOR for values to avoid interpolation.

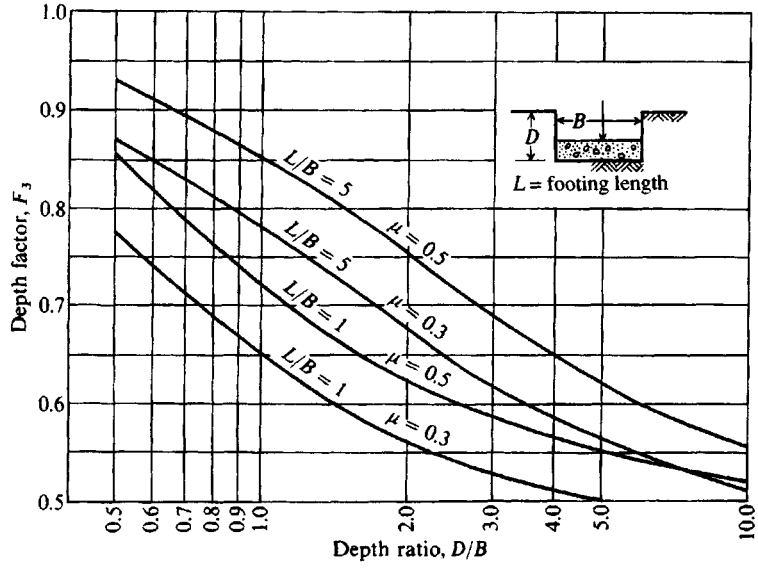

TABLE 5-2

Values of I_1 and I_2 to compute the Steinbrenner influence factor I_s for use in Eq. (5-16*a*) for several $N = H/B'$ and $M = L/B$ ratios

N	M = 1.0	1.1	1.2	1.3	1.4	1.5	1.6	1.7	1.8	1.9	2.0
0.2	I_1 = 0.009	0.008	0.008	0.008	0.008	0.008	0.007	0.007	0.007	0.007	0.007
	I_2 = 0.041	0.042	0.042	0.042	0.042	0.042	0.043	0.043	0.043	0.043	0.043
0.4	0.033	0.032	0.031	0.030	0.029	0.028	0.028	0.027	0.027	0.027	0.027
	0.066	0.068	0.069	0.070	0.070	0.071	0.071	0.072	0.072	0.073	0.073
0.6	0.066	0.064	0.063	0.061	0.060	0.059	0.058	0.057	0.056	0.056	0.055
	0.079	0.081	0.083	0.085	0.087	0.088	0.089	0.090	0.091	0.091	0.092
0.8	0.104	0.102	0.100	0.098	0.096	0.095	0.093	0.092	0.091	0.090	0.089
	0.083	0.087	0.090	0.093	0.095	0.097	0.098	0.100	0.101	0.102	0.103
1.0	0.142	0.140	0.138	0.136	0.134	0.132	0.130	0.129	0.127	0.126	0.125
	0.083	0.088	0.091	0.095	0.098	0.100	0.102	0.104	0.106	0.108	0.109
1.5	0.224	0.224	0.224	0.223	0.222	0.220	0.219	0.217	0.216	0.214	0.213
	0.075	0.080	0.084	0.089	0.093	0.096	0.099	0.102	0.105	0.108	0.110
2.0	0.285	0.288	0.290	0.292	0.292	0.292	0.292	0.292	0.291	0.290	0.289
	0.064	0.069	0.074	0.078	0.083	0.086	0.090	0.094	0.097	0.100	0.102
3.0	0.363	0.372	0.379	0.384	0.389	0.393	0.396	0.398	0.400	0.401	0.402
	0.048	0.052	0.056	0.060	0.064	0.068	0.071	0.075	0.078	0.081	0.084
4.0	0.408	0.421	0.431	0.440	0.448	0.455	0.460	0.465	0.469	0.473	0.476
	0.037	0.041	0.044	0.048	0.051	0.054	0.057	0.060	0.063	0.066	0.069
5.0	0.437	0.452	0.465	0.477	0.487	0.496	0.503	0.510	0.516	0.522	0.526
	0.031	0.034	0.036	0.039	0.042	0.045	0.048	0.050	0.053	0.055	0.058
6.0	0.457	0.474	0.489	0.502	0.514	0.524	0.534	0.542	0.550	0.557	0.563
	0.026	0.028	0.031	0.033	0.036	0.038	0.040	0.043	0.045	0.047	0.050
7.0	0.471	0.490	0.506	0.520	0.533	0.545	0.556	0.566	0.575	0.583	0.590
	0.022	0.024	0.027	0.029	0.031	0.033	0.035	0.037	0.039	0.041	0.043
8.0	0.482	0.502	0.519	0.534	0.549	0.561	0.573	0.584	0.594	0.602	0.611
	0.020	0.022	0.023	0.025	0.027	0.029	0.031	0.033	0.035	0.036	0.038
9.0	0.491	0.511	0.529	0.545	0.560	0.574	0.587	0.598	0.609	0.618	0.627
	0.017	0.019	0.021	0.023	0.024	0.026	0.028	0.029	0.031	0.033	0.034
10.0	0.498	0.519	0.537	0.554	0.570	0.584	0.597	0.610	0.621	0.631	0.641
	0.016	0.017	0.019	0.020	0.022	0.023	0.025	0.027	0.028	0.030	0.031
20.0	0.529	0.553	0.575	0.595	0.614	0.631	0.647	0.662	0.677	0.690	0.702
	0.008	0.009	0.010	0.010	0.011	0.012	0.013	0.013	0.014	0.015	0.016
500.0	**0.560**	0.587	0.612	0.635	0.656	0.677	0.696	0.714	0.731	0.748	0.763
	0.000	0.000	0.000	0.000	0.000	0.000	0.001	0.001	0.001	0.001	0.001

TABLE 5-2
Values of I_1 and I_2 to compute the Steinbrenner influence factor I_s for use in Eq. (5-16*a*) for several $N = H/B'$ and $M = L/B$ ratios *(continued)*

N	M = 2.5	4.0	5.0	6.0	7.0	8.0	9.0	10.0	25.0	50.0	100.0
0.2	I_1 = 0.007	0.006	0.006	0.006	0.006	0.006	0.006	0.006	0.006	0.006	0.006
	I_2 = 0.043	0.044	0.044	0.044	0.044	0.044	0.044	0.044	0.044	0.044	0.044
0.4	0.026	0.024	0.024	0.024	0.024	0.024	0.024	0.024	0.024	0.024	0.024
	0.074	0.075	0.075	0.075	0.076	0.076	0.076	0.076	0.076	0.076	0.076
0.6	0.053	0.051	0.050	0.050	0.050	0.049	0.049	0.049	0.049	0.049	0.049
	0.094	0.097	0.097	0.098	0.098	0.098	0.098	0.098	0.098	0.098	0.098
0.8	0.086	0.082	0.081	0.080	0.080	0.080	0.079	0.079	0.079	0.079	0.079
	0.107	0.111	0.112	0.113	0.113	0.113	0.113	0.114	0.114	0.114	0.114
1.0	0.121	0.115	0.113	0.112	0.112	0.112	0.111	0.111	0.110	0.110	0.110
	0.114	0.120	0.122	0.123	0.123	0.124	0.124	0.124	0.125	0.125	0.125
1.5	0.207	0.197	0.194	0.192	0.191	0.190	0.190	0.189	0.188	0.188	0.188
	0.118	0.130	0.134	0.136	0.137	0.138	0.138	0.139	0.140	0.140	0.140
2.0	0.284	0.271	0.267	0.264	0.262	0.261	0.260	0.259	0.257	0.256	0.256
	0.114	0.131	0.136	0.139	0.141	0.143	0.144	0.145	0.147	0.147	0.148
3.0	0.402	0.392	0.386	0.382	0.378	0.376	0.374	0.373	0.368	0.367	0.367
	0.097	0.122	0.131	0.137	0.141	0.144	0.145	0.147	0.152	0.153	0.154
4.0	0.484	0.484	0.479	0.474	0.470	0.466	0.464	0.462	0.453	0.451	0.451
	0.082	0.110	0.121	0.129	0.135	0.139	0.142	0.145	0.154	0.155	0.156
5.0	0.553	0.554	0.552	0.548	0.543	0.540	0.536	0.534	0.522	0.519	0.519
	0.070	0.098	0.111	0.120	0.128	0.133	0.137	0.140	0.154	0.156	0.157
6.0	0.585	0.609	0.610	0.608	0.604	0.601	0.598	0.595	0.579	0.576	0.575
	0.060	0.087	0.101	0.111	0.120	0.126	0.131	0.135	0.153	0.157	0.157
7.0	0.618	0.653	0.658	0.658	0.656	0.653	0.650	0.647	0.628	0.624	0.623
	0.053	0.078	0.092	0.103	0.112	0.119	0.125	0.129	0.152	0.157	0.158
8.0	0.643	0.688	0.697	0.700	0.700	0.698	0.695	0.692	0.672	0.666	0.665
	0.047	0.071	0.084	0.095	0.104	0.112	0.118	0.124	0.151	0.156	0.158
9.0	0.663	0.716	0.730	0.736	0.737	0.736	0.735	0.732	0.710	0.704	0.702
	0.042	0.064	0.077	0.088	0.097	0.105	0.112	0.118	0.149	0.156	0.158
10.0	0.679	0.740	0.758	0.766	0.770	0.770	0.770	0.768	0.745	0.738	0.735
	0.038	0.059	0.071	0.082	0.091	0.099	0.106	0.112	0.147	0.156	0.158
20.0	0.756	0.856	0.896	0.925	0.945	0.959	0.969	0.977	0.982	0.965	0.957
	0.020	0.031	0.039	0.046	0.053	0.059	0.065	0.071	0.124	0.148	0.156
500.0	0.832	0.977	1.046	1.102	1.150	1.191	1.227	1.259	1.532	1.721	1.879
	0.001	0.001	0.002	0.002	0.002	0.003	0.003	0.003	0.008	0.016	0.031

$$N = \frac{H}{B'}$$

$B' = \frac{B}{2}$ for center; $= B$ for corner I_i

$L' = L/2$ for center; $= L$ for corner I_i

The influence factor I_F is from the Fox (1948*b*) equations, which suggest that the settlement is reduced when it is placed at some depth in the ground, depending on Poisson's ratio and L/B. Figure 5-7 can be used to approximate I_F. You can also use Table 5-2, which gives a select range of I_1 and I_2 values, to compute the composite Steinbrenner influence factor I_s as

$$I_s = I_1 + \frac{1 - 2\mu}{1 - \mu} I_2 \qquad (c)$$

Program FFACTOR (option 6) can be used to obtain both I_F and I_s directly; you have only to input appropriate base dimensions (actual L, B for I_F and B', L' for I_s) and Poisson's ratio μ.

Equation (5-16) can be written more compactly as follows:

$$\Delta H = q_o B' \frac{1 - \mu^2}{E_s} m I_s I_F \qquad (5\text{-}16a)$$

where I_s is defined in Eq. (*c*) and m = number of corners contributing to settlement ΔH. At the footing center $m = 4$; at a side $m = 2$, and at a corner $m = 1$. Not all the rectangles have to have the same L'/B' ratio, but for any footing, use a constant depth H.

This equation is strictly applicable to *flexible bases* on the half-space. The half-space may consist of either cohesionless materials of any water content or unsaturated cohesive soils. The soils may be either inorganic or organic; however, if organic, the amount of organic material should be very small, because both E_s and μ are markedly affected by high organic content. Also, in organic soils the foregoing equation has limited applicability since secondary compression or "creep" is usually the predominating settlement component.

In practice, most foundations are flexible. Even very thick ones deflect when loaded by the superstructure loads. Some theory indicates that if the base is rigid the settlement will be uniform (but may tilt), and the settlement factor I_s will be about 7 percent less than computed by Eq. (*c*). On this basis if your base is "rigid" you should reduce the I_s factor by about 7 percent (that is, $I_{sr} = 0.931 I_s$).

Equation (5-16*a*) is very widely used to compute immediate settlements. These estimates, however, have not agreed well with measured settlements. After analyzing a number of cases, the author concluded that the equation is adequate but the method of using it was incorrect. The equation should be used [see Bowles (1987)] as follows:

1. Make your best estimate of base contact pressure q_o.
2. For round bases, convert to an equivalent square.
3. Determine the point where the settlement is to be computed and divide the base (as in the Newmark stress method) so the point is at the corner or common corner of one or up to 4 contributing rectangles (see Fig. 5-7).

TABLE 5-3

Comparison of computed versus measured settlement for a number of cases provided by the references cited.

Reference	H, ft	B, ft	L/B	D/B	N or q_c	E_s, ksf	μ	Δp, ksf	I_s	I_f	Settlement, in.	
											Computed	Measured
D'Appolonia et al. (1968)	$4B$	12.5	1.6	0.5	25*	1,200	0.33	3.4	0.589	0.75	0.33	0.3–0.4
Schmertmann (1970)												
Case 1	$5B$	8.5	8.8	0.78	40	310	0.4	3.74	0.805	0.87	1.45	1.53
Case 2	$5B$	9.8	4.2	1	120	620	0.3	3.34	0.774	0.75	0.67	0.8–0.9
Case 5	$5B$	62	1.0	0	65	350	0.45	1.56	0.50	1.0	2.64	2.48
Case 6	B	87	2.2	0.1	90	230	0.3	4.14	0.349	0.98	11.7	10.6
Case 8	$5B$	2	1.0	0.55	18	110	0.3	2.28	0.51	0.6	0.35	0.27
Tschebotarioff (1973)	$0.8B$	90	1.1	0.1	12*	270	0.3	7.2	0.152	0.95	3.9	3.9
Davisson and Salley (1972)	90	124	1	0	12–30*	390	0.3	3.14	0.255	1.0	5.6	5.3
Fischer et al. (1972)	1700	500	1	0.2	—	58 200	0.45	7.0	0.472	0.93	0.50	0.50
Webb and Melvill (1971)	150	177	1	0	—	1,100	0.3	4.5	0.161	1.0	1.27	1.50
Swiger (1974)	$4B$	32	1	0	—	3,900	0.3	2.75	0.493	1.0	0.24	0.24
Kantey (1965)	$3.5B$	20	1	0	50	260	0.3	4.0	0.483	1.0	3.25	3.20

Units: Used consistent with references.

*N value, otherwise is q_c. Values not shown use other methods for E_s.

Source: Bowles (1987).

4. Note that the stratum depth actually causing settlement is not at $H/B \rightarrow \infty$, but is at either of the following:
   a. Depth $z = 5B$ where B = least total lateral dimension of base.
   b. Depth to where a hard stratum is encountered. Take "hard" as that where E_s in the hard layer is about $10E_s$ of the adjacent upper layer.
5. Compute the H/B' ratio. For a depth $H = z = 5B$ and for the center of the base we have $H/B' = 5B/0.5B = 10$. For a corner, using the same H, obtain $5B/B = 5$. This computation sets the depth $H = z =$ depth to use for all of the contributing rectangles. Do not use, say, $H = 5B = 15$ m for one rectangle and $H = 5B = 10$ m for two other contributing rectangles—use 15 m in this case for all.
6. Enter Table 5-2, obtain I_1 and I_2, with your best estimate for μ compute I_s, and obtain I_F from Fig. 5-7. Alternatively, use program FFACTOR to compute these factors.
7. Obtain the *weighted average* E_s in the depth $z = H$. The weighted average can be computed (where, for n layers, $H = \sum_i^n H_i$) as

$$E_{s,\text{av}} = \frac{H_1E_{s1} + H_2E_{s2} + \cdots + H_nE_{sn}}{H} \qquad (d)$$

Table 5-3 presents a number of cases reanalyzed by the author using the foregoing procedure. It can be seen that quite good settlement estimates can be made. Earlier estimates were poor owing to two major factors: One was to use a value of E_s just beneath the base and the other was to use a semi-infinite half-space so that $I_s = 0.56$ (but the I_2 contribution was usually neglected—i.e., $\mu = 0.5$). A curve-fitting scheme to obtain I_s used by Gazetas et al. (1985) appeared to have much promise for irregular-shaped bases; however, using the method for some cases in Table 5-3 produced such poor settlement predictions compared with the suggested method that these equations and computation details are not recommended for use. Sufficient computations are given in Bowles (1987) to allow the reader to reproduce E_s and ΔH in this table.

This method for immediate settlements was also used to compute estimated loads for a set of five spread footings [see Briaud and Gibbens (1994)] for purposes of comparison with reported measured values for a settlement of $\Delta H = 25$ mm. A substantial amount of data was taken using the test methods described in Chap. 3, including the SPT, CPT, PMT, DMT, and Iowa stepped blade. For this text the author elected to use only the CPT method with q_c obtained by enlarging the plots, estimating the "average" q_c by eye for each 3 m (10 ft) of depth, and computing a resulting value using

$$\frac{\sum H_i q_{c,i}}{\sum H_i}$$

It was reported that the sandy base soil was very lightly overconsolidated so the cone constant was taken as 5.5 for all footings except the 1×1 m one where the size was such that any soil disturbance would be in the zone of influence. Clearly one can play a numbers game on the coefficient, however, with 3.5 regularly used for normally consolidated soils and from 6 to 30 for overconsolidated soils (refer to Table 5-6), any value from 4 to 7 would appear to apply—5.5 is a reasonable average. With these data and using the program FFACTOR on your diskette for the I_F and I_s (which were all 0.505, because the bases were square and

TABLE 5-4
Comparison of computed versus measured spread footing loads for a 25-mm settlement after 30 min of load. Poisson's ratio $\mu = 0.35$ for all cases.

$B \times B$, m	Cone $q_{c,\text{average}}$, kPa	Cone k	$E_S = kq_{c,\text{average}}$, kPa	B', m	Fox I_F	Soil pressure Δq, kPa	Footing load, kN	
							Computed	Measured
3 × 3	5940	5.5	32700	1.5	0.872	353	3177	4500
3 × 3	9580	5.5	52690	1.5	0.892	555	4995	5200
2 × 2	7185	5.5	39518	1.0	0.836	667	2668	3600
1.5 × 1.5	4790	5.5	26345	0.75	0.788	629	1415	1500
1 × 1	6706	3.5	23471	0.50	0.728	909	909	850

Load test data from Briaud and Gibbens (1994)

because we used an effective influence depth of $5B$) factors, Table 5-4 was developed. Any needed Fps values in the original reference were converted to SI.

Example 5-7. Estimate the settlement of the raft (or mat) foundation for the "Savings Bank Building" given by Kay and Cavagnaro (1983) using the author's procedure. Given data are as follows:

$q_o = 134$ kPa $B \times L = 33.5 \times 39.5$ m measured ΔH = about 18 mm

Soil is layered clays with one sand seam from ground surface to sandstone bedrock at -14 m; mat at -3 m.

E_s from 3 to 6 m = 42.5 MPa E_s from 6 to 14 m = 60 MPa

E_s for sandstone $\geq$ 500 MPa

Solution. For clay, estimate $\mu = 0.35$ (reference used 0.2). Compute

$$E_{s(\text{average})} = \frac{3 \times 42.5 + 8 \times 60}{11} = 55 \text{ MPa}$$

From base to sandstone $H = 14 - 3 = 11$ m.

$$B' = \frac{33.5}{2} = 16.75 \text{ m (for center of mat)} \rightarrow \frac{H}{B'} = \frac{11}{16.75} = 0.66 \text{ (use 0.7)}$$

Interpolating in Table 5-2, we obtain $I_1 = 0.0815$; $I_2 = 0.086$:

$$I_s = 0.0815 + \frac{1 - 2(0.35)}{1 - 0.35}(0.0865) = 0.121$$

$$\frac{D}{B} = \frac{3}{33.5} = 0.09; \text{ use } I_F = 0.95$$

With four contributing corners $m = 4$ and Eq. (5-16a) gives

$$\Delta H = q_o B' \frac{1 - \mu^2}{E_s} 4 I_s I_F$$

$$\Delta H = 134(16.75)\frac{1 - 0.35^2}{55 \times 1000}(4 \times 0.121)(0.95)(1000) = \mathbf{16.5} \text{ mm}$$

(The factor 1000 converts MPa to kPa and m to mm.)

This estimate is rather good when compared to the measured value of 18 mm. If this were made for a semi-infinite elastic half-space (a common practice) we would obtain (using E_s just under the mat)

$$\Delta H = 134\left[16.75\left(\frac{0.878}{42\,500}\right)(4 \times 0.56 \times 0.95 \times 1000)\right] = 98.6 \text{ mm}$$

which is seriously in error. You should study the reference and these computations to appreciate the great difficulty in making settlement predictions and then later trying to verify them—even approximately.

////

5-7 ROTATION OF BASES

It is sometimes necessary to estimate the rotation of a base. This is more of a problem with bases subjected to rocking moments producing vibrations (considered in more detail in Chap. 20), however, for static rotations as when a column applies an overturning moment it may be necessary to make some kind of estimate of the rotation.

A search of the literature produced five different solutions—none of which agreed well with any other—for flexible base rotation under moment. On this basis, and because theoretical solutions require full contact of base with the soil and with overturning often the full base area is not in contact, the best estimate would be made using a finite difference solution. The finite difference solution is recommended since the overturning moment can be modeled using statics to increase the node forces on the pressed side and decrease the node forces on the tension side. The average displacement profile across the base in the direction of the overturning effort can be used to obtain the angle of rotation. This computer program is B-19 in the package of useful programs for Foundation Design noted on your diskette.

Alternatively, the footing rotation can be expressed (see Fig. 5-8) as

$$\tan\theta = \frac{1-\mu^2}{E_s}\frac{M}{B^2L}I_\theta \tag{5-17}$$

where M = overturning moment *resisted by base dimension B*. Influence values I_θ that may be used for a rigid base were given by Taylor (1967) as in Table 5-5. Values of I_θ for a flexible base are given by Tettinek and Matl (1953, see also Frolich in this reference p. 362). These flexible values are intermediate to those of several other authorities. The rotation spring of

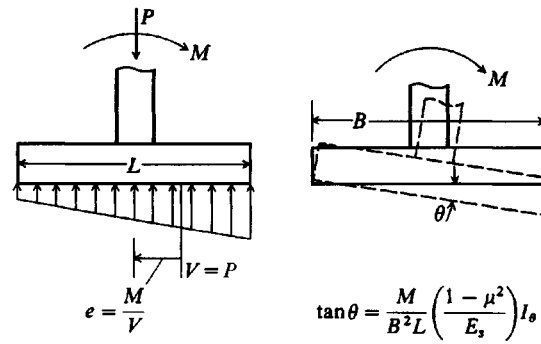

Figure 5-8 Rotation of a footing on an elastic base.

TABLE 5-5
Influence factors I_θ to compute rotation of a footing

L/B	Flexible	Rigid†	
0.1	1.045	1.59	
0.2	1.60	2.42	
0.50	2.51	3.54	
0.75	2.91	3.94	
1.00 (circle)	3.15 (3.00)*	4.17 (5.53)*	For rigid:
1.50	3.43	4.44	$I_\theta = 16/[\pi(1 + 0.22B/L)]$
2.00	3.57	4.59	
3.00	3.70	4.74	
5.00	3.77	4.87	
10.00	3.81	4.98	
100.00	3.82	$5.06 = 16/\pi$	

*For circle B = diameter.

†There are several "rigid" values; these are from equations given by Taylor (1967, Fig. 9, p. 227). They compare reasonably well with those given by Poulos and Davis (1974, p. 169, Table 7.3).

Table 20-2 may also be used to compute base rotation. Most practical footings are intermediate between "rigid" and "flexible" and require engineering judgment for the computed value of footing rotation θ.

Using a computer program such as B19 or the influence factors of Table 5-5 gives a nearly linear displacement profile across the footing length L. This result is approximately correct and will produce the *constant* pressure distribution of Fig. 4-4*a* since the soil will behave similarly to the compression block zone used in concrete beam design using the USD method. In that design the concrete strains are assumed linear but the compression stress block is rectangular. One could actually produce this case using program B19 (FADMATFD) if the nonlinear switch were activated and the correct (or nearly correct) value of maximum linear soil displacement XMAX were used. Enough concrete beam testing has been done to determine that the maximum linear strain is approximately 0.003. Finding an XMAX that would produce an analogous rectangular pressure profile under the pressed part of a footing undergoing rotation would involve trial and error. Making several runs of program B19 with a different XMAX for each trial would eventually produce a reasonable rectangular pressure profile, but this is seldom of more than academic interest. The only XMAX of interest in this type of problem is one that gives

$$q = \text{XMAX} \cdot k_s \leq q_a$$

When this is found the resulting average displacement profile can be used to estimate base and/or superstructure tilt.

Example 5-8.

Given. A rectangular footing with a column moment of 90 kN · m and $P = 500$ kN. Footing is $3 \times 2 \times 0.5$ m thick. The soil parameters are $E_s = 10\,000$ kPa, $\mu = 0.30$. The concrete column is 0.42×0.42 m and has a length of 2.8 m, and $E_c = 27.6 \times 10^6$ kPa. Estimate the footing rotation

 Next Page

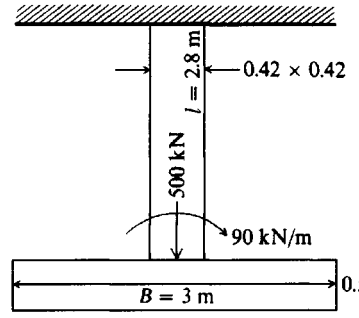

Figure E5-8

and find the footing moment after rotation assuming the upper end of the column is fixed as shown in Fig. E5-8.

Solution.

$$\frac{L}{B} = \frac{2}{3} = 0.67$$

$$I_\theta = 2.8 \text{ (interpolated from Table 5-5, column "Flexible")}$$

$$\tan\theta = \frac{1-\mu^2}{E_s}\frac{M}{B^2L}I_\theta$$

$$\tan\theta = \frac{1-0.3^2}{10\,000}\frac{90}{3^22}(2.8)$$

$$\tan\theta = 0.001\,274 \text{ rad}$$

$$\theta = \mathbf{0.073}^\circ$$

From any text on mechanics of materials the relationship between beam rotation and moment (when the far end is fixed, the induced $M' = M/2$) is

$$\theta = \frac{ML}{4EI}$$

from which the moment to cause a column rotation of θ is

$$M = \frac{4EI}{L}\theta$$

The column moment of inertia is

$$I = \frac{bh^3}{12} = \frac{0.42^3}{12} = 2.593 \times 10^{-3} \text{ m}^4$$

Substitution of I, E_c, L, and θ gives the released column moment of

$$M = 4\frac{(27.6 \times 10^6)(2.593 \times 10^{-3})(1.274 \times 10^{-3})}{2.8} = 130 \text{ kN} \cdot \text{m}$$

Since the rotation is equivalent to applying a moment of 130 kN · m opposite to the given M of 90 kN · m, the footing moment is reduced to zero **and the base $\theta \leq 0.073^\circ$**. There is also a change in the "far-end" column moment that is not considered here.

////

5-8 IMMEDIATE SETTLEMENTS: OTHER CONSIDERATIONS

We can interpret Eq. (5-16*a*) in terms of the Mechanics of Materials equation

$$\Delta H = \frac{PH}{AE} = \sigma\frac{L}{E} = \epsilon H$$

as previously given (and using symbols consistent with this text) where

$$\epsilon = q_o/E_s \qquad H = B(1 - \mu^2)mI_sI_F$$

The major problems, of course, are to obtain the correct E_s and H. It has already been noted with reference to Table 5-3 that one should use the weighted average value of E_s in the influence depth H. Obviously if H is fairly large and one obtains somehow only one value of E_s the resulting computation for ΔH may not be very reliable unless that one value happens to be the "weighted average" on a chance basis.

It is evident that for the usual range of Poisson's ratio μ of 0.2 to 0.4, this parameter has little effect on ΔH (using the extreme range from 0 to 0.5 only produces a maximum difference of 25 percent).

The influence depth H can be estimated reasonably well as noted with reference to Table 5-3 by taking the smaller of $5B$ or the depth to the hard layer, where the "hard" layer was defined as that where the stress-strain modulus was $\geq$ 10 times E_s of the next adjacent layer. One will have to use some judgment if the soil grades from stiff to stiffer so that a factor of 10 is not clearly defined.

Finally we note that the depth factor I_F can reduce computed settlements considerably for $D/B \rightarrow 1$.

Determination of the Stress-Strain Modulus E_s

Several methods are available for determining (actually estimating) the stress-strain modulus:

1. Unconfined compression tests
2. Triaxial compression tests
3. In situ tests
   - *a.* SPT
   - *b.* CPT
   - *c.* Pressuremeter
   - *d.* Flat dilatometer
   - *e.* Iowa stepped blade
   - *f.* Plate-load tests

Unconfined compression tests tend to give conservative values of E_s; i.e., the computed value (usually the initial tangent modulus) is too small, resulting in computed values of ΔH being large compared with any measured value. If the value of ΔH is excessively[2] large, the selection of foundation type may be adversely affected; that is, a recommendation for piles or caissons might be made when, in fact, spread footings would be satisfactory.

[2]Termed *overly conservative* in engineering lexicon.

Triaxial tests tend to produce more usable values of E_s since any confining pressure "stiffens" the soil so that a larger initial tangent modulus is obtained. Other factors such as whether the triaxial test is a U, CU, or CK_oU tend to affect the E_s obtained (see Sec. 2-14). Generally triaxial tests will also be conservative but not quite so much as unconfined compression tests. This observation was somewhat confirmed by Crawford and Burn (1962), where E_s in situ was estimated to be 4 to 13 times as large as that obtained from laboratory q_u test plots and about 1 to 1.5 times those obtained from triaxial U tests.

The in situ tests of SPT and CPT tend to use empirical correlations to obtain E_s. Other in situ tests such as the pressuremeter, the flat dilatometer, and the Iowa stepped blade tend to obtain more direct measurements of E_s. The value of stress-strain modulus E_s obtained from these tests is generally the horizontal value—but the vertical value is usually needed for settlements. Most soils are anisotropic, so the horizontal E_{sh} value may be considerably different from the vertical value E_{sv}.[3] Overconsolidation may also alter the vertical and horizontal values of stress-strain modulus.

Anisotropy, stress history, natural cementation, and overconsolidation are likely to be very significant factors in determining E_s, especially for cohesionless soils. In cohesionless soils cementation is particularly significant; for individual soil grains the effect can be very small, but the statistical accumulation for the mass can have a large effect. Cementation (also called "aging") can be easily lost in recovered cohesionless samples. Drilling disturbances in cohesionless soils for the purpose of performing pressuremeter, dilatometer, or other tests may sufficiently destroy the cementation/aging in the vicinity of the hole to reduce E_s to little more than an estimate.

Because the laboratory values of E_s are expensive to obtain and are generally not very good anyway owing to sampling disturbance, the standard penetration test (SPT) and cone penetration test (CPT) have been widely used to obtain the stress-strain modulus E_s resulting from empirical equations and/or correlations. Table 5-6 gives a number of equations for possible use in several test methods. The value to use should be based on local experience with that equation giving the best fit for that locality. Referring to Table 5-6, we can see that a good estimate for the SPT is

$$E_s = C_1(N + C_2)$$

where values of $C_2 = 6$ and 15 are shown and C_1 ranges from 250 upward. This equation can also be written (see again Table 5-6) as

$$E_s = C_2' + C_1 N \qquad C_2' = C_1 C_2$$

For best results one should attempt to determine the C_i constants for the local area. The increase for $E_{s,\text{OCR}}$ using the multiplier $\sqrt{\text{OCR}}$ seems to be reasonably valid (and substantially used), although again local materials/practice might produce a slightly better multiplier.

For the CPT test the stress-strain modulus in Table 5-6 is of the general form

$$E_s = C_3 + C_4 q_c$$

where C_3 ranges from 0 upward and C_4 may be one of the values also shown in Table 5-6. Values of $C_3 = 0$ and $C_4 = 2.5$ to 3.0 for normally consolidated sands seem rather widely used.

[3] Always used as E_s in this text unless specifically noted otherwise.

A significant factor for the CPT is that there may be some critical depth below which the cone resistance q_c is nearly constant. This has a theoretical basis in that, below this depth, a local bearing failure develops in a small zone around the tip of the cone. Obviously the soil stiffens with depth (but not beyond bound). Depth increases may not be very large owing to "local" failure around the cone tip. Thus, the use of an equation of the general form

$$E_s = C_3 + C_4 q_c \tan^{-1}\left(\frac{z}{D}\right)^n$$

may be necessary to maintain reasonable values for E_s at the several depth increments z through the test zone depth of D.

For this reason values of E_s obtained using N values from the SPT may be more reliable than those from the CPT. We also note that the cone test is essentially a measure of ultimate bearing capacity on the cone tip (which has an area of only 10 cm^2). This phenomenon is illustrated on Figs. 3-14, 3-17, and in the cone data of Table P3-11, where nearly constant q_c values are shown at large D/B ratios. This observation means that one may not obtain very good estimates of E_s at depths beyond the critical depth (usually in the form of a depth ratio such as 15 to 100 D/B)[4] of the cone unless the overburden pressure over the depth of interest is somehow included, perhaps by using a variable C_5 ranging from 0 to 100 as follows:

$$C_4 = \left(\frac{C_5 + p'_o}{p'_o}\right)^n \qquad \text{or} \qquad C_4 = C_5 + \log p'_o$$

where p'_o = the effective overburden pressure at the depth D (or D/B) of interest as previously defined in Chap. 2

n = exponent with a value usually ranging from 0.4 to 0.7 (but other values might be used)

The Effect of the Overconsolidation Ratio (OCR) on E_s

Table 5-6 gives the commonly used multiplier $\sqrt{\text{OCR}}$ used to increase the normally consolidated value of stress-strain modulus $E_{s,\text{nc}}$. By using the square root of OCR the effect is certainly not so great as using OCR as the multiplier. When the soil is *overconsolidated* the following occur:

1. The soil $E_{s,\text{OCR}}$ should be larger than $E_{s,\text{nc}}$. However, we are usually concerned with the vertical value, so that the "OCR" value may not be much larger than the normally consolidated vertical value of E_s.
2. If in situ tests are used, the horizontal value of E_{sh} is obtained. For an overconsolidated soil this value may be very much larger than the vertical value, but this estimate depends heavily on how much soil disturbance (or lateral expansion) occurred when the hole was drilled and/or test device inserted.
3. In overconsolidated soils if the soil is excavated (as for a large and/or deep basement) and expands from loss of overburden, the resulting E_s is smaller than before and may be very much smaller, perhaps requiring a new test(s).

[4]Noting that the cone diameter B (= 35.6 mm) is not great, only a shallow depth D will produce a large D/B ratio for a cone test.

TABLE 5-6
Equations for stress-strain modulus E_s by several test methods

E_s in kPa for SPT and units of q_c for CPT; divide kPa by 50 to obtain ksf. The N values should be estimated as N_{55} and not N_{70}. Refer also to Tables 2-7 and 2-8.

Soil	SPT	CPT
Sand (normally consolidated)	$E_s = 500(N + 15)$ $= 7000\sqrt{N}$ $= 6000N$ — — — ‡$E_s = (15\,000 \text{ to } 22\,000) \cdot \ln N$	$E_s = (2 \text{ to } 4)q_u$ $= 8000\sqrt{q_c}$ — — — $E_s = 1.2(3D_r^2 + 2)q_c$ *$E_s = (1 + D_r^2)q_c$
Sand (saturated)	$E_s = 250(N + 15)$	$E_s = Fq_c$ $e = 1.0 \quad F = 3.5$ $e = 0.6 \quad F = 7.0$
Sands, all (norm. consol.)	¶$E_s = (2600 \text{ to } 2900)N$	
Sand (overconsolidated)	†$E_s = 40\,000 + 1050N$ $E_{s(\text{OCR})} \approx E_{s,\text{nc}}\sqrt{\text{OCR}}$	$E_s = (6 \text{ to } 30)q_c$
Gravelly sand	$E_s = 1200(N + 6)$ $= 600(N + 6) \quad N \le 15$ $= 600(N + 6) + 2000 \quad N > 15$	
Clayey sand	$E_s = 320(N + 15)$	$E_s = (3 \text{ to } 6)q_c$
Silts, sandy silt, or clayey silt	$E_s = 300(N + 6)$ If $q_c < 2500$ kPa use $\quad$ $^{\$}E'_s = 2.5q_c$ $2500 < q_c < 5000$ use $\quad E'_s = 4q_c + 5000$ where E'_s = constrained modulus $= \dfrac{E_s(1-\mu)}{(1+\mu)(1-2\mu)} = \dfrac{1}{m_v}$	$E_s = (1 \text{ to } 2)q_c$
Soft clay or clayey silt		$E_s = (3 \text{ to } 8)q_c$

4. It is not easy to determine if a cohesionless deposit is overconsolidated or what the OCR might be. Cementation may be less difficult to discover, particularly if during drilling or excavation sand "lumps" are present. Carefully done consolidation tests will aid in obtaining the OCR of cohesive deposits as noted in Chap. 2.

In general, with an OCR > 1 you should carefully ascertain the site conditions that will prevail at the time settlement becomes the design concern. This evaluation is, of course, true for any site, but particularly so if OCR > 1.

5-9 SIZE EFFECTS ON SETTLEMENTS AND BEARING CAPACITY

5-9.1 Effects on Settlements

A major problem in foundation design is to proportion the footings and/or contact pressure so that settlements between adjacent footings are nearly equal. Figure 5-9 illustrates the problem

TABLE 5-6

Equations for stress-strain modulus E_s by several test methods (*continued*)

E_s in kPa for SPT and units of q_c for CPT; divide kPa by 50 to obtain ksf. The N values should be estimated as N_{55} and not N_{70}. Refer also to Tables 2-7 and 2-8.

Soil		
	Use the undrained shear strength s_u in units of s_u	
Clay and silt	$I_P > 30$ or *organic*	$E_s = (100 \text{ to } 500)s_u$
Silty or sandy clay	$I_P < 30$ or *stiff*	$E_s = (500 \text{ to } 1500)s_u$ Again, $E_{s,\text{OCR}} \approx E_{s\,\text{nc}}\sqrt{\text{OCR}}$ Use smaller s_u-coefficient for highly plastic clay.

Of general application in clays is

$$E_s = Ks_u \quad \text{(units of } s_u\text{)} \tag{a}$$

where K is defined as

$$K = 4200 - 142.54I_P + 1.73I_P^2 - 0.007\,1I_P^3 \tag{b}$$

and I_P = plasticity index in **percent.** Use $20\% \le I_P \le 100\%$ and round K to the nearest multiple of 10.

Another equation of general application is

$$E_s = 9400 - 8900I_P + 11\,600I_c - 8800S \quad \text{(kPa)} \tag{c}$$

I_P, I_c, S = previously defined above and/or in Chap. 2

*Vesić (1970).

†Author's equation from plot of D'Appolonia et al. (1970).

‡USSR (may not be standard blow count N).

¶Japanese Design Standards (lower value for structures).

$Senneset et al. (1988)

General sources: First European Conference on Standard Penetration Testing (1974), vol. 2.1, pp. 150–151; *CGJ,* November 1983, pp. 726–737; *Use of In Situ Tests in Geotechnical Engineering,* ASCE (1986), p. 1173; Mitchell and Gardner (1975); *Penetration Testing (Second European Conference)* (1982), vol. 1, p. 160; 11th ICSMFE (1985), vol. 2, pp. 462, 765; vol. 4, p. 2185; *International Symposium on Penetration Testing* (1988), 2 vols.

Notes:

1. For q_c generally use $(2.5 \text{ to } 3)q_c$ for normally consolidated sand and about 4 to 6 q_c for overconsolidated sand.
2. Can use Eqs. (*a*) and (*b*) above for all clay. They are particularly applicable for OCR > 1. Probably should use both Eqs. (*a*) and (*c*), and if results differ significantly either use an average or compute another E_s using a different equation.
3. For sands try to use more than one equation or else use one of the equations and compare the computed E_s to published table (see Table 2-8) values.
4. For silts use any of the above equations, but if the equations are given for sand use smaller coefficients.
5. For sand, using $E_s = 250$ or $500(N + 15)$ may give a modulus that is too small (but conservative). Suggest when you use equations of this form you compute E_s by one or more additional equations and average the results.
6. Note: Using $\sqrt{\text{OCR}}$ is the same as $(\text{OCR})^{1/2}$, so that exponent $n = 0.5$. You can use other values for the exponent from about 0.3 to 0.5. However, since all the equations for E_s are approximations the use of $n = 0.5$ is sufficiently accurate unless you have good-quality field or laboratory test values.

(and why plate load tests have little real value). It is evident that if the depth of influence is $H = 5B$, a 0.3-m square plate has an influence depth of $5 \times 0.3 = 1.5$ m, whereas a 2-m prototype would have a depth of $5 \times 2 = 10$ m. Considerable changes in the soil can occur in that amount of depth increase.

To address this problem theoretically, let us rewrite Eq. (5.16*a*) [taking $(1 - \mu^2)/E_s = E'_s$] as

$$\Delta H_1 = q_{o1} B'_1 m I_{s1} I_{F1} E'_{s1} \qquad (a)$$

$$\Delta H_2 = q_{02} B'_2 m I_{s2} I_{F2} E'_{s2} \qquad (b)$$

where q_{oi} = base contact pressure (usually using the allowable bearing pressure q_a)
B'_i = base widths as defined with Eq. (5-16*a*)
I_{si} = settlement influence factors based on $H/B'_{i,i}$ and L'/B'
m = number of I_{si} contributions, 1, 4, etc.
I_{Fi} = factors based on the D/B_i ratio
E'_{si} = average stress-strain modulus over the effective depths H (= $5B$ or actual H to hard stratum). In general, $E'_{s2} < E'_{s1}$ for $B'_2 > B'_1$ but the increase will not usually be linear.

Dividing Eq. (*b*) by Eq. (*a*) we obtain

$$\frac{\Delta H_2}{\Delta H_1} = \frac{q_{o2}}{q_{o1}} \frac{B'_2}{B'_1} \frac{m I_{s2}}{m I_{s1}} \frac{I_{F2}}{I_{F1}} \frac{E'_{s2}}{E'_{s1}} \qquad (5\text{-}18)$$

This equation is as theoretically correct as the basic settlement equations. What has been done in the past is this:

1. For clay soils assume constant E'_{si}, I_{Fi}, and mI_{si} so that we have

$$\frac{\Delta H_2}{\Delta H_1} = \frac{q_{o2}}{q_{o1}} \frac{B'_2}{B'_1} \qquad (c)$$

which simplifies for constant contact pressure $q_o (= q_{o1} = q_{o2})$ to

$$\Delta H_2 = \Delta H_1 (B'_2/B'_1) \qquad (d)$$

This equation has been very widely used for clay soils. It simply states in equation form that the settlement of a footing of width B_2 is the settlement of a footing of width

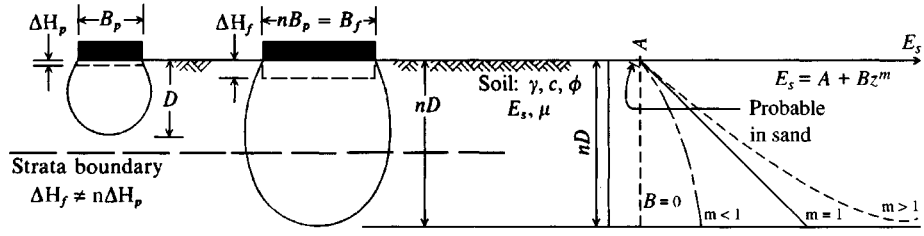

Figure 5-9 Influence of footing size on the depth of the stress zone and E_S. Note that, with an underlying stratum of different soil, the plate settlement does not reflect stresses in this material; thus, the settlement of the full-size footing can be seriously underestimated.

$B_1(=\Delta H_1)$ times the ratio of the footing widths B_2/B_1. Experience indicates the use of this approximation has been reasonably satisfactory.

2. For sand soils the same assumptions of constant values except for B_i' were made but this procedure did not predict very well. Multipliers were sought, and one of the most popular [Terzaghi and Peck (1967), p. 489] was

$$\Delta H_2 = \Delta H_1 \left(\frac{2B_2'}{B_2' + B_1'} \right)^2 \tag{e}$$

Usually B_1' was a load test plate of size 1×1 ft or 0.3×0.3 m and B_2' was the prototype footing of dimension B. The influence of this equation can be seen with the bearing-capacity equation [Eq. (4-12)]. This equation did not provide very good estimates, so another proposal changes the ΔH_1 multiplier to

$$\left(\frac{B_2'}{B_1'} \right)^n \qquad \text{or} \qquad \left(\frac{A_2}{A_1} \right)^n$$

where A_i = base areas and values of 0.4 to 0.7 are often suggested for the exponent n (0.5 is most common).

It should be evident that there is little chance of producing a reasonable multiplier—particularly if the B_2/B_1 ratio is very large, as for using a 0.3-m square plate to extrapolate to a 2- to 3-m square base (or to a 20- or 30-m square mat). The reason is that sand requires confinement to develop strength (or E_s). If we assume that 75 mm (or 3 in.) around the perimeter of any size plate provides the "confinement" to the interior sand, then only one-fourth of a 0.3-m square plate is effective. Thus, the apparent E_s is too small at the surface compared to the prototype, which may be of size 2×2 m and which, with the edge loss, is about 93 percent effective. Therefore, the E_{s2}'/E_{s1}' ratio would be in error and the anticipated settlements of the large plate B_2' too large (but conservative). A literature survey by the author indicates that for large B_2'/B_1' ratios the increased settlement ΔH_2 should not exceed about $1.6(\Delta H_1)$ or the reduced allowable bearing capacity q_{a2} should not be less than about $0.4q_{a1}$. For small footing ratios of about 1.1 to 3 the settlement ratios should be about 1.1 to 1.2 and the pressure ratios about 0.9 to 0.8.

For these reasons, and because Eq. (5-18) is theoretically exact, its use is recommended.

5-9.2 Effects on Bearing Capacity

Another use of Eq. (5-18) is for bearing capacity. Here we take $\Delta H_1 = \Delta H_2$ so settlements are equal and replace $q_{o1} = q_{a1}$; $q_{o2} = q_{a2}$. Rearranging terms we obtain

$$q_{a2} = q_{a1} \frac{B_1'}{B_2'} \frac{E_{s1}'}{E_{s2}'} \frac{mI_{s1}}{mI_{s2}} \frac{I_{F1}}{I_{F2}} \tag{5-19}$$

The analogy of Eq. (e), taking settlement directly proportional to q_a, gives

$$q_{a2} = q_{a1} \left(\frac{B_2 + B_1'}{2B} \right)^2 \tag{f}$$

The effect of base width was included in Eq. (4-12), somewhat similarly to Eq. (f). Equation (f) tends to be too conservative—particularly for extrapolating plate-load tests to prototype

bases—and is not much used at present. The author recommends using Eq. (5-19) for theoretical accuracy, and the additional parameters seldom produce great difficulty because q_a is usually obtained from SPT or CPT data and it is a trivial exercise to obtain the stress-strain modulus additionally from tables such as Table 5-6.

Example 5-9. The geotechnical consultant on a foundation project has obtained the soil data and profile as shown on Fig. E5-9. A best average of N values (they were nearly constant as in Fig. P3-10) gave $N'_{70} = 20$ shown. Column loads including dead and live loads are estimated in the range of 450 to 900 kN (100 to 200 kips).

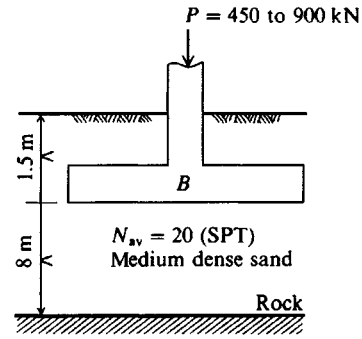

Figure E5-9

Required. Recommend q_a for this project so that ΔH is limited to not over 25 mm.

Solution.

Step 1. Find a tentative q_a using Eq. (4-12). Convert N_{70} to N_{55}, giving $N_{55} = 20(70/55) = 25.45$. Use $N_{55} = 25$.

From Eq. (4-12),

$$q_a = \frac{N_{55}}{0.08}\left(\frac{B+0.3}{B}\right)^2\left(1+0.33\frac{D}{B}\right) \qquad \text{but} \qquad 1+0.33\frac{D}{B} \le 1.33$$

B, m	$1+0.33\frac{D}{B}$	q_a, kPa (rounded)
1.2	1.33	650 [probably no $B < 1.2$ m]
2.0	1.25	515
3.0	1.17	440

The actual soil pressure q for the given range of column loads and for $B = 1.5$ m is from

$$q = \frac{P}{A} = \frac{450}{1.5 \times 1.5} = 200 \text{ kPa}$$

to

$$q = \frac{900}{2.25} = 400 \text{ kPa}$$

Both of these soil pressures are much less than q_a in the foregoing table. *Tentatively recommend* $q_a = \mathbf{250}$ kPa. The maximum allowable soil pressure, as an *approximate* average of the three table values, is about **500** kPa (actual average = 535) with a maximum settlement $\Delta H \approx 25$ mm.

Step 2. Check settlement for $q_a = 250$ kPa.

$$B^2 q_a = P_{av}$$

$$B = \sqrt{\frac{450 + 900}{2 \times 250}} = 1.6 \text{ m as the average width } B$$

For $B = 1.6 \times 1.6$ m we have $L/B = 1$

$$B' = \frac{1.6}{2} = 0.8 \qquad \text{and} \qquad \frac{H}{B'} = \frac{8}{0.8} = 10 \qquad \left(\text{or } \frac{H}{B} = 5\right)$$

From Table 5-2 at $H/B' = 10$ and $L/B = 1$ we obtain

$$I_1 = 0.498 \qquad I_2 = 0.016 \qquad \text{For sand, estimate } \mu = 0.3$$

$$I_s = I_1 + \frac{1 - 2\mu}{1 - \mu} I_2 \qquad I_s = 0.498 + \frac{0.4}{0.7}(0.016) = 0.507$$

From Fig. 5-7 at $D/B = 1.5/1.6 = 0.94$ we obtain $I_F = 0.65$ (using program FFACTOR we obtain 0.66). From Table 5-6 we estimate E_s for a normally consolidated sand as

$$E_s = 500(N + 15) = 500(25 + 15) = 20\,000 \text{ kPa} \qquad \text{(note use of } N_{55})$$

Using $E_s = 2600\,N$, we write

$$E_s = 2600 \text{ N} = 2600(25) = 65\,000 \text{ kPa} \qquad \text{(also } N_{55})$$

and if $E_s = 7000\sqrt{\text{N}}$, we have

$$E_s = 7000\,N = 7000\sqrt{25} = 35\,000 \text{ kPa}$$

From Table 2-7 the value of 20 MPa appears reasonable (and conservative). Substituting values into Eq. (5-16*a*) with $q_a = q_o$, we have

$$\Delta H = q_o B' \frac{1 - \mu^2}{E_s} m I_s I_F$$

and, noting $m = 4$ for the center settlement we have

$$\Delta H = 250(0.8)\frac{1 - 0.3^2}{20\,000}(4 \times 0.507)(0.65)(1000) = \mathbf{12} \text{ mm}$$

The factor 1000 converts ΔH in m to mm. For $E_s = 65\,000$,

$$\Delta H = 12\left(\frac{20}{65}\right) = 3.7 \text{ mm}$$

Here we can also ratio q_a (maximum $q_a \approx 500$ kPa for $\Delta H = 25$ mm) to obtain

$$\frac{\Delta H}{25 \text{ mm}} = \frac{q_{a,\text{used}}}{q_{a,\max}} \rightarrow \Delta H = 25(250/500) = \mathbf{12.5} \text{ mm}$$

It would appear that in the range of $B = 1.5$ to 2.5 m the settlements will be well under 25 mm and differential settlements (difference in settlements between adjacent footings of different size) will be acceptable. An "averaged" E_s could have been used but was not needed as the minimum value gives acceptable ΔH and great computational refinement is not needed at this preliminary stage of design.

Recommend: $q_a = 250$ kPa (about 5 ksf)

$\Delta H =$ under 25 mm

////

Example 5-10.

Given. Spread footings on an overconsolidated (or very heavily compacted) dune sand [D'Appolonia et al. (1968) and in Table 5-3].

Required. Estimate the probable footing settlements.

Solution. From careful reading of the reference we obtain the average $B = 12.5$ ft and $L/B = 1.6$; also $\mu = 0.33$ was given.

From the boring log of Fig. 6 and soil profile of Fig. 2 of the reference we can estimate $H = 4B$. Also take $N_{55} = 25$ as the estimated weighted average in depth $H = 4B$, noting that borings stopped at approximately $N_{55} = 40$ before the full depth of $4B$. From the data given the preconsolidation was from dunes to elevations of 650 and 700 from the base elevations of 607 ft. Using $\gamma = 0.110$ kcf and an average depth of 6 ft below footing base we can estimate the OCR at between 7 and 15. We will take OCR = 9 as a reasonable "average." The footing load q_o at the time settlement measurements were taken was approximately 3.4 ksf (about 55 percent of the design load). Finally, the D/B ratio was given as 0.5 on average.

With these data we can proceed with a solution.

For $H/B' = 2(4B)/B = 8$ and $L/B = 1.6$ we obtain from Table 5-2

$$I_1 = 0.573 \quad \text{and} \quad I_2 = 0.031$$

Also for $D/B = 0.5$ we obtain $I_F = 0.75$ from Fig. 5-7. Then

$$I_s = 0.573 + \frac{1 - 2(0.33)}{1 - 0.33}(0.031) = 0.589$$

For E_s use Table 5-5 with OCR = 9

$$E_s = 10(N + 15)\text{OCR}^{1/2} \qquad \text{(obtain } 10 = 500/50 \text{ for ksf)}$$

$$E_s = 10(25 + 15)(9)^{1/2} = 1200 \text{ ksf}$$

$$\Delta H = 3.4\left(\frac{12.5}{2}\right)\left(\frac{1 - 0.33^2}{1200}\right)(4 \times 0.589)(0.75)(12) = \mathbf{0.335} \text{ in.}$$

The "measured" values as shown in Table 5-3 ranged from 0.3 to 0.4 inches.

////

Example 5-11. What is the expected *corner* settlement of the footing of Ex. 5-9?

Solution. For $q_a = 250$ kPa $= q_o$; $\mu = 0.3$; $E_s = 20\,000$ kPa, and using the "average" $B = 1.6 \times 1.6$ m of step 2, we have

$$D/B = 1.5/1.6 = 0.94 \qquad \text{and} \qquad I_F = 0.65 \qquad \text{(as before)}$$

$$H/B' = H/B = 8/1.6 = 5 \qquad \text{(with } L/B = 1\text{)}$$

using program FFACTOR, obtain

$$I_1 = 0.437 \quad \text{and} \quad I_2 = 0.031 \qquad I_s = 0.437 + \frac{0.4}{0.7}(0.031) = \mathbf{0.455}$$

Substituting into Eq. (5-16*a*) using $B' = B$ for the corner and noting with a corner there is only one contribution ($m = 1$), we obtain

$$\Delta H = 250(1.6)\left(\frac{1-0.3^2}{20\,000}\right)(1 \times 0.455)(0.65)(1000) = \mathbf{5.4}\text{ mm}$$

Observe that the corner settlement is not equal to the center settlement divided by four (12/4 = 3 mm < 5.4 mm computed here).

////

5-10 ALTERNATIVE METHODS OF COMPUTING ELASTIC SETTLEMENTS

Since the elastic settlement is simply

$$\Delta H = \int_0^H \epsilon\, dh = \sum_{i=1}^{n} \epsilon_i H_i$$

any method that accurately gives the strains in the identified influence depth H would give an accurate evaluation of the settlement ΔH. As can be seen in Table 5-3 there is at present no better procedure than that proposed using Eq. (5.16*a*); however, in foundation engineering local practice sometimes prevails over any "best" method. For this reason the following two alternatives are given—not as any author recommendation—so that the reader has familiarity with the procedures.

One method is that proposed by Schmertmann (1970) wherein the change in the Boussinesq pressure bulb was interpreted as related to the strain. Since the pressure bulb changes more rapidly from about 0.4 to 0.6B, this depth is interpreted to have the largest strains. Schmertmann then proposed using a triangular relative-strain diagram to model this strain distribution with ordinates of 0, 0.6, and 0 at 0B, 0.5B, and 2B, respectively. The area of the diagram is related to the settlement, and for constant E_s, which is the same assumption used to develop the strain profile, one may directly compute the settlement as the area of the triangle × strain to obtain

$$\Delta H = 0.6B\frac{\Delta q}{E_s} = 0.6B\epsilon \tag{5-20}$$

Schmertmann also incorporated two correction factors for embedment depth and time as follows:

$$\text{For embedment} \qquad C_1 = 1 - 0.5\frac{\overline{q}}{q_o - \overline{q}}$$

$$\text{For time} \qquad C_2 = 1 + 0.2\log\frac{t}{0.1}$$

where $\overline{q}$ and q_o have been previously defined and t is time > 0.1 in years. With these correction factors Eq. (5-20) now is written as

$$\Delta H = C_1 C_2 (0.6B)\epsilon \tag{5-20a}$$

If E_s is not constant, Schmertmann proposed to plot the strain profile and obtain influence factors I_z at the center of each change in E_s over a depth increment Δz to obtain

$$\Delta H = C_1 C_2 \Delta q \sum \frac{I_z \Delta z}{E_s} \tag{5-20b}$$

This calculation would obviously give a conservative ΔH if E_s is constant or increases with depth. If lower layers have a much smaller E_s the solution could give ΔH that is underpredicted. With these two correction factors and $E_s = 2q_c$ (using cone data), Schmertmann computed a number of cases from the literature (some of which are used by the author in Table 5-3) and obtained only fair agreement between computed and measured values of ΔH.

Another procedure is to use the stress path method of Sec. 2-13. In this method one performs a series of triaxial tests at in situ CK_oUC conditions and plots $2q = \sigma_1 - \sigma_3$ versus the strain ϵ for points along the vertical center line of the foundation at depths of, say,

$$B/4,\ B/2,\ B,\ 1.5B,\ 2B,\ 3B, \text{ and } 4B, \text{ or similar}$$

Fewer tests can be used, but confinement ($K_o\sigma_1$) is a significant parameter that has a considerable effect on the strain ϵ, requiring that enough tests be made in the upper depth of $z = 0$ to $4B$ to provide a reliable strain profile so one can use

$$\Delta H = \sum_{1}^{n} \epsilon_i H_i$$

This method requires careful construction of sand samples or use of good-quality "undisturbed" clay samples. It may give good results for normally consolidated sands but not for overconsolidated and/or cemented sands because sample reconstruction will be impossible. According to Lambe and Whitman (1979, p. 218) the settlement can be rather well predicted, but their example used eight triaxial tests in a medium to fine sand that apparently was not preconsolidated ($K_o = 0.4$) to find the displacement beneath a round tank. D'Appolonia et al. (1968) in the overconsolidated dune sand (of Example 5-9) used this procedure with two series of footings with seven triaxial tests each at the minimum and maximum estimated OCRs on the site with only fair correlation.

Since we start the triaxial tests from in situ K_o consolidated conditions it is evident that the triaxial test stress $\Delta\sigma_1$ has a 1 : 1 correspondence to the footing stress Δq at that depth. The Boussinesq method is commonly used to estimate Δq. Unless the stress path procedure is perceived to give substantially better settlement estimates, its cost will be far out of proportion to results because of the large number of triaxial tests required.

Example 5-12. Compute the immediate elastic settlement for the soil–footing system shown in Fig. E5-12*a*.

Preliminary work. A series of triaxial (or direct shear) tests must be run to establish ϕ. With ϕ the K_o soil pressure can be computed so that the triaxial tests are performed at that value of cell pressure σ_3. Plot the initial part of the stress-strain curve to a large scale as shown in Fig. E5-12*b*. For cyclic tests plot the last cycle and shift the ordinate so the curve passes through the origin. For this example take

$$\phi = 35^\circ \qquad \gamma_1 = 17.3 \qquad \gamma_2 = 19.1 \text{ kN/m}^3$$
$$K_o = 1 - \sin 35^\circ = 0.426$$

Use a single value of ϕ even though it has been previously noted that ϕ varies with soil density.

Test 1: $p_o = 2(17.3) = 34.6$ kPa $\qquad \sigma_3 = 0.426(34.6) = 14.7$ kPa

Use cell pressure = 20 kPa (approx. 3 psi)

Test 2: $p_o = 3(17.3) + 1.5(19.1) = 80.6$ kPa (estimating density)

Use cell pressure = 40 kPa

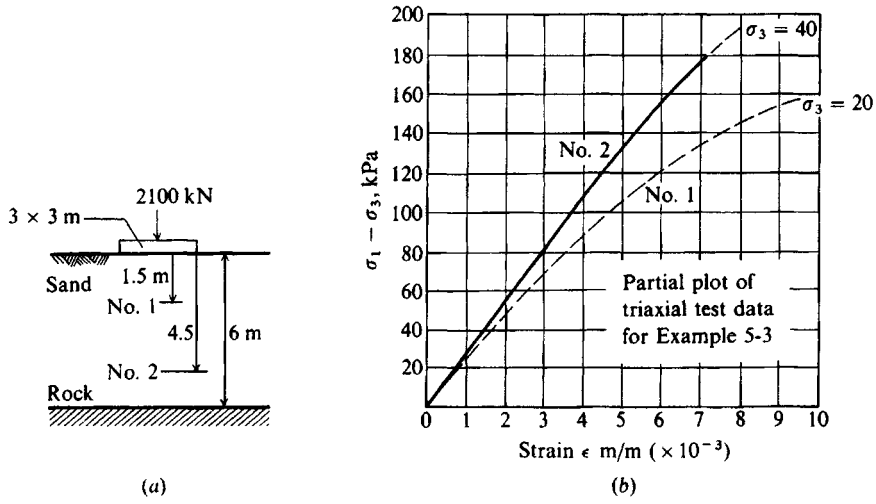

Figure E5-12

It is not a simple matter to test reliably at very low cell pressures. Usually it is not easy to build sand samples to specific densities. At low cell pressures the vacuum used to hold the sample in place until the cell pressure can be applied can "preconsolidate" the sample some amount. Probably three or four tests would be better for this foundation but two are sufficient to illustrate the procedure.

Required. Estimate footing settlement using

a. Stress path method.

b. $\Delta H = \Delta\sigma_1 L/E_s$. Use a secant modulus of elasticity passing through the origin and stress point.

Solution. Divide the 6-m stratum into four increments and make Table E5-12. Obtain q/q_o from Fig. 5-4;

$$q_h = q_v K_o \qquad \text{obtain } \epsilon \text{ from stress-strain plot at } \Delta\sigma_1$$

$$\Delta\sigma_1 = q_v - q_h = q_v(1 - K_o) = \sigma_1 - \sigma_3$$

$$q_o = \frac{2100}{9} = 233.3 \text{ kPa}$$

At $D/B = 0.0$, $\Delta\sigma_1 = q_v(1 - K_o) = 233.3(1 - 0.426) = 133.9$ kPa. From the stress-strain plot (curve 1) in Fig. E5-12*b*, we obtain $\epsilon_1 = 7 \times 10^{-3}$. The corresponding secant modulus $E_s = \Delta\sigma_1/\epsilon_1 = 133.9/0.007 = 19\,130$ kPa, etc.

TABLE E5-12

Curve	D	D/B	q/q_o	q_v, kPa	$\Delta\sigma_1$	$\epsilon \times 10^{-3}$	$E_s \times 10^3$ kPa
1	0	0	1	233.3	133.9	7.0	19.13
1	1.5	0.5	0.7	163.3	93.7	4.6	20.4
1	3.0	1.0	0.33	77.0	44.1	1.8	24.5
2	4.5	1.5	0.19	44.0	25.3	1.0	25.3
2	6.0	2.0	0.12	28.0	16.1	0.6	26.8

We can now compute the settlement using the stress path method by using the strains and the contributory depths (from a depth plot not shown) as

$$\Delta H = 0.75 \text{ m} \times 7.0 + 1.5 \text{ m} \times (4.6 + 1.8 + 1.0) + 0.75 \text{ m} \times 0.6 = \mathbf{16.8} \text{ mm}$$

We note that m $\times$ 1000 $\times$ 10^{-3} cancels, so this computation directly gives the settlement in mm.

For the secant modulus of elasticity method we will numerically integrate the modulus of elasticity using Eq. (5-22) of Sec. 5-12 to find the average E_s as

$$E_s = \frac{1.5}{6}\left(\frac{19.13 + 26.8}{2} + 20.4 + 24.5 + 25.3\right)10^3 = 23.29 \times 10^3 \text{ kPa}$$

A similar computation for $\Delta\sigma_1$ gives 59.525 (using $\Delta\sigma_1$ to be compatible with E_s):

$$\Delta H = \frac{\Delta\sigma L}{E_s} = \frac{(59.525)(6)}{23\,290} = 15.3 \times 10^{-3} \text{ m} = \mathbf{15.3} \text{ mm}$$

This small discrepancy between the two methods is principally due to using the secant instead of the tangent modulus of elasticity. How this compares with a field ΔH will depend on how realistic K_o is compared to field lateral restraint beneath the base. If we used Eq. (5-1*a*) to modify $E_{s,\text{tr}}$ (and strain) both ΔH values would be reduced approximately 1/1.6 = 0.62 (10.4 and 9.5 mm).

////

5-11 STRESSES AND DISPLACEMENTS IN LAYERED AND ANISOTROPIC SOILS

There are numerous elastic solutions for special cases of stresses and displacements in layered or anisotropic soils. Special cases are sometimes useful to obtain an indication of probable (or possible) magnitude of error from using an idealized soil mass (isotropic, homogeneous, etc.). Generally, the special cases in the literature [Poulos and Davis (1974) summarize a large amount of curves, charts, and tables] are not found in nature, or by the time the necessary interpolations from curves and tables are made, the problem would be solved.

The author proposes that one of the best uses of the finite-element method (FEM) is to solve this type of problem. A computer program FEM2D is noted on your program diskette. One solves this type of problem as follows:

1. Model a reasonable size of half-space, once for all, and use a data generator to develop the data to define the x, y coordinates of the nodes and the node numbers defining each element and the soil for that element. The model should have provision for about five different layers of soil (for fewer layers one simply uses the same soil properties for more than one layer).
2. Solve the problem for a point load at one node where the footing is placed and for a "one" soil mass. This is either in the ground or at the ground surface (or both) depending on whether it is desired to obtain depth effects.
3. Re-solve the problem with the point load at the same location but with the correct soil stratification.
4. From the Boussinesq pressure bulbs obtain the stress at the desired point beneath the footing (now we are incorporating the shape and three-dimensional effect of the load into the problem).
5. From steps 2 and 3 find the point load stress at the same point as obtained in step 4.

6. Compute the stress due to stratification at any depth z as a proportion to obtain

$$q_{fL} = q_b\left(\frac{q_3}{q_2}\right) \tag{5-21}$$

where q_b = Boussinesq value for a footing of same dimension and applicable corrections for depth, etc., in a homogeneous soil mass at the depth of interest

q_{fL} = stresses due to footing in layered soil at the depth of interest

q_3, q_2 = stresses from the FEM solutions for the layered (step 3) and homogeneous (step 2) cases at the same depth of interest.

This solution is at least as good as the soil parameters E_s and μ used in the FEM. This method allows using a simpler two-dimensional plane-strain or plane-stress solution rather than a much more complex three-dimensional analysis. Deflections can be computed in an analogous manner.

Example 5-13.

Given. A 3.7 m wide × 24.4 m O.D. foundation ring as shown in Fig. E5-13*a*. This example is taken from Bhushan and Boniadi (1988) and some units have been converted to SI but the field

Figure E5-13*a* Ring foundation geometry and other data. Uses 11 equally spaced columns with pedestals located on center line of ring (not on centerline of area).

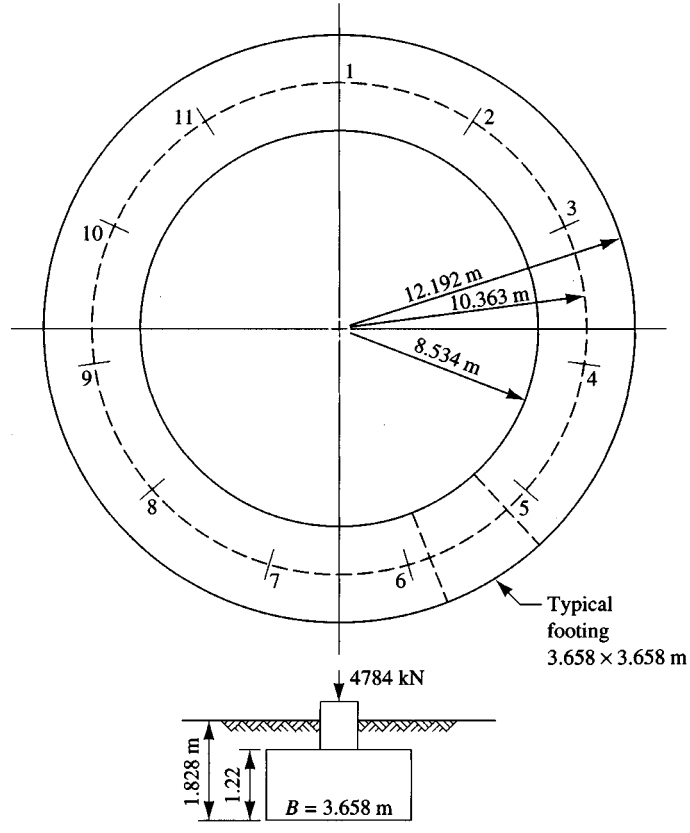

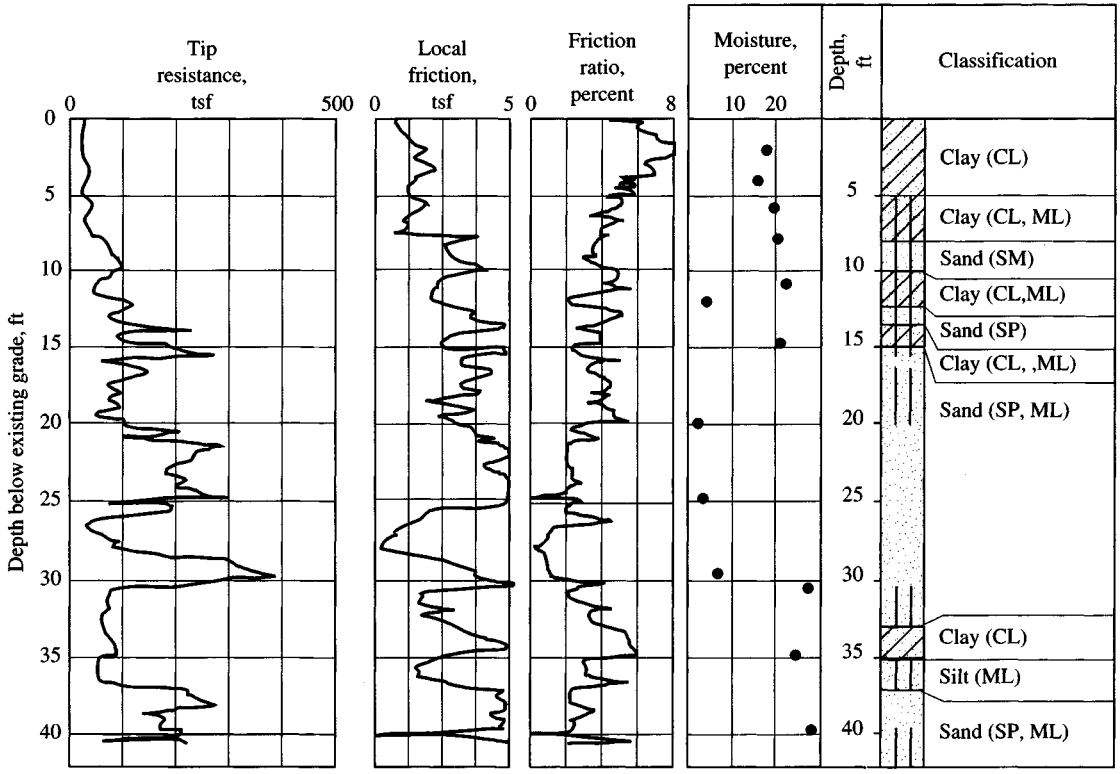

Figure E5-13*b* Typical subsurface exploration (boring) log. Note use of Fps units (1 tsf = 96 kPa).

log is retained in the manner obtained and presented by them. Appropriate conversions to SI will be made as necessary. The measured settlement during preload was 10 to 17 mm and the average given by the reference was 15.2 mm.

Required. Estimate the settlement under the preload stress of 252.8 kPa given by the reference. The preload stress is somewhat larger than the working load stress but will only be temporary.

Solution. We will use a modification of the method given by Bowles (1987) and in the previous edition of this textbook.

Assumptions.

1. Take effective $H = 5B' = 9.144$ m, giving $H/B' = 5$.
2. Since a ring closes on itself an L value has no significance so use an approximate square as shown by dashed lines on the ring in Fig. E5-13*a*. This gives $B \times B = 3.658 \times 3.658$ m ($B' = 1.829$ m). If the inside diameter of the ring were smaller than 17.1 m we might be justified in using B = outside diameter but not here.
3. From an inspection of the "typical" cone penetration resistance q_c profile of Fig. E5-13*b* estimate an "average" $q_c = 150$ tsf, which converts to

$$q_{c,\text{SI}} = 150(2)(47.88) = 14\,364 \text{ kPa}$$

Then estimate $E_s = 3q_c$ since the zone of interest from -6 ft to -36 ft (1.83 to 11 m) for a depth of $5B$ includes both clay and sand layers. This process gives

$$E_s = 3 \times 14\,364 = 43\,092 \rightarrow \mathbf{44\,000}\ \text{kPa}$$

4. $D/B = 1.82/3.66 = 0.5$ (given, not an assumption).
5. I will use Eq. (5-16*a*) with $\mu = 0.3$ and with the Fox embedment reduction factor I_F.

With these data and using program FFACTOR for $D/B = 0.5$, $\mu = 0.3$, and $L/B = 1$, obtain $I_F = 0.77$ and the Steinbrenner influence factor $I_s = 0.455$. One could also have used Table 1 of Bowles (1987) for I_s and Table 5-7 for I_F. Making a direct substitution into Eq. (5-16*a*), we have

$$\Delta H = qB' \frac{(1 - \mu^2)}{E_s} m I_s I_F \qquad (5\text{-}16)$$

$$= 252.8(1.83)\frac{(1 - 0.3^2)}{44\,000}(4)(0.455)(0.77)(1000) = 13.4\ \text{mm}$$

This result compares to the average $\Delta H = 15.2$ mm (0.6 in., and in the range of displacements) reported in the reference. The reader should redo this example using $E_s = 2q_c$ and also inspect Fig. E5-13*b* and see if the author made a selection for the average $q_c = 150$ tsf that is reasonable.

////

5-12 CONSOLIDATION SETTLEMENTS

The settlements of fine-grained, saturated cohesive soils will be time-dependent, and consolidation theory is usually used, although elastic methods can be, and sometimes are, used. Equation (2-44) or (2-45) is usually used for consolidation settlements, however, the alternate form given by Eq. (2-43) as

$$\Delta H = m_v \Delta p H = \epsilon H$$

is also used. Some authorities routinely use this latter equation format for settlement computations both for clay and fine-to-medium sand since $m_v = 1/E_s$ (the constrained modulus of elasticity) where m_v is determined in a consolidation test. The sample, being on the order of only 20 to 25 mm thick, may give results that are not very representative; and in sands, the SPT or CPT is generally preferable since a large number of values can be obtained at relatively low cost compared with the effort in a consolidation test—even if the loads can be changed rapidly.

In applying consolidation theory to compute settlements in clay we have three factors to consider:

1. Whether the soil is normally consolidated or preconsolidated (OCR > 1)
2. Estimating the in situ void ratio e_o and obtaining sufficient compression indexes to profile the clay layer(s) adequately
3. Estimating the average stress increase Δq in the stratum of thickness H

Section 2-10 has adequately considered what to do for preconsolidated strata. That section also detailed obtaining e_o and the compression indexes. Here we are primarily concerned with practical application of the theory.

The in situ void ratio e_o can usually be determined reasonably well using w_N and G_s and/or volumetric-gravimetric data from the soil sample in the consolidation ring used for the test. It is usual to use values at the midheight of the consolidating layer, so if the consolidation test sample were at a different location, the void ratio at midheight can be computed from

rearranging Eq. (2-42) and defining $\Delta e = e_o - e$ and $p_2 = p'_o + \Delta p'_o$ to obtain

$$e = e_o - C_c \log \frac{p'_o + \Delta p'_o}{p'_o}$$

where e_o = void ratio test depth z
$p'_o = \gamma' z$ = effective overburden pressure at depth z
$\Delta p'_o = \gamma'(dz)$ = increase or decrease in p'_o from depth z
dz = depth from test depth z to midheight of stratum and may be (+) if below or (−) if above

It can be seen that the void ratio is not linear (and probably the compression indexes are not either), so one should not use a very large stratum thickness H over which Δq, e_o, and C_c are averaged at $H/2$.

The average pressure increase in the stratum of thickness H from the foundation load can be obtained by simply averaging the top and bottom value from Boussinesq theory for H values up to about 1 m. For greater thickness one should use a numerical integration process. The trapezoidal-rule formula is well suited for this (and other numerical integration) where a depth (or space) increment Δh = constant is taken with end values p_1, p_n and interior points at Δh spacing. This gives the area A of the pressure profile as

$$A = H\Delta p = \Delta h\left(\frac{p_1 + p_n}{2} + p_2 + p_3 + \cdots + p_{n-1}\right) \tag{5-22}$$

from which the average pressure increase Δp in stratum thickness H is

$$\Delta p = \frac{A}{H}$$

It is, of course, necessary to compute p'_o at the midheight of the layer as well. Where the layer(s) are over about 2-m thick, one should give consideration to obtaining additional values of C_c and e_o so that the layer can be subdivided into layers of thickness H_i and the total settlement computed as

$$\Delta H = \sum_1^n \Delta H_i$$

These additional values can result in a large number of computations, and it may be worthwhile to program the steps so that the work is semiautomated.

One may question the validity of using the Boussinesq method when the actual case is one or more layers of clay soils with different C_c (or one or more layers of soils where immediate settlements occur) overlying one or more consolidating clay layers. Although the method is certainly not exact, unless there is a significant difference, say by a factor of five times or more in the stress-strain modulus of the two materials, more refined computation will improve the computed stress increase very little [see Morgan and Gerrard (1971)].

Example 5-14.

Given. The consolidation test, soil profile, and other data shown in Fig. E5-14. Note that original data are given in Fps units and not converted, as emphasis is on procedures.

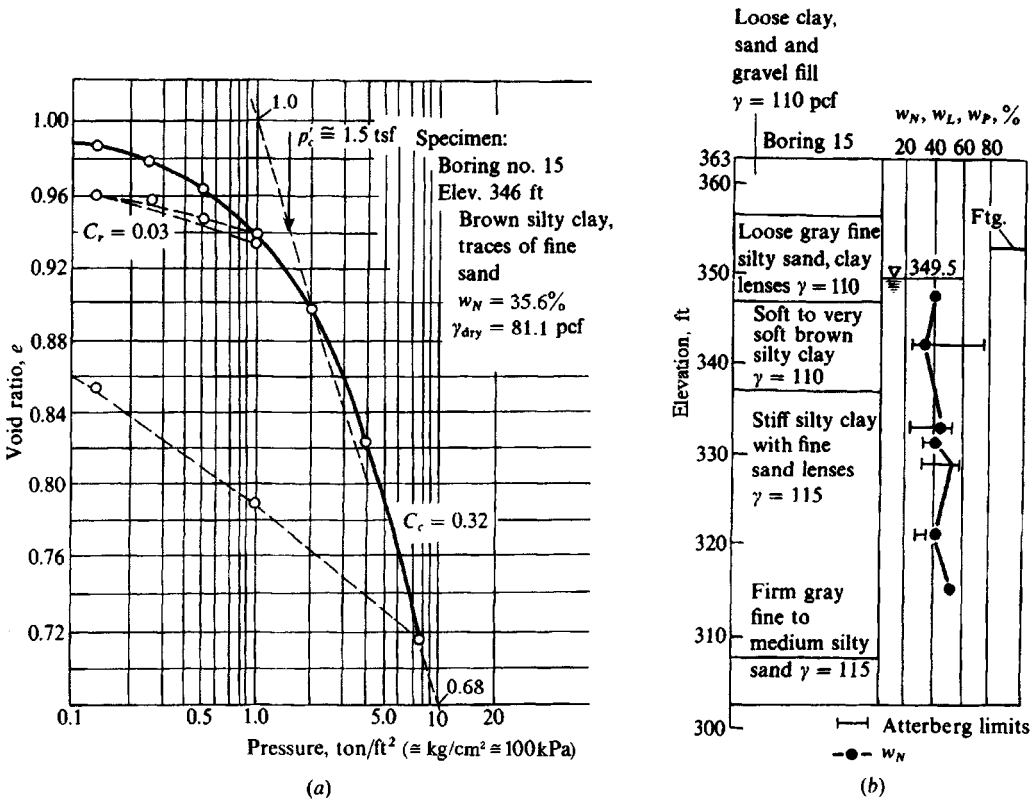

Figure E5-14

Required. Estimate the settlement of an 8 × 8 ft footing carrying 375 kips at elevation 353 ft on the "soft to very soft brown silty clay" (elevation 347 ft to 337 ft).

Solution. Note that the author of this book estimated p_c' using as a guide both the first and second reload cycles since the e versus log p curve does not have a distinct "sharp-curved" portion. It is possible that a better estimate might have been made using either Method 3 or Method 4 of Sec. 2-10.3. The Casagrande method would not be any better than the "eye" method used by the author of this book, since a sharply curving part of the curve is not clearly identified. Even the "virgin" curve part of this e versus log p plot is somewhat curved, and the slope for computing C_c is some approximate. With these comments we shall continue with a solution.

Estimate the initial (or in situ) void ratio e_o. The value at the first plotted point (0.985) is high since the soil has expanded from loss of overburden pressure. Obtain the value of 0.96 at the end of the first rebound cycle as a better estimate. We will check this estimated e_o, since the soil is approximately saturated, using an equation from Chap. 2. This equation requires the specific gravity G_s (estimated 2.70) and the natural water content (35.6% from Fig. E5-14*a*):

$$e_o = \frac{w_N G_s}{100} \approx 0.356(2.70) = \mathbf{0.961} \qquad \text{(coincidence ??)}$$

Compute the slope of the rebound curve C_r as a best estimate of the slope, which the user should lightly pencil in but is not shown here, to obtain the void ratio values and pressure change. A better

value might have been obtained using the average of both the initial and rebound "slopes," but that task is left as a reader exercise.

$$C_r = \frac{\Delta e}{\log p_2/p_1} = \frac{0.960 - 0.930}{\log 1/0.14} = \frac{0.030}{0.854} = \mathbf{0.035}$$

(Note that this slope could have been extended across one log cycle, but points will be used to illustrate alternative).

Compute C_c as the slope of the curve beyond p_c'; extend dashed line shown on Fig. E5-14*a* across one log cycle and obtain

$$C_c = \frac{1.00 - 0.68}{\log 10/1} = \frac{0.32}{1} = \mathbf{0.32}$$

As a check use equations from Table 2-5:

$$C_c = 0.009(w_L - 10) = 0.009(78 - 10) = 0.612 \qquad (a)$$

$$C_c = 0.37(e_o + 0.003w_L + 0.004w_N - 0.34)$$
$$= 0.37[0.96 + 0.003(78) + 0.004(35.6) - 0.34] = 0.37 \qquad (b)$$

Eq. (*a*) is probably in error because the soil is preconsolidated. Eq. (*b*) differs from the plot value because of plot interpretation, but it is not a bad estimate, because it somewhat accounts for preconsolidation by taking into account the liquid and natural water contents as well as the initial void ratio.

Now find the *average* increase in stratum pressure Δp from base load [contact pressure q_o = 375/(8 × 8) = 5.859 ksf (rather high)]:

1. Use the 2 : 1 method [see Eqs. (5-2*a, b*)]. With the footing at elevation 353, the depth to the top of the clay layer is 353 − 347 = 6.0 ft; to the bottom, the depth is 353 − 337 = 16 ft. Thus,

$$\Delta pH = \int_6^{16} \frac{375}{(8+z)^2}\,dx = \left| -\frac{375}{8+z} \right|_6^{16}$$

Inserting the limits, we have

$$\Delta p = \frac{1}{10}\left(-\frac{375}{24} + \frac{375}{14}\right) = \mathbf{1.12}\ \text{ksf}$$

2. Using the Boussinesq pressure bulbs (Fig. 5-4) and computer program SMBWVP we can construct the following table:

Elevation, ft	*D/B*	$\Delta q/q_o$	Fig. 5-4 Δq	Δq* (SMBWVP)
−6.0	6/8 = 0.75	0.50	2.93	2.87
8.5	1.06	0.33	1.93	1.82
11.0	1.375	0.23	1.35	1.22
13.5	1.68	0.16	0.94	0.86
−16.0	2.00	0.12	0.70	0.64

Compute the average stress increase $\Delta p(= \Delta q)$ using Eq. 5-22 and the computer-generated values (but the pressure bulb values are reasonable considering the small text scale—and probably

about as accurate):

$$A = \Delta qH = 2.5\left(\frac{2.87 + 0.64}{2} + 1.82 + 1.22 + 0.86\right) = 14.14$$

with $H = 10$ ft; $\Delta p = 14.14/10 = \mathbf{1.41}$ ksf (pressure bulbs = 1.51)

Next find the *effective* overburden pressure at midheight of the consolidating stratum (refer to Fig. E5-14*b*) referenced to the ground surface, not the footing base:

$$\begin{aligned} p'_o &= 0.110(363.0 - 349.5) &&= 1.485 \\ &\quad + (0.110 - 0.624)(349.5 - 342.0) &&= 0.356 \\ &\text{Total } \textit{effective} \text{ pressure } p'_o &&= \mathbf{1.841} \text{ ksf} \end{aligned}$$

From the e versus log p plot we obtain (method previously noted)

$$p'_c = 1.5 \text{ tsf} = 3.00 \text{ ksf} \qquad \text{OCR} = 3.00/1.84 = 1.6$$

and

$$\begin{aligned} p'_o + \Delta p &= 1.84 + 1.41 = 3.25 \text{ ksf} \\ \Delta p_2 &= 0.25 \text{ ksf} \qquad p'_o = p'_c = 3.00 \text{ ksf} \\ \Delta p_1 &= 1.41 - 0.25 = 1.16 \text{ ksf} \qquad p'_o = 1.84 \text{ ksf} \qquad C_c = C_r \end{aligned}$$

Inserting values into Eqs. (2-45*a*), we have

$$\begin{aligned} \Delta H_1 &= \frac{0.035(10)}{1 + 0.96} \log \frac{1.84 + 1.16}{1.84} &&= \mathbf{0.038} \text{ ft} \\ \Delta H_2 &= \frac{0.32(10)}{1.96} \log \frac{3.00 + 0.25}{3.00} &&= \mathbf{0.057} \\ \Delta H_{total} &&&= \mathbf{0.095} \text{ ft} \qquad (0.095 \times 12 \approx 1.14 \text{ in.}) \end{aligned}$$

This settlement is probably a little too large, and it is quite possible that the soil below elevation 337 ft ("stiff silty clay . . . ") would contribute additional consolidation settlement. The contact pressure $q_o = 5.86$ ksf is rather high, and the base should probably be rechecked for settlement using dimensions of either 9×9 or 10×10 ft.

////

5-12.1 Proportioning Footings for Equal Consolidation Settlement

We considered the problem of sizing footings for equal immediate settlements in developing Eq. (5-18). For footings located over a consolidating clay layer, finding the dimensions of $B \times L$ to obtain equal settlements becomes a trial procedure, as illustrated in the following example.

Example 5-15. Proportion a footing such that the consolidation settlement is not over 40 mm for the given conditions of Fig. E5-15*a*.

Solution. Assume that the net increase in soil pressure due to the concrete displacement of the soil is negligible. Since the settlement depends on the contact pressure and footing size and is nonlinear,

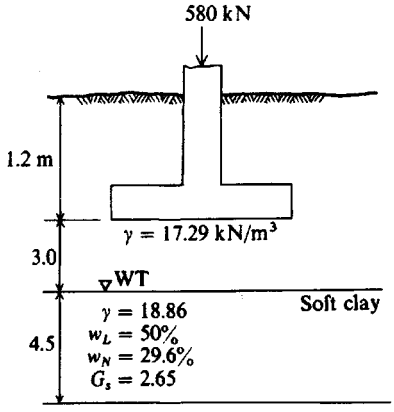

Figure E5-15*a*

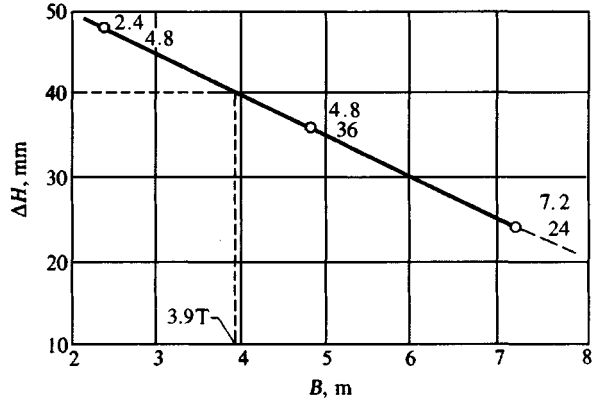

Figure E5-15*b*

several trials will be required, and it will be most convenient to use the average stress increase in the stratum Δp. The results of ΔH versus B will be plotted to find the required footing size.

$$p'_o = (3.0 + 1.2)(17.29) + \frac{4.5}{2}(18.86 - 9.807) = \mathbf{93}\text{ kPa}$$

Take $C_c = 0.009(w_L - 10) = 0.009(50 - 10) = \mathbf{0.36}$ (but soil may have OCR > 1).
Also:

$$e_o = wG_s = \frac{29.6}{100}(2.65) = \mathbf{0.784} \qquad \text{assuming } S = 100 \text{ percent}$$

$$\Delta H = \frac{C_c H}{1 + e_o} \log \frac{p'_o + \Delta p}{p'_o} = \frac{0.36(4.5)}{1.784} \log \frac{p'_o + \Delta p}{p'_o} = 0.91 \log \frac{93 + \Delta p}{93}$$

Use the Boussinesq method (Fig. 5-4), and obtain data in Table E5-15.

TABLE E5-15

	B = 2.4 m		B = 4.8 m		B = 7.2 m	
D, m	D/B	q/q_o	D/B	q/q_o	D/B	q/q_o
−3.0	1.25	0.25	0.62	0.6	0.42	0.77
−4.5	1.87	0.13	0.94	0.4	0.62	0.60
−6.0	2.5	0.08	1.25	0.25	0.83	0.40
−7.5	3.12	0.06	1.56	0.17	1.04	0.34

Computing the average stress Δp by the trapezoidal rule [Eq. (5-22)], we find

$$\Delta p = \frac{1}{15}\left(\frac{15}{3}\right)\left(\frac{0.25 + 0.06}{2} + 0.13 + 0.08\right) = \frac{0.36}{3} = 0.12q_o \qquad B = 2.4 \text{ m}$$

$$= \frac{1}{3}\left(\frac{0.6 + 0.17}{2} + 0.4 + 0.25\right) = 0.35q_o \qquad B = 4.8 \text{ m}$$

$$= \frac{1}{3}\left(\frac{0.77 + 0.34}{2} + 0.6 + 0.40\right) = 0.52q_o \qquad B = 7.2 \text{ m}$$

$$q_{2.4} = 0.12\frac{580}{2.4^2} = 12 \text{ kPa} \qquad q_{4.8} = 0.35\frac{580}{4.8^2} = 8.8 \text{ kPa}$$

$$q_{7.2} = 0.52\frac{580}{7.2^2} = 5.8 \text{ kPa}$$

$$\Delta H_{2.4} = 0.91 \log \frac{93 + 12}{93} = 0.91(0.053) = 0.048 \text{ m or } \mathbf{48} \text{ mm}$$

$$\Delta H_{4.8} = 0.91 \log \frac{93 + 8.8}{93} = 0.91(0.039) = 0.036 \text{ m or } \mathbf{36} \text{ mm}$$

$$\Delta H_{7.2} = 0.91 \log \frac{93 + 5.8}{93} = 0.91(0.026) = 0.024 \text{ m or } \mathbf{24} \text{ mm}$$

Plotting these three points to obtain Fig. E5-15*b*, we can interpolate to obtain $B = 4$ m. Although it might appear that $B = 2, 3$, and 4 m might be better trials, the best choices are not known initially and larger values will more rapidly bracket B with at least as good accuracy as the known settlement data. Note the nearly linear plot, which somewhat justifies Eq. (*d*) of Sec. 5-9.1.

////

It should be evident at this point that it is impossible to proportion footings so that the settlements will be exactly equal unless the footings are the same size and with the same contact pressure. The following points are important:

1. If the footings are of different size, and with the same contact pressure, the larger base will settle more.
2. The stress profile is based on a depth of approximately $5B$, so clearly there is a greater depth undergoing strain (and ΔH) for larger bases.
3. If the layer H is the same depth beneath two footings of q_o = same but with different B, the larger B will settle more, as there is a larger concentration of Boussinesq settlement (the H/B is smaller for the larger footing). For immediate settlements the influence factor is smaller but B' is larger.

5-12.2 Secondary Compression Settlements

In addition to the primary compression of a base as illustrated in Example 5-14, secondary compression (or creep) also occurs. This phenomenon is associated with both immediate and consolidation-type settlements, although it is usually not of much significance with immediate settlements.

At least a part of the settlement causing the Leaning Tower of Pisa to tilt is probably due to secondary compression, with consolidation providing the remainder of the vertical (and differential) movement.

As previously stated in Chap. 2, secondary compression is the continuing readjustment of the soil grains into a closer (or more dense) state under the compressive load. It occurs after the excess pore pressure has dissipated and may continue for many years.

Secondary compression may be the larger component of settlement in some soils, *particularly in soils with a large organic content.* It can be estimated using Eq. (2-49) of Sec. 2-10.6.[5] The major problem is obtaining the secondary compression index C_a of Eq. (2-49).

[5]Stinnette (1992) made an extensive study of organic soils in Florida (USA) and provided an extensive literature survey. Both Eq. (2-49) and the methods of Tan et al. (1991) were shown to provide reasonable results but several other methods were also given.

High-quality consolidation tests, if continued for a sufficient time for the appropriate load increment, may give the best value. These are often not done and an estimated value is used, either from one of the equations given in Table 2-5 or from a lesser-quality consolidation test (if any are done).

Example 5-16.

Given. The data of Example 5-14 and a laboratory value of $t_{100} \approx 100$ minutes (from a plot of ΔH versus log time, not shown).

Required. Compute an estimate of secondary consolidation.

Solution. We will use the value from Table 2-5 of

$$C_\alpha/C_c = 0.032$$

and from Example 5-14 we have $C_c = 0.32$, giving

$$C_\alpha = 0.032C_c = 0.032(0.32) = \mathbf{0.010}$$

Now we need some preliminary computations:

1. $t_{\text{lab}} = 100$ min. There are $24 \times 60 \times 365 = 525\,600$ min in 1 year.
2. Use the following:

$$\frac{t_{\text{field}}}{t_{\text{lab}}} = \frac{H^2_{\text{field}}}{H^2_{\text{lab}}}$$

   This ratio is obtained from using Eq. (2-38), cancelling T_i and c_v and using the appropriate subscripts. The ratio is needed to estimate when secondary compression begins.
3. For a lab sample of $H_{\text{lab}} = 0.75/2$ inches (*two*-way drainage) and a field $H_{\text{field}} = 10$ ft $= 120$ inches (*one*-way drainage from inspection of boring log), the time for 100 percent consolidation before secondary compression starts (using $t_{\text{lab}} = 100$ min)—at least in theory—is

$$\begin{aligned} t_{\text{field}} &= 100(120/0.375)^2 = 10\,240\,000 \text{ min} \\ &= 10\,240\,000/525\,600 = \mathbf{19.5} \text{ years} \end{aligned}$$

   Using Eq. (2-49), we have

$$\Delta H_s = H_s C_\alpha \log \frac{t_2}{t_1}$$

and using $t_2 = 30$ yr (arbitrary), $t_1 = 19.5$ yr, and the consolidating layer as 10 ft (given), we have an *estimated secondary compression* of

$$\Delta H_s = 10(0.010)\log(30/19.5) = \mathbf{0.019} \text{ ft} = 0.23 \text{ in.}$$

which is almost negligible.

It is very likely that the secondary compression will be larger than this, as some will occur during primary consolidation. Theoretically, at the end of 19.5 years there is no excess pore pressure anywhere in the 10-ft layer; however, during this time period dissipation occurs from the top down, with secondary compression beginning before 19.5 years have elapsed in the upper regions. No easily developed theory that is practical to use is currently available to take this into account. It is therefore quite possible that there could be as much as 1 inch of secondary compression, and it could occur well before the time when it is supposed to start, at 19.5 years.

This example and discussion, together with the observation that the consolidation settlement from Example 5-14 is 1.14 in., indicates that there should be more than one consolidation test done in this layer—that is, use at least two 5-foot-thick layers with a test in each. It also would be most prudent to obtain samples and perform one or more additional tests within the $5B$ depth region that penetrates into the "stiff silty clay" underlying this soft clay layer.

////

5-13 RELIABILITY OF SETTLEMENT COMPUTATIONS

Settlements are generally made up of immediate, consolidation, and secondary compression (or creep) components as

$$\Delta H = \Delta H_i + \Delta H_c + \Delta H_s$$

In cohesionless soils and unsaturated clays the immediate settlement predominates with perhaps some creep ΔH_s. The consolidation settlement predominates for saturated cohesive soils unless the soil is very organic, in which case the creep term may predominate.

Immediate settlement computations can vary widely but as shown in Table 5-3 can, with some care, be used to predict the settlement ΔH_i quite satisfactorily.

Consolidation theory tends to predict the amount of settlement ΔH_c rather well if care is taken to obtain representative soil parameters. In most cases the settlement prediction is conservative (i.e., is overpredicted) but within acceptable limits. A study of recent Geotechnical Division Journals and papers given at the ASCE conventions (too numerous to cite specifically) gives an overview that consolidation settlements are adequately predicted. The predictions are better for inorganic, insensitive clays than for others. The prediction requires much care if the e versus log p curve is curved throughout or the clay is very sensitive. Much care is also required if the clay is highly organic, as the creep component will be substantial.

The time rate for consolidation settlement is not well-predicted because the coefficient of permeability is a significant factor. In the laboratory a thin sample with any compression undergoes a large void ratio change relative to in situ. Since the coefficient of consolidation c_v depends on the void ratio [$c_v = f(e)$], the laboratory value tends to be too small, so the time for consolidation is overpredicted; e.g., based on a laboratory test to obtain c_v, the field prediction for a site is 6 years using Eq. (2-38), whereas actual measurements give about 3 years for most of the settlement to occur. While overpredicted times are usually acceptable, there will be cases in which, if the consolidation occurs too rapidly, the superstructure members will crack rather than "creep" into a deformed position.

5-14 STRUCTURES ON FILLS

It is often advantageous, and sometimes necessary, to place the structure or parts of it on filled-in areas. These sites may be sanitary landfills, rubble dumps from demolished buildings, or fills constructed according to engineering criteria. In the situations where sanitary fills or rubble dumps are used, it is doubtful that a structure can be placed on this material and not undergo detrimental settlement unless the fill has had time to decompose and fully consolidate. For most cases of foundations on fills the loads will have to be carried through the fill material utilizing piles or caissons of a noncorrosive material (usually concrete or treated wood).

A well-constructed earth fill, using quality control with regard to both material and compaction, often produces a better foundation base than the original material underlying the fill. Many persons have been reluctant to place a footing on or in fills because of two main factors:

1. Unpleasant results from placing footings on poorly placed fills. With no quality control it is not unusual to get a fill with a hard crust over 0.5 to 1 or more meters of loose fill, as a result of compacting only the last lift, or from placing a lift too thick to be compacted with the available equipment.
2. Placing a footing in the fill with unpleasant results obtained not from the fill settlement but from settlement of the underlying soil due to the weight of both the fill and the structure.

There are precautions one must take with a fill, in addition to exercising compaction control, such as eliminating soils of large volume change; providing adequate drainage; and, if construction is to proceed relatively soon after the fill is placed, making sure that consolidation settlements have been considered. Under consolidation processes the structure and fill will subside from the weight of the fill alone; and this will take place whether the footings are placed on the natural soil or in the fill. Excessive differential settlements may also result from consolidation in the underlying soft strata if the fill varies considerably in thickness and particularly if part of the structure is on an excavation or virgin soil and part is on fill. A poorly constructed fill will also undergo settlements with time, and there is no theory available that can be used to estimate the amount of or the length of time for the settlement to be completed.

The determination of the bearing capacity (and settlements) proceeds as with the virgin soil. If the fill is placed before exploration takes place, the usual exploration methods of Chap. 3 (standard penetration tests on recovered samples) are applicable. When the field exploration has already been performed, the bearing capacity of the fill may be determined by performing laboratory tests on specimens compacted to the proposed in situ density. Building code values, coupled with successful experience on soils of similar properties and density, may also be used as a guide.

5-15 STRUCTURAL TOLERANCE TO SETTLEMENT AND DIFFERENTIAL SETTLEMENTS

Theoretical settlements can be computed for various points such as corner, center, or beneath the lightest- and heaviest-loaded footings to obtain the total settlement and the differential settlement between adjacent points. If the entire structure moves vertically some amount or rotates as a plane rigid body, this movement will not generally cause structural or architectural distress. For example, if a structure settles 20 mm on one side and 100 mm on the other with a linear settlement variation between the two points, structural damage is not likely to develop, although there are aesthetic and public confidence considerations. The building will have settled 20 mm and tilted an amount $\zeta = (100 - 20)/L$. Local settlements below the tilt line between the two sides of the structure will be the cause of any building distress. These local settlements below either the settlement or tilt line are the differential settlements that the foundation designer must control, since they will determine the acceptability of the structure. The initial settlements that occur during construction (or shortly after) can usually

TABLE 5-7
Tolerable differential settlement of buildings, mm*
Recommended maximum values in parentheses

Criterion	Isolated foundations	Rafts
Angular distortion (cracking)	1/300	
Greatest differential settlement		
Clays	45 (35)	
Sands	32 (25)	
Maximum settlement		
Clays	75	75–125 (65–100)
Sands	50	50–75 (35–65)

*After MacDonald and Skempton (1955) but see also Wahls (1981).

be landscaped into concealment when the building is completed or later. A cracked wall or warped roof is much more difficult to conceal.

Differential settlement can be computed as the difference in settlement between two adjacent points. It may be estimated as three-fourths of the computed maximum total settlement; i.e., maximum total settlement = 40 mm; expected differential settlement, $\Delta h = \frac{3}{4}(40) = 30$ mm.

MacDonald and Skempton (1955) made a study of 98 buildings, mostly older structures of load-bearing wall, steel, and reinforced concrete construction to provide the data of Table 5-7. This study was substantiated by Grant et al. (1974) from a study of 95 additional buildings of more recent construction (some were constructed after 1950). Feld (1965) cited a rather large number of specific structures with given amounts of settlement and structural response, which might be of interest in considering a specific problem. Combining all sources, one can conclude [see Wahls (1981)] that

1. The values in Table 5-7 should be adequate most of the time. The values in brackets are recommended for design; others are the range of settlements found for satisfactory structural performance.
2. One must carefully look at the differential movement between two adjacent points in assessing what constitutes an acceptable slope.
3. Residual stresses in the structure may be important, as it has been observed that there is a range of tolerable differential settlements between similar buildings.
4. Construction materials that are more ductile—for example, steel—can tolerate larger movements than either concrete or load-bearing masonry walls.
5. Time interval during which settlement occurs can be important—long time spans allow the structure to adjust and better resist differential movement.

If computed differential settlements are kept within the values in parentheses in Table 5-7, statistically the structure should adequately resist that deformation. Values of acceptable slopes between two adjacent points from the U.S.S.R. building code are in Table 5-8.

One might use the following, a composite from several sources, as a guide in estimating differential settlement. Define L = column spacing and δ = differential displacement

TABLE 5-8
Permissible differential building slopes by the USSR code on both unfrozen and frozen ground

All values to be multiplied by L = length between two adjacent points under consideration. H = height of wall above foundation.*

Structure	On sand or hard clay	On plastic clay	Average max. settlement, mm	
Crane runway	0.003	0.003		
Steel and concrete frames	0.002	0.002	100	
End rows of brick-clad frame	0.0007	0.001	150	
Where strain does not occur	0.005	0.005		
Multistory brick wall			25	$L/H \geq 2.5$
L/H to 3	0.0003	0.0004	100	$L/H \leq 1.5$
Multistory brick wall				
L/H over 5	0.0005	0.0007		
One-story mill buildings	0.001	0.001		
Smokestacks, water towers, ring foundations	0.004	0.004	300	
Structures on permafrost				
Reinforced concrete	0.002–0.0015		150 at 40 mm/year†	
Masonry, precast concrete	0.003–0.002		200 at 60 mm/year	
Steel frames	0.004–0.0025		250 at 80 mm/year	
Timber	0.007–0.005		400 at 129 mm/year	

*From Mikhejev et al. (1961) and Polshin and Tokar (1957).

†Not to exceed this rate per year.

between any two adjacent columns. Use $\delta = 0.75\delta_{max}$ if you only have estimates of settlements at the columns (or edges and center of the structure).

Construction and/or material	Maximum δ/L
Masonry (center sag)	1/250–1/700
(edge sag)	1/500–1/1000
Masonry and steel	1/500
Steel with metal siding	1/250
Tall structures	< 1/300 (so tilt not noticeable)
Storage tanks (center-to-edge)	< 1/300

Although the values in Table 5-8 *may appear dated,* an examination by the author of several current (as of 1995) building codes (BOCA, National, Uniform, etc.) reveals no guidance on tolerable, or allowable, building distortions.

5-16 GENERAL COMMENTS ON SETTLEMENTS

It is a rare event when footings all settle the amount computed by the designer. This is true for footings on sand, on slopes, or on sand and clay where there is a combination of immediate and long-term consolidation settlements.

Soil is too heterogeneous to make settlement predictions with any great accuracy. What is hoped is to design site footings with a 95 to 98 percent reliability such that any given footing settlement is within about ±20 percent of some amount considered tolerable for that structure. It is preferable that settlements all be within less than 20 percent.

Using simple statistics and assuming the work has been reasonably done, if there are 20 to 25 footings in an area, the average settlement will probably be within about ±20 percent (taken as the standard deviation) of the computed value, but there will be at least one whose settlement is about twice as large as the smallest settlement, thus establishing the extremes.

For this ±20 percent settlement range to occur it is necessary to use representative soil properties from the given site. Statistics may be employed to obtain the most probable value. There are a number of statistical procedures given in the literature, but most use symbols and terminology not familiar to engineers, causing them to underutilize these methods. The statistical methods of simple averaging or weighted averaging are easy to apply but are somewhat time-consuming.

Finally, field construction methods may be significant in the settlement outcome. For example, most footings require some soil excavation. If the soil is freestanding, the footing perimeter is often excavated slightly larger so that mechanical excavation equipment can be used, but the excavated pit walls serve as forms. If the soil is not free standing, excess perimeter excavation is required so that the footing forms can be set. In either case the soil beneath the footing must be recompacted. Depending on the compactor and amount of compaction, the soil state can be changed significantly (increase in density, apparent overconsolidation, stiffness, etc.). These state changes can substantially reduce the settlements, particularly on sand. On the other hand, if there is no compaction before the base is placed, the settlements can greatly exceed the computed values.

PROBLEMS

Problems 5-1 to 5-3 are to be assigned by the instructor from the following table by key number, which provides the thickness of the strata in the soil profile given in Fig. P5-1, in feet or meters.

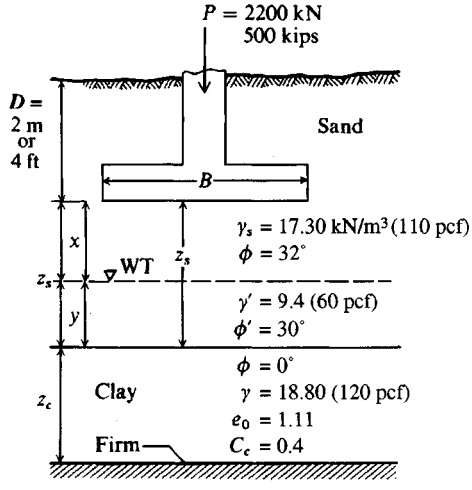

Figure P5-1

B = 2.5 × 2.5 m or 10 × 10

Key Number	z_s	x	y	z_c
1	1.5	1.5	0	1.5
2	2.5	2.5	0	2
3	4	3	1.2	1.2
4*	5	3	2	6
5	4.6	3	1.5	3
6	2	1	1	3
7*	10	6	4	15
8	2	2	0	5
9*	2	2	0	10
10	1	1	0	4

*Dimension in ft.

5-1. Referring to Fig. P5-1, compute the average increase in stress Δq for the clay stratum for the assigned key number from table of strata thickness by (*a*) Boussinesq method; (*b*) Westergaard method (and use $\mu = 0.45$ for saturated clay); (*c*) by 2 : 1 method [for this use Eq. (5-2*b*)].

Partial answer:

Problems	(*a*)	(*b*)	(*c*)
5-1(1)	144.2	202.1	100.0 kPa
5-1(2)	75.4	143.3	62.9
5-1(9)	2.81	3.25	1.89 ksf
5-1(10)	117.2	199.0	83.8

5-2. Compute the consolidation settlement using the Δq obtained from Prob. 5-1. Comment on any differences in the computed settlement.

Partial answers: (mm or in.)

Problems	(*a*)	(*b*)	(*c*)	p'_o
5-1(1)	141.4	171.3	112.5	67.3
5-1(2)	103.0	160.5	89.7	86.8
5-1(4)	6.91	8.02	5.82	1.06 ksf
5-1(6)	122.0	140.4	154.9	74.8
5-1(10)	259.5	362.7	443.7	69.9

5-3. What size footing in Prob. 5-1 (assign only key numbers 1 through 4) is required to limit the consolidation settlement to not over 1.5 in. or 40 mm?

Partial answer:

Problem		*B*
5-1(1)	(*b*)*	$\cong$ 9 m
5-1(2)	(*b*)*	$\cong$ 8.5 m
5-1(4)	(*w*)	$\cong$ 40 ft

*(*b*) = Boussinesq; (*w*) = Westergaard

5-4. What footing load can be used for Prob. 5-1(1), using the Boussinesq pressure profile, to limit the 2.5 × 2.5 m square base to a settlement of 40 mm. The current load is 2200 kN. What load is the maximum allowable using the 2 : 1 method?

Partial answer: 2 : 1: $Q \simeq 570$ kN [by trial $Q_{\text{Boussinesq}} = 450$ kN (40.7 mm)]

5-5. If it will take a $B = 9$ m square (very large) base to carry 2200 kN, what might be an alternative solution to carry the 2200-kN column load?

5-6. Verify the centerline stress ratios of Fig. 5-4 using Eq. (5-5) (Boussinesq equation). Note along the center line $r = 0$ and $z = D/B$.

5-7. Assume in Example 5-14 that instead of 1.5 tsf, $p'_c = 1.0$ tsf and recompute the expected consolidation settlement ΔH_c. Next assume the given $p'_c = 1.5$ tsf and $C_c = 0.40$ instead of 0.32 and compute the settlement. Compare the two settlement values and see if you can draw any conclusions as to the relative effect of error in p'_c versus error in C_c.

5-8. Using either Method 3 or Method 4 of Sec. 2-10.3 compare p'_c to your best construction of Casagrande's Method 2. For both methods make an enlargement of Fig. E5-14*a* on a copy (or other) machine so you can pick off the data points with some confidence. Use the enlarged plot

directly for the Casagrande construction. Comment on the preconsolidation pressure p'_c obtained by these two methods compared with that used by the author.

5-9. Using the Tan and Inove data set on Fig. 2-23, verify select additional plot points and replot the data on a sheet of graph paper and compute the expected settlement ΔH at the end of 2 years.

5-10. Referring to Sec. 5-12.2, what would be the secondary compression settlement and about how long would it take if instead of 100 minutes for t_{100} in the laboratory the plot of ΔH versus $\log t$ gives $t_{100} = 10$ minutes? For C_α use 0.032 and then compute a second value using the equation given in Table 2-5 with $I_P \approx 56$ (obtained from Fig. E5-14*b*). Average the two values for C_α for this problem. Can you draw any conclusions between the computations of Sec. 5-12.2 and here?

5-11. Rework Example 5-5 for $z = 5$ ft.

5-12. Rework Example 5-8 if the moment is resisted by $B = 2$ m.

5-13. Rework Example 5-9 if column loads are expected in the range of 900 to 1800 kN.

5-14. Referring to Example 5-12, if B increases to 6 m, what should the contact pressure q_o be to hold ΔH = constant = 16.8 mm?

5-15. The allowable bearing pressure on a 30-ft thick (below base of footing) medium dense sand (take $\phi = 36°$, $\gamma = 112$ pcf) is 3 ksf. Column A has design load of 430 kips and Column B has 190 kips. What size footings would you use and what might one expect for differential settlement? By using Table 5-7, is this differential settlement satisfactory?

5-16. Two CU triaxial tests were performed on a light brown silty clay obtained from a depth of 5 m and the test data shown following. Footings are to be placed 1.8 m below ground surface on this material, which extends to a depth of approximately 7.3 m. The water table is at 9.3 m in a medium dense sand underlying this clay. Footing loads are 1000 to 1500 kN. What do you recommend for bearing capacity and what do you estimate for total and differential settlements? Is the soil in the CU tests saturated?

	Test No. 1 $\sigma_3 = 70$	**Test No. 3** $\sigma_3 = 140$ kPa
ϵ	$\Delta\sigma_1$	$\Delta\sigma_1$, kPa
0	0	0
0.010	26	17
0.014	39	39
0.02	93	93
0.03	134	131
0.04	142	150
0.05	168	197
0.07	185	221
0.09	205	233
0.12	235	234
0.14	239	245
0.16	241	259
0.19	265	244
0.21	266	228

5-17. Verify the assigned case from Table 5-3 for predicted settlement and make any appropriate comments. Use the author's procedure for the verification process.

CHAPTER 6

IMPROVING SITE SOILS FOR FOUNDATION USE

6-1 INTRODUCTION

The centuries-old problem of land scarcity in the vicinity of existing urban areas often necessitates the use of sites with soils of marginal quality. In many cases these sites can be utilized for the proposed project by using some kind of soil improvement. This chapter will focus on several of the more widely used methods of improving soils for bearing capacity. An extremely large number of methods have been used and/or reported in the literature—many of which have been patented—and at an individual site one may use a mix of several methods to achieve the desired result. Chapter 12 will consider methods for increasing lateral stability.

For a given site a first step is to make a literature review of at least some of the methods reported. This together with a reasonable knowledge of geotechnical fundamentals allows the engineer to use either an existing method, a mix of methods, or some method coupled with modest ingenuity (unless limited by a governmental agency) to produce an adequate solution for almost any site.

Of principal interest in this chapter is the identification of means to obtain a significant increase in the bearing capacity of a soil. This can be achieved by altering the soil properties of ϕ, cohesion c, or density ρ. Usually an increase in density (or unit weight γ) is accompanied by an increase in either ϕ or c or both (assuming the soil is cohesive). Particle packing (compaction) always increases the density, with a resulting decrease in void ratio, and reduces long-term settlements. Particle packing usually increases the stress-strain modulus so that any "immediate" settlements are also reduced.

The rest of this section considers approaches to soil property modification.

Mechanical stabilization. In this method the grain size gradation of the site soil is altered. Where the site soil is predominantly gravel (say, from 75 mm down to 1 mm) binder material is added. *Binder* is defined as material passing either the No. 40 (0.425 mm) or No. 100

(0.150 mm) sieve. The binder is used to fill the voids and usually adds mass cohesion. Where the soil is predominantly cohesive (No. 40 and smaller sieve size) granular soil is imported and blended with the site soil.

In either case the amount of improvement is usually determined by trial, and experience shows that the best improvement results when the binder (or filler) occupies between 75 and 90 percent of the voids of the coarse material. It usually requires much more granular materials to stabilize cohesive deposits than binder for cohesionless deposits and as a result other stabilizing methods are usually used for clayey soils.

Compaction. This method is usually the most economical means to achieve particle packing for both cohesionless and cohesive soils and usually uses some kind of rolling equipment. *Dynamic compaction* is a special type of compaction consisting of dropping heavy weights on the soil.

Preloading. This step is taken primarily to reduce future settlement but may also be used to increase shear strength. It is usually used in combination with drainage.

Drainage. This method is undertaken to remove soil water and to speed up settlements under preloading. It may also increase shear strength since s_u, in particular, depends on water content. For example, consolidation without drainage may take several years to occur whereas with drainage facilities installed the consolidation may occur in 6 to 12 months.

Densification using vibratory equipment. Densification is particularly useful in sand, silty sand, and gravelly sand deposits with D_r less than about 50 to 60 percent. This method uses some type of vibrating probe, which is inserted into the soil mass and withdrawn. Quality fill is added to the site to bring the soil surface to the required grade since the site soil usually settles around and in the vicinity of the vibrating probe.

Use of in situ reinforcement. This approach is used with stone, sand, cement, or lime columns. This treatment produces what is sometimes called *composite* ground. Sometimes small amounts of short lengths of plastic fibers or fiberglass can be mixed with the soil for strength improvement. The major precaution is to use a fiber material that has an adequate durability in the hostile soil environment.

Grouting. Initially this was the name for injection of a viscous fluid to reduce the void ratio (and k) or to cement rock cracks [see ASCE (1962)]. Currently this term is loosely used to describe a number of processes to improve certain soil properties by injection of a viscous fluid, sometimes mixed with a volume of soil. Most commonly, the viscous fluid is a mix of water and cement or water and lime, and/or with additives such as fine sand, bentonite clay, or fly ash.[1] Bitumen and certain chemicals are also sometimes used. Additives are used either to reduce costs or to enhance certain desired effects. Since the term *grout* is so loosely used in construction, the context of usage is important to define the process.

Use of geotextiles. These function primarily as reinforcement but sometimes in other beneficial modes.

Chemical stabilization. This means of stiffening soil is seldom employed because of cost. The use of chemical stabilizers is also termed *chemical grouting*. The more commonly used chemical agents are phosphoric acid, calcium chloride, and sodium silicate (or water

[1] A by-product from burning coal, primarily in electric power generating plants.

glass). Some laboratory tests indicate certain metallic powders (aluminum, iron) may produce beneficial effects as well [Hoshiya and Mandal (1984)]. ASCE (1957,1966) cited usage of an extremely large number of chemical grouting procedures (mostly patented, but most of the patents have probably expired by now).

Strictly, soil-cement and lime-soil treatment (often together with fly ash and/or sand) is a *chemical stabilization* treatment, but it is usually classified separately.

Several of the foregoing methods of soil improvement will be taken up in additional detail in the following sections. The primary emphasis, however, is on improving soils for use in building foundations. Additional background on the preceding methods may be obtained from the three ASCE conferences on "Soil Improvement," the latest being published by ASCE as Geotechnical Special Publication No. 12 (1987).

Appropriate references will be cited so the interested reader may obtain additional depth for a particular application.

6-2 LIGHTWEIGHT AND STRUCTURAL FILLS

A method that allows construction of relatively light structures (such as residences and one- or two-story structures with lightly loaded foundation slabs) on very soft base soil is to use either a lightweight fill or a carefully placed structural fill onto which the foundation is placed.

Lightweight fills may use expanded shale, certain industrial slags, and fly ash. A reduction in γ from 18.5 to 16.5 kN/m^3 in a fill 1 m thick allows a 2 kPa foundation load increase for the same contact pressure of 18.5 kPa. These materials may be mixed with sand and/or gravel to produce a fill of the desired density and durability.

There are two "soft soil" cases to consider:

1. The site soil has such an extremely low shear strength that any surface load produces a shear failure (sinks into the mud). In this case it will be necessary to pretreat a surface thickness on the order of 150$^+$ mm by sand (or a sand-gravel mixture) that is mixed with the top soil to produce a final mix with some load-supporting capacity.
2. The site soil has sufficient shear strength that it can support small surface loads.

For either of these cases a support fill is first placed by spreading imported fill to a loose depth between 0.5 and 1 m from hauling equipment as it is backed onto the site. Care is used that the soil underlying the fill is not much rutted in this operation. That is, the imported fill provides the necessary spreading of the hauler wheel loads to a pressure the underlying soil can support.

Lightweight or small spreaders are then used to bring the fill to the desired depth with minimal damage to the underlying soft base soil. Compaction is done with light- to medium-weight rollers once the layer (usually called *lift*) thickness is sufficient that the equipment weight does not cause the underlying soil to fail.

Construction of the building commences after the desired settlement has occurred under the *preload* of the fill. Vertical drains and a sand blanket beneath the fill may be used to speed consolidation. Fill thicknesses range from about 0.5 m to 1$^+$ m.

Fills may be the most economical site improvement method available when used in conjunction with careful monitoring of the field work for floor slab-type buildings.

This method was used for a housing site near San Francisco on bay mud with an s_u on the order of 15 to 25 kPa [Garbe and Tsai (1972)]. With a compacted fill of about 0.6 m the preload pressure on the underlying mud was on the order of 10 to 14 kPa. With the fill in place about 12 months prior to erecting the houses (using slabs on grade—no basements obviously), the soil consolidated sufficiently that the increase in s_u could carry the building foundations and access roads.

Preloading, however, may not always produce a successful outcome. Duncan (1993—but see also "discussion" in 1995) described another housing development in the San Francisco Bay area where the outcome was rather uncertain. After about 12 years of preloading there was an estimate that subsequent differential settlement over a 23-m distance could approach 100 mm. The developer was required to provide an escrow account should later settlements require housing repairs.

Foundation loads from residential buildings are seldom over 15 to 20 kPa for wall footings and perhaps one-tenth of this for slabs on grade. Service roads should be of asphalt to allow deformation with minimal cracking and to allow repaving of bumps and potholes at minimum cost. It would also be necessary to stipulate a maximum truck load to avoid rutting.

6-3 COMPACTION

Compaction is usually an economical method of improving the bearing capacity of site soils. It may be accomplished by excavating to some depth, then carefully backfilling in controlled lift thicknesses, each of which is compacted with the appropriate compaction equipment. The backfill soil may be the excavated soil dried (or wetted) as necessary, possibly mixed with an admixture such as cement or lime, with or without fly ash or sand filler; or it may be imported soil from a nearby borrow pit. The standard compaction tests (ASTM, vol. 4.08) that may be used to establish the field density are these:

ASTM D 698	ASTM D 1557 (Modified)
24.4-N (5.5-lb) rammer	44.5-N (10-lb) rammer
305-mm (12-in.) drop	457-mm (18-in.) drop
944 cm^3 (1/30 ft^3) mold*	
3 layers of soil	5 layers of soil
25 blows/layer	15 blows/layer

*Mold diameter = 101.6 mm for Methods *A* and *B* or 152.4 mm for Method *C*, which allows particles larger than 20 mm (3/4 in.).

The foregoing procedures are for ASTM test Methods *A* and *B*, which are for soil with grains smaller than 10 mm ($\frac{3}{8}$ in. nominal). Refer to the ASTM test Method *C* if larger soil particles are used.

The modified compaction test (D 1557) just listed is not used much in building construction since there is seldom enough soil improvement to justify the additional compaction effort and necessary quality control. Figure 6-1 presents typical compaction curves for several soils obtained using Method *A* from both ASTM standards.

For fills that will later support any structure it is usual to perform compaction tests to establish the required compacted density and *optimum moisture content* (OMC) for the field

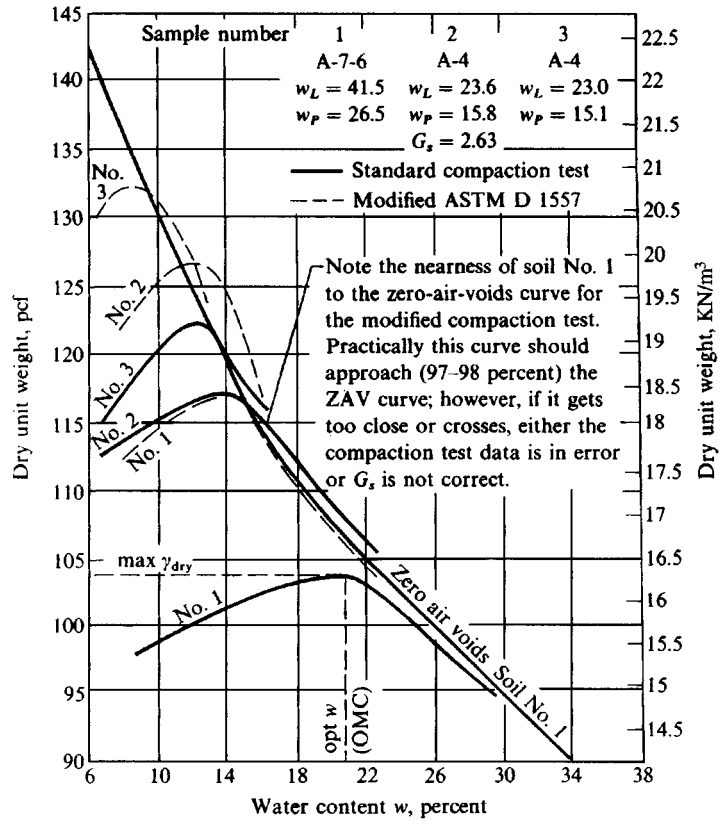

Figure 6-1 Typical compaction curves for three soils classified as indicated on the graph and by both standard (ASTM D 698) and modified (ASTM D 1557) methods. The zero-air-voids (ZAV) curve is shown only for soil sample no. 1.

soil. Field density tests (quality control) are then performed to ensure the desired unit weight γ is obtained. With compaction control, the fill is often of better quality than the underlying soil. The underlying soil will undergo settlements of varying magnitude depending on its characteristics and the depth of fill D_{fill} which produces a settlement/consolidation pressure of γD_{fill}.

Settlements will be *nonuniform* if the fill depth varies or if the site consists of both cut and fill. Settlements may be of long duration unless special steps are taken to speed up the process such as overfill (or *preloading*) to increase the settlement pressure and/or installation of drainage to speed consolidation.

Compaction of cohesive soils can be accomplished using sheeps-foot or rubber-tired rollers. Lifts are commonly 150 to 200 mm thick. It may be necessary either to aerate the soil by disking to reduce the water content or to add water from mobile water tanks if the field w_N is too low. Minimum compaction effort is required when the field w_N is near (or at) the OMC.

Compaction of cohesionless soils can be accomplished using smooth wheel rollers, commonly with a vibratory device inside, so the compaction is a combination of confinement, pressure, and vibration. Lift depths up to about 1.5 to 2 m can be compacted with this

equipment. Better results are obtained, however, for lift thicknesses of 0.6 to 1 m. Where there is an ample supply of water and its use does not adversely affect the surrounding soil, flooding (100 percent saturation) will substantially reduce the required compaction effort—particularly if the in situ sand is slightly damp where surface tension impedes densification.

In confined spaces, it is necessary to use hand-powered equipment for compacting the soil. This requirement reduces the lift thickness so that if density has been specified, lift thicknesses should not exceed 75 to 100 mm. For lifts that are too thick, compacting by hand—or any method—results in a dense upper crust overlying uncompacted soil which will later settle under self-weight and/or applied load, regardless of the type of equipment used or soil location.

Specific details of compaction methods and equipment necessary to compact various soils, laboratory tests to establish compaction specifications, and field tests for verification are beyond the scope of the overview presented here. The interested reader may wish to consult publications (with included references) such as these:

"Criteria for Compacted Fills," Building Research Advisory Board, National Academy of Sciences, Washington, DC, 1965.

Symposium on Compaction of Earthwork and Granular Bases, Highway Research Record no. 177, National Academy of Sciences, Washington, DC, 1967.

Soil Compaction and Corrugations, Highway Research Record no. 438, National Academy of Sciences, Washington, DC, 1973.

"Compacted Clay: A Symposium," *Trans. ASCE,* vol. 125, pp. 681-756, 1960.

"Sand Compaction with Vibratory Rollers," D'Appolonia, D.J., et al., *JSMFD*, ASCE, vol. 95, no. 1, January, pp. 263–284, 1969.

One of the recent textbooks on Geotechnical Engineering such as Bowles (1984).

Although these references are somewhat dated, this soil improvement method was one of the earliest that was heavily researched. There is little that can be added to the current knowledge base.

The bottom of any footing trench or basement excavation should always be compacted either using hand or full-size equipment. Although this precaution does not recover heave (expansion due to loss of overburden) it does place the base soil loosened by the excavation equipment into a dense state.

6-3.1 Consolidation Settlements of Compacted Fill

Early geotechnical engineers knew that a compacted fill would undergo some subsidence due to self-weight producing grain readjustment and/or some squeezing (or creep). Any consolidation settlements were supposed to be developed in the underlying soil supporting the fill. It is now known that both the underlying soil *and* the compacted fill undergo consolidation. The consolidation of the underlying soil is similar to that described in Secs. 2-10 and 5-12.

Fill settlements can range from about 60 mm to well over 500 mm depending on the depth and the following factors:

1. Soil fabric (how much particle packing, type of particles, etc.); related to the compaction effort.

2. The compaction water content, and later change in water content. Factors 1 and 2 are, of course, related.
3. The fill height (or depth for a self-weight component) and any surcharge or applied vertical stress as from a foundation.

The fill consolidation usually involves later mass saturation and may occur a number of years after construction. After a long period of time the vertical movements may not always be correctly attributed to consolidation settlement within the fill.

It appears that one might estimate the probable consolidation settlement in the fill by compacting soil samples in the laboratory to the field density and field compaction water content. These samples can then be put into a consolidation test device, saturated, and then tested for swell and for both primary and secondary compression. It may be necessary to use backpressure to speed the saturation process if the consolidation device allows it. Some of this methodology is described by Brandon et al. (1990) and Lawton et al. (1989).

6-3.2 Dynamic Compaction

A widely used method of compaction using a mobile crane to lift and drop a heavy tamper onto the soil is called *dynamic compaction* (some persons call the procedure *dynamic consolidation*). Although the dropping of a weight on the soil had probably been in use for centuries, it was reintroduced to the profession and patented by L. Ménard in France ca. 1970 [see Ménard and Broise (1975)]. Compaction can be achieved to a substantial depth depending on weight (or mass) of the tamper, height of fall, and the type of soil.

Although the dynamic compaction tamper can have a mass up to 150,000 kg (or 150 tonnes), the usual mass is on the order of 10 to 20 tonnes and is dropped from heights ranging up to 40 m (usually 10 to 20 m) onto a grid spacing so that the site requiring improvement is adequately covered. Craters ranging from 0.5 to 2 m in depth are produced at the points of impact.

After a selected part of the area to be compacted is covered by a pass (drop in each grid point) it is graded with a bulldozer using imported fill as necessary to smooth the surface, the next pass is made, and so on until the desired density is obtained. Density is usually specified based on before and after penetration tests (either SPT or CPT). After the site improvement is completed, the area is brought to grade and compacted with ordinary compaction equipment.

Most saturated soils that can be classified through silty and/or clay sands and gravels can be considerably improved by this method. The amount of compaction tends to decrease with an increase in silt or clay content. Saturated clays tend toward almost no improvement because the impact results in an instantaneously high pore pressure, an immediate loss of shear strength, and remolding. Partially saturated clays may be improved, at least in the region above the GWT.

In practice several trial grid sections are used to determine the optimum drop spacing, drop weight (and/or height of fall), and number of drops.

For cohesionless soils Leonards et al. (1980) suggested the depth of compaction influence D_i is approximately

$$D_i = \frac{1}{2}\sqrt{Wh} \qquad \text{(m)} \tag{6-1}$$

In cohesive soils Ménard and Broise (1975) suggested

$$D_i = \sqrt{Wh} \quad \text{(m)} \tag{6-2}$$

where W = mass of tamper in tonnes (1 tonne = 1000 kg)
h = height of fall, m

Both of these equations are in current use.

Mayne et al. (1984) give a review of a large number of sites where dynamic compaction was used; Rollins and Rogers (1991) present a more recent example of the method for a collapsible alluvial soil. See Greenwood and Thomson (1984) for additional dynamic compaction details if necessary.

It is evident that the improvement will range in quality from the point of impact and grade into untreated soil at the depth D_i. The depth D_i should be on the order of $2B$ of the least lateral foundation dimension for smaller bases, but engineering judgment and available equipment will determine the influence depth D_i for large bases such as mats that cover large foundation areas. Grid spacings are commonly on the order of 1.5 to 4 meters.

Ordinarily, dynamic compaction/consolidation is only economical when

1. Site plan involves an area of some 5000 to 10 000 m^2.
2. Depth of soil is too great to use excavation and replacement.
3. Impact vibrations that are on the order of 2 to 12 Hz will not cause damage to nearby developments.

Where the water table is near the ground surface or there is a soft clay surface deposit, it may be necessary first to lay a free-draining granular blanket on the order of 200 to 1000 mm thick over the area to be dynamically compacted.

6-4 SOIL-CEMENT, LIME, AND FLY ASH

In many cases where slab-on-grade construction is to be used the most economical solution to increase the bearing capacity may be to do one of two things.

1. Use soil-cement, with or without a sand or fly ash filler. In this procedure soil samples are mixed with varying percentages of cement and/or sand and/or fly ash, cured in a manner somewhat similar to concrete control test cylinders,[2] and tested to obtain the unconfined compression strength q_u. That mix providing the required strength becomes the job mix. The cement and/or other admixtures are either deposited on the soil and thoroughly mixed at the necessary water content with discs and similar farm equipment or run through a traveling soil processor where the chemicals and water are added, blended and redeposited on the soil for grading and compaction. Depths to about 1.5 m can be treated in this manner;

[2]ASTM has a number of standards relating to "soil-cement".

greater depths usually require some alternative method. The required cement by weight is seldom over 5 percent.

2. Use lime or a mix of lime and sand, with or without fly ash, in a manner similar to soil-cement.

6-5 PRECOMPRESSION TO IMPROVE SITE SOILS

A relatively inexpensive, effective method to improve poor foundation soils in advance of construction of permanent facilities is *preloading*. The preload may consist of soil, sand, or gravel; and in the case of oil or water tanks, gradual filling of the tanks may be used for the preload. Sometimes the preload may be accomplished by lowering the groundwater table. It may also be accomplished by "ponding," that is, building a watertight containment that is filled with water [but requires protection against vandalism and unauthorized recreation (such as swimming)].

How or what to use to accomplish preloading will be determined by relative economics. Aldrich (1965) [see also Johnson (1970)] conducted a survey among several organizations to produce a report on preload practices that were current at that time.

Precompression (or preloading) accomplishes two major goals:

1. Temporary surcharge loads are used to eliminate settlements that would otherwise occur after the structure is completed.
2. Preloading improves the shear strength of the subsoil by increasing the density, reducing the void ratio, and decreasing the natural water content w_N.

Preloading is most effective on normal to lightly overconsolidated silts, clays, and organic deposits. If the deposits are thick and do not have alternating sand seams, the preloading may necessitate using sand drains (see Sec. 6-6) to reduce the time necessary to effect consolidation.

The amount of settlement eliminated by using preloading should be 100 percent of primary consolidation. As much secondary compression is removed as practical so that, in combination with the eliminated settlement, any remaining after project completion will be tolerable. The primary consolidation can be computed by obtaining the stress increase using the Boussinesq method of Chap. 5 for several points beneath the loaded area and using Eq. (2-44). The secondary compression may be estimated using Eq. (2-49) repeated here, expanded, and terms reidentified to obtain

$$\Delta H_s = \frac{C_\alpha H}{1 + e_o} \log \frac{t_f - t_i}{t_i} \tag{6-3}$$

where ΔH_s = secondary compression settlement, in units of H
H = thickness of stratum in field, m
C_α = coefficient of secondary compression
t_f = time of interest when ΔH_s occurs, days or years
t_i = time at the end of primary consolidation or slightly later, days or years.

The total settlement for the preload is the sum of the primary and secondary settlements [the sum of Eqs. (2-44) and (6-3)].

Shear strength tests before and after preloading are necessary to evaluate the improvement in strength with preconsolidation. These are best run on undisturbed tube samples in either unconfined or triaxial tests. The in situ vane may not give much indication of any shear strength improvement, for the vane measures horizontal rather than vertical shear strengths. Since the lateral improvement is likely to be on the order of $K\sigma_v$, with K usually less than 0.5, preload improvement that may be sufficient for vertical loads may be too small to be detected by the shear vane test with sufficient accuracy or reliability to be of value [Law (1979)].

Normally the preload surcharge would be greater than the estimated weight of the proposed structure so that postconstruction settlements are negligible. There may be some rebound and recompression as any preload is removed and before the building load is applied.

Preloading does not seem to be much used at present since a number of other procedures can be used to improve the soil that are comparable in cost, allow more rapid access to the site, and do not require disposal of the excess preload material.

In extremely soft cohesive and peaty deposits such as glacial lakes, river deltas, and peat bogs a procedure called *displacement preloading* may be used where haulers back to the site edge and dump the quality fill. The fill load induces a shear failure in the in situ soil, which causes it to displace laterally away from the fill. The lateral displacement usually produces viscous waves in the soil called mud waves. When there is enough fill accumulated it is compacted and the process continued until the desired area is stabilized. This procedure is of use for shoreline construction and has been used to produce causeways across lakes for railroad tracks and roadways.

6-6 DRAINAGE USING SAND BLANKETS AND DRAINS

When either a fill or a soil preload is placed on a saturated cohesive deposit, the length of the drainage path may be increased—perhaps to the top of the fill. Since the length of the drainage path determines the time for consolidation, this should be as short as possible.

When the water table is very near the ground surface, either the site should be graded so it slopes to one side or a series of shallow collection ditches should be cut. Next a layer of sand (called a *sand blanket*) 100 to 150 mm thick is placed on top of the site and in the drainage ditches, and then the preload. Water squeezed from the soil being consolidated then flows up to the ditches or sand blanket and drains to the edge for disposal. This will greatly speed the drainage process, since the coefficient of permeability is larger in sand.

6-6.1 Sand Drains

We can extend this concept further and install vertical columns of sand at selected intervals in the existing soil. Under the hydraulic gradient produced by the fill (or preload) the water flows from a higher to a lower energy potential. Since the water can move faster through the sand than through the in situ soil, the sand columns (sand drains) become points of low energy potential.

Maximum flow rate is obtained by incorporating a sand blanket with the sand drains. Sand drains can be installed even where the consolidating stratum is some depth below the surface to speed up the consolidating process. Here, however, it may not be desirable or necessary to use a sand blanket.

Consolidation theory of Sec. 2-10 is the basis for both sand blankets and sand drains. The time t_c for consolidation is estimated from a rearrangement of Eq. (2-38) to obtain

$$t_c = \frac{TH^2}{c_v} \tag{6-4}$$

The dimensionless factor T depends on the percent consolidation U (see Table 2-4) and is about 0.848 and 0.197 for 90 and 50 percent consolidation, respectively. The coefficient of consolidation c_v is usually back-computed from a consolidation test by solving Eq. (6-4) for c_v. The coefficient is also

$$c_v = \frac{k}{\gamma_w m_v} \qquad (2\text{-}35)$$

where all terms have been defined in Chap. 2. For radial drainage as in sand drains, the coefficient of permeability (or *hydraulic conductivity)* k in Eq. (2-35) would be the horizontal value, which is often four or five times as large as the vertical value.

The theory of radial drainage into sand drains, including allowance for "smear" effects on the sides of the holes from soil on the auger flights that reduce inflow, has been presented by Richart (1959) [see also Landau (1978)]. Since one is fortunate to determine the order of magnitude of k (the exponent of 10), for practical purposes the time for consolidation of a layer can be computed as follows:

1. Take $H = \frac{1}{2}$ the longest distance between sand drains, m.
2. Compute c_v using Eq. (2-35) with k = horizontal coefficient of permeability (or your best estimate of that value), m/day.
3. Use T from Table 2-4 for the appropriate percentage of consolidation. For 90 percent consolidation use $T = 0.848$.
4. Solve Eq. (6-4) for t_c in the time unit of days.

The calculated time will be somewhat in error from factors such as vertical drainage within the consolidating layer, presence of thin sand seams, one- or two-way vertical drainage, how the distance H compares with the clay thickness, etc.

Sand drains are installed by several procedures in diameters ranging from 150 to 750 mm. Landau (1966) describes several that are still current:

1. *Mandrel-driven pipes.* The pipe is driven with the mandrel closed. Sand is put in the pipe, which then falls out the bottom as the pile is withdrawn, forming the drain. Air pressure is often used to ensure continuity and densify the sand.
2. *Driven pipes.* The soil inside is then removed using high-pressure water jets. The rest of the procedure is the same as method 1.
3. *Rotary drill.* A casing is used as required, then the boring is filled with sand. Any casing used is pulled as the boring is filled. The sand may be rammed as necessary to increase its density, producing some enlargement of the column over the drilled diameter.
4. *Continuous-flight hollow auger.* The sand may be introduced using air pressure through the hollow stem to fill the cavity as the auger is withdrawn.

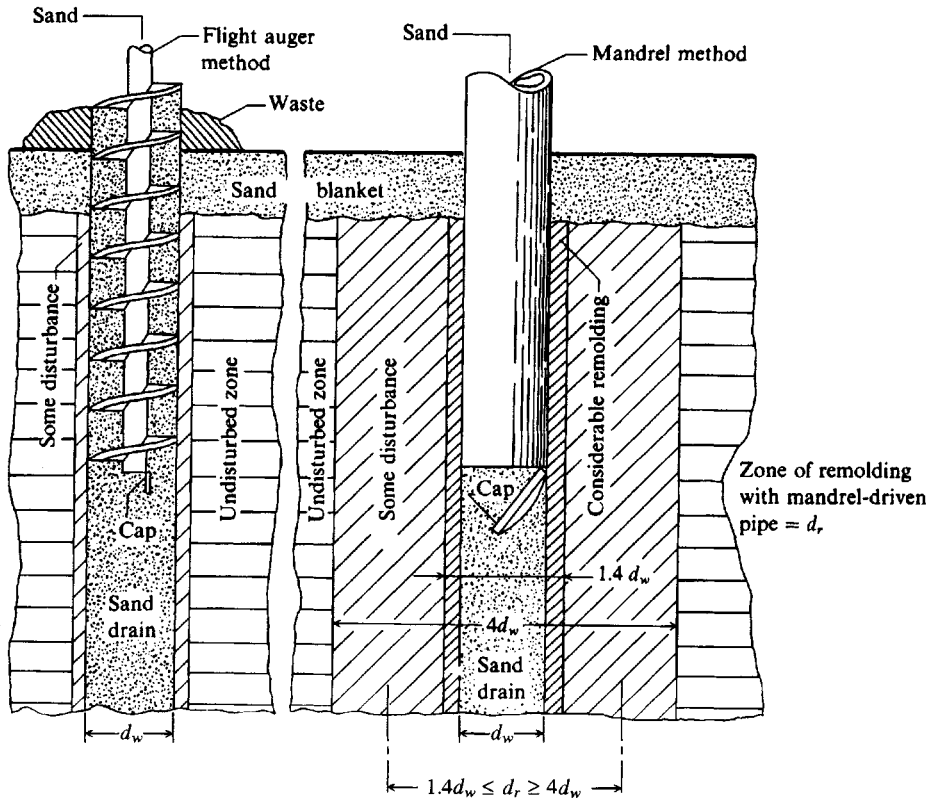

Figure 6-2 Two commonly used methods of constructing sand drains. [Landau (1966).]

Figure 6-2 illustrates methods 1 and 4.

Note that if we construct a pattern of sand drains using displacement-driven columns and then later construct the interior drains (also using displacement columns) the site drainage should be much more rapid since the excess pore pressure produced when installing the interior drains can drain laterally into the existing drains as well as back into the just-installed drains.

Soil drainage is related to settlement (volume change), and the larger the settlement under preload, the less to be expected when the structure is built. Drainage is also related to the change in the natural water content since a change in void space results in a permanent change in water content for saturated soils. The change in water content is also a measure of the improvement in the undrained shear strength s_u.

6-6.2 Wick Drains

Wick drains are now being widely used in lieu of sand columns for soil drainage. A wick drain is a geotextile consisting of a grooved plastic or paper core covered by plastic or paper membranes to produce a "wick" ranging from about 100 to 300 mm wide × 4 to 6 mm thick and of the necessary length. The membrane cover provides a permeable soil barrier to reduce core clogging. The core provides a ready conduit to the surface into a sand or textile filter blanket or into horizontal trench drains.

The particular attraction of wick drains is economy since installation costs per meter are typically one-quarter to one-fifth those of sand drains. They can be installed to depths up to 30 m using a conventional vibratory hammer (as used for pile driving) and a special wick installation rig. According to Morrison (1982) wick drains have about 80 percent of the soil consolidation market—probably about 80–85 percent in 1995. Several references and some design theory on wick drains are cited by Koerner (1990). For current materials consult recent issues of the "Geotechnical Fabrics Report" published monthly by the Industrial Fabrics Association International (see footnote 5 on p. 368).

The same approximate equations for sand drains can be used for wick drains to establish spacing and estimate time for consolidation to occur.

Wick drains provide no strengthening effect on the soil (unless they are laid horizontally) except for that resulting from the reduced water content and for the void ratio reduction that may result from any increase in effective stresses within the soil mass.

Note that the drainage process can be considerably speeded by installing mandrel-driven pipe displacement sand drains interior to the peripheral wicks.

6-7 SAND COLUMNS TO INCREASE SOIL STIFFNESS

Outside the United States—particularly in the Asian and Pacific Rim regions—sand columns are widely used to increase soil stiffness in both sand and clay deposits. Soil stiffness (or improvement) is directly related to the increase in either the SPT blow count N or the CPT cone resistance q_c. That is, if the initial soil resistance (N or q_c) is too low to give an adequate bearing capacity, sand columns might be an economical solution, i.e., use the N after installing the columns for computing the bearing capacity.

The use of sand columns is mostly a trial-experience combination process where their use is appropriate. That is, a trial spacing is chosen and sand columns are inserted. Sand columns are usually drilled at diameters D_o between 600 and 800 mm, but after construction the actual column diameters D_f range from 1.5 to $1.6D_o$. Column depths usually range from about 3 to 8 m but depend on site and purpose.

The before and after stiffness is measured along with the amount of sand needed to produce the required end product. That spacing and/or column density producing the required degree of soil improvement is then specified for that site. Barksdale and Takefumi (1991) cite some equations (see Fig. 6-3) that attempt to quantify some of this process, but the several assumptions used make it necessary to always verify the improvement using either the SPT or CPT. It is also necessary for contractor payment to measure the actual volume of sand used.

To quantify a project approximately one would make a best estimate of the current in situ void ratio e_o. Next one would make an estimate of the final void ratio e_f based on available information or by simply deciding the void ratio should be some value.

You should refer to the previously cited reference for the use of sand columns to strengthen clay deposits.

Stone columns can also be used in sand deposits and they are constructed in a similar manner. Their use is not recommended in sand, however, since the sand column can be constructed more economically. The reason is that the in situ sand can be used as the primary source for the column material, which can then be supplemented with a smaller amount of imported material, whereas the full volume of the stone column would have to be imported.

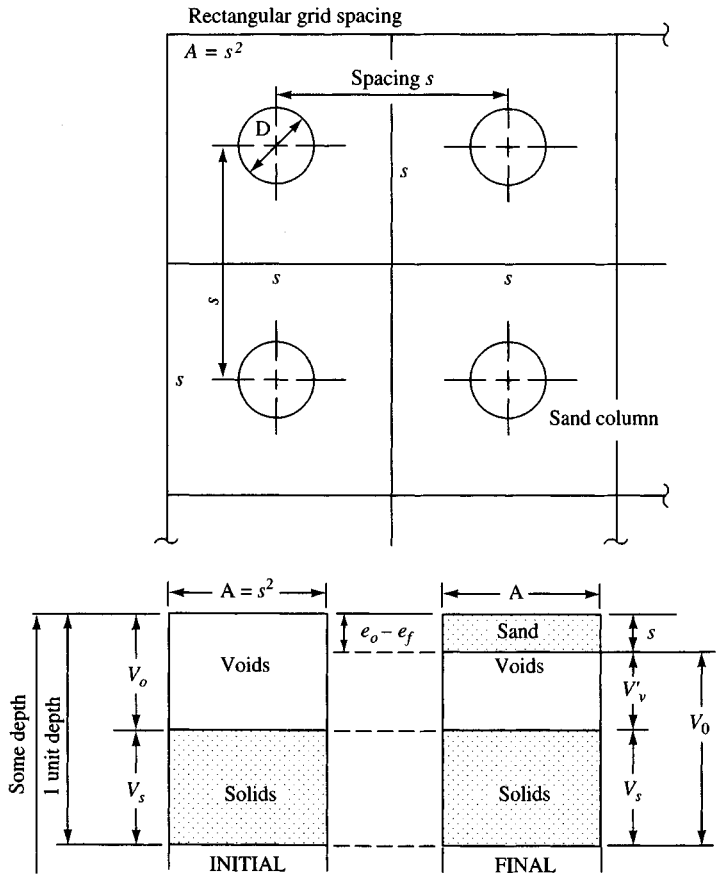

For the initial conditions:

$$e_o = \frac{V_v}{V_s} \rightarrow V_v = e_o V_s$$

The initial volume is

$$\begin{aligned} V_o &= V_s + V_o \\ &= V_s + e_o V_s \\ &= V_s(1 + e_o) \end{aligned}$$

For the final conditions:

Noting that the total volume is now $V_o = V_s + V'_v + s$ we can find the sand volume $\bar{s}$ per unit of depth by proportion as follows:

$$\frac{\bar{s}}{e_o - e_f} = \frac{V_v}{e_o} \rightarrow \bar{s} = \frac{V_v}{e_o}\ (e_o - e_f)$$

The sand ratio as per unit treatment (sand column) depth is:

$$a_s = \frac{\bar{s}}{A}$$

A tentative column spacing distance s for square grid (as shown in the figure) is $s = \sqrt{V_o}$

Figure 6-3 Sand columns for soil strength improvement. [After Barksdale and Takefumi (1991).]

Example 6-1. We have somehow found $e_o = 0.8$ in a sand deposit and have estimated the desired $e_f = 0.5$ and a trial grid spacing of 3 m.

Required. Make an estimate of the amount of sand fill required per meter of improvement depth D_i.

Solution. For this problem we have $A = 3 \times 3 = 9\ \text{m}^2$ and for a 1-m depth,

$$V_o = 9 \times 1 = 9\ \text{m}^3$$

From $V_o = V_s + e_o V_s = V_s(1 + e_o)$ (see Fig. 6-3) we obtain

$$V_s = 9/1.8 = \mathbf{5}\ \text{m}^3$$

The original $V_v = V_o - V_s = 9 - 5 = \mathbf{4}\ \text{m}^3$. The theoretical volume of sand required *per meter of depth* is

$$\bar{s} = \frac{V_v}{A}(e_o - e_f) = \frac{4}{0.8}(0.8 - 0.5) = 5(0.3) = \mathbf{1.5}\ \text{m}^3$$

Still to be determined is the drill diameter, the depth of the sand column, and whether a final void ratio $e_f = 0.5$ is obtainable.

////

6-8 STONE COLUMNS

If, instead of using sand for the column, gravel or stones are used, the result is a *stone column*. The vibratory devices or procedure no. 1 used to install sand drains and sand columns can also be used to insert gravel or stone columns into the soil. The granular material commonly ranges in gradation from about 6 to 40 mm ($\frac{1}{4}$ to $1\frac{1}{2}$ inches).

Stone columns may be used in sand deposits but have particular application in soft, inorganic, cohesive soils. They are generally inserted on a volume displacement basis, that is, a 600- to 800-mm diameter hole is excavated to the desired depth L_c. The depth may be on the order of 5 to 8 m, and sometimes the hole requires casing to maintain the shaft diameter. Stone is introduced into the cavity in small quantities and rammed (while simultaneously withdrawing any casing). The rammed stone increases the drilled diameter of the stone column shaft, and it is necessary to record the hole depth L_c and volume of stone V_c used for the column so that the final nominal shaft diameter can be approximately computed. The lateral expansion of the column due to ramming will induce excess pore pressures in clay, but these rapidly dissipate back into the much larger voids in the granular column. The net effect is to produce a fairly rigid vertical stone mass (the stone column) surrounded by a perimeter zone of somewhat stronger material which has a slightly reduced void ratio. This insertion method also ensures intimate contact between soil and column.

The vibroflotation (see Fig. 6-6) method can be used to produce a stone column by sinking the device, backfilling the cavity with stone, and then raising and lowering the vibroflot while adding additional stone. The result is a densely compacted stone column of some depth with a diameter on the order of 0.5 m to 0.75 m.

Similarly, a closed end pipe mandrel can be driven to the desired depth and a trip valve opened to discharge the stone. Either a rammer packs the soil through the pipe as it is withdrawn and with stone added as needed, or the mandrel is withdrawn until the valve can be closed and this used to ram against the stone to expand and densify the column.

Stone columns are spaced from 1.2 m to about 3 m on center on a grid covering the site. There is no theoretical procedure for predicting the combined improvement obtained, so it is usual to assume that the foundation loads are carried only by the several stone columns with no contribution from the intermediate ground. Work on pile caps by the author indicates that this is reasonable when the stone columns are more than about 10 times as stiff as the surrounding soil. Also a compacted layer of granular material should be placed over the site prior to placing the footings.

An approximate formula for the allowable bearing pressure q_a of stone columns is given by Hughes et al. (1975)

$$q_a = \frac{K_p}{\text{SF}}(4c + \sigma_r') \tag{6-5}$$

where $K_p = \tan^2(45° + \phi/2)$

ϕ' = drained angle of internal friction of stone

c = either drained cohesion (suggested for small column spacings) or the undrained shear strength s_u when the column spacing is over about 2 m

σ_r' = effective radial stress as measured by a pressuremeter (but may use $2c$ if pressuremeter data are not available)

SF = safety factor—use about 1.5 to 2 since Eq. (6-5) is fairly conservative

The allowable load P_a on the stone column of average cross-sectional area $A_c = 0.7854D_{\text{col}}^2$ is

$$P_a = q_a A_c \tag{6-5a}$$

where q_a = allowable bearing pressure from Eq. (6-5)

We can also write the general case of the allowable column load P_a as

$$P_a = (c_s A_s + A_c c_p N_c) \cdot \frac{1}{\text{SF}} \tag{6-5b}$$

where c_s = side cohesion in clay—generally use a "drained" value if available; c_s is the side resistance ($\gamma z K \tan \delta$) in sand

c_p = soil cohesion at base or point of stone column

A_s = average stone column perimeter area

To compute A_s, use the in-place volume of stone V_c and initial column depth L_c as follows:

$$A_c L_c = 0.7854 D_{\text{col}}^2 L_c = V_c \qquad \text{and} \qquad D_{\text{col}} = \sqrt{\frac{V_c}{0.7854 L_c}}$$

$$A_s = \pi D_{\text{col}} L_c$$

Observe that, by using the volume of stone V_c, the diameter D_{col} computed here is the *nominal* value. In Eq. (6-5*a*),

N_c = bearing capacity factor as used in Chap. 4, but use 9 for clay soils if $L_c/D_{\text{col}} \geq 3$ (value between 5.14 and 9 for smaller L/D)

The allowable *total* foundation load is the sum of the several stone column contributions beneath the foundation area (perhaps 1, 2, 4, 5, etc.).

Stone columns should extend through soft clay to firm strata to control settlements. If the end-bearing term ($A_c c_p N_c$) of Eq. (6-5*b*) is included when the column base is on firm strata, a lateral bulging failure along the shaft may result. The bulge failure can develop from using a column load that is too large unless the confinement pressure from the soil surrounding the column is adequate. The failure is avoided by load testing a stone column to failure to obtain a P_{ult} from which the design load is obtained as P_{ult}/SF or by using a large SF in Eq. (6-5*b*) or by not including the end-bearing term (now one can use a smaller SF).

Taking this factor into consideration gives a limiting column length L_c (in clay based on ultimate resistance) of

$$P_{ult} \leq \pi D_{col} L_c c_s + 9 c_p A_c \qquad A_c = 0.7854 D_{col}^2$$

Solving for L_c, we obtain

$$L_c \geq \frac{P_{ult} - 7.07 d_p D_{col}^2}{\pi D_{col} c_s} \tag{6-6}$$

where all terms have been previously identified.

Settlement is generally the principal concern with stone columns since their bearing capacity is usually quite adequate. No method is currently available to compute settlement on a theoretical basis. Settlements are estimated on the basis of empirical methods, of which Fig. 6-4 is typical. From this figure we see that stone columns can reduce the settlement to nearly zero depending on column area, spacing, and initial soil strength.

Note that any substantial improvement in settlement may require placing a granular surcharge over the treated area and rolling it prior to placing the foundation. A surcharge may be necessary because the upper column depth to approximately 0.6 m is often somewhat loose from the placing process and if not compacted may allow an unacceptable settlement.

Stone columns are not applicable to thick deposits of peat or highly organic silts or clays.

6-9 SOIL-CEMENT PILES/COLUMNS

The soil-cement pile (or column), SCP, is a relatively recent innovation for soil improvement that uses a special (proprietary) soil drill bit. The drill bit advances into the soil, cutting and grinding the soil and simultaneously injecting the cement (and any additives) slurry into the cuttings. A shear (or fixed) blade somewhat larger than the hole diameter is located above the drill head and is fixed into the sides of the boring to keep the soil between the drill and shear blade held in place so that it can be well-mixed with the cement slurry (see Fig. 6-5*a*). When the column depth is reached a soil-cement pile has been formed; the drill is withdrawn, with the counterrotation further blending the soil cuttings with the injected cement slurry.

The process is extremely rapid and SCP diameters from 0.6 to 1 m can be readily produced in lengths varying from about 1.5 to 10 m, but maximum depths to 35 m are possible. A typical side view of an SCP is shown in Fig. 6-5*b*.

The design process is as follows:

1. Obtain representative samples of the soil to be improved, including unconfined compression q_u and/or SPT blow counts N.

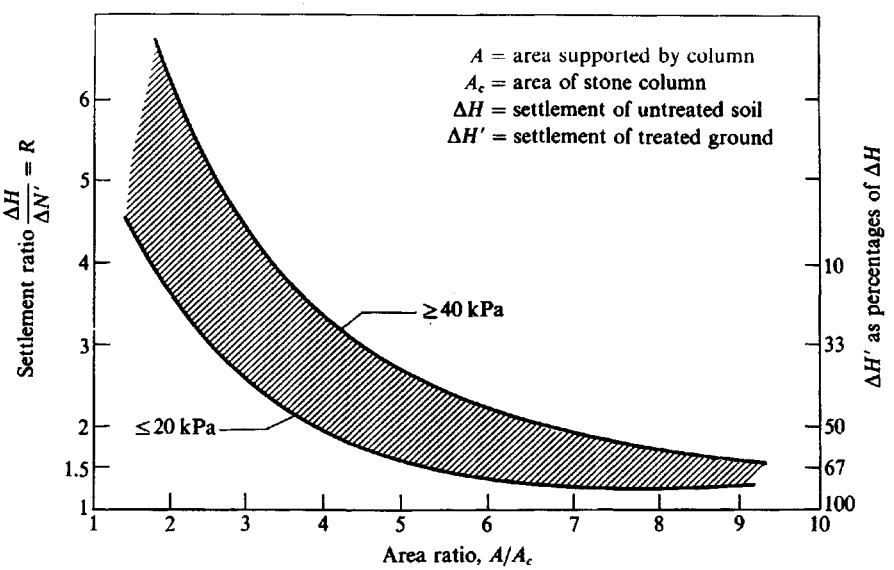

Figure 6-4 Approximate settlement reduction for ground reinforced with stone columns. [After Greenwood and Thomson (1984).]

Example

Stone columns in soil with $s_u = 25$ kPa
Average column diam. = 1 m
Average column spacing = 2 m center-to-center
ΔH of untreated ground estimated at 125 mm

Required: Estimate $\Delta H'$ of treated ground

$$A_c = 0.7854(1)^2 = 0.7854$$
$$A = 2 \times 2 = 4$$
$$A/A_c = 4/0.7854 = 5.09 \text{ use } 5.1$$

From figure interpolating into hatched zone at $s_u = 25$ obtain

$$R = \Delta H/\Delta H' = 2 \text{ (or } 50\%)$$
$$\Delta H' = 125/2 = 125(0.5) = 65 \text{ mm}$$

Note generous rounding since method is inexact.

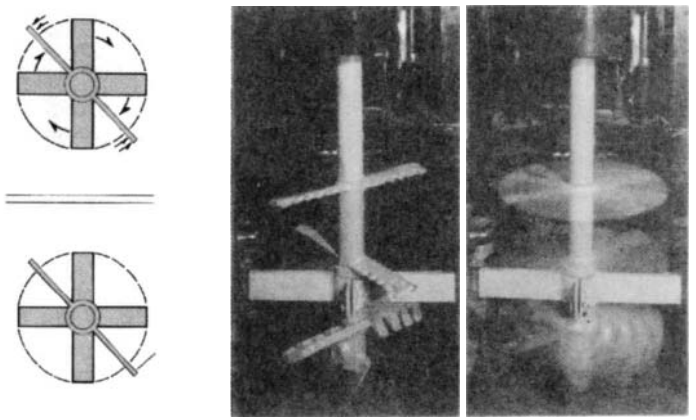

(*a*) Proprietary soil-cement pile drill

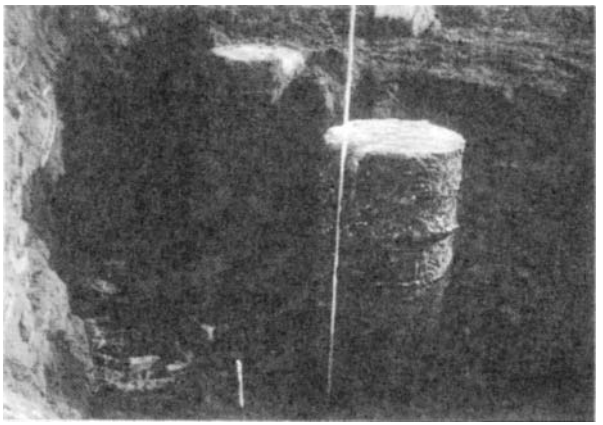

(*b*) Side view of a 1.52 m partially excavated SCP

Figure 6-5 Soil-cement piles. (Photos courtesy O. Taki, SCC Technology, Inc., Belmont, CA.)

2. Mix soil samples with different amounts of cement slurry and produce soil-cement cylinders, which are cured as for any type of soil-cement project. Refer to ASTM D 1633 for compressive strength tests and to D 2901 for cement content.
3. From cylinder compression tests determine the appropriate cement-slurry proportions (water-cement ratio) and slurry injection per unit volume of pile.
4. When the SCPs have been installed and cured, obtain sufficient cores to ascertain the unconfined compression core strength to verify quality.

Soil-cement piles may be used alone or, more commonly, in a closely spaced line to form a wall to maintain an open excavation or basement space. If the spacing produces pile overlap or the spacing is such that a jet-grout operation (of Sec. 6-10) can fill the space between any two piles, a nearly water-tight wall can be formed. Basically a SCP wall [see Taki (1992)] consists in obtaining the unconfined compression strength of the soil-cement cylinders q_{sc}. The unconfined shear strength is taken as

$$s_{u,sc} = \tfrac{1}{2} q_{sc} \qquad \text{(same as for soil)}$$

The allowable compressive strength for column design (without any reinforcement) is taken as

$$f_{c,sc} = \frac{s_{u,sc}}{3} \tag{6-7}$$

using an SF = 3 (actually a little over 6, based on the unconfined compression strength). The allowable side shear or skin resistance is computed as

$$f_{s,sc} = \frac{q_{sc}}{30} \lambda_1 \tag{6-7a}$$

where λ_1 is as follows:

Clay soil	Sandy soil	λ_1
$q_u < 20$ kPa	$N_{55} < 5$	0.25
> 20 kPa	≥ 5	0.75

Point bearing capacity is computed as in Chap. 4 or Chap. 16. Settlements may be computed based on methods given in Chap. 5 or in Chap. 16, and group stresses may be estimated using the methods shown in Fig. 18-4.

Reinforcing bars can be inserted into the fresh SCP if it is necessary to attach a footing or mat securely to the pile or pile group or if the pile(s) must resist bending.

The SCP is particularly suited to anchor floor slabs of dwellings and other buildings in areas where there is a high GWT, possibility of wind shifting the structure or of wave action eroding the soil from beneath the slab. It is also suited for use as an alternative to sand or stone columns if drainage is not a consideration. It may also be used in intermediate locations with sand or stone columns.

6-10 JET GROUTING

This procedure is now (1995) being used somewhat in the United States but it has been used elsewhere since the early 1970s. There are several variations on this method. One procedure

consists in using a special drill bit with vertical and horizontal high-pressure water jets to excavate through the soil. Cement based grout is then forced through the lateral jets to mix with the small remaining amount of foundation material loosened during excavation. When the grout sets the end result is a fairly hard, impervious column. Clearly this procedure is somewhat similar to the soil-cement columns described earlier.

There are at least four procedures for producing jet-grouted columns, but the two principal methods are

1. Breaking up the soil and mixing it in situ with the grout. A borehole of about the same diameter as the grout rods is used and grout columns up to about 1 m in diameter can be produced.
2. Breaking up and partially removing the in situ material—usually using boreholes much larger than the grout rods—so that the resulting column is mostly grout. Grout columns up to about 3 m in diameter can be produced by this method.

The grout columns (also called *grout piles*) have been used considerably in underpinning structures to provide additional foundation support. The method is also used for general foundation improvement, and very small diameter shafts are sometimes called *root piles*. Closely spaced columns are sometimes used for excavation support (but would require the insertion of reinforcing rods in the wet grout for bending resistance) and for groundwater control; however, the soil-cement columns previously described are probably better suited in most cases. A more comprehensive description of this method is given in ASCE SP 12 [see ASCE (1987)].

6-11 FOUNDATION GROUTING AND CHEMICAL STABILIZATION

In addition to the previously described uses of grouting, this term also describes the several techniques of inserting some kind of stabilizing agent into the soil mass under pressure. The pressure forces the agent into the soil voids in a limited space around the injection tube. The agent reacts with the soil and/or itself to form a stable mass. The most common grout is a mixture of cement[3] and water, with or without fine sand.

In general, although grouting is one of the most expensive methods of treating a soil, it has application in

1. Control of water problems by filling cracks and pores; that is, produce a reduction in permeability
2. Prevention of sand densification beneath adjacent structures due to pile driving
3. Reducing both pile driving and operating machinery vibrations by stiffening the soil

Generally this type of grouting can be used if the permeability of the deposit is greater than 10^{-5} m/s. One of the principal precautions with grouting is that the injection pressure should not cause the ground surface to heave. In using compaction grouting where a very stiff displacement volume is injected into the ground under high pressure, however, lifting of the ground surface as a grout lens forms is of minor consequence.

[3]Strictly, cement is a complex chemical agent.

Various chemicals can be used as grouting and/or stabilizing agents. Most chemical agents are very expensive for use in foundation treatment. Many, however, have offsetting advantages where low viscosity and setting time must be controlled. An in-depth discussion of the advantages, disadvantages, and availability of chemical stabilizing agents other than those previously described is beyond the scope of this text. The reader is referred to ASCE (1957, 1966) for very extensive bibliographies by the ASCE Committee on Grouting. A more current status report is given by ASCE (1987, pp. 121–135). The following materials are widely used as grout in soil stabilization for road and street work:

Lime

Cement

Fly ash (refer to *Fly Ash: A Highway Construction Material*, U.S. Department of Transportation, June 1976)

Combinations of the above

They can also be used for building construction to improve the soil. Lime, for example, will reduce the plasticity of most clays (by an ion exchange mechanism, usually Ca for Na), which in return reduces volume-change potential (Secs. 7-1 and 7-9).

6-12 VIBRATORY METHODS TO INCREASE SOIL DENSITY

The allowable bearing capacity of sands depends heavily on the soil conditions. This is reflected in the penetration number or cone resistance value as well as in the angle of internal friction ϕ. It is usually not practical to place a footing on loose sand because the allowable bearing capacity (based on settlements) will be too low to be economical.

Additionally, in *earthquake* analyses the local building code may not allow construction unless the relative density is above a certain value. Table 6-1 gives liquefaction-potential relationships between magnitude of earthquake and relative density for a water table about 1.5 m below ground surface. This table can be used for the GWT up to about 3 m below ground surface with slight error. The relative density is related to penetration testing as shown in Table 3-4 after correcting the measured SPT N to N'_{70} [see Eq. (3-3)].

The methods most commonly used to densify cohesionless deposits of sand and gravel with not over 20 percent silt or 10 percent clay are vibroflotation and insertion and withdrawal of a vibrating pile [termed Terra-Probing, see Janes (1973)].

Vibroflotation (patented by the Vibroflotation Foundation Co.) utilizes a cylindrical penetrator 432 mm in diameter, 1.83 m long, and weighing about 17.8 kN. An eccentric mass rotates inside the cylinder at about 1,800 rpm to develop a horizontal centrifugal vibration force of about 90 kN. The device has water jets top and bottom with a flow rate of between 225 and 300 L/min at a pressure of 430 to 580 kPa. Figure 6-6 illustrates the general procedure for using vibroflotation to densify a granular soil mass. The device sinks at a rate of between 1 and 2 m/min into the ground into the "quick" zone under the point caused by a combination of excess water from the lower water jet and vibration. When the Vibroflot reaches the desired depth, depending on footing size and stratum thickness, say 2 to 3B, and after a few moments of operation, the top jet is turned on and the Vibroflot is withdrawn at the rate of about 0.3 m/min. Sand is added to the crater formed at the top from densification as the device is withdrawn, typically about 10 percent of the compacted volume. Compaction volumes of 7500 to 15 000 m^3 in an 8-hr work shift are common. The probe is inserted in a

TABLE 6-1

Approximate relationship between earthquake magnitude, relative density, and liquefaction potential for water table 1.5 m below ground surface*

Earthquake acceleration	High liquefaction probability	Potential for liquefaction depends on soil type and earthquake acceleration	Low liquefaction probability
$0.10g$	$D_r < 33\%$	$33 < D_r \leq 54$	$D_r > 54\%$
$0.15g$	< 48	$48 < D_r \leq 73$	> 73
$0.20g$	< 60	$60 < D_r \leq 85$	> 85
$0.25g$	< 70	$70 < D_r \leq 92$	> 92

*From Seed and Idriss (1971).

Figure 6-6 Vibroflotation.

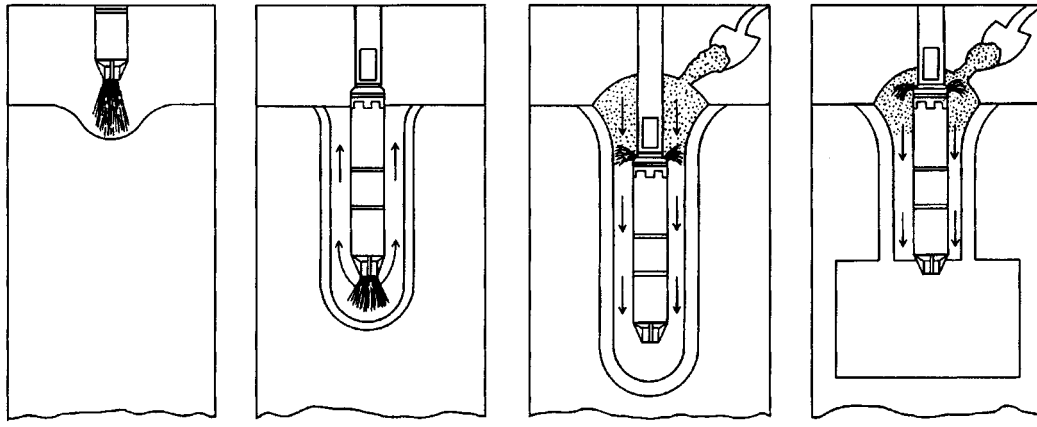

(*a*) Vibroflot is positioned over spot to be compacted, and its lower jet is then opened full.

(*b*) Water is pumped in faster than it can drain away into the subsoil. This creates a momentary "quick" condition beneath the jet which permits the Vibroflot to settle of its own weight and vibration. On typical sites the Vibroflot can penetrate 4.5 to 7.6 m in approximately 2 min.

(*c*) Water is switched from the lower to the top jets, and the pressure is reduced enough to allow water to be returned to the surface, eliminating any arching of backfill material and facilitating the continuous feed of backfill.

(*d*) Compaction takes place during the 0.3 m per minute lifts that return the Vibroflot to the surface. First, the vibrator is allowed to operate at the bottom of the crater. As the sand particles densify, they assume their most compact state. By raising the vibrator step by step and simultaneously back-filling with sand, the entire depth of soil is compacted into a hard core.

grid on 1- to 3- or 5-m centers depending on densification desired, maximum densification being in the immediate vicinity of the probe hole. Bearing capacities of 250 to 400 kPa can be obtained using this method.

The Terra-Probe (patented by the L. B. Foster Co.) method involves mounting a vibratory pile driver on a probe (pile) and vibrating it into and out of the soil to be densified. This device can be used in all soils where the vibroflotation method is applicable. This device is also applicable in underwater work, e.g., shoreline construction. The probe is inserted on spacings of 1.2 to 5 m depending on the amount of densification required.

Whether densification is adequate is determined by comparing in situ N or CPT data before and after vibration. Generally it is necessary to field-test a grid to determine optimum spacing, depth, and any other factors that might affect the efficiency of the process.

6-13 USE OF GEOTEXTILES TO IMPROVE SOIL

A *geotextile* (also geofabric) may be defined as a synthetic fabric that is sufficiently durable to last a reasonable length of time in the hostile soil environment. A number of synthetic fabrics made from polyester, nylon, polyethylene, and polypropylene are used to improve the soil in some manner. The fabrics may be woven or knitted into *sheets* and used in either sheets or strips or formed into *geogrids*[4] to reinforce the soil mass. They may be made impermeable for use as waste pond or sanitary landfill liners.

They may be permeable sheets or rods used to drain the soil. For drainage the geotextile depends on having a much larger coefficient of permeability k than the surrounding soil so that the geotextile attracts water by producing a hydraulic gradient between the textile and the soil to be dewatered. For example, placing a permeable fabric against the back of a retaining wall will reduce the lateral (hydrostatic) pressure against the wall as the water intersects the fabric, drains down to drain pipes or holes in the wall, and exits. Permeable rods (wick drains) can be inserted into the soil mass, on spacings somewhat similar to sand drains but much more rapidly, to increase drainage. The water flows laterally to the drain and easily upward to the ground surface since the k of the drain is several orders of magnitude larger than that of the soil being drained. This type of drainage can be used in conjunction with surcharging (similar to sand drains). Certain fabric sheets may be installed in the soil in lieu of sand blankets for soil drainage.

Much of the present use of geotextiles is involved with soil protection or reinforcement. The former involves control of erosion but may also entail isolating a soil mass from water. A particular installation may include excavating 0.5 to 1.5 m of soil that is susceptible to volume change, installing a plastic film, then carefully backfilling. Subsurface water migrating to the surface is blocked by the film so that the upper soil does not become saturated and undergo volume change. Obviously, careful site grading and protection against water entry from above are also required. A similar installation in colder regions can be used to control frost heave. A film of plastic may be used beneath 100 to 150 mm of coarse granular base beneath basement slabs to control basement dampness.

Geotextiles can be used in strips (or sheets or geogrids) to reinforce a soil mass. This usage is common for reinforced earth walls considered in Chap. 12 but may be carried out

[4] A geotextile grid is a section of specified dimensions consisting of bars of some size intersecting at right angles. Grids are similar to welded wire fabric except that usually the grid rods in one direction do not lie on top of the rods in the orthogonal direction.

for embankments so that steeper slopes can be used or so that compaction can be made to the edge of the slope, or to improve the bearing capacity of poor soil underlying the embankment.

Geotextiles and geogrids have potential application beneath footings and across culverts, both to improve bearing capacity and to spread the loaded area. The interaction of the fabric (dimensions large relative to soil grains) and soil effectively increases the angle of internal friction (between fabric and soil) and cohesion (fabric tension). Current problems with using geotextile sheets/strips or geogrids to increase bearing capacity are in determining the horizontal and vertical spacings of the reinforcement and in controlling settlement. Since improvement is being made on poor ground, the reinforcement will carry substantial tensile stresses. Geotextiles in tension tend to deform considerably (they stretch) under relatively small stresses. Foundation reinforcements would, as a consequence, have to be relatively thick in order to control vertical movement—and thickness is directly related to cost. Alternatives such as piles or soil excavation and replacement with imported fill may be more economical than excavation and replacement with existing soil and geotextile reinforcement.

At the present time, an abundance of theory is not available to compute the required amount, type, or geometry of geotextile reinforcement.

For hazardous fill and similar lining applications strength is not the major consideration, but great care must be exercised to ensure that sheet laps are sealed so that contaminated leachate cannot escape. It is necessary to lap and seal sheets since liners may cover several hectares (or acres) of ground and sheets are available in finite widths usually under about 5 m.

Geotextiles have not yet been in use for a long service period, but their use is spreading very rapidly. There have been, to date, several international conferences on geotextile usage, a textbook by Koerner (1990), occasional papers in the several applicable journals cited in this text, the ASCE (1987) special publication, as well as a Geotextile Fabrics Report.[5] There are also regularly scheduled international conferences on geotextiles.

6-14 ALTERING GROUNDWATER CONDITIONS

From the concept of submerged unit weight it is evident that the intergranular pressure can be increased by removing the buoyant effect of water. This can be accomplished by lowering the water table. In many cases this may not be feasible or perhaps only as a temporary expediency. Where it is possible, one obtains the immediate increase in intergranular pressure of $\gamma_w z_w$, where z_w is the change in GWT elevation.

It is usually impossible to lower the GWT exactly within the limits of one's own property. Thus, the increase in effective pressure also occurs beneath adjacent properties and can result in damage to those owners. The result may be cracked pavements and/or buildings, and the owners will certainly seek damages.

Note that it may be possible to raise the GWT. This process can also have an adverse effect on adjacent properties and requires careful analysis before being undertaken.

Since any activity that alters the GWT location will have some kind of effect on the environment, it will usually be necessary to get permission from appropriate environmental agencies. Otherwise litigation is almost certain to follow.

---

[5]Published by the Industrial Fabrics Association International, 345 Cedar Street, Suite 800, St. Paul, MN 55101 [Tel.: (612)-222-2508]. This monthly magazine usually describes one or more geotextile applications. A yearly summary volume containing a list of manufacturers, geotextile products available, and selected engineering data on the several products such as strength, deformation characteristics, sheet widths, etc., is also published.

PROBLEMS

6-1. The penetration number N of a loose sand varies from 7 at elevation -1.5 m to 16 at elevation -7.0 m. It is necessary to have a D_r of at least 0.75 for this soil. The area to be covered is 40×50 m. Vibroflotation or Terra-Probing will be used. What will be the expected N'_{70} values after densification? About how many cubic meters of sand will be required to maintain the existing ground elevation? (*Note:* Your answer depends on your assumptions.)

6-2. What is the additional settlement due to lowering the water table of Example 5-14 from 349.5 to 344.0? Comment on the effect of raising the water table to elevation 354.5 ft.

6-3. Compute the zero-air-voids curve for soil no. 2 of Fig. 6-1 using $G_s = 2.65$ and plot it on a copy of the figure (or an overlay that shows the compaction curves together with the ZAV curve). Is this G_s reasonably correct for this soil? If not what would you use for G_s?

6-4. A soft clay deposit with $s_u = 20$ kPa (from q_u tests) is 8.0 m thick and is underlain by a dense sandy gravel. The site is to be used for oil storage tanks. The water table is approximately at ground surface. The area is 400×550 m. Other soil data include the following:

$$k_h = 4 \times 10^{-6} \text{ m/s} \qquad w_L = 62\% \qquad w_P = 31\% \qquad w_N = 58\%$$
$$G_s = 2.63 \qquad c_v = 8.64 \times 10^{-4} \text{ m}^2\text{/day}$$

Describe how you would prepare this site for use. How would you either remove 700 mm of anticipated settlement in the clay prior to installing the storage tanks or otherwise control settlement? The tank pressure loading including tank and oil is 110 kPa. The tank has a diameter of 10 m, and it is desirable that the tanks not settle over 25 mm additional from the preload position when filled.

6-5. In referring to Sec. 6-5.1, sand or wick drains are spaced on 3-m centers in a clay soil. Tests indicate the vertical $c_v = 1 \times 10^{-3}$ m^2/day and the horizontal value $= 4c_v$. Estimate how long it will take for a 3-m depth of this clay to undergo 80 percent consolidation.

Answer: ≈ 0.87 years

6-6. What drain spacing in Problem 6-5 would be required to reduce the consolidation time to 0.5 years (6 months)?

6-7. Redo Example 6-1 with a final void ratio $e_f = 0.45$ (instead of 0.5), and estimate the volume of sand required if the sand columns have a depth of 3 m.

Answer: 5.25 m^3(for each 3×3 m grid)

6-8. For a stone column we have $\phi' = 42°$ and a clay cohesion $c = 1$ kPa. For a SF $= 2$, what might the allowable bearing pressure be using Eq. (6-5)? Hint: Assume a diameter D_{col} and length L_c.

6-9. A stone column is installed in a soft clay. The drill diameter $= 800$ mm and the shaft depth $L_c = 3.5$ m. If the volume of stone used to construct the column $V_c = 2.8$ m^3, what is the nominal column diameter D_c?

Answer: ≈ 1.0 m

6-10. A 2.5-m diameter stone column is installed in a clay soil with $c_s = 1.1$ and $c_p = 0.8$ kPa. If the ultimate load $P_{\text{ult}} = 90$ kN and a SF $= 1.5$ is used, what is the required column depth L_c? *Hint:* The working load $P_w = P_{\text{ult/SF}}$.

Answer: ≈ 6.0 m

6-11. A 3-m length of geotextile fabric is installed in a pull-out (tension) condition. The soil has a $\phi = 34°$, and the vertical pressure on the strip is 25 kPa. The coefficient of friction $f = \tan\phi$.

What is the approximate pull-out force on the fabric strip if it is 100 mm wide? *Hint:* Friction acts on both the top and bottom of the strip.

Answer: ≈ 10.1 kN

CHAPTER 7

FACTORS TO CONSIDER IN FOUNDATION DESIGN

7-1 FOOTING DEPTH AND SPACING

Footings should be carried below

1. The frost line
2. Zones of high volume change due to moisture fluctuations
3. Topsoil or organic material
4. Peat and muck
5. Unconsolidated material such as abandoned (or closed) garbage dumps and similar filled-in areas.

Footings should be placed below the frost line because of possible frost heave of the buildings and because alternate freezing and thawing of the soil tends to maintain it in an unconsolidated or loose state. Footings should also be placed below any topsoil layer, for topsoil is loose and usually contains organic matter.

However, aside from the consideration that the soil may be loose, interior footings may be placed at convenient depths since the building warmth should control frost. Figure 7-1 presents approximate maximum frost depths for various parts of the United States; local building codes should be consulted for design values, which may be based on local experience and therefore would be more realistic. Recent weather extremes may be obtained from weather records as a check that possible cold-weather cycles are not increasing the frost depth.

When footings are to be placed adjacent to an existing structure, as indicated in Fig. 7-2, the line from the base of the new footing to the bottom edge of the existing footing should be 45° or less with the horizontal plane. From this requirement it follows that the distance m of Fig. 7-2*a* should be greater than the difference in elevation of the two footings, z_f.

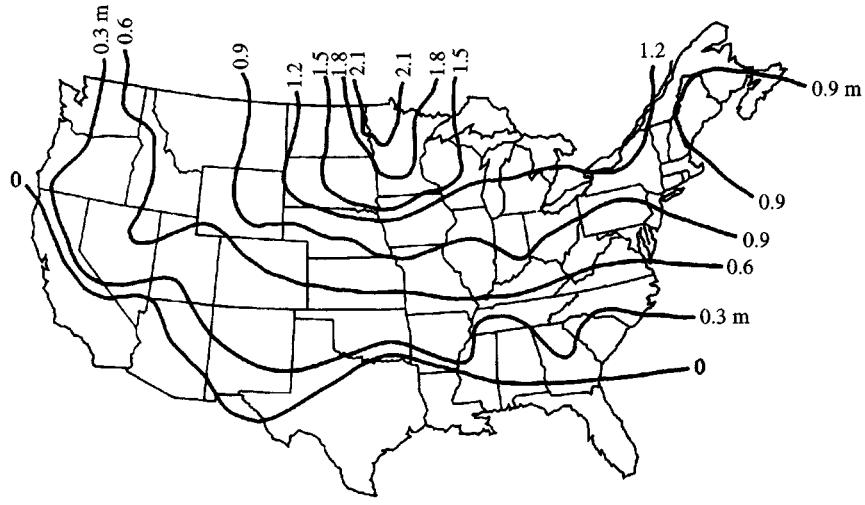

Figure 7-1 Approximate frost-depth contours in meters for the United States, based on a survey by the author of a selected group of cities.

This approximation should produce very conservative pressures in that zone where there is a contribution from more than one footing.

Conversely, Fig. 7-2*b* indicates that if the new footing is lower than the existing footing, there is a possibility that the soil may flow laterally from beneath the existing footing. This may increase the amount of excavation somewhat but, more importantly, may result in settlement cracks in the existing building. This problem is difficult to analyze; however, an approximation of the safe depth z_f may be made for a ϕ–c soil using Eqs. (2-54) and (2-55) since $\sigma_3 = 0$ on the vertical face of the excavation. The vertical pressure σ_1 would include the pressure from the existing footing. This analysis is as follows:

$$\sigma_1 \approx \gamma z_f + q_o$$

$$\sigma_3 = 0 = \sigma_1 K - 2c\sqrt{K} \qquad \text{[Using Eqs. (2-54) and (2-55)]}$$

$$= \gamma z_f K + q_o K - 2c\sqrt{K}$$

Solving for excavation depth z_f (and using a SF), we obtain

$$z_f = \frac{2c}{(\text{SF})\gamma\sqrt{K}} - \frac{q_o}{(\text{SF})\gamma}$$

This equation indicates two factors for consideration:

1. If the soil is a sand (does not have cohesion) one cannot excavate to a depth greater than that of the existing foundation.
2. The excavation depth of a ϕ–c soil is limited by the preceding equation.

The K in these equations is a lateral pressure coefficient of $K_a \leq K \leq K_p$ and considered in some detail in Chap. 11.

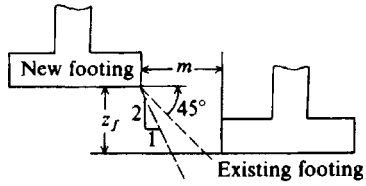

(*a*) An approximation for the spacing of footings to avoid interference between old and new footings. If the "new" footing is in the relative position of the "existing" footing of this figure, interchange the words "existing" and "new." Make $m > z_f$.

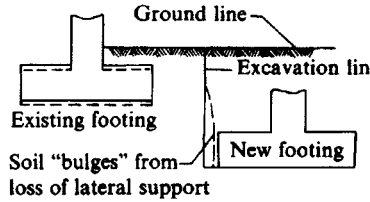

(*b*) Possible settlement of "existing" footing because of loss of lateral support of soil wedge beneath existing footing.

Figure 7-2 Location considerations for spread footings.

Figure 7-3 illustrates how a problem can develop if the excavation for the foundation of the new structure is too close to the existing building. In this case the $\bar{q}N_q$ term of the bearing-capacity equation is lost; for most foundations below the ground surface this is a major component of the bearing capacity as shown in the illustrative bearing-capacity examples of Chap. 4.

It is difficult to compute how close one may excavate to existing footings such as those of Figs. 7-2 or 7-3 before the adjacent structure is distressed. The problem may be avoided by constructing a wall (sheet pile or other material; Chap. 13 or 14) to retain the soil in essentially the K_o state outside the excavation.

One of the major problems in making an excavation for new construction in urban areas is to do so without causing damage to adjacent properties from the construction work or vibrations developed during construction. These may be either real or imagined and where possible a photographer should obtain pre- and postconstruction photographs for the project files.

Underground defects or utilities may affect the foundation depth, for example, limestone caverns, old mine tunnels, soft material, sewer tunnels, telephone-cable conduits, and pos-

Figure 7-3 Potential settlement or instability from loss of overburden pressure.

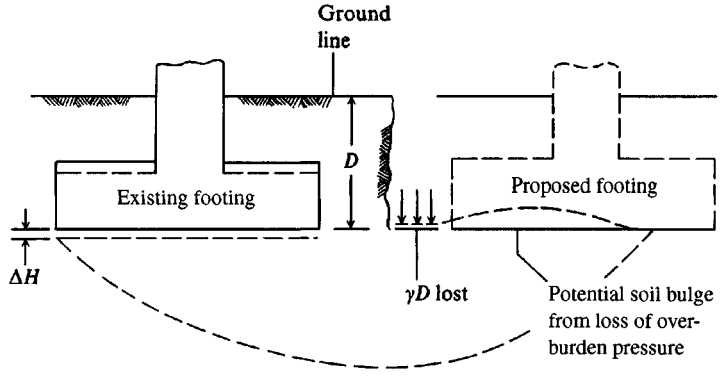

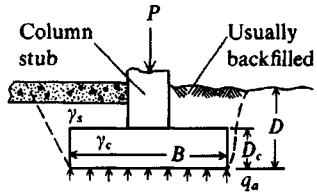

(a)

In general:
γ_s = unit weight of soil
Existing pressure = $\gamma_s D$
Increase in pressure due to $P = P/B^2 = q_1$
Increase due to displaced soil = $(\gamma_c - \gamma_s) D_c = q_2$
Net increase = $q_n = q_1 + q_2 \leq q_a$

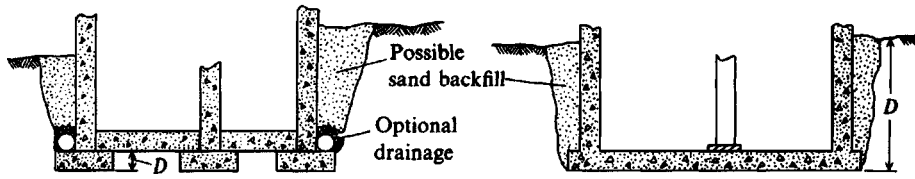

(b) Spread footings with basement.

(c) Mat foundation.

Figure 7-4 Footing placement and significance of q_a if value is "net" pressure increase. *Note:* In both (*b*) and (*c*) we should consider loss of a part of $\gamma_s D$ when computing the *net* pressure increase from the building.

sible flaws created by pumping out soil fluids (oil, water). Bridging action may be adequate for some cavities or across soft lenses but should be relied on only after a careful study of the underground conditions.

In other cases, the solution may require a different type of foundation (such as piles or caissons) or even an abandonment of the site.

7-2 DISPLACED SOIL EFFECTS

Soil is always displaced by installing a foundation. In the case of spread footings the displacement is the volume of the footing pad and the negligible amount from the column resting on the footing. In cases where a basement is involved, the basement floor slab usually rests directly on top of the footing pad. In other cases, a hole is excavated for the footing, the footing and column are installed, and the remainder of the hole is backfilled to the ground surface as illustrated in Fig. 7-4*a*. When the footing is below ground, a concrete pedestal is used to connect to steel columns to avoid corrosion; for concrete columns, the column is simply attached to the footing with dowels at the footing level. Figure 7-4*b* illustrates the condition of footings beneath basements and walls. Figure 7-4*c* illustrates placing of a mat foundation. The backfill soil should be carefully compacted over the footing (Fig. 7-4*a*) if a floor slab is to rest on the ground surface. Select free-draining backfill is carefully placed around the basement walls as shown in Figs. 7-4*b* and *c*, usually with a system of perimeter drainage to control any hydrostatic pressure.

7-3 NET VERSUS GROSS SOIL PRESSURE: DESIGN SOIL PRESSURES

When the soil engineer gives an allowable bearing pressure (or a set of curves of q_a versus B) to the structural designer, as is often the practice, what is the significance of q_a?

1. Is it a net pressure, i.e., pressure in excess of the existing overburden pressure that can be safely carried at the foundation depth D (based on settlement limitations)?
2. Is it a gross pressure, i. e., the total pressure that can be carried at the foundation depth, including the existing overburden pressure (and based on soil strength considerations)?

The bearing-capacity equations are based on gross soil pressure q_{ult}, which is everything above the foundation level. Settlements are caused only by net increases in pressure over the existing overburden pressure. Therefore,

a. If the allowable pressure is based on the bearing-capacity equations of Chap. 4, the pressure is a *gross* pressure.
b. If the allowable pressure is based on settlement considerations, it is a *net* pressure.

The computations then proceed according to whether the given conditions use *gross* or *net* pressures. Whether the pressure is a gross (depends on soil strength) or a net (depends on settlement limitations) value should be stated in the foundation report submitted to the designer; however, it often is not.

Most designers tend to treat the bearing pressure provided by the soils engineer as an accurate value that cannot be exceeded. In fact, from material presented in Chaps. 2, 3, and 4 relating to sampling, testing, and computation difficulties, the bearing pressure is hardly an exact value at all. Thus, it makes little difference if we exceed by 2 to about 10 kPa (0.1 to 0.2 ksf) the given values unless these are under 50 kPa (1 ksf). In this case we probably should not exceed the recommended values by over 2 kPa. We should be aware that if the geotechnical consultant has recommended an allowable bearing pressure of 50 kPa or under, the testing to obtain q_a has been done with more than routine care; but the report to the client should state whether q_a is based on settlement or soil strength limitations.

By noting that bearing-capacity recommendations contain both approximations and empiricism, the computations for footing design in the following chapters can be greatly simplified. For example, the author tends to omit the additional small pressure contribution from the footing volume of soil displaced by the footing concrete. Generally, by rounding the footing dimension to the next larger multiple of 10 mm (or 3 in.) the recommended "allowable" soil pressure is not exceeded. A further mitigating factor is the common practice in ϕ–c soils of digging a slightly oversized hole for directly pouring the concrete without using forms since the labor and material costs for forms greatly exceed the small amount of additional concrete required.

Obviously, one should look at the individual problem before neglecting or exceeding allowable values. One should not neglect the additional pressure from the concrete-displaced soil if, say, the footing is 2 m thick or if a greater depth of backfill is replaced than removed.

On the other hand, an inspection of Fig. 7-4*b* and *c* indicates that we can remove a greater mass of soil and the net pressure can be increased without causing settlement if this mass is not replaced. In the extreme case we can remove enough soil mass to equalize the building mass and "float" the building onto the soil underlying the basement with little or no settlement. This is called a *floating foundation.* The reason for stating "little or no settlement" is that in the usual case of this much excavation, the soil underlying the basement will expand (or *heave*) from loss of overburden pressure. Any mass placed on this expanded soil will result in recovery of some of the expansion.

7-4 EROSION PROBLEMS FOR STRUCTURES ADJACENT TO FLOWING WATER

Bridge piers, abutments, bases for retaining walls, and footings for other structures adjacent to or located in flowing water must be located at a depth such that erosion or scour does not undercut the soil and cause a failure. The scour depth will depend on the geological history of the site (depth of prior erosion to bedrock and subsequent redeposition of sediments, stream velocity, and area runoff).

Where the redeposition of sediments in the stream bed is on the order of 30 to 50 m, a careful analysis of borings into the sediments to predict the depth of maximum scour is necessary in order to provide a foundation that is economical.

It may be possible to use spread footings if they can be placed at sufficient depth, but normally piles are required to support the foundation. An accurate prediction of scour depth is necessary so as to use the shortest possible pile lengths. If careful records of driving resistances are kept, one may predict the scour depth as being where the penetration (SPT or CPT) resistance increases substantially [see Kuhn and Williams (1961)].

An NCHRP (1970) report lists some 13 equations proposed by several authorities including those of Laursen and Toch (1956) and later proposals by Laursen (1962). This report indicates that engineering judgment is used more than any other method for estimating scour depth. The equations by different authorities for the same problem can compute scour depths differing by as much as 1000 percent!

Scour occurs principally during floods, but some scour may occur at other times; in either case a scoured-out pit (or depression) in the stream bed may result. Scour holes formed during floods are usually refilled as high water falls. Scour is accelerated if the foundation creates channel obstruction; thus, to reduce scour the foundation should create a minimum obstruction to normal streamflow patterns.

Normally the approach to scour is as follows:

1. Determine the foundation type.
2. Estimate the probable depth of scour, effects, etc.
3. Estimate the cost of foundations for normal and various scour conditions.
4. Determine the cost versus risk, and revise the design accordingly.

Because scour has been attributed to several bridge foundation failures with some loss of life, this phenomena has received some additional subsidized research, starting ca. 1989, to find some means of better quantifying—preferably by measuring—stream-bed scour during high water periods. Lagasse et al. (1995) cite two reasonably low-cost measuring devices for approximately measuring scour at bridge abutments and/or piers that are now available.

It should be self-evident that a device to measure stream-bed scour must be rugged to survive high water velocity and debris impacts. The device also should have sufficient reliability that the necessary information can be taken at the bridge deck level so that a diver is not required for underwater verification. Since stream-bed scour depends on the amount and shape of the channel obstruction, and this is known only after the structure has been built, it is still necessary to utilize the foregoing four design steps. Direct measuring of actual scour (*for that highwater stage*) is only possible after construction. Direct measurements are useful, however, both for confidence and for remedial measures if the measured scour depth is greater than the design scour depth.

7-5 CORROSION PROTECTION

In polluted ground areas such as old sanitary landfills, shorelines near sewer outfall lines from older industrial plants, or backwater areas where water stands over dead vegetation, there can be corrosion problems with metal foundation members as well as with concrete. Concrete is normally resistant to corrosion; however, if sulfates are present, it may be necessary to use sulfate-resistant concrete. It may occasionally be necessary to use air-entrained concrete for foundation members.

Use of treated timber piling instead of metal piling may be required where the soil has a pH much above 9.5 or below 4.0 (7 being neutral).

The only publications treating corrosion of steel piles are Monographs 58 (dated 1962) and 127 (dated 1972) published by the National Bureau of Standards,[1] and Technical Manual 27 published by the U.S. Army Corps of Engineers, May 1969. All of these publications are probably out of print.

Initial concerns in these references were formulated into design recommendations to install steel piles only in situations where they were completely submerged (this also applies to timber piling). They were not suggested for use in sea water unless coated and not allowed to undergo wet-dry cycles. These conditions are nearly impossible to meet in areas where substantial elevation differences occur from tidal action. In these cases concrete piles were recommended.

The problem is that time-dependent corrosion is now becoming a factor for steel piles installed on the basis of the foregoing. They are approaching an age where corrosion accumulation is to the point that many piles are becoming unsafe.

7-6 WATER TABLE FLUCTUATION

A lowered water table increases the effective pressure and may cause additional settlements. A raised water table may create problems for the owner from the following:

1. Floating the structure (making it unstable or tilting it)
2. Reducing the effective pressure (causing excessive settlements)
3. Creating a wet basement if the basement walls are not watertight

These problems can usually be solved by introducing some type of drainage so that water does not accumulate around the building walls or produce hydrostatic uplift beneath the basement. The use of drain tile around the basement perimeter is common for residential dwellings and some larger buildings. In other cases a sloping basement excavation that is backfilled with granular material to the required horizontal level in combination with a well (called a sump pit) at the low point that is fitted with a pump (a sump pump system) can be used. The pump is preset to start pumping water as it rises to a critical level in the sump pit. Where to pump the water may be a major concern as some municipalities do not allow this kind of water to be emptied into sanitary sewers.

---

[1]Currently known as the National Institute of Standards and Technology, U.S. Department of Commerce, Washington, DC.

A permanent lowering of the water table can sometimes be effected, but with the current status of environmental concerns this will probably not be allowed.

7-7 FOUNDATIONS IN SAND AND SILT DEPOSITS

Foundations on sand and silt[2] will require consideration of the following:

1. Bearing capacity.
2. Densification of loose deposits to control settlement.
3. Placing the footing at a sufficient depth that the soil beneath the footing is confined. If silt or sand is not confined, it will roll out from the footing perimeter with a loss of density and bearing capacity. Wind and water may erode sand or silt from beneath a footing that is too near the ground surface.
4. Uncontaminated glacial silt deposits can have a large capillary rise because of the small particle sizes. Sometimes these deposits can be stabilized by excavation to a depth of 0.6 to 1 m, followed by placement of a geotextile water barrier. The silt is then backfilled and compacted to provide a suitable foundation. An overlying water barrier or other drainage may also be necessary since downward-percolating water will be trapped by the lower geotextile.

Foundations on silt or sand deposits may consist of spread footings, mats, or piles, depending on the density, thickness, and cost of densifying the deposit, and on the building loads. Solid-section, large-volume piles may be used both to carry loads to greater depth in the deposit and as a means of compacting the deposit. Small-volume piles are normally used to carry near-surface loads through loose sand deposits to firm underlying strata. In both sands and silts the soil-cement pile, SCP, may be an economical alternative.

Spread footings are used if the deposit is dense enough to support the loads without excessive settlements. Rapid or immediate settlements occur on noncohesive silt or sand deposits. Much of the settlement resulting from construction loads and associated vibrations is built out during erection—most of the remainder is landscaped.

It is poor practice to place foundations on sand deposits where the relative density is not at least 60 percent or to a density of about 90 percent or more of the maximum density obtained in a laboratory test. This dense state reduces the possibility of both load settlements and settlement damage due to vibrations from passing equipment, earthquakes, or the like.

An inorganic (nearly pure) silt in a saturated condition cannot be compacted. The compaction effort produces a wave in front of the compactor and the entire mass may quiver (a soil state sometimes called "bull liver"). When this type of deposit is encountered, the deposit must be excavated and replaced with competent soil or else excavated and dried to a water content that will allow compaction. Soil replacement is usually impossible so alternatives

[2]The principal difference between sand and silt is grain size. Sand sizes go down to about 0.05 mm, and silt begins at about 0.05 mm and goes down to about 0.006 mm (see Table 2-2). Pure silt is inert (has no particle attraction), but deposits seldom exist in nature that are not contaminated with clay particles or cementation agents from organic materials. As a result of these contaminants, one can obtain plasticity indexes. Deposits with plasticity indexes are usually treated as cohesive materials.

consist in drying the silt and encasing it in a geotextile to control water, mixing it with sand and gravel sufficient to produce a stable condition when saturated, or using piles to carry the load through the deposit to competent soil.

The allowable bearing capacity and estimated settlements for footings and mats on competent sand and/or silt are computed using methods given in Chaps. 4 and 5.

7-8 FOUNDATIONS ON LOESS AND OTHER COLLAPSIBLE SOILS

Collapsible soils are generally wind-blown (aeolian) deposits of silts, dune sands, and volcanic ash. Typically they are loose but stable, with contact points well-cemented with a water-soluble bonding agent, so that certain conditions of load + wetting produce a collapse of the soil structure with a resulting large settlement.

Loess is a special—but widely distributed—case of a silt deposit characterized by having been deposited by wind. The grain distribution of loess deposits tends to be limited to approximately the range of 0.01 to 0.10 mm and is usually contaminated with clay and sand particles (< 0.05 mm) and later by organic leachates. Nonsaturated, aged deposits are capable of standing on vertical cuts or banks due to interparticle cementation, but saturation can produce slough-offs and/or a large vertical settlement, termed *soil collapse*. The collapse of the soil structure may occur interior to any bank or vertical cut (i.e., is confined by K_o lateral pressures) as noted by Feda et al (1995).

Loess is the predominating collapsible soil that engineers are confronted with. It is very widespread, covering about 17 percent of the United States (see Fig. 7-5)—principally adjacent to the major rivers (Mississippi and Missouri). About 15 to 17 percent of Western Europe, including parts of Belgium and France as well as portions of Germany, and Eastern Europe (Slovakia, Romania, Hungary) are covered with loess deposits. The European deposits are generally found adjacent to the major rivers, such as the Danube, the Rhine, and their larger contributories. About 10 to 15 percent of the Russian Federation (south and southwest of Moscow to the Caucasus mountains) and a part of Ukraine is covered by loessial deposits, as well as large parts of China. Very little loess is found in Canada and none in Australia or Africa (but both the latter have other wind-blown deposits), according to Flint (1971).

Figure 7-5 Location of major loess deposits in the United States. [Gibbs and Holland (1960).]

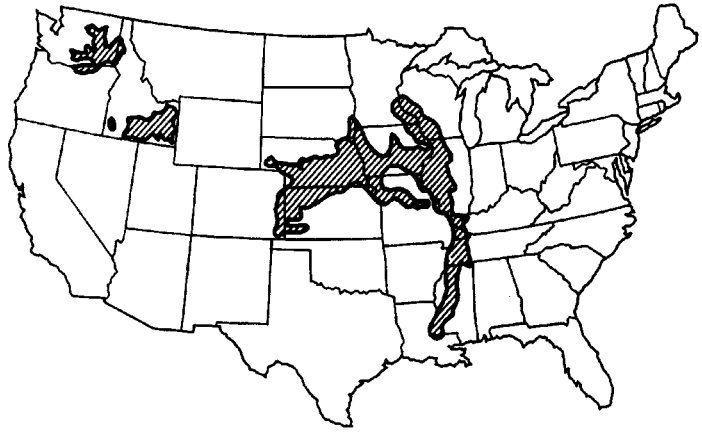

Loess appears to have been formed from the wind picking up inert pulverized silt-sized rock particles produced by glacial action. These were carried to locales where either glacial outwash or a flowing stream produced sufficient humidity in the air that the wind-borne soil grains precipitated—usually on the eastern, or leeward sides of flowing water (at least in the United States). It follows that nonglacial areas do not have loess deposits. Depths of loess deposits range from less than 1 meter to more than 50 meters. Depths of 2 to 3 meters are very common.

Loess and other collapsible deposits are characterized by a complete absence of gravel or pebbles, with most of the material passing the No. 200 sieve (0.075 mm). The specific gravity ranges from 2.60 to 2.80, but most values lie between 2.65 and 2.72. In situ dry densities range from about 10 to 16.5 kN/m^3.

Atterberg limits depend on the clay and/or organic contamination, and commonly w_L ranges from 25 to 55 and w_P from 15 to 30 percent. Standard compaction tests (ASTM D 698) produce γ_{dry} on the order of 15.5 to 17.5 kN/m^3 at optimum moisture contents from 12 to 20 percent according to Sheeler (1968).

Loess has a high in situ porosity, often more than 50 percent (or void ratio > 1.0), and is thus highly susceptible to collapse upon saturation. Most in situ void ratios e_o are in the range from 0.67 to 1.50, according to Drannikov (1967).

The density of loess (and other collapsible soils) is one of the most significant parameters in estimating collapse. Holtz and Hilf (1961) suggest that this be used together with the liquid limit w_L to estimate collapse potential. This suggestion in equation form from a chart and somewhat linearized by the author is

$$\gamma_{dry} = 17.3 - 0.186(w_L - 16) \qquad \text{kN/m}^3 \tag{7-1}$$

where w_L is in percent. When the in situ density is less than that given by Eq. (7-1) the soil is susceptible to collapse, with the severity of susceptibility increasing with a decrease in γ. It is not easy to predict the amount of collapse. One might use the following equation:

$$C_p = \frac{h_p - h'_p}{h_p} \times 100\% \tag{7-2}$$

where C_p = estimated height change in percent

h_p = length change from using an undisturbed tube sample subjected to the consolidation pressure anticipated in the field

h'_p = length change from using an undisturbed, saturated tube sample subjected to the same consolidation pressure as for h_p. Both samples are of the same initial length h.

Major problems in using Eq. (7-2) are obtaining undisturbed tube samples, cutting and placing them into a device, and loading them to the required pressure (and with minimum lateral restraint or side friction). In the field a major problem is associated with how deep is the saturation zone that participates in the collapse.

Problem recognition is considered in some detail by Clemence and Finbarr (1981). One procedure they gave suggests using a consolidation (or oedometer) test where the sample is placed in the confining ring at the in situ water content and consolidated in increments to about 200 kPa; then the ring is flooded with water and the load maintained for 24 hr. If there is a large displacement, this is an indication of a structure collapse within the sample.

In general, after recognition of the collapse potential, one may use the site by doing one of the following:

1. Compact (excavate and replace) the soil to $\gamma_{dry} \geq 15.5$ kN/m^3.
2. Use an admixture during compaction. Admixtures may be lime, lime/fly ash, or Portland cement.
3. Use some means to ensure that the collapsible soil does not get wet (often not practical).
4. Use piles through the collapsing soils to a more competent underlying stratum.

7-9 FOUNDATIONS ON UNSATURATED SOILS SUBJECT TO VOLUME CHANGE WITH CHANGE IN WATER CONTENT

Expansive soils undergo volume changes upon wetting and drying. For a volume change to occur these soils must be initially *unsaturated* at some water content w_o. When the water content changes to a new value w_1, the volume increases if $w_1 > w_o$ or decreases if $w_1 < w_o$ unless w_o is the shrinkage limit where $w_o = w_S$.

These soils occur in an *active zone*, which starts at the ground surface and goes down to the saturated part of the zone of capillary rise above the ground water table. Figure 7-6 is a qualitative chart of variation of water content in the active zone.

Expansive soils are mostly found in arid and semiarid areas worldwide and contain large amounts of lightly weathered clay minerals. Low rainfall has hindered the weathering of more active clay minerals such as the smectite family to less active clay types such as illite or kaolinite, and the rainfall has not been enough to leach the clay particles far enough into the strata that the overburden pressure can control the swell.

In general, all clayey soils tend to shrink on drying and expand when the degree of saturation S increases. Usually, the lower the shrinkage limit w_S and the wider the range of the plasticity index I_P, the more likely is volume change to occur (Table 7-1) and the greater the amount of such change.

Volume change is particularly troublesome in large areas of the southwestern United States, India, and Australia, and in parts of Africa and the Middle East that are subject to long dry periods and periodic heavy rains of short duration. The dry periods tend to desiccate the soil; then the sudden rainy season(s) cause large amounts of swelling near the ground surface. There is not enough regular rainfall to leach and weather the troublesome clay minerals to greater depths; thus, they remain unaltered near the ground surface. During the rainy season(s) they are rapidly wetted and quickly swell to form a water barrier to further water entry, thus keeping the problem near the ground surface.

Soils in these areas are particularly troublesome to build on as they appear competent during dry periods (with the possible exception of surface tension cracks). They would of course remain competent if their water content is controlled in some manner, a difficult task. What happens is that water vapor migrating from the ground water table, which may be at a depth of many meters, condenses on the bottom sides of the floor slabs and footings. Anyone can readily observe this phenomenon by turning over a flat rock in the field (even after a prolonged dry spell) and noting the dampness on the underside.

Since a building is somewhat impermeable, similar to the flat rock in the field, the soil in the interior zone eventually becomes wet to saturated from the condensation of upward-rising

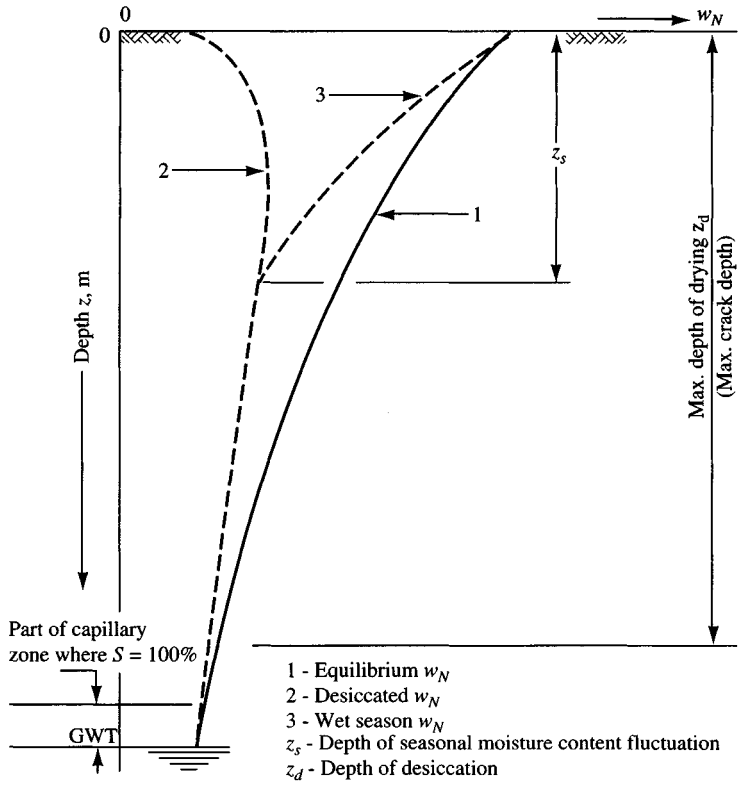

Figure 7-6 Relative variation in field water content w_N with depth z above the water table and the saturated part of the capillary zone, i.e., in the active zone.

water vapor. The soil will then swell unless the building provides sufficient weight to restrain the swelling pressure, and buildings seldom provide the huge restraining pressures required to control swelling.[3]

Cold storage buildings with an uninsulated thermal gradient may cause condensation of the water vapor in the soil or create an upward flow of water vapor from the water table. Ice lenses may form. These typically are more serious from either of two reasons: amplifying swell or producing a semifluid zone when they melt if the temperature is sufficiently low.

With buildings, in addition to possible evaporation of soil water from the perimeter zone, there is also the problem of soil in this region becoming dessicated from water absorption through the roots of adjacent shrubbery and/or trees used in landscaping. Loss in soil moisture by evaporation from heating the building or from beneath or adjacent to heating units such as boilers can also create shrinkage volume changes.

Shrinkage tends to produce perimeter settlements (unless from heating units where the interior may settle), which, in combination with any interior swell, develop larger differential

[3]The rock in the field moves up and down with the varying amount of dampness beneath it, but who notices it?

TABLE 7-1
Potential soil volume change* as related to the plasticity index I_P, liquid limit w_L*, and expansion index E_I

Potential for volume change	Plasticity index I_P	Shrinkage limit w_S, %	Liquid limit w_L, %	Expansion index E_I
Low	< 18	> 15	20–35	21–50
Medium	15–28	10–15	35–50	51–90
High	25–41	7–12	50–70	91–130
Very high	> 35	< 11	> 70	> 130

*From Holtz (1959), Dakshanamurthy and Raman (1973), and Anderson and Lade (1981).

settlements than would be obtained from swelling action alone. By the way, the field rock also has this problem (it is seldom wet from edge to edge) but is of no consequence. Figure 7-7 illustrates the typical case for buildings where the differential settlement is exaggerated from interior swell and edge shrinkage.

In all of the shrinkage cases the amount of volume change is referenced to the initial natural water content w_o of the soil and the current natural water content w_1. Volume changes produced from shrinkage ($w_1 < w_o$) are usually smaller than volume changes from swell ($w_1 > w_o$).

Table 7-1 may be used as a guide in evaluating the potential for volume change of soils based on easily determined index properties. In part, this table is a summary of data from Holtz (1959) on several soils, which are correlated with some 50 soils from other areas, including a large number of Indian black cotton soils by Dakshanamurthy and Raman (1973). In terms of relative values a "low" volume change might be taken as not more than 5 percent whereas "very high" could be interpreted as over 25 percent.

Figure 7-7 Idealized expansion soil problem for a building. The two end zones AB and CD are shrinkage regions of indeterminate length at the foundation edges. Soil is shown in contact with the slab ends but this may not always occur (i.e., there may be a crack between the slab and the soil). The interior region BC represents swell (or heave) from upward-migrating moisture. An estimate of the crack-producing tension stresses might be obtained by using either a solution for a beam on elastic foundation (diskette program B-5) or for a plate (diskette program B-6). In this type of analysis, assume a zone (or interior slab region) of length BC with $k_s > 0$ and the two end zones (or a perimeter zone for slabs) AB, CD with $k_S = 0$.

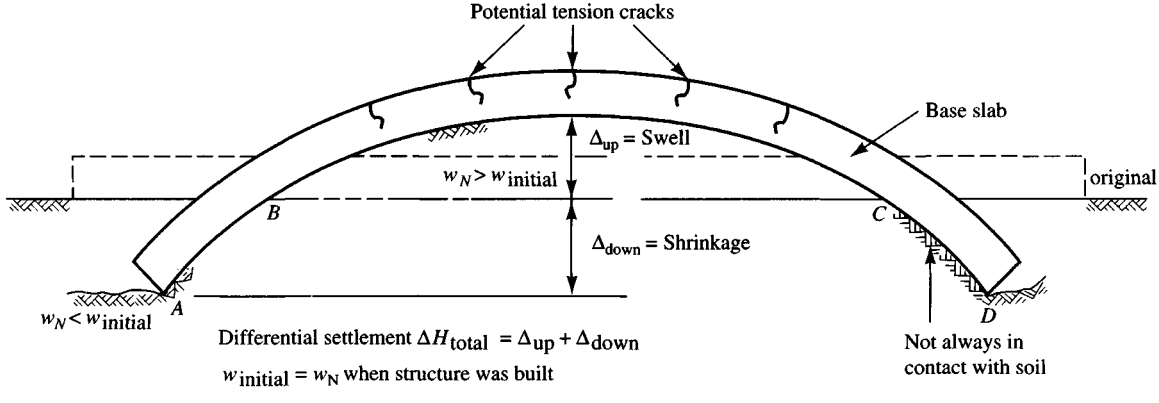

7-9.1 Volume-Change-Related Consolidation Test (ASTM D 4546)

An approximation of the consolidation test (ASTM D 4546) can be used to estimate soil heave or shrinkage. There are three different methods—*A*, *B*, and *C*—of performing this test. Basically, this test uses standard consolidation (ASTM D 2435) equipment; a plot of e versus $\log p$ is made, from which the necessary swell/shrinkage data are obtained. One may use the consolidation ring sample from the compaction test outlined in the next section for the Expansion Index. It is necessary to obtain the in situ void ratio e_o and the void ratio e_f after swell or compression. Best results are obtained by dividing the active zone z_d of Fig. 7-6 into several sublayers of thickness H_i, determining the void ratio of each as e_i, and performing the test on a sample obtained from each sublayer. When this procedure is done, the following equation is used:

$$V_c = \frac{\Delta H_i}{H_{iL}} = \frac{e_{fi} - e_{oi}}{1 + e_{oi}} \cdot 100 \qquad (\%) \tag{7-3}$$

where ΔH_i = change in height of laboratory sample of thickness H_{iL}
e_{fi} = final void ratio of the laboratory sample
e_{oi} = both initial void ratio of laboratory sample and the field void ratio

Using the laboratory percentage change from Eq. (7-3) to represent the field settlement (−) percent or swell (+) percent, we find the field settlement can be directly computed as

$$\Delta H = \sum_{1}^{n} \left(\frac{V_c}{100}\right) H_i \qquad \text{(in units of } H_i\text{)} \tag{7-4}$$

Volume change V_c is used as a percent (division by 100 converts V_c to a decimal).

7-9.2 Volume Change Related to the Expansion Index E_I

Anderson and Lade (1981) suggest using a parameter called the Expansion Index both to recognize and to quantify soil volume change in a relative manner.

The expansion index E_I is obtained from using a standard compaction mold (dimensions of 944 cm^3) but cut and fitted in the midheight part with a removable 25-mm high ring. This setup allows one to compact the soil using a method such as D 698 or D 1557. The soil used is that passing the No. 4 (4.75-mm) sieve and the percent passing is defined as D_4. After compaction (and necessary weighing to determine compaction density and water content) the top part of the mold is removed and soil is trimmed down to the 25-mm ring. The bottom is also removed and the soil trimmed to the base of the 25-mm ring. Water content is obtained from the trimmings, using two or three samples.

The 25-mm ring is then placed in a consolidation-type test configuration and put into a device capable of providing substantial pressure to the sample. This is done to bring the water content in the ring into a range of 49 to 51 percent. If the pressure device cannot apply sufficient pressure to reduce the soil in the ring to a volume that yields the required water content of 49 to 51 percent, the compaction part of the test is repeated using a higher initial water content.

Once the ring sample has been compressed to a volume such that the water content is in the 49 to 51 percent range, it is fitted with a dial gauge or LVDT to measure expansion. It is then loaded with a 6.9-kPa (1-psi) pressure and flooded with distilled water. The one-dimensional expansion δH is determined either after 24 hr or after the rate of expansion (plotted on graph paper) decreases to 0.005 mm/hr. An expansion index can now be computed as

$$E_I = 39.37(\delta H)D_4 \tag{7-5}$$

Here δH = mm and D_4 = decimal value of percent passing the No. 4 sieve. For layered soil an E_i is computed for each layer, multiplied by a weighting factor, and summed. Weighting factors from Anderson and Lade (1981) are as follows:

Depth, m	Weight factor
0 < 0.3	0.4
0.3 < 0.6	0.3
0.6 < 0.9	0.2
0.9 < 1.2	0.1
> 1.2 m	0.0

The E_I can be used as shown in Table 7-1 to estimate volume change potential.

7-9.3 Volume Change Based on Soil Suction

To the present there have been seven international conferences on expansive soils. The seventh conference[4] was held in 1992. From these conferences it appears that soil suction holds substantial promise for estimating a quantitative volume change. It does appear, however, that the volume change equations tend to be more complicated with increasing conference number. An additional major problem is that the equation authors tend to use different symbols.

Once the major deterrent to using soil suction was the difficulty in obtaining the suction stress. Now there are a number of procedures and equipment for obtaining the soil suction, both in the laboratory and in the field. The following are available from commercial sources: filter paper method (ASTM D 5298, in vol. 4.09), pressure plate apparatus, thermocouple psychrometer; heat dissipation sensor, gypsum block, and fiberglass moisture cell.[5] Equipment (and some of their sources) for these procedures is briefly described by Lee and Wray (1992).

Soil suction is currently defined in two ways:

1. In terms of pF, the equivalent capillary rise of water in cm

For example : 100 cm of H_2O gives $pF = 2.0$

10 000 cm gives $pF = 4.0$

[4]Conference proceedings were published and are available (as of 1994) from Civil Engineering Department, Texas Tech University, Lubbock, Texas 79409.

[5]Filter paper for that suction test can be obtained from a number of laboratory suppliers. Some of the equipment is available from sources cited in the literature.

2. In an equation as follows:

$$h = (u_a - u_w) \qquad \text{(in units of } u_i\text{)} \tag{7-6}$$

where h = soil suction (usually termed *matric suction*) and usually (−)
u_a = air pressure in soil pores—usually atmospheric
u_w = pore water pressure in units consistent with u_a

When the soil is saturated, $S \rightarrow 100$ percent and we have $h \rightarrow 0$.

When there is no moisture change **or** the soil is saturated, soil suction has no real significance and the usual equations for bearing capacity and settlement can be used. When the soil is saturated, either or both the $\bar{q}N_q$ and the $\frac{1}{2}\gamma BN_\gamma$ terms in the bearing-capacity equation will be reduced. For bearing capacity, unless there is some means to eliminate water changes in the unsaturated region one should assume the soil is saturated, as this will be conservative.

Additional theoretical considerations may be obtained from the ASCE publication GT SP No. 39, "*Unsaturated Soils,*" or from the *International Conferences on Expansive Soils*—especially the later ones from 4 to 7.

Of considerable interest is the volume change in situations where it is anticipated that the soil above the groundwater table may undergo a change in the initial natural water content w_o that can range from $0 < (w_o - w_f)$. The maximum possible for the final natural water content w_f is a saturated state of $S = 100$ percent and the minimum is $w_f \rightarrow 0$.

Of additional interest is the depth in which this water content change occurs. At some depth z_d (see Fig. 7-6) the saturated zone above any groundwater table is encountered. The depth z_s represents the approximate depth of the active zone, in which water content varies with the season. These water content changes may be drying or wetting from infiltration of surface water during rainy periods.

A number of methods using soil suction as a significant parameter have been proposed to estimate the volume change. Four of these are described by Snethen and Huang (1992), and the two that seemed to provide the best predictions are given by the following:

Method 1. This method is given by Snethen and Huang (1992), who obtained it from Mitchell and Avalle from the Fifth Conference on Expansive Soils in 1984. The equation[6] is

$$\Delta H = \sum_{1}^{n} \epsilon_i H_i \tag{7-7}$$

where ϵ = linear strain as $\Delta L/L_o$; L_o = initial sample length; ΔL = change in length during drying, usually until no further length change occurs (at about a water content = w_S)
H_i = thickness of sublayer i of depth z_s made up of n layers

Equipment for performing the linear shrinkage test is available from several laboratory equipment suppliers. The linear strain required here can be obtained indirectly from the

[6]This is not the form given by them in the reference but is obtained by combining the values as given and canceling terms to produce this form (which does not include a soil suction parameter).

standard shrinkage limit test (ASTM D 427 or D 4943) using equations given by Bowles (1992). Using linear shrinkage equipment will produce a better estimate of linear strain than back-computing it from a standard shrinkage limit test.

Method 2. This is Snethen and Johnson's method and the equation is as follows:[7]

$$\frac{\Delta H}{H_i} = \frac{C_t}{1 + e_o} \log \frac{h_o}{h_f + \alpha \sigma_f} \tag{7-8}$$

where (in these equations)

C_t = suction compression index = $\alpha G_s/100B$

α = slope of a curve of $(1 + e_o)/G_s$ versus water content w_o occurring at void ratio e_o (see Fig. E7-1*b*)

B = obtained from the slope of a curve of log h versus corresponding water content w_o

$\log h_o = A - Bw_N$, obtained from the curve slope

A typical set of plots and computations for $\log h_o$ is shown on Fig. E7-1*a*.

Other Methods.

McKeen (1992) gives an equation of the following form:

$$\Delta H = \sum_{1}^{n} C_h \cdot \Delta h \cdot H_i \cdot f \cdot s \qquad \text{units of } H_i \tag{7-9}$$

where C_h = suction compression index. It can be obtained from a plot of ΔV versus soil suction pF, where pF ranges from about 5.5 at the shrinkage limit w_S to field values from about 2 to 2.5. Clearly volume change increases when the field water content goes from $pF = 5.5$ down to $pF = 2.0$ to 2.5. The linear part of the plot gives the slope defined as $C_h = \Delta V/\Delta pF$.

Δh = some change in suction measured as change in pF.

H_i = thickness of ith layer, m or mm, and gives units of ΔH.

f = lateral restraint factor as $f = (1 + 2K_o)/3$ or similar.

s = coefficient of load effect defined as

$$s = 1.0 - 0.01P_s \qquad P_s \leq 50\% \qquad (s = 0, \text{ at } P_s = 100\%)$$

Estimate the swell pressure P_s, or measure it, or use Eq. (7-10).

Fredlund and Rahardjo (1993, but suggested earlier by Fredlund in the *Canadian Geotechnical Journal*, vol. 1, 1979) suggest an equation in the general format of the consolidation equation of Sec. 2-10. It is too complicated to include here, but the interested reader can consult the 1993 reference and work back.

[7]Other forms of this equation are given in the reference, but this is the simplest.

Example 7-1.

Given. The soil data with properties shown in Table E7-1*a*.

TABLE E7-1*a*
Properties of the soils from the Wynnewood site

Depth, cm	Specific gravity, G_s	Percent (−) 0.002 mm C_p, %	w_L, %	I_P, %	Natural water content w_N, %	γ_{dry}, kN/m^3	Field soil suction h_o, kPa
0							
	—	—	—				
15							
	2.73	31	37	21	18.5	16.7	1978
50							
	2.74	41	48	33	18.9	17.4	2716
90							
	2.75	37	39	26	16.3	18.2	4428
140							
	2.76	32	32	19	15.6	18.8	6048
180							
	2.77	31	30	17	15.8	18.3	1984
230							
	2.78	31	27	14	15.2	18.4	1502
270*							
	2.79	42	31	19	18.2	18.0	2557
320							

*Groundwater table stabilized at 3.0 meter depth after testing.
Source: Snethen and Huang (1992).

Required. Estimate the settlement for a depth of 2.36 m (236 cm) as used in Table E7-1*a*. Use *Snethen and Johnson*'s method.

Step 1. Obtain the necessary soil suction and water content data shown in Tables E7-1*a, b*. Plot these data as indicated in Figs. E7-1*a, b*.

Step 2. From the figures obtain the necessary $\log h$ and α values. Typical computations are shown on the figure. Note that it is difficult to obtain the figure values (obtained from the reference cited) owing to the small scale. Several values shown in Table E7-1*a* and *b* are identified as follows:

h_f = final measured matric soil suction after wetting or drying, kPa. These were estimated in this example.
e_o = initial void ratio, measured or calculated as $Se_o \approx w_N G_s$
σ_f = final estimated field pressure (includes overburden down to the layer of interest + external load). These were estimated in this example.

Let us consider some typical computations. From Figs. E7-1*a* and E7-1*b*, we have

$$\alpha = \frac{\Delta S_v}{\Delta w} = \frac{0.645 - 0.588}{25 - 15} = \frac{0.057}{10/100} = 0.57 \qquad \text{(as in Table 7-1}b\text{)}$$

Figure E7-1*a* displays the equation $\log h = A - Bw_i$, where B can be obtained as the slope of the curve between two ordinates. Note that these curves can be plotted to a semilog scale with h values

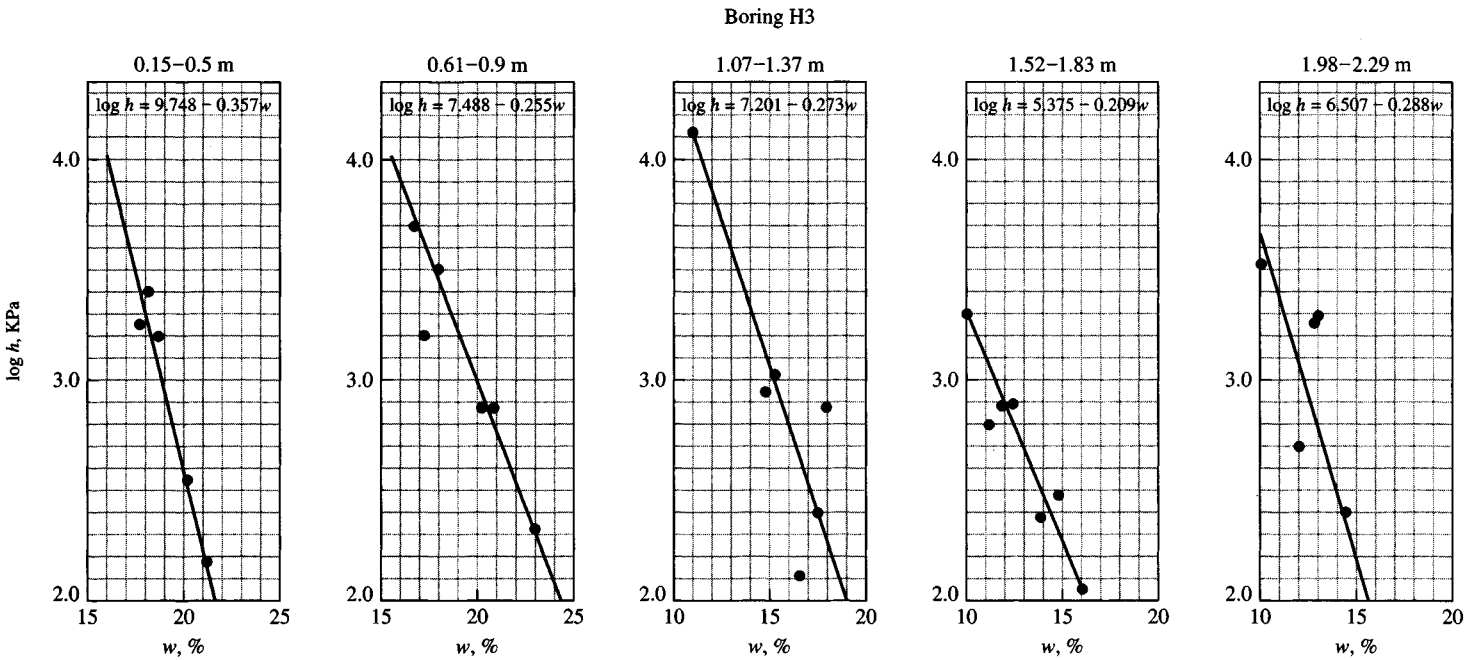

Figure E7-1*a* Suction log h versus water content (%). For example, at $w = 17.5\%$, $h = 2{,}512$ kPa, $\log 2{,}512 = 3.4$ as plotted on first figure. Suction values are obtained from lab drying of the several samples tested per boring depth shown. One draws a "best fit" curve through the plotted points. These plots used to obtain $\log h = A + Bw_i$. Obtain $B = \Delta h/\Delta w$ (use w in decimal although it is plotted in percent). Use convenient points along the slope for both the h and w values. *Note:* If one uses values from the plot to verify A, B the results may be slightly different, but these differences are insignificant if they are small. If they are large, check your work. [Snethen and Huang (1992).]

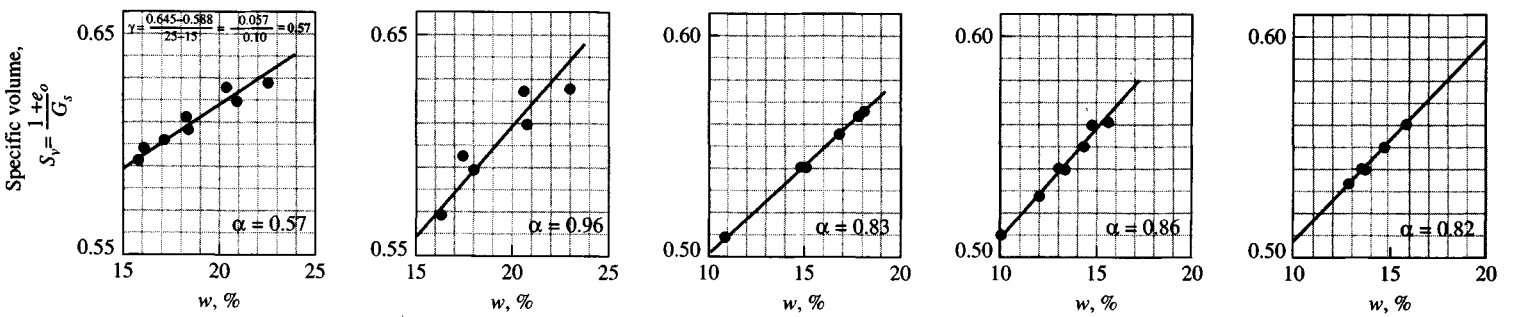

Figure E7-1*b* Plot of specific volume $S_v = (1 + e_o)/G_s$ versus water content w_i (at that e_o) in percent. Compute $\alpha = \Delta S_v/\Delta w$ = slope of curve that is drawn as a "best fit" through the several data points (from drying stages). A typical computation is shown on the first figure. *Note:* If one reads values from the plot one can get slightly different α values from those shown. Small discrepancies are insignificant.

TABLE E7-1*b*
Compilation of suction data* in form for convenient computations

Depth, cm	H_i, cm	Suction index, C_t	Void ratio e_o	Initial soil suction h_o, kPa	α†	Final stress σ_f, kPa	Final assumed soil suction, h_f	Predicted swell/heave: Swell, %	Predicted swell/heave: ΔH, cm
0									
	15	—	—	— sandy					
15									
	38	0.044	0.600	1978	0.57	4.5	2	7.25%	2.76
53									
	46	0.103	0.546	2716	0.96	12.9	11	13.75	6.32
99									
	46	0.084	0.479	4428	0.83	21.1	46	10.47	4.82
145									
	46	0.114	0.438	6048	0.86	29.5	200	11.33	5.17
191									
	45	0.079	0.485	1984	0.82	38.0	871	1.82	0.82
236								Total ΔH =	19.89 cm

*Data obtained and revised from Snethen and Huang (1992).

†Obtained from Fig. E7-1*b* as curve slope. Values are shown on the figure that are used in this table. You will have difficulty obtaining exactly the same values as a result of scaling effects but with care you should get approximately the given α's.

used, such as 1978, 2716, etc., along with others obtained from samples dried to lower water contents w_i during the test. Smaller plots using arithmetic scales with the logarithms of h taken are plotted as here. Note you can use either $\log h$ or $(A - Bw_i)$ in Eq. (7-8). From the first figure (in Fig. E7-1*a*) obtain

$$B = \frac{\Delta \log h}{\delta w} \approx \frac{3.78 - 2.0}{22 - 17} = \frac{1.78}{5} = 0.356 w_i \qquad \text{(vs. } 0.357 w_i \text{ shown)}$$

Now solve for A. Take a convenient point (if using semilog plots extend the curve to the log 1 line and directly read A). For this case use log 3 as the point of interest, so we have

$$3.0 = A - Bw_i \rightarrow \text{read } w_i \approx 19.2\% \text{ at log 3, giving}$$
$$A = 3.0 + 0.356(19.2) = 3.0 + 6.84 = 9.84 \qquad \text{(vs. 9.748 shown)}$$

This computation illustrates the great difficulty in using data presented by others. Either 9.748 shown or 9.84 just computed are sufficiently accurate for suction computations.

Next compute

$$C_t = \frac{\alpha G_B}{100B} = \frac{0.57(2.73)}{100(0.357)} = 0.043\,59 \rightarrow \mathbf{0.044} \qquad \text{(in Table E7-1}b\text{)}$$

Finally compute the percent swell and the swell. Using Eq. (7-8), we write

$$\frac{\Delta H}{H} = \frac{C_t}{1 + e_o} \log \frac{h_o}{h_f + \alpha \sigma_f}$$
$$= \frac{0.044}{1 + 0.60} \log \left[\frac{1978}{2 + 0.57(4.5)} \right]$$

$$= 0.0275 \log \frac{1978}{4.565}$$

$$= 0.0725 \rightarrow 7.25\%$$

$$\Delta H = 38(0.0725) = \mathbf{2.76}\ \text{cm} \rightarrow 27.6\ \text{mm}$$

Other values in the table are computed similarly and summed to obtain the total heave:

$$\Delta H = \mathbf{19.89}\ \text{cm, strictly } \mathbf{198.9}\ \text{mm (about 8 in.) shown}$$

Note that McKeen (1992, vol 2, pp. 79–81) discussed this example, and he raised the question of whether the actual field-measured swell was ≈ 200 mm or something less.

////

7-9.4 Volume Change Correlations Using Soil Index Properties

Correlations using index properties may give fair estimates of volume change. An estimate of the overburden (or footing) pressure P_s necessary to restrain expansion to a tolerable (tolerable not precisely defined) quantity can be obtained from an equation by Komornik and David (1969, p. 222) based on a statistical analysis of some 200 soils. This equation is

$$\log P_s = 2.132 + 0.0208 w_L + 0.665 \rho_d - 0.0269 w_N \qquad (\text{kg/cm}^2) \qquad (7\text{-}10)$$

where w_L, w_N are liquid limit and natural moisture contents *in percent* and ρ_d is the dry density in g/cm^3.

The percent swell can be used to compute an estimate of differential settlement. An equation used by Johnson and Snethen (1979), which compared reasonably well with measured swell (or heave), is

$$\log S_p = 0.0367 w_L - 0.0833 w_N + 0.458 \qquad (\text{percent}) \qquad (7\text{-}11)$$

An equation presented by O'Neill and Ghazzaly (1977) is

$$S_p = 2.27 + 0.131 w_L - 0.27 w_N \qquad (\text{percent}) \qquad (7\text{-}12)$$

Both Eqs. (7-11) and (7-12) are based on statistics, and the water contents are to be used as *percentages*. The *free swell* obtained from these equations may be reduced for confining pressure σ_v using an equation obtained by the author from interpretation of curves by Gogoll (1970) for percent swell versus confining pressure. This equation is

$$S_p' = S_p\left(1 - A\sqrt{\sigma_v}\right) \qquad (7\text{-}13)$$

where $A = 0.0735$ for SI and 0.52 for Fps units of kPa or ksf.

These equations can be expected to compute on the order of a ± 50 percent error, which might not differ greatly from using consolidation or suction tests. Both of these equations are given for percent swell so that some cross checking might be obtained as illustrated in Example 7-2. Tables 5-6 and 5-7 should be used to see if the proposed structure can tolerate the estimated (differential) heave.

Example 7-2.

Given. A soil with properties in Table 1 of Snethen (1980).

Required. Make an estimate of the probable swell in mm.

Solution. We will use average properties of the soil at the depth of interest, given in Snethen (1980) as 8 ft (2.44 m) and as shown in the following table, edited from that reference. That is, add the seven values of interest and divide by seven. Although this average includes soil properties below the 8-ft depth used by Snethen, those properties are likely to somewhat affect the result and so will be used here. The averaging procedure gives the following:

Boring no.	Sample depth, ft	w_L, %	w_P, %	w_N, %	e_o	G_S	γ_{dry}, lb/ft^3
U-1	1.7–2.7	81	22	23.2	0.629	2.68	102.7
U-2	1.4–3.4	75	24	27.2	0.745	2.75	98.4
U-2	4.1–5.1	69	24	22.1	0.613	2.71	104.9
U-1	6.6–7.9	82	27	21.1	0.589	2.73	107.3
U-2	8.6–9.4	77	24	21.4	0.604	2.73	106.2
U-1	10.0–11.2	69	26	20.6	0.579	2.74	108.3
U-2	12.9–13.8	83	21	22.5	0.678	2.74	101.9

$$w_L = 536/7 = 76.6\%$$
$$w_P = 168/7 = 24\% \qquad \gamma_{dry} = 729.7/7 = 104.2 \text{ pcf}$$
$$w_N = 22.6\% \qquad \rho_d = 104.2/62.4 = 1.67 \text{ g/cm}^3$$
$$\text{Total stratum thickness} = 8 \text{ ft} = 2.44 \text{ m}$$

By Eq. (7-11) (water contents as percent), we can write

$$\log S_p = 0.0367(76.6) - 0.0833(22.6) + 0.458$$
$$= 1.387$$
$$S_p = 10^{1.387} = \mathbf{24.4\%}$$

By Eq. (7-12) (water contents as percent), we have

$$S_p = 2.27 + 0.131(76.6) - 0.274(24) = \mathbf{5.73\%}$$

Let us average the swell values as $S_p = (24.4 + 5.73)/2 = \mathbf{15.1\%}$. Since this is a large swell percent and the stratum is 2.44 m in depth make a pressure reduction using Eqs. (7-10) and (7-13). Using Eq. (7-10), we have

$$\log P_s = \bar{2}.132 + 0.0208(76.6) + 0.665(1.67) - 0.0269(22.6)$$
$$= \bar{2}.132 + 2.096 = 0.226 \text{ kg/cm}^2$$
$$P_s = 10^{0.226} = 1.683 \text{ kg/cm}^2 \rightarrow \mathbf{165} \text{ kPa}$$

Using Eq. (7-13), we can write

$$S_p' = S_p(1 - 0.0735)\sqrt{P_s}) = 15.1(1 - 0.0735\sqrt{165}) = 0.056S_p$$
$$= 0.056(15.1) = \mathbf{0.84\%}$$
$$\Delta H = 2.44(0.0084)(1000) = \mathbf{20.5} \text{ mm}$$

The actual swell measured at this site ranged from −25 to 159 mm, but most values were in the range of 6 to under 50 mm (the greatest number were around 20–25 mm). Note that the w_L values are quite large for a soil with the properties indicated in the table. It may be that the liquid limit machine was out of adjustment (a fall of, say, 8 mm versus the 10-mm standard can easily change w_L by 20 or more percent). I have encountered this problem in the Peoria, Illinois, area where a consultant

obtained w_L's on the order of 60 percent, where they were actually only about 35 percent. Clearly, in this case a smaller w_L would greatly affect direct computation of ΔH.

////

7-9.5 Designing Structures on Soils Susceptible to Volume Change

Structures built on expansive soils require special construction techniques for their foundations. When the problem is identified, one may address it in several ways:

1. Alter the soil. For example, the addition of lime, cement, or other admixture will reduce or eliminate the volume change on wetting or drying.
2. Compact the soil well on the wet side of the optimum moisture content (OMC). This process produces a lower than maximum dry density and if the water content does not change until the structure is built there should be little swell. Remember, it is not the water content but the *change* in water content that produces soil volume change. Soils compacted well on the wet side of the OMC are usually nearly saturated [see Gromko (1974), with large number of references]. Often, however, this compaction state may not have sufficient strength for the design requirements.
3. Control the direction of expansion. By allowing the soil to expand into cavities built in the foundation, the foundation movements may be reduced to tolerable amounts. A common practice is to build "waffle" slabs (see Fig. 7-8) so that the ribs support the structure while the waffle voids allow soil expansion [BRAB (1968), Dawson (1959)]. It may be possible to build foundation walls to some depth into the ground using tiles placed such that the soil can expand laterally into the tile cavities.
4. Control the soil water. The soil may be excavated to a depth such that the excavated overburden mass of soil will control heave, lay a plastic fabric within the excavation, and then backfill. The rising water vapor is trapped by the geotextile, and any subsequent volume change is controlled by the weight of overlying material and construction. The surface moisture will also have to be controlled by paving, grading, etc.
5. Check whether a granular blanket of 0.3 to 1 m or more depth will control capillary water and maintain a nearly constant water content in the clay [Gogoll (1970)].
6. Ignore the heave. By placing the footings at a sufficient depth and leaving an adequate expansion zone between the ground surface and the building, swell can take place without causing detrimental movement.

   A common procedure is to use belled piers (Fig. 7-9) with the bell at sufficient depth in the ground that the soil swell produces pull-out tension on the shaft or the whole system heaves. Small-diameter pipes with end plates for bearing can also be used to isolate smaller structures from expansive soil.

   The pier or pile shaft should be as small as possible to minimize the perimeter of the shaft so that soil expansion against the shaft does not produce tension or compression friction/adhesion stresses from vertical movement sufficient to pull the shaft apart or crush it. Adhesion on the pier shaft can be minimized by using a slightly oversized hole or by surrounding the shaft with straw or other porous material such as sawdust to reduce adhesion. The foundation system movements should be stabilized by the time any organic material used has rotted.

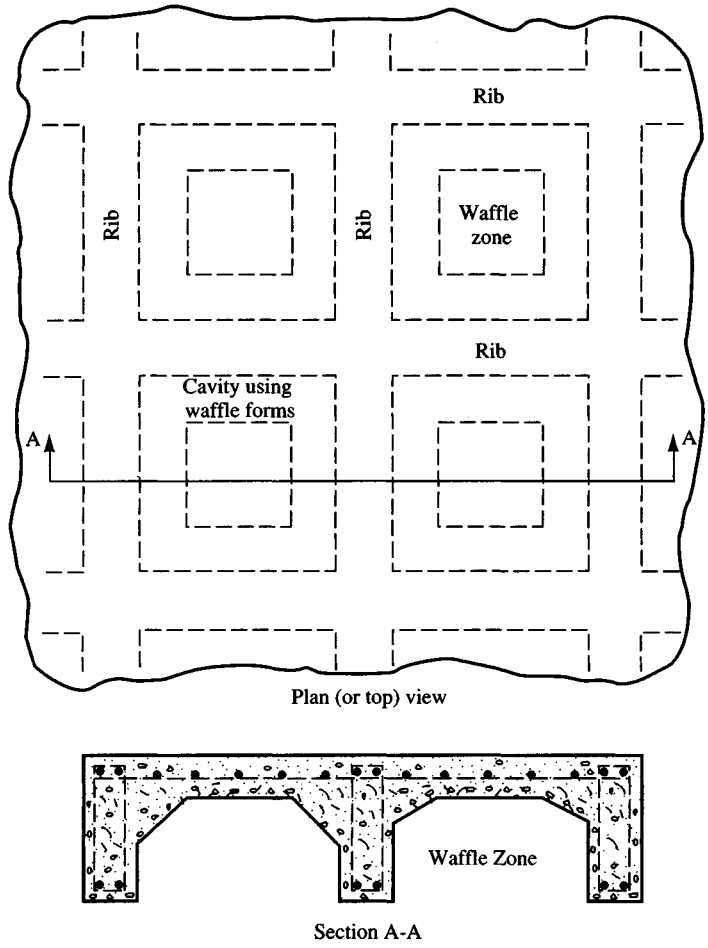

Figure 7-8 General configuration of a waffle slab. Waffle is usually formed by setting waffle forms, which are left in place and form the ribs, which can then be reinforced. Then the concrete is poured. Waffle forms may be of wood or corrugated cardboard.

7. Load the soil to sufficient pressure intensity to balance swell pressures. This method is used in many fills where the fill weight balances the swell pressure. This technique can also be used beneath buildings either by using spread footings of high pressure intensity or by excavating several feet of the clay and backfilling with granular material. The backfill in combination with foundation pressures may contain the swell. This method may not be practical for one-story commercial buildings and residences because of the small soil pressures developed from foundation loads.

Heave of expansive soils is difficult to predict, since the amount depends on the clay mineralogy, particle orientation, confining overburden pressure, and the difference between the current and reference (initial) in situ water content.

Estimates of heave may be obtained from standard 1-D consolidation tests (ASTM D 2435) in which the sample is compressed and then allowed to rebound. The slope of the rebound curve is related to swell.

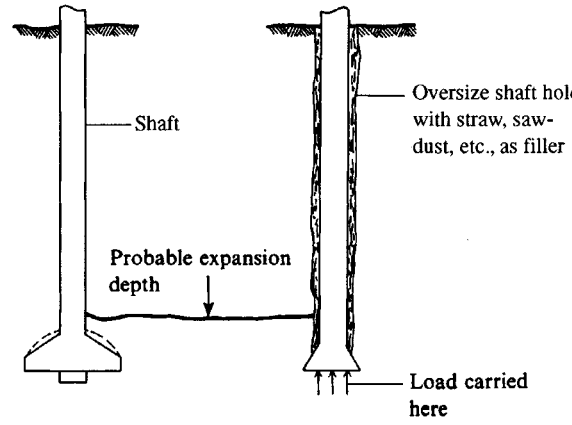

Figure 7-9 Belled piers in expansive soils. The pier shaft should be as small as practical to reduce shaft load from soil expansion.

The ASTM D 4546 method using consolidation test equipment also can be used to obtain swell estimates. It should be used instead of D 2435 where possible since the data obtained is more directly related to swell. Basically we can obtain a swell curve by confining the sample in the ring using a very small confining pressure of about 7 kPa (1 psi) and allowing it to absorb water and swell. If we measure the volume change in these conditions, we have a *free swell test.* If we apply sufficient consolidation pressure to prevent the sample from expanding, we can measure the swell pressure required to maintain the zero volume change. These data can be directly extrapolated to the expected heave or to the footing/overburden pressure required to eliminate, or at least reduce, the swell movements.

The resulting estimates improve with sample quality and careful attention to test details. The estimate also improves if the current natural water content w_o, and the degree of saturation for the laboratory volume change, are representative of the long-term in situ value. The latter is a very important consideration since the laboratory sample is thin and has access to sufficient free water to obtain $S = 100$ percent in a short time; this may never occur in the field, at least through the full depth z_d of the zone (Fig. 7-6) with potential to expand or shrink.

7-10 FOUNDATIONS ON CLAYS AND CLAYEY SILTS

Clays and clayey silts may range from very soft, normally consolidated, to very stiff, highly overconsolidated deposits. Major problems are often associated with the very soft to soft, deposits from both bearing-capacity[8] considerations and consolidation settlements. We should note that "soft" implies that the soil is very wet to saturated. Consolidation settlements occur in these deposits with high water contents as found along lake and ocean fronts, as well as in beds of former lakes and old streams where channels have become relocated but the water table remains high.

Silts with a large I_P and/or w_L may be called plastic silts. These silts exhibit nearly the same characteristics as those of soft clays. The plasticity results from contamination of the

[8] *Note:* Bearing capacity is a measure of soil shear strength. Settlement is a measure of soil stiffness or E_s.

mass with clay minerals and/or organic material. Inorganic silts and silts with little clay content may be loose, but their behavior is more that of sand, and procedures for design and densification are similar as previously noted in Sec. 7-7. Few pure silt deposits are found in nature. Most deposits contain some clay particles (with the resulting plasticity/cohesion) or quantities of fine to medium sand. In passing, note that as little as 5 percent clay can give a silt "cohesion"; 10 to 25 percent clay particles may result in the deposit being a "clay."

In both these types of soil it is necessary to make a best estimate of the allowable bearing capacity to control a shear failure with a suitable factor of safety and to estimate the probable consolidation settlements. The bearing capacity is most often determined using the undrained shear strength as obtained from quality tube samples or from samples obtained from routine SPT. If the soil is highly sensitive (remoulded shear strength one-fourth or less of undisturbed), consideration should be given to in situ strength testing such as the vane shear or the cone penetration test.

Consolidation tests should be made to determine the expected settlement if the structure has a relatively high cost per unit area. For smaller or less important structures, some type of settlement estimate based on the index properties might be justified.

Preconsolidated clays often contain shrinkage cracks and joints (fractured into a quantity of small blocks). The presence of structural defects makes it somewhat difficult to determine the unconfined compression strength. In many cases, and especially above the water table ($S \ll 100$ percent), the q_u strength as determined on occasional intact samples from the SPT or from using a pocket penetrometer will be adequate. If better estimates are required, it may be possible to use plate-load tests since it is very difficult (nearly impossible) to obtain tube samples of sufficient quality that triaxial tests can be performed. The cell pressure in the triaxial test tends to close the fissures so that an approximation to the in situ shear strength can be obtained. If the deposit is not overly fissured and jointed and the foundation is near ground surface, a suitable sample may be trimmed by hand if the cost can be justified. The immediate settlement equations of Chap. 5 can be used for settlement estimates together with empirical values of E_s if the soil is not saturated. These estimates should be adequate if the foundation pressures are not extremely high. If a precise settlement estimate is required, it will be necessary to obtain a reliable value of E_s.

The consolidation settlement of preconsolidated clays can be estimated using consolidation theory and making allowance for preconsolidation as in Example 5-14. Consolidation-settlement estimates based on correlations are not likely to give very good results, since most correlations are for normally consolidated clays.

The net ultimate bearing pressure for vertical loads on clay soils is normally computed as a simplification of either the Meyerhof or Hansen equations of Table 4-1:

$$q_{\text{ult}} = cN_c s_c d_c + \bar{q} N_q s_q d_q - \bar{q}$$

which is often written (after dropping s_q, d_q) as

$$q_{\text{ult}} = cN_c s_c d_c + \bar{q}(N_q - 1)$$

When $c = s_u$ we have $\phi = 0$ and $N_q = 1.0$, giving (see Example 4-4)

$$q_{\text{ult}} = cN_c s_c d_c$$

The combined effect of $N_c s_c d_c$ has a limiting value [Skempton (1951)] of about 9.0 (see Table 14-1) for square and round footings and 7.6 for a strip footing for all $D/B \geq 5$.

7-11 FOUNDATIONS ON RESIDUAL SOILS

Many foundations, particularly near the Atlantic coast, in the southeastern United States, and in parts of South America, Australia, New Zealand, the Middle East, and the Far East (interior parts of southeast Asia, China, and Siberia) are founded on residual soils.

A *residual soil* is produced from physical and chemical weathering of rock. The rock may be sedimentary, metamorphic, or igneous. Soils produced in this manner tend to be sandy silts or silty sands often with some mica particles and clay contamination (depending on the rock type undergoing weathering). The soil particles are more angular than in sedimentary deposits, and frequently the soil contains angular-to-subangular pebbles and larger rock pieces that are still weathering.

Within the mass there may be layers, lenses, or zones of extremely poor material depending on the amount of rainfall and extent of weathering. Near the soil-rock interface there may be a zone where the soil is completely (or nearly so) saturated from water trapped on top of the impermeable rock. Residual soil thickness varies from 0 to about 20 m depending on rock type and climatic conditions over the geological period. These soils are usually competent but again there are exceptions. The upper layers of these soil deposits are seldom saturated, but at the soil-rock interface they may well have $S \rightarrow 100$ percent.

Some residual soils are termed *laterites* or *saprolites*. Laterite soils tend to be reddish from oxidation of certain metallic oxides—principally iron—and are common in the southeastern United States, South America, parts of Africa, and certain other tropical regions.

Saprolites are "soils" that still retain the initial structure and fabric of the rock but have weathered to be so soft that they are treated as soil instead of the parent rock material. These soils are common in the Piedmont region of the United States but also exist in other geographic regions worldwide. Saprolites may contain so much mica that some type of improvement program, such as compaction, may be required so that they can be used.

In any case, to make a reliable design, some soil exploration is necessary in all residual soils. Ordinary drilling may be difficult owing to encounters with rock fragments, and sometimes a hole is abandoned and another one located a few meters away. In saprolites it may be necessary to use rock-coring equipment to obtain samples.

For most residual soils, the sample recovery and laboratory testing methods are the same as for sedimentary deposits to ascertain bearing capacity and estimate probable settlements.

Useful references for use in designing foundations in residual soils are Sowers (1979), Wesley (1990), Loganathan et al. (1992), and Pandian et al. (1993).

7-12 FOUNDATIONS ON SANITARY LANDFILL SITES

As land becomes scarce near urban areas, it may be necessary to use a former sanitary landfill. A sanitary landfill is a euphemistic name for a garbage dump. Landfill sites that are likely to be used now were often placed at some convenient location, generally where the ground was uneven so that the material could be placed in the depression and later covered. Present-day landfills must be located so that groundwater pollution is controlled. Generally daily covering of the refuse accumulation with a layer of earth is required. Good practice requires that 0.6 to 1 m of disposal material be covered with 0.15 to 0.2 m of compacted earth in alternating layers. This goal may not be achieved owing to the practice of dumping old bedding, refrigerators, auto parts, demolition and construction refuse, broken-up pavements, metal cans, and tires as well as smaller materials. In the past dumps were often left uncovered for days at a

time, creating both odor and pest nuisances. Currently, except in smaller communities, health authorities require covering the material daily. When the landfill is closed down, the surface should be covered with ±0.75 m of well-compacted earth and then landscaped. As the refuse decays, the surface may become uneven or the underlying material may form cavities, depending on the rapidity of decomposition (rotting), type of refuse materials, and thickness of fill cover.

In using a landfill for later construction, it may be extremely difficult to avoid settlements as the refuse decomposes and/or consolidates. It is certain that the settlements will be uneven owing to the varied character of the refuse material and the method(s) used to construct the fill. Yen and Scanlon (1975) reported several studies of landfill settlements, but no conclusive method of predicting settlement could be made.

Determination of bearing capacity of the fill will consist in checking to see if the surface cover has adequate thickness to avoid a punching or rotational shear failure as shown in Fig. 7-10*a*. It may be possible to add additional fill to reduce the pressure from the foundation on the refuse zone; this procedure will speed up and increase the fill consolidation and may be desirable for relieving future settlements if sufficient time is available. The additional fill would be on the order of 1.5*B* thick to accomplish the stress reduction on the refuse zone. For light structures such as one- or two-story residential buildings, apartments, office buildings, and stores, where the required bearing capacity may only be 25 to 50 kPa, the use of continuous foundations (with substantial reinforcing bars) may provide adequate bearing capacity and allow bridging over local soft spots or cavities. If this is not sufficient, or the owner does not wish to take a chance on building damage, the only recourse is to use piles or drilled piers (caissons) through the landfill into the underlying soil.

In using piles or piers, it will be necessary to use noncorroding materials, as any moisture in the fill will be contaminated by the garbage and likely to be corrosive to metal and may

Figure 7-10 Considerations for bearing capacity and settlement of foundations on sanitary landfills with thin covers. [Sowers (1968).]

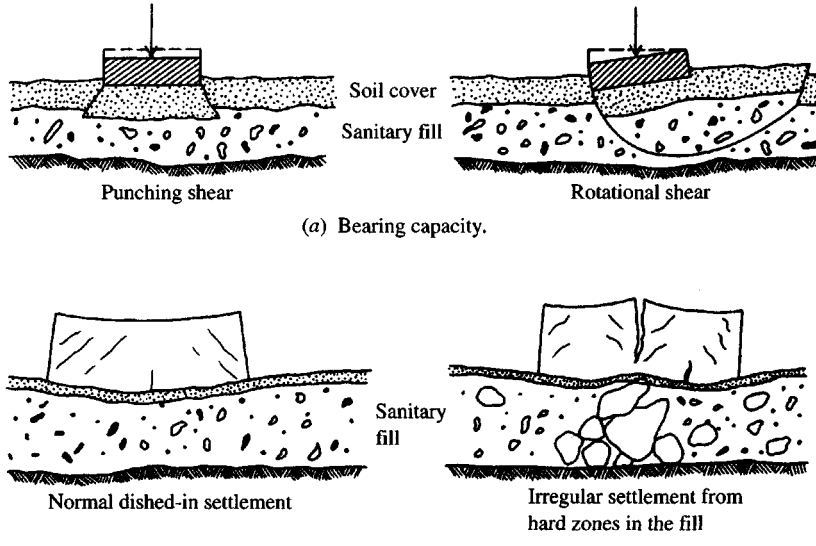

even damage concrete. Generally, only treated wood or precast concrete piles can be used. Driving the piles may be a considerable problem if paving rubble, auto bodies, or tires are encountered.

The foundation construction may create an odor problem as the ground cover is penetrated, and this should be investigated prior to construction as adjacent property owners may be able to obtain a court injunction against the air pollution. Gas (usually methane) is often produced by decay of the landfill contents. This can be an odor problem and a hazard, but also, if a local gas user can be found, an economic advantage. A careful site exploration is required so that the drillers are protected from gas inhalation and so that fumes are not ignited (from a drilling spark or smoking) resulting in an explosion and possible worker injury.

7-13 FROST DEPTH AND FOUNDATIONS ON PERMAFROST

7-13.1 Considerations in Temperate Areas

Figure 7-1 shows frost-depth contours based on a survey of selected cities for frost-depth practices at that location. Building codes may stipulate the depth the footings must be placed in the ground so that differential movement does not take place owing to water freezing in the ground beneath the foundation.

Differential movement is difficult to evaluate, as it depends on the amount of water, the formation of an ice lens, and the soil density. Water expands approximately 10 percent on freezing; thus, an ice lens in dense soil could cause a considerable amount of differential movement.

Unlike soil expansion, controlling ice expansion is impractical for ice forces are quite large (on the order of 2 MPa). Ice adhesion and resulting uplift can be avoided by using granular backfill around the foundation walls or footing pedestals. With insulation [McRoberts (1982)] it may be possible to reduce the depth of foundation or the amount of frost heave.

7-13.2 Foundations on Permafrost

Permafrost is a condition of permanently frozen ground where the ground temperatures are never higher than 0°C. This condition covers large areas of northern Canada, Alaska, most of Siberia, northern parts of Scandinavia, and Antarctica. In many areas an active zone overlies the permafrost, which thaws in season leaving a trapped mass of water-saturated bog, peat, and mud overlying the ice-rich underlying soil. Construction in these areas requires that the foundations be placed below this material and into the permafrost. It is usually necessary to insulate the interface between structure and the permafrost so that thawing of the underlying permafrost does not occur, either from building heat or because of changed environmental conditions.

Where the soil is considered thaw-stable, the foundation design is the same as in temperate regions. Thaw-stable soils are granular materials like coarse sands and gravels. These soils will, of course, have to be of sufficient thickness that the active zone will not penetrate the permafrost. Spread and continuous footings, mats, and beam-and-post construction can be used. Sometimes these foundations can be used for thaw-unstable soils as well [Linnel and Johnston (1973)]. Often the use of these foundations may require the use of a thaw-stable fill or ducting to reduce heat transfer into the underlying permafrost.

Pile foundations are more reliable for permafrost areas but are much more expensive. They may be necessary, however, where large differential settlements cannot be tolerated. Piles are

commonly wood, steel pipe, or **HP** piles. Concrete piles are less common for several reasons: transport cost, problem of curing if cast in place, and the high tensile stresses developed from the soil-water mixture freezing to the piles in the active zone. Pile tensile stresses on the order of 500 kPa have been measured [Linnel and Johnston (1973)]. Piles may be driven or inserted into predrilled holes, using a soil- or sand-water slurry that freezes around the pile to fix it in place.

For both pile foundations and spread footings on permafrost, creep is the significant parameter. With creep (δ_c, mm/time) the long-term settlement ΔH_i some time T_i after construction (and load applied) is

$$\Delta H_i = \delta_c T_i \qquad \text{(mm)} \tag{7-14}$$

The present state of art on the creep factor δ_c gives, at best, only a fair estimate (see Example 16-7 of Sec. 16-11). A number of creep equations and a literature survey are given by Sayles (1985). Lavielle et al. (1985) give a general overview of foundations on frozen ground with references cited from the four (to that time) international conferences on permafrost.

7-14 ENVIRONMENTAL CONSIDERATIONS

Foundation engineers have the responsibility to ensure that their portion of the total design does not have a detrimental effect on the environment. The responsibility may be enforceable by the courts if a laxity on the part of any parties can be ascertained. Although it may not be readily apparent, the foundation engineer does have some effect or potential effect on the environment, for example:

1. Soil borings through sanitary landfills (which may have been constructed on impervious soil to avoid groundwater pollution) can pollute the groundwater via seepage through the boreholes. ASTM D 5434 might be used as a guide in drilling both in natural soil and in sanitary landfills.
2. Soil boring logs should be checked for indication of effect of site excavation on the environment in terms of runoff, pollution in runoff, odor problems, dust, and noise.
3. One should investigate means to salvage topsoil for landscaping.
4. Pile driver noise and vibration can be objectionable.
5. Alternatives to cutting trees either for site work or where trees cause seasonal volume changes from soil desiccation during the growth season and wetting during the dormant season should be established.
6. Effect of soil borings on perched water tables must be identified.
7. It should be determined whether soil borings near streams cause piping problems during high water periods. These may be avoided by careful plugging of the boreholes.
8. Hydraulic fill for cofferdams, roadway approaches, and retaining structures, usually obtained from river bottoms, must not cause pollution of the groundwater through loss of the relatively impervious silt layer in the stream bed.
9. Earth removal for fill from hillsides must not cause landslides, which may destroy scenic areas.
10. The effect of river and marine structures on aquatic life must be minimized.

11. River and marine structures may lead to pollution of groundwater by either river or salt-water intrusions.

Particular sites and potential site development may create environmental considerations supplementing the preceding list.

PROBLEMS

7-1. Verify the computations of Example 7-1.

7-2. Verify the computations of Example 7-2.

7-3. Rework Example 7-2 using only Eq. (7-11) or Eq. (7-12) and assuming the average liquid limit water content $w_L = 42\%$ (instead of 76.6 of the example).

7-4. Average the appropriate water content and γ values of Table E7-1*a* and, using Eqs. (7-11) and (7-12), compute an expected average ΔH and compare it to Example 7-1. Especially note the comments at the end of Example 7-1 when you obtain your results.

7-5. A soil has the following average properties: $w_L = 57.5$ percent; $w_P = 26.0$ percent; $w_N = 29.0$ percent; $\rho_{dry} = 1.67$ g/cm^3. The profile contains 8.0 m of clay overlying a medium dense sand; q_u varies linearly from 125 kPa at -1.5 m to 185 kPa at -7.0 m. Assume this site is near Dallas, Texas.

(*a*) Estimate the swell pressure and heave if the active depth is 3 m.

(*b*) A two-story load-bearing-wall (concrete-block) apartment building consists of 8 units and a plan of 10×48 m. How can this building be constructed to have no differential settlement? Write your recommendations in a short report. Consider the building with and without a basement, and include consideration of floor slabs on grade or basement slab.

7-6. Refer to Fig. 7-4*a* (right side) and take $D = 1.5$ m, $\gamma_{soil} = 17.65$ kN/m^3, concrete $\gamma_c = 23.5$ kN/m^3, $Dc = 0.4$ m, load $P = 1250$ kN, allowable soil pressure $q_a = 300$ kPa, and $B = \sqrt{1150/300}$ and rounded to next larger multiple of 10 mm. If q_a = net allowable soil pressure, what is the difference between q_a and the actual net pressure from foundation load and geometry (make a neat foundation drawing as part of assignment)?

If q_a = gross allowable soil pressure, what is the difference between q_a and actual q_{gross}? Comment on these differences and state what you recommend for footing width B.

7-7. What is the allowable point bearing capacity ($F = 3$) for a 0.45-m diameter belled pier founded at elevation -6 m in the soil of Prob. 7-5?

7-8. What is the allowable bearing capacity for a square footing of $B = 1.75$ m spread footing for elevation -1.5, -3.0, and -4.0 m using the equation given in Sec. 7-10 and the soil of Prob. 7-5?

7-9. A soil investigation in an old sanitary landfill indicated 0.4 m of soil cover; SPT blow counts ranged from 1 to 8 in the depth from the surface to -5 m, except for one boring where $N = 50$ at -3 m. At elevation -5 m approximately 0.6 m of topsoil and organic material was encountered, and from elevation -6 m to -10 m the blow counts ranged from 12 to 20. The soil was a silty, stiff gray clay with traces of sand and gravel. At elevation -10 m (base of fill) the soil became a medium dense sand with blow counts ranging from 26 to 38. At elevation -50 m this soil became very dense and the blow counts ranged from 40 to 45. Boring was terminated at -20 m. The GWT is at elevation -11 m.

A one-story discount store consisting of 5000 m^2 is proposed for this site. Assume the site is near Chicago, Illinois. Draw the "typical" boring log and write a set of recommendations for the foundation design.

7-10. Use the soil boring data of Prob. 7-9. A six-story office building using a steel-frame and curtain-wall construction is proposed for the site. Draw the typical boring log and write a set of foundation recommendations.

7-11. A series of boring logs for a site revealed that the top 10 m was loose sand with blow counts ranging from 5 to 10 for the first 6 m and from 6 to 12 for the remainder. Underlying this is a 10.5-m stiff clay deposit with *average* properties of $w_L = 38.8$, $w_P = 21.3$, $w_N = 25$ percent, and unit weight $\gamma_{soil} = 19.57$ kN/m^3. The water table is at elevation 6.1 m. Assume the site is near Memphis, Tennessee.

A two-story manufacturing plant is proposed with column loads averaging 380 to 450 kN and wall loads of 30 kN/m. Draw the profile and make foundation recommendations. Settlements should be limited to 25 mm, and there will be machinery vibrations.

7-12. A one-story industrial plant is to be built near St. Louis, Missouri, on the east side of the Mississippi River. The site soil is a loess deposit 4 m thick overlying medium dense sand and gravel. Soil samples give $w_L = 42$; $w_P = 26$; $\gamma_{dry} = 14.8$ kN/m^3. The soil can be compacted to $\gamma_{dry} = 16.5$ kN/m^3 using a 3 percent lime admixture. Make tentative site recommendations for foundation loads on the order of 800 to 1200 kN. Estimate the kgs of lime that will be required for the soil improvement assuming that only the upper 2 m of the loess will be treated.

CHAPTER 8

SPREAD FOOTING DESIGN[1]

8-1 FOOTINGS: CLASSIFICATION AND PURPOSE

A footing carrying a single column is called a *spread footing,* since its function is to "spread" the column load laterally to the soil so that the stress intensity is reduced to a value that the soil can safely carry. These members are sometimes called single or isolated footings. Wall footings serve a similar purpose of spreading the wall load to the soil. Often, however, wall footing widths are controlled by factors other than the allowable soil pressure since wall loads (including wall weight) are usually rather low. Foundation members carrying more than one column are considered in Chapters 9 and 10. Concrete is almost universally used for footings because of its durability in a potentially hostile environment and for economy.

Spread footings with tension reinforcing may be called two-way or one-way depending on whether the steel used for bending runs both ways (usual case) or in one direction (as is common for wall footings). Single footings may be of constant thickness or either stepped or sloped. Stepped or sloped footings are most commonly used to reduce the quantity of concrete away from the column where the bending moments are small and when the footing is not reinforced. When labor costs are high relative to material, it is usually more economical to use constant-thickness reinforced footings. Figure 8-1 illustrates several spread footings.

Footings are designed to resist the full dead load delivered by the column. The live load contribution may be either the full amount for one- or two-story buildings or a reduced value

[1] This chapter will retain some Fps units as a reader convenience. This text is widely used as a reference work, and in remodeling/remedial work access to Fps units may be necessary. Also this chapter uses the standard American Institute of Steel Construction (AISC) terminology for rolled sections as given in their AISC (1989) publication for metric shapes based on the ASTM A 6M (SI) standard. For example, a **W** 360 × 79 is a rolled **W**ide flange shape of nominal 360-mm depth (actual depth = 354 mm), has a mass of 79 kg/m, and is usually used as a column.

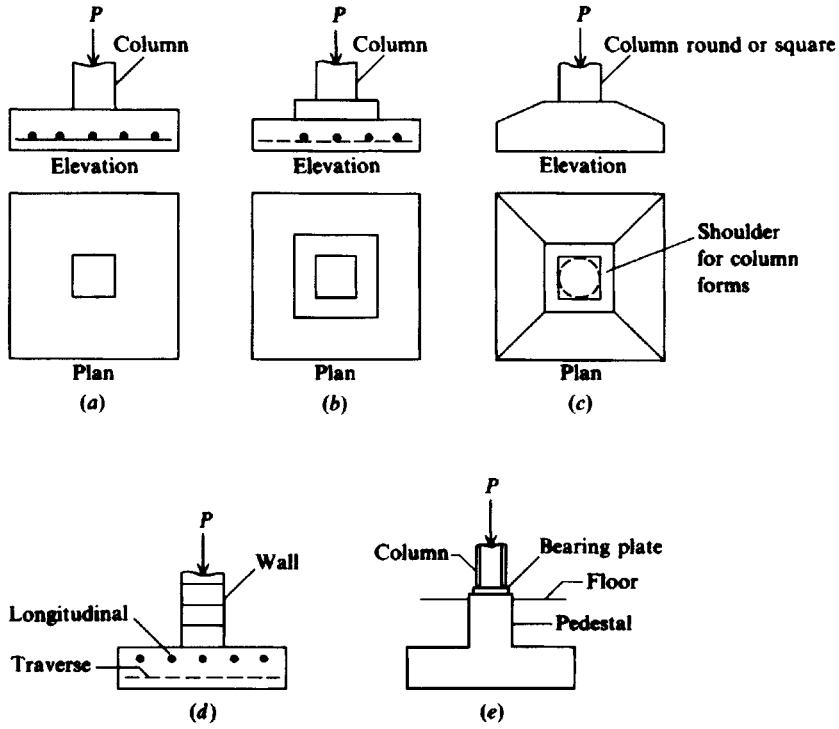

Figure 8-1 Typical footings. (*a*) Single or spread footings; (*b*) stepped footing; (*c*) sloped footing; (*d*) wall footing; (*e*) footing with pedestal.

as allowed by the local building code for multistory structures. Additionally the footing may be required to resist wind or earthquake effects in combination with the dead and live loads. The footing loads may consist of a combination of vertical and horizontal loads (inclined resultant) or these loads in combination with overturning moments. The current ACI[2] Code strength design procedure uses reduced load factors for the several transient loading conditions in lieu of increasing the allowable material stresses.

A pedestal (Fig. 8-1*e*) may be used to interface metal columns with spread or wall footings that are located at the depth in the ground. This prevents possible corrosion of metal through direct contact with the soil.

8-2 ALLOWABLE SOIL PRESSURES IN SPREAD FOOTING DESIGN

The allowable soil pressure for footing design is obtained as the worst case of bearing capacity and settlement as in Example 5-9. Where settlements control, the reported value is the net

[2]American Concrete Institute Building Code 318-. This code is revised every four to eight years. The metric version is designated 318M-. The latest (as of 1995) was issued in 1989 and revised in 1992 [the metric version being designated ACI 318RM-89 (Revised 1992)].

increase in soil pressure that can be allowed. The reason is that settlements are caused by increases in pressure over that currently existing from overburden.

The allowable bearing capacity furnished to the structural designer by the geotechnical engineer will have a suitable factor already applied. The safety factor ranges from 2 to 5 for cohesionless materials depending on density, effects of failure, and consultant caution. The value may range from 3 to 6 for cohesive materials, with the higher values used where consolidation settlements might occur over a long period of time. Note that these safety factors are larger than those cited in Table 4-9. Geotechnical caution should not be viewed as poor practice unless it results in a different type of foundation that is several times more expensive. In general, reduction of q_a from, say, 500 to 300 kPa will result in larger spread footings, but the percent increase in total building cost will be nearly negligible. This can be considered insurance, since a foundation failure requires very expensive remedial measures and structural repairs, whereas a superstructure failure may be localized and easily repaired.

The geotechnical consultant is not usually aware that the footing will be subjected to eccentric load and/or moment, so the allowable bearing pressure may not be found using the B' analysis of Chap. 4. Also if settlement controls, there is no reliable method to account for eccentricity. In these cases the best approach is to avoid any large differential pressure across the base of the footing. Any footing rotation will have a marked effect on the column base moment when the columns are rigidly attached to the footing. The footing rotation will be in a direction to reduce the base moment and may, in fact, reduce it to zero. Equation (5-17) can be used to estimate moment loss due to footing rotation as in Example 5-8.

Any increase in allowable soil pressure for transient load conditions should be verified with the geotechnical consultant. Increasing q_a by one-third as commonly found in design codes for other materials may not be appropriate. Factors such as frequency of overload, soil state, climatic conditions, and type of structure may disallow any large deviation from the recommended q_a.

8-3 ASSUMPTIONS USED IN FOOTING DESIGN

Theory of Elasticity analysis [Borowicka (1963)] and observations [Schultze (1961), Barden (1962)] indicate that the stress distribution beneath symmetrically loaded footings is not uniform. The actual stress distribution depends on both footing rigidity and base soil. For footings on loose sand the grains near the edge tend to displace laterally, whereas the interior soil is relatively confined. This difference results in a pressure diagram qualitatively shown in Fig. 8-2*a*. Figure 8-2*b* is the theoretical pressure distribution for the general case of rigid footings on any material. The high edge pressure may be explained by considering that edge shear must occur before any settlement can take place. Since soil has a low rupture strength, and most footings are of intermediate rigidity, it is not very likely that high edge shear stresses are developed. The edge stress also depends on the thickness H of compressible soil as shown in Fig. 8-2*b*.

The pressure distribution beneath most footings will be rather indeterminate because of the interaction of the footing rigidity with the soil type, state, and time response to stress. For this reason it is common practice to use the linear pressure distribution of Fig. 8-2*c* beneath spread footings. The few field measurements reported indicate this assumption is adequate.

Spread footing design is based almost entirely on the work of Richart (1948) and Moe (1961). Richart's work contributed to locating the critical section for moments; critical

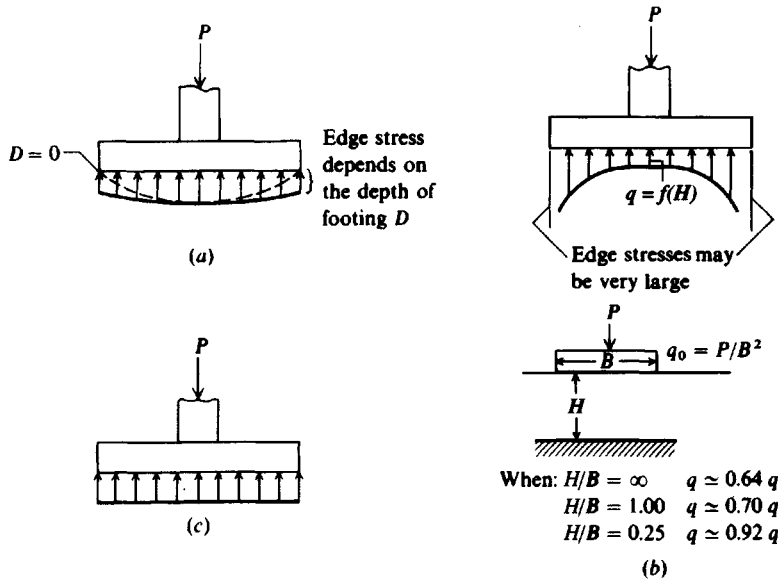

Figure 8-2 Probable pressure distribution beneath a rigid footing. (*a*) On a cohesionless soil; (*b*) generally for cohesive soils; (*c*) usual assumed linear distribution.

sections for shear are based on Moe's work. The ACI, AASHTO, and AREA[3] specifications for footing design are identical for locations of critical sections. AASHTO and ACI use the same design equations and factors for strength design. AREA uses the alternative design method for footings but allowable concrete strengths are about 10 percent less than those allowed by ACI. Because of the similarity in the several codes the ACI code will be the primary reference in this and the following two chapters.

8-4 REINFORCED-CONCRETE DESIGN: USD

The latest revision of the *ACI Standard Building Code Requirements for Reinforced Concrete* (*ACI* 318-), hereinafter termed the Code, places almost total emphasis on ultimate strength-design (USD) methods. The older procedure, termed the *Alternate Design Method* (ADM), is still allowed, and the basic elements are given in Appendix A of the ACI Code. The AASHTO bridge code gives about equal emphasis to both the alternate and the strength design methods. For spread footings, even though the design is reasonably direct, the ADM procedure is simpler to use but produces a more conservative design. When one compares designs by the two methods the ADM will consistently compute a concrete footing thickness on the order of 15 to 25 mm larger and reinforcing bar areas 30 to 50 percent larger. For these two reasons AASHTO gives more emphasis to the ADM than does ACI.

This text uses the ADM for the retaining wall design of Chap. 12—still a widely used procedure in practice—since the ACI code procedure does not give greatly different results

[3]ACI = American Concrete Institute, AASHTO = American Association of State Highway and Transportation Officials, AREA = American Railway Engineering Association.

and there is much uncertainty with that design. We will use the USD for spread footing design; however, footing depth equations [Eqs.(8-5)–(8-9)] are also applicable for the ADM. *The only difference* is whether column loads are factored (USD) or unfactored (ADM).

If you have difficulty factoring column moments for a spread footing design you should use the ADM method. You should also use the ADM where the column loads are not well-defined. The basic procedure is given as previously stated in Appendix A of ACI 318-; select parts and most of the methodology are given in Sec. 12-16 [basic design equations and allowable stresses (in Tables 12-1 and 12-2)].

All notation pertaining to concrete design used in this text will conform to the ACI Code. Where this conflicts with notation previously used, the reader should take note. Strength design requires converting working design dead (D) and live (L) loads (see Table 4-10) to *ultimate* loads through the use of load factors as

$$P_u = 1.4D + 1.7L \qquad (a)$$

$$= 0.75(1.4D + 1.7L + 1.7W) \qquad (b)$$

$$= 0.9D + 1.3W \qquad \text{(alternative with wind)} \qquad (c)$$

For earthquake loading substitute E for W (wind) as applicable. Other load combinations may be used, but the user is referred to Art 9.2 of the Code for their application.

The ultimate concrete strength f_c' in USD is reduced for workmanship and other uncertainties by use of ϕ factors (Art 9.3) as follows:

Design consideration	ϕ
Moment, without axial load	0.90
Two-way action, bond, and anchorage	0.85
Compression members, spiral	0.75
Compression members, tied	0.70
Unreinforced footings	0.65
Bearings on concrete	0.70

Concrete strain at ultimate stress is taken as 0.003 according to Art. 10.3.2, and the yield strength f_y of reinforcing steel is limited to 550 MPa (80 ksi) per Art. 9.4. The most popular grade of reinforcing steel in current use has $f_y = 400$ MPa (Grade 400 or 60 ksi).

ELEMENTS OF USD. For the partial development of the USD equations that follow, refer to Fig. 8-3.

From Fig. 8-3*b* the summing of horizontal forces, $\sum F_H = 0$, yields $C = T$, and, taking the compressive stress block as a rectangle of dimensions shown,

$$C = 0.85 f_c' ba$$

The tensile force in the steel reinforcement T is

$$T = A_s f_y$$

Equating the latter quantities yields an expression for the depth of the compression block as

$$a = \frac{A_s f_y}{0.85 f_c' b} \qquad (8\text{-}1)$$

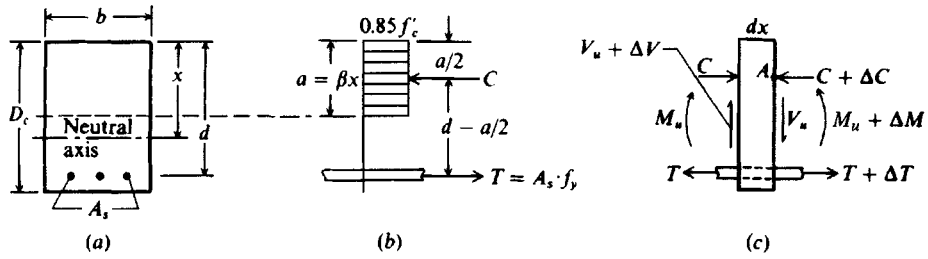

Figure 8-3 Assumptions used for the development of the ACI ultimate-strength-design equations.

For beams, b = width; for footings b = 1 unit (m or ft). From statics and summing moments at a convenient point (either T or C) we obtain

$$T\left(d - \frac{a}{2}\right) = M_u = C\left(d - \frac{a}{2}\right)$$

and solving for the ultimate resisting moment on a section and inserting the work quality factor ϕ, we have

$$M_u = \phi A_s f_y \left(d - \frac{a}{2}\right) \tag{8-2}$$

Alternatively, if steel ratio terms p and q are defined as follows,

$$p = \frac{A_s}{bd} \qquad q = \frac{p f_y}{f'_c}$$

Eq. (8-2) can be written as

$$M_u = \phi b d^2 f'_c q(1 - 0.59q) \tag{8-2a}$$

The steel ratio at a cross section has been defined as $p = A_s/bd$ and the ratio at *balanced* design will be designated as p_b. To ensure a tensile failure rather than a sudden concrete compression failure p_d is taken as not over $0.75p_b$ (Art. 10.3.3) where the balanced reinforcement ratio is computed based on the concrete strain at ultimate stress of 0.003 and E_s = 200,000 MPa or 29×10^6 psi as

$$\text{SI}: p_b = \frac{0.85\beta_1 f'_c}{f_y} \frac{600}{f_y + 600} \qquad \text{Fps}: p_b = \frac{0.85\beta_1 f'_c}{f_y} \frac{87{,}000}{f_y + 87{,}000} \tag{8-3}$$

The factor β_1 in the preceding equation is defined as follows:

$$\text{SI}: = \beta_1 = 0.85 - 0.008(f'_c - 30\text{ MPa}) \geq 0.65$$
$$\text{Fps}: = \beta_1 = 0.85 - 0.05(f'_c - 4\text{ ksi}) \geq 0.65$$

Footings for buildings seldom use $f'_c > 21$ MPa (3 ksi); for bridge footings f'_c is not likely to exceed 30 MPa (4 ksi), so the factor β_1 will, in nearly all cases, be 0.85. The lower-strength concrete is somewhat less costly per cubic meter but, more importantly, will produce a more rigid footing as it will have to be made thicker (larger D_c of Fig. 8-3*a*). Table 8-1 provides values for β_1 for a range of f'_c, which may be of use here and for mat design (Chap. 10), where

TABLE 8-1
Maximum allowable steel ratio ρ_d*

Note: ASTM 615M and 615 now define only two grades of rebars: Grade 300 (40 ksi) and Grade 400 (60 ksi)

		f_y, MPa (ksi)	
f'_c, MPa (ksi)	β_1†	Grade 300 (40 ksi)	Grade 400 (60 ksi)
21 (3.0)	0.85	0.028	0.016
24 (3.5)	0.85	0.032	0.020
30 (4.0)	0.85	0.041	0.024
35 (5.0)	0.81	0.047	0.028
40 (6.0)	0.77	0.054	0.033

*Table ratios shown are $0.75p_b$ for ensuring a tensile rebar failure per ACI Art. 10.3.3.

†Values are slightly approximate for Fps units.

higher-strength concrete may be used on occasion. Also given in Table 8-1 are the several values of $0.75p_b$ (limiting percentage of steel at a cross section), which as shown above depend on both f'_c and f_y. Adequate concrete-to-rebar adhesion (termed *bond*) is provided for in Art. 12.2 by specifying the minimum length of embedment L_d for reinforcing bars in tension depending on diameter or area as follows:

Bar code number or diameter	$L_d \geq$ 300mm (12 in)	SI	Fps
No. 35 (35 mm) and smaller	$C_1 A_b f_y / \sqrt{f'_c}$	$C_1 = 0.02$	0.04
No. 45 (No. 14)	$C_2 f_y / \sqrt{f'_c}$	$C_2 = 25.0$	0.085
No. 55 (No. 18)	$C_3 f_y / \sqrt{f'_c}$	$C_3 = 40.0$	0.125

Note: f'_c = MPa or psi A_b = mm² or in² Max. $\sqrt{f'_c} = \frac{25}{3}$ MPa or 100 psi (Art 12.1.2)
L_d = mm or in.

These development lengths should be multiplied by the following factors as applicable:

Condition	Factor
Top rebars with more than 300 mm or 12 in. of concrete below bar	1.3
Lightweight concrete (seldom used for footings)	$1.3 \geq 1.0$
If bar spacing is at least $5d_b$ on centers and has at least $2.5d_b$ of side cover	0.8
If reinforcement is in excess of that required In all cases the embedment depth $L_d \geq$ 300 mm (12 in.), or	$A_{s,reqd}/A_{s,furn}$
$0.375 d_b f_y / \sqrt{f'_c}$ mm	
$0.03 d_b f_y / \sqrt{f'_c}$ in	

The development length for bond (Art. 12.3) for compression bars is the largest of the following:

SI:	$0.25 f_y d_b / \sqrt{f_c'}$	or	$0.04 f_y d_b$	or	200 mm
Fps:	$0.02 f_y d_b / \sqrt{f_c'}$	or	$0.0003 f_y d_b$	or	8 in.

where A_b = bar area, mm^2 or $in.^2$
d_b = bar diameter, mm or in.
f_y = yield strength of steel, MPa or psi
f_c' = 28-day compressive strength of concrete, MPa or psi

Standard hooks can be used to reduce the required value of L_d from the preceding equations but are not usually used for footings. Hook requirements are given in Art. 12.5 of the Code.

Shear often governs the design of spread footings. The ACI Code allows shear to be computed as

$$v_u = \frac{V_u}{bd} \tag{8-4}$$

where V_u is the ultimate shear force (factored working loads) and bd is the resisting shear area of width b and effective depth d to center of tension steel. The nominal computed value of shear v_u is compared with the allowable values, which are wide-beam and two-way action[4] shear defined on Fig. 8-4. The allowable values of v_c are as follows:

$\phi = 0.85$	SI	Fps	ACI Code Reference
Wide-beam	$\phi \sqrt{f_c'}/6$	$2\phi \sqrt{f_c'}$	Art. 11.3.1.1
Two-way action when $\beta \le 2$	$\left(1 + \frac{2}{\beta}\right)\frac{\phi \sqrt{f_c'}}{6}$	$\left(2 + \frac{4}{\beta}\right)\phi \sqrt{f_c'}$	Art. 11.12.2.1
but not more than:	$v_c = \frac{\phi \sqrt{f_c'}}{3}$ MPa	$4\phi \sqrt{f_c'}$ psi	
	$\beta = \frac{\text{Col. length}}{\text{Col. width}}$		
	f_c' = **MPa**	**psi**	

In most practical design cases the columns have $L_c/B_c \le 2$ (are often square or round with $L_c/B_c = 1$) so that $v_c = \phi \sqrt{f_c'}/3$ (or $4\phi \sqrt{f_c'}$). The ACI Code allows shear reinforcement in footings and it is also obvious that a higher f_c' concrete would reduce or eliminate the need for shear reinforcement. Neither of these alternatives is much used; rather, the effective footing depth d is increased to satisfy shear requirements. This decision has the beneficial effect of increasing the footing rigidity, so the assumption of uniform base pressure is more likely to be obtained, as well as somewhat reducing settlement.

A minimum area of dowels of $0.005 A_{col}$ is required to anchor the column to the footing according to Art. 15.8.2.1. Dowels are sometimes required to transfer column stress into the footing, particularly if the column concrete is substantially stronger than the footing concrete.

[4]This was formerly called diagonal tension or *punching* shear.

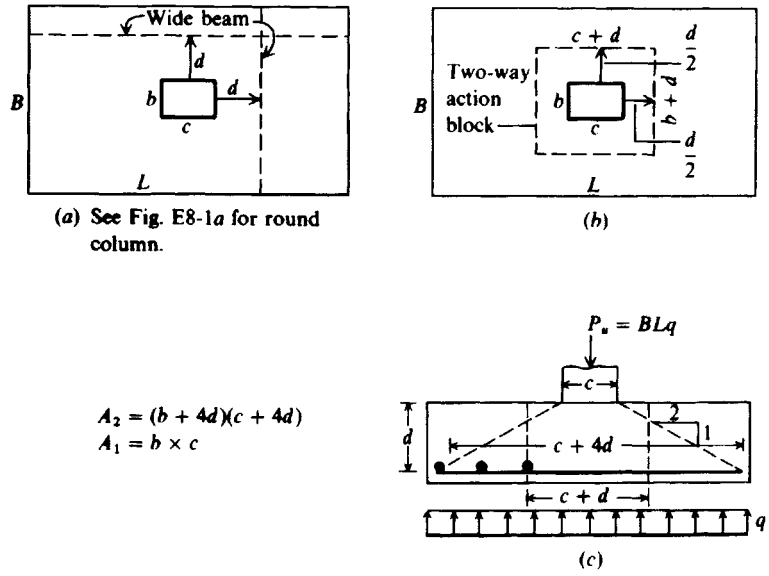

Figure 8-4 (*a*) Section for wide-beam shear; (*b*) section for diagonal-tension shear; (*c*) method of computing area A_2 for allowable column bearing stress.

Dowels are required if the column contact stress exceeds the following:

$$f_c = 0.85\phi f_c' \sqrt{\frac{A_2}{A_1}}$$

The ratio $A_2/A_1 \leq 2$ and the ϕ factor is 0.7. The area A_1 is the column contact area ($b \times c$) or $\pi a^2/4$; the area A_2 is the base of the frustum that can be placed entirely in the footing as shown in Fig. 8-4*c* and defined in Art 10.16.

Table 8-2 gives allowable wide-beam and two-way action shear values for several f_c' values. Table 8-3 summarizes the principal ACI Code requirements particularly applicable to concrete foundation elements (spread footings, mats, retaining walls).

8-5 STRUCTURAL DESIGN OF SPREAD FOOTINGS

The allowable soil pressure controls the plan ($B \times L$) dimensions of a spread footing. Structural (such as a basement) and environmental factors locate the footing vertically in the soil. Shear stresses usually control the footing thickness D. Two-way action shear always controls the depth for centrally loaded square footings. Wide-beam shear may control the depth for rectangular footings when the L/B ratio is greater than about 1.2 and may control for other L/B ratios when there are overturning or eccentric loadings.

The depth of footing for two-way action produces a quadratic equation that is developed from Fig. 8-4*b*, *c* using

$$\sum F_v = 0$$

on the two-way action zone shown. Noting the footing block weight cancels, we have—valid

TABLE 8-2
Allowable limiting two-way action and wide-beam shear v_c by ACI 318 Code for several concrete strengths f'_c for $\beta \leq 2.0$ and the ϕ factor of 0.85 (ACI Art. 9.3.2.3)

$\phi = 0.85$		f'_c, MPa (psi) 21 (3000)	24 (3500)	28 (4000)	35 (5000)
Two-way action (ACI 11.12.2-)					
$\phi\frac{\sqrt{f'_c}}{3}$	(MPa)	**1.298**	**1.388**	**1.499**	**1.676**
$4\phi\sqrt{f'_c}$	(psi)	186.2	201.1	215.0	240.4
	(ksf)	26.8	29.0	31.0	34.6
Wide-beam shear* (ACI 11.3.1.1)					
$\phi\frac{\sqrt{f'_c}}{6}$	(MPa)	**0.649**	**0.694**	**0.750**	**1.676**
$2\phi\sqrt{f'_c}$	(psi)	93.11	100.57	107.52	120.21
	(ksf)	13.41	14.48	15.48	17.31

*For two-way action the ACI Code allowable shear stress (MPa) is the *smallest* of the above and the following two equations:

$$\left(1 + \frac{2}{\beta_c}\right)\phi\frac{\sqrt{f'_c}}{6} \quad \text{[ACI (11-36)]}$$

$$\left(\frac{\alpha_s d}{b_o} + 2\right)\phi\frac{\sqrt{f'_c}}{12} \quad \text{[ACI (11-37)]}$$

where β_c = ratio of long column side over short column side (and must be $\beta_c > 2$ to become the smallest allowable v_c).

α_s = 40 for interior, 30 for edge, and 20 for corner columns.

b_o = two-way action perimeter defined using column dimensions + $\frac{1}{2}d$ distance as appropriate from column face(s).

d = effective depth of member.

for either USD or ADM (select elements of the ADM are given in Sec. 12-16)

$$P_u = 2dv_c(b + d) + 2dv_c(c + d) + (c + d)(b + d)q$$

Substitution of P_u or $P_d = BLq$ and using either the USD or the ADM shear stress v_c gives

$$d^2(4v_c + q) + d(2v_c + q)(b + c) = (BL - cb)q \tag{8-5}$$

For a square column $c = b = w$ we obtain

$$d^2\left(v_c + \frac{q}{4}\right) + d\left(v_c + \frac{q}{2}\right)w = (BL - w^2)\frac{q}{4} \tag{8-6}$$

For a round column, a = diameter, the expression is

$$d^2\left(v_c + \frac{q}{4}\right) + d\left(v_c + \frac{q}{2}\right)a = (BL - A_{\text{col}})\frac{q}{\pi} \tag{8-7}$$

TABLE 8-3
Summary of ACI 318 Code reinforced concrete foundation requirements

		ACI 318
Design factor	**Art. number**	**General requirements**
Bearing (column on footing)	10.15	$q_{brg} \le \psi 0.85\phi f'_c \quad \psi \le 2$
Design load combinations	9.2	E.g., as 1.4 × dead load + 1.7 × live load
Footings		
Column-to-base stress transfer	15.8	With dowels, $w/A_s \ge 0.005A_g$
Location of moment	15.4.2	See Fig. 8-5
Location of shear	15.5	See Fig. 8-4
Minimum edge thickness	15.7	150 mm above reinforcement; 300 mm above pile heads
Round columns on	15.3	Use equivalent square of same area
Grade beams	14.7	Use walls with grade beams
Load factors ϕ	9.3.2	See table in textbook (Sec. 8-4)
Minimum wall thickness	14.5.3.2	Generally 190 mm
Modulus of elasticity E_c	8.5	$E_c = 4700\sqrt{f'_c}$ MPa* $= 57\,000\sqrt{f'_c}$ psi
Reinforcement		
Development length	12.2, 12.6	See equations in text or code
Lap splices in	12.14.2	Not for bars > No. 35
Limits in compression	10.9	$0.01 \le A_{st}/A_g \le 0.08$
Maximum ratio	10.3.3	
Minimum ratio	10.5.1	
Minimum cover	7.7.1	Cast-in-place use 70 mm; with forms 50 mm
Rectangular footings, for	15.4.4	
Spacing of	7.6	Not less than D or 25 mm or 1.33 × max. aggregate size; not more than 3 × D_c or 500 mm
Temperature and shrinkage	7.12	
Shear		
Two-way action	11.12.1:2	$v = V_u/bd$ $v_c = \left(1 + \frac{2}{\beta}\right)\frac{\phi\sqrt{f'_c}}{6} \le \frac{\phi\sqrt{f'_c}}{3}$ $\beta = \frac{\text{Column length}}{\text{Column width}}$
Wide-beam	11.12.1	$v_c = 2\phi\sqrt{f'_c}$ psi
Reinforcement allowed	11.12.3	
β_1 factor	10.2.7.3	$\beta_1 = 0.85$ for $f'_c \le 30$ MPa; reduced by 0.008 for each 1 MPa in excess of 30 MPa but $\beta_1 \ge 0.65$

*$E_c = \gamma_c^{1.5}44\sqrt{f'_c}$ MPa for $14 \le \gamma_c \le 25$ kN/m^3
Values shown of 4700 and 57 000 are for "normal" weight concrete.

If we neglect the upward soil pressure on the diagonal tension block, an *approximate* effective concrete depth d can be obtained for rectangular and round columns as

$$\text{Rectangular:} \qquad 4d^2 + 2(b + c)d = \frac{BLq}{v_c} = \frac{P_v}{v_c} \tag{8-8}$$

$$\text{Round:} \qquad d^2 + ad = \frac{P_u}{\pi v_c} \tag{8-9}$$

The approximate formulas will result in a d value seldom more than 25 mm or 1 in. larger than the "exact" formulas of Eqs. (8-5) and (8-7).

Always use Eq. (8-7) or (8-9) for round columns to obtain the effective footing depth d since using an equivalent square column and Eq. (8-5) gives a smaller value.

Steps in square or rectangular spread footing design with a centrally loaded column and no moments are as follows:

1. Compute the footing plan dimensions $B \times L$ or B using the allowable soil pressure:

$$\text{Square:} \qquad B = \sqrt{\frac{\text{Critical load combination}}{q_a}} = \sqrt{\frac{P}{q_a}}$$

$$\text{Rectangular:} \qquad BL = \frac{P}{q_a}$$

   A rectangular footing may have a number of satisfactory solutions unless either B or L is fixed.

2. Convert the allowable soil pressure q_a to an ultimate value $q_{\text{ult}} = q$ for use in Eqs. (8-5) through (8-9) for footing depth

$$\frac{P_u}{BL} = q = \frac{P_{\text{ult}}}{P_{\text{design}}} q_a$$

   Obtain P_u by applying appropriate load factors to the given design loading.

3. Obtain the allowable two-way action shear stress v_c from Table 8-2 (or compute it) and, using the appropriate Eqs. (8-5) through (8-9), compute the effective footing depth d.

4. If the footing is rectangular, immediately check wide-beam shear. Use the larger d from two-way action (step 3) or wide-beam.

5. Compute the required steel for bending, and use the same amount each way for square footings. Use the effective d to the intersection of the two bar layers for square footings and if $d > 305$ mm or 12 in. For d less than this and for rectangular footings use the actual d for the two directions. The bending moment is computed at the critical section shown in Fig. 8-5. For the length l shown the ultimate bending moment/unit width is

$$M_u = \frac{ql^2}{2}$$

   In Eq. (8-2) use M equals M_u if $q = q_{\text{ult}}$ to obtain the amount of reinforcing bar steel/unit width. Check the steel ratio p to satisfy Temperature and Shrinkage (T and S) and to verify that the maximum steel ratio of Table 8-1 is not exceeded. You should be aware that the ACI 318 has specific T and S requirements for slabs but is somewhat ambiguous about T and S requirements for footings. The commentary R7.12.1 states, "... the provisions of these sections are intended for structural slabs only; they are not intended for 'slabs on grade.'"

   Some designers would routinely put T and S steel in spread footings or mats if the top is not covered with earth. Where the top of the footing is covered by about 400 to 500 mm

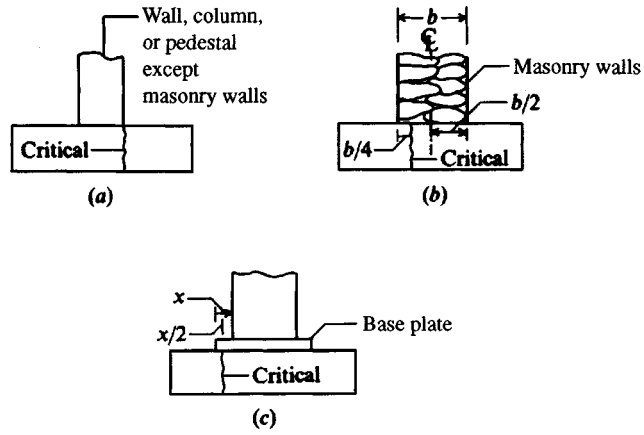

Figure 8-5 Sections for computing bending moment. Bond is computed for section indicated in (*a*) for all cases; however, for convenience use bond at same section as moment.

of earth, there is enough insulation provided that changes in temperature are not wide. Large temperature variations tend to produce tension cracks unless restrained by T and S reinforcement. Regardless of the code, which tends to give minimum requirements, one can always *overdesign,* that is, exceed any minimum code requirements.

6. Compute column bearing and use dowels for bearing if the allowable bearing stress is exceeded. In that case, compute the required dowels based on the difference between actual and allowable stresses × column area. This force, divided by f_y, is the required area of dowels for bearing.

   It is necessary always to use a minimum of $0.005A_{col}$ of dowel steel regardless of the bearing stress.

   If dowels are required to transfer any column load, the length must be adequate for compression bond. The ACI 318 covers the required length in Art. 12.3. If the footing does not have a sufficient d you can put them in a spiral encasement and reduce the required length 25 percent. If that is not adequate you will have to increase the effective footing depth d. The use of 90° bends (whether required or not) is common, as it allows easy attachment of the column dowels to the footing reinforcement by wiring.

7. Detail the design. At least provide enough detail that a draftsperson (or a CAD operator) can produce a working drawing for the construction personnel.

The current ACI Code procedure as outlined in the preceding steps is based primarily on tests by Richart (1948), which showed larger bending moments at the column face for column strips and lesser values on other strips. Bowles (1974*a,* Chap. 7), using finite-difference and finite-element analytical procedures, found that, whereas the bending moment is higher in the column area, for finite-difference methods the average bending moment across the footing at the section taken in Fig. 8-5 is the same as the Code procedure. The maximum computed moment will exceed the average moment by about 30 percent for the finite-difference method and by more than 40 percent using the finite-element method, and assuming column fixity, which is close to reality for concrete columns attached by the Code requirement to the footing as shown later in Example 10-4. It is implicit that readjustment will take place to reduce the cracking effect of the column-zone moment. It may be questionable whether the 40 percent

larger moment can be adequately readjusted without possible cracking and long-term corrosion effects. This problem was less severe when the alternative design method was more popular than at present. The problem is such that one should consider the use of larger load factors than $1.4D$ and $1.7L$ for footings based on the USD method. It is, of course, always permissible to use larger factors since any code provides only minimum values. Alternatively, one could compute the total steel required for the side and put, say, 60 percent in a column zone with a width of about $w + 2d$ and the remainder in the two end zones—similarly for the orthogonal direction.

Example 8-1. Design a plain (unreinforced) concrete spread footing (see Fig. E8-1*a*) for the following data:

$$DL = 90 \text{ kN} \qquad LL = 100 \text{ kN}$$

Column : **W** 200 × 31.3 resting on a 220 × 180 × 18 mm base plate

[Rolled structural shape dimensions are available in ASTM A 6M or AISC (1992).] Also:

$$f'_c = 21 \text{ MPa}$$

Allowable soil pressure $q_a = 200$ kPa

Solution: Note the following:

1. Plain concrete footings must be designed using ACI 318.1 "Building Code Requirements for Structural Plain Concrete." The SI version is ACI 318.1M.
2. Unreinforced footings are only practical and economical for small column loads as in this example.
3. We could step or taper the footing to reduce the volume of concrete slightly but at current labor costs for the additional formwork and shaping; it is usually more economical to use a constant depth footing.
4. Wall footings are very commonly made of plain concrete.

With these comments we will now proceed with the footing design.

Step 1. Size the footing:

$$B^2 q_a = P = 90 + 100 = 190$$

$$B = \sqrt{\frac{190}{200}} = 0.97 \text{ m} \qquad \text{Use } B = 1 \times 1 \text{ m}$$

Figure E8-1*a*

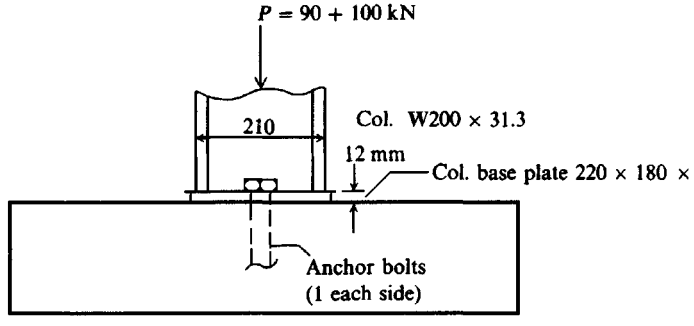

Step 2. Find the footing depth. For plain footings the moment requirement is usually critical, so we will find the depth to satisfy moment and then check shear.

Convert q_a to a pseudo q_{ult} so we can use USD:

$$P_{ult} = 1.4DL + 1.7LL$$

[as one load combination given in ACI 318- (Art. 9.2), which we assume controls in this example]

$$P_{ult} = 1.4(90) + 1.7(100) = 296 \text{ kN} \qquad q_{ult} = \frac{P_{ult}}{A_{ftg}} = \frac{296}{1^2} = \mathbf{296} \text{ kPa}$$

For flexure the maximum tensile stress is $f_t = 0.4\phi\sqrt{f_c'}$ (ACI 318.1M, Art. 6.2.1).

For all cases the ϕ factor = 0.65 for plain concrete (Art. 6.2.2). Thus,

$$f_t + 0.4(0.65)(21)^{1/2} = 1.19 \text{ MPa}$$

The critical section is defined at $\frac{1}{2}$ distance from edge of base plate to column face (Figs. 8-5 and 8-6*b*), which will be taken as $\frac{1}{2}$ distance to center of web that gives the largest moment arm L_m.

Referring to Figs. E8-1*c* and 8-6*b* the distance is

$$L_m = \frac{B}{2} - \frac{0.180}{2} + \frac{0.180}{4} = 0.455 \text{ m}$$

$$M_u = \frac{q_{ult}L_m^2}{2} = \frac{296(0.455)^2}{2} = \mathbf{30.64} \text{ kN} \cdot \text{m/m}$$

Equating allowable stress $f_t \times$ section modulus $\mathbf{S} = M_u$ and for a rectangle

$$\mathbf{S} = bd^2/6$$

Here we will use b = unit width = 1 m giving $f_tS = f_td^2/6 = M_u = 30.64$.

$$f'd^2/6 = 30.64$$

$$d = \sqrt{\frac{30.64(6)}{1.19 \times 1000}} = 0.393 \text{ m}$$

To this thickness d we must add 50 mm according to Art. 6.3.5 (of 318-1M) for concrete in contact with ground, or

$$D_c = d + 0.050 = 0.393 + 0.050 = \mathbf{0.443} \text{ m} \qquad \text{Use } \mathbf{450} \text{ mm}$$

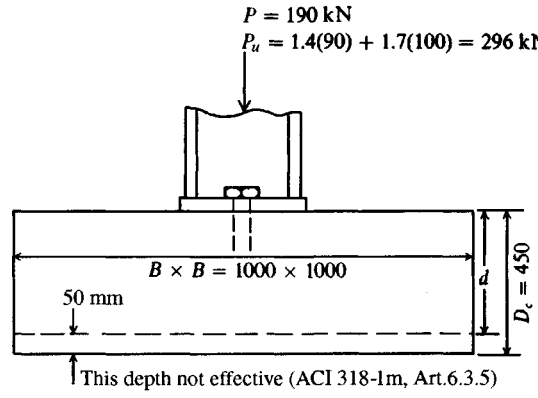

Figure E8-1*b*

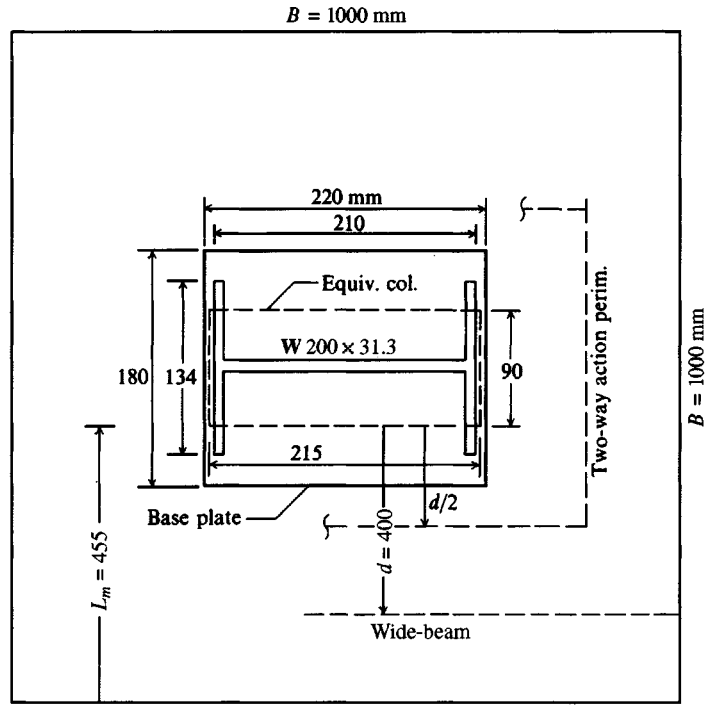

Figure E8-1*c*

Step 3. Check two-way action using $d = 450 - 50 = 400$ mm effective depth.

$$v_c = \left(1 + \frac{2}{\beta}\right)\frac{\phi\sqrt{f'_c}}{6} \le \frac{\sqrt{f'_c}}{3} \qquad \text{(Art. 6.2.1}c\text{ or ACI 318-, Art. 11.12.2.1)}$$

$$\beta = \frac{\text{Col. length}}{\text{Col. width}} = \frac{210}{90} = 2.33 \qquad \text{(using "effective" width)}$$

$$v_c = \left(1 + \frac{2}{2.33}\right)\frac{0.65(21)^{1/2}}{6} = 0.92 \text{ MPa} < \frac{0.65(21)^{1/2}}{3}$$

The average shear perimeter p at $d/2$ from the column with average column dimensions of depth $= (220 + 210)/2 = 215$ mm and width $= 180/2 = 90$ mm (see Fig. E8-1*c*) is

$$p = 2(0.215 + 0.400 + 0.090 + 0.400) = 2.21 \text{ m}$$

The shear resistance (neglecting the upward soil pressure on this area) is

$$R = pdv_c = 2.21(0.40)(0.92 \times 1000) = \mathbf{813} \text{ kN} \gg 296\ (= P_{ult})$$

Step 4. We should check wide-beam shear at distance d from the critical column face.

$$\text{Critical } L' = L_m - d \text{ (by inspection of Fig. E8-1}c\text{)}$$
$$L' = 0.455 - 0.400 = 0.055 \text{ m (negligible)}$$

For a shear force $V = 0.055q_{ult}$, wide-beam shear is not critical.

Step 5. Draw a final design sketch as in Fig. E8-1*c*. A question may arise of whether this plain concrete base should contain temperature and shrinkage (T and S) steel. Strictly, the ACI Code is not

clear on this point; however, if we check Art. 2.1 of 318.1, it defines plain concrete as either unreinforced or containing less reinforcement than the minimum specified in ACI 318. Some authorities are of the opinion that concrete placed in the ground does not require temperature and shrinkage steel since the temperature differentials are not large. For footings, one must make a judgment of effects of temperature and shrinkage cracks. For this and other plain concrete footings a more conservative solution is obtained by using T and S steel both ways. For this problem, and referring to ACI Sec 7.12.2.1, use

T and S reinforcement both ways $= 0.002(0.4 \times 1)10^6 = 800 \text{ mm}^2$ each way
From Table inside front cover try four No. 15 (16 mm diam.) bars each giving

$$A_s = 4 \times 200 = 800 \text{ mm}^2$$

Four equally spaced bars satisfy maximum spacing requirements.

////

Example 8-2. Design a spread footing for the average soil conditions and footing load given in Fig. E8-2*a*. Note the geotechnical consultant provided q_a in Example 8-1; however, in this case the designer preferred to select the allowable soil pressure from a soil profile provided by the geotechnical engineer.

$$DL = 350 \text{ kN} \qquad LL = 450 \text{ kN} 2f_c' = 21 \text{ MPa}$$
Use grade 400 rebars ($f_y = 400$ MPa)

The column has dimensions of 0.35×0.35 m and uses four No. 30 bars (diam. = 29.9 mm, see inside front cover).

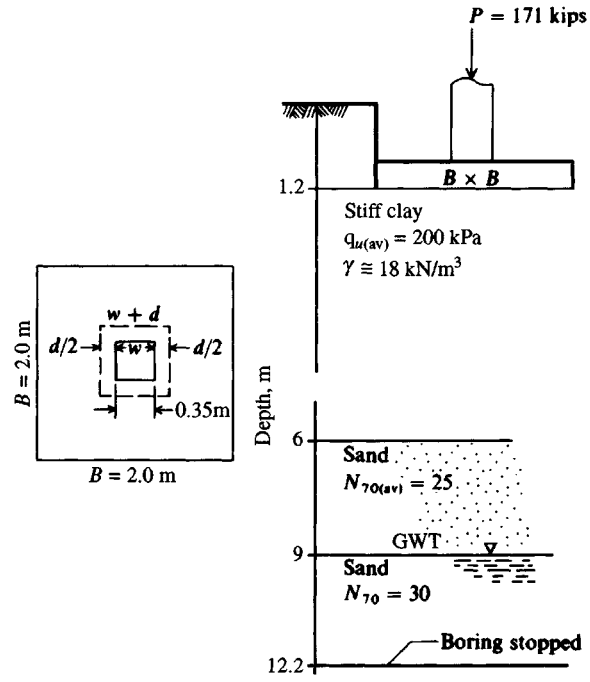

Figure E8-2*a*

Solution.

Step 1. From the soil profile find q_a. To start, we readily obtain $q_a = q_u$ from the average q_u (SF = 3 as in Example 4-4). Estimate $\gamma_{clay} \approx 18.00$ kN/m^3. So, we can include the $\bar{q}N_q$ term (and $N_q = 1.0$):

$$q_a = 200 \text{ kPa} + 1.2(18.00)(1) \approx 220 \text{ kPa} \qquad \text{(Use } \mathbf{200} \text{ kPa)}$$

Step 2. Find tentative base dimensions B using a square footing, or

$$P = 350 + 450 = 800 \text{ kN} \qquad \text{and} \qquad B^2 q_a = P$$

$$B = \sqrt{\frac{800}{200}} = 2.00 \text{ m}$$

Step 3. Check the immediate settlement. Consolidation settlement is not a problem since the water table is at the top of the sand at −12 m. Take

$$E_s = 1000 s_u \text{ since clay is stiff; } s_u = q_u/2 = 100 \text{ kPa}$$
$$E_s = 1000(100) = 100\,000 \text{ kPa}$$

For the sand we must convert N_{70} to N_{55} in order to use Table 5-5. Use a conservative value of $E_s = 500(N_{55} + 15)$:

$$\text{Above GWT: } E_s = 500[25(70/55) + 15] = 23\,409 \text{ kPa}$$
$$\text{Below GWT: } E_s = 500[30(70/55) + 15] = 26\,590 \text{ kPa}$$

The depth of influence is taken as $5B = 10$ m, which is 2 m above the 12-m depth of the boring. Also estimate Poisson's ratio $\mu = 0.35$ (for the clay).

Use a weighted average E_s for the influence depth below the footing base of 8.8 m, based on stratum thickness:

$$E_s = \frac{[6\text{–}1.2)100\,000 + (9\text{–}6)23\,409 + (10\text{–}9)26\,590]}{8.8} = \frac{576\,817}{8.8}$$
$$= \mathbf{65\,500} \text{ kPa (rounding down slightly)}$$

For $10/B' = 10/(2/2) = 10$, we obtain (using Table 5-2)

$$I_s = 0.498 + 0.016\frac{[1 - 2(0.35)]}{[1 - 0.35]} = \mathbf{0.505}$$

For $D/B = 1.2/2 = 0.6$ estimate the Fox embedment factor as

$$I_F = \mathbf{0.75} \text{ (using Fig. 5-7)}$$

Using Eq. (5-16*a*), we see that

$$\Delta H = q_o B' \frac{1 - \mu^2}{E_s} m I_s I_f \qquad \text{(and with } m = 4\text{)}$$
$$= \frac{800}{2^2}\frac{2}{2}\frac{1 - 0.35^2}{65\,000}4(0.505)(0.75)$$
$$= 0.004\,06 \text{ m} \rightarrow \mathbf{4.06} \text{ mm} \qquad \text{(clearly } \Delta H \text{ is not a problem.)}$$

We can now proceed with the footing design using

$$B \times B = 2 \times 2 \text{ m} \qquad \text{and} \qquad q_o = 800/4 = 200 \text{ kPa} < q_a$$

We have made no allowance for soil displaced by concrete, but recall that $q_a \approx 220$ kPa, which should be sufficient.

Step 4. First find the pseudo q_{ult}:

$$q_{ult} = \frac{1.4(350) + 1.7(450)}{2^2} = \frac{1255}{4} = \mathbf{313.8}\ \text{kPa}$$

$$\text{Ratio} = \frac{q_{ult}}{q_a} = \frac{313.8}{200} = 1.57$$

Step 5. Find the depth for two-way action shear using Eq. (8-6):

$$d^2\left(v_c + \frac{q}{4}\right) + d\left(v_c + \frac{q}{2}\right)w = (B^2 - w^2)\frac{q}{4}$$

Allowable concrete shear stress $v_c = \phi\sqrt{f_c'}/3 = 1.30$ MPa. Substituting values $q = 313.8$ kPa; $v_c = 1300$ kPa, and $w = 0.35$ m into Eq. (8-6), we obtain

$$1378.45d^2 + 509.9d = 304.2$$

$$d^2 + 0.37d - 0.2207 = 0$$

$$d = \frac{0.37 \pm \sqrt{0.37^2 - 4(1)(-0.2207)}}{2(1)} = \frac{-0.37 + 1.01}{2} = 0.32\ \text{m}$$

The approximate effective depth by Eq. (8-8) is

$$4d^2 + 2(w + w)d = \frac{BLq}{v_c}$$

Substituting values, we obtain

$$4d^2 + 4(0.35)d = 4(313.8)/1300$$

$$d^2 + 0.35d - 0.241 = 0$$

$$d = 0.346\ \text{m}\ (346\ \text{mm vs. } 320\ \text{mm by "exact" method})$$

For a square, centrally loaded footing it is never necessary to check wide-beam shear and since column $w \simeq d$ it is not necessary to check ACI Eq. (11-37).

Step 6. Find the required steel for bending. We will take d as 0.32 m to the intersection of the bottom of the top bars and the top of the bottom bars, for they will go both ways and will likely be wired together in the shop so that either side of the resulting grid can be the "top" (refer to Fig. 8-2*c*). Refer to Fig. 8-2*b* for the *moment arm* as defined by the ACI 318.

$$L_m = (B - w)/2 = (2.00 - 0.35)/2 = 0.825\ \text{m}$$

$$M_u = \frac{qL_m^2}{2} = \frac{(313.8)(0.825)^2}{2} = 106.8\ \text{kN} \cdot \text{m}$$

$$M_u = \phi A_s f_y\left(d - \frac{a}{2}\right) \qquad (8\text{-}2)$$

$$a = \frac{A_s f_y}{0.85 f_c' b} = \frac{A_s(400)}{0.85(21)(1)} = 22.4A_s$$

Rearranging Eq. (8-2) and substituting, we have

$$A_s\left(0.32 - \frac{22.4}{2}A_s\right) = \frac{106.8}{0.9 \times 400\,000}$$

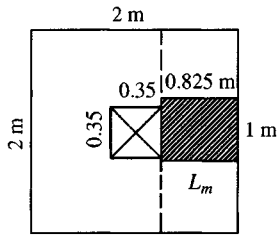

Figure E8-2*b*

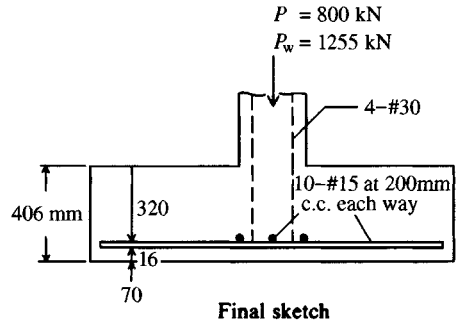

Figure E8-2*c* Final sketch.

Solving, we obtain

$$-11.2A_s^2 + 0.32A_s = 0.000297$$

$$A_s = \frac{0.0286 \pm \sqrt{0.0286^2 - 4(1)(0.0000265)}}{2(1)}$$

$$= 0.000\,96 \text{ m}^2/\text{m} \rightarrow \mathbf{960} \text{ mm}^2/\text{m} \qquad \text{[always use largest (+) value]}$$

Use five No. 15 bars/m to provide $5 \times 200 = 1000 \text{ mm}^2/\text{m}$ of steel at a spacing of $1000/4 = 250$ mm. We could use a lesser number of bars:

$$\text{four No. 20 giving } 4(300) = 1200 \text{ mm}^2/\text{m}$$

$$\text{two No. 25 giving } 2(500) = 1000 \text{ mm}^2/\text{m}$$

This latter value sets the spacing at 1000 mm which is is greater than 500 mm allowed by ACI.

$$A_{s,\text{total}} = 2 \text{ m} \times 1000 \text{ mm}^2/\text{m} = \mathbf{2000} \text{ mm}^2 \text{ (and each way)}$$

Use 10 No. 15 bars at spacing s: $9s + 2(70) + 16 = 2000$; $s = \mathbf{205}$ mm with $10 \times 200 = 2000 \text{ mm}^2$ steel area. Now check steel ratio:

$$p = \frac{1000}{(320)(1000)} = 0.003\,12 > 0.002 \text{ O.K.}$$

$$< 0.016 \text{ Table 8-1 also O.K.}$$

Step 7. Check if the furnished $L = 0.825 - 0.07$ m (clear cover requirement of Art. 7-7.1) $= 0.755 \text{ m} \leq L_d$ of Art. 12.2.2:

$$L_{db} = \frac{0.02A_b f_y}{\sqrt{f_c}} = 0.02(200)(400)/\sqrt{21}$$

$$= \mathbf{349} \text{ mm} > 300 \text{ (minimum length in any case)}$$

$$< 755 \text{ mm furnished}$$

There are no multipliers to increase this computed L_{db} so it will not be larger than the 0.755 m provided by the footing. Thus, the tension bar anchorage is adequate.

Step 8. Check column bearing on the footing per ACI Arts. 10.15 and 15.8. In general allowable bearing pressure is

$$f_c = \phi(0.85)(f_c')\Psi$$

where $\Psi = \sqrt{\frac{A_2}{A_1}} \leq 2$

A_1 = column contact area

A_2 = area of column spread through depth d using the distribution shown in Fig. 8-4*c*.

Inserting values, we compute the allowable bearing stress f_c as

$$f_c = 0.70(0.85)(21)(2) = 25 \text{ MPa}$$

Check the column capacity based on a gross concrete section. If that is adequate, a refined check is not required.

$$P_{comp} = 0.35^2(25 \times 1000) = 3062 \text{ kN}$$
$$P_u = 1.4(350) + 1.7(450) = 1255 \text{ kN} \ll 3062 \qquad \text{O.K.}$$

Step 9. Design dowels. ACI 318 requires a minimum area of dowels of $0.005A_{col}$ (Art. 15-8.2.1) unless a larger amount is needed to transfer compressive forces or moments. In this case the minimum controls:

$$A_{s,dowels} = 0.005(0.35^2) = 0.000\,6125 \text{ m}^2 = \mathbf{612.5} \text{ mm}^2$$

Set four column reinforcing bars with right-angle bends onto the footing reinforcing bars and wire them into position:

$$A_{s,furn} = 4(700) = 2800 \text{ mm}^2 \gg 612.5 \text{ required}$$

Use column reinforcing bar lengths so they either do not have to be spliced in the column zone or will extend above the top of the footing so that the splice length of Art. 12-14 can be satisfied.

Step 10. Make a design sketch as in Fig. E8-2*c*.

It will be necessary to provide at least a 70-mm clear cover from the bottom of the lower reinforcing bar (No. 15 of diam. = 16 mm) to the bottom of the footing. This gives a total depth of

$$D_c = 320 \text{ mm} + 16 \text{ mm} + 70 \text{ mm} = 406 \text{ mm} \rightarrow \mathbf{410} \text{ mm}$$

Note that the top layer of reinforcing bars requires slightly more than 960 mm^2 (actually, 1000 mm^2) and the lower layer requires slightly less than 960 mm^2. This methodology is standard practice, however, since it is seldom that one can obtain a bar schedule that exactly produces the computed (or required) A_s. It is not good practice to mix bar sizes to obtain exactly the required amount of steel area.

We did not check the actual and allowable soil pressures. First, we designed the base on the basis of using 200 kPa when we could have used about 220 kPa. This base is thin (at 406 mm), so soil-concrete displacement pressure is negligible (about 2.3 kPa).

////

It will be useful to compare any cost savings by using the *approximate* base depth equation [Eq. (8-8)] versus the *exact* equation. See the next example.

Example 8-3.

Given. The footing and foundation data of Example 8-2.

Required. Compute the required reinforcement and compare this to Example 8-2.

Solution. All data are exactly the same except d. The approximate value of d computed in Example 8-2 (see Step 5) is $d = 346$ mm → use 350 mm; similarly, $a = 22.4A_s^2$ and constant = 0.000 0297.

Step 1. Substitute values and obtain

$$-11.2A_s^2 + 0.35A_s = 0.000\,297$$

Dividing through by 11.2 and solving the resulting quadratic equation, we have [and again use largest (+) value]

$$A_s = \frac{0.03125 \pm \sqrt{0.031\,25^2 - 4(1)(0.000\,0265)}}{2(1)}$$

$$= (0.031\,25 - 0.0295)/2 = 0.000\,872 \text{ m}^2/\text{m} = \mathbf{872} \text{ mm}^2/\text{m}$$

For $B = 2$ m the required total is

$$A_s = 2(872) = 1744 \text{ mm}^2$$

Use six No. 20 bars giving 6(300) = **1800** mm^2 each way:

$$\text{Spacing} \approx 2000/5 = 400 \text{ mm} < 3(35) < 500 \text{ mm} \qquad \text{(Art. 7-6)}$$

$$\text{Diam. of No. 20 bar} = 19.5 \text{ mm} \rightarrow \text{use } 20 \text{ mm}$$

$$\text{Total depth } D_c = 350 + 20 + 70 = \mathbf{440} \text{ mm}$$

Step 2. Steel mass = 490 lb/ft^3 = 490(3.2808^3)(0.453) = 7840 kg/m^3
From Example 8-2,

$$L_s = 2000 - 2(70) = 1860 \text{ mm} \qquad \text{(clear cover = 70 mm)}$$

$$A_s = 2000 \text{ mm}^2 \text{ each way}$$

$$\text{Vol. of steel } V_s = 2(2000)(1860) = 7\,440\,000 \text{ mm}^3 = 0.007\,44 \text{ m}^3$$

$$\text{Mass of steel } M_1 = 7\,840(0.00744) = 58.3 \text{ kg/footing}$$

$$D_c \text{ of Example 8-2} = 410 \text{ mm}$$

$$\text{Vol. of concrete } V_c = 2 \times 2 \times 0.410 = 1.64 \text{ m}^3$$

For Example 8-3,

$$L_s = 1860 \text{ mm}$$

$$A_s = 1800 \text{ mm}^2 \text{ each way}$$

$$\text{Vol. of steel } V_s = 2(1800)(1860) = 6\,696\,000 \text{ mm}^3 = 0.0067 \text{ m}^3$$

$$\text{Mass of steel } M_2 = 7840(0.0067) = 52.5 \text{ kg/footing}$$

$$\text{Vol. of concrete } V_c = 2 \times 2 \times 0.44 = 1.76 \text{ m}^3$$

Summarizing,

Item	Exact	Approx	Difference
V_{concrete}, m^3	1.64	1.76	0.12
D_c mm	410.	440.	30.
Mass of steel, kg	58.3	52.6	5.8

The "approximate" depth footing is probably about $10 (US) more economical and certainly a small amount stiffer than the "exact" depth footing. Foundations of this type are usually bid on

the basis of volume (m^3) of in-place concrete (currently around \$200 to \$225 per m^3 in-place). There is much to recommend using Eq. (8-8) over the "exact" Eq. (8-7). This consideration will come up later in this chapter for footings with moment.

////

8-6 BEARING PLATES AND ANCHOR BOLTS

Metal column members, including various tower-type elements, require a base plate to spread the very high metal stresses in the small column/tower contact area at the footing interface to a value that the footing or pedestal concrete can safely carry. The bearing plate is cut to size in the steel fabricating shop from rolled plate stock and either shop-welded or field-bolted to the column member. Holes 2- to 5-mm larger in diameter than the anchor rods/bolts are shop-punched in the base plate for later attachment to the footing.

The anchor rods are usually set in nearly exact position in the wet concrete and become fixed in place. The slightly oversized holes allow a small amount of anchor rod misalignment when placing the base plate into position. The plate is then carefully aligned horizontally and to elevation, and nuts are added and tightened to attach the column firmly to the footing.

The AISC (1989) specification[5] provides general guidance in the design of base plates. There is little available design material for anchor bolts aside from that provided by the several manufacturers, which usually is limited to suggested embedment depth and allowable anchor rod force.

8-6.1 Base Plate Design

Base plates can be designed using the AISC specification for axial-loaded columns as follows:

When the base plate covers the concrete support (typically the base plate of a pedestal is the same size as a pedestal) the allowable bearing stress F_p is

$$F_p = 0.35 f'_c \qquad (a)$$

When the base plate covers less than the supporting concrete surface (typical for spread footings carrying steel columns fitted with a base plate), the allowable bearing stress F_p is

$$F_p \leq 0.35 f'_c \sqrt{\frac{A_2}{A_1}} \leq 0.7 f'_c \qquad (b)$$

where F_p = allowable concrete stress; must be greater than the actual bearing stress defined as $f_p = P/A_1$, where P = sum of column loads acting on footing

A_1 = area of base plate in consistent units

A_2 = area of supporting member; is area of pedestal when the base plate is on the pedestal; is area of footing for other cases

A limitation is that $\Psi = \sqrt{A_2/A_1} \leq 2$.

---

[5]Baseplate methodology has changed with the last three editions of the American Institute of Steel Construction (AISC) *A*llowable *S*tress *D*esign manual.

If we substitute for F_p in Eq. (*b*), note the limitation on $\sqrt{A_2/A_1}$ and square both sides, we obtain

$$\left(\frac{P}{0.35f_c'}\right)^2 \leq A_1^2\left(\frac{A_2}{A_1}\right) \leq 4A_1^2 \tag{c}$$

From the left two terms of Eq. (c) we obtain the base plate area as

$$A_1 = \frac{1}{A_2}\left(\frac{P}{0.35f_c'}\right)^2 \tag{8-10}$$

The minimum pedestal dimensions A_2 are obtained from the right two terms of Eq. (*c*) to give

$$A_2 = 4A_1$$

which can be written by making substitution in Eq. (8-10) for A_1 as

$$A_2 = \frac{P}{0.175f_c'} \tag{8-10a}$$

In this equation the area A_2 = both minimum and optimum size of the pedestal.

We may summarize the steps in designing a base plate by the AISC (1989) specifications as follows:

1. Find plate area A_1 as the larger of

$$A_1 = \frac{1}{A_2}\left(\frac{P}{0.35f_c'}\right)^2 \qquad \text{and} \qquad A_1 = \frac{P}{0.7f_c'}$$

   You may first have to find area A_2 using Eq. (8-10*a*) if a pedestal is being used.

2. Find the base plate dimensions (refer to Fig. 8-6 for identification of dimensions) $B \times C \geq A_1$ and use multiples of 5 mm (integers of inches for Fps) for dimensions B, C. Also try to make $m \approx n$ to minimize plate thickness t_p. For m, n use the following:

$$m = \frac{C - 0.95d}{2} \qquad n = \frac{B - 0.80b_f}{2}$$

3. Compute a dimension[6] n' as follows:
   a. Define $L = d + b_f$.
   b. Define $X = \frac{4P_o}{L^2F_b}$ with Bowles' approximations of $P = P_o$; $F_b = F_p$ (plate is heavily loaded if $X \gtrsim 0.64$).
   c. Define $\lambda = \min\left[1.0, \frac{2\sqrt{X}}{1+\sqrt{1-X}}\right]$. Note that $\lambda \leq 1$. If you have a negative square root, lambda is 1.
   d. Compute $n' = 0.25\sqrt{db_f}$.

[6]Here the author deviates from the AISC (1989) ninth edition manual and uses a modification proposed by one of the AISC committee members involved with the Manual [Thornton (1990)]. Except for using λ and n' the computations are exactly as in the AISC manual.

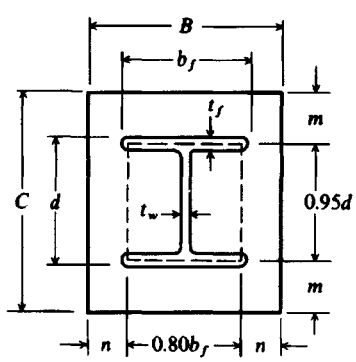

(a) Base plate symbols and term identification. d = column depth.

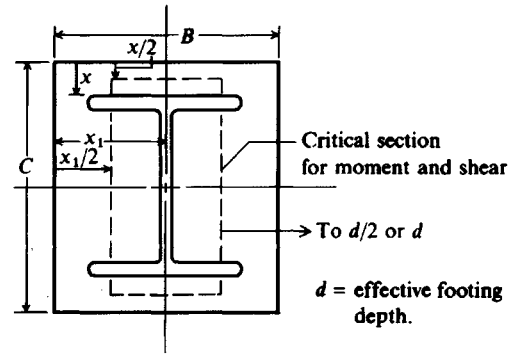

(b) Critical section for shear and moment. Note slight approximation x_1 to $t_w/2$ instead of to web face.

Figure 8-6 Base plate design according to the current AISC design specifications. Symbols are consistent with AISC (1989).

e. Extract the maximum $v = \max[m, n, (\lambda n')]$

f. Compute actual bearing stress $f_p = P/(B \times C)$.

4. Compute the base plate thickness t_p as

$$t_p = 2v\sqrt{\frac{f_p}{F_y}} \qquad \text{(units of } v\text{)} \tag{8-11}$$

Essentially the AISC specification requires sizing the base plate to satisfy the actual bearing pressure f_p. Next the plate thickness is computed based on an allowable bending stress of $0.75F_y$ (F_y = yield stress of base plate steel) using a cantilever moment arm of v and a unit width strip of 1-m or (1-inch) equivalent. After computing plate thickness t_p select a final thickness that is available or round up to the next available plate thickness.

When there is a column moment in addition to the axial load, you must use a form of computations as

$$f_p \leq \frac{P}{B \times C} + \frac{Mc}{I} \tag{8-12}$$

This problem is not addressed directly by AISC so you must use engineering judgment. When there is a column moment, the base plate must be adequately attached to both the column and the foundation. Few steel columns transmit moments to isolated spread footings, but moments into mat foundations are fairly common.

Refer to Example 8-1 and Fig. 8-6 for the shear and moment locations for columns with base plates. It is suggested that the approximate equation for shear depth [Eq. (8-8)] be used for a footing supporting a base plate because of the approximation for locating the critical section.

The previous discussion will be illustrated by a design example.

Example 8-4. Design a reinforced concrete footing with a steel W250 × 67 column (see Fig. E8-4) using the design data of Example 8-2.

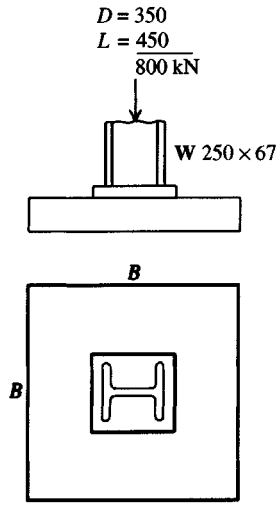

Figure E8-4

General data: $D = 350$ kN $\quad L = 450$ kN $\quad q_a \approx 220$ kPa (used 200)

$f_c' = 21$ MPa $\quad F_y = 250$ MPa (for column)

Rebar F_y = Grade 400 (400 MPa or 60 ksi)

From rolled section tables [AISC (1992)] obtain for a **W**250 × 67:

$d = 257$ mm (depth) $\quad b_f = 204$ mm (width)

$t_w = 8.9$ mm (web) $\quad t_f = 15.7$ mm (flange thickness)

Solution.

Step 1. Find footing area. Since loads and soil pressure are the same as in Example 8-2 we have $B = 2$ m.

Step 2. Since dimensions are same, use the depth $d = 350$ mm and the overall design of steel and $D_c = 440$ mm of Example 8-3.

Step 3. Thus, we need only to size the base plate.

a. Since the base plate is clearly smaller than the footing, it is evident that the ratio $\Psi = A_2/A_1 = 2$ and we have A_1 computed as

$$A_1 = \frac{P}{0.7f_c'} = \frac{800}{0.7 \times 21 \times 1000} = \mathbf{0.0544}\ \text{m}^2$$

The baseplate must fit the column footprint with about 12 mm overhang on all sides in case it is fillet-welded to the column. Thus, tentatively try the following:

$B = 204 + 25 = 230$ mm (rounded) and

$C = 257 + 25 = 285$ mm (rounded to 5 mm)

These values yield

$$A_1 = 0.230(0.285) = 0.0655\ \text{m}^2 > 0.0544 \qquad \text{O.K.}$$

Use $B = 230$ mm × $C = 285$ mm.

b. Find dimensions m and n:

$$m = \frac{285 - 0.95(257)}{2} = 20.4 \text{ mm}$$

$$n = \frac{230 - 0.80(204)}{2} = 33.4 \text{ mm}$$

To obtain $\lambda n'$ we must do some side computations:

$$F_p = 0.35 f_c' \Psi = 0.35(21)(2) = 14.7 \text{ MPa} = (= 0.7 f_c')$$

$$L = (d + b_f) = 257 + 204 = 461 \text{ mm} = 0.461 \text{ m}$$

$$X \approx \frac{4P}{L^2 F_p} = \frac{4(800)}{0.461^2 \times 14.7 \times 1000} = 1.024 \text{ m}$$

$$\lambda = \min\left(1.0, \frac{2\sqrt{X}}{1 + \sqrt{1 - X}}\right)$$

Since $X = 1.024 > 1$ we have a negative root so use

$$\boldsymbol{\lambda = 1.0}$$

$$n' = 0.25\sqrt{257 \times 204} = 57.24 \text{ mm} \rightarrow \lambda n' = 1(57.24) = 57.24 \text{ mm}$$

$$v = \max(20.4, 33.4, 57.24) = \mathbf{57.24} \text{ mm}$$

$$t_p = 2v\sqrt{f_p/F_y} = 2(57.24)\sqrt{\frac{12.7}{250}} = 25.8 \text{ mm}$$

Prior to the 8th ed. of the AISC manual, $t_p = 2(33.4)\sqrt{f_p/F_y} = 15.1$ mm. Use $t_p = 22$ mm ($\approx 1.5 \times 15.1$, or next larger available plate thickness).

c. Complete the design by selecting anchor bolts. Since there is no moment we can probably use two anchor bolts of minimum dimension.

////

8-6.2 Interfacing Base Plate to Footing

So far we have considered the idealized base plate. It still must be interfaced to the footing, the surface of which may be rough or at least rough enough that some base plate leveling is required. Base plate leveling can be accomplished in several ways. One way is to use shims (small, thin strips of tapered steel), which are driven between the plate and footing. Any space remaining is grouted (see Fig. 8-7). Grouting of base plates and machinery has received much attention; and ACI has a committee for this purpose, with the latest report being ACI 351 (1992).

It is not an easy task to grout this gap so that the base plate fully bears on grout—often there is uneven contact from grout shrinkage and trapped air. Holes may be drilled in the base plate to eliminate trapped air. Once grout exits the hole there is no underside cavity.

Another method to level base plates is to use thin metal plates on the order of 5–6 mm thick and slightly larger than the base plate with holes precut for the anchor bolts. These are stacked as required to bring the base to the correct elevation. Again it may be necessary to use a leveling course of grout beneath the first leveling plate for horizontal alignment.

In another method leveling nuts are used, requiring a minimum of four anchor bolts. Leveling is accomplished by putting a nut on each of the anchor bolts and installing the base plate. By adjusting the nuts vertically the base plate can be brought to level. The top nuts are then installed and tightened. The space between the base plate and footing is then grouted.

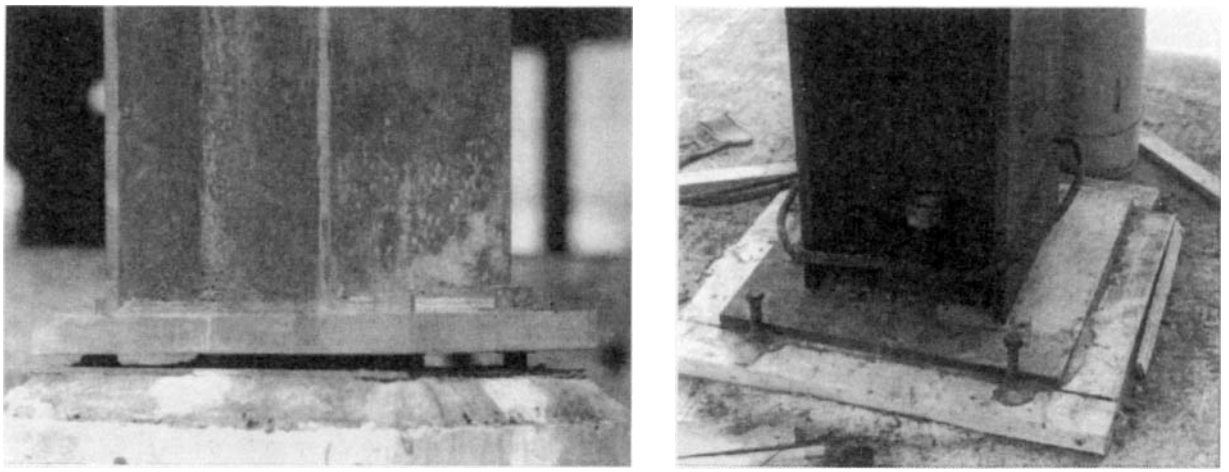

(*a*) (*b*)

Figure 8-7 (*a*) Grout space to be filled when frame alignment is complete. Note that an attempt has already been made to grout space but subsequent realignment has created a new grout gap. *(b)* Base plate grouted using an enclosure to hold grout in position. Some excess grout can be seen around vertical bolt in foreground and between wood containment and base plate.

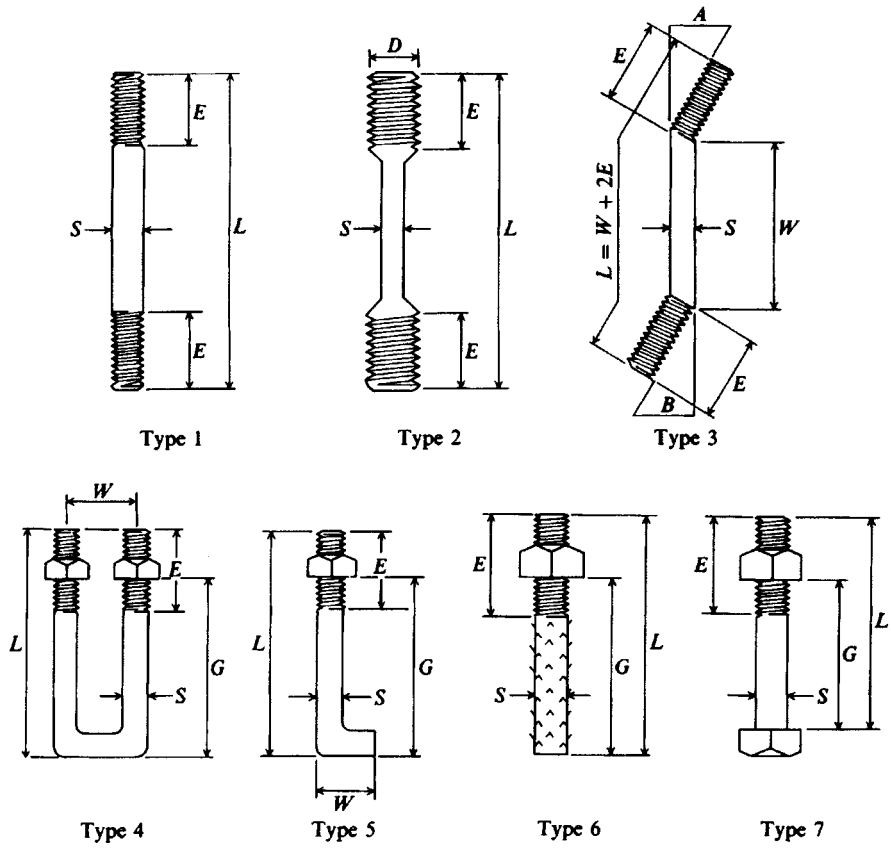

Figure 8-8 Anchor bolts. Types 1 and 2 screw either into a large nut and washer or into a threaded plate to develop pull-out resistance. Type 4 may have rebar threaded through the U to increase pull-out resistance. Type 7 may use a heavy washer or a plate bearing against the nut to increase pullout. Distances shown—*E*, *G*, *L*, *S*, and *W*—are to be specified by designer.

If the base plate is not fitted to the column in the shop the base plate may be grouted into alignment both laterally and vertically onto the footing. Then the column is fastened to the plate during steel erection.

8-6.3 Anchor Bolts

Anchor bolts are required to attach the base plate firmly to the footing or pedestal. Figure 8-8 displays several types of anchor bolts. A number of proprietary types (not shown) are available that work on similar principles but their advantages are mainly to provide additional vertical adjustments and thread protection during concrete placement. Most columns and tower-type structures as well as larger machinery use anchor bolts of the type shown in Fig. 8-8.

Anchor bolts are usually of A307 bolt material grade A (*A*-36 steel of $F_{ult} \approx 400$ MPa and $F_y = 250$ MPa) or grade $B(F_u \approx 690$ MPa). High-strength bolt material in A325 and A490 grades is usually not required since pullout/bond generally controls the design. Anchor bolts

TABLE 8-4
Ultimate tensile strength of selected A307 bolts in diameters most commonly used for base plate anchors.*

Bolt diameter and pitch, mm	Net tensile stress area, A_t, mm²	Tensile force† T_u, kN	
		Grade A	Grade B
16P2	157	63	108
20P2.5	245	98	169
24P3	353	141	244
30P3.5	561	224	387
36P4	817	327	564
42P4.5	1120	448	773
48P5	1470	588	1014
56P5.5	2030	812	1401
64P6	2680	1072	1849
72P6	3460	1384	2387
80P6	4340	1736	2995
90P6	5590	2236	3857
100P6	6990	2796	4823

*From American National Standards Institute (ANSI) SR 17 (it is also ASTM STP 587, dated 1975).

Notes: 16P2 is a nominal bolt diameter of 16 mm with a thread pitch $P = 2$ mm (see inset sketch).

$$A_t = 0.7854(\text{Diam.} - 0.9382P)^2$$

Grade A = 400 MPa (f_u); $f_y = 250$ MPa

Grade B = 690 MPa; $f_y \approx 400$ MPa

For 16P2:

$$A_t = 0.7854(16 - 0.9382 \times 2)^2 = \mathbf{157}\ \text{mm}^2$$

$$T_u = \frac{400}{1000} \times 157\ \text{mm} = 63\ \text{kN}$$

†For design divide the ultimate tensile force T_u to obtain $T_d = T_u/\text{SF}$. Use a SF of about 4.

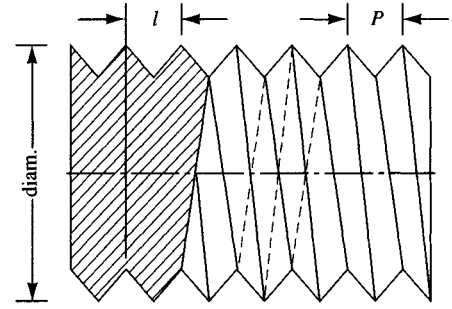

l = nut advance in one complete revolution.

P = thread pitch = distance between corresponding points on adjacent thread forms in mm (or in). A pitch of 2 means there are 2 mm between points, etc.

in A307 material are available from $\frac{1}{4}$- to 4-in. diameter.[7] Most structural applications will fall in the 25- to 100-mm bolt diameter range. Table 8-4 gives selected bolt properties for design use.

In practice the anchor bolt, with the nut(s) and washers attached to avoid loss and to protect the threads, is set in the wet concrete with a sufficient length of the threaded end above the concrete to adjust the baseplate elevation, provide a space to place a grout bed, and allow the nut to be fully effective. To do so, the distance must be large enough for the bolt to elongate while being tightened. Since stress always produces strain, if the anchor bolt were fixed at the top of the concrete and only had an elongation length of the base plate + nut, it might pull apart during the tightening operation.

What is usually done is to slip an oversized cardboard or metal sleeve over the anchor rod so the upper 75 to 90 mm of shaft is not bonded to the hardened concrete. During tightening

[7]When this textbook went to print ASTM had not converted the A307 bolt standard to SI. It will be necessary to soft convert values as necessary.

this length, plus the thickness of the base plate, allows elongation so that the plate can be securely fastened. The sleeve will also allow the smaller-diameter anchor bolts to be bent to fit the predrilled holes in the base plate if there is slight misalignment.

If a sleeve is used, it may or may not be filled with grout after the base plate is attached and the anchor nut tightened. There are major differences of opinion on this:

1. Some think the sleeve should not be grouted so that stress reversals will produce strain changes over a length of bolt rather than locally.
2. Some think that after the bolt is tightened to a proof load (about 70 percent of yield) no strains of any magnitude are developed unless the moment is large enough to separate the base plate from the grout bed.

In any case, if the sleeve is grouted, the distance to develop subsequent strains is limited to roughly the thickness of the base plate. The question is of little importance where no stress reversals occur because the sleeve is used only for alignment in this case and the nut is usually made only snug-tight (about one-fourth turn from tight).

Anchor studs are available that are screwed into expanding sleeves that have been placed in predrilled holes in the footing to a depth of 75 to 300 mm. The studs may expand the sleeve against the concrete, or the sleeve may be driven down over a steel wedge to produce expansion, after which the anchor is screwed in place. Anchor studs can only be tightened a limited amount since the elongation distance is the base plate thickness. They are primarily used for anchoring equipment into permanent position.

Base plate anchor bolts are designed for any tension and/or shear forces that develop when overturning moments are present. Both bolt diameter and depth of embedment require analysis, although the latter is not specifically indicated in most (including ACI) building codes. Where a column has no moment a pair of anchor bolts is used, with the size being somewhat arbitrarily selected by the designer. Some additional information on anchor bolts may be found in Ueda et al. (1991, with references).

8-7 PEDESTALS

A pedestal is used to carry the loads from metal columns through the floor and soil to the footing when the footing is at some depth in the ground. The purpose is to avoid possible corrosion of the metal from the soil. Careful backfill over the footing and around the pedestal will be necessary to avoid subsidence and floor cracks. If the pedestal is very long, a carefully compacted backfill will provide sufficient lateral support to control buckling. The ACI (Art. 7.3 and 318.1) limits the ratio of unsupported length L_u to least lateral dimension h as

$$\frac{L_u}{h} \leq 3$$

for pedestals. The problem is to identify the unsupported length L_u correctly when the member is embedded in the soil.

The code allows both reinforced and unreinforced pedestals. Generally the minimum percentage of steel for columns of $0.01A_{col}$ of Art. 10.9[8] should be used even when the pedestal

[8]The ACI Code specifies gross column area—that is, no area reduction for column reinforcing. The symbol often used is A_g, but this text uses A_{col}.

this length, plus the thickness of the base plate, allows elongation so that the plate can be securely fastened. The sleeve will also allow the smaller-diameter anchor bolts to be bent to fit the predrilled holes in the base plate if there is slight misalignment.

If a sleeve is used, it may or may not be filled with grout after the base plate is attached and the anchor nut tightened. There are major differences of opinion on this:

1. Some think the sleeve should not be grouted so that stress reversals will produce strain changes over a length of bolt rather than locally.
2. Some think that after the bolt is tightened to a proof load (about 70 percent of yield) no strains of any magnitude are developed unless the moment is large enough to separate the base plate from the grout bed.

In any case, if the sleeve is grouted, the distance to develop subsequent strains is limited to roughly the thickness of the base plate. The question is of little importance where no stress reversals occur because the sleeve is used only for alignment in this case and the nut is usually made only snug-tight (about one-fourth turn from tight).

Anchor studs are available that are screwed into expanding sleeves that have been placed in predrilled holes in the footing to a depth of 75 to 300 mm. The studs may expand the sleeve against the concrete, or the sleeve may be driven down over a steel wedge to produce expansion, after which the anchor is screwed in place. Anchor studs can only be tightened a limited amount since the elongation distance is the base plate thickness. They are primarily used for anchoring equipment into permanent position.

Base plate anchor bolts are designed for any tension and/or shear forces that develop when overturning moments are present. Both bolt diameter and depth of embedment require analysis, although the latter is not specifically indicated in most (including ACI) building codes. Where a column has no moment a pair of anchor bolts is used, with the size being somewhat arbitrarily selected by the designer. Some additional information on anchor bolts may be found in Ueda et al. (1991, with references).

8-7 PEDESTALS

A pedestal is used to carry the loads from metal columns through the floor and soil to the footing when the footing is at some depth in the ground. The purpose is to avoid possible corrosion of the metal from the soil. Careful backfill over the footing and around the pedestal will be necessary to avoid subsidence and floor cracks. If the pedestal is very long, a carefully compacted backfill will provide sufficient lateral support to control buckling. The ACI (Art. 7.3 and 318.1) limits the ratio of unsupported length L_u to least lateral dimension h as

$$\frac{L_u}{h} \leq 3$$

for pedestals. The problem is to identify the unsupported length L_u correctly when the member is embedded in the soil.

The code allows both reinforced and unreinforced pedestals. Generally the minimum percentage of steel for columns of $0.01A_{col}$ of Art. 10.9[8] should be used even when the pedestal

[8]The ACI Code specifies gross column area—that is, no area reduction for column reinforcing. The symbol often used is A_g, but this text uses A_{col}.

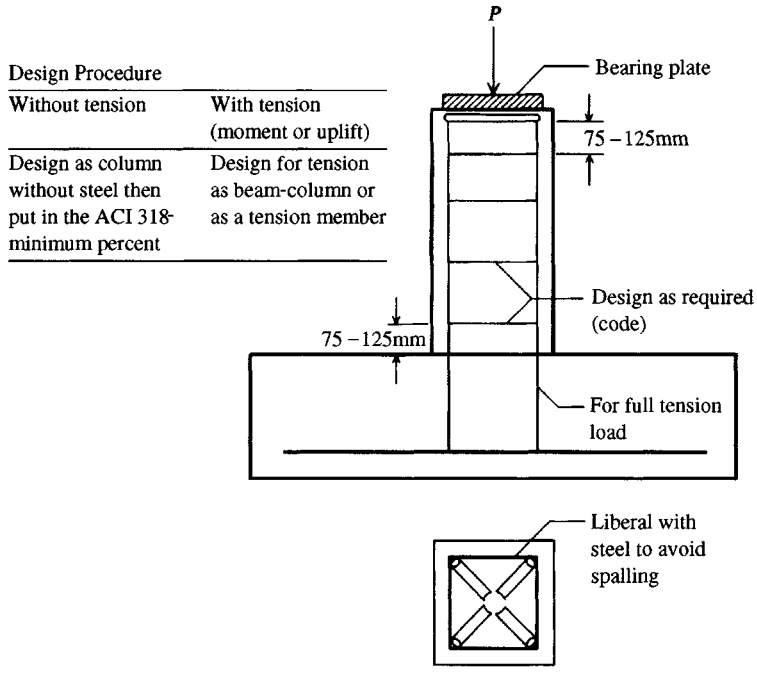

Design Procedure	
Without tension	With tension (moment or uplift)
Design as column without steel then put in the ACI 318-minimum percent	Design for tension as beam-column or as a tension member

Figure 8-9 Pedestal details (approximate). Note that vertical steel should always be designed to carry any tension stresses from moment or uplift

is not designed as a reinforced column-type element. Rather, when the pedestal is designed as an unreinforced member, the minimum column percent steel (4 to 8 bars) is arbitrarily added. When steel base plates are used, this reinforcement should terminate about 70 to 90 mm from the pedestal top in order to minimize point loading on the base plate.

Steel should be liberally added at the top, as in Fig. 8-9, to avoid spalls and to keep the edges from cracking. Room must be left, however, to place the anchor bolts necessary to hold the bearing plate and column in correct position. The anchor bolts should be inside the spiral or tie reinforcement to increase the pullout resistance.

Pedestals are usually considerably overdesigned, since the increase in materials is more than offset by reduced design time and the benefit of the accrued safety factor.

Pedestals can usually be designed as short columns because of the lateral support of the surrounding soil. They may be designed for both axial load and moment, but this feature is beyond the scope of this text. For the rather common condition of the pedestal being designed as a *simply supported* column element interfacing the superstructure to the footing, the following formula may be used:

$$P_u = \phi(0.85 f'_c A_c + A_s f_y) \tag{8-13}$$

where P_u = factored ultimate column design load, kN or kips

A_c = net area of concrete in pedestal ($A_g - A_s$) for unreinforced pedestals $A_s = 0.0$ and A_c = total concrete area

A_s = area of reinforcing steel if designed as a reinforced column

f_y = yield strength of rebar steel

ϕ = 0.70 for tied and 0.75 for spiral reinforcement; 0.65 for nonreinforced pedestals

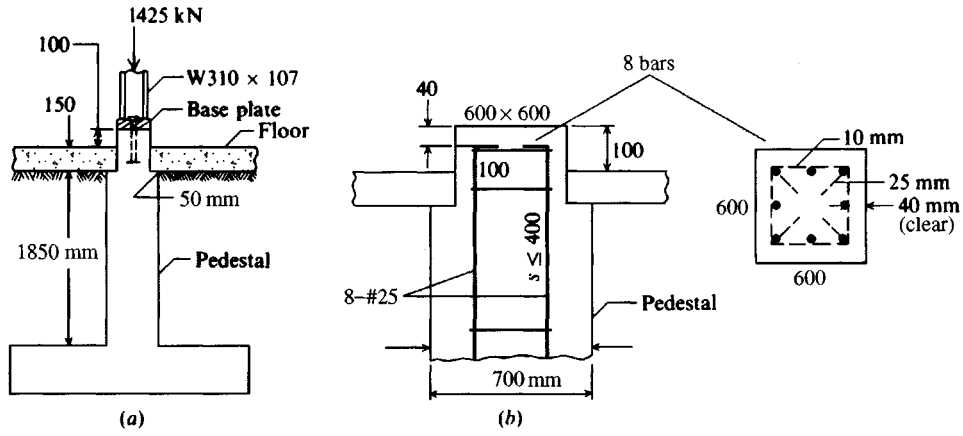

Figure E8-5*a, b*

Example 8-5. Design a pedestal and bearing plate for the following conditions:

$$D = 800 \text{ kN} \qquad L = 625 \text{ kN} \qquad P = \mathbf{1425} \text{ kN}$$

$$\text{W } 310 \times 107 \text{ column} \qquad d = 311 \text{ mm} \qquad b_f = 306 \text{ mm}$$

$F_y = 250$ MPa (A36 steel) for both column and bearing plate

Concrete: $f'_c = 24$ MPa; $\qquad f_y = 400$ MPa (Grade = 400)

Soil: $q_a = 200$ kPa

Solution.

Step 1. We will set dimensions of the pedestal for the base plate but increase (shoulder it out) 50 mm to allow bearing for the floor slab as illustrated in Fig. E8-5*a*. First, find areas A_1 and A_2:

$$A_2 = \frac{P}{0.175 f'_c} = \frac{1425}{0.175 \times 24 \times 1000} = 0.3393 \text{ m}^2 \text{ (1000 converts } f'_c \text{ to kPa)}$$

Next,

$$A_1 = \frac{1}{A^2}\left(\frac{P}{0.35 f'_c}\right)^2 = \frac{1}{0.3393}\left(\frac{1425}{8400}\right)^2 = 0.0848 \text{ m}^2$$

or

$$A_1 = \frac{P}{0.7 f'_c} = \frac{1425}{16\,800} = 0.0848 \text{ m}^2$$

Use a plate area $A_1 \geq 0.0848$ m^2.
Use a pedestal with $A_2 \geq 0.3393$ m^2. For the pedestal try

$$B^2 = 0.3393 \rightarrow B = \sqrt{0.3393} = 0.582 \text{ m}$$

Let us use $B = \mathbf{0.600}$ m;

$$A_2 = 0.60 \times 0.60 = 0.36 \text{ m}^2 > 0.3393 \text{ m}^2 \qquad \text{O.K.}$$

Looking at the column dimensions, let us try a plate of

$$C = d + 25 = 311 + 25 = 336 \rightarrow \mathbf{335} \text{ mm}$$
$$B = b_f + 25 = 306 + 25 = 331 \rightarrow \mathbf{330} \text{ mm}$$

Check the furnished area, that is,

$$A_1 = 0.335 \times 0.330 = \mathbf{0.1106} \text{ m}^2 > 0.0848 \text{ m}^2 \qquad \text{O.K.}$$

The *allowable* concrete bearing stress (base plate area $A_1 < A_2$) is

$$F_p = 0.35 f'_c \sqrt{\frac{A_2}{A_1}} = 0.35(24)\sqrt{\frac{0.360}{0.111}} = 15.13 \text{ MPa} < 0.7 f'_c$$

Let us check:

$$A_1 F_p = 0.111(15.13)(1{,}000) = 1679 > 1425 \text{ kN} \qquad \text{O.K.}$$

Step 2. Find the plate thickness t_p:

$$m = \frac{335 - 0.95d}{2} = \frac{335 - 0.95(311)}{2} = \mathbf{19.8} \text{ mm}$$

$$n = \frac{330 - 0.80 b_f}{2} = \frac{330 - 0.80(306)}{2} = \mathbf{42.6} \text{ mm}$$

$$L = d + b_f = 311 + 306 = 617 \text{ mm} = 0.617 \text{ m}$$

$$X = \frac{4P}{L^2 F_p} = \frac{4(1425)}{0.617^2(15.13 \times 1{,}000)} = 0.9896 \rightarrow \mathbf{0.99}$$

$$\lambda = \min\left(1.0, \frac{2\sqrt{X}}{1 + \sqrt{1 - X}}\right) = \min\left(1.0, \frac{2\sqrt{0.99}}{1 + \sqrt{1 - 0.99}}\right) = \min(1.0, 1.81)$$

$$\lambda = 1.0$$

$$\lambda n' = 1.0(0.25)\sqrt{d_b b_f} = 1.0(0.25)\sqrt{311 \times 306} = \mathbf{77.1} \text{ mm}$$

$$v = \max(m, n, \lambda n') = \max(19.8, 42.6, 77.1) = 77.1 \text{ mm}$$

$$f_p = 1425/A_1 = 1425/0.1106 = 12\,884 \text{ kPa} = \mathbf{12.88} \text{ MPa}$$

The plate thickness is

$$t_p = 2v\sqrt{\frac{f_p}{F_y}} = 2(77.1)\sqrt{\frac{12.88}{250}} = \mathbf{35.0} \text{ mm}$$

Use a base plate of 335 × 330 × 35 mm.

Step 3. Design pedestal reinforcement.

Top area = 600 × 600 mm = 360 000 mm^2

Use minimum of $0.01A_{col} \rightarrow A_s = 0.01(360\,000) = 3600 \text{ mm}^2$

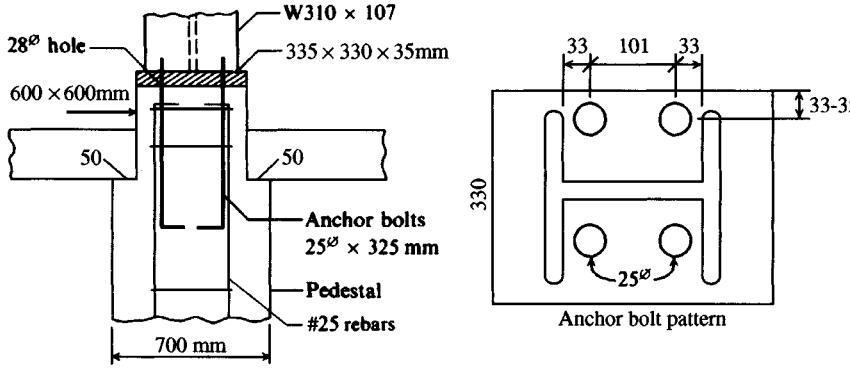

Figure E8-5*c*

Choose eight No. 25 bars, providing 8(500) = 4000 mm^2, which is greater than 3600 m^2 and therefore is acceptable. Place bars in pattern shown in Fig. E8-5*b*.

Step 4. Design anchor rods/bolts. Theoretically no anchorage is required, however, we will arbitrarily use enough to carry $0.1 \times P$ in shear:

$$P_v = 0.1(1425) = 142.5 \text{ kN}$$

Use standard size bolt holes, and from Table 1D of AISC (1989), obtain $F_v = 70$ MPa (10 ksi) for A307 grade steel.

Using 25-mm diameter bolts, we have.

$$P_{\text{bolt}} = 0.7854(0.025^2)(70)(1000) = 34 \text{ kN/bolt}$$

No. of bolts required = 142.5/34 = 4.15 bolts → use **4** bolts

Place anchor bolts in the pattern shown on Fig. E8-5*c*. Use anchor bolt steel of A-307 grade (or better).

////

8-8 BASE PLATE DESIGN WITH OVERTURNING MOMENTS

It is sometimes necessary to design a base plate for a column carrying moment as well as axial force. The AISC and other sources are of little guidance for this type of design. Only a few pre-1970s steel design textbooks addressed the problem. The Gaylord and Gaylord (1972) textbook provided a design alternative using a rectangular pressure distribution as used in this section. Most designs were of the (P/A) ± (Mc/I) type but were generally left to the judgment of the structural engineer. The author will present two methods for guidance.

METHOD 1. For **small** eccentricity where eccentricity $e_x = M/P$, with small e_x arbitrarily defined as less than $C/2$ and C is the base plate length (dimensions B, C) as shown in Fig. 8-10. In this case we make the following definitions:

$$\begin{aligned} C' &= C - 2e_x \\ A_p &= \text{effective plate area} = B \times C' \\ A_{\text{ftg}} &= \text{area of supporting member (footing or pedestal)} \\ P_{\text{col}} &= \text{column axial load} \\ M &= \text{column moment} \\ e_x &= M/P_{\text{col}} = \text{eccentricity} \end{aligned}$$

From these we may compute the following:

$$\text{FAC} = 0.35\sqrt{\frac{A_{\text{ftg}}}{A_p}} \le 0.7$$

$$F_p = \frac{(0.35 + \text{FAC})}{2} \cdot f_c'$$

This F_p is the average allowable bearing pressure to be used for design purposes. By trial, find the footing (or pedestal) dimensions to obtain the footing area A_{ftg}. By trial find the base plate dimensions so that the effective plate area

$$B \times C' \times F_p \ge P_{\text{col}}$$

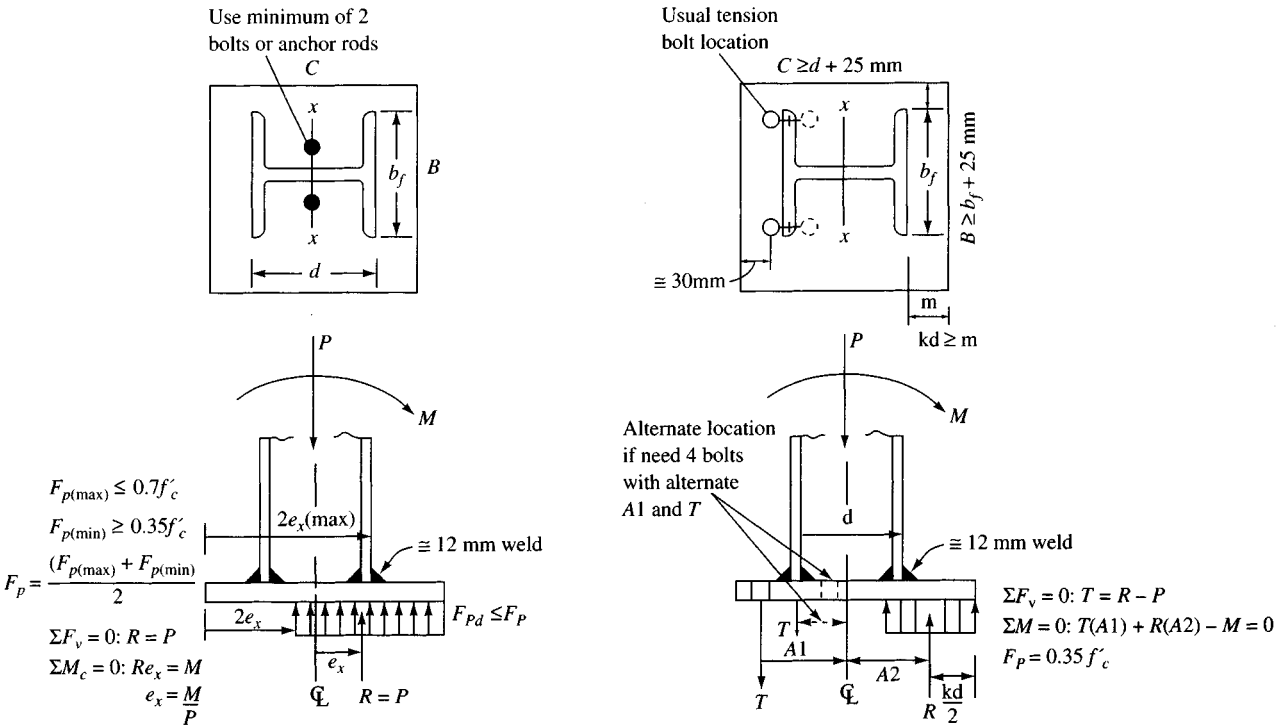

(*a*) Assumptions for column base plate with small eccentricity. F_p depends on area of supporting member (pedestal or footing).

(*b*) Assumptions for large eccentricity.

Figure 8-10 Base plates with eccentricity due to column moment. Bolt pattern is usually symmetrical about column center line when base plate moments are from wind or earthquake.

The assumption of a constant F_p across the effective plate area is made. If you obtain a set of dimensions of $B \times C'$, you can compute the actual contact stress $F_{pa} \leq F_p$. Usually one makes this calculation since a trial case of $B \times C' \times F_p = P_{col}$ is next to impossible. When you have a case of $F_{pa} = P_{col}/(B \times C') \leq F_p$, you have a solution. You may not have the "best" solution, and you might try several other combinations to obtain the minimum plate mass. Clearly a limitation is that the plate must be larger than the column footprint by about 25 mm (1 inch) in both dimensions to allow room for fillet-welding of the column to the base plate in the fabricating shop.

When you have found a $B \times C \times F_{pa}$ combination that works, the $\sum M = 0$ condition for statics is automatically satisfied. The center of the distance C' is always e_x from the column center (or x axis).

Computation of base plate thickness requires using the distances m and n as in Example 8-5 *except* that L is not computed because it has no significance here.

A computer program (the author uses STDBASPL—one suggested on your diskette) is most useful, as it finds several combinations of $B \times C$ that work, computes the resulting mass, and outputs sufficient data for performing any necessary statics checks. The program outputs the largest thickness computed. This distance is not checked against available rolled plate thicknesses since the steel fabricator may have thicker plate stock on hand and it may be more economical to substitute than to order a small quantity for the specific project.

Example 8-6.

Given. A **W** 360 × 162 (**W** 14 × 109) column carries a 500 kN axial load and has a moment of 100 kN·m. The footing dimensions are 1.5 × 2 m. Refer to Fig. E8-6*a*.

Column dimensions (from AISC, 1992): $d = 364$ mm (rounded to 365 mm)

$b_f = 371$ mm (rounded to 375 mm)

Concrete $f'_c = 24$ MPa

$F_y = 250$ MPa (base plate)

Required. Find a minimum weight (or mass) base plate.

I used computer output (but you can make several trials and get the same results) to find

$$e_x = \frac{M}{P_{col}} = \frac{100}{500} = \mathbf{0.200}\ \text{m}$$

Try a plate $B = 450$ mm × C = 500 mm.

$$C' = 500/1000 - 2(0.2) = 0.100\ \text{m}$$

$$B \times C' = 0.450 \times 0.10 = 0.045\ \text{m}^2$$

$$\text{FAC} = 0.35\sqrt{\frac{1.5 \times 2}{0.045}} = 2.86 > 0.7 \text{ use } 0.7$$

$$F_p = \frac{(0.35 + 0.7)}{2} \cdot 24 = \mathbf{12.6}\ \text{MPa}$$

$$\text{Actual } F\text{pa} = \frac{P_{col}}{A_p} = \frac{500}{(1000 \times 0.045)} = \mathbf{11.111}\ \text{MPa}$$

The factor 1000 converted 500 kN to 0.50 MN.

The "actual" column dimensions are used to compute plate thickness based on m and n. Thus,

$$m = (500 - 0.95 \times 364)/2 = 77.1\ \text{mm}$$

$$n = (450 - 0.80 \times 371)/2 = 76.6\ \text{mm}$$

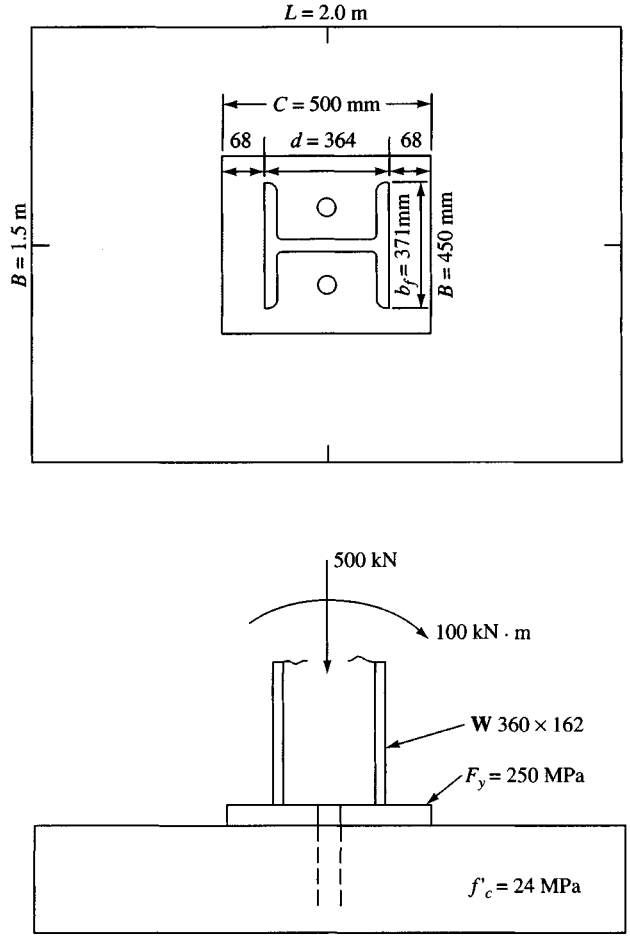

Figure E8-6*a*

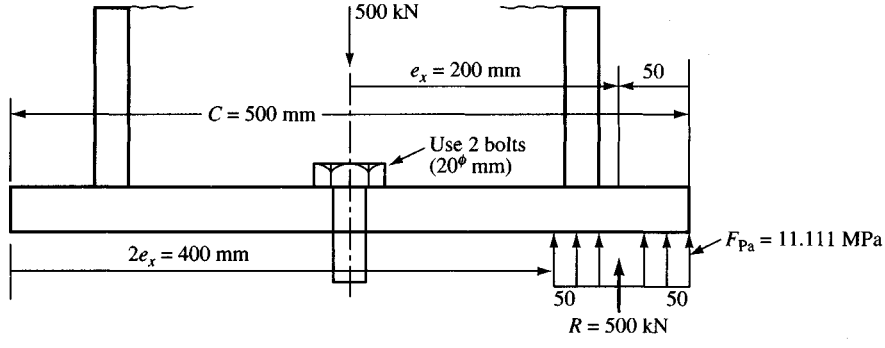

Figure E8-6*b*

Using the larger value, we obtain the plate thickness as

$$t_p = 2m\sqrt{\frac{F_{pa}}{F_y}} = 2(77.1)\sqrt{\frac{11.11}{250}} = \mathbf{32.51}\text{ mm}$$

The plate weight/mass (steel mass = 7850 kg/m^3 or 490 lb/ft^3) is W = $0.500 \times 0.450 \times 0.0325 \times 7850 = 57.42$ kg

Summarizing, we have

Base plate: **500 × 450 × 32.5** mm
and W = **57.42** kg

The reader should verify that $\sum F_v = 0$ and that about the column centerline $\sum M_{cl} = 0$.

Theoretically no base plate anchorage bolts are required, however, at least two 20-mm diameter A307 grade bolts would be used in the web zone of the plate as shown in Fig. E8-6*b*.

////

METHOD 2. Base plate design for **large** eccentricity. When the eccentricity is such that it falls outside one-half the depth of the column, it is necessary to resort to a different type of solution, one that uses heel bolts in tension. The heel bolts may fall behind the heel flange or be centered on both sides of it. The bolt pattern depends on the bolt force required for equilibrium and the designer's prerogative. By making the bolt option part of a computer program interactive either case can be analyzed. The general procedure is as follows (refer to Fig. 8-11):

$$\sum F_v = T + P - R = 0 \qquad T = R - P \tag{a}$$

$$\sum M_{cl} = 0 = T \times X_T + R \times X_R - M \tag{b}$$

Noting that $R = B(F_p)kd$ and substituting Eq. (*a*) for T, we obtain a quadratic equation of the form $(a)kd^2 + (b)kd + c = 0$ from which we can solve for the depth of the rectangular stress block kd. This approach is illustrated by the next example.

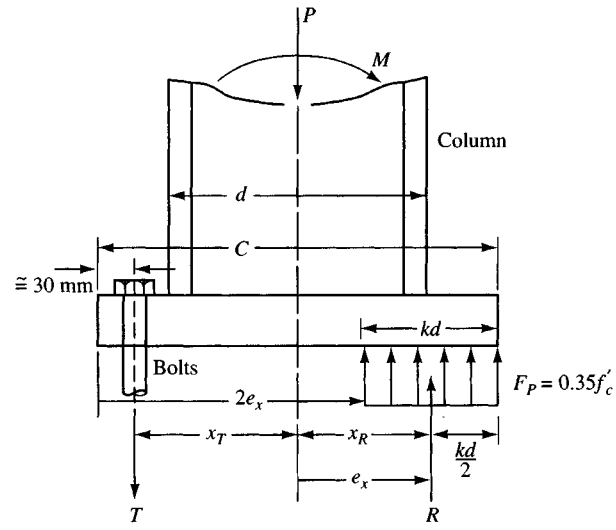

Figure 8-11 Base plate with a large overturning moment and small axial load P. The resulting $e_x = M/P$ is such that $2e_x > d/2$.

There are two additional considerations for large eccentricity. First, the allowable bearing stress $F_p = 0.35f'_c$. This result must occur as part of the solution of the quadratic equation. Second, it is always necessary to check to see whether the bolt tension force T in these equations controls the design of the base plate thickness.

Example 8-7.

Given.

Column load $P = 90$ kN $\quad M = 175$ kN · m

Column : W 360 × 134 $\quad d = 356$ mm $\quad b_f = 369$ mm

$f'_c = 21$ MPa $\quad F_y = 250$ MPa (refer to Fig. E8-7*a*)

Pedestal dimensions: $L = 700$ mm $\quad B = 610$ mm

Initial trial base plate: $B = 610$ mm $\quad C = 700$ mm

Computed eccentricity $e_x = M/P = 175/90 = 1.944$ m $\gg 0.356/2$

The computer program (and hand calculations as well) requires that you "guess" at a set of initial dimensions. If the resulting computed kd is outside the compression flange, that solution is not a

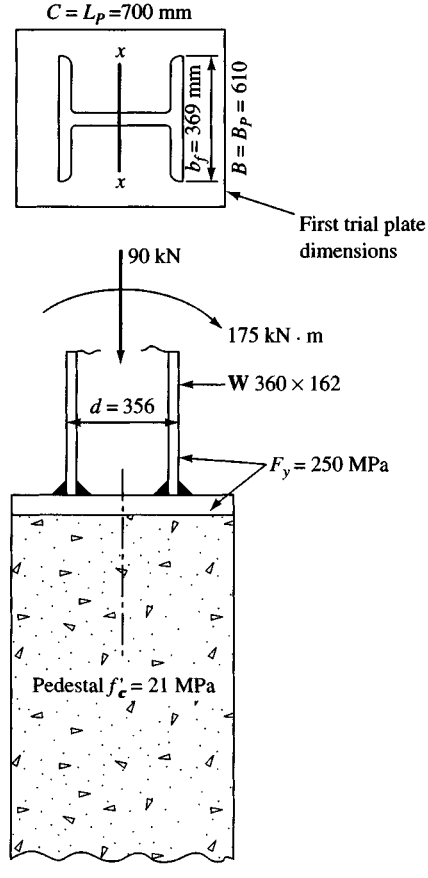

Figure E8-7*a*

good one, so the trial base plate is reduced and a new trial is initiated. This process continues until a solution is obtained where the kd zone is at least partly under the compression flange. The minimum width is, of course, at least the width of the column + 25 mm (1 in.) rounded to an even multiple of 5 mm (or inches in integers).

Required. Design a column base plate for the given conditions. Refer to Fig. E8-7*a*.

Solution. Computer program STDBASPL was again used. A solution can be obtained using

$$C = 550 \text{ mm} \quad \text{and} \quad B = 450 \text{ mm}$$
$$\text{Take } F_p = 0.35 f_c' = 0.35(21) = \mathbf{7.35} \text{ MPa}$$
$$\text{Convert } B, C \text{ to meters} \rightarrow C = 0.550 \text{ m} \quad B = 0.450 \text{ m}$$
$$\text{Define } A1 = T\text{-arm} = C/2 - 0.030 = 0.550/2 - 0.030 = 0.245 \text{ m}$$

The 0.030 provides adequate edge clearance for bolts up to 25 mm in diameter (AISC, 1989) to resist the computed T force. In this example as many as four bolts can be put into the 0.450-m width depending on bolt diameter. Alternatively, of course, we can redefine $A1 = d/2$ and use four bolts (two on each side of the heel flange), producing the following:

$$R = B(F_p)kd = 0.45(7.35)kd = 3.3075kd$$
$$\text{Arm } A2 = C/2 - kd/2 = 0.55/2 - kd/2 = 0.275 - kd/2$$
$$\sum F_v = 0 \quad \text{gives} \quad T = R - 90/1000 = 0$$
$$T = 3.3075kd - 0.09 \text{ (MN)}$$
$$\sum M_{c1} = 0 = T \times A1 + R \times A2 - M = 0 \text{ (units of MN} \cdot \text{m)}$$

Substituting,

$$(3.3075kd - 0.09)(0.245) + (3.3075kd)(0.275 - kd/2) - 0.175 = 0$$

Collecting terms, we obtain

$$-1.654kd^2 + 1.720kd - 0.197 = 0$$

Solving for kd, we find

$$kd = 0.131 \text{ m}$$

Checking, we see that

$$R = 3.3075(0.131) \times 1000 = \mathbf{433.3} \text{ kN}$$
$$\sum F_v = 0\text{: } P_{col} + T - R = 0$$
$$T = 433.3 - 90 = 343.3 \text{ kN}$$
$$\sum M_{c1} = 0\text{: } T \times A1 + R \times A2 - 175 = ?$$
$$343.3(0.245) + 433.3[0.275 - .1311/2] - 175 = ?$$
$$84.1 + 90.8 - 175 = 174.9 - 175 \approx 0 \quad \text{O.K.}$$

Find the required number of bolts and plate thickness for bending produced by bolt tension. In the AISC (1989) text, Table J3.5 indicates we can use bolts of either 22- or 25-mm diameter. We would simply increase the plate length if larger bolts are needed. From Table 8-5 we see that a 20P2.5 Grade B bolt can carry 169 kN for a total of $2 \times 169 = 338 < 343.3$ kN (but O.K.). If Grade B bolts are not available, use alternatives of either A572 or A588 bolt material.

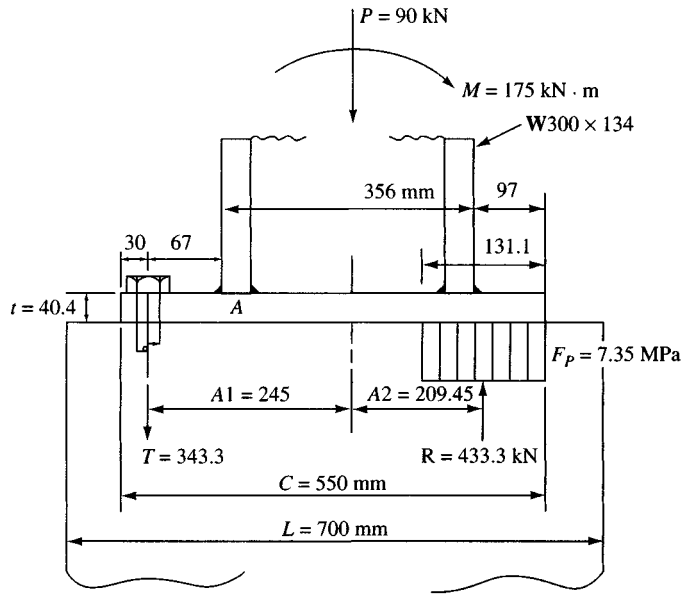

Figure E8-7*b*

No. of bolts required: $T/T_b = 343.3/290 = 1.2 \rightarrow$ use **2** bolts

Maximum bolt spacing of $12d = 12 \times 25 = 300$ mm does not control

Next find the base plate thickness.

$$m = [550 - 0.95(356)]/2 = \mathbf{105.9}\text{ mm} \leftarrow \textbf{controls}$$

$$n = [450 - 0.80(369)]/2 = 77.4\text{ mm} < 105.9$$

$$t_p = 2m\sqrt{\frac{F_p}{F_y}} = 2(105.9)\sqrt{\frac{7.35}{250}} = 36.3\text{ mm}$$

For bending (point A of Fig. E8-7*b*) caused by bolt force, we calculate

$$T = 343.3\text{ kN}$$

$$\text{Arm} = 97 - 30 = 67\text{ mm} = 0.067\text{ m}$$

$$M = 0.067(343.3)/1000 = 0.023\text{ MN} \cdot \text{m (since } F_b \text{ is in MPa)}$$

$$F_b\mathbf{S} = M \rightarrow F_b = 0.75F_y = 0.75(250) = 187.5\text{ MPa}$$

$$\mathbf{S} = Bt_p^2/6 = 0.45t_p^2/6$$

$$t_p^2 = \frac{6M}{0.45 \times 187.5}$$

$$t_p = \sqrt{\frac{6 \times 0.023}{0.45 \times 187.5}} = 0.0404\text{ m} \rightarrow \mathbf{40.4}\text{ mm} \rightarrow \textbf{controls (greater than 36.3)}$$

Provide the following base plate:

$B = \mathbf{450}$ mm $\quad C = \mathbf{550}$ mm $\quad t_p \geq \mathbf{40.4}$ mm

Use two 20P2.5 A-307 Grade B bolts (see Table 8-4) if available

Plate mass $\approx (0.45)(0.55)(0.0404)(7850) = \mathbf{78.5}$ kg

Comments.

a. The plate mass is calculated for purposes of comparison since the thickness t_p must be a value produced by the steel mills (will probably be 45 mm).

b. This solution is adequate if bolts of required length (or end anchorage) can be obtained.

c. The 30-mm edge distance is the minimum required depending on how the plate is cut.

d. It may be possible to reduce the pedestal area beneath the base plate to the plate dimensions unless other factors govern.

////

It should be evident that two design firms can come up with different size base plates (unless they are both using the same computer program) that would be considered acceptable. It should also be evident that these designs are a mixture of "ultimate" and "working stress" designs. It is still a common practice to use $P/A \pm Mc/I$, giving a triangular pressure diagram for this design. One should be aware, however, that the plate toe will always bend and redistribute the compression stresses so that the rectangular compressive pressure block is more realistic.

In most cases the overturning moment is attributable to wind, so that even though the preceding base plate designs considered a moment clockwise about the axis of rotation, the base plate will be symmetrically attached. That is, the same number of heel bolts are placed in the toe region. Also, be aware that with moment the bolts must either have locking washers or be tightened to sufficient tension not to work loose during wind (and stress) reversals. The bolt tension produces additional compression stress in the base plate, so that the sum of the stress from overturning and from bolt tightening may be a rather high value on the order of 0.7 to $0.8f_c'$. In this case the user should check stresses. It may be necessary to redesign the base plate using $0.3f_c'$ instead of $0.35f_c'$. With a computer program it is only necessary to edit one line to change from 0.35 to $0.30f_c'$. Alternatively, one can simply increase the plate dimensions—say, 30 mm for the toe, 30 mm for the heel, and 50 mm for the sides (25 mm on each side).

Finally, note that the AISC design manual does not consider *prying action* for base plates, however, it does for tee hangers and connections. You probably should consider prying action as well for the base plate with large moment. The equation for this purpose is

$$t_{bp} \geq \sqrt{\frac{8T_b b'}{pF_y}}$$

where T_b = bolt force, kN (or MN) or kips
b' = $\frac{1}{2}$ the distance from column flange to bolt line, m or in.
p = tributary width of base plate per bolt, m or in.
F_y = yield strength of base plate, kPa (MPa if T_b in MN) or ksi

If the base plate thickness t from previous computations is less than the t_{bp} just computed, the thickness probably should be increased to t_{bp}.

8-9 RECTANGULAR FOOTINGS

Rectangular footings are necessary where square footings cannot be used because of space limitations. They may be used where an overturning moment is present to produce a more

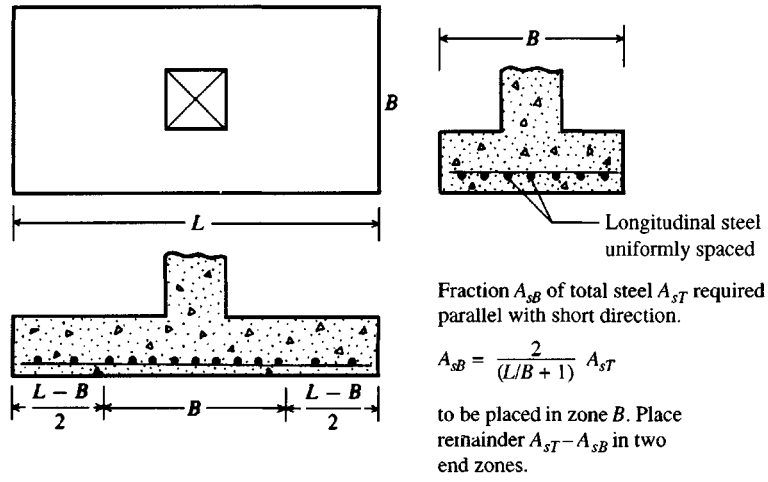

Figure 8-12 Placement of steel in short direction of a rectangular footing based on ACI Code Art. 15.4.4.

economical footing. The design is quite similar to that for a square footing. The depth will be controlled by shear, except that wide-beam action will probably control if the L/B ratio is much greater than 1 or where an overturning moment is present.

One other special consideration for rectangular footings is in the placement of the reinforcement. The reinforcement in the long direction is computed in the same manner as for a square footing, using d to the center of gravity (c.g.) of that steel. Steel in the short direction is computed similarly using the d to the c.g. of the steel, which is usually placed on top of the longitudinal steel for some savings in mass and placing. Additionally, since the footing zone in the column area is more effective in resisting bending, a specified percentage of the total short-side steel is placed in this zone as shown on Fig. 8-12.

Example 8-8. Design a rectangular reinforced concrete footing for the following design data:

Loads:	D = 1110 kN	L = 1022 kN (P_u = 3291.4 kN computed)
Column:	f'_c = 35 MPa	Square w/side = 450 mm
Column steel:	eight No. 25 bars	f_y = 400 MPa
Footing:	f'_c = 21 MPa	q_a = 240 kPa f_y = 400 MPa
	B = 2.20 m (given)	

Solution.

Step 1. Find footing dimension L. Note that if B is not given, then a number of combinations are possible:

$$BLq_a = P = 1110 + 1022$$

$$L = \frac{2132}{2.20 \times 240} = 4.04 \text{ m} \qquad \text{Use } L = \mathbf{4.1} \text{ m}$$

The "ultimate" soil pressure is

$$q_{ult} = \frac{P_u}{BL} = \frac{3291.4}{2.20 \times 4.10} = \mathbf{365} \text{ kPa}$$

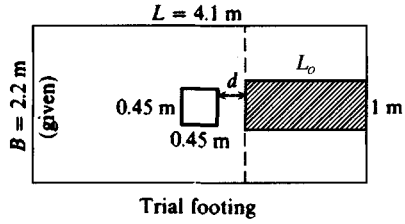

Figure E8-8*a*

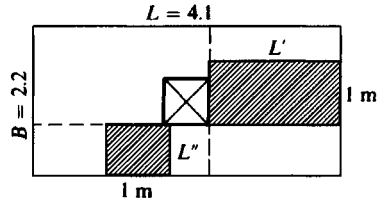

Figure E8-8*b*

As a check,

$$q = \frac{2132}{(2.20)(4.10)} = 236 < 240 \qquad \text{O.K.}$$

Step 2. Find the footing depth for shear. Check wide-beam value first. For a strip 1 m wide as shown in Fig. E8-8*a* and distance d from the column we have

$\sum F_v = 0$ on a 1-m-wide section on right end of footing of length L_o gives

$$d(1.0)v_c - \left(\frac{4.10 - 0.45}{2} - d\right)q_{\text{ult}} = 0$$

Inserting values of $v_c = 0.65$ MPa from Table 8-2 and q_{ult} from the foregoing (in MPa), we obtain

$$0.65d + 0.365d = 0.666$$

$$d = \frac{0.666}{1.015} = \mathbf{0.66}\text{ m}$$

For this value of d let us check the two-way action (approximately by neglecting upward soil pressure on the two-way action block) to obtain

$$\text{Perimeter of two-way action block} = (0.45 + 0.66)4 = 4.4\text{ m}$$

$$P_s = \text{perimeter} \times d \times v_c = 4.4(0.66)(1.30 \times 1000) = 3775\text{ kN} > 3291.4$$

A more refined analysis is not required nor do we need to check ACI Eq. (11-37) since $w < d$. Thus $d = 0.66$ m for longitudinal steel.

Step 3. Find steel required in long direction (longitudinal steel):

$$L' = \frac{4.10 - 0.45}{2} = 1.825\text{ m} \qquad \text{(see Fig. E8-8}b\text{)}$$

and

$$M_u = \frac{q_{\text{ult}}L'^2}{2} = \frac{365 \times 1.825^2}{2} = 608\text{ kN} \cdot \text{m} \qquad a = \frac{400A_s}{0.85 \times 21 \times 1} = 22.41A_s$$

Using Eq. (8-2), we have

$$A_s\left(0.66 - \frac{22.41A_s}{2}\right) = \frac{608}{0.9(400)(1000)}$$

Cleaning up, we obtain

$$A_s^2 - 0.058A_s = -0.000\,15$$

$$A_s = 0.0027\text{ m}^2/\text{m}$$

Checking the percentage of steel, we find

$$p = \frac{0.0027}{1(0.65)} = 0.004 > 0.0018 \qquad \text{(T and S of Art. 7.12.2 for } f_y = 400\text{ MPa)}$$

$$< 0.016 \qquad \text{(Table 8-2)}$$

The total is

$$A_s = 27 \times 10^{-4} \times 2.20 = 5.94 \times 10^{-3} \text{ m}^2$$
$$= 0.005\,94 \times 1000^2 = 5940 \text{ mm}^2$$

From the bar table (inside back cover), use 12 No. 25 bars to furnish:

$$A_{s,\text{ furn}} = 12 \times 500 = \mathbf{6000} \text{ mm}^2 > 5940 \qquad \text{O.K.}$$

Check required development (Art. 12.2.1) length against $L' - 0.07$ m end cover

$$L_d = \frac{0.02A_b f_y}{\sqrt{f_c'}} = \frac{0.02(500)400}{\sqrt{21}} = 873 \text{ mm} < 1.825 - 0.07 \text{ end cover}$$

Space the longitudinal bars at 11 spaces + 0.07 m side clearance + 1 bar:

$$11s + 2(0.07) + 0.025 = 2.20 \text{ m}$$
$$= \mathbf{0.185} \text{ m}$$

Step 4. Find steel in short direction (Fig. E8-8*b*). Place steel on top of longitudinal steel so $d' = 0.66 - 0.025/2 - 0.025/2 = 0.635$ m (assuming the short bars are also No. 25):

$$L'' = \frac{2.20 - 0.45}{2} = 0.875 \text{ m}$$
$$M_u = \frac{365 \times 0.875^2}{2} = 140 \text{ kN} \cdot \text{m}$$

And A_s is found (a = same as for longitudinal steel):

$$A_s\left[0.635 - \frac{22.41A_s}{2}\right] = \frac{140}{0.9(400)(1000)}$$
$$A_s^2 - 0.057A_s = -0.000\,035$$
$$A_s = 0.000\,62 \text{ m}^2/\text{m of width}$$

Checking percent steel furnished, we find

$$p = \frac{0.000\,62}{1(0.635)} = 0.0009 < 0.0018$$

Checking against ACI Art 10.5.2, we see

$$A_s = 1.33(0.000\,62) = 0.000\,825 \rightarrow 825 \text{ mm}^2/\text{m}$$

Since p is less than required for temperature and shrinkage, use A_s based on 0.0018:

$$A_s = 0.0018(1000)(635) = 1143 \text{ mm}^2/\text{m} > 825$$

We will use 1143 but probably could use 825 mm^2/m:

$$A_{s,\text{ total}} = 1143(4.1) = \mathbf{4686} \text{ mm}^2$$

The minimum spacing of bars is $5t$ or 0.457 m for T & S steel. It is not necessary to check L_d or use additional rebars in the zone B centered on the column based on the equation shown on Fig. 8-12.

Let us use sixteen 20-mm bars:

$$A_s = 16(300) = 4800 \text{ mm}^2 > 4686 \qquad \text{and spacing O.K.}$$

Step 5. Check bearing and design dowels:

$$A_1 = 0.45^2 = 0.2025 \text{ m}^2 \qquad A_2 = (0.45 + 4 \times 0.65)^2 = 9.30 \text{ m}^2$$

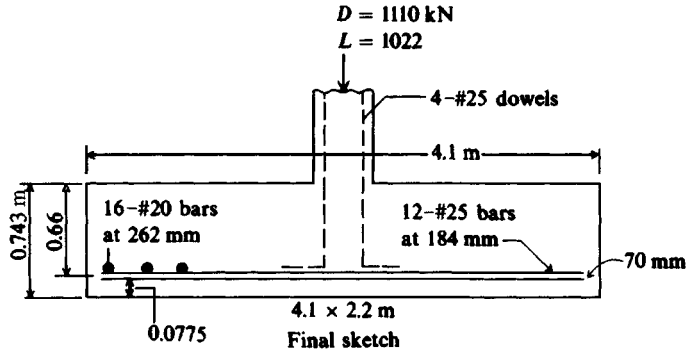

Figure E8-8*c*

$$\psi = \frac{\sqrt{A_2}}{A_1} = \frac{\sqrt{9.30}}{0.2025} = 6.8 \gg 2 \qquad \text{Use } 2$$

$$f_c = 0.85(0.70)(21)(2)(1000) = 24\,990 \text{ kPa}$$

$$f_a = \frac{P_u}{A_1} = \frac{3291}{0.2025} = \mathbf{16\,254} \text{ kPa} < 24\,990 \qquad \text{O.K. for bearing}$$

The minimum of $0.005A_{col}$ (Art. 15.8.2.1) will be used

$$A_s = 0.005(0.2025) \times 1000^2 = 1012 \text{ mm}^2$$

Use four No. 25 bars (same as column):

$$A_s = 4(500 \text{ mm}) = \mathbf{2000} > 1013 \text{ mm}^2 \qquad \text{O.K.}$$

The depth of embedment per Art. 12.3 does not have to be checked since dowels are only for a code requirement to ensure column-to-base anchorage. We will run the dowels using ACI standard 90° bends (for wiring) to the top of the reinforcing bars in the bottom of the footing and wire them in place for alignment.

Step 6. Develop the design sketch (Fig. E8-5*c*). Obtain overall D as

$$D_c \geq 0.66 + \frac{0.025}{2} + 0.070 = 0.7425 \text{ m}$$

Use $D_c = \mathbf{0.743}$ m = **743.0** mm.

////

8-10 ECCENTRICALLY LOADED SPREAD FOOTINGS

When footings have overturning moments as well as axial loads, the resultant soil pressure does not coincide with the centroid of the footing. If we assume the footing is somewhat less than rigid (and most are), the application of the statics equation of

$$\frac{P}{A} \pm \frac{Mc}{I} \tag{8-14}$$

gives a triangular soil pressure and displacement zone *ab*1 as shown in Fig. 8-13. If $q_{max} > q_{ult}$ as shown along the toe as line 1*b*, the soil pressure reduces to its ultimate value and stress is transferred to point 2. When this $q_{max,\,2} > q_{ult}$ the pressure again reduces to q_{ult}, and the process of load redistribution (similar to concrete beam analysis in Strength Design as given by Fig. 8-3) continues until equilibrium (or failure) is obtained.

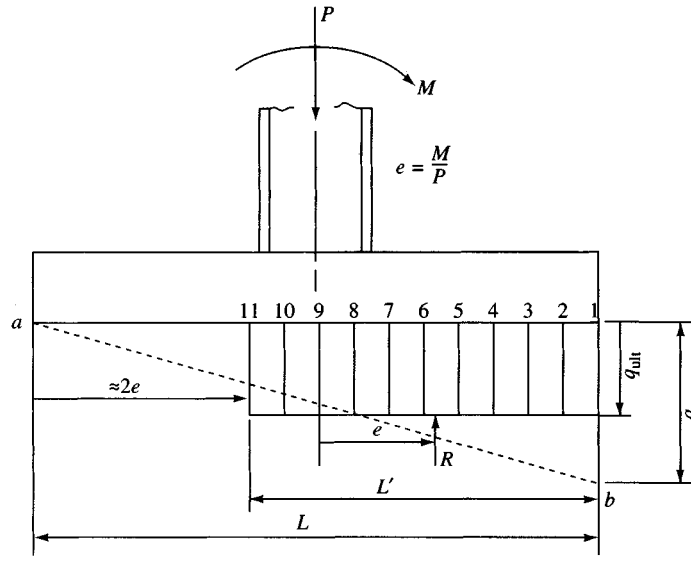

Figure 8-13 Soil yielding under $P/A + Mc/I$ toe stresses to produce an approximate rectangular pressure zone to resist P and to satisfy statics (see also Fig. 4-4). For overturning stability always take a $\sum M$ check about point 1 at toe.

The displacements also initially have a somewhat linear shape as shown by line *ab*. This observation is consistent with concrete design where the compression zone continues to have an approximately linear variation of strain to some "ultimate" value but at the same time the assumed rectangular pressure block of depth a shown in Fig. 8-3*b* is being produced [see also Fig. 4-1 of ACI Committee 336 (1988)]—at least for compressive stresses that are at or somewhat below the ultimate stress of the concrete. The equivalent of depth a of the concrete beam is the length L' of the footing as shown in Fig. 8-13.

Meyerhof at least as early as 1953 [see Meyerhof (1953, 1963)], Hansen in the later 1950s [see Hansen (1961, 1970)], and Vesić (1975*b*) have all suggested computing the bearing capacity of an eccentrically loaded footing using Fig. 4-4 (see also Fig. 8-14). The soil analogy is almost identical to the Strength Design method of concrete.

After careful consideration it appears that the base should be designed consistent with the procedure for obtaining the bearing capacity. That is, use dimension B', L' for the design also.

This procedure ensures four items of considerable concern:

1. The resultant soil R is never out of the middle one-third of the base so that overturning stability is always satisfied (taking moments about point 1 of Fig. 8-13). This R always gives

$$\text{SF} = \frac{M_{\text{resist}}}{M_{\text{overturn}}} = \frac{PL}{2M}$$

2. The toe pressure will always be such that $q_{\text{toe}} \leq q_a$.
3. The design is more easily done when a uniform soil pressure is used to compute design moments.
4. Approximately the same amount of steel is required as in the design using Eq. (8-14). One can never obtain a good comparison since a footing with overturning is heavily dependent

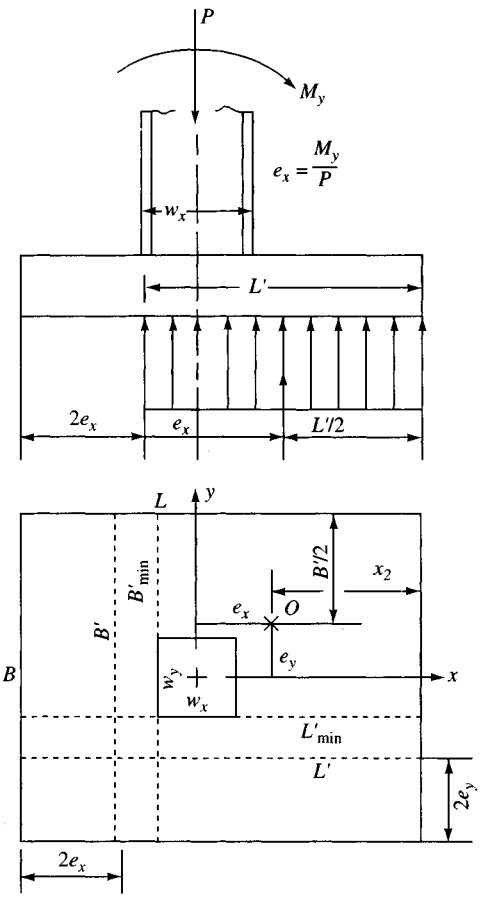

(*a*) General case of a spread footing with overturning – either about *y* or *x* axis (or both).

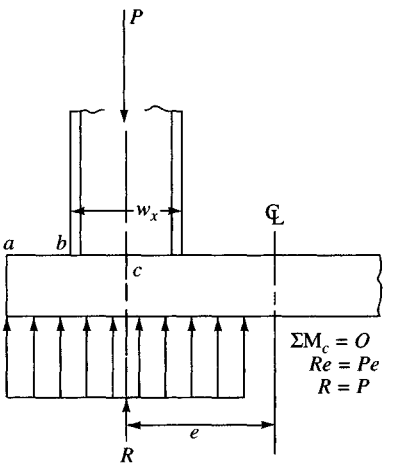

(*b*) Column is offset from centerline. Use a strap footing if column has no edge distance *ab*.

Prove that point *O* is the center of area *B'L'* where $B'L'\,q_a \geq P$:

$L/2 = e_x + x_2$ (1)
$L' = L - 2e_x$ (2)

Substitute (1) into (2): $L' = 2e_x + 2x_2 - 2e_x$
$L' = 2\,x_2$ ←←

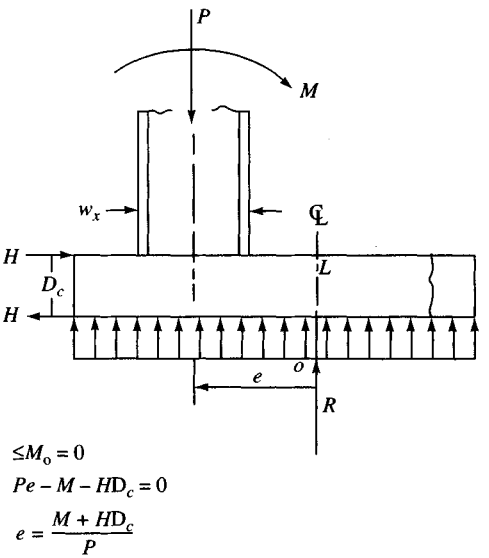

$\leq M_o = 0$
$Pe - M - HD_c = 0$
$e = \frac{M + HD_c}{P}$

(*c*) Offset column at an eccentricity so that a uniform soil pressure results.

Figure 8-14 General case of footings with overturning.

upon the assumptions used by the structural engineer. I was able to achieve some fairly reasonable agreements from the availability of two computer programs—one using Eq. (8-14) and the other using the recommended procedure.

In order to satisfy the ACI 318 Building Code it is necessary to place restrictions on the values of B', L'. These were stated in Chap. 4 and are repeated here for convenience:

$$B_{\min} = 4e_y + w_y \qquad B' = 2e_y + w_y$$
$$L_{\min} = 4e_x + w_x \qquad L' = 2e_x + w_x$$

where the appropriate dimensions are defined on Fig. 8-14*a*. Note in Fig. 8-14*a* that the center of the resultant uniform soil pressure is at the centroid of the B', L' rectangle and is also at the eccentric distance(s) e_x or e_y computed as

$$e_x = \frac{M_y}{P} \qquad e_y = \frac{M_x}{P}$$

from the column center.

By using dimensions of at least $B_{\min}$ and $L_{\min}$ the rectangular pressure zone will always include the column. This allows us to take the moment arms for tension steel on the pressed side, giving for the *minimum* values of B' and L' moment arms of length

$$L_y = B' - w_y \qquad L_x = L' - w_x$$

The amount of steel computed for a unit width is used across the full base dimensions of B and L.

For two-way shear we have two options:

1. Compute an "average" $q = \dfrac{P}{BL}$ and use this q value in Eq. (8-6).
2. Use the approximate Eq. (8-8), which does not use the upward soil pressure in the punch-out zone around the column. The author recommends using approximate Eq. (8-8) both to achieve some small steel economy and to increase the base depth slightly for a somewhat more conservative design.

8-10.1 Can a Spread Footing Carry a Moment?

It should be evident that a column can transmit a moment to the footing only if it is rigidly attached. Nearly all concrete columns satisfy this criterion. Adequate anchorage of the base plate to the footing must be done to transfer a moment when steel columns are used.

The question of whether a spread footing (unless very large in plan) can sustain an applied column moment without undergoing at least some rotation according to Fig. 5-9 is a very important one. From elementary structural analysis, if the footing rotates an amount θ, this results in moments in the opposite direction to that being applied by the column to develop:

$$\text{Near end: } M_r = \frac{4EI_c\theta}{L_c} \qquad \text{Far end: } M_r' = \frac{2EI_c\theta}{L_c}$$

The resultant column end moments are

$$\text{Near end: } M_f = M_o - M_r \geq 0$$
$$\text{Far end: } M_f' = M_o' - M_r' \qquad \text{(with a sign on } M_o')$$

Thus, any footing rotation reduces the moment M_f applied to the footing with a corresponding change to the far-end moment M'_f on the column. Obviously a sufficiently large rotation can reduce the footing moment to zero (but not less than zero).[9] How much rotation is required to reduce the moment to zero depends on the EI_c/L_c of the column. How much rotation actually occurs is somewhat speculative; however, Fig. 5-9 gives a quantitative estimate (see also Example 5-8).

If the structural designer opts to make a rigid base analysis, it is usually done using the following form of Eq. (8-14):

$$q = \frac{P}{BL}\left(1 \pm \frac{6e}{L}\right) \tag{8-14a}$$

where terms are identified on Figs. 8-13 and 8-14. Strictly, when using this type of equation one should include the moment from the footing weight (and any overlying soil) on the resisting side of the footing axis. Doing this will reduce the maximum (toe) pressure slightly and increase the minimum pressure. This is seldom if ever done in practice.

When the eccentricity e of Eq. (8-14) is sufficiently large, the minimum q becomes negative, indicating base-soil separation. Much effort has been expended in developing curves and other design aids to identify the line of zero pressure for those cases where Eq. (8-14*a*) produces a negative q. Clearly, one method is to use some kind of finite element/grid computer program (such as B-6 or B-19; see your diskette) and plot a line through those grid points that after several iterations have either negative or zero displacements (and the next adjacent nodes have positive displacements).

The principal use of Eq. (8-14*a*) in this text is, by rearranging the equation, to solve for the situation where the minimum $q = 0$. When we set $q = 0$ and solve for the eccentricity we find

$$e = L/6$$

Since the author is recommending that the base design proceed according to the same procedure used to obtain the allowable bearing pressure, the following two examples (using computer output from the program identified on your diskette as FOOTDES) are included. Note that select data in these examples are hand-checked, and the procedure is exactly that of Example 8-2. You can readily see this similarity from the sketches accompanying the computer output, giving selected dimensions and showing some of the computed quantities checked by hand. The only difference between Example 8-2 and Examples 8-9 and 8-10 following is that approximate Eq. (8-8) is used to obtain the effective depth d. As shown earlier, this approximation gives a conservative depth d and results in a slight reduction in the mass of footing steel required, thus making the footing slightly more economical at no loss of design safety.

Example 8-9.

Given. The following load, column, footing, and soil data:

$$P_{des} = 800D + 800L = 1600 \text{ kN}$$
$$P_{ult} = 1.4(800) + 1.7(800) = 2480 \text{ kN}$$

[9] As the moment rotates the footing, the rotation reduces the moment, which in turn reduces rotation, etc., until some rotation equilibrium is reached consistent with moment and stiffness of column, footing, and soil.

$M_y = 300D + 500L = 800$ kN · m

$M_{y,\text{ult}} = 1.4(300) + 1.7(500) = 1270$ kN · m

Column dimensions: $AX = 0.50$ m

$AY = 0.40$ m

$f'_c = 21$ MPa $\quad F_y = 400$ (grade 400 rebars)

$s_u = c = 200$ kPa $\quad (\phi = 0) \quad$ Use SF = 3 for q_a

Depth of footing $D = 1$ m $\quad \gamma_{\text{soil}} = 17.50$ kN/m^3

The groundwater table is not a consideration for the design.

Required. Design a spread footing using the Hansen bearing-capacity equations and the effective base area $B' \times L'$.

Solution. A computer program FOOTDES is used with the foregoing data as input. Note (Fig. E8-9) that the data file used for the execution was printed (EXAM89.DTA), so if a parametric study is made a copy of the data set can be made, renamed, and edited.

After the program found a base of dimensions 3.23 m × 2.23 m, a screen request was made if I was satisfied with these dimensions. I decided to round the dimensions to $BX = 3.25$; $BY = 2.25$ m as shown on Fig. E8-9*a*. Using these fixed dimensions the program checked for adequacy and output data indicating the base dimensions are acceptable.

Note that the computer program allowed me to modify the computed dimensions B, L so that reasonable multiples of meters or feet (or inches) result. The program also gave me the opportunity to limit the allowable bearing pressure.

Next the program asked if I wanted a steel design and I responded that I did. The program then computed the allowable concrete two-way shear stress and used Eq. (8-8) to find a depth DE (d). In this type of design wide-beam shear often controls and this was checked. In fact depth d for wide-beam does control at 595 mm (versus 501.73 mm for two-way).

A check for overturning stability (or safety factor SF) is routinely made by taking moments about the appropriate pressed edge. The resisting moment M_r is always

$$M_r = \frac{PL}{2}$$

where L = footing dimension perpendicular to the pressed edge

P = either the working or ultimate column axial load

The overturning moment $M_{\text{o.t.}}$ equals either the working design or ultimate moment producing the edge compression. This check is shown with the output sheets.

The computer program does an internal check and always produces dimensions such that application of Eq. (8-14*a*) places the eccentricity within the middle third of the base. This ensures that the overturning stability will always be adequate, however, always make a routine check to be sure the input is correct.

The program does not design dowels when there is overturning moment. What would normally be done here is to use the column steel as dowels, as this would ensure an adequate column-to-footing interface. Short column bars would either be used and later spliced above the footing at a convenient location or, preferably, be extended the full column height. They would be bent using a standard ACI Code 90° bend at the lower end and set onto the footing steel and wired securely. A bend substantially increases the bar pull-out capacity if the depth d does not provide sufficient length for a straight bar—and it often does not. The portion above the footing would be encased in the column form or, if not convenient to do so, would be held in place using a temporary support until the footing is poured and the concrete hardened.

Figure E8-9*a*

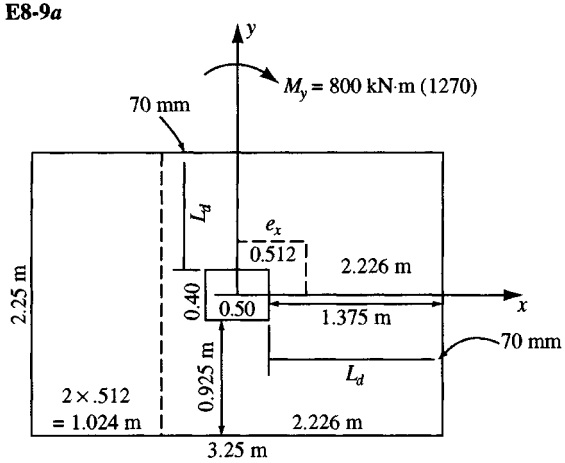

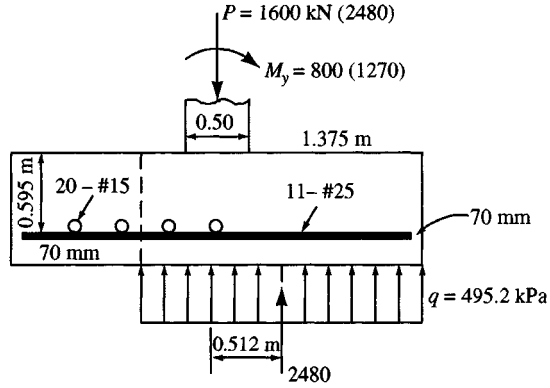

Figure E8-9*b*

```
 ECCENTRICALLY LOADED FOOTING FOR EXAMPLE 8-9 FOR FAD 5/E

     +++++++++++++++++ THIS OUTPUT FOR DATA FILE:  EXAM89A.DTA

++++  HANSEN BEARING CAPACITY METHOD USED--ITYPE = 1

FOOTING DIMENSIONS AND BEARING PRESSURES FOR
 DEPTH OF FTG =     1.00 M        UNIT WT OF SOIL =   17.500 KN/M*3
                                  INITIAL INPUT SF =   3.0

    PHI-ANGLE =    .000 DEG            SOIL COHES =   200.00 KPA

        VERT LOAD =    1600.0 KN     (DESIGN VALUE)
 MOM ABOUT X-AXIS =       .00 KN-M    ECCENTRICITY, ECCY =    .000 M ✓
 MOM ABOUT Y-AXIS =    800.00 KN-M    ECCENTRICITY, ECCX =    .500 M (1)

THE HANSEN N-FACTORS:  NC =   5.14   NQ =     1.0   NG =      .0

ALL SHAPE, DEPTH AND INCLINATION FACTORS FOR HANSEN
              B-DIR      L-DIR              (2)
SCB, SCL =    1.195      1.195
SQB, SQL =    1.000      1.000
SGB, SGL =     .600       .600
DCB, DCL =    1.123      1.178
DQB, DQL =    1.000      1.000
ICB, ICL =    1.000      1.000
IQB, IQL =    1.000      1.000
IGB, IGL =    1.000      1.000
```

Figure E8-9*b* (*continued*)

```
ALLOWABLE BEARING PRESSURE FOR JCOUN = 1
IGB OR IGL (USED VALUE) =  1.000   FOOTING WIDTH USED =   2.25
QULT COMPONENTS:  FCOH =     .00
                  FQBAR =    .00
                  FGAMM =    .00 KPA OR KSF
               QA(JCOUN) =  457.34✓          (3)

*FOOTING DIMENSIONS:  BX =  3.250   BY =  2.250 M     FOR SF =  3.000
                      ALLOW SOIL PRESS =  457.34 KPA
  COMPUTED ALLOW FTG LOAD AS P = B'L'QALL = 2315.29 KN    ( 1600.00)(4)
* = FOOTING DIMENSIONS INPUT OR REVISED--NOT COMPUTED ++++++

++++++++++++++++++++++++++++++++++++++++++++++++++++++++++++++++++

BASED ON THE ULTIMATE LOAD AND ULTIMATE MOMENT
         ECCENTRICITIES, ECCX =    .512✓  ECCY =    .000 M    (5)
REDUCED FOOTING DIMENSIONS BX' =   2.226    BY' =   2.250 M
                      ULTIMATE COLUMN LOAD,PCOL =  2480.0 KN ✓
      ULTIMATE BEARING PRESSURE, PCOL/(BX'*BY') =  495.20 KPA✓ (6)
++++++++++++++++++++++++++++++++++++++++++++++++++++++++++++++++++
++++++++++++++++++++++++++++++++++++++++++++++++++++++++++++++++++

     +++RECTANGULAR FOOTING DESIGN BY ACI 318-89++++

++++++++++++ HAVE SQUARE OR RECTANGULAR COLUMN +++++++++++++++

GIVEN DESIGN DATA:
               COL COLX = 500.000 MM
               COL COLY = 400.000 MM
  YIELD STR OF STEEL FY =   400.0 MPA
    28-DAY CONCRETE STR =    21.0 MPA
   ALLOWABLE SOIL PRESS =  457.34 KPA


FOOTING DIMENSIONS USED FOR DESIGN:  BX =   3.25      BY =   2.25 M

                        FOR FACTORED COLUMN LOAD, PCOL = 2480.00 KN
                          ALLOW TWO-WAY CONC STRESS Vc = 1298.40 KPA
                       EFF DEPTH FOR TWO-WAY SHEAR, DE =  501.73 MM (7)

          FOR SOIL PRESSURE, QULT =  495.20 KPA    PCOL = 2480.00 KN
   THIS SOIL PRESS FOR WIDE-BEAM AND IS BASED ON PCOL/(BX'*BY')

       ALLOW WIDE-BEAM CONC STRESS, Vcw =  649.20 KPA
                    EFF DEPTH FOR WIDE-BEAM SHEAR, DWB =  594.99 MM (8)

                 EFFECTIVE FOOTING DEPTH USED FOR DESIGN =  594.99 MM
               DESIGN EFFECTIVE FOOT DEPTH =   594.99 MM
             AREA STEEL REQD:  LENGTH DIR =  2283.6970 ✓
                                    B DIR =  1189.9720 MM*2/M ✓ (9)

              ACT % STEEL L DIR =  .0038 %
              ACT % STEEL B DIR =  .0020 %
MAX ALLOWABLE % STEEL EITHER DIR =  .0171 %

REINFORCING BARS FOR BENDING--DIR PARALLEL TO L:
          BAR EMBEDMENT LENGTH PROVIDED, LD =  1305.00 MM

BAR      BARS REQD & SPAC CEN-TO-CEN   AS FURN     AS REQD   LD REQD
 MM           NO           MM          MM*2        MM*2       MM
 19.5         18            123.0       5375.67    5138.32✓  398.7
 25.2         11            208.5       5486.36    5138.32   652.4
 29.9          8            297.2       5617.24    5138.32   897.0
++++++++++++++++++++++++++++++++++++++++++++++++++++++++++++++++++
REINFORCING BARS FOR BENDING--DIR PARALLEL TO B:
          BAR EMBEDMENT LENGTH PROVIDED, LD =   855.00 MM ✓
```

Figure E8-9*b* (*continued*)

```
REBARS REQD SHORT SIDE = 1189.9720 MM*2/M
        ACTUAL % STEEL =  .0020 %  (T & S IF 0.002)✓
TOTAL STEEL SHORT SIDE = 3867.4100 MM*2
   STEEL IN COL ZONE B =      .0000 MM*2  (IS 0. FOR NO ZONE)
      LD OF SHORT SIDE =  855.000 MM

SHORT SIDE STEEL--"AS" BASED ON TEMP & SHRINK SO USE
   SAME ROUTINE AS FOR LONG DIRECTION STEEL--NO END ZONES

BAR DIA  BARS REQD AND SPAC CEN-TO-CEN   AS FURN  AS REQD    LD REQD
   MM         ZONE B        EA END ZONE    MM*2     MM*2        MM

 16.0          20            162.8        4021.25   3867.41✓  300.0
 19.5          13            257.5        3882.43   3867.41   415.5
++++++++++++++++++++++++++++++++++++++++++++++++++++++++++++++++++++

OBTAIN TOTAL FOOTING DEPTH BASED ON BARS YOU USE TO ALLOW
   FOR 3-IN OR 70-MM COVER
NOTE THAT REQ'D LD FOR TENSION REBARS IS REDUCED FOR BAR SPACING
   AND RATIO ASFURN/ASREQD ACCORDING TO ACI 318, ART 12.2

DOWELS NOT COMPUTED SINCE A MOMENT IS ON COLUMN
   HAND COMPUTE DOWELS FOR MOMENT TRANSFER
```

The following are selected computations to verify the computer generated output for Example 8-9. Refer to key code and ✓marks on output sheets.

(1): $e_x = \dfrac{M}{P} = \dfrac{800}{1600} = 0.50$ m

$s'_c = 1.195 - 1.000 = 0.195$

(2): $d'_c = 1.123 - 1.000 = 0.123$

$i'_c = 1.000 - 1.000 = 0.000$

(3): Check bearing capacity

$$q_{ult} = cN_c(1 + s'_c + d'_c - i'_c) + \gamma D$$
$$= 200(5.14)(1 + 0.195 + 0.123 - 0.000) + 17.5 \times 1.0$$
$$= \mathbf{1372.4}\ \text{kPa}$$
$$q_a = q_{ult}/SF = 1372.4/3 = \mathbf{457.46}\ \text{kPa}$$

(4): B', L' and $P_{\max}$

$$B' = B = 2.25\ \text{m};\quad L' = 3.25 - 2 \times 0.50 = 2.25\ \text{m}$$
$$P_{\max} = B' \times L' q_{\text{ult}}$$
$$= 2.25 \times 2.25 \times 457.34 = \mathbf{2315.28}\ \text{kN}$$

The actual base contact pressure

$$q = P/B'L' = 1600/(2.25 \times 2.25) = \mathbf{316.0}, \text{KPa} \ll 457.5$$

(5): Now new eccentricity $e_x = \dfrac{M_u}{P_u} = \dfrac{1270}{2480} = 0.512$ m

New $B' = 3.25 - 2(0.512) = \mathbf{2.226}$ m

Computation Check *Continued*

(6): New $q_{ult} = \dfrac{P_u}{B' \times L'} = \dfrac{2480}{.226 \times 2.225} = \mathbf{500.7}$ (vs. 495.2 computer)

(7): Depth for two-way beam shear and using Eq. (8-8):

$$4d^2 + 2(w_x + w_y)d = \frac{P_u}{v_c}$$

$$4d^2 + 2(0.50 + 0.40)d = \frac{2480}{1298.4}$$

$$d^2 + 0.45d = 0.4775$$

$$d = \mathbf{0.5017} \text{ m (501.7 mm)}$$

(8): Depth for wide beam shear in long direction (controls)

$$(L - d)q_{ult} = bdv_{c,wb} \rightarrow L = \frac{3.25 - 0.50}{2} = \mathbf{1.375} \text{ m}$$

$$1.375 - d = \frac{(1.0)(d)(649.2)}{495.2}$$

$$d = 1.375/2.3014 = \mathbf{0.5949} \text{ m } (= 594.9 \text{ mm})$$

(9): ACI 318 Code requirements:

Across footing width of 2.25 m: = L dir = 0.0038 percent

Across footing length of 3.25 m: = B dir = 0.0020 percent

(this is the Art. 7-12 minimum for grade 300—we are using grade 400 so could actually have used 0.0018—this percent also complies with ACI Art. 10-5.3)

$$a = \frac{f_y A_s}{0.85 f'_c b} = \frac{400A_s}{0.85(21)(1)} = 22.41A_s$$

$$M_u = q_{ult}L^2/2 = 495.2(1.375^2)/2 = 468.1 \text{ kN} \cdot \text{m}$$

$$\phi f_y A_s(d - a/2) = M_u$$

$$A_2(0.595 - 22.41A_s/2) = 468.1/(0.9 \times 400 \times 1000)$$

$$0.595A_s - 11.2A_s^2 = 0.0013$$

$$A_s = \frac{0.0531 \pm \sqrt{0.0531^2 - 4(0.00016)}}{2}$$

$$= 0.002283 \text{ m}^2/\text{m}$$

$$= \mathbf{2283} \text{ mm}^2/\text{m}$$

$L_d = (1.375 - 0.70) \times 1000 = \mathbf{1305}$ mm (compare to required L_d)

A_s (req'd for sale) $= 3.25 \times 2283.69 = \mathbf{5138.32}$ mm^2

For short side:

$L = (2.25 - 0.400)/2 = 0.925$ m

Estimate $d \approx 595 - 1$ bar $= 595 - 25 = 570$ mm.

$$M_u = 495.2(0.925^2/2 = \mathbf{211.9} \text{ kN} \cdot \text{m}$$

$$0.570A_s - 11.2A_s^2 = 211.9/(0.9 \times 400 \times 1000) = 0.0005886$$
$$A_s^2 - 0.05089A_s = 0.0000526$$
$$A_s = 0.001055 \text{ m}^2/\text{m}$$
$$= \mathbf{1055} \text{ mm}^2/\text{m}$$

Check against T & S requirements of ACI Art 7.12 (and use $d = 0.595$ m not 0.575 m and 0.002 not 0.0018 as conservative)

$$A_s = 0.002bd = 0.002(1000 \times 595)$$
$$= \mathbf{1190} \text{ mm}^2/\text{m} > 1055 \rightarrow \text{ and controls}$$
$$L_d = (0.925 - 0.070 \times 1000 = \mathbf{855} \text{ mm (compare to required } L_d)$$
$$A_s \text{ (req'd for long side)} = 3.25 \times 1089.972 = \mathbf{3867.41} \text{ mm}^2$$

Finally you must check overturning stability (check about toe of compressed edge)

$$M_{o.t.} = 800 \text{ or } 1270 \text{ kN} \cdot \text{m}$$
$$M_r = (1600 \text{ or } 2480)L/2 =)1600 \text{ or } 2480)3.25/2 = 2600$$
$$= 2600$$
$$\text{S.F.} = M_r/M_{o.t.} = 2600/800 = \mathbf{3.25} \quad \text{(O.K.)}$$
$$= 4030/1270 = \mathbf{3.17} \quad \text{(O.K.)}$$

////

Example 8-10.

Given. Same data as Example 8-9 *except* we have a moment about both axes (see Figure E8-10*b*). Also revise the column dimensions to

$$AX = AY = 0.50 \text{ m}$$

Required. Design the footing.

Solution. Again computer program FOOTDES is used. You should be aware that with equal moments about both axes the optimum footing shape will be a square.

The remainder of the design is almost identical to that of Example 8-9. Note that depth for *two-way* shear again uses Eq. (8-8). The principal difference is that a square column is now used whereas a rectangular one was used in Example 8-9, so the effective depth computes slightly less (484.86 vs. 501.73 mm).

Refer to the computer output sheets (Figure E8-10*a*) for select computations or user checks.

For dowels refer to the comments made in Example 8-9.

```
  TWO-WAY ECCENTRICALLY LOADED FOOTING FOR EXAMPLE 8-10 FOR FAD 5/E

     +++++++++++++++++ THIS OUTPUT FOR DATA FILE:  EXAM89B.DTA

++++  HANSEN BEARING CAPACITY METHOD USED--ITYPE = 1

FOOTING DIMENSIONS AND BEARING PRESSURES FOR
 DEPTH OF FTG =    1.00 M        UNIT WT OF SOIL =  17.500 KN/M*3
                                 INITIAL INPUT SF =  3.0

    PHI-ANGLE =    .000 DEG          SOIL COHES =  200.00 KPA
```

Figure E8-10*a*

Figure E8-10*b*

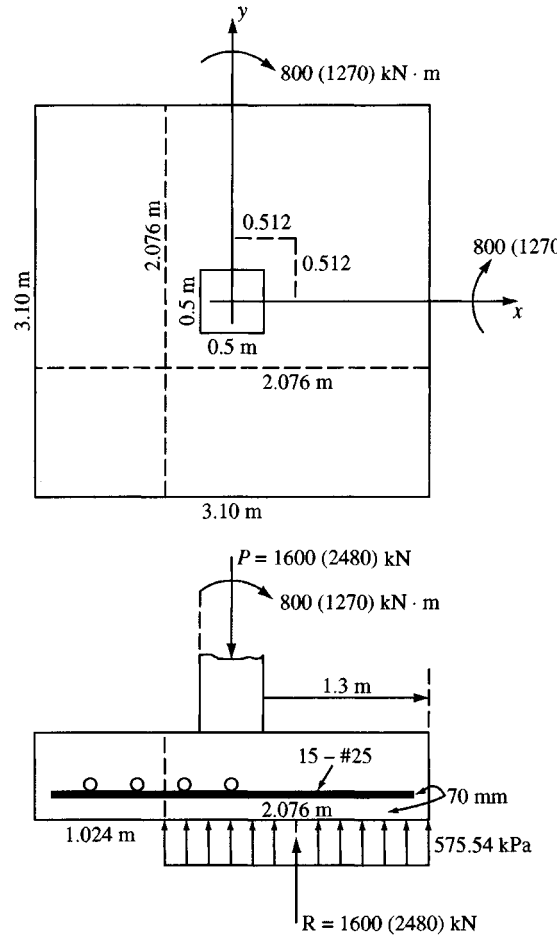

Figure E8-10*a* (*continued*)

```
        VERT LOAD =    1600.0 KN     (DESIGN VALUE)
 MOM ABOUT X-AXIS =    800.00 KN-M    ECCENTRICITY, ECCY =    .500 M
 MOM ABOUT Y-AXIS =    800.00 KN-M    ECCENTRICITY, ECCX =    .500 M


THE HANSEN N-FACTORS:  NC =    5.14    NQ =     1.0    NG =      .0

ALLOWABLE BEARING PRESSURE FOR JCOUN = 1
IGB OR IGL (USED VALUE) =  1.000    FOOTING WIDTH USED =    2.00
QULT COMPONENTS:  FCOH =      .00
                  FQBAR =     .00
                  FGAMM =     .00 KPA OR KSF
                QA(JCOUN) =   460.86
*FOOTING DIMENSIONS:  BX =  3.000    BY =  3.000 M      FOR SF =  3.000
                      ALLOW SOIL PRESS =  460.86 KPA
  COMPUTED ALLOW FTG LOAD AS P = B'L'QALL = 1843.42 KN ✓   ( 1600.00)
* = FOOTING DIMENSIONS INPUT OR REVISED--NOT COMPUTED ++++++
++++++++++++++++++++++++++++++++++++++++++++++++++++++++++++++++

BASED ON THE ULTIMATE LOAD AND ULTIMATE MOMENT
          ECCENTRICITIES, ECCX =    .512    ECCY =    .512 M ✓
REDUCED FOOTING DIMENSIONS BX' =   1.976    BY' =   1.976 M
                      ULTIMATE COLUMN LOAD,PCOL =  2480.0 KN
      ULTIMATE BEARING PRESSURE, PCOL/(BX'*BY') =  635.28 KPA ✓
```

Figure E8-10*a* (*continued*)

```
++++++++++++++++++++++++++++++++++++++++++++++++++++++++++++++++++++++
++++++++++++++++++++++++++++++++++++++++++++++++++++++++++++++++++++++

     +++++SQUARE FOOTING DESIGN BY ACI 318-89-++++

++++++++++++ HAVE SQUARE OR RECTANGULAR COLUMN +++++++++++++++++

GIVEN DESIGN DATA:
               COL COLX = 500.000 MM
               COL COLY = 500.000 MM
  YIELD STR OF STEEL FY =   400.0 MPA
    28-DAY CONCRETE STR =    21.0 MPA
   ALLOWABLE SOIL PRESS =  460.86 KPA

      COL LOADS:  AXIAL =  2480.0 KN     (FACTORED)
                MOMENT = 1270.00 KN-M ABOUT THE X-AXIS
                MOMENT = 1270.00 KN-M ABOUT THE Y-AXIS

FOOTING DIMENSIONS USED FOR DESIGN:  BX =   3.00      BY =   3.00 M

                          FOR FACTORED COLUMN LOAD, PCOL = 2480.00 KN
                            ALLOW TWO-WAY CONC STRESS Vc = 1298.40 KPA

                          EFF DEPTH FOR TWO-WAY SHEAR, DE =  484.86 MM

          FOR SOIL PRESSURE, QULT =  635.28 KPA    PCOL = 2480.00 KN
   THIS SOIL PRESS FOR WIDE-BEAM AND IS BASED ON PCOL/(BX'*BY')

       ALLOW WIDE-BEAM CONC STRESS, Vcw =  649.20 KPA ✓        ✓
                     EFF DEPTH FOR WIDE-BEAM SHEAR, DWB =  618.23 MM

                EFFECTIVE FOOTING DEPTH USED FOR DESIGN =  618.23 MM
              DESIGN EFFECTIVE FOOT DEPTH =   618.23 MM
             AREA STEEL REQD:  LENGTH DIR =  2328.2330 ✓
                                  B DIR =  2328.2330 MM*2/M

              ACT % STEEL L DIR =  .0038 % ✓
              ACT % STEEL B DIR =  .0038 %
MAX ALLOWABLE % STEEL EITHER DIR =  .0171 %

++++++++++++++++++++++++++++++++++++++++++++++++++++++++++++++++++++++

REINF BARS FOR EITHER DIR BENDING (SQ FTG)
         BAR EMBEDMENT LENGTH PROVIDED, LD =  1180.00 MM

BAR      BARS REQD & SPAC CEN-TO-CEN   AS FURN     AS REQD   LD REQD
 MM           NO           MM          MM*2         MM*2      MM
 19.5         24           123.5       7167.56     6984.70 ✓  406.4
 25.2         15           202.5       7481.41     6984.70    650.3

++++++++++++++++++++++++++++++++++++++++++++++++++++++++++++++++++++++

OBTAIN TOTAL FOOTING DEPTH BASED ON BARS YOU USE TO ALLOW
   FOR 3-IN OR 70-MM COVER
NOTE THAT REQ'D LD FOR TENSION REBARS IS REDUCED FOR BAR SPACING
   AND RATIO ASFURN/ASREQD ACCORDING TO ACI 318, ART 12.2

DOWELS NOT COMPUTED SINCE A MOMENT IS ON COLUMN
   HAND COMPUTE DOWELS FOR MOMENT TRANSFER
```

Check overturning stability:

$$M_{o.t} = 800 \text{ or } 1270 \text{ kN} \cdot \text{m (about either axis)}$$

$$\begin{aligned} \text{The resisting moment } M_r &= (1600 \text{ or } 2480)L/2 \\ &= 1600(3.0/2) = 2400 \\ &= 2480(3.0/2) = 3700 \text{ kN} \cdot \text{m} \end{aligned}$$

$$SF = \text{Stability Number} = M_r/M_{o.t}$$
$$= 2400/800 = 3.0$$
$$= 3720/1270 = 2.93 \qquad \text{(both O.K.)}$$

////

Example 8-11. Design a footing $B \times L$ such that the soil pressure will be approximately uniform for the following conditions (see Fig. 8.14*c*):

$D = 419.6$ kN $\qquad L = 535.4$ kN
$M_d = 228$ kN · m $\qquad M_L = 249.5$ kN · m
$H_D = 42.1$ kN $\qquad H_L = 53.2$ kN

Column: Square 500 × 500 mm with eight No. 25 bars
$f'_c = 28$ MPa $\qquad f_y = 400$ MPa

Footing: $f'_c = 21$ MPa $\qquad f_y = 400$ MPa
$q_a = 150$ kPa

Solution.

Step 1. Find footing dimensions $B \times L$:

$$P = 955 \text{ kN}$$
$$M = 477.5 \text{ kN} \cdot \text{m}$$
$$e = \frac{M}{P} = \frac{477.5}{955} = \mathbf{0.50} \text{ m}$$

Note this e should be increased slightly owing to the additional overturning moment from $H_d + H_L$. Use $e = \mathbf{0.55}$ m (see Fig. E8-11*a*).

For $e = 0.55$ m the edge of the column is 0.30 m from the footing centerline. The required footing area for $q = q_a = 150$ kPa is $955/150 = 6.4$ m^2. B for a square footing is 2.52 m. Try $B \times L = \mathbf{2.60} \times \mathbf{2.60}$ m:

$$q_{ult} = \frac{1.4(419.6) + 1.7(535.4)}{2.60^2} = \mathbf{221.5} \text{ kPa}$$

Step 2. Find the footing depth (refer to Fig. E8-11*b*).

Figure E8-11*a*

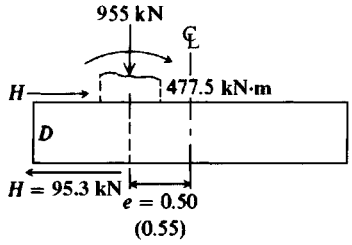

Figure E8-11*b*

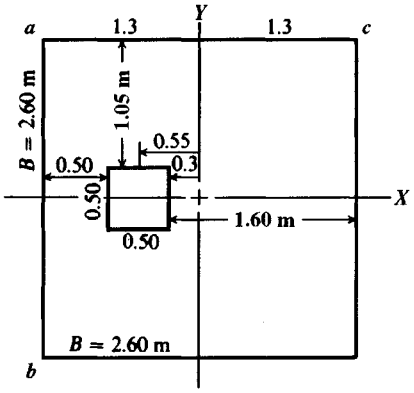

For two-way action (note edge distance limits $d/2 \leq 0.50$) use approximate Eq. (8-8):

$$4d^2 + 2(b + c)d = \frac{BLq}{v_c}$$

$$v_c = 1.30 \text{ MPa}$$

$$4d^2 + 2(0.5 + 0.5)d = \frac{2.60 \times 2.60 \times 221.5}{1300}$$

$$d^2 + 0.5d = 0.2880$$

$$d = \mathbf{0.34} \text{ m} < 0.50 \qquad \text{O.K.}$$

Do not check ACI Eq. (11-37) yet.

Find the depth for wide-beam shear at d from the column for a strip 1 m wide. We could, of course, check $d = 0.34$ m, but it is about as easy to compute the required d:

$$d(1)(v_c) = 1(1.3 + 0.30 - d)q_{\text{ult}}$$

$$v_c = 0.649 \text{ MPa} = 649 \text{ kPa} \qquad \text{(Table 8-2)}$$

Inserting values, we obtain

$$649d = 1.60(221.5) - 221.5d$$

$$d = 0.407 \text{ m} > 0.34 \qquad \text{(therefore, wide-beam shear controls)}$$

Use

$$d = \mathbf{0.410} \text{ m} \qquad (D_c \simeq 0.50 \text{ m})$$

Since wide-beam shear depth controls, it is not necessary to check ACI Eq. (11-37).

Step 3. Check $\sum M$ about centerline using $D_c = 0.50$ m (Fig. 8-14*c*)

$$0.50(62.1 + 53.2) + 228 + 249.5 - 955(0.55) = ?$$

$$47.7 + 477.5 - 525.3 = -0.1 \qquad \text{(should be 0.0)}$$

This small unbalance may be neglected, or e may be reduced and the problem recycled until $\sum M = 0$. Alternatively, since a value of $e \simeq 0.55$ is feasible, directly solve the moment equation for e to obtain $e = 0.5499$ m.

With footing dimensions tentatively established, the sliding stability should be investigated as

$$\frac{H_{\text{resisting}}}{\text{SF}} \geq H_d + H_L$$

Generally,

$$H_{\text{resisting}} = P \tan \delta + c' A_{\text{footing}} + \text{passive pressure}$$

For c', δ see Table 4-5. For passive pressure see Chap. 11.

Step 4. Find the required reinforcing bars for bending. This step is the same as for spread footings. That is, find bars required for bending for the long dimension ($bc + 0.3$ m $= 1.3 + 0.3 = 1.6$ m) and for the short dimension [$(2.60 - 0.50)/2 = 1.05$ m]. For the long direction (length abc) run the required bars the full length of $2.60 - 2(0.07) = 2.46$ m long bars (the 0.07 m is the clear-cover requirement).

For the short direction also run the bars the full distance of 2.46 m (the footing is square). You might here, however, consider placing about 60 percent of the total bars required in the distance ab and the other 40 percent in the distance bc.

Use final footing dimensions

$$\mathbf{2.60} \times \mathbf{2.60} \times D_c \text{ with } d \geq \mathbf{0.41} \text{ m}$$

////

8-10.2 Eccentricity Out of the Middle 1/3 of a Footing

In Sec. 8-10.1 we noted that the eccentrically loaded footings were forced to have the eccentricity

$$e = \frac{M}{P} \le \frac{L}{6} \qquad \left(\text{we have } \pm \frac{L}{6}, \text{ so } 2 \times \frac{L}{6} = \frac{L}{3}\right)$$

This ensures that the overturning stability is adequate.

There are occasions where it is impossible to have the eccentricity $e \le L/6$. In these cases one has two options:

1. Increase the base dimension(s) until the eccentricity is
$$e = L/6$$
2. Make an analysis similar to the base plate design that had a large column moment. Refer to Fig. 8-11 and replace the rectangular pressure diagram for the allowable concrete stress with the allowable soil pressure q_a. Replace the tension bolt(s) with tension piles. Solve the resulting quadratic equation for kd and use that as B' in the bearing-capacity equations and iterate back and forth until the assumed and required soil pressures are $q \le q_a$.

A method used by many structural designers assumes a triangular pressure distribution as shown in Fig. 8-15. The necessary equation for this is derived as follows:

$$L/2 = e + L'/3 \qquad \text{and} \qquad P = \frac{q}{2}(BL')$$

Substituting L' into the expression for P and solving for the soil pressure q at the toe, we obtain

$$q = \frac{2P}{3B(L/2 - e)} \le q'_a \tag{8-15}$$

In this equation P = fixed footing load, and the allowable soil pressure for this type of pressure distribution q'_a is somehow estimated by the geotechnical engineer. With these values set the structural designer solves Eq. (8-15) by trial until a set of dimensions B, L is found. Note carefully that q'_a is *estimated* by the geotechnical engineer. There is no current method to compute the allowable bearing pressure for a linear variable (triangular) pressure diagram.

The solution of Eq. (8-15) is particularly difficult when there is two-way eccentricity, i.e., both e_x and $e_y > L/6$. This is also true when Fig. 8-11 is used for base plates since there are two values of kd_i, where now $kd_1 = B'$, $kd_2 = L'$. Because of these difficultiles in using Eq. (8-15), the method used in Examples 8-9 and 8-10 based on Fig. 8-14 is particularly attractive.

A finite-difference program or program B-6 (Finite Grid on your diskette) might be used in this type of example. Steps include the following:

1. Grid the proposed base into rectangles or squares.
2. Assume or compute or obtain from the geotechnical engineer a value of modulus of subgrade reaction and the allowable bearing pressure q_a.
3. Activate the nonlinear program option and set the maximum soil displacement XMAX such that
$$q_a \le k_s \cdot \text{XMAX}$$

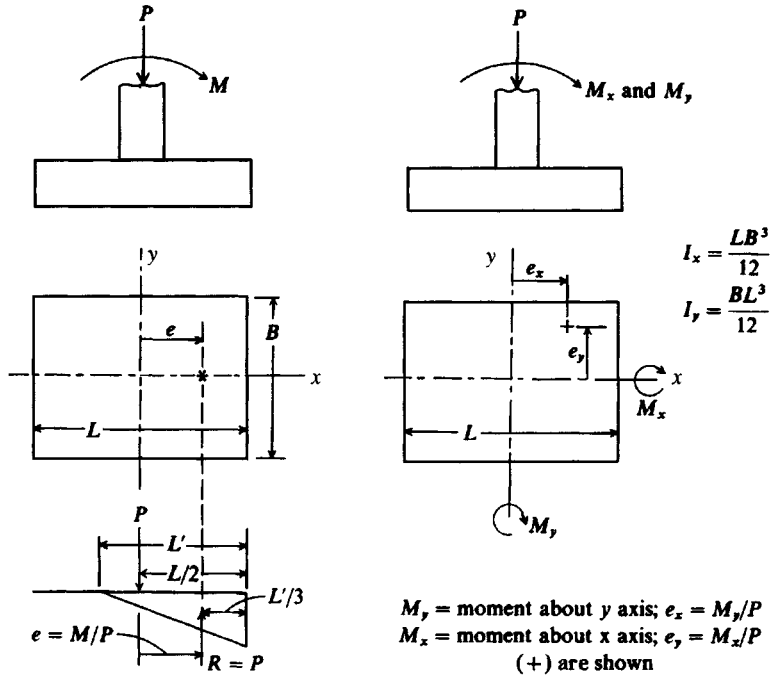

(*a*) Pressure diagram when $e > L/6$.

(*b*) Location of resultant when there is a moment about both the x and y axes. If both $e > L/6$, only part of the footing is effective.

Figure 8-15 An alternate soil pressure profile for footings with large eccentricities.

This step ensures that, regardless of displacement (which may well be linear), the soil will become plastic at displacement XMAX so the ultimate soil pressure is restricted. Of course q_a is less than ultimate for a safety margin.

4. If the foregoing are carefully done, you can then inspect the final computer output and locate the line of zero soil pressure, and at least a part of the pressure diagram will be rectangular. Alternatively, $q_a B' L' = P$, so solve by trial for B', L'.
5. Use the computer output to check statics. Use the base dimensions and given loads to check overturning stability.

8-11 UNSYMMETRICAL FOOTINGS

There are occasions where it is necessary to use a T, L, or other unsymmetrical shape for the foundation. It may also be necessary to cut a notch or hole in an existing footing for some purpose. In these cases it is necessary to estimate the base pressure for $q \leq q_a$ for the design. For the cut base it is also necessary to check that the resulting base pressure $q \leq q_a$.

The current recommendation for solution of this class of problems is to use your mat program B6 using the finite grid method that is presented in Chap. 10. A notched base example there considers both a pinned and fixed column. As with the footing with overturning, the soil, base thickness, and column fixity are significant parameters that are not considered in

the conventional "rigid" unsymmetrical base design still used by some foudation designers. This footing design is very computationally intensive and not recommended by the author.

8-12 WALL FOOTINGS AND FOOTINGS FOR RESIDENTIAL CONSTRUCTION

Load-bearing walls are supported by continuous-strip footings. Sometimes they are corbeled out to accommodate columns integral with the wall. In these cases the columns support a major portion of the interior floor loads; the walls carry self-weight and perimeter floor loads. Figure 8-16 illustrates typical wall footings.

Design of a wall footing consists in providing a depth adequate for wide-beam shear (which will control as long as $d \leq \frac{2}{3} \times$ footing projection). The remainder of the design consists in providing sufficient reinforcing steel for bending requirements of the footing projection. Longitudinal steel is required to satisfy shrinkage requirements. Longitudinal steel will, in general, be more effective in the top of the footing than in the bottom, as shown in Fig. 8-17. Note that as settlement occurs in Fig. 8-17*c* the wall should increase the effective footing I somewhat to resist "dishing."

Wall footings for residential construction are usually of dimensions to satisfy local building codes or Federal Housing Administration (FHA) requirements or to allow placing foundation walls. The contact pressure is usually on the order of 17 to 25 kPa including the wall weight. The FHA requirements are shown in Fig. 8-18. Again longitudinal steel, if used, should be placed in the top rather than the bottom for maximum effectiveness in crack control when the foundation settles.

Interior footings for residential construction are usually nonreinforced and sized to carry not over 20 to 45 kN, resulting in square or rectangular foundations on the order of 0.5 to 1.5 m. Often these footings are concrete-filled predrilled auger holes to a depth below seasonal volume change. Additional information on foundations for residential construction can be found in Bowles (1974*b*).

Figure 8-16 Footings for residential construction.

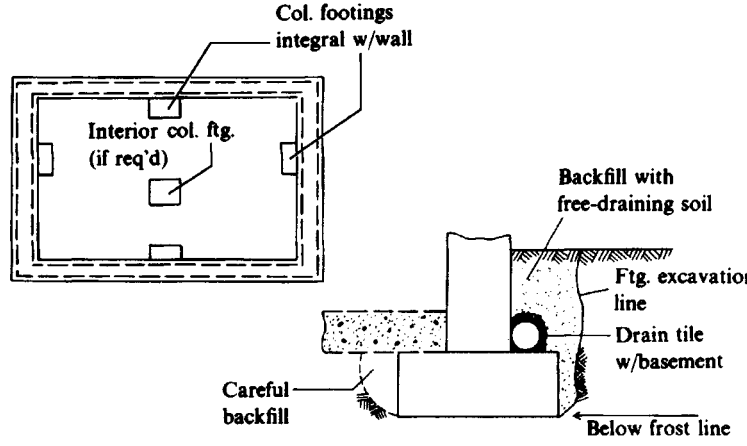

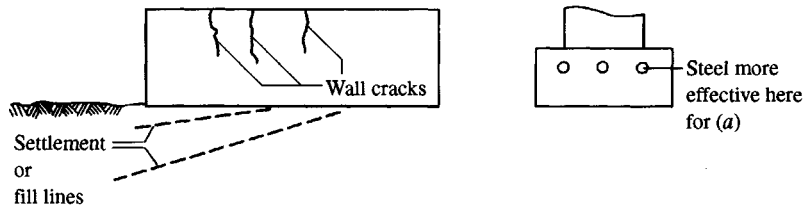

(*a*) The dashed lines represent either varying location of existing ground before filling or the resulting qualitative shape of the ground settlement caused by fill and/or building.

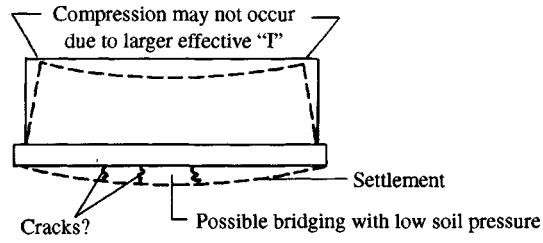

(*b*) Interior settlements may be resisted by larger moment of interia based on wall contribution so that tension stresses in footing are minimal.

Figure 8-17 Settlements of residences.

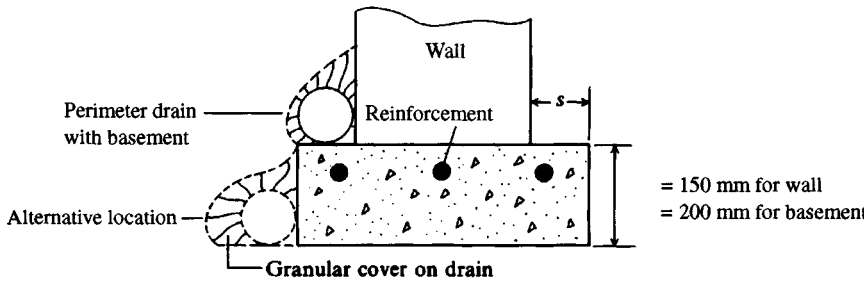

	s, mm	
	Frame construction	**Masonry or veneer**
1-story, basement	75	100
No basement	50	75
2-story, basement	100	125
No basement	75	100

Figure 8-18 Federal Housing Administration (FHA) minimum wall-footing dimensions. Recommend use of at least two No. 10 reinforcing bars (11.3-mm diameter) (author's, not FHA). Always use an outside perimeter drain with a basement. [Further details in Bowles (1974*b*).]

Example 8-12. Design the wall footing for an industrial building for the following data. Wall load consists in 70.1 kN/m (D = 50, L = 20.1 kN/m) including wall, floor, and roof contribution.

f_c' = 21 MPa f_y = 400 MPa
q_a = 200 kPa Wall of concrete block 200 × 300 × 400 mm (8 × 12 × 16 in.)

Solution. From Table 8-2, wide beam v_c = 649 kPa (no two-way action).

Step 1. Find footing width:

$$B = \frac{70.1}{200} = 0.35 \text{ m}$$

Since this is only 50 mm wider than the 300-mm concrete block, we will arbitrarily make the footing project 150 mm on each side of the wall, or

$$B = 300 + 150 + 150 = \mathbf{600} \text{ mm}$$

We will arbitrarily make the total footing depth D_c = 400 mm (d = 400 − 80 = 320 mm). The "pseudo" ultimate soil pressure (neglecting any weight increase from displacing the lighter soil with heavier concrete) is

$$q_{ult} = \frac{P_{ult}}{B} = \frac{1.4(50) + 1.7(20.1)}{600/1000} = \mathbf{174} \text{ kPa/m} < 200 \text{ allowable}$$

Step 2. Check wide-beam shear for the trial depth d = 320 mm. This will be done at the face of the wall (not d out) for the most severe condition: the soil pressure equals 174 kPa and the projected length L' equals 150 mm, giving $V_u = qL' = 174 \times 150/1000 = \mathbf{26.1}$ kN/m. The allowable concrete shear stress is 649 kPa (from Table 8-2), and the actual shear stress for a wall length of L = 1 m is

$$v_a = \frac{V_u}{Ld} = \frac{26.1}{1 \times 320/1000} = 82 \text{ kPa} \ll 649 \qquad \text{depth is OK.}$$

Step 3. Find required steel for transverse bending. Using meters rather than millimeters for computations to avoid huge numbers, we obtain

$$\text{Moment arm } L' = \text{overhang} + \tfrac{1}{4} \text{ concrete block width}$$

$$L' = 0.150 + \tfrac{1}{4}0.300 = 0.225 \text{ m}$$

(See Fig. 8-5*b* for masonry columns.) The resulting "ultimate" moment M_u is

$$M_u = q\frac{L^2}{2} = \frac{174 \times 0.225^2}{2} = \mathbf{4.04} \text{ kN} \cdot \text{m/m}$$

Since the concrete f_c' = 21 and f_y = 400 MPa are the same as used in Example 8-2, we have from that example $a = 22.4A_S$ (see Step 6). Now making substitutions into the previously used rearrangement of Eq. (8-2), we obtain (using d = 320/1000, B = 1 m, and ϕ = 0.9)

$$A_s\left(0.32 - \frac{22.4A_s}{2}\right) = \frac{4.04}{0.9 \times 400 \times 1000}$$

and simplifying obtain $A_s^2 - 0.0286A_s = 1.0 \times 10^{-6}$. Solving the quadratic, we obtain

$$A_s = 0.035 \times 10^{-3} \text{ m}^2/\text{m} = \mathbf{350} \text{ mm}^2/\text{m}.$$

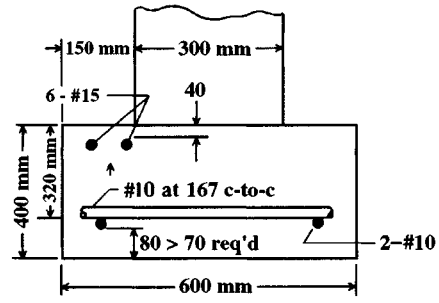

Figure E8-12

Step 4. Check for temperature and shrinkage (T and S) based on ACI Art. 7.12, and grade 400 bars so that the percentage $p = 0.0018$. The steel area A_S per meter of wall length is

$$A_S = pdB = 0.0018 \times 0.320 \times 1.0 = \mathbf{0.576 \times 10^{-3}}\ \text{m}^2/\text{m}$$
$$= 576\ \text{mm}^2 > 350\ \textbf{and controls}$$

Use six No. 10 bars/meter, giving $A_S = 6 \times 100 = 600\ \text{mm}^2/\text{m} > 576$, OK. The spacing will be $1000/6 = 167\ \text{mm} < 5 \times D_c < 500\ \text{mm}$ of ACI Art. 7.12.2.2.

Step 5. Select longitudinal steel. Since there is no moment arm, we will make an arbitrary selection based on a minimum of T and S of 576 mm^2. Let us use eight No. 10 bars as follows:

$$\text{Furnished } A_s = 8 \times 100 = 800\ \text{mm}^2 > 576 \text{ for T and S}$$

Two bars in bottom of wall footing and 80 mm (75 mm clear) above soil. These two bars will provide support for the transverse bars being used at six bars/meter of wall.

Six bars in top part across the width of 600 mm and with 40 mm of clear cover. We are using all the bars of same size to minimize the number of bar sizes on site and reduce any chance of installing an incorrect bar size. The reader should check that we can get six No. 10 bars into the width of 600 mm and not violate any ACI Code spacing requirements.

Step 6. Make a design sketch like Fig. E8-12.

////

PROBLEMS

8-1. Design the assigned problem of Table P8-1 (refer to Fig. P8-1). For this exercise take both columns and footings as square.

TABLE P8-1

	Column data						Footing data		
	w, mm	f_y, MPa	f_c, MPa	Number of bars, type	DL, kN	LL, kN	f_y, MPa	f'_c, MPa	q_a, kPa
a	460	400	28	10 #35	1,300	1,300	400	21	210
b	530	400	24	6 #30	900	1,250	400	21	170
c	360	400	24	4 #35	620	600	400	24	120
d	360	300	24	4 #30	450	580	400	28	200
e	460	300	28	6 #35	800	670	300	28	150

Partial answer:

	B, m	d, mm	A_s, mm²/m
a	3.60	640	1716 (0.0027)*
b	3.60	550	1608 (0.0029)*
c	2.30	346	1189 (0.0034)*

*( ) = p (d rounded to next mm)

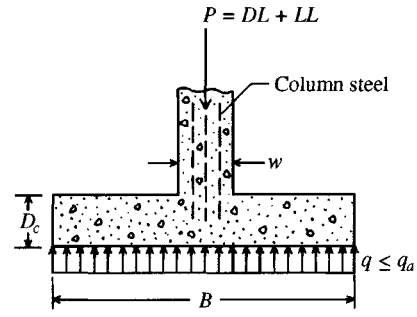

Figure P8-1

8-2. Use the data of Table P8-1 to design a rectangular footing using in all cases $L = 2.75$ m (input one dimension of footing).
Partial answers:

	$2.75 \times L$,	d, mm	$A_{s,\,long}$, mm²/m	$A_{s,\,short}$, mm²/m
a	4.60	682	2923	1363
c	3.70	414	1816	909
d	1.90	350(w-b)	1839	743

8-3. Use the data of Table P8-1 and design a footing if w = diameter.
Partial answers:

	w, mm	B, m	d, mm	A_s, mm²/m
a	460	3.60	747	1508
b	530	3.60	647	1409
e	460	3.20	478	1707

8-4. Design the base plate and pedestal for a W 310×86 column carrying $D = 450$ and $L = 490$ kN. Use $f_y = 250$ MPa steel for column and base plate, $f'_c = 24$ MPa psi for footing and pedestal, and Grade 400 reinforcing bars. The allowable soil pressure is 150 kPa. The pedestal is 1.40 m from the underside of the floor slab. Select two anchor bolts and draw a neat sketch of the column, plate, and anchor bolt locations.

8-5. Using the data of Problem 8-4, design a base plate for the column if it interfaces directly with the footing. Assume the footing is sufficiently large that the allowable concrete bearing stress $f_c = 0.7f'_c$.

8-6. Design the base plate and pedestal for a W 360 × 196 column carrying $D = 1400$ and $L = 1200$ kN. Use $f_y = 345$ MPa for column and base plate, and Grade 300 reinforcing bars. Use $f'_c = 28$ MPa for footing and pedestal and an allowable soil pressure $q_a = 200$ kPa. The pedestal is 1.90 m from underside of floor slab.

8-7. Design the footing and a column base plate for the W 360 × 196 column (no pedestal) data of Prob. 8-6.

8-8. Refer to Example 8-6. Redesign the base plate with the column axial load $P = 600$ kN and the moment $M = 120$ kN · m (instead of the 500 kN and 100 kN · m of the example).

8-9. Refer to Example 8-7. Take the pedestal dimensions at 700×700 mm and rework the example if four bolts that are centered on the heel (tension flange) are used. In the example the bolts are all put into the heel projection of the base plate. Be sure to check the bolt tension to see if it controls the plate thickness.

8-10. Rework Example 8-7 if the column moment $M = 190$ kN · m and all the other data are the same.

8-11. Rework Example 8-9 if the load and moment are increased 10 percent ($800D \times 1.1 = 880$; $800L \times 1.1 = 880$ kN, etc.). Assume the column dimensions are $AX = 0.60$ m and $AY = 0.40$ m. All other data such as f'_c, f_y, q_a, etc. are the same.

8-12. Rework Example 8-10 if the allowable soil pressure $q_a = 450$ kPa (*Remember:* It was set back from about 490^+ to 400). As in Prob. 8-11, assume a 10 percent increase in all loads and moments. *Hint:* The footing will continue to be square and $B' = L'$.

8-13. Design a wall footing for a concrete-block-wall building. The building has a 5-m-high wall; the footing is 1.2 m in the ground and has a plan area of 12 x 36 m. The roof will weigh about 0.9 kPa, and snow load is 1.5 kPa. The allowable soil pressure is 100 kPa, and about one-half of the building length (36 m) is on a fill of varying depth from 0 to 1.2 m.

8-14. Design a wall footing for a two-story office building of concrete block and brick veneer. The building is 16×30 m in plan. The footing is 1 m below ground. The first floor slab rests directly on the ground. Assume the floor dead load averages 2.0 kPa and live load 4.4 kPa. The roof is about 0.75 kPa, and snow is 1.0 kPa. Concrete blocks are $200 \times 300 \times 400$ mm and weigh 4.2 kPa (wall surface). Brick ($100 \times 200 \times 90$ mm) will weigh 1.9 kPa (wall surface). The undrained shear strength s_u may be taken as 60 kPa. *Hint:* estimate wall height.
Partial answer: $B \approx 1.6$ m

8-15. Design the foundation for a residence with approximately 135 m^2 of floor area. A perimeter wall will be used and a single interior post-on-pad. Assume wood frame, aluminum siding, and brick trim. Take snow load at 1.5 kPa. The floor plan is 9.80×13.8 m. Draw a building plan and place the post at a convenient location. Comment on the design as appropriate. You must assume or specify any missing data needed for your design.

CHAPTER 9

SPECIAL FOOTINGS AND BEAMS ON ELASTIC FOUNDATIONS

9-1 INTRODUCTION

This chapter will take up the design of several of the more complicated foundation members such as those required to support several columns in a line or from industrial loadings. Chapter 10 will be concerned with multiple lines of columns supported by mat or plate foundations.

When a footing supports a line of two or more columns, it is called a *combined footing*. A combined footing may have either rectangular or trapezoidal shape or be a series of pads connected by narrow rigid beams called a *strap footing*. We will also briefly consider footings for industrial applications, in particular the round (actually octagonal) footing widely used in the petrochemical industry. These several footing types are illustrated in Fig. 9-1.

Combined footings similar to that shown in Fig. 9-1*f* are fairly common in industrial applications using wide rectangular supports for horizontal tanks and other equipment. In these cases, operational loads, differential temperatures, cleaning operations, and the like can result in both vertical and horizontal loads. The horizontal loads at the equipment level produce support moments that must be resisted by the combined footing.

Both the conventional "rigid" and the beam-on-the-foundation method of combined footing analysis will be presented. The latter method requires a computer program for maximum design efficiency. A reasonably complete program for this type of analysis is included as B-5 (FADBEMLP) on your diskette.

9-2 RECTANGULAR COMBINED FOOTINGS

It may not be possible to place columns at the center of a spread footing if they are near the property line, near mechanical equipment locations, or irregularly spaced. Columns located off-center will usually result in a nonuniform soil pressure. To avoid the nonuniform soil pressure, an alternative is to enlarge the footing and place one or more of the adjacent columns in the same line on it (Fig. 9-2). The footing geometry is made such that the resultant of the

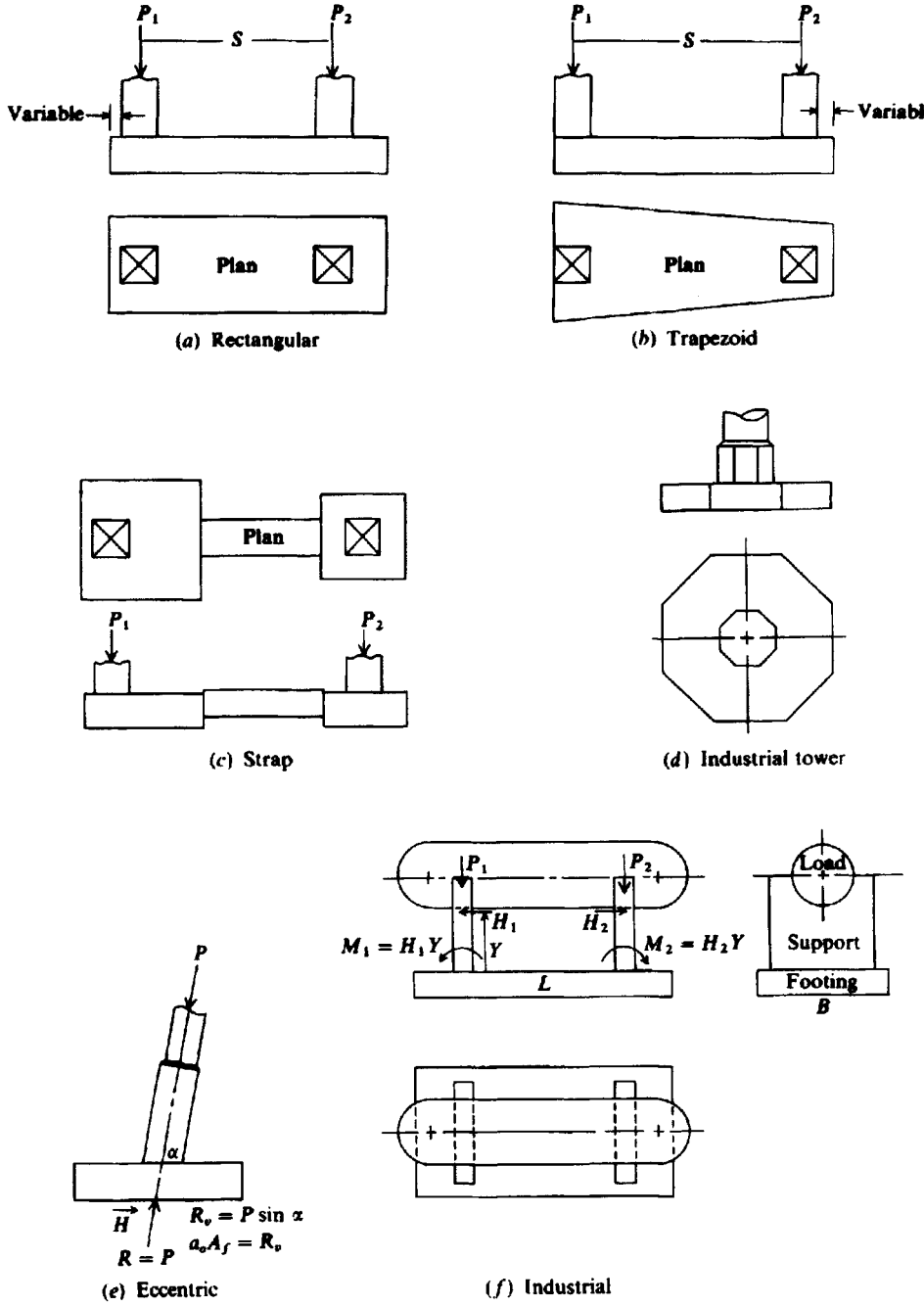

Figure 9-1 Typical special footings considered in this chapter.

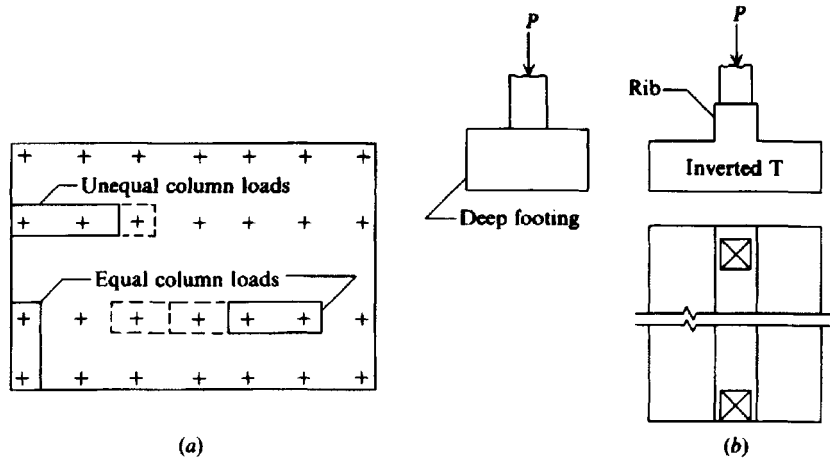

Figure 9-2 (*a*) Typical layout of combined footings for column loads as shown; more than two columns can be used. (*b*) Deep footings for heavy loads and the use of a rib or inverted T beam to reduce footing mass.

several columns is in the center of the footing area. This footing and load geometry allows the designer to assume a uniform soil pressure distribution. The footing can be rectangular if the column that is eccentric with respect to a spread footing carries a smaller load than the interior columns. Bridge piers are also founded on very rigid combined rectangular footings.

The basic assumption for the design of a rectangular combined footing is that it is a rigid member, so that the soil pressure is linear. The pressure will be uniform if the location of the load resultant (including column moments) coincides with the center of area. This assumption is approximately true if the soil is homogeneous and the footing is rigid. In actual practice it is very difficult to make a rigid footing, for the thickness would have to be great; nevertheless, the assumption of a rigid member has been successfully used for many foundation members. Success has probably resulted from a combination of soil creep, concrete stress transfer, and overdesign.

In recognition of the overdesign using the conventional (or "rigid") method, current practice tends to modify the design by a beam-on-elastic-foundation analysis. This produces smaller design moments than those obtained by the rigid method, as will be illustrated later.

The conventional (or rigid) design of a rectangular combined footing consists in determining the location of the center of footing area. Next the length and width can be found. With these dimensions the footing is treated as a beam supported by the two or more columns, and the shear and moment diagrams are drawn. The depth, based on the more critical of two-way action or wide-beam shear, is computed. Critical sections for two-way action and wide-beam shear are the same as for spread footings, i.e., at $d/2$ and d, respectively, from the column face. It is common practice not to use shear reinforcement, both for economy and so that a larger footing thickness is required for greater rigidity. The labor costs to bend and place the shear reinforcement are likely by far to exceed the small savings in concrete that would result from its use.

With the depth selected, the flexural steel can be designed using the critical moments from the moment diagram. Alternatively, the depth and loading can be used in a finite-element analysis to obtain modified moments for the flexural steel. These beam-type members usually have both positive and negative moments, resulting in reinforcing steel in both the top and bottom of the footing. The minimum percentage of steel should be taken as $1.4/f_y$ since the

footing is designed as a "beam" or flexural member. Footings with negative (or top) steel are not economical, so oversized spread footings should be used if possible.

If we compute the short, or transverse, direction bending moments as for a rectangular spread footing, they will be in substantial error. The reason is the soil pressure is larger near the columns, from their stiffening effect on the footing, and lesser in the zone between columns. That zone closest to, and approximately centered on, the column is most effective and should be analyzed somewhat similarly to the ACI Code requirement for rectangular footings. The Code does not directly specify this effective column zone width, but based on inspection of a number of computer printouts using both the finite-difference and finite-element methods the author suggests that the effective zone should be about as shown in Fig. 9-3. Note that as the width of this zone decreases its rigidity increases from the additional reinforcing bars that are required. The increased rigidity will tend to attract moment from the zone between columns but would be difficult to predict since the moment of inertia based on D_c, rather than either the transformed section or effective moment of inertia, is commonly used in finite-element/difference analyses. Making the effective zone reasonably narrow should ensure adequate steel is used to take care of any additional "attracted" moment.

The conventional design method requires computing shears and moments at sufficient locations that a shear and moment diagram can be drawn. It is also standard practice to round computed dimensions to multiples of 75 mm or 0.25 ft. If this is done prior to computing shear and moment diagrams there will be a closure error that depends on the amount the length is changed; thus, it is recommended that footing dimensions be rounded as the final design step.

The column loads are actually distributed over the column width as shown in Fig. 9-4 but should always be taken as point loads. This assumption greatly simplifies the shear and moment computations, and the values at the critical locations are the same by either method.

It should be self-evident that combined footings are statically determinate for any number of columns. With the column loads known and assuming a rigid footing, the resulting soil pressure $q = \sum P/A$. The problem then becomes that of a uniformly loaded continuous beam with all the reactions (the columns) known.

Figure 9-3 Steel for rectangular combined footing. Note the several values of d. Steel in zone a satisfies minimum code requirements, in b satisfies both bending and minimum code requirements.

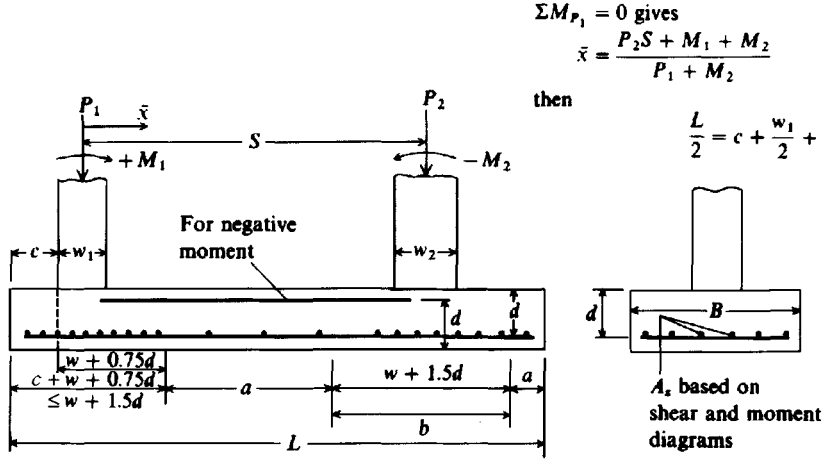

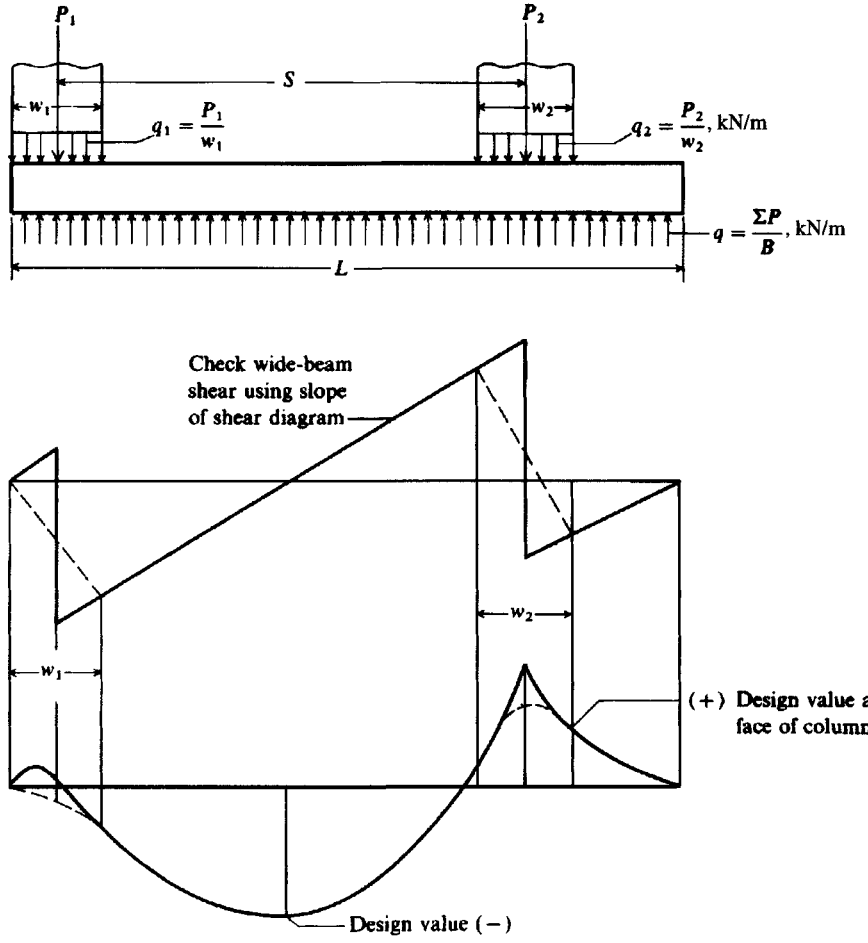

Figure 9-4 Shear and moment diagrams (qualitative) for a combined footing considering the column loads as point loads and as distributed loads (dashed line). It can be seen that in the design areas it makes no difference how the diagrams are drawn, and the point load case is much simpler.

Example 9-1. Design a rectangular combined footing using the conventional method.

Given. $f_c' = 21$ MPa (column and footing) $f_y =$ Grade 400 $q_a = 100$ kPa

Column number	Working loads					P_u, kN	M_u, kN · m
	DL	*LL*, kN	M_D	M_L	*P*		
1	270	270	28	28	540	837	86.8
2	490	400	408	40	890	1366	124
				Total	1430	2203	

Ultimate values = $1.4DL + 1.7LL$, etc.

$$\text{Soil}: \quad q_{ult} = \frac{\sum P_u}{\sum P} q_a = \frac{2203}{1430}(100) = \mathbf{154.1}\ \text{kPa}$$

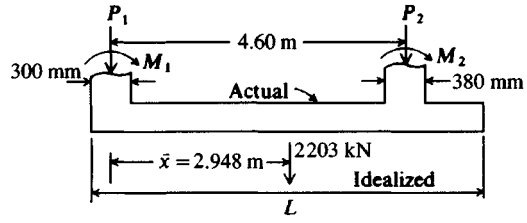

Figure E9-1*a*

It is necessary to use q_{ult} so base eccentricity is not introduced between computing L using q_a and L using q_{ult}.

Solution.

Step 1. Find footing dimensions.

$$\sum M_{col.1} = R\bar{x} \qquad \text{where} \qquad R = \sum P_u = 837 + 1366 = 2203 \text{ kN}$$

For uniform soil pressure R must be at the centroid of the base area (problem in elementary statics), so we compute

$$R\bar{x} = M_1 + M_2 + SP_{ult,2}$$
$$2203\bar{x} = 86.8 + 124.0 + 4.60(1366)$$
$$\bar{x} = \frac{6494.4}{2203} = 2.948 \text{ m}$$

It is evident that if $\bar{x}$ locates the center of pressure the footing length is

$$L = 2 \times (\tfrac{1}{2} \text{ width of col. } 1 + \bar{x}) = 2 \times (0.150 + 2.948) = \mathbf{6.196} \text{ m}$$

Also for a uniform soil pressure $q_{ult} = 154.1$ kPa, the footing width B is computed as

$$BLq_{ult} = P_{ult}$$
$$B = \frac{2203}{6.196 \times 154.1} = \mathbf{2.307} \text{ m}$$

We will have to use these somewhat odd dimensions in subsequent computations so that shear and moment diagrams will close. We would, however, round the dimensions for site use to

$$L = \mathbf{6.200} \text{ m} \qquad B = \mathbf{2.310} \text{ m}$$

Step 2. Obtain data for shear and moment diagrams (or at critical locations). Use any convenient method, e.g., calculus, as

$$V = \int_{x_1}^{x_2} q(dx)$$

$$M = \int_{x_1}^{x_2} V(dx) \qquad \text{with attention to values at the limits}$$

Since calculations for the conventional design of a combined footing involve an enormous amount of busywork (with potential for errors) it is preferable to use a computer program such as B-15 (see supplemental program list on your diskette in file README.DOC). This has been done by the author to obtain the accompanying printout (Fig. E9-1*b*) to which reference will be made with the design steps following.

Step 3. From critical shear find the depth for wide-beam and two-way action. Note that columns may have either a four- (case 1) or three-side (case 2) two-way action perimeter. The computer

```
++++++++++++ NAME OF DATA FILE USED FOR THIS EXECUTION:  EXAM91.DTA

  EXAMPLE 9-1 FOUND. ANALY. AND DESIGN--SI UNITS
FOOTING DESIGN INPUT DATA IS AS FOLLOWS:
COL NO   WIDTH x LEN,  M   LOAD,   KN   MOMENT, KN-M  COL SPAC, M
 1       .300 X   .300         837.0         86.8
                                                          4.600
 2       .380 X   .380        1366.0        124.0

     DIST END FTG TO LT FACE COL 1 =    .000  M
          INPUT FOOTING WIDTH, BF =    .000  M
            LENGTH INCREMENT, DX, =    .500  M
  THE FACTORED ALLOW SOIL PRESSURE = 154.10 KPA

CONCRETE AND STEEL STRESSES:    F1C =     21.0 MPA
                                FY =    400.0 MPA

COMPUTED FOOTING DIMENSIONS:  WIDTH =   2.307  M
                             LENGTH =   6.196  M
                LENGTH/WIDTH RATIO =  2.685
              UNIFORM LOAD ALONG FTG =  355.554 KN/M

 MAX WIDE BEAM SHEAR AT LEFT  FACE COL  2 =   784.327   KN
      DEPTH OF CONCRETE FOR WIDE BEAM = 423.172 MM
                 ALLOW WIDE BEAM SHEAR =    .649 MPA

 DEPTH OF CONCRETE FOR CASE 1 @ COL 1 =    .000 MM(  1.298 MPA)
DEPTH OF CONCRETE FOR CASE 1 @ COL  2 = 342.565 MM
 DEPTH OF CONCRETE FOR CASE 2 @ COL 1 = 369.707 MM(  1.298 MPA)
DEPTH OF CONCRETE FOR CASE 2 @ COL  2 = 225.748 MM

++++++++++++ DEPTH OF CONCRETE USED FOR DESIGN = 423.172 MM

+++ AS = TOTAL STEEL AREA FOR FTG IN WIDTH BF =   2.307  M
DISTANCE
FROM END              SHEAR          MOMENT,KN-M          AS, M**2

    .00LF               .00              .00          .0000E+00*
    .15CL             53.33             4.00          .2626E-04*
    .15CR           -783.67            90.80          .6002E-03*
    .30RF           -730.33           -22.75          .1496E-03*
    .50             -659.22          -161.71          .1075E-02*
   1.00             -481.45          -446.87          .3039E-02*
   1.50             -303.67          -643.15          .4449E-02
   2.00             -125.89          -750.54          .5242E-02
   2.35MM              .00           -772.83          .5409E-02 √
   2.50              51.89           -769.04          .5380E-02
   3.00             229.66           -698.66          .4857E-02
   3.50             407.44           -539.38          .3697E-02
   4.00             585.22           -291.22          .1955E-02*
   4.50             762.99             45.84          .3019E-03*
   4.56LF           784.33             92.26          .6099E-03*
   4.75CL           851.88            247.70          .1657E-02*
   4.75CR          -514.12            371.70          .2512E-02*
   4.94RF          -446.56            280.43          .1881E-02*
   4.50            -603.01            169.84          .1129E-02*
   5.00            -425.23            254.28          .1702E-02*
   5.50            -247.45             86.11          .5689E-03*
   6.00             -69.67              6.83          .4483E-04*
   6.20                .00               .00          .0000E+00*

** = AS > ASMAX--INCREASE D;  * = AS < ASMIN--USE ASMIN

MAX % STEEL = .0171 %    MAX STEEL AREA = .1667E-01 M**2
MIN % STEEL = .0035 %    MIN STEEL AREA = .3417E-02 M**2

TRANSVERSE STEEL IN COLUMN ZONES OF WIDTH BPR FOR DEPTH DCP =  385.17 MM

COL #   PRESS,DQ   ARM, M  WIDTH,BPR, M   AS, M**2   ASMAX    ASMIN, M**2
 1       362.76     1.004       .617        .1412E-02 .4059E-02 .8323E-03
 2       592.04      .964      1.015        .2110E-02 .6672E-02 .1368E-02

   STEEL AREAS FOR WIDTH BPR--IF AS < ASMIN USE ASMIN
```

Figure E9-1*b*

program routinely checks wide-beam and both cases 1 and 2 for each column with depths printed for checking and then selects the largest d for the design value. We see here wide-beam shear controls giving $d = 423.172$ mm on the computer printout.

When wide-beam shear controls d, it may not be necessary to check ACI Eq. (11-36) or (11-37) since the limiting value of two-way shear v_c equals the wide-beam value of $2\phi\sqrt{f_c'}$. It may, however, be necessary to compare the "wide-beam" distances. That is, which is the larger distance, the two-way perimeter of the end (or corner column) or the wide-beam width?

Here the perimeter p_O is calculated as

$$\begin{aligned} p_O &= 0.300 + 0.432 + 0.300 + 0.300 + 2(0.432)/2 \\ &= 1.764 \text{ m} < B = 2.307 \end{aligned}$$

By ACI Eq. (11-37) the allowable two-way shear stress is:

$$\left(\frac{\alpha_s d}{b_o} + 2\right)\phi\sqrt{f_c'} = \left(\frac{30(0.432)}{1.764} + 2\right)\phi\sqrt{f_c'} = 9.35\phi\sqrt{f_c'} \gg 4\phi\sqrt{f_c'}$$

With the column being square, the two-way shear stress is the smaller of these $= 4\phi\sqrt{f_c'}$. Since the column width $w \ll 4d[0.3 \ll 4(0.432)]$, it is evident that the depth will be controlled by wide-beam shear, with the allowable v_c obtained directly from Table 8-2 and using a beam width of $B = 2.307$ m. It is instructive, however, for the reader to make the two-way shear check at least one time.

Step 4. Find the steel for bending. There will be both (+)-bending steel in the bottom of the footing near columns and (−)-bending steel in the top near or in the center portion between columns. Note the signs in the computer printout. The required steel area at each moment location including the maximum (MM) is output. For convenience the program also computes the maximum allowable amount of steel based on p_b (here, 16,670 mm^2, which is far in excess of the A_s required for the largest moment location of 5409 mm^2) and the minimum ACI Code requirement based on $1.4/f_y$, giving 3417 mm^2. Notice that the minimum of 3417 mm^2 controls the bottom longitudinal reinforcing bars since it is larger than any of the A_s values computed for the (+) moments. For longitudinal steel we will use the following:

Top bars :	twenty No. 20 bars (20×300) = **6000** mm^2(5409 required)
Bottom bars :	twelve No. 20 bars (12×300) = **3600** mm^2(3417 required)

We should run all the (−) (or top) bars the full length of the footing, for trying to cut them and satisfy Code requirements for extra length beyond the theoretical is not worth the extra engineering and bar placing effort. We should run about one-half (six bars) of the (+) (or bottom) bars (in the right end zone) all the way as well so that the transverse bars can be supported.

Step 5. Design the transverse steel (refer to Fig. 9-3 for the effective base widths). We will adjust the depth $d = 0.4232 - 0.038$ (approximately 1.5 × No. 25 bar) giving for transverse steel a $d = 0.385$ m for bending. But we will use the initial d for column zone widths.

$$\textbf{Column 1}: \quad B_1' + w + 0.75d = 0.30 + 0.75(0.4232) = 0.6174 \rightarrow \textbf{0.62} \text{ m}$$

The soil pressure in this reduced zone (and rounding $B = 2.31$ m; $L = 0.620$ m) is

$$q_{ult} = \frac{P_{ult}}{B \times B'} = \frac{837}{2.31 \times 0.62} = \textbf{584.4} \text{ kPa} \qquad (587.6 \text{ computer})$$

The effective moment arm is

$$L_1' = \frac{B - w}{2} = \frac{2.31 - 0.30}{2} = 1.01 \text{ m } (1.015)$$

The resulting M_u is

$$M_u = \frac{q_{ult}(L_1')^2}{2} = \frac{584.4(1.01)^2}{2} = \mathbf{298.1}\ \text{kN} \cdot \text{m}$$

For $f_c' = 21$ MPa and $f_y = 400$ MPa, we find that

$$a = \frac{f_y A_s}{0.85 b f_c'} = 22.4 A_s$$

The required steel area in this zone, which is 0.62 m wide, is

$$A_s\left(d - \frac{a}{2}\right) = \frac{M_u}{\phi F_y}$$

$$A_s(0.385d - 22.4A_s/2) = 298.1/(0.9 \times 400 \times 1000)$$

$$11.2A_s^2 - 0.385A_s = 0.000\,828$$

$$A_s = 0.002\,30\ \text{m}^2/\text{m} = 2300\ \text{mm}^2/\text{m}$$

The zone width = 0.62 m, so the required A_s is

$$A_s = 2400(0.62/1)$$

$$= \mathbf{1488}\ \text{mm}^2 \text{ in zone}$$

$$= 1412\ \text{mm}^2 \text{ (by computer)}$$

Use five No. 20 bars, giving $A_s = 5(300) = 1500\ \text{mm}^2 > 1488$. With five bars there will be four spaces, so that

$$s = 620/4 = 155\ \text{mm} > d_b \text{ (Art.7.6)} \qquad \text{O.K.}$$

Column 2: $L_2' = \dfrac{2.31 - 0.380}{2} = \mathbf{0.965}\ \text{m}$

The effective width $B' = w + 1.5d = 0.380 + 1.5(0.4232) = 1.01$ m.

$$q_{ult} = \frac{P_{ult}}{B \times B'} = \frac{1366}{1.01 \times 2.31} = 585.5\ \text{kPa} \qquad (583.4 \text{ computer})$$

$$M_u = \frac{585.5 \times 0.965^2}{2} = 272.6\ \text{kN} \cdot \text{m}$$

$$11.2A_s^2 - 0.385A_s = 272.6/(0.9 \times 400 \times 1000)$$

$$A_s^2 - 0.0344A_s + 0.000\,0676 = 0$$

$$A_s = 0.002\,17\ \text{m}^2/\text{m} \rightarrow 2100\ \text{mm}^2/\text{m}$$

Here we have a zone width of 1.01, so by proportion

$$A_s = 2100(1.01/1.) = \mathbf{2121}\ \text{mm}^2 \text{ for width (2110 computer)}$$

Use eight No. 20 bars $\rightarrow A_s = 8(300) = 2400\ \text{mm}^2 > 2121$. The spacing will satisfy ACI Art. 7.6.

Use T and S steel for the remainder of the short side [$p = 0.0018$ since $f_y = 400$ MPa (Art. 7.12.2.1)]. One might also consider using $1.4/f_y$ of Art. 10.5. The difference is

$$\text{T and S} = 0.0018 \qquad 1.4/400 = 0.0035$$

Compute the total depth (use 50 mm top and 70 mm bottom of clear cover), or

$$D_c = d + \text{bottom bar}/2 + 70 + \text{top bar}/2 + 50$$

$$= 432 + 10 + 70 + 10 + 50 = \mathbf{572}\ \text{mm}$$

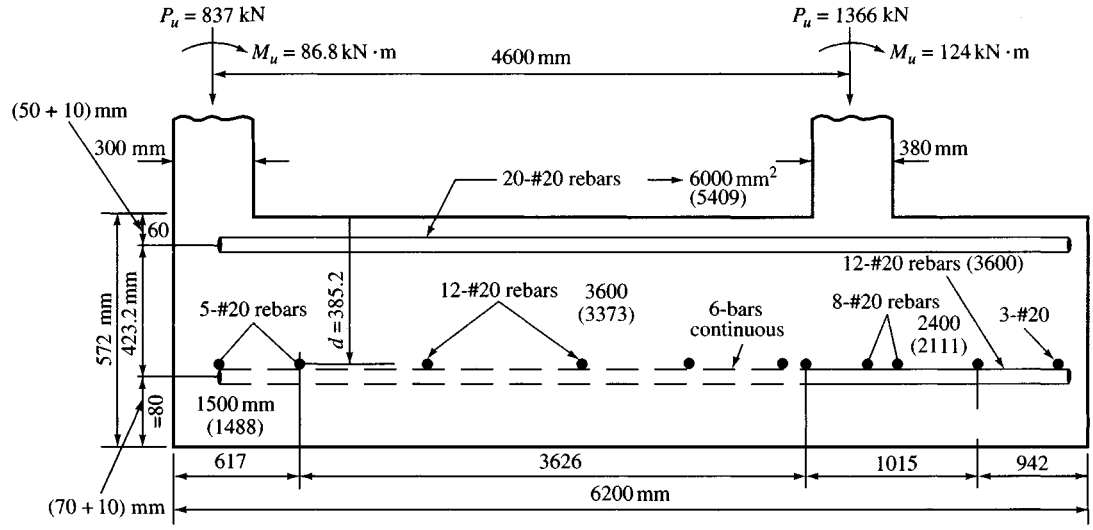

Final design

Figure E9-1*c*

Using 0.0018 × gross area

$$\text{Interior zone} = 0.0018(3626)(572) = 3373 \text{ mm}^2$$
$$\text{Right end zone} = 0.0018(942)(572) = 970 \text{ mm}^2$$

Note: The ACI code specifies the ratio × gross area. Some designers use gross area as width × d whereas others use width × D_c (the total depth). Clearly, using the total depth D_c is conservative.

Step 6. Check columns bearing on the base. At column 1 the area ratio $\sqrt{A_2/A_1} = 1$, and will probably require dowels to assist in transfer of column load into the footing. Column 2 has an area ratio = 2 and should only require the minimum of $0.005A_{col}$ to tie the column to the footing.

Step 7. Prepare a final design sketch as in Fig. E9-1*c* so that the final drawings can be made and the footing constructed. Note these features:

1. Transverse steel uses a different d from longitudinal steel. Here we used 38 mm less (actual reduction is 20 mm). The result is conservative. Note that except for the column zones, T and S steel controls.
2. Top (−) steel uses the same d as (+) bottom steel.
3. Bottom steel clear distance is 70 mm (concrete poured directly on ground).
4. Top steel clear distance is 50 mm (concrete not poured on ground but may be in contact with soil).

////

9-3 DESIGN OF TRAPEZOID-SHAPED FOOTINGS

A combined footing will be trapezoid-shaped if the column that has too limited a space for a spread footing carries the larger load. In this case the resultant of the column loads (including moments) will be closer to the larger column load, and doubling the centroid distance as done for the rectangular footing will not provide sufficient length to reach the interior column. The

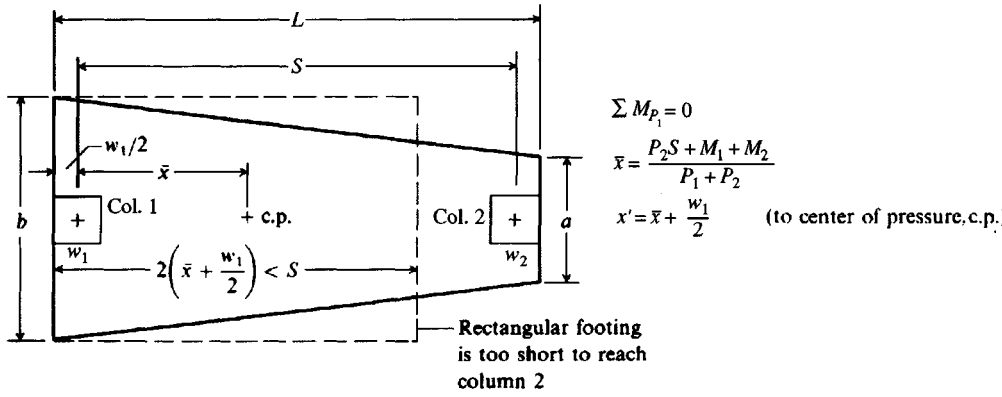

Figure 9-5 A trapezoidal footing is required in this case unless the distance S is so great that a cantilever (or strap) footing would be more economical.

footing geometry necessary for a two-column trapezoid-shaped footing is illustrated in Fig. 9-5 from which we obtain

$$A = \frac{a+b}{2}L \tag{9-1}$$

$$x' = \frac{L}{3}\frac{2a+b}{a+b} \tag{9-2}$$

From Eq. (9-2) and Fig. 9-5 we see that the solution for $a = 0$ is a triangle, and if $a = b$ we have a rectangle. Therefore, it follows that a trapezoid solution exists only for

$$\frac{L}{3} < x' < \frac{L}{2}$$

with the minimum value of L as out-to-out of the column faces. In most cases a trapezoid footing would be used with only two columns as illustrated, but the solution proceeds similarly for more than two columns. The forming and reinforcing steel for a trapezoid footing is somewhat awkward to place. For these reasons it may be preferable to use a strap footing (next section) where possible, since essentially the same goal of producing a computed uniform soil pressure is obtained.

With x' falling at a particular location and defining the center of area, the dimensions a and b have unique values that require a simultaneous solution of Eqs. (9-1) and (9-2). The value of L must be known, and the area A will be based on the soil pressure and column loads ($A = \sum P/q_o$ or $\sum P_u/q_{ult}$).

When the end dimensions a and b are found, the footing is treated similarly to the rectangular footing (as a beam) except that the "beam" pressure diagram will be linear-varying (first-degree) because a and b are not equal. The resulting shear diagram is a second-degree curve and the moment diagram is a third-degree curve. Calculus is a most efficient means to obtain critical ordinates for these diagrams and to treat the columns as point loads. A trapezoid-shaped footing can also be analyzed as a beam on an elastic foundation, only in this case the finite-element widths are average values.

Example 9-2. Proportion and partially design a trapezoidal footing for the given data:

$f'_c = 21$ MPa $\quad f_y = 400$ MPa (grade 400 rebars) $\quad q_a = 190$ kPa

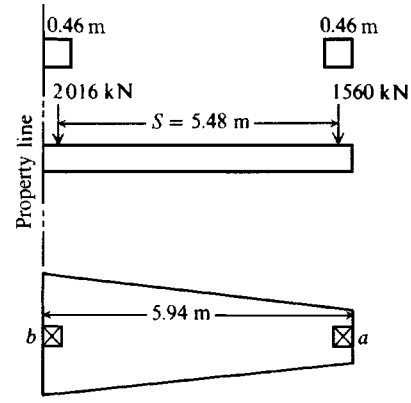

Figure E9-2*a*

Column	*DL*	*LL*	*P*, kN	P_{ult}, kN
1	1200	816	2016	3067.2 (1.4*D*+1.7*L*)
2	900	660	1560	2382.0
		Total	3576	5449.2

$$\text{Soil}: \quad q_{ult} = \frac{P_{ult}}{P}(q_a) = \frac{5449.2}{3576}(190) = \mathbf{289.5}\ \text{kPa}$$

There is much busywork with designing a trapezoid footing, so the only practical modern method is to use a computer program such as B-16.

Solution

Step 1. Find the end dimensions a and b of Fig. E9-2*a*.

First locate the center of area by taking moments through center of col. 1:

$$5449.2\bar{x} = 5.48[1.4(900) + 1.7(660)]$$

$$\bar{x} = \frac{13\,053.4}{5449.2} = 2.395\ \text{m} \qquad \text{and} \qquad x' = 2.395 + \frac{0.46}{2} = 2.625\ \text{m}$$

$$L = 5.48 + 2\frac{(0.46)}{2} = \mathbf{5.94}\ \text{m}$$

Since $L/2 > x' > L/3$ we have a trapezoid. From Eq. (9-1) the area is

$$A = \frac{a+b}{2}L = \frac{a+b}{2}(5.94)$$

but based on q_{ult} and the footing loads,

$$A = \frac{5449.2}{289.5} = 18.823\ \text{m}^2$$

Equating these two A-values, we have

$$\frac{a+b}{2}(5.94) = 18.823 \qquad a + b = \mathbf{6.338}\ \text{m}$$

From Eq. (9-2) and $x' = 2.625$ m,

$$x' = \frac{L}{3}\frac{2a+b}{a+b}$$

$$\frac{2a+b}{a+b} = \frac{3(2.625)}{5.94} = 1.326 \text{ m}$$

but $a + b = 6.338$, from which $b = 6.338 - a$ and substituting for both,

$$\frac{2a + 6.338 - a}{6.338} = 1.326 \text{ m}$$

$$a = \mathbf{2.065} \text{ m}$$

$$b = 6.338 - 2.065 = \mathbf{4.273} \text{ m}$$

One should routinely back-substitute a and b into Eq. (9-1) and compare A.

Step 2. Draw shear and moment diagrams:

$$\text{Pressure big end} = 4.273(289.5) = 1237.03 \text{ kN/m}$$

$$\text{Pressure small end} = 2.065(289.5) = 597.82 \text{ kN/m}$$

$$\text{Slope of the pressure line } s = (1237.0 - 598.0)5.94 = \mathbf{107.6} \text{ kN/m}^2$$

$$q = 1237 - 107.6x$$

$$V = \int_0^x q\,dx = 1237.0x - 107.6\frac{x^2}{2} + C$$

At $x = 0.23$ m, $C = 0$: $V = 1237.0(0.23) - 53.8(0.23)^2 = 282$ kN
At $x = 0.23 + dx$, $C = -3067$: $V = 282 - 3067 = -2785$ kN
At column 2, $x = 5.71$, $C = -3067$: $V = 2242$ kN
And at $x = 5.71 + dx$: $V = -140$ kN

Values of shear at the interior faces of columns 1 and 2 are 2509.4 and 2096.1 kN, respectively (rounded values shown in Fig. E9-2*b*). The maximum moment occurs where the shear diagram is zero (which should be somewhere between cols. 1 and 2), giving

$$V = \int_0^x q(dx) + C_1 = 0$$

Integrating, inserting q and using $P_u = -3067$ kN (col. 1) $= C_1$ we obtain

$$V = 1237.0x - 107.6x^2/2 - 3067 = 0$$

Solving, we find $x = 2.828$ m from left end. Moments are computed similarly,

$$M = \int_0^x V dx = 1237.0\frac{x^2}{2} - 107.6\frac{x^3}{6} - C_1 x''$$

At $x = 0.23$ and x'' = distance from previous discontinuity = 0,

$$M = 32.0 \text{ kN} \cdot \text{m}$$

At the right face of column 1, $M = -576.0$ kN · m. Maximum m is at $x = 2.828$ m, so

$$M = 4946.5 - 405.6 - 3067(2.828 - 0.23) = -3429 \text{ kN} \cdot \text{m}$$

At the left face of column 2, $M = -479$ kN · m. These values are sufficient to draw the shear and moment diagrams of Fig. E9-2*b*.

Step 3. Find the depth for wide-beam shear at the small end and check two-way action at the large end. The reasoning is

$$\frac{V_b}{V_s} = \frac{2509}{2096} = 1.2 \qquad \frac{b}{a} = \frac{4.27}{2.06} = 2.07 \gg 1.2$$

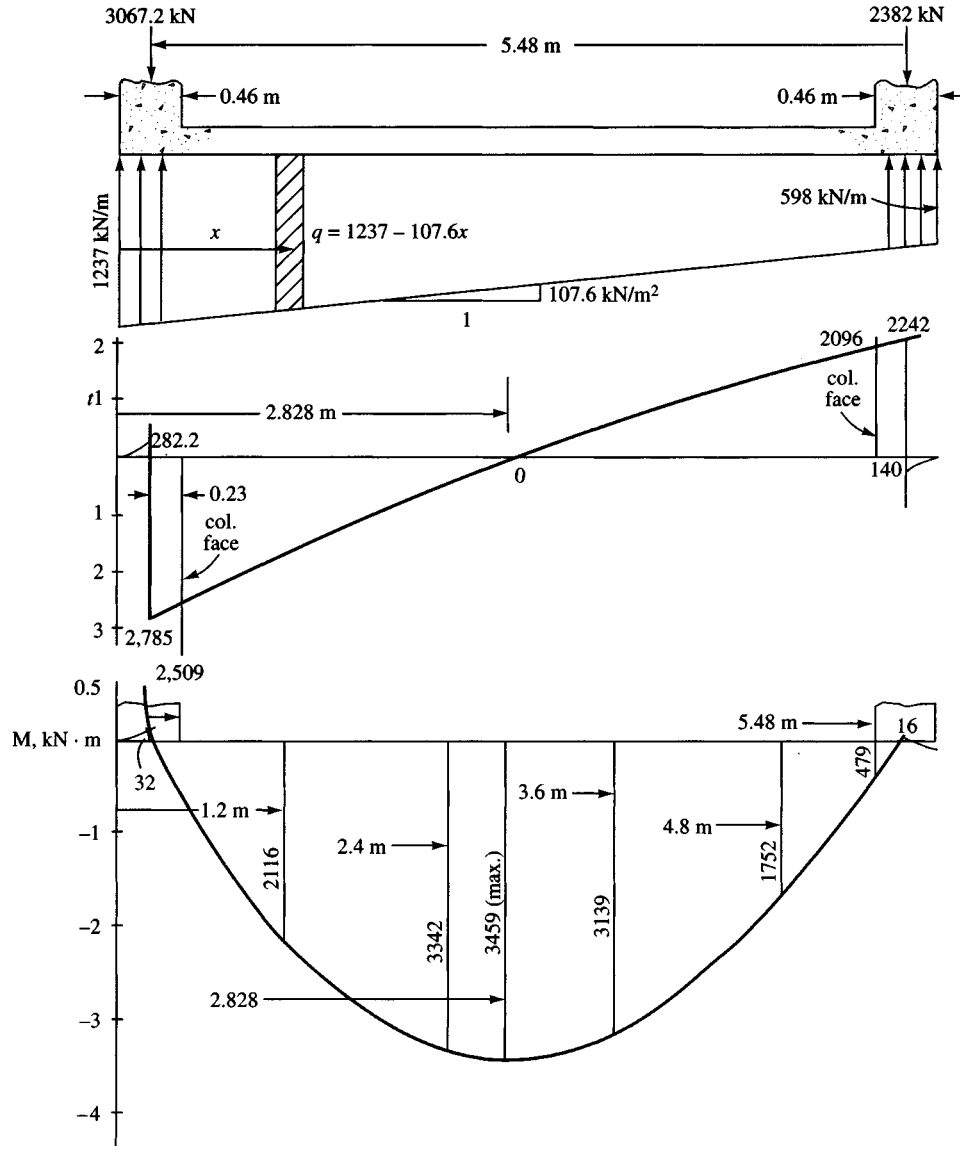

Figure E9-2*b*

Since the width ratio is much larger than the shear ratio, d will probably be based on wide-beam shear at the small end.

$$V = 1237.0x = 107.6\frac{x^2}{2} - 3067 \qquad \text{where} \qquad x = 5.48 - d \qquad \text{(from big end)}$$

$$= 2096 - 647d - 53.8d^2 \qquad \text{(net shear at section at } d \text{ from left face of col. 2)}$$

$$\text{Width} = 2.065 + \frac{4.27 - 2.06}{5.94}(d + 0.46)$$

$$= 2.065 + 0.372d + 0.17 = 2.24 + 0.372d$$

$$v_c = 0.649 \text{ MPa} = 649 \text{ kPa} \quad \text{(Table 8-2)}$$

Equating concrete shear to external shear $(2.24 + 0.372d)d(649) = 2096 - 647d - 53.8d^2$,

$$295d^2 + 2103d = 2096 \qquad d^2 + 7.1d = 7.1 \qquad d = \mathbf{0.89}\text{ m}$$

Two-way action at the large end (not possible to check at small end) requires $d = 0.75$ m. Actually, when wide-beam shear "d" is used it is not necessary to check ACI two-way action since the minimum two-way shear is $2\phi\sqrt{f_c'}$ = wide-beam v_c.

Step 4. Design the flexural steel. Since the width varies, one should check A_s for several locations, resulting in the following table. This table was obtained from a computer printout and there are slight discrepancies between hand and computer computations resulting from rounding for hand computations.

x	V, kN	M, kN · m	w, m	A_s, cm²/m
0	0	0	4.27	0.0
0.6	−2344.6	−916.1	4.05	$6.9 \times 100 = 690$ mm²/m
1.2	−1660.6	−2115.8	3.83	17.0
1.8	−1015.4	−2916.6	3.60	25.2
2.4	−408.9	−3342.0	3.38	31.0
2.828 (max)	0.0	−3428.7	3.22	$33.5 \times 100 = 3350$ mm²/m
3.0	+159.0	−3415.0	3.16	34.1
3.6	688.1	−3159.0	2.94	33.9
4.8	1630.3	−1752.4	2.49	$21.8 \times 100 = 2180$ mm²/m
5.94	0.0	0.0	2.07	0.0

The max. steel = 144.2 cm²/m (based on Table 8-1 and computer printout)
The min. steel = 29.6 cm²/m based on $1.4/f_y$

Step 5. Steel in short direction. Treat same as rectangular footing using appropriate zone of $w + 0.75d$, since columns are at end of footing. Use the average width of footing in this zone for bending, for example, at large end:

$$w + 0.75d = 0.46 + 0.75(0.89) = 1.12\text{ m}$$

$$B_1 = 4.27 \qquad B_2 = 4.27 - 1.12\frac{4.27 - 2.07}{5.94} = 3.85$$

$$\text{Average}: \quad w = \frac{4.27 + 3.85}{2} = \mathbf{4.06}\text{ m}$$

$$L' = \frac{4.06 - 0.46}{2} = \mathbf{1.8}\text{ m}$$

$$M = \frac{289.5}{2}1.8^2 = \mathbf{469}\text{ kN} \cdot \text{m}$$

The remainder of the problem is left for the reader.

////

9-4 DESIGN OF STRAP (OR CANTILEVER) FOOTINGS

A strap footing is used to connect an eccentrically loaded column footing to an interior column as shown in Fig. 9-6. The strap is used to transmit the moment caused from eccentricity to the interior column footing so that a uniform soil pressure is computed beneath both footings. The strap serves the same purpose as the interior portion of a combined footing but is much narrower to save materials. Note again in Fig. 9-6 that the resultant soil pressure is assumed at the centers of both footings so that uniform soil pressure diagrams result. They may not be equal, however.

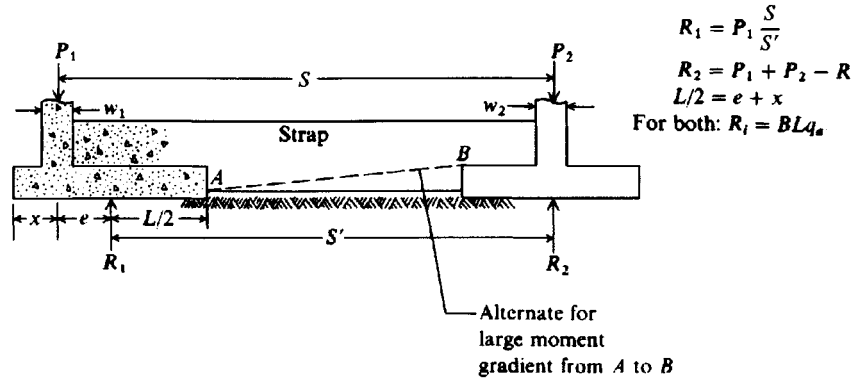

Figure 9-6 Assumed loading and reactions for a strap footing design. Make strap width about the same as the smallest column w.

The strap footing may be used in lieu of a combined rectangular or trapezoid footing if the distance between columns is large and/or the allowable soil pressure is relatively large so that the additional footing area is not needed. Three basic considerations for strap footing design are these:

1. Strap must be rigid—perhaps $I_{strap}/I_{footing} > 2$ (based on work by the author). This rigidity is necessary to control rotation of the exterior footing.
2. Footings should be proportioned for approximately equal soil pressures and avoidance of large differences in B to reduce differential settlement.
3. Strap should be out of contact with soil so that there are no soil reactions to modify the design assumptions shown on Fig. 9-6. It is common to neglect strap weight in the design. Check depth to span (between footing edges) to see if it is a deep beam (ACI Art. 10-7).

A strap footing should be considered only after a careful analysis shows that spread footings—even if oversize—will not work. The extra labor and forming costs for this type of footing make it one to use as a last resort. Again, it is not desirable to use shear reinforcement in either the two footings or the strap so that base rigidity is increased.

The strap may have a number of configurations; however, that shown in Fig. 9-6 should produce the greatest rigidity with the width at least equal to the smallest column width. If the depth is restricted, it may be necessary to increase the strap width to obtain the necessary rigidity. The strap should be securely attached to the column and footing by dowels so that the system acts as a unit.

The strap dimensions to provide adequate rigidity may be most conveniently determined using a beam-on-elastic-foundation computer program such as your diskette program B-5. One would input sufficient data to define the footing and strap stiffness (EI/L) and the program should have an option for no soil reactions against the strap. One then makes a solution and checks the displacement profiles of the two footings. If they are nearly constant across the footing, the strap is sufficiently thick. If there is a nearly linear variation of the displacements, the strap is not rigid enough and is allowing the footing to rotate.

The equations shown in Fig. 9-6 are used to proportion the footing dimensions. The length dimension of the eccentrically loaded footing is dependent upon the designer's arbitrarily selected value of e, so a unique solution is not likely.

Example 9-3. Proportion a strap footing for the column spacing and loading shown in Fig. E9-3*a*. The allowable pressure is 120 kPa. Both columns are 400 mm square.

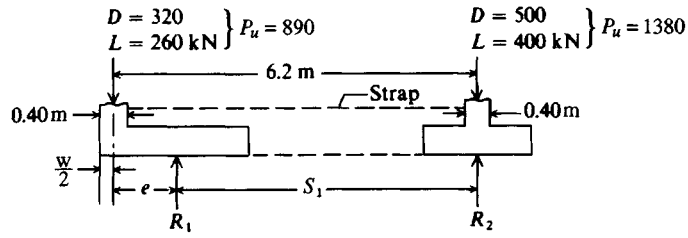

Figure E9-3*a*

Solution.

Step 1. Convert P_w to P_u and try $e = 1.20$ m.
Compute $S_1 = 6.2 - 1.2 = 5.0$ m.

$\sum M$ about column 2 = 0:

$$5R_1 - 6.2(890) = 0 \qquad R_1 = \frac{6.2(890)}{5} = 1103.6 \text{ kN}$$

$\sum M$ about $R_1 = 0$:

$$-1.2(890) + 1380(5) - R_2(5) = 0 \qquad R_2 = 1380 - 890\left(\frac{1.2}{5}\right) = 1166.4 \text{ kN}$$

Check by $\sum F_v = 0$ (note we are deriving equations shown in Fig. 9-6).

$$R_2 = P_1 + P_2 - R_1 = 890 + 1380 - 1103.6 = 1166.4 \text{ kN} \quad \text{(checks)}$$

Step 2. Find footing dimensions:

$$\text{UR} = \frac{P_u}{P_w} = \frac{2270}{1480} = 1.53 \qquad q_{ult} = q_a(\text{UR}) = 120(1.53) = \mathbf{183.6} \text{ kPa}$$

Footing dimensions for column 1:

$$L_1 = 2(e + w/2) = 2(1.2 + 0.2) = 2.8 \text{ m}$$

$$L_1 B_1 q_{ult} = R_1$$

$$B_1 = \frac{1103.6}{(2.80)(183.6)} = 2.147 \text{ m} \qquad \text{use } B = 2.15 \text{ m}$$

Footing dimensions for column 2 (use a square footing):

$$B^2 q_{ult} = R_2$$

$$B = \sqrt{\frac{1166.4}{183.6}} = 2.521 \text{ m} \qquad \text{use } B_2 = 2.52 \text{ m}$$

Use Column 1: $L = \mathbf{2.80}$ m $\quad B = \mathbf{2.15}$ m

Column 2: $B = \mathbf{2.52} \times \mathbf{2.52}$ m

Settlements should be nearly equal, since q is the same for both and the widths B are not greatly different. It is possible an $e = 1.1$ m could provide a closer agreement between B_1 and B_2, but this is left for the reader to verify.

Step 3. Draw shear and moment diagrams as in Fig. E9-3*b*.
Design footing depths for the worst case of two-way action and wide-beam shear; obtain wide-beam shear from V diagram.
Design strap for $V = 213$ kN and $M = 770$ kN · m.
Design footing reinforcing as a spread footing for both directions. Design strap as beam but check if it is a "deep" beam.

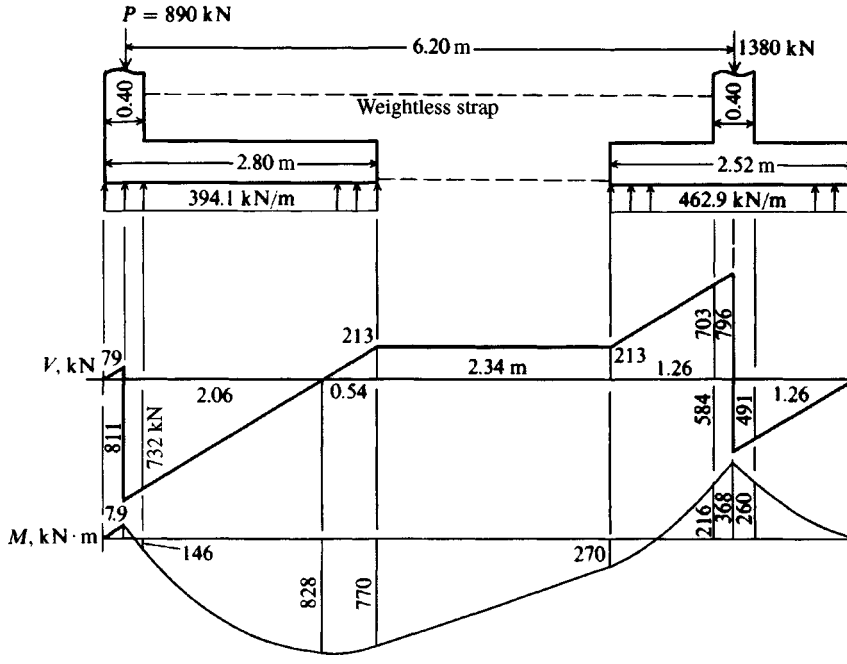

Figure E9-3*b*

////

9-5 FOOTINGS FOR INDUSTRIAL EQUIPMENT

Footings for industrial applications are not directly covered by the ACI Code. On occasion local codes may include some guidance, and certain industries may have recommended standards of practice, but often the engineer has little guidance other than what in-house design experience may exist. These gaps in practice are sometimes filled by handbooks or by professional committees. (ACI, for example, has over 100 committees). ACI Committee 318 is responsible for the ACI "Building Code 318-"; ACI Committee 351 is concerned with foundations for industrial equipment. Professionals who have a mutual interest make up the membership of these committees.

Footings for industrial application are often one of a kind; the loadings are very difficult to define and, as a consequence, the footing is conservatively designed so that, one hopes, the worst possible load condition (or some loading not anticipated at design time) is covered.

Footings in industrial applications often have large horizontal forces and overturning moments in addition to vertical forces. These moments are primarily from wind but may also be from an earthquake analysis or from use. The geotechnical consultant would not know either the moment or horizontal force at this preliminary stage, so that the allowable bearing capacity q_a is not likely to be based on footing eccentricity or any of the refined methods of Chap. 4. (e.g., Fig. 4-4*b*). Rather the allowable bearing capacity is very probably a routine determination using the SPT and/or q_u with some possible reduction to allow for loading uncertainties.

It would be up to the structural designer to accept the recommended q_a or discuss with the consultant whether the value should be further reduced. The designer may also wish to discuss whether an increase may be allowed for wind, and some recommendation for the backfill should be obtained, since this is a substantial contribution to overturning stability and might provide some sliding stability. Two factors usually allow this procedure to work:

1. The critical loading (wind or earthquake) is transitory and represents an upper bound in most cases.
2. The footings are usually embedded in the soil to a substantial depth so that the increase in bearing capacity, which may not be accounted for, more than offsets any reduction from eccentric loadings. If the center of footing area coincides with the resultant (refer to Fig. 9-1*e*) there would be no reduction for eccentricity.

Sliding stability is based on a combination of base adhesion, soil-to-concrete friction, and possibly passive earth pressure (see Chap. 11). Friction resistance depends on the total weight of the system above the base of the footing. Generally the friction factor is tan ϕ but the adhesion should be reduced, with values from 0.6 to 0.8c being commonly used. If the designer includes passive pressure resistance to sliding, great care in backfilling is required so that the perimeter zone soil can provide lateral resistance to translation.

A round base is more economical than other shapes for tall vessels, process towers, and stacks because the direction of overturning from wind or earthquake is not fixed. A pedestal is nearly always used to interface the metal superstructure to the embedded footing. The pedestal is often round to accommodate the base ring, or frame, of the equipment but may be rectangular, hexagonal, or octagonal.

In practice, however, it is difficult to form a round footing member, so an octagon is widely used since it closely fits a circle and can be formed easily. The geometry of an octagon is given in Fig. 9-7 together with a number of section property equations for design use.

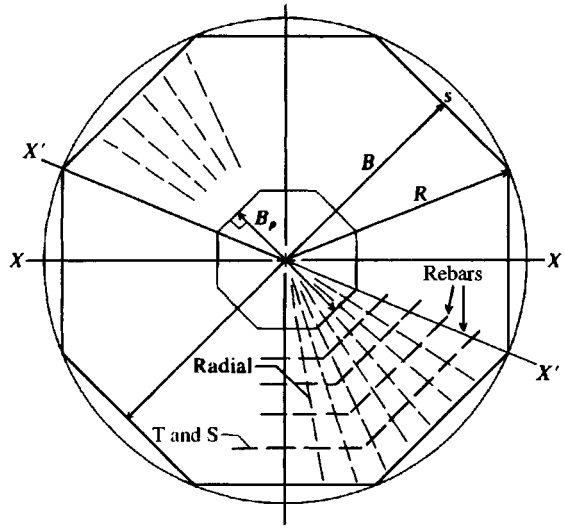

Properties of octagon

$A' = 2B^2 \tan 22.5^\circ = 0.828B^2$
$s = 2R \sin 22.5^\circ = 0.765R$
$B = 2R \cos 22.5^\circ = 1.848R$
$I_{x-x} = I_{x'-x'} = 0.6381R^4$
$r_x = r_{x'} = 0.475R$
$S_x = 0.6906R^3$
$R = 0.5412B$

Figure 9-7 Properties of an octagon. Also shown is the suggested method of placing reinforcement for radial moments and tangential steel either for T and S or for tangential moments. Additional bars may be required on outer radius to meet T and S requirements.

Generally the maximum eccentricity should be limited to about $B/8$ so that the full footing is effective for all but wind on the vessel during erection. If a turnover wind is anticipated during erection, temporary guying can be used.

The design of an octagon-shaped foundation involves sizing the pedestal (diameter and height) and the base. This sizing should take into account the following:

1. Empty condition with and without wind
2. Proof test condition with or without wind
3. Operating conditions with or without wind

The footing soil depth is then tentatively selected. The backfill over the footing has a considerable stabilizing effect and should be included when checking for overturning stability. The weights of the pedestal and footing slab are computed and used in combination with the overturning from wind or earthquake to find the soil pressures at the toe and heel for the several load cases. It is common but no longer recommended by the author to use

$$0 < \frac{P}{A} \pm \frac{Mc}{I} \leq q_a$$

Actually, one should use the equivalent rectangle of Fig. 4-4*b* with a *rectangular* soil pressure distribution and solve for the effective footing area by trial.

Wind and/or earthquake loads are obtained from local building codes, from the client, or from one of the national building codes such as (in the United States) the Uniform Building Code.

The footing is checked for wide-beam shear (most likely to control) and two-way action and for bending with sections as in Fig. 9-8. Noting that two-way action is very difficult to analyze unless one has available curves such as Brown (1968), one can make a rapid approximation by checking for wide-beam and then computing the resisting shear on the curved section, which is first converted into an equivalent square (see step 5 of Example 9-4). If the resisting shear is greater than 90 percent of the factored vertical loads, the depth is adequate. If the resisting shear is less, a more refined analysis is required. At this point one must make a decision either to increase the footing arbitrarily by 25 to 50 mm with some increase in material costs or to refine the analysis with the resulting increase in engineering costs and a possibility of still having to increase the depth. Also carefully note: Shear steel should not be used, for the footing weight has a stabilizing effect on overturning. Most importantly, the footing rigidity is needed to satisfy the linear soil-pressure assumption used in the design.

The most efficient method of round base design is to use a computer program such as B-20 (see your diskette README.DOC file), which uses a radial gridding scheme so that a grid line can be placed at the outer face of the pedestal, which is nearly always used. This program is set up to allow each circular grid line to have a different modulus of subgrade reaction and to allow doubling of the edge springs. This program can iterate to a valid solution by setting node springs that have soil-footing separation to zero. This makes it easy to locate the line of zero pressure without resort to tables or charts and to find bending moments and shear values at the various nodes. In passing, note that it is not a trivial task to compute critical moments by hand when the base supports a pedestal. Moments may be under-computed by close to 30 percent if the pedestal is not considered. By trying several depths a near optimum value can be found and the design continued.

When the footing depth has been fixed, the reinforcing steel is computed. In most cases the minimum amount controls, but note the minimum percent (as a decimal) can be either $1.4/f_y$

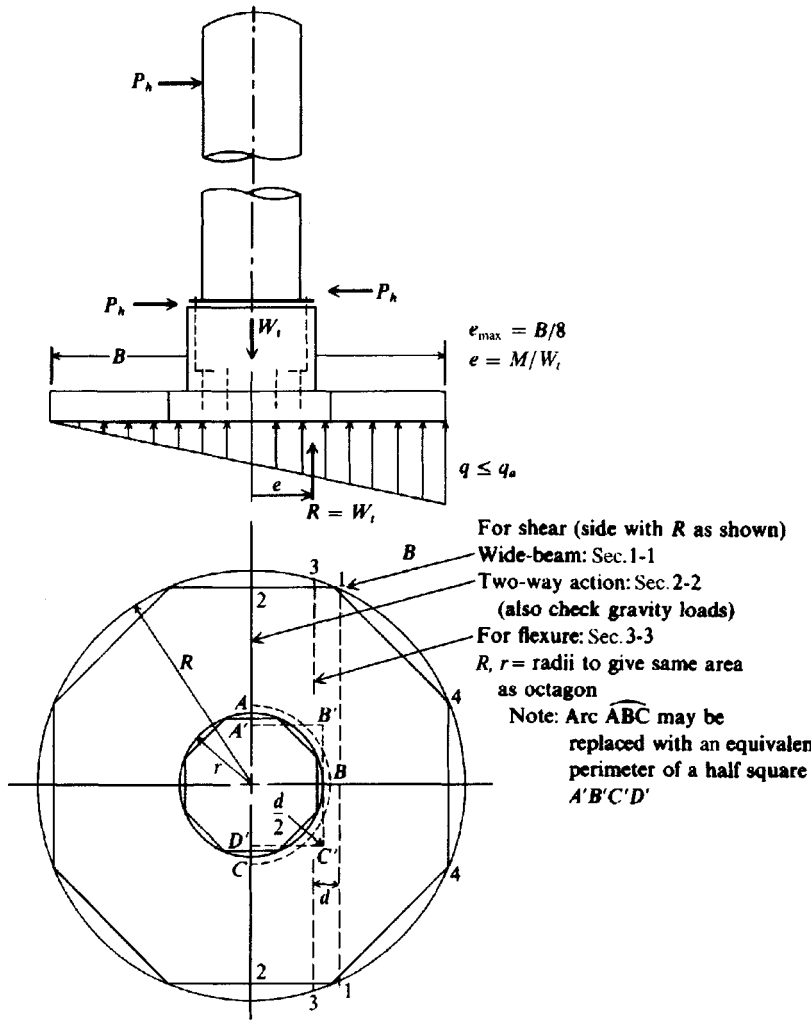

Figure 9-8 Layout of a vertical vessel foundation, critical soil pressure, and sections for shear and bending.

(or $200/f_y$) or a one-third increase in the actual computed amount (ACI Art. 10-5). This steel may be placed radially and distributed across each octagon face (Fig. 9-7). Tangential steel based on temperature and shrinkage (T and S) requirements should be placed parallel to each octagon face. Chu and Afandi (1966) suggest that tangential moments are not likely to exceed $0.05q_oR^2$, so that T and S steel will usually control. Steel requirements for bending moments are computed both for the bottom (with computations based on eccentric soil pressure) and for the top, based on no soil pressure and the weight of backfill and footing acting with full loss of soil pressure.

The pedestal may be hollow but is commonly solid to increase overturning stability. The bearing between base ring and pedestal is checked using the method of Sec. 8-6 for allowable bearing. Depending on base ring dimensions and pedestal configuration this check may set f_c' (which does not have to be same as footing) of the pedestal. The pedestal steel is designed to provide enough steel to resist the overturning moment at the base of the pedestal. This steel

may be computed on the basis of using the section modulus of a *line circle* with r = radius; t = width and is very small compared to r of the reinforcing bar circle. This is obtained as

$$A_{\text{ring}} = 4\int_0^{\pi/2} rt\,d\theta \rightarrow \mathbf{2\pi rt}$$

Similarly the moment of inertia about an axis through the diameter is

$$I_x = 4t\int_0^{\pi/2} r^2 \sin^2\theta d\theta = \boldsymbol{\pi t r^3}$$

and the section modulus $S_x = \pi t r^2$. The line area is also the number of bolts × bolt area as

$$A = 2\pi rt = N_b A_s$$

and multiplying S_x by $A_{\text{ring}}/A_{\text{ring}} = N_b A_s/2\pi rt$, we obtain (with $r = \frac{D_b}{2}$)

$$S_x = \frac{N_b A_s D_b}{4}$$

For combined stresses and with the vertical compressive force W reducing the overturning stresses we obtain

$$T = A_s f_s = \left(\frac{M}{S_x} - \frac{W}{N_b A_s}\right)A_s$$

Substituting and simplifying, we obtain

$$A_s = \frac{1}{f_s}\left(\frac{4M}{N_b D_b} - \frac{W}{N_b}\right) \qquad (a)$$

where A_s = area of a rebar bar or anchor bolt
D_b = diameter of rebar or anchor bolt circle
f_s = allowable steel stresses of bolts or bars in units consistent with A_s and W
M = overturning moment in units consistent with D_b
N_b = number of bars or anchor bolts in circle
W = weight of vessel + pedestal

The pedestal seldom requires reinforcement; however, some designers routinely use a minimum percent steel ($A_s = 0.01A_{\text{ped}}$). A *cracked section* analysis using reinforcement may be required if unreinforced concrete tension stresses exceed some maximum value [given as $f_t \leq 0.4\phi\sqrt{f_c'}$ ($5\phi\sqrt{f_c'}$, psi), $\phi = 0.65$ in ACI 318-1M, Art. 6.2.1]. If a cracked section analysis is necessary, it involves finding the neutral axis (using statics) of the pedestal; the resulting moment of inertia of the composite section and tension stresses in the rebars.

The anchor bolts are designed to resist the tension force from the overturning moment at the base of the vessel or stack. Equation (*a*) may also be used to approximate the anchor bolts.

A general overview of the design of an industrial footing is given in Example 9-4. There is some diversity of opinion on how these designs should be made and what is too conservative a design. One must weigh doubling or tripling engineering costs for a refined design using estimated loads against material savings of perhaps 50 to 150 mm of concrete depth or diameter change. A computer program such as B-20 is particularly useful in analyzing this type of base for node shear, moment, and soil pressures.

Example 9-4.

Given. The following data for the design of a vertical refining vessel:

Diameter (less insulation) = 1.85 m
Insulation thickness = 0.075 m
Height of vessel above pedestal = 33.5 m
Diameter of bolt circle of base ring = 2.00 m
Weights (including anchor or base ring): Shipping = 290 kN
Operating = 580 kN
Test (proofing) = 1160 kN
Allowable net soil pressure q_a = 150 kPa
Unit weight γ of backfill = 16.50 kN/m^3
Materials f'_c = 21 MPa f_y = 400 MPa
γ_c = 23.6 kN/m^3
Vessel location: southern Illinois

Obtain from the Uniform Building Code (UBC, 1994 edition):

Exposure B
Importance factor (hazardous materials), I = 1.15
q_s = 1.80 kPa (wind v = 190 kph and using UBC Table 23-F)

Required. Make a tentative design for this system using both a round base and round pedestal and for the given UBC requirements.

Solution. Some initial computations (not shown) are used to approximate a set of dimensions for the base, pedestal and base thickness. Clearly the pedestal will have to be about 0.15 m larger than tower diameter to provide adequate side cover so the anchor bolts do not split out. The base will have to be large enough to carry the tower load based on allowable soil pressure and the thickness (of 0.70 m) is estimated based on the base diameter (refer to Fig. E9-4*a*).

Step 1. We will only check wind moments (although earthquake moments should also be checked, as this site is in a zone that has an above average earthquake potential). From the Uniform Building Code (UBC) Sec. 2316,[1] we obtain the following equation for wind pressure:

$$p_w = C_e C_q q_s I$$

where C_e = exposure, height and gust factor (use average of (1.13 + 1.20)/2 = 1.17 (using UBC Table 23-G))
C_q = pressure coefficient for structure and for round and elliptical shapes = 0.8 (using UBC Table 23-H)
q_s = wind pressure, at the standard height of 10 m (C_e adjusts for greater heights) and based on the anticipated wind velocity in kph (using UBC Table 23-F). For 190 kph use[2] q_s = **1.80 kPa**
I = Importance factor (1.15 for hazardous materials, UBC Table 23-L)

[1]The UBC method is quite similar to the ANSI A58-1 standard, available from ASCE as ANSI/ASCE 7-88.

[2]At the time this textbook was being prepared, the several available building codes had not converted to SI. The values used by the author are soft conversions from the source and rounded.

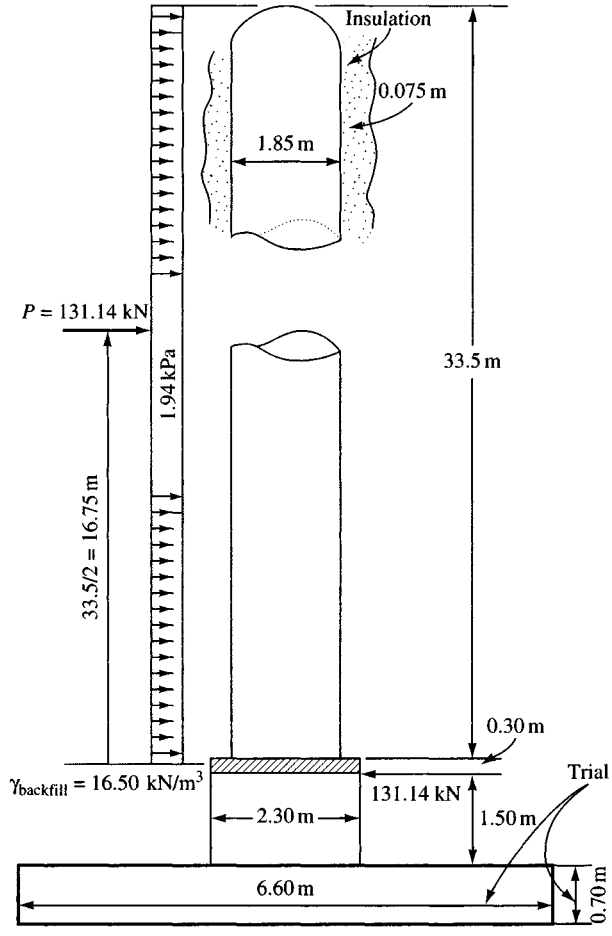

Figure E9-4*a*

Making substitutions, we have the average wind pressure for the tower height as

$$p_w = (1.17)(0.80)(1.80)(1.15) = \mathbf{1.94}\ \text{kPa}$$

The total horizontal wind force is computed as the projected area $\times\ q_s$ with an *increase* factor to account for tower projections of various types. The increase factor may be 1.0, 1.1, 1.2, etc.; we will use a value of 1.0. The general equation format is

$$P_w = \text{height(diam.)(increase factor)}(p_w)$$

Substituting, we obtain the horizontal wind force as

$$P_w = (33.5 + 0.3)[1.85 + 2(0.075)](1)(1.94)$$
$$= 33.8(2.00)(1)(1.94) = \mathbf{131.14}\ \text{kN}$$

This force acts at midheight of the tower and produces a horizontal shear at the anchor ring, as shown in Fig. E9-4*a*. Strictly, the shear is at the top of the ground, but the small height of 0.3 m is negligible, especially since the anchor ring may be between 100 and 150 mm thick.

The 131.14-kN wind load produces an overturning moment, at the top of the anchor ring, of

$$M_{o,r} = 131.14(33.5/2) = \mathbf{2197}\ \text{kN} \cdot \text{m (rounded)}$$

and, about the base (and using initial trial dimensions), of

$$M_{o,b} = 131.14(33.5/2 + 0.30 + 1.50 + 0.70)$$
$$= 131.14(19.25) = \mathbf{2524}\ \text{kN} \cdot \text{m (rounded slightly)}$$

Step 2. Estimate the gravity weights of the several elements in the system that contribute to foundation load. Take pedestal B_p = bolt ring diameter + 0.3 m = 2.30 m and base slab dimensions shown on Fig. E9-4*a*. Concrete $\gamma_c = 23.6$, soil $\gamma_s = 16.5\ \text{kN/m}^3$.

$$\text{Base area (from Fig. 9-7)} = A = 0.828B^2 = 0.828(6.60)^2 = 36.1\ \text{m}^2$$
$$\text{Pedestal weight} = 1.50(0.828)(2.30^2)(23.6) = 155.1\ \text{kN}$$
$$\text{Footing weight} = 36.1(0.70)(23.6) = 596.4\ \text{kN}$$
$$\text{Backfill weight (excluding pedestal zone)} = (36.1 - 4.38)(1.50)(16.5) = 785.1\ \text{kN}$$
$$\text{Total base weight} = \mathbf{1536.6}\ \text{kN}$$

The following load conditions are checked:

1. Erection weight = pedestal + footing + shipping
= 155.1 + 596.4 + 290 = 1042 kN

2. Test weight = Total base + Test weight
= 1536.6 + 1160 = 2697 kN

3. Operating weight = Total base + Operating
= 1536.6 + 580 = 2117 kN

Step 3. Check overturning stability by taking moments about the toe or leading edge (line 4-4 of Fig. 9-8). For all case 1 gravity loads the resisting moment is at $B/2$ from edge to give

$$M_r = (290.0 + 155.1 + 596.4) \times 6.60/2 = \mathbf{3437}\ \text{kN} \cdot \text{m}$$

The worst case for overturning will be **case 1** of tower erection onto a base without backfill. The other two load cases are computed similarly.

$$M_O = \text{wind moment about base} = 2524\ \text{kN} \cdot \text{m (from Step 1)}$$
$$\text{SF} = \text{stability number} = M_r/M_O = 3437/2524 = 1.36$$

The SF is small but > 1. One might consider using some temporary guying during the erection phase.

For working conditions (**case 3**) we find

$$M_r = (580.0 + 1537) \times 6.60/2 = 6986\ \text{kN} \cdot \text{m} \qquad M_O = 2524\ \text{kN} \cdot \text{m as before}$$
$$\text{SF} = 6986/2524 = 2.77 > 1.5 \qquad \text{(O.K.)}$$

Step 4. Find soil pressures beneath toe and heel for cases 2 and 3.

For **case 3**:

$$e = M/P = 2524/(1537 + 580) = 2524/2117 = 1.19\ \text{m}$$
$$B/8 = 6.60/8 = 0.825 < 1.19.$$

Thus, part of the base under operating conditions appears to have soil-base separation. We will continue (in practice I would use program B-20, described on your diskette, and check the toe for q to see if $q > q_a$). Here, to prevent soil-base separation would require $B = 1.19 \times 8 = 9.52$ m—clearly an overdesign.

The effective radius R of the base is (see the equations on Fig. 9-7)

$$R = 0.5412B = 0.5412(6.60) = 3.57\ \text{m}$$

The section modulus about a diameter is (also see Fig. 9-7)

$$S_x = 0.6906R^3 = 0.6906(3.57^3) = 31.42 \text{ m}^3$$

We will compute soil pressures as $q = P/A \pm M/S_x \leq q_a$. Also the base and backfill weight will be neglected, since q_a is a *net* allowable pressure. The resulting error is the difference between the unit weight of concrete and soil and base thickness, $(\gamma_c - \gamma_s)D_c$.

For load test **case 2**, and including only the test load + pedestal weight, we have

$$q = \frac{1160 + 155.1}{36.1} \pm \frac{2524}{31.42}$$

$$= 36.4 \pm 80.3 = \mathbf{116.7} < 150 \quad \text{O.K.}$$

$$= \mathbf{-43.9} < 0 \quad \text{may be O.K.}$$

Since the test load is temporary, any small overstresses would probably not be critical.

At operating conditions (**case 3**) we have the operating load + pedestal weight, giving:

$$q = \frac{580 + 155.1}{36.1} \pm \frac{2524}{31.42}$$

$$= 20.4 \pm 80.3 = \mathbf{100.7} < 150 \quad \text{O.K.}$$

$$= \mathbf{-59.9} \text{ kPa} \quad \text{(base only partly effective)}$$

At this point we have the problem that with the base only partly effective, the section modulus $\mathbf{S}_x$ should be revised. We will not do this, for two reasons:

1. These pressures are only for base bending moment.
2. The actual soil pressure cannot be computed this simply; that is, when the heel begins to lift from the soil, the weight of that part of the base and overlying soil provides a resistance to soil separation. As previously shown it would require an extremely large base diameter to reduce the (−) heel pressure to zero using simple computations of the type used here.

Step 5. Check depth for shear.

We will find the shear value and arbitrarily apply the ACI Code LF = 1.4 (for dead loads) to the working design loads to make them "ultimate." Alternatively, we could recompute the pressures using some ACI factors such as $0.75(1.4D + 1.7W)$ or $0.9D + 1.3W$, but this single factor for the types of loads we have should be an adequate computation.

a. Check wide-beam shear: Take a 1-m wide strip at section 1-1 of Fig. 9-8 (refer also to Fig. E9-4b) as adequate. Take $d = 700 - 70 - 25$ (estimated 25 mm rebar diam both radial and tangential) to obtain a nominal design depth

$$d = 700 - 70 - 25 = 605 \text{ mm} \rightarrow \mathbf{0.605} \text{ m}$$

The shear to be resisted is the area *abcd* of Fig. E9-4*b* under the toe. The slope s of the pressure diagram for case 2 (appears worst case) is

$$s = (q_{\text{toe}} - q_{\text{heel}})/B = [116.7 - (-43.9)]/6.6 = 24.3$$

$$q_{ad} = 116.7 - s(X) = 116.7 - 24.3(1.545) = 79.2 \text{ kPa}$$

For a trapezoid pressure diagram using LF = 1.4, $L = X = 1.545$ m, and a width of 1 m obtain the shear along line *ad* as

$$V_{ad} = 1.4 \times \frac{(116.7 + 79.2)}{2} \times 1.545 = \mathbf{211.9} \text{ kN/m (with LF = 1.4)}$$

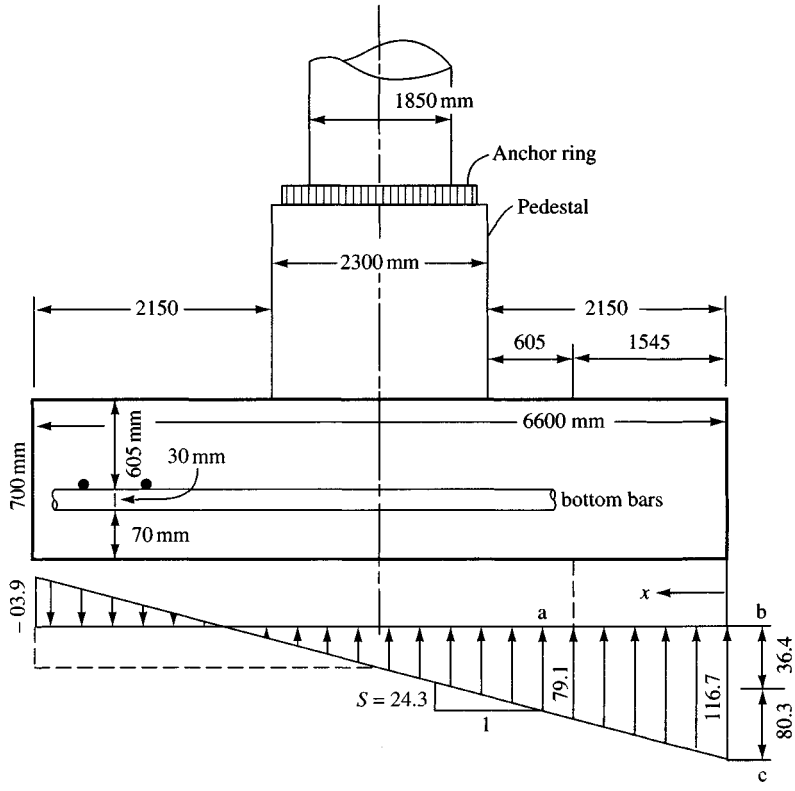

Figure E9-4*b*

Concrete wide-beam resistance is $v_c = 0.649$ MPa (Table 8-2)

$$V_c' = v_c bd = 0.649(1)(0.605)(1000)$$
$$= \mathbf{393}\text{ kN} \gg 211.9 \qquad \text{O.K. wide-beam}$$

b. Check *two-way* action: We should check perimeter shear around arc *ABC* of Fig. 9-8. This arc is often converted into an equivalent one-half square with the same area. The shear on this perimeter is very hard to compute for the overturning case. In many cases its precise value is not necessary. For example, if the resisting shear is larger than about 90 percent of the total vertical load, the precise value is not needed. Let us compute the resisting two-way action shear (allowable $v_c =$ **1.298** MPa from Table 8-2). We will use an equivalent square based on a diameter of

$$B_p + d = 2.300 + 0.605 = 2.905\text{ m}$$

The equivalent side of a square with this diameter is

$$s_s = \sqrt{0.7854(2.905^2)} = 2.57\text{ m}$$
$$p = 2.57 + 2 \times 2.57/2 = 5.14\text{ m (one-half of two-way shear perimeter)}$$

Two-way action shear will be based (using LF = 1.4) on

$$V_l = 1.4\text{ (operating load + pedestal weight)}$$
$$= 1.4(580 + 155.1) = \mathbf{1029}\text{ kN}$$

The resisting shear (include 1000 to convert MPa to kPa) is

$$V_r = v_c pd = 1.298(5.14)(0.605)(1000) = \mathbf{4036}\text{ kN} \gg 1029$$

It appears the base is quite adequate for both wide-beam and two-way shear for all three load cases. Several comments are worthwhile at this point:

1. One could make the footing thinner, but the weight gives additional stability against overturning; thickness gives additional rigidity for satisfying the condition of linear soil pressure distribution.
2. One might consider using $f'_c = 18$ MPa, but when concrete strengths are much less than 21 MPa (3 ksi) the extra quality control needed might cost more than the extra sack or so of cement required for higher strength.
3. Reducing the footing thickness 0.150 m would save about 5.4 m^3 of concrete but would be likely to take an extra day to redesign the footing (especially to check two-way action shear). Obviously the "safety" would be somewhat less with a thinner base slab.

Step 6. Find the required area of bottom reinforcing steel for bending: Take a 1-m strip to the face of the pedestal perpendicular to line 3-3 of Fig. 9-8 (refer also to Fig. E9-4*b*).

$$\text{Cantilever arm } L = 2.15\text{ m}$$

$$q = q_{\max} - sx = 116.7 - 24.3x$$

$$M = \int_0^L \int_0^L q\,dx = \frac{116.7L^2}{2} - \frac{24.3L^3}{6} \text{ (both integration constants} = 0)$$

$$= \frac{116.7 \times 2.15^2}{2} - \frac{24.3 \times 2.15^3}{6} = \mathbf{229.5}\text{ kN} \cdot \text{m/m}$$

For $f'_c = 21$ MPa, $f_y = 400$ MPa $\rightarrow a = 22.4A_s$. Using Eq. (8-2), we have

$$\phi f_y A_s\left(d - \frac{a}{2}\right) = M_u = 1.4M$$

Making substitutions, we have

$$A_s\left(0.605 - \frac{22.4A_s}{2}\right) = \frac{1.4(229.5)}{0.9(400)(1000)}$$

from which

$$A_s^2 - 0.0540A_s = 0.0000797$$

$$A_s = \mathbf{1519}\text{ mm}^2/\text{m}$$

Arbitrarily check the following:

$$\text{T \& S: } A_s = 0.0018(1000)(605) = 1089\text{ mm}^2/\text{m} < 1519$$

Check Min A_s of $1.4/f_y$ (or $200/f_y$) (Art. 10.5.1):

$$A_s = \frac{1.4}{f_y}(0.605)(1)(10^6) = \mathbf{2118}\text{ mm}^2/\text{m} > 1519$$

Check Min A_s (Art. 10.5.2), since $1.4/f_y > 1519$ for bending

$$A_s = 1.33(1519) = \mathbf{2020}\text{ mm}^2/\text{m}$$

From these we see that $1.4f_y$ controls, so use either $A_s \geq 2118$ mm^2/m or $A_s \geq 2020$ mm^2/m. Use four No. 30 bars ($4 \times 700 = 2800$ mm^2/m) and place radially.

The pedestal produces a "fixed-end" rigidity such that the moment computed at the pedestal face of 239.1 kN · m/m could be as much as 30 percent low. ACI Art. 10.5.2 was used in this analysis to provide the required amount of steel. The Code commentary for Art. 10.5.3 states that for slabs supported by soil the one-third increase does not apply unless superstructure loads are transmitted by the slab to the soil. In this case the pedestal transmits the tower load to the footing, so the one-third increase is applicable. It is preferable, of course, to use a computer program and directly obtain the moment at the pedestal face—although the Art. 10.5.2 check would still have to be done.

Step 7. Top steel requirements (side opposite high toe pressure) are based on footing weight + backfill and full loss of soil pressure: Moment arm is same as used in step 6 = 2.15 m, LF = 1.4, and

$$M_u = 1.4(0.7 \times 23.6 + 1.5 \times 16.5) \times \frac{2.15^2}{2} = 133.6 \text{ kN} \cdot \text{m}$$

Based on this small moment and from step 6 it is evident that the minimum $A_s = 1.4/f_y$ will control. Therefore, use $A_s = \mathbf{2118}$ mm^2/m → seven No. 20 bars ($7 \times 300 = 2100$ mm^2/m). This steel is required in any case, as the top steel requirements result from wind, which can come from any direction.

Step 8. Find vertical steel for the pedestal, assuming that the rebars will carry all of the tension stresses. Take pedestal rebar diameter $B_p \approx 2.30 - 0.30 = \mathbf{2.0}$ m.

Find wind moment at top of footing (refer to Fig. E9-4*a*):

$$M_u = 131.14(33.5/2 + 0.3 + 1.5) = 2433 \text{ kN} \cdot \text{m}$$

Using Eq. (*a*) previously given, including the LF = 1.4 and rearranging (the 1000 converts m^2 to mm^2) we have:

$$NA_s = \frac{1.4}{f_s}\left[\frac{4 \times M_o}{B_p} - W\right] = \frac{1.4 \times 1000}{0.9 \times 400}\left[\frac{4 \times 2433}{2.0} - (155.1 + 580)\right]$$

$$= \mathbf{16\,064} \text{ mm}^2 \qquad \text{(total in pedestal)}$$

$$0.01A_g = 0.01(0.828 \times 2.30^2)10^6 = \mathbf{43\,801} \text{ mm}^2$$

Using load factors from ACI Art. 9.2.2, $1.3W + 0.9D$, gives

$$A_s = 22\,027 \text{ mm}^2 > 16\,064 \text{ just computed}$$

Use 24 No. 35 bars ($A_s = 24 \times 1000 = 24\,000$ mm^2) in the pedestal as follows (for octagon shape):

1 at each corner (uses 8)
2 at 1/3 points of each side (uses 16)

These rebars would have to be placed symmetrically, since wind can come from any direction.

The anchor bolts and tangential rebars (probably just T & S) are still to be designed but will be left as a reader exercise. For the anchor bolts the designer would require a plan of the ring support so that the anchorage hole positions are located.

Comment. What should one use for load factors in this type problem? Because the tower is fixed in dimension and volume, there is not an uncertainty factor of 1.7 and probably not of 1.4. The wind load could have a load factor of 1, because it is already estimated from a building code, and it does not make much sense to say, "The wind load is uncertain and may have an additional uncertainty of 30 (1.3), 40 (1.4), or 70 (1.7) percent."

////

9-6 MODULUS OF SUBGRADE REACTION

The modulus of subgrade reaction is a conceptual relationship between soil pressure and deflection that is widely used in the structural analysis of foundation members. It is used for continuous footings, mats, and various types of pilings to be taken up in later chapters. This ratio was defined on Fig. 2-43*c*, and the basic equation when using plate-load test data is

$$k_s = \frac{q}{\delta}$$

with terms identified on both Fig. 2-43*c* and Fig. 9-9*b*. Plots of q versus δ from load tests give curves of the type qualitatively shown in Fig. 9-9*b*. If this type of curve is used to obtain k_s in the preceding equation, it is evident that the value depends on whether it is a tangent or secant modulus and on the location of the coordinates of q and δ.

It is difficult to make a plate-load test except for very small plates because of the reaction load required. Even with small plates of, say, 450-, 600-, and 750-mm diameter it is difficult to obtain δ since the plate tends to be less than rigid so that a constant deflection across the plate (and definition of k_s) is difficult to obtain. Stacking the smaller plates concentric with the larger ones tends to increase the rigidity, but in any case the plot is of load divided by plate contact area (nominal P/A) and the *average measured deflection.*

Figure 9-9*c* is a representation of k_s used by the author where k_s is taken as a constant up to a deflection X_{max}. Beyond X_{max} the soil pressure is a constant value defined by

$$q_{con} = k_s(X_{max})$$

Obviously one could divide the q-δ curve into several regions so that k_s takes on values of the slope in the several regions; however, this approach tends to incorporate too much

Figure 9-9 Determination of modulus of subgrade reaction k_s.

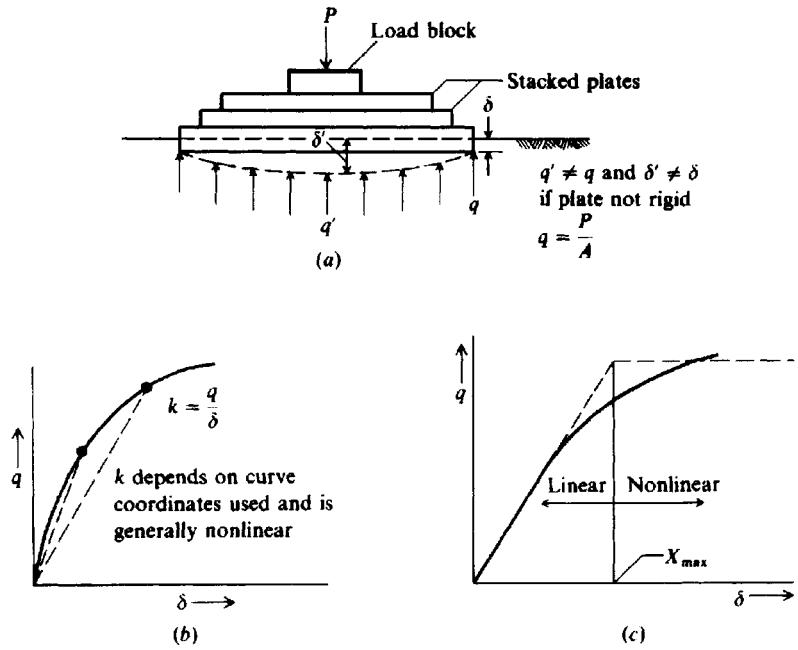

refinement into the problem since most analyses proceed on the basis of estimated values or at best an approximate load test.

A number of persons do not like to use the concept of a modulus of subgrade reaction; rather, they prefer to use E_s (and μ) in some kind of finite-element analysis. The author's experience using both the finite element (of the elastic continuum) and the concept of the modulus of subgrade reaction is that, until the state of the art improves so that accurate values of E_s can be obtained, the modulus of subgrade reaction method is preferable owing to its greater ease of use and to the substantial savings in computer computation time. In the following paragraphs we will see a direct relationship between E_s and k_s.

A major problem is to estimate the numerical value of k_s. One of the early contributions was that of Terzaghi (1955), who proposed that k_s for full-sized footings could be obtained from plate-load tests using the following equations:

For footings on clay[3]

$$k_s = k_1 \frac{B_1}{B} \tag{9-3}$$

For footings on sand (and including size effects)

$$k_s = k_1 \left(\frac{B + B_1}{2B} \right)^2 \tag{9-4}$$

In these two equations use B_1 = side dimension of the square base used in the load test to produce k_1. In most cases $B_1 = 0.3$ m (or 1 ft), but whatever B_1 dimension was used should be input. Also this equation deteriorates when $B/B_1 \approx> 3$.

For a rectangular footing on stiff clay or medium dense sand with dimensions of $B \times L$ with $m = L/B$,

$$k_s = k_1 \frac{m + 0.5}{1.5m} \tag{9-5}$$

where k_s = desired value of modulus of subgrade reaction for the full-size (or prototype) foundation

k_1 = value obtained from a plate-load test using a 0.3×0.3 m (1×1 ft) or other size load plate

Equations (9-3), (9-4), and (9-5) are presented primarily for historical purposes and are not recommended by the author for general use.

Vesić (1961*a*, 1961*b*) proposed that the modulus of subgrade reaction could be computed using the stress-strain modulus E_s as

$$k_s' = 0.65 \sqrt[12]{\frac{E_s B^4}{E_f I_f}} \frac{E_s}{1 - \mu^2} \qquad \text{(units of } E_s\text{)} \tag{9-6}$$

[3]The B_1 is not usually seen in this equation, since at the time it was proposed by Terzaghi (1955) only Fps units were used, and with $B_1 = 1$ ft it did not need to be shown. The equation is dimensionally incorrect, however, without including B_1. Equation (9-3) is not correct in any case, as k_s using a 3.0 m footing would not be $\frac{1}{10}$ the value obtained from a $B_1 = 0.3$ m plate.

where E_s, E_f = modulus of soil and footing, respectively, in consistent units
B, I_f = footing width and its moment of inertia based on cross section (not plan) in consistent units

One can obtain k_s from k_s' as

$$k_s = \frac{k_s'}{B}$$

Since the twelfth root of any value $\times$ 0.65 will be close to 1, for all practical purposes the Vesić equation reduces to

$$k_s = \frac{E_s}{B(1 - \mu^2)} \tag{9-6a}$$

One may rearrange Eq. (5-16*a*) and, using $E_s' = (1 - \mu^2)/E_s$ as in Eqs. (5-18) and (5-19) and $m = 1$, obtain

$$\Delta H = \Delta q B E_s' I_s I_F$$

and, since k_s is defined as $\Delta q/\Delta H$, obtain

$$k_s = \frac{\Delta q}{\Delta H} = \frac{1}{B E_s' I_s I_F} \tag{9-7}$$

but carefully note the definition of E_s'. Now one can correctly incorporate the size effects that are a major concern—particularly for the mat foundations of the next chapter. As for Eqs. (5-18) and (5-19), we can write a k_s ratio from Eq. (9-7) as follows:

$$\frac{k_{s1}}{k_{s2}} = \frac{B_2 E_{s2}' I_{s2} I_{F2}}{B_1 E_{s1}' I_{s1} I_{F1}} \tag{9-8}$$

Equation (9-8) should be used instead of Eqs. (9-3) through (9-5), and Eq. (9-7) is at least as theoretically founded as Eq. (9-6). Carefully note in using these equations that their basis is in the settlement equation [Eq. (5-16*a*)] of Chap. 5, and use B, I_s, and I_F as defined there.

Equations (9-7) and (9-8) show a direct relationship between k_s and E_s. Since one does not often have values of E_s, other approximations are useful and often quite satisfactory if the computed deflection (directly dependent on k_s) can be tolerated for any reasonable value. It has been found that bending moments and the computed soil pressure are not very sensitive to what is used for k_s because the structural member stiffness is usually 10 or more times as great as the soil stiffness as defined by k_s. Recognizing this, the author has suggested the following for approximating k_s from the allowable bearing capacity q_a furnished by the geotechnical consultant:

$$\begin{aligned} \text{SI: } k_s &= 40(\text{SF})q_a \quad && \text{kN/m}^3 \\ \text{Fps: } k_s &= 12(\text{SF})q_a \quad && \text{k/ft}^3 \end{aligned} \tag{9-9}$$

where q_a is furnished in ksf or kPa. This equation is based on $q_a = q_{ult}/\text{SF}$ and the ultimate soil pressure is at a settlement $\Delta H = 0.0254$ m or 1 in. (1/12 ft) and k_s is $q_{ult}/\Delta H$. For $\Delta H = 6, 12, 20$ mm, etc., the factor 40 (or 12) can be adjusted to 160 (or 48), 83 (or 24), 50 (or 16), etc.; 40 is reasonably conservative but smaller assumed displacements can always be used.

The most general form for either a horizontal or lateral modulus of subgrade reaction is

$$k_s = A_s + B_s Z^n \tag{9-10}$$

where A_s = constant for either horizontal or vertical members
B_s = coefficient for depth variation
Z = depth of interest below ground
n = exponent to give k_s the best fit (if load test or other data are available)

Either A_s or B_s in this equation may be zero; at the ground surface A_s is zero for a lateral k_s but at any small depth $A_s > 0$. For footings and mats (plates in general), $A_s > 0$ and $B_s \cong 0$.

Equation (9-10) can be used with the proper interpretation of the bearing-capacity equations of Table 4-1 (with the d_i factors dropped) to give

$$q_{ult} = cN_c s_c + \gamma Z N_q s_q + 0.5\gamma B N_\gamma s_\gamma) \tag{9-10a}$$

Observing that

$$A_s = C(cN_c s_c + 0.5\gamma B N_\gamma s_\gamma) \qquad \text{and} \qquad B_s Z^1 = C(\gamma N_q s_q) Z^1$$

we obtain a ready means to estimate k_s. In these equations the Terzaghi or Hansen bearing-capacity factors can be used. The C factor is 40 for SI units and 12 for Fps, using the same reasoning that q_{ult} occurs at a 0.0254-m and 1-in. settlement but with no SF, since this equation directly gives q_{ult}. Where there is concern that k_s does not increase without bound with depth Z, we may adjust the $B_s Z$ term by one of two simple methods:

$$\text{Method 1: } B_s \tan^{-1} \frac{Z}{D}$$

$$\text{Method 2: } \frac{B_s}{D^n} Z^n = B_s' Z^n$$

where D = maximum depth of interest, say, the length of a pile
Z = current depth of interest
n = your best estimate of the exponent

Table 9-1 may be used to estimate a value of k_s to determine the correct order of magnitude of the subgrade modulus obtained using one of the approximations given here. Obviously if a computed value is two or three times larger than the table range indicates, the computations should be rechecked for a possible gross error. Note, however, if you use a reduced value of displacement (say, 6 mm or 12 mm) instead of 0.0254 m you may well exceed the table range. Other than this, if no computational error (or a poor assumption) is found then use judgment in what value to use. The table values are intended as guides. The reader should not use, say, an average of the range given as a "good" estimate.

The value of X_{max} used in Fig. 9-9*c* (and used in your diskette program FADBEMLP as XMAX) may be directly estimated at some small value of, say, 6 to 25 mm, or from inspection of a load-settlement curve if a load test was done. It might also be estimated from a triaxial test using the strain at "ultimate" or at the maximum pressure from the stress-strain plot. Using the selected strain ϵ_{max} compute

$$X_{max} = \epsilon_{max}(1.5 \text{ to } 2B)$$

TABLE 9-1
Range of modulus of subgrade reaction k_s
Use values as guide and for comparison when using approximate equations

Soil	k_s, kN/m³
Loose sand	4800–16 000
Medium dense sand	9600–80 000
Dense sand	64 000–128 000
Clayey medium dense sand	32 000–80 000
Silty medium dense sand	24 000–48 000
Clayey soil:	
$q_a \leq 200$ kPa	12 000–24 000
$200 < q_a \leq 800$ kPa	24 000–48 000
$q_a > 800$ kPa	> 48 000

The 1.5 to $2B$ dimension is an approximation of the depth of significant stress-strain influence (Boussinesq theory) for the structural member. The structural member may be either a *footing* or a *pile*.

Example 9-5. Estimate the modulus of subgrade reaction k_s for the following design parameters:

$$B = 1.22 \text{ m} \qquad L = 1.83 \text{ m} \qquad D = 0.610 \text{ m}$$
$$q_a = 200 \text{ kPa (clayey sand approximately 10 m deep)}$$
$$E_s = 11.72 \text{ MPa (average in depth } 5B \text{ below base)}$$

Solution. Estimate Poisson's ratio $\mu = 0.30$ so that

$$E_s' = \frac{1 - \mu^2}{E_s} = \frac{1 - 0.3^2}{11.72} = 0.077\,65 \text{ m}^2/\text{MN}$$

For **center:**

$$H/B' = 5B/(B/2) = 10 \text{ (taking } H = 5B \text{ as recommended in Chap. 5)}$$
$$L/B = 1.83/1.22 = 1.5$$

From these we may write

$$I_s = 0.584 + \frac{1 - 2(0.3)}{1 - 0.3}0.023 = \mathbf{0.597}$$

using Eq. (5-16) and Table 5-2 (or your program FFACTOR) for factors 0.584 and 0.023.

At $D/B = 0.61/1.22 = 0.5$, we obtain $I_F = 0.80$ from Fig. 5-7 (or when using FFACTOR for the I_s factors). Substitution into Eq. (9-7) with $B' = 1.22/2 = 0.61$, and $m = 4$ yields

$$k_s = \frac{1}{0.61(0.077\,65)(4 \times 0.597)(0.8)} = \mathbf{11.05} \text{ MN/m}^3$$

You should note that k_s does not depend on the contact pressure of the base q_o.

For **corner:**

$$H/B' = 5B/B = 5(1.22)/1.22 = 5$$

[from Table 5-2 with $L/B = 1.5$ obtained for Eq. (5-16)]

$$I_s = 0.496 + \frac{0.4}{0.7}(0.045) = 0.522 \qquad I_F = 0.8 \text{ (as before)}$$

Again substituting into Eq. (9-7) but with $B' = B = 1.22$ m and one corner contribution, we have

$$k_s = \frac{1}{1.22 \times 0.077\,65 \times 0.522 \times 0.8} = \mathbf{25.28}\ \text{MN/m}^3$$

For an average value we will use weighting, consisting of four center contributions + one corner value, giving

$$k_{s,\text{avg}} + \frac{4(11.5) + 25.28}{5} = \mathbf{13.896}\ \text{MN/m}^3$$

We can also estimate k_s based on SF = 2 for sand to obtain

$$k_s = 40(\text{SF})(q_a) = 40(2)(0.200) = \mathbf{16}\ \text{MN/m}^3$$

For practical usage and since these values of 13.896 and 16.0 are estimates (but reasonably close) we would use

$$k_s = \mathbf{15.0}\ \text{MN/m}^3 \qquad (\mathbf{15\,000}\ \text{kN/m}^3)$$

Comments. It is evident from this example that the "center" k_s is softer (or less stiff) than a corner (or edge). The center being less stiff is consistent with the *dishing* of uniformly loaded plates. One can also *zone* the area beneath a footing by computing a series of k_s values at, say, center, $\frac{1}{4}$, $\frac{1}{8}$, and edge points using for the $\frac{1}{4}$ and $\frac{1}{8}$ point the contributions from four rectangles and for the edge the contributions of two rectangles of the same size.

Note the use of $H = 5B = 5 \times 1.22 = 6.1$ m for both center and corner.

////

9-7 CLASSICAL SOLUTION OF BEAM ON ELASTIC FOUNDATION

When flexural rigidity of the footing is taken into account, a solution can be used that is based on some form of a beam on an elastic foundation. This may be the classical Winkler solution of about 1867, in which the foundation is considered as a bed of springs ("Winkler foundation"), or the finite-element procedure of the next section.

The classical solutions, being of closed form, are not so general in application as the finite-element method. The basic differential equation is (see Fig. 9-10)

$$EI\frac{d^4y}{dx^4} = q = -k_s'y \tag{9-11}$$

where $k_s' = k_sB$. In solving the equations, a variable is introduced:

$$\lambda = \sqrt[4]{\frac{k_s'}{4EI}} \qquad \text{or} \qquad \lambda L = \sqrt[4]{\frac{k_s'L^4}{4EI}}$$

Table 9-2 gives the closed-form solution of the basic differential equations for several loadings shown in Fig. 9-10 utilizing the Winkler concept. It is convenient to express the trigonometric portion of the solutions separately as in the bottom of Table 9-2.

Hetenyi (1946) developed equations for a load at any point along a beam (see Fig. 9-10*b*) measured from the left end as follows:

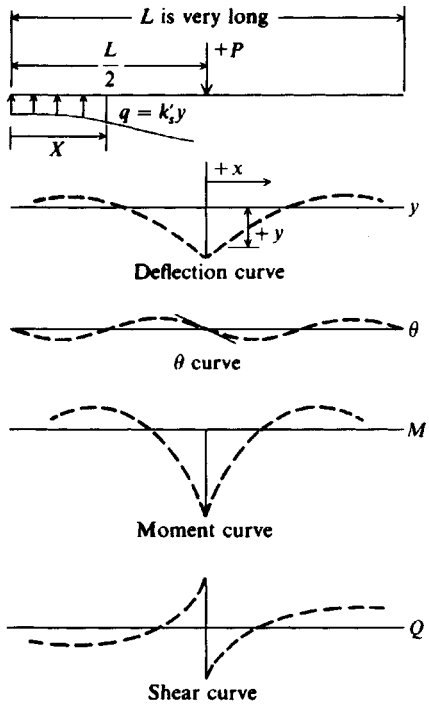

(a) Infinite length beam on an elastic foundation with mid or center loading.

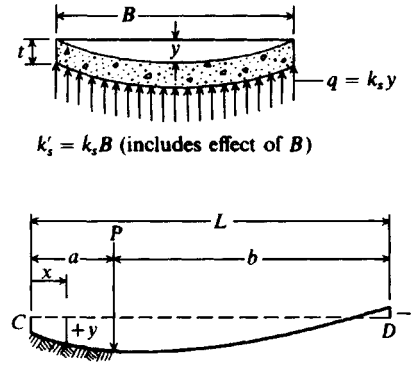

(b) Finite length beam on elastic foundation.

Figure 9-10 Beam on elastic foundation.

$$y = \frac{P\lambda}{k_s'(\sinh^2 \lambda L - \sin^2 \lambda L)}\{2\cosh \lambda x \cos \lambda x(\sinh \lambda L \cos \lambda a \cosh \lambda b - \sin \lambda L \cosh \lambda a \cos \lambda b) + (\cosh \lambda x \sin \lambda x + \sinh \lambda x \cos \lambda x)[\sinh \lambda L(\sin \lambda a \cosh \lambda b - \cos \lambda a \sinh \lambda b) + \sin \lambda L(\sinh \lambda a \cos \lambda b - \cosh \lambda a \sin \lambda b)]\} \quad (9\text{-}12)$$

$$M = \frac{P}{2\lambda(\sinh^2 \lambda L - \sin^2 \lambda L)}\{2\sinh \lambda x \sin \lambda x(\sinh \lambda L \cos \lambda a \cosh \lambda b - \sin \lambda L \cosh \lambda a \cos \lambda b) + (\cosh \lambda x \sin \lambda x - \sinh \lambda x \cos \lambda x) \times [\sinh \lambda L(\sin \lambda a \cosh \lambda b - \cos \lambda a \sinh \lambda b) + \sin \lambda L(\sinh \lambda a \cos \lambda b - \cosh \lambda a \sin \lambda b)]\} \quad (9\text{-}13)$$

$$Q = \frac{P}{\sinh^2 \lambda L - \sin^2 \lambda L}\{(\cosh \lambda x \sin \lambda x + \sinh \lambda x \cos \lambda x) \times (\sinh \lambda L \cos \lambda a \cosh \lambda b - \sin \lambda L \cosh \lambda a \cos \lambda b) + \sinh \lambda x \sin \lambda x[\sinh \lambda L(\sin \lambda a \cosh \lambda b - \cos \lambda a \sinh \lambda b) + \sin \lambda L(\sinh \lambda a \cos \lambda b - \cosh \lambda a \sin \lambda b)]\} \quad (9\text{-}14)$$

The equation for the slope θ of the beam at any point is not presented since it is of little value in the design of a footing. The value of x to use in the equations is from the end of the

TABLE 9-2
Closed-form solutions of infinite beam on elastic foundation (Fig. 9-10*a*)

Concentrated load at end	Moment at end
$y = \frac{2V_1\lambda}{k_s'} D_{\lambda x}$	$y = \frac{-2M_1\lambda^2}{k_s'} C_{\lambda x}$
$\theta = \frac{-2V_1\lambda^2}{k_s'} A_{\lambda x}$	$\theta = \frac{4M_1\lambda^3}{k_s'} D_{\lambda x}$
$M = \frac{-V_1}{\lambda} B_{\lambda x}$	$M = M_1 A_{\lambda x}$
$Q = -V_1 C_{\lambda x}$	$Q = -2M_1\lambda B_{\lambda x}$
Concentrated load at center (+↓)	**Moment at center (+ ↷)**
$y = \frac{P\lambda}{2k_s'} A_{\lambda x}$	$y = \frac{M_0\lambda^2}{k_s'} B_{\lambda x}$ deflection
$\theta = \frac{-P\lambda^2}{k_s'} B_{\lambda x}$	$\theta = \frac{M_0\lambda^3}{k_s'} C_{\lambda x}$ slope
$M = \frac{P}{4\lambda} C_{\lambda x}$	$M = \frac{M_0}{2} D_{\lambda x}$ moment
$Q = \frac{-P}{2} D_{\lambda x}$	$Q = \frac{-M_0\lambda}{2} A_{\lambda x}$ shear

The A, B, C, and D coefficients (use only $+x$) are as follows:

$$A_{\lambda x} = e^{-\lambda x}(\cos \lambda x + \sin \lambda x)$$
$$B_{\lambda x} = e^{-\lambda x} \sin \lambda x$$
$$C_{\lambda x} = e^{-\lambda x}(\cos \lambda x - \sin \lambda x)$$
$$D_{\lambda x} = e^{-\lambda x} \cos \lambda x$$

beam to the point for which the deflection, moment, or shear is desired. If x is less than the distance a of Fig. 9-10*b*, use the equations as given and measure x from C. If x is larger than a, replace a with b in the equations and measure x from D. These equations may be rewritten as

$$y = \frac{P\lambda}{k_s'} A' \qquad M = \frac{P}{2\lambda} B' \qquad Q = PC'$$

where the coefficients A', B', and C' are the values for the hyperbolic and trigonometric remainder of Eqs. (9-12) to (9-14).

It has been proposed that one could use λL previously defined to determine if a foundation should be analyzed on the basis of the conventional rigid procedure or as a beam on an elastic foundation (see combined footing Example 9-1):

Rigid members: $\lambda L < \frac{\pi}{4}$ (bending not influenced much by k_s)

Flexible members: $\lambda L > \pi$ (bending heavily localized)

The author has found these criteria of limited application because of the influence of the number of loads and their locations along the member.

The classical solution presented here has several distinct disadvantages over the finite-element solution presented in the next section, such as

1. Assumes weightless beam (but weight will be a factor when footing tends to separate from the soil)
2. Difficult to remove soil effect when footing tends to separate from soil
3. Difficult to account for boundary conditions of known rotation or deflection at selected points
4. Difficult to apply multiple types of loads to a footing
5. Difficult to change footing properties of I, D, and B along member
6. Difficult to allow for change in subgrade reaction along footing

Although the disadvantages are substantial, some engineers prefer the classical beam-on-elastic-foundation approach over discrete element analyses. Rarely, the classical approach may be a better model than a discrete element analysis, so it is worthwhile to have access to this method of solution.

9-8 FINITE-ELEMENT SOLUTION OF BEAM ON ELASTIC FOUNDATION

The finite-element method (FEM) is the most efficient means for solving a beam-on-elastic-foundation type of problem based on Eq. (9-10) but requires a digital (or personal) computer. It is easy to account for boundary conditions (such as a point where there is no rotation or translation), beam weight, and nonlinear soil effects (either soil-beam separation or a displacement $> X_{max}$).

The FEM is more versatile than the finite-difference method (FDM), because one can write an equation model for one element and use it for each element in the beam model. With the finite-difference method all of the elements must be the same length and cross section. Different equations are required for end elements than for interior ones, and modeling boundary conditions is difficult, as is modeling nonlinear soil effects. The FDM had an initial advantage of not requiring much computer memory, because there is only one unknown at a node—the displacement. With the discovery of band matrix solution methods this advantage was completely nullified.

Only the basic elements of the FEM will be given here, and the reader is referred to Wang (1970) or Bowles (1974a) if more background is required. The computer program B-5 (FADBEMLP) on the enclosed diskette has the necessary routines already coded for the user. This program was used to obtain text output.

General Equations in Solution

For the following development refer to Fig. 9-11. At any node i (junction of two or more members at a point) on the structure we may write

$$P_i = A_i F_i$$

which states that the external node force P is equated to the contributing internal member forces F using bridging constants A. It is understood that P and F are used for either forces

or moments and that this equation is shorthand notation for several values of A_iF_i summed to equal the ith nodal force.

For the full set of nodes on any structure and using matrix notation, where **P**, **F** are column vectors and **A** is a rectangular matrix, this becomes

$$\mathbf{P} = \mathbf{AF} \tag{a}$$

An equation relating internal-member deformation **e** at any node to the external nodal displacements is

$$\mathbf{e} = \mathbf{BX}$$

where both **e** and **X** may be rotations (radians) or translations. From the reciprocal theorem in structural mechanics it can be shown that the **B** matrix is exactly the transpose of the **A** matrix, which is a convenience indeed; thus,

$$\mathbf{e} = \mathbf{A}^{\mathrm{T}}\mathbf{X} \tag{b}$$

The internal-member forces **F** are related to the internal-member displacements **e** and contributing member stiffnesses **S** as

$$\mathbf{F} = \mathbf{Se} \tag{c}$$

These three equations are the fundamental equations in the finite-element method of analysis:

Substituting (*b*) into (*c*),

$$\mathbf{F} = \mathbf{Se} = \mathbf{SA}^{\mathrm{T}}\mathbf{X} \tag{d}$$

Substituting (*d*) into (*a*),

$$\mathbf{P} = \mathbf{AF} = \mathbf{ASA}^{\mathrm{T}}\mathbf{X} \tag{e}$$

Note the order of terms used in developing Eqs. (*d*) and (*e*). Now the only unknowns in this system of equations are the **X**'s; so the $\mathbf{ASA}^{\mathrm{T}}$ is inverted to obtain

$$\mathbf{X} = (\mathbf{ASA}^{\mathrm{T}})^{-1}\mathbf{P} \tag{f}$$

Figure 9-11 External (nodal) and internal (member) finite-element forces.

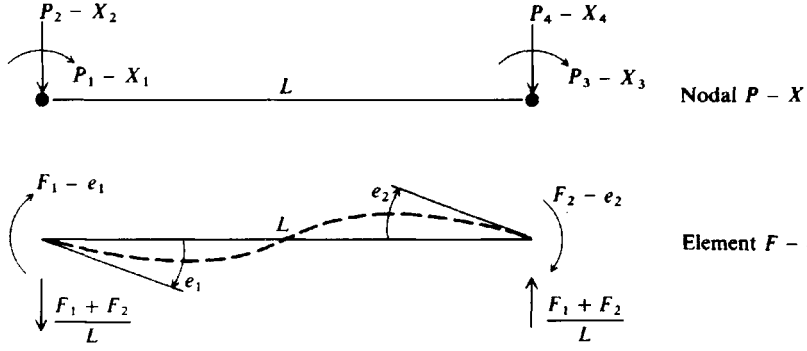

and with the **X**'s we can back-substitute into Eq. (*d*) to obtain the internal-member forces that are necessary for design. This method gives two important pieces of information: (1) design data and (2) deformation data.

The $\mathbf{ASA}^T$ matrix above is often called a global matrix, since it represents the system of equations for each **P** or **X** nodal entry. It is convenient to build it from one finite element of the structure at a time and use superposition to build the global $\mathbf{ASA}^T$ from the element $\mathbf{EASA}^T$. This is easily accomplished, since every entry in both the global and element $\mathbf{ASA}^T$ with a unique set of subscripts is placed into that subscript location in the $\mathbf{ASA}^T$, i.e., for $i = 2, j = 5$ all (2, 5) subscripts in $\mathbf{EASA}^T$ are added into the (2, 5) coordinate location of the global $\mathbf{ASA}^T$.

Developing the Element A Matrix

Consider the single simple beam element shown in Fig. 9-12*b* coded with four values of *P–X* (note that two of these *P–X* values will be common to the next member) and the forces on the element (Fig. 9-12*c*). The forces on the element include two internal bending moments and the shear effect of the bending moments. The sign convention used is consistent with your computer program B-5.

Summing moments on node 1 of Fig. 9-12*d*, we obtain

$$P_1 = F_1 + 0F_2$$

Similarly, summing forces and noting that the soil spring forces are global and will be included separately, we have

$$P_2 = \frac{F_1}{L} + \frac{F_2}{L}$$

$$P_3 = 0F_1 + F_2$$

$$P_4 = -\frac{F_1}{L} - \frac{F_2}{L}$$

Placed into conventional form, the element *A* matrix for element 1 is

$$\mathbf{EA} = \begin{array}{c|cc} \mathbf{P} \backslash \mathbf{F} & 1 & 2 \\ \hline 1 & 1 & 0 \\ 2 & 1/L & 1/L \\ 3 & 0 & 1 \\ 4 & -1/L & -1/L \end{array}$$

The **EA** matrix for member 2 would contain P_3 to P_6; it is not necessary to resubscript the *F* values.

Developing the S Matrix

Referring to Fig. 9-13 and using conjugate-beam (moment-area) principles, we see that the end slopes e_1 and e_2 are

$$\frac{F_1 L}{3EI} - \frac{F_2 L}{6EI} = e_1 \qquad (g)$$

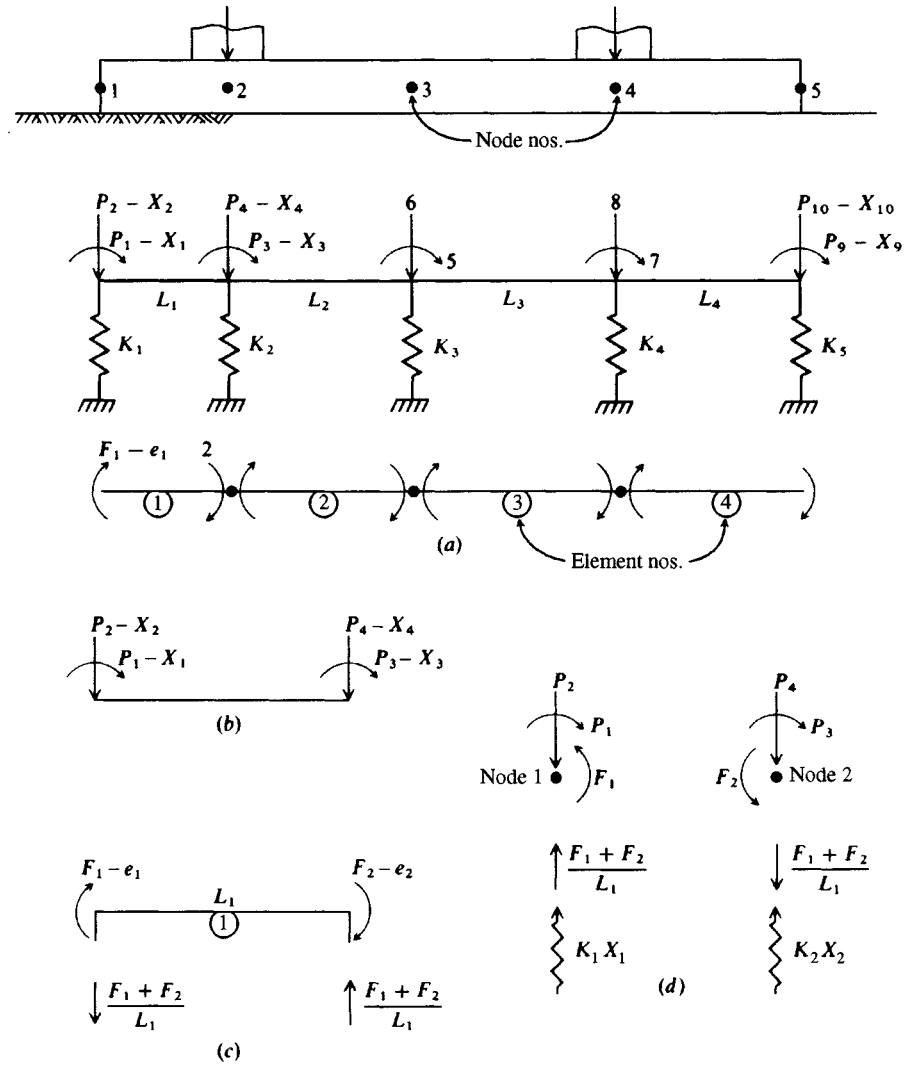

Figure 9-12 (*a*) Structure and structure broken into finite elements with global *P–X*; (*b*) *P–X* of first element; (*c*) element forces of any (including first) element; (*d*) summing nodal forces.

$$-\frac{F_1 L}{6EI} + \frac{F_2 L}{3EI} = e_2 \tag{h}$$

Solving Eqs. (*g*) and (*h*) for **F**, we obtain

$$F_1 = \frac{4EI}{L} e_1 + \frac{2EI}{L} e_2$$

$$F_2 = \frac{2EI}{L} e_1 + \frac{4EI}{L} e_2$$

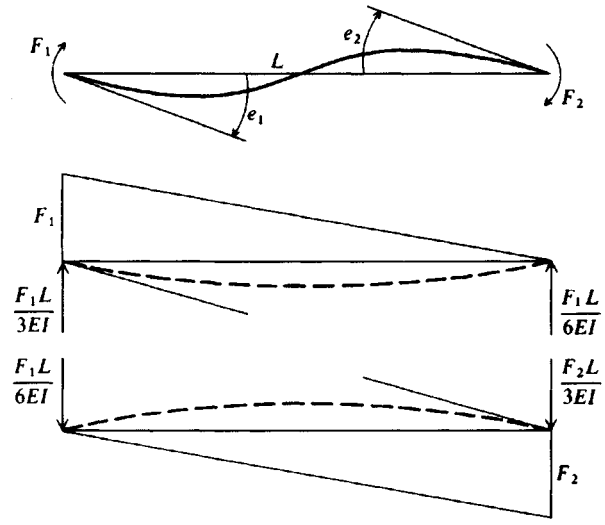

Figure 9-13 Conjugate-beam relationships between end moments and beam rotations.

The element S matrix then becomes

$$\mathbf{ES} = \begin{array}{c|cc} F \backslash e & 1 & 2 \\ \hline 1 & \dfrac{4EI}{L} & \dfrac{2EI}{L} \\ 2 & \dfrac{2EI}{L} & \dfrac{4EI}{L} \end{array}$$

Developing the Element $\mathbf{ESA}^T$ and $\mathbf{EASA}^T$ Matrices

The $\mathbf{ESA}^T$ matrix[4] is formed by multiplying the **ES** and the transpose of the **EA** matrix (in the computer program this is done in place by proper use of subscripting) as shown on the next page and noting that $\mathbf{A}^T$ goes with **e** and **X**. The $\mathbf{EASA}^T$ is obtained in a similar manner[5] as shown opposite.

The node soil "spring" will have units of FL^{-1} obtained from the modulus of subgrade reaction and based on contributory node area. When k_s = constant, they can be computed as

$$K_1 = \frac{L_1}{2}Bk_s \qquad \text{and} \qquad K_2 = \frac{L_1 + L_2}{2}Bk_s$$

[4]The element arrays are prefixed with E to differentiate them from global arrays.

[5]There are several published methods to obtain the element stiffness matrix $\mathbf{EASA}^T$ (sometimes called K), including defining the 16 matrix entries directly. The method given here is easy to understand and program, but more importantly it produces the $\mathbf{ESA}^T$, which can be saved to compute element moments later.

Bowles (1974*a*) shows that *best results are obtained by doubling the end springs.* This was done to make a best fit of the measured data of Vesić and Johnson (1963) with computations. This is incorporated into the computer program on the diskette for beams.

$\mathbf{EA}^{\mathrm{T}} =$

e \ X	1	2	3	4
1	1	$1/L$	0	$-1/L$
2	0	$1/L$	1	$-1/L$

$\mathbf{ES} =$

F \ e	1	2
1	$\frac{4EI}{L}$	$\frac{2EI}{L}$
2	$\frac{2EI}{L}$	$\frac{4EI}{L}$

$\mathbf{ESA}^{\mathrm{T}} =$

$\frac{4EI}{L}$	$\frac{6EI}{L^2}$	$\frac{2EI}{L}$	$\frac{-6EI}{L^2}$
$\frac{2EI}{L}$	$\frac{6EI}{L^2}$	$\frac{4EI}{L}$	$\frac{-6EI}{L^2}$

$\mathbf{EA} =$

1	0
$1/L$	$1/L$
0	1
$-1/L$	$-1/L$

$\mathbf{EASA}^{\mathrm{T}} =$

$\frac{4EI}{L}$	$\frac{6EI}{L^2}$	$\frac{2EI}{L}$	$\frac{-6EI}{L^2}$
$\frac{6EI}{L^2}$	$\frac{12EI}{L^3} + K_1$	$\frac{6EI}{L^2}$	$\frac{-12EI}{L^3}$
$\frac{2EI}{L}$	$\frac{6EI}{L^2}$	$\frac{4EI}{L}$	$\frac{-6EI}{L^2}$
$\frac{-6EI}{L^2}$	$\frac{-12EI}{L^3}$	$\frac{-6EI}{L^2}$	$\frac{+12EI}{L^3} + K_2$

There is some logic in end spring doubling (see also comments at end of Example 9-6), in that if higher edge pressures are obtained for footings, then this translates into "stiffer" end soil springs. For these matrices use $K_1 = L_2 B k_s$ and similarly for K_5 of Fig. 9-12.

From Fig. 9-12 we can see that summing vertical forces on a node (and using node 1 for specific illustration) gives

$$P_2 - \frac{F_1 + F_2}{L} - K_1 X_2 = 0$$

Since $(F_1 + F_2)/L$ is already included in the global $\mathbf{ASA}^{\mathrm{T}}$ we can rewrite the foregoing as

$$P_2 = (\mathbf{ASA}^{\mathrm{T}})_{2,2} X_2 + K_1 X_2 = [(\mathbf{ASA}^{\mathrm{T}})_{2,2} + K_1] X_2$$

or the node spring is directly additive to the appropriate diagonal [subscripted with (i, i)] term. This method is the most efficient way of including the soil springs since they can be built during element input into a "spring" array. Later the global $\mathbf{ASA}^T$ is built (and saved for nonlinear cases) and the springs then added to the appropriate diagonal term (or column 1 of the banded matrix that is usually used).

A check on the correct formation of the $\mathbf{EASA}^T$ and the global $\mathbf{ASA}^T$ is that they are always symmetrical and there cannot be a zero on the diagonal. Note that the soil spring is an additive term to only the appropriate diagonal term in the global $\mathbf{ASA}^T$ matrix. This allows easy removal of a spring for tension effect while still being able to obtain a solution, since there is still the shear effect at the point (not having a zero on the diagonal). This procedure has an additional advantage in that the $\mathbf{ASA}^T$ does not have to be rebuilt for nonlinear soil effects if a copy is saved to call on subsequent cycles for nodal spring adjustments.

Developing the P Matrix

The **P** matrix (a column vector for each load case) is constructed by zeroing the array and then entering those node loads that are nonzero. The usual design problem may involve several different loading cases (or conditions), so the array is of the form $P_{i,j}$ where i identifies the load entry with respect to the node and P–X coding and j the load case. For example, refer to Fig. 9-12 where we have column loads at nodes 2 and 4 and two load cases ($J = 2$) as follows:

	Load case	
Column	**1**	**2**
1 (node 2)	140 kips↓	200 kips↓
1	100 ft · k ↷	110 ft · k ↶
2 (node 4)	200 kips↓	300 kips↓

Our nonzero **P** matrix entries would be (from the P–X coding diagram)

$P_{3,1} = 100$	$P_{3,2} = -110$	(moment entries)
$P_{4,1} = 140$	$P_{4,2} = 200$	(axial loads)
$P_{8,1} = 200$	$P_{8,2} = 300$	(also axial loads)

The loads acting in the same direction as the P–X coding have a (+) sign and opposed a (−) sign as for the second load case moment at column 1.

From the foregoing we see that it is necessary to know the P–X coding used in forming the **EA** matrix, or output may be in substantial error.

For columns that are intermediate between nodes, we may do one of two things:

1. Simply prorate loads to adjacent nodes using a simple beam model.
2. Prorate loads to adjacent nodes as if the element has fixed ends so the values include fixed-end moments and shears (vertical forces). This procedure is strictly correct, but the massive amount of computations is seldom worth the small improvement in computational precision.

Boundary Conditions

The particular advantage of the finite-element method is in allowing boundary conditions of known displacements or rotations. When the displacements are zero, the most expeditious method to account for them is to use *P–X* coding such that if NP = number of *P–X* codings of all the free nodes (thus, NP = 10 in Fig. 9-12) and we want to fix node 5 against both rotation and translation, we would identify

$$\text{NP} = 8$$

and use P_9–X_9 for both rotation and translation *P–X* values at node 5 and instruct the computer that we have NP = 8. The program would then build a 9×9 array but only use the active 8×8 part. When inspecting the output we would, of course, have to know that node 5 has been specified to have zero displacements.

When displacements are of a known value (and including 0.0), a different procedure is required. Here the computer program must be set to allow known displacements. In this case have the program do the following (the computer program uses ASAT for $\mathbf{ASA}^{\mathrm{T}}$):

1. Put a 1 on the diagonal at the point of *P–X* coding (j, j).
2. Zero all the horizontal $\mathbf{ASA}^{\mathrm{T}}_{j,k}$ entries from $k = 1$ to n except $k = j$.
3. Insert the known displacement δ in the $\mathbf{P}$ matrix (so $\mathbf{P}_j = \delta$).
4. Augment all the other $\mathbf{P}$ matrix entries as

$$\mathbf{P}(I) = \mathbf{P}(I) - \mathbf{ASA}^{\mathrm{T}}_{i,j} \times \delta \qquad \text{for } i = 1 \text{ to NP except } i = j$$

Then set $\mathbf{ASA}^{\mathrm{T}}_{i,j} = 0 \qquad \text{for } i = 1, N\mathbf{P} \qquad \text{except } i = j$

When this is done properly, we have an $\mathbf{ASA}^{\mathrm{T}}$ that has a horizontal and vertical row of zeros that intersect at (j, j), where there is a 1.0. The $\mathbf{P}$ matrix has been augmented everywhere except at $\mathbf{P}_j$, where there is the entry δ.

Alternatively, we can use the following (not particularly recommended) approach:

1. Multiply $\mathbf{ASA}^{\mathrm{T}}_{j,j}$ by a very large number N (say $N > 10^{10}$).
2. Replace $\mathbf{P}_j$ by $\mathbf{P}'_j = \mathbf{ASA}^{\mathrm{T}}_{j,j} \times N \times \delta$.

It is common in foundation design to have displacements that are known to be zero (beam on rock, beam embedded in an anchor of some type, etc.). Seldom do we have known displacements where $\delta \neq 0$ other than in "what if" studies.

Node Springs

All the author's finite-element programs using beam elements require concentrating the effect of k_s to the nodes as springs. The concentration method usually used is that suggested by Newmark (1943) for a general parabolic variation of k_s versus length. This method is exact for a parabolic curve and very nearly so for either a linear or cubic curve for k_s if the node spacings are not very large. The error is readily checked because the sum of the node springs (not considering any doubling or reduction of end springs) should equal the volume under the k_s curve. The equations given by Newmark (1943) include a derivation in the Appendix

to his paper. For constant k_s the illustrations for K_1, K_2 previously given can be used, which are essentially average end area computations.

We can readily check the programming for the beam equations by referring to Example 9-6, which lists k_s and all node springs. The sum of the listed node springs is

$$\frac{11\,616}{2} + 11\,616 + 14\,520 + \cdots + 27\,588 + \frac{29\,040}{2} = 370\,550.4$$

The two end values were doubled in the program, since this was a beam. The volume of the k_s curve is

$$V = B \times L \times k_s$$

and, taking L = sum of element lengths = 6.38 m and B = 2.64 m, we obtain

$$V = 2.64 \times 6.38 \times 22\,000 = 370\,550$$

for very nearly an exact check. The reason for this close agreement with using a constant k_s is that the element lengths are rather short.

Spring Coupling

From a Boussinesq analysis it is evident that the base contact pressure contributes to settlements at other points, i.e., causing the center of a flexible uniformly loaded base to settle more than at the edges. Using a constant k_s on a rectangular uniformly loaded base will produce a constant settlement (every node will have the same ΔH within computer round-off) if we compute node springs based on contributing node area. This approach is obviously incorrect, and many persons do not like to use k_s because of this problem. In other words the settlement is "coupled" but the soil springs from k_s have not been coupled.

It is still desirable, however, to use k_s (some persons call this a *Winkler* foundation) in a spring concept because only the diagonal translation terms are affected. When we have true coupling, fractions of the springs K_i are in the off-diagonal terms, making it difficult to perform any kind of nonlinear analysis (soil-base separation or excessive displacements). We can approximately include coupling effects in several ways:

1. Double the end springs, which effectively increases k_s in the end zones. This approach is not applicable to the sides of very long narrow members.
2. Zone k_s with larger values at the ends that transition to a minimum at the center. This concept was illustrated in Example 9-5 where the center k_s was considerably smaller than the corner value.

For beam-on-elastic-foundation problems, where concentrated loads and moments are more common than a uniform load, doubling the end springs is probably sufficient coupling.

Finite Element Computer Program for Beam-on-Elastic Foundation

A computer program would develop the EA and ES for each finite element in turn from input data describing the member so that I, L, and computations (or read in) for K_1 and K_2 can be made. The program performs matrix operations to form the $\mathbf{ESA}^T$ and $\mathbf{EASA}^T$ and with proper instructions identifies the P–X coding so the $\mathbf{EASA}^T$ entries are correctly inserted into the global $\mathbf{ASA}^T$.

When this has been done for all the finite elements (number of members NM, a global $\mathbf{ASA}^T$ of size NP × NP will have been developed as follows:

$$\mathbf{P}_{NP} = \mathbf{A}_{NP\times NF}\mathbf{S}_{NF\times NF}\mathbf{A}^T_{NF\times NP}\mathbf{X}_{NP}$$

and canceling interior terms as shown gives

$$\mathbf{P}_{NP} = \mathbf{ASA}^T_{NP\times NP}\mathbf{X}_{NP}$$

which indicates that the system of equations is just sufficient (that is, a square coefficient matrix, the only type that can be inverted). It also gives a quick estimate of computer needs, as the matrix is always the size of (NP × NP) where NP is the number of *P–X* codings. With proper coding (as in Fig. 9-12) the global $\mathbf{ASA}^T$ is banded with all zeros except for a diagonal strip of nonzero entries that is eight values wide. Of these eight nonzero entries, four are identical (the band is symmetrical). There are matrix reduction routines to solve these types of half-band width problems. As a consequence the actual matrix required (with a band reduction method) is only **NP** × **4** entries instead of NP × NP.

The $\mathbf{ASA}^T$ is inverted (computer program FADBEMLP on the diskette reduces a band matrix) and multiplied by the **P** matrix containing the known externally applied loads. This step gives the nodal displacements of rotation and translation. The computer program then rebuilds the **EA** and **ES** to obtain the $\mathbf{ESA}^T$ and, using Eq. (*d*), computes the element end moments. Node reactions R_i and soil pressures q_i are computed using

$$R_i = K_i X_i \qquad q_i = k_s X_i$$

It may be convenient to store the $\mathbf{ESA}^T$ on a disk file when the $\mathbf{ASA}^T$ is being built and recall it to compute the element end moments of the **F** matrix.

If the footing tends to separate from the soil or the deflections are larger than X_{max} it is desirable to have some means to include the footing weight, zero the soil springs where nodes separate, and apply a constant force to nodes where soil deflections exceed X_{max} of

$$P_i = -K_i(X_{max})$$

Note the sign is negative to indicate the soil reaction opposes the direction of translation. Actual sign of the computed *P* matrix entry is based on the sign convention used in developing the general case as in Fig. 9-12.

A computer program of this type (FADBEMLP on your diskette) can be used to provide the output of Example 9-6 and can also be used to solve a number of structural problems by using 0.0 for k_s.

Example 9-6. Given the general footing and load data shown in Fig. E9-6*a*, assume the loads are factored and might be obtained from some kind of horizontal tank loading where the loads are from the tank supports and are the full width (2.64 m) of the footing. Take $k_s = LF \times k_s = 1.571 \times 14\,000 = 22\,000$ kN/m^3; also $f'_c = 21$ MPa → $E_c = 21\,500$ MPa.

Comments based on Figs. E9-6b, c, and d.

1. The $\sum F_v \approx 0$ (spring forces = 3374.7 vs. 3375 kN input) and is within computer round-off using single precision with 6^+ digits.
2. For the far end of element 9 and near end of element 10,

$$\text{Moment difference} = 549.3 - 468.4 = 80.9\ (81.0\ \text{input})$$

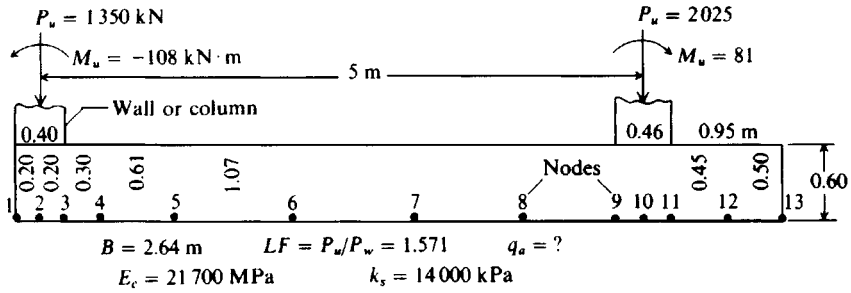

Figure E9-6*a*

3. The moments for the near end of element 1 and far end of element 12 should both be 0.0 (0.014 and −0.004).
4. If the largest soil pressure of 260.1/LF ≤ q_a, the bearing pressure would be O.K. We must use an LF here since factored loads were input.
5. The largest node displacements are

$$\text{Translation} = 11.8 \text{ mm} \qquad \text{(at node 1)}$$
$$\text{Rotation} = -0.002\,53 \text{ rad} \qquad \text{(at nodes 1 \& 2)}$$

6. The output table of displacements from the disk plot file is used to plot the shear V and moment M diagrams shown in Fig. E9-6*c*. You should study these carefully and see how the output is interpreted—particularly at nodes with input moments. Compare the plots to the output checks shown in Fig. E9-6*d*. Refer also to the shear and moment plots of Fig. E13-1*g*.

Comments.

1. The author recently noted that Westergaard (1948) indicated that edge springs probably should be doubled. This suggestion probably did not receive the attention it should have because his observation was the last page of a "Discussion."
2. The question arises of whether one should double the edge springs or double k_s at the ends. Having checked both procedures, the author recommends doubling the edge springs for a beam-on-elastic-foundation problem. For mats one probably should double the edge k_s as that seems to give slightly better values over doubling edge springs. Doubling edge k_s for mats gives large computed edge node soil pressures that include both bearing and edge shear and may (incorrectly) give $q_i > q_a$.
3. There have been some efforts to use only one or two elements by integrating the modulus of subgrade reaction across the beam length. The author does not recommend this for three reasons:
   a. It is difficult to allow for nonlinear effects or for soil-footing separation.
   b. When using a nonlinear analysis with X_{max} the setting of a soil spring to zero introduces a discontinuity into the model. The discontinuity is minimized by using a number of closely spaced elements, the better to transition from the displacements $X > X_{max}$ and displacements $X \le X_{max}$.
   c. It is difficult to produce a shear and moment diagram unless several elements are used. With the availability of computers, there is no justification to use a clever one-element model and have an enormous amount of hand computations to obtain the shear and moment diagrams.

   The author suggests that one should use a minimum of 10 elements for a beam—more for long beams or if it appears that any nonlinear zones are present.

```
 DATA SET FOR EXAMPLE 9-6 SI-UNITS

     ++++++++++++++++++ THIS OUTPUT FOR DATA FILE:  EXAM96.DTA


 SOLUTION FOR BEAM ON ELASTIC FOUNDATION--ITYPE = 0  +++++++

 NO OF NP =  26   NO OF ELEMENTS, NM = 12   NO OF NON-ZERO P, NNZP =  4
   NO OF LOAD CASES, NLC =  1                    NO OF CYCLES NCYC =  1
 NODE SOIL STARTS JTSOIL =  1
      NONLINEAR (IF > 0) =  1            NO OF BOUNDARY CONDIT NZX =  0
           MODULUS KCODE =  1                      LIST BAND IF > 0 =  0
                                                      IMET (SI > 0) =  1

 MOD OF ELASTICITY E =    21500. MPA

MEMNO   NP1   NP2   NP3   NP4   LENGTH     WIDTH     INERTIA, M**4

    1     1     2     3     4      .200     2.640     .47520E-01
    2     3     4     5     6      .200     2.640     .47520E-01
    3     5     6     7     8      .300     2.640     .47520E-01
    4     7     8     9    10      .610     2.640     .47520E-01
    5     9    10    11    12     1.070     2.640     .47520E-01
    6    11    12    13    14     1.070     2.640     .47520E-01
    7    13    14    15    16      .910     2.640     .47520E-01
    8    15    16    17    18      .610     2.640     .47520E-01
    9    17    18    19    20      .230     2.640     .47520E-01
   10    19    20    21    22      .230     2.640     .47520E-01
   11    21    22    23    24      .450     2.640     .47520E-01
   12    23    24    25    26      .500     2.640     .47520E-01

 THE INITIAL INPUT P-MATRIX ENTRIES
 NP    LC     P(NP,LC)
  3     1      -108.000
  4     1      1350.000
 19     1        81.000
 20     1      2025.000

 THE ORIGINAL P-MATRIX WHEN NONLIN > 0 ++++++
     1          .00          .00
     2      -108.00      1350.00
     3          .00          .00
     4          .00          .00
     5          .00          .00
     6          .00          .00
     7          .00          .00
     8          .00          .00
     9          .00          .00
    10        81.00      2025.00
    11          .00          .00
    12          .00          .00
    13          .00          .00

 THE NODE SOIL MODULUS, SPRINGS AND MAX DEFL:
 NODE     SOIL MODULUS     SPRING,KN/M    MAX DEFL, M
    1          22000.0      11616.0          .0500
    2          22000.0      11616.0          .0500
    3          22000.0      14520.0          .0500
    4          22000.0      26426.4          .0500
    5          22000.0      48787.2          .0500
```

Figure E9-6*b*

6	22000.0	62145.6	.0500
7	22000.0	57499.2	.0500
8	22000.0	44140.8	.0500
9	22000.0	24393.6	.0500
10	22000.0	13358.4	.0500
11	22000.0	19747.2	.0500
12	22000.0	27588.0	.0500
13	22000.0	29040.0	.0500

BASE SUM OF NODE SPRINGS = 370550.4 KN/M NO ADJUSTMENTS
* = NODE SPRINGS HAND COMPUTED AND INPUT

MEMBER MOMENTS, NODE REACTIONS, DEFLECTIONS, SOIL PRESSURE, AND LAST USED P-MATRIX FOR LC = 1

MEMNO	MOMENTS--NEAR END 1ST, KN-M		NODE	SPG FORCE, KN	ROT, RADS	DEFL, M	SOIL Q, KPA	P-, KN-M	P-, KN
1	.014	-27.486	1	137.35	-.00253	.01182	260.12	.00	.00
2	-80.742	297.008	2	131.47	-.00253	.01132	248.99	-108.00	1350.00
3	-297.074	574.550	3	157.02	-.00250	.01081	237.91	.00	.00
4	-574.568	976.292	4	266.45	-.00237	.01008	221.82	.00	.00
5	-976.300	1223.258	5	427.76	-.00190	.00877	192.89	.00	.00
6	-1223.256	983.240	6	455.11	-.00075	.00732	161.11	.00	.00
7	-983.243	404.543	7	411.62	.00040	.00716	157.49	.00	.00
8	-404.557	-194.635	8	346.31	.00102	.00785	172.60	.00	.00
9	194.540	-468.397	9	207.48	.00108	.00851	187.13	.00	.00
10	549.286	-384.339	10	116.85	.00101	.00875	192.45	81.00	2025.00
11	384.351	-141.243	11	177.07	.00090	.00897	197.27	.00	.00
12	141.230	-.004	12	257.77	.00079	.00934	205.56	.00	.00
			13	282.44	.00075	.00973	213.97	.00	.00

SUM SPRING FORCES = 3374.71 VS SUM APPLIED FORCES = 3375.00 KN

(*) = SOIL DISPLACEMENT > XMAX SO SPRING FORCE AND Q = XMAX*VALUE ++++++++++++
NOTE THAT P-MATRIX ABOVE INCLUDES ANY EFFECTS FROM X > XMAX ON LAST CYCLE ++++++++++

FOLLOWING IS DATA SAVED TO DATA FILE: BEAM1.PLT

REFER TO "READ" STATEMENT 2040 FOR FORMAT TO USE FOR PLOT PROGRAM ACCESS

NODE	LENGTH	KS	COMP X,MM	XMAX	SHEAR V(I,1),V(I,2) LT OR T	RT OR B	MOMENT MOM(I,1),MOM(I,2) LT OR T	RT OR B
1	.000	22000.0	11.824	50.000	.00	-137.36	.0	.0
2	.200	22000.0	11.318	50.000	-137.36	1081.33	-27.5	80.7
3	.400	22000.0	10.814	50.000	1081.33	924.92	297.0	297.1
4	.700	22000.0	10.083	50.000	924.92	658.56	574.6	574.6
5	1.310	22000.0	8.768	50.000	658.56	230.80	976.3	976.3
6	2.380	22000.0	7.323	50.000	230.80	-224.31	1223.3	1223.3
7	3.450	22000.0	7.159	50.000	-224.31	-635.93	983.2	983.2
8	4.360	22000.0	7.846	50.000	-635.93	-982.28	404.5	404.6
9	4.970	22000.0	8.506	50.000	-982.28	-1190.68	-194.6	-194.5
10	5.200	22000.0	8.748	50.000	-1190.68	717.16	-468.4	-549.3
11	5.430	22000.0	8.967	50.000	717.16	540.24	-384.3	-384.4
12	5.880	22000.0	9.344	50.000	540.24	282.45	-141.2	-141.2
13	6.380	22000.0	9.726	50.000	282.45	.00	.0	.0

Figure E9-6*b* (*continued*)

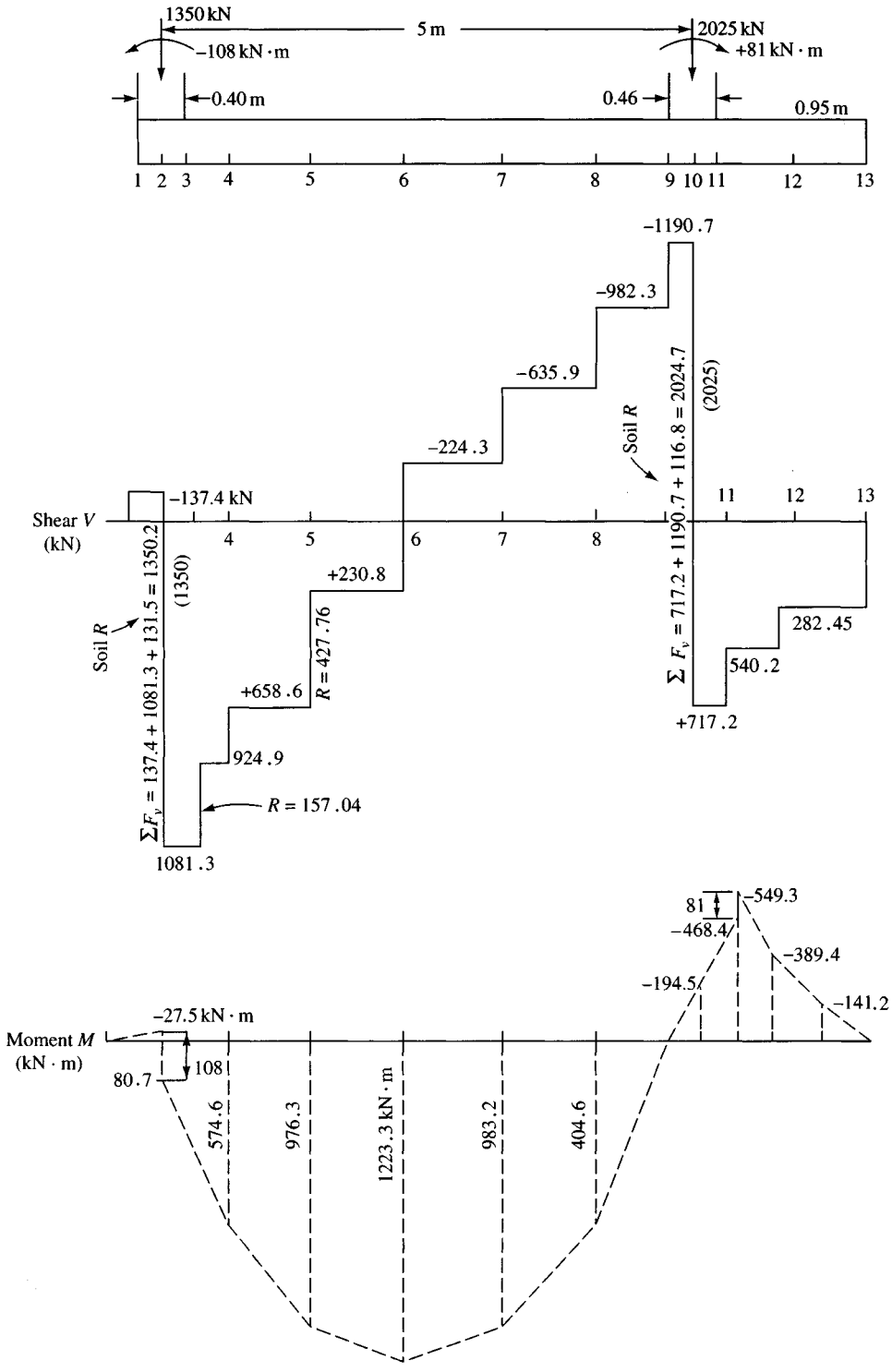
1350 kN
5 m
2025 kN
−108 kN · m
+81 kN · m
0.40 m
0.46
0.95 m
1 2 3 4 5 6 7 8 9 10 11 12 13
−1190.7
−982.3
−635.9
−224.3
Soil R
(2025)
Shear V
(kN)
−137.4 kN
11 12 13
4 5 6 7 8
+230.8
Soil R
(1350)
R = 427.76
+658.6
282.45
540.2
924.9
R = 157.04
+717.2
1081.3
−549.3
81
−468.4
−389.4
−194.5
−141.2
−27.5 kN · m
Moment M
(kN · m)
80.7
108
574.6
976.3
1223.3 kN · m
983.2
404.6

Figure E9-6*c*

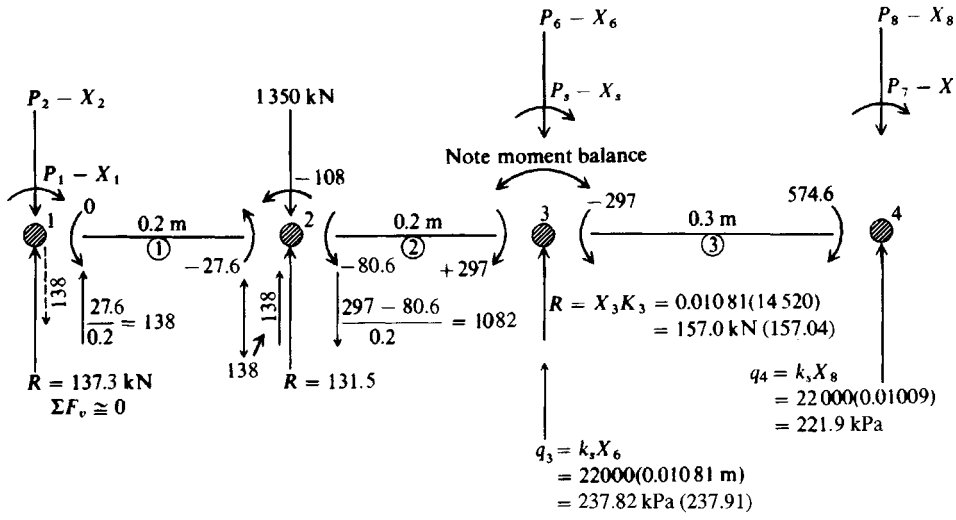

Check node 2:

$\Sigma F_{v2} = 138 + 131.5 + 1082 = 1351.5 \cong 1350$ O.K.

$\Sigma M_2 = 108 - 27.6 - 80.6 \cong 0$ O.K.

$$I = \frac{Bt^3}{12} = \frac{2.64(0.6)^3}{12} = 0.047\,520\ \text{m}^4 \text{ moment of inertia of any element}$$

$$K_1 = 22\,000\left(\frac{0.2}{2}\right)(2.64)(2) = 11\,616\ \text{kN/m}$$

$$K_2 = 22\,000(0.2)(2.64) = 11\,616\ \text{kN/m}$$

} Soil spring computations for first two nodes

R = node spring force

Large numbers in SI produce round-off error using single precision. Also computer values use more digits.

Figure E9-6*d*

////

9-9 RING FOUNDATIONS

Ring foundations can be used for water tower structures, transmission towers, TV antennas, and to support various process tower superstructures. The ring foundation considered here is a relatively narrow circular beam as opposed to the circular mat considered in the next chapter.

The finite-element method (FEM) for a ring foundation is somewhat similar to the beam-on-elastic-foundation method. The node and element numbering are rather straightforward, as shown in Fig. 9-14. The computer program is considerably more lengthy since the P–X coding is somewhat different (see Fig. 9-15) in order to obtain a bandwidth of 9. A bandwidth of 60 is obtained if one proceeds in a continuous manner counterclockwise around the ring from node 1. The element **A** matrix is:

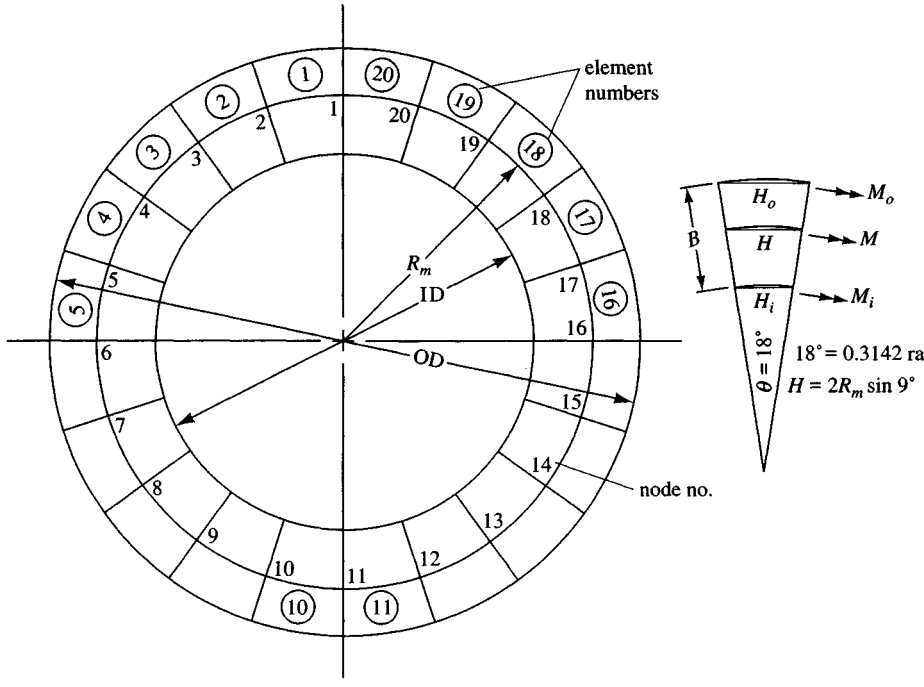

(*a*) Element and node numbering.

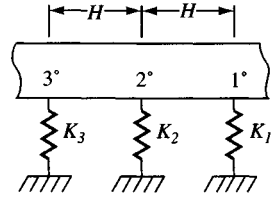

(*b*) Node springs $K = \dfrac{0.7854(\text{OD}^2 - \text{ID}^2)k_s}{20}$

Figure 9-14 Ring foundation configuration and definitions. Note that loads should be placed on mean radius R_m, which divides ring *area* in half, and not on average radius, which divides the ring *width* in half. Always orient your ring so node 1 is at top of page as shown here.

EA =

	1	2	3	4
1	$\sin a$	—	$\cos a$	—
2	$\cos a$	—	$-\sin a$	—
3	$-1/H$	$-1/H$	—	—
4	—	$\sin a$	—	$-\cos a$
5	—	$\cos a$	—	$\sin a$
6	$1/H$	$1/H$	—	—

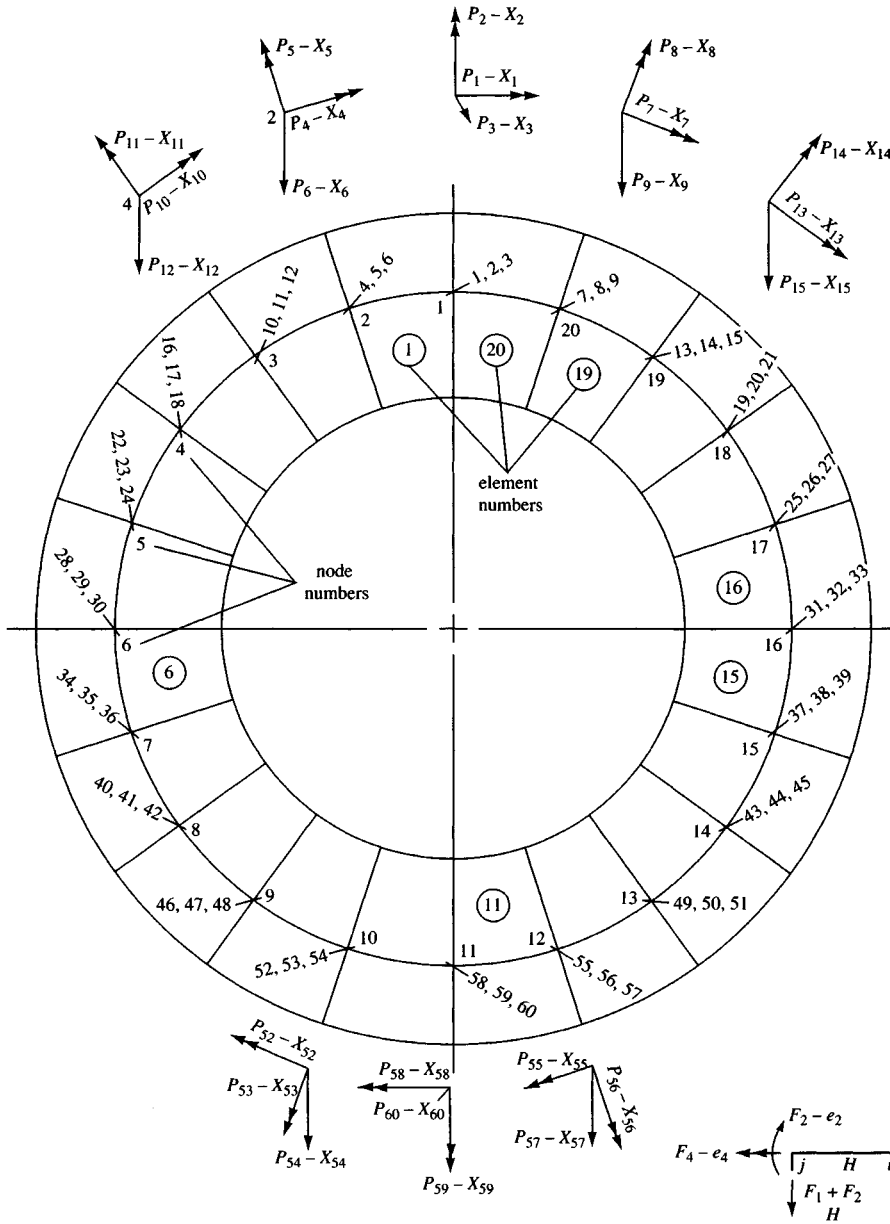

(*a*) General $P - X$ coding. This coding scheme reduces the bandwidth from 60 to 6. For orientation, stand inside ring and look out along any radial line.

(*b*) General forces on element *i*. Note moment F_1 is on near end and F_2 is on far end. Also note far end of element 20 is the near end of element 1.

Figure 9-15 Ring foundation P–X coding and orientation and element forces.

where $\sin a = \sin 9°$

$\cos a = \cos 9°$

$H = 2R_m \sin 9°$

and, allowing for torsion, the element stiffness matrix is

$$\mathbf{ES} =$$

F \ e	1	2	3	4
1	$\frac{4EI}{H}$	$\frac{2EI}{H}$	—	—
2	$\frac{2EI}{H}$	$\frac{4EI}{H}$	—	—
3	—	—	$\frac{GJ}{H}$	—
4	—	—	—	$\frac{GJ}{H}$

The usual matrix multiplications are carried out to produce the element $\mathbf{EASA}^{\mathrm{T}}$, which is then summed into the global $\mathbf{ASA}^{\mathrm{T}}$ matrix, which is then banded and reduced to produce the nodal displacements X_i. The displacements are then used to compute the element forces (moments and shears), soil reactions, and pressures.

To avoid twisting and for a theoretical uniform displacement across the radial line defining any node, one should place the loads on the mean radius R_m, defining the center of area and computed as

$$R_m = \sqrt{\frac{\mathrm{ID}^2 + \mathrm{OD}^2}{8}},$$

rather than on the arithmetic average radius,

$$R_a = \frac{(\mathrm{ID} + \mathrm{OD})}{4}.$$

The moments are computed at the center of area defined by the mean radius R_m (see Fig. 9-14*a*) so that the displacements can be assumed to be constant across the ring radius at the node. Since the inner and outer element lengths are different but with the same end displacements, there should be a different moment according to the central finite-difference expression given as

$$M = \frac{EI}{\Delta x^2}(y_{n+1} - 2y_n + y_{n-1})$$

Replacing Δx^2 by ΔH^2 we can readily see the moment at the inner radius defined by the ID is larger than at the mean radius, and the outer moment at the radius defined by the OD is smaller than the mean radius value. We can adjust for these values as follows:

$$M_i = \left(\frac{2R_m}{\mathrm{ID}}\right)^2 M_m \qquad \text{and} \qquad M_o = \left(\frac{2R_m}{\mathrm{OD}}\right)^2 M_m$$

where M_m = computed value on computer output sheets, and the interior moment M_i and exterior moment M_o can be computed using the preceding expressions.

The finite-element length H is taken as the chord distance and differs slightly from the arc length L_a as follows:

$$L_a = R_m \times 0.314\,16 \qquad H = 2 \times R_m \sin 9^\circ = R_m \times 0.312\,87$$

The node springs (see Fig. 9-14*b*) are computed using a constant value of modulus of subgrade reaction k_s as

$$K_i = \frac{0.7854(\text{OD}^2 - \text{ID}^2)k_s}{20}$$

However, one may input springs for selected nodes in the computer program.

The solution of a ring foundation will be illustrated by Example 9-7, using program B-17, described in the README.DOC file on your diskette.

Example 9-7. Find the bending moments and other data for a ring foundation given the following:

ID = 14.5 m OD = 16.0 m D_c = 0.76 m

E_c = 22 400 MPa k_s = 13 600 + 0Z[1] kN/m^3

(Assume Poisson's ratio of concrete μ = 0.15)

Three equally spaced (120°) loads of 675 kN each

Tangential moment = +200 kPa at node 1 (+) using the right-hand rule (based on the *P–X* coding of Fig. 9-15)

Consider the ring foundation to be *weightless* (although the computer program allows the input of the unit weight of the beam material and will then compute a weight contribution for each node).

Solution.

Step 1. We will put one load on node 1 and the other two will fall on element 7 and on element 14 (as shown on Fig. E9-7*a*). The loads on elements 7 and 14 will have to be prorated to adjacent nodes. We can use either L_a or H for the prorating. Using L_a, we write

$$R_m = \sqrt{\frac{14.5^2 + 16^2}{8}} = 7.634 \text{ m}$$

$$[\text{Average } R_a = (14.5 + 16)/4 = 7.625 \text{ m} < 7.634]$$

$$L_a = 7.634(0.314\,16) = 2.398 \text{ m}$$

Load location = $120^\circ - 6 \times 18^\circ = 120^\circ - 108^\circ = 12^\circ$ into element 7, which is exactly two-thirds of the length (either L_a or H), that is,

$$\frac{2}{3}L_a = \frac{2}{3}(2.398) = 1.599 \text{ m} \qquad \frac{L_a}{3} = \frac{2.398}{3} = 0.799 \text{ m}$$

The column loads are entered in the vertical P's so that

$$\text{Node 7: } P_{36} = \frac{0.799}{2.398}(675) \approx 224.6 \text{ kN}$$

$$\text{Node 8: } P_{42} = \frac{1.599}{2.398}(675) \approx \underline{450.4} \text{ kN}$$

$$\text{Total} = 675.0 \text{ kN}$$

Node 14: Same as node 8 $\rightarrow$ P_{45} = 450.4 kN

Node 15: Same as node 7 $\rightarrow$ P_{39} = 224.6 kN

Node 1: Moment gives P_1 = 200 kN · m

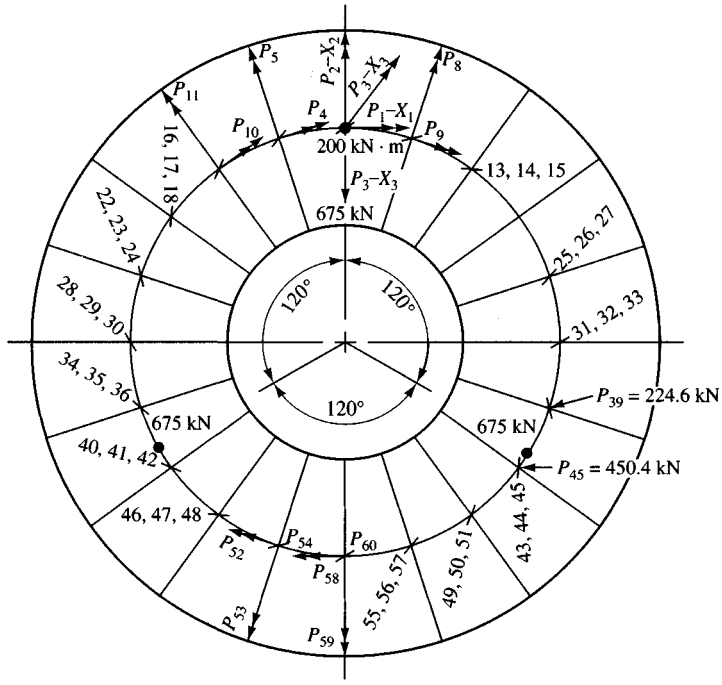

Figure E9-7*a*

These data are shown on Fig. E9-7*b* (computer output pages) where the P matrix is listed.

Step 2. Check the output. The output is partially self-checking. Note that the program converts E_s from MPa to kPa and computes the shear modulus

$$G_c' = \frac{E_c}{2(1+\mu)} = \mathbf{9\,739\,130}\ \text{kPa}$$

1. First check that the sum of input vertical forces = sum of soil springs (the program sums the spring forces).
2. Since the loads are symmetrical and there is a moment only at node 1, there should be some symmetry in the soil springs (which also represents symmetry in the translation displacements).
3. All of the soil springs should be equal (unless some were input (not done here)). The springs should be

$$K_i = \frac{0.7854(16^2 - 14.5^2)(13\,600)}{20} = \mathbf{24\,433.8}\ \text{kN/m}$$

(The computer value of 24 433.72 uses more digits, but in single precision.)

4. The program computes the moment of inertia using a beam with $b = (16 - 14.5)/2 = \mathbf{0.75}$ m as

$$I_i = \frac{bt^3}{12} = \frac{0.75(0.76^3)}{12} = \mathbf{0.027\,436}\ \text{m}^4$$

The torsion inertia J for a rectangle is computed in the program as:

$$J = bt^3\left[\frac{1}{3} - 0.21\frac{t}{b}\left(1 - \frac{t^4}{12b^4}\right)\right],\ \text{m}^4$$

t = thickness, b = width of rectangle, and $t < b$.

```
++++++++++++ NAME OF DATA FILE USED FOR THIS EXECUTION:  EXAM97A.DTA

  EXAMPLE 9-7 RING FOUNDATION OF FAD 5/E--SI UNITS

INPUT CONTROL PARAMETERS:
   NO OF P-MATRIX ENTRIES, NNZP =  6
          NO OF LOAD CASES, NLC =  1
    NO OF BOUND CONDITIONS, NZX =  0
NO OF INPUT SOIL SPRINGS, ISPRG =  0
                NONLIN (IF >0) =  1        IMET (SI>0) =  1


THE ELEMENTS AND NPE(I):
ELEM NO          NPE(I)
    1          1    2    3    4    5    6
    2          4    5    6   10   11   12
    3         10   11   12   16   17   18
    4         16   17   18   22   23   24
    5         22   23   24   28   29   30
    6         28   29   30   34   35   36
    7         34   35   36   40   41   42
    8         40   41   42   46   47   48
    9         46   47   48   52   53   54
   10         52   53   54   58   59   60
   11         58   59   60   55   56   57
   12         55   56   57   49   50   51
   13         49   50   51   43   44   45
   14         43   44   45   37   38   39
   15         37   38   39   31   32   33
   16         31   32   33   25   26   27
   17         25   26   27   19   20   21
   18         19   20   21   13   14   15
   19         13   14   15    7    8    9
   20          7    8    9    1    2    3

RING FOUNDATION DATA AS FOLLOWS:
             DIAMETER: OD =  16.000    ID =  14.500  M
          RING DEPTH, DC =    .760  M
          UNIT WT OF FTG =    .000 KN/M*3
       SOIL MODULUS, SK = 13600.00 KN/M*3
 MAX LINEAR SOIL DEFL, XMAX =  .02000  M
       MOD OF ELAS CONC = 22400000. KPA
           POISSON RATIO =  .150
      SHEAR MODULUS, GC =  9739130. KPA

SELECTED COMPUTED VALUES:
     MOM OF INERTIA: XI = .27436E-01     XJ = .45670E-01  M**4
       NODE SOIL SPRING =  24433.72 KN/M
        MEAN RADIUS, RM =   7.634  M
         ELEMENT: WIDTH =   .750
         W/LENGTHS  ARC =  2.398   CHORD =  2.389  M
       TOTAL RING AREA =    35.932  M**2
     MOMENT RATIOS:  RO =  .9106  RI = 1.1088


FOR CYCLE =  1
   IF NCYC = 1 OUTPUT ORIGINAL P-MATRIX AND SPRING ARRAY
   IN NCYC > 1 OUTPUT MODIFIED P-MATRIX AND SPRING ARRAY
```

Figure E9-7*b* ***(continued on next page)***

5. The nonlinear routines are not activated since X_{max} (XMAX) was set at 0.02 m (20 mm) and the largest displacement, at node 1 (as expected with a full 675 kN located at the point), is 0.007 93 m (7.93 mm).
6. With a symmetrical load and no radial moments the radial rotation at nodes 1 and 11 are both 0.000 00 as expected.
7. Note that even though the node coding is somewhat mixed, the node and element order is recovered for the output. This result makes it easy to check input node springs. Both input node springs and displacements greater than XMAX are identified on the output sheets.

THE P-MATRIX FOR NLC = 1

NODE		TANGEN MOM		RADIAL MOM		VERT P,KN	SPRING,KN/M
1	1	200.000	2	.000	3	675.000	24433.72
2	4	.000	5	.000	6	.000	24433.72
3	10	.000	11	.000	12	.000	24433.72
4	16	.000	17	.000	18	.000	24433.72
5	22	.000	23	.000	24	.000	24433.72
6	28	.000	29	.000	30	.000	24433.72
7	34	.000	35	.000	36	224.600	24433.72
8	40	.000	41	.000	42	450.400	24433.72
9	46	.000	47	.000	48	.000	24433.72
10	52	.000	53	.000	54	.000	24433.72
11	58	.000	59	.000	60	.000	24433.72
12	55	.000	56	.000	57	.000	24433.72
13	49	.000	50	.000	51	.000	24433.72
14	43	.000	44	.000	45	450.400	24433.72
15	37	.000	38	.000	39	224.600	24433.72
16	31	.000	32	.000	33	.000	24433.72
17	25	.000	26	.000	27	.000	24433.72
18	19	.000	20	.000	21	.000	24433.72
19	13	.000	14	.000	15	.000	24433.72
20	7	.000	8	.000	9	.000	24433.72

DISPLACEMENT MATRIX FOR CYCLE = 1 AND NLC = 1

NODE	X1	TANGENT X2		RADIAL X3		VERTICAL	
1	1	.00002	2	.00000	3	.00793	
2	4	-.00004	5	.00131	6	.00595	√
3	10	.00014	11	.00108	12	.00292	
4	16	.00019	17	.00028	18	.00127	
5	22	.00017	23	-.00059	24	.00164	
6	28	.00008	29	-.00120	30	.00385	
7	34	-.00020	35	-.00091	36	.00666	
8	40	-.00036	41	.00045	42	.00738	
9	46	.00002	47	.00128	48	.00491	
10	52	.00016	53	.00084	54	.00226	
11	58	.00019	59	.00000	60	.00124	
12	55	.00016	56	-.00084	57	.00226	
13	49	.00002	50	-.00128	51	.00491	
14	43	-.00036	44	-.00045	45	.00738	
15	37	-.00020	38	.00091	39	.00666	
16	31	.00008	32	.00120	33	.00385	
17	25	.00017	26	.00059	27	.00164	
18	19	.00019	20	-.00028	21	.00127	
19	13	.00014	14	-.00108	15	.00292	
20	7	-.00004	8	-.00131	9	.00595	√

ELEMENT MOMENTS (KN-M) AND OTHER COMPUTED DATA FOR LC = 1

ELEM #	F(1)	F(3)*	F(2)	F(4)*	SHEAR, KN
1	-619.876	3.068	45.214	46.367	-240.595
2	-57.329	30.126	-170.079	5.180	-95.209
3	160.153	57.484	-217.019	-25.966	-23.808
4	214.420	42.368	-197.204	-48.704	7.208
5	202.603	14.619	-89.486	-50.005	47.359
6	100.559	-19.905	237.422	10.376	141.503
7	-229.008	-63.500	419.104	79.895	79.588
8	-423.281	-53.526	-31.873	33.073	-190.561
9	20.093	41.304	-188.497	-4.847	-70.506
10	180.769	53.639	-217.039	-34.376	-15.185
11	217.039	34.376	-180.768	-53.639	15.186
12	188.497	4.847	-20.092	-41.304	70.506
13	31.873	-33.073	423.282	53.526	190.561
14	-419.104	-79.895	229.009	63.500	-79.588
15	-237.422	-10.376	-100.559	19.905	-141.503
16	89.487	50.005	-202.603	-14.619	-47.359
17	197.205	48.704	-214.421	-42.368	-7.208
18	217.019	25.966	-160.153	-57.484	23.808
19	170.079	-5.180	57.330	-30.126	95.210
20	-45.215	-46.367	619.876	-3.068	240.595

* = TORSION MOMENT (MAY NOT BE ZERO WHEN INPUT MOMENTS)
+++ MOMENTS ABOVE AT MEAN RADIUS RM USE RO*F(I) AND RI*F(I) FOR OUTSIDE AND INSIDE VALUES

Figure E9-7*b* *(continued)*

```
NODE SOIL DATA AND DISPLACEMENTS FOR NLC =  1
                                                        ROTAT., RADS
NODE      SOIL Q,KPA   DISPV, M   SPRING R,KN    RADIAL     TANGENT.
 1   3      107.88    .007932      193.81        .000000    .000017
 2   6       80.92    .005950      145.39        .001313   -.000044
 3  12       39.74    .002922       71.40        .001076    .000142
 4  18       17.26    .001269       31.02        .000282    .000186
 5  24       22.35    .001643       40.15       -.000585    .000172
 6  30       52.40    .003853       94.14       -.001200    .000082
 7  36       90.55    .006658      162.68       -.000912   -.000201
 8  42      100.33    .007377      180.25        .000453   -.000363
 9  48       66.82    .004913      120.05        .001277    .000022
10  54       30.79    .002264       55.32        .000837    .000159
11  60       16.90    .001243       30.37        .000000    .000187
12  57       30.79    .002264       55.32       -.000837    .000159
13  51       66.82    .004913      120.05       -.001277    .000022
14  45      100.33    .007377      180.25       -.000453   -.000363
15  39       90.55    .006658      162.68        .000912   -.000201
16  33       52.40    .003853       94.14        .001200    .000082
17  27       22.35    .001643       40.15        .000585    .000172
18  21       17.26    .001269       31.02       -.000282    .000186
19  15       39.74    .002922       71.40       -.001076    .000142
20   9       80.92    .005950      145.39       -.001313   -.000044

* = NON-LINEAR SOIL SPRING FORCE FOR XMAX*SPRNG1(I)

THE SUM OF INPUT VERTICAL LOADS (INCL FTG WT) =   2025.00
                COMPUTED SOIL SPRING REACTIONS =   2025.00 KN
IF INPUT SUM EQUALS COMPUTED SUM YOU HAVE A STATICS CHECK
   CHECK NODE SOIL PRESSURE Q <= QALLOW
```

8. One should never accept FEM output as correct without at least some internal checks. Here Fig. E9-7*c* (next page) illustrates checking nodes 1 and 11 for statics ($\sum M = 0$ and $\sum F_v = 0$). To orient the moments and end shears, you should be inside the ring and look outward at the element or node of interest. Element end shears are computed (but watch the signs—both the moments and shear direction have one) as $(F_1 + F_2)/H$. For any element the shear at each end is the same but reversed in direction (refer also to Figs. 9-11, 9-12, and 9-15*b*). For element 1 we have the numerical value of the shear using $H = 2(7.634)\sin 9° = 2.388$ m as

$$V = \frac{-619.876 + 45.214}{2.388} = -240.6 \text{ kN } (-240.595 \text{ computer})$$

Although the foregoing came out (−), you must look at the element to assign the correct direction (up or down).

Comment. For design one might use the computed displacements from an analysis such as this, depending on how much confidence the user has in the value of k_s. Many designers use some alternative method for computing settlements that often includes both "immediate" and "consolidation" settlement components. A method for "immediate" settlements was illustrated in Example 5-13 using a case history.

////

9-10 GENERAL COMMENTS ON THE FINITE-ELEMENT PROCEDURE

Strictly, the finite-element model used in this chapter should be termed a *beam-element* model. It is a *beam-column* model when axial forces are included as a part of the element force model. The finite-element method is practical only when written into a computer program, because there are usually too many equations for hand solving. The following comments are

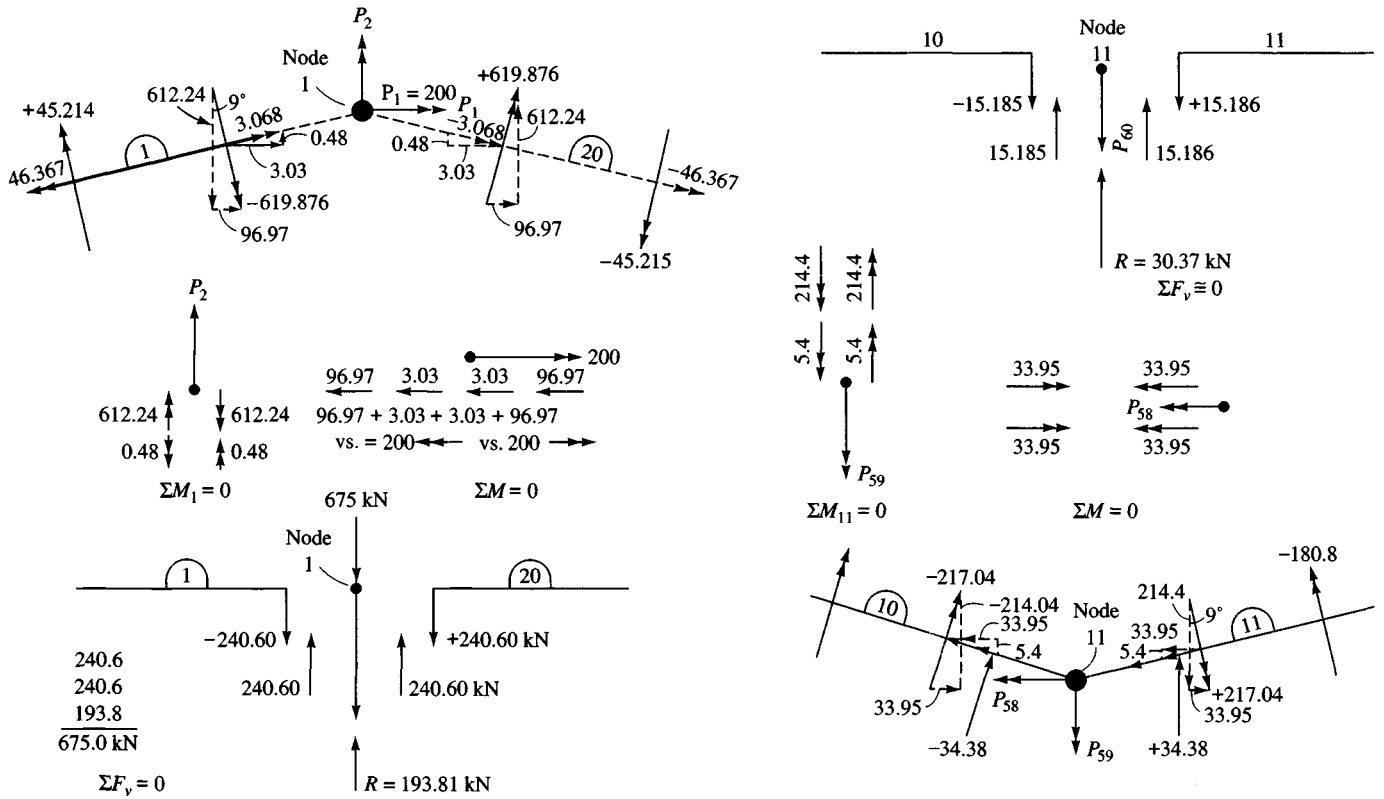
Node
1
P_2
$P_1 = 200$
+619.876
+45.214
612.24
9°
3.068
0.48
3.03
46.367
1
−619.876
96.97
−45.215
20
612.24
−46.367
612.24
0.48
0.48
$\Sigma M_1 = 0$
96.97 3.03 3.03 96.97
200
96.97 + 3.03 + 3.03 + 96.97
vs. = 200
vs. 200
$\Sigma M = 0$
675 kN
−240.60
240.60
240.6
240.6
193.8
675.0 kN
+240.60 kN
240.60 kN
$\Sigma F_y = 0$
$R = 193.81$ kN
10
11
−15.185
15.185
P_{60}
+15.186
15.186
$R = 30.37$ kN
$\Sigma F_y \cong 0$
214.4
5.4
P_{59}
$\Sigma M_{11} = 0$
33.95
P_{58}
$\Sigma M = 0$
−217.04
−214.04
33.95
5.4
214.4
9°
−180.8
+217.04
−34.38
+34.38

Figure E9-7*c*

observations made from solving a large number of different problems using the finite-element method.

1. One must always check finite-element program output. A finite-element computer program should be somewhat self-checking. This is accomplished by echoing back the input and comparing sums of input versus output forces.
   a. Carefully check the input data for correct dimensions, elastic properties, and units.
   b. Check the $\sum M = 0$ at nodes and the sum of soil reactions equal to applied loads ($\sum F_v = 0$). Note how applied moments were treated in Examples 9-6 and 9-7. Also in these examples observe that select nodes were given statics checks.
   c. When the program seems to have been working and a new problem gives obviously incorrect output, compare the *P–X* coding to be sure you are inputting the loads with the correct signs.
2. One should use at a minimum 8 to 10 finite elements, but it is not usually necessary to use more than 20. The number of finite elements used (NM) depends on the length of the member. Also more elements (and closely spaced) are needed if you consider soil nonlinearity or have shear and moment diagrams to plot.
3. One should not use a very short element next to a long element. Use more finite elements and effect a transition between short and long members. Try to keep the ratio

$$\frac{L_{\text{long}}}{L_{\text{short}}} \leq 2 \text{ and not more than } 3.$$

4. The value of k_s directly affects the deflection but has very little effect on the computed bending moments—at least for reasonable values of k_s such as one might obtain from using $k_s = 40(\text{SF})q_a$ (or $k_s = 12(\text{SF})q_a$). If one must obtain accurate displacements one must input a good estimation of k_s.

There are a large number of published solutions claimed by their authors to be better than the simple one proposed here for the beam-on-elastic foundation. A recent claim [Chiwanga and Valsangkar (1988)] has a reference list that may be of some value. Generally, these solutions require additional soil data (which are usually estimated) or obscure soil parameters that are not clearly defined. As a consequence, the solution that is the simplest and requires the minimum of soil properties is going to be the best one—regardless of claims to the contrary. After all, if one must guess at soil values, keep it simple.

As previously stated, a number of beam-on-elastic-foundation solutions claim to allow the user to model the foundation with one or two elements. This is too few for practical purposes in general and too few for realism when including nonlinear effects or where critical values of shear or moment are required for plotting shear and moment curves. In using one or two elements in the beam model these authors do some form of integration, so the result is often a difficult equation containing hyperbolic (and sometimes Bessel and/or Hankel) functions and with strange symbols. These models seldom have any provision for soil-footing separation or for modeling the case where the displacements $X > X_{\max}$.

A note of caution—since k_s is usually estimated—is that the use of refined methods may give undeserved confidence in the computed results.

The only ring solutions known to the author are a closed-form procedure given by Voltera (1952) and Voltera and Chung (1955) and the finite-element method given in the preceding section.

PROBLEMS

TABLE P9-1

Prob.	Col No.	Col Size	Spacing S	Loads DL	Loads LL	f'_c	f_y	Allow soil q_a
a	1	12 in.		100 kip	60			
	2	14	16 ft	160	80	3.0 ksi	50	2.0 ksf
b	1	340 mm		580 kN	310			
	2	380	4.85 m	670	425	21 MPa	400	175 kPa
c	1	340 mm		400 kN	720			
	2	380	5.50 m	780	440	21	350	145
d	1	440 mm		720 kN	890			
	2	440	6.10 m	1120	900	21	400	150

Units: Column Size = in. or mm DL, LL = kips or kN
f'_c = ksi or MPa f_y = ksi or MPa
q_a = ksf or kPa Column spacing S = ft or m

9-1. Design a continuous rectangular footing for the conditions shown in Fig. P9-1 using the assigned data given in Table P9-1 and the method of Sec. 9-2.

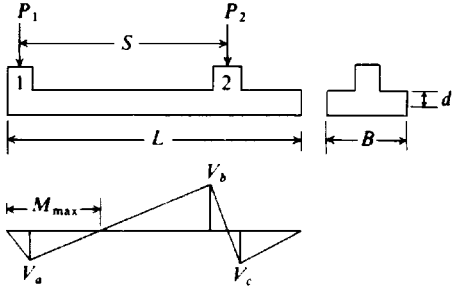

Figure P9-1

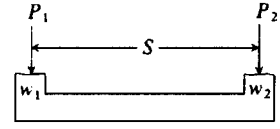

Figure P9-2

9-2. Proportion a trapezoidal-shaped footing using the assigned problem data in Table P9-2, as identified on Fig. P9-2. Draw the shear and moment diagrams.

TABLE P9-2

Prob.	Col	Col Size	Loads DL	Loads LL	Allow soil q_a	Col spacing S
a	1	22 in.	250	200 kips		
	2	18	180	150	4.0 ksf	20.0 ft
b	1	18 in.	180	170 kips		
	2	18	150	110	3.0	15.0 ft
c	1	500 mm	1400	1250 kN		
	2	480	1150	700	120 kPa	5.20 m
d	1	500 mm	2020	1100 kN		
	2	480	1125	1150	195 kPa	4.90 m

Units: Column size: in. or mm DL, LL = kips or kN q_a = ksf or kPa
Column spacing S = ft or m

9-3. Design the trapezoid footing for which the shear and moment diagrams were drawn in Prob. 9-2. Use $f'_c = 21$ MPa or 3 ksi; $f_y = 400$ MPa or 60 ksi.

9-4. What would the dimensions of the two footings of Example 9-3 (strap footing design) be if you used $e =$ value assigned by the instructor (half the class should use 1.0 m and half use 1.4 m) instead of 1.2 m that was used in the example? Compute the volume of concrete for the two footings in Example 9-3 and for your value of e. Swap values of concrete volume with the other group, and for the three points plot e versus concrete volume and see if there might be an optimum e.

9-5. Proportion a strap footing for the following conditions:

	DL	LL
$w_1 =$ 16in. + 6 in. edge distance	50	65 kips
$w_2 =$ 16in.	85	60 kips

9-6. Design d and A_s for footings, and strap for Prob. 9-5. Use $f'_c = 3$ and $f_y = 60$ ksi. Make strap moment of inertia I at least two times I of footing $(BD_c^3/12)$.

9-7. Proportion a strap footing for the following conditions:

	DL	LL
$w_1 =$ 400 mm + 150 mm edge dist	190 kN	300 kN
$w_2 =$ 420 mm	385 kN	270 kN

9-8. Take $f'_c = 21$ and $f_y = 400$ MPa; and design d, A_s, and strap for Prob. 9-7. Make strap moment of inertia I at least two times I of footing $(BD_c^3/12)$.

9-9. Check if $D_c = 0.560$ m is an adequate total depth for the octagon footing for the process tower of Example 9-4.

9-10. Reproportion the octagon footing of Example 9-4 if $q_a = 120$ kPa and the importance factor $I = 1.0$ (instead of 1.15 of the example). Find A_s and make a neat drawing showing how you would place the reinforcing bars.

Modulus of subgrade reaction, k_s

9-11. Referring to Example 9-5, compute k_s for a midside and the $\frac{1}{4}$ and $\frac{1}{8}$ points along the midside to center of the base. Using these three points + the center point of the example, make a plot of k_s versus location and comment on its shape. How close is the edge k_s value to double that of the center?

9-12. Estimate k_s for a soil with $\phi = 34°$ and $c = 25$ kPa.

9-13.* Estimate k_s for the soil of Prob. 3-10.

9-14.* Estimate k_s for the soil of Prob. 3-11.

9-15.* Estimate k_s using the dilatometer data of Prob. 3-14.

* Since there will be a number of different values for any of Problems 9-13, 9-14, and 9-15, the individual values should be turned in or placed on the blackboard, and a statistical average of all the values used should be obtained, with each student computing the statistical class average and comparing it to his or her own value. Any student whose value is more than two standard deviations from the average should give an explanation for the divergence.

Beam-on-elastic foundation

9-16. Refer to the computer output of Fig. E9-6*c* (beam-on-elastic foundation) and perform a statics check at nodes 10 and 13.

9-17. Refer to the computer output of Fig. E9-6*c* and verify the node reaction and soil pressure at nodes 8 and 13.

9-18. Using program B-5 (FADBEMLP) on your program diskette, solve Example 9-1 as a beam-on-elastic foundation. Use nodes at column faces and other locations as necessary and estimate $k_s = 120q_{ult}$. Compare the moments output with those in the table in the example. Also compare the node soil pressures with the uniform values assumed in Example 9-1. Note that you should use ultimate loads and moments for consistency in comparing the example table and computing k_s.

9-19. Make a beam-on-elastic-foundation solution for Example 9-1 using computer program B-5 (FADBEMLP) on your program diskette. For the first trial use $k_s = 120q_{ult}$. Make two additional runs using (*a*) $k_s = 0.5$ and (*b*) two times the initially estimated value. Make one additional run where you input the undoubled values of the two end springs using a program option. Can you draw any conclusions after inspecting the moment and displacement output about the effect of doubling end springs and what is used for k_s?

9-20. Using program B-5 (FADBEMLP) on your program diskette, solve the trapezoidal footing of Example 9-2 as a beam-on-elastic foundation. You will have to use average element widths and estimate $k_s = 120q_i$. Compare the output moments with the moment table in Example 9-2. Also compare the soil node pressures with the uniform value assumed in the example.

9-21. Use program B-5 (FADBEMLP) on the enclosed diskette and analyze the strap footing you designed in Problem 9-6 or 9-8. Use at least four nodes across each footing. Based on the footing displacements, do you think your strap has a sufficient moment of inertia I?

9-22. Refer to the computer output of Fig. E9-6*c* of Example 9-6 and rerun the example using XMAX = 0.011 m. Plot the vertical displacements to a large scale such as 0.01 m = 10 mm (or 2 cm), and superimpose on this displacement plot the horizontal line of XMAX = 0.011 (11 mm).

Ring foundations

9-23. Perform a statics check of the ring foundation of Example 9-7 at node 6 or node 16 as assigned.

9-24. If you have access to the ring foundation computer program (B-17), redo Example 9-6 for k_s = 0.5, 1.5, and 2.0 times the value used of 13 600 kPa. Can you draw any conclusions about the effect of k_s?

9-25. If you have access to computer program B-17, design a ring foundation similar to Example 9-7 assuming a water tower with four equally spaced columns. Other data:

$R_m = 7.5$ m.
The tank holds 378 m^3 of water.
The empty tank, appurtenances, and legs weigh 2200 kN.
The wind moment is 2250 kN · m.
Take the maximum allowable soil pressure (SF = 2) as 200 kPa.
$f'_c = 28$ MPa.
$f_y = 400$ MPa.

Required: Find the ID, OD, and foundation depth D_c of the base. Be sure to check at least two nodes (not adjacent) and draw a neat sketch showing column locations and other critical data.

CHAPTER 10

MAT FOUNDATIONS

10-1 INTRODUCTION

A mat foundation is a large concrete slab used to interface one column, or more than one column in several lines, with the base soil. It may encompass the entire foundation area or only a portion. A mat may be used to support on-grade storage tanks or several pieces of industrial equipment. Mats are commonly used beneath silo clusters, chimneys, and various tower structures. It becomes a matter of definition as to when the dimensions of a spread footing make the transition into being called a mat. Figure 10-1 illustrates several mat configurations as might be used for buildings. Those shown encompass the entire building plan, but this is not a requirement.

A mat foundation may be used where the base soil has a low bearing capacity and/or the column loads are so large that more than 50 percent of the area is covered by conventional spread footings. It is common to use mat foundations for deep basements both to spread the column loads to a more uniform pressure distribution and to provide the floor slab for the basement. A particular advantage for basements at or below the GWT is to provide a water barrier. Depending on local costs, and noting that a mat foundation requires both positive and negative reinforcing steel, one may find it more economical to use spread footings—even if the entire area is covered. Spread footings avoid the use of negative reinforcing steel and can be accomplished as in Fig. 10-2 by pouring alternate footings, to avoid formwork, and using fiber spacer boards to separate the footings poured later.

Mat foundations may be supported by piles in situations such as high groundwater (to control buoyancy) or where the base soil is susceptible to large settlements. We should note that the mat contact stresses will penetrate the ground to a greater depth or have greater relative intensity at a shallower depth (refer to Figs. 5-4 and 5-9). Both factors tend to increase settlements unless there is a stress compensation from excavated soil so that the *net* increase in pressure is controlled.

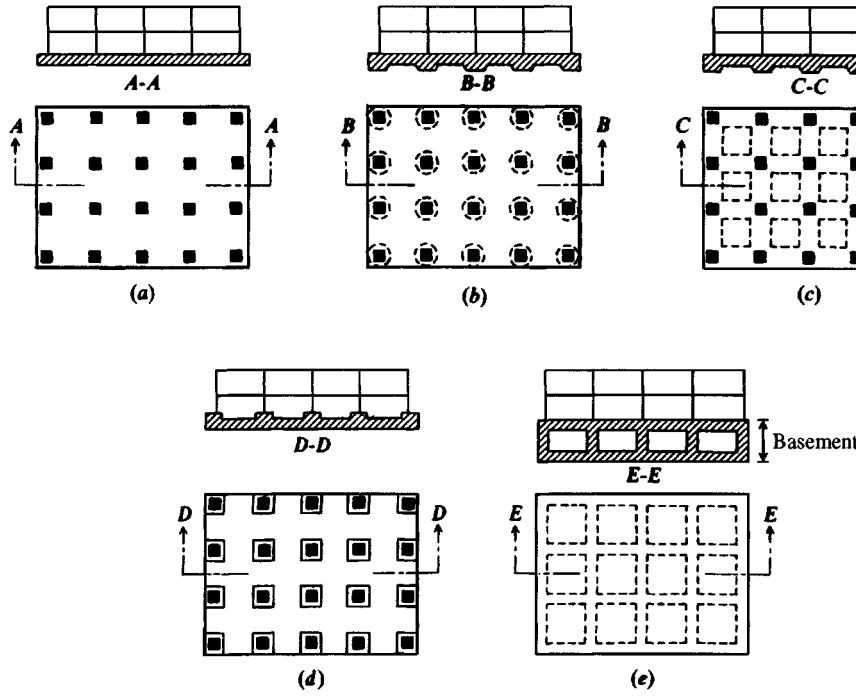

Figure 10-1 Common types of mat foundations. (*a*) Flat plate; (*b*) plate thickened under columns; (*c*) waffle-slab; (*d*) plate with pedestals; (*e*) basement walls as part of mat.

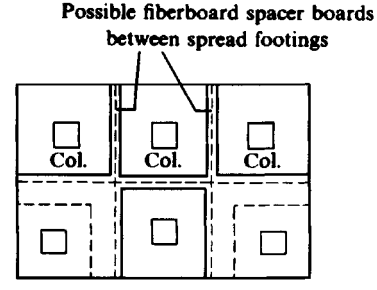

Figure 10-2 Mat versus possible use of spread footings to save labor, forming costs, and negative reinforcing steel.

10-2 TYPES OF MAT FOUNDATIONS

Figure 10-1 illustrates several possible mat-foundation configurations. Probably the most common mat design consists of a flat concrete slab 0.75 to 2 m thick and with continuous two-way reinforcing top and bottom. This type of foundation tends to be heavily overdesigned for three major reasons:

1. Additional cost of analysis methods, which are, however, not exact.
2. The extra cost of a reasonable overdesign of this element of the structure will generally be quite small relative to total project cost.
3. The extra margin of safety provided for the modest additional cost.

10-3 BEARING CAPACITY OF MAT FOUNDATIONS

The mat foundation must be designed to limit settlements to a tolerable amount. These settlements may include the following:

1. Consolidation—including any secondary effects
2. Immediate or elastic
3. A combination of consolidation and immediate amounts

A mat must be stable against a deep shear failure, which may result in either a rotational failure (see Fig. 4-1*a*), typified by the Transcona elevator failure (White, 1953), or a vertical (or punching) failure. A uniform vertical punching failure would not be particularly serious, as the effect would simply be a large settlement that could probably be landscaped; however, as the settlement is not likely to be uniform or predicted as such, this mode should be treated with concern equal to that for the deep-seated shear failure.

The bearing-capacity equations of Table 4-1 may be used to compute the soil capacity, e.g.,

$$q_{\text{ult}} = cN_c s_c i_c d_c + \gamma D N_q s_q i_q d_q + \frac{1}{2}\lambda B N_\gamma s_\gamma i_\gamma d_\gamma$$

or

$$q_{\text{ult}} = 5.14 s_w (1 + s'_c + d'_c - i'_c) + \bar{q}$$

Use B = least mat dimension and D = depth of mat (Fig. 10-3). The allowable soil pressure is obtained by applying a suitable factor of safety (see Table 4-9) and any applicable reduction for mat width B as suggested in Sec. 4-4.

When the bearing capacity is based on penetration tests (e.g., SPT, CPT) *in sands and sandy gravel,* one may use Eq. (4-13) rewritten [see Meyerhof (1965)] as follows:

$$q_a = \frac{N_{55}}{0.08}\left(\frac{\Delta H_a}{25.0}\right)K_d \qquad \text{(kPa)} \tag{10-1}$$

where $K_d = 1 + 0.33D/B \leq 1.33$

ΔH_a = allowable settlement such as 25, 40, 50, 60 mm, etc.

The factor 0.08 converts Meyerhof's original equation to allow a 50 percent increase in bearing capacity and to produce kPa. The bracket ratio of $(\Delta H_a/25.0)$ allows the reader to use any specified settlement, since the original equation was based on a settlement of 25 mm (1 inch). For a mat the ratio $((B + F_3)/B)^2 \approx 1.0$ and is neglected.

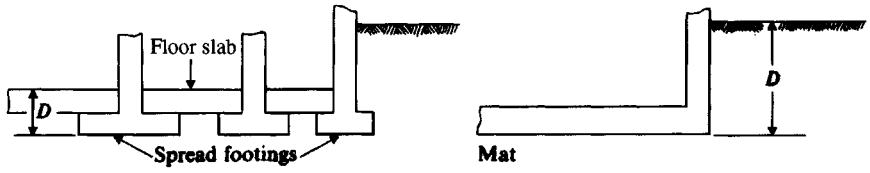

Figure 10-3 Increase in bearing capacity by using a mat foundation.

With q_c (in kPa) from a CPT we can use Fig. 3-23 or Eq. (4-20) to estimate an N_{55} value for use in Eq. (10-1). A typical computation for N_{55}, which you can use as a guide, is given in Fig. 3-23. For CPT in cohesive soil one can use Eq. (3-11) to obtain the undrained shear strength ($\phi = 0°$ case) s_u and use the bearing capacity equations (Meyerhof, Hansen, or Vesić) from Table 4-1 simplified to

$$q_{ult} = 5.14 s_u (1 + s'_c + d'_c - i_c) + \gamma D$$

Alternatively, use Eqs. (4-19) directly with q_c. In most cases the mat will be placed on cohesive soil, where q_u (or q_c) from standard penetration tests is the principal strength data available. In these cases SPT sampling is usually supplemented with several pushed thin-walled tube samples so that laboratory unconfined (or confined triaxial) compression tests can be performed to obtain what are generally considered more reliable strength parameters. Any triaxial laboratory tests may be CK_oXX, as indicated in Sec. 2-11, and either (or both) compression (case 1) and extension (case 3) type of Fig. 2-40. Alternatively, in situ tests may be performed, such as the pressuremeter or borehole shear, to obtain the design strength data.

10-4 MAT SETTLEMENTS

Mat foundations are commonly used where settlements may be a problem, for example, where a site contains erratic deposits or lenses of compressible materials, suspended boulders, etc. The settlement tends to be controlled via the following:

1. Use of a larger foundation to produce lower soil contact pressures.
2. Displaced volume of soil (flotation effect); theoretically if the weight of excavation equals the combined weight of the structure and mat, the system "floats" in the soil mass and no settlement occurs.
3. Bridging effects attributable to
   a. Mat rigidity.
   b. Contribution of superstructure rigidity to the mat.
4. Allowing somewhat larger settlements, say, 50 instead of 25 mm.

The flotation effect should enable most mat settlements, even where consolidation is a problem or piles are used, to be limited to 50 to 80 mm. A problem of more considerable concern is differential settlement. Again the mat tends to reduce this value. We can see in Fig. 10-4 that bending moments ($6EI\Delta/L^2$) and shear forces ($12EI\Delta/L^3$) induced in the superstructure depend on relative movement Δ between beam ends. Mat continuity results in a somewhat lower assumed amount of differential settlement relative to the total expected settlement versus a spread footing as follows:

Foundation type	Expected maximum settlement, mm	Expected differential settlement, mm
Spread	25	20
Mat	50	20

Computer methods that incorporate frame-foundation interaction can allow one to estimate both total and differential settlements. The total settlements will be only as good as the soil

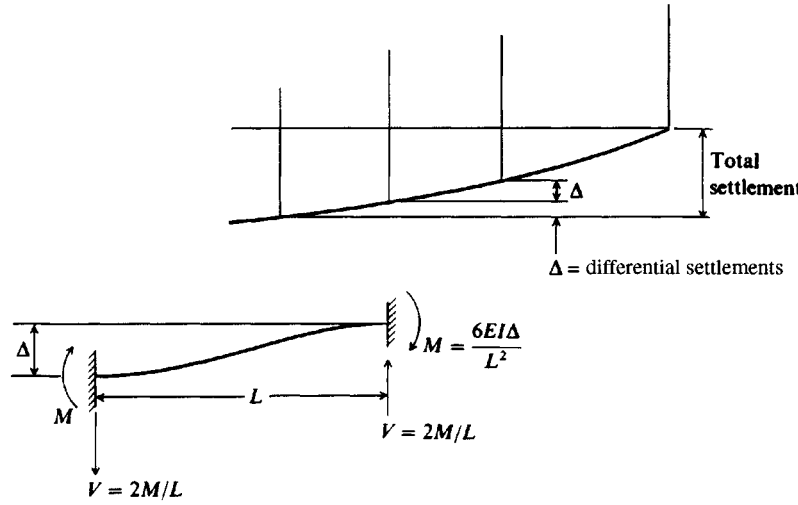

Figure 10-4 Reduction of bending moments in superstructure by using mat foundation. Bending moment M is based on differential settlement between columns and not on total settlement.

data, however, and if other than a strip from the mat is used as a beam-on-elastic foundation type of analysis, the computational effort is substantial.

The differential settlement may be arbitrarily taken as 20 mm (0.75 in.) if the total expected settlement ΔH is not more than 50 mm or may be approximated using a rigidity factor K_r [see ACI Committee 336 (1988)] defined as

$$K_r = \frac{EI_b}{E_s B^3} \tag{10-2}$$

EI_b may be taken as

$$EI_b = EI_f + \sum EI_{bi} + \sum \frac{Eah^3}{12} \tag{10-3}$$

where EI_b = flexural rigidity of the superstructure and mat
E = composite modulus of elasticity of superstructure frame
EI_f = footing or mat flexural rigidity
E_s = modulus of elasticity of soil
$\sum \frac{Eah^3}{12}$ = effective rigidity of shear walls perpendicular to B; h = height; a = wall thickness
$\sum EI_{bi}$ = rigidity of the several members making up the frame resistance perpendicular to B
B = base width of foundation perpendicular to direction of interest

ACI Committee 336 suggests that mat differential settlements are related to both the total estimated foundation settlement ΔH and the structure rigidity factor K_r about as follows:

For K_r	Differential settlement expected	
0	$0.5 \times \Delta H$	for long base
	$0.35 \times \Delta H$	for square base
0.5	$0.1 \times \Delta H$	
> 0.5	Rigid mat; no differential settlement	

Analyses of settlements will have to be performed where the net increase in pressure exceeds the existing in situ pressure p'_o. These may be immediate and/or consolidation settlements adjusted for OCR and depending on the underlying soil stratification.

A major problem—particularly for deep excavations in clay—is expansion and/or lateral flow into the excavation base so that the base elevation rises. This phenomenon is termed *heave,* and values of 25 to 50 mm are very common. Values up to 200 mm (about 8 in.) are reported in the literature. It is difficult to compute settlements when heave has occurred. Theoretically, all the heave should be recovered if we reapply a mat pressure q_o equal to that previously existing. In practice this recovery does not occur, or at least it does not occur with the same rapidity as the heave. It should be expected that if part of the heave occurs from a deep-seated lateral flow (refer to Fig. 4-1 elements 1 and 2) it will be very difficult to predict either the total amount of heave or how much of this will be recovered by elastic recompression. In general, where heave is involved, considerable experience and engineering judgment are necessary in estimating probable soil response, for there are currently no reliable theories for the problem. There is some claim that a finite element of the elastic continuum computation can resolve the dilemma; however, this is a speculative procedure aided by hope of a happy outcome of computations and measurements. The reason is that a finite-element computation is only as good as the input parameters of E_s and μ. Even were we to be able to obtain a reliable initial E_s it will reduce during, and after excavation, as the loss of confining pressure p'_o and expansion produces heave.

Heave can also occur in deep excavations in sand but the amount is usually very small. Heave is usually not a consideration where the excavations are on the order of 2 to 3 m in depth in most soils, but it becomes a major problem for excavations of 10 to 20 m in clay.

Example 10-1. For the soil profile of Fig. E10-1 (a composite of the several site borings to save text space) estimate the allowable bearing capacity for a mat foundation to be located at $D \cong 1.5$ m.

Solution. We will estimate an allowable bearing capacity based on q_u and adjust it so the settlement is approximately adequate.

These data are basically the type a geotechnical consultant would have on which to make an allowable pressure recommendation.

Step 1. Find a q_a based on strength alone with SF = 3 for clay. As in Example 4-4,

$$q_a = \frac{1.3N_c c}{\text{SF}} = 1.3(5.7)\frac{q_u}{2}\frac{1}{3}$$

$$= 1.3(5.14)\frac{300/2}{3} = 334.1 \text{ kPa}$$

Tentatively, q_a = **300** kPa = q_u (see Ex 4-4)

Step 2. Find q_a so mat settlement is on the order of about 50 mm.

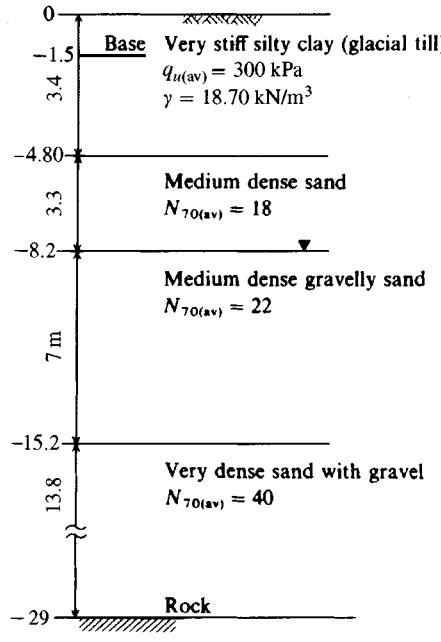

Figure E10-1

a. Find the average E_s.

The depth H from base of mat to rock is

$$H = (4.90 - 1.5) + 3.3 + 7 + 13.8 = 27.5 \text{ m}$$

The average E_s in this depth (and using Table 5-5) is

$$E_{s1} = \frac{1000q_u}{2} = 150\,000 \text{ kPa} \qquad \left(\text{average range of stiff clay and } s_u = \frac{q_u}{2}\right)$$

$$E_{s2} = 500(N_{55} + 15) \qquad \text{(the most conservative equation in Table 5-5)}$$

$$E_{s2} = 500\left[18\left(\frac{70}{55}\right) + 15\right] = 18\,950 \text{ kPa} \qquad \text{(converting } N_{70} \text{ to } N_{55} \text{ and rounding)}$$

$$E_{s3} = 500\left[22\left(\frac{70}{53}\right) + 15\right] = 22\,000 \text{ kPa} \qquad \text{(for 7 m stratum)}$$

$$E_{s4} = 500\left[40\left(\frac{70}{55}\right) + 15\right] = 32\,900 \text{ kPa}$$

The weighted average E_s is

$$E_{s(\text{av})} = \frac{3.4(150\,000) + 3.3(18\,950) + 7.0(22\,000) + 13.8(32\,900)}{27.5}$$

$$= \frac{1\,180\,555}{27.5} = \mathbf{42\,930} \text{ kPa}$$

b. Estimate the mat will be on the order of 14 m, giving

$$\frac{H}{B'} = \frac{27.5}{7} \cong 4 \qquad \frac{L}{B} = 1$$

Estimate $\mu = 0.3$ for all the layers.

From Table 5-2 obtain I_i factors to compute I_s for use in Eq. (5-16*a*); thus,

$$I_s = 0.408 + \frac{1 - 2(0.3)}{1 - 0.3}(0.037) = 0.429$$

Estimating $D/B = 0.1$, we obtain $I_F \cong 0.95$ from your program FFACTOR. Using Eq. (5-16*a*), we write

$$\Delta H = q_o B' \left(\frac{1 - \mu^2}{E_s}\right) m I_s I_F \qquad \text{[Eq. (5-16}a\text{)]}$$

$$\frac{\Delta H}{q_o} = 7\left(\frac{1 - 0.3}{42\,930}\right)^2 (4 \times 0.429)(0.9) = 0.000\,24 \text{ m}^3/\text{kN} \qquad \text{(at center)}$$

For a settlement $\Delta H = 50$ mm (0.050 m) we solve for the required $q_a (= q_o)$ to obtain

$$\frac{\Delta H}{q_a} = 0.000\,24 \rightarrow q_a = \frac{0.050}{0.002\,4} = \mathbf{208} \text{ kPa}$$

This q_a should limit the mat settlement to about 50 mm, which is a common allowable value for mat foundations.

Note: A qualifying statement should be included with this recommendation that if, as the design proceeds and B is found to be substantially different from 14 m, it may be necessary to revise q_a. Recommend $q_a = \mathbf{250}$ kPa.

////

10-5 MODULUS OF SUBGRADE REACTION k_s FOR MATS AND PLATES

All three discrete element methods given in this chapter for mats/plates use the modulus of subgrade reaction k_s to support the plate. The modulus k_s is used to compute node springs based on the contributing plan area of an element to any node as in Fig. 10-5. From the figure we see the following:

Node	Contributing area
1 (corner)	$\frac{1}{4}$ of rectangle *abde*
2 (side)	$\frac{1}{4}$ of *abde* + $\frac{1}{4}$ of *bcef*
3 (interior)	$\frac{1}{4}$ of each rectangle framing to a common node (as node 3)

For a triangle one should arbitrarily use one-third of the triangle area to any corner node. For these area contributions the fraction of k_s node resistance from any element is

$$K_i = k_s, \text{ kN/m}^3, \times \text{Area, m}^2 = \text{units of kN/m (or kips/ft in Fps)}$$

Since this computation gives units of a "spring" it is common to call the effect a *node spring.*

In this form the springs are independent of each other, the system of springs supporting the plate is termed a "Winkler" foundation, and the springs are uncoupled. Uncoupling means that the deflection of any spring is not influenced by adjacent springs.

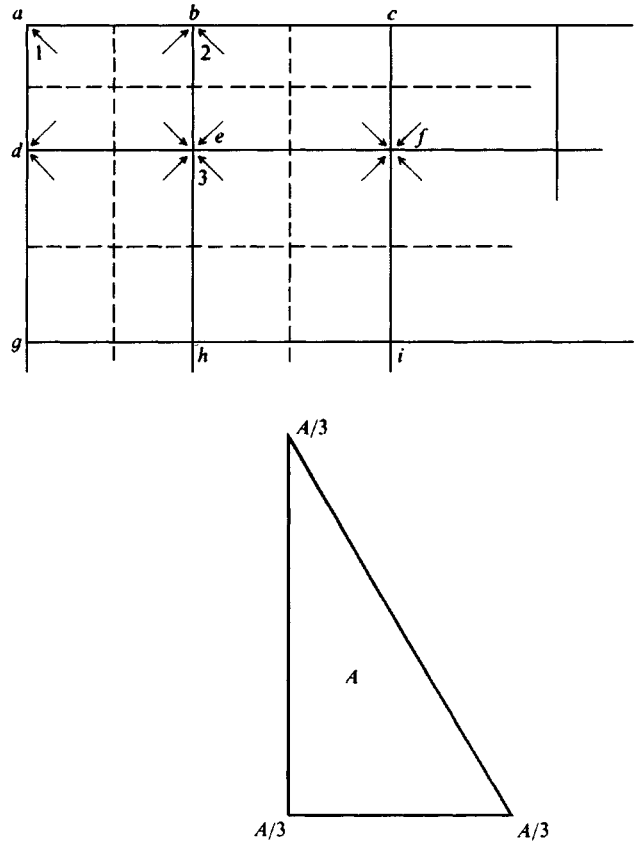

Figure 10-5 Method of prorating k_s to build node springs for rectangles and triangles.

Because the springs are uncoupled, some designers do not like to use the concept of k_s, preferring instead to use a FEM of the elastic continuum with E_s and μ as elastic parameters. This choice does somewhat couple the effects; however, the computations are extensive and only as good as one's estimate of E_s and μ. It has already been shown in Sec. 9-6 that there is a direct relationship between these parameters and k_s. In any case the use of k_s in analyzing mats is rather widespread because of the greater convenience of this parameter. There is actually little computational evidence that the FEM of the elastic continuum provides better solutions than using a "Winkler" foundation.

The author [Bowles (1986)], and as given in previous editions of this textbook, has approximately coupled the springs. In general, coupling can be done as follows:

1. Simply double the edge springs of a mat (we doubled the end springs of the beam-on-elastic foundation in Chap. 9). This should only be done under these conditions:
   a. The plate or mat is uniformly loaded except for edge moments as one would obtain from a tank base.
   b. The plate or mat has only one or at most two column loads.
   c. The computed node soil pressures q are in the range of mat load $\sum P/A_m$, where A_m = area of the mat. If there are large differences do not double the edge springs. How does

one ascertain this? Use computer program B-6 (FADMAT on your diskette), double the edge springs, and inspect the output. If the contact pressures q are questionable, copy the data file, edit the copy to remove the edge spring doubling controls, and rerun. Use the most reasonable output.

2. We can zone the mat area using softer springs in the innermost zone and transitioning to the outer edge. Zoning is computed as in Example 10-2 and usually the three zones computed there are sufficient. Refer to Example 10-6 and data file EXAM106B.DTA for the method.

   The simplest zoning (which effectively doubles the edge springs) is to use two zones—an interior one, which includes all of the nodes except the edge ones, and all the perimeter nodes for the second "zone." Use 1.5 to 2 $\times$ $k_{s,\text{interior}}$ for these edge (or perimeter) nodes. But be aware this will result in large computed edge pressures. Element data generator program B-18 (on your README.DOC file) is particularly well-suited to do these computations.

3. You should not both double the edge springs and zone the mat area for the same program execution. Use either one or the other, or simply use a constant k_s beneath the entire foundation. This latter may be the most nearly correct when there are a number of column loads. There has been some attempt at coupling by using the Boussinesq equation [Eq. (5-3) or (5-4)] in this fashion:
   a. Make a trial run and obtain the node pressures.
   b. Use these node pressures and compute the pressure increase profiles at adjacent nodes.
   c. Use these pressure increase profiles to modify the k_s around these several nodes. This approach requires a very massive amount of computing and is not recommended by the author. It does not make much sense to use an approximation to refine an "estimate."

Example 10-2. For the soil data of Example 10-1 recommend k_s for the 14 $\times$ 14 m mat foundation.

Solution. For many cases a single value of k_s is recommended that may be an average for the base. We will do this but also give the three zone values since very little additional effort is required.

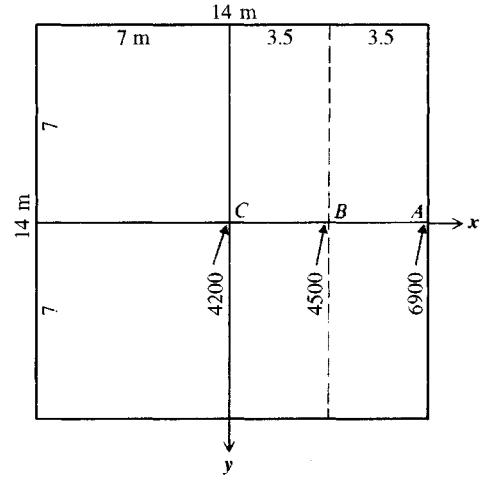

Figure E10-2

Step 1. The center k_s (point C of Fig. E10-2) is readily computed from the same data used to obtain q_a in Example 10-1. From Example 10-1 obtain

$$\frac{1}{k_s} = \frac{\Delta H}{\Delta q} = 0.000\,24 \rightarrow \frac{\Delta q}{\Delta H} = k_s = \frac{1}{0.000\,24}$$

and center $k_s = 4166.7 \rightarrow 4200\ \text{kN/m}^3$.

Step 2. The **edge** (point A of Fig. E10-2) value is obtained by dividing the 14 m mat into two parts of $B \times L = 7 \times 14$ with a common corner $H/B' = 4$ (as before) but $L/B = 2$, $D/B = 0.1$, $\mu = 0.3$, so

$$I_s = 0.476 + \frac{0.4}{0.7}(0.069) = 0.515 \qquad I_F = 0.95 \text{ (using FFACTOR)}$$

$$E_s' = \frac{1 - \mu^2}{42\,930} = \frac{0.91}{42\,930} = 2.12 \times 10^{-5}$$

Rearranging Eq. (5-16a) into Eq. (9-7), we have

$$k_{se} = \frac{1}{B' E_s' m I_s I_f} = \frac{1}{7(2.12 \times 10^{-5})(2 \times 0.515)(0.95)} = 6887 \rightarrow \mathbf{6900}\ \text{kN/m}^3$$

(We used $m = 2$ since there are two common corners.)

Step 3. For the $\frac{1}{4}$ **point** (point B) we have midpoints of two sets of rectangles:

Set 1: $B' = 7$ $L' = 10.5\text{m}$ $L/B = 1.5$ $I_F = 0.95$ $H/B' \cong 4$

$I_s = \mathbf{0.483}$ (program FFACTOR direct)

Set 2: $B' = 3.5$ $L = 7.0\text{ m}$ $L/B = 2$ $H/B = 27.5/3.5 = 7.86$

$I_s = \mathbf{0.630}$

$$k_{s(1/4)} = \frac{1}{7(2.12 \times 10^{-5})(2 \times 0.483)(0.95) + 35(2.12 \times 10^{-5})(2 \times 0.630)(0.95)}$$

(for 2 rectangles)

$$= \frac{1}{2.250 \times 10^{-4}} = 4444.9 \rightarrow \mathbf{4500}\ \text{kN/m}^3$$

The value of $k_{s(1/4)}$ is not the sum of set 1 and set 2 but is actually the reciprocal of the sum of the displacements as given by placing the sum under a single common numerator of 1 as here.

Step 4. If a single value of k_s is to be provided, one might use either

$$k_s = \frac{4200 + 4500 + 6900}{3} = 5200\ \text{kN/m}^3$$

or (weighting the center k_s)

$$k_s = \frac{4(4200) + 6900}{5} = 4740 \rightarrow \mathbf{4700}\ \text{kN/m}^3$$

Comments. This set of computations for k_s is theoretically exact since the displacements are theoretical and the definition of k_s has been strictly followed. The only approximations are in whether E_s and μ are correct.

////

MODULUS OF SUBGRADE REACTION AND CONSOLIDATION SETTLEMENTS. It is not uncommon that a mat is placed on a soil that is analyzed by using k_s, but there are, in addition, consolidation settlements that will occur later.

It is a relatively simple exercise in using the definition of k_s to include the effect of consolidation settlements. This can be done as follows:

$$k_s = \frac{q_o}{\Delta H} \tag{a}$$

Although the base contact pressure q_o remains constant the total settlement is

$$\Delta H' = \Delta H + \Delta H_c$$

giving

$$k_s' = \frac{q_o}{\Delta H + \Delta H_c} \tag{b}$$

Dividing Eq. (*b*) by Eq. (*a*), we obtain

$$k_s' = \frac{k_s \Delta H}{\Delta H + \Delta H_c} \tag{c}$$

We can see that including the consolidation settlement reduces k_s to the lesser k_s' value of Eq. (*c*).

Example 10-3. What is the recommended k_s' (constant value) if the consolidation settlement is estimated to be 50 mm in Example 10-2? Use $k_s = 5200$ kN/m^3.

Solution. From Example 10-1 a contact pressure of $q_o = 205$ kPa produces $\Delta H = 50$ mm $= 0.050$ m. From Example 10-2 we see the elastic k_s was independent of q_a; thus, using Eq. (*c*) we write

$$k_s' = \frac{5200(50)}{50 + 50} = \mathbf{2600}\ \text{kN/m}^3$$

Comments. It is presumed that the consolidation pressure is based on $q_0 = q_a = 200$ kPa. One would probably have to inspect the computer output to find out if the contact pressure in the zone of interest was much different from 200 kPa. If so, a new value of ΔH_c would have to be computed and the problem recycled.

////

10-6 DESIGN OF MAT FOUNDATIONS

There are several methods to design a mat (or plate) foundation.

1. *An approximate method.* The mat is divided into strips loaded by a line of columns and resisted by soil pressure. This strip is then analyzed as a combined footing. This method can be used where the mat is very rigid and the column pattern is fairly uniform in both spacing and loads. This method is not recommended at present because of the substantial amount of approximations and the wide availability of computer programs that are relatively easy to use—the finite grid method (program B6 on your program diskette) in particular. A mat

is generally too expensive and important not to use the most refined analytical methods available.

2. *Approximate flexible method.* This method was suggested by ACI Committee 336 (1988) and is briefly described here, and the essential design aids are provided. If this method is used it should be programmed as for the AIRPAVE computer program noted in subsection 10-6.2 following.
3. *Discrete element methods.* In these the mat is divided into elements by gridding. These methods include the following:
   a. Finite-difference method (FDM)
   b. Finite-element method (FEM)
   c. Finite-grid method (FGM)

10-6.1 Approximate Flexible Method

The approximate flexible method of ACI Committee 336 requires the following steps:

2. Compute the plate rigidity D (unfortunately, same symbol as footing depth).
3. Compute the radius of effective stiffness L (Note: the approximate zone of any column influence is $\approx 4L$).
4. Compute the radial and tangential moments, the shear, and deflection using the following equations (the Z_i factors, from Hetenyi (1946), are not easy to compute) where load P acts:

$$M_r = -\frac{P}{4}\left[Z_4 - \frac{1-\mu_c}{x}Z_3'\right] \tag{10-4}$$

$$M_t = -\frac{P}{4}\left[\mu_c Z_4 + \frac{1-\mu_c}{x}Z_3'\right] \tag{10-5}$$

$$\Delta H = \frac{PL^2}{8D} \qquad \text{(vertical displacement)} \tag{10-6}$$

$$\Delta H = \frac{PL^2}{4D}Z_3 \qquad \text{(at distance } r \text{ from load)} \tag{10-6a}$$

$$V = -\frac{P}{4L}Z_4' \qquad \text{(shear)} \tag{10-7}$$

where P = column load, kN or kips

D = plate stiffness, as

$$D = \frac{E_c t^3}{12(1-\mu_c^2)} \qquad \text{(units of moment)}$$

μ_c = Poisson's ratio for mat or plate (for concrete use 0.15)

x = distance ratio r/L shown on Fig. 10-6

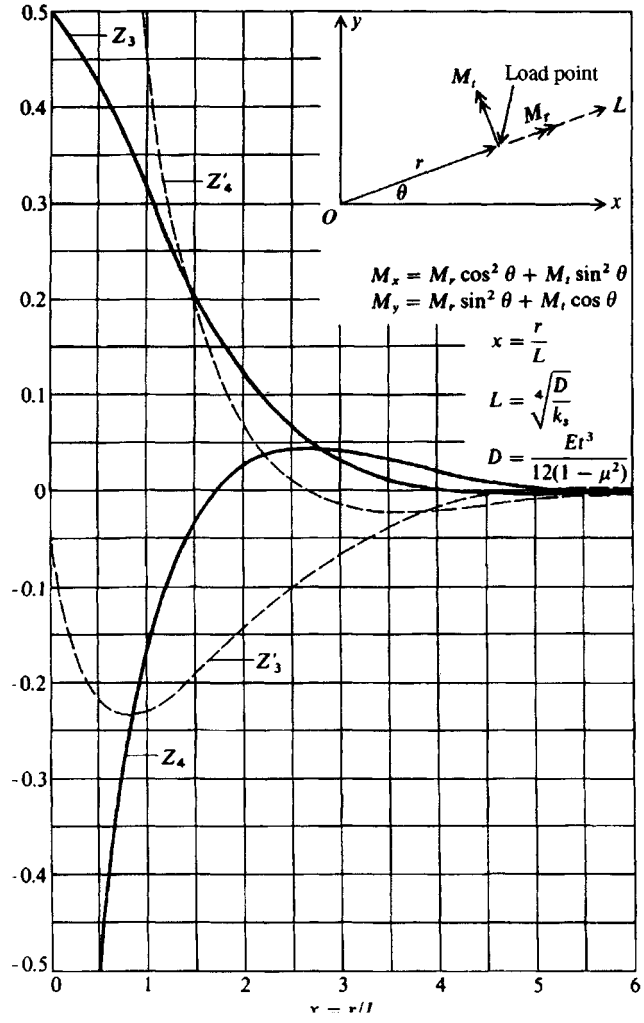

Figure 10-6 Z_i factors for computing deflections, moments, and shears in a flexible plate. [After Hetenyi (1946).]

Z_i = factors from Fig. 10-6 based on x (or from a computer program such as AIRPAVE)

L = influence radius defined as $\sqrt[4]{\frac{D}{k_s}}$

M_r, M_t = radial and tangential moments at the load point of Fig. 10-6, *per unit of width* in units of P, L

V = shear per unit of width of mat or plate in units of P

The radial (M_r) and tangential (M_t) moments in polar coordinates at the load point are converted to rectangular coordinates M_x, M_y, referenced to the origin, using the transfer equations shown in Fig. 10-6. For the several loads in the influence region L these M_x, M_y moment values are summed with attention to sign for design of the plate.

When the edge of the mat is within the radius of influence L, calculate the edge moment and shear. The parallel edge moment and shear are then applied as edge loads with opposite sign. When several columns overlap in the zone L, apply superposition to obtain the net effect.

An illustration of computations for a mat are given by Shukla (1984) using this procedure. The D calculated in this reference is in error, so that the resulting computations are not quite correct; but the general procedure gives an illustration of the method.

10-6.2 Mats or Slabs for Industrial Warehouses and Concrete Airstrips

Industrial floor slabs and concrete airport pavements are somewhat similar and can be designed using the procedure outlined here. One additional step is required. From Westergaard (1948) we can obtain an equation for the bending stresses in the bottom of a slab under a wheel load. This equation is

$$\begin{Bmatrix} \sigma_x \\ \sigma_y \end{Bmatrix} = \frac{3P}{8\pi t^2}\left[(1+\mu_c)\ln\frac{E_c t^3}{k_s\left(\frac{a+b}{2}\right)^4} \mp 2(1-\mu_c)\frac{a-b}{a+b}\right] \tag{10-8}$$

Here terms not defined previously are t = plate thickness; a, b = axis dimensions of an ellipsoid used to model the tire footprint. Approximately [given by PCA (1955)] we have

$$\text{Area} = \text{tire load/tire pressure}$$

$$a = \sqrt{\frac{\text{Area}}{\pi(0.6655)}} \qquad \text{(long axis)}$$

$$b = 0.6655 \times a \qquad \text{(short axis)}$$

Use consistent units for t, a, b of meters or inches. If tire load is in kN use tire pressure in kPa; if load is in pounds use tire pressure in psi. As you can see, there is a sign convention involved with the several equations given here. To understand the significance of the signs you should solve a simple slab where you know there is tension (or compression) in the bottom and compare the result to the signs for stress or moment values given by the equations. Convert the moments of Eqs. (10-4) and (10-5) to stresses by using the conventional

$$f_c = \frac{Mc}{I} = \frac{6M}{t^2} \qquad \text{(since } M_i = \text{ per unit of width)}$$

In usage one would program Eq. (10-8) together with the Z_i factors and Eqs. (10-4) through Eq. (10-7). If the point where the stresses are wanted is under a wheel, include Eq. (10-8) in the analysis. If the point is not under a wheel, use only the equations containing the Z_i factors. You need to program the Z_i factors so that interpolation is not necessary (it is also difficult to obtain reliable values from Fig. 10-6). Figure 10-7 illustrates a set of wheels (these are one landing gear of an airplane) but could be from a wheeled loader in a warehouse. In using this procedure it may be worthwhile to provide suitable load transfer dowels into perimeter wall footings for jointed slabs. For airport runways the common procedure is to use continuously reinforced concrete (CRC) so joints are not used. The pavement edges are usually thickened such that edge formulas do not have to be considered. Floor slab edges in warehouses probably should be thickened as well, partly because of the difficulty in obtaining good compaction adjacent to the perimeter wall footings.

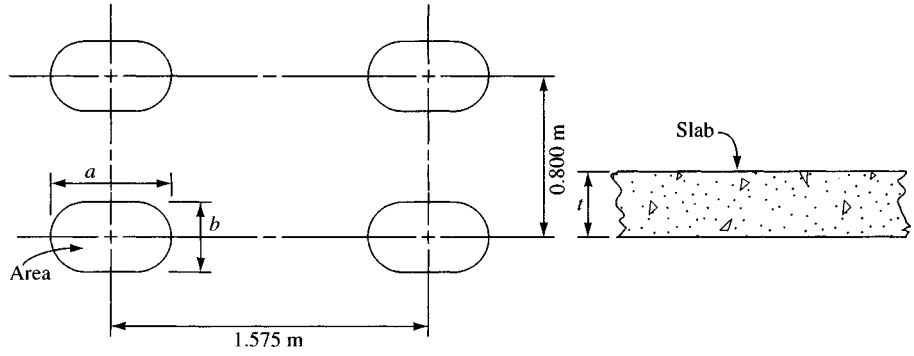

Dual-tandem landing gear
Total load = 667.2 kN (166.8 kN/wheel)

For $P = 166.8$ kN Tire pressure = 690 kPa

$$\text{Area} = \frac{166.8}{690} = 0.2417 \text{ m}^2$$

$$a = \sqrt{\frac{0.2417}{3.14159(0.6655)}} = 0.340 \text{ m} = 340 \text{ mm}$$

$$b = 0.340(0.6655) = 226.3 \text{ mm}$$

Figure 10-7 One part of a landing gear set (nose wheel and other side gear not shown). Also shown are computations for tire load and the approximate ellipse dimensions for use in Eq. (10-8).

10-7 FINITE-DIFFERENCE METHOD FOR MATS

The finite-difference method uses the fourth-order differential equation found in any text on the theory of plates and shells [Timoshenko and Woinowsky-Krieger (1959)]:

$$\frac{\partial^4 w}{\partial x^4} + \frac{2\partial^4 w}{\partial x^2 \partial y^2} + \frac{\partial^4 w}{\partial y^4} = \frac{q}{D} + \frac{P}{D(\partial x \partial y)} \tag{10-9}$$

which can be transposed into a finite-difference equation when $r = 1$ (Fig. 10-8):

$$20w_o - 8(w_T + w_B + w_R + w_L) + 2(w_{TL} + w_{TR} + w_{BL} + w_{BR}) + (w_{TT} + w_{BB} + w_{LL} + w_{RR}) = \frac{qh^4}{D} + \frac{Ph^2}{D} \tag{10-10}$$

When $r \neq 1$, this becomes (as in program B-19, but with much algebra and many steps not shown)

$$\left(\frac{6}{r^4} + \frac{8}{r^2} + 6\right)w_o + \left(-\frac{4}{r^4} - \frac{4}{r^2}\right)(w_L + w_R) + \left(-\frac{4}{r^2} - 4\right)(w_T + w_B) + \frac{2}{r^2}(w_{TL} + w_{TR} + w_{BL} + w_{BR}) + w_{TT} + w_{BB} + \frac{1}{r^4}(w_{LL} + w_{RR}) = \frac{qrh^4}{rD} + \frac{Ph^2}{rD} \tag{10-11}$$

Since $q = -k_s w_o$ we must rearrange the w_o term of Eq. (10-11) to read

$$\left(\frac{6}{r^4} + \frac{8}{r^2} + 6 + \frac{k_s h^4}{D}\right)w_o \tag{a}$$

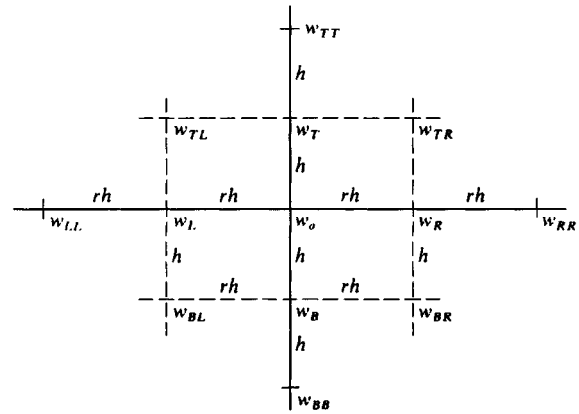

Figure 10-8 Finite-difference grid of elements of $rh \times h$ dimension.

The form shown for the k_s term results from computing a spring using $k_s rh^2$, dividing through by rh^2, and multiplying by h^4. Note that rD does not cancel in the P term.

When $r = 1$ we have the familiar deflection coefficient at any interior node of

$$\left(20 + k_s \frac{h^4}{D}\right) w_o \qquad (b)$$

Referring to Fig. 10-8, we see that the horizontal grid spacing rh can be different from the vertical grid spacing $h (1 \leq r \text{ or } r \leq 1)$. In a computer program, of course, one simply orients the mat so that the minimum grid points are horizontal with the origin of the grid at the lower left corner. The input then consists in the horizontal grid spacing and vertical grid spacing, which are constant, and the band width, which is 2 × horizontal grid points + 1 (thus, a minimum is obtained if the horizontal grid points are the minimum).

The finite-difference method has several advantages:

1. It has been widely used (and should be used as a check on alternative methods where it is practical).
2. It is reliable if the mat can be modeled using a finite-difference grid.
3. It is rapid since the input data are minimal compared with any other discrete method, and the computations to build the stiffness array are not so extensive as other methods. Usually only three to five lines of input data are needed compared with up to several hundred for the other methods.

There are also a number of disadvantages:

1. It is extremely difficult to model boundary conditions of column fixity.
2. It is very difficult to model notches, holes, or reentrant corners.
3. It is difficult to apply a concentrated moment (as from a column) since the difference model uses moment/unit of width.

The following example illustrates typical input and output from an FDM program (e.g., program FADMATFD, B-19).

Example 10-4. Do the Example 10-5 (p. 565) using the finite-difference method (FDM) to illustrate the small amount of input needed and typical output, at least output using program FADMATFD.

```
++++++++++++++ NAME OF DATA FILE USED FOR THIS EXECUTION:  EX104FDM.DTA

      EXAMPLE 10-4-SQUARE PLATE 3 X 3 M--AND NONLIN--FINITE DIFF METHOD--SI UNITS

        MAT FOUNDATION INPUT DATA:
                  NO OF COLS, M =  6
                  NO OF ROWS, N =  6
        NO OF NON-ZERO Q-VALUES =  4
      MAT GRID SPACING:  H =    .600   RH =    .600  M
            PLATE THICK, T =    .600  M
      MOD OF ELASTICITY, E =  22408000. KPA
      POISSON'S RATIO, XMU =  .150
            UNIT WT OF MAT =    .000 KN/M^3
           SOIL MODULUS SK =  15700.0 KN/M^3
      COMPUTED PARAMETERS:  FLEX RIGID D =  .41263E+06
                      FACTOR DD = H^2/R*D =  .87246E-06

         MAT DIMENSIONS ARE:  X =  3.000  M  HORIZ
                              Y =  3.000  M  VERT
      MAX NON-LIN SOIL DEF, XMAX =   .0200  M

      ++++++ BANDWIDTH OF MATRIX =  13  +++++++++++++++

      SOIL SPRING (SOK(I,J) CONSTANTS--EDGES DOUBLED IF IDBLK > 0--IDBLK =  1
                 1          2          3          4          5          6
        1      .00247     .00493     .00493     .00493     .00493     .00247
        2      .00493     .00493     .00493     .00493     .00493     .00493
        3      .00493     .00493     .00493     .00493     .00493     .00493
        4      .00493     .00493     .00493     .00493     .00493     .00493
        5      .00493     .00493     .00493     .00493     .00493     .00493
        6      .00247     .00493     .00493     .00493     .00493     .00247

      THE INPUT FOUNDATION LOADS AND COORDS ARE
     3    3      550.
     3    4      550.
     4    3      550.
     4    4      550.

          FOOTING WT =       .000     SUM OF INPUT LOADS =  2200.000 KN

          THE LOAD ARRAY--AND CORRECTED FOR NON-LINEAR EFFECTS IF CYCLE > 1
            THE CURRENT CYCLE =  1
                 1          2          3          4          5          6
        1      .00000     .00000     .00000     .00000     .00000     .00000
        2      .00000     .00000     .00000     .00000     .00000     .00000
        3      .00000     .00000  550.00000  550.00000     .00000     .00000
        4      .00000     .00000  550.00000  550.00000     .00000     .00000
        5      .00000     .00000     .00000     .00000     .00000     .00000
        6      .00000     .00000     .00000     .00000     .00000     .00000

                          NO OF STIFF(I) ENTRIES =   468
```

Figure E10-4

THE DEFLECTION MATRIX IS (M)

	1	2	3	4	5	6
1	.01107	.01126	.01139	.01139	.01126	.01107
2	.01126	.01146	.01161	.01161	.01146	.01126
3	.01139√	.01161√	.01181√	.01181√	.01161√	.01139√
4	.01139	.01161	.01181	.01181	.01161	.01139
5	.01126	.01146	.01161	.01161	.01146	.01126
6	.01107	.01126	.01139	.01139	.01126	.01107

CURRENT CYCLE = 1 CURRENT NON-LIN COUNT = 0 PREVIOUS COUNT = 0

THE BENDING MOMENTS IN SLAB IN KN-M ARE AS FOLLOWS

COORDS		X-AXIS	Y-AXIS	COORDS		X-AXIS	Y-AXIS
1	1	.0000	.0000	4	1	.0000	-154.0598
1	2	-74.0461	.0000	4	2	-60.4754	-180.3783 √
1	3	-154.0774	.0000	4	3	-259.3937	-259.3710 √
1	4	-154.0733	.0000	4	4	-259.3881	-259.3681 √
1	5	-74.0465	.0000	4	5	-60.4837	-180.3847
1	6	.0000	.0000	4	6	.0000	-154.0587
2	1	.0000	-74.0377	5	1	.0000	-74.0414
2	2	-66.8780	-66.8707	5	2	-66.8739√	-66.8711
2	3	-180.4002	-60.4756	5	3	-180.4066√	-60.4766
2	4	-180.4025	-60.4770	5	4	-180.4068√	-60.4776
2	5	-66.8763	-66.8663	5	5	-66.8683	-66.8620
2	6	.0000	-74.0354	5	6	.0000	-74.0354
3	1	.0000	-154.0615	6	1	.0000	.0000
3	2	-60.4810	-180.3875	6	2	-74.0441	.0000
3	3	-259.3906	-259.3779	6	3	-154.0870	.0000
3	4	-259.3921	-259.3813	6	4	-154.0808	.0000
3	5	-60.4859	-180.3924	6	5	-74.0396	.0000
3	6	.0000	-154.0653	6	6	.0000	.0000

THE NODAL REACTIONS (KN) ARE AS FOLLOWS

	1	2	3	4	5	6
1	31.28732	63.63005	64.36333	64.36211	63.62643	31.2843
2	63.63162	64.78147	65.64455	65.64334	64.77783	63.6255
3	64.36652	65.64617	66.75721	66.75600	65.64252	64.3604
4	64.36701	65.64664	66.75768	66.75645	65.64296	64.3608
5	63.63311	64.78294	65.64601	65.64476	64.77919	63.6268
6	31.28856	63.63249	64.36577	64.36450	63.62873	31.2854

TOTAL SUM OF FOOTING LOADS = 2200.000 KN
SUM OF SOIL REACTIONS = 2200.396 KN

THE NODAL SOIL PRESSURE, KPA , IS

	1	2	3	4	5	6
1	173.81850	176.75010	178.78700	178.78360	176.74010	173.8017
2	176.75450	179.94850	182.34600	182.34260	179.93840	176.7376
3	178.79590	182.35040	185.43670	185.43330	182.34030	178.7789
4	178.79720	182.35180	185.43800	185.43460	182.34150	178.7801
5	176.75860	179.95260	182.35000	182.34650	179.94220	176.7413
6	173.82530	176.75690	178.79380	178.79030	176.74650	173.8080

Figure E10-4 (*continued*)

Solution. Refer to Fig. E10-5*a* for gridding, but for the FDM take the origin at the lower left corner (node 31). Count

$M = 6$ (nodes 31–36) and

$N = 6$ (nodes 31, 25, 19, 13, 7, and 1)

Prorate the column to four nodes as shown giving coordinates of

I	J	Load	I	J	Load
3	3	550 kN	4	3	550 kN
3	4	550 kN	4	4	550 kN

$H = rH = 0.6$ m (square grid) Mat concrete $\mu = 0.15$

Thickness $t = 0.6$ m $E_c = 22\,408$ MPa

The input data set named EX104FDM.DTA is as follows:

```
EXAMPLE 10-4 SQUARE PLATE 3 × 3 M—AND NONLIN—FINITE DIFF METHOD—SI UNITS
6  6    4   0    13  0     0
0  1    1
 .6000      .6000      .6000     22408.0    0.15    15700.    0.0     .02
3  3    550.000
                                    ↑         ↑       ↑               ↑
3  4    550.000
4  3    550.000                   E_c, MPa    μ       k_s           XMAX, m
4  4    550.000
```

The program computes

$$D = \frac{Et^3}{12(1-\mu^2)} = \frac{22\,408\,000 \times 0.6^3}{12(1-\mu^2)}$$

$$= 412\,628.1 \text{ kN} \cdot \text{m (computer output} = .412\,63\text{E}+06)$$

Select data marked with a ✓ from the computer output sheet (Fig. E10-4) is shown on Fig. E10-5*a*.

Note that the program FADMATFD allows a "nonlinear" displacement check, the inclusion of mat weight, the doubling of edge springs, and user input of node springs in the form of $SK \times H^4/D$ (gives $15\,700 \times 0.6^4/412\,628.1 = 0.004\,93$ for interior and doubled side nodes and $0.004\,93/2 = 0.002\,47$ for doubled corner nodes). Here the only option used was doubling of the edge springs so the output could be compared to the output from the other two methods shown on Fig. E10-5*a*. The program always checks for any soil-mat separation and recycles if any nodes separate from the soil regardless of the NONLIN input parameter.

Checking. Perform checks as follows since mat and load are symmetrical.

1. Displacement array is symmetrical. For example, corner nodes of 1,1, 1,6, 6,1, and 6,6 = **0.011 07** m.
2. Moments are symmetrical. For example, the x-moment at nodes 2,2, 2,5, 5,2, and 5, 5 = **−66.87** kN · m.
3. Since the displacements are symmetrical, the node reactions and soil pressures are also equal. The node soil pressure at node 2,2 = $SK \times X(2,2) = 15\,700 \times 0.011\,46 =$ **179.9** kPa.
4. Note the sum of the soil reactions = 2200.396 kN versus the sum of column loads = 2200.000 kN (slight computer round-off error).

////

10-8 FINITE-ELEMENT METHOD FOR MAT FOUNDATIONS

In the *finite-element* analysis, element continuity is maintained through use of displacement functions. The displacement function is of the form

$$u = a_1 + a_2X + a_3Y + a_4X^2 + a_5XY + a_6Y^2 + a_7X^3 + a_8X^2Y + a_9XY^2 + a_{10}Y^3 + a_{11}X^4 + a_{12}X^3Y + a_{13}X^2Y^2 + a_{14}XY^3 + a_{15}Y^4 \quad (10\text{-}12)$$

With a rectangular plate and three general displacements at each corner node (Fig. 10-9) only 12 unknowns of Eq. (10-12) are necessary. This results in reducing the general displacement equation to one with 12 a_i coefficients instead of 15. Which three are best to discard becomes a considerable exercise in both engineering judgment and computational ability/tenacity. Various procedures have been and are being periodically proposed to reduce and solve the resulting matrix such as those proposed at the finite-element conferences at McGill University (1972), Wright Patterson AFB (1965, 1968, 1971), and regular papers in several journals including the *Journal of Structural Division,* ASCE.

One of the major advances in the FEM is using isoparametric element formulation so that a given element may have more nodes than an adjacent one. In any case, the FEM output is very difficult to interpret. Additionally the method is computationally intensive (about four times as long to run a problem of reasonable length as the FGM of the next section). The general methodology uses advanced mathematical concepts with which many civil and structural engineers are not familiar so that identification of incorrect output may be difficult.

Concentrated node moments can be readily input as part of the load array; however, a nodal statics check is difficult. The reason is that the output element node moments are in units of moment/unit of width, whereas the input is the moment at that node. A moment summation is not directly possible because of units incompatibility, and the situation is not helped from having to interpret and apply the twist moment M_{xy} of Fig. 10-9. Similarly a vertical force summation is not easy since element node shears are difficult to compute with the element moments obtained on a unit width basis.

For these several reasons, the author does not recommend use of the FEM for mat and plate problems. There are many design situations where the FEM is particularly suited; however, the FGM following is preferred for the more direct solution of foundation engineering problems.

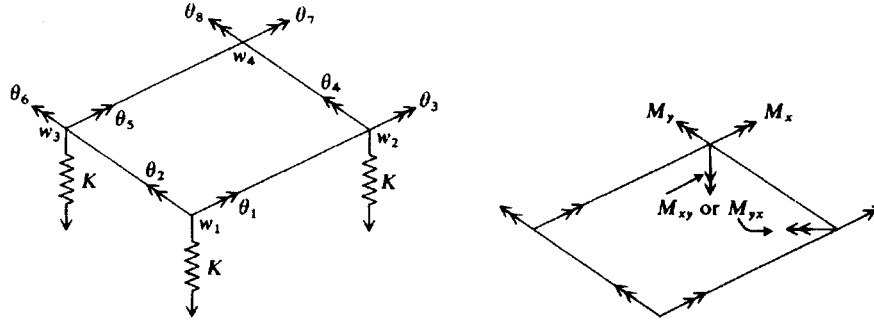

(*a*) Displacements. (*b*) Element moments

Figure 10-9 Finite-element method using a rectangular plate element.

10-9 THE FINITE-GRID METHOD (FGM)

This method is particularly well-suited for use for the analysis of mats and plates. It has these distinct advantages:

1. The output is easy to interpret since beam-column type elements that have only bending and torsion are used. The moment/unit width is simply the node moment (from a node summation) divided by the element width.
2. It is easy to obtain design shears at the ends of the elements. The shear is simply the sum of the element end moments divided by element length. Then one divides the total element shear by the element width to get the shear/unit width.
3. It is easy to input concentrated column moments directly.
4. Boundary cases are as easily modeled as with the FEM.
5. It is relatively simple to extend the 3 degrees of freedom (d.o.f.) nodes of this method to use 6 d.o.f. nodes that are required for pile cap analysis [Bowles (1983)].

Although Table 10-1 (based on Fig. 10-10) established the general validity of the FGM, users have been the ultimate test. The program (your diskette program B-6 but often supplemented by professionals with the data generator program B-18) has been used for silo bases and liquid storage tank bases as well as mat foundations for buildings.[1] A recent comparison was made between the FEM and FGM for a full-scale mat foundation in Australia [Payne et al. (1992)]. This reference compared a modification of B-6 and the commercial computer program NASTRAN. They found a maximum difference of about 10 percent between the stresses computed by the two methods when analyzing a mat on expansive soil. It was not possible to identify the "correct" stress. About the best that could be done was to see if the programs predicted crack locations reasonably well.

The FGM is similar to the beam finite element used in Chap. 9 but extended to a beam column (which has torsion) and used for a plate. The same equations as in Sec. 9-8 are used, namely,

$$\mathbf{P} = \mathbf{AF} \qquad \mathbf{e} = \mathbf{A}^T\mathbf{X} \qquad \mathbf{F} = \mathbf{Se} = \mathbf{SA}^T\mathbf{X}$$
$$\mathbf{P} = \mathbf{ASA}^T\mathbf{X} \qquad \mathbf{X} = (\mathbf{ASA}^T)^{-1}\mathbf{P}$$

As before, it is necessary to develop the element EA and ES matrices, with the computer taking care of the remainder of the work including the building of the global $\mathbf{ASA}^T$ matrix.

Referring to Fig. 10-11, the element EA matrix is built by $\sum F$ at each node. For example, at node 1

$$P_1 = F_1 \sin\alpha + OF_2 - F_3 \cos\alpha$$
$$P_2 = F_1 \cos\alpha + OF_2 - F_3 \sin\alpha$$
$$P_3 = \frac{F_1}{L} + \frac{F_2}{L} + OF_3$$

[1] Since this textbook has been translated into several foreign languages and has been published in an international student edition the usage has been worldwide, not just the United States.

TABLE 10-1

Comparison of finite grid method (FGM) to the FEM using one-quarter of a symmetrical plate (Fig. 10-10) with edge supports indicated and plate *L/B* ratios shown [Bowles (1986*a*)].

Fps units from original source.

Ratio *L/B*	Support type	Element type	For node 9: Deflections, ft			Moment, M_x, k • ft/ft			
			FGM	FEM	Theory*	FGM	FEM	M_{xy}	Net FEM
1	Simple	Square	0.006 41	0.0068	0.006 45	9.0	10.4	−1.2	9.2
1	Simple	Triangle	0.006 25	0.0066	0.006 45				
1	Simple	Square†	0.007 04	0.0066	0.006 45	11.6	12.9	−1.1	11.8
1.2	Simple	Rectangle	0.007 42	0.0080	0.007 52	8.1	9.6	−1.2	8.4
2.0	Simple	Triangle	0.010 25	0.0086	0.009 18				
2.0	Simple	Rectangle	0.009 36	0.0097	0.009 18	5.7	7.2	−1.0	6.2
1.2	Simple	Mixed	0.007 56	—	0.007 52	[Fig. 10-10 with both diagonals (−)]			
1.2	Simple	Mixed	0.007 68	—	0.007 52	[Fig. 10-10 with one diag. (−) and other (+)]			
1.0	Fixed	Triangle	0.003 11	—	0.003 11				
1.0	Fixed	Square‡	0.003 29	0.003 24	0.003 11	7.4	8.6	−1.1	7.5
1.2	Fixed	Mixed	0.004 09	—	0.003 60				
1.4	Fixed	Triangle	0.004 11	—	0.003 84				
1.4	Fixed	Rectangle	0.003 93	0.0042	0.003 84	5.6	7.0	−1.0	6.0
2.0	Fixed	Triangle	0.004 72	—	0.004 01				
2.0	Fixed	Rectangle	0.003 89	0.0043	0.004 01	3.6	5.4	−0.9	4.5

*From Timoshenko and Winowsky-Krieger (1959), pp. 143 and 206.

†Using 25 nodes instead of 9 (finer mesh).

‡Edge moment by FGM gives −4.9 k · ft/ft versus theoretical solution of 0.1257(40) = 5.0 k · ft/ft. The FEM value = −5.4 with M_{xy} = +0.7 to yield a comparable value of M = −4.7 k · ft/ft.

Notes: **1.** Triangle moments not shown since FEM centroid values require interpolation to node values.

2. Net FEM moments are obtained by adding FEM + M_{xy} as shown above.

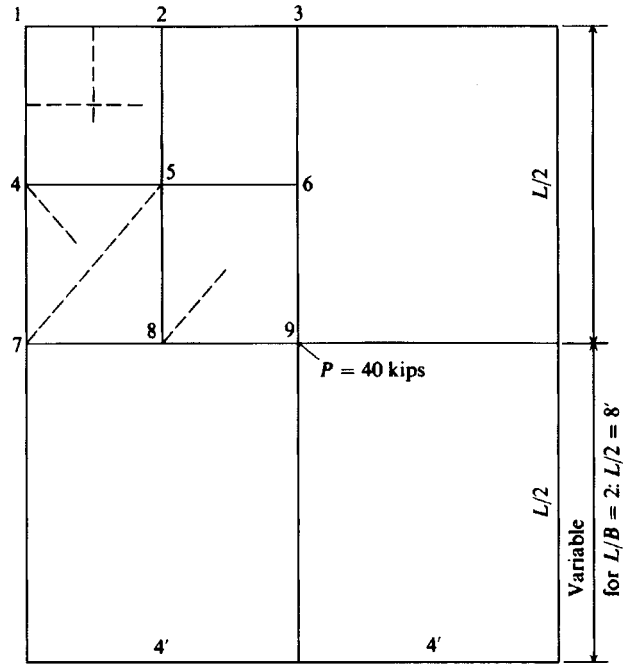

Figure 10-10 Plate with simple and fixed edge supports to illustrate FGM versus FEM with select data given in Table 10-1. Only one-quarter of the plate is used with symmetry. Gridding for finer mesh and to use triangles are shown with dashed lines.

and the resulting matrix (Note: α makes program general but usually $\alpha = 0°$ or $\alpha = 90°$) is

$$EA =$$

P \ F	1	2	3
1	$-\sin\alpha$	0	$-\cos\alpha$
2	$\cos\alpha$	0	$-\sin\alpha$
3	$\frac{1}{L}$	$\frac{1}{L}$	0
4	0	$-\sin\alpha$	$\cos\alpha$
5	0	$\cos\alpha$	$\sin\alpha$
6	$-\frac{1}{L}$	$-\frac{1}{L}$	0

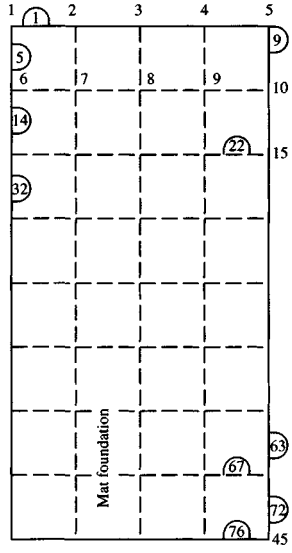

NNODES = 45 NP = 45×3 =**135**
NBAND = 6×3 − 1 + 1 = 18 (Elem 5)
NM = 76 (elements by direct count)
Stiffness matrix = NP × NBAND
= 135×18 = **2430**

(*a*) Plate gridding

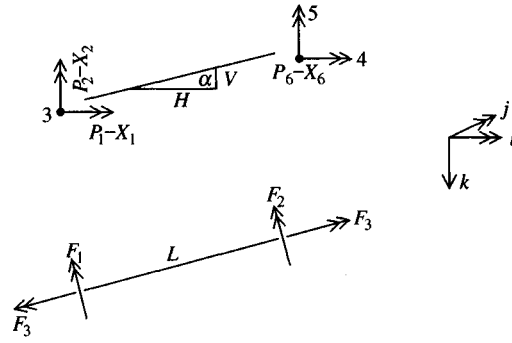

(*b*) *P*–*X* (node) and *F*–*e* (element) coding

Figure 10-11 Method of finite-element (grid) analysis. Note that orientation of node numbers in (*a*) results in a banded stiffness matrix of minimum width of 18. Orient so origin is at upper left corner.

Similar to the ES of Sec. 9-8 but including a torsion adjustment factor Ω for F_3, the mat ES matrix is

$$\mathbf{ES} = \begin{array}{c|ccc} \mathbf{F}\backslash\mathbf{e} & 1 & 2 & 3 \\ \hline 1 & \frac{4EI}{L} & \frac{2EI}{L} & 0 \\ 2 & \frac{2EI}{L} & \frac{4EI}{L} & 0 \\ 3 & 0 & 0 & \frac{\Omega GJ}{L} \end{array}$$

Node springs are built during element input based on node contributory area and saved in a "spring" array. After the global $\mathbf{ASA}^{\mathrm{T}}$ is built (in band form to save computing effort and memory) the node springs are added at the appropriate NP location. All edge springs or, preferably, the perimeter k_s, should be doubled to approximate spring coupling.

The torsion factor J should be computed for a rectangle (see p. 528 unless a T or other shape is involved). The adjust factor Ω is used [along with the double area (see Fig. 10-12)] to make the solution better fit the theoretical solutions as found in Timoshenko and Woinowsky-Krieger (1959), usually used by others to verify FEM solutions. This step is

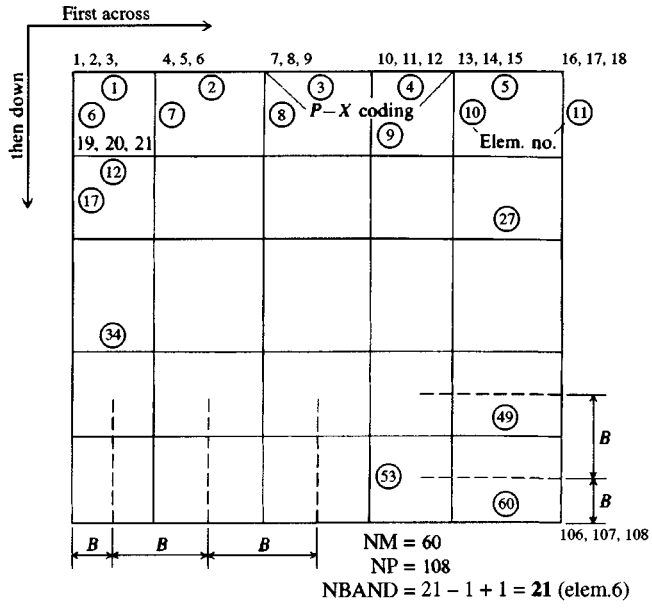

Figure 10-12 Typical coding for a mat. Program "sees" element widths B as shown above. For horizontal members $L = H$ and $V = 0$; vertical members $L = -V$ and $H = 0$. Note use of double the mat area since horizontal and vertical members overlap.

not greatly different from discarding terms in the FEM or using interpolation functions. At present the Ω factor for a best fit is

$$\Omega = \frac{0.75L}{B} \leq 1.1$$

where L, B = grid element length and width, respectively. This method has been extended to allow triangular elements (shown in Table 10-1) and described in more detail in Bowles (1986). As with the beam element, it is necessary to have access to the $P-X$ coding used to develop the EA array so the output can be interpreted.

The concept of subgrade reaction with spring contribution at nodes is easy to modify for soil separation, since the diagonal term is the only coefficient in the stiffness matrix with the soil spring K_i:

$$(A_{ii} + K_i)X_i = P_i$$

Thus, for footing separation we simply make $K_i = 0$, rebuild (or reuse a copy of) the stiffness matrix, and again solve for the displacements X_i.

Generally one should include the mat weight in the analysis. The mat does not cause internal bending moments due to self-weight since the concrete is poured directly on the subbase and in the fluid condition conforms to any surface irregularities prior to hardening. Should the loads cause separation, however, the mat weight tends to counter this. Deflections will be larger when including mat weight, since the soil springs react to all vertical loads.

Preliminary Work

Generally, the depth of the mat is established from shear requirements as in Example 10-6 following. This depth + clear steel cover D_c is used to compute the moment of inertia or D:

$$I = \frac{BD_c^3}{12}(\text{FEM}) \qquad D = \frac{E_c D_c^3}{12(1-\mu^2)}(\text{FEM})$$

The bending moments obtained from the later plate analysis are used to design the mat reinforcement in both directions.

Total deflections are sensitive to the value of k_s used. Bending moments are much less so, but the designer should try to use a realistic minimum and a probable maximum value of k_s and obtain at least two solutions. The design would be based on the best information available or the worst conditions obtained from either of the two solutions (generally when k_s is minimum).

Establishing Finite-Grid Elements (variables in brackets refer to diskette computer program B-6.)

Begin the design by drawing the mat plan to scale and locate all columns and walls. Next lay a grid on this plan such that grid intersections (nodes) occur at any points of zero rotation or displacements (at column faces, wall edges, fixed edges, and similar). Use any convenient gridding if no nodes have unknown rotations or displacements. Grid elements do not have to be the same size, but best results are obtained if very small members are not adjacent to large ones (e.g., a member 0.2 m long connecting to a 2-m-long member is not so satisfactory as a 1-m connecting to a 2-m member). For pinned columns the grid can be at convenient divisions. The load matrix is developed using both column locations and loads. Code the grid starting at the upper left corner, across and then down. Orient the grid so a minimum number of nodes are horizontal for minimum bandwidth.

Develop a data generator to produce element data including the member number (MEMNO) and the six NP values for each element [NPE(I)] and H, V, and B (refer to Fig. 10-12). A data generator (program B-18) is a necessity, since the element input data are enormous.

Develop the nonzero P-matrix entries for each load condition; use simple beam theory for pinned columns between nodes.

Establish if any changes in soil modulus are required. These may be accounted for in the data generator; however, for local soft spots, holes in the ground, hard spots, etc., it may be more convenient to hand-compute the node springs to input into the spring array.

Establish the number of zero boundary conditions (NZX).

Compute the number of NPs in the matrix: NP = 3 × number of nodes; also count the number of members (NM) to be used in the grid.

Compute the bandwidth of the matrix as follows:

1. Find the minimum NP value at various nodes.
2. Find the maximum NP value at adjacent nodes that are interconnected by grid lines.
3. Compute bandwidth as

$$\text{NBAND} = \text{NP}_{\max} - \text{NP}_{\min} + 1$$

As shown on Fig. 10-12, NBAND = 21 − 1 + 1 = 21 (element 6). The size of the resulting band matrix ISIZE is

$$\text{ISIZE} = \text{NBAND} \times \text{NP}$$

The Solution Procedure

With the displacements from $\mathbf{X} = (\mathbf{ASA}^T)^{-1}\mathbf{P}$ we can solve $\mathbf{F} = \mathbf{SA}^T\mathbf{X}$ for each element in turn to find the element forces.

The computer program performs the necessary matrix multiplication to form the element $\mathbf{ESA}^T$ (ESAT) and $\mathbf{EASA}^T$ (EASAT). The element $\mathbf{EASA}^T$ will be of size 6×6. The $\mathbf{EASA}^T$ is then sorted for values to be placed at the appropriate locations in the global $\mathbf{ASA}^T$ (ASAT) for later banding and solution. Normally the $\mathbf{ASA}^T$ will have to be put on a disk or tape file capable of *random access.*

The computer routine next recalls the $\mathbf{ASA}^T$ from disk (or tape) and stores the band in main memory (refer to Fig. 10-13), filling the lower right corner with zeros. Boundary conditions are applied if specified, which result in zeroing the appropriate *row* and *upper diagonal* of the band matrix and placing a 1.0 in the first column as shown here (typical):

$$\begin{array}{cccccc} & & & & & 0. \\ & & & & 0. & \\ & & & 0. & & \\ & & 0. & & & \\ & 0. & & & & \\ 1.0 & 0. & 0. & 0. & 0. & 0. \end{array}$$

With the band reduction method, the displacements are exchanged with the **P** matrix at the end of the reduction. If it is desired to save the original **P** matrix for any reason, it must be stored in some alternative location. The *X*s (or redefined *P*'s) are used to compute the

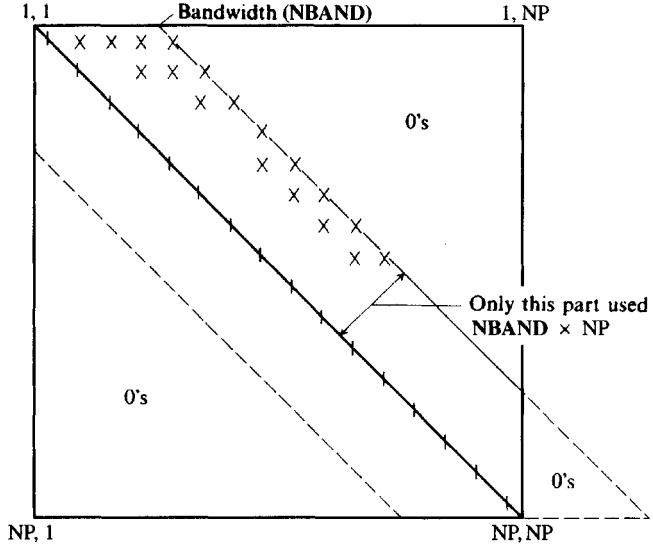

Figure 10-13 Symmetrical $\mathbf{ASA}^T$ matrix. Part used in reduction is as shown.

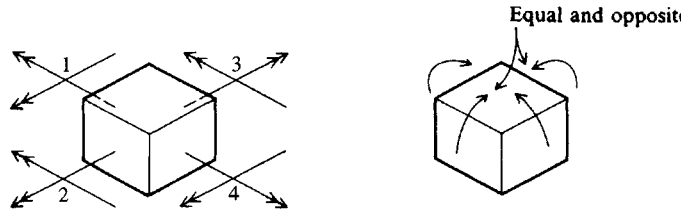

(*a*) Node and moments. (*b*) Node with moments summed for checking.

Figure 10-14 Checking moments in output for statics at a node.

F's. Also they should be scanned to see if mat-soil separation has occurred at any nodes. If negative deflections occur (tension soil springs), the stiffness matrix is rebuilt with no springs ($K = 0$) at those nodes, and the problem is cycled until the solution converges. Convergence is understood to occur when the current number of nodes with soil separation N_i is equal to the N_{i-1} number of nodes with soil separation just used, or

$$N_i = N_{i-1}$$

When convergence is achieved, the program then computes the element bending and torsion forces using

$$\mathbf{F} = \mathbf{ESA}^{\mathrm{T}}\mathbf{X}$$

Here some savings in computation time can be made if the $\mathbf{ESA}^{\mathrm{T}}$ was saved to a disk file when it was computed. But this can be done only if the node springs are added from a spring array; otherwise the element K_i values are included in the $\mathbf{ESA}^{\mathrm{T}}$.

It is helpful to have the program sum soil node forces (X_iK_i) to compare with the input vertical forces as a quick statics check. It is also helpful if the program makes a moment summation (includes both bending and torsion moments) for the several elements framing into a node for a visual $\sum M_i = 0$ within computer round-off at any node i (see Fig. 10-14). These node moments can be directly used in design by dividing by the element width to obtain moment/unit width.

Design shear requires access to a listing of element forces so the two end moment values can be summed (with attention to sign) and divided by the element length and divided by the element width to obtain shear/unit width. In passing we note that at any node the sum of vertical applied force (from **P** matrix) + soil reaction + $\sum$ sum of element shears framing to node = 0 within computer round-off (and with attention to signs).

10-10 MAT FOUNDATION EXAMPLES USING THE FGM

The following several examples are used to illustrate mat analysis using the FGM.

Example 10-5. (*a*) Compare the Bowles finite-grid method (FGM) with the classical finite-element method (FEM) and the finite-difference method (FDM). Both the FDM and the FEM programs are from the author's program library. (*b*) Also compare the bending moments from these elastic

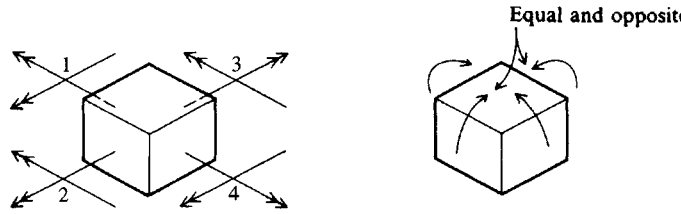

(*a*) Node and moments. (*b*) Node with moments summed for checking.

Figure 10-14 Checking moments in output for statics at a node.

F's. Also they should be scanned to see if mat-soil separation has occurred at any nodes. If negative deflections occur (tension soil springs), the stiffness matrix is rebuilt with no springs ($K = 0$) at those nodes, and the problem is cycled until the solution converges. Convergence is understood to occur when the current number of nodes with soil separation N_i is equal to the N_{i-1} number of nodes with soil separation just used, or

$$N_i = N_{i-1}$$

When convergence is achieved, the program then computes the element bending and torsion forces using

$$\mathbf{F} = \mathbf{ESA}^{\mathrm{T}}\mathbf{X}$$

Here some savings in computation time can be made if the $\mathbf{ESA}^{\mathrm{T}}$ was saved to a disk file when it was computed. But this can be done only if the node springs are added from a spring array; otherwise the element K_i values are included in the $\mathbf{ESA}^{\mathrm{T}}$.

It is helpful to have the program sum soil node forces (X_iK_i) to compare with the input vertical forces as a quick statics check. It is also helpful if the program makes a moment summation (includes both bending and torsion moments) for the several elements framing into a node for a visual $\sum M_i = 0$ within computer round-off at any node i (see Fig. 10-14). These node moments can be directly used in design by dividing by the element width to obtain moment/unit width.

Design shear requires access to a listing of element forces so the two end moment values can be summed (with attention to sign) and divided by the element length and divided by the element width to obtain shear/unit width. In passing we note that at any node the sum of vertical applied force (from **P** matrix) + soil reaction + $\sum$ sum of element shears framing to node = 0 within computer round-off (and with attention to signs).

10-10 MAT FOUNDATION EXAMPLES USING THE FGM

The following several examples are used to illustrate mat analysis using the FGM.

Example 10-5. (*a*) Compare the Bowles finite-grid method (FGM) with the classical finite-element method (FEM) and the finite-difference method (FDM). Both the FDM and the FEM programs are from the author's program library. (*b*) Also compare the bending moments from these elastic

methods with those that would be used in conventional spread footing design of Chap. 8. A large spread footing will be analyzed so that the input/output is not complex. Use the following data:

$B \times B = 3 \times 3$ m Use a 0.6 m grid No footing weight

$P = 2200$ kN Prorate $\frac{1}{4}$ to each adjacent node

$E_c = 22\,408$ MPa $\mu = 0.15$ Thus, $G' = 9740$ MPa

Assume $k_s = 15\,700$ kN/m^3 $D_c = 0.60$ m Double edge springs

Solution. *a.* Make the footing grid as shown in Fig. E10-5*a* and from the coding obtain

NM = 60 (refer also to Fig. 10-11)

NP = 108 NBAND = 21 − 1 + 1 = 21

NNZP = 4 (number of node loads from 500 kN column load)

For 1 load condition NLC = 1

The load matrix and NP is

45	550 kN
48	550
63	550
66	550

One should use a data generator to develop member data entries, since there are 60 lines of input containing NPE(I), *H, V, B*, and element soil springs. From the output, which is symmetrical from loading, obtain the moments and deflections shown in Fig. E10-5*a*. The FGM program output moment for the element has been divided by $B = 0.6$ m to give the moment/unit width shown. Note that you will have to use program FADMAT (B-6) on your diskette with two data sets EXAM105?.DTA to obtain the output for verifying this example.

The actual moment can as easily be determined by the FGM as by the alternative methods. In general, however, the agreement is very good from all three methods. Where the FGM differs from the others, it is on the conservative side. There is some uncertainty as to what the correct moments should be at node 8 since theory indicates odd plate (or membrane) behavior at this location (and also at nodes 11, 26, 29).

b. Compare the moment computed by the ACI 318–suggested procedure with the FGM output. We will do two comparisons: without column fixity (EXAM105A.DTA) and with column fixity (EXAM105B.DTA). Column fixity will assume that the column limits plate rotation at the column corner nodes (15, 16, 21, and 22) to 0.0 radians. This assumption is not unrealistic since the column is 0.6×0.6 m square. For the fixed case a moment at the column face is found to be **307.1** kN · m/m, which is larger than the **272.1** kN · m/m computed without column fixity.

The ACI column face moment will be based on an average soil pressure of $q = 2200/3^2 = \mathbf{244.4}$ kPa. The moment based on a moment length $L = 2(0.6) = 1.2$ m is

$$M = \frac{qL^2}{2} = \frac{244.4(1.2^2)}{2}$$

$= \mathbf{176}$ kN · m/m < 272.1 kN · m/m

$\ll 307.1$ (for fixed column case)

This moment difference is so large that the footing has a real LF close to 1 for the USD method and only slightly over 1.0 for the ADM. At least one non-U.S. footing design standard requires additional reinforcing bars in the column zone for this higher-than-average moment.

c. Now let us do a statics check. For this you must have the output from using program B-6 (on your diskette) with data file EXAM105A.DTA. We will do a statics check at one of the column corner nodes—node 21.

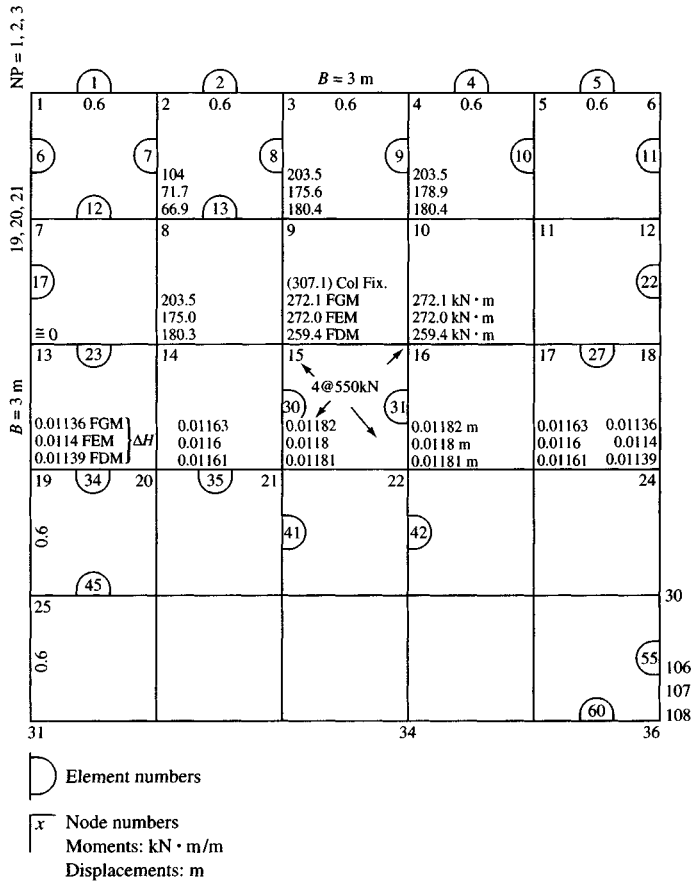

Figure E10-5*a*

1. From Fig. E10-5*a* count the elements (a partial count is shown) so the elements framing into node 21 can be determined (here 30, 35, 36, and 41).

2. Next draw a sketch (as Fig. E10-5*b*) showing the elements framing into node 21 in order, and on the end of those elements draw the bending and torsion moment vector directions. Use the (+) directions as was done in the figure, and from the moment table in the output put the actual moment values and signs on the vectors drawn.

Note you have "far-end" moments (second moment column) for elements 30 and 35, "near-end" moments for elements 36 and 41. The arrowheads on the elements in Fig. E10-5*b* point toward the "far end."

The torsion has a (−) sign if arrow is into the element and (+) if out of the element (sign convention shown in Fig. 10-11).

3. Based on element moments shown, make the following computations:

$$\text{XMX1} = X\text{-}1 = 163.3 + 0 = 163.3$$

Combine the end moment on element 41 and torsion from element 36:

$$\text{XMX2} = X\text{-}2 = -152.6 + (-10.7) = -163.3$$

Combine the end moment on element 30 and torsion from element 35.

From this we see $X\text{-}1 = -X\text{-}2$

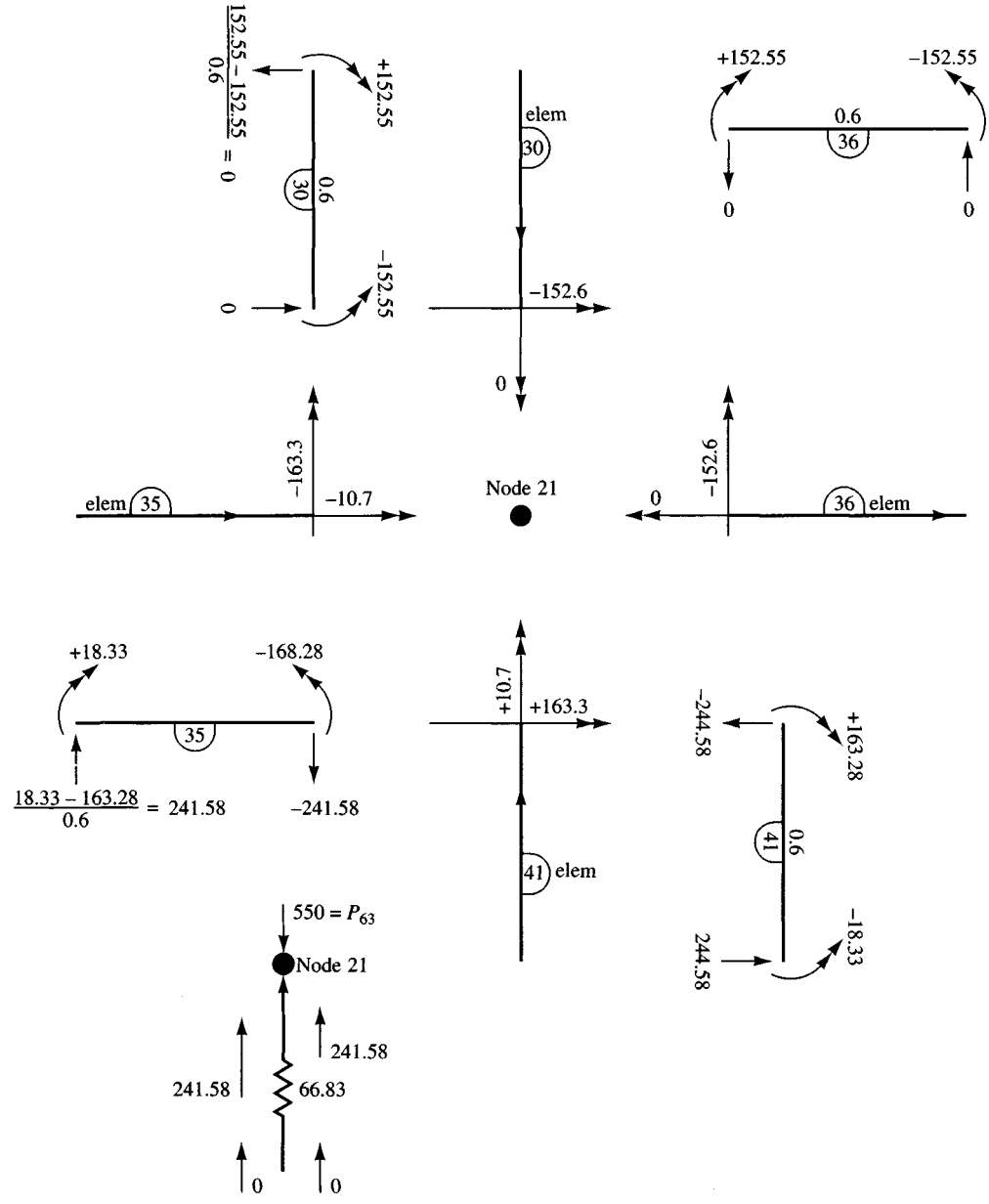

$\uparrow \Sigma F_v = 2(241.58) + 66.83 = 549.99$

$\downarrow F_v = 550$ O.K.

Figure E10-5*b*

These are the horizontal or X values that are output in the combined moment table for direct design use (after the user divides them by element width).

$$\text{Similarly, XMY1} = Y\text{-}1 = -163.3 + 0 = -163.3$$

Combine the vertical moment vector from element 35 with the torsion vector from element 30:

$$\text{Likewise, XMY2} = Y\text{-}2 = 152.6 + 10.7 = 163.3$$

Combine the vertical moment vector from element 36 with the torsion moment from element 41:

$$\text{From this we see } Y\text{-}1 = -Y\text{-}2 \text{ (i.e., equal and opposite)}$$

The sums of the moments at node 21 are satisfied in both the X and Y directions. These are also the values in the node moment table of your computer printout sheets, including sign. There may be small differences (order of 0.01) due to computer rounding.

4. Now we will check $\sum F_V = 0$. For this draw the elements again, somewhat reoriented on Fig. E10-5*b* with the moments shown as circle arcs. Again refer to the element moment table and, using signs, put both the near- and far-end moment values on the arcs and orient the arrowheads on the arcs in the correct direction. *Use the right-hand rule* to establish directions based on Fig. 10-11.

Note that Fig. E10-5*b* shows both the arrowheads in correct direction and the moments labeled with a sign. With the moments on both ends of the element properly oriented, compute the element end shears (there will be a value at each end with one vector up and the other down). You need the moment orientation to get the shear vector signs (or arrowheads) in the correct direction.

Noting that element forces act on the node in the opposite direction, we can draw the node as in the lower left corner of Fig. E10-5*b* and for this node there is an external force (a P matrix entry) of $P_{63} = 550$ kN acting as shown. Putting the several element end shears and the output value of spring force of 66.83 kN from the element moment table (its direction is known, as it always resists downward movement) on node 21, we sum forces and find that the shear + soil reaction gives

$$\sum F\uparrow = 241.58 + 241.58 + 0. + 0. + 66.83 = \mathbf{549.99}\text{ kN}$$

and

$$\sum F\downarrow = 550\text{ kN} \qquad (\text{or } 549.99 \approx 550)$$

This completes the statics check. We have found that the sum of X moments is the same with opposite signs; the sum of the Y moments is the same with opposite signs; and the sum of vertical node forces ≈ 0.

One final note: The moments shown in the node moment table will have a sign reversal for the node. For design divide the node moments by the element width and, on the basis of signs for the element (or the node displacements), you can determine if the top or bottom of the plate has tension; sometimes there is tension in one direction and compression in the other at a node.

5. The element shear values can be used to check two-way action as follows: For either element 35 or 41 (30 and 36 are column elements) we have $V = 241.58$ kN for a width $B = 0.6$ m. This shear is constant over the element length L. $D_c = 0.60$ m so, assuming 70 mm of clear cover and a 25-mm reinforcing bar, the depth $d = 505$ mm or 0.505 m. At $d/2$ from the column face we have (two-way shear $v_c = 1.298$ MPa for $f'_c = 21$ MPa from Table 8-2)

$$\text{Resisting shear} = v_c db = 1.298(0.505)(0.60)(1000, \text{ to convert MN to kN}) = \mathbf{393.3}\text{ kN}$$

$$\text{Actual shear} = 241.6\text{ kN} \ll 393.3\text{ kN} \qquad \text{Two-way shear is O.K.}$$

The footing could probably be made with a smaller D_c but as this decreases, the shear at the column face will increase. You could make one or more trials using data set EXAM105A.DTA edited for slab thickness to find an optimum depth d.

////

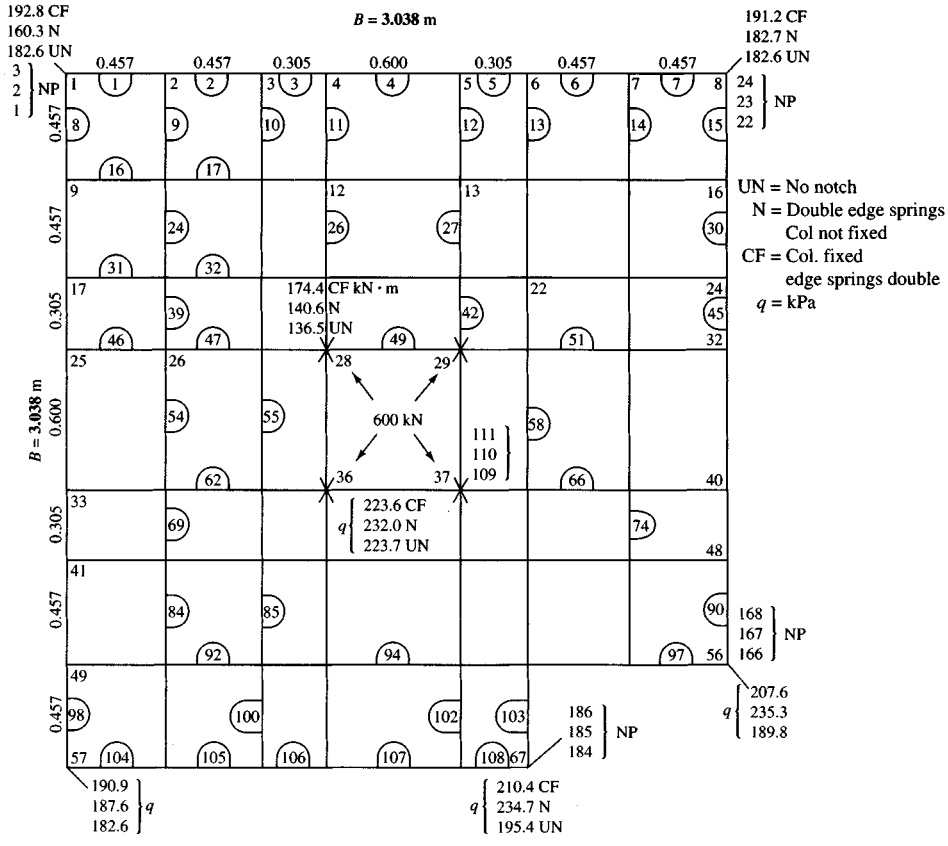

Figure E10-6

Example 10-6. Make a comparison of soil pressure for the notched footing shown in Fig. E10-6 for the following three cases: (1) no notch, (2) a notch but no column fixity, and (3) for notch with column fixed. You should use your program B-6 together with data sets EXAM106.DTA, EXAM106A.DTA, and EXAM106B.DTA from your diskette. Use the output to verify data shown on Fig. E10-5 and for other locations as well. Although the data are assembled into data sets for your convenience the given data are

Column: 600×600 mm with an axial load $P = 2400$ kN

Footing: $B \times B = 3.038 \times 3.038$ m less the corner notch of dimensions shown in Fig. E10-6

Other: $f_c' = 21$ MPa $\quad E_c = 21\,700$ MPa $\quad \mu = 0.15$

$D_c = 510$ mm $\quad q_a = 260$ kPa (sandy-gravelly clay)

Solution. Draw the footing to a large scale and place a grid on it as shown in Fig. E10-6. Try to use symmetry as shown so the output will be somewhat self-checking. Also use enough nodes/elements that there is confidence in the output. I used program B-18 (an element data generator) to produce the element data on a disk file, which was then put into the first B-6 data file (EXAM105.DTA) using the subroutine in B-6 that requests input from the screen when a data file does not exist. Input a 1 at the request location when queried about element data, and later use your editor to include the element data and remove the information line in the data set for B-6. Before editing the output from

program B-18, use the element data set to set up the file for the unnotched base. Next, edit a copy of the data set to create the notch case (by removing some elements and modifying widths of certain others, we have the element data for the notched base). For this we obtain

$$\text{NP} = 186 \qquad \text{Number of elements NM} = 108$$

$$\text{NBAND} = 27 - 1 + 1 = 27 \text{ (using element 8)}$$

$$k_s = 40(\text{SF})q_a = 40(3)(260) = 31\,200 \text{ kN/m}^3$$

$$G' = \frac{E_c}{2(1+\mu)} = \frac{21\,700}{2(1+0.15)} = 9435 \rightarrow \mathbf{9400} \text{ MPa}$$

For fixing the column it is necessary to identify the rotational NPs at the column corner nodes and specify rotation = 0.0 rad. There are eight rotational displacements, of which the last two are 109 and 110, shown on Fig. E10-6. Again we can see that the footing is not quite rigid, for the displacements are larger under the column. Also notice that fixing the column nodes against rotation tends to smooth out the vertical displacements so that the soil pressure is more uniform beneath the footing.

Fixing the column substantially increases the bending moment at the column face over that determined by the pinned column analysis.

////

Example 10-7. An elevated storage bin carrying a total load of 35 600 kN [including bin contents (when full), bin, and columns] is shown in Fig. E10-7*a*. Since steel might require excessive maintenance at this geographic location, reinforced concrete square columns of 760 × 760 mm are used. The soil data for this example are those of Examples 10-1 and 10-2.

We will use column fixity (owing to column dimensions). We should not double the edge springs to account for *soil coupling* when we have a mat with more than two column loads.

Required. Make an approximate mat design. Use your program B-6 (FADMAT) and data file EXAM107.DTA on your diskette to rerun and obtain a set of output. Be careful, however, since the paper output (using $14\frac{1}{2} \times 11$ in. sheets) totals 15 pages [not including the element data list produced when using program B-18, which is about 4 pages, or from setting program control parameter ICHECK = 1 (col 40 in 2nd dataline)].

Solution.

Step 1. Use a load factor LF = 1.5 on loads to convert to ultimate since there is some uncertainty whether the bin contents may be both long-term and transient. The bin and columns are, of course, dead loads with an ACI LF = 1.4.

Step 2. Find tentative mat dimensions. This calculation is no different from the method used in Chap. 8 for spread footings. From the loads and geometry of Fig. 10-7*a* we will try a square mat:

$$B^2 q_a = P \rightarrow B = \sqrt{\frac{P}{q_a}} \text{ (use working loads)}$$

$$B = \frac{\sqrt{35\,600}}{250} = 11.93 \rightarrow \mathbf{12} \text{ m}$$

This slight increase in area serves two purposes: (1) It allows for trucks driving through to load from the hopper; (2) it gives a slight decrease in q_o since the mat will probably be rather thick when carrying an 8900 kN column load.

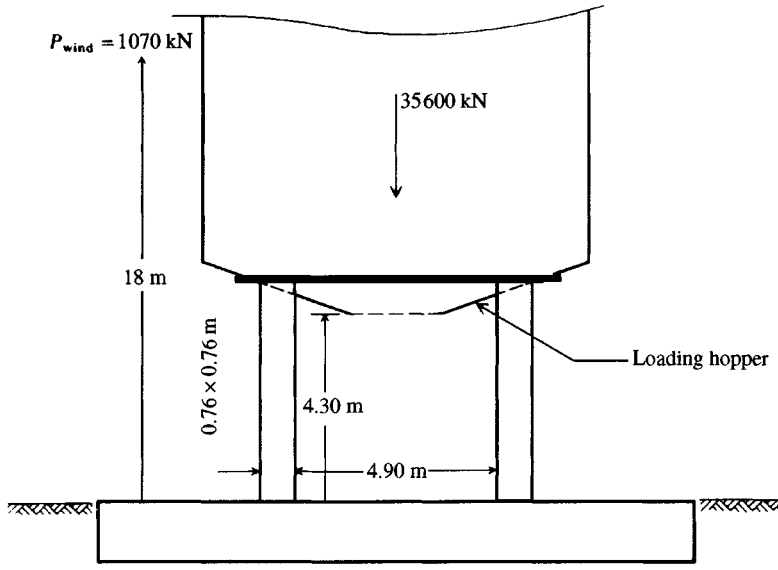

Figure E10-7*a*

Step 3. Find the depth for two-way action. We will use the approximate formula [Eq. (8-8)] since these are large loads and that equation is slightly conservative:

$$4d^2 + 2(w + w)d = P_{ult}/v_c$$

Obtain v_c = 1.499 MPa from Table 8-2 for f'_c = 28 MPa; the column dimensions w = 760 mm = 0.76 m and substitution of values give

$$4d^2 + 2(0.76 + 0.76)d = \frac{(1.5)(8900)}{1.499 \times 1000}$$

Simplifying, we obtain

$$d^2 + 0.76d - 2.226 = 0$$

Solving, we find d = 1.16 m (1160 mm). With a 30-mm rebar each direction + 70 mm of clear cover the total estimated depth is

$$D_c = 1160 + 30 + 70 = 1260 \text{ mm } (\mathbf{1.260} \text{ m}) \text{ as first trial}$$

We could use a thinner base with shear reinforcement but this is difficult both to design and to place and would produce a less rigid mat. We will (or at least try to) use this mat thickness and plan dimensions.

Step 4. From the mat plan dimensions locate the columns (draw to approximate scale) and place the grid lines as shown in Fig. E10-7*b*. Since the columns are large they should be "fixed" to the base. Thus, grid lines must pass through their faces. The remainder should be made as symmetrical as possible and should be chosen to produce elements of reasonable length. For example, the elements

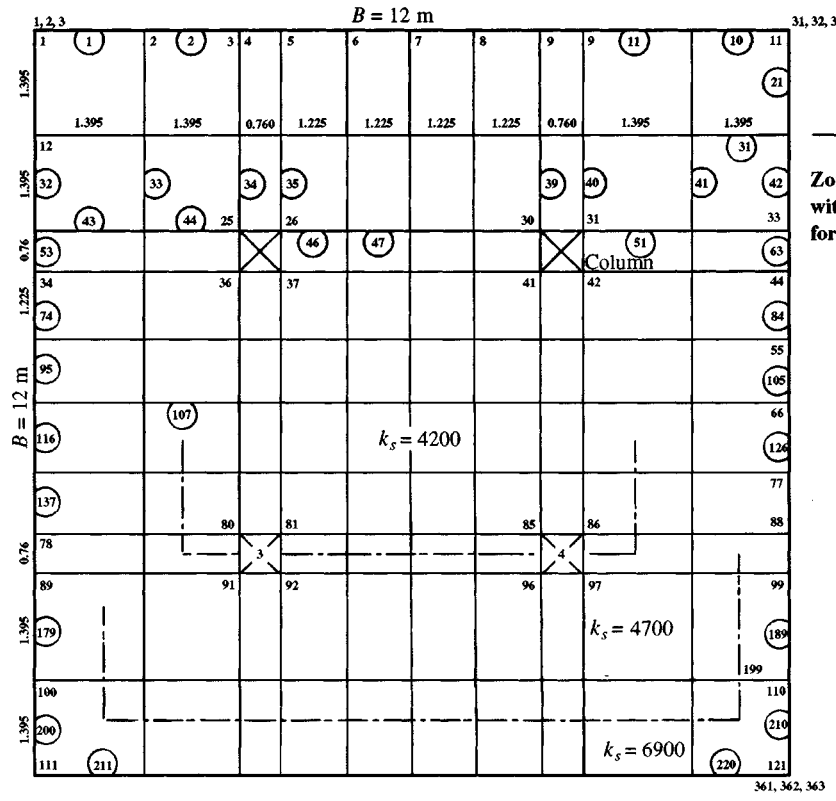

Zone boundaries with k_s values shown for Problem 10-8

Figure E10-7*b*

would be too long (and adjacent to 0.76 mm lengths) if we did not divide the 4.90 m space between column faces as shown or the exterior spacing of 2.79 m into two element lengths of 1.395 m each. This gridding scheme results in 121 nodes and 220 elements. This large number of elements will require an element data generator or an extremely long time to input.

From the *P–X* coding we find that, to fix the columns by setting the two corner rotations = 0 for each of the four column nodes and with four columns, we have

$$\text{NZX} = 4 \times 2 \times 4 = 32 \text{ (8 rotations of } X = 0 \text{ at each column)}$$

$$\text{Number of elements NM} = 220$$

$$\text{Number of NP} = \text{number of nodes} \times 3 = 121 \times 3 = 363$$

The bandwidth can be computed from element 11 as

$$\text{NBAND} = 36 - 1 + 1 = 36$$

The **P** matrix entries will be four values per column for a total of

$$\text{NNZP} = 4 \times 4 = 16 \text{ entries}$$

There are two load cases: (1) gravity, (2) gravity + wind, so

$$\text{LC} = 2$$

For input we have to identify the NP value. A set of P values is input for each load case in turn (refer to the data set). For load case 1 gravity loads P_{gravity} we have

$$35\,600 \text{ kN using 4 columns with 4 nodes per column, so}$$
$$P \text{ value} = 35\,600/(4 \times 4) = \mathbf{2225} \text{ kN}$$

For the load case with wind we will take overturning clockwise as shown on Fig. E10-7*a*. Note that if the bin is round, wind can come from any direction with the force and $\bar{y}$ (of 18 m) shown. It is possible that a more critical loading case obtains with the wind moment taken about an axis through columns 3 and 2. For wind as shown the moment is

$$M = P_w \bar{y} = 1070 \times 18 = 19\,260 \text{ kN} \cdot \text{m}$$

The equivalent vertical force is $P' = 19\,260/(4.90 + 0.76) = 3402.8$ kN. This is divided between two columns on each side, so $P'' = 1701.4$ kN.

Thus the wind moment decreases the vertical load in the windward columns and increases the load in the leeward columns. Typically,

$$P_L = 8900 + 1701.4 = 10\,601.4 \text{ kN}$$
$$P_W = 8900 - 1701.4 = 7198.6 \text{ kN}$$
$$\text{The vertical } P \text{ matrix entry for each column node}$$
$$\text{on the leeward side} = 10\,601.4/4$$
$$= \mathbf{2650.4} \text{ kN}$$
$$P \text{ matrix entry for windward side} = 7198.6/4 = \mathbf{1799.6} \text{ kN}$$

For columns 1 and 2 we have

NP	P_{gravity}, kN	P_{wind}, kN
$25 \times 3 = 75$	2225.0	1799.6
$26 \times 3 = 78$	2225.0	1799.6
$30 \times 3 = 90$	2225.0	2650.4
$31 \times 3 = 93$	2225.0	2650.4
$36 \times 3 = 108$	2225.0	1799.6
$37 \times 3 = 111$	2225.0	1799.6
$41 \times 3 = 123$	2225.0	2650.4
$42 \times 3 = 126$	2225.0	2650.4
$\cdots$ etc.		

At column 1 we have rotation NPs of

73, 74 (75 is translation); 76, 77 (78 is translation);
106, 107 (108 is translation); and 109, 110 (111 is translation)

We should, of course, put these in sequence to minimize program error, not as shown above for illustration of locating the NP numbers where rotation is specified = 0.

You should obtain a direct printout of the data file (several pages in length) to see how the data given here are organized.

Step 5. We must inspect the node moment data, which also include actual soil pressures at nodes and node moments. None of the nodes for load case 1 has a soil pressure $q > 248.8$ kPa (you should

check your output for load case 2). Remember for LC = 2 you have wind, so it is usual to allow an actual $q > q_a$ (how much greater may require discussion with the geotechnical consultant). Here, if $q \leq 1.33q_a$ consider the soil pressures acceptable.

Make a routine inspection of $\sum M \approx 0$ at nodes and

$$\sum F_v \approx 0 \text{ for the entire structure}$$

That is, check if 35 600 input = sum of soil spring reactions (here on the author's computer 35 599.99 kN was output).

Step 6. Compute the required rebars for one node location. From a reasonable examination of the output (LC = 1) find the following:

Node 25: M = 1981.3 with an element width = (1.395 + 0.76)/2 = 1.08 m

Node 26: M = 1522.9 with an element width = (1.225 + 0.76)/2 = 0.99 m

M_{25} = 1981.3/1.08 = 1834.5 kN · m/m

M_{26} = 1522.9/0.99 = 1538.3 kN · m/m

Using 1834.5 kN · m/m to find A_s in both the horizontal and vertical plan orientation in the column regions in the bottom of the mat, we compute using Eq. (8-2) as follows:

$$A_s\left(d - \frac{a}{2}\right) = \frac{M_u}{\phi f_y \times 1000} \qquad a = \frac{A_s f_y}{0.85(b)f_c'}$$

For f_c' = 28 MPa and f_y = 400 MPa, we then have

$$\frac{a}{2} = 0.5\left[\frac{400A_s}{0.85(1)(28)}\right] = 8.40A_s$$

Solving (remember that 1834.5 kN · m/m is an unfactored design value), we have (using d = 1.26 − 0.030 − 0.070 = 1.16 m from step 3)

$$A_s(1.16 - 8.40A_s) = \frac{1.5 \times 1834.5}{0.9 \times 400 \times 1000}$$

Simplifying, we obtain

$$A_s^2 - 0.138A_s + 0.000\,91 = 0$$

Solving, we find A_s = 0.006 943 m²/m → **6943** mm²/m. This requires 6943/700 = 10 No. 30 bars with a spacing of

$$s = 1000/10 = 100 \text{ mm} \qquad \text{(seems satisfactory)}$$

For a *minimum* A_s based on $1.4/f_y \rightarrow 1.4/400 = 0.0035$, we have

$$A_{s,\min} = 0.0035(1000)(1.16 \times 1000) = \mathbf{4060} \text{ mm}^2/\text{m}$$

This computation indicates that most of the mat will require only the minimum percentage of rebars. Only the column zones using a zone distance of about d from each face (2 × 1.16 + 0.76) = 3.84 m centered on each column and each way using 10 No. 30 rebars is required. For the remainder of the mat use six No. 30 reinforcing bars (6 × 700 = 4200 > 4060 required).

Note there is much additional work to be done to complete this design. Even though the minimum percentage of rebars may control, you will have to use them as top bars in zones of (−) moment (top tension).

////

10-11 MAT-SUPERSTRUCTURE INTERACTION

One may include the superstructure rigidity into the problem, as was done in a semiempirical manner using Eq. (10-3), which requires a substantial amount of hand computations.

We may use a regular frame analysis program and add a beam-on-elastic-foundation subroutine so that the global $\mathbf{ASA}^T$ matrix includes nodes for the frame and the foundation. Now one can make a direct solution for node displacements in both the frame and base and from these compute bending moments for the frame and base for design.

Few computer programs do superstructure-foundation coupling at present because of the ease of banding a frame program and the separate narrow bandwidth of a beam-on-elastic foundation. When both the foundation and superstructure are included, the bandwidth may become rather large; however, modern computers can handle large stiffness arrays so size is not a major problem.

We could even do the coupling for a space frame; however, these usually have nodes with 6 d.o.f in the superstructure and do not interface well with the plate where the nodes have 3 d.o.f.

Probably as good a solution as any is to do the following:

1. Code and make an analysis of the superstructure to obtain the axial column forces and applicable column base bending moment(s). Assume a fixed-base condition.
2. Code the foundation (mat or combined footing) with nodes at the superstructure columns. Now use the output from step 1 as the input of this step and make a solution. You will obtain node vertical translations and rotations at the column nodes.
3. Use these data from step 2 as boundary conditions for a rerun of step 1. That is, specify vertical displacement and rotation of the one or more columns. Obtain a new set of axial forces and moments, which are input for step 2.
4. Continue to iterate until the axial forces and moments used are within some specified tolerance (closeness) to the preceding cycle. At this point you have a reasonably good solution for both the superstructure and the foundation.

10-12 CIRCULAR MATS OR PLATES

Circular plates are commonly used for industrial process tower bases (see Example 9-4) and for chimneys. They may also be used to support silos and other similar superstructures. There are few closed-form solutions for a circular plate on an elastic foundation. Timoshenko and Woinowsky-Krieger (1959) give theoretical solutions for a simply supported and a fixed-edge support circular plate but none for a plate on an elastic foundation. Chu and Afandi (1966) and Smith and Zar (1964) provided some practical methods for circular plate (for chimneys) design involving empirical procedures.

The FEM using triangular elements can be used to analyze a circular plate by gridding it into a series of triangles. The particular disadvantage of this is that the moments at the center of any triangle are usually output rather than node values. Since the FEM is difficult to interpret anyway, this creates a truly difficult situation for most designers.

The FGM given here can be fixed (reprogrammed) to solve a circular plate. Referring to Fig. 10-15, we grid the circular plate as shown with radial lines. This gridding produces triangles for the central portion with a common node 1. Next we produce chord-type elements along the circular grid lines. The elements are converted to rectangular elements of average

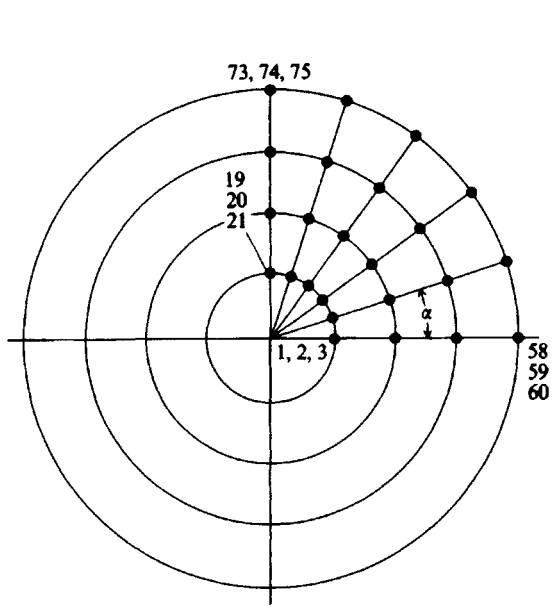

(*a*) Circular mat. Use one-fourth of mat if symmetrical, as a large number of nodes result for even medium-sized alpha angles.

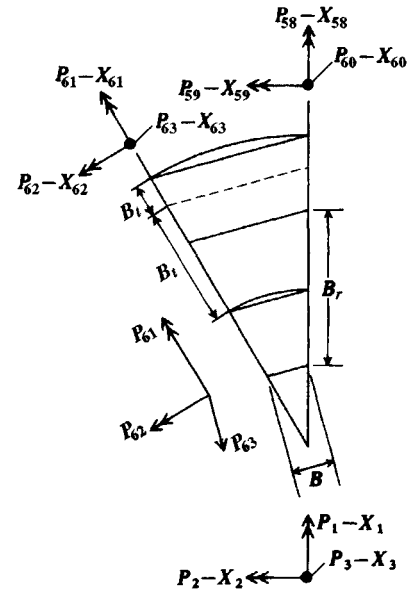

(*b*) A sector showing method of obtaining grid element cross section and coding.

Figure 10-15 A finite-element (grid) method to solve for displacements and bending moments in a circular mat foundation. Matrix is of size 3 × number of nodes. (*a*) Circular mat. Use one-fourth of mat if symmetrical, as a large number of nodes result for even medium-sized alpha angles. (*b*) A sector showing method of obtaining grid element cross section and coding.

width and average length, and the same equations (and $\mathbf{ASA}^{\mathrm{T}}$ formulation) are used as for the rectangular FGM. We note that one-quarter of a plate with the radial lines shown produces NP = 75, but more critical is the bandwidth. It is always determined from the central part, which gives for the figure NBAND = 21 − 1 + 1 = 21; for one-half the plate NBAND = 36 − 1 + 1 = 36. If there are more radial lines, of course, the bandwidth becomes larger. Fortunately, it is seldom necessary to have to use more than one-half the plate. A half-plate is necessary for the overturning case.

Since the element formulation is extremely difficult, it is advantageous to use an element data generator, code one-half the plate, and use that element data for all load cases.

The circular gridding does not have to use an equally divided radius, so that with the *P–X* coding shown it is easy to place one of the circular grid lines at the face of the pedestal or chimney. By careful coding, the elements inside the pedestal/column face grid can have their additional stiffness included into the global stiffness matrix.

To compute the soil springs a special procedure is required that must take into account the contributing arc segment area to any node. The element generator computes the several arc segments and saves them in an array so that they can be multiplied either by the modulus of subgrade reaction k_s to obtain node springs or by γD_c to obtain plate self-weight for the several nodes.

A nonlinear subroutine can be activated for X > XMAX or for soil-base separation. When the soil-base separation stabilizes (number of nodes separated does not change from previous

cycle), one can plot a line approximating the zero-pressure line to see how much of the plate is "effective" in carrying the load.

A pair of programs [B-20, B-21 (element generator)] regularly used by the author for the circular plate has been tested using the simple edge support and fixed edge support plate solutions for comparison, with quite good results. The effect of doubling edge springs (or preferably doubling the edge k_s) can be easily shown to be correct. A round, uniformly loaded plate without edge springs doubled gives a nearly uniform vertical displacement with moments nearly zero around the center. Doubling edge springs gives edge displacements approximately $0.64\delta H_{cen}$ and plate moments that are greater than zero with the magnitude dependent on the uniform load. To model a uniform load, input a unit weight γ such that $\gamma \times$ plate thickness T gives the desired pressure. For flexible plates the center displacements compute nearly exactly according to theory. The theoretical center displacement using Eq. (5-16) is

$$\Delta H = qD\frac{1-\mu^2}{E_s}mI_sI_F \qquad (5\text{-}16)$$

where terms not previously identified in Eq. (5-16) are

D = plate diameter, m or ft
I_s = shape factor for round base
= 1 for center
= 0.64 for edge
= 0.79 to 0.88 for a "rigid" circular plate
m = 1.0

It should be evident that one can find a plate thickness to satisfy "rigid" criteria by simply varying the plate thickness T.

The difference in hand and computer analysis of a round foundation will now be illustrated using the industrial tower footing of Example 9-4 as a circular plate. In Example 10-8 we double edge springs by doubling the outer input value of k_s. This method is the most precise since it is the only one to produce exterior node soil pressures that are correct (i.e., include both edge shear and bearing pressure).

The particular advantage of coding the nodes using radial and tangential rotation NPs is that the edge fixity is much easier to program. Of course for a chimney or pedestal resting on a plate, it will be necessary to be able to fix rotations of a series of interior nodes along some circular grid path. The radial rotations are usually those that are zero when specifying boundary conditions required when using a 1/4 or 1/2 plate from symmetry.

Example 10-8. Reanalyze the industrial/process tower footing of Example 9-4 as a round base using computer program B-20.

Given.

Operating load = 580 kN
Allowable soil pressure q_a = 150 kPa
f'_c = 21 MPa; γ_c = 23.6 kN/m^3
γ_s = 16.50 kN/m^3

Overturning moment from wind at the top of the anchor ring = $131.14 \times 33.5/2 = 2197$ kN · m (see Fig. E9-4a).

Solution.

Step 1. Compute modulus of elasticity of concrete using the ACI equation shown on Table 8-3:

$$E_c = 4700\sqrt{f_c'} = 4700\sqrt{21} = 21\,538 \text{ MPa} \rightarrow \text{ use } \mathbf{21\,500} \text{ MPa}$$

Also compute (using $\mu = 0.15$) the shear modulus

$$G' = \frac{E_s}{2(1+\mu)}\frac{21\,500}{2(1+0.15)} = 9347 \text{ MPa} \rightarrow \text{ use } \mathbf{9350} \text{ MPa}$$

We will estimate $k_s = 40(\text{SF})(q_a) = 40 \times 3 \times 150 = \mathbf{18\,000}$ kN/m^3, and we will double the edge springs by inputting zoned values (this program allows you to input k_s for each radial node along the axis of symmetry), so we have k_s for nodes 1, 2, 13 = 18 000, and for the edge node $k_{s,(24)} = 2 \times 18\,000 = 36\,000$ kN/m^3.

Step 2. There are several load cases to consider. Here for illustration, only the case of working gravity load + wind will be analyzed. *We will use symmetry and only analyze 1/2 the base,* as shown in Fig. E10-8*a*. For this the gravity load from the vessel is

$$\text{Total Load} = 580 \text{ kN} \rightarrow \text{ use } 580/2 = \mathbf{290} \text{ kN}$$

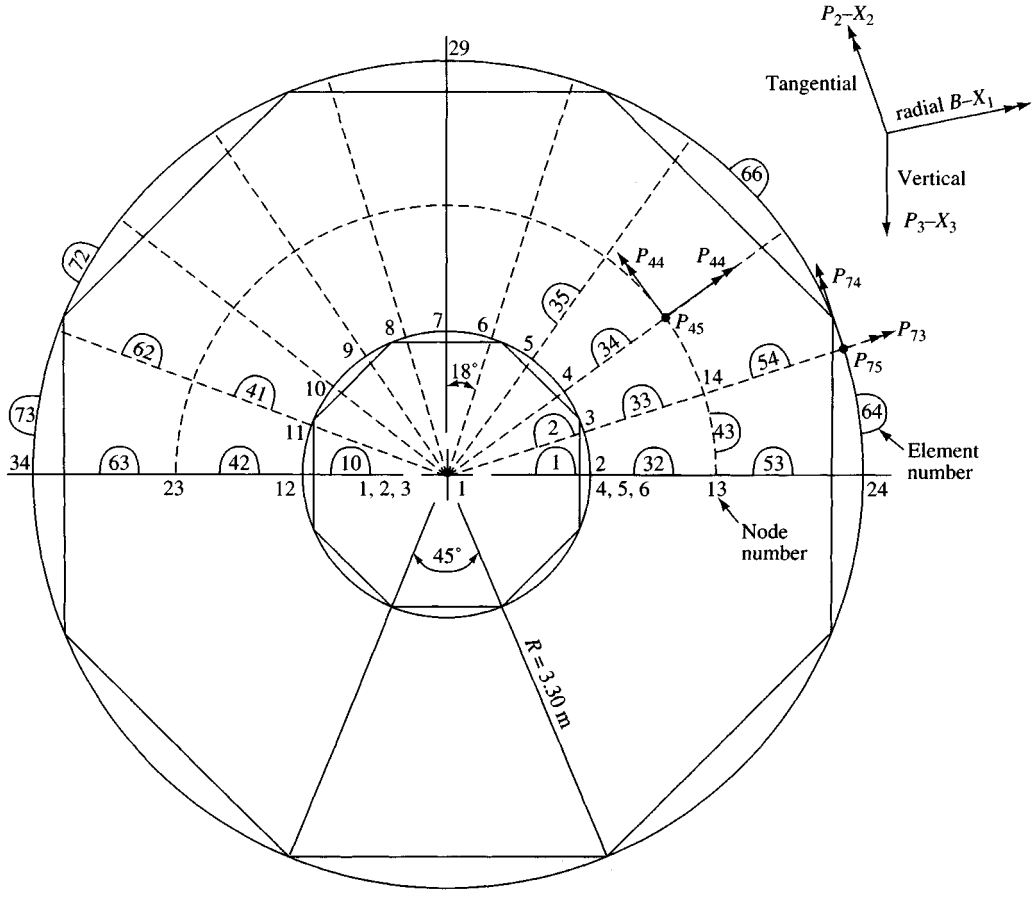

Figure E10-8*a*

For 9 full nodes and 2 half-nodes (on the line of symmetry) the gravity load is

$$P_i = 290/10 = 29.0 \text{ kN} \quad \text{(full node—nodes 3–11)}$$
$$= 29.0/2 = 14.5 \text{ kN} \quad \text{(1/2 nodes—nodes 2 and 12)}$$

The **P** matrix will be developed for 1/2 the base, as shown in the following table. Refer to both Figs. E10-8*a* and *b* for obtaining the NP numbers and both the gravity (vessel) and wind loads shown.

NP	Vessel, kN	Wind Moment, kN	$\sum$ = P matrix, kN
6	14.5	159.2	= 173.7
9	29.0	151.4	180.4
12	29.0	128.8	157.8
15	29.0	93.6	122.6
18	29.0	49.1	78.1
21	29.0	0.0	29.0
24	29.0	−49.1	−20.1
27	29.0	−93.6	−64.6
30	29.0	−128.8	−99.8
33	29.0	−151.4	−122.4
36	14.5	− 159.2	− 144.7
	$\sum$ = 290.0	= 0.0	= 290.0

Refer to the computations shown in Fig. E10-8*b* for the wind moment entries. Other types of overturning moment would be similarly computed.

The base + backfill + pedestal weights will be accounted for by inputting pedestal $H = 1.5 + 0.70 = 2.2$ m with $\gamma_c = 23.6$ kN/m^3.

For the base, input $T = 0.7$ m with an equivalent unit weight based on the soil depth over the base of 1.5 m and base thickness of 0.70 m, giving

$$\gamma_e = \frac{0.70 \times 23.6 + 1.50 \times 16.5}{0.7} = \mathbf{58.96} \text{ kN/m}^3$$

The total weight will be slightly different from Example 9-4 since we are using a "round" base here whereas in that example we used an octagon. For checking we should have:

$$\sum F_v = 0.7854(2.3^2)(1.5 + 0.7)(23.6) + 0.7854(6.60^2 - 2.30^2)(0.7)58.96 + 580$$
$$= 215.7 + 1240.5 + 580 = 2036.2$$

For 1/2 the base the vertical force $F = 2036.2/2 = \mathbf{1018.1}$ kN

Step 3. Check computer output. The output (Fig. E10-8*c*) shows the sum of soil springs:

$$F_v = 1018.8 \text{ kN} \approx 1018.1 \text{ input and is O.K.}$$

We can see from the output that there are no nodes where there is soil-base separation. The soil pressure beneath the base is fairly uniform in the interior. The soil pressure at node 1 is somewhat meaningless, but looking at several other nodes, we have the following pressure values:

Node	Soil *q*, kPa	
2	60.88	Pressed side
13	60.7	
24	120.1	

Node	Soil *q*, kPa	
12	59.9	Tension side
23	58.8	
34	114.2	

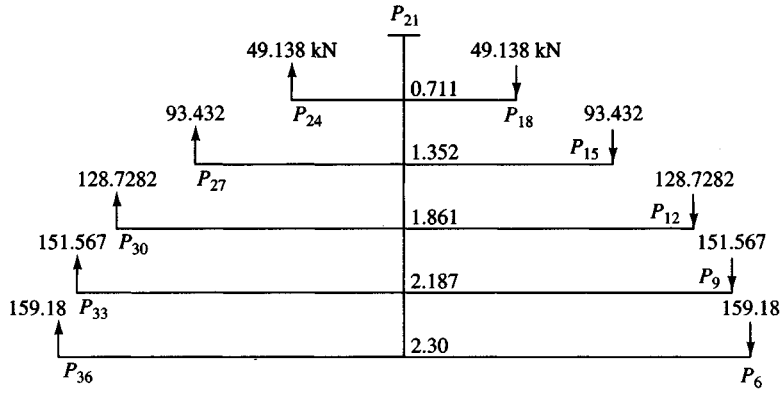

Compute moment arms for each pair of P values (P_{6-36}, P_{9-33}, P_{12-30}, P_{15-27}, and P_{18-24}) as

$$\text{Arm} = 2R\cos\theta\text{: } A_1 = 2(1.15)\cos 0 = 2.30 \text{ m}$$
$$A_2 = 2.30\cos 18 = 2.187 \text{ m}$$
$$A_3 = 2.30\cos 36 = 1.861 \text{ m}$$
$$A_4 = 2.30\cos 54 = 1.352 \text{ m}$$
$$A_5 = 2.30\cos 72 = 0.711 \text{ m}$$

And for $\frac{1}{2}$ wind moment at top of ring $M = 131.14(33.5/2)/2 = \mathbf{1098.2}$ kN · m

$$A_1P_6 + A_2P_9 + A_3P_{12} + A_4P_{15} + A_5P_{18} = 1098.2 \qquad (a)$$

$$P_{18} = \frac{0.71}{2.30}P_6 \qquad P_{15} = \frac{1.352}{2.30}P_6 \qquad P_{12} = \frac{1.861}{2.30}P_6 \qquad P_9 = \frac{2.187}{2.30}P_6$$

Substituting for P_i into Eq. (a) we obtain

$$2.30P_6 + 2.08P_6 + 1.506P_6 + 0.795P_6 + 0.219P_6 = 1098.5$$
$$P_6 = 1098.5/6.901 = \mathbf{159.2} \text{ kN}$$

Back-substitution gives

$$P_9 = \frac{2.187}{2.30}159.2 = 151.4 \text{ kN} \qquad P_{12} = \frac{1.861}{2.30}159.2 = 128.8 \text{ kN}$$
$$P_{15} = \frac{1.352}{2.30}159.2 = 93.6 \text{ kN} \qquad P_{18} = \frac{0.71}{2.30}159.2 = 49.1 \text{ kN}$$

These values are used with the gravity load to produce the full vertical P matrix entry values given in the text.

Figure E10-8*b*

The soil pressures show the effects of the pedestal on "fixing" the base slab. They also show (and based on Example 9-4) that the depth is substantially more than is required for either wide-beam or two-way shear. The high edge node pressures at nodes 24 and 34 result from doubling k_s instead of doubling the soil springs.

Step 4. Find the amount of steel reinforcing required. The radial moment at the face of the pedestal is

$$\text{RM2} = M_r = -13.41 \text{ kN} \cdot \text{m for an element width of } 1.075 \text{ m}$$
$$= -13.41/1.075 = -12.5 \text{ kN} \cdot \text{m/m}$$

```
++++++++++++++ NAME OF DATA FILE USED FOR THIS EXECUTION:  EXAM107A.DTA

 REDO EXAM 9-4 AS A ROUND PLATE WITH EDGE SPRGS DOUBLED USING Ks

NO OF ELEMENTS IN PLATE =   73          NO OF NODES =   34
NO OF NP =  102                  BANDWIDTH, NBAND =   36
          TOTAL STIFF ENTRIES, ISIZE =     3672
          NO OF PEDESTAL NODES, NPED =   12
       PEDESTAL ON RADIAL LINE, IPED =  1
NO OF ELEMENTS ON RADIAL LINE, IRADM =  3
          NO OF RADIAL LINES, IRADL =  11
    NO OF TANGENTIAL ELEMENTS, ITRAN = 10

NO OF NON-ZERO P-MATRIX ENTRIES =   11     NO LOAD CASES, NLC =  1
LIST ELEMENT DATA, LISTA =  1          LIST BAND MATRIX (>0) =  0
NO OF BOUNDARY CONDIT, NZX =   8    CONSIDER NON-LINEAR (> 0) =  1
EDGE SPRINGS DOUBLED (IF > 0), IDBLK =  0       IMST (SI > 0) = 1


MODULUS OF ELASTICITY  E =21500000.0   G = 9350000.0 KPA

UNIT WEIGTHS:  PEDESTAL = 23.600   OF FTG = 58.960 KN/M**3
 CENTRAL ANGLE BETWEEN RADIAL LINES, THET =  18.000 DEG
BASE THICKNESS:  PEDESTAL =   2.200    FOOTING =    .700  M

THE RADIAL NODE VALUES OF Ks ( KN/M**3) ARE:
  18000.0  18000.0  18000.0  36000.0

MAX LINEAR SOIL DEFL, XMAX =  1.000  M
```

MEMNO	NP1	NP2	NP3	NP4	NP5	NP6	ICODE	LEN	BAVG	T	INERTIA	POLAR I
1	1	2	3	4	5	6	0	1.150	.090	2.200	.79771E-01	.57095E-03
2	1	2	3	7	8	9	0	1.150	.180	2.200	.15963	.44542E-02
3	1	2	3	10	11	12	0	1.150	.180	2.200	.15963	.44542E-02
4	1	2	3	13	14	15	0	1.150	.180	2.200	.15963	.44542E-02
5	1	2	3	16	17	18	0	1.150	.180	2.200	.15963	.44542E-02
6	1	2	3	19	20	21	0	1.150	.180	2.200	.15963	.44542E-02
7	1	2	3	22	23	24	0	1.150	.180	2.200	.15963	.44542E-02
8	1	2	3	25	26	27	0	1.150	.180	2.200	.15963	.44542E-02
9	1	2	3	28	29	30	0	1.150	.180	2.200	.15963	.44542E-02
10	1	2	3	31	32	33	0	1.150	.180	2.200	.15963	.44542E-02
11	1	2	3	34	35	36	0	1.150	.090	2.200	.79771E-01	.57095E-03
12	4	5	6	7	8	9	0	.360	.575	2.200	.51022	.72869E-01
13	7	8	9	10	11	12	0	.360	.575	2.200	.51022	.72869E-01
14	10	11	12	13	14	15	0	.360	.575	2.200	.51022	.72869E-01
15	13	14	15	16	17	18	0	.360	.575	2.200	.51022	.72869E-01
16	16	17	18	19	20	21	0	.360	.575	2.200	.51022	.72869E-01
17	19	20	21	22	23	24	0	.360	.575	2.200	.51022	.72869E-01
18	22	23	24	25	26	27	0	.360	.575	2.200	.51022	.72869E-01
19	25	26	27	28	29	30	0	.360	.575	2.200	.51022	.72869E-01
20	28	29	30	31	32	33	0	.360	.575	2.200	.51022	.72869E-01
21	31	32	33	34	35	36	0	.360	.575	2.200	.51022	.72869E-01
22	4	5	6	7	8	9	0	.360	.500	.700	.14292E-01	.11746E-01
23	7	8	9	10	11	12	0	.360	.500	.700	.14292E-01	.11746E-01
24	10	11	12	13	14	15	0	.360	.500	.700	.14292E-01	.11746E-01
25	13	14	15	16	17	18	0	.360	.500	.700	.14292E-01	.11746E-01
26	16	17	18	19	20	21	0	.360	.500	.700	.14292E-01	.11746E-01
27	19	20	21	22	23	24	0	.360	.500	.700	.14292E-01	.11746E-01
28	22	23	24	25	26	27	0	.360	.500	.700	.14292E-01	.11746E-01
29	25	26	27	28	29	30	0	.360	.500	.700	.14292E-01	.11746E-01
30	28	29	30	31	32	33	0	.360	.500	.700	.14292E-01	.11746E-01
31	31	32	33	34	35	36	0	.360	.500	.700	.14292E-01	.11746E-01
32	4	5	6	37	38	39	0	1.000	.258	.700	.73774E-02	.33890E-02
33	7	8	9	40	41	42	0	1.000	.516	.700	.14755E-01	.19303E-01
34	10	11	12	43	44	45	0	1.000	.516	.700	.14755E-01	.19303E-01
35	13	14	15	46	47	48	0	1.000	.516	.700	.14755E-01	.19303E-01
36	16	17	18	49	50	51	0	1.000	.516	.700	.14755E-01	.19303E-01
37	19	20	21	52	53	54	0	1.000	.516	.700	.14755E-01	.19303E-01
38	22	23	24	55	56	57	0	1.000	.516	.700	.14755E-01	.19303E-01
39	25	26	27	58	59	60	0	1.000	.516	.700	.14755E-01	.19303E-01
40	28	29	30	61	62	63	0	1.000	.516	.700	.14755E-01	.19303E-01
41	31	32	33	64	65	66	0	1.000	.516	.700	.14755E-01	.19303E-01
42	34	35	36	67	68	69	0	1.000	.258	.700	.73774E-02	.33890E-02
43	37	38	39	40	41	42	0	.673	1.075	.700	.30727E-01	.45825E-01

Figure E10-8*c* *(4pages of computer output—1/4)*

```
 44   40   41   42   43   44   45       0      .673     1.075      .700   .30727E-01   .45825E-01
 45   43   44   45   46   47   48       0      .673     1.075      .700   .30727E-01   .45825E-01
 46   46   47   48   49   50   51       0      .673     1.075      .700   .30727E-01   .45825E-01
 47   49   50   51   52   53   54       0      .673     1.075      .700   .30727E-01   .45825E-01
 48   52   53   54   55   56   57       0      .673     1.075      .700   .30727E-01   .45825E-01
 49   55   56   57   58   59   60       0      .673     1.075      .700   .30727E-01   .45825E-01
 50   58   59   60   61   62   63       0      .673     1.075      .700   .30727E-01   .45825E-01
 51   61   62   63   64   65   66       0      .673     1.075      .700   .30727E-01   .45825E-01
 52   64   65   66   67   68   69       0      .673     1.075      .700   .30727E-01   .45825E-01
 53   37   38   39   70   71   72       0     1.150      .426      .700   .12185E-01   .12341E-01
 54   40   41   42   73   74   75       0     1.150      .853      .700   .24370E-01   .53855E-01
 55   43   44   45   76   77   78       0     1.150      .853      .700   .24370E-01   .53855E-01
 56   46   47   48   79   80   81       0     1.150      .853      .700   .24370E-01   .53855E-01
 57   49   50   51   82   83   84       0     1.150      .853      .700   .24370E-01   .53855E-01
 58   52   53   54   85   86   87       0     1.150      .853      .700   .24370E-01   .53855E-01
 59   55   56   57   88   89   90       0     1.150      .853      .700   .24370E-01   .53855E-01
 60   58   59   60   91   92   93       0     1.150      .853      .700   .24370E-01   .53855E-01
 61   61   62   63   94   95   96       0     1.150      .853      .700   .24370E-01   .53855E-01
 62   64   65   66   97   98   99       0     1.150      .853      .700   .24370E-01   .53855E-01
 63   67   68   69  100  101  102       0     1.150      .426      .700   .12185E-01   .12341E-01
 64   70   71   72   73   74   75       0     1.033      .575      .700   .16435E-01   .24497E-01
 65   73   74   75   76   77   78       0     1.033      .575      .700   .16435E-01   .24497E-01
 66   76   77   78   79   80   81       0     1.033      .575      .700   .16435E-01   .24497E-01
 67   79   80   81   82   83   84       0     1.033      .575      .700   .16435E-01   .24497E-01
 68   82   83   84   85   86   87       0     1.033      .575      .700   .16435E-01   .24497E-01
 69   85   86   87   88   89   90       0     1.033      .575      .700   .16435E-01   .24497E-01
 70   88   89   90   91   92   93       0     1.033      .575      .700   .16435E-01   .24497E-01
 71   91   92   93   94   95   96       0     1.033      .575      .700   .16435E-01   .24497E-01
 72   94   95   96   97   98   99       0     1.033      .575      .700   .16435E-01   .24497E-01
 73   97   98   99  100  101  102       0     1.033      .575      .700   .16435E-01   .24497E-01

THE FOOTING AREA (AREA(I)) ARRAY IS:

 1     .00  2     .11  3     .22  4     .22  5     .22  6     .22  7     .22

 8     .22  9     .22 10     .22 11     .22 12     .11 13     .37 14     .74

15     .74 16     .74 17     .74 18     .74 19     .74 20     .74 21     .74

22     .74 23     .37 24     .27 25     .54 26     .54 27     .54 28     .54

29     .54 30     .54 31     .54 32     .54 33     .54 34     .27

THE PEDESTAL AREA (AREAP(I)) ARRAY IS:

1     .52  2     .08  3     .16  4     .16  5     .16  6     .16  7     .16

8     .16  9     .16 10     .16 11     .16 12     .08

++++++++++ THE INITIAL SUM OF ALL VERTICAL LOADS INCL FTG WEIGHT =   1019.15   KN


LOAD CONDITION   1   (EVERY 3RD = VERT LOAD)

  1    .000   2    .000   3   26.998   4    .000   5    .000   6   182.394   7    .000   8    .000   9   197.787
 10    .000  11    .000  12  175.187  13    .000  14    .000  15   139.987  16    .000  17    .000  18    95.487
 19    .000  20    .000  21   46.387  22    .000  23    .000  24    -2.713  25    .000  26    .000  27   -47.213
 28    .000  29    .000  30  -82.413  31    .000  32    .000  33  -105.013  34    .000  35    .000  36  -136.006
 37    .000  38    .000  39   15.271  40    .000  41    .000  42    30.541  43    .000  44    .000  45    30.541
 46    .000  47    .000  48   30.541  49    .000  50    .000  51    30.541  52    .000  53    .000  54    30.541
 55    .000  56    .000  57   30.541  58    .000  59    .000  60    30.541  61    .000  62    .000  63    30.541
 64    .000  65    .000  66   30.541  67    .000  68    .000  69    15.271  70    .000  71    .000  72    11.143
 73    .000  74    .000  75   22.287  76    .000  77    .000  78    22.287  79    .000  80    .000  81    22.287
 82    .000  83    .000  84   22.287  85    .000  86    .000  87    22.287  88    .000  89    .000  90    22.287
 91    .000  92    .000  93   22.287  94    .000  95    .000  96    22.287  97    .000  98    .000  99    22.287
100    .000 101    .000 102   11.143

BOUNDARY CONDITIONS OF ZERO DISPLACEMENT AT:
    1    2    4   34   37   67   70  100
IN SUBROUTINE CHECK--NONLIN =    1  XMAX =      1.000

CURRENT CYCLE. JJ =  1   ICOUN(JJ)  =  0   JCOUR (RECYCLE IF > 0) = 0


ELEMENT FORCES FOR LOAD CASE = 1
```

Figure E10-8*c* (*continued*—2/4)

MEMNO	BENDING MOMENTS		TORSION MOMENT	N.E. SHR (-=UP)	ELEM AV WIDTH
1	-100.5205	-19.4522	.0000	-104.32	.090
2	-191.6382	-41.8842	.2721	-203.06	.180
3	-160.7347	-40.6058	.4917	-175.08	.180
4	-112.6487	-34.5627	.6509	-128.01	.180
5	-52.8126	-24.9454	.7471	-67.62	.180
6	12.9680	-13.4578	.7793	-.43	.180
7	78.7540	-1.9765	.7474	66.76	.180
8	138.5960	7.5960	.6513	127.12	.180
9	186.6931	13.6227	.4918	174.19	.180
10	217.6103	14.9189	.2722	202.20	.180
11	113.4990	5.9717	.0000	103.89	.090
12	-13.4998	32.3752	-1.6833	52.46	.575
13	-32.9992	33.1258	-3.0351	.35	.575
14	-34.2300	17.8950	-3.8275	-45.40	.575
15	-18.9657	-9.5907	-4.3013	-79.37	.575
16	8.2991	-43.0759	-4.5260	-96.66	.575
17	41.7519	-76.3731	-4.5280	-96.22	.575
18	74.9879	-103.5121	-4.3107	-79.28	.575
19	102.1349	-118.6151	-3.8324	-45.80	.575
20	117.5873	-117.6627	-3.0330	-.21	.575
21	116.9295	-98.1955	-1.6854	52.07	.575
22	-.3832	.9059	-.2713	1.45	.500
23	-.9214	.9262	-.4892	.01	.500
24	-.9569	.5002	-.6170	-1.27	.500
25	-.5299	-.2643	-.6934	-2.21	.500
26	.2289	-1.2047	-.7296	-2.71	.500
27	1.1711	-2.1375	-.7299	-2.69	.500
28	2.1037	-2.8963	-.6949	-2.20	.500
29	2.8651	-3.3224	-.6178	-1.27	.500
30	3.2926	-3.2933	-.4889	.00	.500
31	3.2739	-2.7535	-.2717	1.45	.500
32	15.3158	-2.2303	.0000	13.09	.258
33	29.8220	-4.7004	.1041	25.12	.516
34	28.8754	-4.7745	.2521	24.10	.516
35	28.1285	-4.6063	.3730	23.52	.516
36	27.5598	-4.2742	.4449	23.29	.516
37	27.0790	-3.8663	.4678	23.21	.516
38	26.5957	-3.4590	.4445	23.14	.516
39	26.0209	-3.1299	.3729	22.89	.516
40	25.2725	-2.9614	.2527	22.31	.516
41	24.3300	-3.0333	.1046	21.30	.516
42	11.7601	-1.6369	.0000	10.12	.258
43	16.9128	-16.4349	.0561	.71	1.075
44	16.6218	-15.8528	.0409	1.14	1.075
45	16.1671	-15.6063	-.0350	.83	1.075
46	15.9786	-15.7597	-.1023	.33	1.075
47	16.1509	-16.1538	-.1370	.00	1.075
48	16.5477	-16.5480	-.1368	.00	1.075
49	16.9405	-16.7138	-.1018	.34	1.075
50	17.0858	-16.5236	-.0348	.84	1.075
51	16.8370	-16.0712	.0401	1.14	1.075
52	16.2549	-15.7783	.0559	.71	1.075
53	4.9314	1.0562	.0000	5.21	.426
54	9.8571	2.0924	-.0640	10.39	.853
55	9.7097	2.0398	-.0559	10.22	.853
56	9.4809	2.0063	-.0147	9.99	.853
57	9.2316	2.0099	.0193	9.78	.853
58	8.9817	2.0379	.0314	9.58	.853
59	8.7329	2.0659	.0193	9.39	.853
60	8.4836	2.0690	-.0150	9.18	.853
61	8.2550	2.0358	-.0559	8.95	.853
62	8.1062	1.9826	-.0638	8.77	.853
63	4.0504	.9813	.0000	4.38	.426
64	6.6812	-6.6645	.0110	.02	.575
65	6.6059	-6.5376	.0275	.07	.575
66	6.4895	-6.4284	.0292	.06	.575
67	6.4212	-6.4192	.0256	.00	.575
68	6.4457	-6.4947	.0231	-.05	.575
69	6.5328	-6.5810	.0231	-.05	.575
70	6.6076	-6.6048	.0256	.00	.575
71	6.5981	-6.5362	.0292	.06	.575
72	6.4885	-6.4188	.0274	.07	.575
73	6.3599	-6.3433	.0110	.02	.575

FOR LOAD CASE = 1
NODE MOMENTS--TM1,TM2 ARE TANG--RM1,RM2 = RADIAL
AT NODE 1 MOMENTS ARE HORIZONTAL AND VERTICAL--GET SIGNS FOR DESIGN BY
CHECKING 1 OR MORE NODES BY HAND

Figure E10-8c (*continued*—3/4)

NODE	TM1	TM2	BTAN	RM1	RM2	BRAD	NODE	DISPLACEMENTS--3RD = DEFL (* = B.C.)				
1	1076.53	.00	.090	.00	82.25	.000	1*	.000000	2*	.000000	3	.003359
2	15.35	-15.32	.258	.00	-13.41	1.075	4*	.000000	5	.000027	6	.003382
3	29.82	-29.82	.516	33.28	-33.22	1.075	7	.000008	8	.000025	9	.003381
4	28.87	-28.88	.516	34.44	-34.55	1.075	10	.000014	11	.000020	12	.003377
5	28.09	-28.13	.516	19.24	-19.13	1.075	13	.000018	14	.000013	15	.003371
6	27.56	-27.56	.516	-8.51	8.50	1.075	16	.000021	17	.000005	18	.003364
7	27.09	-27.08	.516	-42.45	42.44	1.075	19	.000022	20	-.000004	21	.003356
8	26.56	-26.60	.516	-76.28	76.18	1.075	22	.000021	23	-.000014	24	.003349
9	26.02	-26.02	.516	-103.94	103.75	1.075	25	.000018	26	-.000022	27	.003342
10	25.27	-25.27	.516	-119.49	119.45	1.075	28	.000014	29	-.000029	30	.003336
11	24.35	-24.33	.516	-118.81	118.76	1.075	31	.000008	32	-.000034	33	.003332
12	11.75	-11.76	.258	-99.40	.00	1.075	34*	.000000	35	-.000036	36	.003330
13	4.93	-4.93	.426	.00	16.70	1.075	37*	.000000	38	-.000028	39	.003375
14	9.86	-9.86	.853	-16.31	16.31	1.075	40	.000008	41	-.000029	42	.003372
15	9.71	-9.71	.853	-15.72	15.72	1.075	43	.000015	44	-.000033	45	.003364
16	9.48	-9.48	.853	-15.42	15.42	1.075	46	.000020	47	-.000039	48	.003352
17	9.23	-9.23	.853	-15.53	15.53	1.075	49	.000023	50	-.000046	51	.003338
18	8.98	-8.98	.853	-15.90	15.90	1.075	52	.000024	53	-.000053	54	.003321
19	8.73	-8.73	.853	-16.30	16.30	1.075	55	.000023	56	-.000061	57	.003305
20	8.48	-8.48	.853	-16.51	16.51	1.075	58	.000020	59	-.000068	60	.003291
21	8.25	-8.26	.853	-16.37	16.37	1.075	61	.000015	62	-.000073	63	.003279
22	8.10	-8.11	.853	-15.94	15.94	1.075	64	.000008	65	-.000077	66	.003271
23	4.05	-4.05	.426	-15.59	.00	1.075	67*	.000000	68	-.000078	69	.003268
24	.00	.00	.426	.00	6.60	.575	70*	.000000	71	-.000037	72	.003335
25	.00	.00	.853	-6.58	6.58	.575	73	.000008	74	-.000038	75	.003331
26	.00	.00	.853	-6.46	6.46	.575	76	.000015	77	-.000041	78	.003319
27	.00	.00	.853	-6.35	6.35	.575	79	.000020	80	-.000047	81	.003301
28	.00	.00	.853	-6.34	6.34	.575	82	.000023	83	-.000053	84	.003278
29	.00	.00	.853	-6.42	6.42	.575	85	.000024	86	-.000061	87	.003254
30	.00	.00	.853	-6.50	6.50	.575	88	.000023	89	-.000068	90	.003229
31	.00	.00	.853	-6.53	6.53	.575	91	.000020	92	-.000075	93	.003206
32	.00	.00	.853	-6.46	6.46	.575	94	.000015	95	-.000080	96	.003188
33	.00	.00	.853	-6.34	6.34	.575	97	.000008	98	-.000084	99	.003176
34	.00	.00	.426	-6.27	.00	.575	100*	.000000	101	-.000085	102	.003172

SOIL NODE DATA--* = NOT SUMMED, D= SPRING DOUBLED

NODE	SOIL REACT, KN	SOIL SPRING,KN/M	DISPL, M	SOIL PRESS,KPA	Ks,KN/M**3
1	31.40	9348.2	.003359	60.460	18000.0
2	11.44	3381.4	.003382	60.880	18000.0
3	22.86	6762.9	.003381	60.854	18000.0
4	22.84	6762.9	.003377	60.784	18000.0
5	22.80	6762.9	.003371	60.680	18000.0
6	22.75	6762.9	.003364	60.553	18000.0
7	22.70	6762.9	.003356	60.414	18000.0
8	22.65	6762.9	.003349	60.275	18000.0
9	22.60	6762.9	.003342	60.148	18000.0
10	22.56	6762.9	.003336	60.044	18000.0
11	22.53	6762.9	.003332	59.974	18000.0
12	11.26	3381.4	.003330	59.948	18000.0
13	22.44	6648.9	.003375	60.747	18000.0
14	44.84	13297.8	.003372	60.697	18000.0
15	44.74	13297.8	.003364	60.555	18000.0
16	44.58	13297.8	.003352	60.340	18000.0
17	44.38	13297.8	.003338	60.075	18000.0
18	44.17	13297.8	.003321	59.786	18000.0
19	43.95	13297.8	.003305	59.496	18000.0
20	43.76	13297.8	.003291	59.231	18000.0
21	43.60	13297.8	.003279	59.016	18000.0
22	43.49	13297.8	.003271	58.874	18000.0
23	21.73	6648.9	.003268	58.824	18000.0
24	16.33	4897.6	.003335	120.063	36000.0
25	32.63	9795.3	.003331	119.914	36000.0
26	32.51	9795.3	.003319	119.485	36000.0
27	32.33	9795.3	.003301	118.829	36000.0
28	32.11	9795.3	.003278	118.017	36000.0
29	31.87	9795.3	.003254	117.128	36000.0
30	31.63	9795.3	.003229	116.238	36000.0
31	31.41	9795.3	.003206	115.426	36000.0
32	31.23	9795.3	.003188	114.770	36000.0
33	31.11	9795.3	.003176	114.340	36000.0
34	15.54	4897.6	.003172	114.191	36000.0

SUM OF VERTICAL LOADS (ADJ FOR ANY DEFL > XMAX) = 1019.15 KN
THE SUM OF NODAL SOIL REACTIONS (LESS ANY SHOWN ABOVE WITH *) = 1018.75 KN

SUM ANY SOIL REACTIONS WITH * AND ADD TO BOTH TOTALS
THIS SUM + SUM OF VERT LOAD = INPUT SUM OF VERT LOADS

++++ NOTE THAT IF YOU USE NONLIN > 0 AND THERE ARE DISPL > XMAX
THE ORIGINAL P-MATRIX WAS MODIFIED TO INCLUDE -XMAX*SPRNG(I) VALUES
YOU CAN VERIFY THIS BY COMPARING INPUT AND OUTPUT SUM OF VERTICAL FORCES

Figure E10-8*c* (*continued*—4/4)

The tangential moment at the face of the pedestal (node 2 and element 32):

$$\begin{aligned} \text{TM1} &= M_t = 15.35 \text{ kN} \cdot \text{M for an element width of } 0.258 \text{ m} \\ &= 15.35/0.258 = 59.5 \text{ kN} \cdot \text{m/m} \leftarrow \text{use for design} \end{aligned}$$

Applying an LF = 1.5 the design moment = $1.5 \times 59.5 = \mathbf{89.2}$ kN · m/m. From inspection of the element moment table it appears that there are moments producing "tension" in the top of the slab. This table also shows that the largest element bending moments are under the pedestal, but they would not be used for design, since the effective depth here is so large that the minimum steel requirements will control. Critical design moments will be found between element numbers 32 and 73. Since we know that the amount of rebars required in Example 9-4 was based on $1.4/f_y$ and the moments here are substantially less, it is evident that $1.4/f_y$ will control here as well. Therefore the rebar (with $d = 605$ mm from Example 9-4) requirements are

$$\frac{1.4}{f_y} = \frac{1.4}{400} = 0.0035 \qquad \text{and} \qquad A_s = 0.0035 \times 1000 \times 605 = \mathbf{2118} \text{ mm}^2/\text{m}$$

Use 7 No. 30 bars ($7 \times 300 = 2100$ mm^2), radiating from approximately the center to the edge in all directions. Circular (tangential) rebars of the same size and quantity should also be placed for the small twisting moments.

Step 5. Estimate tower tilt. From the computer output we have for the three critical pedestal nodes (1, 2, and 12) the following displacements:

Node	Vertical displacement, m
12	0.003330
1	0.003359
2	0.003382

The slope is obtained from plotting to a large vertical scale; however, a fairly good value can be obtained by taking the displacements at nodes 2 and 12 divided by the pedestal width of 2.30 m to obtain

$$\theta = \frac{0.003\,382 - 0.003\,330}{2.30} = \mathbf{0.000\,0226} \text{ rad}$$

The tower top movement referenced to the bottom of the base (refer to Fig. E9-4*a*) is

$$\delta H = H\theta = (33.5 + 0.30 + 1.50 + 0.70) \times 0.000\,0226 \times 1000 = \mathbf{0.81} \text{ mm}$$

This amount is negligible, but would probably be larger if we tried to save on concrete by using a hollow pedestal and a thinner base.

The pedestal rotations could have been specified as zero using boundary conditions but were not. Probably an execution should have been made setting them to zero (both radial and tangential) and seeing the effect on the output.

Note that the approximate solution of Example 9-4 does not provide a different design (unless we want to use a hollow pedestal with a wall thickness of about 200 mm and reduce the base slab thickness) from the one used here. This analysis, however, gives more confidence in soil pressures and tower tilt.

////

10-13 BOUNDARY CONDITIONS

We have identified boundary conditions of zero rotation or zero displacement. For example, in Example 10-6 we fixed the rotation at the column face nodes to input a total of 32 rotations that were set to zero. We used "boundary conditions" based on symmetry in the round plate analysis by fixing select rotation NPs along the diameter.

Table 10-1 was prepared using boundary conditions to solve only a portion of a plate. One does not arbitrarily select boundary conditions. Rather, one examines the problem carefully to decide intuitively where a nodal rotation will be zero from fixity or from symmetry. Similarly one must recognize when a translation will be zero (as at a fixed edge). For example, if we only solved 1/4 of the circular base of Fig. 10-15 we would specify the radial rotation equals zero at all the horizontal and vertical nodes that are adjacent to the other 3/4 of the base.

At the center node both rotation Xs would be set to zero. Except at the center, the tangential node rotations would not be set to zero. This convention complies with the concept of symmetrical displacements of the full plate so that what one has done produces a correct solution. If one sets boundary conditions to zero that are not consistent with the element model, one can get some strange computed results. For any plate supported only on an elastic foundation, no vertical displacements would be set to zero.

Although the foregoing boundary cases are valid for a symmetrical vertical load, when one has overturning the amount of plate involved for a symmetrical set of displacements changes; one usually must use 1/2 the plate. Example 10-7 was symmetrical for the first load case (four equal loads and symmetrical column spacing), so we could have used only one-quarter of the mat with appropriate zeroing of rotation NPs. However, with wind we would have had to use half the plate. In this case, after considering the difficulty in creating a data file, one is better off to start with half the plate so the data can simply be copied and select entries edited.

If symmetry does not exist for all possible load cases, one probably should ignore symmetry. The additional engineering time to produce extra data sets for the several cases + identification of nodes with symmetry and to do a closer output check will more than offset the slight savings in computational effort— particularly at current costs for computer time.

PROBLEMS

10-1. What would you recommend for q_a in Example 10-1 for plates on the order of 2- to 3-m square?

10-2. For a 3-m square base and data from Examples 10-1 and 10-2, what do you recommend for k_s?

10-3. For a 20-m square mat and data from Example 10-2, what do you recommend for k_s?

10-4. Make a plot of center k_s versus B for values of B from 3 to 30 m. Comment on curve shape; does B have a substantial effect on k_s? Assume $H/B' = 10$ (the stratum depth H is at least 150 m). Also assume the plate is on the ground surface so that $I_F = 1.0$. Take $E_s = 5000 + 1000z$ kPa.

10-5. Use diskette program FADMAT (B-6) and execute the diskette data sets labeled EXAM105A.DTA and EXAM105B.DTA. From the output do a statics check of node 10 or 16 as assigned and for the output set assigned.

10-6. Using a copy of data set EXAM105A.DTA make an execution using k_s = 7850, 31 400, and 47 100 kN/m^3. Can you draw any conclusions concerning the effect of k_s on node moment and displacement of nodes 1 and 21? Make a neat table with values tabulated versus k_s.

10-7. Use program FADMAT and execute the three data sets provided and labeled EXAM106?.DTA (the notched footing). Do a statics check of node 54. How do the computed soil pressures compare to a $q = P/A$ where A = area of footing with notch in it?

10-8. Use program FADMAT and redo Example 10-7 using the three data sets provided (EXAM 107?.DTA where ? represents A, B, C). Compare the moments at node 25 for the three cases (no edge spring doubling, edge spring doubling, and zoning k_s). Which of the three cases do you think provides the best set of design data?

10-9. If you did Problem 10-8 use that output; if not, execute data set EXAM107B.DTA (the mat with two load cases—gravity and gravity with wind). From the output check two-way shear to see if the depth is adequate for the wind load case (LC = 2) for element 51 at the right side of column 2. Also do a statics check for corner nodes 1 and 11.

10-10. Make a plot of the vertical displacement along the diameter of the round base of Example 9-7 (along nodes 34, 23, 1, 13, 24). Using this plot estimate the amount of top drift (movement) during wind and compare this to the value given in the example.

10-11. Verify the **P** matrix entries for the overturning moment for Example 10-8.

10-12. See if you can perform a statics check at node 13 of Example 10-8. There are only three elements (32, 43, and 53) framing into this node.

10-13. Design a chimney foundation for the following data:

Chimney height above ground = 250 m

Bottom OD = 20 m Top ID = 7 m

Bottom wall thickness = 0.8 m Top wall thickness = 0.2 m

Weight above foundation including liner = 104 200 kN

For wind use the values (factors such as velocity, pressure, importance factor, etc.) given in Example 9-4. Take q_a = 400 kPa and place the base of the foundation 4.0 m below ground surface; the base will be backfilled. Use a reasonable estimate for γ_{backfill}.

Make an approximate hand solution, and if you have access to programs B-20 and B-21 (or similar), also analyze the foundation as a round plate. Be sure to make a neat sketch of the chimney and base, and show enough dimensions that your work can be verified.